Wed. May 29, 2019

[E] Poster | P (Space and Planetary Sciences)：P-PS Planetary Sciences

10:45 AM - 12:15 PM JST | 1:45 AM - 3:15 AM UTC | Poster Hall International Exhibition Hall8, Makuhari Messe_2

[P-PS02] Regolith Science

convener:Koji Wada(Planetary Exploration Research Center, Chiba Institute of Technology), Akiko Nakamura(Graduate School of Science, Kobe University), Patrick Michel(Observatoire De La Cote D'Azur), Kevin John Walsh(Southwest Research Institute Boulder)

[PPS02-P01] Abrasion experiments of mineral and meteorite grains: Dependence of particle size and vibration rate on abrasion rate and its application to Itokawa and lunar regolith particles.

*Hirotaka Yamaguchi[1], Akira Tsuchiyama[1], Akiko Nakamura[2] (1.National University Corporation, Kyoto University, 2.National University Corporation,Kobe University)

[PPS02-P02] Measurements of adhesive force of meteorite powders using centrifugal method

*Yuuya Nagaashi[1], Akiko Nakamura[1] (1.Kobe University)

[PPS02-P03] Laboratory impact penetration experiments conducted at simulated reduced gravity

*Akiko Nakamura[1], Kana Morizono[2], Yuuya Nagaashi[1] (1.Graduate School of Science, Kobe University, 2.Faculty of Science, Kobe University)

[PPS02-P04] MARAUDERS: Using instrumented nano-impactors to probe the icy properties of Lunar permanently shadowed regions

*Ronald Ballouz[1], Sarah T Crites[2], Naoya Ozaki[2], Shun Arahata[3], Nicola Baresi[2], Ralf Bolden, Onur Celik[4,2], Yu Himeno[3], Lucie Riu[2], Kevin J Walsh[5] (1.Lunar and Planetary Lab, University of Arizona, Tucson, AZ, USA, 2.Institute of Space and Astronautical Science, Sagamihara, Japan, 3.University of Tokyo, Tokyo, Japan, 4.Sokendai Graduate University, Japan, 5.Southwest Research Institute, Boulder, CO, USA)

[PPS02-P05] Surface size-frequency distribution of accumulating boulders using discrete element simulations of spherical particles in 3D

*Hiroshi Kikuchi[1], Hideaki Miyamoto[1] (1.The University of Tokyo)

[PPS02-P06] Experimental Study to Determine the Best Compression Ratio of High-Resolution Images of Small Bodies for the Martian Moons eXploration (MMX) Mission

*Yuta Shimizu[1], Hiroaki Kamiyoshihara[1], Takafumi Niihara[1], Hideaki Miyamoto[1] (1.University of Tokyo)

[E] Poster | P (Space and Planetary Sciences)：P-PS Planetary Sciences

5:15 PM - 6:30 PM JST | 8:15 AM - 9:30 AM UTC | Poster Hall International Exhibition Hall8, Makuhari Messe_2

[P-PS02] Regolith Science

convener:Koji Wada(Planetary Exploration Research Center, Chiba Institute of Technology), Akiko Nakamura(Graduate School of Science, Kobe University), Patrick Michel(Observatoire De La Cote D'Azur), Kevin John Walsh(Southwest Research Institute Boulder)

[PPS02-P01] Abrasion experiments of mineral and meteorite grains: Dependence of particle size and vibration rate on abrasion rate and its application to Itokawa and lunar regolith particles.

*Hirotaka Yamaguchi[1], Akira Tsuchiyama[1], Akiko Nakamura[2] (1.National University Corporation, Kyoto University, 2.National University Corporation,Kobe University)

[PPS02-P02] Measurements of adhesive force of meteorite powders using centrifugal method

*Yuuya Nagaashi[1], Akiko Nakamura[1] (1.Kobe University)

[PPS02-P03] Laboratory impact penetration experiments conducted at simulated reduced gravity

*Akiko Nakamura[1], Kana Morizono[2], Yuuya Nagaashi[1] (1.Graduate School of Science, Kobe University, 2.Faculty of Science, Kobe University)

[PPS02-P04] MARAUDERS: Using instrumented nano-impactors to probe the icy properties of Lunar permanently shadowed regions

*Ronald Ballouz[1], Sarah T Crites[2], Naoya Ozaki[2], Shun Arahata[3], Nicola Baresi[2], Ralf Bolden, Onur Celik[4,2], Yu Himeno[3], Lucie Riu[2], Kevin J Walsh[5] (1.Lunar and Planetary Lab, University of Arizona, Tucson, AZ, USA, 2.Institute of Space and Astronautical Science, Sagamihara, Japan, 3.University of Tokyo, Tokyo, Japan, 4.Sokendai Graduate University, Japan, 5.Southwest Research Institute, Boulder, CO, USA)

[PPS02-P05] Surface size-frequency distribution of accumulating boulders using discrete element simulations of spherical particles in 3D

*Hiroshi Kikuchi[1], Hideaki Miyamoto[1] (1.The University of Tokyo)

[PPS02-P06] Experimental Study to Determine the Best Compression Ratio of High-Resolution Images of Small Bodies for the Martian Moons eXploration (MMX) Mission

*Yuta Shimizu[1], Hiroaki Kamiyoshihara[1], Takafumi Niihara[1], Hideaki Miyamoto[1] (1.University of Tokyo)

[E] Poster | P (Space and Planetary Sciences)：P-PS Planetary Sciences

3:30 PM - 5:00 PM JST | 6:30 AM - 8:00 AM UTC | Poster Hall International Exhibition Hall8, Makuhari Messe_1

[P-PS03] Solar System Small Bodies: A New Frontier Arising Hayabusa 2, OSIRIS-REx and Other Projects

convener:Masateru Ishiguro(Department of Physics and Astronomy, Seoul National University), Taishi Nakamoto(Tokyo Institute of Technology), Masanao Abe(Institute of Space and Astronautical Science, Japan Aerospace Exploration Agency), Olivier S Barnouin(Johns Hopkins University Applied Physics Laboratory)

[PPS03-P01] Impact experiments on low strength coarse-grained regolith simulating surface materials on asteroid Ryugu

*Yuya Yamamoto[1], Masahiko Arakawa[1], Minami Yasui[1], Sunao Hasegawa[2], Ryo Sugimura[1] (1.Graduate School of Science, Kobe University, 2.ISAS, JAXA)

[PPS03-P02] Reflectance estimation of asteroid Ryugu using MASCOT

*Marika Ishida[1], Koto Amano[1], Keiichi Moroi[1], ERI TATSUMI[2], Tra-Mi Ho[10], Shingo Kameda[1], Seiji Sugita[2], Rie Honda[3], Tomokatsu Morota[4], yokota yasuhiro[5], Toru Kouyama[6], Hidehiko Suzuki[7], Manabu Yamada[8], Naoya Sakatani[5], Chikatoshi Honda[9], Masahiko Hayakawa[5], Kazuo Yoshioka[2], Moe Matsuoka[5], Yuichiro Cho[2], Hirotaka Sawada[5] (1.Rikkyo Univ., 2.Univ. of Tokyo, 3.Kochi Univ., 4.Nagoya Univ., 5.JAXA/ISAS, 6.AIST, 7.Meiji Univ., 8.Chiba Inst. Tech, 9.Univ. of Aizu, 10.DLR)

[PPS03-P03] Flyby observation of Asteroid (3200) Phaethon by DESTINY$^+$ onboard cameras

*Ko Ishibashi[1], Shingo Kameda[2], Masato Kagitani[3], Peng Hong[1], Manabu Yamada[1], Osamu Okudaira[1], Tomoko Arai[1], Fumi Yoshida[1], Shunsuke Sato[4], Takahiro Ishimaru[4], Takaya Okamoto[4], Takahiro Iwata[4], Tatsuaki Okada[4], Takeshi Takashima[4] (1.Chiba Institute of Technology, 2.Rikkyo University, 3.Tohoku Universtiy, 4.Japan Aerospace Exploration Agency)

[PPS03-P04] Polarimetric Study of Asteroids in Comet-Like Orbits (ACOs)

*Jooyeon Geem[1], Masateru Ishiguro[1], Yoonsoo P. Bach[1], Daisuke Kuroda[2], Hiroyuki Naito[3], Hidekazu Hanayama[4], yoonyoung kim[10], Yuna G. Kwon[1], Sunho Jin[1], Tomohiko Sekiguchi[5], Ryo Okazaki[5], Jeremie J. Vaubaillon[6], Masataka Imai[7], Tatsuharu Oono[8], Yuki Futamuts[8], Seiko Takagi[8], Mitsuteru Sato[8], Kiyoshi Kuramoto[8], Makoto Watanabe[9] (1.Astronomy program, Dept of Physics and Astronomy, Seoul National University, 2.Okayama Observatory, Kyoto University, 3.Nayoro Observatory, 4.Ishigakijima Astronomical Observatory, National Astronomical Observatory of Japan, 5.Hokkaido University of Education, 6.Observatoire de Paris, I.M.C.C.E., 7.National Institute of Advanced Industrial Science and Technology, 8.Department of Cosmosciences, Graduate School of Science, Hokkaido University, 9.Department of Applied Physics, Okayama University of Science, 10.Max Planck Institute for Solar System Research)

[PPS03-P05] Dynamical lifetime of the Oort Cloud new comets under planetary perturbation

*Ito Takashi[1], Arika Higuchi[1] (1.National Astronomical Observatory of Japan)

[PPS03-P06] Thermal Infrared Imaging of C-type Asteroid 162173 Ryugu with Porous Surfaces

*Tatsuaki Okada[1,2], Tetsuya Fukuhara[3], Satoshi Tanaka[1], Makoto Taguchi[3], Takehiko Arai[4], Naoya Sakatani[1], Yuri Shimaki[1], Hiroki Senshu[5], Yoshiko Ogawa[6], Hirohide Demura[6], Kentaro Suko[6], Kohei Kitazato[6], Toru Kouyama[7], Tomohiko Sekiguchi[8], Jun Takita[9], Sunao Hasegawa[1], Tsuneo Matsunaga[10], Takehiko Wada[1], Takeshi Imamura[2], Jorn Helbert[11], Thomas G. Mueller[12], Axel Hagermann[13], Jens Biele[11], Matthias Grott[11], Maximiliam Hamm[11], Marco Delbo[14], Yukio Yamamoto[1], Naru Hirata[6], Naoyuki Hirata[15], Fuyuto Terui[1], Takanao Saiki[1], Satoru Nakazawa[1], Makoto Yoshikawa[1], Sei-ichiro WATANABE[1,16], Yuichi Tuda[1] (1.Institute of Space and Astronautical Science, Japan Aerospace Exploration Agency, 2.University of Tokyo, 3.Rikkyo University, 4.Ashikaga University, 5.Chiba Institute of Technology, 6.University of Aizu, 7.National Institute of Advanced Industrial Science and Technology, 8.Hokkaido University of Education, 9.Hokkaido Kitami-Hokuto High School, 10.National Institute for Environmental Studies, 11.German Aerospace Center, 12.Max-Planck Institute for Extraterrestrial Physics, 13.University of Stirling, 14.Observatoire de la Côte d'Azur, 15.Kobe University, 16.Nagoya University)

[PPS03-P07] Data Release of Asteroid 162173 Ryugu by Observation of Thermal Infrared Imager onboard Hayabusa2

*Takehiko Arai[1], Hirohide Demura[2], Toru Kouyama[7], Naoya Sakatani[3], Kentaro Suko[2], Yuri Shimaki[3], Hiroki Senshu[5], Tomohiko Sekiguchi[6], Yoshiko Ogawa[2], Sunao Hasegawa[3], Takehiko Wada[3], Takeshi Imamura[10], Tsuneo Matsunaga[9], Jun Takita[8], Kohei Kitazato[2], Makoto Taguchi[4], Tetsuya Fukuhara[4], Satoshi Tanaka[3], Tatsuaki Okada[3] (1.Ashikaga University, 2.The University of Aizu, 3.Japan Aerospace Exploration Agency (JAXA), 4.Rikkyo University,

5.Chiba Institute of Technology, 6.Hokkaido University of Education, 7.National Institute of Advanced Industrial Science and Technology (AIST), 8.Hokkaido Kitami Hokuto High School, 9.National Institute for Environmental Studies (NIES), 10.The University of Tokyo)

[PPS03-P08] Multi-mission capability of HARMONICS

*Shintaro Tsunoda[1], Hirohide Demura[1], Naru Hirata[1] (1.The University of Aizu)

[PPS03-P09] New interface of verification for calibration and conversion in HEAT : Hayabusa2 Exploration Assistant for TIR

*Tatsuro Kobayashi[1], Kentaro Suko[1], Hirohide Demura[1], Yoshiko Ogawa[1], Takehiko Arai[2], Naoya Sakatani[3], Tatsuaki Okada[3], Satoshi Tanaka[3], Tetsuya Fukuhara[4] (1.The University of Aizu, 2.Ashikaga University, 3.Institute of Space and Astronautical Science, Japan Aerospace Exploration Agency, 4.Rikkyo University)

[PPS03-P10] **Dust particle evolution of a near-Earth object 252P/LINEAR from near-infrared polarimetric observations in 2016**

*Yuna G Kwon[1], Masateru Ishiguro[1], Jungmi Kwon[2], Daisuke Kuroda[3], Myungshin Im[1], Changsu Choi[1], Motohide Tamura[4], Takahiro Nagayama[5], Nobuyuki Kawai[6], Jun-ichi Watanabe[7] (1.Seoul National Univ., 2.ISAS/Japan Aerospace Exploration Agency, 3.Okayama Astrophysical Observatory, 4.The Univ. of Tokyo, 5.Kagoshima Univ., 6.Tokyo Institute of Technology, 7.National Astronomical Observatory of Japan)

[PPS03-P11] **Performance Evaluation of TRIPOL on the 61-cm Telescope at Seoul National University for Polarimetric Observations of Solar System Small Bodies**

*Sunho Jin[1], Masateru Ishiguro[1], Yuna G Kwon[1], Jooyeon Geem[1], Yoonsoo P. Bach[1], Jinguk Seo[1], Hiroshi Sasago[2], Shuji Sato[3] (1.Seoul National University, 2.Sasago Co.,Ltd, 3.Nagoya University)

[PPS03-P12] Smart Interface of HEAT: Hayabusa2 Exploration Assistant for TIR

*Kentaro Suko[1], Tatsuro Kobayashi[1], Hirohide Demura[1], Takehiko Arai[2], Naoya Sakatani[3], Tatsuaki Okada[3], Satoshi Tanaka[3], Tetsuya Fukuhara[4] (1.The University of Aizu, 2.Ashikaga University, 3.Institute of Space and Astronautical Science, Japan Aerospace Exploration Agency, 4.Rikkyo University)

[PPS03-P13] Experimental Study on Collision Crater Formed on Bulge Geography

*Yusaku Yokota[1], Yuya Yamamoto[2], Minami Yasui[2], Masahiko Arakawa[2] (1.Faculty of Science, Kobe University, 2.Graduate School of Science, Kobe University)

[PPS03-P14] Initial analysis plan of soluble organic compounds for the Hayabusa2 sample from asteroid Ryugu

*Hiroshi Naraoka[1], Yoshinori Takano[2], Jason P. Dworkin[3], SOM Analysis Team (1.Department of Earth and Planetary Sciences, Research Center for Planetary Trace Organic Compounds, Kyushu University, 2.Japan Agency for Marine-Earth Science and Technology, 3.Astrochemistry Laboratory NASA Goddard Space Flight Center, Greenbelt, MD 20771 USA)

[PPS03-P15] Radar and optical simultaneous observations of faint meteors with MU radar and Tomo-e Gozen

*Ryou Ohsawa[1], Akira Hirota[2], Shinsuke Abe[2], Daniel Kastinen[3], Kero Johan[3], yasunori Fujiwara[4], Takuji Nakamura[5], Shigeyuki Sako[1], Yuto Kojima[1], Jun-ichi Watanabe[6] (1.Institute of Astronomy, Graduate School of Science, The University of Tokyo, 2.Department of Aerospace Engineering, College of Science & Technology, Nihon University, 3.Swedish Institute of Space Physics, 4.SOKENDAI (The Graduate University for Advanced Studies), 5.National Institute of Polar Research, 6.National Astronomical Observatory of Japan)

[PPS03-P16] Global distribution and spectral characteristics of bright spots on asteroid Ryugu

*Masanori Suemitsu[1], Tomokatsu Morota[1], Rie Honda[2], Singo Kameda[15], Eri Tatsumi[3], Manabu Yamada[4], Naoya Sakatani[5], Toru Kouyama[6], Yokota Yasuhiro[7], Yuichiro Cho[8], Hidehiko Suzuki[9], Masahiko Hayakawa[10], Moe Matsuoka[10], Chikatoshi Honda[11], Tatsuhiro Michikami[12], Kazuo Yoshioka[13], Kazunori Ogawa[14], Hirotaka Sawada[5], Seiji Sugita[3] (1.Graduate School of Environmental Studies, Nagoya University, 2.Department of Science and Technology, System of Natural Science, Kochi Unicversity, 3.Graduate School of Earth and Planetary Science, Tokyo Unicversity, 4.Planetary Exploration Reserch Center, Chiba Institute of Technology, 5.Institute of Space and Astoronautical Science, Japan Aerospace Exploration Agency, 6.National Institute of Advanced Industrial Science and Technology, 7.Kochi University, 8.Department of Earth and Planetary Science, Tokyo University, 9.Depertment of physics, Meiji University , 10.Department of Solar System Science, Institute of Space and Astoronautical Science, Japan Aerospace Exploration Agency, 11.Aizu University, 12.Faculty of Engineering, Kindai University, 13.Graduate School of frontier Science, Tokyo University, 14.Kobe University, 15.Rikkyo University)

[PPS03-P17] Polarimetry of (155140) 2005 UD: the Dynamical Association with (3200) Phaethon

*Masateru Ishiguro[1], Jooyeon Geem[1], Hiroyuki Naito[2], Yoonsoo P. Bach[1], Daisuke Kuroda[3], Tatsuharu Ono[4], Seiko Takagi[4], Mitsuteru Sato[4], Kiyoshi Kuramoto[4], Tomohiko Sekiguchi[5], Masataka Imai[6], Makoto Watanabe[7], Katsuhito Ohtsuka[8], Sunao Hasegawa[9], Takashi Ito[10], Fumi Yoshida[11], Tomoko Arai[11] (1.Department of Physics and Astronomy, Seoul National University, 2.Nayoro Observatory, 3.Okayama Observatory, Kyoto University, 4.Department of Cosmosciences, Graduate School of Science, Hokkaido University, 5.Hokkaido University of Education, 6.National Institute of Advanced Industrial Science and Technology, 7.Department of Applied Physics, Okayama University of Science, 8.Tokyo Meteor Network, 9.Japan Aerospace Exploration Agency, 10.National Astronomical Observatory of Japan, 11.Planetary Exploration Research Center, Chiba Institute of Technology)

[PPS03-P18] **Follow-up observations for AKARI/IRC near-infrared asteroid spectroscopic survey (AcuA-spec)**

*Sunao Hasegawa[1], Daisuke KURODA[2], Kenshi YANAGISAWA[3], Fumihiko Usui[4] (1.Japan Aerospace Exploration Agency, 2.Kyoto University, 3.National Astronomical Observatory of Japan, 4.Kobe University)

[PPS03-P19] Amino acids on witness coupons collected from the ISAS/JAXA curation facility for the assessment and quality control of the Hayabusa2 sampling procedure

*Haruna Sugahara[1,2], Yoshinori Takano[1], Yuzuru Karouji[3], Kazuya Kumagai[4], Toru Yada[3], Naohiko Ohkouchi[1], Masanao Abe[3], Hayabusa2 project team (1.Japan Agency for Marine-Earth Science and Technology (JAMSTEC), 2. Institut de Chimie de Nice, Universite Cote dAzur, 3.Japan Aerospace Exploration Agency (JAXA), 4.Marine Works Japan Ltd.)

[PPS03-P20] Hayabusa2 orbit determination using c5++ software

*Keiko Yamamoto[1], Toshimichi Otsubo[2], Koji Matsumoto[1], Hirotomo Noda[1], Noriyuki Namiki[1], Hiroki Senshu[3], Takahide Mizuno[4], Naoko Ogawa[4], Go Ono[4], Yuya Mimasu[4], Kent Yoshikawa[4], Tadateru Takahashi[4], Yuto Takei[4], Atsushi Fujii[4], Fuyuto Terui[4], Takanao Saiki[4], Satoru Nakazawa[4], Makoto Yoshikawa[4], Yuichi Tsuda[4] (1.National Astronomical Observatory of Japan, 2.Hitotsubashi University, 3.Chiba Institute of Technology, 4.Japan Aerospace Exploration Agency)

[PPS03-P21] **Landing Site Selection for Hayabusa2: Scientific Evaluation of the Candidate Sites on Asteroid (162173) Ryugu**

*Hikaru Yabuta[1], Sei-ichiro WATANABE[2], Tomoki Nakamura[3], Naru Hirata[4], Seiji Sugita[5], Tatsuaki Okada[6], Kohei Kitazato[4], Yoshiaki Ishihara[7], Tomokatsu Morota[2], Naoya Sakatani[6], Koji Matsumoto[8], Koji Wada[9], Shogo Tachibana[5], Mutsumi Komatsu[10], ERI TATSUMI[5], Moe Matsuoka[6], Chikatoshi Honda[4], Takahiro Hiroi[11], Hiroki Senshu[9], Rie Honda[12], Yasuhiro Yokota[6], Rina Noguchi[6], Yuri Shimaki[6], Deborah Lorin Domingue[13], Lucille Le Corre[13], Antonella Barucci[14], Ernest Palomba[15], Shota Kikuchi[6], Akira Miura[6], Tomohiro Yamaguchi[6], Yukio Yamamoto[6], Takanao Saiki[6], Satoshi Tanaka[6], Makoto Yoshikawa[6], Yuichi Tsuda[6] (1.Hiroshima University, Department of Earth and Planetary Systems Science, 2.Nagoya University, 3.Tohoku University, 4.University of Aizu, 5.The University of Tokyo, 6.ISAS/JAXA, 7.NIES, 8.NAOJ, 9.Chiba Institute of Technology, Planetary Exploration Research Center (PERC), 10.Sokendai, 11.Brown University, 12.Kochi University, 13.Planetary Science Institute, USA, 14.Observatoire Paris-Site de Meudon, LESIA, France, 15.INAF-IAPS, Italy.)

[PPS03-P22] Visible Photometric, Spectroscopic and Polarimetric observations of an inactive comet, P/2016 BA14 with the 1.6m Pirka Telescope

*Ryo Yamagata[1], Tomohiko Sekiguchi[1], Ryo Okazaki[1], Kazuya Doi[1], Daisuke Kuroda[2], Masateru Ishiguro[3], Hiroyuki Naito[4] (1.Hokkaido University of Education, 2.Kyoto University, 3.Seoul National University, 4.Nayoro Observatory)

[PPS03-P23] **Polycyclic aromatic hydrocarbons and aliphatic hydrocarbons in Jbilet Winselwan carbonaceous chondrite : Attempt to evaluate the thermal metamorphism degree on the parent body**

Hiroki Kato[1], *Hikaru Yabuta[1] (1.Hiroshima University, Department of Earth and Planetary Systems Science)

[PPS03-P24] Disk-Resolved Photometry Analysis of the Asteroid Ryugu Images Obtained by Hayabusa2 Visible Camera ONC

*yokota yasuhiro[1,2], Rie Honda[1], ERI TATSUMI[3], Deborah Domingue[4], Stefanus E. Schroeder[5], Moe Matsuoka[2], Seiji Sugita[3], Tomokatsu Morota[6], Shingo Kameda[7], Toru Kouyama[8], Hidehiko Suzuki[9], Manabu Yamada[10], Naoya Sakatani[2], Chikatoshi Honda[11], Masahiko Hayakawa[2], Kazuo Yoshioka[3], Yuichiro Cho[3], Hirotaka Sawada[2] (1.Kochi University, 2.ISAS/JAXA, 3.Univ. of Tokyo, 4.Planetary Science Institute, 5.DLR, 6.Nagoya Univ., 7.Rikkyo Univ., 8.AIST, 9.Meiji Univ., 10.Chiba Institute od Technology, 11.Aizu Univ.)

[E] Poster | P (Space and Planetary Sciences)：P-PS Planetary Sciences

5:15 PM - 6:30 PM JST | 8:15 AM - 9:30 AM UTC | Poster Hall International Exhibition Hall8, Makuhari Messe_3

[P-PS03] Solar System Small Bodies: A New Frontier Arising Hayabusa 2, OSIRIS-REx and Other Projects

convener:Masateru Ishiguro(Department of Physics and Astronomy, Seoul National University), Taishi Nakamoto(Tokyo Institute of Technology), Masanao Abe(Institute of Space and Astronautical Science, Japan Aerospace Exploration Agency), Olivier S Barnouin(Johns Hopkins University Applied Physics Laboratory)

[PPS03-P01] Impact experiments on low strength coarse-grained regolith simulating surface materials on asteroid Ryugu

*Yuya Yamamoto[1], Masahiko Arakawa[1], Minami Yasui[1], Sunao Hasegawa[2], Ryo Sugimura[1] (1.Graduate School of Science, Kobe University, 2.ISAS, JAXA)

[PPS03-P02] Reflectance estimation of asteroid Ryugu using MASCOT

*Marika Ishida[1], Koto Amano[1], Keiichi Moroi[1], ERI TATSUMI[2], Tra-Mi Ho[10], Shingo Kameda[1], Seiji Sugita[2], Rie Honda[3], Tomokatsu Morota[4], yokota yasuhiro[5], Toru Kouyama[6], Hidehiko Suzuki[7], Manabu Yamada[8], Naoya Sakatani[5], Chikatoshi Honda[9], Masahiko Hayakawa[5], Kazuo Yoshioka[2], Moe Matsuoka[5], Yuichiro Cho[2], Hirotaka Sawada[5] (1.Rikkyo Univ., 2.Univ. of Tokyo, 3.Kochi Univ., 4.Nagoya Univ., 5.JAXA/ISAS, 6.AIST, 7.Meiji Univ., 8.Chiba Inst. Tech, 9.Univ. of Aizu, 10.DLR)

[PPS03-P03] Flyby observation of Asteroid (3200) Phaethon by DESTINY$^+$ onboard cameras

*Ko Ishibashi[1], Shingo Kameda[2], Masato Kagitani[3], Peng Hong[1], Manabu Yamada[1], Osamu Okudaira[1], Tomoko Arai[1], Fumi Yoshida[1], Shunsuke Sato[4], Takahiro Ishimaru[4], Takaya Okamoto[4], Takahiro Iwata[4], Tatsuaki Okada[4], Takeshi Takashima[4] (1.Chiba Institute of Technology, 2.Rikkyo University, 3.Tohoku Universtiy, 4.Japan Aerospace Exploration Agency)

[PPS03-P04] Polarimetric Study of Asteroids in Comet-Like Orbits (ACOs)

*Jooyeon Geem[1], Masateru Ishiguro[1], Yoonsoo P. Bach[1], Daisuke Kuroda[2], Hiroyuki Naito[3], Hidekazu Hanayama[4], yoonyoung kim[10], Yuna G. Kwon[1], Sunho Jin[1], Tomohiko Sekiguchi[5], Ryo Okazaki[5], Jeremie J. Vaubaillon[6], Masataka Imai[7], Tatsuharu Oono[8], Yuki Futamuts[8], Seiko Takagi[8], Mitsuteru Sato[8], Kiyoshi Kuramoto[8], Makoto Watanabe[9] (1.Astronomy program, Dept of Physics and Astronomy, Seoul National University, 2.Okayama Observatory, Kyoto University, 3.Nayoro Observatory, 4.Ishigakijima Astronomical Observatory, National Astronomical Observatory of Japan, 5.Hokkaido University of Education, 6.Observatoire de Paris, I.M.C.C.E., 7.National Institute of Advanced Industrial Science and Technology, 8.Department of Cosmosciences, Graduate School of Science, Hokkaido University, 9.Department of Applied Physics, Okayama University of Science, 10.Max Planck Institute for Solar System Research)

[PPS03-P05] Dynamical lifetime of the Oort Cloud new comets under planetary perturbation

*Ito Takashi[1], Arika Higuchi[1] (1.National Astronomical Observatory of Japan)

[PPS03-P06] Thermal Infrared Imaging of C-type Asteroid 162173 Ryugu with Porous Surfaces

*Tatsuaki Okada[1,2], Tetsuya Fukuhara[3], Satoshi Tanaka[1], Makoto Taguchi[3], Takehiko Arai[4], Naoya Sakatani[1], Yuri Shimaki[1], Hiroki Senshu[5], Yoshiko Ogawa[6], Hirohide Demura[6], Kentaro Suko[6], Kohei Kitazato[6], Toru Kouyama[7], Tomohiko Sekiguchi[8], Jun Takita[9], Sunao Hasegawa[1], Tsuneo Matsunaga[10], Takehiko Wada[1], Takeshi Imamura[2], Jorn Helbert[11], Thomas G. Mueller[12], Axel Hagermann[13], Jens Biele[11], Matthias Grott[11], Maximiliam Hamm[11], Marco Delbo[14], Yukio Yamamoto[1], Naru Hirata[6], Naoyuki Hirata[15], Fuyuto Terui[1], Takanao Saiki[1], Satoru Nakazawa[1], Makoto Yoshikawa[1], Sei-ichiro WATANABE[1,16], Yuichi Tuda[1] (1.Institute of Space and Astronautical Science, Japan Aerospace Exploration Agency, 2.University of Tokyo, 3.Rikkyo University, 4.Ashikaga University, 5.Chiba Institute of Technology, 6.University of Aizu, 7.National Institute of Advanced Industrial Science and Technology, 8.Hokkaido University of Education, 9.Hokkaido Kitami-Hokuto High School, 10.National Institute for Environmental Studies, 11.German Aerospace Center, 12.Max-Planck Institute for Extraterrestrial Physics, 13.University of Stirling, 14.Observatoire de la Côte d'Azur, 15.Kobe University, 16.Nagoya University)

[PPS03-P07] Data Release of Asteroid 162173 Ryugu by Observation of Thermal Infrared Imager onboard Hayabusa2

*Takehiko Arai[1], Hirohide Demura[2], Toru Kouyama[7], Naoya Sakatani[3], Kentaro Suko[2], Yuri Shimaki[3], Hiroki Senshu[5], Tomohiko Sekiguchi[6], Yoshiko Ogawa[2], Sunao Hasegawa[3], Takehiko Wada[3], Takeshi Imamura[10], Tsuneo Matsunaga[9], Jun Takita[8], Kohei Kitazato[2], Makoto Taguchi[4], Tetsuya Fukuhara[4], Satoshi Tanaka[3], Tatsuaki Okada[3] (1.Ashikaga University, 2.The University of Aizu, 3.Japan Aerospace Exploration Agency (JAXA), 4.Rikkyo University,

5.Chiba Institute of Technology, 6.Hokkaido University of Education, 7.National Institute of Advanced Industrial Science and Technology (AIST), 8.Hokkaido Kitami Hokuto High School, 9.National Institute for Environmental Studies (NIES), 10.The University of Tokyo)

[PPS03-P08] Multi-mission capability of HARMONICS

*Shintaro Tsunoda[1], Hirohide Demura[1], Naru Hirata[1] (1.The University of Aizu)

[PPS03-P09] New interface of verification for calibration and conversion in HEAT : Hayabusa2 Exploration Assistant for TIR

*Tatsuro Kobayashi[1], Kentaro Suko[1], Hirohide Demura[1], Yoshiko Ogawa[1], Takehiko Arai[2], Naoya Sakatani[3], Tatsuaki Okada[3], Satoshi Tanaka[3], Tetsuya Fukuhara[4] (1.The University of Aizu, 2.Ashikaga University, 3.Institute of Space and Astronautical Science, Japan Aerospace Exploration Agency, 4.Rikkyo University)

[PPS03-P10] **Dust particle evolution of a near-Earth object 252P/LINEAR from near-infrared polarimetric observations in 2016**

*Yuna G Kwon[1], Masateru Ishiguro[1], Jungmi Kwon[2], Daisuke Kuroda[3], Myungshin Im[1], Changsu Choi[1], Motohide Tamura[4], Takahiro Nagayama[5], Nobuyuki Kawai[6], Jun-ichi Watanabe[7] (1.Seoul National Univ., 2.ISAS/Japan Aerospace Exploration Agency, 3.Okayama Astrophysical Observatory, 4.The Univ. of Tokyo, 5.Kagoshima Univ., 6.Tokyo Institute of Technology, 7.National Astronomical Observatory of Japan)

[PPS03-P11] **Performance Evaluation of TRIPOL on the 61-cm Telescope at Seoul National University for Polarimetric Observations of Solar System Small Bodies**

*Sunho Jin[1], Masateru Ishiguro[1], Yuna G Kwon[1], Jooyeon Geem[1], Yoonsoo P. Bach[1], Jinguk Seo[1], Hiroshi Sasago[2], Shuji Sato[3] (1.Seoul National University, 2.Sasago Co.,Ltd, 3.Nagoya University)

[PPS03-P12] Smart Interface of HEAT: Hayabusa2 Exploration Assistant for TIR

*Kentaro Suko[1], Tatsuro Kobayashi[1], Hirohide Demura[1], Takehiko Arai[2], Naoya Sakatani[3], Tatsuaki Okada[3], Satoshi Tanaka[3], Tetsuya Fukuhara[4] (1.The University of Aizu, 2.Ashikaga University, 3.Institute of Space and Astronautical Science, Japan Aerospace Exploration Agency, 4.Rikkyo University)

[PPS03-P13] Experimental Study on Collision Crater Formed on Bulge Geography

*Yusaku Yokota[1], Yuya Yamamoto[2], Minami Yasui[2], Masahiko Arakawa[2] (1.Faculty of Science, Kobe University, 2.Graduate School of Science, Kobe University)

[PPS03-P14] Initial analysis plan of soluble organic compounds for the Hayabusa2 sample from asteroid Ryugu

*Hiroshi Naraoka[1], Yoshinori Takano[2], Jason P. Dworkin[3], SOM Analysis Team (1.Department of Earth and Planetary Sciences, Research Center for Planetary Trace Organic Compounds, Kyushu University, 2.Japan Agency for Marine-Earth Science and Technology, 3.Astrochemistry Laboratory NASA Goddard Space Flight Center, Greenbelt, MD 20771 USA)

[PPS03-P15] Radar and optical simultaneous observations of faint meteors with MU radar and Tomo-e Gozen

*Ryou Ohsawa[1], Akira Hirota[2], Shinsuke Abe[2], Daniel Kastinen[3], Kero Johan[3], yasunori Fujiwara[4], Takuji Nakamura[5], Shigeyuki Sako[1], Yuto Kojima[1], Jun-ichi Watanabe[6] (1.Institute of Astronomy, Graduate School of Science, The University of Tokyo, 2.Department of Aerospace Engineering, College of Science & Technology, Nihon University, 3.Swedish Institute of Space Physics, 4.SOKENDAI (The Graduate University for Advanced Studies), 5.National Institute of Polar Research, 6.National Astronomical Observatory of Japan)

[PPS03-P16] Global distribution and spectral characteristics of bright spots on asteroid Ryugu

*Masanori Suemitsu[1], Tomokatsu Morota[1], Rie Honda[2], Singo Kameda[15], Eri Tatsumi[3], Manabu Yamada[4], Naoya Sakatani[5], Toru Kouyama[6], Yokota Yasuhiro[7], Yuichiro Cho[8], Hidehiko Suzuki[9], Masahiko Hayakawa[10], Moe Matsuoka[10], Chikatoshi Honda[11], Tatsuhiro Michikami[12], Kazuo Yoshioka[13], Kazunori Ogawa[14], Hirotaka Sawada[5], Seiji Sugita[3] (1.Graduate School of Environmental Studies, Nagoya University, 2.Department of Science and Technology, System of Natural Science, Kochi Unicversity, 3.Graduate School of Earth and Planetary Science, Tokyo Unicversity, 4.Planetary Exploration Reserch Center, Chiba Institute of Technology, 5.Institute of Space and Astoronautical Science, Japan Aerospace Exploration Agency, 6.National Institute of Advanced Industrial Science and Technology, 7.Kochi University, 8.Department of Earth and Planetary Science, Tokyo University, 9.Depertment of physics, Meiji University , 10.Department of Solar System Science, Institute of Space and Astoronautical Science, Japan Aerospace Exploration Agency, 11.Aizu University, 12.Faculty of Engineering, Kindai University, 13.Graduate School of frontier Science, Tokyo University, 14.Kobe University, 15.Rikkyo University)

[PPS03-P17] Polarimetry of (155140) 2005 UD: the Dynamical Association with (3200) Phaethon

*Masateru Ishiguro[1], Jooyeon Geem[1], Hiroyuki Naito[2], Yoonsoo P. Bach[1], Daisuke Kuroda[3], Tatsuharu Ono[4], Seiko Takagi[4], Mitsuteru Sato[4], Kiyoshi Kuramoto[4], Tomohiko Sekiguchi[5], Masataka Imai[6], Makoto Watanabe[7], Katsuhito Ohtsuka[8], Sunao Hasegawa[9], Takashi Ito[10], Fumi Yoshida[11], Tomoko Arai[11] (1.Department of Physics and Astronomy, Seoul National University, 2.Nayoro Observatory, 3.Okayama Observatory, Kyoto University, 4.Department of Cosmosciences, Graduate School of Science, Hokkaido University, 5.Hokkaido University of Education, 6.National Institute of Advanced Industrial Science and Technology, 7.Department of Applied Physics, Okayama University of Science, 8.Tokyo Meteor Network, 9.Japan Aerospace Exploration Agency, 10.National Astronomical Observatory of Japan, 11.Planetary Exploration Research Center, Chiba Institute of Technology)

[PPS03-P18] **Follow-up observations for AKARI/IRC near-infrared asteroid spectroscopic survey (AcuA-spec)**

*Sunao Hasegawa[1], Daisuke KURODA[2], Kenshi YANAGISAWA[3], Fumihiko Usui[4] (1.Japan Aerospace Exploration Agency, 2.Kyoto University, 3.National Astronomical Observatory of Japan, 4.Kobe University)

[PPS03-P19] Amino acids on witness coupons collected from the ISAS/JAXA curation facility for the assessment and quality control of the Hayabusa2 sampling procedure

*Haruna Sugahara[1,2], Yoshinori Takano[1], Yuzuru Karouji[3], Kazuya Kumagai[4], Toru Yada[3], Naohiko Ohkouchi[1], Masanao Abe[3], Hayabusa2 project team (1.Japan Agency for Marine-Earth Science and Technology (JAMSTEC), 2. Institut de Chimie de Nice, Universite Cote dAzur, 3.Japan Aerospace Exploration Agency (JAXA), 4.Marine Works Japan Ltd.)

[PPS03-P20] Hayabusa2 orbit determination using c5++ software

*Keiko Yamamoto[1], Toshimichi Otsubo[2], Koji Matsumoto[1], Hirotomo Noda[1], Noriyuki Namiki[1], Hiroki Senshu[3], Takahide Mizuno[4], Naoko Ogawa[4], Go Ono[4], Yuya Mimasu[4], Kent Yoshikawa[4], Tadateru Takahashi[4], Yuto Takei[4], Atsushi Fujii[4], Fuyuto Terui[4], Takanao Saiki[4], Satoru Nakazawa[4], Makoto Yoshikawa[4], Yuichi Tsuda[4] (1.National Astronomical Observatory of Japan, 2.Hitotsubashi University, 3.Chiba Institute of Technology, 4.Japan Aerospace Exploration Agency)

[PPS03-P21] **Landing Site Selection for Hayabusa2: Scientific Evaluation of the Candidate Sites on Asteroid (162173) Ryugu**

*Hikaru Yabuta[1], Sei-ichiro WATANABE[2], Tomoki Nakamura[3], Naru Hirata[4], Seiji Sugita[5], Tatsuaki Okada[6], Kohei Kitazato[4], Yoshiaki Ishihara[7], Tomokatsu Morota[2], Naoya Sakatani[6], Koji Matsumoto[8], Koji Wada[9], Shogo Tachibana[5], Mutsumi Komatsu[10], ERI TATSUMI[5], Moe Matsuoka[6], Chikatoshi Honda[4], Takahiro Hiroi[11], Hiroki Senshu[9], Rie Honda[12], Yasuhiro Yokota[6], Rina Noguchi[6], Yuri Shimaki[6], Deborah Lorin Domingue[13], Lucille Le Corre[13], Antonella Barucci[14], Ernest Palomba[15], Shota Kikuchi[6], Akira Miura[6], Tomohiro Yamaguchi[6], Yukio Yamamoto[6], Takanao Saiki[6], Satoshi Tanaka[6], Makoto Yoshikawa[6], Yuichi Tsuda[6] (1.Hiroshima University, Department of Earth and Planetary Systems Science, 2.Nagoya University, 3.Tohoku University, 4.University of Aizu, 5.The University of Tokyo, 6.ISAS/JAXA, 7.NIES, 8.NAOJ, 9.Chiba Institute of Technology, Planetary Exploration Research Center (PERC), 10.Sokendai, 11.Brown University, 12.Kochi University, 13.Planetary Science Institute, USA, 14.Observatoire Paris-Site de Meudon, LESIA, France, 15.INAF-IAPS, Italy.)

[PPS03-P22] Visible Photometric, Spectroscopic and Polarimetric observations of an inactive comet, P/2016 BA14 with the 1.6m Pirka Telescope

*Ryo Yamagata[1], Tomohiko Sekiguchi[1], Ryo Okazaki[1], Kazuya Doi[1], Daisuke Kuroda[2], Masateru Ishiguro[3], Hiroyuki Naito[4] (1.Hokkaido University of Education, 2.Kyoto University, 3.Seoul National University, 4.Nayoro Observatory)

[PPS03-P23] **Polycyclic aromatic hydrocarbons and aliphatic hydrocarbons in Jbilet Winselwan carbonaceous chondrite : Attempt to evaluate the thermal metamorphism degree on the parent body**

Hiroki Kato[1], *Hikaru Yabuta[1] (1.Hiroshima University, Department of Earth and Planetary Systems Science)

[PPS03-P24] Disk-Resolved Photometry Analysis of the Asteroid Ryugu Images Obtained by Hayabusa2 Visible Camera ONC

*yokota yasuhiro[1,2], Rie Honda[1], ERI TATSUMI[3], Deborah Domingue[4], Stefanus E. Schroeder[5], Moe Matsuoka[2], Seiji Sugita[3], Tomokatsu Morota[6], Shingo Kameda[7], Toru Kouyama[8], Hidehiko Suzuki[9], Manabu Yamada[10], Naoya Sakatani[2], Chikatoshi Honda[11], Masahiko Hayakawa[2], Kazuo Yoshioka[3], Yuichiro Cho[3], Hirotaka Sawada[2] (1.Kochi University, 2.ISAS/JAXA, 3.Univ. of Tokyo, 4.Planetary Science Institute, 5.DLR, 6.Nagoya Univ., 7.Rikkyo Univ., 8.AIST, 9.Meiji Univ., 10.Chiba Institute od Technology, 11.Aizu Univ.)

[E] Poster | P (Space and Planetary Sciences)：P-EM Solar-Terrestrial Sciences, Space Electromagnetism & Space Environment

10:45 AM - 12:15 PM JST | 1:45 AM - 3:15 AM UTC | Poster Hall International Exhibition Hall8, Makuhari Messe_3

[P-EM09] Vertical coupling in the atmosphere and Ionosphere

convener:Huixin Liu(Earth and Planetary Science Division, Kyushu University SERC, Kyushu University), Loren Chang(Institute of Space Science, National Central University), Yuichi Otsuka(Institute for Space-Earth Environmental Research, Nagoya University)

[PEM09-P01] Local-time Variabilities of SABER CO_2 in the Mesosphere and Lower Thermosphere Region

*Cornelius Csar Jude Salinas[1], Loren Chang[1], Danie Liang[2], Jia Yue[3], Liying Qian[4], Quan Gan[5], James Russel III[3], Martin G Mlynczak[6] (1.Institute of Space Science, National Central University, 2.Institute of Earth Science, Academia Sinica, 3.Department of Atmospheric Sciences, Hampton University, 4.High Altitude Observatory, National Center for Atmospheric Research, 5.Department of Physics and Astronomy, Clemson University, 6.NASA Langley Research Center)

[PEM09-P02] Enhanced dynamo electric field as a possible cause of ionosphere disturbance before Large Earthquake

*Koichiro Oyama[1,2,3] (1.Institute of Plasma and Space Sciences,National Cheng Kung Univ., Taiwan, 2.International Ceneter for Space Weather Sudy and Education, Kyushu Univ.,, 3.CoLtd. Asia Space Environment Research Consortium, Japan)

[PEM09-P03] Morphology of E1 and E2 Kelvin waves from ECMWF reanalysis

*Chen-Jeih Pan[1], Wei-Sheng Chen[1], Uma Das[2] (1.Institute of Space Science, National Central University, 2.Department of Physics, Indian Institute of Information Technology, Kalyani, India)

[PEM09-P04] Impact of strong ENSO on TEC activity disturbed by ultra-fast Kelvin waves

*Wei-Sheng Chen[1], C.J. Pan[1], Uma Das[2], Chian-Chiau Lin[3] (1.Institute of Space Science, National Central University, Taiwan, 2.Department of Physics, Indian Institute of Information Technology, Kalyani, India, 3.Environmental Research and Information Center, Chang Jung Christian University, Taiwan)

[PEM09-P05] Observation and simulation of propagation of coseismic infrasound to the ionosphere

*Jaroslav Chum[1] (1.Institute of Atmospheric Physics of the Czech Academy of Sciences)

[PEM09-P06] Solar wind influence on tropical cyclones mediated by atmospheric gravity waves

*Paul Prikryl[1,2], Iurii Cherniak[3], Irina Zakharenkova[4,5], James M. Weygand[6], Bharat S. R. Kunduri[7] (1.Physics Department, University of New Brunswick, Fredericton, NB, Canada, 2.Geomagnetic Laboratory, Natural Resources Canada, Ottawa, ON, Canada, 3.COSMIC Program Office, University Corporation for Atmospheric Research, Boulder, CO, USA, 4.West Department of IZMIRAN, Kaliningrad, Russia, 5.University of Warmia and Mazury in Olsztyn, Poland, 6.Earth Planetary and Space Sciences, University of California, Los Angeles, CA, USA, 7.Bradley Dept. of Electrical and Computer Engineering, Virginia Tech, Blacksburg, VA, USA)

[PEM09-P07] VIPIR ionospheric observations in Japan

*Takuya Tsugawa[1], Hideo Maeno[1], Michi Nishioka[1], Takumi Kondo[1], Mamoru Ishii[1] (1.National Institute of Information and Communications Technology)

[PEM09-P08] Simulation Results and Performance Analysis of Phase Velocity Spectral Analysis Software (M-Transform) for Airglow Imaging Data

*Septi Perwitasari[1], Takuji Nakamura[2], Masaru Kogure[2], Yoshihiro Tomikawa[2], Mitsumu K. Ejiri[2] (1.LAPAN, 2.NIPR)

[PEM09-P09] Comparisons of Co-incident Ionospheric Plasma Observations Between FORMOSAT-5/AIP and Millstone Hill Incoherent Scatter Radar

*Yi-Wun Chen[1], Chi-Kuang Chao[1] (1.Graduate Institute of Space Science, National Central University, Taiwan)

[PEM09-P10] Sub-ionospheric effects of volcano eruptions using VLF/LF standard radio waves

*Kei Maruyama[1], Hiroyo Ohya[1], Fuminori Tsuchiya[2], Kenro Nozaki[5], Kozo Yamashita[3], Yukihiro Takahashi[4], Hiroyuki Nakata[1], Toshiaki Takano[1] (1.Chiba University, 2.Tohoku University, 3.Ashikaga University, 4.Hokkaido University, 5.National Institute of Information and Communications Technology)

[PEM09-P11] Observations of ionospheric and mesospheric wave structures by a low-cost airglow imaging system

*Keisuke Hosokawa[1], Nanami Kusuyama[1], Yuta Hozumi[1], Kohei Takami[1], Susumu Saito[2], Yasunobu Ogawa[3], Mamoru Ishii[4], Yuichi Otsuka[5], Takuya Tsugawa[4] (1.University of Electro-Communications, 2.ENRI, 3.NIPR, 4.NICT, 5.ISEE, Nagoya University)

[PEM09-P12] Analysis of characteristics of ionospheric parameters, Sq index and neutral winds over Taiwan

*Yu-Jung Chuo[1] (1.Department of Information Technology, Ling Tung University)

[PEM09-P13] Statistical study on daytime Es observed by ground-ionosonde and RO-COSMIC in magnetic Equator region in 2010

*Zheng Wang [1,2], Huixin Liu[1] (1.Department of Earth and Planetary Sciences, School of Science, Kyushu University, Japan. , 2.National Space Science Center, Chinese Academy of Sciences, China.)

[PEM09-P14] The statistical study of the growth rates of Medium-Scale Traveling Ionospheric Disturbances observed with GPS-TEC

*Takafumi Ikeda[1], Akinori Saito[1], Takuya Tsugawa[2], Hiroyuki Shinagawa[2] (1.Department of Geophysics, Graduate School of Science, Kyoto University, 2.National Institutes of Information and Communications Technology)

[PEM09-P15] Comparison of Gravity Wave Activity in the Mesosphere Observed by OH Airglow Imagers and MF Radars over the Antarctic (Syowa & Davis).

*Masaru Kogure[1], Takuji Nakamura[1,2], Yoshihiro Tomikawa[1,2], Mitsumu K. Ejiri[1,2], Takanori Nishiyama[2,1], Masaki Tsutsumi[1,2], Michael J. Taylor[3], Yucheng Zhao[3], P.-Dominique Pautet[3], Damian Murphy[4] (1.National Institute of Polar Research, 2.Department of Polar Science, Sokendai, 3.Physics Department, Utah State University, 4.Australian Antarctic Division)

[E] Poster | P (Space and Planetary Sciences)：P-EM Solar-Terrestrial Sciences, Space Electromagnetism & Space Environment

5:15 PM - 6:30 PM JST | 8:15 AM - 9:30 AM UTC | Poster Hall International Exhibition Hall8, Makuhari Messe_4

[P-EM09] Vertical coupling in the atmosphere and Ionosphere

convener:Huixin Liu(Earth and Planetary Science Division, Kyushu University SERC, Kyushu University), Loren Chang(Institute of Space Science, National Central University), Yuichi Otsuka(Institute for Space-Earth Environmental Research, Nagoya University)

[PEM09-P01] Local-time Variabilities of SABER CO_2 in the Mesosphere and Lower Thermosphere Region

*Cornelius Csar Jude Salinas[1], Loren Chang[1], Danie Liang[2], Jia Yue[3], Liying Qian[4], Quan Gan[5], James Russel III[3], Martin G Mlynczak[6] (1.Institute of Space Science, National Central University, 2.Institute of Earth Science, Academia Sinica, 3.Department of Atmospheric Sciences, Hampton University, 4.High Altitude Observatory, National Center for Atmospheric Research, 5.Department of Physics and Astronomy, Clemson University, 6.NASA Langley Research Center)

[PEM09-P02] Enhanced dynamo electric field as a possible cause of ionosphere disturbance before Large Earthquake

*Koichiro Oyama[1,2,3] (1.Institute of Plasma and Space Sciences,National Cheng Kung Univ., Taiwan, 2.International Ceneter for Space Weather Sudy and Education, Kyushu Univ.,, 3.CoLtd. Asia Space Environment Research Consortium, Japan)

[PEM09-P03] Morphology of E1 and E2 Kelvin waves from ECMWF reanalysis

*Chen-Jeih Pan[1], Wei-Sheng Chen[1], Uma Das[2] (1.Institute of Space Science, National Central University, 2.Department of Physics, Indian Institute of Information Technology, Kalyani, India)

[PEM09-P04] Impact of strong ENSO on TEC activity disturbed by ultra-fast Kelvin waves

*Wei-Sheng Chen[1], C.J. Pan[1], Uma Das[2], Chian-Chiau Lin[3] (1.Institute of Space Science, National Central University, Taiwan, 2.Department of Physics, Indian Institute of Information Technology, Kalyani, India, 3.Environmental Research and Information Center, Chang Jung Christian University, Taiwan)

[PEM09-P05] Observation and simulation of propagation of coseismic infrasound to the ionosphere

*Jaroslav Chum[1] (1.Institute of Atmospheric Physics of the Czech Academy of Sciences)

[PEM09-P06] Solar wind influence on tropical cyclones mediated by atmospheric gravity waves

*Paul Prikryl[1,2], Iurii Cherniak[3], Irina Zakharenkova[4,5], James M. Weygand[6], Bharat S. R. Kunduri[7] (1.Physics Department, University of New Brunswick, Fredericton, NB, Canada, 2.Geomagnetic Laboratory, Natural Resources Canada, Ottawa, ON, Canada, 3.COSMIC Program Office, University Corporation for Atmospheric Research, Boulder, CO, USA, 4.West Department of IZMIRAN, Kaliningrad, Russia, 5.University of Warmia and Mazury in Olsztyn, Poland, 6.Earth Planetary and Space Sciences, University of California, Los Angeles, CA, USA, 7.Bradley Dept. of Electrical and Computer Engineering, Virginia Tech, Blacksburg, VA, USA)

[PEM09-P07] VIPIR ionospheric observations in Japan

*Takuya Tsugawa[1], Hideo Maeno[1], Michi Nishioka[1], Takumi Kondo[1], Mamoru Ishii[1] (1.National Institute of Information and Communications Technology)

[PEM09-P08] Simulation Results and Performance Analysis of Phase Velocity Spectral Analysis Software (M-Transform) for Airglow Imaging Data

*Septi Perwitasari[1], Takuji Nakamura[2], Masaru Kogure[2], Yoshihiro Tomikawa[2], Mitsumu K. Ejiri[2] (1.LAPAN, 2.NIPR)

[PEM09-P09] Comparisons of Co-incident Ionospheric Plasma Observations Between FORMOSAT-5/AIP and Millstone Hill Incoherent Scatter Radar

*Yi-Wun Chen[1], Chi-Kuang Chao[1] (1.Graduate Institute of Space Science, National Central University, Taiwan)

[PEM09-P10] Sub-ionospheric effects of volcano eruptions using VLF/LF standard radio waves

*Kei Maruyama[1], Hiroyo Ohya[1], Fuminori Tsuchiya[2], Kenro Nozaki[5], Kozo Yamashita[3], Yukihiro Takahashi[4], Hiroyuki Nakata[1], Toshiaki Takano[1] (1.Chiba University, 2.Tohoku University, 3.Ashikaga University, 4.Hokkaido University, 5.National Institute of Information and Communications Technology)

[PEM09-P11] Observations of ionospheric and mesospheric wave structures by a low-cost airglow imaging system

*Keisuke Hosokawa[1], Nanami Kusuyama[1], Yuta Hozumi[1], Kohei Takami[1], Susumu Saito[2], Yasunobu Ogawa[3], Mamoru Ishii[4], Yuichi Otsuka[5], Takuya Tsugawa[4] (1.University of Electro-Communications, 2.ENRI, 3.NIPR, 4.NICT, 5.ISEE, Nagoya University)

[PEM09-P12] Analysis of characteristics of ionospheric parameters, Sq index and neutral winds over Taiwan

*Yu-Jung Chuo[1] (1.Department of Information Technology, Ling Tung University)

[PEM09-P13] Statistical study on daytime Es observed by ground-ionosonde and RO-COSMIC in magnetic Equator region in 2010

*Zheng Wang [1,2], Huixin Liu[1] (1.Department of Earth and Planetary Sciences, School of Science, Kyushu University, Japan. , 2.National Space Science Center, Chinese Academy of Sciences, China.)

[PEM09-P14] The statistical study of the growth rates of Medium-Scale Traveling Ionospheric Disturbances observed with GPS-TEC

*Takafumi Ikeda[1], Akinori Saito[1], Takuya Tsugawa[2], Hiroyuki Shinagawa[2] (1.Department of Geophysics, Graduate School of Science, Kyoto University, 2.National Institutes of Information and Communications Technology)

[PEM09-P15] Comparison of Gravity Wave Activity in the Mesosphere Observed by OH Airglow Imagers and MF Radars over the Antarctic (Syowa & Davis).

*Masaru Kogure[1], Takuji Nakamura[1,2], Yoshihiro Tomikawa[1,2], Mitsumu K. Ejiri[1,2], Takanori Nishiyama[2,1], Masaki Tsutsumi[1,2], Michael J. Taylor[3], Yucheng Zhao[3], P.-Dominique Pautet[3], Damian Murphy[4] (1.National Institute of Polar Research, 2.Department of Polar Science, Sokendai, 3.Physics Department, Utah State University, 4.Australian Antarctic Division)

[E] Poster | P (Space and Planetary Sciences)：P-EM Solar-Terrestrial Sciences, Space Electromagnetism & Space Environment

1:45 PM - 3:15 PM JST | 4:45 AM - 6:15 AM UTC | Poster Hall International Exhibition Hall8, Makuhari Messe_1

[P-EM11] Dynamics of Magnetosphere and Ionosphere

convener:Aoi Nakamizo(Applied Electromagnetic Research Institute, National Institute of Information and Communications Technology), Mitsunori Ozaki(Faculty of Electrical and Computer Engineering, Institute of Science and Engineering, Kanazawa University), Akiko Fujimoto(Kyushu Institute of Technology), Tomoaki Hori(Institute for Space-Earth Environmental Research, Nagoya University)

[PEM11-P01] Effects of Inclination/Rotation of Earth's Magnetic Axis on Magnetosphere Simulated by Global MHD Model

*Aoi Nakamizo[1] (1.Applied Electromagnetic Research Institute, National Institute of Information and Communications Technology)

[PEM11-P02] Asymmetric deformation of the magnetosphere under low-density solar wind

*Masaki N Nishino[1,2], Yoshifumi Saito[2], Kazuo Shiokawa[1], Masaki Fujimoto[2] (1.Institute for Space-Earth Environmental Research, Nagoya University, 2.JAXA/ISAS)

[PEM11-P03] New perspectives on coupling processes in solar-terrestrial system obtained by comprehensive data analysis

*Yoshimasa Tanaka[1], Norio Umemura[2], Shuji Abe[3], Satoru UeNo[4], Masahito Nose[2], Yumi Nakagawa[5] (1.National Institute of Polar Research, 2.Institute for Space-Earth Environmental Research, Nagoya University, 3.International Center for Space Weather Science and Education, 4.Kwasan & Hida Observatories, School of Science, Kyoto University, 5.Ibaraki University)

[PEM11-P04] The interaction between the magnetosphere-ionosphere compound system and the magnetic field topology

*Shigeru Fujita[1], Takashi Tanaka[2], Masakazu Watanabe[2] (1.Meteorological College, Japan Meteorological Agency/ Nationa Institute of Polar Research, 2.Kyushu University)

[PEM11-P05] Effects of the dipole tilt and the interplanetary magnetic field Bx component on the dawn-dusk and interhemispheric asymmetries of the interchange convection cycle

*Masakazu Watanabe[1,2], Takashi Tanaka[2], Shigeru Fujita[3,4] (1.Graduate School of Science, Kyushu University, 2.International Center for Space Weather Science and Education, Kyushu University, 3.Meteorological College, 4.National Institute of Polar Research)

[PEM11-P06] Transient polar ionospheric convection response to negative dynamic pressure pulse

*Jianjun Liu[1] (1.Polar Research Institute of China)

[PEM11-P07] An active ionosphere: a new perspective of field line dipolarization

*Osuke Saka[1] (1.Office Geophysik)

[PEM11-P08] Toward the automatic identification of FLR signals in the SuperDARN data by using the gradient method

*Hideaki Kawano[1,2], Akira Sessai Yukimatu[3,4], Nozomu Nishitani[5], Yoshimasa Tanaka[3,4], Satoko Saita[6], Tomoaki Hori[5] (1.Dept. Earth Planet. Sci., Kyushu Univ., 2.ICSWSE, Kyushu University, 3.National Institute of Polar Research, 4.SOKENDAI, 5.ISEE, Nagoya University, 6.Kitakyushu College)

[PEM11-P09] A statistical study of Pi2 pulsations observed in the upper ionosphere using Swarm magnetic field data

*Park Jaehee[1], Khan-Hyuk Kim[1], Junga Hwang[2] (1.School of Space Research, Kyung Hee University, Gyeonggi, South Korea, 2.Korea Astronomy and Space Science Institute, Daejeon,South Korea)

[PEM11-P10] Study on the global distribution characteristics of Pc 1-2 geomagnetic pulsation with the 10Hz data of the MAGDAS system

*Taisei Kabasawa[1], Akimasa Yoshikawa[1], Teiji Uozumi[1], Akiko Fujimoto[1], Shuji Abe[1] (1.Kyushu University)

[PEM11-P11] In-situ Observations of Reconnection Separatrix Regions in the near-Earth Magnetotail

*Mizuho Araki[1], Masahiro Hoshino[1], Kunihiro Keika[1], Yoshifumi Saito[2] (1.Graduate School of Science, The University of Tokyo, 2.Institude of Space and Astronautical Science)

[PEM11-P12] Flow speed dependence of ion temperature, electron temperature, and their ratio in the near-Earth magnetotail reconnection region

*Kaori Watanabe[1], Masahiro Hoshino[1], Kunihiro Keika[1], Yoshifumi Saito[2], Naritoshi Kitamura[1] (1.Univ. of Tokyo, 2.ISAS/JAXA)

[PEM11-P13] **Examining Minimum Cyclotron Resonant Electron Energy of EMIC Waves with MMS**

*Si Liu[1] (1.Changsha University of Science and Technology)

[PEM11-P14] Small scale whistler mode waves near the magnetic field intensity minimum in the magnetosheath

*Naritoshi Kitamura[1], Takanobu Amano[1], Yoshiharu Omura[2], Satoko Nakamura[2], Chika Umegaki[1], Scott A Boardsen[3,4], Narges Ahmadi[5], Robert E Ergun[5], Olivier Le Contel[6], Per-Arne Lindqvist[7], Yoshifumi Saito[8], Shoichiro Yokota[9], Daniel J Gershman[3], Barbara L Giles[3], Thomas E Moore[3], William R Paterson[3], Craig J Pollock[10], Christopher T Russell[11], Robert J Strangeway[11], James L Burch[12] (1.Department of Earth and Planetary Science, Graduate School of Science, The University of Tokyo, 2.Research Institute for Sustainable Humanosphere, Kyoto University, 3.NASA Goddard Space Flight Center, 4.University of Maryland, 5.Laboratory for Atmospheric and Space Physics, University of Colorado, 6.Laboratoire de Physique des Plasmas, UMR7648 CNRS/Ecole Polytechnique/UPMC/Université Paris-Sud/Observatoire de Paris, 7.Royal Institute of Technology, 8.Institute of Space and Astronautical Science, Japan Aerospace Exploration Agency, 9.Department of Earth and Space Science, Graduate School of Science, Osaka University, 10.Denali Scientific, 11.Institute of Geophysics and Planetary Physics, University of California, Los Angeles, 12.Southwest Research Institute)

[PEM11-P15] Spatial characteristics of the internal modulation of pulsating aurora: multi-point high-speed optical observations in Scandinavia

*Yuki Kawamura[1], Keisuke Hosokawa[1], Shin-ichiro Oyama[2,3], Yoshizumi Miyoshi[2], Yasunobu Ogawa[3], Satoshi Kurita[2], Satoshi Ebukuro[1], Ryoichi Fujii[4] (1.Department of Communication Engineering and Informatics, University of Electro-Communications, 2.Institute for Space-Earth Environmental Research, Nagoya University, 3.National Institute of Polar Research, 4.Research Organization of Information and Systems)

[PEM11-P16] **Large-scale characteristics of pulsating aurora periodicities:multi-point high-speed optical observations in Scandinavia**

*Satoshi Ebukuro[1], Keisuke Hosokawa[1], Shin-ichiro Oyama[2,3,5], Yoshizumi Miyoshi[2], Yasunobu Ogawa[3], Satoshi Kurita[2], Yuki Kawamura[1], Ryoichi Fujii[4] (1.Department of Communication Engineering and Informatics, University of Electro-Communications, 2.Institute for Space-Earth Environmental Research, Nagoya University, 3.National Institute of Polar Research, 4.Research Organization of Information and Systems, 5.University of Oulu)

[PEM11-P17] Variations of cosmic noise absorption (CNA) by energetic electron precipitation (EEP) and changes of the auroral morphology

*Miyamoto Taishiro[1], Shin-ichiro Oyama[1,4,5], Yasunobu Ogawa[2], Keisuke Hosokawa[3], Satoshi Kurita[1], Yoshizumi Miyoshi[1], Ryuho Kataoka[2], Hiroshi Miyaoka[2], Tero Raita[4] (1. Institute for Space-Earth Environmental Research,Nagoya University, 2.National Institute of Polar Research, 3.Department of Communication Engineering and Informatics, University of Electro-Communications, 4.Sodankylä Geophysical Observatory, University of Oulu, 5.Ionosphere Research Unit, University of Oulu)

[PEM11-P18] Spatiotemporal characteristics on the source region of flash aurora using ray tracing analysis

*Tomohiro Inoue[1], Mitsunori Ozaki[1], Yoshitaka Goto[1], Satoshi Yagitani[1], Yoshiya Kasahara[1], Kazuo Shiokawa[2], Yoshizumi Miyoshi[2], Ryuho Kataoka[3], Yusuke Ebihara[4] (1.Kanazawa University , 2.Nagoya University, 3.National Institute of Polar Research, 4.Kyoto University)

[PEM11-P19] Molecular ion supply mechanisms from the low-altitude ionosphere to magnetosphere observed by EISCAT and Arase(ERG)

*Masayoshi Takada[1], Kanako Seki[1], Yasunobu Ogawa[2], Kunihiro Keika[3], Satoshi Kasahara[4], Shoichiro Yokota[5], Tomoaki Hori[7], Kazushi Asamura[6], Yoshizumi Miyoshi[7] (1.Graduate School of Science, Tokyo University, 2.National Institute of Polar Research, 3.Department of Earth and Planetary Science, Graduate School of Science, Tokyo University, 4.The University of Tokyo, 5.Graduate School of Science, Osaka University, 6.Institute of Space and Astronautical Science, Japan Aerospace Exploration Agency, 7.Institute for Space-Earth Environmental Research, Nagoya University)

[PEM11-P20] Optical and radar observation of the dynamic auroral forms

*Yunosuke Nagafusa[1], Tima Sergienko[2], Satoshi Taguchi[1], Urban Braendstroem[2], Masatoshi Yamauchi[2] (1.Graduate School of Science, Kyoto University, 2.Swedish Institute of Space Physics, Kiruna)

[PEM11-P21] Observations of MF/HF auroral radio emissions at three ground-based stations

*Yuka Sato[1], Atsushi Kumamoto[2], Yuto Katoh[2], Akira Kadokura[3,4], Yasunobu Ogawa[3,4], Atsuki Shinbori[5] (1.Nippon Institute of Technology (NIT), 2.Graduate School of Science, Tohoku University, 3.National Institute of Polar Research (NIPR), 4.The Graduate University for Advanced Studies, 5.Institute for Space-Earth Environmental Research (ISEE), Nagoya University)

[PEM11-P22] **Ionospheric F-region Drift Measurements Derived from DPS-4D at Zhongshan Station, Antarctic**

*Xiangcai Chen[1] (1.Polar Research Institute of China)

[PEM11-P23] PARM-HEP Observation of Precipitating High Energy Electrons over Pulsating Aurora

*Taku Namekawa[1], Takefumi Mitani[2], Kazushi Asamura[2], Yoshifumi Saito[2] (1.Department of Earth and Planetary Science, Graduate school of Science, The University of Tokyo, 2.Institute of Space and Astronautical Science, Japan Aerospace Exploration Agency)

[PEM11-P24] Development of the medium-energy electron detector with hemispherical field-of-view and the flight test in the PARM (Pulsating AuRora and Microburst) mission

*Shin Sugo[1], Oya Kawashima[1], Kazushi Asamura[2], Reiko Nomura[3], Yasunobu Ogawa[4], Keisuke Hosokawa[5], Yoshizumi Miyoshi[6], Takefumi Mitani[2], Taku Namekawa[1,2], Takeshi Sakanoi[7], Mizuki Fukizawa[7], Naoshi Yagi[7], Satoshi Kasahara[1] (1.The University of Tokyo, 2.Institute of Space and Astronautical Science, Japan Aerospace Exploration Agency, 3.National Astronomical Observatory of Japan, 4.National Institute of Polar Research, 5.The University of Electro-Communications, 6.Institute for Space-Earth Environmental Research, Nagoya University, 7.Tohoku University)

[PEM11-P25] Auroral substorm onset in satellite-based global images and ground-based all-sky images

*Akimasa Ieda[1], Kirsti Kauristie[2], Yukitoshi Nishimura[3], Yukinaga Miyashita[4], Harald U Frey[5], Liisa Juusola[2], Daniel Whiter[6], Masahito Nose[7], Matthew O Fillingim[5], Farideh Honary[8], Neil C Rogers[8], Yoshizumi Miyoshi[1], Shinobu Machida[1] (1.Institute for Space-Earth Environmental Research, Nagoya University, 2.Finnish Meteorological Institute, 3.Boston university, 4.Korea Astronomy and Space Science Institute, 5.University of California Berkeley, 6.University of Southampton, 7.Graduate School of Science, Kyoto University, 8.Lancaster University)

[PEM11-P26] Automatic Classification of Auroral images using optical flow feature

*Naoto Kashiwagi[1], Akiko Fujimoto[1], Terumasa Tokunaga[1], Yoshizumi Miyoshi[2], Yasunobu Ogawa[3], Keisuke Hosokawa[4] (1.Kyushu Institute of Technology, 2.Nagoya University, 3.National Institute of Polar Research, 4.The University of Electro-Communications)

[PEM11-P27] Fine-scale visualization of aurora in a wide area using color digital camera images from the International Space Station

*Sota Nanjo[1], Yuta Hozumi[1], Keisuke Hosokawa[1] (1.The University of Electro-Communications)

[PEM11-P28] Geospace Imaging via the soft X-ray imager: GEO-X mission

*Yoshizumi Miyoshi[1], Yuichiro Ezoe[2], Satoshi Kasahara[3], Yosuke Matsumoto[4], Kumi Ishikawa[5], Ryuho Kataoka[6], Hiroki Ito[1], Daiki Ishi[2], Masaki Numazawa[2], Atsushi Yamazaki[5], Hiroshi Hasegawa[5], Masaki Fujimoto[5], Kazuhisa Mitsuda[5] (1.Institute for Space-Earth Environmental Research, Nagoya University, 2.Tokyo Metropolitan University, 3.University of Tokyo, 4.Chiba University, 5.ISAS/JAXA, 6.NIPR)

[E] Poster | P (Space and Planetary Sciences)：P-EM Solar-Terrestrial Sciences, Space Electromagnetism & Space Environment

5:15 PM - 6:30 PM JST | 8:15 AM - 9:30 AM UTC | Poster Hall International Exhibition Hall8, Makuhari Messe_5

[P-EM11] Dynamics of Magnetosphere and Ionosphere

convener:Aoi Nakamizo(Applied Electromagnetic Research Institute, National Institute of Information and Communications Technology), Mitsunori Ozaki(Faculty of Electrical and Computer Engineering, Institute of Science and Engineering, Kanazawa University), Akiko Fujimoto(Kyushu Institute of Technology), Tomoaki Hori(Institute for Space-Earth Environmental Research, Nagoya University)

[PEM11-P01] Effects of Inclination/Rotation of Earth's Magnetic Axis on Magnetosphere Simulated by Global MHD Model

*Aoi Nakamizo[1] (1.Applied Electromagnetic Research Institute, National Institute of Information and Communications Technology)

[PEM11-P02] Asymmetric deformation of the magnetosphere under low-density solar wind

*Masaki N Nishino[1,2], Yoshifumi Saito[2], Kazuo Shiokawa[1], Masaki Fujimoto[2] (1.Institute for Space-Earth Environmental Research, Nagoya University, 2.JAXA/ISAS)

[PEM11-P03] New perspectives on coupling processes in solar-terrestrial system obtained by comprehensive data analysis

*Yoshimasa Tanaka[1], Norio Umemura[2], Shuji Abe[3], Satoru UeNo[4], Masahito Nose[2], Yumi Nakagawa[5] (1.National Institute of Polar Research, 2.Institute for Space-Earth Environmental Research, Nagoya University, 3.International Center for Space Weather Science and Education, 4.Kwasan & Hida Observatories, School of Science, Kyoto University, 5.Ibaraki University)

[PEM11-P04] The interaction between the magnetosphere-ionosphere compound system and the magnetic field topology

*Shigeru Fujita[1], Takashi Tanaka[2], Masakazu Watanabe[2] (1.Meteorological College, Japan Meteorological Agency/ Nationa Institute of Polar Research, 2.Kyushu University)

[PEM11-P05] Effects of the dipole tilt and the interplanetary magnetic field Bx component on the dawn-dusk and interhemispheric asymmetries of the interchange convection cycle

*Masakazu Watanabe[1,2], Takashi Tanaka[2], Shigeru Fujita[3,4] (1.Graduate School of Science, Kyushu University, 2.International Center for Space Weather Science and Education, Kyushu University, 3.Meteorological College, 4.National Institute of Polar Research)

[PEM11-P06] Transient polar ionospheric convection response to negative dynamic pressure pulse

*Jianjun Liu[1] (1.Polar Research Institute of China)

[PEM11-P07] An active ionosphere: a new perspective of field line dipolarization

*Osuke Saka[1] (1.Office Geophysik)

[PEM11-P08] Toward the automatic identification of FLR signals in the SuperDARN data by using the gradient method

*Hideaki Kawano[1,2], Akira Sessai Yukimatu[3,4], Nozomu Nishitani[5], Yoshimasa Tanaka[3,4], Satoko Saita[6], Tomoaki Hori[5] (1.Dept. Earth Planet. Sci., Kyushu Univ., 2.ICSWSE, Kyushu University, 3.National Institute of Polar Research, 4.SOKENDAI, 5.ISEE, Nagoya University, 6.Kitakyushu College)

[PEM11-P09] A statistical study of Pi2 pulsations observed in the upper ionosphere using Swarm magnetic field data

*Park Jaehee[1], Khan-Hyuk Kim[1], Junga Hwang[2] (1.School of Space Research, Kyung Hee University, Gyeonggi, South Korea, 2.Korea Astronomy and Space Science Institute, Daejeon,South Korea)

[PEM11-P10] Study on the global distribution characteristics of Pc 1-2 geomagnetic pulsation with the 10Hz data of the MAGDAS system

*Taisei Kabasawa[1], Akimasa Yoshikawa[1], Teiji Uozumi[1], Akiko Fujimoto[1], Shuji Abe[1] (1.Kyushu University)

[PEM11-P11] In-situ Observations of Reconnection Separatrix Regions in the near-Earth Magnetotail

*Mizuho Araki[1], Masahiro Hoshino[1], Kunihiro Keika[1], Yoshifumi Saito[2] (1.Graduate School of Science, The University of Tokyo, 2.Institude of Space and Astronautical Science)

[PEM11-P12] Flow speed dependence of ion temperature, electron temperature, and their ratio in the near-Earth magnetotail reconnection region

*Kaori Watanabe[1], Masahiro Hoshino[1], Kunihiro Keika[1], Yoshifumi Saito[2], Naritoshi Kitamura[1] (1.Univ. of Tokyo, 2.ISAS/JAXA)

[PEM11-P13] **Examining Minimum Cyclotron Resonant Electron Energy of EMIC Waves with MMS**

*Si Liu[1] (1.Changsha University of Science and Technology)

[PEM11-P14] Small scale whistler mode waves near the magnetic field intensity minimum in the magnetosheath

*Naritoshi Kitamura[1], Takanobu Amano[1], Yoshiharu Omura[2], Satoko Nakamura[2], Chika Umegaki[1], Scott A Boardsen[3,4], Narges Ahmadi[5], Robert E Ergun[5], Olivier Le Contel[6], Per-Arne Lindqvist[7], Yoshifumi Saito[8], Shoichiro Yokota[9], Daniel J Gershman[3], Barbara L Giles[3], Thomas E Moore[3], William R Paterson[3], Craig J Pollock[10], Christopher T Russell[11], Robert J Strangeway[11], James L Burch[12] (1.Department of Earth and Planetary Science, Graduate School of Science, The University of Tokyo, 2.Research Institute for Sustainable Humanosphere, Kyoto University, 3.NASA Goddard Space Flight Center, 4.University of Maryland, 5.Laboratory for Atmospheric and Space Physics, University of Colorado, 6.Laboratoire de Physique des Plasmas, UMR7648 CNRS/Ecole Polytechnique/UPMC/Université Paris-Sud/Observatoire de Paris, 7.Royal Institute of Technology, 8.Institute of Space and Astronautical Science, Japan Aerospace Exploration Agency, 9.Department of Earth and Space Science, Graduate School of Science, Osaka University, 10.Denali Scientific, 11.Institute of Geophysics and Planetary Physics, University of California, Los Angeles, 12.Southwest Research Institute)

[PEM11-P15] Spatial characteristics of the internal modulation of pulsating aurora: multi-point high-speed optical observations in Scandinavia

*Yuki Kawamura[1], Keisuke Hosokawa[1], Shin-ichiro Oyama[2,3], Yoshizumi Miyoshi[2], Yasunobu Ogawa[3], Satoshi Kurita[2], Satoshi Ebukuro[1], Ryoichi Fujii[4] (1.Department of Communication Engineering and Informatics, University of Electro-Communications, 2.Institute for Space-Earth Environmental Research, Nagoya University, 3.National Institute of Polar Research, 4.Research Organization of Information and Systems)

[PEM11-P16] **Large-scale characteristics of pulsating aurora periodicities:multi-point high-speed optical observations in Scandinavia**

*Satoshi Ebukuro[1], Keisuke Hosokawa[1], Shin-ichiro Oyama[2,3,5], Yoshizumi Miyoshi[2], Yasunobu Ogawa[3], Satoshi Kurita[2], Yuki Kawamura[1], Ryoichi Fujii[4] (1.Department of Communication Engineering and Informatics, University of Electro-Communications, 2.Institute for Space-Earth Environmental Research, Nagoya University, 3.National Institute of Polar Research, 4.Research Organization of Information and Systems, 5.University of Oulu)

[PEM11-P17] Variations of cosmic noise absorption (CNA) by energetic electron precipitation (EEP) and changes of the auroral morphology

*Miyamoto Taishiro[1], Shin-ichiro Oyama[1,4,5], Yasunobu Ogawa[2], Keisuke Hosokawa[3], Satoshi Kurita[1], Yoshizumi Miyoshi[1], Ryuho Kataoka[2], Hiroshi Miyaoka[2], Tero Raita[4] (1. Institute for Space-Earth Environmental Research,Nagoya University, 2.National Institute of Polar Research, 3.Department of Communication Engineering and Informatics, University of Electro-Communications, 4.Sodankylä Geophysical Observatory, University of Oulu, 5.Ionosphere Research Unit, University of Oulu)

[PEM11-P18] Spatiotemporal characteristics on the source region of flash aurora using ray tracing analysis

*Tomohiro Inoue[1], Mitsunori Ozaki[1], Yoshitaka Goto[1], Satoshi Yagitani[1], Yoshiya Kasahara[1], Kazuo Shiokawa[2], Yoshizumi Miyoshi[2], Ryuho Kataoka[3], Yusuke Ebihara[4] (1.Kanazawa University , 2.Nagoya University, 3.National Institute of Polar Research, 4.Kyoto University)

[PEM11-P19] Molecular ion supply mechanisms from the low-altitude ionosphere to magnetosphere observed by EISCAT and Arase(ERG)

*Masayoshi Takada[1], Kanako Seki[1], Yasunobu Ogawa[2], Kunihiro Keika[3], Satoshi Kasahara[4], Shoichiro Yokota[5], Tomoaki Hori[7], Kazushi Asamura[6], Yoshizumi Miyoshi[7] (1.Graduate School of Science, Tokyo University, 2.National Institute of Polar Research, 3.Department of Earth and Planetary Science, Graduate School of Science, Tokyo University, 4.The University of Tokyo, 5.Graduate School of Science, Osaka University, 6.Institute of Space and Astronautical Science, Japan Aerospace Exploration Agency, 7.Institute for Space-Earth Environmental Research, Nagoya University)

[PEM11-P20] Optical and radar observation of the dynamic auroral forms

*Yunosuke Nagafusa[1], Tima Sergienko[2], Satoshi Taguchi[1], Urban Braendstroem[2], Masatoshi Yamauchi[2] (1.Graduate School of Science, Kyoto University, 2.Swedish Institute of Space Physics, Kiruna)

[PEM11-P21] Observations of MF/HF auroral radio emissions at three ground-based stations

*Yuka Sato[1], Atsushi Kumamoto[2], Yuto Katoh[2], Akira Kadokura[3,4], Yasunobu Ogawa[3,4], Atsuki Shinbori[5] (1.Nippon Institute of Technology (NIT), 2.Graduate School of Science, Tohoku University, 3.National Institute of Polar Research (NIPR), 4.The Graduate University for Advanced Studies, 5.Institute for Space-Earth Environmental Research (ISEE), Nagoya University)

[PEM11-P22] **Ionospheric F-region Drift Measurements Derived from DPS-4D at Zhongshan Station, Antarctic**

*Xiangcai Chen[1] (1.Polar Research Institute of China)

[PEM11-P23] PARM-HEP Observation of Precipitating High Energy Electrons over Pulsating Aurora

*Taku Namekawa[1], Takefumi Mitani[2], Kazushi Asamura[2], Yoshifumi Saito[2] (1.Department of Earth and Planetary Science, Graduate school of Science, The University of Tokyo, 2.Institute of Space and Astronautical Science, Japan Aerospace Exploration Agency)

[PEM11-P24] Development of the medium-energy electron detector with hemispherical field-of-view and the flight test in the PARM (Pulsating AuRora and Microburst) mission

*Shin Sugo[1], Oya Kawashima[1], Kazushi Asamura[2], Reiko Nomura[3], Yasunobu Ogawa[4], Keisuke Hosokawa[5], Yoshizumi Miyoshi[6], Takefumi Mitani[2], Taku Namekawa[1,2], Takeshi Sakanoi[7], Mizuki Fukizawa[7], Naoshi Yagi[7], Satoshi Kasahara[1] (1.The University of Tokyo, 2.Institute of Space and Astronautical Science, Japan Aerospace Exploration Agency, 3.National Astronomical Observatory of Japan, 4.National Institute of Polar Research, 5.The University of Electro-Communications, 6.Institute for Space-Earth Environmental Research, Nagoya University, 7.Tohoku University)

[PEM11-P25] Auroral substorm onset in satellite-based global images and ground-based all-sky images

*Akimasa Ieda[1], Kirsti Kauristie[2], Yukitoshi Nishimura[3], Yukinaga Miyashita[4], Harald U Frey[5], Liisa Juusola[2], Daniel Whiter[6], Masahito Nose[7], Matthew O Fillingim[5], Farideh Honary[8], Neil C Rogers[8], Yoshizumi Miyoshi[1], Shinobu Machida[1] (1.Institute for Space-Earth Environmental Research, Nagoya University, 2.Finnish Meteorological Institute, 3.Boston university, 4.Korea Astronomy and Space Science Institute, 5.University of California Berkeley, 6.University of Southampton, 7.Graduate School of Science, Kyoto University, 8.Lancaster University)

[PEM11-P26] Automatic Classification of Auroral images using optical flow feature

*Naoto Kashiwagi[1], Akiko Fujimoto[1], Terumasa Tokunaga[1], Yoshizumi Miyoshi[2], Yasunobu Ogawa[3], Keisuke Hosokawa[4] (1.Kyushu Institute of Technology, 2.Nagoya University, 3.National Institute of Polar Research, 4.The University of Electro-Communications)

[PEM11-P27] Fine-scale visualization of aurora in a wide area using color digital camera images from the International Space Station

*Sota Nanjo[1], Yuta Hozumi[1], Keisuke Hosokawa[1] (1.The University of Electro-Communications)

[PEM11-P28] Geospace Imaging via the soft X-ray imager: GEO-X mission

*Yoshizumi Miyoshi[1], Yuichiro Ezoe[2], Satoshi Kasahara[3], Yosuke Matsumoto[4], Kumi Ishikawa[5], Ryuho Kataoka[6], Hiroki Ito[1], Daiki Ishi[2], Masaki Numazawa[2], Atsushi Yamazaki[5], Hiroshi Hasegawa[5], Masaki Fujimoto[5], Kazuhisa Mitsuda[5] (1.Institute for Space-Earth Environmental Research, Nagoya University, 2.Tokyo Metropolitan University, 3.University of Tokyo, 4.Chiba University, 5.ISAS/JAXA, 6.NIPR)

[E] Poster | P (Space and Planetary Sciences)：P-EM Solar-Terrestrial Sciences, Space Electromagnetism & Space Environment

3:30 PM - 5:00 PM JST | 6:30 AM - 8:00 AM UTC | Poster Hall International Exhibition Hall8, Makuhari Messe_2

[P-EM13] Inner magnetosphere: Recent understanding and new insights

convener:Yusuke Ebihara(Research Institute for Sustainable Humanosphere, Kyoto University), Danny Summers(Memorial University of Newfoundland), Yoshizumi Miyoshi(Institute for Space-Earth Environmental Research, Nagoya University), Shinji Saito(Graduate School of Science, Nagoya University)

[PEM13-P01] Evaluation of wave normal and Poynting vector analyses for whistler mode waves observed by the waveform capture (WFC) on board the Arase

*Yoshiya Kasahara[1], Satoshi Ikarashi[1], Hiroyuki Nishizawa[1], Shoya Matsuda[2], Fuminori Tsuchiya[3], Atsushi Kumamoto[3], Yasumasa Kasaba[3], Mitsunori Ozaki[1], Ayako Matsuoka[2] (1.Kanazawa University, 2.ISAS/JAXA, 3.Tohoku University)

[PEM13-P02] Calibration of electric fields dedicated to the measurement of the S-WPIA of the Arase Satellite

*Miki Jumpei[1], Hirotsugu Kojima[2], Yuto Katoh[3], Shoya Matsuda[4], Yoshiya Kasahara[5], Mitsuru Hikishima[4], Satoshi Kurita[6], Masahiro Kitahara[3], Satoshi Kasahara[7], Yoshizumi Miyoshi[6], Atsushi Kumamoto[3], Ayako Matsuoka[4], Shoichiro Yokota[8], Tomoaki Hori[6], Kunihiro Keika[7] (1.Space Radio Engineering Laboratory, Division of Electrical Engineering, Kyoto University Graduated School, 2.Research Institute for Sustainable Humanosphere, Kyoto University, 3.Graduate School of Science and Faculty of Science, Tohoku University, 4.Institute of Space and Astronautical Science, JAXA, 5.Information Media Center, Kanazawa University, 6.Institute for Space-Earth Environmental Research, Nagoya University, 7.School of Science, The University of Tokyo, 8.School of Science, Osaka University)

[PEM13-P03] Enhancement of whistler-mode chorus in association with Pc 4-5 ULF waves and related variation of high energy electrons

*Atsuhiro Ono[1], Yuto Katoh[1], Atsushi Kumamoto[1], Fuminori Tsuchiya[1], Mariko Teramoto[2], Yoshiya Kasahara[3], Shoya Matsuda[4], Ayako Matsuoka[4], Takefumi Mitani[4], Tomoaki Hori[2], Satoshi Kasahara[5], Shoichiro Yokota[6], Kunihiro Keika[5], Yoshizumi Miyoshi[2], Iku Shinohara[4] (1.Tohoku University, 2.Nagoya University, 3.Kanazawa University, 4.ISAS/JAXA, 5.The University of Tokyo, 6.Osaka University)

[PEM13-P04] Sudden enhancements of electron cyclotron harmonic waves observed by the Arase satellite

*Shinjo Airi[1], Hirotsugu Kojima[1], Yoshiya Kasahara[2], Yoichi Kazama[3], Hideyuki Usui[4], Yoshizumi Miyoshi[5], Yasumasa Kasaba[6], Shoya Matsuda[7], Tomoaki Hori[5], S. -Y. Wang[8], Sunny W.Y. Tam[9], Atsushi Kumamoto[10], Ayako Matsuoka[11] (1.Research institute for sustainable humanosphere, Kyoto University, 2.Information Media Center, Kanazawa University, 3.ASIAA, 4.Graduate school of system informatics Kobe University, 5.Institute for Space-Earth Environmental Research, Nagoya University, 6.Planetary Plasma and Atmospheric Research Center, Tohoku University, 7.Institute of Space and Astronautical Science/Japan Aerospace Exploration Agency, 8.ASIAA, Taiwan, 9.ISAPS, NCKU, Taiwan, 10.Department of Geophysics, Graduate School of Science, Tohoku University, 11.Research Division for Space Plasma, Institute of Space and Astronautical Science, Japan Aerospace Exploration Agency)

[PEM13-P05] Correlation between pulsating aurora and electrostatic electron cyclotron harmonic waves obtained from coordinated Arase and ground data

*Mizuki Fukizawa[1], Takeshi Sakanoi[1], Yoshizumi Miyoshi[2], Keisuke Hosokawa[3], Yoichi Kazama[4], Yoshiya Kasahara[5], Shoya Matsuda[6], Ayako Matsuoka[7], Wang Shiang-Yu[4], Sunny Wing-Yee Tam[8], Ryuho Kataoka[9] (1.Planetary Plasma and Atmospheric Research Center, Graduate School of Science, Tohoku University, 2.Institute for Space-Earth Environmental Research, Nagoya University, 3.Department of Communication Engineering and Informatics, University of Electro-Communications, 4.Academia Sinica Institute of Astronomy and Astrophysics, 5.Information Media Center, Kanazawa University, 6.Institute of Space and Astronautical Science/Japan Aerospace Exploration Agency, 7.Research Division for Space Plasma, Institute of Space and Astronautical Science, Japan Aerospace Exploration Agency, 8.Institute of Space and Plasma Sciences, College of Sciences, National Cheng Kung University , 9.National Institute of Polar Research)

[PEM13-P06] Automatic determination of Upper Hybrid Resonance Frequencies by Convolutional Neural Network.

*Shoya Matsuda[1], Tatsuhito Hasegawa[2], Atsushi Kumamoto[3], Fuminori Tsuchiya[3], Yoshiya Kasahara[4], Yoshizumi Miyoshi[5], Yasumasa Kasaba[3], Ayako Matsuoka[1] (1.Institute of Space and Astronautical Science/Japan Aerospace Exploration Agency, 2.University of Fukui, 3.Tohoku University, 4.Kanazawa University, 5.ISEE, Nagoya University)

[PEM13-P07] Amplitude dependence of whistler wave motion on electron scattering process

*Yoshiki Ito[1], Yoshizumi Miyoshi[1], Shinji Saito[1] (1.Nagoya University, ISEE)

[PEM13-P08] Two-dimensional simulation of whistler mode wave packets interacting with energetic electrons

*Takeshi Nogi[1], Yoshiharu Omura[1] (1.Reserch Institute for Sustainable Humanosphere, Kyoto University)

[PEM13-P09] Relativistic electron acceleration by whistler-mode chorus waves in 1D, 2D, and 3D magnetic field models.

*Keita Takahashi[1], Yoshiharu Omura[1], Yikai HSIEH[1], Danny Summers[2] (1.Research Institute for Sustainable Humanosphere, Kyoto University , 2.Department of Mathematics and Statistics, Memorial University of Newfoundland)

[PEM13-P10] Study of global spatio-temporal development of magnetospheric ELF/VLF waves for the 26-30 March 2017 storm based on ground and satellite observations and the RAM simulations

*Yuhei Takeshita[1], Kazuo Shiokawa[1], Yoshizumi Miyoshi[1], Mitsunori Ozaki[2], Yoshiya Kasahara[2], Martine Connors[3], Jyrki Manninen[4], Craig Kletzing[5], Vania Jordanova[6] (1.Nagoya University, Institute for Space-Earth Environmental Resarch, 2.Kanazawa University, 3.Athabasca University, 4.Sodankylä Geophysical Observatory, 5.The University of Iowa, 6.Los Alamos National Laboratory)

[PEM13-P11] Flux decrease of outer radiation belt electrons associated with solar wind pressure pulse: A Code coupling simulation of GEMSIS-RB and GEMSIS-GM

*Ito Hiroki[1], Yoshizumi Miyoshi[1], Shinji Saito[2], Yosuke Matsumoto[3], Takanobu Amano[4] (1.Institute for Space-Earth Environmental Research, Nagoya University, 2. Graduate School of Science, Nagoya University, 3. Graduate School of Science, Chiba University, 4.Department of Earth and Planetary Science, University of Tokyo)

[PEM13-P12] Non-diffusive response of outer belt electrons on interplanetary shock

Takuma Toishi[1], *Yusuke Ebihara[1], Takashi Tanaka[2] (1.Research Institute for Sustainable Humanosphere, Kyoto University, 2.Kyushu University)

[PEM13-P13] PARM: Initial result of the auroral camera on the G-CHASER (RockSat-XN) rocket and status of the development of auroral cameras for the LAMP rocket experiment

*Naoshi Yagi[1], Takeshi Sakanoi[1], Fukizawa Mizuki[1], Kazushi Asamura[2], Yoshizumi Miyoshi[3], Keisuke Hosokawa[4], Genki Ishizawa[5] (1.Planetary Plasma and Atmospheric Research Center, Graduate School of Science, Tohoku University, 2.Institute of Space and Astronautical Science, Japan Aerospace Exploration Agency, 3.Institute for Space-Earth Environmental Research, Nagoya University, 4.Department of Communication Engineering and Informatics, University of Electro-Communications, 5.Space & terrestrial plasma pyhsics)

[PEM13-P14] First simultaneous observation of a SAR arc at subauroral latitudes using a ground all-sky camera and the Arase satellite in the inner magnetosphere

*Yudai Inaba[1], Kazuo Shiokawa[1], Shin-ichiro Oyama[1,8,9], Yuichi Otsuka[1], Atsuki Shinbori[1], Yoichi Kazama[2], Shiang-Yu Wang[2], Sunny W. Y. Tam[2], Shoichiro Yokota[3], Satoshi Kasahara[4], Kunihiro Keika[4], Tomoaki Hori[1], Ayako Matsuoka[5], Yoshiya Kasahara[6], Atsushi Kumamoto[7], Yasumasa Kasaba[7], Yoshizumi Miyoshi[1], Iku Shinohara[5], Arto Oksanen[10] (1.Institute for Space-Earth Environmental Research, 2.Academia Sinica, 3.Osaka Univ, 4.Tokyo Univ, 5.JAXA, 6.Kanazawa University, 7.Tohoku University, 8.University of Oulu, Finland, 9.National Institute of Polar Research, 10.Jyväskylän Sirius ry, Finland)

[PEM13-P15] Pi2 pulsations observed by the Arase satellite inside and outside the plasmapause

*Mariko Teramoto[1], Ayako Matsuoka[2], Reiko Nomura[5], Yoshiya Kasahara[3], Yasumasa Kasaba[4], Atsushi Kumamoto[4], Fuminori Tsuchiya[4], Shoya Matsuda[2], Masahito Nose[1], Masafumi Shoji[1], Yasunori Tsugawa[1], Shun Imajo[1], Yoshizumi Miyoshi[1], Iku Shinohara[2] (1.Institute for Space-Earth Environmental Research Nagoya University, 2.Institute of Space and Astronautical Science, Japan Aerospace eXploration Agency, 3.Kanazawa University, 4.Tohoku University, 5.National Astronomical Observatory of Japan)

[PEM13-P16] An extreme erosion of the plasmasphere during the 7–10 September 2017 storm

*Yuki Obana[1], Naomi Maruyama[2,3], Atsuki Shinbori[4], Kumiko K. Hashimoto[5], Mariangel Fedrizzi[2,3], Masahito Nose[4], Yuichi Otsuka[4], Nozomu Nishitani[4], Tomoaki Hori[4], Atsushi Kumamoto[6], Fuminori Tsuchiya[6], Shoya Matsuda[7], Ayako Matsuoka[7], Yoshiya Kasahara[8], Akimasa Yoshikawa[9], Yoshizumi Miyoshi[4], Iku Shinohara[7] (1.Osaka Electro-Communication University, 2.University of Colorado Boulder, 3.NOAA Space Weather Prediction Center, 4.Nagoya

University, 5.Kibi International University, 6.Tohoku University, 7.Japan Aerospace Exploration Agency, 8.Kanazawa University, 9.Kyushu University)

[PEM13-P17] Relative contribution of ULF and chorus waves to the radiation belt variation: Comparison between multi-point observations and BATSRUS + CRCM simulation

*Naoko Takahashi[1], Kanako Seki[1], Mei-Ching Fok[2], Yihua Zheng[2], Yoshizumi Miyoshi[3], David Hartley[4], Ayako Matsuoka[5], Yoshiya Kasahara[6], Yasumasa Kasaba[7], Nana Higashio[8] (1.Graduate School of Science, University of Tokyo, 2.NASA Goddard Space Flight Center, 3.Institute for Space-Earth Environmental Research, Nagoya University, 4.Department of Physics and Astronomy, University of Iowa, 5.Institute of Space and Astronautical Science, Japan Aerospace Exploration Agency, 6.Information Media Center, Kanazawa University, 7.Planetary Plasma and Atmospheric Research Center, Tohoku University, 8.Japan Aerospace Exploration Agency)

[PEM13-P18] Modulation of the D-region ionosphere by Pc5 waves observed by VLF/LF standard radio waves

*Miyashita Takuya[1], Hiroyo Ohya[1], Fuminori Tsuchiya[2], Hiroyuki Nakata[1], Toshiaki Takano[1], Kazuo Shiokawa[3], Yoshizumi Miyoshi[3] (1.Chiba University, 2.Tohoku University, 3.Nagoya University)

[PEM13-P19] Oxygen-proton differences in ion energies dominating plasma pressure: Dependence on storm phases and solar wind drivers

*Kunihiro Keika[1], Satoshi Kasahara[1], Shoichiro Yokota[2], Masahiro Hoshino[1], Kanako Seki[1], Masahito Nose[3], Yoshizumi Miyoshi[3], Iku Shinohara[4] (1.Graduate School of Science, The University of Tokyo , 2.Graduate School of Science, Osaka University, 3.Institute for Space-Earth Environmental Research, Nagoya University, 4.Institute of Space and Astronautical Science, Japan Aerospace Exploration Agency)

[PEM13-P20] Mass dependence of penetration depth of multi-energy ions in the inner magnetosphere during magnetic storms: Arase observations

*Ryosuke Fujii[1], Yoshizumi Miyoshi[1], Masafumi Shoji[1], Kazushi Asamura[2], Lynn Kistler[1,8], Vania Jordanova[9], Tomoaki Hori[1], Satoshi Kurita[1], Mariko Teramoto[1], Yasunori Tsugawa[1], Yoshiya Kasahara[3], Yasumasa Kasaba[4], Atsushi Kumamoto[5], Fuminori Tsuchiya[4], Shoichiro Yokota[6], Kunihiro Keika[7], Ayako Matsuoka[2], Iku Shinohara[2] (1.Institute for Space-Earth Environmental Research, Nagoya University, 2.Institute of Space and Astronautical Science, Japan Aerospace Exploration Agency, 3.Information Media Center, Kanazawa University, 4.Planetary Plasma and Atmospheric Research Center, Tohoku University, 5.Department of Geophysics, Graduate School of Science, Tohoku University, 6.Graduate School of Science, Osaka University, 7.Department of Earth and Planetary Science, Graduate School of Science, The University of Tokyo, 8.University of New Hampshire, 9.Los Alamos National Laboratory)

[PEM13-P21] Relativistic Acceleration of Energetic Protons by Electromagnetic Ion Cyclotron Waves in the Jovian Magnetosphere

*Tomohiro Sekine[1], Yoshiharu Omura[1], Danny Summers[2], Yikai HSIEH[1], Satoko Nakamura[1] (1.Reserach Institute for Sustainable Humanosphere, Kyoto University, 2.Memorial University of Newfoundland)

[PEM13-P22] Statistical study of IPDP type EMIC wave-related electron precipitation at subauroral latitude

*Asuka Hirai[1], Fuminori Tsuchiya[1], Takahiro Obara[1], Yasumasa Kasaba[1], Yuto Katoh[2], Hiroaki Misawa[1], Kazuo Shiokawa[3], Yoshizumi Miyoshi[3], Satoshi Kurita[3], Martin G Connors[4] (1.Planetary Plasma and Atmospheric Research Center, Graduate School of Science, Tohoku Univ. , 2.Department of Geophysics, Graduate School of Science, Tohoku University, 3.Institute for Space-Earth Environmental Research, Nagoya University, 4.Athabasca University)

[PEM13-P23] Meridional distributions of proton plasma and pressure-driven currents in the nightside inner magnetosphere: Arase observations

*Shun Imajo[1], Masahito Nose[1], Satoshi Kasahara[2], Shoichiro Yokota[3], Ayako Matsuoka[4], Kunihiro Keika[2], Tomoaki Hori[1], Mariko Teramoto[1], Kazuhiro Yamamoto[5], Oimatsu Satoshi[5], Reiko Nomura[6], Akiko Fujimoto[7], Iku Shinohara[4], Yoshizumi Miyoshi[1] (1.Institute for Space-Earth Environmental Research, Nagoya University, 2.Graduate School of Science, The University of Tokyo, 3.Graduate School of Science, Osaka University, 4.Institute of Space and Astronautical Science, Japan Aerospace Exploration Agency, 5.Graduate School of Science, Kyoto University, 6.National Astronomical Observatory of Japan, 7.Kyushu Institute of Technology)

[PEM13-P24] Space Weather Effects on Energetic Proton Flux Response in South Atlantic Anomaly

*Kirolosse Mina GIRGIS[1,2], Tohru Hada[1], Shuichi Matsukiyo[1] (1.Earth System Science and Technology (ESST) Department, Interdisciplinary Graduate School of Engineering Sciences (IGSES), Kyushu University, Japan, 2.Aerospace Engineering Department, Faculty of Engineering, Cairo University, Egypt)

[PEM13-P25] Solar-cycle variations of >30 keV electron flux enhancements under the inner radiation belt

*ALLA SUVOROVA[1] (1.National Central University)

[PEM13-P26] Energy spectra variations of high energy electrons in the inner magnetosphere observed by HEP/XEP on ARASE and SEDA-e on HIMAWARI

*Takeshi Takashima[1], Takefumi Mitani[1], Nana Higashio[2], Tsutomu Nagatsuma[3] (1. ISAS/JAXA, 2.Research and Development Directorate/JAXA, 3.NiCT)

[PEM13-P27] Inter-channel calibration of the high-energy electron experiments (HEP) instrument onboard the Arase satellite

*Tomoaki Hori[1], Takefumi Mitani[2], Takeshi Takashima[2], Park Inchun[1], Satoshi Kurita[1], Mariko Teramoto[1], Nana Higashio[3], Satoshi Kasahara[4], Shoichiro Yokota[5], Yoshizumi Miyoshi[1], Iku Shinohara[2] (1.Institute for Space-Earth Environmental Research, Nagoya University, 2.Japan Aerospace Exploration Agency, Institute of Space and Astronautical Science, 3.Japan Aerospace Exploration Agency, 4.Graduate School of Science, The University of Tokyo, 5.Graduate School of Science, Osaka University)

[PEM13-P28] Particle simulation for calibrating the HEP data onboard the ARASE satellite

*PARK INCHUN[1], Yoshizumi Miyoshi[1], Takefumi Mitani[2], Tomoaki Hori[1], Satoshi Kurita[1], Mariko Teramoto[1], Takeshi Takashima[2], Nana Higashio[3], Iku Shinohara[2] (1.Nagoya University Institute for Space-Earth Environmental Research, 2.Japan Aerospace Exploration Agency Institute of Space and Astronautical Science , 3.Japan Aerospace Exploration Agency)

[PEM13-P29] Geant4 model calculation and energetic particle observation with HEP/Arase in the inner radiation belt

*Honoka Toda[1], Wataru Miyake[1], Takefumi Mitani[3], Takeshi Takashima[3], Yoshizumi Miyoshi[2], PARK INCHUN[2], Tomoaki Hori[2] (1.Tokai University, 2.ISEE/Nagoya University, 3.ISAS/JAXA)

[PEM13-P30] Validation of High-energy electron detector simulator for the HEP instruments onboard Arase

*Takefumi Mitani[1], PARK INCHUN[2], Tomoaki Hori[2], Taku Namekawa[1,3], Kazushi Asamura[1], Takeshi Takashima[1], Satoshi Kasahara[3], Satoshi Kurita[2], Mariko Teramoto[2], Nana Higashio[1], Yoshizumi Miyoshi[2], Iku Shinohara[1] (1.Japan Aerospace Exploration Agency, Institute of Space and Astronautical Science, 2.Institute for Space-Earth Environmental Research, Nagoya Univ., 3.The university of Tokyo)

[E] Poster | P (Space and Planetary Sciences)：P-EM Solar-Terrestrial Sciences, Space Electromagnetism & Space Environment

5:15 PM - 6:30 PM JST | 8:15 AM - 9:30 AM UTC | Poster Hall International Exhibition Hall8, Makuhari Messe_6

[P-EM13] Inner magnetosphere: Recent understanding and new insights

convener:Yusuke Ebihara(Research Institute for Sustainable Humanosphere, Kyoto University), Danny Summers(Memorial University of Newfoundland), Yoshizumi Miyoshi(Institute for Space-Earth Environmental Research, Nagoya University), Shinji Saito(Graduate School of Science, Nagoya University)

[PEM13-P01] Evaluation of wave normal and Poynting vector analyses for whistler mode waves observed by the waveform capture (WFC) on board the Arase

*Yoshiya Kasahara[1], Satoshi Ikarashi[1], Hiroyuki Nishizawa[1], Shoya Matsuda[2], Fuminori Tsuchiya[3], Atsushi Kumamoto[3], Yasumasa Kasaba[3], Mitsunori Ozaki[1], Ayako Matsuoka[2] (1.Kanazawa University, 2.ISAS/JAXA, 3.Tohoku University)

[PEM13-P02] Calibration of electric fields dedicated to the measurement of the S-WPIA of the Arase Satellite

*Miki Jumpei[1], Hirotsugu Kojima[2], Yuto Katoh[3], Shoya Matsuda[4], Yoshiya Kasahara[5], Mitsuru Hikishima[4], Satoshi Kurita[6], Masahiro Kitahara[3], Satoshi Kasahara[7], Yoshizumi Miyoshi[6], Atsushi Kumamoto[3], Ayako Matsuoka[4], Shoichiro Yokota[8], Tomoaki Hori[6], Kunihiro Keika[7] (1.Space Radio Engineering Laboratory, Division of Electrical Engineering, Kyoto University Graduated School, 2.Research Institute for Sustainable Humanosphere, Kyoto University, 3.Graduate School of Science and Faculty of Science, Tohoku University, 4.Institute of Space and Astronautical Science, JAXA, 5.Information Media Center, Kanazawa University, 6.Institute for Space-Earth Environmental Research, Nagoya University, 7.School of Science, The University of Tokyo, 8.School of Science, Osaka University)

[PEM13-P03] Enhancement of whistler-mode chorus in association with Pc 4-5 ULF waves and related variation of high energy electrons

*Atsuhiro Ono[1], Yuto Katoh[1], Atsushi Kumamoto[1], Fuminori Tsuchiya[1], Mariko Teramoto[2], Yoshiya Kasahara[3], Shoya Matsuda[4], Ayako Matsuoka[4], Takefumi Mitani[4], Tomoaki Hori[2], Satoshi Kasahara[5], Shoichiro Yokota[6], Kunihiro Keika[5], Yoshizumi Miyoshi[2], Iku Shinohara[4] (1.Tohoku University, 2.Nagoya University, 3.Kanazawa University, 4.ISAS/JAXA, 5.The University of Tokyo, 6.Osaka University)

[PEM13-P04] Sudden enhancements of electron cyclotron harmonic waves observed by the Arase satellite

*Shinjo Airi[1], Hirotsugu Kojima[1], Yoshiya Kasahara[2], Yoichi Kazama[3], Hideyuki Usui[4], Yoshizumi Miyoshi[5], Yasumasa Kasaba[6], Shoya Matsuda[7], Tomoaki Hori[5], S. -Y. Wang[8], Sunny W.Y. Tam[9], Atsushi Kumamoto[10], Ayako Matsuoka[11] (1.Research institute for sustainable humanosphere, Kyoto University, 2.Information Media Center, Kanazawa University, 3.ASIAA, 4.Graduate school of system informatics Kobe University, 5.Institute for Space-Earth Environmental Research, Nagoya University, 6.Planetary Plasma and Atmospheric Research Center, Tohoku University, 7.Institute of Space and Astronautical Science/Japan Aerospace Exploration Agency, 8.ASIAA, Taiwan, 9.ISAPS, NCKU, Taiwan, 10.Department of Geophysics, Graduate School of Science, Tohoku University, 11.Research Division for Space Plasma, Institute of Space and Astronautical Science, Japan Aerospace Exploration Agency)

[PEM13-P05] Correlation between pulsating aurora and electrostatic electron cyclotron harmonic waves obtained from coordinated Arase and ground data

*Mizuki Fukizawa[1], Takeshi Sakanoi[1], Yoshizumi Miyoshi[2], Keisuke Hosokawa[3], Yoichi Kazama[4], Yoshiya Kasahara[5], Shoya Matsuda[6], Ayako Matsuoka[7], Wang Shiang-Yu[4], Sunny Wing-Yee Tam[8], Ryuho Kataoka[9] (1.Planetary Plasma and Atmospheric Research Center, Graduate School of Science, Tohoku University, 2.Institute for Space-Earth Environmental Research, Nagoya University, 3.Department of Communication Engineering and Informatics, University of Electro-Communications, 4.Academia Sinica Institute of Astronomy and Astrophysics, 5.Information Media Center, Kanazawa University, 6.Institute of Space and Astronautical Science/Japan Aerospace Exploration Agency, 7.Research Division for Space Plasma, Institute of Space and Astronautical Science, Japan Aerospace Exploration Agency, 8.Institute of Space and Plasma Sciences, College of Sciences, National Cheng Kung University , 9.National Institute of Polar Research)

[PEM13-P06] Automatic determination of Upper Hybrid Resonance Frequencies by Convolutional Neural Network.

*Shoya Matsuda[1], Tatsuhito Hasegawa[2], Atsushi Kumamoto[3], Fuminori Tsuchiya[3], Yoshiya Kasahara[4], Yoshizumi Miyoshi[5], Yasumasa Kasaba[3], Ayako Matsuoka[1] (1.Institute of Space and Astronautical Science/Japan Aerospace Exploration Agency, 2.University of Fukui, 3.Tohoku University, 4.Kanazawa University, 5.ISEE, Nagoya University)

[PEM13-P07] Amplitude dependence of whistler wave motion on electron scattering process

*Yoshiki Ito[1], Yoshizumi Miyoshi[1], Shinji Saito[1] (1.Nagoya University, ISEE)

[PEM13-P08] Two-dimensional simulation of whistler mode wave packets interacting with energetic electrons

*Takeshi Nogi[1], Yoshiharu Omura[1] (1.Reserch Institute for Sustainable Humanosphere, Kyoto University)

[PEM13-P09] Relativistic electron acceleration by whistler-mode chorus waves in 1D, 2D, and 3D magnetic field models.

*Keita Takahashi[1], Yoshiharu Omura[1], Yikai HSIEH[1], Danny Summers[2] (1.Research Institute for Sustainable Humanosphere, Kyoto University , 2.Department of Mathematics and Statistics, Memorial University of Newfoundland)

[PEM13-P10] Study of global spatio-temporal development of magnetospheric ELF/VLF waves for the 26-30 March 2017 storm based on ground and satellite observations and the RAM simulations

*Yuhei Takeshita[1], Kazuo Shiokawa[1], Yoshizumi Miyoshi[1], Mitsunori Ozaki[2], Yoshiya Kasahara[2], Martine Connors[3], Jyrki Manninen[4], Craig Kletzing[5], Vania Jordanova[6] (1.Nagoya University, Institute for Space-Earth Environmental Resarch, 2.Kanazawa University, 3.Athabasca University, 4.Sodankylä Geophysical Observatory, 5.The University of Iowa, 6.Los Alamos National Laboratory)

[PEM13-P11] Flux decrease of outer radiation belt electrons associated with solar wind pressure pulse: A Code coupling simulation of GEMSIS-RB and GEMSIS-GM

*Ito Hiroki[1], Yoshizumi Miyoshi[1], Shinji Saito[2], Yosuke Matsumoto[3], Takanobu Amano[4] (1.Institute for Space-Earth Environmental Research, Nagoya University, 2. Graduate School of Science, Nagoya University, 3. Graduate School of Science, Chiba University, 4.Department of Earth and Planetary Science, University of Tokyo)

[PEM13-P12] Non-diffusive response of outer belt electrons on interplanetary shock

Takuma Toishi[1], *Yusuke Ebihara[1], Takashi Tanaka[2] (1.Research Institute for Sustainable Humanosphere, Kyoto University, 2.Kyushu University)

[PEM13-P13] PARM: Initial result of the auroral camera on the G-CHASER (RockSat-XN) rocket and status of the development of auroral cameras for the LAMP rocket experiment

*Naoshi Yagi[1], Takeshi Sakanoi[1], Fukizawa Mizuki[1], Kazushi Asamura[2], Yoshizumi Miyoshi[3], Keisuke Hosokawa[4], Genki Ishizawa[5] (1.Planetary Plasma and Atmospheric Research Center, Graduate School of Science, Tohoku University, 2.Institute of Space and Astronautical Science, Japan Aerospace Exploration Agency, 3.Institute for Space-Earth Environmental Research, Nagoya University, 4.Department of Communication Engineering and Informatics, University of Electro-Communications, 5.Space & terrestrial plasma pyhsics)

[PEM13-P14] First simultaneous observation of a SAR arc at subauroral latitudes using a ground all-sky camera and the Arase satellite in the inner magnetosphere

*Yudai Inaba[1], Kazuo Shiokawa[1], Shin-ichiro Oyama[1,8,9], Yuichi Otsuka[1], Atsuki Shinbori[1], Yoichi Kazama[2], Shiang-Yu Wang[2], Sunny W. Y. Tam[2], Shoichiro Yokota[3], Satoshi Kasahara[4], Kunihiro Keika[4], Tomoaki Hori[1], Ayako Matsuoka[5], Yoshiya Kasahara[6], Atsushi Kumamoto[7], Yasumasa Kasaba[7], Yoshizumi Miyoshi[1], Iku Shinohara[5], Arto Oksanen[10] (1.Institute for Space-Earth Environmental Research, 2.Academia Sinica, 3.Osaka Univ, 4.Tokyo Univ, 5.JAXA, 6.Kanazawa University, 7.Tohoku University, 8.University of Oulu, Finland, 9.National Institute of Polar Research, 10.Jyväskylän Sirius ry, Finland)

[PEM13-P15] Pi2 pulsations observed by the Arase satellite inside and outside the plasmapause

*Mariko Teramoto[1], Ayako Matsuoka[2], Reiko Nomura[5], Yoshiya Kasahara[3], Yasumasa Kasaba[4], Atsushi Kumamoto[4], Fuminori Tsuchiya[4], Shoya Matsuda[2], Masahito Nose[1], Masafumi Shoji[1], Yasunori Tsugawa[1], Shun Imajo[1], Yoshizumi Miyoshi[1], Iku Shinohara[2] (1.Institute for Space-Earth Environmental Research Nagoya University, 2.Institute of Space and Astronautical Science, Japan Aerospace eXploration Agency, 3.Kanazawa University, 4.Tohoku University, 5.National Astronomical Observatory of Japan)

[PEM13-P16] An extreme erosion of the plasmasphere during the 7–10 September 2017 storm

*Yuki Obana[1], Naomi Maruyama[2,3], Atsuki Shinbori[4], Kumiko K. Hashimoto[5], Mariangel Fedrizzi[2,3], Masahito Nose[4], Yuichi Otsuka[4], Nozomu Nishitani[4], Tomoaki Hori[4], Atsushi Kumamoto[6], Fuminori Tsuchiya[6], Shoya Matsuda[7], Ayako Matsuoka[7], Yoshiya Kasahara[8], Akimasa Yoshikawa[9], Yoshizumi Miyoshi[4], Iku Shinohara[7] (1.Osaka Electro-Communication University, 2.University of Colorado Boulder, 3.NOAA Space Weather Prediction Center, 4.Nagoya

University, 5.Kibi International University, 6.Tohoku University, 7.Japan Aerospace Exploration Agency, 8.Kanazawa University, 9.Kyushu University)

[PEM13-P17] Relative contribution of ULF and chorus waves to the radiation belt variation: Comparison between multi-point observations and BATSRUS + CRCM simulation

*Naoko Takahashi[1], Kanako Seki[1], Mei-Ching Fok[2], Yihua Zheng[2], Yoshizumi Miyoshi[3], David Hartley[4], Ayako Matsuoka[5], Yoshiya Kasahara[6], Yasumasa Kasaba[7], Nana Higashio[8] (1.Graduate School of Science, University of Tokyo, 2.NASA Goddard Space Flight Center, 3.Institute for Space-Earth Environmental Research, Nagoya University, 4.Department of Physics and Astronomy, University of Iowa, 5.Institute of Space and Astronautical Science, Japan Aerospace Exploration Agency, 6.Information Media Center, Kanazawa University, 7.Planetary Plasma and Atmospheric Research Center, Tohoku University, 8.Japan Aerospace Exploration Agency)

[PEM13-P18] Modulation of the D-region ionosphere by Pc5 waves observed by VLF/LF standard radio waves

*Miyashita Takuya[1], Hiroyo Ohya[1], Fuminori Tsuchiya[2], Hiroyuki Nakata[1], Toshiaki Takano[1], Kazuo Shiokawa[3], Yoshizumi Miyoshi[3] (1.Chiba University, 2.Tohoku University, 3.Nagoya University)

[PEM13-P19] Oxygen-proton differences in ion energies dominating plasma pressure: Dependence on storm phases and solar wind drivers

*Kunihiro Keika[1], Satoshi Kasahara[1], Shoichiro Yokota[2], Masahiro Hoshino[1], Kanako Seki[1], Masahito Nose[3], Yoshizumi Miyoshi[3], Iku Shinohara[4] (1.Graduate School of Science, The University of Tokyo , 2.Graduate School of Science, Osaka University, 3.Institute for Space-Earth Environmental Research, Nagoya University, 4.Institute of Space and Astronautical Science, Japan Aerospace Exploration Agency)

[PEM13-P20] Mass dependence of penetration depth of multi-energy ions in the inner magnetosphere during magnetic storms: Arase observations

*Ryosuke Fujii[1], Yoshizumi Miyoshi[1], Masafumi Shoji[1], Kazushi Asamura[2], Lynn Kistler[1,8], Vania Jordanova[9], Tomoaki Hori[1], Satoshi Kurita[1], Mariko Teramoto[1], Yasunori Tsugawa[1], Yoshiya Kasahara[3], Yasumasa Kasaba[4], Atsushi Kumamoto[5], Fuminori Tsuchiya[4], Shoichiro Yokota[6], Kunihiro Keika[7], Ayako Matsuoka[2], Iku Shinohara[2] (1.Institute for Space-Earth Environmental Research, Nagoya University, 2.Institute of Space and Astronautical Science, Japan Aerospace Exploration Agency, 3.Information Media Center, Kanazawa University, 4.Planetary Plasma and Atmospheric Research Center, Tohoku University, 5.Department of Geophysics, Graduate School of Science, Tohoku University, 6.Graduate School of Science, Osaka University, 7.Department of Earth and Planetary Science, Graduate School of Science, The University of Tokyo, 8.University of New Hampshire, 9.Los Alamos National Laboratory)

[PEM13-P21] Relativistic Acceleration of Energetic Protons by Electromagnetic Ion Cyclotron Waves in the Jovian Magnetosphere

*Tomohiro Sekine[1], Yoshiharu Omura[1], Danny Summers[2], Yikai HSIEH[1], Satoko Nakamura[1] (1.Reserach Institute for Sustainable Humanosphere, Kyoto University, 2.Memorial University of Newfoundland)

[PEM13-P22] Statistical study of IPDP type EMIC wave-related electron precipitation at subauroral latitude

*Asuka Hirai[1], Fuminori Tsuchiya[1], Takahiro Obara[1], Yasumasa Kasaba[1], Yuto Katoh[2], Hiroaki Misawa[1], Kazuo Shiokawa[3], Yoshizumi Miyoshi[3], Satoshi Kurita[3], Martin G Connors[4] (1.Planetary Plasma and Atmospheric Research Center, Graduate School of Science, Tohoku Univ. , 2.Department of Geophysics, Graduate School of Science, Tohoku University, 3.Institute for Space-Earth Environmental Research, Nagoya University, 4.Athabasca University)

[PEM13-P23] Meridional distributions of proton plasma and pressure-driven currents in the nightside inner magnetosphere: Arase observations

*Shun Imajo[1], Masahito Nose[1], Satoshi Kasahara[2], Shoichiro Yokota[3], Ayako Matsuoka[4], Kunihiro Keika[2], Tomoaki Hori[1], Mariko Teramoto[1], Kazuhiro Yamamoto[5], Oimatsu Satoshi[5], Reiko Nomura[6], Akiko Fujimoto[7], Iku Shinohara[4], Yoshizumi Miyoshi[1] (1.Institute for Space-Earth Environmental Research, Nagoya University, 2.Graduate School of Science, The University of Tokyo, 3.Graduate School of Science, Osaka University, 4.Institute of Space and Astronautical Science, Japan Aerospace Exploration Agency, 5.Graduate School of Science, Kyoto University, 6.National Astronomical Observatory of Japan, 7.Kyushu Institute of Technology)

[PEM13-P24] Space Weather Effects on Energetic Proton Flux Response in South Atlantic Anomaly

*Kirolosse Mina GIRGIS[1,2], Tohru Hada[1], Shuichi Matsukiyo[1] (1.Earth System Science and Technology (ESST) Department, Interdisciplinary Graduate School of Engineering Sciences (IGSES), Kyushu University, Japan, 2.Aerospace Engineering Department, Faculty of Engineering, Cairo University, Egypt)

[PEM13-P25] Solar-cycle variations of >30 keV electron flux enhancements under the inner radiation belt

*ALLA SUVOROVA[1] (1.National Central University)

[PEM13-P26] Energy spectra variations of high energy electrons in the inner magnetosphere observed by HEP/XEP on ARASE and SEDA-e on HIMAWARI

*Takeshi Takashima[1], Takefumi Mitani[1], Nana Higashio[2], Tsutomu Nagatsuma[3] (1. ISAS/JAXA, 2.Research and Development Directorate/JAXA, 3.NiCT)

[PEM13-P27] Inter-channel calibration of the high-energy electron experiments (HEP) instrument onboard the Arase satellite

*Tomoaki Hori[1], Takefumi Mitani[2], Takeshi Takashima[2], Park Inchun[1], Satoshi Kurita[1], Mariko Teramoto[1], Nana Higashio[3], Satoshi Kasahara[4], Shoichiro Yokota[5], Yoshizumi Miyoshi[1], Iku Shinohara[2] (1.Institute for Space-Earth Environmental Research, Nagoya University, 2.Japan Aerospace Exploration Agency, Institute of Space and Astronautical Science, 3.Japan Aerospace Exploration Agency, 4.Graduate School of Science, The University of Tokyo, 5.Graduate School of Science, Osaka University)

[PEM13-P28] Particle simulation for calibrating the HEP data onboard the ARASE satellite

*PARK INCHUN[1], Yoshizumi Miyoshi[1], Takefumi Mitani[2], Tomoaki Hori[1], Satoshi Kurita[1], Mariko Teramoto[1], Takeshi Takashima[2], Nana Higashio[3], Iku Shinohara[2] (1.Nagoya University Institute for Space-Earth Environmental Research, 2.Japan Aerospace Exploration Agency Institute of Space and Astronautical Science , 3.Japan Aerospace Exploration Agency)

[PEM13-P29] Geant4 model calculation and energetic particle observation with HEP/Arase in the inner radiation belt

*Honoka Toda[1], Wataru Miyake[1], Takefumi Mitani[3], Takeshi Takashima[3], Yoshizumi Miyoshi[2], PARK INCHUN[2], Tomoaki Hori[2] (1.Tokai University, 2.ISEE/Nagoya University, 3.ISAS/JAXA)

[PEM13-P30] Validation of High-energy electron detector simulator for the HEP instruments onboard Arase

*Takefumi Mitani[1], PARK INCHUN[2], Tomoaki Hori[2], Taku Namekawa[1,3], Kazushi Asamura[1], Takeshi Takashima[1], Satoshi Kasahara[3], Satoshi Kurita[2], Mariko Teramoto[2], Nana Higashio[1], Yoshizumi Miyoshi[2], Iku Shinohara[1] (1.Japan Aerospace Exploration Agency, Institute of Space and Astronautical Science, 2.Institute for Space-Earth Environmental Research, Nagoya Univ., 3.The university of Tokyo)

[E] Poster | A (Atmospheric and Hydrospheric Sciences)：A-AS Atmospheric Sciences, Meteorology & Atmospheric Environment

3:30 PM - 5:00 PM JST | 6:30 AM - 8:00 AM UTC | Poster Hall International Exhibition Hall8, Makuhari Messe_5

[A-AS01] High performance computing for next generation weather, climate, and environmental sc iences

convener:Hiromu Seko(Meteorological Research Institute), Takemasa Miyoshi(RIKEN), Chihiro Kodama(Japan Agency for Marine-Earth Science and Technology), Masayuki Takigawa(Japan Agency for Marine-Earth Science and Technology)

[AAS01-P01] **Categorized correction forecast for accumulative precipitation of heavy rainfall processes based on optimal probability (OPPF) in medium-extended-range forecast time**

*Ruoyun Niu[1] (1.National Meteorological Center)

[AAS01-P02] **Characteristics of temporal and spatial distribution of regional rainstorm processes to the east of 95°E in China during 1981-2015**

*Ruoyun Niu[1], Couhua Liu[1] (1.National Meteorological Center)

[AAS01-P03] Near-real-time SCALE-LETKF forecasts of the record breaking rainfall in Japan in July 2018

*Takumi Honda[1], Guo-Yuan Lien[2,1], Takemasa Miyoshi[1] (1.RIKEN Center for Computational Science, 2.Central Weather Bureau)

[AAS01-P04] An objective Frontal Analysis Techniques and Application in Model Verification

*couhua liu[1] (1.National Meteorology Centre of China Meteorological Administration)

[AAS01-P05] Assimilating every 30-second phased array weather radar data in a torrential rainfall event on July 6, 2018 around Kobe city

*Yasumitsu Maejima[1], Shigenori Otsuka[1], Takemasa Miyoshi[1,2] (1.RIKEN Center for Computational Science, 2.University of Maryland, College Park)

[AAS01-P06] The impact of range sidelobes from phased array weather radar observations to short-range convective forecasts

*James David Taylor[1], Guo-Yuan Lien[1], Shinsuke Satoh[2], Takemasa Miyoshi[1] (1.RIKEN Research center for computational science, 2.NICT National Institute of Information and Communications Technology)

[AAS01-P07] Development of Hydro-debris 2D model for larger area

*Yosuke Alexandre Yamashiki[1], Tsutao OIZUMI[2], Bruno Ribeiro[1], Ryusuke Kuroki[1] (1.Earth & Planetary Water Resources Assessment Laboratory Graduate School of Advanced Integrated Studies in Human Survivability Kyoto University, 2.Japan Association of Marine-Earth Science and Tecnology)

[AAS01-P08] **Research on the application of an improved terrain-following vertical coordinates on GRAPES model**

*chao li[1] (1.NWPC.CMA)

[AAS01-P09] Development of a parallel spherical harmonic transform library: design and performance

*Fuyuki SAITO[1] (1.Japan Agency for Marine-Earth Science and Technology)

[AAS01-P10] Global data assimilation of multi-species satellite measurements for atmospheric chemistry analysis

*Takashi Sekiya[1], Kazuyuki Miyazaki[2,1], Koji Ogochi[1], Kengo Sudo[3,1], Masayuki Takigawa[1] (1.Japan Agency for Marine-Earth Science and Technology, 2.Jet Propulsion Laboratory/California Institute for Technology, 3.Graduate School of Environmental Studies, Nagoya University)

[AAS01-P11] The sensitivity to WRF shortwave radiation parameterizations in prediction of global horizontal irradiance for investigating interactions of atmosphere with croplands

*Ankur Srivastava[1], Sarita Kumari[1], Rajkumar Dhakar[2] (1.Indian Institute of Technology Delhi, 2.Indian Agriculture Research Institute)

[AAS01-P12] The development of an atmospheric aerosol/chemistry–climate model, BCC_AGCM_CUACE2.0, and simulated effective radiative forcing of nitrate aerosols

*QI AN[1,2,4], Hua Zhang[2], Zhili Wang[2], Yi Liu[1,4], Bing Xie[3], Qianxia Liu[3], Zaizhi Wang[3], Sunling Gong[2] (1.LAGEO, IAP, CAS, 2.LaSW, CAMS, 3.NCC,CMA, 4.UCAS)

[AAS01-P13] **Impacts of different types and intensities of El Niño events on winter aerosols over China**

*Xiaochao Yu[1,2], Zhili Wang[2,1], Hua Zhang[2], Shuyun Zhao[3] (1.Collaborative Innovation Center on Forecast and Evaluation of Meteorological Disasters, Nanjing University of Information Science and Technology, Nanjing, 210044, China, 2.State Key Laboratory of Severe Weather and Key Laboratory of Atmospheric Chemistry of CMA, Chinese Academy of Meteorological Sciences, Beijing, 100081, China., 3.National Climate Center, China Meteorological Administration, Beijing, 100081, China)

[AAS01-P14] High Cloud Annual Variation and Its Responses to Global Warming in the NICAM AMIP Experiment

*Ying-Wen Chen[1], Masaki Satoh[1,2], Chihiro Kodama[2], Akira Noda[2], Yohei Yamada[2] (1.Atmospheric and Ocean Research Institute, The University of Tokyo , 2.Japan Agency for Marine-Earth Science and Technology)

[AAS01-P15] Improvements in Simulating the Relationship between ENSO and East Asian Summer Rainfall in the CMIP5 Models

*Yuanhai FU[1], Riyu Lu[1] (1.IAP, CAS)

[E] Poster | A (Atmospheric and Hydrospheric Sciences)：A-AS Atmospheric Sciences, Meteorology & Atmospheric Environment

5:15 PM - 6:30 PM JST | 8:15 AM - 9:30 AM UTC | Poster Hall International Exhibition Hall8, Makuhari Messe_9

[A-AS01] High performance computing for next generation weather, climate, and environmental sc iences

convener:Hiromu Seko(Meteorological Research Institute), Takemasa Miyoshi(RIKEN), Chihiro Kodama(Japan Agency for Marine-Earth Science and Technology), Masayuki Takigawa(Japan Agency for Marine-Earth Science and Technology)

[AAS01-P01] **Categorized correction forecast for accumulative precipitation of heavy rainfall processes based on optimal probability (OPPF) in medium-extended-range forecast time**

*Ruoyun Niu[1] (1.National Meteorological Center)

[AAS01-P02] **Characteristics of temporal and spatial distribution of regional rainstorm processes to the east of 95°E in China during 1981-2015**

*Ruoyun Niu[1], Couhua Liu[1] (1.National Meteorological Center)

[AAS01-P03] Near-real-time SCALE-LETKF forecasts of the record breaking rainfall in Japan in July 2018

*Takumi Honda[1], Guo-Yuan Lien[2,1], Takemasa Miyoshi[1] (1.RIKEN Center for Computational Science, 2.Central Weather Bureau)

[AAS01-P04] An objective Frontal Analysis Techniques and Application in Model Verification

*couhua liu[1] (1.National Meteorology Centre of China Meteorological Administration)

[AAS01-P05] Assimilating every 30-second phased array weather radar data in a torrential rainfall event on July 6, 2018 around Kobe city

*Yasumitsu Maejima[1], Shigenori Otsuka[1], Takemasa Miyoshi[1,2] (1.RIKEN Center for Computational Science, 2.University of Maryland, College Park)

[AAS01-P06] The impact of range sidelobes from phased array weather radar observations to short-range convective forecasts

*James David Taylor[1], Guo-Yuan Lien[1], Shinsuke Satoh[2], Takemasa Miyoshi[1] (1.RIKEN Research center for computational science, 2.NICT National Institute of Information and Communications Technology)

[AAS01-P07] Development of Hydro-debris 2D model for larger area

*Yosuke Alexandre Yamashiki[1], Tsutao OIZUMI[2], Bruno Ribeiro[1], Ryusuke Kuroki[1] (1.Earth & Planetary Water Resources Assessment Laboratory Graduate School of Advanced Integrated Studies in Human Survivability Kyoto University, 2.Japan Association of Marine-Earth Science and Tecnology)

[AAS01-P08] **Research on the application of an improved terrain-following vertical coordinates on GRAPES model**

*chao li[1] (1.NWPC.CMA)

[AAS01-P09] Development of a parallel spherical harmonic transform library: design and performance

*Fuyuki SAITO[1] (1.Japan Agency for Marine-Earth Science and Technology)

[AAS01-P10] Global data assimilation of multi-species satellite measurements for atmospheric chemistry analysis

*Takashi Sekiya[1], Kazuyuki Miyazaki[2,1], Koji Ogochi[1], Kengo Sudo[3,1], Masayuki Takigawa[1] (1.Japan Agency for Marine-Earth Science and Technology, 2.Jet Propulsion Laboratory/California Institute for Technology, 3.Graduate School of Environmental Studies, Nagoya University)

[AAS01-P11] The sensitivity to WRF shortwave radiation parameterizations in prediction of global horizontal irradiance for investigating interactions of atmosphere with croplands

*Ankur Srivastava[1], Sarita Kumari[1], Rajkumar Dhakar[2] (1.Indian Institute of Technology Delhi, 2.Indian Agriculture Research Institute)

[AAS01-P12] The development of an atmospheric aerosol/chemistry–climate model, BCC_AGCM_CUACE2.0, and simulated effective radiative forcing of nitrate aerosols

*QI AN[1,2,4], Hua Zhang[2], Zhili Wang[2], Yi Liu[1,4], Bing Xie[3], Qianxia Liu[3], Zaizhi Wang[3], Sunling Gong[2] (1.LAGEO, IAP, CAS, 2.LaSW, CAMS, 3.NCC,CMA, 4.UCAS)

[AAS01-P13] **Impacts of different types and intensities of El Niño events on winter aerosols over China**

*Xiaochao Yu[1,2], Zhili Wang[2,1], Hua Zhang[2], Shuyun Zhao[3] (1.Collaborative Innovation Center on Forecast and Evaluation of Meteorological Disasters, Nanjing University of Information Science and Technology, Nanjing, 210044, China, 2.State Key Laboratory of Severe Weather and Key Laboratory of Atmospheric Chemistry of CMA, Chinese Academy of Meteorological Sciences, Beijing, 100081, China., 3.National Climate Center, China Meteorological Administration, Beijing, 100081, China)

[AAS01-P14] High Cloud Annual Variation and Its Responses to Global Warming in the NICAM AMIP Experiment

*Ying-Wen Chen[1], Masaki Satoh[1,2], Chihiro Kodama[2], Akira Noda[2], Yohei Yamada[2] (1.Atmospheric and Ocean Research Institute, The University of Tokyo , 2.Japan Agency for Marine-Earth Science and Technology)

[AAS01-P15] Improvements in Simulating the Relationship between ENSO and East Asian Summer Rainfall in the CMIP5 Models

*Yuanhai FU[1], Riyu Lu[1] (1.IAP, CAS)

[E] Poster | A (Atmospheric and Hydrospheric Sciences)：A-OS Ocean Sciences & Ocean Environment

10:45 AM - 12:15 PM JST | 1:45 AM - 3:15 AM UTC | Poster Hall International Exhibition Hall8, Makuhari Messe_4

[A-OS08] ECS-Kuroshio and Ryukyu Current System -Observation, modeling and theory-

convener:Hirohiko Nakamura(Kagoshima University, Faculy of Fisheries), Xiao-Hua Zhu(Second Institute of Oceanography)

[AOS08-P01] **Impact of the mesosacle eddies on the western boundary current over the entire western North Pacific**

*Kako Shinichiro[1], Hirohiko Nakamura[2] (1.Graduate School of Science and Engineering, Kagoshima University, 2.Faculty of Fisheries, Kagoshima University)

[AOS08-P02] Glider observations of interleaving layers in the Kuroshio

*Sen Jan[1], Shih-Hong Wang[1], Kai-Chieh Yang[1], Yiing Jang Yang[1], Ming-Huei Chang[1] (1.Institute of Oceanography, National Taiwan Univ.)

[AOS08-P03] Bottom Pressure in the East China Sea -Observation and modeling

*Hua Zheng[1], Xiao-Hua Zhu[1], Hirohiko Nakamura[2], Jae-Hun Park[3], Chanhyung Jeon[4], Ruixiang Zhao[1], Ayako Nishina[2], Chuanzheng Zhang[1], Hanna Na[5], Ze-Nan Zhu[1], Hong Sik Min[6] (1.Second Institute of Oceanography, Ministry of Natural Resources, China, 2.Faculty of Fisheries, Kagoshima University, Kagoshima, Japan, 3.Department of Ocean Sciences, Inha University, Incheon, South Kore, 4.Department of Marine Science and Biological Engineering, Inha University, Incheon, Korea, 5.School of Earth and Environmental Sciences, Seoul National University, Seoul, Korea, 6.Ocean Circulation and Climate Research Center, Korea Institute of Ocean Science and Technology, Busan, Korea)

[AOS08-P04] A numerical study on the dynamics of seasonal velocity variation in the East China Sea

*ZHENLONG ZHANG[1], Nakamura Hirohiko[1], Xiao-Hua Zhu[2] (1.Kagoshima University, 2.Ministry of Natural Resources, CHINA.)

[AOS08-P05] Temporal and spatial velocity variations over the Kuroshio Extension, Kuroshio and Ryukyu Current System in 1982-2014

*YUXIANG QIAO[1], Hirohiko Nakamura[2], AYAKO NISHINA[2] (1.Kagoshima University, Graduate School of Fisheries, 2.Kagoshima University, Faculty of Fishries)

[AOS08-P06] Characteristics of water in the southern Okinawa Trough.

*Ayako Nishina[1], Hirohiko Nakamura[1], Jae-Hun Park[2], Xiao-Hua Zhu[3], Hong Sik Min[4], Hanna Na[5] (1.Kagoshima University, 2.Inha University, 3.Second Institute of Oceanography, 4.Korea Institute of Ocean Science and Technology, 5.Seoul National University)

[E] Poster | A (Atmospheric and Hydrospheric Sciences)：A-OS Ocean Sciences & Ocean Environment

5:15 PM - 6:30 PM JST | 8:15 AM - 9:30 AM UTC | Poster Hall International Exhibition Hall8, Makuhari Messe_11

[A-OS08] ECS-Kuroshio and Ryukyu Current System -Observation, modeling and theory-

convener:Hirohiko Nakamura(Kagoshima University, Faculy of Fisheries), Xiao-Hua Zhu(Second Institute of Oceanography)

[AOS08-P01] Impact of the mesosacle eddies on the western boundary current over the entire western North Pacific

*Kako Shinichiro[1], Hirohiko Nakamura[2] (1.Graduate School of Science and Engineering, Kagoshima University, 2.Faculty of Fisheries, Kagoshima University)

[AOS08-P02] Glider observations of interleaving layers in the Kuroshio

*Sen Jan[1], Shih-Hong Wang[1], Kai-Chieh Yang[1], Yiing Jang Yang[1], Ming-Huei Chang[1] (1.Institute of Oceanography, National Taiwan Univ.)

[AOS08-P03] Bottom Pressure in the East China Sea -Observation and modeling

*Hua Zheng[1], Xiao-Hua Zhu[1], Hirohiko Nakamura[2], Jae-Hun Park[3], Chanhyung Jeon[4], Ruixiang Zhao[1], Ayako Nishina[2], Chuanzheng Zhang[1], Hanna Na[5], Ze-Nan Zhu[1], Hong Sik Min[6] (1.Second Institute of Oceanography, Ministry of Natural Resources, China, 2.Faculty of Fisheries, Kagoshima University, Kagoshima, Japan, 3.Department of Ocean Sciences, Inha University, Incheon, South Kore, 4.Department of Marine Science and Biological Engineering, Inha University, Incheon, Korea, 5.School of Earth and Environmental Sciences, Seoul National University, Seoul, Korea, 6.Ocean Circulation and Climate Research Center, Korea Institute of Ocean Science and Technology, Busan, Korea)

[AOS08-P04] A numerical study on the dynamics of seasonal velocity variation in the East China Sea

*ZHENLONG ZHANG[1], Nakamura Hirohiko[1], Xiao-Hua Zhu[2] (1.Kagoshima University, 2.Ministry of Natural Resources, CHINA.)

[AOS08-P05] Temporal and spatial velocity variations over the Kuroshio Extension, Kuroshio and Ryukyu Current System in 1982-2014

*YUXIANG QIAO[1], Hirohiko Nakamura[2], AYAKO NISHINA[2] (1.Kagoshima University, Graduate School of Fisheries, 2.Kagoshima University, Faculty of Fishries)

[AOS08-P06] Characteristics of water in the southern Okinawa Trough.

*Ayako Nishina[1], Hirohiko Nakamura[1], Jae-Hun Park[2], Xiao-Hua Zhu[3], Hong Sik Min[4], Hanna Na[5] (1.Kagoshima University, 2.Inha University, 3.Second Institute of Oceanography, 4.Korea Institute of Ocean Science and Technology, 5.Seoul National University)

[E] Poster | A (Atmospheric and Hydrospheric Sciences)：A-OS Ocean Sciences & Ocean Environment

3:30 PM - 5:00 PM JST | 6:30 AM - 8:00 AM UTC | Poster Hall International Exhibition Hall8, Makuhari Messe_7

[A-OS11] Continental-Oceanic Mutual Interaction: Planetary scale Material Circulation

convener:Yosuke Alexandre Yamashiki(Earth & Planetary Water Resources Assessment Laboratory Graduate School of Advanced Integrated Studies in Human Survivability Kyoto University), Yukio Masumoto(Graduate School of Science, The University of Tokyo), Swadhin Behera(Climate Variation Predictability and Applicability Research Group, Application Laboratory, JAMSTEC, 3173-25 Showa-machi, Yokohama 236-0001), Takanori Sasaki(Department of Astronomy, Kyoto University)

[AOS11-P01] Remote Sensing of Chlorophyll-a and Submerged Aquatic Vegetation for a Freshwater Lake in Japan

*Shweta Yadav[1], Yamashiki Yosuke[1], Junichi Susaki[1], Kanako Ishikawa[2] (1.Kyoto University, 2.Lake Biwa Environmental Research Institute)

[AOS11-P02] Hydrological and Debris-flow simulation of Martian Surface in Hesperian & early Amazonian epoch

*Hiroaki Sato[2], Yosuke Alexandre Yamashiki[1], Ryusuke Kuroki[1], Hideaki Miyamoto[3], Ryodo Hemmi[3] (1.Earth & Planetary Water Resources Assessment Laboratory Graduate School of Advanced Integrated Studies in Human Survivability Kyoto University, 2.Faculty of Engineering, Kyoto University, 3.Graduate School of Engineering, The University of Tokyo)

[AOS11-P03] Global Lakes & reservoirs Repository and their application for terrestrial surface environment

*Yosuke Alexandre Yamashiki[1], Ryusuke Kuroki[1], Botong Gao[1], Hina Bando[2], Fuka Takagi[3], Shweta Yadav[4] (1.Earth & Planetary Water Resources Assessment Laboratory Graduate School of Advanced Integrated Studies in Human Survivability Kyoto University, 2.Faculty of Science, Kyoto University, 3.Faculty of Agriculture, Kyoto University, 4.Educational Unit for Studies on Connectivity of Hills, Humans and Ocean, Kyoto University)

[AOS11-P04] Numerical simulation of Tidal Heating using SPH and its application to inner sea formation

*keiya murashima[1], Yosuke Alexandre Yamashiki[1], Natsuki Hosono[2] (1.Kyoto University, 2.Japan Agency for Marine-Earth Science and Technology)

[E] Poster | A (Atmospheric and Hydrospheric Sciences)：A-OS Ocean Sciences & Ocean Environment

5:15 PM - 6:30 PM JST | 8:15 AM - 9:30 AM UTC | Poster Hall International Exhibition Hall8, Makuhari Messe_12

[A-OS11] Continental-Oceanic Mutual Interaction: Planetary scale Material Circulation

convener:Yosuke Alexandre Yamashiki(Earth & Planetary Water Resources Assessment Laboratory Graduate School of Advanced Integrated Studies in Human Survivability Kyoto University), Yukio Masumoto(Graduate School of Science, The University of Tokyo), Swadhin Behera(Climate Variation Predictability and Applicability Research Group, Application Laboratory, JAMSTEC, 3173-25 Showa-machi, Yokohama 236-0001), Takanori Sasaki(Department of Astronomy, Kyoto University)

[AOS11-P01] Remote Sensing of Chlorophyll-a and Submerged Aquatic Vegetation for a Freshwater Lake in Japan

*Shweta Yadav[1], Yamashiki Yosuke[1], Junichi Susaki[1], Kanako Ishikawa[2] (1.Kyoto University, 2.Lake Biwa Environmental Research Institute)

[AOS11-P02] Hydrological and Debris-flow simulation of Martian Surface in Hesperian & early Amazonian epoch

*Hiroaki Sato[2], Yosuke Alexandre Yamashiki[1], Ryusuke Kuroki[1], Hideaki Miyamoto[3], Ryodo Hemmi[3] (1.Earth & Planetary Water Resources Assessment Laboratory Graduate School of Advanced Integrated Studies in Human Survivability Kyoto University, 2.Faculty of Engineering, Kyoto University, 3.Graduate School of Engineering, The University of Tokyo)

[AOS11-P03] Global Lakes & reservoirs Repository and their application for terrestrial surface environment

*Yosuke Alexandre Yamashiki[1], Ryusuke Kuroki[1], Botong Gao[1], Hina Bando[2], Fuka Takagi[3], Shweta Yadav[4] (1.Earth & Planetary Water Resources Assessment Laboratory Graduate School of Advanced Integrated Studies in Human Survivability Kyoto University, 2.Faculty of Science, Kyoto University, 3.Faculty of Agriculture, Kyoto University, 4.Educational Unit for Studies on Connectivity of Hills, Humans and Ocean, Kyoto University)

[AOS11-P04] Numerical simulation of Tidal Heating using SPH and its application to inner sea formation

*keiya murashima[1], Yosuke Alexandre Yamashiki[1], Natsuki Hosono[2] (1.Kyoto University, 2.Japan Agency for Marine-Earth Science and Technology)

[E] Poster | A (Atmospheric and Hydrospheric Sciences)：A-HW Hydrology & Water Environment

3:30 PM - 5:00 PM JST | 6:30 AM - 8:00 AM UTC | Poster Hall International Exhibition Hall8, Makuhari Messe_8

[A-HW23] Hydrology & Water Environment

convener:Isao Machida(Geological Survey of Japan), Dai Yamazaki(Institute of Industrial Sciences, The University of Tokyo), Takeshi Hayashi(Faculty of Education and Human Studies, Akita University), Keisuke Fukushi(Institute of Nature & Environmental Technology, Kanazawa University)

[AHW23-P01] **A multiobjective risk management model for real-time reservoir flood control operation**

*Juan Chen[1,2], Ping-An Zhong[2], XinYu Wan[2], Yu Zhang[2] (1.College of Earth Sciences and Engineering, Hohai University, 2.College of Hydrology and Water Resources, Hohai University)

[AHW23-P02] **Assessment of the Flow Regime of Roanoke River due to Climatic and Anthropogenic Activities**

*Rahul Kumar Singh[1], Dr. Manoj Kumar Jain[1] (1.Indian Institute of Technology, Roorkee, India)

[AHW23-P03] Predictive Analysis of Climate, Water, Health and the Environment Nexus

*Abhishek [1], Deepika [2] (1.Technical University Dresden, GERMANY, 2.BPS Government Medical College for Women, Sonepat, INDIA)

[AHW23-P05] Severe droughts provide huge fuel for widespread wildfires in California in USA

*Linghua Qiu[1], Ji Chen[1], Haiyun Shi[2], Liqun Sun[3], Jun Niu[4] (1.the University of Hong Kong, 2.Southern University of Science and Technology, 3.Shenzhen Institutes of Advanced Technology, Chinese Academy of Sciences, 4.China Agricultural University)

[AHW23-P06] A comprehensive evaluation of MODIS-based water use efficiency with global eddy covariance flux data and a process model

*Shanshan YANG[1,2], Jiahua ZHANG[1], Sha ZHANG[1,2], Jingwen WANG[1,2], Yun BAI[1,2], Fengmei YAO[2], Huadong GUO[1] (1.Institute of Remote Sensing and Digital Earth, Chinese Academy of Sciences, 2.University of Chinese Academy of Sciences, Beijing, China)

[AHW23-P07] Impact of variability and anisotropy in the correlation decay distance for precipitation spatial interpolation in China

*yingxian zhang[1] (1.National Climate Center, China Meteorological Administration)

[AHW23-P08] New Record-Breaking Frequency of Annual Maximum Daily Precipitation of 58 stations in the whole Japan, an increasing of extreme values.

*Chhay Ngorn SEANG[1], Tomohito YAMADA[1] (1.Hokkaido University)

[AHW23-P09] Quantifying stemflow to better express its ecohydrological significance

*Shin'ichi Iida[1], Darryl E. Carlye-Moses[2], Sonja Germer[3], Pilar Llorens[4], Beate Michalzik[5], Kazuki Nanko[1], Alexander Tischer[5], Delphis F. Levia[6] (1.Department of Disaster Prevention, Meteorology and Hydrology, Forestry and Forest Products Research Institute, 2.Department of Geography and Environmental Studies, Thompson Rivers University, Kamloops, British Columbia, Canada, 3.Department of Bioengineering, Leibniz Institute for Agricultural Engineering and Bioeconomy, Potsdam, Germany, 4.Institute of Environmental Assessment and Water Research (IDAEA-CSIC), Barcelona, Spain, 5.Soil Science, Institute of Geography, Friedrich Schiller University Jena, Jena, Germany, 6.Department of Geography and Department of Plant and Soil Sciences, University of Delaware, Newark, DE, USA)

[AHW23-P10] **Hydraulic analysis of overland flow caused by temporally varying rainfall**

*PING-CHENG HSIEH[1], Ming-Chang Wu[1] (1.National Chung Hsing University)

[AHW23-P11] A comparative Study on Water Environment of Isolated Islands - Focusing on Islands in Nagasaki Prefecture - (3)

*Go Yamaki[1], Koji Kodera[2], Kazuki Asami[1], Yoshihiro IGARI[1], Masaki Horiuchi[1] (1.Grad. Student, Hosei Univ., 2.Dep. of Geography, Hosei Univ.)

[AHW23-P12] **Water environment around Kusatsu-Shirane volcano and consideration of the effect of eruption in January 2018**

*Igari Yoshihiro[1], Koji Kodera[2], Kazuki Asami[1] (1.Grad.Student,Hosei Univ., 2.Dep.of Geography Hosei Univ.)

[AHW23-P13] Re-consideration of discharge rate of spring water in Lake Ezu, Kumamoto

*Kimpei Ichiyanagi[1], Kiyoshi Ide[1], Jun Shimada[1], Tsutomu Ichikawa[2] (1.Kumamoto University, 2.Tokai University)

[AHW23-P14] **Evaluating the efficacy of hydrologically and hydrodynamically driven methods of e-flow assessment for Upper Godavari River Basin, India**

*GAURAV KALIDAS PAKHALE[1], Jyoti Punjahari Nale[2], Ashvin Kumar Gosain[3], Rakesh Khosa[3] (1.PhD Research Scholar, Civil Engineering Department, Indian Institute of Technology, Delhi, 2.Project Advisor, IEWP, GIZ India, New Delhi, India, 3.Professor, Civil Engineering Department, Indian Institute of Technology, Delhi)

[AHW23-P15] Presence of pharmaceutical compounds in freshwater lakes and their impact on phytoplankton

*Nandakumar Kanavillil[1], Cassandra Fligg[1], Sreekumari Kurissery[1] (1.Lakehead University, Canada)

[AHW23-P16] **Novel approximate solutions for solute transport due to injections: considering the scale-dependent dispersion and non-integer flow dimension**

*Ye-Chen Lin[1], Hund-Der Yeh[1] (1.National Chiao Tung Univ.)

[AHW23-P17] Experimemtal study on the residual saturation of Porous Media using Pore Doublets Micromodel

*Chun-Wei Peng[1] (1.Taiwan National Chiao Tung University)

[AHW23-P18] Assessment of Synergy between Biomedical Waste and Shallow Groundwater Pollution

*Deepika [1], Abhishek [2] (1.BPS Government Medical College for Women, Sonepat, INDIA, 2.Technical University Dresden, GERMANY)

[AHW23-P19] Erosion and transport processes of earth surface materials in a reservoir-catchment system inferred from atmospheric radionuclides ^{7}Be and ^{210}Pb

*Mikiya Tsuruoka[1], Shinya Ochiai[2], Atsushi Matsuki[2], Seiya Nagao[2] (1.Graduate School of Natural Science and Technology, Kanazawa University, 2.Institute of Nature and Environmental Technology, Kanazawa University)

[AHW23-P20] Fluctuation of groundwater level in a sloping unconfined aquifer due to time varying recharge

*Ming-Chang Wu[1], Ping-Cheng Hsieh[1] (1.National Chung Hsing University)

[AHW23-P21] **Effect of cutoff wall on recharge water storage volume**

*Pei-hsun Tsai[1], Jung-hsing Tai[1] (1.Chaoyang University of Technology)

[AHW23-P22] **Studying Operation Parameters on Flat-Plate Membrane Bioreactor for Sewage Treatment**

*Jen Hung Chiu[1], Wen Chin Chen[1] (1.Studying Operation Parameters on Flat-Plate Membrane Bioreactor for Sewage Treatment)

[AHW23-P23] **Mine-water quality at a tertiary coalfield in India: Characterisation and treatment using novel polyvinyl alcohol (PVA) gel bioreactor**

*Aparna Dutta[1], Sudipta Sarkar[1] (1.Indian Institute of Technology Roorkee)

[E] Poster | A (Atmospheric and Hydrospheric Sciences)：A-HW Hydrology & Water Environment

5:15 PM - 6:30 PM JST | 8:15 AM - 9:30 AM UTC | Poster Hall International Exhibition Hall8, Makuhari Messe_14

[A-HW23] Hydrology & Water Environment

convener:Isao Machida(Geological Survey of Japan), Dai Yamazaki(Institute of Industrial Sciences, The University of Tokyo), Takeshi Hayashi(Faculty of Education and Human Studies, Akita University), Keisuke Fukushi(Institute of Nature & Environmental Technology, Kanazawa University)

[AHW23-P01] **A multiobjective risk management model for real-time reservoir flood control operation**

*Juan Chen[1,2], Ping-An Zhong[2], XinYu Wan[2], Yu Zhang[2] (1.College of Earth Sciences and Engineering, Hohai University, 2.College of Hydrology and Water Resources, Hohai University)

[AHW23-P02] **Assessment of the Flow Regime of Roanoke River due to Climatic and Anthropogenic Activities**

*Rahul Kumar Singh[1], Dr. Manoj Kumar Jain[1] (1.Indian Institute of Technology, Roorkee, India)

[AHW23-P03] Predictive Analysis of Climate, Water, Health and the Environment Nexus

*Abhishek [1], Deepika [2] (1.Technical University Dresden, GERMANY, 2.BPS Government Medical College for Women, Sonepat, INDIA)

[AHW23-P05] Severe droughts provide huge fuel for widespread wildfires in California in USA

*Linghua Qiu[1], Ji Chen[1], Haiyun Shi[2], Liqun Sun[3], Jun Niu[4] (1.the University of Hong Kong, 2.Southern University of Science and Technology, 3.Shenzhen Institutes of Advanced Technology, Chinese Academy of Sciences, 4.China Agricultural University)

[AHW23-P06] A comprehensive evaluation of MODIS-based water use efficiency with global eddy covariance flux data and a process model

*Shanshan YANG[1,2], Jiahua ZHANG[1], Sha ZHANG[1,2], Jingwen WANG[1,2], Yun BAI[1,2], Fengmei YAO[2], Huadong GUO[1] (1.Institute of Remote Sensing and Digital Earth, Chinese Academy of Sciences, 2.University of Chinese Academy of Sciences, Beijing, China)

[AHW23-P07] Impact of variability and anisotropy in the correlation decay distance for precipitation spatial interpolation in China

*yingxian zhang[1] (1.National Climate Center, China Meteorological Administration)

[AHW23-P08] New Record-Breaking Frequency of Annual Maximum Daily Precipitation of 58 stations in the whole Japan, an increasing of extreme values.

*Chhay Ngorn SEANG[1], Tomohito YAMADA[1] (1.Hokkaido University)

[AHW23-P09] Quantifying stemflow to better express its ecohydrological significance

*Shin'ichi Iida[1], Darryl E. Carlye-Moses[2], Sonja Germer[3], Pilar Llorens[4], Beate Michalzik[5], Kazuki Nanko[1], Alexander Tischer[5], Delphis F. Levia[6] (1.Department of Disaster Prevention, Meteorology and Hydrology, Forestry and Forest Products Research Institute, 2.Department of Geography and Environmental Studies, Thompson Rivers University, Kamloops, British Columbia, Canada, 3.Department of Bioengineering, Leibniz Institute for Agricultural Engineering and Bioeconomy, Potsdam, Germany, 4.Institute of Environmental Assessment and Water Research (IDAEA-CSIC), Barcelona, Spain, 5.Soil Science, Institute of Geography, Friedrich Schiller University Jena, Jena, Germany, 6.Department of Geography and Department of Plant and Soil Sciences, University of Delaware, Newark, DE, USA)

[AHW23-P10] **Hydraulic analysis of overland flow caused by temporally varying rainfall**

*PING-CHENG HSIEH[1], Ming-Chang Wu[1] (1.National Chung Hsing University)

[AHW23-P11] A comparative Study on Water Environment of Isolated Islands - Focusing on Islands in Nagasaki Prefecture - (3)

*Go Yamaki[1], Koji Kodera[2], Kazuki Asami[1], Yoshihiro IGARI[1], Masaki Horiuchi[1] (1.Grad. Student, Hosei Univ., 2.Dep. of Geography, Hosei Univ.)

[AHW23-P12] **Water environment around Kusatsu-Shirane volcano and consideration of the effect of eruption in January 2018**

*Igari Yoshihiro[1], Koji Kodera[2], Kazuki Asami[1] (1.Grad.Student,Hosei Univ., 2.Dep.of Geography Hosei Univ.)

[AHW23-P13] Re-consideration of discharge rate of spring water in Lake Ezu, Kumamoto

*Kimpei Ichiyanagi[1], Kiyoshi Ide[1], Jun Shimada[1], Tsutomu Ichikawa[2] (1.Kumamoto University, 2.Tokai University)

[AHW23-P14] **Evaluating the efficacy of hydrologically and hydrodynamically driven methods of e-flow assessment for Upper Godavari River Basin, India**

*GAURAV KALIDAS PAKHALE[1], Jyoti Punjahari Nale[2], Ashvin Kumar Gosain[3], Rakesh Khosa[3] (1.PhD Research Scholar, Civil Engineering Department, Indian Institute of Technology, Delhi, 2.Project Advisor, IEWP, GIZ India, New Delhi, India, 3.Professor, Civil Engineering Department, Indian Institute of Technology, Delhi)

[AHW23-P15] Presence of pharmaceutical compounds in freshwater lakes and their impact on phytoplankton

*Nandakumar Kanavillil[1], Cassandra Fligg[1], Sreekumari Kurissery[1] (1.Lakehead University, Canada)

[AHW23-P16] **Novel approximate solutions for solute transport due to injections: considering the scale-dependent dispersion and non-integer flow dimension**

*Ye-Chen Lin[1], Hund-Der Yeh[1] (1.National Chiao Tung Univ.)

[AHW23-P17] Experimemtal study on the residual saturation of Porous Media using Pore Doublets Micromodel

*Chun-Wei Peng[1] (1.Taiwan National Chiao Tung University)

[AHW23-P18] Assessment of Synergy between Biomedical Waste and Shallow Groundwater Pollution

*Deepika [1], Abhishek [2] (1.BPS Government Medical College for Women, Sonepat, INDIA, 2.Technical University Dresden, GERMANY)

[AHW23-P19] Erosion and transport processes of earth surface materials in a reservoir-catchment system inferred from atmospheric radionuclides ^{7}Be and ^{210}Pb

*Mikiya Tsuruoka[1], Shinya Ochiai[2], Atsushi Matsuki[2], Seiya Nagao[2] (1.Graduate School of Natural Science and Technology, Kanazawa University, 2.Institute of Nature and Environmental Technology, Kanazawa University)

[AHW23-P20] Fluctuation of groundwater level in a sloping unconfined aquifer due to time varying recharge

*Ming-Chang Wu[1], Ping-Cheng Hsieh[1] (1.National Chung Hsing University)

[AHW23-P21] **Effect of cutoff wall on recharge water storage volume**

*Pei-hsun Tsai[1], Jung-hsing Tai[1] (1.Chaoyang University of Technology)

[AHW23-P22] **Studying Operation Parameters on Flat-Plate Membrane Bioreactor for Sewage Treatment**

*Jen Hung Chiu[1], Wen Chin Chen[1] (1.Studying Operation Parameters on Flat-Plate Membrane Bioreactor for Sewage Treatment)

[AHW23-P23] **Mine-water quality at a tertiary coalfield in India: Characterisation and treatment using novel polyvinyl alcohol (PVA) gel bioreactor**

*Aparna Dutta[1], Sudipta Sarkar[1] (1.Indian Institute of Technology Roorkee)

[E] Poster | A (Atmospheric and Hydrospheric Sciences)：A-CG Complex & General

10:45 AM - 12:15 PM JST | 1:45 AM - 3:15 AM UTC | Poster Hall International Exhibition Hall8, Makuhari Messe_6

[A-CG35] Projection and detection of global environmental change

convener:Michio Kawamiya(Japan Agency for Marine-Earth Science and Technology), Hiroaki Tatebe(Japan Agency for Marine-Earth Science and Technology), Kaoru Tachiiri(Japan Agency for Marine-Earth Science and Technology)

[ACG35-P01] **World Regionalization of Climate Change (1961–2010)**

*Shao Sun[1,2], Peijun Shi[2,3,4], Daoyi Gong[2], Tao Zhou[2] (1.National Climate Center, China Meteorological Administration, Beijing 100081, China, 2.State Key Laboratory of Earth Surface Processes and Resource Ecology, Beijing Normal University, Beijing 100875, China, 3.Key Laboratory of Environmental Change and Natural Disaster of Ministry of Education, Beijing Normal University, Beijing 100875, China, 4.Academy of Disaster Reduction and Emergency Management, Ministry of Civil Affairs & Ministry of Education, Beijing 100875, China)

[ACG35-P02] Quantifying and identifying future climate signal, noise, and internal variability at finer temporal scales

*Jongho Kim[1], Manh Van Doi[1] (1.University of Ulsan)

[ACG35-P03] Basic evaluation of MIROC6 and current status of CMIP6 experiments

*Hiroaki Tatebe[1] (1.Japan Agency for Marine-Earth Science and Technology)

[ACG35-P04] **Synchronized increase of extreme cold and warm events in China during the recent global warming slowdown**

*Xiubao Sun[1,3], Chunzai Wang[1], Guoyu Ren[2,3], Panfeng Zhang[2] (1.State Key Laboratory of Tropical Oceanography (LTO), South China Sea Institute of Oceanology(SCSIO), Chinese Academy of Sciences (CAS), 2.Department of Atmospheric Science, School of Environmental Studies, China University of Geosciences (CUG), 3.Laboratory for Climate Studies, National Climate Center (NCC), China Meteorological Administration (CMA))

[ACG35-P05] Quantification of thermodynamical and dynamical contributions to the anthropogenic influences on tropical cyclone rainfall extremes

*Cheng-Ta Chen[1], Shih-How Lo[1], Chung-Chieh Wang[1], Kazuhisa Tsuboki[2] (1.Department of Earth Sciences, National Taiwan Normal University, 2.Hydrospheric-Atmospheric Research Center, Nagoya University)

[ACG35-P06] **Temporal Evolution of the Long-Term Distributional Biases of Climate Models as a Parameter for the Regional Evaluation of the Simulation of Climate Change**

*Martin Gomez-Garcia[1], Akiko Matsumura[1], Shiro Hishinuma[1], Daikichi Ogawada[1] (1.Nippon Koei Co. Ltd., Reasearch and Development Center)

[ACG35-P07] A global simulation of bioenergy crop yield

*Zhipin Ai[1], Naota Hanasaki[1] (1.National Institute for Environmental Studies)

[ACG35-P08] Integrated Research Program for Advancing Climate Models - Theme B: national research program in Japan on earth system modeling

*Michio Kawamiya[1], Tomohiro Hajima[1], Kaoru Tachiiri[1], Jun'ichi Tsutsui[2], Tokuta Yokohata[3], Takashi Arakawa[4], Takahiro Inoue[4] (1.Japan Agency for Marine-Earth Science and Technology, 2.Central Research Institute of Electric Power Industry, 3.National Institute for Environmental Studies, 4.Research Organization for Information Science and Technology)

[ACG35-P09] Towards probabilistic climate projections based on the CMIP6 multi-model ensemble

*Junichi Tsutsui[1] (1.Central Research Institute of Electric Power Industry)

[ACG35-P10] Effect on the earth system of realizing 1.5 degree climate target by overshooting after reaching 2 degree level

*Kaoru Tachiiri[1], Herran Diego Silva[2], Xuanming Su[1], Michio Kawamiya[1] (1.Japan Agency for Marine-Earth Science and Technology, 2.Institute for Global Environmental Strategies)

[ACG35-P11] **Historical regional and sectoral contributions to climate change**

*Xuanming Su[1], Kaoru Tachiiri[1], Katsumasa TANAKA[2], Michio Watanabe[1] (1.Japan Agency for Marine-Earth Science and Technology, 2.National Institute for Environmental Studies)

[ACG35-P12] **Future projection of global climate, water, food, bio-energy, and land investigated with MIROC-INTEG: a global bio-geophysical land surface model with human components**

*Tokuta Yokohata[1], Yusuke Satoh[1], Tsuguki Kinoshita[2], Gen Sakurai[3], Yadu Pokhrel[4], Akihiko Ito[1], Etsushi Kato[5], Masashi Okada[1], Naota Hanasaki[1], Tomoko Nitta[6], Seita Emori[1] (1.National Institute for Environmental Studies, 2.Ibaraki University, 3.National Agriculture and Food Research Organization, 4.Michigan State University, 5.The Institute of Applied Energy, 6.University of Tokyo)

[ACG35-P13] **Downscaling a global agricultural land use model to country level for national SSP analysis**

*Wenchao Wu[1], Tomoko Hasegawa[1], Kiyoshi Takahashi[1], Shinichiro Fujimori[2] (1.National Institute for Environmental Studies, 2.Kyoto Univ.)

[ACG35-P14] Extreme Events and Emergent Trends in Marine Ecosystem Stressors under a historical/RCP8.5 Climate Change Pathway

*Keith Bradley Rodgers[1,2], Sarah Schlunegger[3], Richard Slater[3], Burke Hales[4], Axel Timmermann[1,2] (1.IBS Center for Climate Physics, Busan, South Korea, 2.Pusan National University, Busan, South Korea, 3.AOS Program, Princeton University, Princeton NJ, USA, 4.College of Ocean and Atmospheric Sciences, Oregon State Universitym, Corvallis, OR, USA)

[E] Poster | A (Atmospheric and Hydrospheric Sciences)：A-CG Complex & General

5:15 PM - 6:30 PM JST | 8:15 AM - 9:30 AM UTC | Poster Hall International Exhibition Hall8, Makuhari Messe_16

[A-CG35] Projection and detection of global environmental change

convener:Michio Kawamiya(Japan Agency for Marine-Earth Science and Technology), Hiroaki Tatebe(Japan Agency for Marine-Earth Science and Technology), Kaoru Tachiiri(Japan Agency for Marine-Earth Science and Technology)

[ACG35-P01] **World Regionalization of Climate Change (1961–2010)**

*Shao Sun[1,2], Peijun Shi[2,3,4], Daoyi Gong[2], Tao Zhou[2] (1.National Climate Center, China Meteorological Administration, Beijing 100081, China, 2.State Key Laboratory of Earth Surface Processes and Resource Ecology, Beijing Normal University, Beijing 100875, China, 3.Key Laboratory of Environmental Change and Natural Disaster of Ministry of Education, Beijing Normal University, Beijing 100875, China, 4.Academy of Disaster Reduction and Emergency Management, Ministry of Civil Affairs & Ministry of Education, Beijing 100875, China)

[ACG35-P02] Quantifying and identifying future climate signal, noise, and internal variability at finer temporal scales

*Jongho Kim[1], Manh Van Doi[1] (1.University of Ulsan)

[ACG35-P03] Basic evaluation of MIROC6 and current status of CMIP6 experiments

*Hiroaki Tatebe[1] (1.Japan Agency for Marine-Earth Science and Technology)

[ACG35-P04] **Synchronized increase of extreme cold and warm events in China during the recent global warming slowdown**

*Xiubao Sun[1,3], Chunzai Wang[1], Guoyu Ren[2,3], Panfeng Zhang[2] (1.State Key Laboratory of Tropical Oceanography (LTO), South China Sea Institute of Oceanology(SCSIO), Chinese Academy of Sciences (CAS), 2.Department of Atmospheric Science, School of Environmental Studies, China University of Geosciences (CUG), 3.Laboratory for Climate Studies, National Climate Center (NCC), China Meteorological Administration (CMA))

[ACG35-P05] Quantification of thermodynamical and dynamical contributions to the anthropogenic influences on tropical cyclone rainfall extremes

*Cheng-Ta Chen[1], Shih-How Lo[1], Chung-Chieh Wang[1], Kazuhisa Tsuboki[2] (1.Department of Earth Sciences, National Taiwan Normal University, 2.Hydrospheric-Atmospheric Research Center, Nagoya University)

[ACG35-P06] **Temporal Evolution of the Long-Term Distributional Biases of Climate Models as a Parameter for the Regional Evaluation of the Simulation of Climate Change**

*Martin Gomez-Garcia[1], Akiko Matsumura[1], Shiro Hishinuma[1], Daikichi Ogawada[1] (1.Nippon Koei Co. Ltd., Reasearch and Development Center)

[ACG35-P07] A global simulation of bioenergy crop yield

*Zhipin Ai[1], Naota Hanasaki[1] (1.National Institute for Environmental Studies)

[ACG35-P08] Integrated Research Program for Advancing Climate Models - Theme B: national research program in Japan on earth system modeling

*Michio Kawamiya[1], Tomohiro Hajima[1], Kaoru Tachiiri[1], Jun'ichi Tsutsui[2], Tokuta Yokohata[3], Takashi Arakawa[4], Takahiro Inoue[4] (1.Japan Agency for Marine-Earth Science and Technology, 2.Central Research Institute of Electric Power Industry, 3.National Institute for Environmental Studies, 4.Research Organization for Information Science and Technology)

[ACG35-P09] Towards probabilistic climate projections based on the CMIP6 multi-model ensemble

*Junichi Tsutsui[1] (1.Central Research Institute of Electric Power Industry)

[ACG35-P10] Effect on the earth system of realizing 1.5 degree climate target by overshooting after reaching 2 degree level

*Kaoru Tachiiri[1], Herran Diego Silva[2], Xuanming Su[1], Michio Kawamiya[1] (1.Japan Agency for Marine-Earth Science and Technology, 2.Institute for Global Environmental Strategies)

[ACG35-P11] **Historical regional and sectoral contributions to climate change**

*Xuanming Su[1], Kaoru Tachiiri[1], Katsumasa TANAKA[2], Michio Watanabe[1] (1.Japan Agency for Marine-Earth Science and Technology, 2.National Institute for Environmental Studies)

[ACG35-P12] **Future projection of global climate, water, food, bio-energy, and land investigated with MIROC-INTEG: a global bio-geophysical land surface model with human components**

*Tokuta Yokohata[1], Yusuke Satoh[1], Tsuguki Kinoshita[2], Gen Sakurai[3], Yadu Pokhrel[4], Akihiko Ito[1], Etsushi Kato[5], Masashi Okada[1], Naota Hanasaki[1], Tomoko Nitta[6], Seita Emori[1] (1.National Institute for Environmental Studies, 2.Ibaraki University, 3.National Agriculture and Food Research Organization, 4.Michigan State University, 5.The Institute of Applied Energy, 6.University of Tokyo)

[ACG35-P13] **Downscaling a global agricultural land use model to country level for national SSP analysis**

*Wenchao Wu[1], Tomoko Hasegawa[1], Kiyoshi Takahashi[1], Shinichiro Fujimori[2] (1.National Institute for Environmental Studies, 2.Kyoto Univ.)

[ACG35-P14] Extreme Events and Emergent Trends in Marine Ecosystem Stressors under a historical/RCP8.5 Climate Change Pathway

*Keith Bradley Rodgers[1,2], Sarah Schlunegger[3], Richard Slater[3], Burke Hales[4], Axel Timmermann[1,2] (1.IBS Center for Climate Physics, Busan, South Korea, 2.Pusan National University, Busan, South Korea, 3.AOS Program, Princeton University, Princeton NJ, USA, 4.College of Ocean and Atmospheric Sciences, Oregon State Universitym, Corvallis, OR, USA)

[E] Poster | H (Human Geosciences)：H-GM Geomorphology

3:30 PM - 5:00 PM JST | 6:30 AM - 8:00 AM UTC | Poster Hall International Exhibition Hall8, Makuhari Messe_11

[H-GM03] Geomorphology

convener:Tsuyoshi Hattanji(Faculty of Life and Environmental Sciences, University of Tsukuba), Masayuki Seto(Fukushima Future Center for Regional Revitalization, Fukushima University)

[HGM03-P01] Honeycomb Weathering (Tafoni) of Sandstone and Environmental Factors in Yonaguni Island, Okinawa Prefecture, Japan

*Takayuki Ogata[1] (1.Disaster Prevention Research Center for Island Regions, University of the Ryukyus)

[HGM03-P02] Colluvial deposits in first-order streams and channel head migration by shallow landslides: Case study in granitic basins, Asaminami, Hiroshima, Japan

*Tsuyoshi Hattanji[1], Ryuya Kodama[2], Takahisa Furuichi[3], Shoji Doshida[4], Yasushi Tanaka[5] (1.Faculty of Life and Environmental Sciences, University of Tsukuba, 2.former College of Geoscience, University of Tsukuba, 3.Hokkaido University, 4.National Research Institute of Fire and Disaster, 5.Komazawa University)

[HGM03-P03] Rock restrictions on topographical features of rivers: model experiment

*Yuta Takase[1], Noritaka Endo[1] (1.Kanazawa University)

[HGM03-P04] Stream power incision model and the stage of topographic equilibrium, using physical experiments

*Imamura Akihiro[1], Noritaka Endo[1] (1.Kanazawa University)

[HGM03-P05] Downstream variation in gravel size of the Tenjin River system

*Kazuaki Hori[1], Kazuya Yonehara[1] (1.Department of Geography, Graduate School of Environmental Studies, Nagoya University)

[HGM03-P06] Talus slope development in the time of deglaciation: a case study of the Rev Valley, SW Spitsbergen

*Krzysztof Senderak[1], Marta Kondracka[1], Bogdan Gądek[1] (1.Faculty of Earth Sciences, University of Silesia)

[HGM03-P07] **Distribution of Large Benthic Foraminifers in one of Majuro's Conservation Areas – Drenmeo Island**

*Benedict Yamamura[1], Kazuhiko Fujita[2], Melba White[3], Kyotak Ishiguro[3], Hironobu Kan[1] (1.Kyushu University, Integrated Sciences for Global Society - Research Center for Coastal Seafloor , 2.Department of Physics and Earth Sciences, University of the Ryukyus, 3.Marshall Islands Marine Resources Authority)

[HGM03-P08] Luminescence chronology of fluvial and marine records from subsurface sediment cores: An insight into the geomorphic evolution of Kaveri delta, India

*kartika goswami[1], Anbarasu Kumaresan[2], Sivakumar Krishnan[2], Senthil K. Sadasivam[2], Manoj Kumar Jaiswal[1] (1.Department of Earth Sciences, Indian Institute of Science Education and Reserach Kolkata, 2.National College Tiruchirappalli, India)

[E] Poster | H (Human Geosciences)：H-GM Geomorphology

5:15 PM - 6:30 PM JST | 8:15 AM - 9:30 AM UTC | Poster Hall International Exhibition Hall8, Makuhari Messe_18

[H-GM03] Geomorphology

convener:Tsuyoshi Hattanji(Faculty of Life and Environmental Sciences, University of Tsukuba), Masayuki Seto(Fukushima Future Center for Regional Revitalization, Fukushima University)

[HGM03-P01] Honeycomb Weathering (Tafoni) of Sandstone and Environmental Factors in Yonaguni Island, Okinawa Prefecture, Japan

*Takayuki Ogata[1] (1.Disaster Prevention Research Center for Island Regions, University of the Ryukyus)

[HGM03-P02] Colluvial deposits in first-order streams and channel head migration by shallow landslides: Case study in granitic basins, Asaminami, Hiroshima, Japan

*Tsuyoshi Hattanji[1], Ryuya Kodama[2], Takahisa Furuichi[3], Shoji Doshida[4], Yasushi Tanaka[5] (1.Faculty of Life and Environmental Sciences, University of Tsukuba, 2.former College of Geoscience, University of Tsukuba, 3.Hokkaido University, 4.National Research Institute of Fire and Disaster, 5.Komazawa University)

[HGM03-P03] Rock restrictions on topographical features of rivers: model experiment

*Yuta Takase[1], Noritaka Endo[1] (1.Kanazawa University)

[HGM03-P04] Stream power incision model and the stage of topographic equilibrium, using physical experiments

*Imamura Akihiro[1], Noritaka Endo[1] (1.Kanazawa University)

[HGM03-P05] Downstream variation in gravel size of the Tenjin River system

*Kazuaki Hori[1], Kazuya Yonehara[1] (1.Department of Geography, Graduate School of Environmental Studies, Nagoya University)

[HGM03-P06] Talus slope development in the time of deglaciation: a case study of the Rev Valley, SW Spitsbergen

*Krzysztof Senderak[1], Marta Kondracka[1], Bogdan Gądek[1] (1.Faculty of Earth Sciences, University of Silesia)

[HGM03-P07] **Distribution of Large Benthic Foraminifers in one of Majuro's Conservation Areas – Drenmeo Island**

*Benedict Yamamura[1], Kazuhiko Fujita[2], Melba White[3], Kyotak Ishiguro[3], Hironobu Kan[1] (1.Kyushu University, Integrated Sciences for Global Society - Research Center for Coastal Seafloor , 2.Department of Physics and Earth Sciences, University of the Ryukyus, 3.Marshall Islands Marine Resources Authority)

[HGM03-P08] Luminescence chronology of fluvial and marine records from subsurface sediment cores: An insight into the geomorphic evolution of Kaveri delta, India

*kartika goswami[1], Anbarasu Kumaresan[2], Sivakumar Krishnan[2], Senthil K. Sadasivam[2], Manoj Kumar Jaiswal[1] (1.Department of Earth Sciences, Indian Institute of Science Education and Reserach Kolkata, 2.National College Tiruchirappalli, India)

[E] Poster | H (Human Geosciences)：H-DS Disaster geosciences

10:45 AM - 12:15 PM JST | 1:45 AM - 3:15 AM UTC | Poster Hall International Exhibition Hall8, Makuhari Messe_7

[H-DS10] Natural hazards impacts on human society, economics and technological systems

convener:ELENA PETROVA(Lomonosov Moscow State University, Faculty of Geography), Hajime Matsushima(Research Faculty of Agriculture, Hokkaido University)

[HDS10-P01] **The 2018 Activity of Kamchatka Volcanoes and Danger to Aviation**

*Olga Girina[1], Dmitry Melnikov[1], Alexander Manevich[1], Anton Nuzhdaev[1], Elena Petrova[2] (1.Institute of Volcanology and Seismology, Far East Division, Russian Academy of Sciences, 2.M.V. Lomonosov Moscow State University)

[HDS10-P02] Planning Methodology on the Effective Use of Green Infrastructure for Disaster Risk Reduction

★Invited Papers

*Keita Aragane[1], Satoshi Funakubo[1] (1.National Institute for Land Infrastructure Management)

[HDS10-P03] EMERGENCY CALL PATTERN IN PETROZAVODSK

*Boris Zalmanovich Belashev[1], Natalia Vladimirovna Krutskikh[1], Anna Aleksandrovna Gerasimova[1] (1.Karelian research center of Russian academy of science)

[HDS10-P04] IDENTIFYING “REGIMES” IN THE TIME SEQUENCES OF PROCESSES

*Boris Zalmanovich Belashev[1] (1.Karelian research center of Russian academy of science)

[HDS10-P05] **Investigation of status and demand on public service of earthquake disaster mitigation in China**

*Lina Dong[1], Weiping Lian[1], Weitao Chen[1] (1.Development Research Center, China Earthquake Administration)

[HDS10-P06] Analysis of Eco-DRR and Ecological Services using InVEST at the Disaster Areas of Kumamoto Earthquake

*Minghui Tang[1], Naoko Fujita[1] (1.Kyushu University)

[HDS10-P07] Transformation as praxis: Exploring socially just and transdisciplinary pathways to sustainability in marginal environments (TAPESTRY)

*Nobuhito Ohte[1], Lyla Mehta[2], Synne Movik[3], Devanathan Parthasarathy[4] (1.Department of Social Informatics, Graduate School of Informatics, Kyoto University, 2.Institute of Development Studies at the University of Sussex, 3.Department of Urban and Regional Planning, Norwegian University of Life Sciences, 4.Department of Humanities and Social Sciences, Indian Institute of Technology)

[HDS10-P08] Study for the Establishment of the Design for Disaster prevention through the survey of Recognition of tsunami disaster prevention from the viewpoint of green infrastructure in the coastal area of Kyushu-Pacific region.

*Shanshan Xu[1], Naoko Fujita[1], Minghui Tang[1] (1.Kyushu University)

[HDS10-P09] Design for Green Infrastructure: Analysis of Landscape change in the Kumamoto earthquake area

★Invited Papers

*Naoko Fujita[1] (1.Kyushu University)

[E] Poster | H (Human Geosciences)：H-DS Disaster geosciences

5:15 PM - 6:30 PM JST | 8:15 AM - 9:30 AM UTC | Poster Hall International Exhibition Hall8, Makuhari Messe_21

[H-DS10] Natural hazards impacts on human society, economics and technological systems

convener:ELENA PETROVA(Lomonosov Moscow State University, Faculty of Geography), Hajime Matsushima(Research Faculty of Agriculture, Hokkaido University)

[HDS10-P01] **The 2018 Activity of Kamchatka Volcanoes and Danger to Aviation**

*Olga Girina[1], Dmitry Melnikov[1], Alexander Manevich[1], Anton Nuzhdaev[1], Elena Petrova[2] (1.Institute of Volcanology and Seismology, Far East Division, Russian Academy of Sciences, 2.M.V. Lomonosov Moscow State University)

[HDS10-P02] Planning Methodology on the Effective Use of Green Infrastructure for Disaster Risk Reduction

★Invited Papers

*Keita Aragane[1], Satoshi Funakubo[1] (1.National Institute for Land Infrastructure Management)

[HDS10-P03] EMERGENCY CALL PATTERN IN PETROZAVODSK

*Boris Zalmanovich Belashev[1], Natalia Vladimirovna Krutskikh[1], Anna Aleksandrovna Gerasimova[1] (1.Karelian research center of Russian academy of science)

[HDS10-P04] IDENTIFYING “REGIMES” IN THE TIME SEQUENCES OF PROCESSES

*Boris Zalmanovich Belashev[1] (1.Karelian research center of Russian academy of science)

[HDS10-P05] **Investigation of status and demand on public service of earthquake disaster mitigation in China**

*Lina Dong[1], Weiping Lian[1], Weitao Chen[1] (1.Development Research Center, China Earthquake Administration)

[HDS10-P06] Analysis of Eco-DRR and Ecological Services using InVEST at the Disaster Areas of Kumamoto Earthquake

*Minghui Tang[1], Naoko Fujita[1] (1.Kyushu University)

[HDS10-P07] Transformation as praxis: Exploring socially just and transdisciplinary pathways to sustainability in marginal environments (TAPESTRY)

*Nobuhito Ohte[1], Lyla Mehta[2], Synne Movik[3], Devanathan Parthasarathy[4] (1.Department of Social Informatics, Graduate School of Informatics, Kyoto University, 2.Institute of Development Studies at the University of Sussex, 3.Department of Urban and Regional Planning, Norwegian University of Life Sciences, 4.Department of Humanities and Social Sciences, Indian Institute of Technology)

[HDS10-P08] Study for the Establishment of the Design for Disaster prevention through the survey of Recognition of tsunami disaster prevention from the viewpoint of green infrastructure in the coastal area of Kyushu-Pacific region.

*Shanshan Xu[1], Naoko Fujita[1], Minghui Tang[1] (1.Kyushu University)

[HDS10-P09] Design for Green Infrastructure: Analysis of Landscape change in the Kumamoto earthquake area

★Invited Papers

*Naoko Fujita[1] (1.Kyushu University)

[E] Poster | H (Human Geosciences)：H-TT Technology & Techniques

1:45 PM - 3:15 PM JST | 4:45 AM - 6:15 AM UTC | Poster Hall International Exhibition Hall8, Makuhari Messe_2

[H-TT21] Non-destructive techniques applied to stone cultural heritage

convener:Chiaki T. Oguchi(Institute for Environmental Science and Technology, Graduate School of Science and Engineering, Saitama University), Celine Elise Thomachot-Schneider(Groupe d'etude des environnements naturels, anthropiques et archeologiques - Universite de Reims-Champagne-Ardenne (France)), Wonsuh Song(Waseda University), Miguel Gomez-Heras(Universidad Autonoma de Madrid)

[HTT21-P01] **Comparison and Analysis of GNSS-RTK Combined with 3D LiDAR Technology on Monument Maintenance Project**

*Lih-Shinn Hwang[1], Chien-Hua Chiu[1], Chien-Wen Wang[1], Hsiao-Hung Chen[1] (1.National Defense Univ.)

[HTT21-P02] Non-destructive field measurement for investigation of deteriorated parts of an artificial cave

Kaisei Sakane[1], *Chiaki T. Oguchi[1], Yasuhiko TAMURA[2] (1.Institute for Environmental Science and Technology, Graduate School of Science and Engineering, Saitama University, 2.The Exective Committee for the Preservation of Taya Cavern)

[HTT21-P03] Ultra-portable thermal cameras for moisture detection

*Miguel Gomez-Heras[1], Laura Lopez-Gonzalez[2], Maria Teresa Gil-Muñoz[3] (1.Universidad Autonoma de Madrid, 2.Artfabrik, 3.Universidad Complutense de Madrid)

[HTT21-P04] A laboratory experiment on stone decay by combination of salt and ice crystallization

*Masato Sato[1], Tsuyoshi Hattanji[2] (1.Graduate School of Life and environmental Sciences, 2.Faculty of Life and EnvironmentalSciences, University of Tsukuba)

[HTT21-P05] Study of the micro-climatic monitoring on the Saint-Remi Basilica (Rheims, France)

*Emilie Huby[1], Celine Elise Thomachot-Schneider[1], Patricia Vazquez[1], Gilles Fronteau[1] (1.Universite de Reims-Champagne-Ardenne)

[E] Poster | H (Human Geosciences)：H-TT Technology & Techniques

5:15 PM - 6:30 PM JST | 8:15 AM - 9:30 AM UTC | Poster Hall International Exhibition Hall8, Makuhari Messe_23

[H-TT21] Non-destructive techniques applied to stone cultural heritage

convener:Chiaki T. Oguchi(Institute for Environmental Science and Technology, Graduate School of Science and Engineering, Saitama University), Celine Elise Thomachot-Schneider(Groupe d'etude des environnements naturels, anthropiques et archeologiques - Universite de Reims-Champagne-Ardenne (France)), Wonsuh Song(Waseda University), Miguel Gomez-Heras(Universidad Autonoma de Madrid)

[HTT21-P01] **Comparison and Analysis of GNSS-RTK Combined with 3D LiDAR Technology on Monument Maintenance Project**

*Lih-Shinn Hwang[1], Chien-Hua Chiu[1], Chien-Wen Wang[1], Hsiao-Hung Chen[1] (1.National Defense Univ.)

[HTT21-P02] Non-destructive field measurement for investigation of deteriorated parts of an artificial cave

Kaisei Sakane[1], *Chiaki T. Oguchi[1], Yasuhiko TAMURA[2] (1.Institute for Environmental Science and Technology, Graduate School of Science and Engineering, Saitama University, 2.The Exective Committee for the Preservation of Taya Cavern)

[HTT21-P03] Ultra-portable thermal cameras for moisture detection

*Miguel Gomez-Heras[1], Laura Lopez-Gonzalez[2], Maria Teresa Gil-Muñoz[3] (1.Universidad Autonoma de Madrid, 2.Artfabrik, 3.Universidad Complutense de Madrid)

[HTT21-P04] A laboratory experiment on stone decay by combination of salt and ice crystallization

*Masato Sato[1], Tsuyoshi Hattanji[2] (1.Graduate School of Life and environmental Sciences, 2.Faculty of Life and EnvironmentalSciences, University of Tsukuba)

[HTT21-P05] Study of the micro-climatic monitoring on the Saint-Remi Basilica (Rheims, France)

*Emilie Huby[1], Celine Elise Thomachot-Schneider[1], Patricia Vazquez[1], Gilles Fronteau[1] (1.Universite de Reims-Champagne-Ardenne)

[E] Poster | H (Human Geosciences)：H-CG Complex & General

3:30 PM - 5:00 PM JST | 6:30 AM - 8:00 AM UTC | Poster Hall International Exhibition Hall8, Makuhari Messe_15

[H-CG25] International Comparison of Landscape Appreciation

convener:Anastasia Petrova(Institute of Oriental Studies of the Russian Academy of Sciences), yoji aoki(Open University of Japan)

[HCG25-P01] **The Globally Important Agricultural Heritage of Aso from the perspective of landscape and its supporting systems**

*REIKO MACHIDA[1] (1.TOKYO UNIVERSITY OF AGRICULTURE)

[HCG25-P02] **Hazardous natural phenomena and weather conditions appreciation in Russian landscape painting**

*ELENA PETROVA[1] (1.Lomonosov Moscow State University, Faculty of Geography)

[HCG25-P03] Trends of evaluation items to landscape appreciation until 2017 in the English journals

*yoji aoki[1], keisuke mukagai[2], Anastasia Petrova[3] (1.Open University of Japan, 2.Nagano University, 3.Institute of Oriental Studies, Russian Academy of Sciences)

[E] Poster | H (Human Geosciences)：H-CG Complex & General

5:15 PM - 6:30 PM JST | 8:15 AM - 9:30 AM UTC | Poster Hall International Exhibition Hall8, Makuhari Messe_24

[H-CG25] International Comparison of Landscape Appreciation

convener:Anastasia Petrova(Institute of Oriental Studies of the Russian Academy of Sciences), yoji aoki(Open University of Japan)

[HCG25-P01] **The Globally Important Agricultural Heritage of Aso from the perspective of landscape and its supporting systems**

*REIKO MACHIDA[1] (1.TOKYO UNIVERSITY OF AGRICULTURE)

[HCG25-P02] **Hazardous natural phenomena and weather conditions appreciation in Russian landscape painting**

*ELENA PETROVA[1] (1.Lomonosov Moscow State University, Faculty of Geography)

[HCG25-P03] Trends of evaluation items to landscape appreciation until 2017 in the English journals

*yoji aoki[1], keisuke mukagai[2], Anastasia Petrova[3] (1.Open University of Japan, 2.Nagano University, 3.Institute of Oriental Studies, Russian Academy of Sciences)

[E] Poster | S (Solid Earth Sciences)：S-IT Science of the Earth's Interior & Techtonophysics

10:45 AM - 12:15 PM JST | 1:45 AM - 3:15 AM UTC | Poster Hall International Exhibition Hall8, Makuhari Messe_8

[S-IT26] New perspectives on the geodynamics of East Asia

convener:Timothy B Byrne(University of Connecticut), Asuka Yamaguchi(Atomosphere and Ocean Research Institute, The University of Tokyo), Jonny Wu(University of Houston), Kyoko Okino(Atmosphere and Ocean Research Institute, The University of Tokyo)

[SIT26-P01] Geochemical characteristics of effusive rocks (greenstones) in the Hidaka Belt, Hokkaido, Japan

*Toru Yamasaki[1], Futoshi Nanayama[1] (1.Geol. Survey of Japan (AIST))

[SIT26-P02] Large gas reservoir in continental back-arc basin, revealed by automatic seismic velocity analysis in the Okinawa Trough

*Kota Mukumoto[1], Takeshi Tsuji[1], Andri Hendriyana[1] (1.Kyushu University)

[SIT26-P03] Characterize coseismic deformation of Mw 7.5 Palu earthquake in a triple junction in Sulawesi, Indonesia

*MIN-CHIEN TSAI[1], Ying-Hui Yang[2], Chun-Ying Chiu[3], Jyr-Ching Hu[3] (1.Seismological center, Central Weather Bureau, Taipei, Taiwan, R.O.C., 2.School of Civil Engineering and Architecture, Southwest Petroleum University, Chengdu, China, 3.Department of Geosciences, National Taiwan University, Taipei, Taiwan, R.O.C.)

[E] Poster | S (Solid Earth Sciences)：S-IT Science of the Earth's Interior & Techtonophysics

5:15 PM - 6:30 PM JST | 8:15 AM - 9:30 AM UTC | Poster Hall International Exhibition Hall8, Makuhari Messe_28

[S-IT26] New perspectives on the geodynamics of East Asia

convener:Timothy B Byrne(University of Connecticut), Asuka Yamaguchi(Atomosphere and Ocean Research Institute, The University of Tokyo), Jonny Wu(University of Houston), Kyoko Okino(Atmosphere and Ocean Research Institute, The University of Tokyo)

[SIT26-P01] Geochemical characteristics of effusive rocks (greenstones) in the Hidaka Belt, Hokkaido, Japan

*Toru Yamasaki[1], Futoshi Nanayama[1] (1.Geol. Survey of Japan (AIST))

[SIT26-P02] Large gas reservoir in continental back-arc basin, revealed by automatic seismic velocity analysis in the Okinawa Trough

*Kota Mukumoto[1], Takeshi Tsuji[1], Andri Hendriyana[1] (1.Kyushu University)

[SIT26-P03] Characterize coseismic deformation of Mw 7.5 Palu earthquake in a triple junction in Sulawesi, Indonesia

*MIN-CHIEN TSAI[1], Ying-Hui Yang[2], Chun-Ying Chiu[3], Jyr-Ching Hu[3] (1.Seismological center, Central Weather Bureau, Taipei, Taiwan, R.O.C., 2.School of Civil Engineering and Architecture, Southwest Petroleum University, Chengdu, China, 3.Department of Geosciences, National Taiwan University, Taipei, Taiwan, R.O.C.)

[E] Poster | S (Solid Earth Sciences)：S-GC Geochemistry

10:45 AM - 12:15 PM JST | 1:45 AM - 3:15 AM UTC | Poster Hall International Exhibition Hall8, Makuhari Messe_9

[S-GC40] Volatile Cycles in the Deep Earth - from Subduction Zone to Hot Spot

convener:Hirochika Sumino(Department of Basic Science, Graduate School of Arts and Sciences, The University of Tokyo), Takeshi Hanyu(Japan Agency for Marine-Earth Science and Technology, Department of Solid Earth Geochemistry), Yuji Sano(Division of Ocean and Earth Systems, Atmosphere and Ocean Research Institute, University of Tokyo), Gray E Bebout(Lehigh University)

[SGC40-P01] Continental growth models demystified

*Jun Korenaga[1] (1.Department of Geology and Geophysics, Yale University)

[SGC40-P02] Mass-independent sulfur isotope signature from the 2.7 Ga Belingwe komatiite: Recycling of crustal material in Archean

*Yusuke Kubota[1], Yuichiro Ueno[1,2,3], Kenji Shimizu[3], Fumihiro Matsuura[2], Akira Ishikawa[1,3] (1.Department of Earth and Planetary Sciences, Tokyo Institute of Technology, 2.Earth-Life Science Institute, Tokyo Institute of Technology, 3.Japan Agency for Marine-Earth Science and Technology (JAMSTEC))

[SGC40-P03] Determination of halogens in some standard materials using the neutron irradiation noble gas mass spectrometric technique

*Hirochika Sumino[1], Masahiro Kobayashi[2], Takehiko Saito[3], Keisuke Nagao[3] (1.Department of Basic Science, Graduate School of Arts and Sciences, The University of Tokyo, 2.Tokyo Metropolitan Industrial Technology Research Institute, 3.Geochemical Research Center, Graduate School of Science, University of Tokyo)

[SGC40-P04] FTIR spectroscopy and noble gas mass spectrometry for a single olivine grain

*Sota Niki[1], Hirochika Sumino[2], Masahiro Kobayashi[3], Hiroyuki Kagi[1], Takafumi Hirata[1], Chris J. Ballentine[4] (1.Geochemical Research Center, Grad. School of Science, Univ. of Tokyo, 2.Dept. of Basic Science, Grad. School of Arts and Sciences, Univ. of Tokyo, 3.Tokyo Metropolitan Industrial Technology Research Institute, 4.Dept. of Earth Sciences, Univ. of Oxford)

[SGC40-P05] New halogen incorporation mechanism in serpentine group minerals: Crystal chemical consideration

*Masami Kanzaki[1] (1.Institute for Planetary Matereials, Okayama University)

[SGC40-P06] Mineralogical and geochemical characteristics of cuttings from Taketomi hot spring

*Noriyuki Shingaki[1], Tomohiro Toki[1], Syogo Oshima[2], Masaaki chinen[3], Arito Sakaguchi[4], Naoto Takahata[5], Yuji Sano[5], Shirai Kotaro[5], Kentaro Tanaka[5] (1.University of the Ryukyus , 2.West Japan Engineering Consultants, Inc., 3.MicroRange, 4.Faculty of Science, Yamaguchi University, 5.Atmosphere and Ocean Research Institute, The University of Tokyo)

[SGC40-P07] Variation of helium isotope compositions at Lake Mashu

*Takanori Kagoshima[1], Yuji Sano[1], Atsushi Tanaka[2] (1.Atmosphere and Ocean Research Institute, University of Tokyo, 2.National Institute for Environmental Studies)

[SGC40-P08] Helium isotopes in Tachibana Bay and Shimabara Bay, Nagasaki

*Ma. Teresa Escobar[1], Yama Tomonaga[2], Hajime Obata[1], Shigenobu Takeda[3], Naoto Takahata[1], Yuji Sano[1] (1.Atmosphere and Ocean Research Institute, University of Tokyo, Kashiwanoha, Kashiwa, Chiba, Japan, 2.Eawag,, Swiss Federal Institute of Aquatic Science and Technology, Department of Water Resources and Drinking Water, Überlandstrasse 133 CH-8600 ,Dübendorf, Switzerland, 3.Graduate School of Fisheries and Environmental Sciences, Nagasaki University, Nagasaki, Japan)

[E] Poster | S (Solid Earth Sciences)：S-GC Geochemistry

5:15 PM - 6:30 PM JST | 8:15 AM - 9:30 AM UTC | Poster Hall International Exhibition Hall8, Makuhari Messe_31

[S-GC40] Volatile Cycles in the Deep Earth - from Subduction Zone to Hot Spot

convener:Hirochika Sumino(Department of Basic Science, Graduate School of Arts and Sciences, The University of Tokyo), Takeshi Hanyu(Japan Agency for Marine-Earth Science and Technology, Department of Solid Earth Geochemistry), Yuji Sano(Division of Ocean and Earth Systems, Atmosphere and Ocean Research Institute, University of Tokyo), Gray E Bebout(Lehigh University)

[SGC40-P01] Continental growth models demystified

*Jun Korenaga[1] (1.Department of Geology and Geophysics, Yale University)

[SGC40-P02] Mass-independent sulfur isotope signature from the 2.7 Ga Belingwe komatiite: Recycling of crustal material in Archean

*Yusuke Kubota[1], Yuichiro Ueno[1,2,3], Kenji Shimizu[3], Fumihiro Matsuura[2], Akira Ishikawa[1,3] (1.Department of Earth and Planetary Sciences, Tokyo Institute of Technology, 2.Earth-Life Science Institute, Tokyo Institute of Technology, 3.Japan Agency for Marine-Earth Science and Technology (JAMSTEC))

[SGC40-P03] Determination of halogens in some standard materials using the neutron irradiation noble gas mass spectrometric technique

*Hirochika Sumino[1], Masahiro Kobayashi[2], Takehiko Saito[3], Keisuke Nagao[3] (1.Department of Basic Science, Graduate School of Arts and Sciences, The University of Tokyo, 2.Tokyo Metropolitan Industrial Technology Research Institute, 3.Geochemical Research Center, Graduate School of Science, University of Tokyo)

[SGC40-P04] FTIR spectroscopy and noble gas mass spectrometry for a single olivine grain

*Sota Niki[1], Hirochika Sumino[2], Masahiro Kobayashi[3], Hiroyuki Kagi[1], Takafumi Hirata[1], Chris J. Ballentine[4] (1.Geochemical Research Center, Grad. School of Science, Univ. of Tokyo, 2.Dept. of Basic Science, Grad. School of Arts and Sciences, Univ. of Tokyo, 3.Tokyo Metropolitan Industrial Technology Research Institute, 4.Dept. of Earth Sciences, Univ. of Oxford)

[SGC40-P05] New halogen incorporation mechanism in serpentine group minerals: Crystal chemical consideration

*Masami Kanzaki[1] (1.Institute for Planetary Matereials, Okayama University)

[SGC40-P06] Mineralogical and geochemical characteristics of cuttings from Taketomi hot spring

*Noriyuki Shingaki[1], Tomohiro Toki[1], Syogo Oshima[2], Masaaki chinen[3], Arito Sakaguchi[4], Naoto Takahata[5], Yuji Sano[5], Shirai Kotaro[5], Kentaro Tanaka[5] (1.University of the Ryukyus , 2.West Japan Engineering Consultants, Inc., 3.MicroRange, 4.Faculty of Science, Yamaguchi University, 5.Atmosphere and Ocean Research Institute, The University of Tokyo)

[SGC40-P07] Variation of helium isotope compositions at Lake Mashu

*Takanori Kagoshima[1], Yuji Sano[1], Atsushi Tanaka[2] (1.Atmosphere and Ocean Research Institute, University of Tokyo, 2.National Institute for Environmental Studies)

[SGC40-P08] Helium isotopes in Tachibana Bay and Shimabara Bay, Nagasaki

*Ma. Teresa Escobar[1], Yama Tomonaga[2], Hajime Obata[1], Shigenobu Takeda[3], Naoto Takahata[1], Yuji Sano[1] (1.Atmosphere and Ocean Research Institute, University of Tokyo, Kashiwanoha, Kashiwa, Chiba, Japan, 2.Eawag,, Swiss Federal Institute of Aquatic Science and Technology, Department of Water Resources and Drinking Water, Überlandstrasse 133 CH-8600 ,Dübendorf, Switzerland, 3.Graduate School of Fisheries and Environmental Sciences, Nagasaki University, Nagasaki, Japan)

[E] Poster | S (Solid Earth Sciences)：S-CG Complex & General

10:45 AM - 12:15 PM JST | 1:45 AM - 3:15 AM UTC | Poster Hall International Exhibition Hall8, Makuhari Messe_10

[S-CG48] Science of slow earthquakes: Toward unified understandings of whole earthquake process

convener:Satoshi Ide(Department of Earth an Planetary Science, University of Tokyo), Hitoshi Hirose(Research Center for Urban Safety and Security, Kobe University), Kohtaro Ujiie(Graduate School of Life and Environmental Sciences, University of Tsukuba), Takahiro Hatano(Earthquake Research Institute, University of Tokyo)

[SCG48-P01] Off the Kii Peninsula Shallow Low Frequency Earthquake in 2004 revealed by Ocean Bottom Seismometer

*Koji Tamaribuchi[1], Akio Kobayashi[1], Takahito Nishimiya[1], Satoshi Annoura[2] (1.Meteorological Research Institute, 2.Japan Meteorological Agency)

[SCG48-P02] The development of pressure vessel on gouges for rock deformation at seismic rates under water-saturated conditions

*Wei-Ting Lin[1], Li-Wei Kuo[1], Wen-Jie Wu[1], Jia-Jyun Dong[1], Yi-Hung Huang[2] (1.National Central University, 2.MATSUKI HYDRAULIC INDUSTRIAL CO. LTD)

[SCG48-P03] Spatial variations of shallow very low-frequency earthquake activity along the Nankai Trough based on CMT inversion using the 3D heterogeneous model

*Shunsuke Takemura[1], Takanori Matsuzawa[1], Akemi Noda[1], Takashi Tonegawa[2], Youichi Asano[1], Takeshi Kimura[1], Katsuhiko Shiomi[1] (1.National Research Institute for Earth Science and Disaster Resilience, 2.Japan Agency for Marine-Earth Science and Technology)

[SCG48-P04] Evaluation of Magnitude and Characteristics of Seismicity of Low Frequency Earthquakes in Parkfield

*Miki Aso[1,3], Naofumi Aso[2], Satoshi Ide[1] (1.Department of Earth and Planetary Science, The University of Tokyo, 2.Tokyo Institute of Technology, School of Science, 3.OYO RMS Corporation)

[SCG48-P05] Tectonic tremor catalog in the Tohoku-Hokkaido-Oki region using S-net

*Satoshi Ide[1], Tomoaki Nishikawa[2], Takanori Matsuzawa[3], Kazuaki Ohta[2], Naoki Uchida[4], Takuya NISHIMURA[2] (1.Department of Earth an Planetary Science, University of Tokyo, 2.Disaster Prevention Research Institute, Kyoto University, 3.National Research Institute for Earth Science and Disaster Resilience, 4.Graduate School of Science and International Research Institute of Disaster Science, Tohoku University)

[SCG48-P06] Spontaneous Slow Slip and Runaway Slip in Laboratory

*Miki Takahashi[1] (1.Institute of Earthquake and Volcano Geology, Geological Survey of Japan, AIST)

[SCG48-P07] Hydration and amorphization of quartz rocks during high-velocity frictional sliding: An examination of fault gouge from friction experiments of synthetic quartz

*Yuko Onoe[1], Hirotaka Iida[2], Akito Tsutsumi[1], Aki Takigawa[1] (1.Graduate School of Science, Kyoto University, 2.Geothermal Engineering Co., Ltd.)

[SCG48-P08] Constraining S Wave Velocity of the Source Region of Shallow Very Low-Frequency Earthquakes

*Takeshi Akuhara[1], Takashi Tonegawa[2] (1.Earthquake Research Institute, The University of Tokyo, 2.Research and Development center for Earthquake and Tsunami, Japan Agency for Marine-Earth Science and Technology)

[SCG48-P09] Quantitative relationship between aseismic slip propagation speed and frictional properties

*Keisuke Ariyoshi[1], Jean-Paul Ampuero[2,3], Roland Burgmann[4], Toru Matsuzawa[5], Akira Hasegawa[5], Ryota Hino[5], Takane Hori[1] (1.Japan Agency for Marine-Earth Science and Technology, 2.Université Côte d'Azur, 3.California Institute of Technology, 4.University of California, Berkeley, 5.Graduate School of Science, Tohoku University)

[SCG48-P10] Comprehensive detection of very low frequency earthquakes off the Pacific coasts of Hokkaido and Tohoku, northeastern Japan

*Satoru Baba[1], Akiko Takeo[1], Kazushige Obara[1], Takanori Matsuzawa[2], Takuto Maeda[3] (1.Earthquake Research Institute, University of Tokyo, 2.National Research Institute for Earth Science and Disaster Resilience, 3.Graduate School of Science and Technology, Hirosaki University)

[SCG48-P11] **Spatio-temporal evolution of long- and short-term slow slip events in the Tokai region, central Japan estimated from a very dense GNSS network, during 1997-2017**

*Hiromu Sakaue[1], Takuya NISHIMURA[2], Jun'ichi Fukuda[3], Teruyuki Kato[4] (1.Graduate School of Science, Kyoto University, 2.Disaster Prevention Research Institute Kyoto University, 3.Earthquake Research Institute,The University of Tokyo, 4.Hot Springs Research Institute of Kanagawa Prefecture)

[SCG48-P12] Broadband excitation of acoustic emission in granular stick-slip : experiments and spectral analyses

*Hidekazu Fukumizu[1], Ikuro Sumita[2] (1.Earth and Environmental Science Course, Division of Natural System, Graduate school of Natural Science and Technology, Kanazawa University, 2.School of Geosciences and Civil Engineering, Kanazawa University)

[SCG48-P13] Episodic tremor and slip silently invades strongly locked megathrust in the Nankai Trough

*Masayuki Kano[1], Aitaro Kato[2], Kazushige Obara[2] (1.Graduate school of science, Tohoku University, 2.Earthquake Research Institute, The University of Tokyo)

[SCG48-P14] Spatial distribution of the electrical resistivity beneath western part of Shikoku Island where long-term SSE events have repeatedly occurred

*Makoto Uyeshima[1], Maki Hata[1], Hiroshi Ichihara[2], Ryokei Yoshimura[3], Koki Aizawa[4] (1.Earthquake Research Institute, The University of Tokyo, 2.Graduate School of Environmental Studies, Nagoya University, 3.Disaster Prevention Research Institute, Kyoto University, 4.Institute of Seismology and Volcanology, Faculty of Sciences, Kyushu University)

[SCG48-P15] Variations of scaling relationships for shallow tremor observed along the Nankai trough

*Masaru Nakano[1], Suguru Yabe[1] (1.Japan Agency for Marine-Earth Science and Technology)

[SCG48-P16] Low-frequency earthquakes triggered by teleseismic surface waves by Ryukyu subduction zone.

Ayumi Kinjo[1], *Mamoru Nakamura[1] (1.Faculty of Science, University of the Ryukyus)

[SCG48-P17] Detection of small surface displacement accompanying deep low-frequency tremor in Shikoku region, southwest Japan

*Yutaro Okada[1], Takao Tabei[2] (1.Faculty of Science, Kochi University, 2.Faculty of Science and Technology, Kochi University)

[SCG48-P18] Long-term temporal change in crustal resistivity beneath western Shikoku

*Futoshi Yamashita[1], Yoshimori Honkura[1] (1.National Research Institute for Earth Science and Disaster Resilience)

[SCG48-P19] Slow decay of postseismic deformation compared with aftershocks following the 2011 Tohoku-oki Earthquake

*Yuta Mitsui[1], Shunsuke Morikami[2] (1.Department of Geosciences, Shizuoka University, 2.Formerly at Graduate School of Science and Technology, Shizuoka University)

[SCG48-P20] Serpentinite dehydration in subduction shear zones formed at source depths of slow earthquakes

*Yasushi Mori[1], Miki Shigeno[1], Kohtaro Ujiie[2], Kazuya Noro[2], Tadao Nishiyama[3] (1.Kitakyushu Museum of Natural History and Human History, 2.University of Tsukuba, 3.Kumamoto University)

[SCG48-P21] Earthquake swarms following very low-frequency earthquakes in the central Ryukyu Trench

*Mamoru Nakamura[1] (1.Faculty of Science, University of the Ryukyus)

[SCG48-P22] Seismic imaging in the central Nankai trough, off Shionomisaki to Kii channel

*Yasuyuki Nakamura[1], Shuichi Kodaira[1], Tetsuo No[1], Yuka Kaiho[1], Gou Fujie[1], Seiichi Miura[1], Kazuya Shiraishi[1] (1.Japan Agency for Marine Earth Science and Technology)

[SCG48-P23] Attempt to Detect Intra-plate SSEs Based on F3 Solution of GEONET

*Yusaku Tanaka[1] (1.Earthquake Research Institute)

[SCG48-P24] A new hydrothermal, low to high speed rotary-shearing apparatus: Reproduction of slow/megathrust earthquakes in laboratory

*Takehiro Hirose[1], Wataru Tanikawa[1], Yohei Hamada[1], Keishi Okazaki[1] (1.Kochi Institute for Core Sample Research, Japan Agency for Marine-Earth Science and Technology)

[SCG48-P25] Very low-frequency earthquakes in western Shikoku remotely triggered by the 2016 Mw5.9 off-Kii Peninsula earthquake

*Masatoshi Miyazawa[1] (1.Disaster Prevention Research Institute, Kyoto University)

[SCG48-P26] **Underground structure around source region of slow earthquakes in western Shikoku obtained by receiver function analysis**

Akira Hikita[1], Aitaro Kato[1], *Kazushige Obara[1], Akiko Takeo[1], Takeshi Akuhara[1] (1.Earthquake Research Institute, The University of Tokyo)

[SCG48-P27] Hypocenter determination of deep low frequency tremors beneath the Kii Peninsula by backprojection of seismic array data

*Kodai Sagae[1], Hisashi Nakahara[1], Takeshi Nishimura[1], Kazutoshi Imanishi[2] (1.Graduate School of Science,Tohoku University, 2.National Institute of Advanced Industrial Science and Technology (AIST))

[SCG48-P28] Triggered tremors and stress perturbations due to surface waves

*Ryohei Ikeda[1], Naoki Suda[1] (1.Hiroshima University)

[SCG48-P29] Numerical modeling of long- and shallow slow slip events including shallow region in Hyuganada and western Nankai, Japan

*Takanori Matsuzawa[1], Bunichiro Shibazaki[2] (1.National Research Institute for Earth Science and Disaster Resilience, 2.Building Research Institute)

[SCG48-P30] Further evidence for the influence of a subducting-ridge on the spatial strain accumulation and release pattern in the shallow eastern Nankai Trough, based on VLFE distribution

*Akiko Toh[1], Chen Wan-Jou [2], Doug Dreger[3], Wu-Cheng Chi[2], Satoshi Ide[1] (1.University of Tokyo, 2.Institute of Earth Sciences, Academia Sinica, 3.UC Berkeley)

[SCG48-P31] Evidence for semi-brittle flow in mantle-wedge serpentinites under high pore fluid pressure and their implications for deep low frequency earthquakes

Kengo Kataoka[1], Yurina Nagata[1], *Ken-ichi Hirauchi[1], Ryosuke Oyanagi[2], Atsushi Okamoto[3], Katsuyoshi Michibayashi[4] (1.Department of Geosciences, Faculty of Science, Shizuoka University, 2.Japan Agency for Marine-Earth Science and Technology, 3.Graduate School of Environmental studies, Tohoku University, 4.Department of Earth and Planetary Sciences, Nagoya University)

[SCG48-P32] Spatial distribution of slow slip events off the Boso peninsula from 1996 to 2018 under sparsity constraints

*Ryoko Nakata[1], Hideitsu Hino[2], Tatsu Kuwatani[3,4], Takahiro Akiyama[5], Shoichi Yoshioka[6], Masato Okada[7], Takane Hori[1] (1.Japan Agency for Marine-Earth Science and Technology, 2.The Institute of Statistical Mathematics, 3.Department of Solid Earth Geochemistry, Japan Agency for Marine-Earth Science and Technology, 4.PRESTO, Japan Science and Technology Agency, 5.Graduate School of Science, Kobe University, 6.Research Center for Urban Safety and Security, Kobe University, 7.Graduate School of Frontier Sciences, The University of Tokyo)

[SCG48-P33] Marine electromagnetic observations around a slow earthquake region in the western Nankai trough

*Hiroshi Ichihara[1], Tada-nori Goto[2], Tetsuo Matsuno[3], Noriko Tada[4], Shinya Sato[2] (1.Earthquake and Volcano Research Center, Nagoya University, 2.Graduate School of Engineering, Kyoto University, 3.Ocean Bottom Exploration Center, Kobe University, 4.JAMSTEC)

[SCG48-P34] Dynamics of precipitating injection fronts inside of structured medium

*Yutaka Sumino[1], Shunsuke Tanaka[1], Miyuki Kunihiro[1] (1.Tokyo University of Science)

[SCG48-P35] Permeability changes of simulated low permeable fault rocks induced by intermediate velocity friction test

*Wataru Tanikawa[1] (1.Japan Agency for Marine-Earth Science and Technology, Kochi Instutute for Core Sample Research)

[SCG48-P36] Modified relation between the coupling and tremor rates around the Shikoku region

*Tadafumi Ochi[1] (1.Institute of Earthquake and Volcano Geology, Geological Survey of Japan, The National Institute of Advanced Industrial Science and Technology)

[SCG48-P37] Spatiotemporal distribution of regular and very low-frequency earthquakes in the northern part of the Ryukyu subduction zone

*Youichi Asano[1], Kazuhiko Goto[2], Hiroshi Yakiwara[3], Shuichiro Hirano[3] (1.National Research Institute for Earth Science and Disaster Resilience, 2.Association for the development of earthquake prediction, 3.Nansei-toko Observatory for Earthquakes and Volcanoes, Kagoshima University)

[SCG48-P38] Possible tectonic tremor activities near the VLFE epicenters in the Sanriku-Oki region in 2011

*Hidenobu Takahashi[1], Ryota Hino[1], Yusaku Ohta[1], Naoki Uchida[1], Syuichi Suzuki[1], Masanao Shinohara[2], Takanori Matsuzawa[3] (1.Graduate school of Science Tohoku University , 2.Earthquake Research Institute, University of Tokyo, 3.National Research Institute for Earth Science and Disaster Resilience)

[SCG48-P39] Heterogeneous structure around a region of slow earthquake activity off Ibaraki prefecture along the Japan Trench

*Kimihiro Mochizuki[1], Tomoaki Yamada[1], Masanao Shinohara[1], Ryota Hino[2], Ryosuke Azuma[2], Yoshihiro Ito[3], Yoshio Murai[4], Kenji Uehira[5], Toshinori Sato[6] (1.ERI, Univ. of Tokyo, 2.Graduate School of Science, Tohoku Univ., 3.DPRI, Kyoto Univ., 4.Faculty of Science, Hokkaido Univ., 5.NIED, 6.Graduate School of Science, Chiba Univ.)

[SCG48-P40] Shallow low-frequency tremor triggered by nearby moderate earthquakes off Sanriku

*Sachiko Tanaka[1], Takanori Matsuzawa[1], Youichi Asano[1] (1.National Research Institute for Earth Science and Disaster Resilience)

[SCG48-P41] Slow slip events in the Bungo Channel over 15 years as inferred from GNSS data (1996-2011)

Takatoshi Yokoi[1], *SHINICHI MIYAZAKI[1], Hiromu Sakaue[1], Jun'ichi Fukuda[2] (1.Graduate School of Science, Kyoto University, 2.Earthquake Research Institute, The University of Tokyo)

[SCG48-P42] Investigations of sensor orientation and a possibility of detecting crustal deformation based on accelerometer records of S-net

*Ryota Takagi[1], Naoki Uchida[1], Takashi NAKAYAMA[1], Ryosuke Azuma[1], Akira Ishigami[1], Tomomi Okada[1], Yusaku Ohta[1], Ryota Hino[1] (1.Research Center for Prediction of Earthquakes and Volcanic Eruptions, Graduate School of Science, Tohoku University)

[SCG48-P43] Spatiotemporal variation of released seismic energy from shallow low-frequency tremor in Hyuga-nada, revealed by ocean bottom seismological observation

*Yusuke Yamashita[1], Saki Watanabe[2], Tomoaki Yamada[3], Masanao Shinohara[3], Takeshi Matsushima[2] (1.Disaster Prevention Research Institute, Kyoto University, 2.Institute of Seismology and Volcanology, Kyushu University, 3.Earthquake Research Institute, The University of Tokyo)

[SCG48-P44] Unified description of fast and slow earthquakes using velocity strengthening patches

*So Ozawa[1], Takahiro Hatano[1] (1.Earthquake Research Institute, the University of Tokyo)

[SCG48-P45] The b-value of the earthquake swarm activities accompanied by the Boso slow slip events

*Yuki Noda[1], Hitoshi Hirose[2,1] (1.Department of Planetology, Faculty of Science, Kobe University , 2.Research Center for Urban Safety and Security, Kobe University)

[SCG48-P46] **Three-dimensional thermal modeling associated with subduction of the Philippine Sea plate at the Ryukyu Trench, and its relation to the occurrence of interplate seismic events**

*Nobuaki Suenaga[1], Shoichi Yoshioka[2,1], Yinfeng Ji[3] (1.Graduate School of Science, Kobe University, Japan, 2.Research Center for Urban Safety and Security, Kobe University, Japan, 3.Chinese Academy of Science, Beijin, China)

[E] Poster | S (Solid Earth Sciences)：S-CG Complex & General

5:15 PM - 6:30 PM JST | 8:15 AM - 9:30 AM UTC | Poster Hall International Exhibition Hall8, Makuhari Messe_33

[S-CG48] Science of slow earthquakes: Toward unified understandings of whole earthquake process

convener:Satoshi Ide(Department of Earth an Planetary Science, University of Tokyo), Hitoshi Hirose(Research Center for Urban Safety and Security, Kobe University), Kohtaro Ujiie(Graduate School of Life and Environmental Sciences, University of Tsukuba), Takahiro Hatano(Earthquake Research Institute, University of Tokyo)

[SCG48-P01] Off the Kii Peninsula Shallow Low Frequency Earthquake in 2004 revealed by Ocean Bottom Seismometer

*Koji Tamaribuchi[1], Akio Kobayashi[1], Takahito Nishimiya[1], Satoshi Annoura[2] (1.Meteorological Research Institute, 2.Japan Meteorological Agency)

[SCG48-P02] The development of pressure vessel on gouges for rock deformation at seismic rates under water-saturated conditions

*Wei-Ting Lin[1], Li-Wei Kuo[1], Wen-Jie Wu[1], Jia-Jyun Dong[1], Yi-Hung Huang[2] (1.National Central University, 2.MATSUKI HYDRAULIC INDUSTRIAL CO. LTD)

[SCG48-P03] Spatial variations of shallow very low-frequency earthquake activity along the Nankai Trough based on CMT inversion using the 3D heterogeneous model

*Shunsuke Takemura[1], Takanori Matsuzawa[1], Akemi Noda[1], Takashi Tonegawa[2], Youichi Asano[1], Takeshi Kimura[1], Katsuhiko Shiomi[1] (1.National Research Institute for Earth Science and Disaster Resilience, 2.Japan Agency for Marine-Earth Science and Technology)

[SCG48-P04] Evaluation of Magnitude and Characteristics of Seismicity of Low Frequency Earthquakes in Parkfield

*Miki Aso[1,3], Naofumi Aso[2], Satoshi Ide[1] (1.Department of Earth and Planetary Science, The University of Tokyo, 2.Tokyo Institute of Technology, School of Science, 3.OYO RMS Corporation)

[SCG48-P05] Tectonic tremor catalog in the Tohoku-Hokkaido-Oki region using S-net

*Satoshi Ide[1], Tomoaki Nishikawa[2], Takanori Matsuzawa[3], Kazuaki Ohta[2], Naoki Uchida[4], Takuya NISHIMURA[2] (1.Department of Earth an Planetary Science, University of Tokyo, 2.Disaster Prevention Research Institute, Kyoto University, 3.National Research Institute for Earth Science and Disaster Resilience, 4.Graduate School of Science and International Research Institute of Disaster Science, Tohoku University)

[SCG48-P06] **Spontaneous Slow Slip and Runaway Slip in Laboratory**

*Miki Takahashi[1] (1.Institute of Earthquake and Volcano Geology, Geological Survey of Japan, AIST)

[SCG48-P07] Hydration and amorphization of quartz rocks during high-velocity frictional sliding: An examination of fault gouge from friction experiments of synthetic quartz

*Yuko Onoe[1], Hirotaka Iida[2], Akito Tsutsumi[1], Aki Takigawa[1] (1.Graduate School of Science, Kyoto University, 2.Geothermal Engineering Co., Ltd.)

[SCG48-P08] Constraining S Wave Velocity of the Source Region of Shallow Very Low-Frequency Earthquakes

*Takeshi Akuhara[1], Takashi Tonegawa[2] (1.Earthquake Research Institute, The University of Tokyo, 2.Research and Development center for Earthquake and Tsunami, Japan Agency for Marine-Earth Science and Technology)

[SCG48-P09] **Quantitative relationship between aseismic slip propagation speed and frictional properties**

*Keisuke Ariyoshi[1], Jean-Paul Ampuero[2,3], Roland Burgmann[4], Toru Matsuzawa[5], Akira Hasegawa[5], Ryota Hino[5], Takane Hori[1] (1.Japan Agency for Marine-Earth Science and Technology, 2.Université Côte d'Azur, 3.California Institute of Technology, 4.University of California, Berkeley, 5.Graduate School of Science, Tohoku University)

[SCG48-P10] Comprehensive detection of very low frequency earthquakes off the Pacific coasts of Hokkaido and Tohoku, northeastern Japan

*Satoru Baba[1], Akiko Takeo[1], Kazushige Obara[1], Takanori Matsuzawa[2], Takuto Maeda[3] (1.Earthquake Research Institute, University of Tokyo, 2.National Research Institute for Earth Science and Disaster Resilience, 3.Graduate School of Science and Technology, Hirosaki University)

[SCG48-P11] **Spatio-temporal evolution of long- and short-term slow slip events in the Tokai region, central Japan estimated from a very dense GNSS network, during 1997-2017**

*Hiromu Sakaue[1], Takuya NISHIMURA[2], Jun'ichi Fukuda[3], Teruyuki Kato[4] (1.Graduate School of Science, Kyoto University, 2.Disaster Prevention Research Institute Kyoto University, 3.Earthquake Research Institute,The University of Tokyo, 4.Hot Springs Research Institute of Kanagawa Prefecture)

[SCG48-P12] Broadband excitation of acoustic emission in granular stick-slip : experiments and spectral analyses

*Hidekazu Fukumizu[1], Ikuro Sumita[2] (1.Earth and Environmental Science Course, Division of Natural System, Graduate school of Natural Science and Technology, Kanazawa University, 2.School of Geosciences and Civil Engineering, Kanazawa University)

[SCG48-P13] Episodic tremor and slip silently invades strongly locked megathrust in the Nankai Trough

*Masayuki Kano[1], Aitaro Kato[2], Kazushige Obara[2] (1.Graduate school of science, Tohoku University, 2.Earthquake Research Institute, The University of Tokyo)

[SCG48-P14] Spatial distribution of the electrical resistivity beneath western part of Shikoku Island where long-term SSE events have repeatedly occurred

*Makoto Uyeshima[1], Maki Hata[1], Hiroshi Ichihara[2], Ryokei Yoshimura[3], Koki Aizawa[4] (1.Earthquake Research Institute, The University of Tokyo, 2.Graduate School of Environmental Studies, Nagoya University, 3.Disaster Prevention Research Institute, Kyoto University, 4.Institute of Seismology and Volcanology, Faculty of Sciences, Kyushu University)

[SCG48-P15] Variations of scaling relationships for shallow tremor observed along the Nankai trough

*Masaru Nakano[1], Suguru Yabe[1] (1.Japan Agency for Marine-Earth Science and Technology)

[SCG48-P16] Low-frequency earthquakes triggered by teleseismic surface waves by Ryukyu subduction zone.

Ayumi Kinjo[1], *Mamoru Nakamura[1] (1.Faculty of Science, University of the Ryukyus)

[SCG48-P17] Detection of small surface displacement accompanying deep low-frequency tremor in Shikoku region, southwest Japan

*Yutaro Okada[1], Takao Tabei[2] (1.Faculty of Science, Kochi University, 2.Faculty of Science and Technology, Kochi University)

[SCG48-P18] Long-term temporal change in crustal resistivity beneath western Shikoku

*Futoshi Yamashita[1], Yoshimori Honkura[1] (1.National Research Institute for Earth Science and Disaster Resilience)

[SCG48-P19] Slow decay of postseismic deformation compared with aftershocks following the 2011 Tohoku-oki Earthquake

*Yuta Mitsui[1], Shunsuke Morikami[2] (1.Department of Geosciences, Shizuoka University, 2.Formerly at Graduate School of Science and Technology, Shizuoka University)

[SCG48-P20] Serpentinite dehydration in subduction shear zones formed at source depths of slow earthquakes

*Yasushi Mori[1], Miki Shigeno[1], Kohtaro Ujiie[2], Kazuya Noro[2], Tadao Nishiyama[3] (1.Kitakyushu Museum of Natural History and Human History, 2.University of Tsukuba, 3.Kumamoto University)

[SCG48-P21] Earthquake swarms following very low-frequency earthquakes in the central Ryukyu Trench

*Mamoru Nakamura[1] (1.Faculty of Science, University of the Ryukyus)

[SCG48-P22] Seismic imaging in the central Nankai trough, off Shionomisaki to Kii channel

*Yasuyuki Nakamura[1], Shuichi Kodaira[1], Tetsuo No[1], Yuka Kaiho[1], Gou Fujie[1], Seiichi Miura[1], Kazuya Shiraishi[1] (1.Japan Agency for Marine Earth Science and Technology)

[SCG48-P23] Attempt to Detect Intra-plate SSEs Based on F3 Solution of GEONET

*Yusaku Tanaka[1] (1.Earthquake Research Institute)

[SCG48-P24] A new hydrothermal, low to high speed rotary-shearing apparatus: Reproduction of slow/megathrust earthquakes in laboratory

*Takehiro Hirose[1], Wataru Tanikawa[1], Yohei Hamada[1], Keishi Okazaki[1] (1.Kochi Institute for Core Sample Research, Japan Agency for Marine-Earth Science and Technology)

[SCG48-P25] Very low-frequency earthquakes in western Shikoku remotely triggered by the 2016 Mw5.9 off-Kii Peninsula earthquake

*Masatoshi Miyazawa[1] (1.Disaster Prevention Research Institute, Kyoto University)

[SCG48-P26] **Underground structure around source region of slow earthquakes in western Shikoku obtained by receiver function analysis**

Akira Hikita[1], Aitaro Kato[1], *Kazushige Obara[1], Akiko Takeo[1], Takeshi Akuhara[1] (1.Earthquake Research Institute, The University of Tokyo)

[SCG48-P27] Hypocenter determination of deep low frequency tremors beneath the Kii Peninsula by backprojection of seismic array data

*Kodai Sagae[1], Hisashi Nakahara[1], Takeshi Nishimura[1], Kazutoshi Imanishi[2] (1.Graduate School of Science,Tohoku University, 2.National Institute of Advanced Industrial Science and Technology (AIST))

[SCG48-P28] Triggered tremors and stress perturbations due to surface waves

*Ryohei Ikeda[1], Naoki Suda[1] (1.Hiroshima University)

[SCG48-P29] Numerical modeling of long- and shallow slow slip events including shallow region in Hyuganada and western Nankai, Japan

*Takanori Matsuzawa[1], Bunichiro Shibazaki[2] (1.National Research Institute for Earth Science and Disaster Resilience, 2.Building Research Institute)

[SCG48-P30] Further evidence for the influence of a subducting-ridge on the spatial strain accumulation and release pattern in the shallow eastern Nankai Trough, based on VLFE distribution

*Akiko Toh[1], Chen Wan-Jou [2], Doug Dreger[3], Wu-Cheng Chi[2], Satoshi Ide[1] (1.University of Tokyo, 2.Institute of Earth Sciences, Academia Sinica, 3.UC Berkeley)

[SCG48-P31] Evidence for semi-brittle flow in mantle-wedge serpentinites under high pore fluid pressure and their implications for deep low frequency earthquakes

Kengo Kataoka[1], Yurina Nagata[1], *Ken-ichi Hirauchi[1], Ryosuke Oyanagi[2], Atsushi Okamoto[3], Katsuyoshi Michibayashi[4] (1.Department of Geosciences, Faculty of Science, Shizuoka University, 2.Japan Agency for Marine-Earth Science and Technology, 3.Graduate School of Environmental studies, Tohoku University, 4.Department of Earth and Planetary Sciences, Nagoya University)

[SCG48-P32] Spatial distribution of slow slip events off the Boso peninsula from 1996 to 2018 under sparsity constraints

*Ryoko Nakata[1], Hideitsu Hino[2], Tatsu Kuwatani[3,4], Takahiro Akiyama[5], Shoichi Yoshioka[6], Masato Okada[7], Takane Hori[1] (1.Japan Agency for Marine-Earth Science and Technology, 2.The Institute of Statistical Mathematics, 3.Department of Solid Earth Geochemistry, Japan Agency for Marine-Earth Science and Technology, 4.PRESTO, Japan Science and Technology Agency, 5.Graduate School of Science, Kobe University, 6.Research Center for Urban Safety and Security, Kobe University, 7.Graduate School of Frontier Sciences, The University of Tokyo)

[SCG48-P33] Marine electromagnetic observations around a slow earthquake region in the western Nankai trough

*Hiroshi Ichihara[1], Tada-nori Goto[2], Tetsuo Matsuno[3], Noriko Tada[4], Shinya Sato[2] (1.Earthquake and Volcano Research Center, Nagoya University, 2.Graduate School of Engineering, Kyoto University, 3.Ocean Bottom Exploration Center, Kobe University, 4.JAMSTEC)

[SCG48-P34] Dynamics of precipitating injection fronts inside of structured medium

*Yutaka Sumino[1], Shunsuke Tanaka[1], Miyuki Kunihiro[1] (1.Tokyo University of Science)

[SCG48-P35] Permeability changes of simulated low permeable fault rocks induced by intermediate velocity friction test

*Wataru Tanikawa[1] (1.Japan Agency for Marine-Earth Science and Technology, Kochi Instutute for Core Sample Research)

[SCG48-P36] Modified relation between the coupling and tremor rates around the Shikoku region

*Tadafumi Ochi[1] (1.Institute of Earthquake and Volcano Geology, Geological Survey of Japan, The National Institute of Advanced Industrial Science and Technology)

[SCG48-P37] Spatiotemporal distribution of regular and very low-frequency earthquakes in the northern part of the Ryukyu subduction zone

*Youichi Asano[1], Kazuhiko Goto[2], Hiroshi Yakiwara[3], Shuichiro Hirano[3] (1.National Research Institute for Earth Science and Disaster Resilience, 2.Association for the development of earthquake prediction, 3.Nansei-toko Observatory for Earthquakes and Volcanoes, Kagoshima University)

[SCG48-P38] Possible tectonic tremor activities near the VLFE epicenters in the Sanriku-Oki region in 2011

*Hidenobu Takahashi[1], Ryota Hino[1], Yusaku Ohta[1], Naoki Uchida[1], Syuichi Suzuki[1], Masanao Shinohara[2], Takanori Matsuzawa[3] (1.Graduate school of Science Tohoku University , 2.Earthquake Research Institute, University of Tokyo, 3.National Research Institute for Earth Science and Disaster Resilience)

[SCG48-P39] Heterogeneous structure around a region of slow earthquake activity off Ibaraki prefecture along the Japan Trench

*Kimihiro Mochizuki[1], Tomoaki Yamada[1], Masanao Shinohara[1], Ryota Hino[2], Ryosuke Azuma[2], Yoshihiro Ito[3], Yoshio Murai[4], Kenji Uehira[5], Toshinori Sato[6] (1.ERI, Univ. of Tokyo, 2.Graduate School of Science, Tohoku Univ., 3.DPRI, Kyoto Univ., 4.Faculty of Science, Hokkaido Univ., 5.NIED, 6.Graduate School of Science, Chiba Univ.)

[SCG48-P40] Shallow low-frequency tremor triggered by nearby moderate earthquakes off Sanriku

*Sachiko Tanaka[1], Takanori Matsuzawa[1], Youichi Asano[1] (1.National Research Institute for Earth Science and Disaster Resilience)

[SCG48-P41] Slow slip events in the Bungo Channel over 15 years as inferred from GNSS data (1996-2011)

Takatoshi Yokoi[1], *SHINICHI MIYAZAKI[1], Hiromu Sakaue[1], Jun'ichi Fukuda[2] (1.Graduate School of Science, Kyoto University, 2.Earthquake Research Institute, The University of Tokyo)

[SCG48-P42] Investigations of sensor orientation and a possibility of detecting crustal deformation based on accelerometer records of S-net

*Ryota Takagi[1], Naoki Uchida[1], Takashi NAKAYAMA[1], Ryosuke Azuma[1], Akira Ishigami[1], Tomomi Okada[1], Yusaku Ohta[1], Ryota Hino[1] (1.Research Center for Prediction of Earthquakes and Volcanic Eruptions, Graduate School of Science, Tohoku University)

[SCG48-P43] Spatiotemporal variation of released seismic energy from shallow low-frequency tremor in Hyuga-nada, revealed by ocean bottom seismological observation

*Yusuke Yamashita[1], Saki Watanabe[2], Tomoaki Yamada[3], Masanao Shinohara[3], Takeshi Matsushima[2] (1.Disaster Prevention Research Institute, Kyoto University, 2.Institute of Seismology and Volcanology, Kyushu University, 3.Earthquake Research Institute, The University of Tokyo)

[SCG48-P44] Unified description of fast and slow earthquakes using velocity strengthening patches

*So Ozawa[1], Takahiro Hatano[1] (1.Earthquake Research Institute, the University of Tokyo)

[SCG48-P45] The b-value of the earthquake swarm activities accompanied by the Boso slow slip events

*Yuki Noda[1], Hitoshi Hirose[2,1] (1.Department of Planetology, Faculty of Science, Kobe University , 2.Research Center for Urban Safety and Security, Kobe University)

[SCG48-P46] **Three-dimensional thermal modeling associated with subduction of the Philippine Sea plate at the Ryukyu Trench, and its relation to the occurrence of interplate seismic events**

*Nobuaki Suenaga[1], Shoichi Yoshioka[2,1], Yinfeng Ji[3] (1.Graduate School of Science, Kobe University, Japan, 2.Research Center for Urban Safety and Security, Kobe University, Japan, 3.Chinese Academy of Science, Beijin, China)

[E] Poster | M (Multidisciplinary and Interdisciplinary)：M-GI General Geosciences, Information Geosciences & Simulations

10:45 AM - 12:15 PM JST | 1:45 AM - 3:15 AM UTC | Poster Hall International Exhibition Hall8, Makuhari Messe_11

[M-GI30] Data assimilation: A fundamental approach in geosciences

convener:Shin ya Nakano(The Institute of Statistical Mathematics), Yosuke Fujii(Meteorological Research Institute, Japan Meteorological Agency), SHINICHI MIYAZAKI(Graduate School of Science, Kyoto University), Takemasa Miyoshi(RIKEN)

[MGI30-P01] Superposition of atmospheric states using information redundancy for Numerical Weather Prediction

*Toshiyuki Ishibashi[1] (1.Meteorological Research Institute/Japan Meteorological Agency)

[MGI30-P02] **Numerical Weather Prediction Experiments using a Coupled Atmosphere-Ocean Data Assimilation System in JMA/MRI** (3)

*Toshiyuki Ishibashi[1], Takeshi Iriguchi[1], Yosuke Fujii[1], Tamaki Yasuda[1], Yuhei Takaya[1], Naoki Saito[1], Toshikazu Onogi[1] (1.Meteorological Research Institute/Japan Meteorological Agency)

[MGI30-P03] **Accurate estimation of posterior error covariance in a 4D-Var inverse analysis**

*Yosuke Niwa[1,2], Yosuke Fujii[2,3] (1.National Institute for Environmental Studies, 2.Meteorological Research Institute, Japan Meteorological Agency, 3.The Institute of Statistical Mathematics)

[MGI30-P04] Assimilation CO_2 concentration data in the Kanto region using AIST-MM model and for the estimation of CO_2 emissions

*Yutaka Arai[1], Ryoichi Imasu[1], Hiroaki Kondo[2], Yosuke Niwa[3] (1.Atmosphere and Ocean Research Institute, The University of Tokyo, 2.National Institute of Advanced Industrial Science and Technology, 3.National Institute for Environmental Studies, Independent Administrative Institutions)

[MGI30-P05] **Application of data assimilation method on parameter estimation of flow and nutrient behavior in watershed model**

*Yosuke Horie[1] (1.Nippon Koei Co., Ltd.)

[MGI30-P06] Bayesian inference of grain growth prediction via multi-phase-field models

*Shin-ichi Ito[1], Hiromichi Nagao[1], Takashi Kurokawa[1], Tadashi Kasuya[1], Junya Inoue[1] (1.The University of Tokyo)

[MGI30-P07] GNSS data assimilation for the Bungo channel Long-term SSEs using Ensemble Kalman Filter (EnKF)

*Megumi Fujita[1], Takuya NISHIMURA[2], Kazuro Hirahara[3], SHINICHI MIYAZAKI[1] (1.Graduate School of Science , Kyoto University, 2.Disaster Prevention Research Institute, Kyoto University, 3.Institute of Education, Research and Regional Cooperation for crisis Management Shikoku, Kagawa University)

[MGI30-P08] A data assimilation library with Python for parallel computing

*Shin ya Nakano[1], Yuya Ariyoshi[2], Tomoyuki Higuchi[1] (1.The Institute of Statistical Mathematics, 2.Faculty of Engineering, Nippon Bunri University)

[E] Poster | M (Multidisciplinary and Interdisciplinary)：M-GI General Geosciences, Information Geosciences & Simulations

5:15 PM - 6:30 PM JST | 8:15 AM - 9:30 AM UTC | Poster Hall International Exhibition Hall8, Makuhari Messe_37

[M-GI30] Data assimilation: A fundamental approach in geosciences

convener:Shin ya Nakano(The Institute of Statistical Mathematics), Yosuke Fujii(Meteorological Research Institute, Japan Meteorological Agency), SHINICHI MIYAZAKI(Graduate School of Science, Kyoto University), Takemasa Miyoshi(RIKEN)

[MGI30-P01] Superposition of atmospheric states using information redundancy for Numerical Weather Prediction

*Toshiyuki Ishibashi[1] (1.Meteorological Research Institute/Japan Meteorological Agency)

[MGI30-P02] **Numerical Weather Prediction Experiments using a Coupled Atmosphere-Ocean Data Assimilation System in JMA/MRI** (3)

*Toshiyuki Ishibashi[1], Takeshi Iriguchi[1], Yosuke Fujii[1], Tamaki Yasuda[1], Yuhei Takaya[1], Naoki Saito[1], Toshikazu Onogi[1] (1.Meteorological Research Institute/Japan Meteorological Agency)

[MGI30-P03] **Accurate estimation of posterior error covariance in a 4D-Var inverse analysis**

*Yosuke Niwa[1,2], Yosuke Fujii[2,3] (1.National Institute for Environmental Studies, 2.Meteorological Research Institute, Japan Meteorological Agency, 3.The Institute of Statistical Mathematics)

[MGI30-P04] Assimilation CO_2 concentration data in the Kanto region using AIST-MM model and for the estimation of CO_2 emissions

*Yutaka Arai[1], Ryoichi Imasu[1], Hiroaki Kondo[2], Yosuke Niwa[3] (1.Atmosphere and Ocean Research Institute, The University of Tokyo, 2.National Institute of Advanced Industrial Science and Technology, 3.National Institute for Environmental Studies, Independent Administrative Institutions)

[MGI30-P05] **Application of data assimilation method on parameter estimation of flow and nutrient behavior in watershed model**

*Yosuke Horie[1] (1.Nippon Koei Co., Ltd.)

[MGI30-P06] Bayesian inference of grain growth prediction via multi-phase-field models

*Shin-ichi Ito[1], Hiromichi Nagao[1], Takashi Kurokawa[1], Tadashi Kasuya[1], Junya Inoue[1] (1.The University of Tokyo)

[MGI30-P07] GNSS data assimilation for the Bungo channel Long-term SSEs using Ensemble Kalman Filter (EnKF)

*Megumi Fujita[1], Takuya NISHIMURA[2], Kazuro Hirahara[3], SHINICHI MIYAZAKI[1] (1.Graduate School of Science , Kyoto University, 2.Disaster Prevention Research Institute, Kyoto University, 3.Institute of Education, Research and Regional Cooperation for crisis Management Shikoku, Kagawa University)

[MGI30-P08] A data assimilation library with Python for parallel computing

*Shin ya Nakano[1], Yuya Ariyoshi[2], Tomoyuki Higuchi[1] (1.The Institute of Statistical Mathematics, 2.Faculty of Engineering, Nippon Bunri University)

[E] Poster | M (Multidisciplinary and Interdisciplinary)：M-TT Technology & Techniques

1:45 PM - 3:15 PM JST | 4:45 AM - 6:15 AM UTC | Poster Hall International Exhibition Hall8, Makuhari Messe_6

[M-TT45] Cryoseismology - a new proxy for detecting surface environmental variations of the Earth -

convener:Genti Toyokuni(Research Center for Prediction of Earthquakes and Volcanic Eruptions, Graduate School of Science, Tohoku University), Masaki Kanao(National Institute of Polar Research), Seiji Tsuboi(JAMSTEC, Center for Earth Information Science and Technology)

[MTT45-P01] Application of neural network and theoretical seismograms as training data to locate ice quakes

*Seiji Tsuboi[1], DAISUKE SUGIYAMA[1] (1.JAMSTEC, Center for Earth Information Science and Technology)

[MTT45-P02] **P-wave tomography beneath Greenland**

*Takaya Matsuno[1], Genti Toyokuni[1], Dapeng Zhao[1] (1.Research Center for Prediction of Earthquakes and Volcanic Eruptions, Graduate School of Science, Tohoku University)

[MTT45-P03] **Seismic observations in Greenland by a joint USA and Japanese GLISN team (2011–2018)**

*Genti Toyokuni[1], Masaki Kanao[2], Seiji Tsuboi[3], Yoko Tono[4] (1.RCPEVE, Tohoku Univ., 2.NIPR, 3.JAMSTEC, 4.ERI, Univ. Tokyo)

[E] Poster | M (Multidisciplinary and Interdisciplinary)：M-TT Technology & Techniques

5:15 PM - 6:30 PM JST | 8:15 AM - 9:30 AM UTC | Poster Hall International Exhibition Hall8, Makuhari Messe_40

[M-TT45] Cryoseismology - a new proxy for detecting surface environmental variations of the Earth -

convener:Genti Toyokuni(Research Center for Prediction of Earthquakes and Volcanic Eruptions, Graduate School of Science, Tohoku University), Masaki Kanao(National Institute of Polar Research), Seiji Tsuboi(JAMSTEC, Center for Earth Information Science and Technology)

[MTT45-P01] Application of neural network and theoretical seismograms as training data to locate ice quakes

*Seiji Tsuboi[1], DAISUKE SUGIYAMA[1] (1.JAMSTEC, Center for Earth Information Science and Technology)

[MTT45-P02] **P-wave tomography beneath Greenland**

*Takaya Matsuno[1], Genti Toyokuni[1], Dapeng Zhao[1] (1.Research Center for Prediction of Earthquakes and Volcanic Eruptions, Graduate School of Science, Tohoku University)

[MTT45-P03] **Seismic observations in Greenland by a joint USA and Japanese GLISN team (2011–2018)**

*Genti Toyokuni[1], Masaki Kanao[2], Seiji Tsuboi[3], Yoko Tono[4] (1.RCPEVE, Tohoku Univ., 2.NIPR, 3.JAMSTEC, 4.ERI, Univ. Tokyo)

[E] Poster | P (Space and Planetary Sciences)：P-PS Planetary Sciences

Wed. May 29, 2019 10:45 AM - 12:15 PM JST | Wed. May 29, 2019 1:45 AM - 3:15 AM UTC | Poster Hall International Exhibition Hall8, Makuhari Messe_2

[P-PS02] Regolith Science

convener:Koji Wada(Planetary Exploration Research Center, Chiba Institute of Technology), Akiko Nakamura(Graduate School of Science, Kobe University), Patrick Michel(Observatoire De La Cote D'Azur), Kevin John Walsh(Southwest Research Institute Boulder)

Recent planetary explorations have revealed that almost all solid bodies in the solar system are covered with small particles, called regolith. The surface geology, especially regolith behavior on the surfaces of solid bodies, becomes increasingly more important as represented by Hayabusa mission and other on-going and planned sample-return missions such as Hayabusa2, OSIRIS-REx, and MMX.

For fully understanding the regolith science, it is required to know and compare the regolith conditions on various celestial bodies, from asteroids to planets, with various methods.

Therefore, this session welcomes broad topics related to regolith on various celestial bodies, such as asteroids, comets, the Moon, the martian moons, Mars, etc. Papers on the formation, evolution, and alteration processes of regolith particles and regolith systems on the surface of planetary bodies, remote and in-situ observational results and techniques, analyses and results of returned samples, and laboratory, numerical, and theoretical studies on the fundamental physical and chemical processes are all welcome.

Note that what we call regolith is not just fine grains: all kinds of materials (more or less loose) that lie on the surface, from cobbles to finer grains, are our targets.

[PPS02-P01] Abrasion experiments of mineral and meteorite grains: Dependence of particle size and vibration rate on abrasion rate and its application to Itokawa and lunar regolith particles.

*Hirotaka Yamaguchi[1], Akira Tsuchiyama[1], Akiko Nakamura[2] (1.National University Corporation, Kyoto University, 2.National University Corporation,Kobe University)

[PPS02-P02] Measurements of adhesive force of meteorite powders using centrifugal method

*Yuuya Nagaashi[1], Akiko Nakamura[1] (1.Kobe University)

[PPS02-P03] Laboratory impact penetration experiments conducted at simulated reduced gravity

*Akiko Nakamura[1], Kana Morizono[2], Yuuya Nagaashi[1] (1.Graduate School of Science, Kobe University, 2.Faculty of Science, Kobe University)

[PPS02-P04] MARAUDERS: Using instrumented nano-impactors to probe the icy properties of Lunar permanently shadowed regions

*Ronald Ballouz[1], Sarah T Crites[2], Naoya Ozaki[2], Shun Arahata[3], Nicola Baresi[2], Ralf Bolden, Onur Celik[4,2], Yu Himeno[3], Lucie Riu[2], Kevin J Walsh[5] (1.Lunar and Planetary Lab, University of Arizona, Tucson, AZ, USA, 2.Institute of Space and Astronautical Science, Sagamihara, Japan, 3.University of Tokyo, Tokyo, Japan, 4.Sokendai Graduate University, Japan, 5.Southwest Research Institute, Boulder, CO, USA)

[PPS02-P05] Surface size-frequency distribution of accumulating boulders using discrete element simulations of spherical particles in 3D

*Hiroshi Kikuchi[1], Hideaki Miyamoto[1] (1.The University of Tokyo)

[PPS02-P06] Experimental Study to Determine the Best Compression Ratio of High-Resolution Images of Small Bodies for the Martian Moons eXploration (MMX) Mission

*Yuta Shimizu[1], Hiroaki Kamiyoshihara[1], Takafumi Niihara[1], Hideaki Miyamoto[1] (1.University of Tokyo)

Abrasion experiments of mineral and meteorite grains: Dependence of particle size and vibration rate on abrasion rate and its application to Itokawa and lunar regolith particles.

*Hirotaka Yamaguchi[1], Akira Tsuchiyama[1], Akiko Nakamura[2]

1. National University Corporation, Kyoto University, 2. National University Corporation,Kobe University

Rounded edges were found in some regolith particles collected from asteroid Itokawa [1] and Moon [2]. These particles should be formed by mechanical abrasion [1]. Seismic-induced grain motion by micrometeoroid impacts [1] and YORP effect [3] were proposed for the abrasion process on Itokawa. However, it is not clear how these processes actually work on the surfaces of the airless celestial bodies.

In order to understand detailed process of the abrasion, our research group have carried out abrasion experiments using mineral, rock and meteorite grains (grain size: 1-2 mm) [4]. Samples used were quartz, olivine, corundum, marble, L5 chondrite meteorite (Sayh al Uhaymir 001) and CM chondrite meteorite (Murchison). These particles were put into a vessel of 10 mL with the filling ratio of ~50 % and the sample was vibrated with the rate from 1000 to 3000 rpm using a multi-beads-shocker (YASUIKIKAI Co.). The proportion of powder (<250 μm) produced by vibration at first 1 min., ΔP_1, was adopted as the measure of abrasion and its dependence of the vibration rate and the sample strength was examined. However, the particle size used in the experiments (1-2 mm) is larger than Itokawa particles (< a few hundred μm). In addition, the vibration rates used in the experiments are larger than those estimated for Itokawa(~100 rpm) and Moon (~700 rpm) by considering the maximum seismic acceleration due to micrometeoroidimpacts onto their surface [5]. In the present study, therefore, we conducted new experiments with different parameters such as particle size and vibration rate using the same experimental procedure as [4]. In the present experiments, we used quartz grains for examining the effect of packing ratio in the vessel (Exp-1), particle size (Exp-2), mixing ratio of large and small particles (Exp-3). The effect of lower vibration rate (100 - 1000 rpm) was examined using olivine and basalt as well as quartz (Exp-4). Experiments using basalt at higher vibration rates were also made.

We obtained following results. Exp-1: $\Delta P_1$was constant in a wide range of the filling rate except for the filling rate of 2/3, where ΔP_1showed a peak value. Exp-2: $\Delta P_1$is proportional to the particle size. Exp-3: When the proportion of large particles is larger than 25%, $\Delta P_1$is almost constant and the same as $\Delta P_1$for the large particles. Exp-4: In the previous experiments, ΔP_1increases with the vibration rate with the power of 1.1-2.9 for large vibration rates (>~1000 rpm) [4] while the power becomes smaller (0.67-0.77) for smaller vibration rates (<~1000 rpm). This result shows that the abrasion mode changed at ~1000 rpm. In order to understand abrasion modes, SEM observation of powder particles produced in the abrasion experiments were also made. It was found that chipping of particle edges occurred at low vibration rate (~100 rpm) and the proportion of gradual wearing on the whole particle surface gradually increased as the vibration rate increased.

We estimated the amount of abrasion of Itokawa and lunar regolith particles in a regolith layer by impact based on the present experiments. ΔP_1values of basalt at 100 and 700 rpm, which corresponding to Itokawa and Moon [4], are ~0.1 %and ~1 %, respectively (Exp-4). If we consider the size of Itokawa and Moon particle (~100 μm), ΔP_1on Itokawa and Moon should be ~0.01%and ~0.1%, respectively(Exp-2). These values are larger than those estimated from the previous experiments [4] by the order of about 1.

©2019. Japan Geoscience Union. All Right Reserved.

The present results suggest that abrasion is possible on the Moon and may occur on Itokawa as well.

[1] Tsuchiyama et al. 2011. Science, 333, 1125-1128.

[2] Sakurama et al. 2016. JpGU, Abstract, PPS03-13.

[3] Connolly et al. 2015. Earth Planet and Space, 67: 12.

[4] Tsuchiyama et al. 2018. LPSC, Abstract 1844.

[5] Yasui et al. 2015. Icarus, 260: 320-331.

©2019. Japan Geoscience Union. All Right Reserved.

Measurements of adhesive force of meteorite powders using centrifugal method

*Yuuya Nagaashi[1], Akiko Nakamura[1]

1. Kobe University

Introduction: Layer of fine particles in the laboratory shows fluffy structure owing to interparticle force (e.g., Kiuchi and Nakamura, 2014). On small bodies, interparticle forces are thought to be dominant compared to gravitational force for small particles. Fast rotators spin in excess of what gravity alone could hold together were shown to be explained by cohesive force between constituent particles (Sánchez & Scheeres, 2016). Measurements of cohesive force between micron-size spherical silica particles using an atomic force microscope cantilever (Heim et al., 1999) showed that the results agree with predictions of the JKR model (Johnson et al., 1971). On the other hand, measurements of cohesive force between 50 or 100 μm glass beads and a glass plate using centrifugal method showed that the results are by several orders of magnitude smaller than predictions of the JKR theory (Nagaashi et al., 2018). In addition, it was also shown that ~ 70 μm irregularly-shaped silica and alumina grains have the range of adhesive force similar to the glass beads, indicating that the adhesive force of the spherical and the irregular particles used in the measurement is dependent not on the macroscopic shape but on the microscopic surface roughness. However, it is not clear whether the adhesive force of the particles that actually form the asteroids is similar to those of silica grains. Measurements of adhesive force of meteorite powders will bring important knowledge of adhesive force of the asteroid-forming particles for understanding physical processes occurring on asteroids.

Experimental method: In this study, we used centrifugal method as in our previous study (Nagaashi et al., 2018) in order to measure cohesive or adhesive force between a particle and a plate. This method can directly measure the cohesive or adhesive force of many particles at the same time, which enables us to statistically analyze the results. Additionally, it can also deal with irregularly shaped particles. The measurements were conducted for carbonaceous chondrite (CV3: Allende, CM2: Murchison), ordinary chondrite (LL3.5: NWA 539, LL5: NWA 1794, LL6: NWA 542), and Eucrite (Millbillillie) powders of median diameter ~ 50 μm. We discretely increased the centrifugal acceleration from 10g to 5000g (g: the Earth's gravitational acceleration) and took optical microscope images of the same location of the plate before and after applying centrifugal force at each centrifugal acceleration. We determined the range of centrifugal acceleration within which the particle separated from the plate based on the microscope images and estimated the cohesive or adhesive force between the particle and the plate. More detail description of the procedure is described in Nagaashi et al. (2018).

Results: As compared with the JKR adhesion force $F_{ad} = 3\pi\gamma R$ (γ: surface energy, R: reduced radius of particle) for a spherical particle of silica composition, we calculated the effective surface energy of particles which reproduces the measurement value, and compared the results of each type of meteorite powders. Similar to the previous results described in the above (Nagaashi et al., 2018), the measurements of meteorite powders showed a wide range of adhesive force distributions over several orders of magnitude for all measured meteorite types. In addition, we found that the effective surface energy of Allende and Murchison meteorite particles were several times smaller than those for the particles of the other meteorite types. There is no difference in the axial ratio of each type of meteorite powders, and therefore this is likely due to differences in material composition or micro-topography of the particles.

©2019. Japan Geoscience Union. All Right Reserved.

©2019. Japan Geoscience Union. All Right Reserved.

Laboratory impact penetration experiments conducted at simulated reduced gravity

*Akiko Nakamura[1], Kana Morizono[2], Yuuya Nagaashi[1]

1. Graduate School of Science, Kobe University, 2. Faculty of Science, Kobe University

Small bodies are covered with a layer of regolith made up of particles of various sizes. It is important to understand the interactions that occur with surface regolith when a spacecraft lands on or when a block secondarily collide with the regolith layer at low velocity. Penetration depth of an impactor in granular layer was investigated under Earth’ s gravity and an empirical relationship between the drop height and penetration depth was shown to reproduce the experimental results for various granular materials (Uehara et al., 2013). Deceleration of spherical impactor in granular layer was experimentally and theoretically investigated and deceleration formulae were proposed (Katsuragi and Durian 2007, Nakamura et al., 2013; Katsuragi and Durian 2013). On the other hand, interactions of spheres with simulated regolith have been studied at reduced gravity and micro-gravity conditions (Murdoch et al., 2016; Brisset et al., 2018). However, more data of penetration depth of impactor are required to establish quantitative understanding of the penetration process in regolith under low gravity.

We conducted laboratory low-velocity impact experiments of a sphere into granular layer at reduced gravity. Impactor was a glass sphere with a diameter of 16.7 mm and granular layer consisted of glass beads with a diameter of 1 mm. The glass beads were packed in a bucket having a diameter of 15 cm and a depth of 15 cm. The bucket was hung with three constant load springs. The bucket was fixed with two electromagnets, and when the electromagnet was switched off, it dropped vertically downward with the gravity reduced. The simulated reduced gravity level was monitored by an accelerometer placed in a bucket and found to be on average 0.26 G. A plastic straw with horizontal line drawing was glued to the glass sphere. The glass sphere collided with the glass bead layer at a relative velocity between 2 and 4 ms $^{-1}$. The penetration process of the glass sphere with the straw was imaged at 240 fps by a camera attached to the bucket. The final depth of the glass sphere was found to be systematically deeper than the depth found in the experiment conducted at 1 G.

Keywords: regolith, low gravity, impact

©2019. Japan Geoscience Union. All Right Reserved.

MARAUDERS: Using instrumented nano-impactors to probe the icy properties of Lunar permanently shadowed regions

*Ronald Ballouz[1], Sarah T Crites[2], Naoya Ozaki[2], Shun Arahata[3], Nicola Baresi[2], Ralf Bolden, Onur Celik[4,2], Yu Himeno[3], Lucie Riu[2], Kevin J Walsh[5]

1. Lunar and Planetary Lab, University of Arizona, Tucson, AZ, USA, 2. Institute of Space and Astronautical Science, Sagamihara, Japan, 3. University of Tokyo, Tokyo, Japan, 4. Sokendai Graduate University, Japan, 5. Southwest Research Institute, Boulder, CO, USA

The Mini lAndeRs And boUncers Deployed for Exploration and Regolith Science (MARAUDERS) is a small satellite concept that aims to characterize the surface and volatile properties of regolith in permanently shadowed regions (PSRs) around the Moon's poles. Large PSRs are cold enough to trap scientifically and economically valuable volatiles such as water ice. However, despite ongoing studies, the distribution, abundance, and physical phase of volatiles at the Moon's poles remains elusive [1]. *In-situ* measurements are required to conclusively determine the geotechnical and physical properties of lunar polar volatiles. To address these needs, the MARAUDERS team is currently developing a technique using instrumented nano-impactors to determine the mechanical properties of regolith at the impact point.

Small spacecraft equipped with penetrators or inertial measurement units (IMU) can characterize the strength and structure of the planetary surface that they impact. Early space exploration used penetrometers to determine the surface properties of the Moon and Mars before the arrival of astronauts and rovers. In recent decades, spacecraft equipped with IMUs characterized the surface of Titan [1], and determined the sub-surface stratification of ice and rock on the comet 67P/C-G [2]. While this technique is unable to relay the detailed mineralogical and elemental composition at the impact point, it obtains a first-order structural knowledge of potentially hazardous surfaces and sub-surfaces that cannot be obtained through remote sensing. This is highly relevant for PSRs due to extreme environmental conditions such as the lack of solar illumination, cold temperatures, and challenging communications.

Here, we present preliminary analysis on the instrument capabilities based on the potential deployment scenarios to PSRs, and the possible mechanical properties of the regolith found within these regions (Fig. 1). We present a computational study of the varying response of an instrumented impactor impacting regolith with variable i) water ice content (0-10%), ii) impactor speeds (50-250 m/s], and iii) impact angles (45-90˚), using a discrete element method code [4]. Furthermore, we analyse the ejecta properties and resulting crater morphology in order to gain a better understanding of impact processes on icy bodies. Our next steps will be to conduct laboratory impact experiments using prototypes of our instrumented impactors to calibrate the impact response on lunar simulant with variable water-ice content.

References:

1. Lorenz, R. et al. (1994) Meas. Sci. Technol. 5, 1033-1041

2. Biele, J. et al. (2016), Science, 349, 6247.

3. Holsapple, K.A. (1994) LPSC 25, 559.

©2019. Japan Geoscience Union. All Right Reserved.

4. Richardson, D.C. et al. (2011) Icarus, 212, 427–437.

Acknowledgements:

This material is based upon work supported by ISAS/JAXA’s start-up fund for international collaborations, the Aerospace Project Research Associate Program, and the International Top Young Fellow Program.

Keywords: Moon, Permanently Shadowed Regions, Volatiles, Regolith Characterization

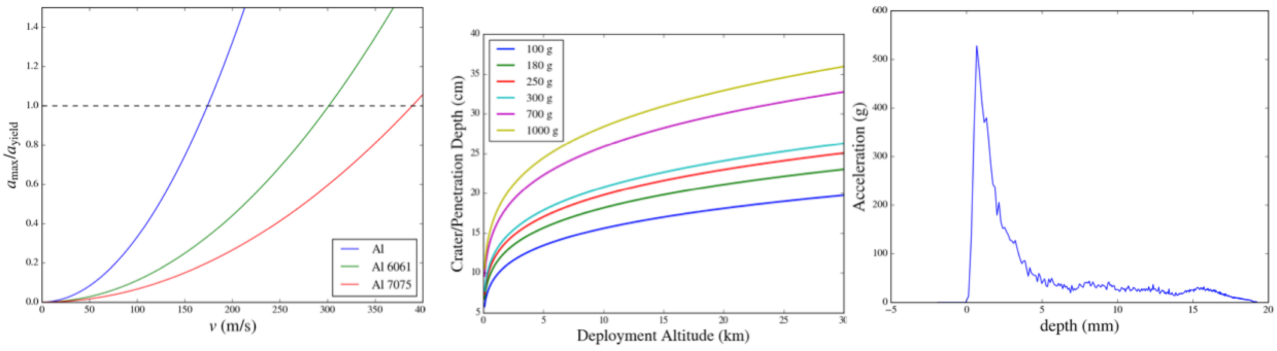

Fig. 1. Preliminary analysis showing shock tolerance, penetration depth, and instrument response for different instrument designs and impact speeds. Left: Maximum shock tolerance before material failure for three different aluminum alloy instrument housings. An Al-7075 housing can withstand impact speeds greater than 350 m/s. Middle: Penetrations depths for a 250 m/s impact for different impactor masses (100 - 1000 grams). For a nominal impactor mass of 180 g, a deployment from 15 km from the lunar surface results in a penetration depth of < 20 cm (based on [3]). Right: Simulated response of a 180 g impactor using a particle dynamics simulation.

©2019. Japan Geoscience Union. All Right Reserved.

Surface size-frequency distribution of accumulating boulders using discrete element simulations of spherical particles in 3D

*Hiroshi Kikuchi[1], Hideaki Miyamoto[1]

1. The University of Tokyo

Several spacecraft have revealed new detail about small bodies such as asteroids, comets, and small satellites. Images from Hayabusa, Hayabusa2, and OSIRIS-REx showed more boulders on the surfaces than originally expected. Owing to the high resolution at which images were taken, a number of boulders could often be observed in clusters. In future explorations, because we expect to observe more cases of boulder-rich surfaces, the characterization of the size-frequency distribution (SFD) will be important especially for the missions involving a lander such as MMX. Basically, measuring the SFD of boulders on a surface is expected to represent that of the interior. However, considering that surface boulders can hide the underlying boulder, it is not clear that the SFD in a volume can adequately be represented by its surface. Therefore, in this work, we focus on how accumulating boulders with a known SFD appear from above.
In order to compare the SFD on a surface with that of a volume, the initial SFD has to be known. For the initial study, numerical simulations are convenient, because they can easily prepare the suitable conditions. In the previous studies, spherical boulders were randomly distributed in three-dimensional space, and only those on the surface were automatically extracted and measured (Tancredi et al., 2015). It was found that the particle distribution on the surface well reproduces the overall particle distribution. We consider that there is room for improvement in the arrangement of particles and the measurement of particles. Thus, we implement a three-dimensional discrete element method using rigid spherical particles to simulate the accumulation of a boulder-rich regolith. We then measure particles one by one manually when viewed from above the surface. For initial conditions, we set the size and the number of boulders randomly as specified by the power law index of -3. During a simulation, particles are not initially adjacent to each other and are instead dropped from the height of 30 m above the 54 x 54 m planar surface. The total number of particles is changed from 3000 to 7000 in 1000 increments. After the simulation, the size and number of the particles are measured manually when viewing the surface from the vertical direction. Then we refer to Clauset et al. (2009) for fitting and evaluating the data using the p-value metric.
We find that the power law index of the SFD is low when the number of particles is 3000. This may be because the larger particles are not buried in the smaller particles, resulting in only the number of smaller particles being reduced when viewed from above. When the total number is 4000 or more in a volume and p-value is high, the surface power law index from the multiple simulations is consistent with the specified value of -3 for some cases.
The SFD observed on the surface corresponds to the SFD in the interior of the body for the following conditions: the thickness of the deposited particles is larger than the largest particle and the p-value is high. For more detailed analyses, investigating the effects of the number of simulations, the complicated shapes of boulders, and parameter studies are needed. In addition, for a deeper understanding of the problem, experiments in a similar condition to the airless bodies using simulated regolith particles such as UTPS-TB and UTPS-IB (Miyamoto et al., 2018) are also required.

Keywords: Discrete element method, Boulder size-frequency distribution, Interior of small bodies

©2019. Japan Geoscience Union. All Right Reserved.

Experimental Study to Determine the Best Compression Ratio of High-Resolution Images of Small Bodies for the Martian Moons eXploration (MMX) Mission

*Yuta Shimizu[1], Hiroaki Kamiyoshihara[1], Takafumi Niihara[1], Hideaki Miyamoto[1]

1. University of Tokyo

Data transmission rate becomes one of the biggest limiting factors in space explorations; technological advance in increasing pixel numbers of camera images dominates the improvement of the data transmission rate. Yet, high demand exists for high-resolution images especially in geological studies, and thus there is a tradeoff between the spatial resolutions (or pixel numbers) and the number of images to be transmitted to Earth. The telecommunications issue is critical for Martian Moons eXploration (MMX) mission that explore either/both Phobos and Deimos and return samples. Especially, timely transmission of high-resolution images is required for the selection of sampling site both in terms of scientific impacts and of the landing safety. The highest image resolution of the current camera configuration is as good as several tens of centimeters per pixel and the size of image is 3296 x 2472 pixels, which means 7 color (3 bands) images can be up to 1 GB if no compression is considered. During the landing phase, such large data have to be sent at the limited bitrate (< 32 kbps) to select landing and sampling sites, while the landing duration is about 4 hours. Thus, considering the best compression scheme of images is a big issue for landing operation. Lossy compression can significantly reduce the sizes of images, though images can be scientifically worthless when compressed too much. The best compression ratio should make the sizes of images as small as possible without losing scientific importance.

Here, we develop a method of rapidly determining the best compression ratio of high-resolution images of the surface of small bodies. For preparing the image studied in this research, we take an experimental scheme, where we develop a simulated Phobos surface by using a high-quality simulant of Phobos regolith (UTPS-TB) and take simulated images of the surface of Phobos in somehow similar condition with the camera of the MMX mission. The images are compressed by JPEG2000, which is planned to be used in MMX mission, and the influence of the compression is analyzed by objective methods such as Structural SIMilarity (SSIM) and entropy of image. The results shows that they are able to rapidly detect the exact ratio, in which the quality of the images started to be diminished.

Moreover, by defining scientific value of images as detectability of rock gravel on the surface of celestial bodies and showing that the loss of scientific value can be expressed by the change in the value of slope of Cumulative Size-Frequency Distribution (CSFD) of gravel, we carefully confirm whether the decrease in the image quality is truly connected with the loss of scientific information such as for landing operations and conclude that those objective methods can determine the best compression ratio. By using those methods, the spacecraft can autonomously complete the process of finding the best compression ratio, compressing images and sending it to the ground within a few minutes even if it has only a limited transmission rate.

Keywords: the best compression ratio, Cumulative Size-Frequency Distribution (CSFD), Martian Moons eXploration (MMX)

©2019. Japan Geoscience Union. All Right Reserved.

[E] Poster | P (Space and Planetary Sciences)：P-PS Planetary Sciences

Wed. May 29, 2019 5:15 PM - 6:30 PM JST | Wed. May 29, 2019 8:15 AM - 9:30 AM UTC | Poster Hall International Exhibition Hall8, Makuhari Messe_2

[P-PS02] Regolith Science

convener:Koji Wada(Planetary Exploration Research Center, Chiba Institute of Technology), Akiko Nakamura(Graduate School of Science, Kobe University), Patrick Michel(Observatoire De La Cote D'Azur), Kevin John Walsh(Southwest Research Institute Boulder)

Recent planetary explorations have revealed that almost all solid bodies in the solar system are covered with small particles, called regolith. The surface geology, especially regolith behavior on the surfaces of solid bodies, becomes increasingly more important as represented by Hayabusa mission and other on-going and planned sample-return missions such as Hayabusa2, OSIRIS-REx, and MMX.

For fully understanding the regolith science, it is required to know and compare the regolith conditions on various celestial bodies, from asteroids to planets, with various methods.

Therefore, this session welcomes broad topics related to regolith on various celestial bodies, such as asteroids, comets, the Moon, the martian moons, Mars, etc. Papers on the formation, evolution, and alteration processes of regolith particles and regolith systems on the surface of planetary bodies, remote and in-situ observational results and techniques, analyses and results of returned samples, and laboratory, numerical, and theoretical studies on the fundamental physical and chemical processes are all welcome.

Note that what we call regolith is not just fine grains: all kinds of materials (more or less loose) that lie on the surface, from cobbles to finer grains, are our targets.

[PPS02-P01] Abrasion experiments of mineral and meteorite grains: Dependence of particle size and vibration rate on abrasion rate and its application to Itokawa and lunar regolith particles.

*Hirotaka Yamaguchi[1], Akira Tsuchiyama[1], Akiko Nakamura[2] (1.National University Corporation, Kyoto University, 2.National University Corporation,Kobe University)

[PPS02-P02] Measurements of adhesive force of meteorite powders using centrifugal method

*Yuuya Nagaashi[1], Akiko Nakamura[1] (1.Kobe University)

[PPS02-P03] Laboratory impact penetration experiments conducted at simulated reduced gravity

*Akiko Nakamura[1], Kana Morizono[2], Yuuya Nagaashi[1] (1.Graduate School of Science, Kobe University, 2.Faculty of Science, Kobe University)

[PPS02-P04] MARAUDERS: Using instrumented nano-impactors to probe the icy properties of Lunar permanently shadowed regions

*Ronald Ballouz[1], Sarah T Crites[2], Naoya Ozaki[2], Shun Arahata[3], Nicola Baresi[2], Ralf Bolden, Onur Celik[4,2], Yu Himeno[3], Lucie Riu[2], Kevin J Walsh[5] (1.Lunar and Planetary Lab, University of Arizona, Tucson, AZ, USA, 2.Institute of Space and Astronautical Science, Sagamihara, Japan, 3.University of Tokyo, Tokyo, Japan, 4.Sokendai Graduate University, Japan, 5.Southwest Research Institute, Boulder, CO, USA)

[PPS02-P05] Surface size-frequency distribution of accumulating boulders using discrete element simulations of spherical particles in 3D

*Hiroshi Kikuchi[1], Hideaki Miyamoto[1] (1.The University of Tokyo)

[PPS02-P06] Experimental Study to Determine the Best Compression Ratio of High-Resolution Images of Small Bodies for the Martian Moons eXploration (MMX) Mission

*Yuta Shimizu[1], Hiroaki Kamiyoshihara[1], Takafumi Niihara[1], Hideaki Miyamoto[1] (1.University of Tokyo)

Abrasion experiments of mineral and meteorite grains: Dependence of particle size and vibration rate on abrasion rate and its application to Itokawa and lunar regolith particles.

*Hirotaka Yamaguchi[1], Akira Tsuchiyama[1], Akiko Nakamura[2]

1. National University Corporation, Kyoto University, 2. National University Corporation,Kobe University

Rounded edges were found in some regolith particles collected from asteroid Itokawa [1] and Moon [2]. These particles should be formed by mechanical abrasion [1]. Seismic-induced grain motion by micrometeoroid impacts [1] and YORP effect [3] were proposed for the abrasion process on Itokawa. However, it is not clear how these processes actually work on the surfaces of the airless celestial bodies.

In order to understand detailed process of the abrasion, our research group have carried out abrasion experiments using mineral, rock and meteorite grains (grain size: 1-2 mm) [4]. Samples used were quartz, olivine, corundum, marble, L5 chondrite meteorite (Sayh al Uhaymir 001) and CM chondrite meteorite (Murchison). These particles were put into a vessel of 10 mL with the filling ratio of ~50 % and the sample was vibrated with the rate from 1000 to 3000 rpm using a multi-beads-shocker (YASUIKIKAI Co.). The proportion of powder (<250 μm) produced by vibration at first 1 min., ΔP_1, was adopted as the measure of abrasion and its dependence of the vibration rate and the sample strength was examined. However, the particle size used in the experiments (1-2 mm) is larger than Itokawa particles (< a few hundred μm). In addition, the vibration rates used in the experiments are larger than those estimated for Itokawa(~100 rpm) and Moon (~700 rpm) by considering the maximum seismic acceleration due to micrometeoroidimpacts onto their surface [5]. In the present study, therefore, we conducted new experiments with different parameters such as particle size and vibration rate using the same experimental procedure as [4]. In the present experiments, we used quartz grains for examining the effect of packing ratio in the vessel (Exp-1), particle size (Exp-2), mixing ratio of large and small particles (Exp-3). The effect of lower vibration rate (100 - 1000 rpm) was examined using olivine and basalt as well as quartz (Exp-4). Experiments using basalt at higher vibration rates were also made.

We obtained following results. Exp-1: $\Delta P_1$was constant in a wide range of the filling rate except for the filling rate of 2/3, where ΔP_1showed a peak value. Exp-2: $\Delta P_1$is proportional to the particle size. Exp-3: When the proportion of large particles is larger than 25%, $\Delta P_1$is almost constant and the same as $\Delta P_1$for the large particles. Exp-4: In the previous experiments, ΔP_1increases with the vibration rate with the power of 1.1-2.9 for large vibration rates (>~1000 rpm) [4] while the power becomes smaller (0.67-0.77) for smaller vibration rates (<~1000 rpm). This result shows that the abrasion mode changed at ~1000 rpm. In order to understand abrasion modes, SEM observation of powder particles produced in the abrasion experiments were also made. It was found that chipping of particle edges occurred at low vibration rate (~100 rpm) and the proportion of gradual wearing on the whole particle surface gradually increased as the vibration rate increased.

We estimated the amount of abrasion of Itokawa and lunar regolith particles in a regolith layer by impact based on the present experiments. ΔP_1values of basalt at 100 and 700 rpm, which corresponding to Itokawa and Moon [4], are ~0.1 %and ~1 %, respectively (Exp-4). If we consider the size of Itokawa and Moon particle (~100 μm), ΔP_1on Itokawa and Moon should be ~0.01%and ~0.1%, respectively(Exp-2). These values are larger than those estimated from the previous experiments [4] by the order of about 1.

©2019. Japan Geoscience Union. All Right Reserved.

The present results suggest that abrasion is possible on the Moon and may occur on Itokawa as well.

[1] Tsuchiyama et al. 2011. Science, 333, 1125-1128.

[2] Sakurama et al. 2016. JpGU, Abstract, PPS03-13.

[3] Connolly et al. 2015. Earth Planet and Space, 67: 12.

[4] Tsuchiyama et al. 2018. LPSC, Abstract 1844.

[5] Yasui et al. 2015. Icarus, 260: 320-331.

©2019. Japan Geoscience Union. All Right Reserved.

Measurements of adhesive force of meteorite powders using centrifugal method

*Yuuya Nagaashi[1], Akiko Nakamura[1]

1. Kobe University

Introduction: Layer of fine particles in the laboratory shows fluffy structure owing to interparticle force (e.g., Kiuchi and Nakamura, 2014). On small bodies, interparticle forces are thought to be dominant compared to gravitational force for small particles. Fast rotators spin in excess of what gravity alone could hold together were shown to be explained by cohesive force between constituent particles (Sánchez & Scheeres, 2016). Measurements of cohesive force between micron-size spherical silica particles using an atomic force microscope cantilever (Heim et al., 1999) showed that the results agree with predictions of the JKR model (Johnson et al., 1971). On the other hand, measurements of cohesive force between 50 or 100 μm glass beads and a glass plate using centrifugal method showed that the results are by several orders of magnitude smaller than predictions of the JKR theory (Nagaashi et al., 2018). In addition, it was also shown that ~ 70 μm irregularly-shaped silica and alumina grains have the range of adhesive force similar to the glass beads, indicating that the adhesive force of the spherical and the irregular particles used in the measurement is dependent not on the macroscopic shape but on the microscopic surface roughness. However, it is not clear whether the adhesive force of the particles that actually form the asteroids is similar to those of silica grains. Measurements of adhesive force of meteorite powders will bring important knowledge of adhesive force of the asteroid-forming particles for understanding physical processes occurring on asteroids.

Experimental method: In this study, we used centrifugal method as in our previous study (Nagaashi et al., 2018) in order to measure cohesive or adhesive force between a particle and a plate. This method can directly measure the cohesive or adhesive force of many particles at the same time, which enables us to statistically analyze the results. Additionally, it can also deal with irregularly shaped particles. The measurements were conducted for carbonaceous chondrite (CV3: Allende, CM2: Murchison), ordinary chondrite (LL3.5: NWA 539, LL5: NWA 1794, LL6: NWA 542), and Eucrite (Millbillillie) powders of median diameter ~ 50 μm. We discretely increased the centrifugal acceleration from 10g to 5000g (g: the Earth's gravitational acceleration) and took optical microscope images of the same location of the plate before and after applying centrifugal force at each centrifugal acceleration. We determined the range of centrifugal acceleration within which the particle separated from the plate based on the microscope images and estimated the cohesive or adhesive force between the particle and the plate. More detail description of the procedure is described in Nagaashi et al. (2018).

Results: As compared with the JKR adhesion force $F_{ad} = 3\pi\gamma R$ (γ: surface energy, R: reduced radius of particle) for a spherical particle of silica composition, we calculated the effective surface energy of particles which reproduces the measurement value, and compared the results of each type of meteorite powders. Similar to the previous results described in the above (Nagaashi et al., 2018), the measurements of meteorite powders showed a wide range of adhesive force distributions over several orders of magnitude for all measured meteorite types. In addition, we found that the effective surface energy of Allende and Murchison meteorite particles were several times smaller than those for the particles of the other meteorite types. There is no difference in the axial ratio of each type of meteorite powders, and therefore this is likely due to differences in material composition or micro-topography of the particles.

©2019. Japan Geoscience Union. All Right Reserved.

©2019. Japan Geoscience Union. All Right Reserved.

Laboratory impact penetration experiments conducted at simulated reduced gravity

*Akiko Nakamura[1], Kana Morizono[2], Yuuya Nagaashi[1]

1. Graduate School of Science, Kobe University, 2. Faculty of Science, Kobe University

Small bodies are covered with a layer of regolith made up of particles of various sizes. It is important to understand the interactions that occur with surface regolith when a spacecraft lands on or when a block secondarily collide with the regolith layer at low velocity. Penetration depth of an impactor in granular layer was investigated under Earth’ s gravity and an empirical relationship between the drop height and penetration depth was shown to reproduce the experimental results for various granular materials (Uehara et al., 2013). Deceleration of spherical impactor in granular layer was experimentally and theoretically investigated and deceleration formulae were proposed (Katsuragi and Durian 2007, Nakamura et al., 2013; Katsuragi and Durian 2013). On the other hand, interactions of spheres with simulated regolith have been studied at reduced gravity and micro-gravity conditions (Murdoch et al., 2016; Brisset et al., 2018). However, more data of penetration depth of impactor are required to establish quantitative understanding of the penetration process in regolith under low gravity.

We conducted laboratory low-velocity impact experiments of a sphere into granular layer at reduced gravity. Impactor was a glass sphere with a diameter of 16.7 mm and granular layer consisted of glass beads with a diameter of 1 mm. The glass beads were packed in a bucket having a diameter of 15 cm and a depth of 15 cm. The bucket was hung with three constant load springs. The bucket was fixed with two electromagnets, and when the electromagnet was switched off, it dropped vertically downward with the gravity reduced. The simulated reduced gravity level was monitored by an accelerometer placed in a bucket and found to be on average 0.26 G. A plastic straw with horizontal line drawing was glued to the glass sphere. The glass sphere collided with the glass bead layer at a relative velocity between 2 and 4 ms $^{-1}$. The penetration process of the glass sphere with the straw was imaged at 240 fps by a camera attached to the bucket. The final depth of the glass sphere was found to be systematically deeper than the depth found in the experiment conducted at 1 G.

Keywords: regolith, low gravity, impact

©2019. Japan Geoscience Union. All Right Reserved.

MARAUDERS: Using instrumented nano-impactors to probe the icy properties of Lunar permanently shadowed regions

*Ronald Ballouz[1], Sarah T Crites[2], Naoya Ozaki[2], Shun Arahata[3], Nicola Baresi[2], Ralf Bolden, Onur Celik[4,2], Yu Himeno[3], Lucie Riu[2], Kevin J Walsh[5]

1. Lunar and Planetary Lab, University of Arizona, Tucson, AZ, USA, 2. Institute of Space and Astronautical Science, Sagamihara, Japan, 3. University of Tokyo, Tokyo, Japan, 4. Sokendai Graduate University, Japan, 5. Southwest Research Institute, Boulder, CO, USA

The Mini lAndeRs And boUncers Deployed for Exploration and Regolith Science (MARAUDERS) is a small satellite concept that aims to characterize the surface and volatile properties of regolith in permanently shadowed regions (PSRs) around the Moon's poles. Large PSRs are cold enough to trap scientifically and economically valuable volatiles such as water ice. However, despite ongoing studies, the distribution, abundance, and physical phase of volatiles at the Moon's poles remains elusive [1]. *In-situ* measurements are required to conclusively determine the geotechnical and physical properties of lunar polar volatiles. To address these needs, the MARAUDERS team is currently developing a technique using instrumented nano-impactors to determine the mechanical properties of regolith at the impact point.

Small spacecraft equipped with penetrators or inertial measurement units (IMU) can characterize the strength and structure of the planetary surface that they impact. Early space exploration used penetrometers to determine the surface properties of the Moon and Mars before the arrival of astronauts and rovers. In recent decades, spacecraft equipped with IMUs characterized the surface of Titan [1], and determined the sub-surface stratification of ice and rock on the comet 67P/C-G [2]. While this technique is unable to relay the detailed mineralogical and elemental composition at the impact point, it obtains a first-order structural knowledge of potentially hazardous surfaces and sub-surfaces that cannot be obtained through remote sensing. This is highly relevant for PSRs due to extreme environmental conditions such as the lack of solar illumination, cold temperatures, and challenging communications.

Here, we present preliminary analysis on the instrument capabilities based on the potential deployment scenarios to PSRs, and the possible mechanical properties of the regolith found within these regions (Fig. 1). We present a computational study of the varying response of an instrumented impactor impacting regolith with variable i) water ice content (0-10%), ii) impactor speeds (50-250 m/s], and iii) impact angles (45-90˚), using a discrete element method code [4]. Furthermore, we analyse the ejecta properties and resulting crater morphology in order to gain a better understanding of impact processes on icy bodies. Our next steps will be to conduct laboratory impact experiments using prototypes of our instrumented impactors to calibrate the impact response on lunar simulant with variable water-ice content.

References:

1. Lorenz, R. et al. (1994) Meas. Sci. Technol. 5, 1033-1041

2. Biele, J. et al. (2016), Science, 349, 6247.

3. Holsapple, K.A. (1994) LPSC 25, 559.

©2019. Japan Geoscience Union. All Right Reserved.

4. Richardson, D.C. et al. (2011) Icarus, 212, 427–437.

Acknowledgements:

This material is based upon work supported by ISAS/JAXA’s start-up fund for international collaborations, the Aerospace Project Research Associate Program, and the International Top Young Fellow Program.

Keywords: Moon, Permanently Shadowed Regions, Volatiles, Regolith Characterization

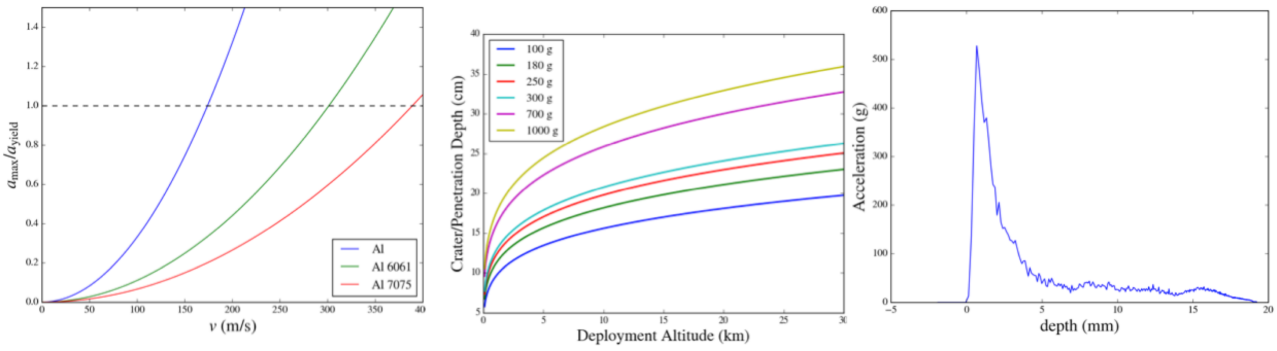

Fig. 1. Preliminary analysis showing shock tolerance, penetration depth, and instrument response for different instrument designs and impact speeds. Left: Maximum shock tolerance before material failure for three different aluminum alloy instrument housings. An Al-7075 housing can withstand impact speeds greater than 350 m/s. Middle: Penetrations depths for a 250 m/s impact for different impactor masses (100 - 1000 grams). For a nominal impactor mass of 180 g, a deployment from 15 km from the lunar surface results in a penetration depth of < 20 cm (based on [3]). Right: Simulated response of a 180 g impactor using a particle dynamics simulation.

©2019. Japan Geoscience Union. All Right Reserved.

Surface size-frequency distribution of accumulating boulders using discrete element simulations of spherical particles in 3D

*Hiroshi Kikuchi[1], Hideaki Miyamoto[1]

1. The University of Tokyo

Several spacecraft have revealed new detail about small bodies such as asteroids, comets, and small satellites. Images from Hayabusa, Hayabusa2, and OSIRIS-REx showed more boulders on the surfaces than originally expected. Owing to the high resolution at which images were taken, a number of boulders could often be observed in clusters. In future explorations, because we expect to observe more cases of boulder-rich surfaces, the characterization of the size-frequency distribution (SFD) will be important especially for the missions involving a lander such as MMX. Basically, measuring the SFD of boulders on a surface is expected to represent that of the interior. However, considering that surface boulders can hide the underlying boulder, it is not clear that the SFD in a volume can adequately be represented by its surface. Therefore, in this work, we focus on how accumulating boulders with a known SFD appear from above.
In order to compare the SFD on a surface with that of a volume, the initial SFD has to be known. For the initial study, numerical simulations are convenient, because they can easily prepare the suitable conditions. In the previous studies, spherical boulders were randomly distributed in three-dimensional space, and only those on the surface were automatically extracted and measured (Tancredi et al., 2015). It was found that the particle distribution on the surface well reproduces the overall particle distribution. We consider that there is room for improvement in the arrangement of particles and the measurement of particles. Thus, we implement a three-dimensional discrete element method using rigid spherical particles to simulate the accumulation of a boulder-rich regolith. We then measure particles one by one manually when viewed from above the surface. For initial conditions, we set the size and the number of boulders randomly as specified by the power law index of -3. During a simulation, particles are not initially adjacent to each other and are instead dropped from the height of 30 m above the 54 x 54 m planar surface. The total number of particles is changed from 3000 to 7000 in 1000 increments. After the simulation, the size and number of the particles are measured manually when viewing the surface from the vertical direction. Then we refer to Clauset et al. (2009) for fitting and evaluating the data using the p-value metric.
We find that the power law index of the SFD is low when the number of particles is 3000. This may be because the larger particles are not buried in the smaller particles, resulting in only the number of smaller particles being reduced when viewed from above. When the total number is 4000 or more in a volume and p-value is high, the surface power law index from the multiple simulations is consistent with the specified value of -3 for some cases.
The SFD observed on the surface corresponds to the SFD in the interior of the body for the following conditions: the thickness of the deposited particles is larger than the largest particle and the p-value is high. For more detailed analyses, investigating the effects of the number of simulations, the complicated shapes of boulders, and parameter studies are needed. In addition, for a deeper understanding of the problem, experiments in a similar condition to the airless bodies using simulated regolith particles such as UTPS-TB and UTPS-IB (Miyamoto et al., 2018) are also required.

Keywords: Discrete element method, Boulder size-frequency distribution, Interior of small bodies

©2019. Japan Geoscience Union. All Right Reserved.

Experimental Study to Determine the Best Compression Ratio of High-Resolution Images of Small Bodies for the Martian Moons eXploration (MMX) Mission

*Yuta Shimizu[1], Hiroaki Kamiyoshihara[1], Takafumi Niihara[1], Hideaki Miyamoto[1]

1. University of Tokyo

Data transmission rate becomes one of the biggest limiting factors in space explorations; technological advance in increasing pixel numbers of camera images dominates the improvement of the data transmission rate. Yet, high demand exists for high-resolution images especially in geological studies, and thus there is a tradeoff between the spatial resolutions (or pixel numbers) and the number of images to be transmitted to Earth. The telecommunications issue is critical for Martian Moons eXploration (MMX) mission that explore either/both Phobos and Deimos and return samples. Especially, timely transmission of high-resolution images is required for the selection of sampling site both in terms of scientific impacts and of the landing safety. The highest image resolution of the current camera configuration is as good as several tens of centimeters per pixel and the size of image is 3296 x 2472 pixels, which means 7 color (3 bands) images can be up to 1 GB if no compression is considered. During the landing phase, such large data have to be sent at the limited bitrate (< 32 kbps) to select landing and sampling sites, while the landing duration is about 4 hours. Thus, considering the best compression scheme of images is a big issue for landing operation. Lossy compression can significantly reduce the sizes of images, though images can be scientifically worthless when compressed too much. The best compression ratio should make the sizes of images as small as possible without losing scientific importance.

Here, we develop a method of rapidly determining the best compression ratio of high-resolution images of the surface of small bodies. For preparing the image studied in this research, we take an experimental scheme, where we develop a simulated Phobos surface by using a high-quality simulant of Phobos regolith (UTPS-TB) and take simulated images of the surface of Phobos in somehow similar condition with the camera of the MMX mission. The images are compressed by JPEG2000, which is planned to be used in MMX mission, and the influence of the compression is analyzed by objective methods such as Structural SIMilarity (SSIM) and entropy of image. The results shows that they are able to rapidly detect the exact ratio, in which the quality of the images started to be diminished.

Moreover, by defining scientific value of images as detectability of rock gravel on the surface of celestial bodies and showing that the loss of scientific value can be expressed by the change in the value of slope of Cumulative Size-Frequency Distribution (CSFD) of gravel, we carefully confirm whether the decrease in the image quality is truly connected with the loss of scientific information such as for landing operations and conclude that those objective methods can determine the best compression ratio. By using those methods, the spacecraft can autonomously complete the process of finding the best compression ratio, compressing images and sending it to the ground within a few minutes even if it has only a limited transmission rate.

Keywords: the best compression ratio, Cumulative Size-Frequency Distribution (CSFD), Martian Moons eXploration (MMX)

©2019. Japan Geoscience Union. All Right Reserved.

[E] Poster | P (Space and Planetary Sciences)：P-PS Planetary Sciences

Wed. May 29, 2019 3:30 PM - 5:00 PM JST | Wed. May 29, 2019 6:30 AM - 8:00 AM UTC | Poster Hall International Exhibition Hall8, Makuhari Messe_1

[P-PS03] Solar System Small Bodies: A New Frontier Arising Hayabusa 2, OSIRIS-REx and Other Projects

convener:Masateru Ishiguro(Department of Physics and Astronomy, Seoul National University), Taishi Nakamoto(Tokyo Institute of Technology), Masanao Abe(Institute of Space and Astronautical Science, Japan Aerospace Exploration Agency), Olivier S Barnouin(Johns Hopkins University Applied Physics Laboratory)

In June 2018, the Hayabusa 2 spacecraft arrived at the target asteroid Ryugu after three and half years journey. In addition, another spacecraft, OSIRIS-REx will soon arrive at its destination Bennu. With these arrivals, the solar system research is about to enter a new era. We have organized this small bodies session since 2012 and had a broad range of discussions from viewpoints of laboratory experiments, observations, space explorations, theoretical modeling, and sample analyses. In particular, this time, we aim to hold this session to bring the latest research on solar system small bodies, focusing on the initial results of Hayabusa 2 and OSIRIS-REx. Presentations in the related fields other than these two asteroidal missions are also welcomed.

[PPS03-P01] Impact experiments on low strength coarse-grained regolith simulating surface materials on asteroid Ryugu

*Yuya Yamamoto[1], Masahiko Arakawa[1], Minami Yasui[1], Sunao Hasegawa[2], Ryo Sugimura[1] (1.Graduate School of Science, Kobe University, 2.ISAS, JAXA)

[PPS03-P02] Reflectance estimation of asteroid Ryugu using MASCOT

*Marika Ishida[1], Koto Amano[1], Keiichi Moroi[1], ERI TATSUMI[2], Tra-Mi Ho[10], Shingo Kameda[1], Seiji Sugita[2], Rie Honda[3], Tomokatsu Morota[4], yokota yasuhiro[5], Toru Kouyama[6], Hidehiko Suzuki[7], Manabu Yamada[8], Naoya Sakatani[5], Chikatoshi Honda[9], Masahiko Hayakawa[5], Kazuo Yoshioka[2], Moe Matsuoka[5], Yuichiro Cho[2], Hirotaka Sawada[5] (1.Rikkyo Univ., 2.Univ. of Tokyo, 3.Kochi Univ., 4.Nagoya Univ., 5.JAXA/ISAS, 6.AIST, 7.Meiji Univ., 8.Chiba Inst. Tech, 9.Univ. of Aizu, 10.DLR)

[PPS03-P03] Flyby observation of Asteroid (3200) Phaethon by DESTINY$^+$ onboard cameras

*Ko Ishibashi[1], Shingo Kameda[2], Masato Kagitani[3], Peng Hong[1], Manabu Yamada[1], Osamu Okudaira[1], Tomoko Arai[1], Fumi Yoshida[1], Shunsuke Sato[4], Takahiro Ishimaru[4], Takaya Okamoto[4], Takahiro Iwata[4], Tatsuaki Okada[4], Takeshi Takashima[4] (1.Chiba Institute of Technology, 2.Rikkyo University, 3.Tohoku Universtiy, 4.Japan Aerospace Exploration Agency)

[PPS03-P04] Polarimetric Study of Asteroids in Comet-Like Orbits (ACOs)

*Jooyeon Geem[1], Masateru Ishiguro[1], Yoonsoo P. Bach[1], Daisuke Kuroda[2], Hiroyuki Naito[3], Hidekazu Hanayama[4], yoonyoung kim[10], Yuna G. Kwon[1], Sunho Jin[1], Tomohiko Sekiguchi[5], Ryo Okazaki[5], Jeremie J. Vaubaillon[6], Masataka Imai[7], Tatsuharu Oono[8], Yuki Futamuts[8], Seiko Takagi[8], Mitsuteru Sato[8], Kiyoshi Kuramoto[8], Makoto Watanabe[9] (1.Astronomy program, Dept of Physics and Astronomy, Seoul National University, 2.Okayama Observatory, Kyoto University, 3.Nayoro Observatory, 4.Ishigakijima Astronomical Observatory, National Astronomical Observatory of Japan, 5.Hokkaido University of Education, 6.Observatoire de Paris, I.M.C.C.E., 7.National Institute of Advanced Industrial Science and Technology, 8.Department of Cosmosciences, Graduate School of Science, Hokkaido University, 9.Department of Applied Physics, Okayama University of Science, 10.Max Planck Institute for Solar System Research)

[PPS03-P05] Dynamical lifetime of the Oort Cloud new comets under planetary perturbation

*Ito Takashi[1], Arika Higuchi[1] (1.National Astronomical Observatory of Japan)

[PPS03-P06] Thermal Infrared Imaging of C-type Asteroid 162173 Ryugu with Porous Surfaces

*Tatsuaki Okada[1,2], Tetsuya Fukuhara[3], Satoshi Tanaka[1], Makoto Taguchi[3], Takehiko Arai[4], Naoya Sakatani[1], Yuri Shimaki[1], Hiroki Senshu[5], Yoshiko Ogawa[6], Hirohide Demura[6], Kentaro Suko[6], Kohei Kitazato[6], Toru Kouyama[7], Tomohiko Sekiguchi[8], Jun Takita[9], Sunao Hasegawa[1], Tsuneo Matsunaga[10], Takehiko Wada[1], Takeshi Imamura[2], Jorn Helbert[11], Thomas G. Mueller[12], Axel Hagermann[13], Jens Biele[11], Matthias Grott[11], Maximiliam Hamm[11], Marco Delbo[14], Yukio Yamamoto[1], Naru Hirata[6], Naoyuki Hirata[15], Fuyuto Terui[1], Takanao Saiki[1], Satoru Nakazawa[1], Makoto Yoshikawa[1], Sei-ichiro WATANABE[1,16], Yuichi Tuda[1] (1.Institute of Space and Astronautical Science, Japan Aerospace Exploration Agency, 2.University of Tokyo, 3.Rikkyo University, 4.Ashikaga University, 5.Chiba Institute of Technology, 6.University of Aizu, 7.National Institute of Advanced Industrial Science and Technology, 8.Hokkaido University of Education, 9.Hokkaido Kitami-Hokuto High School, 10.National Institute for Environmental Studies, 11.German Aerospace Center, 12.Max-Planck Institute for Extraterrestrial Physics, 13.University of Stirling, 14.Observatoire de la Côte d'Azur, 15.Kobe University, 16.Nagoya University)

[PPS03-P07] Data Release of Asteroid 162173 Ryugu by Observation of Thermal Infrared Imager onboard Hayabusa2

*Takehiko Arai[1], Hirohide Demura[2], Toru Kouyama[7], Naoya Sakatani[3], Kentaro Suko[2], Yuri Shimaki[3], Hiroki Senshu[5], Tomohiko Sekiguchi[6], Yoshiko Ogawa[2], Sunao Hasegawa[3], Takehiko Wada[3], Takeshi Imamura[10], Tsuneo Matsunaga[9], Jun Takita[8], Kohei Kitazato[2], Makoto Taguchi[4], Tetsuya Fukuhara[4], Satoshi Tanaka[3], Tatsuaki Okada[3] (1.Ashikaga University, 2.The University of Aizu, 3.Japan Aerospace Exploration Agency (JAXA), 4.Rikkyo University, 5.Chiba Institute of Technology, 6.Hokkaido University of Education, 7.National Institute of Advanced Industrial Science and Technology (AIST), 8.Hokkaido Kitami Hokuto High School, 9.National Institute for Environmental Studies (NIES), 10.The University of Tokyo)

[PPS03-P08] Multi-mission capability of HARMONICS

*Shintaro Tsunoda[1], Hirohide Demura[1], Naru Hirata[1] (1.The University of Aizu)

[PPS03-P09] New interface of verification for calibration and conversion in HEAT : Hayabusa2 Exploration Assistant for TIR

*Tatsuro Kobayashi[1], Kentaro Suko[1], Hirohide Demura[1], Yoshiko Ogawa[1], Takehiko Arai[2], Naoya Sakatani[3], Tatsuaki Okada[3], Satoshi Tanaka[3], Tetsuya Fukuhara[4] (1.The University of Aizu, 2.Ashikaga University, 3.Institute of Space and Astronautical Science, Japan Aerospace Exploration Agency, 4.Rikkyo University)

[PPS03-P10] **Dust particle evolution of a near-Earth object 252P/LINEAR from near-infrared polarimetric observations in 2016**

*Yuna G Kwon[1], Masateru Ishiguro[1], Jungmi Kwon[2], Daisuke Kuroda[3], Myungshin Im[1], Changsu Choi[1], Motohide Tamura[4], Takahiro Nagayama[5], Nobuyuki Kawai[6], Jun-ichi Watanabe[7] (1.Seoul National Univ., 2.ISAS/Japan Aerospace Exploration Agency, 3.Okayama Astrophysical Observatory, 4.The Univ. of Tokyo, 5.Kagoshima Univ., 6.Tokyo Institute of Technology, 7.National Astronomical Observatory of Japan)

[PPS03-P11] **Performance Evaluation of TRIPOL on the 61-cm Telescope at Seoul National University for Polarimetric Observations of Solar System Small Bodies**

*Sunho Jin[1], Masateru Ishiguro[1], Yuna G Kwon[1], Jooyeon Geem[1], Yoonsoo P. Bach[1], Jinguk Seo[1], Hiroshi Sasago[2], Shuji Sato[3] (1.Seoul National University, 2.Sasago Co.,Ltd, 3.Nagoya University)

[PPS03-P12] Smart Interface of HEAT: Hayabusa2 Exploration Assistant for TIR

*Kentaro Suko[1], Tatsuro Kobayashi[1], Hirohide Demura[1], Takehiko Arai[2], Naoya Sakatani[3], Tatsuaki Okada[3], Satoshi Tanaka[3], Tetsuya Fukuhara[4] (1.The University of Aizu, 2.Ashikaga University, 3.Institute of Space and Astronautical Science, Japan Aerospace Exploration Agency, 4.Rikkyo University)

[PPS03-P13] Experimental Study on Collision Crater Formed on Bulge Geography

*Yusaku Yokota[1], Yuya Yamamoto[2], Minami Yasui[2], Masahiko Arakawa[2] (1.Faculty of Science, Kobe University, 2.Graduate School of Science, Kobe University)

[PPS03-P14] Initial analysis plan of soluble organic compounds for the Hayabusa2 sample from asteroid Ryugu

*Hiroshi Naraoka[1], Yoshinori Takano[2], Jason P. Dworkin[3], SOM Analysis Team (1.Department of Earth and Planetary Sciences, Research Center for Planetary Trace Organic Compounds, Kyushu University, 2.Japan Agency for Marine-Earth Science and Technology, 3.Astrochemistry Laboratory NASA Goddard Space Flight Center, Greenbelt, MD 20771 USA)

[PPS03-P15] Radar and optical simultaneous observations of faint meteors with MU radar and Tomo-e Gozen

*Ryou Ohsawa[1], Akira Hirota[2], Shinsuke Abe[2], Daniel Kastinen[3], Kero Johan[3], yasunori Fujiwara[4], Takuji Nakamura[5], Shigeyuki Sako[1], Yuto Kojima[1], Jun-ichi Watanabe[6] (1.Institute of Astronomy, Graduate School of Science, The University of Tokyo, 2.Department of Aerospace Engineering, College of Science & Technology, Nihon University, 3.Swedish Institute of Space Physics, 4.SOKENDAI (The Graduate University for Advanced Studies), 5.National Institute of Polar Research, 6.National Astronomical Observatory of Japan)

[PPS03-P16] Global distribution and spectral characteristics of bright spots on asteroid Ryugu

*Masanori Suemitsu[1], Tomokatsu Morota[1], Rie Honda[2], Singo Kameda[15], Eri Tatsumi[3], Manabu Yamada[4], Naoya Sakatani[5], Toru Kouyama[6], Yokota Yasuhiro[7], Yuichiro Cho[8], Hidehiko Suzuki[9], Masahiko Hayakawa[10], Moe Matsuoka[10], Chikatoshi Honda[11], Tatsuhiro Michikami[12], Kazuo Yoshioka[13], Kazunori Ogawa[14], Hirotaka Sawada[5], Seiji Sugita[3] (1.Graduate School of Environmental Studies, Nagoya University, 2.Department of Science and Technology, System of Natural Science, Kochi Unicversity, 3.Graduate School of Earth and Planetary Science, Tokyo Unicversity, 4.Planetary Exploration Reserch Center, Chiba Institute of Technology, 5.Institute of Space and Astoronautical Science, Japan Aerospace Exploration Agency, 6.National Institute of Advanced Industrial Science and Technology, 7.Kochi University, 8.Department of Earth and Planetary Science, Tokyo University, 9.Depertment of physics, Meiji University , 10.Department of Solar System Science, Institute of Space and Astoronautical Science, Japan Aerospace Exploration Agency, 11.Aizu University, 12.Faculty of Engineering, Kindai University, 13.Graduate School of frontier Science, Tokyo University, 14.Kobe University, 15.Rikkyo University)

[PPS03-P17] Polarimetry of (155140) 2005 UD: the Dynamical Association with (3200) Phaethon

*Masateru Ishiguro[1], Jooyeon Geem[1], Hiroyuki Naito[2], Yoonsoo P. Bach[1], Daisuke Kuroda[3], Tatsuharu Ono[4], Seiko Takagi[4], Mitsuteru Sato[4], Kiyoshi Kuramoto[4], Tomohiko Sekiguchi[5], Masataka Imai[6], Makoto Watanabe[7], Katsuhito Ohtsuka[8], Sunao Hasegawa[9], Takashi Ito[10], Fumi Yoshida[11], Tomoko Arai[11] (1.Department of Physics and Astronomy, Seoul National University, 2.Nayoro Observatory, 3.Okayama Observatory, Kyoto University, 4.Department of Cosmosciences, Graduate School of Science, Hokkaido University, 5.Hokkaido University of Education, 6.National Institute of Advanced Industrial Science and Technology, 7.Department of Applied Physics, Okayama University of Science, 8.Tokyo Meteor Network, 9.Japan Aerospace Exploration Agency, 10.National Astronomical Observatory of Japan, 11.Planetary Exploration Research Center, Chiba Institute of Technology)

[PPS03-P18] **Follow-up observations for AKARI/IRC near-infrared asteroid spectroscopic survey (AcuA-spec)**

*Sunao Hasegawa[1], Daisuke KURODA[2], Kenshi YANAGISAWA[3], Fumihiko Usui[4] (1.Japan Aerospace Exploration Agency, 2.Kyoto University, 3.National Astronomical Observatory of Japan, 4.Kobe University)

[PPS03-P19] Amino acids on witness coupons collected from the ISAS/JAXA curation facility for the assessment and quality control of the Hayabusa2 sampling procedure

*Haruna Sugahara[1,2], Yoshinori Takano[1], Yuzuru Karouji[3], Kazuya Kumagai[4], Toru Yada[3], Naohiko Ohkouchi[1], Masanao Abe[3], Hayabusa2 project team (1.Japan Agency for Marine-Earth Science and Technology (JAMSTEC), 2. Institut de Chimie de Nice, Universite Cote dAzur, 3.Japan Aerospace Exploration Agency (JAXA), 4.Marine Works Japan Ltd.)

[PPS03-P20] Hayabusa2 orbit determination using c5++ software

*Keiko Yamamoto[1], Toshimichi Otsubo[2], Koji Matsumoto[1], Hirotomo Noda[1], Noriyuki Namiki[1], Hiroki Senshu[3], Takahide Mizuno[4], Naoko Ogawa[4], Go Ono[4], Yuya Mimasu[4], Kent Yoshikawa[4], Tadateru Takahashi[4], Yuto Takei[4], Atsushi Fujii[4], Fuyuto Terui[4], Takanao Saiki[4], Satoru Nakazawa[4], Makoto Yoshikawa[4], Yuichi Tsuda[4] (1.National Astronomical Observatory of Japan, 2.Hitotsubashi University, 3.Chiba Institute of Technology, 4.Japan Aerospace Exploration Agency)

[PPS03-P21] **Landing Site Selection for Hayabusa2: Scientific Evaluation of the Candidate Sites on Asteroid (162173) Ryugu**

*Hikaru Yabuta[1], Sei-ichiro WATANABE[2], Tomoki Nakamura[3], Naru Hirata[4], Seiji Sugita[5], Tatsuaki Okada[6], Kohei Kitazato[4], Yoshiaki Ishihara[7], Tomokatsu Morota[2], Naoya Sakatani[6], Koji Matsumoto[8], Koji Wada[9], Shogo Tachibana[5], Mutsumi Komatsu[10], ERI TATSUMI[5], Moe Matsuoka[6], Chikatoshi Honda[4], Takahiro Hiroi[11], Hiroki Senshu[9], Rie Honda[12], Yasuhiro Yokota[6], Rina Noguchi[6], Yuri Shimaki[6], Deborah Lorin Domingue[13], Lucille Le Corre[13], Antonella Barucci[14], Ernest Palomba[15], Shota Kikuchi[6], Akira Miura[6], Tomohiro Yamaguchi[6], Yukio Yamamoto[6], Takanao Saiki[6], Satoshi Tanaka[6], Makoto Yoshikawa[6], Yuichi Tsuda[6] (1.Hiroshima University, Department of Earth and Planetary Systems Science, 2.Nagoya University, 3.Tohoku University, 4.University of Aizu, 5.The University of Tokyo, 6.ISAS/JAXA, 7.NIES, 8.NAOJ, 9.Chiba Institute of Technology, Planetary Exploration Research Center (PERC), 10.Sokendai, 11.Brown University, 12.Kochi University, 13.Planetary Science Institute, USA, 14.Observatoire Paris-Site de Meudon, LESIA, France, 15.INAF-IAPS, Italy.)

[PPS03-P22] Visible Photometric, Spectroscopic and Polarimetric observations of an inactive comet, P/2016 BA14 with the 1.6m Pirka Telescope

*Ryo Yamagata[1], Tomohiko Sekiguchi[1], Ryo Okazaki[1], Kazuya Doi[1], Daisuke Kuroda[2], Masateru Ishiguro[3], Hiroyuki Naito[4] (1.Hokkaido University of Education, 2.Kyoto University, 3.Seoul National University, 4.Nayoro Observatory)

[PPS03-P23] **Polycyclic aromatic hydrocarbons and aliphatic hydrocarbons in Jbilet Winselwan carbonaceous chondrite : Attempt to evaluate the thermal metamorphism degree on the parent body**

Hiroki Kato[1], *Hikaru Yabuta[1] (1.Hiroshima University, Department of Earth and Planetary Systems Science)

[PPS03-P24] Disk-Resolved Photometry Analysis of the Asteroid Ryugu Images Obtained by Hayabusa2 Visible Camera ONC

*yokota yasuhiro[1,2], Rie Honda[1], ERI TATSUMI[3], Deborah Domingue[4], Stefanus E. Schroeder[5], Moe Matsuoka[2], Seiji Sugita[3], Tomokatsu Morota[6], Shingo Kameda[7], Toru Kouyama[8], Hidehiko Suzuki[9], Manabu Yamada[10], Naoya Sakatani[2], Chikatoshi Honda[11], Masahiko Hayakawa[2], Kazuo Yoshioka[3], Yuichiro Cho[3], Hirotaka Sawada[2] (1.Kochi University, 2.ISAS/JAXA, 3.Univ. of Tokyo, 4.Planetary Science Institute, 5.DLR, 6.Nagoya Univ., 7.Rikkyo Univ., 8.AIST, 9.Meiji Univ., 10.Chiba Institute od Technology, 11.Aizu Univ.)

Impact experiments on low strength coarse-grained regolith simulating surface materials on asteroid Ryugu

*Yuya Yamamoto[1], Masahiko Arakawa[1], Minami Yasui[1], Sunao Hasegawa[2], Ryo Sugimura[1]

1. Graduate School of Science, Kobe University, 2. ISAS, JAXA

Impact cratering is one of the most important physical processes, then we study crater scaling laws and impact induced seismic waves in order to elucidate various flow processes on asteroids caused by impacts. The conventional crater scaling laws are categorized into two regions according to the controlling physics for the crater growth: they are gravity and material strength. A crater formed on regolith layer is surely controlled by the gravity, however when the regolith layer was filled with coarse particles with low mechanical strength, then the several coarse grains might be disrupted to consume the Ek. Thus, the crater size could be affected by the disruptions of the coarse grains. We speculate that not only the gravity but also the grain strength could affect the final crater size. Then, we made cratering experiments by using the target made of weak particles, and studied the effects of the particle strength on the crater scaling law and the impact induced seismic wave.

Experiments: Cratering experiments were conducted by using a gas gun set at Kobe University and ISAS. Granular targets were prepared by using weathered tuff granules with the size of 1 to 4mm (small particle) and the size of 1 to 4cm (large particle). The crush strength of these tuff particles was measured to be about 60 kPa. A spherical projectile with the size of 3mm which is made of iron, zirconia, alumina, glass, and nylon) was lunched at the impact velocity from 40 to 200m/s, and a spherical Al projectile with the size of 2mm was impacted at the impact velocity from 1.2 to 4.5km/s, then these two types of the projectile were impacted on the target surface at the normal direction. Impact cratering process and ejecta curtain growth were observed by a high-speed camera at 10^3-10^5 fps, and the video images were used to analyze ejecta particles to reconstruct the trajectories. After the shot, the crater morphology was recorded and the diameter and the depth were measured. Impact induced seismic waves were measured by using 3 accelerometers (specific frequency is 30kHz) set at different positions from the impact point, and a data logger was used to record the seismic data through charge amplifiers (data acquisition rate is 100kHz) connecting to the accelerometer.

Results: The crater size was found to increase with the projectile kinetic energy (Ek) at lower than 0.14J and at higher than 0.63J, so that the crater size was almost constant among them, and more the crater size obtained at very high Ek was almost on the extrapolated line from the relationship given by the low Ek data. The pi-scaling law was used to construct the relationship between normalized radius (πR) and normalized gravity (π2), and πR at small π2 was found to be rather smaller than that obtained for sand and glass beads targets, and more πR at large π2 was found to be consistent with that for sand and glass beads. More detail analysis tells us that all the data separated into two trends with large offset according to the impact velocity and the projectile material. This offset might be caused by the disruption of several tuff particles. The ejection velocities of each tuff particle were so scattered, then the distinctive relationship between initial position of particle and the ejection velocity was not derived in the low velocity range. The propagation velocity of the impact induced seismic wave was about 30 m/s, and it is 1/3 of that for glass beads. Furthermore, we found that the relationship between the maximum acceleration and the distance from the impact point was about 1/10 of that obtained for glass beads: the seismic wave in the tuff granules attenuated so quickly compared to the glass beads. But, when the distance is normalized by the crater radius, these relationships almost consistent each other, so that the

©2019. Japan Geoscience Union. All Right Reserved.

normalized distance could be a good parameter for the scaling of the acceleration of seismic wave.

Keywords: impact cratering experiment, low strength, impact-induced seismic shaking, crater scaling law

©2019. Japan Geoscience Union. All Right Reserved.

Reflectance estimation of asteroid Ryugu using MASCOT

*Marika Ishida[1], Koto Amano[1], Keiichi Moroi[1], ERI TATSUMI[2], Tra-Mi Ho[10], Shingo Kameda[1], Seiji Sugita[2], Rie Honda[3], Tomokatsu Morota[4], yokota yasuhiro[5], Toru Kouyama[6], Hidehiko Suzuki[7], Manabu Yamada[8], Naoya Sakatani[5], Chikatoshi Honda[9], Masahiko Hayakawa[5], Kazuo Yoshioka[2], Moe Matsuoka[5], Yuichiro Cho[2], Hirotaka Sawada[5]

1. Rikkyo Univ., 2. Univ. of Tokyo, 3. Kochi Univ., 4. Nagoya Univ., 5. JAXA/ISAS, 6. AIST, 7. Meiji Univ., 8. Chiba Inst. Tech, 9. Univ. of Aizu, 10. DLR

Hayabusa2 is a sample-return mission for the C-type asteroid 162173 Ryugu. Hayabusa2 arrived at Ryugu on 27 June 2018, and various observations are still being conducted. Hayabusa2 performs multiband spectral observation by employing the optical navigation camera telescope (ONC-T)and can thereby obtain spectral map of Ryugu, which enables the study of material distribution and degree of space weathering of Ryugu. However, the sensitivity of ONC-T has been previously calibrated by incorporating the inflight data of stars with significant uncertainty. Hence, the authors aim to estimate the reflectance of Ryugu by employing Mobile Asteroid Surface Scout (MASCOT).
MASCOT comprises four instruments (MASCAM, MicrOmega, MARA, and MASMAG) that are employed for analyzing the soil of Ryugu. The upper side of the MASCOT landeris coated with white paint, and its spectral image was captured by ONC-T after its release from Hayabusa2 to Ryugu. The authors conducted on-ground reflectance measurement of a white plate whose white paint is identical to that of MASCOT. Hence, the primary objective of the proposed study is to estimate the reflectance of Ryugu by comparing MASCOT’ s white side’ s spectrum captured by ONC-T with the on-ground reflectance measurement of the white plate that has identical paint as MASCOT, and thus evaluate the validity.

Keywords: Hayabusa2, ONC-T, MASCOT

©2019. Japan Geoscience Union. All Right Reserved.

Flyby observation of Asteroid (3200) Phaethon by DESTINY$^+$ onboard cameras

*Ko Ishibashi[1], Shingo Kameda[2], Masato Kagitani[3], Peng Hong[1], Manabu Yamada[1], Osamu Okudaira[1], Tomoko Arai[1], Fumi Yoshida[1], Shunsuke Sato[4], Takahiro Ishimaru[4], Takaya Okamoto[4], Takahiro Iwata[4], Tatsuaki Okada[4], Takeshi Takashima[4]

1. Chiba Institute of Technology, 2. Rikkyo University, 3. Tohoku Universtiy, 4. Japan Aerospace Exploration Agency

DESTINY$^+$ (Demonstration and Experiment of Space Technology for INterplanetary voYage, Phaethon fLy-by and dUst Science) is a mission proposed for JAXA/ISAS Epsilon class small program, currently in the pre-project phase (Phase-A) with a launch targeted for 2023. DESTINY$^+$ is a joint mission of technology demonstration and scientific observation. The near-Earth asteroid (3200) Phaethon, the flyby target, is known as a parent body of the Geminid meteor shower, the size of which is approximately 5 to 6 km in diameter.

In this mission, spatially resolved images of Phaethon will be taken by two onboard cameras, the Telescopic CAmera for Phaethon (TCAP) and the Multiband CAmera for Phaethon (MCAP) during the flyby, in order to understand the nature of a meteor shower's parent body, which is one of the sources of interplanetary dust particles that are thought to be an important transport medium of organic matter to the Earth. The spacecraft flybys Phaethon with a relative speed of 30 to 40 km/s. Despite such a high flyby speed, the cameras are required to take un-blurred images of Phaethon.

The main purposes of the DESTINY$^+$ flyby observation of Phaethon is to understand the geology of a parent body of a meteor shower, and in particular constrain the dust ejection mechanisms from active (i.e., dust-ejecting) asteroids. The specific objectives of the camera observation are taking images for (1) obtaining the light curve of Phaethon in order to estimate the rotational period, (2) measuring the outline shape of Phaeton, (3) making a 3D shape model of Phaethon, (4) observing the surface geological features of Phaethon including dust ejection features, and (5) observing the surface material distribution of Phaethon. The observations (1) to (4) will be conducted by TCAP, and (5) by MCAP.

TCAP is a telescopic panchromatic camera for high spatial resolution imaging of the surface of Phaethon and have a rotational mirror for asteroid tracking during flyby. The rotational mirror can change the direction of the line of sight from 0 deg to 180 deg. This enables to observe Phaethon throughout the flyby with wide solar phase angles, which is extremely important to image and understand the surfaces of planetary bodies because the solar phase angle affects significantly the appearance of geological features in taken images.

MCAP is a multiband camera, the wavelengths of which are 400, 480, 550, 700, 850, and 950 nm (480 and 950 nm are optional bands) and has multiple optical systems and sensors in order to take all band images simultaneously. This is because there is not enough time to take each band image in turn with changing bandpass filters using such as a filter wheel in this high speed flyby mission. MCAP does not have a tracking mirror due to the weight limitation, and the line of sight of MCAP is fixed to the spacecraft with 40 deg off the relative velocity vector of the spacecraft.

We will explain the flyby imaging sequence of DESTINY$^+$, and show the conceptual designs of TCAP and MCAP.

©2019. Japan Geoscience Union. All Right Reserved.

Keywords: Phaethon, DESTINY+, Flyby, Camera

©2019. Japan Geoscience Union. All Right Reserved.

Polarimetric Study of Asteroids in Comet-Like Orbits (ACOs)

*Jooyeon Geem[1], Masateru Ishiguro[1], Yoonsoo P. Bach[1], Daisuke Kuroda[2], Hiroyuki Naito[3], Hidekazu Hanayama[4], yoonyoung kim[10], Yuna G. Kwon[1], Sunho Jin[1], Tomohiko Sekiguchi[5], Ryo Okazaki[5], Jeremie J. Vaubaillon[6], Masataka Imai[7], Tatsuharu Oono[8], Yuki Futamuts[8], Seiko Takagi[8], Mitsuteru Sato[8], Kiyoshi Kuramoto[8], Makoto Watanabe[9]

1. Astronomy program, Dept of Physics and Astronomy, Seoul National University, 2. Okayama Observatory, Kyoto University, 3. Nayoro Observatory, 4. Ishigakijima Astronomical Observatory, National Astronomical Observatory of Japan, 5. Hokkaido University of Education, 6. Observatoire de Paris, I.M.C.C.E., 7. National Institute of Advanced Industrial Science and Technology, 8. Department of Cosmosciences, Graduate School of Science, Hokkaido University, 9. Department of Applied Physics, Okayama University of Science, 10. Max Planck Institute for Solar System Research

It is important to determine the taxonomic types of small bodies in the solar system and further to study the spatial distribution of the planetary system. Among the small bodies, it is considered that there should be dormant comets that have lost a significant fraction of volatile materials in their subsurface layers. As a result, they are unable to produce any detectable coma and recognized as asteroids. It has been challenging to find out such dormant comet population from a list of known asteroids because of the asteroidal appearances. There are several attempts to find the dormant comet nuclei from asteroidal catalogs, for example, by using their reflectance spectra or orbital elements. However, little has been studied via polarimetry.
We conduct a polarimetric study of three candidates of dormant comet nuclei, (331471) 1984 QY1, (3552) Don Quixote and (944) Hidalgo, by using the 1.6-m Pirka Telescope at the Nayoro observatory (operated by Hokkaido University, Japan). We chose these asteroids in comet-like orbits (ACOs) based on the orbital elements (i.e., the Tisserand parameter with respect to Jupiter $T_J < 3$). We found that 1984 QY1 has a polarimetric albedo (geometric albedo determined via polarimetry) $p_V = 0.16 \pm 0.06$ while both Don Quixote and Hidalgo have Rc-band polarimetric albedo $p_R < 0.05$. Based on the polarimetric result together with a dynamical analysis, we conjectured that 1984 QY1 could be an S-type asteroid transported into the current orbit via 3:1 mean motion resonance with Jupiter. From the previous spectroscopic study, Don Quixote and Hidalgo are classified into D-type taxonomic group, which are typical of comet nuclei. In this presentation, we will introduce our polarimetric observations of ACOs and emphasize that polarimetry is a powerful tool for discriminating the asteroidal and cometary origins.

Keywords: Polarimetry, Asteroid

©2019. Japan Geoscience Union. All Right Reserved.

Dynamical lifetime of the Oort Cloud new comets under planetary perturbation

*Ito Takashi[1], Arika Higuchi[1]

1. National Astronomical Observatory of Japan

Nearly isotropic comets with very long orbital period are supposed to come from the Oort Cloud. Recent observational and theoretical studies have greatly revealed the dynamical nature of this cloud and its evolutionally history, but many issues are yet to be known. Our goal is to trace the dynamical evolution of the Oort Cloud new comets (OCNCs) produced by evolving comet cloud, hopefully estimating the fraction of OCNCs embedded in the current populations of the solar system small bodies. We combine two models to follow the dynamical evolution of OCNCs beginning from their production until their ejection out of the solar system, obtaining statistics of the dynamical lifetime of OCNCs: The first model is a semi-analytical one about the OCNC production in an evolving comet cloud under the perturbation of the galactic tide and stellar encounters. The second model numerically deals with planetary perturbation over OCNCs' dynamics in planetary region. The main results of the present study are: (1) Typical dynamical lifetime of OCNCs in our models turned out to be O(10^7) years. Once entering into the planetary region, most OCNCs stay there just for this timespan, then get ejected out of the solar system on hyperbolic orbits. (2) While averaged orbital inclination of OCNCs is small, the so-called "planet barrier" works rather effectively, preventing some OCNCs from penetrating into the terrestrial planetary region.

Keywords: Oort Cloud, comet, orbital dynamics

©2019. Japan Geoscience Union. All Right Reserved.

Thermal Infrared Imaging of C-type Asteroid 162173 Ryugu with Porous Surfaces

*Tatsuaki Okada[1,2], Tetsuya Fukuhara[3], Satoshi Tanaka[1], Makoto Taguchi[3], Takehiko Arai[4], Naoya Sakatani[1], Yuri Shimaki[1], Hiroki Senshu[5], Yoshiko Ogawa[6], Hirohide Demura[6], Kentaro Suko[6], Kohei Kitazato[6], Toru Kouyama[7], Tomohiko Sekiguchi[8], Jun Takita[9], Sunao Hasegawa[1], Tsuneo Matsunaga[10], Takehiko Wada[1], Takeshi Imamura[2], Jorn Helbert[11], Thomas G. Mueller[12], Axel Hagermann[13], Jens Biele[11], Matthias Grott[11], Maximiliam Hamm[11], Marco Delbo[14], Yukio Yamamoto[1], Naru Hirata[6], Naoyuki Hirata[15], Fuyuto Terui[1], Takanao Saiki[1], Satoru Nakazawa[1], Makoto Yoshikawa[1], Sei-ichiro WATANABE[1,16], Yuichi Tuda[1]

1. Institute of Space and Astronautical Science, Japan Aerospace Exploration Agency, 2. University of Tokyo, 3. Rikkyo University, 4. Ashikaga University, 5. Chiba Institute of Technology, 6. University of Aizu, 7. National Institute of Advanced Industrial Science and Technology, 8. Hokkaido University of Education, 9. Hokkaido Kitami-Hokuto High School, 10. National Institute for Environmental Studies, 11. German Aerospace Center, 12. Max-Planck Institute for Extraterrestrial Physics, 13. University of Stirling, 14. Observatoire de la Côte d'Azur, 15. Kobe University, 16. Nagoya University

Thermal images from global to close-up scales taken by the Thermal Infrared Imager TIR [1] on Hayabusa2 [2] have revealed thermophysical properties of the C-type Near-Earth Asteroid 162173 Ryugu. On 27 June 2018, Hayabusa2 arrived at Ryugu and started remote sensing to characterize the nature of the asteroid and find the proper landing sites. *In situ* surface experiments were conducted using the robotic landers Minerva-II and Mascot [3]. *In situ* radiometry was conducted by MARA on MASCOT during a day-night cycle to derive the thermal inertia of a single boulder [4]. Ground-based observations [5] have been informed that the averaged thermal inertia of the asteroid is from 150 to 300 [tiu = J m^{-2} $s^{-0.5}$ K^{-1}] [5,6], corresponding to the surface covered with cm-sized granules.

TIR is the same design as the LIR on Akatsuki Venus climate orbiter [6], with 8 to 12 μm wavelength range, 328 x 248 effective pixels, and the FOV and IFOV of 16.7˚ x 12.7˚ and 0.051˚ per pixel, respectively. The first image of Ryugu detected by TIR was a point source on 6 June 2018, as was previously predicted [7]. Disc-resolved thermal images of Ryugu was taken from the HP on 30 June. The surface temperature was measured at 300 to 370K at about 1AU from the Sun, and gradually decreased with the solar distance. Comparison of the results with modeling [8] shows that the surface of Ryugu is not like fine regolith nor base rocks. Most of large boulders on Ryugu show temperatures almost the same as the surrounding surfaces. Diurnal temperature profiles of Ryugu are rather flatter than expected for a smooth terrain. Apparent thermal inertia is ~300 tiu or larger, but probably lower than the value when the surface roughness is considered. All these facts are consistent with a very rough and porous surface with low porosity (~35 ±10 %) [9] and the surrounding surface is dominated by porous rocks larger than several centimeters. Macro porosity should be 30 to 50 % to account for the bulk density of Ryugu ~1200 kg m^{-3}.

During the descent operations for the release of landers and the touchdowns for sample collection, TIR has taken close-up thermal images of the local sites, continually from the altitude of 500 m until the start of final descent at 10 or 20 m altitude. Close-up thermal images show the surface physical state and a variety of boulders. Most of the boulders in close-up images have temperatures similar to the surroundings but with more variety. A small number of boulders are remarkably colder than the surroundings, indicating dense rocks with lower porosity.

©2019. Japan Geoscience Union. All Right Reserved.

These facts indicate that Ryugu is probably a rubble pile of loosely-bound porous rocks, which might originate from the outer layer of parent body where compaction did not occur effectively, while the dense boulders might originate the compacted center region of parent body or from the different parent body. A different composition (e.g., organic rich materials) cannot be ruled out so far to account for such a low thermal inertia (and low density) of Ryugu.

Acknowledgments: The authors appreciate all the members of the Hayabusa2 Project and supporting staff for their technical assistance and scientific discussions. This research is partly supported by the JSPS KAKENHI No. J26287108, No. J17H06459 (Aqua Planetology), and the Core-to-Core program “International Network of Planetary Sciences”. MDB acknowledges support from CNES.

References: [1] Okada T. et al. (2017) *SSR.,* 208, 255-286. [2] Tsuda Y. et al. (2013) *Acta. Astronautica, 91* , 356-362. [3] Ho T.M. et al. (2017) *SSR.,* 208, 255-286. [4] Grott, M. et al. (2019), submitted to Nature. [5] Mueller T.G. et al. (2016) Astronon. Astrophys., doi:10.1051/0004-6361/201629143. [6] Fukuhara T. et al. (2011) *EPS,* 63, 1009-1018. [7] Okada T. et al. (2018) *PSS., 158, 46-52.* [8] Takita J., et al. SSR, 2018, 287-315. [9] Okada T. (2016) *LPSC.*, 47, #1457.

Keywords: Hayabsua2, Thermal Infrared Imager, Thermal Inertia

©2019. Japan Geoscience Union. All Right Reserved.

Data Release of Asteroid 162173 Ryugu by Observation of Thermal Infrared Imager onboard Hayabusa2

*Takehiko Arai[1], Hirohide Demura[2], Toru Kouyama[7], Naoya Sakatani[3], Kentaro Suko[2], Yuri Shimaki[3], Hiroki Senshu[5], Tomohiko Sekiguchi[6], Yoshiko Ogawa[2], Sunao Hasegawa[3], Takehiko Wada[3], Takeshi Imamura[10], Tsuneo Matsunaga[9], Jun Takita[8], Kohei Kitazato[2], Makoto Taguchi[4], Tetsuya Fukuhara[4], Satoshi Tanaka[3], Tatsuaki Okada[3]

1. Ashikaga University, 2. The University of Aizu, 3. Japan Aerospace Exploration Agency (JAXA), 4. Rikkyo University, 5. Chiba Institute of Technology, 6. Hokkaido University of Education, 7. National Institute of Advanced Industrial Science and Technology (AIST), 8. Hokkaido Kitami Hokuto High School, 9. National Institute for Environmental Studies (NIES), 10. The University of Tokyo

The thermal infrared imager (TIR) onboard the Hayabusa2 spacecraft performed thermography of the asteroid 162173 Ryugu through in-situ observations from 2018 to 2019. The primary purpose of TIR is to determine the global thermophysical properties of the asteroid and to reveal the evolutional history such as physical properties of the coalesced bodies, orbital changes due to radiation force, and the thermal evolution. This study introduces observed data of TIR and public data for scientists. The data are released by JAXA data archives (DARTS) and NASA PDS.

Keywords: Hayabusa2, Thermal Infrared Imager, Asteroid Ryugu

©2019. Japan Geoscience Union. All Right Reserved.

Multi-mission capability of HARMONICS

*Shintaro Tsunoda[1], Hirohide Demura[1], Naru Hirata[1]

1. The University of Aizu

This research has updated HARMONICS from a viewpoint of multi-mission capability, such as the Martian satellite exploration mission MMX in 2020s. Newly additional function is Switching on the shape model interface.
Bird view and visualization of FOV is important in robotics control. This technology is also used for deep space explorer missions.
HARMONICS is visualization tool of FOV(Field Of View) of scientific instruments and spacecraft’s position for HAYABUSA mission. The software has been updated by University of Aizu students of the past. The original HARMONICS had been developed by Nemoto(2006). GUI of HARMONICS had been replaced GUI library from GKT to Qt and added new functions, such as interactive modification of input mission plan by Ueno+(2017). The software had been add FOV frustum function by Aoki(2017). HARMONICS has tried to manage data for each project based on preference file in 2018.
HARMONICS should improved scalability to be compatible for ongoing mission. HARMONICS had been used to decide shutter chance by Camera Science Team in the asteroid Itokawa rendezvous of HAYABUSA. This software has not used in the asteroid Ryugu rendezvous of HAYABUSA2. The proven software should be use for future ongoing missions other than HAYABUSA. This research is development to HARMONICS adapt to ongoing missions.
I separated the designation of the data set from the source code and clarified the part edited by the user and the part edited by the developer.
HARMONICS has the function to switch and display data of different missions by this research. When users extend HARMONICS for multiple missions, users don’t need edit source code. User needs only kernel and the shape model of spacecraft and target asteroid. User do not need tough coding. User can use easily HARMONICS by editing preference file and kernel.

Keywords: Hayabusa2, Ryugu, Software, visualization

©2019. Japan Geoscience Union. All Right Reserved.

New interface of verification for calibration and conversion in HEAT : Hayabusa2 Exploration Assistant for TIR

*Tatsuro Kobayashi[1], Kentaro Suko[1], Hirohide Demura[1], Yoshiko Ogawa[1], Takehiko Arai[2], Naoya Sakatani[3], Tatsuaki Okada[3], Satoshi Tanaka[3], Tetsuya Fukuhara[4]

1. The University of Aizu, 2. Ashikaga University, 3. Institute of Space and Astronautical Science, Japan Aerospace Exploration Agency, 4. Rikkyo University

Hayabusa2 is an ongoing mission for sample return from the asteroid Ryugu.
Candidates of sampling sites are selected based on surface mapping by optical instruments such as Thermal Camera (TIR). TIR observes surface infrared radiation from the asteroid. A software package peculiar to TIR is HEAT: Hayabusa2 Exploration Assistant for TIR. The software has four functions; Database for ground tests, calibration of flight data based on the ground tests, conversion from raw data to temperature one, and analysis for verifying the calibration and conversion. The converted data products are divided into some levels: Lv1 Raw data [DN], Lv2a Temperature [K], Lv2b is Brightness [W/m2], and higher thermal model with VTK format [K]. This research implements new interface of verification for calibration and conversion based on hearing and survey for requirements from TIR science team. The environment of implementation is following tool. OS: macOS Mojave 10.14.2. Computing language: C++, OpenGL. Frameworks: Qt5.4. Tools: Fits, Qt creator, SPICE toolkit, Visualization Toolkit, QcustomPlot, Xcode10.1.

Keywords: Hayabusa2, Software, Ryugu, Calibration

©2019. Japan Geoscience Union. All Right Reserved.

Dust particle evolution of a near-Earth object 252P/LINEAR from near-infrared polarimetric observations in 2016

*Yuna G Kwon[1], Masateru Ishiguro[1], Jungmi Kwon[2], Daisuke Kuroda[3], Myungshin Im[1], Changsu Choi[1], Motohide Tamura[4], Takahiro Nagayama[5], Nobuyuki Kawai[6], Jun-ichi Watanabe[7]

1. Seoul National Univ., 2. ISAS/Japan Aerospace Exploration Agency, 3. Okayama Astrophysical Observatory, 4. The Univ. of Tokyo, 5. Kagoshima Univ., 6. Tokyo Institute of Technology, 7. National Astronomical Observatory of Japan

Comets, one of the least-altered leftovers from the early solar system, have probably preserved the primitive structure inside, whereas their surfaces become differentiated from initial states after repetitive orbital revolutions around the sun. Resurfacing makes the surface drier and more consolidated than the bulk nuclei, creating inert refractory dust layer (so-called “dust mantle”). Near-Infrared (NIR) polarimetry is theoretically expected to maximize the contrast of the porosity between inner fresh and evolved dust particles, by harboring more dust constituents in the single wavelength than the optical, and thus intensifying electromagnetic interference in dust agglomerates. Despite the advantage, only few studies have been conducted in this approach at multiple observation epochs. Herein, we present our new multi-band NIR polarimetric (1.25—2.25 microns) study of near-Earth object 252P/LINEAR over 12 days near perihelion; alongside broadband optical photometric (0.48—0.80 microns) data over four months in 2016 and a subsidiary dynamical simulation over 1000 year backward in time. 252P/LINEAR drew attention due to (1) its close approach to the Earth (~0.036 au on 2016 March 16), (2) its possible pairing to a comet P/2016 BA14 (PanSTARRS), and (3) its very low activity level despite its relatively young dynamical age. In this study, we detected two discontinuous brightness enhancements of 252P/LINEAR, particularly, the former of which accompanied a significant increase of NIR polarization degree of the comet (by ~13 % at most) with unusual blue polarimetric color. We will discuss the most probable scenario of the observed results, together with the orbital evolution of the comet and a dynamical association with its pair.

Keywords: Comet, Near-earth object, Polarimetry, Dust

©2019. Japan Geoscience Union. All Right Reserved.

Performance Evaluation of TRIPOL on the 61-cm Telescope at Seoul National University for Polarimetric Observations of Solar System Small Bodies

*Sunho Jin[1], Masateru Ishiguro[1], Yuna G Kwon[1], Jooyeon Geem[1], Yoonsoo P. Bach[1], Jinguk Seo[1], Hiroshi Sasago[2], Shuji Sato[3]

1. Seoul National University, 2. Sasago Co.,Ltd, 3. Nagoya University

Polarimetry of solar system small bodies is a powerful technique for investigating their physical properties, such as albedos, particle sizes, and porosities of these bodies. Observational opportunities arise sometimes suddenly, that is, just after unforeseeable activations of comets and discoveries of near-miss asteroids. Here, we introduce our activity to install the polarimetric instrument, TRIPOL (Triple-Range Imager and POLarimeter) on the 61-cm telescope (a Ritchey-Chretien reflector with f/7.0) at the Center for Astronomy and Space Science, Seoul National University, and report an observational result of three comets. This combination provides an 8.0’ ´8.0’ field of view and pixel resolution of 0.94” pixel^{-1}. Throughout photometric observations, we determined the limiting magnitudes (defined as magnitudes for S/N=5) of 15.17±0.06 (g’-band), 15.68±0.01 (r’-band), 16.24±0.03 (I’-band), respectively, with total 240-seconds exposure (four 60-seconds exposure images, each was taken at different rotation angle for the half-wave plate). We also found that the instrumental polarizations are negligibly small, that is, -0.32±0.04% (g’-band), -0.36±0.05% (r’-band) and -0.21±0.04% (I’-band), while the polarization efficiencies are large enough to maximize the performance, that is, 97.52±0.03% (g’-band), 98.83±0.02% (r’-band) and 99.15±0.02% (I’-band).

With this instrument, we conducted polarimetric observations of three Jupiter-family comets, 21P/Giacobini-Zinner, 38P/Stephan-Oterma, and 46P/Wirtanen on a trial basis. It is known from a recent study that the polarization degrees of cometary dust particles are significantly influenced by gas emissions [1] With multiband data taken with TRIPOL, we eliminated an influence of gas contaminations and found that the dust polarization degrees of these three comets coincide with those of so-called ‘dust-rich comets’. From this result, we conjecture that the polarimetric property of Jupiter-family comets is broadly homogeneous, unlike asteroids. We plan to describe our future plan using the polarimetric system.

[1] Kwon, Y. G. et al. Astronomical Journal, 154, 4, 173, 2017

Keywords: Comet, Instrument, Polarimetry

©2019. Japan Geoscience Union. All Right Reserved.

Smart Interface of HEAT: Hayabusa2 Exploration Assistant for TIR

*Kentaro Suko[1], Tatsuro Kobayashi[1], Hirohide Demura[1], Takehiko Arai[2], Naoya Sakatani[3], Tatsuaki Okada[3], Satoshi Tanaka[3], Tetsuya Fukuhara[4]

1. The University of Aizu, 2. Ashikaga University, 3. Institute of Space and Astronautical Science, Japan Aerospace Exploration Agency, 4. Rikkyo University

The Hayabusa2 project is a sample return mission to the asteroid Ryugu. It was launched on Dec. 3, 2014, and it has been at Ryugu since June 27, 2018. Hayabusa2 has optical instrument called Thermal Infrared Imager (TIR). These main functions are to know natures of the asteroid and to select the candidate of safe landing sites for sampling based on thermos-physical properties of the surface. TIR records infrared radiation from the target as a digital number (DN). The infrared signal is affected by sensor-surrounding objects; lens, shutter, package, and case. TIR requires consideration about this effect when converts DN images to temperature one. This study improved conversion system to increase conversion efficiency.

Hayabusa2 TIR Science Team has developed an analysis supporting tool called Hayabusa2 Exploration Assistant for TIR (HEAT). HEAT is used to search TIR data interactively, display TIR images, and visualize thermal models. We receive TIR raw images (Product Level 1) from ISAS/JAXA and convert them to brightness temperature images (Level 2a) and radiance images (Level 2b) using HEAT at Univ. of Aizu. The converted images are provided to the Hayabusa2 project data server.

This part introduces a concept model. The spectral radiance emitted from a blackbody B(λ ,T) (W s r-1m-2) is given by the Planck function based on wavelength λ (m) and temperature T(K) as follows:

$$B(\lambda,T) = (2hc2/\lambda 5)^* (1/(\exp(\lambda kBT)-1))$$

H = 6.63*1034 (m2 kg s-2 s-1) is the Planck constant, c=2.9972*108(ms-1) is the speed of light, and KB= 1.38*10-23 (m2 kg s-2K-1) is the Boltzmann constant. The observed radiance L(T) (W sr−1 m−2) is as follows:

$$L(T)= \varepsilon \int BR(\lambda)d\lambda$$

ε is the spectral thermal emissivity, and R(λ) is the response function such as the detection efficiency of the bolometer, the measured transmittance of optics including the band-pass filter and the germanium lens. The calibration formula with two regressed parameters A and B is written as follows:

$$DN=A * L(T) + B$$

The converted temperatures of the Moon were lower than expected because each pixel did not cover the sunlit area entirely or due to roughness effect of the cratered terrain. TIR has been observing Ryugu in approach and rendezvous phases. The altitudes of TIR observations during the rendezvous phase range from 20 km to less than 10 m. This study has processed about 3000 Ryugu images observed by TIR since June 2018.

©2019. Japan Geoscience Union. All Right Reserved.

This study improved conversion system. Previous conversion system converts a TIR image one by one, but current conversion system converts TIR images in selected directory at once.

Keywords: Hayabusa2, TIR, HEAT, Software

©2019. Japan Geoscience Union. All Right Reserved.

Experimental Study on Collision Crater Formed on Bulge Geography

*Yusaku Yokota[1], Yuya Yamamoto[2], Minami Yasui[2], Masahiko Arakawa[2]

1. Faculty of Science, Kobe University, 2. Graduate School of Science, Kobe University

An equatorial bulge was found on the surface of asteroid Ryugu and Bennu by recent spacecrafts of Hayabusa2 and OSIRIS-Rex, and ridge structures with various scales originated by geological activities have been recognized on icy satellites. Impact craters are dominant geological features on solid planets such as asteroids and satellites, and a crater rim are also recognized as a ridge or bulge with a circular shape. These bulges and ridges are shown to be erased with time because small scale impacts excavate and disrupt these topographies. It is well known that old craters gradually degraded by small impacts to get blurred and could be completely erased. We can expect the similar degradation process on large bulges and ridge structures, so that the life time of these structures by small impacts is a good indicator of the formation age of these structure by geologic activities. So far, the effect of small impacts on the degradation is estimated by using the results on the flat surface, but actually the surface of the bulge is curved and there is a summit on the bulge. Therefore, if we estimate the life time of the bulge structure, we should consider the effect of the topography such as a summit and curvature. Then, the impacts on the bulge structure was studied to clarify how the bulge structure affected the crater formation efficiency. In this study, we suppose the bulge made from regolith and boulders, such as an equatorial bulge of Ryugu and assume the crater formation process dominated by not the strength but the gravity.

We prepared a triangular prism target to simulate the bilge structure, and set it like that the base of this prism is rectangle, then it looks triangle when we look it at the horizontal direction, and we can look at the linear summit from the top view. Quartz sands with the size of 100μm was used to build the target and the angle of repose for this quartz sand is about 30 degree. The slope of the prism was measured from the base, and we set the angle from 20 to 30 degree. The quartz sands were filled into a transparent water tank with the depth of 20 cm to prepare the bulge structure. Impact experiments were conducted by using a vertical type gas gun, and the water tank was set in the chamber to evacuate below 1000 Pa. A alumina sphere projectile with the size of 3mm was launched at the velocity from 70 to 200 m/s, and it was impacted on the bulge in the vertical direction: the impact angle measured from the target surface was about 60 degree when the slope was 30 degree. The distance from the impact pint to the summit (deviation distance, d_d) was changed from 0 to 20mm.

We found that the crater shape strongly depended on the d_d, so the crater shape was an ellipsoid when the impact point was near the summit. Th major axis appeared along the linear summit and the minor axis appeared across the summit. The aspect ratio of the major axis to the minor axis gradually changed toward 1 with the increase of d_d. Moreover, the aspect ratio becomes large at the same d_d when the impact velocity increased. The major axis of the ellipsoid crater formed on the bulge was slightly larger than the crater diameter formed on the flat surface, and the slope angle might affect the size of the ellipsoid because we found that the crater formed on the slope of 30 degree was systematically larger than that formed on the slope of 20 degree. We also observed an asymmetric ejecta curtain from the impact point on the bulge, moreover the ejecta curtain was notice to be deformed so much at the impact point near the summit because of the effect of curvature of the bulge on the crater flow.

Angle of repose, Impact crater, Bulge and ridge structure, Ejecta curtain

©2019. Japan Geoscience Union. All Right Reserved.

©2019. Japan Geoscience Union. All Right Reserved.

Initial analysis plan of soluble organic compounds for the Hayabusa2 sample from asteroid Ryugu

*Hiroshi Naraoka[1], Yoshinori Takano[2], Jason P. Dworkin[3], SOM Analysis Team

1. Department of Earth and Planetary Sciences, Research Center for Planetary Trace Organic Compounds, Kyushu University, 2. Japan Agency for Marine-Earth Science and Technology, 3. Astrochemistry Laboratory NASA Goddard Space Flight Center, Greenbelt, MD 20771 USA

The spectra of asteroid 162173 Ryugu taken by Near-Infrared Spectrometer (NIRS3) onboard Hayabusa2 are nearly featureless and consistent with carbonaceous chondrites (Matsuoka et al., 2018). The Hayabusa2 spacecraft will collect surface samples of Ryugu and deliver to the Earth during late 2020. The initial analysis of the Ryugu samples will focus on (1) detailed chemical and mineralogical characterization of the samples and (2) understanding the history of Ryugu and the Solar System in order to maximize the scientific achievement of the project and (3) to prove the scientific potential of the samples to the community for the analytical opportunity (Tachibana et al., 2014). We have organized an international team, consisting of 24 members currently, for the initial analysis of soluble organic matter (SOM) for the returned samples.
The primitive asteroidal materials are expected to contain diverse and complex (e.g. elemental, structural, and optical) organic matter all at low concentrations. The occurrence of SOM will provide clues to the origins of organic compounds as well as prebiotic molecules of potential relevance to origins of life on Earth and possibly elsewhere in the Solar System. We propose the comprehensive SOM analyses to reveal the chemical evolution of Ryugu using high-sensitive and high-resolution analytical methods as follows:

1) High-resolution mass spectrometry (HRMS) of various solvent extracts with electrospray ionization (ESI) coupled with or without nano-liquid chromatography.
2) Enantiomerically resolved amino acid analysis using high-resolution column chromatography with high-sensitive fluorescence spectroscopy coupled with HRMS.
3) *In situ* organic compound analysis and molecular imaging using desorption electrospray ionization (DESI) and/or direct analysis in real time (DART) equipped with HRMS.
4) Spatial resolution imaging of organic compounds using time of flight-secondary ion mass spectrometry (ToF-SIMS; Naraoka et al., 2015).

In addition, if the sample is available, we will also perform the following additional analyses:

5) Compound-specific isotope analysis using gas chromatography/combustion or pyrolysis /isotope ratio mass spectrometry (GC/C or pyrolysis/IRMS).
6) Bulk chemical and isotopic analysis of organic matter (C, H, N and S) using nano-EA/IRMS system and laser-tunable FT-IR spectroscopy.

Depending to the sample size available to the initial analysis, we will perform preliminary analytical tests using 30 mg, 10 mg, and 1 mg samples of the Murchison meteorite (CM2, positive SOM-rich), Yamato 793321 meteorite (heated CM2, positive SOM-depleted), and baked serpentine (negative SOM-depleted) as well as procedural blank. The analytical protocol will be discussed in the meeting.

< References >
Tachibana, S. et al. (2014) Hayabusa2: Scientific importance of samples returned from C-type near-Earth

©2019. Japan Geoscience Union. All Right Reserved.

asteroid (162173) 1999 JU3. Geochemical Journal. 48. 571-581. 10.2343/geochemj.2.0350.
Matsuoka, M. et al. (2018) Spectral comparison between asteroid (162173) Ryugu and carbonaceous meteorites. American Astronomical Society, DPS meeting #50.
Naraoka, H. et al. (2015) ToF-SIMS analysis of carbonaceous particles in the sample catcher of the Hayabusa spacecraft. Earth, Planets and Space, 67:67. DOI 10.1186/s40623-015-0224-0.
Naraoka, H. and Hashiguchi, M. (2018) *In situ* organic compound analysis on a meteorite surface by desorption electrospray ionization coupled with an Orbitrap mass spectrometer. Rapid Commun. Mass Spectrom. 32, 959-964.

Keywords: Hayabusa2, Ryugu, Carbonaceous Asteroid, Soluble Organic Matter

©2019. Japan Geoscience Union. All Right Reserved.

Radar and optical simultaneous observations of faint meteors with MU radar and Tomo-e Gozen

*Ryou Ohsawa[1], Akira Hirota[2], Shinsuke Abe[2], Daniel Kastinen[3], Kero Johan[3], yasunori Fujiwara[4], Takuji Nakamura[5], Shigeyuki Sako[1], Yuto Kojima[1], Jun-ichi Watanabe[6]

1. Institute of Astronomy, Graduate School of Science, The University of Tokyo, 2. Department of Aerospace Engineering, College of Science & Technology, Nihon University, 3. Swedish Institute of Space Physics, 4. SOKENDAI (The Graduate University for Advanced Studies), 5. National Institute of Polar Research, 6. National Astronomical Observatory of Japan

The Earth is surrounded by small dust grains produced by comets and asteroids. Tons of such grains plunge into the Earth's atmosphere hourly. Part of their kinetic energy excites and ionizes the surrounding atmosphere, which is observed as a meteor phenomenon. A simultaneous radar and optical observation is promising to constrain the motion and mass of a meteor at a time. We launched a project to observe faint meteors with Middle and Upper Atmosphere Radar (MU radar) and a wide-field CMOS mosaic camera Tomo-e Gozen installed on the 105 cm Kiso Schmidt telescope. The observations were carried out in 18--21, April, 2018. From tons of the detected meteors, the simultaneous detections were extracted in terms of the times, loci, and directions of the meteors. Finally, we identified the 894 meteor events simultaneously detected in the both sites. The optical brightness of the simultaneous meteors ranged from about 3--11 mag. in the V-band, which is about 5 magnitude fainter than in previous studies. We confirmed a clear correlation between the meteor brightnesses and the radar cross sections.

Keywords: meteor, interplanetary dust

©2019. Japan Geoscience Union. All Right Reserved.

Global distribution and spectral characteristics of bright spots on asteroid Ryugu

*Masanori Suemitsu[1], Tomokatsu Morota[1], Rie Honda[2], Singo Kameda[15], Eri Tatsumi[3], Manabu Yamada[4], Naoya Sakatani[5], Toru Kouyama[6], Yokota Yasuhiro[7], Yuichiro Cho[8], Hidehiko Suzuki[9], Masahiko Hayakawa[10], Moe Matsuoka[10], Chikatoshi Honda[11], Tatsuhiro Michikami[12], Kazuo Yoshioka[13], Kazunori Ogawa[14], Hirotaka Sawada[5], Seiji Sugita[3]

1. Graduate School of Environmental Studies, Nagoya University, 2. Department of Science and Technology, System of Natural Science, Kochi Unicversity, 3. Graduate School of Earth and Planetary Science, Tokyo Unicversity, 4. Planetary Exploration Reserch Center, Chiba Institute of Technology, 5. Institute of Space and Astoronautical Science, Japan Aerospace Exploration Agency, 6. National Institute of Advanced Industrial Science and Technology, 7. Kochi University, 8. Department of Earth and Planetary Science, Tokyo University, 9. Depertment of physics, Meiji University , 10. Department of Solar System Science, Institute of Space and Astoronautical Science, Japan Aerospace Exploration Agency, 11. Aizu University, 12. Faculty of Engineering, Kindai University, 13. Graduate School of frontier Science, Tokyo University, 14. Kobe University, 15. Rikkyo University

On June 27, 2018, the asteroid explorer Hayabusa2 arrived at the target C-type asteroid 162173 Ryugu. The telescopic optical navigation camera (ONC-T) on-board Hayabusa2 has acquired the multiband image data for the entire surface of Ryugu with spatial resolutions better than 2 m/pixel. These data show that the Ryugu surface has the very low surface reflectance, flat spectra, and its spatial homogeneity [Sugita et al. 2019]. However, more detailed observations on Ryugu have revealed that many boulders exhibit different spectral properties and that a number of spots with distinctively brighter than the surroundings [Sugita et al. 2019]. Although larger boulders have been analyzed to show that they form two distinctive spectral trends, no substantial spectral analyses on bright spots have been conducted. Determining whether or not these bright spots are one of the materials that originate from the parent body of Ryugu is important to understand the differentiation and geologic processes on the parent body. In this study, in order to understand origins of the bright spots, we investigated spectral characteristics of the bright spots and compared those of the boulders on Ryugu. We used the ONC-T multiband images obtained in Box-A (20 km altitude) and mid-altitude (5 km altitude) operations.

We found seven meter-sized bright spots that have radiance factor 1.3 to 2.0 times higher than that of the surrounding area. The spectra of these bright spots were classified into two types, one being a flat spectrum type and another being a convex spectrum type. The former type has spectrum similar to but flatter and brighter than the mean spectra of the whole Ryugu and boulders, suggesting that the bright spots originate from parent body of Ryugu. The latter type has spectrum similar to those of S-type asteroids, suggesting their exogenous origin.

Keywords: asteroids, Ryugu, bright spot, spectrum, boulder

©2019. Japan Geoscience Union. All Right Reserved.

Polarimetry of (155140) 2005 UD: the Dynamical Association with (3200) Phaethon

*Masateru Ishiguro[1], Jooyeon Geem[1], Hiroyuki Naito[2], Yoonsoo P. Bach[1], Daisuke Kuroda[3], Tatsuharu Ono[4], Seiko Takagi[4], Mitsuteru Sato[4], Kiyoshi Kuramoto[4], Tomohiko Sekiguchi[5], Masataka Imai[6], Makoto Watanabe[7], Katsuhito Ohtsuka[8], Sunao Hasegawa[9], Takashi Ito[10], Fumi Yoshida[11], Tomoko Arai[11]

1. Department of Physics and Astronomy, Seoul National University, 2. Nayoro Observatory, 3. Okayama Observatory, Kyoto University, 4. Department of Cosmosciences, Graduate School of Science, Hokkaido University, 5. Hokkaido University of Education, 6. National Institute of Advanced Industrial Science and Technology, 7. Department of Applied Physics, Okayama University of Science, 8. Tokyo Meteor Network, 9. Japan Aerospace Exploration Agency, 10. National Astronomical Observatory of Japan, 11. Planetary Exploration Research Center, Chiba Institute of Technology

An Apollo-type near--Earth asteroid, (155140) 2005 UD, is considered as a possible fragment from (3200) Phaethon, suggesting that Phaethon precursor body might undergo a catastrophic disruption in the past. Here we present our new observational evidence for supporting these two are common origin. We thus conducted a polarimetric observation in 2018 September-October and found that 2005 UD exhibited a polarimetric property significantly different from those of major taxonomic classes of NEAs (i.e., S- and C-type) but similar to that of Phaethon at a wide range of the solar phase angles. Using the polarimetric data, we derived the geometric albedo of ~0.1. In addition, we made a photometric observation at the opposition (the zero phase angle), and determined the mean absolute magnitude of 17.2, the synodic rotational period 5.23 hr, and the effective diameter 1.5 km in combination with the derived geometric albedo. From these evidence, we found that the Phaethon precursor body might have lost more than a few percents of the mass via a disruption if 2005 UD was indeed ejected from the Phaethon precursor.

Keywords: Asteroids, Space Mission (Destiny+)

©2019. Japan Geoscience Union. All Right Reserved.

Follow-up observations for AKARI/IRC near-infrared asteroid spectroscopic survey (AcuA-spec)

*Sunao Hasegawa[1], Daisuke KURODA[2], Kenshi YANAGISAWA[3], Fumihiko Usui[4]

1. Japan Aerospace Exploration Agency, 2. Kyoto University, 3. National Astronomical Observatory of Japan, 4. Kobe University

In the range from 1 to 2.5 μm, we made the spectroscopic observations of the AcuA-spec asteroids (Hasegawa et al. 2017, PASJ, 69, 9), whose spectra were obtained in continuous covered between 2.5 and 5.0 μm by NIR/IRC/AKARI (Usui et al. 2019, PASJ, 71, 1). Candidates of AcuA-spec asteroids were selected from only main-belt asteroids classified based on visible spectrophotometric and spectroscopic observations (Tholen 1984, PhD thesis, Arizona University; Bus & Binzel 2002, Icarus, 158, 146; Lazzaro et al. 2004, Icarus, 172, 179). About 200 classified asteroids were raised as observational candidates. Spectroscopic observations for 65 AcuA-spec asteroids which were selected among the AcuA-spec candidate catalogue in taking account of signal-noise ratio and target opportunity by AKARI were executed.
Section work of the AcuA-spec candidate catalogue was done around 2005, yet there were not many spectroscopic observations of asteroids in the near-infrared wavelength range. As a result of survey of published paper for near-infrared spectroscopic observations of asteroids, howevwer, it was found that spectroscopic observations in the near-infrared region of 1–2.5 μm for most AcuA-spec asteroids are performed except for several asteroids.
If data in near-infrared wavelength range of the lacked AcuA-spec asteroids were acquired, all AcuA-spec asteroids will have 0.35–5 μm of data available. Obtaining continuous reflectance of asteroids is essential data to compare with those such as meteorites. Based on the Bus-DeMeo taxonomy (DeMeo et al. 2009, Icarus, 202, 160), we conducted classification of all AcuA-spec asteroids using published and our observational data.

Keywords: asteroids, spectroscopy

©2019. Japan Geoscience Union. All Right Reserved.

Amino acids on witness coupons collected from the ISAS/JAXA curation facility for the assessment and quality control of the Hayabusa2 sampling procedure

*Haruna Sugahara[1,2], Yoshinori Takano[1], Yuzuru Karouji[3], Kazuya Kumagai[4], Toru Yada[3], Naohiko Ohkouchi[1], Masanao Abe[3], Hayabusa2 project team

1. Japan Agency for Marine-Earth Science and Technology (JAMSTEC), 2. Institut de Chimie de Nice, Universite Cote dAzur, 3. Japan Aerospace Exploration Agency (JAXA), 4. Marine Works Japan Ltd.

The Hayabusa2 spacecraft is visiting a near-Earth carbonaceous type (C-type) asteroid, 162173 Ryugu, and planning to return the pristine samples to the Earth. C-type asteroids are considered to be related with carbonaceous chondrites that are enriched in organic and volatile materials. The one of the scientific goals of Hayabusa2 mission is to understand the origin and evolution of organic materials through interactions with water and minerals in the early solar system [e.g., 1]. Thus, the characterization of organic materials in the returned sample has great importance for this purpose. However, the analysis of small quantities of extraterrestrial organic materials in the returned samples requires a great care to avoid the introduction of terrestrial contaminants and any artifact materials to the pristine samples. Thus, the assessment of the degrees of the terrestrial contaminants to the samples as well as the comprehensive and specific managements to minimize the terrestrial contamination throughout the mission is essential.

The purpose of the study is to investigate the potential terrestrial organic contamination in a clean chamber for the Hayabusa2 returned samples in an Institute of Space and Astronautical Science/Japan Aerospace Exploration Agency (ISAS/JAXA) curation room [2-4]. As the indicator of the terrestrial organic contaminants, we selected amino acids that ubiquitously exist in the terrestrial environments and are also the target molecules in the Hayabusa2 mission. In the study, we used witness coupons made of aluminum foil to collect the contaminants in the clean chamber. The witness coupons were collected at different exposure times, ranging from 1 day to 1 month to examine the accumulation rate of the contaminants. After the collection, amino acids on the witness coupons were extracted in hot water, hydrolysed with HCl, and then converted to *N*-pivaloyl isopropyl (Pv/iPr) ester derivatives for gas chromatographic (GC) analysis [5].

On the witness coupons, eight terrestrially common amino acids (glycine, alanine, valine, leucine, isoleucine, proline, aspartic acid and glutamic acid) were detected and seven of them, except valine due to the under quantification limit, were quantified. Among them, glycine was the most abundant species with the highest concentration of 10 pmol/cm^2. A time-dependent profile of the four major amino acids (glycine, alanine, aspartic acid and glutamic acid) showed the increasing trend between 1 to 7 days. The average accumulation rates are 1.2 pmol/cm^2/day for glycine, 0.6 pmol/cm^2/day for alanine, 0.1 pmol/cm^2/day for aspartic acid and 0.2 pmol/cm^2/day for glutamic acid. The species and the concentrations of amino acids on our witness coupons are similar to those reported by the National Aeronautics and Space Administration/Johnson Space Center (NASA/JSC) OSIRIS-REx team [6]. Thus, the quality control against terrestrial contaminants in ISAS/JAXA curation facility is at the same quantitative level as in their facility. This inter-laboratory evaluation [7] about the terrestrial organic contamination will provide important information for the curation procedure of the Hayabusa2-returned samples.

©2019. Japan Geoscience Union. All Right Reserved.

References: [1] Tachibana S. et al. (2014) Geochem. J., 48, 571-587. doi: 10.2343/geochemj.2.0350. [2] Yada T. et al. (2014) Meteorit. Planet. Sci., 49, 135-153. doi: 10.1111/maps.12027. [3] Sawada H. et al. (2017) Space Sci. Rev. 208, 81–106. doi: 10.1007/s11214-017-0338-8. [4] Okazaki R. et al. (2017) Space Sci. Rev. 208, 107–124. doi: 10.1007/s11214-016-0289-5. [5] Chikaraishi Y. et al. (2010) in *Earth, Life, Isotopes*, Kyoto Univ. Press, pp.367-386. [6] Dworkin et al. (2018) Space Sci. Rev. 214, 9. doi: 10.1007/s11214-017-0439-4. [7] Sugahara et al. (2018) Earth, Planets Space, 70, 194. doi: 10.1186/s40623-018-0965-7.

Keywords: Amino acid, Hayabusa2, Curation, Witness coupons, Quality control

©2019. Japan Geoscience Union. All Right Reserved.

Hayabusa2 orbit determination using c5++ software

*Keiko Yamamoto[1], Toshimichi Otsubo[2], Koji Matsumoto[1], Hirotomo Noda[1], Noriyuki Namiki[1], Hiroki Senshu[3], Takahide Mizuno[4], Naoko Ogawa[4], Go Ono[4], Yuya Mimasu[4], Kent Yoshikawa[4], Tadateru Takahashi[4], Yuto Takei[4], Atsushi Fujii[4], Fuyuto Terui[4], Takanao Saiki[4], Satoru Nakazawa[4], Makoto Yoshikawa[4], Yuichi Tsuda[4]

1. National Astronomical Observatory of Japan, 2. Hitotsubashi University, 3. Chiba Institute of Technology, 4. Japan Aerospace Exploration Agency

Hayabusa2 arrived at the target asteroid Ryugu in June 2018 and is currently conducting remote sensing observations with various onboard instruments. So far, we have improved orbit determination software c5++, originally developed for the analysis of satellite laser ranging (SLR) data of the Earth, so that it can be used for the analysis of laser ranging data between Hayabusa2 and Ryugu obtained by Hayabusa2 LIDAR. Then we used it for the estimation of Hayabusa2 trajectory and the GM value of Ryugu. However, in the case of Hayabusa2, it is difficult to determine all of the 6 components of the initial state vector precisely if only LIDAR range data was used, and the simultaneously estimated GM value also had large uncertainty. To overcome this problem, in addition to LIDAR ranging data, we used Automated-Image-Tracking (AIT) data obtained by wide-angle optical navigation camera (ONC-W1) for the estimation of Hayabusa2 trajectory. In principle, LIDAR data gives information on the radial direction and AIT data give the ones on the across and along track directions. Thus, both data sets are complementary and help to improve the precision of the trajectory estimation. For this purpose, we improved c5 ++ so that it can deal with AIT data as observation data. In the presentation, we will show the results of trajectory and GM estimations using LIDAR and AIT data, and show how much the precision and accuracy are improved compared to the case using LIDAR data only.

Keywords: Hayabusa2, Orbit Determination, Ryugu

©2019. Japan Geoscience Union. All Right Reserved.

Landing Site Selection for Hayabusa2: Scientific Evaluation of the Candidate Sites on Asteroid (162173) Ryugu

*Hikaru Yabuta[1], Sei-ichiro WATANABE[2], Tomoki Nakamura[3], Naru Hirata[4], Seiji Sugita[5], Tatsuaki Okada[6], Kohei Kitazato[4], Yoshiaki Ishihara[7], Tomokatsu Morota[2], Naoya Sakatani[6], Koji Matsumoto[8], Koji Wada[9], Shogo Tachibana[5], Mutsumi Komatsu[10], ERI TATSUMI[5], Moe Matsuoka[6], Chikatoshi Honda[4], Takahiro Hiroi[11], Hiroki Senshu[9], Rie Honda[12], Yasuhiro Yokota[6], Rina Noguchi[6], Yuri Shimaki[6], Deborah Lorin Domingue[13], Lucille Le Corre[13], Antonella Barucci[14], Ernest Palomba[15], Shota Kikuchi[6], Akira Miura[6], Tomohiro Yamaguchi[6], Yukio Yamamoto[6], Takanao Saiki[6], Satoshi Tanaka[6], Makoto Yoshikawa[6], Yuichi Tsuda[6]

1. Hiroshima University, Department of Earth and Planetary Systems Science, 2. Nagoya University, 3. Tohoku University, 4. University of Aizu, 5. The University of Tokyo, 6. ISAS/JAXA, 7. NIES, 8. NAOJ, 9. Chiba Institute of Technology, Planetary Exploration Research Center (PERC), 10. Sokendai, 11. Brown University, 12. Kochi University, 13. Planetary Science Institute, USA, 14. Observatoire Paris-Site de Meudon, LESIA, France, 15. INAF-IAPS, Italy.

On June 27, 2018, JAXA’s Hayabusa2 spacecraft arrived at its target C-type asteroid Ryugu. Immediately after arrival, remote-sensing observations were carried out with the Optical Navigation Camera (ONC), the Near Infrared Spectrometer (NIRS3), the Thermal Infrared Imager (TIR), and the Laser Altimeter (LIDAR). Based on data from this suite of instruments, we carried out the landing site selection for the first touch-down (TD1). Since the mission aims to understand i) the origin and chemical evolution of the solar system and ii) the formation process and structure of the asteroid, we have set the most scientifically valuable TD1 site as the least altered region where water and/or carbon are potentially abundant.

Landing candidate sites were first selected by engineering evaluation for operational safety followed by scientific evaluations based on criteria such as science and samplability for the most interesting sites. The process was repeated using the observations from the altitudes of 20 km, 6 km, and 5 km.

Scientific evaluations of the landing site candidates were conducted based on the data products from ONC, NIRS3, TIR, and LIDAR. The shape modeling team produced two different shape models. ONC produced multiband images and reflectance spectra, as well as maps of spectral indices and X-means clustering analysis. Measurements of boulder size-frequency and Hapke parameters in the candidate landing areas were examined. NIRS3 produced four types of spectral feature maps. TIR provided maps of maximum temperature from the October 22, 2018 TD1 practice operations, apparent thermal inertia, and typical grain size determinations. LIDAR provided time series ranging data, topography, and corrected spacecraft trajectory.

Engineering evaluation: The possible landing site candidates were selected from the engineering safety score map evaluated based on the sub-Earth distance, local solar angle, local slope and elevation maximum difference. Thermal prediction results for TD1 were obtained by TIR. Temperatures of each site are < 350 K, confirming the safe conditions. The regions that satisfied all the conditions were, L05, L07, L08, L12, M01, M03 and M04.

Scientific evaluation:
1) Boulders. Based on the distribution of boulders with a diameter larger than 3 m for each potential landing site, regions L07, L08, and M04 show smaller percentages of boulder coverage than other areas, and are regarded as safer sites for landing.

©2019. Japan Geoscience Union. All Right Reserved.

2) Geology. Ryugu exhibits a variety of topographic features and geologic settings. From a scientific perspective, it is of interest to be able to study various materials representing the evolution of Ryugu.
3) Hydrous minerals. The NIR spectral properties are nearly homogeneous across Ryugu’ s surface, especially between the candidate sites. The near-infrared reflectance spectra of Ryugu is similar to experimentally heated Murchison meteorite at 400˚C.
4) Carbon contents. It is likely that visible reflectance at 0.55 μm (R(0.55)) is influenced mostly by carbon content. R(0.55) is almost homogeneous across the surface with a low value, regardless of the candidate sites.
5) Secondary processes. Although the surface of Ryugu is almost homogeneous at the macro scale in the map of spectral slope from 0.48 to 0.86 μm, a slight heterogeneity is observed across the candidate regions. L-regions are relatively bluish and M-regions are reddish. Considering that spectral reddening is observed by laser irradiation of dehydrated carbonaceous chondrites, L regions are probably less altered and preferable for sampling.

In the total evaluation, L08, L07 and M04 were selected as the TD1 candidates on August 17, 2018. In September 2018, many boulders > 50 cm were additionally found for the sites during the rehearsal of TD1. Thus, the originally scheduled TD1 in October was postponed. Further search for a flat and safe site continued, and L08-E1 was determined as the TD1 site. The TD1 will be scheduled on Feb 22, 2019.

Keywords: Hayabusa2, Landing Site Selection

©2019. Japan Geoscience Union. All Right Reserved.

Visible Photometric, Spectroscopic and Polarimetric observations of an inactive comet, P/2016 BA14 with the 1.6m Pirka Telescope

*Ryo Yamagata[1], Tomohiko Sekiguchi[1], Ryo Okazaki[1], Kazuya Doi[1], Daisuke Kuroda[2], Masateru Ishiguro[3], Hiroyuki Naito[4]

1. Hokkaido University of Education, 2. Kyoto University, 3. Seoul National University, 4. Nayoro Observatory

We performed photometric, spectroscopic and polarimetric observations of an inactive comet, P/2016 BA14 with the 1.6m Pirka Telescope, Hokkaido.

P/2016 BA14 (a=3.02 au, e=0.67, i=18.9 deg.) was discovered as an unusual asteroid with a cometary orbit by the PANSTAARS on 2016 January 21.Since Knight et al. 2016 detected its cometary tail when the object close to sun(r=1.018au). It was classified into a Jupiter Family Comets. It can be regarded as a bare nucleus invisible coma because very weak comet activity that is different from general comet. There is a remarkable similarity between the orbits of 252P/LINEAR (a=3.05au, e=0.67, i=10.4deg) and P/2016 BA14. Jupiter Tisserand parameter is 252P/LINEAR and that of P/2016 BA14 are 2.82. P/2016 BA14 and 252P/LINEAR is division comet that is originally same comet (Jian-Yang.2017).

In this study, surface reflection properties of P/2016 BA14 classify D-type asteroids (Bus-DeMeo taxonomy) from result of visible spectroscopy (435-820nm). Color of surface is little red as D-type asteroid, but very blue as comet nucleus from result of BVRI photometry. The linear polarization Pr=10.46.±0.11% (α=46°) is in close accord with that of D-type asteroids and comet nucleus.

Keywords: P/2016 BA14, Photometric, Spectroscopic, Polarimetric, D-type

©2019. Japan Geoscience Union. All Right Reserved.

Polycyclic aromatic hydrocarbons and aliphatic hydrocarbons in Jbilet Winselwan carbonaceous chondrite : Attempt to evaluate the thermal metamorphism degree on the parent body

Hiroki Kato[1], *Hikaru Yabuta[1]

1. Hiroshima University, Department of Earth and Planetary Systems Science

Introduction: On June 27, 2018, Hayabusa2 spacecraft arrived at the C-type asteroid Ryugu. The surface of Ryugu has been thought to have experienced dehydration at least partially, according to the grand-based observation (Vilas et al. 2008; Hiroi et al. 1993). Therefore, it is important to investigate the chemical compositions of dehydrated carbonaceous CM chondrites for understanding the surface process of asteroid Ryugu. Although the extents of thermal metamorphism of CM chondrites have been evaluated by mineralogical compositions (e.g., Nakamura et al. 2006) and elemental and molecular compositions of insoluble organic matter (IOM) (e.g., Naraoka et al. 2004; Yabuta et al. 2005), the estimated temperature varies widely. On the other hand, soluble organic molecules from the dehydrated CM chondrites have not been quantified or below detection (e.g. Shimoyama et al. 1989), and there has been no study which evaluated thermal metamorphism based on the compositions of soluble organic molecules. Therefore, in this study, we analyzed aliphatic hydrocarbons and polycyclic aromatic hydrocarbons (PAHs) in Jbilet Winselwan CM chondrite, which is a dehydrated CM chondrite (Zolensky et al 2016) and show similar reflectance spectrum to that of asteroid Ryugu (Kameda et al. 2015), for precise evaluation of parent body thermal metamorphism. The relative abundances of the hydrocarbons were compared with those of Murray meteorite, which is a primitive CM chondrite.

Samples and Methods: Powdered samples of Jbilet Winselwan meteorite and Murray meteorite (0.2 - 0.4g) were extracted with dichloromethane/methanol (9:1) by sonication. The extracts were applied to a silica gel column. From the column, aliphatic hydrocarbons were eluated with hexane and then PAHs were eluated with dichloromethane. The hexane and dichloromethane eluates were concentrated to 100 μl individually under a nitrogen flow for analysis by a gas chromatography coupled with mass spectrometry (GC-MS). Identification and quantification of compounds were made by comparison of peak retention times on mass chromatograms and mass spectra, and peak areas, respectively, with those of standard compounds. For compounds without standard compounds, identification was made by comparison of mass spectra with library data.

Results and discussion: Total concentration of *n*-alkanes from Jbilet Winselwan meteorite (1.85 μg/g meteorite) was 40 times lower than those from Murray meteorite (80.7 μg/g meteorite). Relative abundances of short-chain *n*-alkanes (C_{15}-C_{16}) were dominant in Jbilet Winselwan meteorite, while those of long-chain *n*-alkanes (C_{17}-C_{21}) were dominant in Murray meteorite. This difference implies that short-chain *n*-alkanes were resulted from cracking of long-chain *n*-alkanes and/or IOM during thermal metamorphism of the parent body of Jbilet Winselwan meteorite. Total concentration of PAHs from Jbilet Winselwan meteorite (0.05 μg/ meteorite) was 1000 times lower than those from Murray meteorite (62.0 μg/g meteorite). Dimethylnaphthalene, fluorine, phenanthrene, pyrene, fluoranthene, methylbiphenyl (0.003-0.039 μg/g meteorite) were identified, while low molecular weight PAHs, such as naphthalene, methylnaphthalene, and acenaphthene, were not detected. The results suggest that PAHs with high volatility in Jbilet Winselwan meteorite were lost or involved in further aromatization during thermal metamorphism. Distributions of dimethylnaphthalene and methylbiphenyl isomers in Jbilet Winselwan

©2019. Japan Geoscience Union. All Right Reserved.

and Murray meteorites were similar, respectively, which indicates that the parent body of Jbilet Winselwan meteorite experienced relatively mild thermal metamorphism.

Keywords: Jbilet Winselwan meteorite, Soluble organic molecules, Dehydration

©2019. Japan Geoscience Union. All Right Reserved.

Disk-Resolved Photometry Analysis of the Asteroid Ryugu Images Obtained by Hayabusa2 Visible Camera ONC

*yokota yasuhiro[1,2], Rie Honda[1], ERI TATSUMI[3], Deborah Domingue[4], Stefanus E. Schroeder[5], Moe Matsuoka[2], Seiji Sugita[3], Tomokatsu Morota[6], Shingo Kameda[7], Toru Kouyama[8], Hidehiko Suzuki[9], Manabu Yamada[10], Naoya Sakatani[2], Chikatoshi Honda[11], Masahiko Hayakawa[2], Kazuo Yoshioka[3], Yuichiro Cho[3], Hirotaka Sawada[2]

1. Kochi University, 2. ISAS/JAXA, 3. Univ. of Tokyo, 4. Planetary Science Institute, 5. DLR, 6. Nagoya Univ., 7. Rikkyo Univ., 8. AIST, 9. Meiji Univ., 10. Chiba Institute od Technology, 11. Aizu Univ.

Since June 2018, the Optical Navigation Camera (ONC) onboard Hayabusa2, has observed the C-type asteroid 162173 Ryugu at a distance below 20 km. ONC-T and ONC-W1 are used for surface imaging operations, and their images allow us to investigate the disk-resolved photometric properties of the surface. A narrow-angle camera ONC-T has 7 broad-band filters ranging in wavelength from 0.39–0.95 μm. ONC-W1 is a wide-angle (> 65˚) pan-chromatic camera mainly used for optical navigation during cruise and low-altitude (< 20km) operations. We are proceeding the analysis of both dataset, ONC-T and ONC-W1.

Since Hayabusa2’s position is nominally fixed on the line connecting Ryugu and the Earth, the available solar phase angle range by ONC-T changes seasonally with the orbits of Earth and Ryugu around the sun. Therefore, we are collecting a large number of ONC-T images over a long period of time to cover a wide phase angle range.

ONC-W1 data has a strong point that it covers a wide phase angle range within a single frame during the descent operations, because of its wide field of view. One of our current challenges is deriving a precise viewing geometries (incidence angle, emission angle, and phase angle) at each pixel. Additionally, comparison of the absolute brightness value (radiance factor) with ONC-T is an ongoing issue.

Keywords: Asteroid, Photometry, Ryugu, Hayabusa2

©2019. Japan Geoscience Union. All Right Reserved.

[E] Poster | P (Space and Planetary Sciences)：P-PS Planetary Sciences

Wed. May 29, 2019 5:15 PM - 6:30 PM JST | Wed. May 29, 2019 8:15 AM - 9:30 AM UTC | Poster Hall International Exhibition Hall8, Makuhari Messe_3

[P-PS03] Solar System Small Bodies: A New Frontier Arising Hayabusa 2, OSIRIS-REx and Other Projects

convener:Masateru Ishiguro(Department of Physics and Astronomy, Seoul National University), Taishi Nakamoto(Tokyo Institute of Technology), Masanao Abe(Institute of Space and Astronautical Science, Japan Aerospace Exploration Agency), Olivier S Barnouin(Johns Hopkins University Applied Physics Laboratory)

In June 2018, the Hayabusa 2 spacecraft arrived at the target asteroid Ryugu after three and half years journey. In addition, another spacecraft, OSIRIS-REx will soon arrive at its destination Bennu. With these arrivals, the solar system research is about to enter a new era. We have organized this small bodies session since 2012 and had a broad range of discussions from viewpoints of laboratory experiments, observations, space explorations, theoretical modeling, and sample analyses. In particular, this time, we aim to hold this session to bring the latest research on solar system small bodies, focusing on the initial results of Hayabusa 2 and OSIRIS-REx. Presentations in the related fields other than these two asteroidal missions are also welcomed.

[PPS03-P01] Impact experiments on low strength coarse-grained regolith simulating surface materials on asteroid Ryugu

*Yuya Yamamoto[1], Masahiko Arakawa[1], Minami Yasui[1], Sunao Hasegawa[2], Ryo Sugimura[1] (1.Graduate School of Science, Kobe University, 2.ISAS, JAXA)

[PPS03-P02] Reflectance estimation of asteroid Ryugu using MASCOT

*Marika Ishida[1], Koto Amano[1], Keiichi Moroi[1], ERI TATSUMI[2], Tra-Mi Ho[10], Shingo Kameda[1], Seiji Sugita[2], Rie Honda[3], Tomokatsu Morota[4], yokota yasuhiro[5], Toru Kouyama[6], Hidehiko Suzuki[7], Manabu Yamada[8], Naoya Sakatani[5], Chikatoshi Honda[9], Masahiko Hayakawa[5], Kazuo Yoshioka[2], Moe Matsuoka[5], Yuichiro Cho[2], Hirotaka Sawada[5] (1.Rikkyo Univ., 2.Univ. of Tokyo, 3.Kochi Univ., 4.Nagoya Univ., 5.JAXA/ISAS, 6.AIST, 7.Meiji Univ., 8.Chiba Inst. Tech, 9.Univ. of Aizu, 10.DLR)

[PPS03-P03] Flyby observation of Asteroid (3200) Phaethon by DESTINY$^+$ onboard cameras

*Ko Ishibashi[1], Shingo Kameda[2], Masato Kagitani[3], Peng Hong[1], Manabu Yamada[1], Osamu Okudaira[1], Tomoko Arai[1], Fumi Yoshida[1], Shunsuke Sato[4], Takahiro Ishimaru[4], Takaya Okamoto[4], Takahiro Iwata[4], Tatsuaki Okada[4], Takeshi Takashima[4] (1.Chiba Institute of Technology, 2.Rikkyo University, 3.Tohoku Universtiy, 4.Japan Aerospace Exploration Agency)

[PPS03-P04] Polarimetric Study of Asteroids in Comet-Like Orbits (ACOs)

*Jooyeon Geem[1], Masateru Ishiguro[1], Yoonsoo P. Bach[1], Daisuke Kuroda[2], Hiroyuki Naito[3], Hidekazu Hanayama[4], yoonyoung kim[10], Yuna G. Kwon[1], Sunho Jin[1], Tomohiko Sekiguchi[5], Ryo Okazaki[5], Jeremie J. Vaubaillon[6], Masataka Imai[7], Tatsuharu Oono[8], Yuki Futamuts[8], Seiko Takagi[8], Mitsuteru Sato[8], Kiyoshi Kuramoto[8], Makoto Watanabe[9] (1.Astronomy program, Dept of Physics and Astronomy, Seoul National University, 2.Okayama Observatory, Kyoto University, 3.Nayoro Observatory, 4.Ishigakijima Astronomical Observatory, National Astronomical Observatory of Japan, 5.Hokkaido University of Education, 6.Observatoire de Paris, I.M.C.C.E., 7.National Institute of Advanced Industrial Science and Technology, 8.Department of Cosmosciences, Graduate School of Science, Hokkaido University, 9.Department of Applied Physics, Okayama University of Science, 10.Max Planck Institute for Solar System Research)

[PPS03-P05] Dynamical lifetime of the Oort Cloud new comets under planetary perturbation

*Ito Takashi[1], Arika Higuchi[1] (1.National Astronomical Observatory of Japan)

[PPS03-P06] Thermal Infrared Imaging of C-type Asteroid 162173 Ryugu with Porous Surfaces

*Tatsuaki Okada[1,2], Tetsuya Fukuhara[3], Satoshi Tanaka[1], Makoto Taguchi[3], Takehiko Arai[4], Naoya Sakatani[1], Yuri Shimaki[1], Hiroki Senshu[5], Yoshiko Ogawa[6], Hirohide Demura[6], Kentaro Suko[6], Kohei Kitazato[6], Toru Kouyama[7], Tomohiko Sekiguchi[8], Jun Takita[9], Sunao Hasegawa[1], Tsuneo Matsunaga[10], Takehiko Wada[1], Takeshi Imamura[2], Jorn Helbert[11], Thomas G. Mueller[12], Axel Hagermann[13], Jens Biele[11], Matthias Grott[11], Maximiliam Hamm[11], Marco Delbo[14], Yukio Yamamoto[1], Naru Hirata[6], Naoyuki Hirata[15], Fuyuto Terui[1], Takanao Saiki[1], Satoru Nakazawa[1], Makoto Yoshikawa[1], Sei-ichiro WATANABE[1,16], Yuichi Tuda[1] (1.Institute of Space and Astronautical Science, Japan Aerospace Exploration Agency, 2.University of Tokyo, 3.Rikkyo University, 4.Ashikaga University, 5.Chiba Institute of Technology, 6.University of Aizu, 7.National Institute of Advanced Industrial Science and Technology, 8.Hokkaido University of Education, 9.Hokkaido Kitami-Hokuto High School, 10.National Institute for Environmental Studies, 11.German Aerospace Center, 12.Max-Planck Institute for Extraterrestrial Physics, 13.University of Stirling, 14.Observatoire de la Côte d'Azur, 15.Kobe University, 16.Nagoya University)

[PPS03-P07] Data Release of Asteroid 162173 Ryugu by Observation of Thermal Infrared Imager onboard Hayabusa2

*Takehiko Arai[1], Hirohide Demura[2], Toru Kouyama[7], Naoya Sakatani[3], Kentaro Suko[2], Yuri Shimaki[3], Hiroki Senshu[5], Tomohiko Sekiguchi[6], Yoshiko Ogawa[2], Sunao Hasegawa[3], Takehiko Wada[3], Takeshi Imamura[10], Tsuneo Matsunaga[9], Jun Takita[8], Kohei Kitazato[2], Makoto Taguchi[4], Tetsuya Fukuhara[4], Satoshi Tanaka[3], Tatsuaki Okada[3] (1.Ashikaga University, 2.The University of Aizu, 3.Japan Aerospace Exploration Agency (JAXA), 4.Rikkyo University, 5.Chiba Institute of Technology, 6.Hokkaido University of Education, 7.National Institute of Advanced Industrial Science and Technology (AIST), 8.Hokkaido Kitami Hokuto High School, 9.National Institute for Environmental Studies (NIES), 10.The University of Tokyo)

[PPS03-P08] Multi-mission capability of HARMONICS

*Shintaro Tsunoda[1], Hirohide Demura[1], Naru Hirata[1] (1.The University of Aizu)

[PPS03-P09] New interface of verification for calibration and conversion in HEAT : Hayabusa2 Exploration Assistant for TIR

*Tatsuro Kobayashi[1], Kentaro Suko[1], Hirohide Demura[1], Yoshiko Ogawa[1], Takehiko Arai[2], Naoya Sakatani[3], Tatsuaki Okada[3], Satoshi Tanaka[3], Tetsuya Fukuhara[4] (1.The University of Aizu, 2.Ashikaga University, 3.Institute of Space and Astronautical Science, Japan Aerospace Exploration Agency, 4.Rikkyo University)

[PPS03-P10] **Dust particle evolution of a near-Earth object 252P/LINEAR from near-infrared polarimetric observations in 2016**

*Yuna G Kwon[1], Masateru Ishiguro[1], Jungmi Kwon[2], Daisuke Kuroda[3], Myungshin Im[1], Changsu Choi[1], Motohide Tamura[4], Takahiro Nagayama[5], Nobuyuki Kawai[6], Jun-ichi Watanabe[7] (1.Seoul National Univ., 2.ISAS/Japan Aerospace Exploration Agency, 3.Okayama Astrophysical Observatory, 4.The Univ. of Tokyo, 5.Kagoshima Univ., 6.Tokyo Institute of Technology, 7.National Astronomical Observatory of Japan)

[PPS03-P11] **Performance Evaluation of TRIPOL on the 61-cm Telescope at Seoul National University for Polarimetric Observations of Solar System Small Bodies**

*Sunho Jin[1], Masateru Ishiguro[1], Yuna G Kwon[1], Jooyeon Geem[1], Yoonsoo P. Bach[1], Jinguk Seo[1], Hiroshi Sasago[2], Shuji Sato[3] (1.Seoul National University, 2.Sasago Co.,Ltd, 3.Nagoya University)

[PPS03-P12] Smart Interface of HEAT: Hayabusa2 Exploration Assistant for TIR

*Kentaro Suko[1], Tatsuro Kobayashi[1], Hirohide Demura[1], Takehiko Arai[2], Naoya Sakatani[3], Tatsuaki Okada[3], Satoshi Tanaka[3], Tetsuya Fukuhara[4] (1.The University of Aizu, 2.Ashikaga University, 3.Institute of Space and Astronautical Science, Japan Aerospace Exploration Agency, 4.Rikkyo University)

[PPS03-P13] Experimental Study on Collision Crater Formed on Bulge Geography

*Yusaku Yokota[1], Yuya Yamamoto[2], Minami Yasui[2], Masahiko Arakawa[2] (1.Faculty of Science, Kobe University, 2.Graduate School of Science, Kobe University)

[PPS03-P14] Initial analysis plan of soluble organic compounds for the Hayabusa2 sample from asteroid Ryugu

*Hiroshi Naraoka[1], Yoshinori Takano[2], Jason P. Dworkin[3], SOM Analysis Team (1.Department of Earth and Planetary Sciences, Research Center for Planetary Trace Organic Compounds, Kyushu University, 2.Japan Agency for Marine-Earth Science and Technology, 3.Astrochemistry Laboratory NASA Goddard Space Flight Center, Greenbelt, MD 20771 USA)

[PPS03-P15] Radar and optical simultaneous observations of faint meteors with MU radar and Tomo-e Gozen

*Ryou Ohsawa[1], Akira Hirota[2], Shinsuke Abe[2], Daniel Kastinen[3], Kero Johan[3], yasunori Fujiwara[4], Takuji Nakamura[5], Shigeyuki Sako[1], Yuto Kojima[1], Jun-ichi Watanabe[6] (1.Institute of Astronomy, Graduate School of Science, The University of Tokyo, 2.Department of Aerospace Engineering, College of Science & Technology, Nihon University, 3.Swedish Institute of Space Physics, 4.SOKENDAI (The Graduate University for Advanced Studies), 5.National Institute of Polar Research, 6.National Astronomical Observatory of Japan)

[PPS03-P16] Global distribution and spectral characteristics of bright spots on asteroid Ryugu

*Masanori Suemitsu[1], Tomokatsu Morota[1], Rie Honda[2], Singo Kameda[15], Eri Tatsumi[3], Manabu Yamada[4], Naoya Sakatani[5], Toru Kouyama[6], Yokota Yasuhiro[7], Yuichiro Cho[8], Hidehiko Suzuki[9], Masahiko Hayakawa[10], Moe Matsuoka[10], Chikatoshi Honda[11], Tatsuhiro Michikami[12], Kazuo Yoshioka[13], Kazunori Ogawa[14], Hirotaka Sawada[5], Seiji Sugita[3] (1.Graduate School of Environmental Studies, Nagoya University, 2.Department of Science and Technology, System of Natural Science, Kochi Unicversity, 3.Graduate School of Earth and Planetary Science, Tokyo Unicversity, 4.Planetary Exploration Reserch Center, Chiba Institute of Technology, 5.Institute of Space and Astoronautical Science, Japan Aerospace Exploration Agency, 6.National Institute of Advanced Industrial Science and Technology, 7.Kochi University, 8.Department of Earth and Planetary Science, Tokyo University, 9.Depertment of physics, Meiji University , 10.Department of Solar System Science, Institute of Space and Astoronautical Science, Japan Aerospace Exploration Agency, 11.Aizu University, 12.Faculty of Engineering, Kindai University, 13.Graduate School of frontier Science, Tokyo University, 14.Kobe University, 15.Rikkyo University)

[PPS03-P17] Polarimetry of (155140) 2005 UD: the Dynamical Association with (3200) Phaethon

*Masateru Ishiguro[1], Jooyeon Geem[1], Hiroyuki Naito[2], Yoonsoo P. Bach[1], Daisuke Kuroda[3], Tatsuharu Ono[4], Seiko Takagi[4], Mitsuteru Sato[4], Kiyoshi Kuramoto[4], Tomohiko Sekiguchi[5], Masataka Imai[6], Makoto Watanabe[7], Katsuhito Ohtsuka[8], Sunao Hasegawa[9], Takashi Ito[10], Fumi Yoshida[11], Tomoko Arai[11] (1.Department of Physics and Astronomy, Seoul National University, 2.Nayoro Observatory, 3.Okayama Observatory, Kyoto University, 4.Department of Cosmosciences, Graduate School of Science, Hokkaido University, 5.Hokkaido University of Education, 6.National Institute of Advanced Industrial Science and Technology, 7.Department of Applied Physics, Okayama University of Science, 8.Tokyo Meteor Network, 9.Japan Aerospace Exploration Agency, 10.National Astronomical Observatory of Japan, 11.Planetary Exploration Research Center, Chiba Institute of Technology)

[PPS03-P18] **Follow-up observations for AKARI/IRC near-infrared asteroid spectroscopic survey (AcuA-spec)**

*Sunao Hasegawa[1], Daisuke KURODA[2], Kenshi YANAGISAWA[3], Fumihiko Usui[4] (1.Japan Aerospace Exploration Agency, 2.Kyoto University, 3.National Astronomical Observatory of Japan, 4.Kobe University)

[PPS03-P19] Amino acids on witness coupons collected from the ISAS/JAXA curation facility for the assessment and quality control of the Hayabusa2 sampling procedure

*Haruna Sugahara[1,2], Yoshinori Takano[1], Yuzuru Karouji[3], Kazuya Kumagai[4], Toru Yada[3], Naohiko Ohkouchi[1], Masanao Abe[3], Hayabusa2 project team (1.Japan Agency for Marine-Earth Science and Technology (JAMSTEC), 2. Institut de Chimie de Nice, Universite Cote dAzur, 3.Japan Aerospace Exploration Agency (JAXA), 4.Marine Works Japan Ltd.)

[PPS03-P20] Hayabusa2 orbit determination using c5++ software

*Keiko Yamamoto[1], Toshimichi Otsubo[2], Koji Matsumoto[1], Hirotomo Noda[1], Noriyuki Namiki[1], Hiroki Senshu[3], Takahide Mizuno[4], Naoko Ogawa[4], Go Ono[4], Yuya Mimasu[4], Kent Yoshikawa[4], Tadateru Takahashi[4], Yuto Takei[4], Atsushi Fujii[4], Fuyuto Terui[4], Takanao Saiki[4], Satoru Nakazawa[4], Makoto Yoshikawa[4], Yuichi Tsuda[4] (1.National Astronomical Observatory of Japan, 2.Hitotsubashi University, 3.Chiba Institute of Technology, 4.Japan Aerospace Exploration Agency)

[PPS03-P21] **Landing Site Selection for Hayabusa2: Scientific Evaluation of the Candidate Sites on Asteroid (162173) Ryugu**

*Hikaru Yabuta[1], Sei-ichiro WATANABE[2], Tomoki Nakamura[3], Naru Hirata[4], Seiji Sugita[5], Tatsuaki Okada[6], Kohei Kitazato[4], Yoshiaki Ishihara[7], Tomokatsu Morota[2], Naoya Sakatani[6], Koji Matsumoto[8], Koji Wada[9], Shogo Tachibana[5], Mutsumi Komatsu[10], ERI TATSUMI[5], Moe Matsuoka[6], Chikatoshi Honda[4], Takahiro Hiroi[11], Hiroki Senshu[9], Rie Honda[12], Yasuhiro Yokota[6], Rina Noguchi[6], Yuri Shimaki[6], Deborah Lorin Domingue[13], Lucille Le Corre[13], Antonella Barucci[14], Ernest Palomba[15], Shota Kikuchi[6], Akira Miura[6], Tomohiro Yamaguchi[6], Yukio Yamamoto[6], Takanao Saiki[6], Satoshi Tanaka[6], Makoto Yoshikawa[6], Yuichi Tsuda[6] (1.Hiroshima University, Department of Earth and Planetary Systems Science, 2.Nagoya University, 3.Tohoku University, 4.University of Aizu, 5.The University of Tokyo, 6.ISAS/JAXA, 7.NIES, 8.NAOJ, 9.Chiba Institute of Technology, Planetary Exploration Research Center (PERC), 10.Sokendai, 11.Brown University, 12.Kochi University, 13.Planetary Science Institute, USA, 14.Observatoire Paris-Site de Meudon, LESIA, France, 15.INAF-IAPS, Italy.)

[PPS03-P22] Visible Photometric, Spectroscopic and Polarimetric observations of an inactive comet, P/2016 BA14 with the 1.6m Pirka Telescope

*Ryo Yamagata[1], Tomohiko Sekiguchi[1], Ryo Okazaki[1], Kazuya Doi[1], Daisuke Kuroda[2], Masateru Ishiguro[3], Hiroyuki Naito[4] (1.Hokkaido University of Education, 2.Kyoto University, 3.Seoul National University, 4.Nayoro Observatory)

[PPS03-P23] **Polycyclic aromatic hydrocarbons and aliphatic hydrocarbons in Jbilet Winselwan carbonaceous chondrite : Attempt to evaluate the thermal metamorphism degree on the parent body**

Hiroki Kato[1], *Hikaru Yabuta[1] (1.Hiroshima University, Department of Earth and Planetary Systems Science)

[PPS03-P24] Disk-Resolved Photometry Analysis of the Asteroid Ryugu Images Obtained by Hayabusa2 Visible Camera ONC

*yokota yasuhiro[1,2], Rie Honda[1], ERI TATSUMI[3], Deborah Domingue[4], Stefanus E. Schroeder[5], Moe Matsuoka[2], Seiji Sugita[3], Tomokatsu Morota[6], Shingo Kameda[7], Toru Kouyama[8], Hidehiko Suzuki[9], Manabu Yamada[10], Naoya Sakatani[2], Chikatoshi Honda[11], Masahiko Hayakawa[2], Kazuo Yoshioka[3], Yuichiro Cho[3], Hirotaka Sawada[2] (1.Kochi University, 2.ISAS/JAXA, 3.Univ. of Tokyo, 4.Planetary Science Institute, 5.DLR, 6.Nagoya Univ., 7.Rikkyo Univ., 8.AIST, 9.Meiji Univ., 10.Chiba Institute od Technology, 11.Aizu Univ.)

Impact experiments on low strength coarse-grained regolith simulating surface materials on asteroid Ryugu

*Yuya Yamamoto[1], Masahiko Arakawa[1], Minami Yasui[1], Sunao Hasegawa[2], Ryo Sugimura[1]

1. Graduate School of Science, Kobe University, 2. ISAS, JAXA

Impact cratering is one of the most important physical processes, then we study crater scaling laws and impact induced seismic waves in order to elucidate various flow processes on asteroids caused by impacts. The conventional crater scaling laws are categorized into two regions according to the controlling physics for the crater growth: they are gravity and material strength. A crater formed on regolith layer is surely controlled by the gravity, however when the regolith layer was filled with coarse particles with low mechanical strength, then the several coarse grains might be disrupted to consume the Ek. Thus, the crater size could be affected by the disruptions of the coarse grains. We speculate that not only the gravity but also the grain strength could affect the final crater size. Then, we made cratering experiments by using the target made of weak particles, and studied the effects of the particle strength on the crater scaling law and the impact induced seismic wave.

Experiments: Cratering experiments were conducted by using a gas gun set at Kobe University and ISAS. Granular targets were prepared by using weathered tuff granules with the size of 1 to 4mm (small particle) and the size of 1 to 4cm (large particle). The crush strength of these tuff particles was measured to be about 60 kPa. A spherical projectile with the size of 3mm which is made of iron, zirconia, alumina, glass, and nylon) was lunched at the impact velocity from 40 to 200m/s, and a spherical Al projectile with the size of 2mm was impacted at the impact velocity from 1.2 to 4.5km/s, then these two types of the projectile were impacted on the target surface at the normal direction. Impact cratering process and ejecta curtain growth were observed by a high-speed camera at 10^3-10^5 fps, and the video images were used to analyze ejecta particles to reconstruct the trajectories. After the shot, the crater morphology was recorded and the diameter and the depth were measured. Impact induced seismic waves were measured by using 3 accelerometers (specific frequency is 30kHz) set at different positions from the impact point, and a data logger was used to record the seismic data through charge amplifiers (data acquisition rate is 100kHz) connecting to the accelerometer.

Results: The crater size was found to increase with the projectile kinetic energy (Ek) at lower than 0.14J and at higher than 0.63J, so that the crater size was almost constant among them, and more the crater size obtained at very high Ek was almost on the extrapolated line from the relationship given by the low Ek data. The pi-scaling law was used to construct the relationship between normalized radius (πR) and normalized gravity (π2), and πR at small π2 was found to be rather smaller than that obtained for sand and glass beads targets, and more πR at large π2 was found to be consistent with that for sand and glass beads. More detail analysis tells us that all the data separated into two trends with large offset according to the impact velocity and the projectile material. This offset might be caused by the disruption of several tuff particles. The ejection velocities of each tuff particle were so scattered, then the distinctive relationship between initial position of particle and the ejection velocity was not derived in the low velocity range. The propagation velocity of the impact induced seismic wave was about 30 m/s, and it is 1/3 of that for glass beads. Furthermore, we found that the relationship between the maximum acceleration and the distance from the impact point was about 1/10 of that obtained for glass beads: the seismic wave in the tuff granules attenuated so quickly compared to the glass beads. But, when the distance is normalized by the crater radius, these relationships almost consistent each other, so that the

©2019. Japan Geoscience Union. All Right Reserved.

normalized distance could be a good parameter for the scaling of the acceleration of seismic wave.

Keywords: impact cratering experiment, low strength, impact-induced seismic shaking, crater scaling law

©2019. Japan Geoscience Union. All Right Reserved.

Reflectance estimation of asteroid Ryugu using MASCOT

*Marika Ishida[1], Koto Amano[1], Keiichi Moroi[1], ERI TATSUMI[2], Tra-Mi Ho[10], Shingo Kameda[1], Seiji Sugita[2], Rie Honda[3], Tomokatsu Morota[4], yokota yasuhiro[5], Toru Kouyama[6], Hidehiko Suzuki[7], Manabu Yamada[8], Naoya Sakatani[5], Chikatoshi Honda[9], Masahiko Hayakawa[5], Kazuo Yoshioka[2], Moe Matsuoka[5], Yuichiro Cho[2], Hirotaka Sawada[5]

1. Rikkyo Univ., 2. Univ. of Tokyo, 3. Kochi Univ., 4. Nagoya Univ., 5. JAXA/ISAS, 6. AIST, 7. Meiji Univ., 8. Chiba Inst. Tech, 9. Univ. of Aizu, 10. DLR

Hayabusa2 is a sample-return mission for the C-type asteroid 162173 Ryugu. Hayabusa2 arrived at Ryugu on 27 June 2018, and various observations are still being conducted. Hayabusa2 performs multiband spectral observation by employing the optical navigation camera telescope (ONC-T)and can thereby obtain spectral map of Ryugu, which enables the study of material distribution and degree of space weathering of Ryugu. However, the sensitivity of ONC-T has been previously calibrated by incorporating the inflight data of stars with significant uncertainty. Hence, the authors aim to estimate the reflectance of Ryugu by employing Mobile Asteroid Surface Scout (MASCOT).
MASCOT comprises four instruments (MASCAM, MicrOmega, MARA, and MASMAG) that are employed for analyzing the soil of Ryugu. The upper side of the MASCOT landeris coated with white paint, and its spectral image was captured by ONC-T after its release from Hayabusa2 to Ryugu. The authors conducted on-ground reflectance measurement of a white plate whose white paint is identical to that of MASCOT. Hence, the primary objective of the proposed study is to estimate the reflectance of Ryugu by comparing MASCOT’ s white side’ s spectrum captured by ONC-T with the on-ground reflectance measurement of the white plate that has identical paint as MASCOT, and thus evaluate the validity.

Keywords: Hayabusa2, ONC-T, MASCOT

©2019. Japan Geoscience Union. All Right Reserved.

Flyby observation of Asteroid (3200) Phaethon by DESTINY$^+$ onboard cameras

*Ko Ishibashi[1], Shingo Kameda[2], Masato Kagitani[3], Peng Hong[1], Manabu Yamada[1], Osamu Okudaira[1], Tomoko Arai[1], Fumi Yoshida[1], Shunsuke Sato[4], Takahiro Ishimaru[4], Takaya Okamoto[4], Takahiro Iwata[4], Tatsuaki Okada[4], Takeshi Takashima[4]

1. Chiba Institute of Technology, 2. Rikkyo University, 3. Tohoku Universtiy, 4. Japan Aerospace Exploration Agency

DESTINY$^+$ (Demonstration and Experiment of Space Technology for INterplanetary voYage, Phaethon fLy-by and dUst Science) is a mission proposed for JAXA/ISAS Epsilon class small program, currently in the pre-project phase (Phase-A) with a launch targeted for 2023. DESTINY$^+$ is a joint mission of technology demonstration and scientific observation. The near-Earth asteroid (3200) Phaethon, the flyby target, is known as a parent body of the Geminid meteor shower, the size of which is approximately 5 to 6 km in diameter.

In this mission, spatially resolved images of Phaethon will be taken by two onboard cameras, the Telescopic CAmera for Phaethon (TCAP) and the Multiband CAmera for Phaethon (MCAP) during the flyby, in order to understand the nature of a meteor shower's parent body, which is one of the sources of interplanetary dust particles that are thought to be an important transport medium of organic matter to the Earth. The spacecraft flybys Phaethon with a relative speed of 30 to 40 km/s. Despite such a high flyby speed, the cameras are required to take un-blurred images of Phaethon.

The main purposes of the DESTINY$^+$ flyby observation of Phaethon is to understand the geology of a parent body of a meteor shower, and in particular constrain the dust ejection mechanisms from active (i.e., dust-ejecting) asteroids. The specific objectives of the camera observation are taking images for (1) obtaining the light curve of Phaethon in order to estimate the rotational period, (2) measuring the outline shape of Phaeton, (3) making a 3D shape model of Phaethon, (4) observing the surface geological features of Phaethon including dust ejection features, and (5) observing the surface material distribution of Phaethon. The observations (1) to (4) will be conducted by TCAP, and (5) by MCAP.

TCAP is a telescopic panchromatic camera for high spatial resolution imaging of the surface of Phaethon and have a rotational mirror for asteroid tracking during flyby. The rotational mirror can change the direction of the line of sight from 0 deg to 180 deg. This enables to observe Phaethon throughout the flyby with wide solar phase angles, which is extremely important to image and understand the surfaces of planetary bodies because the solar phase angle affects significantly the appearance of geological features in taken images.

MCAP is a multiband camera, the wavelengths of which are 400, 480, 550, 700, 850, and 950 nm (480 and 950 nm are optional bands) and has multiple optical systems and sensors in order to take all band images simultaneously. This is because there is not enough time to take each band image in turn with changing bandpass filters using such as a filter wheel in this high speed flyby mission. MCAP does not have a tracking mirror due to the weight limitation, and the line of sight of MCAP is fixed to the spacecraft with 40 deg off the relative velocity vector of the spacecraft.

We will explain the flyby imaging sequence of DESTINY$^+$, and show the conceptual designs of TCAP and MCAP.

©2019. Japan Geoscience Union. All Right Reserved.

Keywords: Phaethon, DESTINY+, Flyby, Camera

©2019. Japan Geoscience Union. All Right Reserved.

Polarimetric Study of Asteroids in Comet-Like Orbits (ACOs)

*Jooyeon Geem[1], Masateru Ishiguro[1], Yoonsoo P. Bach[1], Daisuke Kuroda[2], Hiroyuki Naito[3], Hidekazu Hanayama[4], yoonyoung kim[10], Yuna G. Kwon[1], Sunho Jin[1], Tomohiko Sekiguchi[5], Ryo Okazaki[5], Jeremie J. Vaubaillon[6], Masataka Imai[7], Tatsuharu Oono[8], Yuki Futamuts[8], Seiko Takagi[8], Mitsuteru Sato[8], Kiyoshi Kuramoto[8], Makoto Watanabe[9]

1. Astronomy program, Dept of Physics and Astronomy, Seoul National University, 2. Okayama Observatory, Kyoto University, 3. Nayoro Observatory, 4. Ishigakijima Astronomical Observatory, National Astronomical Observatory of Japan, 5. Hokkaido University of Education, 6. Observatoire de Paris, I.M.C.C.E., 7. National Institute of Advanced Industrial Science and Technology, 8. Department of Cosmosciences, Graduate School of Science, Hokkaido University, 9. Department of Applied Physics, Okayama University of Science, 10. Max Planck Institute for Solar System Research

It is important to determine the taxonomic types of small bodies in the solar system and further to study the spatial distribution of the planetary system. Among the small bodies, it is considered that there should be dormant comets that have lost a significant fraction of volatile materials in their subsurface layers. As a result, they are unable to produce any detectable coma and recognized as asteroids. It has been challenging to find out such dormant comet population from a list of known asteroids because of the asteroidal appearances. There are several attempts to find the dormant comet nuclei from asteroidal catalogs, for example, by using their reflectance spectra or orbital elements. However, little has been studied via polarimetry.
We conduct a polarimetric study of three candidates of dormant comet nuclei, (331471) 1984 QY1, (3552) Don Quixote and (944) Hidalgo, by using the 1.6-m Pirka Telescope at the Nayoro observatory (operated by Hokkaido University, Japan). We chose these asteroids in comet-like orbits (ACOs) based on the orbital elements (i.e., the Tisserand parameter with respect to Jupiter $T_J < 3$). We found that 1984 QY1 has a polarimetric albedo (geometric albedo determined via polarimetry) $p_V = 0.16 \pm 0.06$ while both Don Quixote and Hidalgo have Rc-band polarimetric albedo $p_R < 0.05$. Based on the polarimetric result together with a dynamical analysis, we conjectured that 1984 QY1 could be an S-type asteroid transported into the current orbit via 3:1 mean motion resonance with Jupiter. From the previous spectroscopic study, Don Quixote and Hidalgo are classified into D-type taxonomic group, which are typical of comet nuclei. In this presentation, we will introduce our polarimetric observations of ACOs and emphasize that polarimetry is a powerful tool for discriminating the asteroidal and cometary origins.

Keywords: Polarimetry, Asteroid

©2019. Japan Geoscience Union. All Right Reserved.

Dynamical lifetime of the Oort Cloud new comets under planetary perturbation

*Ito Takashi[1], Arika Higuchi[1]

1. National Astronomical Observatory of Japan

Nearly isotropic comets with very long orbital period are supposed to come from the Oort Cloud. Recent observational and theoretical studies have greatly revealed the dynamical nature of this cloud and its evolutionally history, but many issues are yet to be known. Our goal is to trace the dynamical evolution of the Oort Cloud new comets (OCNCs) produced by evolving comet cloud, hopefully estimating the fraction of OCNCs embedded in the current populations of the solar system small bodies. We combine two models to follow the dynamical evolution of OCNCs beginning from their production until their ejection out of the solar system, obtaining statistics of the dynamical lifetime of OCNCs: The first model is a semi-analytical one about the OCNC production in an evolving comet cloud under the perturbation of the galactic tide and stellar encounters. The second model numerically deals with planetary perturbation over OCNCs' dynamics in planetary region. The main results of the present study are: (1) Typical dynamical lifetime of OCNCs in our models turned out to be O(10^7) years. Once entering into the planetary region, most OCNCs stay there just for this timespan, then get ejected out of the solar system on hyperbolic orbits. (2) While averaged orbital inclination of OCNCs is small, the so-called "planet barrier" works rather effectively, preventing some OCNCs from penetrating into the terrestrial planetary region.

Keywords: Oort Cloud, comet, orbital dynamics

©2019. Japan Geoscience Union. All Right Reserved.

Thermal Infrared Imaging of C-type Asteroid 162173 Ryugu with Porous Surfaces

*Tatsuaki Okada[1,2], Tetsuya Fukuhara[3], Satoshi Tanaka[1], Makoto Taguchi[3], Takehiko Arai[4], Naoya Sakatani[1], Yuri Shimaki[1], Hiroki Senshu[5], Yoshiko Ogawa[6], Hirohide Demura[6], Kentaro Suko[6], Kohei Kitazato[6], Toru Kouyama[7], Tomohiko Sekiguchi[8], Jun Takita[9], Sunao Hasegawa[1], Tsuneo Matsunaga[10], Takehiko Wada[1], Takeshi Imamura[2], Jorn Helbert[11], Thomas G. Mueller[12], Axel Hagermann[13], Jens Biele[11], Matthias Grott[11], Maximiliam Hamm[11], Marco Delbo[14], Yukio Yamamoto[1], Naru Hirata[6], Naoyuki Hirata[15], Fuyuto Terui[1], Takanao Saiki[1], Satoru Nakazawa[1], Makoto Yoshikawa[1], Sei-ichiro WATANABE[1,16], Yuichi Tuda[1]

1. Institute of Space and Astronautical Science, Japan Aerospace Exploration Agency, 2. University of Tokyo, 3. Rikkyo University, 4. Ashikaga University, 5. Chiba Institute of Technology, 6. University of Aizu, 7. National Institute of Advanced Industrial Science and Technology, 8. Hokkaido University of Education, 9. Hokkaido Kitami-Hokuto High School, 10. National Institute for Environmental Studies, 11. German Aerospace Center, 12. Max-Planck Institute for Extraterrestrial Physics, 13. University of Stirling, 14. Observatoire de la Côte d'Azur, 15. Kobe University, 16. Nagoya University

Thermal images from global to close-up scales taken by the Thermal Infrared Imager TIR [1] on Hayabusa2 [2] have revealed thermophysical properties of the C-type Near-Earth Asteroid 162173 Ryugu. On 27 June 2018, Hayabusa2 arrived at Ryugu and started remote sensing to characterize the nature of the asteroid and find the proper landing sites. *In situ* surface experiments were conducted using the robotic landers Minerva-II and Mascot [3]. *In situ* radiometry was conducted by MARA on MASCOT during a day-night cycle to derive the thermal inertia of a single boulder [4]. Ground-based observations [5] have been informed that the averaged thermal inertia of the asteroid is from 150 to 300 [tiu = J m^{-2} $s^{-0.5}$ K^{-1}] [5,6], corresponding to the surface covered with cm-sized granules.

TIR is the same design as the LIR on Akatsuki Venus climate orbiter [6], with 8 to 12 μm wavelength range, 328 x 248 effective pixels, and the FOV and IFOV of 16.7˚ x 12.7˚ and 0.051˚ per pixel, respectively. The first image of Ryugu detected by TIR was a point source on 6 June 2018, as was previously predicted [7]. Disc-resolved thermal images of Ryugu was taken from the HP on 30 June. The surface temperature was measured at 300 to 370K at about 1AU from the Sun, and gradually decreased with the solar distance. Comparison of the results with modeling [8] shows that the surface of Ryugu is not like fine regolith nor base rocks. Most of large boulders on Ryugu show temperatures almost the same as the surrounding surfaces. Diurnal temperature profiles of Ryugu are rather flatter than expected for a smooth terrain. Apparent thermal inertia is ~300 tiu or larger, but probably lower than the value when the surface roughness is considered. All these facts are consistent with a very rough and porous surface with low porosity (~35 ±10 %) [9] and the surrounding surface is dominated by porous rocks larger than several centimeters. Macro porosity should be 30 to 50 % to account for the bulk density of Ryugu ~1200 kg m^{-3}.

During the descent operations for the release of landers and the touchdowns for sample collection, TIR has taken close-up thermal images of the local sites, continually from the altitude of 500 m until the start of final descent at 10 or 20 m altitude. Close-up thermal images show the surface physical state and a variety of boulders. Most of the boulders in close-up images have temperatures similar to the surroundings but with more variety. A small number of boulders are remarkably colder than the surroundings, indicating dense rocks with lower porosity.

©2019. Japan Geoscience Union. All Right Reserved.

These facts indicate that Ryugu is probably a rubble pile of loosely-bound porous rocks, which might originate from the outer layer of parent body where compaction did not occur effectively, while the dense boulders might originate the compacted center region of parent body or from the different parent body. A different composition (e.g., organic rich materials) cannot be ruled out so far to account for such a low thermal inertia (and low density) of Ryugu.

Acknowledgments: The authors appreciate all the members of the Hayabusa2 Project and supporting staff for their technical assistance and scientific discussions. This research is partly supported by the JSPS KAKENHI No. J26287108, No. J17H06459 (Aqua Planetology), and the Core-to-Core program “International Network of Planetary Sciences”. MDB acknowledges support from CNES.

References: [1] Okada T. et al. (2017) *SSR.,* 208, 255-286. [2] Tsuda Y. et al. (2013) *Acta. Astronautica, 91* , 356-362. [3] Ho T.M. et al. (2017) *SSR.,* 208, 255-286. [4] Grott, M. et al. (2019), submitted to Nature. [5] Mueller T.G. et al. (2016) Astronon. Astrophys., doi:10.1051/0004-6361/201629143. [6] Fukuhara T. et al. (2011) *EPS,* 63, 1009-1018. [7] Okada T. et al. (2018) *PSS., 158, 46-52.* [8] Takita J., et al. SSR, 2018, 287-315. [9] Okada T. (2016) *LPSC.*, 47, #1457.

Keywords: Hayabsua2, Thermal Infrared Imager, Thermal Inertia

©2019. Japan Geoscience Union. All Right Reserved.

Data Release of Asteroid 162173 Ryugu by Observation of Thermal Infrared Imager onboard Hayabusa2

*Takehiko Arai[1], Hirohide Demura[2], Toru Kouyama[7], Naoya Sakatani[3], Kentaro Suko[2], Yuri Shimaki[3], Hiroki Senshu[5], Tomohiko Sekiguchi[6], Yoshiko Ogawa[2], Sunao Hasegawa[3], Takehiko Wada[3], Takeshi Imamura[10], Tsuneo Matsunaga[9], Jun Takita[8], Kohei Kitazato[2], Makoto Taguchi[4], Tetsuya Fukuhara[4], Satoshi Tanaka[3], Tatsuaki Okada[3]

1. Ashikaga University, 2. The University of Aizu, 3. Japan Aerospace Exploration Agency (JAXA), 4. Rikkyo University, 5. Chiba Institute of Technology, 6. Hokkaido University of Education, 7. National Institute of Advanced Industrial Science and Technology (AIST), 8. Hokkaido Kitami Hokuto High School, 9. National Institute for Environmental Studies (NIES), 10. The University of Tokyo

The thermal infrared imager (TIR) onboard the Hayabusa2 spacecraft performed thermography of the asteroid 162173 Ryugu through in-situ observations from 2018 to 2019. The primary purpose of TIR is to determine the global thermophysical properties of the asteroid and to reveal the evolutional history such as physical properties of the coalesced bodies, orbital changes due to radiation force, and the thermal evolution. This study introduces observed data of TIR and public data for scientists. The data are released by JAXA data archives (DARTS) and NASA PDS.

Keywords: Hayabusa2, Thermal Infrared Imager, Asteroid Ryugu

©2019. Japan Geoscience Union. All Right Reserved.

Multi-mission capability of HARMONICS

*Shintaro Tsunoda[1], Hirohide Demura[1], Naru Hirata[1]

1. The University of Aizu

This research has updated HARMONICS from a viewpoint of multi-mission capability, such as the Martian satellite exploration mission MMX in 2020s. Newly additional function is Switching on the shape model interface.
Bird view and visualization of FOV is important in robotics control. This technology is also used for deep space explorer missions.
HARMONICS is visualization tool of FOV(Field Of View) of scientific instruments and spacecraft’s position for HAYABUSA mission. The software has been updated by University of Aizu students of the past. The original HARMONICS had been developed by Nemoto(2006). GUI of HARMONICS had been replaced GUI library from GKT to Qt and added new functions, such as interactive modification of input mission plan by Ueno+(2017). The software had been add FOV frustum function by Aoki(2017). HARMONICS has tried to manage data for each project based on preference file in 2018.
HARMONICS should improved scalability to be compatible for ongoing mission. HARMONICS had been used to decide shutter chance by Camera Science Team in the asteroid Itokawa rendezvous of HAYABUSA. This software has not used in the asteroid Ryugu rendezvous of HAYABUSA2. The proven software should be use for future ongoing missions other than HAYABUSA. This research is development to HARMONICS adapt to ongoing missions.
I separated the designation of the data set from the source code and clarified the part edited by the user and the part edited by the developer.
HARMONICS has the function to switch and display data of different missions by this research. When users extend HARMONICS for multiple missions, users don’t need edit source code. User needs only kernel and the shape model of spacecraft and target asteroid. User do not need tough coding. User can use easily HARMONICS by editing preference file and kernel.

Keywords: Hayabusa2, Ryugu, Software, visualization

©2019. Japan Geoscience Union. All Right Reserved.

New interface of verification for calibration and conversion in HEAT : Hayabusa2 Exploration Assistant for TIR

*Tatsuro Kobayashi[1], Kentaro Suko[1], Hirohide Demura[1], Yoshiko Ogawa[1], Takehiko Arai[2], Naoya Sakatani[3], Tatsuaki Okada[3], Satoshi Tanaka[3], Tetsuya Fukuhara[4]

1. The University of Aizu, 2. Ashikaga University, 3. Institute of Space and Astronautical Science, Japan Aerospace Exploration Agency, 4. Rikkyo University

Hayabusa2 is an ongoing mission for sample return from the asteroid Ryugu.
Candidates of sampling sites are selected based on surface mapping by optical instruments such as Thermal Camera (TIR). TIR observes surface infrared radiation from the asteroid. A software package peculiar to TIR is HEAT: Hayabusa2 Exploration Assistant for TIR. The software has four functions; Database for ground tests, calibration of flight data based on the ground tests, conversion from raw data to temperature one, and analysis for verifying the calibration and conversion. The converted data products are divided into some levels: Lv1 Raw data [DN], Lv2a Temperature [K], Lv2b is Brightness [W/m2], and higher thermal model with VTK format [K]. This research implements new interface of verification for calibration and conversion based on hearing and survey for requirements from TIR science team. The environment of implementation is following tool. OS: macOS Mojave 10.14.2. Computing language: C++, OpenGL. Frameworks: Qt5.4. Tools: Fits, Qt creator, SPICE toolkit, Visualization Toolkit, QcustomPlot, Xcode10.1.

Keywords: Hayabusa2, Software, Ryugu, Calibration

©2019. Japan Geoscience Union. All Right Reserved.

Dust particle evolution of a near-Earth object 252P/LINEAR from near-infrared polarimetric observations in 2016

*Yuna G Kwon[1], Masateru Ishiguro[1], Jungmi Kwon[2], Daisuke Kuroda[3], Myungshin Im[1], Changsu Choi[1], Motohide Tamura[4], Takahiro Nagayama[5], Nobuyuki Kawai[6], Jun-ichi Watanabe[7]

1. Seoul National Univ., 2. ISAS/Japan Aerospace Exploration Agency, 3. Okayama Astrophysical Observatory, 4. The Univ. of Tokyo, 5. Kagoshima Univ., 6. Tokyo Institute of Technology, 7. National Astronomical Observatory of Japan

Comets, one of the least-altered leftovers from the early solar system, have probably preserved the primitive structure inside, whereas their surfaces become differentiated from initial states after repetitive orbital revolutions around the sun. Resurfacing makes the surface drier and more consolidated than the bulk nuclei, creating inert refractory dust layer (so-called “dust mantle”). Near-Infrared (NIR) polarimetry is theoretically expected to maximize the contrast of the porosity between inner fresh and evolved dust particles, by harboring more dust constituents in the single wavelength than the optical, and thus intensifying electromagnetic interference in dust agglomerates. Despite the advantage, only few studies have been conducted in this approach at multiple observation epochs. Herein, we present our new multi-band NIR polarimetric (1.25—2.25 microns) study of near-Earth object 252P/LINEAR over 12 days near perihelion; alongside broadband optical photometric (0.48—0.80 microns) data over four months in 2016 and a subsidiary dynamical simulation over 1000 year backward in time. 252P/LINEAR drew attention due to (1) its close approach to the Earth (~0.036 au on 2016 March 16), (2) its possible pairing to a comet P/2016 BA14 (PanSTARRS), and (3) its very low activity level despite its relatively young dynamical age. In this study, we detected two discontinuous brightness enhancements of 252P/LINEAR, particularly, the former of which accompanied a significant increase of NIR polarization degree of the comet (by ~13 % at most) with unusual blue polarimetric color. We will discuss the most probable scenario of the observed results, together with the orbital evolution of the comet and a dynamical association with its pair.

Keywords: Comet, Near-earth object, Polarimetry, Dust

©2019. Japan Geoscience Union. All Right Reserved.

Performance Evaluation of TRIPOL on the 61-cm Telescope at Seoul National University for Polarimetric Observations of Solar System Small Bodies

*Sunho Jin[1], Masateru Ishiguro[1], Yuna G Kwon[1], Jooyeon Geem[1], Yoonsoo P. Bach[1], Jinguk Seo[1], Hiroshi Sasago[2], Shuji Sato[3]

1. Seoul National University, 2. Sasago Co.,Ltd, 3. Nagoya University

Polarimetry of solar system small bodies is a powerful technique for investigating their physical properties, such as albedos, particle sizes, and porosities of these bodies. Observational opportunities arise sometimes suddenly, that is, just after unforeseeable activations of comets and discoveries of near-miss asteroids. Here, we introduce our activity to install the polarimetric instrument, TRIPOL (Triple-Range Imager and POLarimeter) on the 61-cm telescope (a Ritchey-Chretien reflector with f/7.0) at the Center for Astronomy and Space Science, Seoul National University, and report an observational result of three comets. This combination provides an 8.0’ ´8.0’ field of view and pixel resolution of 0.94” pixel^{-1}. Throughout photometric observations, we determined the limiting magnitudes (defined as magnitudes for S/N=5) of 15.17±0.06 (g’-band), 15.68±0.01 (r’-band), 16.24±0.03 (I’-band), respectively, with total 240-seconds exposure (four 60-seconds exposure images, each was taken at different rotation angle for the half-wave plate). We also found that the instrumental polarizations are negligibly small, that is, -0.32±0.04% (g’-band), -0.36±0.05% (r’-band) and -0.21±0.04% (I’-band), while the polarization efficiencies are large enough to maximize the performance, that is, 97.52±0.03% (g’-band), 98.83±0.02% (r’-band) and 99.15±0.02% (I’-band).

With this instrument, we conducted polarimetric observations of three Jupiter-family comets, 21P/Giacobini-Zinner, 38P/Stephan-Oterma, and 46P/Wirtanen on a trial basis. It is known from a recent study that the polarization degrees of cometary dust particles are significantly influenced by gas emissions [1] With multiband data taken with TRIPOL, we eliminated an influence of gas contaminations and found that the dust polarization degrees of these three comets coincide with those of so-called ‘dust-rich comets’. From this result, we conjecture that the polarimetric property of Jupiter-family comets is broadly homogeneous, unlike asteroids. We plan to describe our future plan using the polarimetric system.

[1] Kwon, Y. G. et al. Astronomical Journal, 154, 4, 173, 2017

Keywords: Comet, Instrument, Polarimetry

©2019. Japan Geoscience Union. All Right Reserved.

Smart Interface of HEAT: Hayabusa2 Exploration Assistant for TIR

*Kentaro Suko[1], Tatsuro Kobayashi[1], Hirohide Demura[1], Takehiko Arai[2], Naoya Sakatani[3], Tatsuaki Okada[3], Satoshi Tanaka[3], Tetsuya Fukuhara[4]

1. The University of Aizu, 2. Ashikaga University, 3. Institute of Space and Astronautical Science, Japan Aerospace Exploration Agency, 4. Rikkyo University

The Hayabusa2 project is a sample return mission to the asteroid Ryugu. It was launched on Dec. 3, 2014, and it has been at Ryugu since June 27, 2018. Hayabusa2 has optical instrument called Thermal Infrared Imager (TIR). These main functions are to know natures of the asteroid and to select the candidate of safe landing sites for sampling based on thermos-physical properties of the surface. TIR records infrared radiation from the target as a digital number (DN). The infrared signal is affected by sensor-surrounding objects; lens, shutter, package, and case. TIR requires consideration about this effect when converts DN images to temperature one. This study improved conversion system to increase conversion efficiency.

Hayabusa2 TIR Science Team has developed an analysis supporting tool called Hayabusa2 Exploration Assistant for TIR (HEAT). HEAT is used to search TIR data interactively, display TIR images, and visualize thermal models. We receive TIR raw images (Product Level 1) from ISAS/JAXA and convert them to brightness temperature images (Level 2a) and radiance images (Level 2b) using HEAT at Univ. of Aizu. The converted images are provided to the Hayabusa2 project data server.

This part introduces a concept model. The spectral radiance emitted from a blackbody B(λ ,T) (W s r-1m-2) is given by the Planck function based on wavelength λ (m) and temperature T(K) as follows:

$$B(\lambda,T) = (2hc2/\lambda 5)^* (1/(\exp(\lambda kBT)-1))$$

H = 6.63*1034 (m2 kg s-2 s-1) is the Planck constant, c=2.9972*108(ms-1) is the speed of light, and KB= 1.38*10-23 (m2 kg s-2K-1) is the Boltzmann constant. The observed radiance L(T) (W sr−1 m−2) is as follows:

$$L(T)= \varepsilon \int BR(\lambda)d\lambda$$

ε is the spectral thermal emissivity, and R(λ) is the response function such as the detection efficiency of the bolometer, the measured transmittance of optics including the band-pass filter and the germanium lens. The calibration formula with two regressed parameters A and B is written as follows:

$$DN=A * L(T) + B$$

The converted temperatures of the Moon were lower than expected because each pixel did not cover the sunlit area entirely or due to roughness effect of the cratered terrain. TIR has been observing Ryugu in approach and rendezvous phases. The altitudes of TIR observations during the rendezvous phase range from 20 km to less than 10 m. This study has processed about 3000 Ryugu images observed by TIR since June 2018.

©2019. Japan Geoscience Union. All Right Reserved.

This study improved conversion system. Previous conversion system converts a TIR image one by one, but current conversion system converts TIR images in selected directory at once.

Keywords: Hayabusa2, TIR, HEAT, Software

©2019. Japan Geoscience Union. All Right Reserved.

Experimental Study on Collision Crater Formed on Bulge Geography

*Yusaku Yokota[1], Yuya Yamamoto[2], Minami Yasui[2], Masahiko Arakawa[2]

1. Faculty of Science, Kobe University, 2. Graduate School of Science, Kobe University

An equatorial bulge was found on the surface of asteroid Ryugu and Bennu by recent spacecrafts of Hayabusa2 and OSIRIS-Rex, and ridge structures with various scales originated by geological activities have been recognized on icy satellites. Impact craters are dominant geological features on solid planets such as asteroids and satellites, and a crater rim are also recognized as a ridge or bulge with a circular shape. These bulges and ridges are shown to be erased with time because small scale impacts excavate and disrupt these topographies. It is well known that old craters gradually degraded by small impacts to get blurred and could be completely erased. We can expect the similar degradation process on large bulges and ridge structures, so that the life time of these structures by small impacts is a good indicator of the formation age of these structure by geologic activities. So far, the effect of small impacts on the degradation is estimated by using the results on the flat surface, but actually the surface of the bulge is curved and there is a summit on the bulge. Therefore, if we estimate the life time of the bulge structure, we should consider the effect of the topography such as a summit and curvature. Then, the impacts on the bulge structure was studied to clarify how the bulge structure affected the crater formation efficiency. In this study, we suppose the bulge made from regolith and boulders, such as an equatorial bulge of Ryugu and assume the crater formation process dominated by not the strength but the gravity.

We prepared a triangular prism target to simulate the bilge structure, and set it like that the base of this prism is rectangle, then it looks triangle when we look it at the horizontal direction, and we can look at the linear summit from the top view. Quartz sands with the size of 100μm was used to build the target and the angle of repose for this quartz sand is about 30 degree. The slope of the prism was measured from the base, and we set the angle from 20 to 30 degree. The quartz sands were filled into a transparent water tank with the depth of 20 cm to prepare the bulge structure. Impact experiments were conducted by using a vertical type gas gun, and the water tank was set in the chamber to evacuate below 1000 Pa. A alumina sphere projectile with the size of 3mm was launched at the velocity from 70 to 200 m/s, and it was impacted on the bulge in the vertical direction: the impact angle measured from the target surface was about 60 degree when the slope was 30 degree. The distance from the impact pint to the summit (deviation distance, d_d) was changed from 0 to 20mm.

We found that the crater shape strongly depended on the d_d, so the crater shape was an ellipsoid when the impact point was near the summit. Th major axis appeared along the linear summit and the minor axis appeared across the summit. The aspect ratio of the major axis to the minor axis gradually changed toward 1 with the increase of d_d. Moreover, the aspect ratio becomes large at the same d_d when the impact velocity increased. The major axis of the ellipsoid crater formed on the bulge was slightly larger than the crater diameter formed on the flat surface, and the slope angle might affect the size of the ellipsoid because we found that the crater formed on the slope of 30 degree was systematically larger than that formed on the slope of 20 degree. We also observed an asymmetric ejecta curtain from the impact point on the bulge, moreover the ejecta curtain was notice to be deformed so much at the impact point near the summit because of the effect of curvature of the bulge on the crater flow.

Angle of repose, Impact crater, Bulge and ridge structure, Ejecta curtain

©2019. Japan Geoscience Union. All Right Reserved.

©2019. Japan Geoscience Union. All Right Reserved.

Initial analysis plan of soluble organic compounds for the Hayabusa2 sample from asteroid Ryugu

*Hiroshi Naraoka[1], Yoshinori Takano[2], Jason P. Dworkin[3], SOM Analysis Team

1. Department of Earth and Planetary Sciences, Research Center for Planetary Trace Organic Compounds, Kyushu University, 2. Japan Agency for Marine-Earth Science and Technology, 3. Astrochemistry Laboratory NASA Goddard Space Flight Center, Greenbelt, MD 20771 USA

The spectra of asteroid 162173 Ryugu taken by Near-Infrared Spectrometer (NIRS3) onboard Hayabusa2 are nearly featureless and consistent with carbonaceous chondrites (Matsuoka et al., 2018). The Hayabusa2 spacecraft will collect surface samples of Ryugu and deliver to the Earth during late 2020. The initial analysis of the Ryugu samples will focus on (1) detailed chemical and mineralogical characterization of the samples and (2) understanding the history of Ryugu and the Solar System in order to maximize the scientific achievement of the project and (3) to prove the scientific potential of the samples to the community for the analytical opportunity (Tachibana et al., 2014). We have organized an international team, consisting of 24 members currently, for the initial analysis of soluble organic matter (SOM) for the returned samples.
The primitive asteroidal materials are expected to contain diverse and complex (e.g. elemental, structural, and optical) organic matter all at low concentrations. The occurrence of SOM will provide clues to the origins of organic compounds as well as prebiotic molecules of potential relevance to origins of life on Earth and possibly elsewhere in the Solar System. We propose the comprehensive SOM analyses to reveal the chemical evolution of Ryugu using high-sensitive and high-resolution analytical methods as follows:

1) High-resolution mass spectrometry (HRMS) of various solvent extracts with electrospray ionization (ESI) coupled with or without nano-liquid chromatography.
2) Enantiomerically resolved amino acid analysis using high-resolution column chromatography with high-sensitive fluorescence spectroscopy coupled with HRMS.
3) *In situ* organic compound analysis and molecular imaging using desorption electrospray ionization (DESI) and/or direct analysis in real time (DART) equipped with HRMS.
4) Spatial resolution imaging of organic compounds using time of flight-secondary ion mass spectrometry (ToF-SIMS; Naraoka et al., 2015).

In addition, if the sample is available, we will also perform the following additional analyses:

5) Compound-specific isotope analysis using gas chromatography/combustion or pyrolysis /isotope ratio mass spectrometry (GC/C or pyrolysis/IRMS).
6) Bulk chemical and isotopic analysis of organic matter (C, H, N and S) using nano-EA/IRMS system and laser-tunable FT-IR spectroscopy.

Depending to the sample size available to the initial analysis, we will perform preliminary analytical tests using 30 mg, 10 mg, and 1 mg samples of the Murchison meteorite (CM2, positive SOM-rich), Yamato 793321 meteorite (heated CM2, positive SOM-depleted), and baked serpentine (negative SOM-depleted) as well as procedural blank. The analytical protocol will be discussed in the meeting.

< References >
Tachibana, S. et al. (2014) Hayabusa2: Scientific importance of samples returned from C-type near-Earth

©2019. Japan Geoscience Union. All Right Reserved.

asteroid (162173) 1999 JU3. Geochemical Journal. 48. 571-581. 10.2343/geochemj.2.0350.
Matsuoka, M. et al. (2018) Spectral comparison between asteroid (162173) Ryugu and carbonaceous meteorites. American Astronomical Society, DPS meeting #50.
Naraoka, H. et al. (2015) ToF-SIMS analysis of carbonaceous particles in the sample catcher of the Hayabusa spacecraft. Earth, Planets and Space, 67:67. DOI 10.1186/s40623-015-0224-0.
Naraoka, H. and Hashiguchi, M. (2018) *In situ* organic compound analysis on a meteorite surface by desorption electrospray ionization coupled with an Orbitrap mass spectrometer. Rapid Commun. Mass Spectrom. 32, 959-964.

Keywords: Hayabusa2, Ryugu, Carbonaceous Asteroid, Soluble Organic Matter

©2019. Japan Geoscience Union. All Right Reserved.

Radar and optical simultaneous observations of faint meteors with MU radar and Tomo-e Gozen

*Ryou Ohsawa[1], Akira Hirota[2], Shinsuke Abe[2], Daniel Kastinen[3], Kero Johan[3], yasunori Fujiwara[4], Takuji Nakamura[5], Shigeyuki Sako[1], Yuto Kojima[1], Jun-ichi Watanabe[6]

1. Institute of Astronomy, Graduate School of Science, The University of Tokyo, 2. Department of Aerospace Engineering, College of Science & Technology, Nihon University, 3. Swedish Institute of Space Physics, 4. SOKENDAI (The Graduate University for Advanced Studies), 5. National Institute of Polar Research, 6. National Astronomical Observatory of Japan

The Earth is surrounded by small dust grains produced by comets and asteroids. Tons of such grains plunge into the Earth's atmosphere hourly. Part of their kinetic energy excites and ionizes the surrounding atmosphere, which is observed as a meteor phenomenon. A simultaneous radar and optical observation is promising to constrain the motion and mass of a meteor at a time. We launched a project to observe faint meteors with Middle and Upper Atmosphere Radar (MU radar) and a wide-field CMOS mosaic camera Tomo-e Gozen installed on the 105 cm Kiso Schmidt telescope. The observations were carried out in 18--21, April, 2018. From tons of the detected meteors, the simultaneous detections were extracted in terms of the times, loci, and directions of the meteors. Finally, we identified the 894 meteor events simultaneously detected in the both sites. The optical brightness of the simultaneous meteors ranged from about 3--11 mag. in the V-band, which is about 5 magnitude fainter than in previous studies. We confirmed a clear correlation between the meteor brightnesses and the radar cross sections.

Keywords: meteor, interplanetary dust

©2019. Japan Geoscience Union. All Right Reserved.

Global distribution and spectral characteristics of bright spots on asteroid Ryugu

*Masanori Suemitsu[1], Tomokatsu Morota[1], Rie Honda[2], Singo Kameda[15], Eri Tatsumi[3], Manabu Yamada[4], Naoya Sakatani[5], Toru Kouyama[6], Yokota Yasuhiro[7], Yuichiro Cho[8], Hidehiko Suzuki[9], Masahiko Hayakawa[10], Moe Matsuoka[10], Chikatoshi Honda[11], Tatsuhiro Michikami[12], Kazuo Yoshioka[13], Kazunori Ogawa[14], Hirotaka Sawada[5], Seiji Sugita[3]

1. Graduate School of Environmental Studies, Nagoya University, 2. Department of Science and Technology, System of Natural Science, Kochi Unicversity, 3. Graduate School of Earth and Planetary Science, Tokyo Unicversity, 4. Planetary Exploration Reserch Center, Chiba Institute of Technology, 5. Institute of Space and Astoronautical Science, Japan Aerospace Exploration Agency, 6. National Institute of Advanced Industrial Science and Technology, 7. Kochi University, 8. Department of Earth and Planetary Science, Tokyo University, 9. Depertment of physics, Meiji University , 10. Department of Solar System Science, Institute of Space and Astoronautical Science, Japan Aerospace Exploration Agency, 11. Aizu University, 12. Faculty of Engineering, Kindai University, 13. Graduate School of frontier Science, Tokyo University, 14. Kobe University, 15. Rikkyo University

On June 27, 2018, the asteroid explorer Hayabusa2 arrived at the target C-type asteroid 162173 Ryugu. The telescopic optical navigation camera (ONC-T) on-board Hayabusa2 has acquired the multiband image data for the entire surface of Ryugu with spatial resolutions better than 2 m/pixel. These data show that the Ryugu surface has the very low surface reflectance, flat spectra, and its spatial homogeneity [Sugita et al. 2019]. However, more detailed observations on Ryugu have revealed that many boulders exhibit different spectral properties and that a number of spots with distinctively brighter than the surroundings [Sugita et al. 2019]. Although larger boulders have been analyzed to show that they form two distinctive spectral trends, no substantial spectral analyses on bright spots have been conducted. Determining whether or not these bright spots are one of the materials that originate from the parent body of Ryugu is important to understand the differentiation and geologic processes on the parent body. In this study, in order to understand origins of the bright spots, we investigated spectral characteristics of the bright spots and compared those of the boulders on Ryugu. We used the ONC-T multiband images obtained in Box-A (20 km altitude) and mid-altitude (5 km altitude) operations.

We found seven meter-sized bright spots that have radiance factor 1.3 to 2.0 times higher than that of the surrounding area. The spectra of these bright spots were classified into two types, one being a flat spectrum type and another being a convex spectrum type. The former type has spectrum similar to but flatter and brighter than the mean spectra of the whole Ryugu and boulders, suggesting that the bright spots originate from parent body of Ryugu. The latter type has spectrum similar to those of S-type asteroids, suggesting their exogenous origin.

Keywords: asteroids, Ryugu, bright spot, spectrum, boulder

©2019. Japan Geoscience Union. All Right Reserved.

Polarimetry of (155140) 2005 UD: the Dynamical Association with (3200) Phaethon

*Masateru Ishiguro[1], Jooyeon Geem[1], Hiroyuki Naito[2], Yoonsoo P. Bach[1], Daisuke Kuroda[3], Tatsuharu Ono[4], Seiko Takagi[4], Mitsuteru Sato[4], Kiyoshi Kuramoto[4], Tomohiko Sekiguchi[5], Masataka Imai[6], Makoto Watanabe[7], Katsuhito Ohtsuka[8], Sunao Hasegawa[9], Takashi Ito[10], Fumi Yoshida[11], Tomoko Arai[11]

1. Department of Physics and Astronomy, Seoul National University, 2. Nayoro Observatory, 3. Okayama Observatory, Kyoto University, 4. Department of Cosmosciences, Graduate School of Science, Hokkaido University, 5. Hokkaido University of Education, 6. National Institute of Advanced Industrial Science and Technology, 7. Department of Applied Physics, Okayama University of Science, 8. Tokyo Meteor Network, 9. Japan Aerospace Exploration Agency, 10. National Astronomical Observatory of Japan, 11. Planetary Exploration Research Center, Chiba Institute of Technology

An Apollo-type near--Earth asteroid, (155140) 2005 UD, is considered as a possible fragment from (3200) Phaethon, suggesting that Phaethon precursor body might undergo a catastrophic disruption in the past. Here we present our new observational evidence for supporting these two are common origin. We thus conducted a polarimetric observation in 2018 September-October and found that 2005 UD exhibited a polarimetric property significantly different from those of major taxonomic classes of NEAs (i.e., S- and C-type) but similar to that of Phaethon at a wide range of the solar phase angles. Using the polarimetric data, we derived the geometric albedo of ~0.1. In addition, we made a photometric observation at the opposition (the zero phase angle), and determined the mean absolute magnitude of 17.2, the synodic rotational period 5.23 hr, and the effective diameter 1.5 km in combination with the derived geometric albedo. From these evidence, we found that the Phaethon precursor body might have lost more than a few percents of the mass via a disruption if 2005 UD was indeed ejected from the Phaethon precursor.

Keywords: Asteroids, Space Mission (Destiny+)

©2019. Japan Geoscience Union. All Right Reserved.

Follow-up observations for AKARI/IRC near-infrared asteroid spectroscopic survey (AcuA-spec)

*Sunao Hasegawa[1], Daisuke KURODA[2], Kenshi YANAGISAWA[3], Fumihiko Usui[4]

1. Japan Aerospace Exploration Agency, 2. Kyoto University, 3. National Astronomical Observatory of Japan, 4. Kobe University

In the range from 1 to 2.5 μm, we made the spectroscopic observations of the AcuA-spec asteroids (Hasegawa et al. 2017, PASJ, 69, 9), whose spectra were obtained in continuous covered between 2.5 and 5.0 μm by NIR/IRC/AKARI (Usui et al. 2019, PASJ, 71, 1). Candidates of AcuA-spec asteroids were selected from only main-belt asteroids classified based on visible spectrophotometric and spectroscopic observations (Tholen 1984, PhD thesis, Arizona University; Bus & Binzel 2002, Icarus, 158, 146; Lazzaro et al. 2004, Icarus, 172, 179). About 200 classified asteroids were raised as observational candidates. Spectroscopic observations for 65 AcuA-spec asteroids which were selected among the AcuA-spec candidate catalogue in taking account of signal-noise ratio and target opportunity by AKARI were executed.
Section work of the AcuA-spec candidate catalogue was done around 2005, yet there were not many spectroscopic observations of asteroids in the near-infrared wavelength range. As a result of survey of published paper for near-infrared spectroscopic observations of asteroids, howevwer, it was found that spectroscopic observations in the near-infrared region of 1–2.5 μm for most AcuA-spec asteroids are performed except for several asteroids.
If data in near-infrared wavelength range of the lacked AcuA-spec asteroids were acquired, all AcuA-spec asteroids will have 0.35–5 μm of data available. Obtaining continuous reflectance of asteroids is essential data to compare with those such as meteorites. Based on the Bus-DeMeo taxonomy (DeMeo et al. 2009, Icarus, 202, 160), we conducted classification of all AcuA-spec asteroids using published and our observational data.

Keywords: asteroids, spectroscopy

©2019. Japan Geoscience Union. All Right Reserved.

Amino acids on witness coupons collected from the ISAS/JAXA curation facility for the assessment and quality control of the Hayabusa2 sampling procedure

*Haruna Sugahara[1,2], Yoshinori Takano[1], Yuzuru Karouji[3], Kazuya Kumagai[4], Toru Yada[3], Naohiko Ohkouchi[1], Masanao Abe[3], Hayabusa2 project team

1. Japan Agency for Marine-Earth Science and Technology (JAMSTEC), 2. Institut de Chimie de Nice, Universite Cote dAzur, 3. Japan Aerospace Exploration Agency (JAXA), 4. Marine Works Japan Ltd.

The Hayabusa2 spacecraft is visiting a near-Earth carbonaceous type (C-type) asteroid, 162173 Ryugu, and planning to return the pristine samples to the Earth. C-type asteroids are considered to be related with carbonaceous chondrites that are enriched in organic and volatile materials. The one of the scientific goals of Hayabusa2 mission is to understand the origin and evolution of organic materials through interactions with water and minerals in the early solar system [e.g., 1]. Thus, the characterization of organic materials in the returned sample has great importance for this purpose. However, the analysis of small quantities of extraterrestrial organic materials in the returned samples requires a great care to avoid the introduction of terrestrial contaminants and any artifact materials to the pristine samples. Thus, the assessment of the degrees of the terrestrial contaminants to the samples as well as the comprehensive and specific managements to minimize the terrestrial contamination throughout the mission is essential.

The purpose of the study is to investigate the potential terrestrial organic contamination in a clean chamber for the Hayabusa2 returned samples in an Institute of Space and Astronautical Science/Japan Aerospace Exploration Agency (ISAS/JAXA) curation room [2-4]. As the indicator of the terrestrial organic contaminants, we selected amino acids that ubiquitously exist in the terrestrial environments and are also the target molecules in the Hayabusa2 mission. In the study, we used witness coupons made of aluminum foil to collect the contaminants in the clean chamber. The witness coupons were collected at different exposure times, ranging from 1 day to 1 month to examine the accumulation rate of the contaminants. After the collection, amino acids on the witness coupons were extracted in hot water, hydrolysed with HCl, and then converted to *N*-pivaloyl isopropyl (Pv/iPr) ester derivatives for gas chromatographic (GC) analysis [5].

On the witness coupons, eight terrestrially common amino acids (glycine, alanine, valine, leucine, isoleucine, proline, aspartic acid and glutamic acid) were detected and seven of them, except valine due to the under quantification limit, were quantified. Among them, glycine was the most abundant species with the highest concentration of 10 pmol/cm^2. A time-dependent profile of the four major amino acids (glycine, alanine, aspartic acid and glutamic acid) showed the increasing trend between 1 to 7 days. The average accumulation rates are 1.2 pmol/cm^2/day for glycine, 0.6 pmol/cm^2/day for alanine, 0.1 pmol/cm^2/day for aspartic acid and 0.2 pmol/cm^2/day for glutamic acid. The species and the concentrations of amino acids on our witness coupons are similar to those reported by the National Aeronautics and Space Administration/Johnson Space Center (NASA/JSC) OSIRIS-REx team [6]. Thus, the quality control against terrestrial contaminants in ISAS/JAXA curation facility is at the same quantitative level as in their facility. This inter-laboratory evaluation [7] about the terrestrial organic contamination will provide important information for the curation procedure of the Hayabusa2-returned samples.

©2019. Japan Geoscience Union. All Right Reserved.

References: [1] Tachibana S. et al. (2014) Geochem. J., 48, 571-587. doi: 10.2343/geochemj.2.0350. [2] Yada T. et al. (2014) Meteorit. Planet. Sci., 49, 135-153. doi: 10.1111/maps.12027. [3] Sawada H. et al. (2017) Space Sci. Rev. 208, 81–106. doi: 10.1007/s11214-017-0338-8. [4] Okazaki R. et al. (2017) Space Sci. Rev. 208, 107–124. doi: 10.1007/s11214-016-0289-5. [5] Chikaraishi Y. et al. (2010) in *Earth, Life, Isotopes*, Kyoto Univ. Press, pp.367-386. [6] Dworkin et al. (2018) Space Sci. Rev. 214, 9. doi: 10.1007/s11214-017-0439-4. [7] Sugahara et al. (2018) Earth, Planets Space, 70, 194. doi: 10.1186/s40623-018-0965-7.

Keywords: Amino acid, Hayabusa2, Curation, Witness coupons, Quality control

©2019. Japan Geoscience Union. All Right Reserved.

Hayabusa2 orbit determination using c5++ software

*Keiko Yamamoto[1], Toshimichi Otsubo[2], Koji Matsumoto[1], Hirotomo Noda[1], Noriyuki Namiki[1], Hiroki Senshu[3], Takahide Mizuno[4], Naoko Ogawa[4], Go Ono[4], Yuya Mimasu[4], Kent Yoshikawa[4], Tadateru Takahashi[4], Yuto Takei[4], Atsushi Fujii[4], Fuyuto Terui[4], Takanao Saiki[4], Satoru Nakazawa[4], Makoto Yoshikawa[4], Yuichi Tsuda[4]

1. National Astronomical Observatory of Japan, 2. Hitotsubashi University, 3. Chiba Institute of Technology, 4. Japan Aerospace Exploration Agency

Hayabusa2 arrived at the target asteroid Ryugu in June 2018 and is currently conducting remote sensing observations with various onboard instruments. So far, we have improved orbit determination software c5++, originally developed for the analysis of satellite laser ranging (SLR) data of the Earth, so that it can be used for the analysis of laser ranging data between Hayabusa2 and Ryugu obtained by Hayabusa2 LIDAR. Then we used it for the estimation of Hayabusa2 trajectory and the GM value of Ryugu. However, in the case of Hayabusa2, it is difficult to determine all of the 6 components of the initial state vector precisely if only LIDAR range data was used, and the simultaneously estimated GM value also had large uncertainty. To overcome this problem, in addition to LIDAR ranging data, we used Automated-Image-Tracking (AIT) data obtained by wide-angle optical navigation camera (ONC-W1) for the estimation of Hayabusa2 trajectory. In principle, LIDAR data gives information on the radial direction and AIT data give the ones on the across and along track directions. Thus, both data sets are complementary and help to improve the precision of the trajectory estimation. For this purpose, we improved c5 ++ so that it can deal with AIT data as observation data. In the presentation, we will show the results of trajectory and GM estimations using LIDAR and AIT data, and show how much the precision and accuracy are improved compared to the case using LIDAR data only.

Keywords: Hayabusa2, Orbit Determination, Ryugu

©2019. Japan Geoscience Union. All Right Reserved.

Landing Site Selection for Hayabusa2: Scientific Evaluation of the Candidate Sites on Asteroid (162173) Ryugu

*Hikaru Yabuta[1], Sei-ichiro WATANABE[2], Tomoki Nakamura[3], Naru Hirata[4], Seiji Sugita[5], Tatsuaki Okada[6], Kohei Kitazato[4], Yoshiaki Ishihara[7], Tomokatsu Morota[2], Naoya Sakatani[6], Koji Matsumoto[8], Koji Wada[9], Shogo Tachibana[5], Mutsumi Komatsu[10], ERI TATSUMI[5], Moe Matsuoka[6], Chikatoshi Honda[4], Takahiro Hiroi[11], Hiroki Senshu[9], Rie Honda[12], Yasuhiro Yokota[6], Rina Noguchi[6], Yuri Shimaki[6], Deborah Lorin Domingue[13], Lucille Le Corre[13], Antonella Barucci[14], Ernest Palomba[15], Shota Kikuchi[6], Akira Miura[6], Tomohiro Yamaguchi[6], Yukio Yamamoto[6], Takanao Saiki[6], Satoshi Tanaka[6], Makoto Yoshikawa[6], Yuichi Tsuda[6]

1. Hiroshima University, Department of Earth and Planetary Systems Science, 2. Nagoya University, 3. Tohoku University, 4. University of Aizu, 5. The University of Tokyo, 6. ISAS/JAXA, 7. NIES, 8. NAOJ, 9. Chiba Institute of Technology, Planetary Exploration Research Center (PERC), 10. Sokendai, 11. Brown University, 12. Kochi University, 13. Planetary Science Institute, USA, 14. Observatoire Paris-Site de Meudon, LESIA, France, 15. INAF-IAPS, Italy.

On June 27, 2018, JAXA’s Hayabusa2 spacecraft arrived at its target C-type asteroid Ryugu. Immediately after arrival, remote-sensing observations were carried out with the Optical Navigation Camera (ONC), the Near Infrared Spectrometer (NIRS3), the Thermal Infrared Imager (TIR), and the Laser Altimeter (LIDAR). Based on data from this suite of instruments, we carried out the landing site selection for the first touch-down (TD1). Since the mission aims to understand i) the origin and chemical evolution of the solar system and ii) the formation process and structure of the asteroid, we have set the most scientifically valuable TD1 site as the least altered region where water and/or carbon are potentially abundant.

Landing candidate sites were first selected by engineering evaluation for operational safety followed by scientific evaluations based on criteria such as science and samplability for the most interesting sites. The process was repeated using the observations from the altitudes of 20 km, 6 km, and 5 km.

Scientific evaluations of the landing site candidates were conducted based on the data products from ONC, NIRS3, TIR, and LIDAR. The shape modeling team produced two different shape models. ONC produced multiband images and reflectance spectra, as well as maps of spectral indices and X-means clustering analysis. Measurements of boulder size-frequency and Hapke parameters in the candidate landing areas were examined. NIRS3 produced four types of spectral feature maps. TIR provided maps of maximum temperature from the October 22, 2018 TD1 practice operations, apparent thermal inertia, and typical grain size determinations. LIDAR provided time series ranging data, topography, and corrected spacecraft trajectory.

Engineering evaluation: The possible landing site candidates were selected from the engineering safety score map evaluated based on the sub-Earth distance, local solar angle, local slope and elevation maximum difference. Thermal prediction results for TD1 were obtained by TIR. Temperatures of each site are < 350 K, confirming the safe conditions. The regions that satisfied all the conditions were, L05, L07, L08, L12, M01, M03 and M04.

Scientific evaluation:
1) Boulders. Based on the distribution of boulders with a diameter larger than 3 m for each potential landing site, regions L07, L08, and M04 show smaller percentages of boulder coverage than other areas, and are regarded as safer sites for landing.

©2019. Japan Geoscience Union. All Right Reserved.

2) Geology. Ryugu exhibits a variety of topographic features and geologic settings. From a scientific perspective, it is of interest to be able to study various materials representing the evolution of Ryugu.
3) Hydrous minerals. The NIR spectral properties are nearly homogeneous across Ryugu’ s surface, especially between the candidate sites. The near-infrared reflectance spectra of Ryugu is similar to experimentally heated Murchison meteorite at 400˚C.
4) Carbon contents. It is likely that visible reflectance at 0.55 μm (R(0.55)) is influenced mostly by carbon content. R(0.55) is almost homogeneous across the surface with a low value, regardless of the candidate sites.
5) Secondary processes. Although the surface of Ryugu is almost homogeneous at the macro scale in the map of spectral slope from 0.48 to 0.86 μm, a slight heterogeneity is observed across the candidate regions. L-regions are relatively bluish and M-regions are reddish. Considering that spectral reddening is observed by laser irradiation of dehydrated carbonaceous chondrites, L regions are probably less altered and preferable for sampling.

In the total evaluation, L08, L07 and M04 were selected as the TD1 candidates on August 17, 2018. In September 2018, many boulders > 50 cm were additionally found for the sites during the rehearsal of TD1. Thus, the originally scheduled TD1 in October was postponed. Further search for a flat and safe site continued, and L08-E1 was determined as the TD1 site. The TD1 will be scheduled on Feb 22, 2019.

Keywords: Hayabusa2, Landing Site Selection

©2019. Japan Geoscience Union. All Right Reserved.

Visible Photometric, Spectroscopic and Polarimetric observations of an inactive comet, P/2016 BA14 with the 1.6m Pirka Telescope

*Ryo Yamagata[1], Tomohiko Sekiguchi[1], Ryo Okazaki[1], Kazuya Doi[1], Daisuke Kuroda[2], Masateru Ishiguro[3], Hiroyuki Naito[4]

1. Hokkaido University of Education, 2. Kyoto University, 3. Seoul National University, 4. Nayoro Observatory

We performed photometric, spectroscopic and polarimetric observations of an inactive comet, P/2016 BA14 with the 1.6m Pirka Telescope, Hokkaido.

P/2016 BA14 (a=3.02 au, e=0.67, i=18.9 deg.) was discovered as an unusual asteroid with a cometary orbit by the PANSTAARS on 2016 January 21.Since Knight et al. 2016 detected its cometary tail when the object close to sun(r=1.018au). It was classified into a Jupiter Family Comets. It can be regarded as a bare nucleus invisible coma because very weak comet activity that is different from general comet. There is a remarkable similarity between the orbits of 252P/LINEAR (a=3.05au, e=0.67, i=10.4deg) and P/2016 BA14. Jupiter Tisserand parameter is 252P/LINEAR and that of P/2016 BA14 are 2.82. P/2016 BA14 and 252P/LINEAR is division comet that is originally same comet (Jian-Yang.2017).

In this study, surface reflection properties of P/2016 BA14 classify D-type asteroids (Bus-DeMeo taxonomy) from result of visible spectroscopy (435-820nm). Color of surface is little red as D-type asteroid, but very blue as comet nucleus from result of BVRI photometry. The linear polarization Pr=10.46.±0.11% (α=46°) is in close accord with that of D-type asteroids and comet nucleus.

Keywords: P/2016 BA14, Photometric, Spectroscopic, Polarimetric, D-type

©2019. Japan Geoscience Union. All Right Reserved.

Polycyclic aromatic hydrocarbons and aliphatic hydrocarbons in Jbilet Winselwan carbonaceous chondrite : Attempt to evaluate the thermal metamorphism degree on the parent body

Hiroki Kato[1], *Hikaru Yabuta[1]

1. Hiroshima University, Department of Earth and Planetary Systems Science

Introduction: On June 27, 2018, Hayabusa2 spacecraft arrived at the C-type asteroid Ryugu. The surface of Ryugu has been thought to have experienced dehydration at least partially, according to the grand-based observation (Vilas et al. 2008; Hiroi et al. 1993). Therefore, it is important to investigate the chemical compositions of dehydrated carbonaceous CM chondrites for understanding the surface process of asteroid Ryugu. Although the extents of thermal metamorphism of CM chondrites have been evaluated by mineralogical compositions (e.g., Nakamura et al. 2006) and elemental and molecular compositions of insoluble organic matter (IOM) (e.g., Naraoka et al. 2004; Yabuta et al. 2005), the estimated temperature varies widely. On the other hand, soluble organic molecules from the dehydrated CM chondrites have not been quantified or below detection (e.g. Shimoyama et al. 1989), and there has been no study which evaluated thermal metamorphism based on the compositions of soluble organic molecules. Therefore, in this study, we analyzed aliphatic hydrocarbons and polycyclic aromatic hydrocarbons (PAHs) in Jbilet Winselwan CM chondrite, which is a dehydrated CM chondrite (Zolensky et al 2016) and show similar reflectance spectrum to that of asteroid Ryugu (Kameda et al. 2015), for precise evaluation of parent body thermal metamorphism. The relative abundances of the hydrocarbons were compared with those of Murray meteorite, which is a primitive CM chondrite.

Samples and Methods: Powdered samples of Jbilet Winselwan meteorite and Murray meteorite (0.2 - 0.4g) were extracted with dichloromethane/methanol (9:1) by sonication. The extracts were applied to a silica gel column. From the column, aliphatic hydrocarbons were eluated with hexane and then PAHs were eluated with dichloromethane. The hexane and dichloromethane eluates were concentrated to 100 μl individually under a nitrogen flow for analysis by a gas chromatography coupled with mass spectrometry (GC-MS). Identification and quantification of compounds were made by comparison of peak retention times on mass chromatograms and mass spectra, and peak areas, respectively, with those of standard compounds. For compounds without standard compounds, identification was made by comparison of mass spectra with library data.

Results and discussion: Total concentration of *n*-alkanes from Jbilet Winselwan meteorite (1.85 μg/g meteorite) was 40 times lower than those from Murray meteorite (80.7 μg/g meteorite). Relative abundances of short-chain *n*-alkanes (C_{15}-C_{16}) were dominant in Jbilet Winselwan meteorite, while those of long-chain *n*-alkanes (C_{17}-C_{21}) were dominant in Murray meteorite. This difference implies that short-chain *n*-alkanes were resulted from cracking of long-chain *n*-alkanes and/or IOM during thermal metamorphism of the parent body of Jbilet Winselwan meteorite. Total concentration of PAHs from Jbilet Winselwan meteorite (0.05 μg/ meteorite) was 1000 times lower than those from Murray meteorite (62.0 μg/g meteorite). Dimethylnaphthalene, fluorine, phenanthrene, pyrene, fluoranthene, methylbiphenyl (0.003-0.039 μg/g meteorite) were identified, while low molecular weight PAHs, such as naphthalene, methylnaphthalene, and acenaphthene, were not detected. The results suggest that PAHs with high volatility in Jbilet Winselwan meteorite were lost or involved in further aromatization during thermal metamorphism. Distributions of dimethylnaphthalene and methylbiphenyl isomers in Jbilet Winselwan

©2019. Japan Geoscience Union. All Right Reserved.

and Murray meteorites were similar, respectively, which indicates that the parent body of Jbilet Winselwan meteorite experienced relatively mild thermal metamorphism.

Keywords: Jbilet Winselwan meteorite, Soluble organic molecules, Dehydration

©2019. Japan Geoscience Union. All Right Reserved.

Disk-Resolved Photometry Analysis of the Asteroid Ryugu Images Obtained by Hayabusa2 Visible Camera ONC

*yokota yasuhiro[1,2], Rie Honda[1], ERI TATSUMI[3], Deborah Domingue[4], Stefanus E. Schroeder[5], Moe Matsuoka[2], Seiji Sugita[3], Tomokatsu Morota[6], Shingo Kameda[7], Toru Kouyama[8], Hidehiko Suzuki[9], Manabu Yamada[10], Naoya Sakatani[2], Chikatoshi Honda[11], Masahiko Hayakawa[2], Kazuo Yoshioka[3], Yuichiro Cho[3], Hirotaka Sawada[2]

1. Kochi University, 2. ISAS/JAXA, 3. Univ. of Tokyo, 4. Planetary Science Institute, 5. DLR, 6. Nagoya Univ., 7. Rikkyo Univ., 8. AIST, 9. Meiji Univ., 10. Chiba Institute od Technology, 11. Aizu Univ.

Since June 2018, the Optical Navigation Camera (ONC) onboard Hayabusa2, has observed the C-type asteroid 162173 Ryugu at a distance below 20 km. ONC-T and ONC-W1 are used for surface imaging operations, and their images allow us to investigate the disk-resolved photometric properties of the surface. A narrow-angle camera ONC-T has 7 broad-band filters ranging in wavelength from 0.39–0.95 μm. ONC-W1 is a wide-angle (> 65˚) pan-chromatic camera mainly used for optical navigation during cruise and low-altitude (< 20km) operations. We are proceeding the analysis of both dataset, ONC-T and ONC-W1.

Since Hayabusa2’s position is nominally fixed on the line connecting Ryugu and the Earth, the available solar phase angle range by ONC-T changes seasonally with the orbits of Earth and Ryugu around the sun. Therefore, we are collecting a large number of ONC-T images over a long period of time to cover a wide phase angle range.

ONC-W1 data has a strong point that it covers a wide phase angle range within a single frame during the descent operations, because of its wide field of view. One of our current challenges is deriving a precise viewing geometries (incidence angle, emission angle, and phase angle) at each pixel. Additionally, comparison of the absolute brightness value (radiance factor) with ONC-T is an ongoing issue.

Keywords: Asteroid, Photometry, Ryugu, Hayabusa2

©2019. Japan Geoscience Union. All Right Reserved.

[E] Poster | P (Space and Planetary Sciences)：P-EM Solar-Terrestrial Sciences, Space Electromagnetism & Space Environment

Wed. May 29, 2019 10:45 AM - 12:15 PM JST | Wed. May 29, 2019 1:45 AM - 3:15 AM UTC | Poster Hall International Exhibition Hall8, Makuhari Messe_3

[P-EM09] Vertical coupling in the atmosphere and Ionosphere

convener:Huixin Liu(Earth and Planetary Science Division, Kyushu University SERC, Kyushu University), Loren Chang(Institute of Space Science, National Central University), Yuichi Otsuka(Institute for Space-Earth Environmental Research, Nagoya University)

Vertical coupling mechanisms throughout the whole atmosphere are critical to understanding the near Earth space environment, as well as its sensitivity to the solar, geomagnetic, and atmospheric drivers. This international session focuses on physical/chemical processes occurring in the mesosphere, thermosphere, and ionosphere (MTI). Both quiet and disturbed states in response to lower atmospheric forcing or solar forcing are important for understanding the MTI system and its coupling to other regions. We invite presentations of observations and observational concepts with ground-based and/or space-borne instruments, theoretical studies, numerical simulations, and development of data analysis systems for various kinds of temporal and spatial variations in atmosphere-ionosphere coupled system.

[PEM09-P01] Local-time Variabilities of SABER CO_2 in the Mesosphere and Lower Thermosphere Region

*Cornelius Csar Jude Salinas[1], Loren Chang[1], Danie Liang[2], Jia Yue[3], Liying Qian[4], Quan Gan[5], James Russel III[3], Martin G Mlynczak[6] (1.Institute of Space Science, National Central University, 2.Institute of Earth Science, Academia Sinica, 3.Department of Atmospheric Sciences, Hampton University, 4.High Altitude Observatory, National Center for Atmospheric Research, 5.Department of Physics and Astronomy, Clemson University, 6.NASA Langley Research Center)

[PEM09-P02] Enhanced dynamo electric field as a possible cause of ionosphere disturbance before Large Earthquake

*Koichiro Oyama[1,2,3] (1.Institute of Plasma and Space Sciences,National Cheng Kung Univ., Taiwan, 2.International Ceneter for Space Weather Sudy and Education, Kyushu Univ.,, 3.CoLtd. Asia Space Environment Research Consortium, Japan)

[PEM09-P03] Morphology of E1 and E2 Kelvin waves from ECMWF reanalysis

*Chen-Jeih Pan[1], Wei-Sheng Chen[1], Uma Das[2] (1.Institute of Space Science, National Central University, 2.Department of Physics, Indian Institute of Information Technology, Kalyani, India)

[PEM09-P04] Impact of strong ENSO on TEC activity disturbed by ultra-fast Kelvin waves

*Wei-Sheng Chen[1], C.J. Pan[1], Uma Das[2], Chian-Chiau Lin[3] (1.Institute of Space Science, National Central University, Taiwan, 2.Department of Physics, Indian Institute of Information Technology, Kalyani, India, 3.Environmental Research and Information Center, Chang Jung Christian University, Taiwan)

[PEM09-P05] Observation and simulation of propagation of coseismic infrasound to the ionosphere

*Jaroslav Chum[1] (1.Institute of Atmospheric Physics of the Czech Academy of Sciences)

[PEM09-P06] Solar wind influence on tropical cyclones mediated by atmospheric gravity waves

*Paul Prikryl[1,2], Iurii Cherniak[3], Irina Zakharenkova[4,5], James M. Weygand[6], Bharat S. R. Kunduri[7] (1.Physics Department, University of New Brunswick, Fredericton, NB, Canada, 2.Geomagnetic Laboratory, Natural Resources Canada, Ottawa, ON, Canada, 3.COSMIC Program Office, University Corporation for Atmospheric Research, Boulder, CO, USA, 4.West Department of IZMIRAN, Kaliningrad, Russia, 5.University of Warmia and Mazury in Olsztyn, Poland, 6.Earth Planetary and Space Sciences, University of California, Los Angeles, CA, USA, 7.Bradley Dept. of Electrical and Computer Engineering, Virginia Tech, Blacksburg, VA, USA)

[PEM09-P07] VIPIR ionospheric observations in Japan

*Takuya Tsugawa[1], Hideo Maeno[1], Michi Nishioka[1], Takumi Kondo[1], Mamoru Ishii[1] (1.National Institute of Information and Communications Technology)

[PEM09-P08] Simulation Results and Performance Analysis of Phase Velocity Spectral Analysis Software (M-Transform) for Airglow Imaging Data

*Septi Perwitasari[1], Takuji Nakamura[2], Masaru Kogure[2], Yoshihiro Tomikawa[2], Mitsumu K. Ejiri[2] (1.LAPAN, 2.NIPR)

[PEM09-P09] Comparisons of Co-incident Ionospheric Plasma Observations Between FORMOSAT-5/AIP and Millstone Hill Incoherent Scatter Radar

*Yi-Wun Chen[1], Chi-Kuang Chao[1] (1.Graduate Institute of Space Science, National Central University, Taiwan)

[PEM09-P10] Sub-ionospheric effects of volcano eruptions using VLF/LF standard radio waves

*Kei Maruyama[1], Hiroyo Ohya[1], Fuminori Tsuchiya[2], Kenro Nozaki[5], Kozo Yamashita[3], Yukihiro Takahashi[4], Hiroyuki Nakata[1], Toshiaki Takano[1] (1.Chiba University, 2.Tohoku University, 3.Ashikaga University, 4.Hokkaido University, 5.National Institute of Information and Communications Technology)

[PEM09-P11] Observations of ionospheric and mesospheric wave structures by a low-cost airglow imaging system

*Keisuke Hosokawa[1], Nanami Kusuyama[1], Yuta Hozumi[1], Kohei Takami[1], Susumu Saito[2], Yasunobu Ogawa[3], Mamoru Ishii[4], Yuichi Otsuka[5], Takuya Tsugawa[4] (1.University of Electro-Communications, 2.ENRI, 3.NIPR, 4.NICT, 5.ISEE, Nagoya University)

[PEM09-P12] Analysis of characteristics of ionospheric parameters, Sq index and neutral winds over Taiwan

*Yu-Jung Chuo[1] (1.Department of Information Technology, Ling Tung University)

[PEM09-P13] Statistical study on daytime Es observed by ground-ionosonde and RO-COSMIC in magnetic Equator region in 2010

*Zheng Wang [1,2], Huixin Liu[1] (1.Department of Earth and Planetary Sciences, School of Science, Kyushu University, Japan. , 2.National Space Science Center, Chinese Academy of Sciences, China.)

[PEM09-P14] The statistical study of the growth rates of Medium-Scale Traveling Ionospheric Disturbances observed with GPS-TEC

*Takafumi Ikeda[1], Akinori Saito[1], Takuya Tsugawa[2], Hiroyuki Shinagawa[2] (1.Department of Geophysics, Graduate School of Science, Kyoto University, 2.National Institutes of Information and Communications Technology)

[PEM09-P15] Comparison of Gravity Wave Activity in the Mesosphere Observed by OH Airglow Imagers and MF Radars over the Antarctic (Syowa & Davis).

*Masaru Kogure[1], Takuji Nakamura[1,2], Yoshihiro Tomikawa[1,2], Mitsumu K. Ejiri[1,2], Takanori Nishiyama[2,1], Masaki Tsutsumi[1,2], Michael J. Taylor[3], Yucheng Zhao[3], P.-Dominique Pautet[3], Damian Murphy[4] (1.National Institute of Polar Research, 2.Department of Polar Science, Sokendai, 3.Physics Department, Utah State University, 4.Australian Antarctic Division)

Local-time Variabilities of SABER CO_2 in the Mesosphere and Lower Thermosphere Region

*Cornelius Csar Jude Salinas[1], Loren Chang[1], Danie Liang[2], Jia Yue[3], Liying Qian[4], Quan Gan[5], James Russel III[3], Martin G Mlynczak[6]

1. Institute of Space Science, National Central University, 2. Institute of Earth Science, Academia Sinica, 3. Department of Atmospheric Sciences, Hampton University, 4. High Altitude Observatory, National Center for Atmospheric Research, 5. Department of Physics and Astronomy, Clemson University, 6. NASA Langley Research Center

This work presents the local-time variabilities of CO_2 in the Mesosphere and Lower Thermosphere region (MLT region) as observed by the Sounding of the Atmosphere using Broadband Emission Radiometry (SABER) onboard the Thermosphere Ionosphere Mesosphere Energetics and Dynamics Satellite (TIMED Satellite). These are then compared to CO_2 as modeled by the Whole Atmosphere Community Climate Model –eXtended (WACCM-X). Also using WACCM-X, a tendency analysis using the continuity equation is done to explain the local-time variabilities of CO_2 in the MLT region. Finally, consequences of including a significant local-time variability in CO_2 when retrieving SABER temperature profiles are determined.

Keywords: Carbon Dioxide, Mesosphere and Lower Thermosphere Region, Tides

©2019. Japan Geoscience Union. All Right Reserved.

Enhanced dynamo electric field as a possible cause of ionosphere disturbance before Large Earthquake

*Koichiro Oyama[1,2,3]

1. Institute of Plasma and Space Sciences,National Cheng Kung Univ., Taiwan, 2. International Ceneter for Space Weather Sudy and Education, Kyushu Univ.,, 3. CoLtd. Asia Space Environment Research Consortium, Japan

Disturbance of ionosphere before large earthquakes has been very often reported. One of the possible disturbing drivers is electric field, which explains most of the ionosphere features we reported so far. However, the origin of the electric field is still in the darkness. One idea of electric field generation exists inside earth interior (Freund et a., 2006). We propose here that the electric field is dynamo field at the height of ≈100 km, which simply intensified before earthquake; intensified eastward (westward)electric field during daytime(nighttime). This idea explains satellite data (Oyama et al.,2008; Oyama et al.,2011; Ryu et al., 2014; Ryu et al., 2016; Oyama et al.,2016; Oyama et al., 2019).

Next question on the electric field generation is the mechanism which modifies the dynamo field. We speculate that modification of E field is a result of modification of neutral wind system, which is originally caused by internal gravity waves which propagate from below. Then again next question is on the origin of the internal gravity waves. The waves might be originally caused by the ground motion, and these waves which propagate upward might interact with planetary wave, and amplified. We show several side evidence of ground motions before earthquakes.

Keywords: Earthquake, Electric field, Ionosphere, Disturbance

©2019. Japan Geoscience Union. All Right Reserved.

Morphology of E1 and E2 Kelvin waves from ECMWF reanalysis

*Chen-Jeih Pan[1], Wei-Sheng Chen[1], Uma Das[2]

1. Institute of Space Science, National Central University, 2. Department of Physics, Indian Institute of Information Technology, Kalyani, India

Kelvin waves are planetary waves traveling eastwards and confined in the equatorial latitudes. The waves play an important role in middle atmosphere dynamics because they transfer energy and momentum from lower to higher altitudes, which contributes to the quasi-biennial oscillation (QBO) and further influences the global climate. Kelvin waves have been studied for many decades, and the most of studies were focused on the waves of wavenumber 1 (E1). On the other hand, the wavenumber-2 Kelvin waves (E2) are also an important part of Kelvin wave activities although their amplitude less than the E1. In this study, we analyzed the long-term European Centre for Medium-Range Weather Forecasts (ECMWF) reanalysis data and reported the morphology of E1 and E2 Kelvin waves in the stratospheric altitudes individually. The temperature from ECMWF reanalysis was used to extract the wave properties. Temperatures between latitudes of 10S and 10N were firstly gridded into the structure of day-altitude-longitude, and then subtract background (longitudinal means) to get equatorial temperature fluctuations. For each altitude, the two-dimensional fast Fourier transform was applied to each 96-day data segment and stepped forward in time by 1 day. The output spectra were then analyzed to get primary wave periods and amplitude variations. From spectra, the E1 amplitude is 1.5 to 2.0 times larger than the E2 in average. The E1 primary periods are 12 to 25 days and are restricted under the 20-km altitude. The periods of 8 to 14 days are the secondary group. They can propagate upward to the 40-km altitude. Regarding the E2, the primary periods are 7 to 12 days and are also restricted under the 20-km altitude. Its secondary group is the periods of 5 to 8 days, which also can propagate upward to the 40-km altitude. Furthermore, the altitude-time-amplitude variation show that the E2 waves are influenced strictly by the QBO westerly. Finally, the cross correlation between E1 and E2 show that the E1 and E2 have high correlation at altitudes close to the tropopause, which implies they are excited simultaneously.

Keywords: Kelvin waves, QBO

©2019. Japan Geoscience Union. All Right Reserved.

Impact of strong ENSO on TEC activity disturbed by ultra-fast Kelvin waves

*Wei-Sheng Chen[1], C.J. Pan[1], Uma Das[2], Chian-Chiau Lin[3]

1. Institute of Space Science, National Central University, Taiwan, 2. Department of Physics, Indian Institute of Information Technology, Kalyani, India, 3. Environmental Research and Information Center, Chang Jung Christian University, Taiwan

Ultra-fast Kelvin waves (UFKW) are a subclass of Kelvin waves that they have the shortest periods (2-5 days) and thus can propagate into the ionosphere. UFKW relate to ionospheric variations have been reported, which include ionospheric minimum virtual height (h'F), F2 maximum critical frequency (foF2), total electron content (TEC), S4 scintillations, etc. In the study, we analyzed the UFKW activities using SABER (Sounding of the Atmosphere using Broadband Emission Radiometry) temperatures and GIM (Global Ionospheric Maps) TEC from 2009 to 2011 to see how UFKW influence the ionosphere. The period 2009-2011 belongs to the strong ENSO period. Previous studies have shown that Kelvin waves were highly active in this period, especially in the early of 2010. Therefore, this study can implicitly reveal how the ionosphere responds to the ENSO. The wave signatures in SABER temperatures were extracted using the fast Fourier transform (FFT). Temperatures in the geographic equatorial latitudes were gridded into the day-altitude-longitude structure and then removed background to get temperature fluctuations. The two-dimensional FFT was applied to each 96-day data segment for each altitude and stepped forward in time by one day. Regarding TEC, the Lomb-Scargle periodogram was used to extract UFKW signatures. Because TEC has a strong local time variation and constrains by the geomagnetic configuration, TEC at 16 local time and low geomagnetic latitudes were selected. The background was removed firstly from the data and then fed TEC fluctuations into the Lomb-Scargle process, which also stepped forward in time by one day. The FFT and Lomb-Scargle process both outputted spectra, which revealed UFKW activities in the mesosphere and lower thermosphere (MLT) region (90-100 km) and the ionosphere (about 150-600 km). The results show that UFKW activities at two equatorial ionization anomalies (EIA) were almost identical, and both were higher than that at geomagnetic equator. Most of wave activities in the temperature field in the MLT region have corresponding activities in TEC. However, there are a lot of small amplitude activities only in TEC.

Keywords: ultra-fast Kelvin waves, ENSO, TEC

©2019. Japan Geoscience Union. All Right Reserved.

Observation and simulation of propagation of coseismic infrasound to the ionosphere

*Jaroslav Chum[1]

1. Institute of Atmospheric Physics of the Czech Academy of Sciences

Vertical motion of the ground surface caused by seismic waves generates acoustic waves that propagate nearly vertically upward owing to supersonic speed of seismic waves. As the air density decreases with height, the amplitude of acoustic waves increases to conserve the energy flux up to the altitudes where the air is so rarefied that it cannot sustain the propagation and the waves start dissipating. For distances up to about 1500 km from the epicenter of the strong earthquakes (M>7), the amplitude (oscillation velocity) of infrasound waves reaches significant values in the upper atmosphere. Consequently, the nonlinear phenomena start to play an important role. Spectral content of the wave packet is changed and the energy is transferred to lower frequencies, which can cause the formation of roughly bipolar N-shaped pulse. The simulation results are compared with observation for selected examples. It is also shown that only infrasound with periods larger than about 10 s (generated by long period seismic waves) can reach the ionospheric heights, namely the F layer where it can be easily detected.

Keywords: coseismic perturbation in the ionosphere, infrasound, nonlinear propagation

©2019. Japan Geoscience Union. All Right Reserved.

Solar wind influence on tropical cyclones mediated by atmospheric gravity waves

*Paul Prikryl[1,2], Iurii Cherniak[3], Irina Zakharenkova[4,5], James M. Weygand[6], Bharat S. R. Kunduri[7]

1. Physics Department, University of New Brunswick, Fredericton, NB, Canada, 2. Geomagnetic Laboratory, Natural Resources Canada, Ottawa, ON, Canada, 3. COSMIC Program Office, University Corporation for Atmospheric Research, Boulder, CO, USA, 4. West Department of IZMIRAN, Kaliningrad, Russia, 5. University of Warmia and Mazury in Olsztyn, Poland, 6. Earth Planetary and Space Sciences, University of California, Los Angeles, CA, USA, 7. Bradley Dept. of Electrical and Computer Engineering, Virginia Tech, Blacksburg, VA, USA

Solar wind coupling to the magnetosphere-ionosphere-atmosphere (MIA) system generates medium- and large-scale atmospheric gravity waves (AGWs) propagating globally from sources in the lower thermosphere at high latitudes. The AGWs propagate globally [1,2] upward and downward, are observed in the ionosphere as traveling ionospheric disturbances [3], can be ducted in lower atmosphere over long distances and reach troposphere. At the reflection point in the troposphere they can trigger moist instabilities to initiate convective bursts, with the latent heat release leading to intensification of storms [4]. In the follow-up studies [5,6,7] it was shown that explosive extratropical cyclones and rapid intensification of tropical cyclones tend to follow arrivals of solar wind high-speed streams (HSS) and/or interplanetary coronal mass ejections (ICMEs). The coupling of solar wind to MIA is most intense during the arrivals of co-rotating interaction regions (CIRs) and/or interplanetary shocks at the leading edges of HSSs and ICMEs when the amplitudes of aurorally-generated AGWs are largest. Ray tracing of AGWs in a model atmosphere show that they can reach tropical cyclones. Spiral gravity waves in typhoons were observed and simulated to propagate radially outward from the typhoon core [8]. The spectra of waves in surface pressure and surface wind measured by the Impacts of Typhoons on the Ocean in the Pacific (ITOP) buoy during the nearby passages of intense typhoons are similar to those of incoming aurorally-generated AGWs. It is suggested that the interaction of aurorally-generated gravity waves with the tropical cyclone vortex and the inner primary eyewall plays a role in the intensification process.

[1] Mayr H.G., et al., J. Geophys. Res., 89, 10929–10959, 1984.
[2] Prikryl P., et al., Ann. Geophys., 23, 401-417, 2005. doi:10.5194/angeo-23-401-2005
[3] Cherniak Iu., Zakharenkova I., Space Weather, 16, 2018. https://doi.org/10.1029/2018SW001869.
[4] Prikryl P., et al., Ann. Geophys. 27, 31–57, 2009. https://doi.org/10.5194/angeo-27-31-2009.
[5] Prikryl P., et al., J. Atmos. Sol.-Terr. Phys., 149, 219–231, 2016.
[6] Prikryl P., et al., J. Atmos. Sol.-Terr. Phys., 171, 94–110, 2018.
[7] Prikryl P., et al., J. Atmos. Sol.-Terr. Phys., 183, 36-60, https://doi.org/10.1016/j.jastp.2018.12.009.
[8] Nolan D.S., Zhang J.A., Geophys. Res. Lett., 44, 3924–3931, 2017. doi:10.1002/2017GL073572

Keywords: Solar wind-magnetosphere-ionosphere-atmosphere coupling, High-speed solar wind stream, Atmospheric gravity wave, Extratropical and tropical cyclones

©2019. Japan Geoscience Union. All Right Reserved.

VIPIR ionospheric observations in Japan

*Takuya Tsugawa[1], Hideo Maeno[1], Michi Nishioka[1], Takumi Kondo[1], Mamoru Ishii[1]

1. National Institute of Information and Communications Technology

National Institute of Information and Communications Technology (NICT) has observed ionosphere by ionosondes more than 70 years in Japan. At present, four ionosondes at Wakkanai (Sarobetsu), Kokubunji, Yamagawa, Okinawa (Ogimi) are automatically operated and controlled from Tokyo. Major ionospheric parameters such as foF2 and foEs are scaled from the ionograms automatically on a realtime basis and scaled manually for the final values. These scaled parameters are provided through our web site (http://wdc.nict.go.jp/IONO/). In 2017, we replaced the 10C ionosondes with Vertical Incidence Pulsed Ionospheric Radar 2 (VIPIR2) which can separate the O- and X-modes of ionospheric echoes which have improved the availability of automatic scaling of the ionogram. Our automatic scaling method has been improved using new O- and X-modes separated ionograms. As for future plans, we try to expand observation area by oblique sounding observations with VIPIRs in Japan and neighboring countries. We have also tried to detect arrival directions of ionospheric echo by using the 8ch receiving data as a interferometry. In this presentation, we will introduce current status and future plans of ionospheric observation in NICT.

Keywords: Ionosphere, Ionosonde, Space Weather

©2019. Japan Geoscience Union. All Right Reserved.

Simulation Results and Performance Analysis of Phase Velocity Spectral Analysis Software (M-Transform) for Airglow Imaging Data

*Septi Perwitasari[1], Takuji Nakamura[2], Masaru Kogure[2], Yoshihiro Tomikawa[2], Mitsumu K. Ejiri[2]

1. LAPAN, 2. NIPR

We have developed a user-friendly software based on *Matsuda et al.*, 2014's 3D-FFT method (M-Transform) for airglow data analysis as a function on Interactive Data Language (IDL). Input of this function is 3-D array of a time series of airglow image that have already been converted to geographical coordinate (*x*, *y*, *t*). The user can customize the wave parameters (e.g. horizontal wavelength (λ_h), wave period (τ), phase speed (*c*), image resolution in space (*dx*,*dy*) and time (*dt*)) in one-line command when executing the program, which depends on their analysis purpose. In order to exhibit this new function's performance and the characteristics/interpretation of the spectral analysis, we have run several test cases using artificial wave. The first case is artificial wave with constant speed (40 m/s) and different wave period (8, 15, 30 min) and horizontal wavelength. In second case, we applied Gaussian shape wave-packet with different FWHM (50, 100, 200 km). For the third test case, with a fixed wave packet size (100 km), we changed the wave packet duration (30, 60, 120 min). The results from the various simulations showed reasonable characteristics of the spectral analysis for different scenarios. We showed that the increase of wave period and horizontal wavelength lead to the wider spectrum with total power difference of ~10%. By changing the wave packet size, we showed that the bigger the wave packet size, the sharper and narrower the spectrum became with the total power increase 2x of the increase size of the wave packet. The result of changing the wave packet duration showed that the longer the duration of wave packet, the spectrum becomes sharper and the total power is proportional to the wave packet length. We also examined the aliasing and zero padding effect on the spectral analysis. In order to avoid the aliasing effect, it is recommended to set the period minimum to at least 2 x image interval (*dt*). More detailed analysis will be discussed during the presentation.

Keywords: Airglow, Gravity wave, Analysis software

©2019. Japan Geoscience Union. All Right Reserved.

Comparisons of Co-incident Ionospheric Plasma Observations Between FORMOSAT-5/AIP and Millstone Hill Incoherent Scatter Radar

*Yi-Wun Chen[1], Chi-Kuang Chao[1]

1. Graduate Institute of Space Science, National Central University, Taiwan

Advanced Ionospheric Probe (AIP) onboard FORMOSAT-5 satellite has routinely measured ionospheric plasma parameters, like ion concentration, velocity, and temperature in a sun-synchronous circular orbit at 720 km altitude along 2230 local-time sector since November 2017. AIP has found that the satellite has a much lower potential with respective to environmental plasma from measured current-voltage curves. A comparison study shall be performed to identify possible bias on the derived AIP parameters. Co-incident observations have been scheduled with Millstone Hill incoherent scatter radar during 30 January to 1 February 2019. In this poster, preliminary comparison results will be outlined and will be used to improve accuracy of the AIP measurement in the future.

Keywords: FORMOSAT-5, AIP, ionosphere

©2019. Japan Geoscience Union. All Right Reserved.

Sub-ionospheric effects of volcano eruptions using VLF/LF standard radio waves

*Kei Maruyama[1], Hiroyo Ohya[1], Fuminori Tsuchiya[2], Kenro Nozaki[5], Kozo Yamashita[3], Yukihiro Takahashi[4], Hiroyuki Nakata[1], Toshiaki Takano[1]

1. Chiba University, 2. Tohoku University, 3. Ashikaga University, 4. Hokkaido University, 5. National Institute of Information and Communications Technology

Several studies for the F-region ionosphere associated with volcano eruptions based on GPS-TEC data have been reported so far (e.g., Heki, 2006; Dautermann et al., 2009; Heki et al., 2010). These studies reported that acoustic waves excited by volcano eruptions reach up to the F-region ionosphere, and caused F-region perturbations. After eruption of the Kelud Volcano, Indonesia, in February 2014, acoustic resonance between the Earth’ s surface and lower thermosphere was reported based on TEC data and the seismic wave data (Nakashima et al., 2015). However, little studies on the D-region ionosphere associated with volcano eruptions have been reported. In this study, we investigate the D-region effects of eruptions of Sakurajima volcano (31.59N, 130.66E), Japan, at 04:11 UT on June 6, 2014, using intensity perturbation of VLF/LF transmitter signals. The VLF/LF propagation paths use in this study are JJY (JJY 60 kHz) - Tainan (TNN, Taiwan), and JJI (22.2 kHz) - TNN. Based on wavelet spectra, the perturbation of both transmitter signals had a frequency of 2-6 mHz during 04:12-04:30 UT after the eruptions (04:11 UT).We compared the perturbations with atmospheric pressure data obtained by an infrasonic meter observed by Sakurajima Volcano Research Center, Kyoto University, and seismic waves in the NIED F-net data (FUK, STM, and SBR) located close to the JJY-TNN path. The atmospheric pressure and vertical velocity of the seismic waves had the similar frequencies of 2-10 mHz during 04:12-04:47 UT. These similar frequencies suggest that the perturbations would be caused by acoustic resonance between the Earth's surface and lower thermosphere, or by acoustic and atmospheric gravity waves generated by volcanic eruptions. In the presentation, we will discuss the cause of the VLF/LF perturbations in more detail.

©2019. Japan Geoscience Union. All Right Reserved.

Observations of ionospheric and mesospheric wave structures by a low-cost airglow imaging system

*Keisuke Hosokawa[1], Nanami Kusuyama[1], Yuta Hozumi[1], Kohei Takami[1], Susumu Saito[2], Yasunobu Ogawa[3], Mamoru Ishii[4], Yuichi Otsuka[5], Takuya Tsugawa[4]

1. University of Electro-Communications, 2. ENRI, 3. NIPR, 4. NICT, 5. ISEE, Nagoya University

In the last two decades, all-sky airglow imagers with cooled CCD cameras have widely been used to observe large-scale wave structures in the F-region ionosphere, for example medium-scale traveling ionospheric disturbances (MSTIDs). Such wavy features are seen in the oxygen emission at 630.0 nm from altitudes slightly below the F-region peak. Similar optical observations of OH band emission have also enabled us to visualize atmospheric gravity waves at the mesospheric height. Deploying airglow imagers in multiple places is one of the cost-effective ways to visualize the large-scale structure of these wave structures at both the F-region ionosphere and mesosphere [e.g., Kubota et al., 2001; Suzuki et al., 2013]. However, ground-based airglow imagers equipped with a cooled CCD camera is still expensive; thus, it is rather difficult to deploy such systems in a wide area and carry out a network observation. To overcome this limitation, we recently developed a low-cost airglow imaging system (Low-Cost Airglow imaging System: LCAS) which consists of a small camera (WAT-910HX), fisheye lens and optical filter. We then confirmed its capability of imaging the spatial structure of polar cap patches and plasma bubble in the 630.0 nm emission from the F-region. But, still, it is unclarified if the system is also capable of detecting the two-dimensional structure of MSTIDs. On the night of May 12, 2018, we identified a weak wavy signature in the 630.0 nm airglow images from one of our LCAS stations in Ishigaki Island, Japan. The wave structure in the 630.0 nm images was smoothly connected to the structure of MSTIDs in the GPS-TEC data, which confirmed the ability of LCAS for detecting MSTIDs. We also identified smaller scale wave structures in the 630.0 nm images, showing characteristic concentric wave fronts. We speculate that gravity waves in the mesosphere were captured in the 630.0 nm images as a contamination of the OH airglow. This is mainly because we make use of an optical filter having 10 nm FWHM, which enables us to detect several spectral peaks of OH emission near the 630.0 nm oxygen emission. We have estimated the center of the concentric wave structures by using the curvature of the wave fronts, and then confirmed that active rain fall took place in a localized area close to the estimated center of the concentric waves. This result supports our hypothesis that the OH emission containing signatures of mesospheric gravity waves were detected in the 630.0 nm images. In summary, the 630.0 nm airglow observation of LCAS is able to observe MSTIDs and mesospheric gravity waves. This will allow us to monitor such wavy structures at two different altitudes by distributing the similar system in a wide area.

Keywords: Airglow, Traveling Ionospheric Disturbances

©2019. Japan Geoscience Union. All Right Reserved.

Analysis of characteristics of ionospheric parameters, Sq index and neutral winds over Taiwan

*Yu-Jung Chuo[1]

1. Department of Information Technology, Ling Tung University

In this paper, we examine the variation of thermospheric neutral winds and solar quiet (Sq) current of the geomagnetic fields for the equatorial ionospheric anomaly area (EIA) during the solar activity period in 1999. The thermospheric neutral winds are derived from the ionospheric F_2-layer peak height, hmF_2, by using the servo model method. The variability of the amplitude ofSq fields is derived from the ground geomagnetic fields in the components H and Z, respectively. Theresults of the current system show a same diurnal variation, which that peaks / valleys in the local noon time for Sq(H) / Sq(Z) in the low latitudes, respectively.The results also indicate a weak seasonal variation that peaks appear at the local summer of the Sq currents in H and Z components, respectively. The Sq current system is associated with the change of the equatorial electrojet (EEJ). Further, the variability is probably attributed to local thermospheric winds. The study also shows that the zonal and meridional components of the neutral winds at the EIA over Taiwan area. Furthermore, the study examines the variations of Sq(H), Sq(Z), neutral winds, and ionospheric parameters foE_s, NmF_2, and hmF_2during the disturbed geophysical conditions such as geomagnetic storm and earthquake. The result shows the variationsof ionospheric Sq(H), Sq(Z) and thermospheric neutral winds are different between the seismo-ionospheric and solar-terrestrial disturbed periods, even they lead the same decreasing electron density reaction in the ionosphere at the EIA over Taiwan area.

Keywords: Sq current, ionosphere, neutral winds

©2019. Japan Geoscience Union. All Right Reserved.

Statistical study on daytime Es observed by ground-ionosonde and RO-COSMIC in magnetic Equator region in 2010

*Zheng Wang [1,2], Huixin Liu[1]

1. Department of Earth and Planetary Sciences, School of Science, Kyushu University, Japan. , 2. National Space Science Center, Chinese Academy of Sciences, China.

Scintillations under 150 km height shown by radio occultation (RO) of COSMIC are considered to be associated with ionospheric sporadic E (Es) layer. In this paper, we make a Statistical study on daytime Es observed by ground-ionosonde at five stations in magnetic Equator region in 2010, and make a comparison with S4 index from RO-COSMIC within 6 degree of each station. The results show that: At each station the diurnal variation of foEs from ionosonde decrease a little around LT 0600 and then increase, having maximum around LT 1200, decrease around LT 1800 and then increase near LT 2000-2200; All the S4>=0.3 observations during daytime come from RO-COSMIC under 150 km height; The diurnal variation of S4 index under 150 km height from RO-COSMIC over each station has similar trend with that of foEs at the same station; S4 index over 150 km height from RO-COSMIC is only high during nighttime; For the stations at different longitudes, Es occurrences from ionosonde are positively associated with S4>=0.3 from RO-COSMIC. The comparison shows that the S4 index from RO-COSMIC could show some features of daytime Es layer in magnetic Equator region without the location limitation of ground stations.

Keywords: daytime ionospheric sporadic E, ground-ionosonde , radio occultation of COSMIC , magnetic Equator region

©2019. Japan Geoscience Union. All Right Reserved.

The statistical study of the growth rates of Medium-Scale Traveling Ionospheric Disturbances observed with GPS-TEC

*Takafumi Ikeda[1], Akinori Saito[1], Takuya Tsugawa[2], Hiroyuki Shinagawa[2]

1. Department of Geophysics, Graduate School of Science, Kyoto University, 2. National Institutes of Information and Communications Technology

We think two mechanism, E-F coupling and Perkins Instability, will relate to growth for nighttime-MSTID in mid-latitude [Tsunoda and Cosgrove., 2001 ; Perkins., 1973]. Linear growth rate of perturbation intensity of Pedersen conductivity expected from E-F coupling is around 15 minutes [Yokoyama et al., 2009], which is far shorter than one expected from Perkins Instability [Fukao and Kelley, 1991 ; Miller et al., 1997 ; Shiokawa et al., 2003]. However, Es layer’ s spatial and temporal scale is less than 100km and 15min [Maeda et al., 2013 ; S.Saito et al., 2007]. They are different from MSTID’ s ones, which are 200-400 km and around 2hours [Otsuka et al., 2011]. To decide which instability is responsible for growth of nighttime MSTID, the growth rate of MSTID was observationally determined with ground-based GPS network data.

We statistically investigated the growth rate of nighttime-MSTID in Japan in 2014 observed with GPS-TEC. The growth rate of nighttime -MSTID observed was 1.0 - 6.0 $\times 10^{-4}$ s^{-1} during 1800LT-2400LT in summer.Linear growth rate of Perkins instability in summer was 1.0 - 6.0 $\times 10^{-4}$ s^{-1} during 1800LT - 2400LT, so they were less than one of the E-F coupling instability. Also,Seasonal distribution of observed growth rate before midnight was similar to that of linear growth rate.U×B derived by GAIA model was high in spring - summer and seasonal distribution of U×B was similar to that of linear growth rate. Therefore, the growth of MSTID when propagating is not determined by E-F coupling instability but Perkins instability and neutral wind.

Keywords: MSTID, GPS-TEC, Ionosphere

©2019. Japan Geoscience Union. All Right Reserved.

Comparison of Gravity Wave Activity in the Mesosphere Observed by OH Airglow Imagers and MF Radars over the Antarctic (Syowa & Davis).

*Masaru Kogure[1], Takuji Nakamura[1,2], Yoshihiro Tomikawa[1,2], Mitsumu K. Ejiri[1,2], Takanori Nishiyama[2,1], Masaki Tsutsumi[1,2], Michael J. Taylor[3], Yucheng Zhao[3], P.-Dominique Pautet[3], Damian Murphy[4]

1. National Institute of Polar Research, 2. Department of Polar Science, Sokendai, 3. Physics Department, Utah State University, 4. Australian Antarctic Division

Gravity waves transport momentum and energy from the lower atmosphere to the upper atmosphere and drive the general circulation, which significantly changes the temperature in the middle atmosphere [Fritts and Alexander, 2003]. To understand this role quantitatively will improve the modern general circulation models [Garcia et al., 2017].

The polar night jet region is known to have high gravity-wave activity. However, sources of gravity waves, their propagation, and their spectra are poorly understood because of a lack of observations. In particular, little is known about the dependence of their characteristics on their spectra (i.e., wavenumber and frequency) and on interactions among waves with several wavenumbers and frequencies [Fritts and Alexander, 2003]. To understand these, our group has observed gravity waves at different sites over the Antarctic.

Observation techniques have limitations due to the breadth of the gravity wave spectrum and the target and physical parameter sensed by the observing system [Alexander et al., 1998]. In this study an OH imager and an MF radar are used. Both instruments cover the OH layer (~87 km altitude), but both cover quite different ranges of the wave spectrum. The OH imager can observe waves with shorter ground-based periods (8-60 min) and shorter horizontal wavelengths (2-100 km) [Matsuda et al., 2017]. On the other hand, the MF radar can observe waves with the longer ground-based periods (>~30 min). It also has a preference for the waves with longer horizontal wavelength because of its observational volume.

This study derives gravity-wave perturbations, over Syowa and Davis, from the OH imager data based on Matsuda et al. [2014] and the MF radar data based on Murphy et al. [2007], respectively. In this presentation, we would like to show the gravity wave activity, over Syowa and Davis, with the shorter horizontal wavelength (i.e., observed by the OH imagers) and with the longer horizontal wavelength (i.e., observed by the MF radars). The correlation and relationship between both wave activities will be discussed. Also, we would like to discuss the local variation of that relationship.

Keywords: Gravity Wave, Middle Atmosphere, OH Imager

©2019. Japan Geoscience Union. All Right Reserved.

[E] Poster | P (Space and Planetary Sciences)：P-EM Solar-Terrestrial Sciences, Space Electromagnetism & Space Environment

Wed. May 29, 2019 5:15 PM - 6:30 PM JST | Wed. May 29, 2019 8:15 AM - 9:30 AM UTC | Poster Hall International Exhibition Hall8, Makuhari Messe_4

[P-EM09] Vertical coupling in the atmosphere and Ionosphere

convener:Huixin Liu(Earth and Planetary Science Division, Kyushu University SERC, Kyushu University), Loren Chang(Institute of Space Science, National Central University), Yuichi Otsuka(Institute for Space-Earth Environmental Research, Nagoya University)

Vertical coupling mechanisms throughout the whole atmosphere are critical to understanding the near Earth space environment, as well as its sensitivity to the solar, geomagnetic, and atmospheric drivers. This international session focuses on physical/chemical processes occurring in the mesosphere, thermosphere, and ionosphere (MTI). Both quiet and disturbed states in response to lower atmospheric forcing or solar forcing are important for understanding the MTI system and its coupling to other regions. We invite presentations of observations and observational concepts with ground-based and/or space-borne instruments, theoretical studies, numerical simulations, and development of data analysis systems for various kinds of temporal and spatial variations in atmosphere-ionosphere coupled system.

[PEM09-P01] Local-time Variabilities of SABER CO_2 in the Mesosphere and Lower Thermosphere Region

*Cornelius Csar Jude Salinas[1], Loren Chang[1], Danie Liang[2], Jia Yue[3], Liying Qian[4], Quan Gan[5], James Russel III[3], Martin G Mlynczak[6] (1.Institute of Space Science, National Central University, 2.Institute of Earth Science, Academia Sinica, 3.Department of Atmospheric Sciences, Hampton University, 4.High Altitude Observatory, National Center for Atmospheric Research, 5.Department of Physics and Astronomy, Clemson University, 6.NASA Langley Research Center)

[PEM09-P02] Enhanced dynamo electric field as a possible cause of ionosphere disturbance before Large Earthquake

*Koichiro Oyama[1,2,3] (1.Institute of Plasma and Space Sciences,National Cheng Kung Univ., Taiwan, 2.International Ceneter for Space Weather Sudy and Education, Kyushu Univ.,, 3.CoLtd. Asia Space Environment Research Consortium, Japan)

[PEM09-P03] Morphology of E1 and E2 Kelvin waves from ECMWF reanalysis

*Chen-Jeih Pan[1], Wei-Sheng Chen[1], Uma Das[2] (1.Institute of Space Science, National Central University, 2.Department of Physics, Indian Institute of Information Technology, Kalyani, India)

[PEM09-P04] Impact of strong ENSO on TEC activity disturbed by ultra-fast Kelvin waves

*Wei-Sheng Chen[1], C.J. Pan[1], Uma Das[2], Chian-Chiau Lin[3] (1.Institute of Space Science, National Central University, Taiwan, 2.Department of Physics, Indian Institute of Information Technology, Kalyani, India, 3.Environmental Research and Information Center, Chang Jung Christian University, Taiwan)

[PEM09-P05] Observation and simulation of propagation of coseismic infrasound to the ionosphere

*Jaroslav Chum[1] (1.Institute of Atmospheric Physics of the Czech Academy of Sciences)

[PEM09-P06] Solar wind influence on tropical cyclones mediated by atmospheric gravity waves

*Paul Prikryl[1,2], Iurii Cherniak[3], Irina Zakharenkova[4,5], James M. Weygand[6], Bharat S. R. Kunduri[7] (1.Physics Department, University of New Brunswick, Fredericton, NB, Canada, 2.Geomagnetic Laboratory, Natural Resources Canada, Ottawa, ON, Canada, 3.COSMIC Program Office, University Corporation for Atmospheric Research, Boulder, CO, USA, 4.West Department of IZMIRAN, Kaliningrad, Russia, 5.University of Warmia and Mazury in Olsztyn, Poland, 6.Earth Planetary and Space Sciences, University of California, Los Angeles, CA, USA, 7.Bradley Dept. of Electrical and Computer Engineering, Virginia Tech, Blacksburg, VA, USA)

[PEM09-P07] VIPIR ionospheric observations in Japan

*Takuya Tsugawa[1], Hideo Maeno[1], Michi Nishioka[1], Takumi Kondo[1], Mamoru Ishii[1] (1.National Institute of Information and Communications Technology)

[PEM09-P08] Simulation Results and Performance Analysis of Phase Velocity Spectral Analysis Software (M-Transform) for Airglow Imaging Data

*Septi Perwitasari[1], Takuji Nakamura[2], Masaru Kogure[2], Yoshihiro Tomikawa[2], Mitsumu K. Ejiri[2] (1.LAPAN, 2.NIPR)

[PEM09-P09] Comparisons of Co-incident Ionospheric Plasma Observations Between FORMOSAT-5/AIP and Millstone Hill Incoherent Scatter Radar

*Yi-Wun Chen[1], Chi-Kuang Chao[1] (1.Graduate Institute of Space Science, National Central University, Taiwan)

[PEM09-P10] Sub-ionospheric effects of volcano eruptions using VLF/LF standard radio waves

*Kei Maruyama[1], Hiroyo Ohya[1], Fuminori Tsuchiya[2], Kenro Nozaki[5], Kozo Yamashita[3], Yukihiro Takahashi[4], Hiroyuki Nakata[1], Toshiaki Takano[1] (1.Chiba University, 2.Tohoku University, 3.Ashikaga University, 4.Hokkaido University, 5.National Institute of Information and Communications Technology)

[PEM09-P11] Observations of ionospheric and mesospheric wave structures by a low-cost airglow imaging system

*Keisuke Hosokawa[1], Nanami Kusuyama[1], Yuta Hozumi[1], Kohei Takami[1], Susumu Saito[2], Yasunobu Ogawa[3], Mamoru Ishii[4], Yuichi Otsuka[5], Takuya Tsugawa[4] (1.University of Electro-Communications, 2.ENRI, 3.NIPR, 4.NICT, 5.ISEE, Nagoya University)

[PEM09-P12] Analysis of characteristics of ionospheric parameters, Sq index and neutral winds over Taiwan

*Yu-Jung Chuo[1] (1.Department of Information Technology, Ling Tung University)

[PEM09-P13] Statistical study on daytime Es observed by ground-ionosonde and RO-COSMIC in magnetic Equator region in 2010

*Zheng Wang [1,2], Huixin Liu[1] (1.Department of Earth and Planetary Sciences, School of Science, Kyushu University, Japan. , 2.National Space Science Center, Chinese Academy of Sciences, China.)

[PEM09-P14] The statistical study of the growth rates of Medium-Scale Traveling Ionospheric Disturbances observed with GPS-TEC

*Takafumi Ikeda[1], Akinori Saito[1], Takuya Tsugawa[2], Hiroyuki Shinagawa[2] (1.Department of Geophysics, Graduate School of Science, Kyoto University, 2.National Institutes of Information and Communications Technology)

[PEM09-P15] Comparison of Gravity Wave Activity in the Mesosphere Observed by OH Airglow Imagers and MF Radars over the Antarctic (Syowa & Davis).

*Masaru Kogure[1], Takuji Nakamura[1,2], Yoshihiro Tomikawa[1,2], Mitsumu K. Ejiri[1,2], Takanori Nishiyama[2,1], Masaki Tsutsumi[1,2], Michael J. Taylor[3], Yucheng Zhao[3], P.-Dominique Pautet[3], Damian Murphy[4] (1.National Institute of Polar Research, 2.Department of Polar Science, Sokendai, 3.Physics Department, Utah State University, 4.Australian Antarctic Division)

Local-time Variabilities of SABER CO_2 in the Mesosphere and Lower Thermosphere Region

*Cornelius Csar Jude Salinas[1], Loren Chang[1], Danie Liang[2], Jia Yue[3], Liying Qian[4], Quan Gan[5], James Russel III[3], Martin G Mlynczak[6]

1. Institute of Space Science, National Central University, 2. Institute of Earth Science, Academia Sinica, 3. Department of Atmospheric Sciences, Hampton University, 4. High Altitude Observatory, National Center for Atmospheric Research, 5. Department of Physics and Astronomy, Clemson University, 6. NASA Langley Research Center

This work presents the local-time variabilities of CO_2 in the Mesosphere and Lower Thermosphere region (MLT region) as observed by the Sounding of the Atmosphere using Broadband Emission Radiometry (SABER) onboard the Thermosphere Ionosphere Mesosphere Energetics and Dynamics Satellite (TIMED Satellite). These are then compared to CO_2 as modeled by the Whole Atmosphere Community Climate Model –eXtended (WACCM-X). Also using WACCM-X, a tendency analysis using the continuity equation is done to explain the local-time variabilities of CO_2 in the MLT region. Finally, consequences of including a significant local-time variability in CO_2 when retrieving SABER temperature profiles are determined.

Keywords: Carbon Dioxide, Mesosphere and Lower Thermosphere Region, Tides

©2019. Japan Geoscience Union. All Right Reserved.

Enhanced dynamo electric field as a possible cause of ionosphere disturbance before Large Earthquake

*Koichiro Oyama[1,2,3]

1. Institute of Plasma and Space Sciences,National Cheng Kung Univ., Taiwan, 2. International Ceneter for Space Weather Sudy and Education, Kyushu Univ.,, 3. CoLtd. Asia Space Environment Research Consortium, Japan

Disturbance of ionosphere before large earthquakes has been very often reported. One of the possible disturbing drivers is electric field, which explains most of the ionosphere features we reported so far. However, the origin of the electric field is still in the darkness. One idea of electric field generation exists inside earth interior (Freund et a., 2006). We propose here that the electric field is dynamo field at the height of ≈100 km, which simply intensified before earthquake; intensified eastward (westward)electric field during daytime(nighttime). This idea explains satellite data (Oyama et al.,2008; Oyama et al.,2011; Ryu et al., 2014; Ryu et al., 2016; Oyama et al.,2016; Oyama et al., 2019).

Next question on the electric field generation is the mechanism which modifies the dynamo field. We speculate that modification of E field is a result of modification of neutral wind system, which is originally caused by internal gravity waves which propagate from below. Then again next question is on the origin of the internal gravity waves. The waves might be originally caused by the ground motion, and these waves which propagate upward might interact with planetary wave, and amplified. We show several side evidence of ground motions before earthquakes.

Keywords: Earthquake, Electric field, Ionosphere, Disturbance

©2019. Japan Geoscience Union. All Right Reserved.

Morphology of E1 and E2 Kelvin waves from ECMWF reanalysis

*Chen-Jeih Pan[1], Wei-Sheng Chen[1], Uma Das[2]

1. Institute of Space Science, National Central University, 2. Department of Physics, Indian Institute of Information Technology, Kalyani, India

Kelvin waves are planetary waves traveling eastwards and confined in the equatorial latitudes. The waves play an important role in middle atmosphere dynamics because they transfer energy and momentum from lower to higher altitudes, which contributes to the quasi-biennial oscillation (QBO) and further influences the global climate. Kelvin waves have been studied for many decades, and the most of studies were focused on the waves of wavenumber 1 (E1). On the other hand, the wavenumber-2 Kelvin waves (E2) are also an important part of Kelvin wave activities although their amplitude less than the E1. In this study, we analyzed the long-term European Centre for Medium-Range Weather Forecasts (ECMWF) reanalysis data and reported the morphology of E1 and E2 Kelvin waves in the stratospheric altitudes individually. The temperature from ECMWF reanalysis was used to extract the wave properties. Temperatures between latitudes of 10S and 10N were firstly gridded into the structure of day-altitude-longitude, and then subtract background (longitudinal means) to get equatorial temperature fluctuations. For each altitude, the two-dimensional fast Fourier transform was applied to each 96-day data segment and stepped forward in time by 1 day. The output spectra were then analyzed to get primary wave periods and amplitude variations. From spectra, the E1 amplitude is 1.5 to 2.0 times larger than the E2 in average. The E1 primary periods are 12 to 25 days and are restricted under the 20-km altitude. The periods of 8 to 14 days are the secondary group. They can propagate upward to the 40-km altitude. Regarding the E2, the primary periods are 7 to 12 days and are also restricted under the 20-km altitude. Its secondary group is the periods of 5 to 8 days, which also can propagate upward to the 40-km altitude. Furthermore, the altitude-time-amplitude variation show that the E2 waves are influenced strictly by the QBO westerly. Finally, the cross correlation between E1 and E2 show that the E1 and E2 have high correlation at altitudes close to the tropopause, which implies they are excited simultaneously.

Keywords: Kelvin waves, QBO

©2019. Japan Geoscience Union. All Right Reserved.

Impact of strong ENSO on TEC activity disturbed by ultra-fast Kelvin waves

*Wei-Sheng Chen[1], C.J. Pan[1], Uma Das[2], Chian-Chiau Lin[3]

1. Institute of Space Science, National Central University, Taiwan, 2. Department of Physics, Indian Institute of Information Technology, Kalyani, India, 3. Environmental Research and Information Center, Chang Jung Christian University, Taiwan

Ultra-fast Kelvin waves (UFKW) are a subclass of Kelvin waves that they have the shortest periods (2-5 days) and thus can propagate into the ionosphere. UFKW relate to ionospheric variations have been reported, which include ionospheric minimum virtual height (h'F), F2 maximum critical frequency (foF2), total electron content (TEC), S4 scintillations, etc. In the study, we analyzed the UFKW activities using SABER (Sounding of the Atmosphere using Broadband Emission Radiometry) temperatures and GIM (Global Ionospheric Maps) TEC from 2009 to 2011 to see how UFKW influence the ionosphere. The period 2009-2011 belongs to the strong ENSO period. Previous studies have shown that Kelvin waves were highly active in this period, especially in the early of 2010. Therefore, this study can implicitly reveal how the ionosphere responds to the ENSO. The wave signatures in SABER temperatures were extracted using the fast Fourier transform (FFT). Temperatures in the geographic equatorial latitudes were gridded into the day-altitude-longitude structure and then removed background to get temperature fluctuations. The two-dimensional FFT was applied to each 96-day data segment for each altitude and stepped forward in time by one day. Regarding TEC, the Lomb-Scargle periodogram was used to extract UFKW signatures. Because TEC has a strong local time variation and constrains by the geomagnetic configuration, TEC at 16 local time and low geomagnetic latitudes were selected. The background was removed firstly from the data and then fed TEC fluctuations into the Lomb-Scargle process, which also stepped forward in time by one day. The FFT and Lomb-Scargle process both outputted spectra, which revealed UFKW activities in the mesosphere and lower thermosphere (MLT) region (90-100 km) and the ionosphere (about 150-600 km). The results show that UFKW activities at two equatorial ionization anomalies (EIA) were almost identical, and both were higher than that at geomagnetic equator. Most of wave activities in the temperature field in the MLT region have corresponding activities in TEC. However, there are a lot of small amplitude activities only in TEC.

Keywords: ultra-fast Kelvin waves, ENSO, TEC

©2019. Japan Geoscience Union. All Right Reserved.

Observation and simulation of propagation of coseismic infrasound to the ionosphere

*Jaroslav Chum[1]

1. Institute of Atmospheric Physics of the Czech Academy of Sciences

Vertical motion of the ground surface caused by seismic waves generates acoustic waves that propagate nearly vertically upward owing to supersonic speed of seismic waves. As the air density decreases with height, the amplitude of acoustic waves increases to conserve the energy flux up to the altitudes where the air is so rarefied that it cannot sustain the propagation and the waves start dissipating. For distances up to about 1500 km from the epicenter of the strong earthquakes (M>7), the amplitude (oscillation velocity) of infrasound waves reaches significant values in the upper atmosphere. Consequently, the nonlinear phenomena start to play an important role. Spectral content of the wave packet is changed and the energy is transferred to lower frequencies, which can cause the formation of roughly bipolar N-shaped pulse. The simulation results are compared with observation for selected examples. It is also shown that only infrasound with periods larger than about 10 s (generated by long period seismic waves) can reach the ionospheric heights, namely the F layer where it can be easily detected.

Keywords: coseismic perturbation in the ionosphere, infrasound, nonlinear propagation

©2019. Japan Geoscience Union. All Right Reserved.

Solar wind influence on tropical cyclones mediated by atmospheric gravity waves

*Paul Prikryl[1,2], Iurii Cherniak[3], Irina Zakharenkova[4,5], James M. Weygand[6], Bharat S. R. Kunduri[7]

1. Physics Department, University of New Brunswick, Fredericton, NB, Canada, 2. Geomagnetic Laboratory, Natural Resources Canada, Ottawa, ON, Canada, 3. COSMIC Program Office, University Corporation for Atmospheric Research, Boulder, CO, USA, 4. West Department of IZMIRAN, Kaliningrad, Russia, 5. University of Warmia and Mazury in Olsztyn, Poland, 6. Earth Planetary and Space Sciences, University of California, Los Angeles, CA, USA, 7. Bradley Dept. of Electrical and Computer Engineering, Virginia Tech, Blacksburg, VA, USA

Solar wind coupling to the magnetosphere-ionosphere-atmosphere (MIA) system generates medium- and large-scale atmospheric gravity waves (AGWs) propagating globally from sources in the lower thermosphere at high latitudes. The AGWs propagate globally [1,2] upward and downward, are observed in the ionosphere as traveling ionospheric disturbances [3], can be ducted in lower atmosphere over long distances and reach troposphere. At the reflection point in the troposphere they can trigger moist instabilities to initiate convective bursts, with the latent heat release leading to intensification of storms [4]. In the follow-up studies [5,6,7] it was shown that explosive extratropical cyclones and rapid intensification of tropical cyclones tend to follow arrivals of solar wind high-speed streams (HSS) and/or interplanetary coronal mass ejections (ICMEs). The coupling of solar wind to MIA is most intense during the arrivals of co-rotating interaction regions (CIRs) and/or interplanetary shocks at the leading edges of HSSs and ICMEs when the amplitudes of aurorally-generated AGWs are largest. Ray tracing of AGWs in a model atmosphere show that they can reach tropical cyclones. Spiral gravity waves in typhoons were observed and simulated to propagate radially outward from the typhoon core [8]. The spectra of waves in surface pressure and surface wind measured by the Impacts of Typhoons on the Ocean in the Pacific (ITOP) buoy during the nearby passages of intense typhoons are similar to those of incoming aurorally-generated AGWs. It is suggested that the interaction of aurorally-generated gravity waves with the tropical cyclone vortex and the inner primary eyewall plays a role in the intensification process.

[1] Mayr H.G., et al., J. Geophys. Res., 89, 10929–10959, 1984.
[2] Prikryl P., et al., Ann. Geophys., 23, 401-417, 2005. doi:10.5194/angeo-23-401-2005
[3] Cherniak Iu., Zakharenkova I., Space Weather, 16, 2018. https://doi.org/10.1029/2018SW001869.
[4] Prikryl P., et al., Ann. Geophys. 27, 31–57, 2009. https://doi.org/10.5194/angeo-27-31-2009.
[5] Prikryl P., et al., J. Atmos. Sol.-Terr. Phys., 149, 219–231, 2016.
[6] Prikryl P., et al., J. Atmos. Sol.-Terr. Phys., 171, 94–110, 2018.
[7] Prikryl P., et al., J. Atmos. Sol.-Terr. Phys., 183, 36-60, https://doi.org/10.1016/j.jastp.2018.12.009.
[8] Nolan D.S., Zhang J.A., Geophys. Res. Lett., 44, 3924–3931, 2017. doi:10.1002/2017GL073572

Keywords: Solar wind-magnetosphere-ionosphere-atmosphere coupling, High-speed solar wind stream, Atmospheric gravity wave, Extratropical and tropical cyclones

©2019. Japan Geoscience Union. All Right Reserved.

VIPIR ionospheric observations in Japan

*Takuya Tsugawa[1], Hideo Maeno[1], Michi Nishioka[1], Takumi Kondo[1], Mamoru Ishii[1]

1. National Institute of Information and Communications Technology

National Institute of Information and Communications Technology (NICT) has observed ionosphere by ionosondes more than 70 years in Japan. At present, four ionosondes at Wakkanai (Sarobetsu), Kokubunji, Yamagawa, Okinawa (Ogimi) are automatically operated and controlled from Tokyo. Major ionospheric parameters such as foF2 and foEs are scaled from the ionograms automatically on a realtime basis and scaled manually for the final values. These scaled parameters are provided through our web site (http://wdc.nict.go.jp/IONO/). In 2017, we replaced the 10C ionosondes with Vertical Incidence Pulsed Ionospheric Radar 2 (VIPIR2) which can separate the O- and X-modes of ionospheric echoes which have improved the availability of automatic scaling of the ionogram. Our automatic scaling method has been improved using new O- and X-modes separated ionograms. As for future plans, we try to expand observation area by oblique sounding observations with VIPIRs in Japan and neighboring countries. We have also tried to detect arrival directions of ionospheric echo by using the 8ch receiving data as a interferometry. In this presentation, we will introduce current status and future plans of ionospheric observation in NICT.

Keywords: Ionosphere, Ionosonde, Space Weather

©2019. Japan Geoscience Union. All Right Reserved.

Simulation Results and Performance Analysis of Phase Velocity Spectral Analysis Software (M-Transform) for Airglow Imaging Data

*Septi Perwitasari[1], Takuji Nakamura[2], Masaru Kogure[2], Yoshihiro Tomikawa[2], Mitsumu K. Ejiri[2]

1. LAPAN, 2. NIPR

We have developed a user-friendly software based on *Matsuda et al.*, 2014's 3D-FFT method (M-Transform) for airglow data analysis as a function on Interactive Data Language (IDL). Input of this function is 3-D array of a time series of airglow image that have already been converted to geographical coordinate (*x*, *y*, *t*). The user can customize the wave parameters (e.g. horizontal wavelength (λ_h), wave period (τ), phase speed (*c*), image resolution in space (*dx*,*dy*) and time (*dt*)) in one-line command when executing the program, which depends on their analysis purpose. In order to exhibit this new function's performance and the characteristics/interpretation of the spectral analysis, we have run several test cases using artificial wave. The first case is artificial wave with constant speed (40 m/s) and different wave period (8, 15, 30 min) and horizontal wavelength. In second case, we applied Gaussian shape wave-packet with different FWHM (50, 100, 200 km). For the third test case, with a fixed wave packet size (100 km), we changed the wave packet duration (30, 60, 120 min). The results from the various simulations showed reasonable characteristics of the spectral analysis for different scenarios. We showed that the increase of wave period and horizontal wavelength lead to the wider spectrum with total power difference of ~10%. By changing the wave packet size, we showed that the bigger the wave packet size, the sharper and narrower the spectrum became with the total power increase 2x of the increase size of the wave packet. The result of changing the wave packet duration showed that the longer the duration of wave packet, the spectrum becomes sharper and the total power is proportional to the wave packet length. We also examined the aliasing and zero padding effect on the spectral analysis. In order to avoid the aliasing effect, it is recommended to set the period minimum to at least 2 x image interval (*dt*). More detailed analysis will be discussed during the presentation.

Keywords: Airglow, Gravity wave, Analysis software

©2019. Japan Geoscience Union. All Right Reserved.

Comparisons of Co-incident Ionospheric Plasma Observations Between FORMOSAT-5/AIP and Millstone Hill Incoherent Scatter Radar

*Yi-Wun Chen[1], Chi-Kuang Chao[1]

1. Graduate Institute of Space Science, National Central University, Taiwan

Advanced Ionospheric Probe (AIP) onboard FORMOSAT-5 satellite has routinely measured ionospheric plasma parameters, like ion concentration, velocity, and temperature in a sun-synchronous circular orbit at 720 km altitude along 2230 local-time sector since November 2017. AIP has found that the satellite has a much lower potential with respective to environmental plasma from measured current-voltage curves. A comparison study shall be performed to identify possible bias on the derived AIP parameters. Co-incident observations have been scheduled with Millstone Hill incoherent scatter radar during 30 January to 1 February 2019. In this poster, preliminary comparison results will be outlined and will be used to improve accuracy of the AIP measurement in the future.

Keywords: FORMOSAT-5, AIP, ionosphere

©2019. Japan Geoscience Union. All Right Reserved.

Sub-ionospheric effects of volcano eruptions using VLF/LF standard radio waves

*Kei Maruyama[1], Hiroyo Ohya[1], Fuminori Tsuchiya[2], Kenro Nozaki[5], Kozo Yamashita[3], Yukihiro Takahashi[4], Hiroyuki Nakata[1], Toshiaki Takano[1]

1. Chiba University, 2. Tohoku University, 3. Ashikaga University, 4. Hokkaido University, 5. National Institute of Information and Communications Technology

Several studies for the F-region ionosphere associated with volcano eruptions based on GPS-TEC data have been reported so far (e.g., Heki, 2006; Dautermann et al., 2009; Heki et al., 2010). These studies reported that acoustic waves excited by volcano eruptions reach up to the F-region ionosphere, and caused F-region perturbations. After eruption of the Kelud Volcano, Indonesia, in February 2014, acoustic resonance between the Earth’ s surface and lower thermosphere was reported based on TEC data and the seismic wave data (Nakashima et al., 2015). However, little studies on the D-region ionosphere associated with volcano eruptions have been reported. In this study, we investigate the D-region effects of eruptions of Sakurajima volcano (31.59N, 130.66E), Japan, at 04:11 UT on June 6, 2014, using intensity perturbation of VLF/LF transmitter signals. The VLF/LF propagation paths use in this study are JJY (JJY 60 kHz) - Tainan (TNN, Taiwan), and JJI (22.2 kHz) - TNN. Based on wavelet spectra, the perturbation of both transmitter signals had a frequency of 2-6 mHz during 04:12-04:30 UT after the eruptions (04:11 UT).We compared the perturbations with atmospheric pressure data obtained by an infrasonic meter observed by Sakurajima Volcano Research Center, Kyoto University, and seismic waves in the NIED F-net data (FUK, STM, and SBR) located close to the JJY-TNN path. The atmospheric pressure and vertical velocity of the seismic waves had the similar frequencies of 2-10 mHz during 04:12-04:47 UT. These similar frequencies suggest that the perturbations would be caused by acoustic resonance between the Earth's surface and lower thermosphere, or by acoustic and atmospheric gravity waves generated by volcanic eruptions. In the presentation, we will discuss the cause of the VLF/LF perturbations in more detail.

©2019. Japan Geoscience Union. All Right Reserved.

Observations of ionospheric and mesospheric wave structures by a low-cost airglow imaging system

*Keisuke Hosokawa[1], Nanami Kusuyama[1], Yuta Hozumi[1], Kohei Takami[1], Susumu Saito[2], Yasunobu Ogawa[3], Mamoru Ishii[4], Yuichi Otsuka[5], Takuya Tsugawa[4]

1. University of Electro-Communications, 2. ENRI, 3. NIPR, 4. NICT, 5. ISEE, Nagoya University

In the last two decades, all-sky airglow imagers with cooled CCD cameras have widely been used to observe large-scale wave structures in the F-region ionosphere, for example medium-scale traveling ionospheric disturbances (MSTIDs). Such wavy features are seen in the oxygen emission at 630.0 nm from altitudes slightly below the F-region peak. Similar optical observations of OH band emission have also enabled us to visualize atmospheric gravity waves at the mesospheric height. Deploying airglow imagers in multiple places is one of the cost-effective ways to visualize the large-scale structure of these wave structures at both the F-region ionosphere and mesosphere [e.g., Kubota et al., 2001; Suzuki et al., 2013]. However, ground-based airglow imagers equipped with a cooled CCD camera is still expensive; thus, it is rather difficult to deploy such systems in a wide area and carry out a network observation. To overcome this limitation, we recently developed a low-cost airglow imaging system (Low-Cost Airglow imaging System: LCAS) which consists of a small camera (WAT-910HX), fisheye lens and optical filter. We then confirmed its capability of imaging the spatial structure of polar cap patches and plasma bubble in the 630.0 nm emission from the F-region. But, still, it is unclarified if the system is also capable of detecting the two-dimensional structure of MSTIDs. On the night of May 12, 2018, we identified a weak wavy signature in the 630.0 nm airglow images from one of our LCAS stations in Ishigaki Island, Japan. The wave structure in the 630.0 nm images was smoothly connected to the structure of MSTIDs in the GPS-TEC data, which confirmed the ability of LCAS for detecting MSTIDs. We also identified smaller scale wave structures in the 630.0 nm images, showing characteristic concentric wave fronts. We speculate that gravity waves in the mesosphere were captured in the 630.0 nm images as a contamination of the OH airglow. This is mainly because we make use of an optical filter having 10 nm FWHM, which enables us to detect several spectral peaks of OH emission near the 630.0 nm oxygen emission. We have estimated the center of the concentric wave structures by using the curvature of the wave fronts, and then confirmed that active rain fall took place in a localized area close to the estimated center of the concentric waves. This result supports our hypothesis that the OH emission containing signatures of mesospheric gravity waves were detected in the 630.0 nm images. In summary, the 630.0 nm airglow observation of LCAS is able to observe MSTIDs and mesospheric gravity waves. This will allow us to monitor such wavy structures at two different altitudes by distributing the similar system in a wide area.

Keywords: Airglow, Traveling Ionospheric Disturbances

©2019. Japan Geoscience Union. All Right Reserved.

Analysis of characteristics of ionospheric parameters, Sq index and neutral winds over Taiwan

*Yu-Jung Chuo[1]

1. Department of Information Technology, Ling Tung University

In this paper, we examine the variation of thermospheric neutral winds and solar quiet (Sq) current of the geomagnetic fields for the equatorial ionospheric anomaly area (EIA) during the solar activity period in 1999. The thermospheric neutral winds are derived from the ionospheric F_2-layer peak height, hmF_2, by using the servo model method. The variability of the amplitude ofSq fields is derived from the ground geomagnetic fields in the components H and Z, respectively. Theresults of the current system show a same diurnal variation, which that peaks / valleys in the local noon time for Sq(H) / Sq(Z) in the low latitudes, respectively.The results also indicate a weak seasonal variation that peaks appear at the local summer of the Sq currents in H and Z components, respectively. The Sq current system is associated with the change of the equatorial electrojet (EEJ). Further, the variability is probably attributed to local thermospheric winds. The study also shows that the zonal and meridional components of the neutral winds at the EIA over Taiwan area. Furthermore, the study examines the variations of Sq(H), Sq(Z), neutral winds, and ionospheric parameters foE_s, NmF_2, and hmF_2during the disturbed geophysical conditions such as geomagnetic storm and earthquake. The result shows the variationsof ionospheric Sq(H), Sq(Z) and thermospheric neutral winds are different between the seismo-ionospheric and solar-terrestrial disturbed periods, even they lead the same decreasing electron density reaction in the ionosphere at the EIA over Taiwan area.

Keywords: Sq current, ionosphere, neutral winds

©2019. Japan Geoscience Union. All Right Reserved.

Statistical study on daytime Es observed by ground-ionosonde and RO-COSMIC in magnetic Equator region in 2010

*Zheng Wang [1,2], Huixin Liu[1]

1. Department of Earth and Planetary Sciences, School of Science, Kyushu University, Japan. , 2. National Space Science Center, Chinese Academy of Sciences, China.

Scintillations under 150 km height shown by radio occultation (RO) of COSMIC are considered to be associated with ionospheric sporadic E (Es) layer. In this paper, we make a Statistical study on daytime Es observed by ground-ionosonde at five stations in magnetic Equator region in 2010, and make a comparison with S4 index from RO-COSMIC within 6 degree of each station. The results show that: At each station the diurnal variation of foEs from ionosonde decrease a little around LT 0600 and then increase, having maximum around LT 1200, decrease around LT 1800 and then increase near LT 2000-2200; All the S4>=0.3 observations during daytime come from RO-COSMIC under 150 km height; The diurnal variation of S4 index under 150 km height from RO-COSMIC over each station has similar trend with that of foEs at the same station; S4 index over 150 km height from RO-COSMIC is only high during nighttime; For the stations at different longitudes, Es occurrences from ionosonde are positively associated with S4>=0.3 from RO-COSMIC. The comparison shows that the S4 index from RO-COSMIC could show some features of daytime Es layer in magnetic Equator region without the location limitation of ground stations.

Keywords: daytime ionospheric sporadic E, ground-ionosonde , radio occultation of COSMIC , magnetic Equator region

©2019. Japan Geoscience Union. All Right Reserved.

The statistical study of the growth rates of Medium-Scale Traveling Ionospheric Disturbances observed with GPS-TEC

*Takafumi Ikeda[1], Akinori Saito[1], Takuya Tsugawa[2], Hiroyuki Shinagawa[2]

1. Department of Geophysics, Graduate School of Science, Kyoto University, 2. National Institutes of Information and Communications Technology

We think two mechanism, E-F coupling and Perkins Instability, will relate to growth for nighttime-MSTID in mid-latitude [Tsunoda and Cosgrove., 2001 ; Perkins., 1973]. Linear growth rate of perturbation intensity of Pedersen conductivity expected from E-F coupling is around 15 minutes [Yokoyama et al., 2009], which is far shorter than one expected from Perkins Instability [Fukao and Kelley, 1991 ; Miller et al., 1997 ; Shiokawa et al., 2003]. However, Es layer’ s spatial and temporal scale is less than 100km and 15min [Maeda et al., 2013 ; S.Saito et al., 2007]. They are different from MSTID’ s ones, which are 200-400 km and around 2hours [Otsuka et al., 2011]. To decide which instability is responsible for growth of nighttime MSTID, the growth rate of MSTID was observationally determined with ground-based GPS network data.

We statistically investigated the growth rate of nighttime-MSTID in Japan in 2014 observed with GPS-TEC. The growth rate of nighttime -MSTID observed was 1.0 - 6.0 $\times 10^{-4}$ s^{-1} during 1800LT-2400LT in summer.Linear growth rate of Perkins instability in summer was 1.0 - 6.0 $\times 10^{-4}$ s^{-1} during 1800LT - 2400LT, so they were less than one of the E-F coupling instability. Also,Seasonal distribution of observed growth rate before midnight was similar to that of linear growth rate.U×B derived by GAIA model was high in spring - summer and seasonal distribution of U×B was similar to that of linear growth rate. Therefore, the growth of MSTID when propagating is not determined by E-F coupling instability but Perkins instability and neutral wind.

Keywords: MSTID, GPS-TEC, Ionosphere

©2019. Japan Geoscience Union. All Right Reserved.

Comparison of Gravity Wave Activity in the Mesosphere Observed by OH Airglow Imagers and MF Radars over the Antarctic (Syowa & Davis).

*Masaru Kogure[1], Takuji Nakamura[1,2], Yoshihiro Tomikawa[1,2], Mitsumu K. Ejiri[1,2], Takanori Nishiyama[2,1], Masaki Tsutsumi[1,2], Michael J. Taylor[3], Yucheng Zhao[3], P.-Dominique Pautet[3], Damian Murphy[4]

1. National Institute of Polar Research, 2. Department of Polar Science, Sokendai, 3. Physics Department, Utah State University, 4. Australian Antarctic Division

Gravity waves transport momentum and energy from the lower atmosphere to the upper atmosphere and drive the general circulation, which significantly changes the temperature in the middle atmosphere [Fritts and Alexander, 2003]. To understand this role quantitatively will improve the modern general circulation models [Garcia et al., 2017].

The polar night jet region is known to have high gravity-wave activity. However, sources of gravity waves, their propagation, and their spectra are poorly understood because of a lack of observations. In particular, little is known about the dependence of their characteristics on their spectra (i.e., wavenumber and frequency) and on interactions among waves with several wavenumbers and frequencies [Fritts and Alexander, 2003]. To understand these, our group has observed gravity waves at different sites over the Antarctic.

Observation techniques have limitations due to the breadth of the gravity wave spectrum and the target and physical parameter sensed by the observing system [Alexander et al., 1998]. In this study an OH imager and an MF radar are used. Both instruments cover the OH layer (~87 km altitude), but both cover quite different ranges of the wave spectrum. The OH imager can observe waves with shorter ground-based periods (8-60 min) and shorter horizontal wavelengths (2-100 km) [Matsuda et al., 2017]. On the other hand, the MF radar can observe waves with the longer ground-based periods (>~30 min). It also has a preference for the waves with longer horizontal wavelength because of its observational volume.

This study derives gravity-wave perturbations, over Syowa and Davis, from the OH imager data based on Matsuda et al. [2014] and the MF radar data based on Murphy et al. [2007], respectively. In this presentation, we would like to show the gravity wave activity, over Syowa and Davis, with the shorter horizontal wavelength (i.e., observed by the OH imagers) and with the longer horizontal wavelength (i.e., observed by the MF radars). The correlation and relationship between both wave activities will be discussed. Also, we would like to discuss the local variation of that relationship.

Keywords: Gravity Wave, Middle Atmosphere, OH Imager

©2019. Japan Geoscience Union. All Right Reserved.

[E] Poster | P (Space and Planetary Sciences)：P-EM Solar-Terrestrial Sciences, Space Electromagnetism & Space Environment

Wed. May 29, 2019 1:45 PM - 3:15 PM JST | Wed. May 29, 2019 4:45 AM - 6:15 AM UTC | Poster Hall International Exhibition Hall8, Makuhari Messe_1

[P-EM11] Dynamics of Magnetosphere and Ionosphere

convener:Aoi Nakamizo(Applied Electromagnetic Research Institute, National Institute of Information and Communications Technology), Mitsunori Ozaki(Faculty of Electrical and Computer Engineering, Institute of Science and Engineering, Kanazawa University), Akiko Fujimoto(Kyushu Institute of Technology), Tomoaki Hori(Institute for Space-Earth Environmental Research, Nagoya University)

This session provides an opportunity to present recent results from satellite and ground-based observations and theoretical and simulation studies on the magnetosphere, ionosphere, and their coupling processes. We invite talks and posters discussing various phenomena related to the magnetosphere-ionosphere system: solar wind-magnetosphere interaction, magnetosphere-ionosphere convection, field-aligned current, magnetic storms/substorms, neutral-plasma interaction, ionospheric ion inflow and outflow, aurora phenomena, and so forth. Discussions on planetary and satellite ionosphere and magnetospheres, future missions and instrument developments are also welcome.

[PEM11-P01] Effects of Inclination/Rotation of Earth's Magnetic Axis on Magnetosphere Simulated by Global MHD Model

*Aoi Nakamizo[1] (1.Applied Electromagnetic Research Institute, National Institute of Information and Communications Technology)

[PEM11-P02] Asymmetric deformation of the magnetosphere under low-density solar wind

*Masaki N Nishino[1,2], Yoshifumi Saito[2], Kazuo Shiokawa[1], Masaki Fujimoto[2] (1.Institute for Space-Earth Environmental Research, Nagoya University, 2.JAXA/ISAS)

[PEM11-P03] New perspectives on coupling processes in solar-terrestrial system obtained by comprehensive data analysis

*Yoshimasa Tanaka[1], Norio Umemura[2], Shuji Abe[3], Satoru UeNo[4], Masahito Nose[2], Yumi Nakagawa[5] (1.National Institute of Polar Research, 2.Institute for Space-Earth Environmental Research, Nagoya University, 3.International Center for Space Weather Science and Education, 4.Kwasan & Hida Observatories, School of Science, Kyoto University, 5.Ibaraki University)

[PEM11-P04] The interaction between the magnetosphere-ionosphere compound system and the magnetic field topology

*Shigeru Fujita[1], Takashi Tanaka[2], Masakazu Watanabe[2] (1.Meteorological College, Japan Meteorological Agency/ Nationa Institute of Polar Research, 2.Kyushu University)

[PEM11-P05] Effects of the dipole tilt and the interplanetary magnetic field Bx component on the dawn-dusk and interhemispheric asymmetries of the interchange convection cycle

*Masakazu Watanabe[1,2], Takashi Tanaka[2], Shigeru Fujita[3,4] (1.Graduate School of Science, Kyushu University, 2.International Center for Space Weather Science and Education, Kyushu University, 3.Meteorological College, 4.National Institute of Polar Research)

[PEM11-P06] Transient polar ionospheric convection response to negative dynamic pressure pulse

*Jianjun Liu[1] (1.Polar Research Institute of China)

[PEM11-P07] An active ionosphere: a new perspective of field line dipolarization

*Osuke Saka[1] (1.Office Geophysik)

[PEM11-P08] Toward the automatic identification of FLR signals in the SuperDARN data by using the gradient method

*Hideaki Kawano[1,2], Akira Sessai Yukimatu[3,4], Nozomu Nishitani[5], Yoshimasa Tanaka[3,4], Satoko Saita[6], Tomoaki Hori[5] (1.Dept. Earth Planet. Sci., Kyushu Univ., 2.ICSWSE, Kyushu University, 3.National Institute of Polar Research, 4.SOKENDAI, 5.ISEE, Nagoya University, 6.Kitakyushu College)

[PEM11-P09] A statistical study of Pi2 pulsations observed in the upper ionosphere using Swarm magnetic field data

*Park Jaehee[1], Khan-Hyuk Kim[1], Junga Hwang[2] (1.School of Space Research, Kyung Hee University, Gyeonggi, South Korea, 2.Korea Astronomy and Space Science Institute, Daejeon,South Korea)

[PEM11-P10] Study on the global distribution characteristics of Pc 1-2 geomagnetic pulsation with the 10Hz data of the MAGDAS system

*Taisei Kabasawa[1], Akimasa Yoshikawa[1], Teiji Uozumi[1], Akiko Fujimoto[1], Shuji Abe[1] (1.Kyushu University)

[PEM11-P11] In-situ Observations of Reconnection Separatrix Regions in the near-Earth Magnetotail

*Mizuho Araki[1], Masahiro Hoshino[1], Kunihiro Keika[1], Yoshifumi Saito[2] (1.Graduate School of Science, The University of Tokyo, 2.Institude of Space and Astronautical Science)

[PEM11-P12] Flow speed dependence of ion temperature, electron temperature, and their ratio in the near-Earth magnetotail reconnection region

*Kaori Watanabe[1], Masahiro Hoshino[1], Kunihiro Keika[1], Yoshifumi Saito[2], Naritoshi Kitamura[1] (1.Univ. of Tokyo, 2.ISAS/JAXA)

[PEM11-P13] **Examining Minimum Cyclotron Resonant Electron Energy of EMIC Waves with MMS**

*Si Liu[1] (1.Changsha University of Science and Technology)

[PEM11-P14] Small scale whistler mode waves near the magnetic field intensity minimum in the magnetosheath

*Naritoshi Kitamura[1], Takanobu Amano[1], Yoshiharu Omura[2], Satoko Nakamura[2], Chika Umegaki[1], Scott A Boardsen[3,4], Narges Ahmadi[5], Robert E Ergun[5], Olivier Le Contel[6], Per-Arne Lindqvist[7], Yoshifumi Saito[8], Shoichiro Yokota[9], Daniel J Gershman[3], Barbara L Giles[3], Thomas E Moore[3], William R Paterson[3], Craig J Pollock[10], Christopher T Russell[11], Robert J Strangeway[11], James L Burch[12] (1.Department of Earth and Planetary Science, Graduate School of Science, The University of Tokyo, 2.Research Institute for Sustainable Humanosphere, Kyoto University, 3.NASA Goddard Space Flight Center, 4.University of Maryland, 5.Laboratory for Atmospheric and Space Physics, University of Colorado, 6.Laboratoire de Physique des Plasmas, UMR7648 CNRS/Ecole Polytechnique/UPMC/Université Paris-Sud/Observatoire de Paris, 7.Royal Institute of Technology, 8.Institute of Space and Astronautical Science, Japan Aerospace Exploration Agency, 9.Department of Earth and Space Science, Graduate School of Science, Osaka University, 10.Denali Scientific, 11.Institute of Geophysics and Planetary Physics, University of California, Los Angeles, 12.Southwest Research Institute)

[PEM11-P15] Spatial characteristics of the internal modulation of pulsating aurora: multi-point high-speed optical observations in Scandinavia

*Yuki Kawamura[1], Keisuke Hosokawa[1], Shin-ichiro Oyama[2,3], Yoshizumi Miyoshi[2], Yasunobu Ogawa[3], Satoshi Kurita[2], Satoshi Ebukuro[1], Ryoichi Fujii[4] (1.Department of Communication Engineering and Informatics, University of Electro-Communications, 2.Institute for Space-Earth Environmental Research, Nagoya University, 3.National Institute of Polar Research, 4.Research Organization of Information and Systems)

[PEM11-P16] **Large-scale characteristics of pulsating aurora periodicities:multi-point high-speed optical observations in Scandinavia**

*Satoshi Ebukuro[1], Keisuke Hosokawa[1], Shin-ichiro Oyama[2,3,5], Yoshizumi Miyoshi[2], Yasunobu Ogawa[3], Satoshi Kurita[2], Yuki Kawamura[1], Ryoichi Fujii[4] (1.Department of Communication Engineering and Informatics, University of Electro-Communications, 2.Institute for Space-Earth Environmental Research, Nagoya University, 3.National Institute of Polar Research, 4.Research Organization of Information and Systems, 5.University of Oulu)

[PEM11-P17] Variations of cosmic noise absorption (CNA) by energetic electron precipitation (EEP) and changes of the auroral morphology

*Miyamoto Taishiro[1], Shin-ichiro Oyama[1,4,5], Yasunobu Ogawa[2], Keisuke Hosokawa[3], Satoshi Kurita[1], Yoshizumi Miyoshi[1], Ryuho Kataoka[2], Hiroshi Miyaoka[2], Tero Raita[4] (1. Institute for Space-Earth Environmental Research,Nagoya University, 2.National Institute of Polar Research, 3.Department of Communication Engineering and Informatics, University of Electro-Communications, 4.Sodankylä Geophysical Observatory, University of Oulu, 5.Ionosphere Research Unit, University of Oulu)

[PEM11-P18] Spatiotemporal characteristics on the source region of flash aurora using ray tracing analysis

*Tomohiro Inoue[1], Mitsunori Ozaki[1], Yoshitaka Goto[1], Satoshi Yagitani[1], Yoshiya Kasahara[1], Kazuo Shiokawa[2], Yoshizumi Miyoshi[2], Ryuho Kataoka[3], Yusuke Ebihara[4] (1.Kanazawa University , 2.Nagoya University, 3.National Institute of Polar Research, 4.Kyoto University)

[PEM11-P19] Molecular ion supply mechanisms from the low-altitude ionosphere to magnetosphere observed by EISCAT and Arase(ERG)

*Masayoshi Takada[1], Kanako Seki[1], Yasunobu Ogawa[2], Kunihiro Keika[3], Satoshi Kasahara[4], Shoichiro Yokota[5], Tomoaki Hori[7], Kazushi Asamura[6], Yoshizumi Miyoshi[7] (1.Graduate School of Science, Tokyo University, 2.National Institute of Polar Research, 3.Department of Earth and Planetary Science, Graduate School of Science, Tokyo University, 4.The University of Tokyo, 5.Graduate School of Science, Osaka University, 6.Institute of Space and Astronautical Science, Japan Aerospace Exploration Agency, 7.Institute for Space-Earth Environmental Research, Nagoya University)

[PEM11-P20] Optical and radar observation of the dynamic auroral forms

*Yunosuke Nagafusa[1], Tima Sergienko[2], Satoshi Taguchi[1], Urban Braendstroem[2], Masatoshi Yamauchi[2] (1.Graduate School of Science, Kyoto University, 2.Swedish Institute of Space Physics, Kiruna)

[PEM11-P21] Observations of MF/HF auroral radio emissions at three ground-based stations

*Yuka Sato[1], Atsushi Kumamoto[2], Yuto Katoh[2], Akira Kadokura[3,4], Yasunobu Ogawa[3,4], Atsuki Shinbori[5] (1.Nippon Institute of Technology (NIT), 2.Graduate School of Science, Tohoku University, 3.National Institute of Polar Research (NIPR), 4.The Graduate University for Advanced Studies, 5.Institute for Space-Earth Environmental Research (ISEE), Nagoya University)

[PEM11-P22] **Ionospheric F-region Drift Measurements Derived from DPS-4D at Zhongshan Station, Antarctic**

*Xiangcai Chen[1] (1.Polar Research Institute of China)

[PEM11-P23] PARM-HEP Observation of Precipitating High Energy Electrons over Pulsating Aurora

*Taku Namekawa[1], Takefumi Mitani[2], Kazushi Asamura[2], Yoshifumi Saito[2] (1.Department of Earth and Planetary Science, Graduate school of Science, The University of Tokyo, 2.Institute of Space and Astronautical Science, Japan Aerospace Exploration Agency)

[PEM11-P24] Development of the medium-energy electron detector with hemispherical field-of-view and the flight test in the PARM (Pulsating AuRora and Microburst) mission

*Shin Sugo[1], Oya Kawashima[1], Kazushi Asamura[2], Reiko Nomura[3], Yasunobu Ogawa[4], Keisuke Hosokawa[5], Yoshizumi Miyoshi[6], Takefumi Mitani[2], Taku Namekawa[1,2], Takeshi Sakanoi[7], Mizuki Fukizawa[7], Naoshi Yagi[7], Satoshi Kasahara[1] (1.The University of Tokyo, 2.Institute of Space and Astronautical Science, Japan Aerospace Exploration Agency, 3.National Astronomical Observatory of Japan, 4.National Institute of Polar Research, 5.The University of Electro-Communications, 6.Institute for Space-Earth Environmental Research, Nagoya University, 7.Tohoku University)

[PEM11-P25] Auroral substorm onset in satellite-based global images and ground-based all-sky images

*Akimasa Ieda[1], Kirsti Kauristie[2], Yukitoshi Nishimura[3], Yukinaga Miyashita[4], Harald U Frey[5], Liisa Juusola[2], Daniel Whiter[6], Masahito Nose[7], Matthew O Fillingim[5], Farideh Honary[8], Neil C Rogers[8], Yoshizumi Miyoshi[1], Shinobu Machida[1] (1.Institute for Space-Earth Environmental Research, Nagoya University, 2.Finnish Meteorological Institute, 3.Boston university, 4.Korea Astronomy and Space Science Institute, 5.University of California Berkeley, 6.University of Southampton, 7.Graduate School of Science, Kyoto University, 8.Lancaster University)

[PEM11-P26] Automatic Classification of Auroral images using optical flow feature

*Naoto Kashiwagi[1], Akiko Fujimoto[1], Terumasa Tokunaga[1], Yoshizumi Miyoshi[2], Yasunobu Ogawa[3], Keisuke Hosokawa[4] (1.Kyushu Institute of Technology, 2.Nagoya University, 3.National Institute of Polar Research, 4.The University of Electro-Communications)

[PEM11-P27] Fine-scale visualization of aurora in a wide area using color digital camera images from the International Space Station

*Sota Nanjo[1], Yuta Hozumi[1], Keisuke Hosokawa[1] (1.The University of Electro-Communications)

[PEM11-P28] Geospace Imaging via the soft X-ray imager: GEO-X mission

*Yoshizumi Miyoshi[1], Yuichiro Ezoe[2], Satoshi Kasahara[3], Yosuke Matsumoto[4], Kumi Ishikawa[5], Ryuho Kataoka[6], Hiroki Ito[1], Daiki Ishi[2], Masaki Numazawa[2], Atsushi Yamazaki[5], Hiroshi Hasegawa[5], Masaki Fujimoto[5], Kazuhisa Mitsuda[5] (1.Institute for Space-Earth Environmental Research, Nagoya University, 2.Tokyo Metropolitan University, 3.University of Tokyo, 4.Chiba University, 5.ISAS/JAXA, 6.NIPR)

Effects of Inclination/Rotation of Earth’s Magnetic Axis on Magnetosphere Simulated by Global MHD Model

*Aoi Nakamizo[1]

1. Applied Electromagnetic Research Institute, National Institute of Information and Communications Technology

Recently, we have shown that the ionospheric Hall conductance distribution, owing to the polarization field generated by its nonuniformity, largely control the magnetospheric configuration and dynamics by using a global MHD model. The effects of the ionospheric conductance on the magnetosphere were also reported by previous studies based on other global models; for example, the current-voltage relationship in the solar wind-magnetosphere-ionosphere [Fedder and Lyon, 1987] and the plasma pressure distribution in the near-Earth region [Ridley et al., 2004]. These studies indicate that the ionospheric conductance is one of the most important settings in the global models to accurately simulate the magnetosphere.

On the other hand, in the development/improvement of the global MHD model in NICT, which was originally developed by Tanaka [1994] and Tanaka et al. [2010], introducing the inclination and rotation of Earth’s magnetic axis with respect to the rotation axis has been remained as one of the most difficult problems. In other words, in the present model, the precession between the magnetic axis and the rotation axis is not included. This means that the simulated magnetosphere will show a different structure and temporal development than the actual magnetosphere.

We, for the first time, equivalently introduce the precession by rotating the background conductance distribution due to solar illumination (i.e., depending on the geographic coordinate) with respect to the geomagnetic coordinate. (Improvement of the conductance setting in the auroral region is the next challenge.) In this paper, we will show how the simulated magnetosphere is changed by this improvement, focusing on the near-Earth plasma environment.

Keywords: M-I Coupling, Global MHD Simulation, Ionospheric Effect

©2019. Japan Geoscience Union. All Right Reserved.

Asymmetric deformation of the magnetosphere under low-density solar wind

*Masaki N Nishino[1,2], Yoshifumi Saito[2], Kazuo Shiokawa[1], Masaki Fujimoto[2]

1. Institute for Space-Earth Environmental Research, Nagoya University, 2. JAXA/ISAS

The density of the solar wind around the Earth's magnetosphere sometimes decreases to only several percent of the usual value, and such density extrema results in a significant reduction of dynamic pressure and Alfvenic Mach number of the solar wind flow. While simple expansion of the Earth's magnetosphere by the low dynamic pressure was assumed in previous studies, a global-MHD simulation study predicted a remarkable dawn-dusk asymmetry of the magnetosphere in shape under low-density solar wind and Parker-spiral IMF configuration. Here we present evidence of asymmetric deformation of the magnetosphere under low-density solar wind and Parker-spiral IMF conditions, based on several events of GEOTAIL observations. As predicted by the global-MHD simulation, the magnetosphere on the dawnside expands much further than the magnetopause location of simple (symmetric) expansion, while no significant expansion is detected in the dusk tail flank. Fast ion beams detected at the flank magnetopause suggest that magnetic reconnection frequently occurs due to the low-beta environment of the magnetosheath.

Keywords: Low density solar wind, Magnetosphere, Plasma transport

©2019. Japan Geoscience Union. All Right Reserved.

New perspectives on coupling processes in solar-terrestrial system obtained by comprehensive data analysis

*Yoshimasa Tanaka[1], Norio Umemura[2], Shuji Abe[3], Satoru UeNo[4], Masahito Nose[2], Yumi Nakagawa[5]

1. National Institute of Polar Research, 2. Institute for Space-Earth Environmental Research, Nagoya University, 3. International Center for Space Weather Science and Education, 4. Kwasan & Hida Observatories, School of Science, Kyoto University, 5. Ibaraki University

In the Earth’ s upper atmosphere above 60 km, including magnetosphere and ionosphere, various phenomena are generated by energy inputs from solar radiation (including solar wind) and atmospheric waves propagating from the lower atmosphere. Thus, comprehensive analysis of various kinds of satellite and ground-based observational data using advanced methods is required to understand physical mechanism of the phenomena. For such interdisciplinary studies, it is important to share data distributed across many universities and institutes and use advanced tools, such as metadata database for cross-searching a variety of datasets and analysis software for analyzing various types of data in an integrated fashion. In fact, many scientific papers on the upper atmosphere have recently been obtained by comprehensive analysis of various data with such analysis tools.
We present some examples of scientific results achieved by comprehensively analyzing data from multiple regions. These examples include the effect of solar coronal holes on the Earth’ s geomagnetic activity and the interaction between solar wind, magnetosphere, ionosphere and neutral atmosphere. The former study investigated long-term trends of coronal boles, solar wind parameters, and Earth’ s geomagnetic indices during two solar cycles. It showed the possibility that the solar wind speed and geomagnetic activities may be controlled by the size and latitudinal distribution of coronal holes. The latter analyzed multi-instrument data simultaneously obtained from interplanetary space, magnetosphere, and ionosphere and mesosphere in both northern and southern hemispheres. They newly found that the polar mesosphere is affected by relativistic electron precipitation caused by the interaction with magnetospheric plasma waves during the high-speed solar wind stream. These studies demonstrate that sharing and comprehensive analysis of long-term, multiple-sphere, and multi-instrument data using sophisticated tools are very effective to produce scientific outcomes. At present there are data gap areas in the Asia and African regions. Therefore, we believe that filling in the data gap by international collaborations could be a breakthrough for unsolved issues in the upper atmosphere.

Keywords: upper atmosphere, coupling between multiple regions, comprehensive analysis, long-term observational data

©2019. Japan Geoscience Union. All Right Reserved.

The interaction between the magnetosphere-ionosphere compound system and the magnetic field topology

*Shigeru Fujita[1], Takashi Tanaka[2], Masakazu Watanabe[2]

1. Meteorological College, Japan Meteorological Agency/ Nationa Institute of Polar Research, 2. Kyushu University

The steady convection in the magnetosphere-ionosphere coupling system is composed of the following self-consistent elementary processes; dynamo in the cusp-mantle region, the field-perpendicular current system in the magnetosphere, the field-aligned current system connecting the ionosphere, the ionospheric electric field, the magnetospheric convection corresponding to the ionospheric electric field, and the high plasma pressure distribution in the cusp region [Tanaka, 2007].

The energy of the convection is transported from the solar wind across the magnetopause where the magnetic field configures the null-separator structure. Since the magnetic field configuration of the null-separator structure is originally derived from the superposition of two scalar fields [Stern, 1973], say, the dipole field and the uniform field, the magnetic field of the null-separator would not have free energy necessary for plasma acceleration. However, the simulation reveals that the magnetic field has a tension force near the null point. Therefore, we need a mechanism that transports the energy to this region.

It is revealed from the simulation that the bow shock supplies the energy. Indeed, the current from the bow shock deforms the magnetic field of the null-separator structure. In addition, it is noted that the Chapman-Ferraro current also deforms the magnetic field configuration in the magnetopause. This fact indicates that the convection system in the magnetosphere contributes to deformation of the null-separator structure. That is to say, energy transport from the solar wind to the magnetosphere-ionosphere compound system is affected by the physical processes in the convection. Therefore, as a result of the interaction between the magnetosphere-ionosphere convection and the null-separator structure, the magnetosphere-ionosphere compound system can be extended to the solar wind-magnetosphere-ionosphere compound system.

References

T. Tanaka (2007), Magnetosphere-Ionosphere Convection as a Compound System, Space Sci Rev, 133, 1-72, DOI 10.1007/s11214-007-9168-4.

Stern, D. P. (1973), A study of the electric field in an open magnetospheric model, J. Geophys. Res., 78(31), 7292-7305, doi:10.1029/JA078i031p07292.

Keywords: global MHD simulation, compound system

©2019. Japan Geoscience Union. All Right Reserved.

Effects of the dipole tilt and the interplanetary magnetic field Bx component on the dawn-dusk and interhemispheric asymmetries of the interchange convection cycle

*Masakazu Watanabe[1,2], Takashi Tanaka[2], Shigeru Fujita[3,4]

1. Graduate School of Science, Kyushu University, 2. International Center for Space Weather Science and Education, Kyushu University, 3. Meteorological College, 4. National Institute of Polar Research

The interchange cycle is a mode of magnetic flux circulation that appears for periods of northward interplanetary magnetic field (IMF). It is made up of IMF-to-open reconnection in one hemisphere and open-to-closed reconnection in the other hemisphere. The two reconnection processes have the same topological nature in that the roles of the two reconnecting field lines interchange at the time of reconnection. The interchange cycle is characterized by reciprocation of open magnetic flux between the two hemispheres. One observable signature of the interchange cycle is an appearance of a reverse cell circulating in the closed field line region of the ionosphere, which is named the “reciprocal cell.” The reciprocal cell appears in the open-to-closed reconnection hemisphere, whereas in the opposite IMF-to-open reconnection hemisphere, there appears a lobe cell circulating exclusively on open field lines. For given (1) IMF By, (2) IMF Bx, and (3) dipole tilt conditions, two interchange cycles concur, one on the dawnside and the other on the duskside. For an ideal case, one can easily expect the mode of the interchange cycles to occur. For example, for the case of due northward IMF with significant dipole tilt, the twin reverse cells in the summer hemisphere are both lobe cells, while in the winter hemisphere the twin reverse cells are both reciprocal cells. For the general case, however, one cannot predict the mode of the interchange cycles without quantitative modeling. The purpose of this study is to examine how the presence of dipole tilt or IMF Bx alters the dawn-dusk and north-south pattern of the twin reverse cells. For this purpose, we perform numerical magnetohydrodynamic simulations using the REPPU (Reproduce Plasma Universe) code developed by T. Tanaka. In the presentation, we discuss the dipole tilt and IMF Bx effects revealed by the numerical modeling.

Keywords: ionospheric convection, interchange reconnection, reciprocal cell

©2019. Japan Geoscience Union. All Right Reserved.

Transient polar ionospheric convection response to negative dynamic pressure pulse

*Jianjun Liu[1]

1. Polar Research Institute of China

The response of the high latitude ionospheric convection to a sudden decrease in solar wind dynamic pressure provides a unique opportunity to investigate how the solar wind couples to the dayside magnetosphere and ionosphere. Here, the event shows three IMF components do not have prominent changes, but the solar wind plasma went down to near zero magnitude, which leads to very weak solar wind driving during northward IMF. However, ionospheric convection observed by SuperDARN radars showed enhanced plasma flow speed in the central polar cap region just after the negative pressure pulse arrival to the magnetosphere. Simultaneous convection map generated by SuperDARN measurement presents enlarged convection cell with obvious equatorward moving Heppner-Maynard boundary. It is noted that cross polar cap potential enhanced instantly and this enhanced feature continued almost 10 min. The distribution of total electron content (TEC) exhibited typical auroral oval signature especially on dayside ionosphere, TEC density in auroral oval showed a noticeable decrease after the arrival of the negative pressure pulse. Both ionospheric convection and TEC distribution reveal that negative pressure pulse impacts the magnetosphere-ionosphere coupling system directly and dramatically. Moreover, the TIEGCM model also showed an enhanced polar potential pattern.

Keywords: Dynamic pressure, Ionospheric convection, Auroral oval

©2019. Japan Geoscience Union. All Right Reserved.

An active ionosphere: a new perspective of field line dipolarization

*Osuke Saka[1]

1. Office Geophysik

Transient westward electric fields from the magnetosphere generate equatorward plasma drifts of the order of kilometers per second in the auroral ionosphere. This flow channel extends in north-south directions and is produced in the initial pulse of Pi2 pulsations associated with the filed line dipolarization. Drifts in the ionosphere of the order of kilometers per second that accumulated plasmas at the low latitude end of the flow channel are of such large degree that possible vertical transport effects (including precipitation) along the field lines may be ignored. We suggest that plasma compression in the ionosphere implemented the ionosphere to be active. Active ionosphere generates field-aligned currents to satisfy the quasi-neutrality of the ionosphere, ion acoustic wave for ion outflows and the inverted-V type electron precipitations in the topside ionosphere, and poleward expansion of auroras due to a nonlinear evolution of the ionosphere. We will study auroral expansion in this acoustic regime.

Keywords: Substorm, Auroral substorm, Ionosphere

©2019. Japan Geoscience Union. All Right Reserved.

Toward the automatic identification of FLR signals in the SuperDARN data by using the gradient method

*Hideaki Kawano[1,2], Akira Sessai Yukimatu[3,4], Nozomu Nishitani[5], Yoshimasa Tanaka[3,4], Satoko Saita[6], Tomoaki Hori[5]

1. Dept. Earth Planet. Sci., Kyushu Univ., 2. ICSWSE, Kyushu University, 3. National Institute of Polar Research, 4. SOKENDAI, 5. ISEE, Nagoya University, 6. Kitakyushu College

The FLR (Field Line Resonance) takes place where the frequency of an incoming wave matches the eigen-frequency of magnetospheric magnetic field lines, and excites the eigen-oscillation of the field lines. The FLR can be identified by using the unique manner of change in the amplitude and the phase of thus excited eigen-oscillation across the resonant point. That is, the amplitude is maximum at the resonant point, and the phase changes the most steeply across the resonance point. The FLR-generated eigen-oscillations can be identified in the ground magnetic field data and the ionospheric plasma velocity data. From thus identified eigen-frequency ("FLR frequency" below) one can estimate the magnetospheric plasma density along the field line which passes through the ground/ionospheric observation point.

In this study we use the SuperDARN radar data to identify FLR: For each radar beam from each SuperDARN radar, the velocity of the ionospheric plasma flow along the line of sight (VLOS) of the beam is obtained; we use the VLOS data to identify the FLR and estimate the magnetospheric plasma density. Unlike the ground magnetometer data, the SuperDARN data is two-dimensional, enabling two-dimensional estimates of the magnetospheric equatorial plasma density and magnetospheric region identification.

To achieve that, it is important to identify as many FLR events as possible. Overwrapping of non-FLR waves/perturbations hides FLR events. As a countermeasure to this problem, the so-called gradient method has been applied to the ground magnetometer data; this method cancels out the overwrapping signals by dividing the data from a magnetometer by the data from another magnetometer having an adequate latitudinal distance from the other. The division yields the amplitude ratio and the phase difference. The gradient method is effective since the FLR frequency tends to depend on the latitude more strongly than the overwrapping signals.

The gradient method is also applicable to the SuperDARN VLOS data. The field of view of each beam is divided into Range Gates (RGs below) having the same length along the beam. The identification number of the RGs increases with increasing distance from the radar. The VLOS is obtained for each RG. Thus, each RG can be regarded as a "virtual observatory."

As an initial study, we have selected an FLR event which was identified in the VLOS data of a radar (at Hankasalmi) without the use of the gradient method, selected a beam, and selected a few pairs of RGs of the beam. We then have manually applied the gradient method to the VLOS data of the above-selected RG pairs, and successfully identified the FLR. In more detail, the identification has been successful only for two paired RGs whose RG numbers differs by two. This suggest that, since the length of the RG, mapped to the meridional plane, was about 40km for this event, about 80km distance was the best (with the resolution of 40km) for this event. This distance reflects the resonance width, which is an important quantity reflecting the diffusion and dissipation of the FLR energy.

©2019. Japan Geoscience Union. All Right Reserved.

In order to identify as many FLR events as possible, it is also important to automatically identify the FLR events, since visual identification is time-consuming. The gradient method enables automatic identification more easily than analyses of VLOS itself, since the gradient method yields peaks in both the amplitude ratio and the phase difference. We have started making a program for automatic identification by applying the gradient method to VLOS; the version at the time of this abstract has successfully identified FLRs for all of the above-stated pairs of RGs.

©2019. Japan Geoscience Union. All Right Reserved.

A statistical study of Pi2 pulsations observed in the upper ionosphere using Swarm magnetic field data

*Park Jaehee[1], Khan-Hyuk Kim[1], Junga Hwang[2]

1. School of Space Research, Kyung Hee University, Gyeonggi, South Korea, 2. Korea Astronomy and Space Science Institute, Daejeon,South Korea

The properties of Pi2 pulsations observed in the upper ionosphere are studied using magnetic field data acquired by the Swarm-A spacecraft in low Earth orbit (LEO) and at the low-latitude Bohyun ground station (BOH, L = 1,3) for January 2014-Jun 2015. From time intervals when Swarm-A was on the nightside (magnetic local time (MLT) = 1800-0600 hrs) and the BOH station was near midnight (MLT = 2100-0300 hrs), we identified 623 Pi2 events in the horizontal H component of the BOH data. For each event we examine the coherence between the horizontal H component on the ground and the B_x (radial) azimuthal B_y (azimuthal), or B_z (compressional) components at Swarm-A. Out of 623 events, the B_x-H high coherence (> 0.7) events are ~6%, the B_y-H high coherence events are ~4%, and the B_z-H high coherence events are ~25%. The ground-satellite high coherence events occurred when the spacecraft was located within a magnetic latitude range of ±50°. Using the ground-satellite high coherence events, we examined the latitudinal structure of the relative amplitude and phase of the ionospheric Pi2 pulsations detected at Swarm-A. Confirming previous observations at LEO, we found that the ionospheric Pi2 pulsations are characterized by symmetric odd mode standing oscillations in the north-south direction, having a node for B_x oscillation and an antinode for B_z oscillation, respectively, at the equator. This indicates that the source of ionospheric Pi2 pulsations is the plasmaspheric resonance.

Keywords: Pi2 pulsations

©2019. Japan Geoscience Union. All Right Reserved.

Study on the global distribution characteristics of Pc 1-2 geomagnetic pulsation with the 10Hz data of the MAGDAS system

*Taisei Kabasawa[1], Akimasa Yoshikawa[1], Teiji Uozumi[1], Akiko Fujimoto[1], Shuji Abe[1]

1. Kyushu University

The magnetic field observed on the ground is affected by the space weather phenomena such as magnetic storms and auroral storms.

The Pc1 geomagnetic pulsation (frequency range of 0.2-5.0 seconds) activated mainly around a high-latitude region is understood as a phenomenon accompanied by the excitation of EMIC waves to cause the particle acceleration in the equatorial region of the magnetosphere. Also, it is well known that Pc1 waves propagate horizontally in the ionospheric at the F layer. However, it is not clarified about the global occurrence and propagation properties of Pc1 geomagnetic pulsation on the ground. Moreover, although induction magnetometers are used to observe the high-frequency magnetic field disturbance phenomenon like Pc1 and Pc2 (frequency range of 5.0-10.0 seconds) geomagnetic pulsation, the global observation network with induction magnetometers covering from high-latitude to low-latitude area and equator domain does not exist at this stage. On the other hand, although it is common to use Fluxgate magnetometers for the observation of global space weather phenomenon, it is considered to be unsuitable for analysis of the high-frequency Pc1-2 geomagnetic pulsation because its time accuracy is usually one second value.

The ground multipoint magnetic field observation network which Kyushu University has developed (MAGDAS-9 magnetometer) acquire a 250Hz sampling and 10Hz mean data. Also, it is the only geomagnetic observation network that can investigate the global aspects of Pc1-2 geomagnetic pulsation.

In this study, we investigated the global distribution of Pc1-2 pulsation from polar region to equatorial region with magnetic field data provided by MAGDAS and Dst/AE index provided by the WDC for Geomagnetism, Kyoto. As a result, when the substorm have occurred during a magnetic storm time, generation of Pc1-2 pulsation from high-latitude to middle-and-low latitude region and further arrival of Pc2 pulsation to the dip-equator are identified. The elucidation of occurrence characteristic of the Pc1-2 pulsation on the ground with the EMIC waves excitation is very important not only for space weather application to be able to monitor particle energization process via EMIC excitation but also the elucidation of the super global coupling process from inner magnetosphere to the global ionosphere from polar to equatorial region. In this presentation, we will report the preliminary results of observational analysis of Pc1-2 pulsation by using MAGDAS network. We also discuss the comprehensive approach for understanding global coupling process among inner magnetosphere and high-middle-low latitude to the equatorial region by using FM-CW radar data, PWING induction magnetometer data, and the geo-space environment data from the ERG satellite.

Keywords: Pc1-2 pulsation, EMIC waves, global coupling

©2019. Japan Geoscience Union. All Right Reserved.

In-situ Observations of Reconnection Separatrix Regions in the near-Earth Magnetotail

*Mizuho Araki[1], Masahiro Hoshino[1], Kunihiro Keika[1], Yoshifumi Saito[2]

1. Graduate School of Science, The University of Tokyo, 2. Institude of Space and Astronautical Science

Magnetic reconnection which converts magnetic energy into thermal and kinetic energy of plasmas is an important physical mechanism of plasma heating and acceleration. Particularly in the Petschek-type reconnection, plasma acceleration and heating in the slow-mode shocks formed at the separatrices must be taken into consideration. The structure of the slow-mode shocks in the distant tail of the Earth’s magnetosphere was investigated with in-situ observations made by the GEOTAIL satellite (Saito et.al, 1995). It is observationally suggested that about 10% of the plasma sheet boundary layer (PSBL) is slow-mode shocks. It is, however, not fully understood what determines this percentage and what is the difference in the ion and electron temperature changes between slow-mode shocks and others separatrix regions.
In this study, we utilized multi-spacecraft in-situ observations of separatrix regions at magnetic reconnection in the near-Earth magnetotail (GSM-X is between ~13 and ~25RE). We used data obtained from FPI (Fast Plasma Investigation) and FGM (Fluxgate Magnetometer) on board the MMS satellite from June 1, 2017to August 31, 2017. We examined occurrence locations, ion flow directions and velocity of ion flow in downstream regions of observed events. We also examined changes in ion and electron temperatures and the ion-to-electron temperature ratio.

We classified their events into 2 types according to plasma beta in the in-flow regions: below 0.1 or around 1. We term them “lobe reconnection” and “plasma sheet reconnection”, respectively. In the former type, plasmas in the in-flow regions are cold and tenuous. In the latter type, plasmas in the in-flow regions are hot and dense. In both types, we observed increases in ion and electron temperatures increase, but their characteristics are different. In the lobe reconnection, ion temperatures increase from several hundred eV to several keV. In the plasma sheet reconnection, ion temperatures also increase from about 1 keV to several keV. The increase rate of the electron temperature is less than one order of magnitude for both types, smaller than that of the ion temperature; the electron temperature increases up to at most 1 keV. The ion-to-electron temperature ratio in the out-flow regions in both types is about 5 for both types. We then examined changes of the ion-to-electron temperature ratio and found that the changes are consistent with the result reported by Wang et al. (2012).

In this presentation, we will show the results of separatrix crossing events (both lobe and plasma sheet reconnection events) that occur in 2017 and 2018. We will identify whether each of the separatrices is a slow shock or not and how the separatrix conditions affect ion and electron heating. These characteristics will provide insights into heating mechanisms and energy conversion through separatrix regions.

Reference:

Yoshifumi Saito, Toshifumi Mukai, Toshio Terasawa, Atsuhiro Nishida, Shinobu Machida, Masafumi Hirahara, Kiyoshi Maezawa, Susumu Kokubun, and Tatsundo Yamamoto, Slow-mode shocks in the magneto, J. Geophys. Res., 100, A12, 23,567, 1995

©2019. Japan Geoscience Union. All Right Reserved.

Chih-Ping Wang, Matina Gkioulidou, Larry R. Lyons and Vassilis Angelopoulos, Spatial distributions of ion to electron temperature ratio in the magnetosheath and plasma sheet, J. Geophys. Res., 117, A08215, 2012

Keywords: Magnetic Reconnection, MMS satellite, Earth's Magnetotail

©2019. Japan Geoscience Union. All Right Reserved.

Flow speed dependence of ion temperature, electron temperature, and their ratio in the near-Earth magnetotail reconnection region

*Kaori Watanabe[1], Masahiro Hoshino[1], Kunihiro Keika[1], Yoshifumi Saito[2], Naritoshi Kitamura[1]

1. Univ. of Tokyo, 2. ISAS/JAXA

Plasma in the Earth's magnetotail are heated up to 1-10 keV and stored in the plasma sheet. One of the heating or acceleration mechanisms is the magnetic reconnection. Heated or accelerated plasma are transported both earthward and tailward as fast flow with a speed of several hundred kilometers per second. However, what determines the partition among ion and electron thermal energy and kinetic energy is an unresolved problem. It has been reported that ion temperature T_i, electron temperature T_e, and their ratio T_i/T_e vary spatially and depend on the conditions of fast flows [Wang et al., 2012, Runov et al., 2018] but there are few studies which focus on macroscopic profiles of them in reconnection regions in the magnetotail.

In this study, we examine the relation between flow speed and average profiles of T_i, T_e, and T_i/T_e in the magnetotail reconnection region by using data obtained from FPI and FGM on board the MMS spacecraft. We use the observations for a period from May to August 2017 and take out the data in the region of $X_{GSM} < -15$ Re, -10 Re $< Y_{GSM} < 10$ Re, and beta > 0.1. We then divide them into different groups according to flow speed normalized by alfven speed and show B_z/B_{lobe}– B_x/B_{lobe} maps of T_i, T_e, and T_i/T_e of each group. The results show that ion temperature increase with increasing flow speed while electron temperature decrease. Ion temperature are hotter around the X-point. The structure of inflow and outflow regions is pronounced in the profile of electron temperature. T_i/T_e in inflow region are greater than in outflow region, which means that ion and electron temperatures become comparable by passing through the diffusion region. The results suggest that electron get less energy when more energy is partitioned into plasma kinetic energy. We will discuss about the profiles of anisotropy of plasma temperatures to know more details about the heating mechanisms.

Keywords: temperature ratio, flow, MMS

©2019. Japan Geoscience Union. All Right Reserved.

Examining Minimum Cyclotron Resonant Electron Energy of EMIC Waves with MMS

*Si Liu[1]

1. Changsha University of Science and Technology

Electromagnetic ion cyclotron (EMIC) waves can be in cyclotron resonance with relativistic electrons, causing relativistic electron precipitation. The four ideal Magnetospheric Multiscale (MMS) spacecraft provide great opportunity to directly calculate the wave vector ***k*** of EMIC waves by phase differencing technique and hence estimate the minimum resonant energy by the resonance condition. Deriving a simplified analytic solution, we find that the phase differencing method can still provide an estimate of the dominant wave number when a finite wave number spread or a finite frequency spread is present. Numerical calculations indicate that quasi-antiparallel propagation dominates the EMIC event on 20 November 2015, which is consistent with the FFT spectral analysis results. We also find that obtained wave vectors, roughly agreeing with the validity of cold plasma theory, might significantly vary from wave packet to wave packet. Moreover, minimum resonant electron energies gradually increase from 0.5 MeV to tens of MeV with a decreasing parallel componet of ***k***. Current results provide evidence that EMIC waves can be in resonance with the electrons of energies down to hundreds of keV. It further demonstrates that EMIC waves in a narrow frequency band can effectively interact with the relativistic electrons with a broad energy range.

Keywords: EMIC waves, minimum resonant electron energy, wave vector, phase differencing

©2019. Japan Geoscience Union. All Right Reserved.

Small scale whistler mode waves near the magnetic field intensity minimum in the magnetosheath

*Naritoshi Kitamura[1], Takanobu Amano[1], Yoshiharu Omura[2], Satoko Nakamura[2], Chika Umegaki[1], Scott A Boardsen[3,4], Narges Ahmadi[5], Robert E Ergun[5], Olivier Le Contel[6], Per-Arne Lindqvist[7], Yoshifumi Saito[8], Shoichiro Yokota[9], Daniel J Gershman[3], Barbara L Giles[3], Thomas E Moore[3], William R Paterson[3], Craig J Pollock[10], Christopher T Russell[11], Robert J Strangeway[11], James L Burch[12]

1. Department of Earth and Planetary Science, Graduate School of Science, The University of Tokyo, 2. Research Institute for Sustainable Humanosphere, Kyoto University, 3. NASA Goddard Space Flight Center, 4. University of Maryland, 5. Laboratory for Atmospheric and Space Physics, University of Colorado, 6. Laboratoire de Physique des Plasmas, UMR7648 CNRS/Ecole Polytechnique/UPMC/Université Paris-Sud/Observatoire de Paris, 7. Royal Institute of Technology, 8. Institute of Space and Astronautical Science, Japan Aerospace Exploration Agency, 9. Department of Earth and Space Science, Graduate School of Science, Osaka University, 10. Denali Scientific, 11. Institute of Geophysics and Planetary Physics, University of California, Los Angeles, 12. Southwest Research Institute

Wave-particle interactions are thought to play a crucial role in energy transfer in collisionless space plasmas in which the motion of charged particles is controlled by electromagnetic fields. In the terrestrial magnetosheath, intense whistler mode waves, called 'Lion roars', are often detected by spacecraft around minima of semi-periodic fluctuations of magnetic field intensity due to mirror mode structures and motion of the structures. It is expected that whistler mode waves are efficiently generated near a local minimum of magnetic field intensity due to the smallest cyclotron resonance velocity. We report the detailed characteristics of such whistler mode waves using the data obtained by the four MMS (Magnetospheric Multiscale) spacecraft. Because reversals of field-aligned component of Poynting flux around minima in mirror mode structures correspond to reversals of gradient of magnetic field intensity along the magnetic field, whistler mode events with reversals of the field-aligned component of Poynting flux are good candidates of observations of effective wave generation regions along field lines. Even in such events, phase difference and change of amplitude of whistler mode waves observed by the four spacecraft do not have a clear correlation in cases of ~40 km separation, which is much smaller than the spatial scale of magnetic field depression due to mirror mode structures and is even smaller than the local thermal ion gyro scale. This result indicates that the coherent whistler wave generation in mirror mode structures has very limited spatial scale across field lines and is probably affected by any electron scale process. A plane wave approximation can be usable only in a very small scale. Because some events in cases of ~7 km separation showed good correlation among four spacecraft, the typical scale of coherent whistler wave across field lines can be at least an order of 10 km in mirror mode structures in the terrestrial magnetosheath. The whistler mode waves observed by a spacecraft in a mirror mode structure are a cluster of waves from multiple spatially small sources.

Keywords: Whistler mode wave, Plasma wave, MMS spacecraft, Wave-particle interaction

©2019. Japan Geoscience Union. All Right Reserved.

Spatial characteristics of the internal modulation of pulsating aurora: multi-point high-speed optical observations in Scandinavia

*Yuki Kawamura[1], Keisuke Hosokawa[1], Shin-ichiro Oyama[2,3], Yoshizumi Miyoshi[2], Yasunobu Ogawa[3], Satoshi Kurita[2], Satoshi Ebukuro[1], Ryoichi Fujii[4]

1. Department of Communication Engineering and Informatics, University of Electro-Communications, 2. Institute for Space-Earth Environmental Research, Nagoya University, 3. National Institute of Polar Research, 4. Research Organization of Information and Systems

Pulsating aurora (PsA) is a kind of diffuse aurora which almost always appears in the morning side during the recovery phase of auroral substorm. PsA typically has two characteristic temporal variations. One is so-called main pulsation whose period ranges from a few to a few tens of seconds. The other is a few Hz brightness modulation (internal modulation) which is often seen during the ON time of the main pulsation. Previous studies have suggested that the temporal variation of PsA is characterized by wave-particle interaction between whistler-mode chorus waves and high energy electrons in the magnetosphere. Especially, it has been indicated that there is one to one correspondence between the amplitude variation of chorus waves and the luminosity modulation of PsA.
Recent studies revealed the occurrence distribution of the frequency of the internal modulation. However, there have been no studies which analyzed the spatial distribution of the internal modulation.

To reveal the spatial characteristics of the internal modulation, we need to perform a frequency analysis of the internal modulation by using data from high speed optical instruments having wide spatial coverage. For this purpose, we make use of highly sensitive EMCCD cameras which have been operated in Sodankylä and Kevo in Finland, Tromsø in Norway, and Tjautjas in Sweden. In these observations, all-sky images are taken with a sampling rate of 100 Hz, which is sufficient to identify temporal variations of the internal modulation.

In the frequency analysis, we have employed all-sky images taken on March 15, 2018 (00:00 –01:30 UT) in Sodankylä, Kevo, Tromsø, and Tjautjas. We computed the average frequency of the internal modulation from each pixel of the EMCCD cameras and derived the spatial distribution of their dominant frequencies. Regardless of the latitude, each pulsating patch was fluctuating at a similar frequency. We also derived the frequency spectrum of several pulsating patches existing at different positions in the north-south direction and found that those frequency spectrums of pulsating patches have peaks at about 3 Hz. These results indicate that the frequency of the internal modulation does not depend on the magnetic latitude, and the frequency of the internal modulation is collimated on 3 Hz.
In the presentation, we discuss why the frequency of the internal modulation concentrate on 3 Hz by taking into account the time of flight of PsA electrons.

Keywords: Pulsating aurora, Internal modulation

©2019. Japan Geoscience Union. All Right Reserved.

Large-scale characteristics of pulsating aurora periodicities: multi-point high-speed optical observations in Scandinavia

*Satoshi Ebukuro[1], Keisuke Hosokawa[1], Shin-ichiro Oyama[2,3,5], Yoshizumi Miyoshi[2], Yasunobu Ogawa[3], Satoshi Kurita[2], Yuki Kawamura[1], Ryoichi Fujii[4]

1. Department of Communication Engineering and Informatics, University of Electro-Communications, 2. Institute for Space-Earth Environmental Research, Nagoya University, 3. National Institute of Polar Research, 4. Research Organization of Information and Systems, 5. University of Oulu

It has been known that most of diffuse aurorae in the morning side are composed of luminous patches whose brightness modulates quasi-periodically. Such aurorae are termed as pulsating aurora (PsA) and have been studied extensively in the last decade. PsA patches have a scale size of a few hundreds of km and are usually observed during the late recovery phase of substorms. The entire temporal variation of PsA consists of two individual modulations: main pulsation and internal modulation. The periodicity of the main pulsation ranges from a few to a few tens of seconds and the internal modulation, showing a few Hz scintillating luminosity changes, is often embedded within the ON time of the main pulsation. Previous studies using satellites indicated one-to-one correlation between PsA and chorus wave near the equatorial plane of the magnetosphere, suggesting that ground-based observations of PsA can be used for mapping the activity of chorus in the magnetosphere in 2D fashion. In the past, the spatial characteristics of chorus wave have not visualized in detail because satellite observations only cover a single point in the magnetosphere. To overcome this limitation, we derive the spatial distribution of chorus waves by using ground-based optical observations of PsA and discuss the ambient parameters which characterize the nature of chorus.
For this purpose, we have employed data from electron multiplying charge-coupled device (EMCCD) cameras deployed at multiple sites in Scandinavia to derive the large-scale characteristics of PsA. EMCCD cameras have been operative in Kevo and Sodankyla in Finland, Tromsoe in Norway, and Tjautjas in Sweden and their temporal resolution is 100 Hz. We conducted a frequency analysis for a PsA event on March 28, 2017 (23:30 to 24:10 UT). During the event studied, there existed three different regions of PsA, regions A, B and C, showing different modulation periods. It was also found that the boundaries between these three regions were sharp. We derived the 2D frequency map by using data from all the available stations. As a result, it became clear that the higher latitude region (region C) showed faster internal modulation than the lower latitude region (region A). In addition, region B, which was sandwiched by regions A and C, did not show any internal modulations (i.e., main pulsation without internal modulation). In the presentation, we discuss why the three regions showed different modulation periods with sharp boundaries. In particular, we address what ambient conditions can control the absence of internal modulation in region B. We also derived similar frequency maps of chorus waves by tracing the PsA modulation with the Tsyganenko 04 magnetic field model, which could be used to estimate the spatial extent of chorus wave generation region.

Keywords: Pulsating aurora, Chorus wave, Main pulsation, Internal modulation

©2019. Japan Geoscience Union. All Right Reserved.

Variations of cosmic noise absorption (CNA) by energetic electron precipitation (EEP) and changes of the auroral morphology

*Miyamoto Taishiro[1], Shin-ichiro Oyama[1,4,5], Yasunobu Ogawa[2], Keisuke Hosokawa[3], Satoshi Kurita[1], Yoshizumi Miyoshi[1], Ryuho Kataoka[2], Hiroshi Miyaoka[2], Tero Raita[4]

1. Institute for Space-Earth Environmental Research,Nagoya University, 2. National Institute of Polar Research, 3. Department of Communication Engineering and Informatics, University of Electro-Communications, 4. Sodankylä Geophysical Observatory, University of Oulu, 5. Ionosphere Research Unit, University of Oulu

Temporal and spatial variations of aurora morphology in association with substorm have been studied for more than half a century. Various types of aurora are known, such as discrete arc emitting at relatively high intensity and elongating along the zonal direction, and diffuse aurora with darker but more widely spreading in the sky. Pulsating aurora, which is characterized by quasi-periodic oscillations in the emission intensity at periods of a few to tens seconds, and auroral patches observed embedding in the pulsating aurora tend to appear at the recovery phase of substorm, especially from midnight to dawn. It is known that these types of aurora are accompanied by energetic electron precipitation exceeding several hundreds keV. Elucidation of the causality to produce pulsating aurora and energetic electron precipitation is an important theme to understand relationships between the radiation belt and upper-middle atmosphere of the earth. Analyzing measurements from satellite observations (e.g., Arase) and ground-based optical/radio technique observations, the generation mechanism is thought to be mainly attributed to wave particle interactions due to plasma wave and electrons in the magnetosphere. In this study, we focus on relationships between auroral morphological changes, in particular spatiotemporal evolutions to patches and coinciding precipitations of the energetic electron.

Some previous studies have presented changes in morphology from pulsating aurora to patch structures [e.g., Shiokawa et al., 2014] and temporal variations of energetic electron precipitation [e.g., Hosokawa and Ogawa, 2015]. As mentioned above, the wave-particle interaction has been widely accepted with experimental evidences to support generation of pulsating aurora and energetic electron precipitation. However, our understanding has not yet reached its maturity of presenting spatiotemporal evolutions of auroral morphology and associated electron precipitation. Oyama et al. [2017] presented enhancements of CNA (cosmic noise absorption) coinciding with appearance of the patch structure but with only two events. Furthermore, due to measurements with intensive diagnostic instruments, the result was based on information of a part of the auroral ionosphere. In this study, we conducted observations to capture simultaneously time evolutions and spatial distributions of auroral morphology and energetic electron precipitation by utilizing a network of EMCCD (Electron Multiplying Charge Coupled Device) cameras and riometers deployed in Northern Europe.

This study will present three events (February 19-20, 2018, March 6-7, 2017, and March 29-30, 2017). On the way of all events, after substorm onsets twice near Northern Europe, another onset occurred again at more west side (near Iceland or Greenland area) but at dawn in the Northern Europe. In this study, we have focused on the aurora and CNA associated with the latter onset, and at that time, the aurora spatially and temporally shifted from diffuse to pulsation and patch structures. This suggests that substorm activities occurred in the distance can induce these auroral morphological changes seen in the Northern Europe. CNA at that time is characterized by gradual variations with time scale of several hours. This trend cannot be seen at substorm onset near the Northern Europe. Moreover, in the latitude distribution, the feature was confirmed that CNA increases at the latitude where patch structure is seen, and CNA keeps

©2019. Japan Geoscience Union. All Right Reserved.

constant value at the latitude where patch structure is not seen. In the presentation, based on these observations, we will discuss physical mechanisms to cause changes in the auroral morphology and energetic electron precipitation, which can be seen as increases of CNA.

Keywords: Ionosphere, Aurora, Energetic Electron Precipitation (EEP)

©2019. Japan Geoscience Union. All Right Reserved.

Spatiotemporal characteristics on the source region of flash aurora using ray tracing analysis

*Tomohiro Inoue[1], Mitsunori Ozaki[1], Yoshitaka Goto[1], Satoshi Yagitani[1], Yoshiya Kasahara[1], Kazuo Shiokawa[2], Yoshizumi Miyoshi[2], Ryuho Kataoka[3], Yusuke Ebihara[4]

1. Kanazawa University , 2. Nagoya University, 3. National Institute of Polar Research, 4. Kyoto University

Whistler mode waves cause precipitation of high-energy electrons via wave-particle interactions in the magnetosphere. The scattered particles precipitate to the ground along the geomagnetic field line. Then, flush aurora, which is a rapid (less than 1 s) auroral phenomenon, is happened. Flash aurora is important for understanding the spatial evolution of wave-particle interaction region in the magnetosphere. We observed the mainly southward spread of flush aurora. In order to understand the spatial-time variation of wave-particle interaction region, we analyze the propagation effects of whistler mode waves near the magnetic equator region using ray tracing analysis. We calculated the ray paths of whistler mode waves (0.2 fce and 0.4 fce) near the magnetic equator (-10 to +10 degrees of geographic latitude), where fce is the electron cyclotron frequency at the magnetic equator. The initial ray paths put in the assumption of a spatial spread with the wave normal angles of tens of degrees along the magnetic field line at the magnetic equator (a point source). Then, we traced the magnetic field lines from the ray paths of whistler mode waves and estimated the precipitation area of electrons in the ionosphere using the IGRF model. The calculation results showed the precipitation area was not mainly spread southward, but evolved northward in the preliminary study.
In this presentation, we will present the spatiotemporal characteristics of flash aurora and the analysis results of ray tracing in detail.

Keywords: Flush aurora, Whistler mode wave, Ray tracing, Wave-particle interaction

©2019. Japan Geoscience Union. All Right Reserved.

Molecular ion supply mechanisms from the low-altitude ionosphere to magnetosphere observed by EISCAT and Arase(ERG)

*Masayoshi Takada[1], Kanako Seki[1], Yasunobu Ogawa[2], Kunihiro Keika[3], Satoshi Kasahara[4], Shoichiro Yokota[5], Tomoaki Hori[7], Kazushi Asamura[6], Yoshizumi Miyoshi[7]

1. Graduate School of Science, Tokyo University, 2. National Institute of Polar Research, 3. Department of Earth and Planetary Science, Graduate School of Science, Tokyo University, 4. The University of Tokyo, 5. Graduate School of Science, Osaka University, 6. Institute of Space and Astronautical Science, Japan Aerospace Exploration Agency, 7. Institute for Space-Earth Environmental Research, Nagoya University

Molecular ions ($O_2^+/NO^+/N_2^+$) in the magnetosphere have been observed during magnetic storms [Peterson et al., 1994; Klecker et al., 1986]. These molecular ions are considered to originate from the Earth’ s ionosphere. It is considered that they have been transported upward by some heating processes in the ionosphere. However, due to the larger mass than atomic ions (O^+), the molecular ions usually exist only in the low-altitude ionosphere below 300 km altitude. It is hence difficult to transport these molecular ions by overcoming loss by chemical reactions to the high-altitude ionosphere where the ion upflow and outflows usually take place [Peterson et al., 1994]. Therefore, it is necessary to reveal what mechanism causes molecular ion upflow during the magnetic storms. In this study, we aim at the observational assessments of the supply processes of the molecular ions from the low-altitude ionosphere to the magnetosphere based on conjugate observations by EISCAT radar and the Arase (ERG) satellite.

The EISCAT radar and the Arase (ERG) satellite have the conjunction event during the large magnetic storm with the minimum Dst of -124 nT on September 8, 2017. During the event, the Arase satellite was located in the dusk-side inner magnetosphere and observed molecular ions in the energy range of 12-180 keV/q. The EISCAT radar simultaneously observed the ion upflow (with the upward velocity of ~50-150 m/s) from the low-altitude ionosphere (~250-400 km) together with strong ion heating (>2000 K). The convective electric field was also enhanced by a factor of 2 in the same region. We estimated each term in the equation of motion for ions. The result indicates that the ion upflow reached stable equilibrium because the upward ion and electron pressure gradients are balanced with the downward gravitational force. It is suggested that the ion upflow can take place from the low-altitude ionosphere due to strong ion pressure gradient. We also estimated the flux decrease of molecular ions due to dissociative recombination. The flux decreased to ~1 % at 350 km compared with 280 km. The estimated upflow flux of molecular ions at 350 km is $>10^{10}$ m^{-2} s^{-1} . Comparison between distribution functions observed by Arase satellite and EISCAT radar suggests that acceleration by 3 orders of magnitudes is necessary during the outflow process. These results indicate that the strong ion frictional heating during magnetic storms enabled molecular ions to be transported upward from the low-altitude ionosphere and provide a source of molecular ion outflows into the magnetosphere.

Keywords: Molecular ion, EISCAT radar, Arase (ERG) satellite, Ion upflow, Ionospheric heating

©2019. Japan Geoscience Union. All Right Reserved.

Optical and radar observation of the dynamic auroral forms

*Yunosuke Nagafusa[1], Tima Sergienko[2], Satoshi Taguchi[1], Urban Braendstroem[2], Masatoshi Yamauchi[2]

1. Graduate School of Science, Kyoto University, 2. Swedish Institute of Space Physics, Kiruna

Ionosphere disturbances caused by the auroral electron precipitations are studied using auroral images taken by Auroral Large Imaging System (ALIS) and ionospheric parameters measured by EISCAT UHF radar that were conjugate with ALIS field-of-view. ALIS consists of several remote controlled stations located in northern Scandinavia, separated by approximately 50 km. Each station is equipped with a high-resolution CCD detector with 1024×1024 pixels, and a filter wheel with six positions for narrow-band interference filters. In this study we use the data obtained with the 557.7 nm filter, which show the auroral emission originated from the atomic oxygen. EISCAT UHF radar located in northern Norway near Tromsø operating in the BEATA program provides the ionospheric electron density, electron and ion temperatures, and ion velocity with the time resolution of 5 s and the spatial resolution of 1.5 km. The auroral images from the different ALIS stations were used for triangulation of the auroral forms in order to determine the aurora position in relation to the radar beam. For each auroral arc, the electron density, the electron and ion temperatures measured inside and in the vicinity of the auroral forms were analyzed with the aim of understanding the ionospheric response to the different types of auroral electron precipitations.

Keywords: aurora, ionospheric parameters, electron precipitations

©2019. Japan Geoscience Union. All Right Reserved.

Observations of MF/HF auroral radio emissions at three ground-based stations

*Yuka Sato[1], Atsushi Kumamoto[2], Yuto Katoh[2], Akira Kadokura[3,4], Yasunobu Ogawa[3,4], Atsuki Shinbori[5]

1. Nippon Institute of Technology (NIT), 2. Graduate School of Science, Tohoku University, 3. National Institute of Polar Research (NIPR), 4. The Graduate University for Advanced Studies, 5. Institute for Space-Earth Environmental Research (ISEE), Nagoya University

We started ground-based observations of MF/HF auroral radio emissions about 10 years ago at two stations (The Husafell Station, Iceland, September 2005; The Kjell Henriksen Observatory, Svalbard, September 2008) and found multiple unknown properties of MF/HF auroral radio emissions, e.g. polarization features [*Sato et al.*, 2008, 2015] and existence of a higher frequency component [*Sato et al.*, 2012]. To make a next siginificant step for a futher understanding of MF/HF auroral radio emissions, we installed a new dedicated instrumentation at the KAIRA (Kilpisjärvi Atmospheric Imaging Receiver Array) site in Kilpisjärvi, Finland (Latitude: 60.07 N, Longitude: 20.76 E) in the summer of 2018. It is a passive receiving system designed to realize a high-resolution spectral, interferometric and polarization measurements using 4 loop antennas and a software-defined radio (SDR) receiver. This SDR receiver can implement high-speed, flexible digital signal processing of RF signals and obtain high-resolution spectra pauselessly throughout the night in a wide frequency range up to 6 MHz. One of the main research subjects of this project is radio emission spontaneously emitted from aurora. There are long-known three types of MF/HF auroral radio emissions identified at ground level: auroral hiss, medium frequency burst (MFB), and auroral roar. Investigation into the generation of these emissions not only offers a tool of great promise for remote sensing of ionospheric plasma processes and parameters but also gives the foundation for understanding various radiation mechanisms that occur in planetary magnetospheres and plasma in space. In combination with the long-term continuous observations in Iceland and Svalbard and future EISCAT_3D experiments, observation with this new instrumentation will provide a first-time opportunity to reveal spatiotemporal variations of macro and fine structures of MF/HF auroral radio emissions associated with substorm evolution. In this presentation, we show detailed specification of this new instrumentation and some initial results.

Keywords: auroral phenomena, radio wave propagation, wave-particle interaction

©2019. Japan Geoscience Union. All Right Reserved.

Ionospheric F-region Drift Measurements Derived from DPS-4D at Zhongshan Station, Antarctic

*Xiangcai Chen[1]

1. Polar Research Institute of China

By means of high-frequency radio sounding, the ionospheric plasma drift can be measured by the Doppler frequency shift of signal. In this paper we analyze the ionospheric F-region plasma motion performed by Digisonde Portable Sounder (DPS-4D) at cusp latitude over Zhongshan Station in Antarctic. By restricting the echo arrival angle, and selecting the reflection height range at 175 –475 km, we present the variation of the F-region plasma drift measurements by setting limits on the Doppler frequency shift. Base on the 7.5 min interval Digisonde drift data from November 2011 to February 2012, we considered the variations of the plasma drift in F-region under the different geomagnetic activity (Kp) and magnetic local time, as well as it correlation with interplanetary magnetic field (IMF). The results indicate that properly restricting the Doppler frequency shift of the echo has a strong effect that contributes to the accurate and robust measurements of the ionospheric plasma drift. The mean value of horizontal drift mostly leveled off to about 600 m/s at altitude around of 230 km, while the field-aligned component of drift showed mean values of -25 m/s near pre-noon and +40 m/s during the night. These strong diurnal variations have dependence on the sign and strength of the IMF B_y and B_z components. It implies that the contraction and expansion of the polar cap with Kp and the convection in the proximity of the throat with different IMF conditions have a profound influence on the observed drift velocities.

Keywords: Digisonde DPS 4, Doppler frequency shift, remote sensing, polar ionosphere, plasma drift

©2019. Japan Geoscience Union. All Right Reserved.

PARM-HEP Observation of Precipitating High Energy Electrons over Pulsating Aurora

*Taku Namekawa[1], Takefumi Mitani[2], Kazushi Asamura[2], Yoshifumi Saito[2]

1. Department of Earth and Planetary Science, Graduate school of Science, The University of Tokyo, 2. Institute of Space and Astronautical Science, Japan Aerospace Exploration Agency

The phenomenon called microbursts that radiation belt particles precipitate to the Earth’ s atmosphere is thought to be largely related to the dissipation of high energy electrons in radiation belt. It is suggested that this phenomenon is caused by pitch angle scattering of the magnetospheric particles by plasma waves, which is a mechanism similar to the cause of the pulsating aurora observed in the Earth’ s polar region. There is a possibility that the origin of microburst can be clarified by proving simultaneous occurrence of microburst and pulsating aurora, but observational verification has not been made yet. For that purpose, we have developed a high-energy electron detector (HEP) for the observation of sub-relativistic - relativistic energy electrons that make up the microburst. HEP is designed to measure electrons between 300 keV and 2 MeV with energy resolution of 20% or less and with signal processing time of ~ 5 μs. Energy analysis is performed by the detection part of this instrument using SSD (Solid State Detector). Performance tests of this instrument are carried out using a sealed radiation source and a high energy electron beam line. This instrument is installed as one of the core instruments of the PARM instrument package developed for the simultaneous observation of the pulsating aurora and microburst by an international student sounding rocket experiment RockSat-XN and LAMP (Loss through Auroral Microburst Pulsation) sounding rocket experiment. We have succeeded in obtaining the flight data on 13 January 2019 from RockSat-XN sounding rocket experiment. In parallel, we are now preparing HEP analyzer for LAMP sounding rocket experiment. In this presentation, we will show the outline and observation results of RockSat-XN-HEP as well as the LAMP-HEP development status.

Keywords: Microburst, PARM, RockSat-XN, LAMP, Sounding rocket, Pulsating aurora

©2019. Japan Geoscience Union. All Right Reserved.

Development of the medium-energy electron detector with hemispherical field-of-view and the flight test in the PARM (Pulsating AuRora and Microburst) mission

*Shin Sugo[1], Oya Kawashima[1], Kazushi Asamura[2], Reiko Nomura[3], Yasunobu Ogawa[4], Keisuke Hosokawa[5], Yoshizumi Miyoshi[6], Takefumi Mitani[2], Taku Namekawa[1,2], Takeshi Sakanoi[7], Mizuki Fukizawa[7], Naoshi Yagi[7], Satoshi Kasahara[1]

1. The University of Tokyo, 2. Institute of Space and Astronautical Science, Japan Aerospace Exploration Agency, 3. National Astronomical Observatory of Japan, 4. National Institute of Polar Research, 5. The University of Electro-Communications, 6. Institute for Space-Earth Environmental Research, Nagoya University, 7. Tohoku University

Energetic electrons significantly affect ionospheric dynamics and the long-term evolution of surfaces and atmospheres of planets and moons. Since the energetic electron flux is not necessarily isotropic, it is important to cover the broad solid angle to quantitatively evaluate the effects on solar system bodies. With future planetary explorations in mind, we developed the medium-energy (20 - 100 keV) electron detector (MED) which can cover almost 2-pi steradian without the spacecraft spin. In order to test the performance of this analyzer in the relevant environment, we participated in the PARM mission, which aimed to measure electron precipitation using NASA’s sounding rocket RockSat-XN. In this presentation we report on MED observation results obtained through the flight on 13 January 2019.

©2019. Japan Geoscience Union. All Right Reserved.

Auroral substorm onset in satellite-based global images and ground-based all-sky images

*Akimasa Ieda[1], Kirsti Kauristie[2], Yukitoshi Nishimura[3], Yukinaga Miyashita[4], Harald U Frey[5], Liisa Juusola[2], Daniel Whiter[6], Masahito Nose[7], Matthew O Fillingim[5], Farideh Honary[8], Neil C Rogers[8], Yoshizumi Miyoshi[1], Shinobu Machida[1]

1. Institute for Space-Earth Environmental Research, Nagoya University, 2. Finnish Meteorological Institute, 3. Boston university, 4. Korea Astronomy and Space Science Institute, 5. University of California Berkeley, 6. University of Southampton, 7. Graduate School of Science, Kyoto University, 8. Lancaster University

Substorm onset has originally been defined as a longitudinally extended sudden auroral brightening (Akasofu initial brightening: AIB) followed a few minutes later by an auroral poleward expansion in ground-based all-sky images (ASIs). In contrast, such clearly marked two-stage development has not been evident in satellite-based global images (GIs). Instead, substorm onsets have been identified as localized sudden brightenings that expand immediately poleward.
To resolve these differences, optical substorm onset signatures in GIs and ASIs are compared in this study for a substorm that occurred on December 7, 1999. For this substorm, the Polar satellite ultraviolet global imager was operated with a fixed-filter (170 nm) mode, enabling a higher time resolution (37 s) than usual to resolve the possible two-stage development. These data were compared with 20-s resolution green-line (557.7 nm) ASIs at Muonio in Finland. The ASIs revealed the AIB at 2124:50 UT and the subsequent poleward expansion at 2127:50 UT, whereas the GIs revealed only an onset brightening that started at 2127:49 UT.
Thus, the onset in the GIs was delayed relative to the AIB and in fact agreed with the poleward expansion in the ASIs. The fact that the AIB was not evident in the GIs may be attributed to the limited spatial resolution of GIs for thin auroral arc brightenings. The implications of these results for the definition of substorm onset are discussed herein.

Keywords: substorm, auroral breakup, aurora

©2019. Japan Geoscience Union. All Right Reserved.

Original substorm onset (Akasofu 1964; 2010)

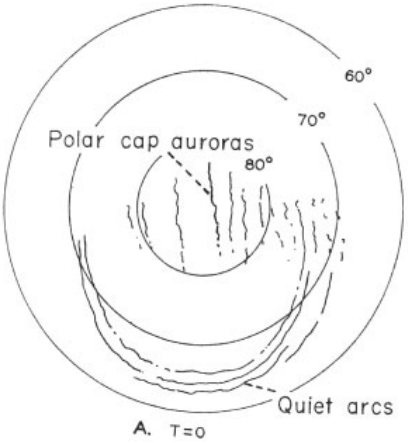

FIG. 2. THE DISTRIBUTION OF THE AURORAS DURING THE QUIET PHASE.

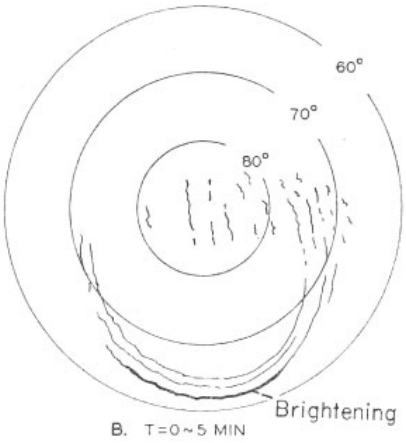

FIG. 3. AURORAS DURING THE EXPANSIVE PHASE (STAGE I).

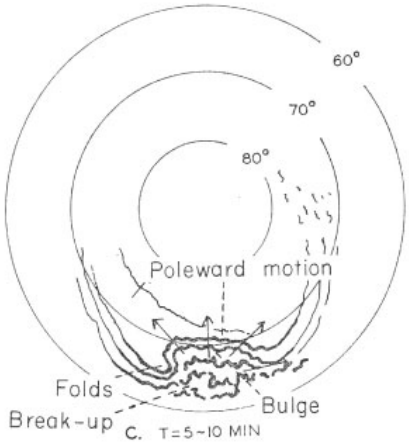

FIG. 4. AURORAS DURING THE EXPANSIVE PHASE (STAGE II).

a Time < 0
Before onset
Quiet arc

b T = 0 ~ 5 min
Expansion phase stage 1
Initial brightening
T = 0: Substorm onset

c T = 5 ~ 10 min
Expansion phase stage 2
Poleward expansion
(Auroral breakup)

Ground and satellite observations (Ieda et al. 2018: 10.1186/s40623-018-0843-3)

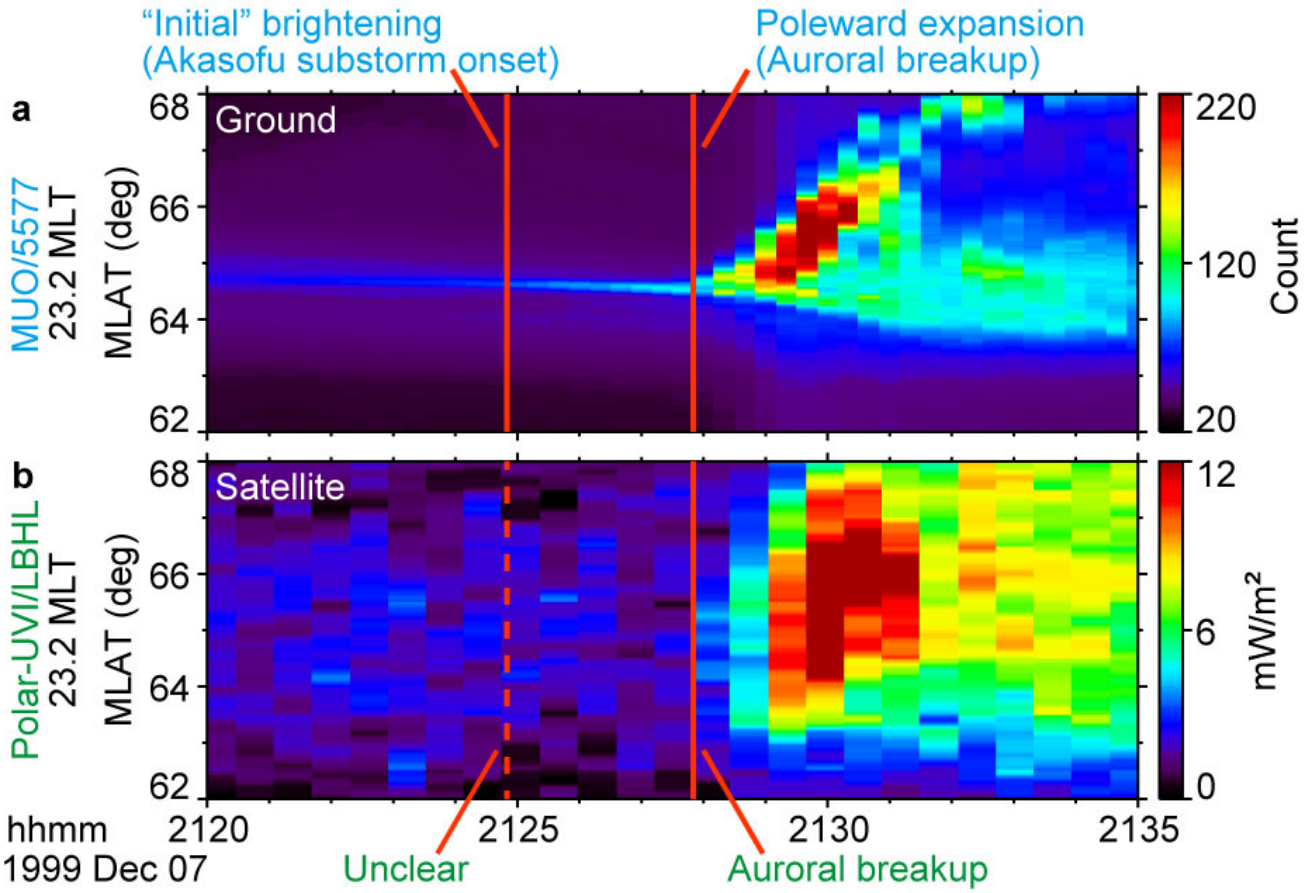

©2019. Japan Geoscience Union. All Right Reserved.

Automatic Classification of Auroral images using optical flow feature

*Naoto Kashiwagi[1], Akiko Fujimoto[1], Terumasa Tokunaga[1], Yoshizumi Miyoshi[2], Yasunobu Ogawa[3], Keisuke Hosokawa[4]

1. Kyushu Institute of Technology, 2. Nagoya University, 3. National Institute of Polar Research, 4. The University of Electro-Communications

The machine learning technique including the deep learning has been developed and the practical uses have increased on various field. On the study of auroral detection, the concern over the automatic image classification has risen using the approach of machine learning technique for the large statistical analysis of auroral images. The automatic auroral image classification has tried to use some techniques from computer vision, machine vision and pattern recognition. There are roughly two kinds of the selected feature: the color of image and the motion of aurora image sequences. The works based on the color feature of aurora image have been performed by Rao et al. (2014) and Tanaka et al. (2015). Rao et al. (2014) performed Support Vector Machines (SVM) classification with several local feature extraction techniques, and found that Scale Invariant Feature Transform (SIFT), OpponentSIFT, is the most effective feature for the automated classification of color aurora images. Tanaka et al. (2015) used the aurora area using the HSV model. They mentioned that it is difficult to classify the images including the diffuse aurora and cloud area. The color feature work well for the color auroral image, while the gray-scale (optically filtered) auroral images need other features on the automated classification. Blixt et al. (2006) applied the optical flow estimation to auroral image sequences. Their case study showed the useful tool for representing the motion of the aurora. In this study, we validate the optical flow estimation to extract the feature of auroral image, and automatically classify the large gray-scale auroral images using the machine learning with Convolution Neural Network (CNN). We use 63,486 gray-scale aurora images in total and use five categories for the preparation of supervised learning data, 1) aurora, 2) aurora and cloudy, 3) aurora and moon, 4) aurora, cloudy and moon, 5) noaurora. We perform the Hold-out and the Cross Validation to evaluate our classification performance. We obtained 98.58% of the classification accuracy based on Hold-out and 98.47% of the classification accuracy based on Cross Validation.

Keywords: Aurora, Optical flow, Convolution Neural Network

©2019. Japan Geoscience Union. All Right Reserved.

Fine-scale visualization of aurora in a wide area using color digital camera images from the International Space Station

*Sota Nanjo[1], Yuta Hozumi[1], Keisuke Hosokawa[1]

1. The University of Electro-Communications

Various ground-based and space-based imagers have been used to observe aurora borealis and australis. So far, however, it has been difficult to observe the detailed spatial structure of auroras in a wide area with sufficient spatial and temporal resolution. Since the photographs taken from the International Space Station (ISS) have sufficient spatial and temporal resolution, it is possible to visualize the fine-scale structures of aurora in a wide area. A calibration of imaging parameters of the photographs using star lights was proposed by a previous research. The accuracy in the timestamp was not guaranteed by the method based on the star lights because the position of the star lights in the image did not change with elapsed time. Thus, it is still difficult to use the mapped data for studying fast variations of aurora, for example pulsating aurora (PsA). Therefore, in this study, we calibrated the images from the ISS using city lights which change their apparent positions with elapsed time. In order to validate the calibration method using city light positions, we mapped two PsA events in the photographs to the geographical coordinate, and compared with those from ground-based all-sky imagers in Alaska and Canada. We found that the approximate shape of discrete aurora and the temporal variation of PsA derived from the ISS images are consistent with those from the ground-based observation. The accuracy in the timestamp is less than 0.5 sec and that in space in the direction perpendicular to the line of sight of the camera is within 5 km. In the presentation, we will also address how the mapped full-color images can be used for studies of PsA in the future work.

Keywords: aurora, ISS

©2019. Japan Geoscience Union. All Right Reserved.

PARM: Investigation of precipitating high-energy electrons into the auroral ionosphere with sounding rockets

*Kazushi Asamura[1], Yoshizumi Miyoshi[2], Keisuke Hosokawa[3], Takefumi Mitani[1], Taku Namekawa[1,5], Takeshi Sakanoi[4], Naoshi Yagi[4], Mizuki Fukizawa[4], Genki Ishizawa[4], Satoshi Kasahara[5], Shin Sugo[5], Oya Kawashima[5], Reiko Nomura[6], Masahito Nose[2], Mariko Teramoto[2], Yasunobu Ogawa[7], Shinji Saito[2], Ryoichi Fujii[8]

1. ISAS / JAXA, 2. ISEE, Nagoya University, 3. The University of Electro-Communications, 4. Tohoku University, 5. The University of Tokyo, 6. NAOJ / NINS, 7. NiPR / ROIS, 8. ROIS

Bursty precipitations of high-energy electrons into the polar ionopshere have been observed by low-altitude satellite, for example, SAMPEX and FIREBIRD II. These precipitations, called microburst, may contribute to the loss of the terrestrial radiation belt through the collisional energy loss with the dense, cold atmospheric particles. Recent numerical simulations successfully reproduce these microburst precipitations with a few Hz modulations by taking into account the pitch angle scattering with the whistler chorus elements at off-equator regions in the inner magnetosphere. Therefore, one can expect that the miscroburst precipitations have properties depending on auroral activities especially the pulsating auroras. In order to investigate the mechanisms of the microburst precipitations by in-situ observations, we are developing two instrument packages: PARM (Pulsating AuRora and Microbursts; already developed) and PARM-2 (being developed), both of which are designed suitable for sounding rocket experiments. PARM consists of four sensors; HEP (high-energy electron energy spectrometer), MED (medium-energy electron detector), AIC (auroral camera), and AFG (ASIC-based fluxgate magnetometer). PARM was onboard the NASA's RockSat-XN sounding rocket, and launched from Andoya, Norway at 09:13UT, Jan 13, 2019. On the other hand, PARM-2 is under development. It consists of HEP, two AICs, and MIM (magneto-impedance magnetometer). PARM-2 is to be onboard the NASA's LAMP sounding rocket which will fly from Poker Flat, Alaska in the period between the end of 2019 and the beginning of 2020.

We will present the overview of PARM missions including the initial results of RockSat-XN/PARM with ground-based observations and preparation status of LAMP/PARM-2.

Keywords: electron microburst precipitation, sounding rocket, pulsating aurora

©2019. Japan Geoscience Union. All Right Reserved.

[E] Poster | P (Space and Planetary Sciences)：P-EM Solar-Terrestrial Sciences, Space Electromagnetism & Space Environment

Wed. May 29, 2019 5:15 PM - 6:30 PM JST | Wed. May 29, 2019 8:15 AM - 9:30 AM UTC | Poster Hall International Exhibition Hall8, Makuhari Messe_5

[P-EM11] Dynamics of Magnetosphere and Ionosphere

convener:Aoi Nakamizo(Applied Electromagnetic Research Institute, National Institute of Information and Communications Technology), Mitsunori Ozaki(Faculty of Electrical and Computer Engineering, Institute of Science and Engineering, Kanazawa University), Akiko Fujimoto(Kyushu Institute of Technology), Tomoaki Hori(Institute for Space-Earth Environmental Research, Nagoya University)

This session provides an opportunity to present recent results from satellite and ground-based observations and theoretical and simulation studies on the magnetosphere, ionosphere, and their coupling processes. We invite talks and posters discussing various phenomena related to the magnetosphere-ionosphere system: solar wind-magnetosphere interaction, magnetosphere-ionosphere convection, field-aligned current, magnetic storms/substorms, neutral-plasma interaction, ionospheric ion inflow and outflow, aurora phenomena, and so forth. Discussions on planetary and satellite ionosphere and magnetospheres, future missions and instrument developments are also welcome.

[PEM11-P01] Effects of Inclination/Rotation of Earth's Magnetic Axis on Magnetosphere Simulated by Global MHD Model

*Aoi Nakamizo[1] (1.Applied Electromagnetic Research Institute, National Institute of Information and Communications Technology)

[PEM11-P02] Asymmetric deformation of the magnetosphere under low-density solar wind

*Masaki N Nishino[1,2], Yoshifumi Saito[2], Kazuo Shiokawa[1], Masaki Fujimoto[2] (1.Institute for Space-Earth Environmental Research, Nagoya University, 2.JAXA/ISAS)

[PEM11-P03] New perspectives on coupling processes in solar-terrestrial system obtained by comprehensive data analysis

*Yoshimasa Tanaka[1], Norio Umemura[2], Shuji Abe[3], Satoru UeNo[4], Masahito Nose[2], Yumi Nakagawa[5] (1.National Institute of Polar Research, 2.Institute for Space-Earth Environmental Research, Nagoya University, 3.International Center for Space Weather Science and Education, 4.Kwasan & Hida Observatories, School of Science, Kyoto University, 5.Ibaraki University)

[PEM11-P04] The interaction between the magnetosphere-ionosphere compound system and the magnetic field topology

*Shigeru Fujita[1], Takashi Tanaka[2], Masakazu Watanabe[2] (1.Meteorological College, Japan Meteorological Agency/ Nationa Institute of Polar Research, 2.Kyushu University)

[PEM11-P05] Effects of the dipole tilt and the interplanetary magnetic field Bx component on the dawn-dusk and interhemispheric asymmetries of the interchange convection cycle

*Masakazu Watanabe[1,2], Takashi Tanaka[2], Shigeru Fujita[3,4] (1.Graduate School of Science, Kyushu University, 2.International Center for Space Weather Science and Education, Kyushu University, 3.Meteorological College, 4.National Institute of Polar Research)

[PEM11-P06] Transient polar ionospheric convection response to negative dynamic pressure pulse

*Jianjun Liu[1] (1.Polar Research Institute of China)

[PEM11-P07] An active ionosphere: a new perspective of field line dipolarization

*Osuke Saka[1] (1.Office Geophysik)

[PEM11-P08] Toward the automatic identification of FLR signals in the SuperDARN data by using the gradient method

*Hideaki Kawano[1,2], Akira Sessai Yukimatu[3,4], Nozomu Nishitani[5], Yoshimasa Tanaka[3,4], Satoko Saita[6], Tomoaki Hori[5] (1.Dept. Earth Planet. Sci., Kyushu Univ., 2.ICSWSE, Kyushu University, 3.National Institute of Polar Research, 4.SOKENDAI, 5.ISEE, Nagoya University, 6.Kitakyushu College)

[PEM11-P09] A statistical study of Pi2 pulsations observed in the upper ionosphere using Swarm magnetic field data

*Park Jaehee[1], Khan-Hyuk Kim[1], Junga Hwang[2] (1.School of Space Research, Kyung Hee University, Gyeonggi, South Korea, 2.Korea Astronomy and Space Science Institute, Daejeon,South Korea)

[PEM11-P10] Study on the global distribution characteristics of Pc 1-2 geomagnetic pulsation with the 10Hz data of the MAGDAS system

*Taisei Kabasawa[1], Akimasa Yoshikawa[1], Teiji Uozumi[1], Akiko Fujimoto[1], Shuji Abe[1] (1.Kyushu University)

[PEM11-P11] In-situ Observations of Reconnection Separatrix Regions in the near-Earth Magnetotail

*Mizuho Araki[1], Masahiro Hoshino[1], Kunihiro Keika[1], Yoshifumi Saito[2] (1.Graduate School of Science, The University of Tokyo, 2.Institude of Space and Astronautical Science)

[PEM11-P12] Flow speed dependence of ion temperature, electron temperature, and their ratio in the near-Earth magnetotail reconnection region

*Kaori Watanabe[1], Masahiro Hoshino[1], Kunihiro Keika[1], Yoshifumi Saito[2], Naritoshi Kitamura[1] (1.Univ. of Tokyo, 2.ISAS/JAXA)

[PEM11-P13] **Examining Minimum Cyclotron Resonant Electron Energy of EMIC Waves with MMS**

*Si Liu[1] (1.Changsha University of Science and Technology)

[PEM11-P14] Small scale whistler mode waves near the magnetic field intensity minimum in the magnetosheath

*Naritoshi Kitamura[1], Takanobu Amano[1], Yoshiharu Omura[2], Satoko Nakamura[2], Chika Umegaki[1], Scott A Boardsen[3,4], Narges Ahmadi[5], Robert E Ergun[5], Olivier Le Contel[6], Per-Arne Lindqvist[7], Yoshifumi Saito[8], Shoichiro Yokota[9], Daniel J Gershman[3], Barbara L Giles[3], Thomas E Moore[3], William R Paterson[3], Craig J Pollock[10], Christopher T Russell[11], Robert J Strangeway[11], James L Burch[12] (1.Department of Earth and Planetary Science, Graduate School of Science, The University of Tokyo, 2.Research Institute for Sustainable Humanosphere, Kyoto University, 3.NASA Goddard Space Flight Center, 4.University of Maryland, 5.Laboratory for Atmospheric and Space Physics, University of Colorado, 6.Laboratoire de Physique des Plasmas, UMR7648 CNRS/Ecole Polytechnique/UPMC/Université Paris-Sud/Observatoire de Paris, 7.Royal Institute of Technology, 8.Institute of Space and Astronautical Science, Japan Aerospace Exploration Agency, 9.Department of Earth and Space Science, Graduate School of Science, Osaka University, 10.Denali Scientific, 11.Institute of Geophysics and Planetary Physics, University of California, Los Angeles, 12.Southwest Research Institute)

[PEM11-P15] Spatial characteristics of the internal modulation of pulsating aurora: multi-point high-speed optical observations in Scandinavia

*Yuki Kawamura[1], Keisuke Hosokawa[1], Shin-ichiro Oyama[2,3], Yoshizumi Miyoshi[2], Yasunobu Ogawa[3], Satoshi Kurita[2], Satoshi Ebukuro[1], Ryoichi Fujii[4] (1.Department of Communication Engineering and Informatics, University of Electro-Communications, 2.Institute for Space-Earth Environmental Research, Nagoya University, 3.National Institute of Polar Research, 4.Research Organization of Information and Systems)

[PEM11-P16] **Large-scale characteristics of pulsating aurora periodicities:multi-point high-speed optical observations in Scandinavia**

*Satoshi Ebukuro[1], Keisuke Hosokawa[1], Shin-ichiro Oyama[2,3,5], Yoshizumi Miyoshi[2], Yasunobu Ogawa[3], Satoshi Kurita[2], Yuki Kawamura[1], Ryoichi Fujii[4] (1.Department of Communication Engineering and Informatics, University of Electro-Communications, 2.Institute for Space-Earth Environmental Research, Nagoya University, 3.National Institute of Polar Research, 4.Research Organization of Information and Systems, 5.University of Oulu)

[PEM11-P17] Variations of cosmic noise absorption (CNA) by energetic electron precipitation (EEP) and changes of the auroral morphology

*Miyamoto Taishiro[1], Shin-ichiro Oyama[1,4,5], Yasunobu Ogawa[2], Keisuke Hosokawa[3], Satoshi Kurita[1], Yoshizumi Miyoshi[1], Ryuho Kataoka[2], Hiroshi Miyaoka[2], Tero Raita[4] (1. Institute for Space-Earth Environmental Research,Nagoya University, 2.National Institute of Polar Research, 3.Department of Communication Engineering and Informatics, University of Electro-Communications, 4.Sodankylä Geophysical Observatory, University of Oulu, 5.Ionosphere Research Unit, University of Oulu)

[PEM11-P18] Spatiotemporal characteristics on the source region of flash aurora using ray tracing analysis

*Tomohiro Inoue[1], Mitsunori Ozaki[1], Yoshitaka Goto[1], Satoshi Yagitani[1], Yoshiya Kasahara[1], Kazuo Shiokawa[2], Yoshizumi Miyoshi[2], Ryuho Kataoka[3], Yusuke Ebihara[4] (1.Kanazawa University , 2.Nagoya University, 3.National Institute of Polar Research, 4.Kyoto University)

[PEM11-P19] Molecular ion supply mechanisms from the low-altitude ionosphere to magnetosphere observed by EISCAT and Arase(ERG)

*Masayoshi Takada[1], Kanako Seki[1], Yasunobu Ogawa[2], Kunihiro Keika[3], Satoshi Kasahara[4], Shoichiro Yokota[5], Tomoaki Hori[7], Kazushi Asamura[6], Yoshizumi Miyoshi[7] (1.Graduate School of Science, Tokyo University, 2.National Institute of Polar Research, 3.Department of Earth and Planetary Science, Graduate School of Science, Tokyo University, 4.The University of Tokyo, 5.Graduate School of Science, Osaka University, 6.Institute of Space and Astronautical Science, Japan Aerospace Exploration Agency, 7.Institute for Space-Earth Environmental Research, Nagoya University)

[PEM11-P20] Optical and radar observation of the dynamic auroral forms

*Yunosuke Nagafusa[1], Tima Sergienko[2], Satoshi Taguchi[1], Urban Braendstroem[2], Masatoshi Yamauchi[2] (1.Graduate School of Science, Kyoto University, 2.Swedish Institute of Space Physics, Kiruna)

[PEM11-P21] Observations of MF/HF auroral radio emissions at three ground-based stations

*Yuka Sato[1], Atsushi Kumamoto[2], Yuto Katoh[2], Akira Kadokura[3,4], Yasunobu Ogawa[3,4], Atsuki Shinbori[5] (1.Nippon Institute of Technology (NIT), 2.Graduate School of Science, Tohoku University, 3.National Institute of Polar Research (NIPR), 4.The Graduate University for Advanced Studies, 5.Institute for Space-Earth Environmental Research (ISEE), Nagoya University)

[PEM11-P22] **Ionospheric F-region Drift Measurements Derived from DPS-4D at Zhongshan Station, Antarctic**

*Xiangcai Chen[1] (1.Polar Research Institute of China)

[PEM11-P23] PARM-HEP Observation of Precipitating High Energy Electrons over Pulsating Aurora

*Taku Namekawa[1], Takefumi Mitani[2], Kazushi Asamura[2], Yoshifumi Saito[2] (1.Department of Earth and Planetary Science, Graduate school of Science, The University of Tokyo, 2.Institute of Space and Astronautical Science, Japan Aerospace Exploration Agency)

[PEM11-P24] Development of the medium-energy electron detector with hemispherical field-of-view and the flight test in the PARM (Pulsating AuRora and Microburst) mission

*Shin Sugo[1], Oya Kawashima[1], Kazushi Asamura[2], Reiko Nomura[3], Yasunobu Ogawa[4], Keisuke Hosokawa[5], Yoshizumi Miyoshi[6], Takefumi Mitani[2], Taku Namekawa[1,2], Takeshi Sakanoi[7], Mizuki Fukizawa[7], Naoshi Yagi[7], Satoshi Kasahara[1] (1.The University of Tokyo, 2.Institute of Space and Astronautical Science, Japan Aerospace Exploration Agency, 3.National Astronomical Observatory of Japan, 4.National Institute of Polar Research, 5.The University of Electro-Communications, 6.Institute for Space-Earth Environmental Research, Nagoya University, 7.Tohoku University)

[PEM11-P25] Auroral substorm onset in satellite-based global images and ground-based all-sky images

*Akimasa Ieda[1], Kirsti Kauristie[2], Yukitoshi Nishimura[3], Yukinaga Miyashita[4], Harald U Frey[5], Liisa Juusola[2], Daniel Whiter[6], Masahito Nose[7], Matthew O Fillingim[5], Farideh Honary[8], Neil C Rogers[8], Yoshizumi Miyoshi[1], Shinobu Machida[1] (1.Institute for Space-Earth Environmental Research, Nagoya University, 2.Finnish Meteorological Institute, 3.Boston university, 4.Korea Astronomy and Space Science Institute, 5.University of California Berkeley, 6.University of Southampton, 7.Graduate School of Science, Kyoto University, 8.Lancaster University)

[PEM11-P26] Automatic Classification of Auroral images using optical flow feature

*Naoto Kashiwagi[1], Akiko Fujimoto[1], Terumasa Tokunaga[1], Yoshizumi Miyoshi[2], Yasunobu Ogawa[3], Keisuke Hosokawa[4] (1.Kyushu Institute of Technology, 2.Nagoya University, 3.National Institute of Polar Research, 4.The University of Electro-Communications)

[PEM11-P27] Fine-scale visualization of aurora in a wide area using color digital camera images from the International Space Station

*Sota Nanjo[1], Yuta Hozumi[1], Keisuke Hosokawa[1] (1.The University of Electro-Communications)

[PEM11-P28] Geospace Imaging via the soft X-ray imager: GEO-X mission

*Yoshizumi Miyoshi[1], Yuichiro Ezoe[2], Satoshi Kasahara[3], Yosuke Matsumoto[4], Kumi Ishikawa[5], Ryuho Kataoka[6], Hiroki Ito[1], Daiki Ishi[2], Masaki Numazawa[2], Atsushi Yamazaki[5], Hiroshi Hasegawa[5], Masaki Fujimoto[5], Kazuhisa Mitsuda[5] (1.Institute for Space-Earth Environmental Research, Nagoya University, 2.Tokyo Metropolitan University, 3.University of Tokyo, 4.Chiba University, 5.ISAS/JAXA, 6.NIPR)

Effects of Inclination/Rotation of Earth’s Magnetic Axis on Magnetosphere Simulated by Global MHD Model

*Aoi Nakamizo[1]

1. Applied Electromagnetic Research Institute, National Institute of Information and Communications Technology

Recently, we have shown that the ionospheric Hall conductance distribution, owing to the polarization field generated by its nonuniformity, largely control the magnetospheric configuration and dynamics by using a global MHD model. The effects of the ionospheric conductance on the magnetosphere were also reported by previous studies based on other global models; for example, the current-voltage relationship in the solar wind-magnetosphere-ionosphere [Fedder and Lyon, 1987] and the plasma pressure distribution in the near-Earth region [Ridley et al., 2004]. These studies indicate that the ionospheric conductance is one of the most important settings in the global models to accurately simulate the magnetosphere.

On the other hand, in the development/improvement of the global MHD model in NICT, which was originally developed by Tanaka [1994] and Tanaka et al. [2010], introducing the inclination and rotation of Earth’s magnetic axis with respect to the rotation axis has been remained as one of the most difficult problems. In other words, in the present model, the precession between the magnetic axis and the rotation axis is not included. This means that the simulated magnetosphere will show a different structure and temporal development than the actual magnetosphere.

We, for the first time, equivalently introduce the precession by rotating the background conductance distribution due to solar illumination (i.e., depending on the geographic coordinate) with respect to the geomagnetic coordinate. (Improvement of the conductance setting in the auroral region is the next challenge.) In this paper, we will show how the simulated magnetosphere is changed by this improvement, focusing on the near-Earth plasma environment.

Keywords: M-I Coupling, Global MHD Simulation, Ionospheric Effect

©2019. Japan Geoscience Union. All Right Reserved.

Asymmetric deformation of the magnetosphere under low-density solar wind

*Masaki N Nishino[1,2], Yoshifumi Saito[2], Kazuo Shiokawa[1], Masaki Fujimoto[2]

1. Institute for Space-Earth Environmental Research, Nagoya University, 2. JAXA/ISAS

The density of the solar wind around the Earth's magnetosphere sometimes decreases to only several percent of the usual value, and such density extrema results in a significant reduction of dynamic pressure and Alfvenic Mach number of the solar wind flow. While simple expansion of the Earth's magnetosphere by the low dynamic pressure was assumed in previous studies, a global-MHD simulation study predicted a remarkable dawn-dusk asymmetry of the magnetosphere in shape under low-density solar wind and Parker-spiral IMF configuration. Here we present evidence of asymmetric deformation of the magnetosphere under low-density solar wind and Parker-spiral IMF conditions, based on several events of GEOTAIL observations. As predicted by the global-MHD simulation, the magnetosphere on the dawnside expands much further than the magnetopause location of simple (symmetric) expansion, while no significant expansion is detected in the dusk tail flank. Fast ion beams detected at the flank magnetopause suggest that magnetic reconnection frequently occurs due to the low-beta environment of the magnetosheath.

Keywords: Low density solar wind, Magnetosphere, Plasma transport

©2019. Japan Geoscience Union. All Right Reserved.

New perspectives on coupling processes in solar-terrestrial system obtained by comprehensive data analysis

*Yoshimasa Tanaka[1], Norio Umemura[2], Shuji Abe[3], Satoru UeNo[4], Masahito Nose[2], Yumi Nakagawa[5]

1. National Institute of Polar Research, 2. Institute for Space-Earth Environmental Research, Nagoya University, 3. International Center for Space Weather Science and Education, 4. Kwasan & Hida Observatories, School of Science, Kyoto University, 5. Ibaraki University

In the Earth’ s upper atmosphere above 60 km, including magnetosphere and ionosphere, various phenomena are generated by energy inputs from solar radiation (including solar wind) and atmospheric waves propagating from the lower atmosphere. Thus, comprehensive analysis of various kinds of satellite and ground-based observational data using advanced methods is required to understand physical mechanism of the phenomena. For such interdisciplinary studies, it is important to share data distributed across many universities and institutes and use advanced tools, such as metadata database for cross-searching a variety of datasets and analysis software for analyzing various types of data in an integrated fashion. In fact, many scientific papers on the upper atmosphere have recently been obtained by comprehensive analysis of various data with such analysis tools.
We present some examples of scientific results achieved by comprehensively analyzing data from multiple regions. These examples include the effect of solar coronal holes on the Earth’ s geomagnetic activity and the interaction between solar wind, magnetosphere, ionosphere and neutral atmosphere. The former study investigated long-term trends of coronal boles, solar wind parameters, and Earth’ s geomagnetic indices during two solar cycles. It showed the possibility that the solar wind speed and geomagnetic activities may be controlled by the size and latitudinal distribution of coronal holes. The latter analyzed multi-instrument data simultaneously obtained from interplanetary space, magnetosphere, and ionosphere and mesosphere in both northern and southern hemispheres. They newly found that the polar mesosphere is affected by relativistic electron precipitation caused by the interaction with magnetospheric plasma waves during the high-speed solar wind stream. These studies demonstrate that sharing and comprehensive analysis of long-term, multiple-sphere, and multi-instrument data using sophisticated tools are very effective to produce scientific outcomes. At present there are data gap areas in the Asia and African regions. Therefore, we believe that filling in the data gap by international collaborations could be a breakthrough for unsolved issues in the upper atmosphere.

Keywords: upper atmosphere, coupling between multiple regions, comprehensive analysis, long-term observational data

©2019. Japan Geoscience Union. All Right Reserved.

The interaction between the magnetosphere-ionosphere compound system and the magnetic field topology

*Shigeru Fujita[1], Takashi Tanaka[2], Masakazu Watanabe[2]

1. Meteorological College, Japan Meteorological Agency/ Nationa Institute of Polar Research, 2. Kyushu University

The steady convection in the magnetosphere-ionosphere coupling system is composed of the following self-consistent elementary processes; dynamo in the cusp-mantle region, the field-perpendicular current system in the magnetosphere, the field-aligned current system connecting the ionosphere, the ionospheric electric field, the magnetospheric convection corresponding to the ionospheric electric field, and the high plasma pressure distribution in the cusp region [Tanaka, 2007].

The energy of the convection is transported from the solar wind across the magnetopause where the magnetic field configures the null-separator structure. Since the magnetic field configuration of the null-separator structure is originally derived from the superposition of two scalar fields [Stern, 1973], say, the dipole field and the uniform field, the magnetic field of the null-separator would not have free energy necessary for plasma acceleration. However, the simulation reveals that the magnetic field has a tension force near the null point. Therefore, we need a mechanism that transports the energy to this region.

It is revealed from the simulation that the bow shock supplies the energy. Indeed, the current from the bow shock deforms the magnetic field of the null-separator structure. In addition, it is noted that the Chapman-Ferraro current also deforms the magnetic field configuration in the magnetopause. This fact indicates that the convection system in the magnetosphere contributes to deformation of the null-separator structure. That is to say, energy transport from the solar wind to the magnetosphere-ionosphere compound system is affected by the physical processes in the convection. Therefore, as a result of the interaction between the magnetosphere-ionosphere convection and the null-separator structure, the magnetosphere-ionosphere compound system can be extended to the solar wind-magnetosphere-ionosphere compound system.

References

T. Tanaka (2007), Magnetosphere-Ionosphere Convection as a Compound System, Space Sci Rev, 133, 1-72, DOI 10.1007/s11214-007-9168-4.

Stern, D. P. (1973), A study of the electric field in an open magnetospheric model, J. Geophys. Res., 78(31), 7292-7305, doi:10.1029/JA078i031p07292.

Keywords: global MHD simulation, compound system

©2019. Japan Geoscience Union. All Right Reserved.

Effects of the dipole tilt and the interplanetary magnetic field Bx component on the dawn-dusk and interhemispheric asymmetries of the interchange convection cycle

*Masakazu Watanabe[1,2], Takashi Tanaka[2], Shigeru Fujita[3,4]

1. Graduate School of Science, Kyushu University, 2. International Center for Space Weather Science and Education, Kyushu University, 3. Meteorological College, 4. National Institute of Polar Research

The interchange cycle is a mode of magnetic flux circulation that appears for periods of northward interplanetary magnetic field (IMF). It is made up of IMF-to-open reconnection in one hemisphere and open-to-closed reconnection in the other hemisphere. The two reconnection processes have the same topological nature in that the roles of the two reconnecting field lines interchange at the time of reconnection. The interchange cycle is characterized by reciprocation of open magnetic flux between the two hemispheres. One observable signature of the interchange cycle is an appearance of a reverse cell circulating in the closed field line region of the ionosphere, which is named the “reciprocal cell.” The reciprocal cell appears in the open-to-closed reconnection hemisphere, whereas in the opposite IMF-to-open reconnection hemisphere, there appears a lobe cell circulating exclusively on open field lines. For given (1) IMF By, (2) IMF Bx, and (3) dipole tilt conditions, two interchange cycles concur, one on the dawnside and the other on the duskside. For an ideal case, one can easily expect the mode of the interchange cycles to occur. For example, for the case of due northward IMF with significant dipole tilt, the twin reverse cells in the summer hemisphere are both lobe cells, while in the winter hemisphere the twin reverse cells are both reciprocal cells. For the general case, however, one cannot predict the mode of the interchange cycles without quantitative modeling. The purpose of this study is to examine how the presence of dipole tilt or IMF Bx alters the dawn-dusk and north-south pattern of the twin reverse cells. For this purpose, we perform numerical magnetohydrodynamic simulations using the REPPU (Reproduce Plasma Universe) code developed by T. Tanaka. In the presentation, we discuss the dipole tilt and IMF Bx effects revealed by the numerical modeling.

Keywords: ionospheric convection, interchange reconnection, reciprocal cell

©2019. Japan Geoscience Union. All Right Reserved.

Transient polar ionospheric convection response to negative dynamic pressure pulse

*Jianjun Liu[1]

1. Polar Research Institute of China

The response of the high latitude ionospheric convection to a sudden decrease in solar wind dynamic pressure provides a unique opportunity to investigate how the solar wind couples to the dayside magnetosphere and ionosphere. Here, the event shows three IMF components do not have prominent changes, but the solar wind plasma went down to near zero magnitude, which leads to very weak solar wind driving during northward IMF. However, ionospheric convection observed by SuperDARN radars showed enhanced plasma flow speed in the central polar cap region just after the negative pressure pulse arrival to the magnetosphere. Simultaneous convection map generated by SuperDARN measurement presents enlarged convection cell with obvious equatorward moving Heppner-Maynard boundary. It is noted that cross polar cap potential enhanced instantly and this enhanced feature continued almost 10 min. The distribution of total electron content (TEC) exhibited typical auroral oval signature especially on dayside ionosphere, TEC density in auroral oval showed a noticeable decrease after the arrival of the negative pressure pulse. Both ionospheric convection and TEC distribution reveal that negative pressure pulse impacts the magnetosphere-ionosphere coupling system directly and dramatically. Moreover, the TIEGCM model also showed an enhanced polar potential pattern.

Keywords: Dynamic pressure, Ionospheric convection, Auroral oval

©2019. Japan Geoscience Union. All Right Reserved.

An active ionosphere: a new perspective of field line dipolarization

*Osuke Saka[1]

1. Office Geophysik

Transient westward electric fields from the magnetosphere generate equatorward plasma drifts of the order of kilometers per second in the auroral ionosphere. This flow channel extends in north-south directions and is produced in the initial pulse of Pi2 pulsations associated with the filed line dipolarization. Drifts in the ionosphere of the order of kilometers per second that accumulated plasmas at the low latitude end of the flow channel are of such large degree that possible vertical transport effects (including precipitation) along the field lines may be ignored. We suggest that plasma compression in the ionosphere implemented the ionosphere to be active. Active ionosphere generates field-aligned currents to satisfy the quasi-neutrality of the ionosphere, ion acoustic wave for ion outflows and the inverted-V type electron precipitations in the topside ionosphere, and poleward expansion of auroras due to a nonlinear evolution of the ionosphere. We will study auroral expansion in this acoustic regime.

Keywords: Substorm, Auroral substorm, Ionosphere

©2019. Japan Geoscience Union. All Right Reserved.

Toward the automatic identification of FLR signals in the SuperDARN data by using the gradient method

*Hideaki Kawano[1,2], Akira Sessai Yukimatu[3,4], Nozomu Nishitani[5], Yoshimasa Tanaka[3,4], Satoko Saita[6], Tomoaki Hori[5]

1. Dept. Earth Planet. Sci., Kyushu Univ., 2. ICSWSE, Kyushu University, 3. National Institute of Polar Research, 4. SOKENDAI, 5. ISEE, Nagoya University, 6. Kitakyushu College

The FLR (Field Line Resonance) takes place where the frequency of an incoming wave matches the eigen-frequency of magnetospheric magnetic field lines, and excites the eigen-oscillation of the field lines. The FLR can be identified by using the unique manner of change in the amplitude and the phase of thus excited eigen-oscillation across the resonant point. That is, the amplitude is maximum at the resonant point, and the phase changes the most steeply across the resonance point. The FLR-generated eigen-oscillations can be identified in the ground magnetic field data and the ionospheric plasma velocity data. From thus identified eigen-frequency ("FLR frequency" below) one can estimate the magnetospheric plasma density along the field line which passes through the ground/ionospheric observation point.

In this study we use the SuperDARN radar data to identify FLR: For each radar beam from each SuperDARN radar, the velocity of the ionospheric plasma flow along the line of sight (VLOS) of the beam is obtained; we use the VLOS data to identify the FLR and estimate the magnetospheric plasma density. Unlike the ground magnetometer data, the SuperDARN data is two-dimensional, enabling two-dimensional estimates of the magnetospheric equatorial plasma density and magnetospheric region identification.

To achieve that, it is important to identify as many FLR events as possible. Overwrapping of non-FLR waves/perturbations hides FLR events. As a countermeasure to this problem, the so-called gradient method has been applied to the ground magnetometer data; this method cancels out the overwrapping signals by dividing the data from a magnetometer by the data from another magnetometer having an adequate latitudinal distance from the other. The division yields the amplitude ratio and the phase difference. The gradient method is effective since the FLR frequency tends to depend on the latitude more strongly than the overwrapping signals.

The gradient method is also applicable to the SuperDARN VLOS data. The field of view of each beam is divided into Range Gates (RGs below) having the same length along the beam. The identification number of the RGs increases with increasing distance from the radar. The VLOS is obtained for each RG. Thus, each RG can be regarded as a "virtual observatory."

As an initial study, we have selected an FLR event which was identified in the VLOS data of a radar (at Hankasalmi) without the use of the gradient method, selected a beam, and selected a few pairs of RGs of the beam. We then have manually applied the gradient method to the VLOS data of the above-selected RG pairs, and successfully identified the FLR. In more detail, the identification has been successful only for two paired RGs whose RG numbers differs by two. This suggest that, since the length of the RG, mapped to the meridional plane, was about 40km for this event, about 80km distance was the best (with the resolution of 40km) for this event. This distance reflects the resonance width, which is an important quantity reflecting the diffusion and dissipation of the FLR energy.

©2019. Japan Geoscience Union. All Right Reserved.

In order to identify as many FLR events as possible, it is also important to automatically identify the FLR events, since visual identification is time-consuming. The gradient method enables automatic identification more easily than analyses of VLOS itself, since the gradient method yields peaks in both the amplitude ratio and the phase difference. We have started making a program for automatic identification by applying the gradient method to VLOS; the version at the time of this abstract has successfully identified FLRs for all of the above-stated pairs of RGs.

©2019. Japan Geoscience Union. All Right Reserved.

A statistical study of Pi2 pulsations observed in the upper ionosphere using Swarm magnetic field data

*Park Jaehee[1], Khan-Hyuk Kim[1], Junga Hwang[2]

1. School of Space Research, Kyung Hee University, Gyeonggi, South Korea, 2. Korea Astronomy and Space Science Institute, Daejeon,South Korea

The properties of Pi2 pulsations observed in the upper ionosphere are studied using magnetic field data acquired by the Swarm-A spacecraft in low Earth orbit (LEO) and at the low-latitude Bohyun ground station (BOH, L = 1,3) for January 2014-Jun 2015. From time intervals when Swarm-A was on the nightside (magnetic local time (MLT) = 1800-0600 hrs) and the BOH station was near midnight (MLT = 2100-0300 hrs), we identified 623 Pi2 events in the horizontal H component of the BOH data. For each event we examine the coherence between the horizontal H component on the ground and the B_x (radial) azimuthal B_y (azimuthal), or B_z (compressional) components at Swarm-A. Out of 623 events, the B_x-H high coherence (> 0.7) events are ~6%, the B_y-H high coherence events are ~4%, and the B_z-H high coherence events are ~25%. The ground-satellite high coherence events occurred when the spacecraft was located within a magnetic latitude range of ±50°. Using the ground-satellite high coherence events, we examined the latitudinal structure of the relative amplitude and phase of the ionospheric Pi2 pulsations detected at Swarm-A. Confirming previous observations at LEO, we found that the ionospheric Pi2 pulsations are characterized by symmetric odd mode standing oscillations in the north-south direction, having a node for B_x oscillation and an antinode for B_z oscillation, respectively, at the equator. This indicates that the source of ionospheric Pi2 pulsations is the plasmaspheric resonance.

Keywords: Pi2 pulsations

©2019. Japan Geoscience Union. All Right Reserved.

Study on the global distribution characteristics of Pc 1-2 geomagnetic pulsation with the 10Hz data of the MAGDAS system

*Taisei Kabasawa[1], Akimasa Yoshikawa[1], Teiji Uozumi[1], Akiko Fujimoto[1], Shuji Abe[1]

1. Kyushu University

The magnetic field observed on the ground is affected by the space weather phenomena such as magnetic storms and auroral storms.

The Pc1 geomagnetic pulsation (frequency range of 0.2-5.0 seconds) activated mainly around a high-latitude region is understood as a phenomenon accompanied by the excitation of EMIC waves to cause the particle acceleration in the equatorial region of the magnetosphere. Also, it is well known that Pc1 waves propagate horizontally in the ionospheric at the F layer. However, it is not clarified about the global occurrence and propagation properties of Pc1 geomagnetic pulsation on the ground. Moreover, although induction magnetometers are used to observe the high-frequency magnetic field disturbance phenomenon like Pc1 and Pc2 (frequency range of 5.0-10.0 seconds) geomagnetic pulsation, the global observation network with induction magnetometers covering from high-latitude to low-latitude area and equator domain does not exist at this stage. On the other hand, although it is common to use Fluxgate magnetometers for the observation of global space weather phenomenon, it is considered to be unsuitable for analysis of the high-frequency Pc1-2 geomagnetic pulsation because its time accuracy is usually one second value.

The ground multipoint magnetic field observation network which Kyushu University has developed (MAGDAS-9 magnetometer) acquire a 250Hz sampling and 10Hz mean data. Also, it is the only geomagnetic observation network that can investigate the global aspects of Pc1-2 geomagnetic pulsation.

In this study, we investigated the global distribution of Pc1-2 pulsation from polar region to equatorial region with magnetic field data provided by MAGDAS and Dst/AE index provided by the WDC for Geomagnetism, Kyoto. As a result, when the substorm have occurred during a magnetic storm time, generation of Pc1-2 pulsation from high-latitude to middle-and-low latitude region and further arrival of Pc2 pulsation to the dip-equator are identified. The elucidation of occurrence characteristic of the Pc1-2 pulsation on the ground with the EMIC waves excitation is very important not only for space weather application to be able to monitor particle energization process via EMIC excitation but also the elucidation of the super global coupling process from inner magnetosphere to the global ionosphere from polar to equatorial region. In this presentation, we will report the preliminary results of observational analysis of Pc1-2 pulsation by using MAGDAS network. We also discuss the comprehensive approach for understanding global coupling process among inner magnetosphere and high-middle-low latitude to the equatorial region by using FM-CW radar data, PWING induction magnetometer data, and the geo-space environment data from the ERG satellite.

Keywords: Pc1-2 pulsation, EMIC waves, global coupling

©2019. Japan Geoscience Union. All Right Reserved.

In-situ Observations of Reconnection Separatrix Regions in the near-Earth Magnetotail

*Mizuho Araki[1], Masahiro Hoshino[1], Kunihiro Keika[1], Yoshifumi Saito[2]

1. Graduate School of Science, The University of Tokyo, 2. Institude of Space and Astronautical Science

Magnetic reconnection which converts magnetic energy into thermal and kinetic energy of plasmas is an important physical mechanism of plasma heating and acceleration. Particularly in the Petschek-type reconnection, plasma acceleration and heating in the slow-mode shocks formed at the separatrices must be taken into consideration. The structure of the slow-mode shocks in the distant tail of the Earth’s magnetosphere was investigated with in-situ observations made by the GEOTAIL satellite (Saito et.al, 1995). It is observationally suggested that about 10% of the plasma sheet boundary layer (PSBL) is slow-mode shocks. It is, however, not fully understood what determines this percentage and what is the difference in the ion and electron temperature changes between slow-mode shocks and others separatrix regions.
In this study, we utilized multi-spacecraft in-situ observations of separatrix regions at magnetic reconnection in the near-Earth magnetotail (GSM-X is between ~13 and ~25RE). We used data obtained from FPI (Fast Plasma Investigation) and FGM (Fluxgate Magnetometer) on board the MMS satellite from June 1, 2017to August 31, 2017. We examined occurrence locations, ion flow directions and velocity of ion flow in downstream regions of observed events. We also examined changes in ion and electron temperatures and the ion-to-electron temperature ratio.

We classified their events into 2 types according to plasma beta in the in-flow regions: below 0.1 or around 1. We term them “lobe reconnection” and “plasma sheet reconnection”, respectively. In the former type, plasmas in the in-flow regions are cold and tenuous. In the latter type, plasmas in the in-flow regions are hot and dense. In both types, we observed increases in ion and electron temperatures increase, but their characteristics are different. In the lobe reconnection, ion temperatures increase from several hundred eV to several keV. In the plasma sheet reconnection, ion temperatures also increase from about 1 keV to several keV. The increase rate of the electron temperature is less than one order of magnitude for both types, smaller than that of the ion temperature; the electron temperature increases up to at most 1 keV. The ion-to-electron temperature ratio in the out-flow regions in both types is about 5 for both types. We then examined changes of the ion-to-electron temperature ratio and found that the changes are consistent with the result reported by Wang et al. (2012).

In this presentation, we will show the results of separatrix crossing events (both lobe and plasma sheet reconnection events) that occur in 2017 and 2018. We will identify whether each of the separatrices is a slow shock or not and how the separatrix conditions affect ion and electron heating. These characteristics will provide insights into heating mechanisms and energy conversion through separatrix regions.

Reference:

Yoshifumi Saito, Toshifumi Mukai, Toshio Terasawa, Atsuhiro Nishida, Shinobu Machida, Masafumi Hirahara, Kiyoshi Maezawa, Susumu Kokubun, and Tatsundo Yamamoto, Slow-mode shocks in the magneto, J. Geophys. Res., 100, A12, 23,567, 1995

©2019. Japan Geoscience Union. All Right Reserved.

Chih-Ping Wang, Matina Gkioulidou, Larry R. Lyons and Vassilis Angelopoulos, Spatial distributions of ion to electron temperature ratio in the magnetosheath and plasma sheet, J. Geophys. Res., 117, A08215, 2012

Keywords: Magnetic Reconnection, MMS satellite, Earth's Magnetotail

©2019. Japan Geoscience Union. All Right Reserved.

Flow speed dependence of ion temperature, electron temperature, and their ratio in the near-Earth magnetotail reconnection region

*Kaori Watanabe[1], Masahiro Hoshino[1], Kunihiro Keika[1], Yoshifumi Saito[2], Naritoshi Kitamura[1]

1. Univ. of Tokyo, 2. ISAS/JAXA

Plasma in the Earth's magnetotail are heated up to 1-10 keV and stored in the plasma sheet. One of the heating or acceleration mechanisms is the magnetic reconnection. Heated or accelerated plasma are transported both earthward and tailward as fast flow with a speed of several hundred kilometers per second. However, what determines the partition among ion and electron thermal energy and kinetic energy is an unresolved problem. It has been reported that ion temperature T_i, electron temperature T_e, and their ratio T_i/T_e vary spatially and depend on the conditions of fast flows [Wang et al., 2012, Runov et al., 2018] but there are few studies which focus on macroscopic profiles of them in reconnection regions in the magnetotail.

In this study, we examine the relation between flow speed and average profiles of T_i, T_e, and T_i/T_e in the magnetotail reconnection region by using data obtained from FPI and FGM on board the MMS spacecraft. We use the observations for a period from May to August 2017 and take out the data in the region of $X_{GSM} < -15$ Re, -10 Re $< Y_{GSM} < 10$ Re, and beta > 0.1. We then divide them into different groups according to flow speed normalized by alfven speed and show B_z/B_{lobe}– B_x/B_{lobe} maps of T_i, T_e, and T_i/T_e of each group. The results show that ion temperature increase with increasing flow speed while electron temperature decrease. Ion temperature are hotter around the X-point. The structure of inflow and outflow regions is pronounced in the profile of electron temperature. T_i/T_e in inflow region are greater than in outflow region, which means that ion and electron temperatures become comparable by passing through the diffusion region. The results suggest that electron get less energy when more energy is partitioned into plasma kinetic energy. We will discuss about the profiles of anisotropy of plasma temperatures to know more details about the heating mechanisms.

Keywords: temperature ratio, flow, MMS

©2019. Japan Geoscience Union. All Right Reserved.

Examining Minimum Cyclotron Resonant Electron Energy of EMIC Waves with MMS

*Si Liu[1]

1. Changsha University of Science and Technology

Electromagnetic ion cyclotron (EMIC) waves can be in cyclotron resonance with relativistic electrons, causing relativistic electron precipitation. The four ideal Magnetospheric Multiscale (MMS) spacecraft provide great opportunity to directly calculate the wave vector ***k*** of EMIC waves by phase differencing technique and hence estimate the minimum resonant energy by the resonance condition. Deriving a simplified analytic solution, we find that the phase differencing method can still provide an estimate of the dominant wave number when a finite wave number spread or a finite frequency spread is present. Numerical calculations indicate that quasi-antiparallel propagation dominates the EMIC event on 20 November 2015, which is consistent with the FFT spectral analysis results. We also find that obtained wave vectors, roughly agreeing with the validity of cold plasma theory, might significantly vary from wave packet to wave packet. Moreover, minimum resonant electron energies gradually increase from 0.5 MeV to tens of MeV with a decreasing parallel componet of ***k***. Current results provide evidence that EMIC waves can be in resonance with the electrons of energies down to hundreds of keV. It further demonstrates that EMIC waves in a narrow frequency band can effectively interact with the relativistic electrons with a broad energy range.

Keywords: EMIC waves, minimum resonant electron energy, wave vector, phase differencing

©2019. Japan Geoscience Union. All Right Reserved.

Small scale whistler mode waves near the magnetic field intensity minimum in the magnetosheath

*Naritoshi Kitamura[1], Takanobu Amano[1], Yoshiharu Omura[2], Satoko Nakamura[2], Chika Umegaki[1], Scott A Boardsen[3,4], Narges Ahmadi[5], Robert E Ergun[5], Olivier Le Contel[6], Per-Arne Lindqvist[7], Yoshifumi Saito[8], Shoichiro Yokota[9], Daniel J Gershman[3], Barbara L Giles[3], Thomas E Moore[3], William R Paterson[3], Craig J Pollock[10], Christopher T Russell[11], Robert J Strangeway[11], James L Burch[12]

1. Department of Earth and Planetary Science, Graduate School of Science, The University of Tokyo, 2. Research Institute for Sustainable Humanosphere, Kyoto University, 3. NASA Goddard Space Flight Center, 4. University of Maryland, 5. Laboratory for Atmospheric and Space Physics, University of Colorado, 6. Laboratoire de Physique des Plasmas, UMR7648 CNRS/Ecole Polytechnique/UPMC/Université Paris-Sud/Observatoire de Paris, 7. Royal Institute of Technology, 8. Institute of Space and Astronautical Science, Japan Aerospace Exploration Agency, 9. Department of Earth and Space Science, Graduate School of Science, Osaka University, 10. Denali Scientific, 11. Institute of Geophysics and Planetary Physics, University of California, Los Angeles, 12. Southwest Research Institute

Wave-particle interactions are thought to play a crucial role in energy transfer in collisionless space plasmas in which the motion of charged particles is controlled by electromagnetic fields. In the terrestrial magnetosheath, intense whistler mode waves, called 'Lion roars', are often detected by spacecraft around minima of semi-periodic fluctuations of magnetic field intensity due to mirror mode structures and motion of the structures. It is expected that whistler mode waves are efficiently generated near a local minimum of magnetic field intensity due to the smallest cyclotron resonance velocity. We report the detailed characteristics of such whistler mode waves using the data obtained by the four MMS (Magnetospheric Multiscale) spacecraft. Because reversals of field-aligned component of Poynting flux around minima in mirror mode structures correspond to reversals of gradient of magnetic field intensity along the magnetic field, whistler mode events with reversals of the field-aligned component of Poynting flux are good candidates of observations of effective wave generation regions along field lines. Even in such events, phase difference and change of amplitude of whistler mode waves observed by the four spacecraft do not have a clear correlation in cases of ~40 km separation, which is much smaller than the spatial scale of magnetic field depression due to mirror mode structures and is even smaller than the local thermal ion gyro scale. This result indicates that the coherent whistler wave generation in mirror mode structures has very limited spatial scale across field lines and is probably affected by any electron scale process. A plane wave approximation can be usable only in a very small scale. Because some events in cases of ~7 km separation showed good correlation among four spacecraft, the typical scale of coherent whistler wave across field lines can be at least an order of 10 km in mirror mode structures in the terrestrial magnetosheath. The whistler mode waves observed by a spacecraft in a mirror mode structure are a cluster of waves from multiple spatially small sources.

Keywords: Whistler mode wave, Plasma wave, MMS spacecraft, Wave-particle interaction

©2019. Japan Geoscience Union. All Right Reserved.

Spatial characteristics of the internal modulation of pulsating aurora: multi-point high-speed optical observations in Scandinavia

*Yuki Kawamura[1], Keisuke Hosokawa[1], Shin-ichiro Oyama[2,3], Yoshizumi Miyoshi[2], Yasunobu Ogawa[3], Satoshi Kurita[2], Satoshi Ebukuro[1], Ryoichi Fujii[4]

1. Department of Communication Engineering and Informatics, University of Electro-Communications, 2. Institute for Space-Earth Environmental Research, Nagoya University, 3. National Institute of Polar Research, 4. Research Organization of Information and Systems

Pulsating aurora (PsA) is a kind of diffuse aurora which almost always appears in the morning side during the recovery phase of auroral substorm. PsA typically has two characteristic temporal variations. One is so-called main pulsation whose period ranges from a few to a few tens of seconds. The other is a few Hz brightness modulation (internal modulation) which is often seen during the ON time of the main pulsation. Previous studies have suggested that the temporal variation of PsA is characterized by wave-particle interaction between whistler-mode chorus waves and high energy electrons in the magnetosphere. Especially, it has been indicated that there is one to one correspondence between the amplitude variation of chorus waves and the luminosity modulation of PsA.
Recent studies revealed the occurrence distribution of the frequency of the internal modulation. However, there have been no studies which analyzed the spatial distribution of the internal modulation.

To reveal the spatial characteristics of the internal modulation, we need to perform a frequency analysis of the internal modulation by using data from high speed optical instruments having wide spatial coverage. For this purpose, we make use of highly sensitive EMCCD cameras which have been operated in Sodankylä and Kevo in Finland, Tromsø in Norway, and Tjautjas in Sweden. In these observations, all-sky images are taken with a sampling rate of 100 Hz, which is sufficient to identify temporal variations of the internal modulation.

In the frequency analysis, we have employed all-sky images taken on March 15, 2018 (00:00 –01:30 UT) in Sodankylä, Kevo, Tromsø, and Tjautjas. We computed the average frequency of the internal modulation from each pixel of the EMCCD cameras and derived the spatial distribution of their dominant frequencies. Regardless of the latitude, each pulsating patch was fluctuating at a similar frequency. We also derived the frequency spectrum of several pulsating patches existing at different positions in the north-south direction and found that those frequency spectrums of pulsating patches have peaks at about 3 Hz. These results indicate that the frequency of the internal modulation does not depend on the magnetic latitude, and the frequency of the internal modulation is collimated on 3 Hz.
In the presentation, we discuss why the frequency of the internal modulation concentrate on 3 Hz by taking into account the time of flight of PsA electrons.

Keywords: Pulsating aurora, Internal modulation

©2019. Japan Geoscience Union. All Right Reserved.

Large-scale characteristics of pulsating aurora periodicities: multi-point high-speed optical observations in Scandinavia

*Satoshi Ebukuro[1], Keisuke Hosokawa[1], Shin-ichiro Oyama[2,3,5], Yoshizumi Miyoshi[2], Yasunobu Ogawa[3], Satoshi Kurita[2], Yuki Kawamura[1], Ryoichi Fujii[4]

1. Department of Communication Engineering and Informatics, University of Electro-Communications, 2. Institute for Space-Earth Environmental Research, Nagoya University, 3. National Institute of Polar Research, 4. Research Organization of Information and Systems, 5. University of Oulu

It has been known that most of diffuse aurorae in the morning side are composed of luminous patches whose brightness modulates quasi-periodically. Such aurorae are termed as pulsating aurora (PsA) and have been studied extensively in the last decade. PsA patches have a scale size of a few hundreds of km and are usually observed during the late recovery phase of substorms. The entire temporal variation of PsA consists of two individual modulations: main pulsation and internal modulation. The periodicity of the main pulsation ranges from a few to a few tens of seconds and the internal modulation, showing a few Hz scintillating luminosity changes, is often embedded within the ON time of the main pulsation. Previous studies using satellites indicated one-to-one correlation between PsA and chorus wave near the equatorial plane of the magnetosphere, suggesting that ground-based observations of PsA can be used for mapping the activity of chorus in the magnetosphere in 2D fashion. In the past, the spatial characteristics of chorus wave have not visualized in detail because satellite observations only cover a single point in the magnetosphere. To overcome this limitation, we derive the spatial distribution of chorus waves by using ground-based optical observations of PsA and discuss the ambient parameters which characterize the nature of chorus.
For this purpose, we have employed data from electron multiplying charge-coupled device (EMCCD) cameras deployed at multiple sites in Scandinavia to derive the large-scale characteristics of PsA. EMCCD cameras have been operative in Kevo and Sodankyla in Finland, Tromsoe in Norway, and Tjautjas in Sweden and their temporal resolution is 100 Hz. We conducted a frequency analysis for a PsA event on March 28, 2017 (23:30 to 24:10 UT). During the event studied, there existed three different regions of PsA, regions A, B and C, showing different modulation periods. It was also found that the boundaries between these three regions were sharp. We derived the 2D frequency map by using data from all the available stations. As a result, it became clear that the higher latitude region (region C) showed faster internal modulation than the lower latitude region (region A). In addition, region B, which was sandwiched by regions A and C, did not show any internal modulations (i.e., main pulsation without internal modulation). In the presentation, we discuss why the three regions showed different modulation periods with sharp boundaries. In particular, we address what ambient conditions can control the absence of internal modulation in region B. We also derived similar frequency maps of chorus waves by tracing the PsA modulation with the Tsyganenko 04 magnetic field model, which could be used to estimate the spatial extent of chorus wave generation region.

Keywords: Pulsating aurora, Chorus wave, Main pulsation, Internal modulation

©2019. Japan Geoscience Union. All Right Reserved.

Variations of cosmic noise absorption (CNA) by energetic electron precipitation (EEP) and changes of the auroral morphology

*Miyamoto Taishiro[1], Shin-ichiro Oyama[1,4,5], Yasunobu Ogawa[2], Keisuke Hosokawa[3], Satoshi Kurita[1], Yoshizumi Miyoshi[1], Ryuho Kataoka[2], Hiroshi Miyaoka[2], Tero Raita[4]

1. Institute for Space-Earth Environmental Research,Nagoya University, 2. National Institute of Polar Research, 3. Department of Communication Engineering and Informatics, University of Electro-Communications, 4. Sodankylä Geophysical Observatory, University of Oulu, 5. Ionosphere Research Unit, University of Oulu

Temporal and spatial variations of aurora morphology in association with substorm have been studied for more than half a century. Various types of aurora are known, such as discrete arc emitting at relatively high intensity and elongating along the zonal direction, and diffuse aurora with darker but more widely spreading in the sky. Pulsating aurora, which is characterized by quasi-periodic oscillations in the emission intensity at periods of a few to tens seconds, and auroral patches observed embedding in the pulsating aurora tend to appear at the recovery phase of substorm, especially from midnight to dawn. It is known that these types of aurora are accompanied by energetic electron precipitation exceeding several hundreds keV. Elucidation of the causality to produce pulsating aurora and energetic electron precipitation is an important theme to understand relationships between the radiation belt and upper-middle atmosphere of the earth. Analyzing measurements from satellite observations (e.g., Arase) and ground-based optical/radio technique observations, the generation mechanism is thought to be mainly attributed to wave particle interactions due to plasma wave and electrons in the magnetosphere. In this study, we focus on relationships between auroral morphological changes, in particular spatiotemporal evolutions to patches and coinciding precipitations of the energetic electron.

Some previous studies have presented changes in morphology from pulsating aurora to patch structures [e.g., Shiokawa et al., 2014] and temporal variations of energetic electron precipitation [e.g., Hosokawa and Ogawa, 2015]. As mentioned above, the wave-particle interaction has been widely accepted with experimental evidences to support generation of pulsating aurora and energetic electron precipitation. However, our understanding has not yet reached its maturity of presenting spatiotemporal evolutions of auroral morphology and associated electron precipitation. Oyama et al. [2017] presented enhancements of CNA (cosmic noise absorption) coinciding with appearance of the patch structure but with only two events. Furthermore, due to measurements with intensive diagnostic instruments, the result was based on information of a part of the auroral ionosphere. In this study, we conducted observations to capture simultaneously time evolutions and spatial distributions of auroral morphology and energetic electron precipitation by utilizing a network of EMCCD (Electron Multiplying Charge Coupled Device) cameras and riometers deployed in Northern Europe.

This study will present three events (February 19-20, 2018, March 6-7, 2017, and March 29-30, 2017). On the way of all events, after substorm onsets twice near Northern Europe, another onset occurred again at more west side (near Iceland or Greenland area) but at dawn in the Northern Europe. In this study, we have focused on the aurora and CNA associated with the latter onset, and at that time, the aurora spatially and temporally shifted from diffuse to pulsation and patch structures. This suggests that substorm activities occurred in the distance can induce these auroral morphological changes seen in the Northern Europe. CNA at that time is characterized by gradual variations with time scale of several hours. This trend cannot be seen at substorm onset near the Northern Europe. Moreover, in the latitude distribution, the feature was confirmed that CNA increases at the latitude where patch structure is seen, and CNA keeps

©2019. Japan Geoscience Union. All Right Reserved.

constant value at the latitude where patch structure is not seen. In the presentation, based on these observations, we will discuss physical mechanisms to cause changes in the auroral morphology and energetic electron precipitation, which can be seen as increases of CNA.

Keywords: Ionosphere, Aurora, Energetic Electron Precipitation (EEP)

©2019. Japan Geoscience Union. All Right Reserved.

Spatiotemporal characteristics on the source region of flash aurora using ray tracing analysis

*Tomohiro Inoue[1], Mitsunori Ozaki[1], Yoshitaka Goto[1], Satoshi Yagitani[1], Yoshiya Kasahara[1], Kazuo Shiokawa[2], Yoshizumi Miyoshi[2], Ryuho Kataoka[3], Yusuke Ebihara[4]

1. Kanazawa University , 2. Nagoya University, 3. National Institute of Polar Research, 4. Kyoto University

Whistler mode waves cause precipitation of high-energy electrons via wave-particle interactions in the magnetosphere. The scattered particles precipitate to the ground along the geomagnetic field line. Then, flush aurora, which is a rapid (less than 1 s) auroral phenomenon, is happened. Flash aurora is important for understanding the spatial evolution of wave-particle interaction region in the magnetosphere. We observed the mainly southward spread of flush aurora. In order to understand the spatial-time variation of wave-particle interaction region, we analyze the propagation effects of whistler mode waves near the magnetic equator region using ray tracing analysis. We calculated the ray paths of whistler mode waves (0.2 fce and 0.4 fce) near the magnetic equator (-10 to +10 degrees of geographic latitude), where fce is the electron cyclotron frequency at the magnetic equator. The initial ray paths put in the assumption of a spatial spread with the wave normal angles of tens of degrees along the magnetic field line at the magnetic equator (a point source). Then, we traced the magnetic field lines from the ray paths of whistler mode waves and estimated the precipitation area of electrons in the ionosphere using the IGRF model. The calculation results showed the precipitation area was not mainly spread southward, but evolved northward in the preliminary study.
In this presentation, we will present the spatiotemporal characteristics of flash aurora and the analysis results of ray tracing in detail.

Keywords: Flush aurora, Whistler mode wave, Ray tracing, Wave-particle interaction

©2019. Japan Geoscience Union. All Right Reserved.

Molecular ion supply mechanisms from the low-altitude ionosphere to magnetosphere observed by EISCAT and Arase(ERG)

*Masayoshi Takada[1], Kanako Seki[1], Yasunobu Ogawa[2], Kunihiro Keika[3], Satoshi Kasahara[4], Shoichiro Yokota[5], Tomoaki Hori[7], Kazushi Asamura[6], Yoshizumi Miyoshi[7]

1. Graduate School of Science, Tokyo University, 2. National Institute of Polar Research, 3. Department of Earth and Planetary Science, Graduate School of Science, Tokyo University, 4. The University of Tokyo, 5. Graduate School of Science, Osaka University, 6. Institute of Space and Astronautical Science, Japan Aerospace Exploration Agency, 7. Institute for Space-Earth Environmental Research, Nagoya University

Molecular ions ($O_2^+/NO^+/N_2^+$) in the magnetosphere have been observed during magnetic storms [Peterson et al., 1994; Klecker et al., 1986]. These molecular ions are considered to originate from the Earth’ s ionosphere. It is considered that they have been transported upward by some heating processes in the ionosphere. However, due to the larger mass than atomic ions (O^+), the molecular ions usually exist only in the low-altitude ionosphere below 300 km altitude. It is hence difficult to transport these molecular ions by overcoming loss by chemical reactions to the high-altitude ionosphere where the ion upflow and outflows usually take place [Peterson et al., 1994]. Therefore, it is necessary to reveal what mechanism causes molecular ion upflow during the magnetic storms. In this study, we aim at the observational assessments of the supply processes of the molecular ions from the low-altitude ionosphere to the magnetosphere based on conjugate observations by EISCAT radar and the Arase (ERG) satellite.

The EISCAT radar and the Arase (ERG) satellite have the conjunction event during the large magnetic storm with the minimum Dst of -124 nT on September 8, 2017. During the event, the Arase satellite was located in the dusk-side inner magnetosphere and observed molecular ions in the energy range of 12-180 keV/q. The EISCAT radar simultaneously observed the ion upflow (with the upward velocity of ~50-150 m/s) from the low-altitude ionosphere (~250-400 km) together with strong ion heating (>2000 K). The convective electric field was also enhanced by a factor of 2 in the same region. We estimated each term in the equation of motion for ions. The result indicates that the ion upflow reached stable equilibrium because the upward ion and electron pressure gradients are balanced with the downward gravitational force. It is suggested that the ion upflow can take place from the low-altitude ionosphere due to strong ion pressure gradient. We also estimated the flux decrease of molecular ions due to dissociative recombination. The flux decreased to ~1 % at 350 km compared with 280 km. The estimated upflow flux of molecular ions at 350 km is $>10^{10}$ m^{-2} s^{-1} . Comparison between distribution functions observed by Arase satellite and EISCAT radar suggests that acceleration by 3 orders of magnitudes is necessary during the outflow process. These results indicate that the strong ion frictional heating during magnetic storms enabled molecular ions to be transported upward from the low-altitude ionosphere and provide a source of molecular ion outflows into the magnetosphere.

Keywords: Molecular ion, EISCAT radar, Arase (ERG) satellite, Ion upflow, Ionospheric heating

©2019. Japan Geoscience Union. All Right Reserved.

Optical and radar observation of the dynamic auroral forms

*Yunosuke Nagafusa[1], Tima Sergienko[2], Satoshi Taguchi[1], Urban Braendstroem[2], Masatoshi Yamauchi[2]

1. Graduate School of Science, Kyoto University, 2. Swedish Institute of Space Physics, Kiruna

Ionosphere disturbances caused by the auroral electron precipitations are studied using auroral images taken by Auroral Large Imaging System (ALIS) and ionospheric parameters measured by EISCAT UHF radar that were conjugate with ALIS field-of-view. ALIS consists of several remote controlled stations located in northern Scandinavia, separated by approximately 50 km. Each station is equipped with a high-resolution CCD detector with 1024×1024 pixels, and a filter wheel with six positions for narrow-band interference filters. In this study we use the data obtained with the 557.7 nm filter, which show the auroral emission originated from the atomic oxygen. EISCAT UHF radar located in northern Norway near Tromsø operating in the BEATA program provides the ionospheric electron density, electron and ion temperatures, and ion velocity with the time resolution of 5 s and the spatial resolution of 1.5 km. The auroral images from the different ALIS stations were used for triangulation of the auroral forms in order to determine the aurora position in relation to the radar beam. For each auroral arc, the electron density, the electron and ion temperatures measured inside and in the vicinity of the auroral forms were analyzed with the aim of understanding the ionospheric response to the different types of auroral electron precipitations.

Keywords: aurora, ionospheric parameters, electron precipitations

©2019. Japan Geoscience Union. All Right Reserved.

Observations of MF/HF auroral radio emissions at three ground-based stations

*Yuka Sato[1], Atsushi Kumamoto[2], Yuto Katoh[2], Akira Kadokura[3,4], Yasunobu Ogawa[3,4], Atsuki Shinbori[5]

1. Nippon Institute of Technology (NIT), 2. Graduate School of Science, Tohoku University, 3. National Institute of Polar Research (NIPR), 4. The Graduate University for Advanced Studies, 5. Institute for Space-Earth Environmental Research (ISEE), Nagoya University

We started ground-based observations of MF/HF auroral radio emissions about 10 years ago at two stations (The Husafell Station, Iceland, September 2005; The Kjell Henriksen Observatory, Svalbard, September 2008) and found multiple unknown properties of MF/HF auroral radio emissions, e.g. polarization features [*Sato et al.*, 2008, 2015] and existence of a higher frequency component [*Sato et al.*, 2012]. To make a next siginificant step for a futher understanding of MF/HF auroral radio emissions, we installed a new dedicated instrumentation at the KAIRA (Kilpisjärvi Atmospheric Imaging Receiver Array) site in Kilpisjärvi, Finland (Latitude: 60.07 N, Longitude: 20.76 E) in the summer of 2018. It is a passive receiving system designed to realize a high-resolution spectral, interferometric and polarization measurements using 4 loop antennas and a software-defined radio (SDR) receiver. This SDR receiver can implement high-speed, flexible digital signal processing of RF signals and obtain high-resolution spectra pauselessly throughout the night in a wide frequency range up to 6 MHz. One of the main research subjects of this project is radio emission spontaneously emitted from aurora. There are long-known three types of MF/HF auroral radio emissions identified at ground level: auroral hiss, medium frequency burst (MFB), and auroral roar. Investigation into the generation of these emissions not only offers a tool of great promise for remote sensing of ionospheric plasma processes and parameters but also gives the foundation for understanding various radiation mechanisms that occur in planetary magnetospheres and plasma in space. In combination with the long-term continuous observations in Iceland and Svalbard and future EISCAT_3D experiments, observation with this new instrumentation will provide a first-time opportunity to reveal spatiotemporal variations of macro and fine structures of MF/HF auroral radio emissions associated with substorm evolution. In this presentation, we show detailed specification of this new instrumentation and some initial results.

Keywords: auroral phenomena, radio wave propagation, wave-particle interaction

©2019. Japan Geoscience Union. All Right Reserved.

Ionospheric F-region Drift Measurements Derived from DPS-4D at Zhongshan Station, Antarctic

*Xiangcai Chen[1]

1. Polar Research Institute of China

By means of high-frequency radio sounding, the ionospheric plasma drift can be measured by the Doppler frequency shift of signal. In this paper we analyze the ionospheric F-region plasma motion performed by Digisonde Portable Sounder (DPS-4D) at cusp latitude over Zhongshan Station in Antarctic. By restricting the echo arrival angle, and selecting the reflection height range at 175 –475 km, we present the variation of the F-region plasma drift measurements by setting limits on the Doppler frequency shift. Base on the 7.5 min interval Digisonde drift data from November 2011 to February 2012, we considered the variations of the plasma drift in F-region under the different geomagnetic activity (Kp) and magnetic local time, as well as it correlation with interplanetary magnetic field (IMF). The results indicate that properly restricting the Doppler frequency shift of the echo has a strong effect that contributes to the accurate and robust measurements of the ionospheric plasma drift. The mean value of horizontal drift mostly leveled off to about 600 m/s at altitude around of 230 km, while the field-aligned component of drift showed mean values of -25 m/s near pre-noon and +40 m/s during the night. These strong diurnal variations have dependence on the sign and strength of the IMF B_y and B_z components. It implies that the contraction and expansion of the polar cap with Kp and the convection in the proximity of the throat with different IMF conditions have a profound influence on the observed drift velocities.

Keywords: Digisonde DPS 4, Doppler frequency shift, remote sensing, polar ionosphere, plasma drift

©2019. Japan Geoscience Union. All Right Reserved.

PARM-HEP Observation of Precipitating High Energy Electrons over Pulsating Aurora

*Taku Namekawa[1], Takefumi Mitani[2], Kazushi Asamura[2], Yoshifumi Saito[2]

1. Department of Earth and Planetary Science, Graduate school of Science, The University of Tokyo, 2. Institute of Space and Astronautical Science, Japan Aerospace Exploration Agency

The phenomenon called microbursts that radiation belt particles precipitate to the Earth’ s atmosphere is thought to be largely related to the dissipation of high energy electrons in radiation belt. It is suggested that this phenomenon is caused by pitch angle scattering of the magnetospheric particles by plasma waves, which is a mechanism similar to the cause of the pulsating aurora observed in the Earth’ s polar region. There is a possibility that the origin of microburst can be clarified by proving simultaneous occurrence of microburst and pulsating aurora, but observational verification has not been made yet. For that purpose, we have developed a high-energy electron detector (HEP) for the observation of sub-relativistic - relativistic energy electrons that make up the microburst. HEP is designed to measure electrons between 300 keV and 2 MeV with energy resolution of 20% or less and with signal processing time of ~ 5 μs. Energy analysis is performed by the detection part of this instrument using SSD (Solid State Detector). Performance tests of this instrument are carried out using a sealed radiation source and a high energy electron beam line. This instrument is installed as one of the core instruments of the PARM instrument package developed for the simultaneous observation of the pulsating aurora and microburst by an international student sounding rocket experiment RockSat-XN and LAMP (Loss through Auroral Microburst Pulsation) sounding rocket experiment. We have succeeded in obtaining the flight data on 13 January 2019 from RockSat-XN sounding rocket experiment. In parallel, we are now preparing HEP analyzer for LAMP sounding rocket experiment. In this presentation, we will show the outline and observation results of RockSat-XN-HEP as well as the LAMP-HEP development status.

Keywords: Microburst, PARM, RockSat-XN, LAMP, Sounding rocket, Pulsating aurora

©2019. Japan Geoscience Union. All Right Reserved.

Development of the medium-energy electron detector with hemispherical field-of-view and the flight test in the PARM (Pulsating AuRora and Microburst) mission

*Shin Sugo[1], Oya Kawashima[1], Kazushi Asamura[2], Reiko Nomura[3], Yasunobu Ogawa[4], Keisuke Hosokawa[5], Yoshizumi Miyoshi[6], Takefumi Mitani[2], Taku Namekawa[1,2], Takeshi Sakanoi[7], Mizuki Fukizawa[7], Naoshi Yagi[7], Satoshi Kasahara[1]

1. The University of Tokyo, 2. Institute of Space and Astronautical Science, Japan Aerospace Exploration Agency, 3. National Astronomical Observatory of Japan, 4. National Institute of Polar Research, 5. The University of Electro-Communications, 6. Institute for Space-Earth Environmental Research, Nagoya University, 7. Tohoku University

Energetic electrons significantly affect ionospheric dynamics and the long-term evolution of surfaces and atmospheres of planets and moons. Since the energetic electron flux is not necessarily isotropic, it is important to cover the broad solid angle to quantitatively evaluate the effects on solar system bodies. With future planetary explorations in mind, we developed the medium-energy (20 - 100 keV) electron detector (MED) which can cover almost 2-pi steradian without the spacecraft spin. In order to test the performance of this analyzer in the relevant environment, we participated in the PARM mission, which aimed to measure electron precipitation using NASA’s sounding rocket RockSat-XN. In this presentation we report on MED observation results obtained through the flight on 13 January 2019.

©2019. Japan Geoscience Union. All Right Reserved.

Auroral substorm onset in satellite-based global images and ground-based all-sky images

*Akimasa Ieda[1], Kirsti Kauristie[2], Yukitoshi Nishimura[3], Yukinaga Miyashita[4], Harald U Frey[5], Liisa Juusola[2], Daniel Whiter[6], Masahito Nose[7], Matthew O Fillingim[5], Farideh Honary[8], Neil C Rogers[8], Yoshizumi Miyoshi[1], Shinobu Machida[1]

1. Institute for Space-Earth Environmental Research, Nagoya University, 2. Finnish Meteorological Institute, 3. Boston university, 4. Korea Astronomy and Space Science Institute, 5. University of California Berkeley, 6. University of Southampton, 7. Graduate School of Science, Kyoto University, 8. Lancaster University

Substorm onset has originally been defined as a longitudinally extended sudden auroral brightening (Akasofu initial brightening: AIB) followed a few minutes later by an auroral poleward expansion in ground-based all-sky images (ASIs). In contrast, such clearly marked two-stage development has not been evident in satellite-based global images (GIs). Instead, substorm onsets have been identified as localized sudden brightenings that expand immediately poleward.
To resolve these differences, optical substorm onset signatures in GIs and ASIs are compared in this study for a substorm that occurred on December 7, 1999. For this substorm, the Polar satellite ultraviolet global imager was operated with a fixed-filter (170 nm) mode, enabling a higher time resolution (37 s) than usual to resolve the possible two-stage development. These data were compared with 20-s resolution green-line (557.7 nm) ASIs at Muonio in Finland. The ASIs revealed the AIB at 2124:50 UT and the subsequent poleward expansion at 2127:50 UT, whereas the GIs revealed only an onset brightening that started at 2127:49 UT.
Thus, the onset in the GIs was delayed relative to the AIB and in fact agreed with the poleward expansion in the ASIs. The fact that the AIB was not evident in the GIs may be attributed to the limited spatial resolution of GIs for thin auroral arc brightenings. The implications of these results for the definition of substorm onset are discussed herein.

Keywords: substorm, auroral breakup, aurora

©2019. Japan Geoscience Union. All Right Reserved.

Original substorm onset (Akasofu 1964; 2010)

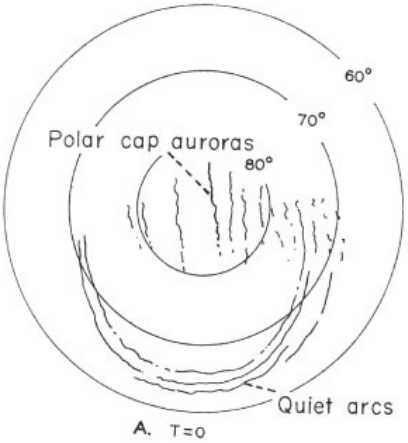

FIG. 2. THE DISTRIBUTION OF THE AURORAS DURING THE QUIET PHASE.

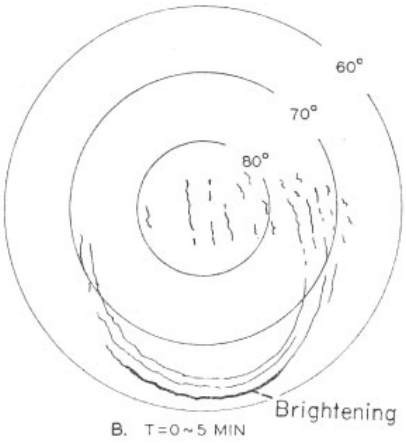

FIG. 3. AURORAS DURING THE EXPANSIVE PHASE (STAGE I).

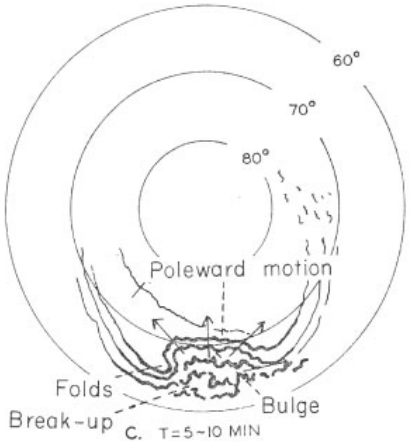

FIG. 4. AURORAS DURING THE EXPANSIVE PHASE (STAGE II).

a Time < 0
Before onset
Quiet arc

b T = 0 ~ 5 min
Expansion phase stage 1
Initial brightening
T = 0: Substorm onset

c T = 5 ~ 10 min
Expansion phase stage 2
Poleward expansion
(Auroral breakup)

Ground and satellite observations (Ieda et al. 2018: 10.1186/s40623-018-0843-3)

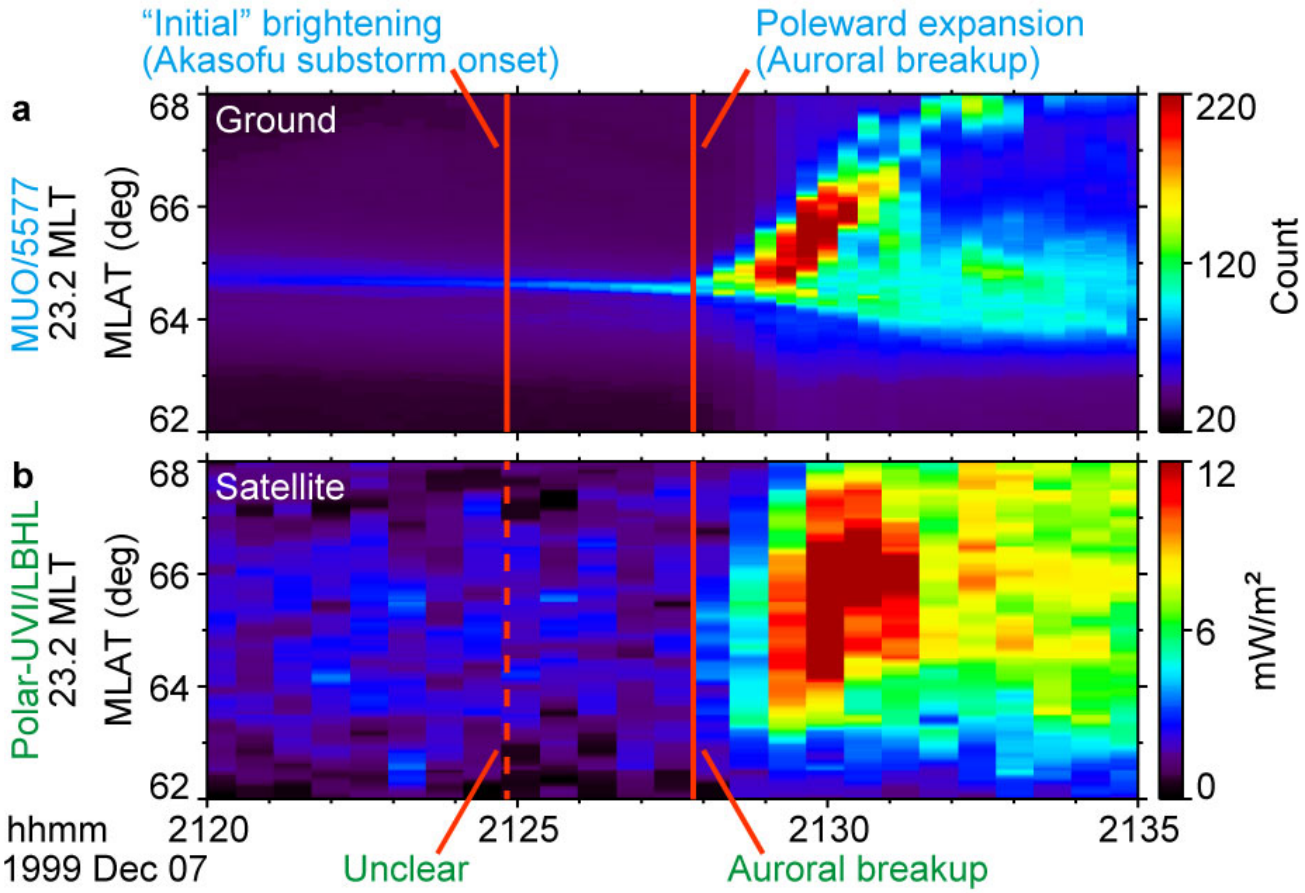

©2019. Japan Geoscience Union. All Right Reserved.

Automatic Classification of Auroral images using optical flow feature

*Naoto Kashiwagi[1], Akiko Fujimoto[1], Terumasa Tokunaga[1], Yoshizumi Miyoshi[2], Yasunobu Ogawa[3], Keisuke Hosokawa[4]

1. Kyushu Institute of Technology, 2. Nagoya University, 3. National Institute of Polar Research, 4. The University of Electro-Communications

The machine learning technique including the deep learning has been developed and the practical uses have increased on various field. On the study of auroral detection, the concern over the automatic image classification has risen using the approach of machine learning technique for the large statistical analysis of auroral images. The automatic auroral image classification has tried to use some techniques from computer vision, machine vision and pattern recognition. There are roughly two kinds of the selected feature: the color of image and the motion of aurora image sequences. The works based on the color feature of aurora image have been performed by Rao et al. (2014) and Tanaka et al. (2015). Rao et al. (2014) performed Support Vector Machines (SVM) classification with several local feature extraction techniques, and found that Scale Invariant Feature Transform (SIFT), OpponentSIFT, is the most effective feature for the automated classification of color aurora images. Tanaka et al. (2015) used the aurora area using the HSV model. They mentioned that it is difficult to classify the images including the diffuse aurora and cloud area. The color feature work well for the color auroral image, while the gray-scale (optically filtered) auroral images need other features on the automated classification. Blixt et al. (2006) applied the optical flow estimation to auroral image sequences. Their case study showed the useful tool for representing the motion of the aurora. In this study, we validate the optical flow estimation to extract the feature of auroral image, and automatically classify the large gray-scale auroral images using the machine learning with Convolution Neural Network (CNN). We use 63,486 gray-scale aurora images in total and use five categories for the preparation of supervised learning data, 1) aurora, 2) aurora and cloudy, 3) aurora and moon, 4) aurora, cloudy and moon, 5) noaurora. We perform the Hold-out and the Cross Validation to evaluate our classification performance. We obtained 98.58% of the classification accuracy based on Hold-out and 98.47% of the classification accuracy based on Cross Validation.

Keywords: Aurora, Optical flow, Convolution Neural Network

©2019. Japan Geoscience Union. All Right Reserved.

Fine-scale visualization of aurora in a wide area using color digital camera images from the International Space Station

*Sota Nanjo[1], Yuta Hozumi[1], Keisuke Hosokawa[1]

1. The University of Electro-Communications

Various ground-based and space-based imagers have been used to observe aurora borealis and australis. So far, however, it has been difficult to observe the detailed spatial structure of auroras in a wide area with sufficient spatial and temporal resolution. Since the photographs taken from the International Space Station (ISS) have sufficient spatial and temporal resolution, it is possible to visualize the fine-scale structures of aurora in a wide area. A calibration of imaging parameters of the photographs using star lights was proposed by a previous research. The accuracy in the timestamp was not guaranteed by the method based on the star lights because the position of the star lights in the image did not change with elapsed time. Thus, it is still difficult to use the mapped data for studying fast variations of aurora, for example pulsating aurora (PsA). Therefore, in this study, we calibrated the images from the ISS using city lights which change their apparent positions with elapsed time. In order to validate the calibration method using city light positions, we mapped two PsA events in the photographs to the geographical coordinate, and compared with those from ground-based all-sky imagers in Alaska and Canada. We found that the approximate shape of discrete aurora and the temporal variation of PsA derived from the ISS images are consistent with those from the ground-based observation. The accuracy in the timestamp is less than 0.5 sec and that in space in the direction perpendicular to the line of sight of the camera is within 5 km. In the presentation, we will also address how the mapped full-color images can be used for studies of PsA in the future work.

Keywords: aurora, ISS

©2019. Japan Geoscience Union. All Right Reserved.

PARM: Investigation of precipitating high-energy electrons into the auroral ionosphere with sounding rockets

*Kazushi Asamura[1], Yoshizumi Miyoshi[2], Keisuke Hosokawa[3], Takefumi Mitani[1], Taku Namekawa[1,5], Takeshi Sakanoi[4], Naoshi Yagi[4], Mizuki Fukizawa[4], Genki Ishizawa[4], Satoshi Kasahara[5], Shin Sugo[5], Oya Kawashima[5], Reiko Nomura[6], Masahito Nose[2], Mariko Teramoto[2], Yasunobu Ogawa[7], Shinji Saito[2], Ryoichi Fujii[8]

1. ISAS / JAXA, 2. ISEE, Nagoya University, 3. The University of Electro-Communications, 4. Tohoku University, 5. The University of Tokyo, 6. NAOJ / NINS, 7. NiPR / ROIS, 8. ROIS

Bursty precipitations of high-energy electrons into the polar ionopshere have been observed by low-altitude satellite, for example, SAMPEX and FIREBIRD II. These precipitations, called microburst, may contribute to the loss of the terrestrial radiation belt through the collisional energy loss with the dense, cold atmospheric particles. Recent numerical simulations successfully reproduce these microburst precipitations with a few Hz modulations by taking into account the pitch angle scattering with the whistler chorus elements at off-equator regions in the inner magnetosphere. Therefore, one can expect that the miscroburst precipitations have properties depending on auroral activities especially the pulsating auroras. In order to investigate the mechanisms of the microburst precipitations by in-situ observations, we are developing two instrument packages: PARM (Pulsating AuRora and Microbursts; already developed) and PARM-2 (being developed), both of which are designed suitable for sounding rocket experiments. PARM consists of four sensors; HEP (high-energy electron energy spectrometer), MED (medium-energy electron detector), AIC (auroral camera), and AFG (ASIC-based fluxgate magnetometer). PARM was onboard the NASA's RockSat-XN sounding rocket, and launched from Andoya, Norway at 09:13UT, Jan 13, 2019. On the other hand, PARM-2 is under development. It consists of HEP, two AICs, and MIM (magneto-impedance magnetometer). PARM-2 is to be onboard the NASA's LAMP sounding rocket which will fly from Poker Flat, Alaska in the period between the end of 2019 and the beginning of 2020.

We will present the overview of PARM missions including the initial results of RockSat-XN/PARM with ground-based observations and preparation status of LAMP/PARM-2.

Keywords: electron microburst precipitation, sounding rocket, pulsating aurora

©2019. Japan Geoscience Union. All Right Reserved.

[E] Poster | P (Space and Planetary Sciences)：P-EM Solar-Terrestrial Sciences, Space Electromagnetism & Space Environment

Wed. May 29, 2019 3:30 PM - 5:00 PM JST | Wed. May 29, 2019 6:30 AM - 8:00 AM UTC | Poster Hall International Exhibition Hall8, Makuhari Messe_2

[P-EM13] Inner magnetosphere: Recent understanding and new insights

convener:Yusuke Ebihara(Research Institute for Sustainable Humanosphere, Kyoto University), Danny Summers(Memorial University of Newfoundland), Yoshizumi Miyoshi(Institute for Space-Earth Environmental Research, Nagoya University), Shinji Saito(Graduate School of Science, Nagoya University)

The inner magnetosphere is characterized by the dominance of intrinsic dipolar Earth's magnetic field. The dipolar magnetic field traps charged particles, resulting in the formation of unique particle environment known as the plasmasphere, the ring current, and the radiation belt. The inner magnetosphere is always changing because of incoming energy from the outer magnetosphere and the ionosphere in the forms of particles and electromagnetic fields. In the inner magnetosphere, the particle energy is transferred to the field energy, and vice versa. The mutual coupling between particles and fields also makes the inner magnetosphere unique. The outgoing energy to these regions is also known to be significant, such as precipitation into the upper atmosphere and sub-auroral disturbances. A number of satellites (e.g., DMSP, NOAA, Geotail, Cluster, THEMIS, Van Allen Probes, MMS, and Arase), ground-based instruments (e.g., SuperDARN and EISCAT radars, magnetometers, and cameras), and numerical simulations (e.g., global particle simulation, PIC simulation, and hybrid simulation) have successfully surveyed the inner magnetosphere, which deepen our knowledge significantly. USAF DSX, UCLA Elfin and NASA CeRES will be launched soon, being expected to provide important information. We solicit papers describing recent results on the inner magnetosphere and/or its coupling with the other regions, including the ionosphere and the outer magnetosphere.

[PEM13-P01] Evaluation of wave normal and Poynting vector analyses for whistler mode waves observed by the waveform capture (WFC) on board the Arase

*Yoshiya Kasahara[1], Satoshi Ikarashi[1], Hiroyuki Nishizawa[1], Shoya Matsuda[2], Fuminori Tsuchiya[3], Atsushi Kumamoto[3], Yasumasa Kasaba[3], Mitsunori Ozaki[1], Ayako Matsuoka[2] (1.Kanazawa University, 2.ISAS/JAXA, 3.Tohoku University)

[PEM13-P02] Calibration of electric fields dedicated to the measurement of the S-WPIA of the Arase Satellite

*Miki Jumpei[1], Hirotsugu Kojima[2], Yuto Katoh[3], Shoya Matsuda[4], Yoshiya Kasahara[5], Mitsuru Hikishima[4], Satoshi Kurita[6], Masahiro Kitahara[3], Satoshi Kasahara[7], Yoshizumi Miyoshi[6], Atsushi Kumamoto[3], Ayako Matsuoka[4], Shoichiro Yokota[8], Tomoaki Hori[6], Kunihiro Keika[7] (1.Space Radio Engineering Laboratory, Division of Electrical Engineering, Kyoto University Graduated School, 2.Research Institute for Sustainable Humanosphere, Kyoto University, 3.Graduate School of Science and Faculty of Science, Tohoku University, 4.Institute of Space and Astronautical Science, JAXA, 5.Information Media Center, Kanazawa University, 6.Institute for Space-Earth Environmental Research, Nagoya University, 7.School of Science, The University of Tokyo, 8.School of Science, Osaka University)

[PEM13-P03] Enhancement of whistler-mode chorus in association with Pc 4-5 ULF waves and related variation of high energy electrons

*Atsuhiro Ono[1], Yuto Katoh[1], Atsushi Kumamoto[1], Fuminori Tsuchiya[1], Mariko Teramoto[2], Yoshiya Kasahara[3], Shoya Matsuda[4], Ayako Matsuoka[4], Takefumi Mitani[4], Tomoaki Hori[2], Satoshi Kasahara[5], Shoichiro Yokota[6], Kunihiro Keika[5], Yoshizumi Miyoshi[2], Iku Shinohara[4] (1.Tohoku University, 2.Nagoya University, 3.Kanazawa University, 4.ISAS/JAXA, 5.The University of Tokyo, 6.Osaka University)

[PEM13-P04] Sudden enhancements of electron cyclotron harmonic waves observed by the Arase satellite

*Shinjo Airi[1], Hirotsugu Kojima[1], Yoshiya Kasahara[2], Yoichi Kazama[3], Hideyuki Usui[4], Yoshizumi Miyoshi[5], Yasumasa Kasaba[6], Shoya Matsuda[7], Tomoaki Hori[5], S. -Y. Wang[8], Sunny W.Y. Tam[9], Atsushi

Kumamoto[10], Ayako Matsuoka[11] (1.Research institute for sustainable humanosphere, Kyoto University, 2.Information Media Center, Kanazawa University, 3.ASIAA, 4.Graduate school of system informatics Kobe University, 5.Institute for Space-Earth Environmental Research, Nagoya University, 6.Planetary Plasma and Atmospheric Research Center, Tohoku University, 7.Institute of Space and Astronautical Science/Japan Aerospace Exploration Agency, 8.ASIAA, Taiwan, 9.ISAPS, NCKU, Taiwan, 10.Department of Geophysics, Graduate School of Science, Tohoku University, 11.Research Division for Space Plasma, Institute of Space and Astronautical Science, Japan Aerospace Exploration Agency)

[PEM13-P05] Correlation between pulsating aurora and electrostatic electron cyclotron harmonic waves obtained from coordinated Arase and ground data

*Mizuki Fukizawa[1], Takeshi Sakanoi[1], Yoshizumi Miyoshi[2], Keisuke Hosokawa[3], Yoichi Kazama[4], Yoshiya Kasahara[5], Shoya Matsuda[6], Ayako Matsuoka[7], Wang Shiang-Yu[4], Sunny Wing-Yee Tam[8], Ryuho Kataoka[9] (1.Planetary Plasma and Atmospheric Research Center, Graduate School of Science, Tohoku University, 2.Institute for Space-Earth Environmental Research, Nagoya University, 3.Department of Communication Engineering and Informatics, University of Electro-Communications, 4.Academia Sinica Institute of Astronomy and Astrophysics, 5.Information Media Center, Kanazawa University, 6.Institute of Space and Astronautical Science/Japan Aerospace Exploration Agency, 7.Research Division for Space Plasma, Institute of Space and Astronautical Science, Japan Aerospace Exploration Agency, 8.Institute of Space and Plasma Sciences, College of Sciences, National Cheng Kung University , 9.National Institute of Polar Research)

[PEM13-P06] Automatic determination of Upper Hybrid Resonance Frequencies by Convolutional Neural Network.

*Shoya Matsuda[1], Tatsuhito Hasegawa[2], Atsushi Kumamoto[3], Fuminori Tsuchiya[3], Yoshiya Kasahara[4], Yoshizumi Miyoshi[5], Yasumasa Kasaba[3], Ayako Matsuoka[1] (1.Institute of Space and Astronautical Science/Japan Aerospace Exploration Agency, 2.University of Fukui, 3.Tohoku University, 4.Kanazawa University, 5.ISEE, Nagoya University)

[PEM13-P07] Amplitude dependence of whistler wave motion on electron scattering process

*Yoshiki Ito[1], Yoshizumi Miyoshi[1], Shinji Saito[1] (1.Nagoya University, ISEE)

[PEM13-P08] Two-dimensional simulation of whistler mode wave packets interacting with energetic electrons

*Takeshi Nogi[1], Yoshiharu Omura[1] (1.Reserch Institute for Sustainable Humanosphere, Kyoto University)

[PEM13-P09] Relativistic electron acceleration by whistler-mode chorus waves in 1D, 2D, and 3D magnetic field models.

*Keita Takahashi[1], Yoshiharu Omura[1], Yikai HSIEH[1], Danny Summers[2] (1.Research Institute for Sustainable Humanosphere, Kyoto University , 2.Department of Mathematics and Statistics, Memorial University of Newfoundland)

[PEM13-P10] Study of global spatio-temporal development of magnetospheric ELF/VLF waves for the 26-30 March 2017 storm based on ground and satellite observations and the RAM simulations

*Yuhei Takeshita[1], Kazuo Shiokawa[1], Yoshizumi Miyoshi[1], Mitsunori Ozaki[2], Yoshiya Kasahara[2], Martine Connors[3], Jyrki Manninen[4], Craig Kletzing[5], Vania Jordanova[6] (1.Nagoya University, Institute for Space-Earth Environmental Resarch, 2.Kanazawa University, 3.Athabasca University, 4.Sodankylä Geophysical Observatory, 5.The University of Iowa, 6.Los Alamos National Laboratory)

[PEM13-P11] Flux decrease of outer radiation belt electrons associated with solar wind pressure pulse: A Code coupling simulation of GEMSIS-RB and GEMSIS-GM

*Ito Hiroki[1], Yoshizumi Miyoshi[1], Shinji Saito[2], Yosuke Matsumoto[3], Takanobu Amano[4] (1.Institute for Space-Earth Environmental Research, Nagoya University, 2. Graduate School of Science, Nagoya

University, 3. Graduate School of Science, Chiba University, 4.Department of Earth and Planetary Science, University of Tokyo)

[PEM13-P12] Non-diffusive response of outer belt electrons on interplanetary shock

Takuma Toishi[1], *Yusuke Ebihara[1], Takashi Tanaka[2] (1.Research Institute for Sustainable Humanosphere, Kyoto University, 2.Kyushu University)

[PEM13-P13] PARM: Initial result of the auroral camera on the G-CHASER (RockSat-XN) rocket and status of the development of auroral cameras for the LAMP rocket experiment

*Naoshi Yagi[1], Takeshi Sakanoi[1], Fukizawa Mizuki[1], Kazushi Asamura[2], Yoshizumi Miyoshi[3], Keisuke Hosokawa[4], Genki Ishizawa[5] (1.Planetary Plasma and Atmospheric Research Center, Graduate School of Science, Tohoku University, 2.Institute of Space and Astronautical Science, Japan Aerospace Exploration Agency, 3.Institute for Space-Earth Environmental Research, Nagoya University, 4.Department of Communication Engineering and Informatics, University of Electro-Communications, 5.Space & terrestrial plasma pyhsics)

[PEM13-P14] First simultaneous observation of a SAR arc at subauroral latitudes using a ground all-sky camera and the Arase satellite in the inner magnetosphere

*Yudai Inaba[1], Kazuo Shiokawa[1], Shin-ichiro Oyama[1,8,9], Yuichi Otsuka[1], Atsuki Shinbori[1], Yoichi Kazama[2], Shiang-Yu Wang[2], Sunny W. Y. Tam[2], Shoichiro Yokota[3], Satoshi Kasahara[4], Kunihiro Keika[4], Tomoaki Hori[1], Ayako Matsuoka[5], Yoshiya Kasahara[6], Atsushi Kumamoto[7], Yasumasa Kasaba[7], Yoshizumi Miyoshi[1], Iku Shinohara[5], Arto Oksanen[10] (1.Institute for Space-Earth Environmental Research, 2.Academia Sinica, 3.Osaka Univ, 4.Tokyo Univ, 5.JAXA, 6.Kanazawa University, 7.Tohoku University, 8.University of Oulu, Finland, 9.National Institute of Polar Research, 10.Jyväskylän Sirius ry, Finland)

[PEM13-P15] Pi2 pulsations observed by the Arase satellite inside and outside the plasmapause

*Mariko Teramoto[1], Ayako Matsuoka[2], Reiko Nomura[5], Yoshiya Kasahara[3], Yasumasa Kasaba[4], Atsushi Kumamoto[4], Fuminori Tsuchiya[4], Shoya Matsuda[2], Masahito Nose[1], Masafumi Shoji[1], Yasunori Tsugawa[1], Shun Imajo[1], Yoshizumi Miyoshi[1], Iku Shinohara[2] (1.Institute for Space-Earth Environmental Research Nagoya University, 2.Institute of Space and Astronautical Science, Japan Aerospace eXploration Agency, 3.Kanazawa University, 4.Tohoku University, 5.National Astronomical Observatory of Japan)

[PEM13-P16] An extreme erosion of the plasmasphere during the 7–10 September 2017 storm

*Yuki Obana[1], Naomi Maruyama[2,3], Atsuki Shinbori[4], Kumiko K. Hashimoto[5], Mariangel Fedrizzi[2,3], Masahito Nose[4], Yuichi Otsuka[4], Nozomu Nishitani[4], Tomoaki Hori[4], Atsushi Kumamoto[6], Fuminori Tsuchiya[6], Shoya Matsuda[7], Ayako Matsuoka[7], Yoshiya Kasahara[8], Akimasa Yoshikawa[9], Yoshizumi Miyoshi[4], Iku Shinohara[7] (1.Osaka Electro-Communication University, 2.University of Colorado Boulder, 3.NOAA Space Weather Prediction Center, 4.Nagoya University, 5.Kibi International University, 6.Tohoku University, 7.Japan Aerospace Exploration Agency, 8.Kanazawa University, 9.Kyushu University)

[PEM13-P17] Relative contribution of ULF and chorus waves to the radiation belt variation: Comparison between multi-point observations and BATSRUS + CRCM simulation

*Naoko Takahashi[1], Kanako Seki[1], Mei-Ching Fok[2], Yihua Zheng[2], Yoshizumi Miyoshi[3], David Hartley[4], Ayako Matsuoka[5], Yoshiya Kasahara[6], Yasumasa Kasaba[7], Nana Higashio[8] (1.Graduate School of Science, University of Tokyo, 2.NASA Goddard Space Flight Center, 3.Institute for Space-Earth Environmental Research, Nagoya University, 4.Department of Physics and Astronomy, University of Iowa, 5.Institute of Space and Astronautical Science, Japan Aerospace Exploration Agency, 6.Information Media Center, Kanazawa University, 7.Planetary Plasma and Atmospheric Research Center, Tohoku University, 8.Japan Aerospace Exploration Agency)

[PEM13-P18] Modulation of the D-region ionosphere by Pc5 waves observed by VLF/LF standard radio waves

*Miyashita Takuya[1], Hiroyo Ohya[1], Fuminori Tsuchiya[2], Hiroyuki Nakata[1], Toshiaki Takano[1], Kazuo Shiokawa[3], Yoshizumi Miyoshi[3] (1.Chiba University, 2.Tohoku University, 3.Nagoya University)

[PEM13-P19] Oxygen-proton differences in ion energies dominating plasma pressure: Dependence on storm phases and solar wind drivers

*Kunihiro Keika[1], Satoshi Kasahara[1], Shoichiro Yokota[2], Masahiro Hoshino[1], Kanako Seki[1], Masahito Nose[3], Yoshizumi Miyoshi[3], Iku Shinohara[4] (1.Graduate School of Science, The University of Tokyo , 2.Graduate School of Science, Osaka University, 3.Institute for Space-Earth Environmental Research, Nagoya University, 4.Institute of Space and Astronautical Science, Japan Aerospace Exploration Agency)

[PEM13-P20] Mass dependence of penetration depth of multi-energy ions in the inner magnetosphere during magnetic storms: Arase observations

*Ryosuke Fujii[1], Yoshizumi Miyoshi[1], Masafumi Shoji[1], Kazushi Asamura[2], Lynn Kistler[1,8], Vania Jordanova[9], Tomoaki Hori[1], Satoshi Kurita[1], Mariko Teramoto[1], Yasunori Tsugawa[1], Yoshiya Kasahara[3], Yasumasa Kasaba[4], Atsushi Kumamoto[5], Fuminori Tsuchiya[4], Shoichiro Yokota[6], Kunihiro Keika[7], Ayako Matsuoka[2], Iku Shinohara[2] (1.Institute for Space-Earth Environmental Research, Nagoya University, 2.Institute of Space and Astronautical Science, Japan Aerospace Exploration Agency, 3.Information Media Center, Kanazawa University, 4.Planetary Plasma and Atmospheric Research Center, Tohoku University, 5.Department of Geophysics, Graduate School of Science, Tohoku University, 6.Graduate School of Science, Osaka University, 7.Department of Earth and Planetary Science, Graduate School of Science, The University of Tokyo, 8.University of New Hampshire, 9.Los Alamos National Laboratory)

[PEM13-P21] Relativistic Acceleration of Energetic Protons by Electromagnetic Ion Cyclotron Waves in the Jovian Magnetosphere

*Tomohiro Sekine[1], Yoshiharu Omura[1], Danny Summers[2], Yikai HSIEH[1], Satoko Nakamura[1] (1.Reserach Institute for Sustainable Humanosphere, Kyoto University, 2.Memorial University of Newfoundland)

[PEM13-P22] Statistical study of IPDP type EMIC wave-related electron precipitation at subauroral latitude

*Asuka Hirai[1], Fuminori Tsuchiya[1], Takahiro Obara[1], Yasumasa Kasaba[1], Yuto Katoh[2], Hiroaki Misawa[1], Kazuo Shiokawa[3], Yoshizumi Miyoshi[3], Satoshi Kurita[3], Martin G Connors[4] (1.Planetary Plasma and Atmospheric Research Center, Graduate School of Science, Tohoku Univ. , 2.Department of Geophysics, Graduate School of Science, Tohoku University, 3.Institute for Space-Earth Environmental Research, Nagoya University, 4.Athabasca University)

[PEM13-P23] Meridional distributions of proton plasma and pressure-driven currents in the nightside inner magnetosphere: Arase observations

*Shun Imajo[1], Masahito Nose[1], Satoshi Kasahara[2], Shoichiro Yokota[3], Ayako Matsuoka[4], Kunihiro Keika[2], Tomoaki Hori[1], Mariko Teramoto[1], Kazuhiro Yamamoto[5], Oimatsu Satoshi[5], Reiko Nomura[6], Akiko Fujimoto[7], Iku Shinohara[4], Yoshizumi Miyoshi[1] (1.Institute for Space-Earth Environmental Research, Nagoya University, 2.Graduate School of Science, The University of Tokyo, 3.Graduate School of Science, Osaka University, 4.Institute of Space and Astronautical Science, Japan Aerospace Exploration Agency, 5.Graduate School of Science, Kyoto University, 6.National Astronomical Observatory of Japan, 7.Kyushu Institute of Technology)

[PEM13-P24] Space Weather Effects on Energetic Proton Flux Response in South Atlantic Anomaly

*Kirolosse Mina GIRGIS[1,2], Tohru Hada[1], Shuichi Matsukiyo[1] (1.Earth System Science and Technology (ESST) Department, Interdisciplinary Graduate School of Engineering Sciences (IGSES), Kyushu University, Japan, 2.Aerospace Engineering Department, Faculty of Engineering, Cairo University, Egypt)

[PEM13-P25] Solar-cycle variations of >30 keV electron flux enhancements under the inner radiation belt

*ALLA SUVOROVA[1] (1.National Central University)

[PEM13-P26] Energy spectra variations of high energy electrons in the inner magnetosphere observed by HEP/XEP on ARASE and SEDA-e on HIMAWARI

*Takeshi Takashima[1], Takefumi Mitani[1], Nana Higashio[2], Tsutomu Nagatsuma[3] (1. ISAS/JAXA, 2.Research and Development Directorate/JAXA, 3.NiCT)

[PEM13-P27] Inter-channel calibration of the high-energy electron experiments (HEP) instrument onboard the Arase satellite

*Tomoaki Hori[1], Takefumi Mitani[2], Takeshi Takashima[2], Park Inchun[1], Satoshi Kurita[1], Mariko Teramoto[1], Nana Higashio[3], Satoshi Kasahara[4], Shoichiro Yokota[5], Yoshizumi Miyoshi[1], Iku Shinohara[2] (1.Institute for Space-Earth Environmental Research, Nagoya University, 2.Japan Aerospace Exploration Agency, Institute of Space and Astronautical Science, 3.Japan Aerospace Exploration Agency, 4.Graduate School of Science, The University of Tokyo, 5.Graduate School of Science, Osaka University)

[PEM13-P28] Particle simulation for calibrating the HEP data onboard the ARASE satellite

*PARK INCHUN[1], Yoshizumi Miyoshi[1], Takefumi Mitani[2], Tomoaki Hori[1], Satoshi Kurita[1], Mariko Teramoto[1], Takeshi Takashima[2], Nana Higashio[3], Iku Shinohara[2] (1.Nagoya University Institute for Space-Earth Environmental Research, 2.Japan Aerospace Exploration Agency Institute of Space and Astronautical Science , 3.Japan Aerospace Exploration Agency)

[PEM13-P29] Geant4 model calculation and energetic particle observation with HEP/Arase in the inner radiation belt

*Honoka Toda[1], Wataru Miyake[1], Takefumi Mitani[3], Takeshi Takashima[3], Yoshizumi Miyoshi[2], PARK INCHUN[2], Tomoaki Hori[2] (1.Tokai University, 2.ISEE/Nagoya University, 3.ISAS/JAXA)

[PEM13-P30] Validation of High-energy electron detector simulator for the HEP instruments onboard Arase

*Takefumi Mitani[1], PARK INCHUN[2], Tomoaki Hori[2], Taku Namekawa[1,3], Kazushi Asamura[1], Takeshi Takashima[1], Satoshi Kasahara[3], Satoshi Kurita[2], Mariko Teramoto[2], Nana Higashio[1], Yoshizumi Miyoshi[2], Iku Shinohara[1] (1.Japan Aerospace Exploration Agency, Institute of Space and Astronautical Science, 2.Institute for Space-Earth Environmental Research, Nagoya Univ., 3.The university of Tokyo)

Evaluation of wave normal and Poynting vector analyses for whistler mode waves observed by the waveform capture (WFC) on board the Arase

*Yoshiya Kasahara[1], Satoshi Ikarashi[1], Hiroyuki Nishizawa[1], Shoya Matsuda[2], Fuminori Tsuchiya[3], Atsushi Kumamoto[3], Yasumasa Kasaba[3], Mitsunori Ozaki[1], Ayako Matsuoka[2]

1. Kanazawa University, 2. ISAS/JAXA, 3. Tohoku University

The Plasma Wave Experiment (PWE) is one of scientific instruments on board the Arase (ERG) satellite to measure electric field from DC to 10 MHz and magnetic field from a few Hz to 100 kHz in the inner magnetosphere. It is well known that chorus wave, one of typical plasma waves in VLF range observed in the inner magnetosphere, is a plausible candidate that accelerates relativistic electrons in the radiation belt. Besides the chorus, the Arase has observed various kinds of plasma waves such as lightning whistlers and hiss waves. It is very important to study the propagation characteristics of these waves.

In the present paper, we developed a direction finding system applicable to whistler mode waves using the data from waveform capture (WFC), which is one of receivers covering the frequency range below 20kHz implemented in the PWE. The absolute directions of the wave normal and Poynting vectors were derived in the coordinate system referring the ambient magnetic field and geomagnetic meridian plane. We also estimated the Poynting vector theoretically using the derived wave normal vector, electron density and ambient magnetic field intensity to confirm the validity of the results from the observation data.

We demonstrated that the results were generally reliable, but further calibration is necessary for electric field to improve the accuracy of Poynting vector because the waveform of electric field is now calibrated under the assumptions of theoretical antenna capacitance in a vacuum and typical plasma impedance. In other words, we expect to be able to correct the calibration table for electric field measurements from the direction finding results.

In the presentation, we introduce some typical results which have been derived from the observation data of upper- and lower-band chorus, and lightning whistlers.

Keywords: Whistler mode wave, Waveform Capture, Direction finding, Plasma wave

©2019. Japan Geoscience Union. All Right Reserved.

Calibration of electric fields dedicated to the measurement of the S-WPIA of the Arase Satellite

*Miki Jumpei[1], Hirotsugu Kojima[2], Yuto Katoh[3], Shoya Matsuda[4], Yoshiya Kasahara[5], Mitsuru Hikishima[4], Satoshi Kurita[6], Masahiro Kitahara[3], Satoshi Kasahara[7], Yoshizumi Miyoshi[6], Atsushi Kumamoto[3], Ayako Matsuoka[4], Shoichiro Yokota[8], Tomoaki Hori[6], Kunihiro Keika[7]

1. Space Radio Engineering Laboratory, Division of Electrical Engineering, Kyoto University Graduated School, 2. Research Institute for Sustainable Humanosphere, Kyoto University, 3. Graduate School of Science and Faculty of Science, Tohoku University, 4. Institute of Space and Astronautical Science, JAXA, 5. Information Media Center, Kanazawa University, 6. Institute for Space-Earth Environmental Research, Nagoya University, 7. School of Science, The University of Tokyo, 8. School of Science, Osaka University

The outer radiation belt consists of high-energy electrons. They are strongly affected by geomagnetic activities in the relation to solar wind conditions. The important science target of the Arase mission is to clarify generation/loss mechanisms of relativistic electrons in the outer radiation belt. Wave-particle interactions are thought to be a plausible mechanism for generation/loss processes of relativistic electrons. S-WPIA (Software-type Wave-Particle Interaction Analyzer) is installed in the Arase satellite. The WPIA is a newly developed observation system that enables us to quantitatively understand the interaction between plasma waves and electrons. The WPIA has the capability to identify a relative phase angle of a plasma wave vector and a velocity vector of each detected particle. Since phase information of observed plasma waves is essential to the WPIA, precise calibrations of plasma wave data are important. While the calibration data for the magnetic field sensors are identical to those we obtained during the ground tests of the instruments, the calibration data for electric field sensors strongly depend on plasma parameters around the satellite. Furthermore, there are still unclear parameters at the inputs of preamplifiers relating to the connection with electric field sensors. The calibration for electric field data needs to be performed carefully consulting observation data after the launch.

The present paper focuses on the calibration of plasma wave data for the S-WPIA’s data processing. We picked up events including whistler-mode chorus emissions and lightning-whistler waves. They all are electromagnetic waves, so-called whistler mode waves. The amplitude ratios of their electric field and magnetic field components can be theoretically calculated referring to the Appleton-Hartlee equations. Poynting vectors of whistler mode waves can be also theoretically obtained. We compared the observation results of the picked up events with the theoretical ones. The results show the precise calibration for the magnetic field data have been made. On the other hand, the calibration for the electric field data should be further modified consulting plasma parameters and other uncertain parameters at the input of preamplifiers. In the present paper, we will discuss the improvement of the calibration for electric field data by correcting the calibration table to aim the precise S-WPIA data processing.

©2019. Japan Geoscience Union. All Right Reserved.

Enhancement of whistler-mode chorus in association with Pc 4-5 ULF waves and related variation of high energy electrons

*Atsuhiro Ono[1], Yuto Katoh[1], Atsushi Kumamoto[1], Fuminori Tsuchiya[1], Mariko Teramoto[2], Yoshiya Kasahara[3], Shoya Matsuda[4], Ayako Matsuoka[4], Takefumi Mitani[4], Tomoaki Hori[2], Satoshi Kasahara[5], Shoichiro Yokota[6], Kunihiro Keika[5], Yoshizumi Miyoshi[2], Iku Shinohara[4]

1. Tohoku University, 2. Nagoya University, 3. Kanazawa University, 4. ISAS/JAXA, 5. The University of Tokyo, 6. Osaka University

Whistler-mode chorus emissions play significant roles in the acceleration and loss of energetic electrons in the magnetosphere. One of the important factors which control periodic enhancement of chorus emissions is ULF (Ultra Low Frequency) waves. Previous studies reported that the compressional component of Pc4-5 ULF waves modulates the intensity of chorus waves [Li et al., 2011] and that the toroidal and poloidal components of Pc4-5 ULF waves as well [Jaynes et al., 2015]. Previous studies also suggested that enhancement of the temperature anisotropy of energetic electrons in the wave generation region should be required for the chorus generation. In order to understand the reported correspondence, in addition to the wave observation, we should examine simultaneously observed variations of the flux and the pitch angle distribution of energetic electrons.

In the present study, we investigate the relationship between chorus emissions and ULF waves using particle and electromagnetic field observations made by the Arase satellite. First, we analyze data observed by the Onboard Frequency Analyzer (OFA) of the Plasma Wave Experiment (PWE) and the Magnetic Field Experiment (MGF) during the campaign observation period of the Arase satellite with ground stations from March to April in 2017. As a result, we identified the simultaneous enhancement of chorus emissions and Pc4-5 ULF waves, which was dominated by the toroidal component, from 2130 to 2200 UT on March 27, 2017. The Arase satellite was located at the magnetic local time about 04:00, the magnetic latitude about -10 degrees, and the L-value about 6 during the event. We find that there is one-to-one correspondence between chorus emissions and the toroidal component of ULF waves; chorus emissions enhanced at the timings when the toroidal magnetic field component of ULF waves had a peak in the westward direction. The identified phase relationship is different from that reported by Jaynes et al. (2015), which isn't one-to-one correspondence. Next, we evaluate the resonance energy of the observed chorus emissions, using the ratio of the plasma frequency to the electron cyclotron frequency (f_p/f_{ce}) based on the upper-hybrid resonance frequency derived from the spectra observed by the High Frequency Analyzer (HFA) of PWE and the ambient magnetic field intensity observed by MGF. We find that f_p/f_{ce} is 3.3-3.4 during the event and that the resonance energy for whistler-mode waves in the frequency range of 0.1-0.2 f_{ce} is estimated to be about 100-400keV, which is larger than typical energies of resonating electrons observed in the inner magnetosphere. The estimated large resonant energy can be explained by the frequency range of the observed chorus emissions, approximately 0.1 - 0.2 f_{ce}, is relatively lower than that observed in typical cases.
We also analyze variations of the flux and the pitch angle distribution of energetic electrons during the event using data observed by the High-energy electron experiments (HEP) instrument onboard Arase. The result shows that both the flux and the pitch angle distribution of electrons in the kinetic energy range from 100 to 400 keV, which corresponds to the estimated resonance energy, did not fluctuate with the intensity variation of the chorus emissions and the ULF waves. In addition, we analyze the data observed by the Medium-energy particle experiments - electron analyzer (MEP-e) for energetic electrons in the energy range of 10-80 keV, lower than the estimated resonance energy. Then we identify the

©2019. Japan Geoscience Union. All Right Reserved.

corresponding variation of both the flux and the pitch angle distribution in the 40-60 keV energy range. One of the possible reasons why no significant variations were observed in the hundred keV range would be that the Arase satellite was located in the off-equatorial region during the event, and that the satellite was away from the wave generation region.

Keywords: ULF waves, chorus emissions

©2019. Japan Geoscience Union. All Right Reserved.

Sudden enhancements of electron cyclotron harmonic waves observed by the Arase satellite

*Shinjo Airi[1], Hirotsugu Kojima[1], Yoshiya Kasahara[2], Yoichi Kazama[3], Hideyuki Usui[4], Yoshizumi Miyoshi[5], Yasumasa Kasaba[6], Shoya Matsuda[7], Tomoaki Hori[5], S. -Y. Wang[8], Sunny W.Y. Tam[9], Atsushi Kumamoto[10], Ayako Matsuoka[11]

1. Research institute for sustainable humanosphere, Kyoto University, 2. Information Media Center, Kanazawa University, 3. ASIAA, 4. Graduate school of system informatics Kobe University, 5. Institute for Space-Earth Environmental Research, Nagoya University, 6. Planetary Plasma and Atmospheric Research Center, Tohoku University, 7. Institute of Space and Astronautical Science/Japan Aerospace Exploration Agency, 8. ASIAA, Taiwan, 9. ISAPS, NCKU, Taiwan, 10. Department of Geophysics, Graduate School of Science, Tohoku University, 11. Research Division for Space Plasma, Institute of Space and Astronautical Science, Japan Aerospace Exploration Agency

Electron cyclotron harmonic (ECH) waves are commonly observed in the low latitude region just outside the terrestrial plasmapause. They are purely electrostatic and their frequency spectra show harmonic structures. The harmonic structures are believed to depend on the temperature and density ratio between cold and hot background electrons. The Plasma Wave Experiment (PWE) onboard the Arase satellite has observed ECH waves since the start of its operation. The observed ECH waves are classified into two types. They are the diffuse ECH waves and the enhanced ECH waves. The diffuse ECH waves are weak and they appear as continuous emissions that last for more than a few minutes. The enhanced ECH waves are the sudden enhancements of the diffuse ECH in shorter periods. The present paper focuses on the enhanced ECH waves observed by the Arase satellite.

Kazama et al. (2018) introduced the event that the repeated enhancement of ECH waves is associated with density depletions near the plasmapause. They succeeded in revealing the good correlation of the enhancement of the ECH waves and the sudden decrease of the cold electrons with energies lower than the lowest energy limit of the particle detector. The observed electron features are clear in the relation to the enhancement of ECH waves, but the mechanism of the enhancement is still unclear. We searched for such events of the enhanced ECH waves and examined the correlation of wave intensities, spacecraft potentials and electron velocity distributions observed by the Arase satellite. Some of the events show the features similar to those of Kazama et al. (2018), but there are also many other events with no correlation between the enhancements of the ECH waves and the density depletions. In the present paper, we examine velocity distribution functions of electrons observed by the low-energy particle experiments-electron analyzer (LEPe) onboard Arase. Velocity distribution functions allow us to examine temperature anisotropies of electrons and calculate linear dispersion relations for the ECH waves. Once we get electron temperatures, resonance velocities are calculated. On the other hand, since the wavelength of the ECH waves is very short, the relation of the wavelength and the length of the Arase electric field sensors is also important in evaluating the time variations of the ECH wave intensity. We study the enhanced ECH waves in various viewpoints using wave and electron data observed by the Arase satellite and discuss the generation mechanism in the present paper.

©2019. Japan Geoscience Union. All Right Reserved.

Correlation between pulsating aurora and electrostatic electron cyclotron harmonic waves obtained from coordinated Arase and ground data

*Mizuki Fukizawa[1], Takeshi Sakanoi[1], Yoshizumi Miyoshi[2], Keisuke Hosokawa[3], Yoichi Kazama[4], Yoshiya Kasahara[5], Shoya Matsuda[6], Ayako Matsuoka[7], Wang Shiang-Yu[4], Sunny Wing-Yee Tam[8], Ryuho Kataoka[9]

1. Planetary Plasma and Atmospheric Research Center, Graduate School of Science, Tohoku University, 2. Institute for Space-Earth Environmental Research, Nagoya University, 3. Department of Communication Engineering and Informatics, University of Electro-Communications, 4. Academia Sinica Institute of Astronomy and Astrophysics, 5. Information Media Center, Kanazawa University, 6. Institute of Space and Astronautical Science/Japan Aerospace Exploration Agency, 7. Research Division for Space Plasma, Institute of Space and Astronautical Science, Japan Aerospace Exploration Agency, 8. Institute of Space and Plasma Sciences, College of Sciences, National Cheng Kung University , 9. National Institute of Polar Research

Pulsating auroras (PsAs) are thought to be generated by precipitating electrons scattered by lower-band chorus (LBC) waves near the magnetic equator through cyclotron resonance. Previous studies showed one-to-one correlation between LBC wave intensity observed by satellites near the magnetic equator and PsA intensity obtained by ground-based all-sky imager [e.g., Nishimura et al., Science, 2010, Nishimura et al., JGR, 2011]. In addition, electrostatic electron cyclotron harmonic (ECH) waves can also interact with magnetospheric electrons and scatter their pitch angle theoretically [e.g., Lyons, JGR, 1974]. However, characteristics of aurora caused by ECH are not understood. In our study, we report for the first time in the world that not only LBC but also ECH wave intensity has correlation with the PsA intensity using coordinated Arase and ground-based imager observations. The first campaign observations between the Arase satellite and ground-based optical imager were conducted in March 2017. A typical substorm occurred on 27 March 2017 and the ionospheric footprint of Arase traversed the field of view of all-sky imager at Sodankylä during 00:00–03:15 UT on 29 March 2017. Quasi-periodic LBC and ECH waves were observed by Arase near the magnetic equator and PsA was detected by the all-sky imager during 01:30–02:00 UT. We calculated the cross-correlation coefficients between auroral intensity and LBC or ECH wave intensity from 01:30 UT to 02:00 UT with a time window of every 2 minutes. The highest cross-correlation coefficient between auroral intensity and LBC wave intensity was 0.73 and that between auroral intensity and ECH wave intensity was 0.62 from 01:46 UT to 01:48 UT, and they were statistically significant. The period of auroral intensity which correlated with LBC intensity was shorter than 10 s and that correlated with ECH intensity was 10–20 s. We estimated the precipitating electron energy assuming that the time lag when the cross-correlation coefficient became the highest equals to the travel time of electrons from the modulated source region to the auroral emission height. We shifted the variation of auroral intensity against that of ECH or LBC wave intensity with a time step of 0.01 s using 100 Hz sampling image data taken by the all-sky imager. The estimated energy of precipitating electron interacted with LBC waves was ~20–67 keV and that interacted with ECH waves was ~3–4 keV. On the other hand, we independently estimated the cyclotron resonance energy of LBC and ECH waves from the Arase's observation data and geomagnetic field model by TS04 Model [Tsyganenko and Sitnov, JGR, 2005]. The estimated cyclotron resonance energy of LBC waves was ~30 keV. Although the cyclotron resonance energy of ECH waves could not be estimated because it was difficult to obtain the electron temperature and wave normal angle of ECH waves from Arase data, we suggest the cyclotron resonance energy of ECH waves to be a few keV with probable assumptions. From these results, we suggest that LBC waves interact with high energy electrons which cause auroral emission at lower altitudes, while ECH waves interact with

©2019. Japan Geoscience Union. All Right Reserved.

relatively low energy electrons which cause auroral emission at higher altitudes. These results were published in Fukizawa et al. [GRL, 2018].
To verify whether ECH waves indeed scatter the pitch angle of electrons, we compared ECH wave intensity with electron flux in the loss cone obtained with low-energy particle experiments-electron analyzer onboard Arase. We also give results of other coordinated observation events.

Keywords: pulsating aurora, ECH waves, wave-particle interaction

©2019. Japan Geoscience Union. All Right Reserved.

Automatic determination of Upper Hybrid Resonance Frequencies by Convolutional Neural Network.

*Shoya Matsuda[1], Tatsuhito Hasegawa[2], Atsushi Kumamoto[3], Fuminori Tsuchiya[3], Yoshiya Kasahara[4], Yoshizumi Miyoshi[5], Yasumasa Kasaba[3], Ayako Matsuoka[1]

1. Institute of Space and Astronautical Science/Japan Aerospace Exploration Agency, 2. University of Fukui, 3. Tohoku University, 4. Kanazawa University, 5. ISEE, Nagoya University

Electron number density is a key parameter for discussions of plasma wave generation/propagation, and wave-particle interaction in the inner magnetosphere. The High Frequency Analyzer (HFA) is a subsystem of Plasma Wave Experiment (PWE) aboard Arase [Kasahara et al. (2018), Kumamoto et al. (2018), Miyoshi et al. (2018)]. The HFA measures electric field spectra in a frequency range from 10 kHz to 10 MHz, which covers a typical frequency range of Upper Hybrid Resonance (UHR) frequency in the inner magnetosphere. Kumamoto et al. (2018) proposed the semiautomatic method for the identification of UHR frequency by computer and a human operator. However, it takes a enormous effort of a human operator.

We propose an automatic determination system of UHR frequency by machine learning. Machine learning is a technique in the field of artificial intelligence to give computers the ability to learn with data. In this study, we defined a task of UHR frequency determination as supervised regression that a computer estimates UHR frequencies using the dataset composed of electric field dynamic spectra with correct UHR frequency labels. We adopted Convolutional Neural Network (CNN) as a machine learning algorithm. In this study, we introduce our machine learning approach and initial results for determining UHR frequency from electric field spectra observed by PWE/HFA.

Keywords: Arase satellite, UHR frequency, Machine learning

©2019. Japan Geoscience Union. All Right Reserved.

Amplitude dependence of whistler wave motion on electron scattering process

*Yoshiki Ito[1], Yoshizumi Miyoshi[1], Shinji Saito[1]

1. Nagoya University, ISEE

Whistler mode chorus waves cause scattering and acceleration of energetic electrons in the inner magnetosphere. The interaction processes have been modeled as diffusive process. The pitch angle diffusion coefficients of the pitch angle scattering depend on the power of chorus waves, so that it is expected that the scattering rate also depends on the wave amplitude. On the other hand, several previous studies indicated that the Lorentz force by the wave magnetic field is larger than the mirror force if the wave amplitudes increase and the electron trajectories in the velocity space are different from the diffusive distributions. In this study, we investigate chorus wave amplitude dependence of electron scattering using the GEMSIS-RBW simulation code. The RBW simulation demonstrates generation of periodical rising-tone chorus waves propagating along a magnetic field line to higher latitudes, and calculates local pitch angle and energy change by the imposed waves on the field line. At small wave amplitudes, time variations of pitch angle and energy of electrons are similar to diffusive process. At large wave amplitudes, some electrons increase both pitch angle and energy at interaction with the first rising tone, and then they decrease these parameters at interaction with the second rising tone. The process in the first rising tone seems to be the phase trapping, while the process in the second rising tone seems to be dislocation. Therefore, nonlinear scattering processes, which are phase trapping and dislocations, occur during the interactions with periodical rising-tone chorus waves with large amplitudes, which are quite different from quasi-linear scattering process.

©2019. Japan Geoscience Union. All Right Reserved.

Two-dimensional simulation of whistler mode wave packets interacting with energetic electrons

*Takeshi Nogi[1], Yoshiharu Omura[1]

1. Reserch Institute for Sustainable Humanosphere, Kyoto University

We perform two-dimensional electromagnetic particle simulations to study basic characteristics of whistler-mode wave particle interaction involved in the generation and propagation processes of chorus emissions with wave normal angles oblique to the static magnetic field. We assume a simple periodic (x, y) system with the magnetic field taken in the x-direction. We find the linear phase of the instability is much affected by electrostatic thermal fluctuations. It is necessary to put many super-particles in a grid cell to suppress the thermal fluctuation. We next put an array of antennas perpendicular to the background magnetic field, and oscillate the antenna current to generate obliquely propagating waves. In addition to the nonlinear trapping of energetic electrons through the cyclotron resonance, another nonlinear trapping of electrons takes place through the Landau resonance. Structures of the nonlinear trapping potentials change with the varying frequency, affecting efficiency of energy transfer between the wave and energetic electrons. We study nonlinear evolution of the wave packet, and competing processes of both resonances in accelerating energetic electrons to higher energies.

©2019. Japan Geoscience Union. All Right Reserved.

Relativistic electron acceleration by whistler-mode chorus waves in 1D, 2D, and 3D magnetic field models.

*Keita Takahashi[1], Yoshiharu Omura[1], Yikai HSIEH[1], Danny Summers[2]

1. Research Institute for Sustainable Humanosphere, Kyoto University , 2. Department of Mathematics and Statistics, Memorial University of Newfoundland

We evaluate the acceleration efficiencies of relativistic electrons under a 1D, 2D, and 3D model magnetic fields. We perform test-particle simulations and analyze nonlinear trapping motions of resonant electrons in each model. As a chorus wave model, we assume that a chorus wave packet generated at the magnetic equator propagates along the magnetic field to higher latitudes. When we perform simulations with the whistler mode wave, the cyclotron resonance with energetic electrons occurs at the similar timing in each model. Although we find relativistic turning acceleration (RTA) [1] to take place in each model, acceleration efficiencies of resonant electrons are different in these models. In terms of the numerical Green's function[2], we find a clear difference in time evolution of the distribution function in energy and equatorial pitch angle. The energy gap between resonant electrons and non-resonant electrons in the 1D model is slightly different from those in the 2D and 3D models. The energy gap in the 3D model is the largest among the three magnetic field models. This difference is due to additional oscillations in the velocity phase space, which only occur in the 2D and 3D models. These oscillations occur because the magnitude of the magnetic field changes during one period of relativistic cyclotron motion, affecting the nonlinear trapping conditions of resonant electrons.

References:

[1] Y. Omura, N. Furuya, D. Summers, Relativistic turning acceleration of resonant electrons by coherent whistler-mode waves in a dipole magnetic field, Journal Geophysical Research, Vol. 112, A06236, doi:10.1029/2006JA012243, 2007.

[2] Y. Omura, Y. Miyashita, M. Yoshikawa, D. Summers, M. Hikishima, Y. Ebihara, and Y. Kubota (2015), Formation process of relativistic electron flux through interaction with chorus emissions in the Earth's inner magnetosphere, J. Geophys. Res. Space Physics, 120, 9545–9562, doi:10.1002/2015JA021563, 2015.

©2019. Japan Geoscience Union. All Right Reserved.

Study of global spatio-temporal development of magnetospheric ELF/VLF waves for the 26-30 March 2017 storm based on ground and satellite observations and the RAM simulations

*Yuhei Takeshita[1], Kazuo Shiokawa[1], Yoshizumi Miyoshi[1], Mitsunori Ozaki[2], Yoshiya Kasahara[2], Martine Connors[3], Jyrki Manninen[4], Craig Kletzing[5], Vania Jordanova[6]

1. Nagoya University, Institute for Space-Earth Environmental Resarch, 2. Kanazawa University, 3. Athabasca University, 4. Sodankylä Geophysical Observatory, 5. The University of Iowa, 6. Los Alamos National Laboratory

The magnetospheric ELF/VLF waves are plasma waves generated by energetic electrons from several keV to tens keV with temperature anisotropy at magnetospheric equatorial plane of the inner magnetosphere. These ELF/VLF waves with frequencies lower than local half gyro frequency (lower-band) can propagate to the ground along magnetic field line. It is also known that the ELF/VLF waves interact with electrons drifting longitudinally in the inner magnetosphere, and help accelerating them to relativistic energies. Takeshita et al. [SGEPSS, 2018] statistically investigated the longitudinal extent of the magnetospheric ELF/VLF waves using six ground-based stations for two months, and showed the average extent of the ELF/VLF waves as ~90 degrees in longitude. However, Jordanova et al. [JGR, 2010] investigated the global distribution of linear growth rate of whistler mode chorus waves using global ring current-atmosphere interactions model (RAM), and showed that the region of large linear growth rate can extend ~180 degrees in longitude during the geomagnetic storm of 22 April 2001.

In this study we investigate the spatio-temporal distibution of the source region of magnetospheric ELF/VLF waves based on ground and satellite observations during the geomagnetic storm period from 26-30 March 2017, and compare it with global distribution of non-linear waves proxy of whistler mode chorus waves obtained by the RAM simulation. In this preliminary simulation, the simple dipole field and the Volland-Stern electric field are used as ambient magnetic and electric fields. And we assumed simply the Maxwell distribution as an energy spectrum using the empirical model of Tsyganenko and Mukai [2003]. In order to evaluate the non-linear wave excitation, we have estimated the optimum amplitude and the threshold value indicated by Omura and Nunn [2011]. We investigated the existence of lower band chorus waves using ground based observations at Athabasca (ATH; 54.7N, 246.4E, MLAT: 61.3N), Kapuskasing (KAP; 49.4N, 277.8E, MLAT: 58.7N), Kannuslehto (KAN: 67.7N, 26.3E, MLAT: 64.5N) and satellite-based observations by ERG with an apogee in the pre-dawn sector and RBSP-A and RBSP-B with an apogees in the post-dusk sector. We found the magnetospheric ELF/VLF waves exist from 3 MLT to 12 MLT for most periods from main- to recovery-phases of the magnetic storm. However, the RAM simulation did not predict wave generation during recovery phase of the storm. We compare the simulation and the ground-satellite observation in detail, and calculate the over-estimate rate (the ratio of wave existence period on the simulation to no wave period on the observation) and under-estimate rate (the ratio of no wave period on the simulation to wave existence period on the observation). We found the over-estimate rate become high (0.2~0.9) and under-estimate rate become low (0~0.4) in the main phase of the storm. This indicates that the longitudinal size of chorus source region predicted by simulation is larger than the observed size at the main phase. We also found that the over-estimate rate becomes low (0~0.2) and under-estimate rate becomes high (~1) during the recovery phase of the storm. This indicates that the simulation does not reproduce the wave existence during the recovery phase of the storm. Looking into the MLT distribution, the simulation predicts the wave existence from dusk to the midnight sector, but the

©2019. Japan Geoscience Union. All Right Reserved.

waves were not observed in this local time sector during the main phase. In case of recovery phase, the simulation did not predict wave existence but the observation showed continuous wave existence from dawn to the noon sector.

Keywords: chorus, ERG satellite, ground based observation

©2019. Japan Geoscience Union. All Right Reserved.

Flux decrease of outer radiation belt electrons associated with solar wind pressure pulse: A Code coupling simulation of GEMSIS-RB and GEMSIS-GM

*Ito Hiroki[1], Yoshizumi Miyoshi[1], Shinji Saito[2], Yosuke Matsumoto[3], Takanobu Amano[4]

1. Institute for Space-Earth Environmental Research, Nagoya University, 2. Graduate School of Science, Nagoya University, 3. Graduate School of Science, Chiba University, 4. Department of Earth and Planetary Science, University of Tokyo

Relativistic electron flux of the outer radiation belt dynamically changes in response to solar wind variations. There exist several conditions to cause the flux drop-out of the outer belt electrons. The magnetopause shadowing (MPS) is one of the processes to cause the rapid loss of outer belt electrons (e.g.,Kim et al.,2008). In this study, we investigate how radiation belt electrons are lost through the MPS process with a code-coupling simulation using GEMSIS-RB test particle simulation code (Saito et al., 2010) and GEMSIS-GM global MHD magnetosphere simulation code (Matsumoto et al., 2010) by focusing the equatorial pitch angle and local time dependence. We calculate trajectories of electrons in electromagnetic fields calculated from GEMSIS-GM with initial L-shells from 6 to 11, initial energies from 1 MeV to 10 MeV, and initial pitch angles between 50 degrees and 90 degrees, using the relativistic guiding-center equation. The simulation consists of the following three phases associated with variations of the solar wind dynamic pressure; [i] The standoff distance of magnetopause at the subsolar point is 12 Re with the initial dynamic pressure of 1.0 nPa. [ii] The solar wind dynamic pressure becomes 2.5 nPa, and the magnetopause moves to 9 Re. [iii] The solar wind dynamic pressure decreases, so that the inflation of the magnetopause takes place and the standoff distance of the magnetopause is 10 Re. During phase [ii], the high-latitude reconnections occur at dawn-side firstly and many electrons escape from the magnetosphere to the interplanetary magnetic field along the field line in the dawn side. Subsequently, the high-latitude reconnections occur at the high-latitude in the dusk side. In phase [iii], the remained electrons in the magnetosphere escape into the interplanetary in both the dawn and dusk sides. The loss at the dusk-side is outward motion of the trapped electrons caused by the dawn-to-dusk electric fields associated with the inflation of the magnetosphere. The study showed detailed process of the electron escape into the interplanetary magnetic field and the electron escape occur in both enhancement/decrease of the dynamic pressure.

Keywords: Magnetopause Shadowing, global MHD magnetosphere simulation, test particle simulation

©2019. Japan Geoscience Union. All Right Reserved.

Non-diffusive response of outer belt electrons on interplanetary shock

Takuma Toishi[1], *Yusuke Ebihara[1], Takashi Tanaka[2]

1. Research Institute for Sustainable Humanosphere, Kyoto University, 2. Kyushu University

Test particle simulation is performed in the electric and magnetic fields given by a global magnetohydrodynamics (MHD) simulation. When an interplanetary shock strikes the magnetosphere, a compressional wave propagates tailward. Pre-existing relativistic electrons that are initially located at fixed radial distances are redistributed by the electric and magnetic fields associated with the compressional wave. When the electrons encounter the nightside, they undergo complicated paths under the complicated distribution of the electric and the magnetic fields. Consequently, a group of isolated electrons forms, suggesting non-diffusive response. We discuss the redistribution processes in terms of the magnetospheric processes.

Keywords: radiation belt, MHD simulation, Test particle simulation

©2019. Japan Geoscience Union. All Right Reserved.

PARM: Initial result of the auroral camera on the G-CHASER (RockSat-XN) rocket and status of the development of auroral cameras for the LAMP rocket experiment

*Naoshi Yagi[1], Takeshi Sakanoi[1], Fukizawa Mizuki[1], Kazushi Asamura[2], Yoshizumi Miyoshi[3], Keisuke Hosokawa[4], Genki Ishizawa[5]

1. Planetary Plasma and Atmospheric Research Center, Graduate School of Science, Tohoku University, 2. Institute of Space and Astronautical Science, Japan Aerospace Exploration Agency, 3. Institute for Space-Earth Environmental Research, Nagoya University, 4. Department of Communication Engineering and Informatics, University of Electro-Communications, 5. Space & terrestrial plasma pyhsics

We developed an Aurora Imaging Camera (AIC) for NASA’ s G-CHASER (RockSat-XN) sounding rocket launched on 13th January, 2019. In addition, LAMP sounding rocket scheduled to be launched from December 2019 to February 2020 to reveal the spatio-temporal relationship between PsA and relativistic electrons, namely microbursts. In this presentation, we report the development of AIC, the result f the G-CHASER (RockSat-XN) rocket, as well as the current status of LAMP rocket project.

On the G-CHASER rocket experiment, 7 scientific and educational instruments were provided from Japan, U.S., Norway and Puerto Rico. Japanese instrument, called PARM, consists of an intermediate energy (20 - 100 keV) electron detector MED, high energy (several hundred keV - 2 MeV) electron detector HEP, fluxgate magnetometer AFG, and auroral camera AIC. Concerning development of AIC, we carried out sensitivity calibration experiment, electrical function test, fabrications, focus adjustment and environmental (vibration, vacuum and thermal) tests from January to July 2018. AIC consists of detector unit AIC-S and power/data processing electric unit AIC-E. AIC-S consists of a CCD camera (Watec 910 HX), wide-angle lens (F-number: 1.6, focal length: 3.5 mm, field of view: 96.4˚x75˚) and a glass filter (RG665) that transmits light with a wavelength longer than 665 nm.

NASA decided to launch the G-CHASER rocket at 9:00UT on 13rd January 2019 from Andoya Space Center, Norway (69.3˚N, 16.0˚E in the geographic coordinate). At this time, the solar elevation was -4˚, hence twilight had been already started and the region above 15km was sunlit. AIC detected leak light from the rocket skirt until the separation of skirt at an altitude of 82.9km. From time variation of AIC data, rocket spin frequencies were estimated to be ~5Hz at ~20km altitude and ~1Hz at ~80km altitude. This is consistent with the modulation period of magnetic field data observed by AFG. Because AIC was designed to measure weak pulsating aurora with hundreds Rayleigh, the AIC data was saturated above 82.9km after separation of rocket in the sunlit region, and no aurora was observed.

We are also conducting the LAMP sounding rocket project whose PI is Dr. Sarah Jones in NASA/GSFC. This is scheduled to be launched at Poker Flat Research Range in Alaska in 2019 winter. Japanese PARM2 team will provide high energy (several hundred keV - 2 MeV) electron detector HEP, fluxgate magnetometer MIM, and auroral cameras AIC2. We concern AIC2 that consists of two cameras AIC2-S1/AIC2-S2 and power/data processing electric unit AIC2-E. AIC2-S1/S2 and AIC2-E will be installed on a despun platform to derotate rocket spin. AIC2-S1 measures N2 1stPG emission with a narrow FOV lens (F value: 0.95, focal length:17mm, field of view 27x27deg), and AIC-S2 measures OI 844.6nm emission with a wide-angle lens (F value:1.6, focal length:3.5 mm, diagonal field of view:120x120˚). AIC2-S1 will take fine structure of PsA in the region more than 100 x 100 km area around the magnetic footprint with a few kilometer resolution, while AIC2-S2 will obtain an altitude distribution of

©2019. Japan Geoscience Union. All Right Reserved.

PsA in the F-region as well as wide-range distribution of PsA. The characteristic energy of precipitating electron can be estimated from the ration of OI844.6 and N2 1stPG. The cameras are conducted by a single board computer NanoPi M4 via USB3.0 high speed interface. We confirmed to get frame sampling rate with approximately 10Hz with this system. Region-of-interest (ROI) of 3660 x 3660 pixel area is binned with 61x61pixels, and finally image data with 60 x 60 bin (16 bit/bin) is recorded at 10 Hz. The precise imaging and altitude distribution of PsA are obtained with AIC2 at two wavelengths with 10Hz sampling. The imaging data combined with precipitating electron data in the wide energy range enable us to investigate the relativistic electron precipitation in microbursts that is probably caused by chorus waves in the magnetosphere.

Keywords: auroral camera, rocket experiment

©2019. Japan Geoscience Union. All Right Reserved.

First simultaneous observation of a SAR arc at subauroral latitudes using a ground all-sky camera and the Arase satellite in the inner magnetosphere

*Yudai Inaba[1], Kazuo Shiokawa[1], Shin-ichiro Oyama[1,8,9], Yuichi Otsuka[1], Atsuki Shinbori[1], Yoichi Kazama[2], Shiang-Yu Wang[2], Sunny W. Y. Tam[2], Shoichiro Yokota[3], Satoshi Kasahara[4], Kunihiro Keika[4], Tomoaki Hori[1], Ayako Matsuoka[5], Yoshiya Kasahara[6], Atsushi Kumamoto[7], Yasumasa Kasaba[7], Yoshizumi Miyoshi[1], Iku Shinohara[5], Arto Oksanen[10]

1. Institute for Space-Earth Environmental Research, 2. Academia Sinica, 3. Osaka Univ, 4. Tokyo Univ, 5. JAXA, 6. Kanazawa University, 7. Tohoku University, 8. University of Oulu, Finland, 9. National Institute of Polar Research, 10. Jyväskylän Sirius ry, Finland

Stable Auroral Red (SAR) arc is characterized by a 630.0 nm emission observed at subauroral latitudes. The energy of precipitating electrons that cause the SAR arc emission is several electron volts (eV). Precipitation of low-energy electrons is expected to occur due to spatial overlap between the plasmasphere and the ring current, where high-energy (more than 10 keV) ring current ions heat low-energy (less than 1 eV) electrons in the plasmasphere. Simultaneous observations of SAR arcs using the ionospheric satellite and ground all-sky cameras have been already done [e.g., Foster et al., 1994]. However, there has been no reports on in-situ measurements of plasma and electromagnetic fields in the inner magnetosphere, where the plasmaspheric plasma is heated by the ring current. In this study, we report simultaneous observations of a SAR arc at 22:04 UT on March 28, 2017, by using an all-sky camera at Nyrola (62.34 N, 25.51 E, MLAT 59.4 N) at subauroral latitudes and the Arase satellite. We analyze the all-sky camera data and the satellite data of this event to investigate the generation mechanism of the SAR arc. We find interesting features in the electric field data and the energy flux of electrons observed by the electric field detector of the plasma wave experiment (EFD/PWE) and the low-energy particle experiments–electron analyzer (LEP-e), respectively, onboard the Arase satellite at the crossing of the SAR arc. A negative excursion of the Ez component of the electric field (GSE coordinate system) with an amplitude of ~2.4 mV/m was observed at the crossing time. The Bx component of the magnetic field (GSE coordinate system) was negative. Thus the direction of the E ×B drift is westward, which is consistent with the westward auroral motion observed in the SAR arc by the ground all-sky camera. At the SAR arc crossing, the energy flux of electrons below 100-eV electrons is slightly intensified. We will discuss these observations in relation to the proposed SAR-arc generation mechanisms.

Keywords: ERG, SAR arc, All-sky imager, Simultaneous observation

©2019. Japan Geoscience Union. All Right Reserved.

Pi2 pulsations observed by the Arase satellite inside and outside the plasmapause

*Mariko Teramoto[1], Ayako Matsuoka[2], Reiko Nomura[5], Yoshiya Kasahara[3], Yasumasa Kasaba[4], Atsushi Kumamoto[4], Fuminori Tsuchiya[4], Shoya Matsuda[2], Masahito Nose[1], Masafumi Shoji[1], Yasunori Tsugawa[1], Shun Imajo[1], Yoshizumi Miyoshi[1], Iku Shinohara[2]

1. Institute for Space-Earth Environmental Research Nagoya University, 2. Institute of Space and Astronautical Science, Japan Aerospace eXploration Agency, 3. Kanazawa University, 4. Tohoku University, 5. National Astronomical Observatory of Japan

The spatial structure of Pi2 pulsation relative to the plasmasphere has been studied using the magnetic and electric field observed from the equatorial orbiting satellite in the inner magnetosphere by Takahashi et al (2003; 1995). They showed that the nightside Pi2 pulsations in the inner magnetosphere, which have high coherence with those at low-latitude ground station, are dominated by the poloidal component (the radial and compressional components for the magnetic field and azimuthal component for the electric field). The amplitudes of the compressional magnetic field has maximum and azimuthal electric field and the compressional magnetic field have maximum and minimum in the vicinity of the plasmaspause, respectively. The phase of the azimuthal electric field relative to low-latitude Pi2 pulsations on ground is 90 degrees in the plasmasphere. Such radial profile of the amplitude and phase of Pi2 pulsations can be explained by a plasmaspheric cavity mode resonance. However, the latitudinal structure of Pi2 pulsations in the electric field has not been examined. We investigate the latitudinal characteristics of off-equatorial Pi2 pulsations on the nightside and their relation to the plasmapause using the magnetic field measured by the fluxgate magnetometer measured by the Magnetic Field Experiment (MGF), the electric field measured by the Electric field Detector (EFD), and electron density derived from the spectra measured by the High Frequency Analyzer (HFA) from the Arase satellite.

©2019. Japan Geoscience Union. All Right Reserved.

An extreme erosion of the plasmasphere during the 7–10 September 2017 storm

*Yuki Obana[1], Naomi Maruyama[2,3], Atsuki Shinbori[4], Kumiko K. Hashimoto[5], Mariangel Fedrizzi[2,3], Masahito Nose[4], Yuichi Otsuka[4], Nozomu Nishitani[4], Tomoaki Hori[4], Atsushi Kumamoto[6], Fuminori Tsuchiya[6], Shoya Matsuda[7], Ayako Matsuoka[7], Yoshiya Kasahara[8], Akimasa Yoshikawa[9], Yoshizumi Miyoshi[4], Iku Shinohara[7]

1. Osaka Electro-Communication University, 2. University of Colorado Boulder, 3. NOAA Space Weather Prediction Center, 4. Nagoya University, 5. Kibi International University, 6. Tohoku University, 7. Japan Aerospace Exploration Agency, 8. Kanazawa University, 9. Kyushu University

We report an extreme erosion of the plasmasphere arising from the September 2017 storm. The cold electron density is identified from the upper limit frequency of UHR waves observed by the HFA of the PWE instrument onboard the Arase spacecraft. The HFA provides the spectrograms of electric fields in a frequency range from 10 kHz to 10 MHz with an 8-sec time resolution (Kasahara et al., 2018; Kumamoto et al., 2018). Such wide frequency coverage allows observation of the UHR frequency even deep inside the plasmasphere.
The electron density profiles reveal that the plasmasphere was severely eroded during the recovery phase of the storm and the plasmapause was located at L~1.7 at 23 UT on 8 Sep 2017. This is the first report of such deep erosion of the plasmasphere (L_{PP}<2) with the in-situ observation of the electron density. The degree of the severity is much more than what is expected from the SYM-H minimum (−146 nT) of the event.
We further study absolute GNSS-TEC, ground-based magnetic field, the doppler velocity obtained from the SuperDARN Hokkaido Radars to investigate the location of the midlatitude ionospheric trough, the penetration of the convection electric field to the equator and middle latitudes, respectively. Our results suggest that the middle latitude electric field was penetrated from the high-latitude storm time convection for several hours. Futhermore, the Ionosphere-Plasmasphere-Electrodynamics (IPE) model (Sun et al., 2015; Maruyama et al., 2016) is used to understand the dynamics of the plasmasphere. The IPE results suggest that the middle latitude electric field penetrates from the high-latitude storm time convection that lasts for several hours can explain the degree of severity during the September 7-11 2017 storm.

Keywords: plasmasphere, innner magnetosphere, Magnetosphere-ionosphere coupling

©2019. Japan Geoscience Union. All Right Reserved.

Relative contribution of ULF and chorus waves to the radiation belt variation: Comparison between multi-point observations and BATSRUS + CRCM simulation

*Naoko Takahashi[1], Kanako Seki[1], Mei-Ching Fok[2], Yihua Zheng[2], Yoshizumi Miyoshi[3], David Hartley[4], Ayako Matsuoka[5], Yoshiya Kasahara[6], Yasumasa Kasaba[7], Nana Higashio[8]

1. Graduate School of Science, University of Tokyo, 2. NASA Goddard Space Flight Center, 3. Institute for Space-Earth Environmental Research, Nagoya University, 4. Department of Physics and Astronomy, University of Iowa, 5. Institute of Space and Astronautical Science, Japan Aerospace Exploration Agency, 6. Information Media Center, Kanazawa University, 7. Planetary Plasma and Atmospheric Research Center, Tohoku University, 8. Japan Aerospace Exploration Agency

Earth’ s radiation belt is the area where electrons with energies from hundreds of keV to several MeV are trapped. When, where, and how the radiation belt exhibits a dramatic variation during a magnetic storm is of global interest. The dynamic variation of the radiation belt is caused by various wave-particle interactions: (1) the radial diffusion of electrons driven by ultra-low-frequency (ULF) waves in Pc5 frequency ranges (1.6–6.7 mHz) and (2) the local acceleration caused by wave-particle interactions between whistler-mode chorus waves and radiation belt particles. Over the past decade, multi-point observations and numerical simulations have provided evidence to support above physical processes. However, it is debatable how much each wave contributes to the radiation belt variation during a magnetic storm. A few previous studies have quantitatively compared roles of local acceleration and radial transport by calculating diffusion coefficients, whereas the global context between the wave growth and the relativistic electron flux enhancement has not been extensively studied. To address these issues, the comprehensive study using multi-point observations and numerical simulations (not empirical models) makes essential and significant contributions.

We focus on the magnetic storm on 27-30 May 2017. This magnetic storm is triggered by coronal mass ejections and induces a clear interplanetary shock. Fortunately, several satellites are scattered in the inner magnetosphere and detect both ULF and chorus waves during this magnetic storm. Arase and Van Allen Probes also detect variations of relativistic electron fluxes associated with the Dst index variation. We examine L-value dependence of ULF and chorus wave powers and find the difference of wave activity during the recovery phase. The chorus wave activity is large during the early recovery phase, while the ULF wave activity is large during the late recovery phase. The difference of wave activity may contribute to the radial profile in the phase space density of relativistic electrons. To grasp the extent of individual wave contribution, we also perform the comprehensive ring current model (CRCM) coupled with Block-Adaptive-Tree Solar-Wind Roe-Type Upwind Scheme (BATSRUS) simulation. BATSRUS with CRCM well reproduces global characteristics of energetic electron fluxes and wave growth during this magnetic storm. We will further evaluate global distribution of simulated wave power comparing to the observation, and then discuss the temporal and spatial context between each wave growth and the radiation belt variation.

©2019. Japan Geoscience Union. All Right Reserved.

Modulation of the D-region ionosphere by Pc5 waves observed by VLF/LF standard radio waves

*Miyashita Takuya[1], Hiroyo Ohya[1], Fuminori Tsuchiya[2], Hiroyuki Nakata[1], Toshiaki Takano[1], Kazuo Shiokawa[3], Yoshizumi Miyoshi[3]

1. Chiba University, 2. Tohoku University, 3. Nagoya University

Ionospheric modulation due to ultra low frequency (ULF) Pc5 waves have been observed by GPS-total electron content (TEC), high frequency (HF) Doppler sounders, and SuperDARN HF radars [e.g., Pilipenko et al., 2014; Belakhovsky et al., 2016]. However, there are few reports for the modulation of the lower ionospheric associated with the ULF Pc5 waves using VLF/LF transmitter signals. In this study, we investigate the D-region signatures of the modulation due to the ULF Pc5 waves using a network of very low frequency (VLF)/low frequency (LF) standard radio waves. We show oscillations in intensities of the VLF/LF waves with a period of 4-6 minutes during substorms on 27 April, 2017. The transmitter signals from NAA (USA, 24.0 kHz, L = 2.88), NLK (USA, 24.8 kHz, L = 2.88), NDK (USA, 25.2 kHz, L = 2.98) and WWVB (USA, 60.0 kHz, L = 2.26) were observed by the receivers at ATH (Athabasca, L=4.31) and PKR (Poker Flat, L=5.95). The substorm occurred at 04:30 UT. Based on the wavelet analysis, we found that the intensities for the NDK-ATH and WWVB-ATH paths showed oscillations with a period of 4-6 minutes during the substorm growth phase (05:00-06:00 UT). Magnetic field variations observed by ground magnetometers around the NDK-ATH and WWVB-ATH paths also showed the same periodicity, which means that the variations in the VLF/LF intensities would be caused by Pc5 modulations. The magnetic field oscillations were observed in wide latitude range. The intensity of the oscillation was larger at high latitude magnetometers than those around the location of the NDK-ATH and WWVB-ATH path (mid-latitude). The Pc5 oscillations could be excited by solar wind because solar wind speed had similar period of the 4-6 minutes. In this presentation, we will discuss the cause of these VLF/LF oscillations.

Keywords: VLF/LF standard radio waves, Pc5, ULF

©2019. Japan Geoscience Union. All Right Reserved.

Oxygen-proton differences in ion energies dominating plasma pressure: Dependence on storm phases and solar wind drivers

*Kunihiro Keika[1], Satoshi Kasahara[1], Shoichiro Yokota[2], Masahiro Hoshino[1], Kanako Seki[1], Masahito Nose[3], Yoshizumi Miyoshi[3], Iku Shinohara[4]

1. Graduate School of Science, The University of Tokyo , 2. Graduate School of Science, Osaka University, 3. Institute for Space-Earth Environmental Research, Nagoya University, 4. Institute of Space and Astronautical Science, Japan Aerospace Exploration Agency

The ion pressure in the inner magnetosphere is generally dominated by protons with energies of a few to a few 100s keV. Oxygen ions of ionospheric origin, O+, can make a significant contribution to the ion pressure during geomagnetically active periods. Our previous study (Keika et al., 2018, GRL) examined the radial dependence of contributing energies, which we term an energy range that makes the dominant contribution to the plasma pressure, during the main phase of the six magnetic storms in Year 2017. We found clear oxygen-proton differences in the contributing energies in the outer part (L>5) of the ring current region. The contributing energies were higher for O+ than for H+. The results provided in situ evidence of the contribution from mass-dependent/selective acceleration processes to the energization of the outer part of the ring current.

The present study extends this analysis toward a larger database obtained from a longer period of magnetic storm times including the recovery phase. We also compare mass-dependent/selective energization between different solar wind drivers such as coronal mass ejections and corotational interaction regions. We primarily use data from the MEP-i (Medium-Energy Particle experiments - ion mass analyzer) on board the Arase spacecraft. MEP-i measures ions with energies of 10 to 180 keV/q and distinguishes between different ion species. Arase observed the nightside near-Earth magnetosphere (L<10) during 7 CME-driven and 7 CIR-driven storms with the Dst minimum of smaller than -50 nT in Years 2017 and 2018. The dependence on storm phases and solar wind drivers helps identify magnetospheric conditions favorable for mass-dependent/selective acceleration and in turn provides clues for understanding important physical mechanisms. Utilizing observations made by the MMS spacecraft in the near-Earth plasma sheet, we also compare oxygen-to-proton differences inside earthward bursty bulk flows with the Arase/MEP-i observations. The multi-spacecraft observations help better understand the temporal evolution of the mass-dependent/selective acceleration processes.

Keywords: Magnetic storms, Substorms, RIng current, Oxygen ions, Ion transport and acceleration

©2019. Japan Geoscience Union. All Right Reserved.

Mass dependence of penetration depth of multi-energy ions in the inner magnetosphere during magnetic storms: Arase observations

*Ryosuke Fujii[1], Yoshizumi Miyoshi[1], Masafumi Shoji[1], Kazushi Asamura[2], Lynn Kistler[1,8], Vania Jordanova[9], Tomoaki Hori[1], Satoshi Kurita[1], Mariko Teramoto[1], Yasunori Tsugawa[1], Yoshiya Kasahara[3], Yasumasa Kasaba[4], Atsushi Kumamoto[5], Fuminori Tsuchiya[4], Shoichiro Yokota[6], Kunihiro Keika[7], Ayako Matsuoka[2], Iku Shinohara[2]

1. Institute for Space-Earth Environmental Research, Nagoya University, 2. Institute of Space and Astronautical Science, Japan Aerospace Exploration Agency, 3. Information Media Center, Kanazawa University, 4. Planetary Plasma and Atmospheric Research Center, Tohoku University, 5. Department of Geophysics, Graduate School of Science, Tohoku University, 6. Graduate School of Science, Osaka University, 7. Department of Earth and Planetary Science, Graduate School of Science, The University of Tokyo, 8. University of New Hampshire, 9. Los Alamos National Laboratory

During magnetic storms, the ring current ions move toward the Earth, and the inner edge position of the ring current depends on the convection electric field. We investigate variations of the inner edge of the ring current ions, so-called, penetration depth, during magnetic storms using the ion measurements made by the Low-energy particle experiments-ion mass analyzer (LEP-i)/Medium-energy particle experiments-ion mass analyzer (MEP-i) instruments onboard the Arase satellite. The Arase satellite typically observes the earthward penetration of the ring current protons associated with the enhancement of the dawn-to-dusk electric field in the inner magnetosphere during the storm main phase. The plasmapause moves earthward during the main phase. On the other hand, the convection electric field decreases during the storm recovery phase in which the flux of ring current protons decreases. We identify that the penetration depth of protons depends on the minimum Dst index during the storms as well as the proton energy.

We also investigate the penetration depth of other ions, i.e., helium and oxygen ions. Because the life times of helium and oxygen ions due to charge exchange reaction for are longer than that of protons, it is expected that these ions can penetrate deeper than protons and temporal and spatial evolution can be observed clearly. We will also discuss the relation between the position of ring current inner edge and cross polar cap potential.

Keywords: The Arase satellite, Ring current, Ions

©2019. Japan Geoscience Union. All Right Reserved.

Relativistic Acceleration of Energetic Protons by Electromagnetic Ion Cyclotron Waves in the Jovian Magnetosphere

*Tomohiro Sekine[1], Yoshiharu Omura[1], Danny Summers[2], Yikai HSIEH[1], Satoko Nakamura[1]

1. Reserach Institute for Sustainable Humanosphere, Kyoto University, 2. Memorial University of Newfoundland

We perform test particle simulations of nonlinear interaction between energetic protons and EMIC waves. We assume a coherent EMIC waves that have a constant frequency and propagate parallel to the magnetic field. We find that protons can be trapped and accelerated by EMIC waves. We find a very efficient acceleration process of protons in which kinetic energy of protons increases while directions of parallel velocities reverses when we assume parameters in the Jovian magnetosphere. We notice that this phenomenon is very similar to the interaction process between relativistic electrons and whistler-mode waves, which is called Relativistic Turning Acceleration (RTA) [1]. In order to analyze the phenomena, we have developed nonlinear trapping theory of interaction between relativistic protons and EMIC waves. Next, we compare the theory and simulation results. We confirm that the results satisfy the conditions for RTA. Following the trajectories of many resonant protons, we obtain time evolution of the distribution function of relativistic protons as a function of energy and equatorial pitch angle based on the numerical Green’ s function method [2].

References:

[1] Y. Omura, N. Furuya, D. Summers, Relativistic turning acceleration of resonant electrons by coherent whistler-mode waves in a dipole magnetic field, Journal Geophysical Research, Vol. 112, A06236, doi:10.1029/2006JA012243, 2007.

[2] Y. Omura, Y. Miyashita, M. Yoshikawa, D. Summers, M. Hikishima, Y. Ebihara, and Y. Kubota (2015), Formation process of relativistic electron flux through interaction with chorus emissions in the Earth’ s inner magnetosphere, J. Geophys. Res. Space Physics, 120, 9545–9562, doi:10.1002/2015JA021563, 2015.

©2019. Japan Geoscience Union. All Right Reserved.

Statistical study of IPDP type EMIC wave-related electron precipitation at subauroral latitude

*Asuka Hirai[1], Fuminori Tsuchiya[1], Takahiro Obara[1], Yasumasa Kasaba[1], Yuto Katoh[2], Hiroaki Misawa[1], Kazuo Shiokawa[3], Yoshizumi Miyoshi[3], Satoshi Kurita[3], Martin G Connors[4]

1. Planetary Plasma and Atmospheric Research Center, Graduate School of Science, Tohoku Univ. , 2. Department of Geophysics, Graduate School of Science, Tohoku University, 3. Institute for Space-Earth Environmental Research, Nagoya University, 4. Athabasca University

The outer radiation belt electrons disappear during the main phase of geomagnetic storms. One of the loss mechanisms of electrons from the outer belt is precipitation into the atmosphere due to wave-particle interactions. Electromagnetic ion cyclotron (EMIC) waves are believed to be important plasma waves that contribute to the loss of the outer radiation belt due to pitch angle scattering. They can scatter relativistic and ultra-relativistic electrons. However, there are still questions left about the contribution of EMIC waves to the whole loss of radiation belt electrons and possible conditions favorable to pitch angle scattering.

EMIC waves mainly propagate along magnetic field lines and are observed on the ground as Pc1 geomagnetic pulsations. Intervals of pulsations of diminishing periods (IPDP) are Pc1/EMIC waves that are characterized by frequency rise from 0.1 to 1–2 Hz in a period of ~1 h, and often occur during substorms. Recent studies reported that IPDP are preferentially associated with relativistic electron precipitation. However, the statistical relation between IPDP waves and relativistic electron precipitation, and their physical mechanism, remain open issues.

We investigated differences in characteristics between IPDP and other types of Pc1 by using an induction magnetometer and VLF radio wave data that is a proxy of electron precipitations at subauroral latitude from 1 November 2016 to 30 June 2018. We used the induction magnetometer of PWING (study of dynamical variation of Particles and Waves in the INner magnetosphere using Ground-based network observations) at Athabasca, Canada (54.6˚N, 246.36˚E, L = 4.39). VLF radio waves propagate from transmitters to receivers in subionospheric waveguide. The modulations of VLF signals are detected as occurrence of sub-relativistic and relativistic electron (>100 keV) precipitation due to ionization changes in the lower ionosphere along the radio wave propagation path. VLF radio waves are transmitter from NDK, U.S. (46.367˚N, 261.467˚E, L =3.13) and NLK, U.S. (48.2˚N, 238.083˚E, L =2.84) and received at Athabasca. We selected EMIC wave events on the basis of the following criteria: (1) EMIC wave power is higher than 10^{-5} nT^2/Hz. (2) Duration of EMIC waves is longer than 20 min. (3) Interval between one EMIC wave event and the next one is longer than 30 min. Electron precipitation was identified as a decrease in amplitude of VLF signals from the quiet day curve (QDC). We counted as EMIC wave-driven electron precipitation if we detect temporal correspondence with EMIC waves. In this period, we found 950 EMIC wave events, and 87 of total EMIC wave events were IPDP events (9.2%). Local time dependence of EMIC waves shows that IPDP often occurs in the afternoon and evening sector, while other types of Pc1 occur in all local time range, but with a maximum in 12–16 MLT, which is consistent with previous studies. Simultaneous observation of the magnetometer and VLF radio waves were available for 286 days, and we found 163 EMIC wave events. 19 of 163 EMIC wave events were clearly associated with electron precipitation (12%). Among 19 electron precipitation events, 15 events were caused by IPDP (79%). Also, the electron precipitation events were observed in the evening sector with similar local time dependence to IPDP. This result suggests that IPDP is more likely to cause electron precipitation than other Pc1 wave types. In previous studies, IPDP occurs due to ion cyclotron instability of ring current ions in the evening sector, and favorable region for electron scattering by EMIC waves is high density duskside plasmapause

©2019. Japan Geoscience Union. All Right Reserved.

and plasmaspheric plume because dense plasma lowers minimum resonant energy of electrons. It is assumed that occurrence region of IPDP is coincident with the preferential region for MeV electron scattering by EMIC waves. For this reason, it is expected that IPDP type EMIC waves significantly cause relativistic electron precipitations in the duskside.

Keywords: EMIC waves, electron precipitation, subionospheric VLF radio waves

©2019. Japan Geoscience Union. All Right Reserved.

Meridional distributions of proton plasma and pressure-driven currents in the nightside inner magnetosphere: Arase observations

*Shun Imajo[1], Masahito Nose[1], Satoshi Kasahara[2], Shoichiro Yokota[3], Ayako Matsuoka[4], Kunihiro Keika[2], Tomoaki Hori[1], Mariko Teramoto[1], Kazuhiro Yamamoto[5], Oimatsu Satoshi[5], Reiko Nomura[6], Akiko Fujimoto[7], Iku Shinohara[4], Yoshizumi Miyoshi[1]

1. Institute for Space-Earth Environmental Research, Nagoya University, 2. Graduate School of Science, The University of Tokyo, 3. Graduate School of Science, Osaka University, 4. Institute of Space and Astronautical Science, Japan Aerospace Exploration Agency, 5. Graduate School of Science, Kyoto University, 6. National Astronomical Observatory of Japan, 7. Kyushu Institute of Technology

We examine the averaged meridional distributions of proton plasma parameters and pressure-driven currents in the nightside (20–04 h magnetic local time) ring current region during disturbed times (-80 < SYM-H* < -40 nT) using ion measurements covering energy range of 10–180 keV by the Arase satellite. Because the Arase satellite has a large inclination orbit of 31°, it covers the absolute value of magnetic latitude (|MLAT|) range of 0–40° and the radial distance of < 6 Re. We find that the plasma pressure decreases significantly with MLAT. The plasma pressure on the same L^* shell at 30°<|MLAT|<40° is about 10–60% of that at 0°<|MLAT|<10°, and the percentage of decrease is larger on lower L^* shells. The pressure anisotropy which is defined by the perpendicular pressure divided by the parallel pressure decreases with radial distance and shows a weak dependence on |MLAT|. The magnitude of the plasma beta at 30°<|MLAT|<40° is one or two order smaller than that at 0°<|MLAT|<10°. The relative plasma pressure distribution predicted from the magnetic strength and anisotropy is roughly consistent with the observed plasma pressure for L^*=3.5–5.5. The azimuthal pressure-gradient current derived from the plasma pressure distribution spreads over ~-20° |MLAT|, while the curvature current is limited in ~0–10° |MLAT|. We suggest that the latitudinal dependences should be taken into account when considering a temporal evolution of ring current particles from L distributions of successive orbits.

Keywords: meridional distributions, plasma pressure, pressure-driven currents, Arase satellite

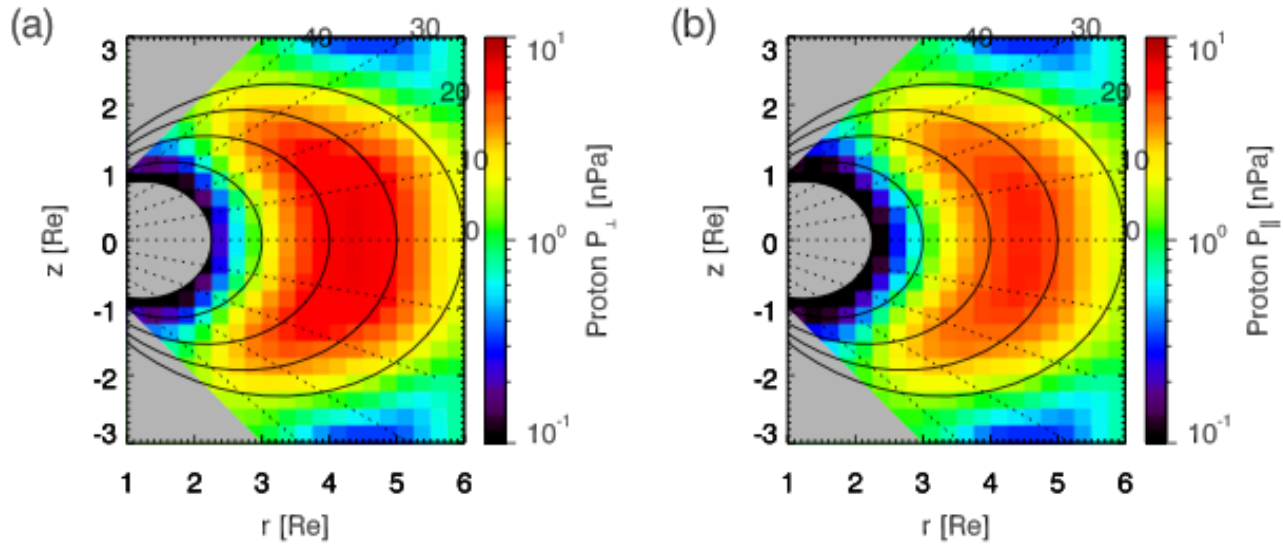

©2019. Japan Geoscience Union. All Right Reserved.

Space Weather Effects on Energetic Proton Flux Response in South Atlantic Anomaly

*Kirolosse Mina GIRGIS[1,2], Tohru Hada[1], Shuichi Matsukiyo[1]

1. Earth System Science and Technology (ESST) Department, Interdisciplinary Graduate School of Engineering Sciences (IGSES), Kyushu University, Japan, 2. Aerospace Engineering Department, Faculty of Engineering, Cairo University, Egypt

In this research, energetic proton flux in the inner radiation belt, is studied inside the South Atlantic Anomaly (SAA) by performing test particle simulations, where the background time-varying magnetic field is provided by Tsyganenko model, according to *Dst* index and altitudes. The objective of this investigation, is to estimate and forecast the additional radiation dose, occurring on spacecraft and human bodies, due to their passage inside the anomaly, and precisely, during intense solar storms. It was found that within minutes, proton flux in the SAA, penetrated deeper downward by about 200 km, when the *Dst* index is decreased (< -210 nT), and a after few more minutes, it was significantly reduced at all the altitudes; the last conclusion was confirmed by satellite observations.

Keywords: South Atlantic Anomaly, Space Weather, Dst Index, Radiation Dose, Proton Flux

©2019. Japan Geoscience Union. All Right Reserved.

Solar-cycle variations of >30 keV electron flux enhancements under the inner radiation belt

*ALLA SUVOROVA[1]

1. National Central University

Intense fluxes of 30-300 electrons can arise in the equatorial ionosphere outside the South Atlantic Anomaly. It was established that the electrons were injected from the inner radiation belt probably due to a mechanism of fast radial transport in the crossed electric and magnetic fields. Continuous monitoring of energetic particles at low heights of ~850 km with the MEPED instrument onboard the NOAA/POES satellites allowed compiling large statistics of the >30 keV electron enhancements from 1998 to 2018. We studied particle flux variations with geomagnetic activity and solar cycle. We found that geomagnetic activity measured by Dst and AE indices are not key factors of occurrence rate increase for electron injections, but influence on intensity of particles. The occurrence rate is controlled by auroral conductivity on the dayside and significantly enhanced during northern summer. Descending phase of solar cycle plays a major role in the occurrence rate increase.

Keywords: magnetosphere-ionosphere, energetic electrons, low latitudes, solar cycle

©2019. Japan Geoscience Union. All Right Reserved.

Energy spectra variations of high energy electrons in the inner magnetosphere observed by HEP/XEP on ARASE and SEDA-e on HIMAWARI

*Takeshi Takashima[1], Takefumi Mitani[1], Nana Higashio[2], Tsutomu Nagatsuma[3]

1. ISAS/JAXA, 2. Research and Development Directorate/JAXA, 3. NiCT

The relativistic electrons in the outer radiation belt were disappeared/increased and their energy spectra were changed dynamically in some storms observed by XEP/HEP onboard the ARASE spacecraft. In the same time, SEDA-e with energy range 200keV-4.5MeV for electron on board the HIMAWARI-8, Japanese weather satellite on GEO, observed increase of relativistic electron in different local time.
When comparing the energy spectra, there are times when the spectrum matches or does not match. It is also observed that the change in the slope of the energy spectrum differs with time. These phenomena are observed even when there are two satellites at the same local time.
We will report on energy spectra variations of high energy electrons including calibrations of differential flux between XEP and HEP and discuss comparisons with energy spectra between ARAE and HIMAWARI that observed each storm in different local time.

Keywords: relativistic electron, inner magnetosphere, ARASE

©2019. Japan Geoscience Union. All Right Reserved.

Inter-channel calibration of the high-energy electron experiments (HEP) instrument onboard the Arase satellite

*Tomoaki Hori[1], Takefumi Mitani[2], Takeshi Takashima[2], Park Inchun[1], Satoshi Kurita[1], Mariko Teramoto[1], Nana Higashio[3], Satoshi Kasahara[4], Shoichiro Yokota[5], Yoshizumi Miyoshi[1], Iku Shinohara[2]

1. Institute for Space-Earth Environmental Research, Nagoya University, 2. Japan Aerospace Exploration Agency, Institute of Space and Astronautical Science, 3. Japan Aerospace Exploration Agency, 4. Graduate School of Science, The University of Tokyo, 5. Graduate School of Science, Osaka University

An inter-channel comparison of electron fluxes measured by the HEP instrument onboard the Arase satellite is conducted with a focus on the apparent non-uniformity in detection efficiency and relative offset of the background flux level between the channels, which was partly reported previously. We extend the data set to cover the entire two-year period since the start of the regular observations. The flux ratio of different channels is sorted by the electron flux level of much higher energies that was simultaneously measured by the extremely high-energy electron experiment (XEP) instrument onboard Arase. The result shows that the HEP flux of all azimuthal channels is more or less affected by MeV electrons which are most likely to have penetrated into the instrument box and directly hit the detectors. However, it is also revealed that the non-uniform count distribution over the channels still remains even when the penetrating electrons are absent. We conduct a set of Geant-4 simulations to trace electrons with various energies and incident angles to the detector plane in order to give a quantitative interpretation for the resultant count distributions, in terms of the effects of penetrating electrons and obliquely-colliding incident electrons.

Keywords: Arase satellite, particle instrument, calibration

©2019. Japan Geoscience Union. All Right Reserved.

Particle simulation for calibrating the HEP data onboard the ARASE satellite

*PARK INCHUN[1], Yoshizumi Miyoshi[1], Takefumi Mitani[2], Tomoaki Hori[1], Satoshi Kurita[1], Mariko Teramoto[1], Takeshi Takashima[2], Nana Higashio[3], Iku Shinohara[2]

1. Nagoya University Institute for Space-Earth Environmental Research, 2. Japan Aerospace Exploration Agency Institute of Space and Astronautical Science , 3. Japan Aerospace Exploration Agency

Understanding the detailed characteristics of the HEP (High-Energy electron Experiment) instrument onboard the Arase satellite is crucial for data calibration. Due to difficulties of reproducing the severe radiation environment of the inner magnetosphere on the ground, computer simulation is the best method to understand instrument responses to the ambient radiation environment. Through Monte-Carlo simulations using the Geant4 tool, we have reconstructed the geometry of the HEP instrument and modeled the high-energy particle environment. Using the developed model, we have studied the efficiency of the detectors, the angular resolution, and the g-factors, which depend on the particle energy and the sensor channels. While the previous studies were based on a uni-direction simulation with electron pencil beams, this study adopted all the detector channels and energy bends of HEP thus resulting in more advanced simulations. Based on the results, we have made a new calibration table depending on the angle of incident particles. We have also estimated the g-factor which depends on the incident particle energy. The updated calibration table and g-factors are important for calibrating the HEP data as well as inter-calibrations with other particle instruments' data.

Keywords: ARASE, Geant4, HEP

©2019. Japan Geoscience Union. All Right Reserved.

Geant4 model calculation and energetic particle observation with HEP/Arase in the inner radiation belt

*Honoka Toda[1], Wataru Miyake[1], Takefumi Mitani[3], Takeshi Takashima[3], Yoshizumi Miyoshi[2], PARK INCHUN[2], Tomoaki Hori[2]

1. Tokai University, 2. ISEE/Nagoya University, 3. ISAS/JAXA

The high-energy electron experiments (HEP) instrument installed on the Arase is designed to observe energetic electrons of 70 keV to 2 MeV. The HEP registers high electron counts for the MeV energy range, not only in the outer belt but also in the inner belt, in MeV energy range. On the contrary, Van Allen Probes have hardly detected MeV electrons in the inner radiation belt. A probable interpretation is that the counts of HEP are caused due to contamination of high-energy protons. In order to verify this idea, we have modeled the HEP instrument a Geant4 simulation to determine the energy of penetrating protons. The result clearly shows that high-energy protons, it has become clear that high-energy protons of a few to a few tens of MeV can contribute to the apparent high counts of HEP. No instrument for measuring protons in this energy range is installed on the satellite. We will discuss the possibility of research on the spatial distribution and time variation of high-energy protons in the inner belt based on observation data from the HEP instrument.

Keywords: Arase, Proton Radiation Belt, HEP

©2019. Japan Geoscience Union. All Right Reserved.

Validation of High-energy electron detector simulator for the HEP instruments onboard Arase

*Takefumi Mitani[1], PARK INCHUN[2], Tomoaki Hori[2], Taku Namekawa[1,3], Kazushi Asamura[1], Takeshi Takashima[1], Satoshi Kasahara[3], Satoshi Kurita[2], Mariko Teramoto[2], Nana Higashio[1], Yoshizumi Miyoshi[2], Iku Shinohara[1]

1. Japan Aerospace Exploration Agency, Institute of Space and Astronautical Science, 2. Institute for Space-Earth Environmental Research, Nagoya Univ., 3. The university of Tokyo

The high-energy electron experiments (HEP) onboard the Arase satellite detects 70 keV-2 MeV electrons and generates a three-dimensional velocity distribution for these electrons in every period of the satellite's rotation. Electrons are detected by two instruments, namely, HEP-L and HEP-H, which differ in their geometric factor (G-factor) and range of energies they detect. HEP-L detects 70 keV–1 MeV electrons and its G-factor is 9.3 $\times 10^{-4}$ cm^2 sr at maximum, while HEP-H observes 0.7 MeV–2 MeV electrons and its G-factor is 9.3 $\times 10^{-3}$ cm^2 sr at maximum. The instruments utilize silicon strip detectors and application-specific integrated circuits to readout the incident charge signal from each strip.

In order to deduce the distribution of incident electrons from the direction and energy detections in orbit, we have developed a detector simulator using the Geant4 toolkit. Especially contamination due to high energy particles must be considered quantitatively. We have also been working on electron beam experiments using HEP detector modules which are almost the same as the flight model in order to compare detailed simulations and experimental data.

We will present a comparison between results from the electron beam experiments and those from the detector simulator. And we will discuss its influence on the interpretation of the observational data obtained in orbit.

Keywords: high-energy electron, Arase, Geant4

©2019. Japan Geoscience Union. All Right Reserved.

[E] Poster | P (Space and Planetary Sciences)：P-EM Solar-Terrestrial Sciences, Space Electromagnetism & Space Environment

Wed. May 29, 2019 5:15 PM - 6:30 PM JST | Wed. May 29, 2019 8:15 AM - 9:30 AM UTC | Poster Hall International Exhibition Hall8, Makuhari Messe_6

[P-EM13] Inner magnetosphere: Recent understanding and new insights

convener:Yusuke Ebihara(Research Institute for Sustainable Humanosphere, Kyoto University), Danny Summers(Memorial University of Newfoundland), Yoshizumi Miyoshi(Institute for Space-Earth Environmental Research, Nagoya University), Shinji Saito(Graduate School of Science, Nagoya University)

The inner magnetosphere is characterized by the dominance of intrinsic dipolar Earth's magnetic field. The dipolar magnetic field traps charged particles, resulting in the formation of unique particle environment known as the plasmasphere, the ring current, and the radiation belt. The inner magnetosphere is always changing because of incoming energy from the outer magnetosphere and the ionosphere in the forms of particles and electromagnetic fields. In the inner magnetosphere, the particle energy is transferred to the field energy, and vice versa. The mutual coupling between particles and fields also makes the inner magnetosphere unique. The outgoing energy to these regions is also known to be significant, such as precipitation into the upper atmosphere and sub-auroral disturbances. A number of satellites (e.g., DMSP, NOAA, Geotail, Cluster, THEMIS, Van Allen Probes, MMS, and Arase), ground-based instruments (e.g., SuperDARN and EISCAT radars, magnetometers, and cameras), and numerical simulations (e.g., global particle simulation, PIC simulation, and hybrid simulation) have successfully surveyed the inner magnetosphere, which deepen our knowledge significantly. USAF DSX, UCLA Elfin and NASA CeRES will be launched soon, being expected to provide important information. We solicit papers describing recent results on the inner magnetosphere and/or its coupling with the other regions, including the ionosphere and the outer magnetosphere.

[PEM13-P01] Evaluation of wave normal and Poynting vector analyses for whistler mode waves observed by the waveform capture (WFC) on board the Arase

*Yoshiya Kasahara[1], Satoshi Ikarashi[1], Hiroyuki Nishizawa[1], Shoya Matsuda[2], Fuminori Tsuchiya[3], Atsushi Kumamoto[3], Yasumasa Kasaba[3], Mitsunori Ozaki[1], Ayako Matsuoka[2] (1.Kanazawa University, 2.ISAS/JAXA, 3.Tohoku University)

[PEM13-P02] Calibration of electric fields dedicated to the measurement of the S-WPIA of the Arase Satellite

*Miki Jumpei[1], Hirotsugu Kojima[2], Yuto Katoh[3], Shoya Matsuda[4], Yoshiya Kasahara[5], Mitsuru Hikishima[4], Satoshi Kurita[6], Masahiro Kitahara[3], Satoshi Kasahara[7], Yoshizumi Miyoshi[6], Atsushi Kumamoto[3], Ayako Matsuoka[4], Shoichiro Yokota[8], Tomoaki Hori[6], Kunihiro Keika[7] (1.Space Radio Engineering Laboratory, Division of Electrical Engineering, Kyoto University Graduated School, 2.Research Institute for Sustainable Humanosphere, Kyoto University, 3.Graduate School of Science and Faculty of Science, Tohoku University, 4.Institute of Space and Astronautical Science, JAXA, 5.Information Media Center, Kanazawa University, 6.Institute for Space-Earth Environmental Research, Nagoya University, 7.School of Science, The University of Tokyo, 8.School of Science, Osaka University)

[PEM13-P03] Enhancement of whistler-mode chorus in association with Pc 4-5 ULF waves and related variation of high energy electrons

*Atsuhiro Ono[1], Yuto Katoh[1], Atsushi Kumamoto[1], Fuminori Tsuchiya[1], Mariko Teramoto[2], Yoshiya Kasahara[3], Shoya Matsuda[4], Ayako Matsuoka[4], Takefumi Mitani[4], Tomoaki Hori[2], Satoshi Kasahara[5], Shoichiro Yokota[6], Kunihiro Keika[5], Yoshizumi Miyoshi[2], Iku Shinohara[4] (1.Tohoku University, 2.Nagoya University, 3.Kanazawa University, 4.ISAS/JAXA, 5.The University of Tokyo, 6.Osaka University)

[PEM13-P04] Sudden enhancements of electron cyclotron harmonic waves observed by the Arase satellite

*Shinjo Airi[1], Hirotsugu Kojima[1], Yoshiya Kasahara[2], Yoichi Kazama[3], Hideyuki Usui[4], Yoshizumi Miyoshi[5], Yasumasa Kasaba[6], Shoya Matsuda[7], Tomoaki Hori[5], S. -Y. Wang[8], Sunny W.Y. Tam[9], Atsushi

Kumamoto[10], Ayako Matsuoka[11] (1.Research institute for sustainable humanosphere, Kyoto University, 2.Information Media Center, Kanazawa University, 3.ASIAA, 4.Graduate school of system informatics Kobe University, 5.Institute for Space-Earth Environmental Research, Nagoya University, 6.Planetary Plasma and Atmospheric Research Center, Tohoku University, 7.Institute of Space and Astronautical Science/Japan Aerospace Exploration Agency, 8.ASIAA, Taiwan, 9.ISAPS, NCKU, Taiwan, 10.Department of Geophysics, Graduate School of Science, Tohoku University, 11.Research Division for Space Plasma, Institute of Space and Astronautical Science, Japan Aerospace Exploration Agency)

[PEM13-P05] Correlation between pulsating aurora and electrostatic electron cyclotron harmonic waves obtained from coordinated Arase and ground data

*Mizuki Fukizawa[1], Takeshi Sakanoi[1], Yoshizumi Miyoshi[2], Keisuke Hosokawa[3], Yoichi Kazama[4], Yoshiya Kasahara[5], Shoya Matsuda[6], Ayako Matsuoka[7], Wang Shiang-Yu[4], Sunny Wing-Yee Tam[8], Ryuho Kataoka[9] (1.Planetary Plasma and Atmospheric Research Center, Graduate School of Science, Tohoku University, 2.Institute for Space-Earth Environmental Research, Nagoya University, 3.Department of Communication Engineering and Informatics, University of Electro-Communications, 4.Academia Sinica Institute of Astronomy and Astrophysics, 5.Information Media Center, Kanazawa University, 6.Institute of Space and Astronautical Science/Japan Aerospace Exploration Agency, 7.Research Division for Space Plasma, Institute of Space and Astronautical Science, Japan Aerospace Exploration Agency, 8.Institute of Space and Plasma Sciences, College of Sciences, National Cheng Kung University , 9.National Institute of Polar Research)

[PEM13-P06] Automatic determination of Upper Hybrid Resonance Frequencies by Convolutional Neural Network.

*Shoya Matsuda[1], Tatsuhito Hasegawa[2], Atsushi Kumamoto[3], Fuminori Tsuchiya[3], Yoshiya Kasahara[4], Yoshizumi Miyoshi[5], Yasumasa Kasaba[3], Ayako Matsuoka[1] (1.Institute of Space and Astronautical Science/Japan Aerospace Exploration Agency, 2.University of Fukui, 3.Tohoku University, 4.Kanazawa University, 5.ISEE, Nagoya University)

[PEM13-P07] Amplitude dependence of whistler wave motion on electron scattering process

*Yoshiki Ito[1], Yoshizumi Miyoshi[1], Shinji Saito[1] (1.Nagoya University, ISEE)

[PEM13-P08] Two-dimensional simulation of whistler mode wave packets interacting with energetic electrons

*Takeshi Nogi[1], Yoshiharu Omura[1] (1.Reserch Institute for Sustainable Humanosphere, Kyoto University)

[PEM13-P09] Relativistic electron acceleration by whistler-mode chorus waves in 1D, 2D, and 3D magnetic field models.

*Keita Takahashi[1], Yoshiharu Omura[1], Yikai HSIEH[1], Danny Summers[2] (1.Research Institute for Sustainable Humanosphere, Kyoto University , 2.Department of Mathematics and Statistics, Memorial University of Newfoundland)

[PEM13-P10] Study of global spatio-temporal development of magnetospheric ELF/VLF waves for the 26-30 March 2017 storm based on ground and satellite observations and the RAM simulations

*Yuhei Takeshita[1], Kazuo Shiokawa[1], Yoshizumi Miyoshi[1], Mitsunori Ozaki[2], Yoshiya Kasahara[2], Martine Connors[3], Jyrki Manninen[4], Craig Kletzing[5], Vania Jordanova[6] (1.Nagoya University, Institute for Space-Earth Environmental Resarch, 2.Kanazawa University, 3.Athabasca University, 4.Sodankylä Geophysical Observatory, 5.The University of Iowa, 6.Los Alamos National Laboratory)

[PEM13-P11] Flux decrease of outer radiation belt electrons associated with solar wind pressure pulse: A Code coupling simulation of GEMSIS-RB and GEMSIS-GM

*Ito Hiroki[1], Yoshizumi Miyoshi[1], Shinji Saito[2], Yosuke Matsumoto[3], Takanobu Amano[4] (1.Institute for Space-Earth Environmental Research, Nagoya University, 2. Graduate School of Science, Nagoya

University, 3. Graduate School of Science, Chiba University, 4.Department of Earth and Planetary Science, University of Tokyo)

[PEM13-P12] Non-diffusive response of outer belt electrons on interplanetary shock

Takuma Toishi[1], *Yusuke Ebihara[1], Takashi Tanaka[2] (1.Research Institute for Sustainable Humanosphere, Kyoto University, 2.Kyushu University)

[PEM13-P13] PARM: Initial result of the auroral camera on the G-CHASER (RockSat-XN) rocket and status of the development of auroral cameras for the LAMP rocket experiment

*Naoshi Yagi[1], Takeshi Sakanoi[1], Fukizawa Mizuki[1], Kazushi Asamura[2], Yoshizumi Miyoshi[3], Keisuke Hosokawa[4], Genki Ishizawa[5] (1.Planetary Plasma and Atmospheric Research Center, Graduate School of Science, Tohoku University, 2.Institute of Space and Astronautical Science, Japan Aerospace Exploration Agency, 3.Institute for Space-Earth Environmental Research, Nagoya University, 4.Department of Communication Engineering and Informatics, University of Electro-Communications, 5.Space & terrestrial plasma pyhsics)

[PEM13-P14] First simultaneous observation of a SAR arc at subauroral latitudes using a ground all-sky camera and the Arase satellite in the inner magnetosphere

*Yudai Inaba[1], Kazuo Shiokawa[1], Shin-ichiro Oyama[1,8,9], Yuichi Otsuka[1], Atsuki Shinbori[1], Yoichi Kazama[2], Shiang-Yu Wang[2], Sunny W. Y. Tam[2], Shoichiro Yokota[3], Satoshi Kasahara[4], Kunihiro Keika[4], Tomoaki Hori[1], Ayako Matsuoka[5], Yoshiya Kasahara[6], Atsushi Kumamoto[7], Yasumasa Kasaba[7], Yoshizumi Miyoshi[1], Iku Shinohara[5], Arto Oksanen[10] (1.Institute for Space-Earth Environmental Research, 2.Academia Sinica, 3.Osaka Univ, 4.Tokyo Univ, 5.JAXA, 6.Kanazawa University, 7.Tohoku University, 8.University of Oulu, Finland, 9.National Institute of Polar Research, 10.Jyväskylän Sirius ry, Finland)

[PEM13-P15] Pi2 pulsations observed by the Arase satellite inside and outside the plasmapause

*Mariko Teramoto[1], Ayako Matsuoka[2], Reiko Nomura[5], Yoshiya Kasahara[3], Yasumasa Kasaba[4], Atsushi Kumamoto[4], Fuminori Tsuchiya[4], Shoya Matsuda[2], Masahito Nose[1], Masafumi Shoji[1], Yasunori Tsugawa[1], Shun Imajo[1], Yoshizumi Miyoshi[1], Iku Shinohara[2] (1.Institute for Space-Earth Environmental Research Nagoya University, 2.Institute of Space and Astronautical Science, Japan Aerospace eXploration Agency, 3.Kanazawa University, 4.Tohoku University, 5.National Astronomical Observatory of Japan)

[PEM13-P16] An extreme erosion of the plasmasphere during the 7–10 September 2017 storm

*Yuki Obana[1], Naomi Maruyama[2,3], Atsuki Shinbori[4], Kumiko K. Hashimoto[5], Mariangel Fedrizzi[2,3], Masahito Nose[4], Yuichi Otsuka[4], Nozomu Nishitani[4], Tomoaki Hori[4], Atsushi Kumamoto[6], Fuminori Tsuchiya[6], Shoya Matsuda[7], Ayako Matsuoka[7], Yoshiya Kasahara[8], Akimasa Yoshikawa[9], Yoshizumi Miyoshi[4], Iku Shinohara[7] (1.Osaka Electro-Communication University, 2.University of Colorado Boulder, 3.NOAA Space Weather Prediction Center, 4.Nagoya University, 5.Kibi International University, 6.Tohoku University, 7.Japan Aerospace Exploration Agency, 8.Kanazawa University, 9.Kyushu University)

[PEM13-P17] Relative contribution of ULF and chorus waves to the radiation belt variation: Comparison between multi-point observations and BATSRUS + CRCM simulation

*Naoko Takahashi[1], Kanako Seki[1], Mei-Ching Fok[2], Yihua Zheng[2], Yoshizumi Miyoshi[3], David Hartley[4], Ayako Matsuoka[5], Yoshiya Kasahara[6], Yasumasa Kasaba[7], Nana Higashio[8] (1.Graduate School of Science, University of Tokyo, 2.NASA Goddard Space Flight Center, 3.Institute for Space-Earth Environmental Research, Nagoya University, 4.Department of Physics and Astronomy, University of Iowa, 5.Institute of Space and Astronautical Science, Japan Aerospace Exploration Agency, 6.Information Media Center, Kanazawa University, 7.Planetary Plasma and Atmospheric Research Center, Tohoku University, 8.Japan Aerospace Exploration Agency)

[PEM13-P18] Modulation of the D-region ionosphere by Pc5 waves observed by VLF/LF standard radio waves

*Miyashita Takuya[1], Hiroyo Ohya[1], Fuminori Tsuchiya[2], Hiroyuki Nakata[1], Toshiaki Takano[1], Kazuo Shiokawa[3], Yoshizumi Miyoshi[3] (1.Chiba University, 2.Tohoku University, 3.Nagoya University)

[PEM13-P19] Oxygen-proton differences in ion energies dominating plasma pressure: Dependence on storm phases and solar wind drivers

*Kunihiro Keika[1], Satoshi Kasahara[1], Shoichiro Yokota[2], Masahiro Hoshino[1], Kanako Seki[1], Masahito Nose[3], Yoshizumi Miyoshi[3], Iku Shinohara[4] (1.Graduate School of Science, The University of Tokyo , 2.Graduate School of Science, Osaka University, 3.Institute for Space-Earth Environmental Research, Nagoya University, 4.Institute of Space and Astronautical Science, Japan Aerospace Exploration Agency)

[PEM13-P20] Mass dependence of penetration depth of multi-energy ions in the inner magnetosphere during magnetic storms: Arase observations

*Ryosuke Fujii[1], Yoshizumi Miyoshi[1], Masafumi Shoji[1], Kazushi Asamura[2], Lynn Kistler[1,8], Vania Jordanova[9], Tomoaki Hori[1], Satoshi Kurita[1], Mariko Teramoto[1], Yasunori Tsugawa[1], Yoshiya Kasahara[3], Yasumasa Kasaba[4], Atsushi Kumamoto[5], Fuminori Tsuchiya[4], Shoichiro Yokota[6], Kunihiro Keika[7], Ayako Matsuoka[2], Iku Shinohara[2] (1.Institute for Space-Earth Environmental Research, Nagoya University, 2.Institute of Space and Astronautical Science, Japan Aerospace Exploration Agency, 3.Information Media Center, Kanazawa University, 4.Planetary Plasma and Atmospheric Research Center, Tohoku University, 5.Department of Geophysics, Graduate School of Science, Tohoku University, 6.Graduate School of Science, Osaka University, 7.Department of Earth and Planetary Science, Graduate School of Science, The University of Tokyo, 8.University of New Hampshire, 9.Los Alamos National Laboratory)

[PEM13-P21] Relativistic Acceleration of Energetic Protons by Electromagnetic Ion Cyclotron Waves in the Jovian Magnetosphere

*Tomohiro Sekine[1], Yoshiharu Omura[1], Danny Summers[2], Yikai HSIEH[1], Satoko Nakamura[1] (1.Reserach Institute for Sustainable Humanosphere, Kyoto University, 2.Memorial University of Newfoundland)

[PEM13-P22] Statistical study of IPDP type EMIC wave-related electron precipitation at subauroral latitude

*Asuka Hirai[1], Fuminori Tsuchiya[1], Takahiro Obara[1], Yasumasa Kasaba[1], Yuto Katoh[2], Hiroaki Misawa[1], Kazuo Shiokawa[3], Yoshizumi Miyoshi[3], Satoshi Kurita[3], Martin G Connors[4] (1.Planetary Plasma and Atmospheric Research Center, Graduate School of Science, Tohoku Univ. , 2.Department of Geophysics, Graduate School of Science, Tohoku University, 3.Institute for Space-Earth Environmental Research, Nagoya University, 4.Athabasca University)

[PEM13-P23] Meridional distributions of proton plasma and pressure-driven currents in the nightside inner magnetosphere: Arase observations

*Shun Imajo[1], Masahito Nose[1], Satoshi Kasahara[2], Shoichiro Yokota[3], Ayako Matsuoka[4], Kunihiro Keika[2], Tomoaki Hori[1], Mariko Teramoto[1], Kazuhiro Yamamoto[5], Oimatsu Satoshi[5], Reiko Nomura[6], Akiko Fujimoto[7], Iku Shinohara[4], Yoshizumi Miyoshi[1] (1.Institute for Space-Earth Environmental Research, Nagoya University, 2.Graduate School of Science, The University of Tokyo, 3.Graduate School of Science, Osaka University, 4.Institute of Space and Astronautical Science, Japan Aerospace Exploration Agency, 5.Graduate School of Science, Kyoto University, 6.National Astronomical Observatory of Japan, 7.Kyushu Institute of Technology)

[PEM13-P24] Space Weather Effects on Energetic Proton Flux Response in South Atlantic Anomaly

*Kirolosse Mina GIRGIS[1,2], Tohru Hada[1], Shuichi Matsukiyo[1] (1.Earth System Science and Technology (ESST) Department, Interdisciplinary Graduate School of Engineering Sciences (IGSES), Kyushu University, Japan, 2.Aerospace Engineering Department, Faculty of Engineering, Cairo University, Egypt)

[PEM13-P25] Solar-cycle variations of >30 keV electron flux enhancements under the inner radiation belt

*ALLA SUVOROVA[1] (1.National Central University)

[PEM13-P26] Energy spectra variations of high energy electrons in the inner magnetosphere observed by HEP/XEP on ARASE and SEDA-e on HIMAWARI

*Takeshi Takashima[1], Takefumi Mitani[1], Nana Higashio[2], Tsutomu Nagatsuma[3] (1. ISAS/JAXA, 2.Research and Development Directorate/JAXA, 3.NiCT)

[PEM13-P27] Inter-channel calibration of the high-energy electron experiments (HEP) instrument onboard the Arase satellite

*Tomoaki Hori[1], Takefumi Mitani[2], Takeshi Takashima[2], Park Inchun[1], Satoshi Kurita[1], Mariko Teramoto[1], Nana Higashio[3], Satoshi Kasahara[4], Shoichiro Yokota[5], Yoshizumi Miyoshi[1], Iku Shinohara[2] (1.Institute for Space-Earth Environmental Research, Nagoya University, 2.Japan Aerospace Exploration Agency, Institute of Space and Astronautical Science, 3.Japan Aerospace Exploration Agency, 4.Graduate School of Science, The University of Tokyo, 5.Graduate School of Science, Osaka University)

[PEM13-P28] Particle simulation for calibrating the HEP data onboard the ARASE satellite

*PARK INCHUN[1], Yoshizumi Miyoshi[1], Takefumi Mitani[2], Tomoaki Hori[1], Satoshi Kurita[1], Mariko Teramoto[1], Takeshi Takashima[2], Nana Higashio[3], Iku Shinohara[2] (1.Nagoya University Institute for Space-Earth Environmental Research, 2.Japan Aerospace Exploration Agency Institute of Space and Astronautical Science , 3.Japan Aerospace Exploration Agency)

[PEM13-P29] Geant4 model calculation and energetic particle observation with HEP/Arase in the inner radiation belt

*Honoka Toda[1], Wataru Miyake[1], Takefumi Mitani[3], Takeshi Takashima[3], Yoshizumi Miyoshi[2], PARK INCHUN[2], Tomoaki Hori[2] (1.Tokai University, 2.ISEE/Nagoya University, 3.ISAS/JAXA)

[PEM13-P30] Validation of High-energy electron detector simulator for the HEP instruments onboard Arase

*Takefumi Mitani[1], PARK INCHUN[2], Tomoaki Hori[2], Taku Namekawa[1,3], Kazushi Asamura[1], Takeshi Takashima[1], Satoshi Kasahara[3], Satoshi Kurita[2], Mariko Teramoto[2], Nana Higashio[1], Yoshizumi Miyoshi[2], Iku Shinohara[1] (1.Japan Aerospace Exploration Agency, Institute of Space and Astronautical Science, 2.Institute for Space-Earth Environmental Research, Nagoya Univ., 3.The university of Tokyo)

Evaluation of wave normal and Poynting vector analyses for whistler mode waves observed by the waveform capture (WFC) on board the Arase

*Yoshiya Kasahara[1], Satoshi Ikarashi[1], Hiroyuki Nishizawa[1], Shoya Matsuda[2], Fuminori Tsuchiya[3], Atsushi Kumamoto[3], Yasumasa Kasaba[3], Mitsunori Ozaki[1], Ayako Matsuoka[2]

1. Kanazawa University, 2. ISAS/JAXA, 3. Tohoku University

The Plasma Wave Experiment (PWE) is one of scientific instruments on board the Arase (ERG) satellite to measure electric field from DC to 10 MHz and magnetic field from a few Hz to 100 kHz in the inner magnetosphere. It is well known that chorus wave, one of typical plasma waves in VLF range observed in the inner magnetosphere, is a plausible candidate that accelerates relativistic electrons in the radiation belt. Besides the chorus, the Arase has observed various kinds of plasma waves such as lightning whistlers and hiss waves. It is very important to study the propagation characteristics of these waves.

In the present paper, we developed a direction finding system applicable to whistler mode waves using the data from waveform capture (WFC), which is one of receivers covering the frequency range below 20kHz implemented in the PWE. The absolute directions of the wave normal and Poynting vectors were derived in the coordinate system referring the ambient magnetic field and geomagnetic meridian plane. We also estimated the Poynting vector theoretically using the derived wave normal vector, electron density and ambient magnetic field intensity to confirm the validity of the results from the observation data.

We demonstrated that the results were generally reliable, but further calibration is necessary for electric field to improve the accuracy of Poynting vector because the waveform of electric field is now calibrated under the assumptions of theoretical antenna capacitance in a vacuum and typical plasma impedance. In other words, we expect to be able to correct the calibration table for electric field measurements from the direction finding results.

In the presentation, we introduce some typical results which have been derived from the observation data of upper- and lower-band chorus, and lightning whistlers.

Keywords: Whistler mode wave, Waveform Capture, Direction finding, Plasma wave

©2019. Japan Geoscience Union. All Right Reserved.

Calibration of electric fields dedicated to the measurement of the S-WPIA of the Arase Satellite

*Miki Jumpei[1], Hirotsugu Kojima[2], Yuto Katoh[3], Shoya Matsuda[4], Yoshiya Kasahara[5], Mitsuru Hikishima[4], Satoshi Kurita[6], Masahiro Kitahara[3], Satoshi Kasahara[7], Yoshizumi Miyoshi[6], Atsushi Kumamoto[3], Ayako Matsuoka[4], Shoichiro Yokota[8], Tomoaki Hori[6], Kunihiro Keika[7]

1. Space Radio Engineering Laboratory, Division of Electrical Engineering, Kyoto University Graduated School, 2. Research Institute for Sustainable Humanosphere, Kyoto University, 3. Graduate School of Science and Faculty of Science, Tohoku University, 4. Institute of Space and Astronautical Science, JAXA, 5. Information Media Center, Kanazawa University, 6. Institute for Space-Earth Environmental Research, Nagoya University, 7. School of Science, The University of Tokyo, 8. School of Science, Osaka University

The outer radiation belt consists of high-energy electrons. They are strongly affected by geomagnetic activities in the relation to solar wind conditions. The important science target of the Arase mission is to clarify generation/loss mechanisms of relativistic electrons in the outer radiation belt. Wave-particle interactions are thought to be a plausible mechanism for generation/loss processes of relativistic electrons. S-WPIA (Software-type Wave-Particle Interaction Analyzer) is installed in the Arase satellite. The WPIA is a newly developed observation system that enables us to quantitatively understand the interaction between plasma waves and electrons. The WPIA has the capability to identify a relative phase angle of a plasma wave vector and a velocity vector of each detected particle. Since phase information of observed plasma waves is essential to the WPIA, precise calibrations of plasma wave data are important. While the calibration data for the magnetic field sensors are identical to those we obtained during the ground tests of the instruments, the calibration data for electric field sensors strongly depend on plasma parameters around the satellite. Furthermore, there are still unclear parameters at the inputs of preamplifiers relating to the connection with electric field sensors. The calibration for electric field data needs to be performed carefully consulting observation data after the launch.

The present paper focuses on the calibration of plasma wave data for the S-WPIA’s data processing. We picked up events including whistler-mode chorus emissions and lightning-whistler waves. They all are electromagnetic waves, so-called whistler mode waves. The amplitude ratios of their electric field and magnetic field components can be theoretically calculated referring to the Appleton-Hartlee equations. Poynting vectors of whistler mode waves can be also theoretically obtained. We compared the observation results of the picked up events with the theoretical ones. The results show the precise calibration for the magnetic field data have been made. On the other hand, the calibration for the electric field data should be further modified consulting plasma parameters and other uncertain parameters at the input of preamplifiers. In the present paper, we will discuss the improvement of the calibration for electric field data by correcting the calibration table to aim the precise S-WPIA data processing.

©2019. Japan Geoscience Union. All Right Reserved.

Enhancement of whistler-mode chorus in association with Pc 4-5 ULF waves and related variation of high energy electrons

*Atsuhiro Ono[1], Yuto Katoh[1], Atsushi Kumamoto[1], Fuminori Tsuchiya[1], Mariko Teramoto[2], Yoshiya Kasahara[3], Shoya Matsuda[4], Ayako Matsuoka[4], Takefumi Mitani[4], Tomoaki Hori[2], Satoshi Kasahara[5], Shoichiro Yokota[6], Kunihiro Keika[5], Yoshizumi Miyoshi[2], Iku Shinohara[4]

1. Tohoku University, 2. Nagoya University, 3. Kanazawa University, 4. ISAS/JAXA, 5. The University of Tokyo, 6. Osaka University

Whistler-mode chorus emissions play significant roles in the acceleration and loss of energetic electrons in the magnetosphere. One of the important factors which control periodic enhancement of chorus emissions is ULF (Ultra Low Frequency) waves. Previous studies reported that the compressional component of Pc4-5 ULF waves modulates the intensity of chorus waves [Li et al., 2011] and that the toroidal and poloidal components of Pc4-5 ULF waves as well [Jaynes et al., 2015]. Previous studies also suggested that enhancement of the temperature anisotropy of energetic electrons in the wave generation region should be required for the chorus generation. In order to understand the reported correspondence, in addition to the wave observation, we should examine simultaneously observed variations of the flux and the pitch angle distribution of energetic electrons.

In the present study, we investigate the relationship between chorus emissions and ULF waves using particle and electromagnetic field observations made by the Arase satellite. First, we analyze data observed by the Onboard Frequency Analyzer (OFA) of the Plasma Wave Experiment (PWE) and the Magnetic Field Experiment (MGF) during the campaign observation period of the Arase satellite with ground stations from March to April in 2017. As a result, we identified the simultaneous enhancement of chorus emissions and Pc4-5 ULF waves, which was dominated by the toroidal component, from 2130 to 2200 UT on March 27, 2017. The Arase satellite was located at the magnetic local time about 04:00, the magnetic latitude about -10 degrees, and the L-value about 6 during the event. We find that there is one-to-one correspondence between chorus emissions and the toroidal component of ULF waves; chorus emissions enhanced at the timings when the toroidal magnetic field component of ULF waves had a peak in the westward direction. The identified phase relationship is different from that reported by Jaynes et al. (2015), which isn't one-to-one correspondence. Next, we evaluate the resonance energy of the observed chorus emissions, using the ratio of the plasma frequency to the electron cyclotron frequency (f_p/f_{ce}) based on the upper-hybrid resonance frequency derived from the spectra observed by the High Frequency Analyzer (HFA) of PWE and the ambient magnetic field intensity observed by MGF. We find that f_p/f_{ce} is 3.3-3.4 during the event and that the resonance energy for whistler-mode waves in the frequency range of 0.1-0.2 f_{ce} is estimated to be about 100-400keV, which is larger than typical energies of resonating electrons observed in the inner magnetosphere. The estimated large resonant energy can be explained by the frequency range of the observed chorus emissions, approximately 0.1 - 0.2 f_{ce}, is relatively lower than that observed in typical cases.
We also analyze variations of the flux and the pitch angle distribution of energetic electrons during the event using data observed by the High-energy electron experiments (HEP) instrument onboard Arase. The result shows that both the flux and the pitch angle distribution of electrons in the kinetic energy range from 100 to 400 keV, which corresponds to the estimated resonance energy, did not fluctuate with the intensity variation of the chorus emissions and the ULF waves. In addition, we analyze the data observed by the Medium-energy particle experiments - electron analyzer (MEP-e) for energetic electrons in the energy range of 10-80 keV, lower than the estimated resonance energy. Then we identify the

©2019. Japan Geoscience Union. All Right Reserved.

corresponding variation of both the flux and the pitch angle distribution in the 40-60 keV energy range. One of the possible reasons why no significant variations were observed in the hundred keV range would be that the Arase satellite was located in the off-equatorial region during the event, and that the satellite was away from the wave generation region.

Keywords: ULF waves, chorus emissions

©2019. Japan Geoscience Union. All Right Reserved.

Sudden enhancements of electron cyclotron harmonic waves observed by the Arase satellite

*Shinjo Airi[1], Hirotsugu Kojima[1], Yoshiya Kasahara[2], Yoichi Kazama[3], Hideyuki Usui[4], Yoshizumi Miyoshi[5], Yasumasa Kasaba[6], Shoya Matsuda[7], Tomoaki Hori[5], S. -Y. Wang[8], Sunny W.Y. Tam[9], Atsushi Kumamoto[10], Ayako Matsuoka[11]

1. Research institute for sustainable humanosphere, Kyoto University, 2. Information Media Center, Kanazawa University, 3. ASIAA, 4. Graduate school of system informatics Kobe University, 5. Institute for Space-Earth Environmental Research, Nagoya University, 6. Planetary Plasma and Atmospheric Research Center, Tohoku University, 7. Institute of Space and Astronautical Science/Japan Aerospace Exploration Agency, 8. ASIAA, Taiwan, 9. ISAPS, NCKU, Taiwan, 10. Department of Geophysics, Graduate School of Science, Tohoku University, 11. Research Division for Space Plasma, Institute of Space and Astronautical Science, Japan Aerospace Exploration Agency

Electron cyclotron harmonic (ECH) waves are commonly observed in the low latitude region just outside the terrestrial plasmapause. They are purely electrostatic and their frequency spectra show harmonic structures. The harmonic structures are believed to depend on the temperature and density ratio between cold and hot background electrons. The Plasma Wave Experiment (PWE) onboard the Arase satellite has observed ECH waves since the start of its operation. The observed ECH waves are classified into two types. They are the diffuse ECH waves and the enhanced ECH waves. The diffuse ECH waves are weak and they appear as continuous emissions that last for more than a few minutes. The enhanced ECH waves are the sudden enhancements of the diffuse ECH in shorter periods. The present paper focuses on the enhanced ECH waves observed by the Arase satellite.

Kazama et al. (2018) introduced the event that the repeated enhancement of ECH waves is associated with density depletions near the plasmapause. They succeeded in revealing the good correlation of the enhancement of the ECH waves and the sudden decrease of the cold electrons with energies lower than the lowest energy limit of the particle detector. The observed electron features are clear in the relation to the enhancement of ECH waves, but the mechanism of the enhancement is still unclear. We searched for such events of the enhanced ECH waves and examined the correlation of wave intensities, spacecraft potentials and electron velocity distributions observed by the Arase satellite. Some of the events show the features similar to those of Kazama et al. (2018), but there are also many other events with no correlation between the enhancements of the ECH waves and the density depletions. In the present paper, we examine velocity distribution functions of electrons observed by the low-energy particle experiments-electron analyzer (LEPe) onboard Arase. Velocity distribution functions allow us to examine temperature anisotropies of electrons and calculate linear dispersion relations for the ECH waves. Once we get electron temperatures, resonance velocities are calculated. On the other hand, since the wavelength of the ECH waves is very short, the relation of the wavelength and the length of the Arase electric field sensors is also important in evaluating the time variations of the ECH wave intensity. We study the enhanced ECH waves in various viewpoints using wave and electron data observed by the Arase satellite and discuss the generation mechanism in the present paper.

©2019. Japan Geoscience Union. All Right Reserved.

Correlation between pulsating aurora and electrostatic electron cyclotron harmonic waves obtained from coordinated Arase and ground data

*Mizuki Fukizawa[1], Takeshi Sakanoi[1], Yoshizumi Miyoshi[2], Keisuke Hosokawa[3], Yoichi Kazama[4], Yoshiya Kasahara[5], Shoya Matsuda[6], Ayako Matsuoka[7], Wang Shiang-Yu[4], Sunny Wing-Yee Tam[8], Ryuho Kataoka[9]

1. Planetary Plasma and Atmospheric Research Center, Graduate School of Science, Tohoku University, 2. Institute for Space-Earth Environmental Research, Nagoya University, 3. Department of Communication Engineering and Informatics, University of Electro-Communications, 4. Academia Sinica Institute of Astronomy and Astrophysics, 5. Information Media Center, Kanazawa University, 6. Institute of Space and Astronautical Science/Japan Aerospace Exploration Agency, 7. Research Division for Space Plasma, Institute of Space and Astronautical Science, Japan Aerospace Exploration Agency, 8. Institute of Space and Plasma Sciences, College of Sciences, National Cheng Kung University , 9. National Institute of Polar Research

Pulsating auroras (PsAs) are thought to be generated by precipitating electrons scattered by lower-band chorus (LBC) waves near the magnetic equator through cyclotron resonance. Previous studies showed one-to-one correlation between LBC wave intensity observed by satellites near the magnetic equator and PsA intensity obtained by ground-based all-sky imager [e.g., Nishimura et al., Science, 2010, Nishimura et al., JGR, 2011]. In addition, electrostatic electron cyclotron harmonic (ECH) waves can also interact with magnetospheric electrons and scatter their pitch angle theoretically [e.g., Lyons, JGR, 1974]. However, characteristics of aurora caused by ECH are not understood. In our study, we report for the first time in the world that not only LBC but also ECH wave intensity has correlation with the PsA intensity using coordinated Arase and ground-based imager observations. The first campaign observations between the Arase satellite and ground-based optical imager were conducted in March 2017. A typical substorm occurred on 27 March 2017 and the ionospheric footprint of Arase traversed the field of view of all-sky imager at Sodankylä during 00:00–03:15 UT on 29 March 2017. Quasi-periodic LBC and ECH waves were observed by Arase near the magnetic equator and PsA was detected by the all-sky imager during 01:30–02:00 UT. We calculated the cross-correlation coefficients between auroral intensity and LBC or ECH wave intensity from 01:30 UT to 02:00 UT with a time window of every 2 minutes. The highest cross-correlation coefficient between auroral intensity and LBC wave intensity was 0.73 and that between auroral intensity and ECH wave intensity was 0.62 from 01:46 UT to 01:48 UT, and they were statistically significant. The period of auroral intensity which correlated with LBC intensity was shorter than 10 s and that correlated with ECH intensity was 10–20 s. We estimated the precipitating electron energy assuming that the time lag when the cross-correlation coefficient became the highest equals to the travel time of electrons from the modulated source region to the auroral emission height. We shifted the variation of auroral intensity against that of ECH or LBC wave intensity with a time step of 0.01 s using 100 Hz sampling image data taken by the all-sky imager. The estimated energy of precipitating electron interacted with LBC waves was ~20–67 keV and that interacted with ECH waves was ~3–4 keV. On the other hand, we independently estimated the cyclotron resonance energy of LBC and ECH waves from the Arase's observation data and geomagnetic field model by TS04 Model [Tsyganenko and Sitnov, JGR, 2005]. The estimated cyclotron resonance energy of LBC waves was ~30 keV. Although the cyclotron resonance energy of ECH waves could not be estimated because it was difficult to obtain the electron temperature and wave normal angle of ECH waves from Arase data, we suggest the cyclotron resonance energy of ECH waves to be a few keV with probable assumptions. From these results, we suggest that LBC waves interact with high energy electrons which cause auroral emission at lower altitudes, while ECH waves interact with

©2019. Japan Geoscience Union. All Right Reserved.

relatively low energy electrons which cause auroral emission at higher altitudes. These results were published in Fukizawa et al. [GRL, 2018].
To verify whether ECH waves indeed scatter the pitch angle of electrons, we compared ECH wave intensity with electron flux in the loss cone obtained with low-energy particle experiments-electron analyzer onboard Arase. We also give results of other coordinated observation events.

Keywords: pulsating aurora, ECH waves, wave-particle interaction

©2019. Japan Geoscience Union. All Right Reserved.

Automatic determination of Upper Hybrid Resonance Frequencies by Convolutional Neural Network.

*Shoya Matsuda[1], Tatsuhito Hasegawa[2], Atsushi Kumamoto[3], Fuminori Tsuchiya[3], Yoshiya Kasahara[4], Yoshizumi Miyoshi[5], Yasumasa Kasaba[3], Ayako Matsuoka[1]

1. Institute of Space and Astronautical Science/Japan Aerospace Exploration Agency, 2. University of Fukui, 3. Tohoku University, 4. Kanazawa University, 5. ISEE, Nagoya University

Electron number density is a key parameter for discussions of plasma wave generation/propagation, and wave-particle interaction in the inner magnetosphere. The High Frequency Analyzer (HFA) is a subsystem of Plasma Wave Experiment (PWE) aboard Arase [Kasahara et al. (2018), Kumamoto et al. (2018), Miyoshi et al. (2018)]. The HFA measures electric field spectra in a frequency range from 10 kHz to 10 MHz, which covers a typical frequency range of Upper Hybrid Resonance (UHR) frequency in the inner magnetosphere. Kumamoto et al. (2018) proposed the semiautomatic method for the identification of UHR frequency by computer and a human operator. However, it takes a enormous effort of a human operator.

We propose an automatic determination system of UHR frequency by machine learning. Machine learning is a technique in the field of artificial intelligence to give computers the ability to learn with data. In this study, we defined a task of UHR frequency determination as supervised regression that a computer estimates UHR frequencies using the dataset composed of electric field dynamic spectra with correct UHR frequency labels. We adopted Convolutional Neural Network (CNN) as a machine learning algorithm. In this study, we introduce our machine learning approach and initial results for determining UHR frequency from electric field spectra observed by PWE/HFA.

Keywords: Arase satellite, UHR frequency, Machine learning

©2019. Japan Geoscience Union. All Right Reserved.

Amplitude dependence of whistler wave motion on electron scattering process

*Yoshiki Ito[1], Yoshizumi Miyoshi[1], Shinji Saito[1]

1. Nagoya University, ISEE

Whistler mode chorus waves cause scattering and acceleration of energetic electrons in the inner magnetosphere. The interaction processes have been modeled as diffusive process. The pitch angle diffusion coefficients of the pitch angle scattering depend on the power of chorus waves, so that it is expected that the scattering rate also depends on the wave amplitude. On the other hand, several previous studies indicated that the Lorentz force by the wave magnetic field is larger than the mirror force if the wave amplitudes increase and the electron trajectories in the velocity space are different from the diffusive distributions. In this study, we investigate chorus wave amplitude dependence of electron scattering using the GEMSIS-RBW simulation code. The RBW simulation demonstrates generation of periodical rising-tone chorus waves propagating along a magnetic field line to higher latitudes, and calculates local pitch angle and energy change by the imposed waves on the field line. At small wave amplitudes, time variations of pitch angle and energy of electrons are similar to diffusive process. At large wave amplitudes, some electrons increase both pitch angle and energy at interaction with the first rising tone, and then they decrease these parameters at interaction with the second rising tone. The process in the first rising tone seems to be the phase trapping, while the process in the second rising tone seems to be dislocation. Therefore, nonlinear scattering processes, which are phase trapping and dislocations, occur during the interactions with periodical rising-tone chorus waves with large amplitudes, which are quite different from quasi-linear scattering process.

©2019. Japan Geoscience Union. All Right Reserved.

Two-dimensional simulation of whistler mode wave packets interacting with energetic electrons

*Takeshi Nogi[1], Yoshiharu Omura[1]

1. Reserch Institute for Sustainable Humanosphere, Kyoto University

We perform two-dimensional electromagnetic particle simulations to study basic characteristics of whistler-mode wave particle interaction involved in the generation and propagation processes of chorus emissions with wave normal angles oblique to the static magnetic field. We assume a simple periodic (x, y) system with the magnetic field taken in the x-direction. We find the linear phase of the instability is much affected by electrostatic thermal fluctuations. It is necessary to put many super-particles in a grid cell to suppress the thermal fluctuation. We next put an array of antennas perpendicular to the background magnetic field, and oscillate the antenna current to generate obliquely propagating waves. In addition to the nonlinear trapping of energetic electrons through the cyclotron resonance, another nonlinear trapping of electrons takes place through the Landau resonance. Structures of the nonlinear trapping potentials change with the varying frequency, affecting efficiency of energy transfer between the wave and energetic electrons. We study nonlinear evolution of the wave packet, and competing processes of both resonances in accelerating energetic electrons to higher energies.

©2019. Japan Geoscience Union. All Right Reserved.

Relativistic electron acceleration by whistler-mode chorus waves in 1D, 2D, and 3D magnetic field models.

*Keita Takahashi[1], Yoshiharu Omura[1], Yikai HSIEH[1], Danny Summers[2]

1. Research Institute for Sustainable Humanosphere, Kyoto University , 2. Department of Mathematics and Statistics, Memorial University of Newfoundland

We evaluate the acceleration efficiencies of relativistic electrons under a 1D, 2D, and 3D model magnetic fields. We perform test-particle simulations and analyze nonlinear trapping motions of resonant electrons in each model. As a chorus wave model, we assume that a chorus wave packet generated at the magnetic equator propagates along the magnetic field to higher latitudes. When we perform simulations with the whistler mode wave, the cyclotron resonance with energetic electrons occurs at the similar timing in each model. Although we find relativistic turning acceleration (RTA) [1] to take place in each model, acceleration efficiencies of resonant electrons are different in these models. In terms of the numerical Green's function[2], we find a clear difference in time evolution of the distribution function in energy and equatorial pitch angle. The energy gap between resonant electrons and non-resonant electrons in the 1D model is slightly different from those in the 2D and 3D models. The energy gap in the 3D model is the largest among the three magnetic field models. This difference is due to additional oscillations in the velocity phase space, which only occur in the 2D and 3D models. These oscillations occur because the magnitude of the magnetic field changes during one period of relativistic cyclotron motion, affecting the nonlinear trapping conditions of resonant electrons.

References:

[1] Y. Omura, N. Furuya, D. Summers, Relativistic turning acceleration of resonant electrons by coherent whistler-mode waves in a dipole magnetic field, Journal Geophysical Research, Vol. 112, A06236, doi:10.1029/2006JA012243, 2007.

[2] Y. Omura, Y. Miyashita, M. Yoshikawa, D. Summers, M. Hikishima, Y. Ebihara, and Y. Kubota (2015), Formation process of relativistic electron flux through interaction with chorus emissions in the Earth's inner magnetosphere, J. Geophys. Res. Space Physics, 120, 9545–9562, doi:10.1002/2015JA021563, 2015.

©2019. Japan Geoscience Union. All Right Reserved.

Study of global spatio-temporal development of magnetospheric ELF/VLF waves for the 26-30 March 2017 storm based on ground and satellite observations and the RAM simulations

*Yuhei Takeshita[1], Kazuo Shiokawa[1], Yoshizumi Miyoshi[1], Mitsunori Ozaki[2], Yoshiya Kasahara[2], Martine Connors[3], Jyrki Manninen[4], Craig Kletzing[5], Vania Jordanova[6]

1. Nagoya University, Institute for Space-Earth Environmental Resarch, 2. Kanazawa University, 3. Athabasca University, 4. Sodankylä Geophysical Observatory, 5. The University of Iowa, 6. Los Alamos National Laboratory

The magnetospheric ELF/VLF waves are plasma waves generated by energetic electrons from several keV to tens keV with temperature anisotropy at magnetospheric equatorial plane of the inner magnetosphere. These ELF/VLF waves with frequencies lower than local half gyro frequency (lower-band) can propagate to the ground along magnetic field line. It is also known that the ELF/VLF waves interact with electrons drifting longitudinally in the inner magnetosphere, and help accelerating them to relativistic energies. Takeshita et al. [SGEPSS, 2018] statistically investigated the longitudinal extent of the magnetospheric ELF/VLF waves using six ground-based stations for two months, and showed the average extent of the ELF/VLF waves as ~90 degrees in longitude. However, Jordanova et al. [JGR, 2010] investigated the global distribution of linear growth rate of whistler mode chorus waves using global ring current-atmosphere interactions model (RAM), and showed that the region of large linear growth rate can extend ~180 degrees in longitude during the geomagnetic storm of 22 April 2001.

In this study we investigate the spatio-temporal distibution of the source region of magnetospheric ELF/VLF waves based on ground and satellite observations during the geomagnetic storm period from 26-30 March 2017, and compare it with global distribution of non-linear waves proxy of whistler mode chorus waves obtained by the RAM simulation. In this preliminary simulation, the simple dipole field and the Volland-Stern electric field are used as ambient magnetic and electric fields. And we assumed simply the Maxwell distribution as an energy spectrum using the empirical model of Tsyganenko and Mukai [2003]. In order to evaluate the non-linear wave excitation, we have estimated the optimum amplitude and the threshold value indicated by Omura and Nunn [2011]. We investigated the existence of lower band chorus waves using ground based observations at Athabasca (ATH; 54.7N, 246.4E, MLAT: 61.3N), Kapuskasing (KAP; 49.4N, 277.8E, MLAT: 58.7N), Kannuslehto (KAN: 67.7N, 26.3E, MLAT: 64.5N) and satellite-based observations by ERG with an apogee in the pre-dawn sector and RBSP-A and RBSP-B with an apogees in the post-dusk sector. We found the magnetospheric ELF/VLF waves exist from 3 MLT to 12 MLT for most periods from main- to recovery-phases of the magnetic storm. However, the RAM simulation did not predict wave generation during recovery phase of the storm. We compare the simulation and the ground-satellite observation in detail, and calculate the over-estimate rate (the ratio of wave existence period on the simulation to no wave period on the observation) and under-estimate rate (the ratio of no wave period on the simulation to wave existence period on the observation). We found the over-estimate rate become high (0.2~0.9) and under-estimate rate become low (0~0.4) in the main phase of the storm. This indicates that the longitudinal size of chorus source region predicted by simulation is larger than the observed size at the main phase. We also found that the over-estimate rate becomes low (0~0.2) and under-estimate rate becomes high (~1) during the recovery phase of the storm. This indicates that the simulation does not reproduce the wave existence during the recovery phase of the storm. Looking into the MLT distribution, the simulation predicts the wave existence from dusk to the midnight sector, but the

©2019. Japan Geoscience Union. All Right Reserved.

waves were not observed in this local time sector during the main phase. In case of recovery phase, the simulation did not predict wave existence but the observation showed continuous wave existence from dawn to the noon sector.

Keywords: chorus, ERG satellite, ground based observation

©2019. Japan Geoscience Union. All Right Reserved.

Flux decrease of outer radiation belt electrons associated with solar wind pressure pulse: A Code coupling simulation of GEMSIS-RB and GEMSIS-GM

*Ito Hiroki[1], Yoshizumi Miyoshi[1], Shinji Saito[2], Yosuke Matsumoto[3], Takanobu Amano[4]

1. Institute for Space-Earth Environmental Research, Nagoya University, 2. Graduate School of Science, Nagoya University, 3. Graduate School of Science, Chiba University, 4. Department of Earth and Planetary Science, University of Tokyo

Relativistic electron flux of the outer radiation belt dynamically changes in response to solar wind variations. There exist several conditions to cause the flux drop-out of the outer belt electrons. The magnetopause shadowing (MPS) is one of the processes to cause the rapid loss of outer belt electrons (e.g.,Kim et al.,2008). In this study, we investigate how radiation belt electrons are lost through the MPS process with a code-coupling simulation using GEMSIS-RB test particle simulation code (Saito et al., 2010) and GEMSIS-GM global MHD magnetosphere simulation code (Matsumoto et al., 2010) by focusing the equatorial pitch angle and local time dependence. We calculate trajectories of electrons in electromagnetic fields calculated from GEMSIS-GM with initial L-shells from 6 to 11, initial energies from 1 MeV to 10 MeV, and initial pitch angles between 50 degrees and 90 degrees, using the relativistic guiding-center equation. The simulation consists of the following three phases associated with variations of the solar wind dynamic pressure; [i] The standoff distance of magnetopause at the subsolar point is 12 Re with the initial dynamic pressure of 1.0 nPa. [ii] The solar wind dynamic pressure becomes 2.5 nPa, and the magnetopause moves to 9 Re. [iii] The solar wind dynamic pressure decreases, so that the inflation of the magnetopause takes place and the standoff distance of the magnetopause is 10 Re. During phase [ii], the high-latitude reconnections occur at dawn-side firstly and many electrons escape from the magnetosphere to the interplanetary magnetic field along the field line in the dawn side. Subsequently, the high-latitude reconnections occur at the high-latitude in the dusk side. In phase [iii], the remained electrons in the magnetosphere escape into the interplanetary in both the dawn and dusk sides. The loss at the dusk-side is outward motion of the trapped electrons caused by the dawn-to-dusk electric fields associated with the inflation of the magnetosphere. The study showed detailed process of the electron escape into the interplanetary magnetic field and the electron escape occur in both enhancement/decrease of the dynamic pressure.

Keywords: Magnetopause Shadowing, global MHD magnetosphere simulation, test particle simulation

©2019. Japan Geoscience Union. All Right Reserved.

Non-diffusive response of outer belt electrons on interplanetary shock

Takuma Toishi[1], *Yusuke Ebihara[1], Takashi Tanaka[2]

1. Research Institute for Sustainable Humanosphere, Kyoto University, 2. Kyushu University

Test particle simulation is performed in the electric and magnetic fields given by a global magnetohydrodynamics (MHD) simulation. When an interplanetary shock strikes the magnetosphere, a compressional wave propagates tailward. Pre-existing relativistic electrons that are initially located at fixed radial distances are redistributed by the electric and magnetic fields associated with the compressional wave. When the electrons encounter the nightside, they undergo complicated paths under the complicated distribution of the electric and the magnetic fields. Consequently, a group of isolated electrons forms, suggesting non-diffusive response. We discuss the redistribution processes in terms of the magnetospheric processes.

Keywords: radiation belt, MHD simulation, Test particle simulation

©2019. Japan Geoscience Union. All Right Reserved.

PARM: Initial result of the auroral camera on the G-CHASER (RockSat-XN) rocket and status of the development of auroral cameras for the LAMP rocket experiment

*Naoshi Yagi[1], Takeshi Sakanoi[1], Fukizawa Mizuki[1], Kazushi Asamura[2], Yoshizumi Miyoshi[3], Keisuke Hosokawa[4], Genki Ishizawa[5]

1. Planetary Plasma and Atmospheric Research Center, Graduate School of Science, Tohoku University, 2. Institute of Space and Astronautical Science, Japan Aerospace Exploration Agency, 3. Institute for Space-Earth Environmental Research, Nagoya University, 4. Department of Communication Engineering and Informatics, University of Electro-Communications, 5. Space & terrestrial plasma pyhsics

We developed an Aurora Imaging Camera (AIC) for NASA’ s G-CHASER (RockSat-XN) sounding rocket launched on 13th January, 2019. In addition, LAMP sounding rocket scheduled to be launched from December 2019 to February 2020 to reveal the spatio-temporal relationship between PsA and relativistic electrons, namely microbursts. In this presentation, we report the development of AIC, the result f the G-CHASER (RockSat-XN) rocket, as well as the current status of LAMP rocket project.

On the G-CHASER rocket experiment, 7 scientific and educational instruments were provided from Japan, U.S., Norway and Puerto Rico. Japanese instrument, called PARM, consists of an intermediate energy (20 - 100 keV) electron detector MED, high energy (several hundred keV - 2 MeV) electron detector HEP, fluxgate magnetometer AFG, and auroral camera AIC. Concerning development of AIC, we carried out sensitivity calibration experiment, electrical function test, fabrications, focus adjustment and environmental (vibration, vacuum and thermal) tests from January to July 2018. AIC consists of detector unit AIC-S and power/data processing electric unit AIC-E. AIC-S consists of a CCD camera (Watec 910 HX), wide-angle lens (F-number: 1.6, focal length: 3.5 mm, field of view: 96.4˚x75˚) and a glass filter (RG665) that transmits light with a wavelength longer than 665 nm.

NASA decided to launch the G-CHASER rocket at 9:00UT on 13rd January 2019 from Andoya Space Center, Norway (69.3˚N, 16.0˚E in the geographic coordinate). At this time, the solar elevation was -4˚, hence twilight had been already started and the region above 15km was sunlit. AIC detected leak light from the rocket skirt until the separation of skirt at an altitude of 82.9km. From time variation of AIC data, rocket spin frequencies were estimated to be ~5Hz at ~20km altitude and ~1Hz at ~80km altitude. This is consistent with the modulation period of magnetic field data observed by AFG. Because AIC was designed to measure weak pulsating aurora with hundreds Rayleigh, the AIC data was saturated above 82.9km after separation of rocket in the sunlit region, and no aurora was observed.

We are also conducting the LAMP sounding rocket project whose PI is Dr. Sarah Jones in NASA/GSFC. This is scheduled to be launched at Poker Flat Research Range in Alaska in 2019 winter. Japanese PARM2 team will provide high energy (several hundred keV - 2 MeV) electron detector HEP, fluxgate magnetometer MIM, and auroral cameras AIC2. We concern AIC2 that consists of two cameras AIC2-S1/AIC2-S2 and power/data processing electric unit AIC2-E. AIC2-S1/S2 and AIC2-E will be installed on a despun platform to derotate rocket spin. AIC2-S1 measures N2 1stPG emission with a narrow FOV lens (F value: 0.95, focal length:17mm, field of view 27x27deg), and AIC-S2 measures OI 844.6nm emission with a wide-angle lens (F value:1.6, focal length:3.5 mm, diagonal field of view:120x120˚). AIC2-S1 will take fine structure of PsA in the region more than 100 x 100 km area around the magnetic footprint with a few kilometer resolution, while AIC2-S2 will obtain an altitude distribution of

©2019. Japan Geoscience Union. All Right Reserved.

PsA in the F-region as well as wide-range distribution of PsA. The characteristic energy of precipitating electron can be estimated from the ration of OI844.6 and N2 1stPG. The cameras are conducted by a single board computer NanoPi M4 via USB3.0 high speed interface. We confirmed to get frame sampling rate with approximately 10Hz with this system. Region-of-interest (ROI) of 3660 x 3660 pixel area is binned with 61x61pixels, and finally image data with 60 x 60 bin (16 bit/bin) is recorded at 10 Hz. The precise imaging and altitude distribution of PsA are obtained with AIC2 at two wavelengths with 10Hz sampling. The imaging data combined with precipitating electron data in the wide energy range enable us to investigate the relativistic electron precipitation in microbursts that is probably caused by chorus waves in the magnetosphere.

Keywords: auroral camera, rocket experiment

©2019. Japan Geoscience Union. All Right Reserved.

First simultaneous observation of a SAR arc at subauroral latitudes using a ground all-sky camera and the Arase satellite in the inner magnetosphere

*Yudai Inaba[1], Kazuo Shiokawa[1], Shin-ichiro Oyama[1,8,9], Yuichi Otsuka[1], Atsuki Shinbori[1], Yoichi Kazama[2], Shiang-Yu Wang[2], Sunny W. Y. Tam[2], Shoichiro Yokota[3], Satoshi Kasahara[4], Kunihiro Keika[4], Tomoaki Hori[1], Ayako Matsuoka[5], Yoshiya Kasahara[6], Atsushi Kumamoto[7], Yasumasa Kasaba[7], Yoshizumi Miyoshi[1], Iku Shinohara[5], Arto Oksanen[10]

1. Institute for Space-Earth Environmental Research, 2. Academia Sinica, 3. Osaka Univ, 4. Tokyo Univ, 5. JAXA, 6. Kanazawa University, 7. Tohoku University, 8. University of Oulu, Finland, 9. National Institute of Polar Research, 10. Jyväskylän Sirius ry, Finland

Stable Auroral Red (SAR) arc is characterized by a 630.0 nm emission observed at subauroral latitudes. The energy of precipitating electrons that cause the SAR arc emission is several electron volts (eV). Precipitation of low-energy electrons is expected to occur due to spatial overlap between the plasmasphere and the ring current, where high-energy (more than 10 keV) ring current ions heat low-energy (less than 1 eV) electrons in the plasmasphere. Simultaneous observations of SAR arcs using the ionospheric satellite and ground all-sky cameras have been already done [e.g., Foster et al., 1994]. However, there has been no reports on in-situ measurements of plasma and electromagnetic fields in the inner magnetosphere, where the plasmaspheric plasma is heated by the ring current. In this study, we report simultaneous observations of a SAR arc at 22:04 UT on March 28, 2017, by using an all-sky camera at Nyrola (62.34 N, 25.51 E, MLAT 59.4 N) at subauroral latitudes and the Arase satellite. We analyze the all-sky camera data and the satellite data of this event to investigate the generation mechanism of the SAR arc. We find interesting features in the electric field data and the energy flux of electrons observed by the electric field detector of the plasma wave experiment (EFD/PWE) and the low-energy particle experiments–electron analyzer (LEP-e), respectively, onboard the Arase satellite at the crossing of the SAR arc. A negative excursion of the Ez component of the electric field (GSE coordinate system) with an amplitude of ~2.4 mV/m was observed at the crossing time. The Bx component of the magnetic field (GSE coordinate system) was negative. Thus the direction of the E ×B drift is westward, which is consistent with the westward auroral motion observed in the SAR arc by the ground all-sky camera. At the SAR arc crossing, the energy flux of electrons below 100-eV electrons is slightly intensified. We will discuss these observations in relation to the proposed SAR-arc generation mechanisms.

Keywords: ERG, SAR arc, All-sky imager, Simultaneous observation

©2019. Japan Geoscience Union. All Right Reserved.

Pi2 pulsations observed by the Arase satellite inside and outside the plasmapause

*Mariko Teramoto[1], Ayako Matsuoka[2], Reiko Nomura[5], Yoshiya Kasahara[3], Yasumasa Kasaba[4], Atsushi Kumamoto[4], Fuminori Tsuchiya[4], Shoya Matsuda[2], Masahito Nose[1], Masafumi Shoji[1], Yasunori Tsugawa[1], Shun Imajo[1], Yoshizumi Miyoshi[1], Iku Shinohara[2]

1. Institute for Space-Earth Environmental Research Nagoya University, 2. Institute of Space and Astronautical Science, Japan Aerospace eXploration Agency, 3. Kanazawa University, 4. Tohoku University, 5. National Astronomical Observatory of Japan

The spatial structure of Pi2 pulsation relative to the plasmasphere has been studied using the magnetic and electric field observed from the equatorial orbiting satellite in the inner magnetosphere by Takahashi et al (2003; 1995). They showed that the nightside Pi2 pulsations in the inner magnetosphere, which have high coherence with those at low-latitude ground station, are dominated by the poloidal component (the radial and compressional components for the magnetic field and azimuthal component for the electric field). The amplitudes of the compressional magnetic field has maximum and azimuthal electric field and the compressional magnetic field have maximum and minimum in the vicinity of the plasmaspause, respectively. The phase of the azimuthal electric field relative to low-latitude Pi2 pulsations on ground is 90 degrees in the plasmasphere. Such radial profile of the amplitude and phase of Pi2 pulsations can be explained by a plasmaspheric cavity mode resonance. However, the latitudinal structure of Pi2 pulsations in the electric field has not been examined. We investigate the latitudinal characteristics of off-equatorial Pi2 pulsations on the nightside and their relation to the plasmapause using the magnetic field measured by the fluxgate magnetometer measured by the Magnetic Field Experiment (MGF), the electric field measured by the Electric field Detector (EFD), and electron density derived from the spectra measured by the High Frequency Analyzer (HFA) from the Arase satellite.

©2019. Japan Geoscience Union. All Right Reserved.

An extreme erosion of the plasmasphere during the 7–10 September 2017 storm

*Yuki Obana[1], Naomi Maruyama[2,3], Atsuki Shinbori[4], Kumiko K. Hashimoto[5], Mariangel Fedrizzi[2,3], Masahito Nose[4], Yuichi Otsuka[4], Nozomu Nishitani[4], Tomoaki Hori[4], Atsushi Kumamoto[6], Fuminori Tsuchiya[6], Shoya Matsuda[7], Ayako Matsuoka[7], Yoshiya Kasahara[8], Akimasa Yoshikawa[9], Yoshizumi Miyoshi[4], Iku Shinohara[7]

1. Osaka Electro-Communication University, 2. University of Colorado Boulder, 3. NOAA Space Weather Prediction Center, 4. Nagoya University, 5. Kibi International University, 6. Tohoku University, 7. Japan Aerospace Exploration Agency, 8. Kanazawa University, 9. Kyushu University

We report an extreme erosion of the plasmasphere arising from the September 2017 storm. The cold electron density is identified from the upper limit frequency of UHR waves observed by the HFA of the PWE instrument onboard the Arase spacecraft. The HFA provides the spectrograms of electric fields in a frequency range from 10 kHz to 10 MHz with an 8-sec time resolution (Kasahara et al., 2018; Kumamoto et al., 2018). Such wide frequency coverage allows observation of the UHR frequency even deep inside the plasmasphere.
The electron density profiles reveal that the plasmasphere was severely eroded during the recovery phase of the storm and the plasmapause was located at L~1.7 at 23 UT on 8 Sep 2017. This is the first report of such deep erosion of the plasmasphere (L_{PP}<2) with the in-situ observation of the electron density. The degree of the severity is much more than what is expected from the SYM-H minimum (−146 nT) of the event.
We further study absolute GNSS-TEC, ground-based magnetic field, the doppler velocity obtained from the SuperDARN Hokkaido Radars to investigate the location of the midlatitude ionospheric trough, the penetration of the convection electric field to the equator and middle latitudes, respectively. Our results suggest that the middle latitude electric field was penetrated from the high-latitude storm time convection for several hours. Futhermore, the Ionosphere-Plasmasphere-Electrodynamics (IPE) model (Sun et al., 2015; Maruyama et al., 2016) is used to understand the dynamics of the plasmasphere. The IPE results suggest that the middle latitude electric field penetrates from the high-latitude storm time convection that lasts for several hours can explain the degree of severity during the September 7-11 2017 storm.

Keywords: plasmasphere, innner magnetosphere, Magnetosphere-ionosphere coupling

©2019. Japan Geoscience Union. All Right Reserved.

Relative contribution of ULF and chorus waves to the radiation belt variation: Comparison between multi-point observations and BATSRUS + CRCM simulation

*Naoko Takahashi[1], Kanako Seki[1], Mei-Ching Fok[2], Yihua Zheng[2], Yoshizumi Miyoshi[3], David Hartley[4], Ayako Matsuoka[5], Yoshiya Kasahara[6], Yasumasa Kasaba[7], Nana Higashio[8]

1. Graduate School of Science, University of Tokyo, 2. NASA Goddard Space Flight Center, 3. Institute for Space-Earth Environmental Research, Nagoya University, 4. Department of Physics and Astronomy, University of Iowa, 5. Institute of Space and Astronautical Science, Japan Aerospace Exploration Agency, 6. Information Media Center, Kanazawa University, 7. Planetary Plasma and Atmospheric Research Center, Tohoku University, 8. Japan Aerospace Exploration Agency

Earth’ s radiation belt is the area where electrons with energies from hundreds of keV to several MeV are trapped. When, where, and how the radiation belt exhibits a dramatic variation during a magnetic storm is of global interest. The dynamic variation of the radiation belt is caused by various wave-particle interactions: (1) the radial diffusion of electrons driven by ultra-low-frequency (ULF) waves in Pc5 frequency ranges (1.6–6.7 mHz) and (2) the local acceleration caused by wave-particle interactions between whistler-mode chorus waves and radiation belt particles. Over the past decade, multi-point observations and numerical simulations have provided evidence to support above physical processes. However, it is debatable how much each wave contributes to the radiation belt variation during a magnetic storm. A few previous studies have quantitatively compared roles of local acceleration and radial transport by calculating diffusion coefficients, whereas the global context between the wave growth and the relativistic electron flux enhancement has not been extensively studied. To address these issues, the comprehensive study using multi-point observations and numerical simulations (not empirical models) makes essential and significant contributions.

We focus on the magnetic storm on 27-30 May 2017. This magnetic storm is triggered by coronal mass ejections and induces a clear interplanetary shock. Fortunately, several satellites are scattered in the inner magnetosphere and detect both ULF and chorus waves during this magnetic storm. Arase and Van Allen Probes also detect variations of relativistic electron fluxes associated with the Dst index variation. We examine L-value dependence of ULF and chorus wave powers and find the difference of wave activity during the recovery phase. The chorus wave activity is large during the early recovery phase, while the ULF wave activity is large during the late recovery phase. The difference of wave activity may contribute to the radial profile in the phase space density of relativistic electrons. To grasp the extent of individual wave contribution, we also perform the comprehensive ring current model (CRCM) coupled with Block-Adaptive-Tree Solar-Wind Roe-Type Upwind Scheme (BATSRUS) simulation. BATSRUS with CRCM well reproduces global characteristics of energetic electron fluxes and wave growth during this magnetic storm. We will further evaluate global distribution of simulated wave power comparing to the observation, and then discuss the temporal and spatial context between each wave growth and the radiation belt variation.

©2019. Japan Geoscience Union. All Right Reserved.

Modulation of the D-region ionosphere by Pc5 waves observed by VLF/LF standard radio waves

*Miyashita Takuya[1], Hiroyo Ohya[1], Fuminori Tsuchiya[2], Hiroyuki Nakata[1], Toshiaki Takano[1], Kazuo Shiokawa[3], Yoshizumi Miyoshi[3]

1. Chiba University, 2. Tohoku University, 3. Nagoya University

Ionospheric modulation due to ultra low frequency (ULF) Pc5 waves have been observed by GPS-total electron content (TEC), high frequency (HF) Doppler sounders, and SuperDARN HF radars [e.g., Pilipenko et al., 2014; Belakhovsky et al., 2016]. However, there are few reports for the modulation of the lower ionospheric associated with the ULF Pc5 waves using VLF/LF transmitter signals. In this study, we investigate the D-region signatures of the modulation due to the ULF Pc5 waves using a network of very low frequency (VLF)/low frequency (LF) standard radio waves. We show oscillations in intensities of the VLF/LF waves with a period of 4-6 minutes during substorms on 27 April, 2017. The transmitter signals from NAA (USA, 24.0 kHz, L = 2.88), NLK (USA, 24.8 kHz, L = 2.88), NDK (USA, 25.2 kHz, L = 2.98) and WWVB (USA, 60.0 kHz, L = 2.26) were observed by the receivers at ATH (Athabasca, L=4.31) and PKR (Poker Flat, L=5.95). The substorm occurred at 04:30 UT. Based on the wavelet analysis, we found that the intensities for the NDK-ATH and WWVB-ATH paths showed oscillations with a period of 4-6 minutes during the substorm growth phase (05:00-06:00 UT). Magnetic field variations observed by ground magnetometers around the NDK-ATH and WWVB-ATH paths also showed the same periodicity, which means that the variations in the VLF/LF intensities would be caused by Pc5 modulations. The magnetic field oscillations were observed in wide latitude range. The intensity of the oscillation was larger at high latitude magnetometers than those around the location of the NDK-ATH and WWVB-ATH path (mid-latitude). The Pc5 oscillations could be excited by solar wind because solar wind speed had similar period of the 4-6 minutes. In this presentation, we will discuss the cause of these VLF/LF oscillations.

Keywords: VLF/LF standard radio waves, Pc5, ULF

©2019. Japan Geoscience Union. All Right Reserved.

Oxygen-proton differences in ion energies dominating plasma pressure: Dependence on storm phases and solar wind drivers

*Kunihiro Keika[1], Satoshi Kasahara[1], Shoichiro Yokota[2], Masahiro Hoshino[1], Kanako Seki[1], Masahito Nose[3], Yoshizumi Miyoshi[3], Iku Shinohara[4]

1. Graduate School of Science, The University of Tokyo , 2. Graduate School of Science, Osaka University, 3. Institute for Space-Earth Environmental Research, Nagoya University, 4. Institute of Space and Astronautical Science, Japan Aerospace Exploration Agency

The ion pressure in the inner magnetosphere is generally dominated by protons with energies of a few to a few 100s keV. Oxygen ions of ionospheric origin, O+, can make a significant contribution to the ion pressure during geomagnetically active periods. Our previous study (Keika et al., 2018, GRL) examined the radial dependence of contributing energies, which we term an energy range that makes the dominant contribution to the plasma pressure, during the main phase of the six magnetic storms in Year 2017. We found clear oxygen-proton differences in the contributing energies in the outer part (L>5) of the ring current region. The contributing energies were higher for O+ than for H+. The results provided in situ evidence of the contribution from mass-dependent/selective acceleration processes to the energization of the outer part of the ring current.

The present study extends this analysis toward a larger database obtained from a longer period of magnetic storm times including the recovery phase. We also compare mass-dependent/selective energization between different solar wind drivers such as coronal mass ejections and corotational interaction regions. We primarily use data from the MEP-i (Medium-Energy Particle experiments - ion mass analyzer) on board the Arase spacecraft. MEP-i measures ions with energies of 10 to 180 keV/q and distinguishes between different ion species. Arase observed the nightside near-Earth magnetosphere (L<10) during 7 CME-driven and 7 CIR-driven storms with the Dst minimum of smaller than -50 nT in Years 2017 and 2018. The dependence on storm phases and solar wind drivers helps identify magnetospheric conditions favorable for mass-dependent/selective acceleration and in turn provides clues for understanding important physical mechanisms. Utilizing observations made by the MMS spacecraft in the near-Earth plasma sheet, we also compare oxygen-to-proton differences inside earthward bursty bulk flows with the Arase/MEP-i observations. The multi-spacecraft observations help better understand the temporal evolution of the mass-dependent/selective acceleration processes.

Keywords: Magnetic storms, Substorms, RIng current, Oxygen ions, Ion transport and acceleration

©2019. Japan Geoscience Union. All Right Reserved.

Mass dependence of penetration depth of multi-energy ions in the inner magnetosphere during magnetic storms: Arase observations

*Ryosuke Fujii[1], Yoshizumi Miyoshi[1], Masafumi Shoji[1], Kazushi Asamura[2], Lynn Kistler[1,8], Vania Jordanova[9], Tomoaki Hori[1], Satoshi Kurita[1], Mariko Teramoto[1], Yasunori Tsugawa[1], Yoshiya Kasahara[3], Yasumasa Kasaba[4], Atsushi Kumamoto[5], Fuminori Tsuchiya[4], Shoichiro Yokota[6], Kunihiro Keika[7], Ayako Matsuoka[2], Iku Shinohara[2]

1. Institute for Space-Earth Environmental Research, Nagoya University, 2. Institute of Space and Astronautical Science, Japan Aerospace Exploration Agency, 3. Information Media Center, Kanazawa University, 4. Planetary Plasma and Atmospheric Research Center, Tohoku University, 5. Department of Geophysics, Graduate School of Science, Tohoku University, 6. Graduate School of Science, Osaka University, 7. Department of Earth and Planetary Science, Graduate School of Science, The University of Tokyo, 8. University of New Hampshire, 9. Los Alamos National Laboratory

During magnetic storms, the ring current ions move toward the Earth, and the inner edge position of the ring current depends on the convection electric field. We investigate variations of the inner edge of the ring current ions, so-called, penetration depth, during magnetic storms using the ion measurements made by the Low-energy particle experiments-ion mass analyzer (LEP-i)/Medium-energy particle experiments-ion mass analyzer (MEP-i) instruments onboard the Arase satellite. The Arase satellite typically observes the earthward penetration of the ring current protons associated with the enhancement of the dawn-to-dusk electric field in the inner magnetosphere during the storm main phase. The plasmapause moves earthward during the main phase. On the other hand, the convection electric field decreases during the storm recovery phase in which the flux of ring current protons decreases. We identify that the penetration depth of protons depends on the minimum Dst index during the storms as well as the proton energy.

We also investigate the penetration depth of other ions, i.e., helium and oxygen ions. Because the life times of helium and oxygen ions due to charge exchange reaction for are longer than that of protons, it is expected that these ions can penetrate deeper than protons and temporal and spatial evolution can be observed clearly. We will also discuss the relation between the position of ring current inner edge and cross polar cap potential.

Keywords: The Arase satellite, Ring current, Ions

©2019. Japan Geoscience Union. All Right Reserved.

Relativistic Acceleration of Energetic Protons by Electromagnetic Ion Cyclotron Waves in the Jovian Magnetosphere

*Tomohiro Sekine[1], Yoshiharu Omura[1], Danny Summers[2], Yikai HSIEH[1], Satoko Nakamura[1]

1. Reserach Institute for Sustainable Humanosphere, Kyoto University, 2. Memorial University of Newfoundland

We perform test particle simulations of nonlinear interaction between energetic protons and EMIC waves. We assume a coherent EMIC waves that have a constant frequency and propagate parallel to the magnetic field. We find that protons can be trapped and accelerated by EMIC waves. We find a very efficient acceleration process of protons in which kinetic energy of protons increases while directions of parallel velocities reverses when we assume parameters in the Jovian magnetosphere. We notice that this phenomenon is very similar to the interaction process between relativistic electrons and whistler-mode waves, which is called Relativistic Turning Acceleration (RTA) [1]. In order to analyze the phenomena, we have developed nonlinear trapping theory of interaction between relativistic protons and EMIC waves. Next, we compare the theory and simulation results. We confirm that the results satisfy the conditions for RTA. Following the trajectories of many resonant protons, we obtain time evolution of the distribution function of relativistic protons as a function of energy and equatorial pitch angle based on the numerical Green’ s function method [2].

References:

[1] Y. Omura, N. Furuya, D. Summers, Relativistic turning acceleration of resonant electrons by coherent whistler-mode waves in a dipole magnetic field, Journal Geophysical Research, Vol. 112, A06236, doi:10.1029/2006JA012243, 2007.

[2] Y. Omura, Y. Miyashita, M. Yoshikawa, D. Summers, M. Hikishima, Y. Ebihara, and Y. Kubota (2015), Formation process of relativistic electron flux through interaction with chorus emissions in the Earth’ s inner magnetosphere, J. Geophys. Res. Space Physics, 120, 9545–9562, doi:10.1002/2015JA021563, 2015.

©2019. Japan Geoscience Union. All Right Reserved.

Statistical study of IPDP type EMIC wave-related electron precipitation at subauroral latitude

*Asuka Hirai[1], Fuminori Tsuchiya[1], Takahiro Obara[1], Yasumasa Kasaba[1], Yuto Katoh[2], Hiroaki Misawa[1], Kazuo Shiokawa[3], Yoshizumi Miyoshi[3], Satoshi Kurita[3], Martin G Connors[4]

1. Planetary Plasma and Atmospheric Research Center, Graduate School of Science, Tohoku Univ. , 2. Department of Geophysics, Graduate School of Science, Tohoku University, 3. Institute for Space-Earth Environmental Research, Nagoya University, 4. Athabasca University

The outer radiation belt electrons disappear during the main phase of geomagnetic storms. One of the loss mechanisms of electrons from the outer belt is precipitation into the atmosphere due to wave-particle interactions. Electromagnetic ion cyclotron (EMIC) waves are believed to be important plasma waves that contribute to the loss of the outer radiation belt due to pitch angle scattering. They can scatter relativistic and ultra-relativistic electrons. However, there are still questions left about the contribution of EMIC waves to the whole loss of radiation belt electrons and possible conditions favorable to pitch angle scattering.

EMIC waves mainly propagate along magnetic field lines and are observed on the ground as Pc1 geomagnetic pulsations. Intervals of pulsations of diminishing periods (IPDP) are Pc1/EMIC waves that are characterized by frequency rise from 0.1 to 1–2 Hz in a period of ~1 h, and often occur during substorms. Recent studies reported that IPDP are preferentially associated with relativistic electron precipitation. However, the statistical relation between IPDP waves and relativistic electron precipitation, and their physical mechanism, remain open issues.

We investigated differences in characteristics between IPDP and other types of Pc1 by using an induction magnetometer and VLF radio wave data that is a proxy of electron precipitations at subauroral latitude from 1 November 2016 to 30 June 2018. We used the induction magnetometer of PWING (study of dynamical variation of Particles and Waves in the INner magnetosphere using Ground-based network observations) at Athabasca, Canada (54.6˚N, 246.36˚E, L = 4.39). VLF radio waves propagate from transmitters to receivers in subionospheric waveguide. The modulations of VLF signals are detected as occurrence of sub-relativistic and relativistic electron (>100 keV) precipitation due to ionization changes in the lower ionosphere along the radio wave propagation path. VLF radio waves are transmitter from NDK, U.S. (46.367˚N, 261.467˚E, L =3.13) and NLK, U.S. (48.2˚N, 238.083˚E, L =2.84) and received at Athabasca. We selected EMIC wave events on the basis of the following criteria: (1) EMIC wave power is higher than 10^{-5} nT^2/Hz. (2) Duration of EMIC waves is longer than 20 min. (3) Interval between one EMIC wave event and the next one is longer than 30 min. Electron precipitation was identified as a decrease in amplitude of VLF signals from the quiet day curve (QDC). We counted as EMIC wave-driven electron precipitation if we detect temporal correspondence with EMIC waves. In this period, we found 950 EMIC wave events, and 87 of total EMIC wave events were IPDP events (9.2%). Local time dependence of EMIC waves shows that IPDP often occurs in the afternoon and evening sector, while other types of Pc1 occur in all local time range, but with a maximum in 12–16 MLT, which is consistent with previous studies. Simultaneous observation of the magnetometer and VLF radio waves were available for 286 days, and we found 163 EMIC wave events. 19 of 163 EMIC wave events were clearly associated with electron precipitation (12%). Among 19 electron precipitation events, 15 events were caused by IPDP (79%). Also, the electron precipitation events were observed in the evening sector with similar local time dependence to IPDP. This result suggests that IPDP is more likely to cause electron precipitation than other Pc1 wave types. In previous studies, IPDP occurs due to ion cyclotron instability of ring current ions in the evening sector, and favorable region for electron scattering by EMIC waves is high density duskside plasmapause

©2019. Japan Geoscience Union. All Right Reserved.

and plasmaspheric plume because dense plasma lowers minimum resonant energy of electrons. It is assumed that occurrence region of IPDP is coincident with the preferential region for MeV electron scattering by EMIC waves. For this reason, it is expected that IPDP type EMIC waves significantly cause relativistic electron precipitations in the duskside.

Keywords: EMIC waves, electron precipitation, subionospheric VLF radio waves

©2019. Japan Geoscience Union. All Right Reserved.

Meridional distributions of proton plasma and pressure-driven currents in the nightside inner magnetosphere: Arase observations

*Shun Imajo[1], Masahito Nose[1], Satoshi Kasahara[2], Shoichiro Yokota[3], Ayako Matsuoka[4], Kunihiro Keika[2], Tomoaki Hori[1], Mariko Teramoto[1], Kazuhiro Yamamoto[5], Oimatsu Satoshi[5], Reiko Nomura[6], Akiko Fujimoto[7], Iku Shinohara[4], Yoshizumi Miyoshi[1]

1. Institute for Space-Earth Environmental Research, Nagoya University, 2. Graduate School of Science, The University of Tokyo, 3. Graduate School of Science, Osaka University, 4. Institute of Space and Astronautical Science, Japan Aerospace Exploration Agency, 5. Graduate School of Science, Kyoto University, 6. National Astronomical Observatory of Japan, 7. Kyushu Institute of Technology

We examine the averaged meridional distributions of proton plasma parameters and pressure-driven currents in the nightside (20–04 h magnetic local time) ring current region during disturbed times (-80 < SYM-H* < -40 nT) using ion measurements covering energy range of 10–180 keV by the Arase satellite. Because the Arase satellite has a large inclination orbit of 31°, it covers the absolute value of magnetic latitude (|MLAT|) range of 0–40° and the radial distance of < 6 Re. We find that the plasma pressure decreases significantly with MLAT. The plasma pressure on the same L^* shell at 30°<|MLAT|<40° is about 10–60% of that at 0°<|MLAT|<10°, and the percentage of decrease is larger on lower L^* shells. The pressure anisotropy which is defined by the perpendicular pressure divided by the parallel pressure decreases with radial distance and shows a weak dependence on |MLAT|. The magnitude of the plasma beta at 30°<|MLAT|<40° is one or two order smaller than that at 0°<|MLAT|<10°. The relative plasma pressure distribution predicted from the magnetic strength and anisotropy is roughly consistent with the observed plasma pressure for L^*=3.5–5.5. The azimuthal pressure-gradient current derived from the plasma pressure distribution spreads over ~-20° |MLAT|, while the curvature current is limited in ~0–10° |MLAT|. We suggest that the latitudinal dependences should be taken into account when considering a temporal evolution of ring current particles from L distributions of successive orbits.

Keywords: meridional distributions, plasma pressure, pressure-driven currents, Arase satellite

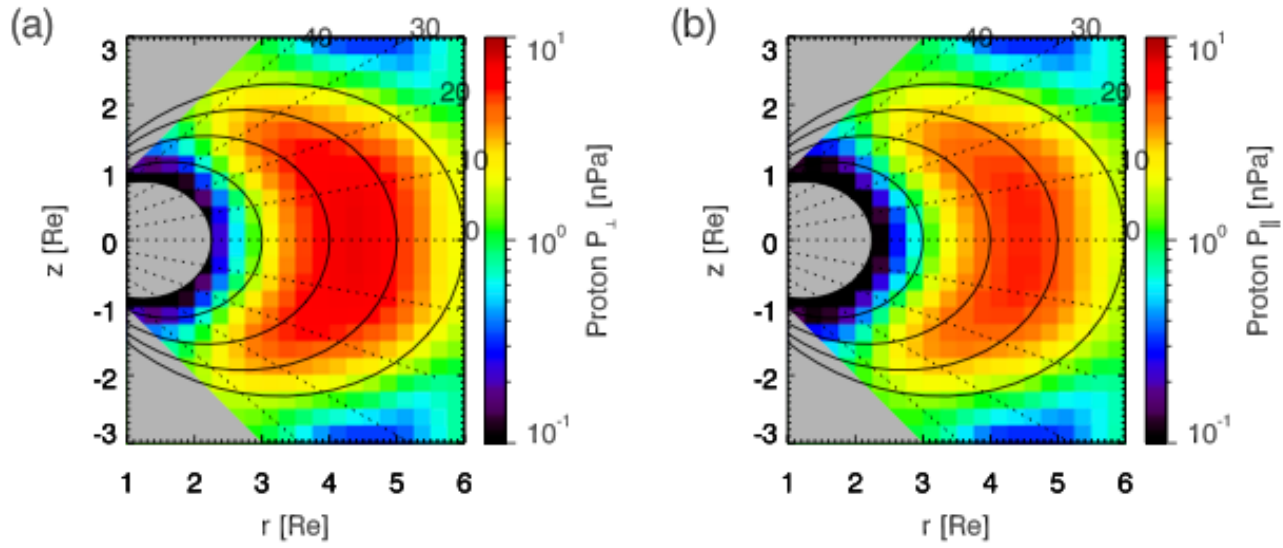

©2019. Japan Geoscience Union. All Right Reserved.

Space Weather Effects on Energetic Proton Flux Response in South Atlantic Anomaly

*Kirolosse Mina GIRGIS[1,2], Tohru Hada[1], Shuichi Matsukiyo[1]

1. Earth System Science and Technology (ESST) Department, Interdisciplinary Graduate School of Engineering Sciences (IGSES), Kyushu University, Japan, 2. Aerospace Engineering Department, Faculty of Engineering, Cairo University, Egypt

In this research, energetic proton flux in the inner radiation belt, is studied inside the South Atlantic Anomaly (SAA) by performing test particle simulations, where the background time-varying magnetic field is provided by Tsyganenko model, according to *Dst* index and altitudes. The objective of this investigation, is to estimate and forecast the additional radiation dose, occurring on spacecraft and human bodies, due to their passage inside the anomaly, and precisely, during intense solar storms. It was found that within minutes, proton flux in the SAA, penetrated deeper downward by about 200 km, when the *Dst* index is decreased (< -210 nT), and a after few more minutes, it was significantly reduced at all the altitudes; the last conclusion was confirmed by satellite observations.

Keywords: South Atlantic Anomaly, Space Weather, Dst Index, Radiation Dose, Proton Flux

©2019. Japan Geoscience Union. All Right Reserved.

Solar-cycle variations of >30 keV electron flux enhancements under the inner radiation belt

*ALLA SUVOROVA[1]

1. National Central University

Intense fluxes of 30-300 electrons can arise in the equatorial ionosphere outside the South Atlantic Anomaly. It was established that the electrons were injected from the inner radiation belt probably due to a mechanism of fast radial transport in the crossed electric and magnetic fields. Continuous monitoring of energetic particles at low heights of ~850 km with the MEPED instrument onboard the NOAA/POES satellites allowed compiling large statistics of the >30 keV electron enhancements from 1998 to 2018. We studied particle flux variations with geomagnetic activity and solar cycle. We found that geomagnetic activity measured by Dst and AE indices are not key factors of occurrence rate increase for electron injections, but influence on intensity of particles. The occurrence rate is controlled by auroral conductivity on the dayside and significantly enhanced during northern summer. Descending phase of solar cycle plays a major role in the occurrence rate increase.

Keywords: magnetosphere-ionosphere, energetic electrons, low latitudes, solar cycle

©2019. Japan Geoscience Union. All Right Reserved.

Energy spectra variations of high energy electrons in the inner magnetosphere observed by HEP/XEP on ARASE and SEDA-e on HIMAWARI

*Takeshi Takashima[1], Takefumi Mitani[1], Nana Higashio[2], Tsutomu Nagatsuma[3]

1. ISAS/JAXA, 2. Research and Development Directorate/JAXA, 3. NiCT

The relativistic electrons in the outer radiation belt were disappeared/increased and their energy spectra were changed dynamically in some storms observed by XEP/HEP onboard the ARASE spacecraft. In the same time, SEDA-e with energy range 200keV-4.5MeV for electron on board the HIMAWARI-8, Japanese weather satellite on GEO, observed increase of relativistic electron in different local time.
When comparing the energy spectra, there are times when the spectrum matches or does not match. It is also observed that the change in the slope of the energy spectrum differs with time. These phenomena are observed even when there are two satellites at the same local time.
We will report on energy spectra variations of high energy electrons including calibrations of differential flux between XEP and HEP and discuss comparisons with energy spectra between ARAE and HIMAWARI that observed each storm in different local time.

Keywords: relativistic electron, inner magnetosphere, ARASE

©2019. Japan Geoscience Union. All Right Reserved.

Inter-channel calibration of the high-energy electron experiments (HEP) instrument onboard the Arase satellite

*Tomoaki Hori[1], Takefumi Mitani[2], Takeshi Takashima[2], Park Inchun[1], Satoshi Kurita[1], Mariko Teramoto[1], Nana Higashio[3], Satoshi Kasahara[4], Shoichiro Yokota[5], Yoshizumi Miyoshi[1], Iku Shinohara[2]

1. Institute for Space-Earth Environmental Research, Nagoya University, 2. Japan Aerospace Exploration Agency, Institute of Space and Astronautical Science, 3. Japan Aerospace Exploration Agency, 4. Graduate School of Science, The University of Tokyo, 5. Graduate School of Science, Osaka University

An inter-channel comparison of electron fluxes measured by the HEP instrument onboard the Arase satellite is conducted with a focus on the apparent non-uniformity in detection efficiency and relative offset of the background flux level between the channels, which was partly reported previously. We extend the data set to cover the entire two-year period since the start of the regular observations. The flux ratio of different channels is sorted by the electron flux level of much higher energies that was simultaneously measured by the extremely high-energy electron experiment (XEP) instrument onboard Arase. The result shows that the HEP flux of all azimuthal channels is more or less affected by MeV electrons which are most likely to have penetrated into the instrument box and directly hit the detectors. However, it is also revealed that the non-uniform count distribution over the channels still remains even when the penetrating electrons are absent. We conduct a set of Geant-4 simulations to trace electrons with various energies and incident angles to the detector plane in order to give a quantitative interpretation for the resultant count distributions, in terms of the effects of penetrating electrons and obliquely-colliding incident electrons.

Keywords: Arase satellite, particle instrument, calibration

©2019. Japan Geoscience Union. All Right Reserved.

Particle simulation for calibrating the HEP data onboard the ARASE satellite

*PARK INCHUN[1], Yoshizumi Miyoshi[1], Takefumi Mitani[2], Tomoaki Hori[1], Satoshi Kurita[1], Mariko Teramoto[1], Takeshi Takashima[2], Nana Higashio[3], Iku Shinohara[2]

1. Nagoya University Institute for Space-Earth Environmental Research, 2. Japan Aerospace Exploration Agency Institute of Space and Astronautical Science , 3. Japan Aerospace Exploration Agency

Understanding the detailed characteristics of the HEP (High-Energy electron Experiment) instrument onboard the Arase satellite is crucial for data calibration. Due to difficulties of reproducing the severe radiation environment of the inner magnetosphere on the ground, computer simulation is the best method to understand instrument responses to the ambient radiation environment. Through Monte-Carlo simulations using the Geant4 tool, we have reconstructed the geometry of the HEP instrument and modeled the high-energy particle environment. Using the developed model, we have studied the efficiency of the detectors, the angular resolution, and the g-factors, which depend on the particle energy and the sensor channels. While the previous studies were based on a uni-direction simulation with electron pencil beams, this study adopted all the detector channels and energy bends of HEP thus resulting in more advanced simulations. Based on the results, we have made a new calibration table depending on the angle of incident particles. We have also estimated the g-factor which depends on the incident particle energy. The updated calibration table and g-factors are important for calibrating the HEP data as well as inter-calibrations with other particle instruments' data.

Keywords: ARASE, Geant4, HEP

©2019. Japan Geoscience Union. All Right Reserved.

Geant4 model calculation and energetic particle observation with HEP/Arase in the inner radiation belt

*Honoka Toda[1], Wataru Miyake[1], Takefumi Mitani[3], Takeshi Takashima[3], Yoshizumi Miyoshi[2], PARK INCHUN[2], Tomoaki Hori[2]

1. Tokai University, 2. ISEE/Nagoya University, 3. ISAS/JAXA

The high-energy electron experiments (HEP) instrument installed on the Arase is designed to observe energetic electrons of 70 keV to 2 MeV. The HEP registers high electron counts for the MeV energy range, not only in the outer belt but also in the inner belt, in MeV energy range. On the contrary, Van Allen Probes have hardly detected MeV electrons in the inner radiation belt. A probable interpretation is that the counts of HEP are caused due to contamination of high-energy protons. In order to verify this idea, we have modeled the HEP instrument a Geant4 simulation to determine the energy of penetrating protons. The result clearly shows that high-energy protons, it has become clear that high-energy protons of a few to a few tens of MeV can contribute to the apparent high counts of HEP. No instrument for measuring protons in this energy range is installed on the satellite. We will discuss the possibility of research on the spatial distribution and time variation of high-energy protons in the inner belt based on observation data from the HEP instrument.

Keywords: Arase, Proton Radiation Belt, HEP

©2019. Japan Geoscience Union. All Right Reserved.

Validation of High-energy electron detector simulator for the HEP instruments onboard Arase

*Takefumi Mitani[1], PARK INCHUN[2], Tomoaki Hori[2], Taku Namekawa[1,3], Kazushi Asamura[1], Takeshi Takashima[1], Satoshi Kasahara[3], Satoshi Kurita[2], Mariko Teramoto[2], Nana Higashio[1], Yoshizumi Miyoshi[2], Iku Shinohara[1]

1. Japan Aerospace Exploration Agency, Institute of Space and Astronautical Science, 2. Institute for Space-Earth Environmental Research, Nagoya Univ., 3. The university of Tokyo

The high-energy electron experiments (HEP) onboard the Arase satellite detects 70 keV-2 MeV electrons and generates a three-dimensional velocity distribution for these electrons in every period of the satellite's rotation. Electrons are detected by two instruments, namely, HEP-L and HEP-H, which differ in their geometric factor (G-factor) and range of energies they detect. HEP-L detects 70 keV–1 MeV electrons and its G-factor is 9.3 $\times 10^{-4}$ cm^2 sr at maximum, while HEP-H observes 0.7 MeV–2 MeV electrons and its G-factor is 9.3 $\times 10^{-3}$ cm^2 sr at maximum. The instruments utilize silicon strip detectors and application-specific integrated circuits to readout the incident charge signal from each strip.

In order to deduce the distribution of incident electrons from the direction and energy detections in orbit, we have developed a detector simulator using the Geant4 toolkit. Especially contamination due to high energy particles must be considered quantitatively. We have also been working on electron beam experiments using HEP detector modules which are almost the same as the flight model in order to compare detailed simulations and experimental data.

We will present a comparison between results from the electron beam experiments and those from the detector simulator. And we will discuss its influence on the interpretation of the observational data obtained in orbit.

Keywords: high-energy electron, Arase, Geant4

©2019. Japan Geoscience Union. All Right Reserved.

[E] Poster | A (Atmospheric and Hydrospheric Sciences)：A-AS Atmospheric Sciences, Meteorology & Atmospheric Environment

Wed. May 29, 2019 3:30 PM - 5:00 PM JST | Wed. May 29, 2019 6:30 AM - 8:00 AM UTC | Poster Hall International Exhibition Hall8, Makuhari Messe_5

[A-AS01] High performance computing for next generation weather, climate, and environmental sc iences

convener:Hiromu Seko(Meteorological Research Institute), Takemasa Miyoshi(RIKEN), Chihiro Kodama(Japan Agency for Marine-Earth Science and Technology), Masayuki Takigawa(Japan Agency for Marine-Earth Science and Technology)

A lot of advanced simulation studies are being conducted by high performance supercomputers, such as K computer and Earth Simulator, in various fields including meteorology. The high performance supercomputers enable us to conduct numerical simulations and data assimilation of observation big-data (huge high-density and high-frequency data) with an order of magnitude higher resolutions and ensemble numbers than those with the previous supercomputers. In addition, the post-K computer will be available as a successor of K, and studies for the post-K computer are in progress. At this session, we comprehensively pick up the topics in the Atmospheric and Hydrospheric Sciences Sessions of the 2019 Union Meeting that comprise the atmospheric, oceanic and land sciences. This session aims to promote recent studies related to the issues on high performance computing in weather, climate, and environmental studies using the K computer and other supercomputers, and to enhance discussions on future directions of numerical simulations in meteorology.

[AAS01-P01] **Categorized correction forecast for accumulative precipitation of heavy rainfall processes based on optimal probability (OPPF) in medium-extended-range forecast time**

*Ruoyun Niu[1] (1.National Meteorological Center)

[AAS01-P02] **Characteristics of temporal and spatial distribution of regional rainstorm processes to the east of 95°E in China during 1981-2015**

*Ruoyun Niu[1], Couhua Liu[1] (1.National Meteorological Center)

[AAS01-P03] Near-real-time SCALE-LETKF forecasts of the record breaking rainfall in Japan in July 2018

*Takumi Honda[1], Guo-Yuan Lien[2,1], Takemasa Miyoshi[1] (1.RIKEN Center for Computational Science, 2.Central Weather Bureau)

[AAS01-P04] An objective Frontal Analysis Techniques and Application in Model Verification

*couhua liu[1] (1.National Meteorology Centre of China Meteorological Administration)

[AAS01-P05] Assimilating every 30-second phased array weather radar data in a torrential rainfall event on July 6, 2018 around Kobe city

*Yasumitsu Maejima[1], Shigenori Otsuka[1], Takemasa Miyoshi[1,2] (1.RIKEN Center for Computational Science, 2.University of Maryland, College Park)

[AAS01-P06] The impact of range sidelobes from phased array weather radar observations to short-range convective forecasts

*James David Taylor[1], Guo-Yuan Lien[1], Shinsuke Satoh[2], Takemasa Miyoshi[1] (1.RIKEN Research center for computational science, 2.NICT National Institute of Information and Communications Technology)

[AAS01-P07] Development of Hydro-debris 2D model for larger area

*Yosuke Alexandre Yamashiki[1], Tsutao OIZUMI[2], Bruno Ribeiro[1], Ryusuke Kuroki[1] (1.Earth & Planetary Water Resources Assessment Laboratory Graduate School of Advanced Integrated Studies in Human Survivability Kyoto University, 2.Japan Association of Marine-Earth Science and Tecnology)

[AAS01-P08] **Research on the application of an improved terrain-following vertical coordinates on GRAPES model**

*chao li[1] (1.NWPC.CMA)

[AAS01-P09] Development of a parallel spherical harmonic transform library: design and performance

*Fuyuki SAITO[1] (1.Japan Agency for Marine-Earth Science and Technology)

[AAS01-P10] Global data assimilation of multi-species satellite measurements for atmospheric chemistry analysis

*Takashi Sekiya[1], Kazuyuki Miyazaki[2,1], Koji Ogochi[1], Kengo Sudo[3,1], Masayuki Takigawa[1] (1.Japan Agency for Marine-Earth Science and Technology, 2.Jet Propulsion Laboratory/California Institute for Technology, 3.Graduate School of Environmental Studies, Nagoya University)

[AAS01-P11] The sensitivity to WRF shortwave radiation parameterizations in prediction of global horizontal irradiance for investigating interactions of atmosphere with croplands

*Ankur Srivastava[1], Sarita Kumari[1], Rajkumar Dhakar[2] (1.Indian Institute of Technology Delhi, 2.Indian Agriculture Research Institute)

[AAS01-P12] The development of an atmospheric aerosol/chemistry–climate model, BCC_AGCM_CUACE2.0, and simulated effective radiative forcing of nitrate aerosols

*QI AN[1,2,4], Hua Zhang[2], Zhili Wang[2], Yi Liu[1,4], Bing Xie[3], Qianxia Liu[3], Zaizhi Wang[3], Sunling Gong[2] (1.LAGEO, IAP, CAS, 2.LaSW, CAMS, 3.NCC,CMA, 4.UCAS)

[AAS01-P13] **Impacts of different types and intensities of El Niño events on winter aerosols over China**

*Xiaochao Yu[1,2], Zhili Wang[2,1], Hua Zhang[2], Shuyun Zhao[3] (1.Collaborative Innovation Center on Forecast and Evaluation of Meteorological Disasters, Nanjing University of Information Science and Technology, Nanjing, 210044, China, 2.State Key Laboratory of Severe Weather and Key Laboratory of Atmospheric Chemistry of CMA, Chinese Academy of Meteorological Sciences, Beijing, 100081, China., 3.National Climate Center, China Meteorological Administration, Beijing, 100081, China)

[AAS01-P14] High Cloud Annual Variation and Its Responses to Global Warming in the NICAM AMIP Experiment

*Ying-Wen Chen[1], Masaki Satoh[1,2], Chihiro Kodama[2], Akira Noda[2], Yohei Yamada[2] (1.Atmospheric and Ocean Research Institute, The University of Tokyo , 2.Japan Agency for Marine-Earth Science and Technology)

[AAS01-P15] Improvements in Simulating the Relationship between ENSO and East Asian Summer Rainfall in the CMIP5 Models

*Yuanhai FU[1], Riyu Lu[1] (1.IAP, CAS)

Categorized correction forecast for accumulative precipitation of heavy rainfall processes based on optimal probability (OPPF) in medium-extended-range forecast time

*Ruoyun Niu[1]

1. National Meteorological Center

By taking the ensemble prediction data from ECMWF and the intensive observations of precipitation in China, the technology of categorized correction forecast for accumulative precipitation of heavy rainfall processes based on optimal probability(OPPF) is developed, and 3 calculation schemes of OPPF are designed according to overall technical route. Then the reforecast test are carried for the accumulative precipitation of 67 heavy rainfall processes from May to September during 1981 to 2015 in China, and the forecast performance of the 3 OPPFs against that of ensemble mean (EMPF) and control number (CTPF) is evaluated and contrasted. The results show that:(1) In the medium-extended-range (096-360h) forecast time, the performance of the 3 OPPFs are better than that of EMPF and CTPF for heavy precipitation forecast and clear-rain forecast. the performance of OPPF1 and OPPF2 is close to that of EMPF for Moderate precipitation and larger precipitation. OPPF3 produces the best performance among the 3 OPPFs. (2) There are obvious regional differences in forecast performances. TS of OPPF3 in southern China are higher than in northern China, and the performance of OPPF3 for heavy precipitation is better than that of EMPF in southern China. During 096-240h forecast time, the performance of OPPF3 for heavy precipitation is also better than that of EMPF in eastern part of Northeast China.

Keywords: optimal probability, accumulative precipitation of heavy precipitation processes, categorized correction forecast, comparative evaluation of forecast performance

©2019. Japan Geoscience Union. All Right Reserved.

Characteristics of temporal and spatial distribution of regional rainstorm processes to the east of 95ºE in China during 1981-2015

*Ruoyun Niu[1], Couhua Liu[1]

1. National Meteorological Center

The events of the regional rainstorm processes (RRP) to the east of 95ºE in China over 1981-2015 are constructed based on intensive daily observations of precipitation in China and NCEP/NCAR reanalysis data by means of subjective and objective analyses. Temporal and spatial characteristic distribution of RRP in China are further investigated using the methods of wavelet power spectrum, nine-point binomial smoothing and Ward cluster analysis. The main conclusions are as follows. (1) The annual average number of RRP to the east of 95ºE in China is nearly 30. RRP in the Yangtze-Huaihe River valley occur most frequently among the six subareas with an annual average number of about 19, followed by that in South China and the eastern part of Southwest China with the annual average number of RRP 10.5 and 5.8 times respectively. Annual average number of RRP are only about 1-3 times in other subareas. (2) The inter-annual and inter-decadal variations of the annual number of RRP exhibit distinct fluctuation characteristics. The inter-annual and inter-decadal fluctuating variation in the Yangtze-Huaihe River valley is the most consistent with that to the east of 95E in China. Moreover, the fluctuating variations have a significant positive correlation between South China and eastern part of Southwest China, and also between Northeast China and North China. The annual number of RRP over the east of 95E in China and its subareas demonstrates a periodic variation of 2-4a, and also shows a periodic variation of 6-10a in the Yangtze-Huaihe River valley and South China and eastern part of Northwest China, while a 13-17a oscillation can be found in North China.(3) On the whole, the occurrence frequency of RRP to the east of 95E in China is the most in summer (especially in July), the least in winter, and higher in spring than in autumn. The months when RRP occur most frequently are June and July in the Yangtze-Huaihe River valley and eastern part of Southwest China, and May and June in South China. RRP mainly appear in July and August in other subareas.(4) The distribution patterns of RRP to the east of 95E in China are divided into 7 types. The heavy precipitation areas for pattern Ⅰ-Ⅳ migrate northward step by step from South China and southern part of Yangtze River valley to Huanghuai Basin and eastern part of Sichuan Basin.The heavy precipitation areas of pattern Ⅴ-Ⅶ all are located at the Coastal region of Southeast China.

Keywords: Regional rainstorm processes, Method for distinguishing, Temporal and spatial distribution, Patterns of extremely regional rainstorm processes

©2019. Japan Geoscience Union. All Right Reserved.

Near-real-time SCALE-LETKF forecasts of the record breaking rainfall in Japan in July 2018

*Takumi Honda[1], Guo-Yuan Lien[2,1], Takemasa Miyoshi[1]

1. RIKEN Center for Computational Science, 2. Central Weather Bureau

In July 2018, a stationary precipitation band associated with the Baiu front induced a record breaking rainfall and caused catastrophic destruction in Japan. This event was successfully captured by the near-real-time (NRT) SCALE-LETKF system (Lien et al. 2017) consisting of the Scalable Computing for Advanced Library and Environment-Regional Model (SCALE-RM, Nishizawa et al. 2015; Sato et al. 2015) and the Local Ensemble Transform Kalman Filter (LETKF, Hunt et al. 2007; Miyoshi and Yamane 2007). This system has been continuously operated since 2015 with an 18-km mesh model domain and the ensemble size of 50. In the NRT SCALE-LETKF system, only conventional observations are assimilated every 6 hours. By conducting a series of 50-member ensemble forecasts from the 6-hourly SCALE-LETKF analyses, this study aims to investigate predictability of this torrential rainfall event and important factors that contributed to the heavy precipitation. In general, the NRT SCALE-LETKF system provides skillful ensemble forecasts of the rainfall a few days in advance. Interestingly, the forecast skill exhibits sudden improvement due to assimilating conventional observations at a single location far southwest from the peak accumulated rainfall location. Forecast differences and ensemble correlations suggest that an extratropical cyclone over the Sea of Japan and a low-level trough near Taiwan play important roles in determining the front location.

Keywords: Data assimilation, Numerical Weather Prediction

©2019. Japan Geoscience Union. All Right Reserved.

An objective Frontal Analysis Techniques and Application in Model Verification

*Couhua Liu[1]

1. National Meteorology Centre of China Meteorological Administration

This paper presents an objective Frontal analysis method based on pressure field for east Asia. Comparing to methods based on thermo-dynamical elements such as temperature, the method developed in this paper can avoid the complex affection from sea-land and landform. The method will be used to identification of fronts in analysis and prediction of ECMWF model all over 2015, and then model error of predicted fronts will be verification. The verification result show that, comparing to analysis field, the moving speed of fronts in prediction field of ECMWF model is slower and strength is weaker.

Keywords: front, model, verification

©2019. Japan Geoscience Union. All Right Reserved.

Assimilating every 30-second phased array weather radar data in a torrential rainfall event on July 6, 2018 around Kobe city

*Yasumitsu Maejima[1], Shigenori Otsuka[1], Takemasa Miyoshi[1,2]

1. RIKEN Center for Computational Science, 2. University of Maryland, College Park

To investigate the impact of every 30-second phased array weather radar (PAWR; Yoshikawa et al. 2013, Ushio et al. 2014) observation on a simulation of a severe rainfall event occurred on July 6, 2018 around Kobe city, we perform 30-second-update 100-m-mesh data assimilation (DA) experiments using the Local Ensemble Transform Kalman Filter with the Scalable Computing for Advanced Library and Environment regional numerical weather prediction model. Two experiments were performed: the test experiment with every 30-second PAWR observation (TEST), and the other without observation (NO-DA).

The TEST analysis shows intense rainfalls with detailed structure of active convection, better matching with the PAWR observation compared to NO-DA analysis. In the forecast experiment, the forecast initialized by the ensemble mean analysis of TEST is skillful for 20 minutes compared with NO-DA, although the skill is decreased rapidly. The results suggest that the PAWR DA have a potential to improve the numerical simulation for this torrential rainfall event.

Keywords: Data assimilation, Heavy rainfall forecast, High performance computing

©2019. Japan Geoscience Union. All Right Reserved.

The impact of range sidelobes from phased array weather radar observations to short-range convective forecasts

*James David Taylor[1], Guo-Yuan Lien[1], Shinsuke Satoh[2], Takemasa Miyoshi[1]

1. RIKEN Research center for computational science, 2. NICT National Institute of Information and Communications Technology

Range sidelobes are an erroneous feature of radar observations that are generated by the pulse compression process used to improve the range resolution of target echoes in high resolution radar systems. Phased array weather radar (PAWR) is an advanced radar system providing very dense observations of reflectivity and Doppler radial velocity at 100m range resolution for over 100 elevation angles every 30 seconds. The use of pulse compression in PAWR to provide very high range resolution data makes it subject to these types of errors, which can result in false echoes observed at other ranges.

In this study we investigate the impact of assimilating range sidelobes from PAWR observations to short-range convective forecasts. This happens frequently in the current QC algorithm, although we plan to improve the QC in the future. We employ the use of the SCALE-LETKF system which couples the Local Ensemble Transform Kalman Filter (LETKF) with the Scalable Computing for Advanced Library and Environment (SCALE)-RM model. We focus on a convective rainfall event in August 2016 that brought heavy, intense rainfall over Osaka. PAWRs located in Suita, Osaka and in Kobe well-captured the convective system over its life cycle but featured prominent range sidelobes as part of their observations. Here, observations from both radars are first used to identify the range sidelobes before performing a series of 30-second update cycling experiments using observations from the Suita PAWR both with and without range sidelobes within a high-resolution 100-m mesh. As well as investigating their impact on short-range forecasts, we aim to show how we can further the usefulness of having two sets of PAWR observations to observe the same convective system by using them to identify and remove range sidelobes and improve short-range forecasts of severe convective events through the assimilation of this data.

Keywords: LETKF, Assimilation, Forecasts, Convection, Sidelobes

©2019. Japan Geoscience Union. All Right Reserved.

Development of Hydro-debris 2D model for larger area

*Yosuke Alexandre Yamashiki[1], Tsutao OIZUMI[2], Bruno Ribeiro[1], Ryusuke Kuroki[1]

1. Earth & Planetary Water Resources Assessment Laboratory Graduate School of Advanced Integrated Studies in Human Survivability Kyoto University, 2. Japan Association of Marine-Earth Science and Tecnology

The Hydro-debris 2D model has been developed and applied for both larger and limited zones in the Hiroshima debris-flow disasters that occurred both in 2014 & 2018. The model application for hindcast for wider and limited areas with the same scheme is tested in order to obtain better and precise hindcast as well as a future forecast of rainfall-induced debris flow disasters by improving the geological classification module for the initiation of the debris flow. A universal algorithm for predicting the debris flow disasters solely by the initial geological boundary conditions and forecasted rainfall distribution may contribute to improving early warnings in this field.

Keywords: Debris flow, Hindcast

©2019. Japan Geoscience Union. All Right Reserved.

Research on the application of an improved terrain-following vertical coordinates on GRAPES model

*chao li[1]

1. NWPC.CMA

Errors caused by topographic feathers of the coordinate planes can be reduced with the Smoothed-level terrain-following coordinate(T-F coordinate for short). On higher layors,coordinate planes of T-F coordinate based on trigonometric function of cos (COS coordinate for short)are horizontal with almost none errors. However,on the lower layers,thickness between planes is too small to keep the model stability.At the same time,it will bring larger calculating errors which result in bad performance of the model.Considering all above,an improved COS coordinate is designed to average the thickness of COS coordinate planes.
Ideal and real case tests are conducted with the GRAPES_Meso model using the improved COS coordinate.The results of the tests indicate that:compared with the COS coordinate, the improved COS coordinate ,on one hand ,keep the planes horizontal on the higher layers ,on the other hand, lead the distribute of the coordinate planes more uniformity , which greatly reduced the errors on the lower layers;The coordinate can reproduce in general the mountain induced gravity waves in comparison to the analytic solution. However, the shapes,vertical structures and intensity of the waves are better simulated by the improved COS coordinate, in the lower levels where the COS coordinate didn’ t behave so better. In the one-month real case tests, the improved COS coordinate gives the better results in terms of smaller forecast bias and root mean square error, and higher anomaly correlation coefficients than the COS coordinate. In conclusion, the improved COS coordinate solves the calculation problems of the COS coordinate ,and improves the prediction ability.

Keywords: GRAPES Model, Terrain-following coordinate, Dynamic Core, Numerical Modelling

©2019. Japan Geoscience Union. All Right Reserved.

Development of a parallel spherical harmonic transform library: design and performance

*Fuyuki SAITO[1]

1. Japan Agency for Marine-Earth Science and Technology

The spherical harmonic transform (SHT) is a typical method to describe the dynamical core in climate models (e.g. MIROC). SHT is a combination of two transformation: a Fourier transformation in longitude and an associate Legendre transformation in latitude. Therefore, a simple way to introduce SHT in parallel computing is to apply domain decomposition in latitudes only, involving a relocation in latitudes before/after the Legendre transformation. However, the number of maximum processors is limited by the size of latitude dimension, which is an obstacle to more efficient computing. Recently the `physics' routines in a climate model have become more and more complex and expensive, thus the heavy computation significantly suffers from the limitation. A new (yet-another) library, Flageolet, has been developed to help parallel processing of SHT in particular for climate models like MIROC, to support more flexible domain decomposition, following the approach adopted in several 3D FFT libraries and also some climate models. As a continuation of last-year's presentation, which reports the design and performance of FFT part, those of SHT part as well as transposition part between FFT and ALT are reported in this study for various sizes of domain around T213 etc, examined on the Earth simulator.

Keywords: spherical harmonic transform

©2019. Japan Geoscience Union. All Right Reserved.

Global data assimilation of multi-species satellite measurements for atmospheric chemistry analysis

*Takashi Sekiya[1], Kazuyuki Miyazaki[2,1], Koji Ogochi[1], Kengo Sudo[3,1], Masayuki Takigawa[1]

1. Japan Agency for Marine-Earth Science and Technology, 2. Jet Propulsion Laboratory/California Institute for Technology, 3. Graduate School of Environmental Studies, Nagoya University

Information on tropospheric ozone and its precursors are important for human health, ecosystem, and climate studies. The combined use of satellite measurements of ozone and its precursors has great potential to provide comprehensive information on the tropospheric chemistry system on various spatial scales. In this study, we present the results of global data assimilation of multi-species measurements (O_3, NO_2, CO, HNO_3, and SO_2) from multi-satellite sensors (OMI, GOME-2, SCIAMACHY, MOPITT, TES, and MLS) using the ensemble Kalman filter approach (Miyazaki et al., 2015). We demonstrated that increasing horizontal resolution from 2.8 to 0.56 degree is necessary for capturing high concentrations of NO_2 in the megacities, whereas 1.1-degree resolution is more suitable for optimizing tropospheric chemistry system on regional and global scales considering the current computational resources (computational cost was larger by a factor of 10 at 0.56-dgree resolution than at 1.1-degree resolution). Using the data assimilation system at 1.1-degree resolution, we constructed an updated version of tropospheric chemistry reanalysis (TCR-2; Miyazaki et al., in prep.) data for 2005—2017, which provide valuable information on decadal changes in air pollutant concentrations and emissions. The estimated NO_x emissions were strongly increased from 2005 to 2011 (+37%/decade) and decreased from 2011 to 2017 (-37%/decade) in China, while the emissions exhibited decreasing trends in Europe (-11%/decade) and the United States (-27%/decade) and an increasing trend in India (+23%/decade) during 2005—2017. A post peta-scale supercomputer such as post-K computer will facilitate the data assimilation calculation to produce tropospheric chemistry reanalysis data at 0.56-degree resolution for air pollutions on a megacity scale globally in a consistent way, which will benefit future study of atmospheric environment on various spatial scales.

Keywords: Data assimilation, Atmospheric chemistry, Atmospheric environment

©2019. Japan Geoscience Union. All Right Reserved.

The sensitivity to WRF shortwave radiation parameterizations in prediction of global horizontal irradiance for investigating interactions of atmosphere with croplands

*Ankur Srivastava[1], Sarita Kumari[1], Rajkumar Dhakar[2]

1. Indian Institute of Technology Delhi, 2. Indian Agriculture Research Institute

The present study intends to evaluate the Advanced Research Weather Research Forecating (ARW) model performance in representing the observed global horizontal irradiance (GHI) measurements while using different shortwave radiation (SWR) parameterization schemes. Two cases are considered, first case is ‘clear sky condition’ which includes model simulation of a clear/ cloudless day and second case is ‘all sky condition’ which includes model simulations of a cloudy and a rainy day. The above two cases are formulated on the basis that amount of incoming SWR will be different in each case owing to the differences in atmospheric conditions.
For the mentioned instances dates of 23rd February, 9th January and 12th March of 2016, which are clear, cloudy and rainy days respectively, are chosen for WRF model simulation. The shortwave radiation schemes that were evaluated are: Dudhia, Community Atmosphere Model (CAM), the updated Rapid Radiative Transfer Model (RRTMG), the updated Goddard and the
Goddard Fluid Dynamics Laboratory (GFDL) schemes. The model generated predictions are verified against the GHI measurements at weather station of Indian Agriculture Research Institute (IARI), New Delhi.
All schemes perform better under ‘clear sky condition’ i.e. for clear/cloudless day. For both the cases Dudhia scheme performs best with Mean Bias (MB) of 62.84 Wm^{-2} for clear day, 86.44 Wm^{-2} for cloudy day and 89.44 Wm^{-2} for rainy day. All-inclusive, the model derived predictions are over estimated in all the schemes.

Keywords: global horizontal irradiance , parameterization, shortwave radiation

©2019. Japan Geoscience Union. All Right Reserved.

The development of an atmospheric aerosol/chemistry–climate model, BCC_AGCM_CUACE2.0, and simulated effective radiative forcing of nitrate aerosols

*QI AN[1,2,4], Hua Zhang[2], Zhili Wang[2], Yi Liu[1,4], Bing Xie[3], Qianxia Liu[3], Zaizhi Wang[3], Sunling Gong[2]

1. LAGEO, IAP, CAS, 2. LaSW, CAMS, 3. NCC,CMA, 4. UCAS

As important components of total anthropogenic aerosols, nitrate aerosols have large impacts on aerosol radiative forcing and climate at regional and seasonal scales, but few current climate models coupled nitrate chemical modules online. This study developed a next-generation atmospheric aerosol/chemistry–climate model, the BCC_AGCM_CUACE2.0. Then, the performance of the model for nitrate was evaluated, and the direct radiative forcing (DRF) and effective radiative forcing (ERF) due to nitrate were simulated for the present day (2010), near future (2030) and middle future (2050) under the Representative Concentration Pathway (RCP) 4.5, 6.0, and 8.5 scenarios relative to the pre-industrial era (1850). The model reproduced the distributions and seasonal changes in nitrate loading well and simulated surface concentrations matched observations in Europe and North America. Current global mean annual loading of nitrates was predicted to increase by 1.12 mg m^{-2} relative to 1850, with the largest increases occurring in East Asia (3.89 mg m^{-2}), Europe (3.6 mg m^{-2}), and South Asia (1.86 mg m^{-2}). The current global mean annual ERF of nitrates was −0.21 W m^{-2} relative to 1850. Due to global reductions in pollutant emissions, the nitrate ERF values were predicted to decrease to −0.17 and −0.20 W m^{-2} in 2030, −0.07 and −0.18 W m^{-2} in 2050 for RCP4.5 and 6.0 relative to 1850, respectively. Under RCP8.5, nitrate ERF values were −0.24 and −0.19 W m^{-2} in 2030 and 2050, respectively. Although global mean nitrate values showed a declining trend, future nitrate loading remained high in East Asia and South Asia.

Keywords: Effective radiative forcing, Nitrate

©2019. Japan Geoscience Union. All Right Reserved.

Impacts of different types and intensities of El Niño events on winter aerosols over China

*Xiaochao Yu[1,2], Zhili Wang[2,1], Hua Zhang[2], Shuyun Zhao[3]

1. Collaborative Innovation Center on Forecast and Evaluation of Meteorological Disasters, Nanjing University of Information Science and Technology, Nanjing, 210044, China, 2. State Key Laboratory of Severe Weather and Key Laboratory of Atmospheric Chemistry of CMA, Chinese Academy of Meteorological Sciences, Beijing, 100081, China., 3. National Climate Center, China Meteorological Administration, Beijing, 100081, China

El Niño is a strong signal of interannual climate variability. The occurrence of an El Niño event may have an important impact on atmospheric pollutant concentrations in China through changes to the regional climate. This study quantitatively examines the differences among the effects of different types and intensities of El Niño events on winter mean aerosol concentration and severe haze days in China. It is found that Central Pacific (CP) El Niño events lead to larger increases in the aerosol burden over southern China relative to the same intensity of Eastern Pacific (EP) events. For El Niño events of the same type but with different intensities, moderate events induce large increases in surface aerosol concentrations over the entire eastern China, while strong and weak events lead to obvious decreases in the surface aerosol concentration over northern China. These differences are mainly attributed to changes in atmospheric circulation, with the resulting changes in aerosol mass transport occurring in response to the different types of El Niño event. Except for moderate CP events, all kinds of El Niño events lead to an increase in severe haze days in winter over northern China. Strong and weak EP El Niño events and weak CP El Niño events lead to an increase in severe haze days in winter over southern China. A change in the south-north transport of aerosols caused by El Niño events also play a dominate role in changing the occurrence of winter haze days in China.

Keywords: Eastern Pacific El Niño, Central Pacific El Niño, aerosol concentration, severe haze day

©2019. Japan Geoscience Union. All Right Reserved.

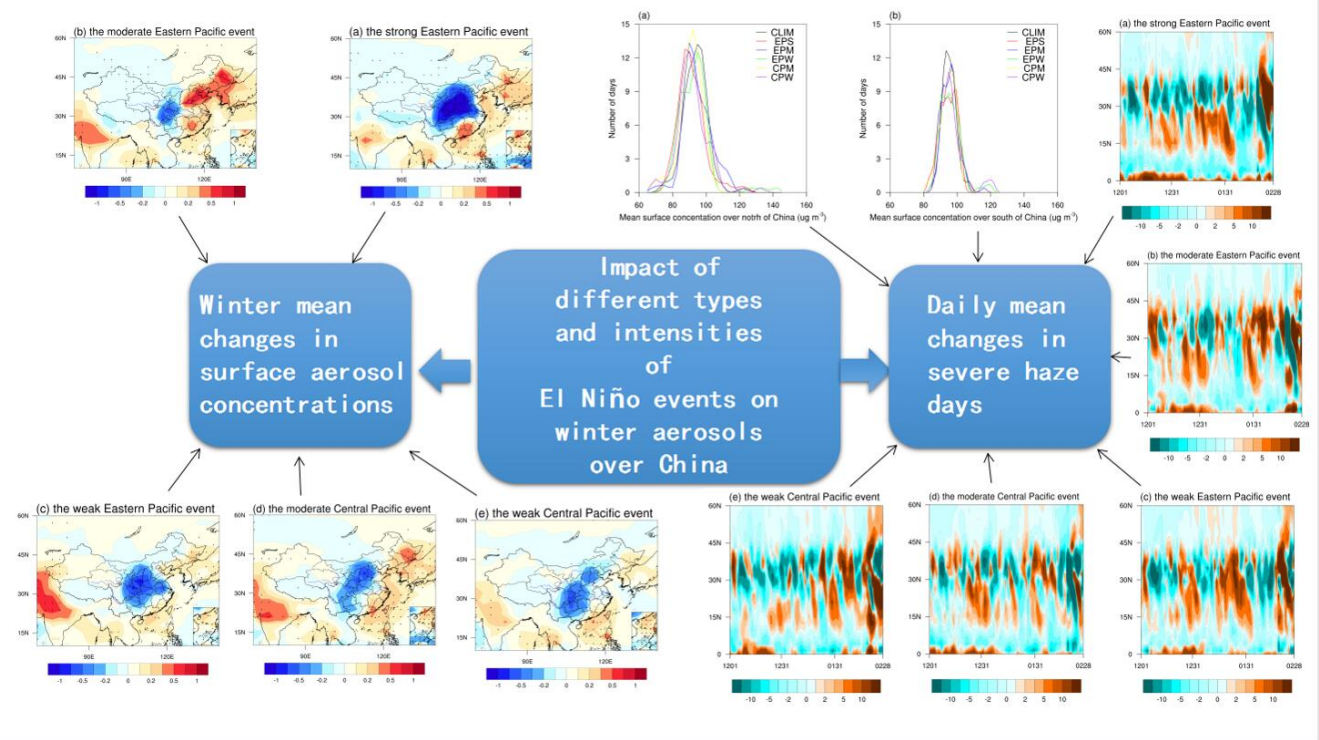

©2019. Japan Geoscience Union. All Right Reserved.

High Cloud Annual Variation and Its Responses to Global Warming in the NICAM AMIP Experiment

*Ying-Wen Chen[1], Masaki Satoh[1,2], Chihiro Kodama[2], Akira Noda[2], Yohei Yamada[2]

1. Atmospheric and Ocean Research Institute, The University of Tokyo , 2. Japan Agency for Marine-Earth Science and Technology

Uncertainties in climate sensitivity mainly come from the ambiguities in simulations of both high- and low-level clouds. The previous studies using NICAM’s short time simulation showed that the both the altitudes and amount of high clouds increase under the global warming condition, while other climate models show high cloud amount contrarily decreases.
Due to the progress in computer performance, long term climate simulation with $x < 20$ km becomes available. A pair of 25-year climate simulation (present and warming climate) with 14-km horizontal resolution (NICAM AMIP-like simulation, Kodama et al. 2015) has been performed by K computer. In this study, we analyze how the annual variation in high clouds is presented in the NICAM AMIP-like simulation. Satellite and in-situ data are used to investigate whether NICAM captures the observed responses of high clouds to the mean sea surface temperature (SST). Regressions between the high cloud amount variation and the SST variation is different with altitudes; positive regressions appear at altitudes above 100 hPa while negative regressions are found in altitudes below 100 hPa. The results are consistent with previous study based on observations (Zelinka and Hartmann 2011). Further analysis showed that the spatial pattern of high clouds is mainly associated with the El Nino response; as SST warmer, the high clouds shift in the eastern Pacific with higher. The increase of high clouds is associated with the increase of ice water content of cloud ice and snow. We argue that the response of high clouds to global warming is also explained by the change in the spatial distribution of the high clouds.

Keywords: Global Warming, Cloud-Resolving Model

©2019. Japan Geoscience Union. All Right Reserved.

Improvements in Simulating the Relationship between ENSO and East Asian Summer Rainfall in the CMIP5 Models

*Yuanhai FU[1], Riyu Lu[1]

1. IAP, CAS

There is a significant relationship between the preceding winter El Niño–Southern Oscillation (ENSO) and the subsequent East Asian summer rainfall (EASR), and this relationship is helpful for seasonal forecasting in East Asia. This study investigated the relationship between the preceding winter ENSO and EASR in the Coupled Model Intercomparison Project Phase 5 (CMIP5) models and compared the results with those from the CMIP3 models. In general, the CMIP5 models capture the ENSO–EASR relationship more realistically than the CMIP3 models. For instance, approximately two-thirds of the CMIP5 models capture the ENSO–EASR relationship, while less than one-third of the CMIP3 models capture the relationship. Further investigation suggests that the improvement could be attributed to simulating the physical processes of ENSO's impact on the EASR more realistically in the CMIP5 models, particularly the effect of ENSO on tropical Indian Ocean SST and the effect of Indian Ocean SST anomalies on the atmospheric convection over the Philippine Sea. However, there is large diversity in the ENSO–EASR relationship in the CMIP5 models, and most of the models underestimate the relationship. This underestimation comes from the underestimation of the physical processes, particularly from the underestimated impact of the atmospheric convection over the Philippine Sea on the EASR. The CMIP5 models that capture the ENSO–EASR relationship well/bad also show high/low skill in representing the physical processes.

Keywords: East Asian summer rainfall, ENSO, CMIP5 model

©2019. Japan Geoscience Union. All Right Reserved.

[E] Poster | A (Atmospheric and Hydrospheric Sciences)：A-AS Atmospheric Sciences, Meteorology & Atmospheric Environment

Wed. May 29, 2019 5:15 PM - 6:30 PM JST | Wed. May 29, 2019 8:15 AM - 9:30 AM UTC | Poster Hall International Exhibition Hall8, Makuhari Messe_9

[A-AS01] High performance computing for next generation weather, climate, and environmental sc iences

convener:Hiromu Seko(Meteorological Research Institute), Takemasa Miyoshi(RIKEN), Chihiro Kodama(Japan Agency for Marine-Earth Science and Technology), Masayuki Takigawa(Japan Agency for Marine-Earth Science and Technology)

A lot of advanced simulation studies are being conducted by high performance supercomputers, such as K computer and Earth Simulator, in various fields including meteorology. The high performance supercomputers enable us to conduct numerical simulations and data assimilation of observation big-data (huge high-density and high-frequency data) with an order of magnitude higher resolutions and ensemble numbers than those with the previous supercomputers. In addition, the post-K computer will be available as a successor of K, and studies for the post-K computer are in progress. At this session, we comprehensively pick up the topics in the Atmospheric and Hydrospheric Sciences Sessions of the 2019 Union Meeting that comprise the atmospheric, oceanic and land sciences. This session aims to promote recent studies related to the issues on high performance computing in weather, climate, and environmental studies using the K computer and other supercomputers, and to enhance discussions on future directions of numerical simulations in meteorology.

[AAS01-P01] **Categorized correction forecast for accumulative precipitation of heavy rainfall processes based on optimal probability (OPPF) in medium-extended-range forecast time**

*Ruoyun Niu[1] (1.National Meteorological Center)

[AAS01-P02] **Characteristics of temporal and spatial distribution of regional rainstorm processes to the east of 95°E in China during 1981-2015**

*Ruoyun Niu[1], Couhua Liu[1] (1.National Meteorological Center)

[AAS01-P03] Near-real-time SCALE-LETKF forecasts of the record breaking rainfall in Japan in July 2018

*Takumi Honda[1], Guo-Yuan Lien[2,1], Takemasa Miyoshi[1] (1.RIKEN Center for Computational Science, 2.Central Weather Bureau)

[AAS01-P04] An objective Frontal Analysis Techniques and Application in Model Verification

*couhua liu[1] (1.National Meteorology Centre of China Meteorological Administration)

[AAS01-P05] Assimilating every 30-second phased array weather radar data in a torrential rainfall event on July 6, 2018 around Kobe city

*Yasumitsu Maejima[1], Shigenori Otsuka[1], Takemasa Miyoshi[1,2] (1.RIKEN Center for Computational Science, 2.University of Maryland, College Park)

[AAS01-P06] The impact of range sidelobes from phased array weather radar observations to short-range convective forecasts

*James David Taylor[1], Guo-Yuan Lien[1], Shinsuke Satoh[2], Takemasa Miyoshi[1] (1.RIKEN Research center for computational science, 2.NICT National Institute of Information and Communications Technology)

[AAS01-P07] Development of Hydro-debris 2D model for larger area

*Yosuke Alexandre Yamashiki[1], Tsutao OIZUMI[2], Bruno Ribeiro[1], Ryusuke Kuroki[1] (1.Earth & Planetary Water Resources Assessment Laboratory Graduate School of Advanced Integrated Studies in Human Survivability Kyoto University, 2.Japan Association of Marine-Earth Science and Tecnology)

[AAS01-P08] **Research on the application of an improved terrain-following vertical coordinates on GRAPES model**

*chao li[1] (1.NWPC.CMA)

[AAS01-P09] Development of a parallel spherical harmonic transform library: design and performance

*Fuyuki SAITO[1] (1.Japan Agency for Marine-Earth Science and Technology)

[AAS01-P10] Global data assimilation of multi-species satellite measurements for atmospheric chemistry analysis

*Takashi Sekiya[1], Kazuyuki Miyazaki[2,1], Koji Ogochi[1], Kengo Sudo[3,1], Masayuki Takigawa[1] (1.Japan Agency for Marine-Earth Science and Technology, 2.Jet Propulsion Laboratory/California Institute for Technology, 3.Graduate School of Environmental Studies, Nagoya University)

[AAS01-P11] The sensitivity to WRF shortwave radiation parameterizations in prediction of global horizontal irradiance for investigating interactions of atmosphere with croplands

*Ankur Srivastava[1], Sarita Kumari[1], Rajkumar Dhakar[2] (1.Indian Institute of Technology Delhi, 2.Indian Agriculture Research Institute)

[AAS01-P12] The development of an atmospheric aerosol/chemistry–climate model, BCC_AGCM_CUACE2.0, and simulated effective radiative forcing of nitrate aerosols

*QI AN[1,2,4], Hua Zhang[2], Zhili Wang[2], Yi Liu[1,4], Bing Xie[3], Qianxia Liu[3], Zaizhi Wang[3], Sunling Gong[2] (1.LAGEO, IAP, CAS, 2.LaSW, CAMS, 3.NCC,CMA, 4.UCAS)

[AAS01-P13] **Impacts of different types and intensities of El Niño events on winter aerosols over China**

*Xiaochao Yu[1,2], Zhili Wang[2,1], Hua Zhang[2], Shuyun Zhao[3] (1.Collaborative Innovation Center on Forecast and Evaluation of Meteorological Disasters, Nanjing University of Information Science and Technology, Nanjing, 210044, China, 2.State Key Laboratory of Severe Weather and Key Laboratory of Atmospheric Chemistry of CMA, Chinese Academy of Meteorological Sciences, Beijing, 100081, China., 3.National Climate Center, China Meteorological Administration, Beijing, 100081, China)

[AAS01-P14] High Cloud Annual Variation and Its Responses to Global Warming in the NICAM AMIP Experiment

*Ying-Wen Chen[1], Masaki Satoh[1,2], Chihiro Kodama[2], Akira Noda[2], Yohei Yamada[2] (1.Atmospheric and Ocean Research Institute, The University of Tokyo , 2.Japan Agency for Marine-Earth Science and Technology)

[AAS01-P15] Improvements in Simulating the Relationship between ENSO and East Asian Summer Rainfall in the CMIP5 Models

*Yuanhai FU[1], Riyu Lu[1] (1.IAP, CAS)

Categorized correction forecast for accumulative precipitation of heavy rainfall processes based on optimal probability (OPPF) in medium-extended-range forecast time

*Ruoyun Niu[1]

1. National Meteorological Center

By taking the ensemble prediction data from ECMWF and the intensive observations of precipitation in China, the technology of categorized correction forecast for accumulative precipitation of heavy rainfall processes based on optimal probability(OPPF) is developed, and 3 calculation schemes of OPPF are designed according to overall technical route. Then the reforecast test are carried for the accumulative precipitation of 67 heavy rainfall processes from May to September during 1981 to 2015 in China, and the forecast performance of the 3 OPPFs against that of ensemble mean (EMPF) and control number (CTPF) is evaluated and contrasted. The results show that:(1) In the medium-extended-range (096-360h) forecast time, the performance of the 3 OPPFs are better than that of EMPF and CTPF for heavy precipitation forecast and clear-rain forecast. the performance of OPPF1 and OPPF2 is close to that of EMPF for Moderate precipitation and larger precipitation. OPPF3 produces the best performance among the 3 OPPFs. (2) There are obvious regional differences in forecast performances. TS of OPPF3 in southern China are higher than in northern China, and the performance of OPPF3 for heavy precipitation is better than that of EMPF in southern China. During 096-240h forecast time, the performance of OPPF3 for heavy precipitation is also better than that of EMPF in eastern part of Northeast China.

Keywords: optimal probability, accumulative precipitation of heavy precipitation processes, categorized correction forecast, comparative evaluation of forecast performance

©2019. Japan Geoscience Union. All Right Reserved.

Characteristics of temporal and spatial distribution of regional rainstorm processes to the east of 95ºE in China during 1981-2015

*Ruoyun Niu[1], Couhua Liu[1]

1. National Meteorological Center

The events of the regional rainstorm processes (RRP) to the east of 95ºE in China over 1981-2015 are constructed based on intensive daily observations of precipitation in China and NCEP/NCAR reanalysis data by means of subjective and objective analyses. Temporal and spatial characteristic distribution of RRP in China are further investigated using the methods of wavelet power spectrum, nine-point binomial smoothing and Ward cluster analysis. The main conclusions are as follows. (1) The annual average number of RRP to the east of 95ºE in China is nearly 30. RRP in the Yangtze-Huaihe River valley occur most frequently among the six subareas with an annual average number of about 19, followed by that in South China and the eastern part of Southwest China with the annual average number of RRP 10.5 and 5.8 times respectively. Annual average number of RRP are only about 1-3 times in other subareas. (2) The inter-annual and inter-decadal variations of the annual number of RRP exhibit distinct fluctuation characteristics. The inter-annual and inter-decadal fluctuating variation in the Yangtze-Huaihe River valley is the most consistent with that to the east of 95E in China. Moreover, the fluctuating variations have a significant positive correlation between South China and eastern part of Southwest China, and also between Northeast China and North China. The annual number of RRP over the east of 95E in China and its subareas demonstrates a periodic variation of 2-4a, and also shows a periodic variation of 6-10a in the Yangtze-Huaihe River valley and South China and eastern part of Northwest China, while a 13-17a oscillation can be found in North China.(3) On the whole, the occurrence frequency of RRP to the east of 95E in China is the most in summer (especially in July), the least in winter, and higher in spring than in autumn. The months when RRP occur most frequently are June and July in the Yangtze-Huaihe River valley and eastern part of Southwest China, and May and June in South China. RRP mainly appear in July and August in other subareas.(4) The distribution patterns of RRP to the east of 95E in China are divided into 7 types. The heavy precipitation areas for pattern Ⅰ-Ⅳ migrate northward step by step from South China and southern part of Yangtze River valley to Huanghuai Basin and eastern part of Sichuan Basin.The heavy precipitation areas of pattern Ⅴ-Ⅶ all are located at the Coastal region of Southeast China.

Keywords: Regional rainstorm processes, Method for distinguishing, Temporal and spatial distribution, Patterns of extremely regional rainstorm processes

©2019. Japan Geoscience Union. All Right Reserved.

Near-real-time SCALE-LETKF forecasts of the record breaking rainfall in Japan in July 2018

*Takumi Honda[1], Guo-Yuan Lien[2,1], Takemasa Miyoshi[1]

1. RIKEN Center for Computational Science, 2. Central Weather Bureau

In July 2018, a stationary precipitation band associated with the Baiu front induced a record breaking rainfall and caused catastrophic destruction in Japan. This event was successfully captured by the near-real-time (NRT) SCALE-LETKF system (Lien et al. 2017) consisting of the Scalable Computing for Advanced Library and Environment-Regional Model (SCALE-RM, Nishizawa et al. 2015; Sato et al. 2015) and the Local Ensemble Transform Kalman Filter (LETKF, Hunt et al. 2007; Miyoshi and Yamane 2007). This system has been continuously operated since 2015 with an 18-km mesh model domain and the ensemble size of 50. In the NRT SCALE-LETKF system, only conventional observations are assimilated every 6 hours. By conducting a series of 50-member ensemble forecasts from the 6-hourly SCALE-LETKF analyses, this study aims to investigate predictability of this torrential rainfall event and important factors that contributed to the heavy precipitation. In general, the NRT SCALE-LETKF system provides skillful ensemble forecasts of the rainfall a few days in advance. Interestingly, the forecast skill exhibits sudden improvement due to assimilating conventional observations at a single location far southwest from the peak accumulated rainfall location. Forecast differences and ensemble correlations suggest that an extratropical cyclone over the Sea of Japan and a low-level trough near Taiwan play important roles in determining the front location.

Keywords: Data assimilation, Numerical Weather Prediction

©2019. Japan Geoscience Union. All Right Reserved.

An objective Frontal Analysis Techniques and Application in Model Verification

*Couhua Liu[1]

1. National Meteorology Centre of China Meteorological Administration

This paper presents an objective Frontal analysis method based on pressure field for east Asia. Comparing to methods based on thermo-dynamical elements such as temperature, the method developed in this paper can avoid the complex affection from sea-land and landform. The method will be used to identification of fronts in analysis and prediction of ECMWF model all over 2015, and then model error of predicted fronts will be verification. The verification result show that, comparing to analysis field, the moving speed of fronts in prediction field of ECMWF model is slower and strength is weaker.

Keywords: front, model, verification

©2019. Japan Geoscience Union. All Right Reserved.

Assimilating every 30-second phased array weather radar data in a torrential rainfall event on July 6, 2018 around Kobe city

*Yasumitsu Maejima[1], Shigenori Otsuka[1], Takemasa Miyoshi[1,2]

1. RIKEN Center for Computational Science, 2. University of Maryland, College Park

To investigate the impact of every 30-second phased array weather radar (PAWR; Yoshikawa et al. 2013, Ushio et al. 2014) observation on a simulation of a severe rainfall event occurred on July 6, 2018 around Kobe city, we perform 30-second-update 100-m-mesh data assimilation (DA) experiments using the Local Ensemble Transform Kalman Filter with the Scalable Computing for Advanced Library and Environment regional numerical weather prediction model. Two experiments were performed: the test experiment with every 30-second PAWR observation (TEST), and the other without observation (NO-DA).

The TEST analysis shows intense rainfalls with detailed structure of active convection, better matching with the PAWR observation compared to NO-DA analysis. In the forecast experiment, the forecast initialized by the ensemble mean analysis of TEST is skillful for 20 minutes compared with NO-DA, although the skill is decreased rapidly. The results suggest that the PAWR DA have a potential to improve the numerical simulation for this torrential rainfall event.

Keywords: Data assimilation, Heavy rainfall forecast, High performance computing

©2019. Japan Geoscience Union. All Right Reserved.

The impact of range sidelobes from phased array weather radar observations to short-range convective forecasts

*James David Taylor[1], Guo-Yuan Lien[1], Shinsuke Satoh[2], Takemasa Miyoshi[1]

1. RIKEN Research center for computational science, 2. NICT National Institute of Information and Communications Technology

Range sidelobes are an erroneous feature of radar observations that are generated by the pulse compression process used to improve the range resolution of target echoes in high resolution radar systems. Phased array weather radar (PAWR) is an advanced radar system providing very dense observations of reflectivity and Doppler radial velocity at 100m range resolution for over 100 elevation angles every 30 seconds. The use of pulse compression in PAWR to provide very high range resolution data makes it subject to these types of errors, which can result in false echoes observed at other ranges.

In this study we investigate the impact of assimilating range sidelobes from PAWR observations to short-range convective forecasts. This happens frequently in the current QC algorithm, although we plan to improve the QC in the future. We employ the use of the SCALE-LETKF system which couples the Local Ensemble Transform Kalman Filter (LETKF) with the Scalable Computing for Advanced Library and Environment (SCALE)-RM model. We focus on a convective rainfall event in August 2016 that brought heavy, intense rainfall over Osaka. PAWRs located in Suita, Osaka and in Kobe well-captured the convective system over its life cycle but featured prominent range sidelobes as part of their observations. Here, observations from both radars are first used to identify the range sidelobes before performing a series of 30-second update cycling experiments using observations from the Suita PAWR both with and without range sidelobes within a high-resolution 100-m mesh. As well as investigating their impact on short-range forecasts, we aim to show how we can further the usefulness of having two sets of PAWR observations to observe the same convective system by using them to identify and remove range sidelobes and improve short-range forecasts of severe convective events through the assimilation of this data.

Keywords: LETKF, Assimilation, Forecasts, Convection, Sidelobes

©2019. Japan Geoscience Union. All Right Reserved.

Development of Hydro-debris 2D model for larger area

*Yosuke Alexandre Yamashiki[1], Tsutao OIZUMI[2], Bruno Ribeiro[1], Ryusuke Kuroki[1]

1. Earth & Planetary Water Resources Assessment Laboratory Graduate School of Advanced Integrated Studies in Human Survivability Kyoto University, 2. Japan Association of Marine-Earth Science and Tecnology

The Hydro-debris 2D model has been developed and applied for both larger and limited zones in the Hiroshima debris-flow disasters that occurred both in 2014 & 2018. The model application for hindcast for wider and limited areas with the same scheme is tested in order to obtain better and precise hindcast as well as a future forecast of rainfall-induced debris flow disasters by improving the geological classification module for the initiation of the debris flow. A universal algorithm for predicting the debris flow disasters solely by the initial geological boundary conditions and forecasted rainfall distribution may contribute to improving early warnings in this field.

Keywords: Debris flow, Hindcast

©2019. Japan Geoscience Union. All Right Reserved.

Research on the application of an improved terrain-following vertical coordinates on GRAPES model

*chao li[1]

1. NWPC.CMA

Errors caused by topographic feathers of the coordinate planes can be reduced with the Smoothed-level terrain-following coordinate(T-F coordinate for short). On higher layors,coordinate planes of T-F coordinate based on trigonometric function of cos (COS coordinate for short)are horizontal with almost none errors. However,on the lower layers,thickness between planes is too small to keep the model stability.At the same time,it will bring larger calculating errors which result in bad performance of the model.Considering all above,an improved COS coordinate is designed to average the thickness of COS coordinate planes.
Ideal and real case tests are conducted with the GRAPES_Meso model using the improved COS coordinate.The results of the tests indicate that:compared with the COS coordinate, the improved COS coordinate ,on one hand ,keep the planes horizontal on the higher layers ,on the other hand, lead the distribute of the coordinate planes more uniformity , which greatly reduced the errors on the lower layers;The coordinate can reproduce in general the mountain induced gravity waves in comparison to the analytic solution. However, the shapes,vertical structures and intensity of the waves are better simulated by the improved COS coordinate, in the lower levels where the COS coordinate didn’ t behave so better. In the one-month real case tests, the improved COS coordinate gives the better results in terms of smaller forecast bias and root mean square error, and higher anomaly correlation coefficients than the COS coordinate. In conclusion, the improved COS coordinate solves the calculation problems of the COS coordinate ,and improves the prediction ability.

Keywords: GRAPES Model, Terrain-following coordinate, Dynamic Core, Numerical Modelling

©2019. Japan Geoscience Union. All Right Reserved.

Development of a parallel spherical harmonic transform library: design and performance

*Fuyuki SAITO[1]

1. Japan Agency for Marine-Earth Science and Technology

The spherical harmonic transform (SHT) is a typical method to describe the dynamical core in climate models (e.g. MIROC). SHT is a combination of two transformation: a Fourier transformation in longitude and an associate Legendre transformation in latitude. Therefore, a simple way to introduce SHT in parallel computing is to apply domain decomposition in latitudes only, involving a relocation in latitudes before/after the Legendre transformation. However, the number of maximum processors is limited by the size of latitude dimension, which is an obstacle to more efficient computing. Recently the `physics' routines in a climate model have become more and more complex and expensive, thus the heavy computation significantly suffers from the limitation. A new (yet-another) library, Flageolet, has been developed to help parallel processing of SHT in particular for climate models like MIROC, to support more flexible domain decomposition, following the approach adopted in several 3D FFT libraries and also some climate models. As a continuation of last-year's presentation, which reports the design and performance of FFT part, those of SHT part as well as transposition part between FFT and ALT are reported in this study for various sizes of domain around T213 etc, examined on the Earth simulator.

Keywords: spherical harmonic transform

©2019. Japan Geoscience Union. All Right Reserved.

Global data assimilation of multi-species satellite measurements for atmospheric chemistry analysis

*Takashi Sekiya[1], Kazuyuki Miyazaki[2,1], Koji Ogochi[1], Kengo Sudo[3,1], Masayuki Takigawa[1]

1. Japan Agency for Marine-Earth Science and Technology, 2. Jet Propulsion Laboratory/California Institute for Technology, 3. Graduate School of Environmental Studies, Nagoya University

Information on tropospheric ozone and its precursors are important for human health, ecosystem, and climate studies. The combined use of satellite measurements of ozone and its precursors has great potential to provide comprehensive information on the tropospheric chemistry system on various spatial scales. In this study, we present the results of global data assimilation of multi-species measurements (O_3, NO_2, CO, HNO_3, and SO_2) from multi-satellite sensors (OMI, GOME-2, SCIAMACHY, MOPITT, TES, and MLS) using the ensemble Kalman filter approach (Miyazaki et al., 2015). We demonstrated that increasing horizontal resolution from 2.8 to 0.56 degree is necessary for capturing high concentrations of NO_2 in the megacities, whereas 1.1-degree resolution is more suitable for optimizing tropospheric chemistry system on regional and global scales considering the current computational resources (computational cost was larger by a factor of 10 at 0.56-dgree resolution than at 1.1-degree resolution). Using the data assimilation system at 1.1-degree resolution, we constructed an updated version of tropospheric chemistry reanalysis (TCR-2; Miyazaki et al., in prep.) data for 2005—2017, which provide valuable information on decadal changes in air pollutant concentrations and emissions. The estimated NO_x emissions were strongly increased from 2005 to 2011 (+37%/decade) and decreased from 2011 to 2017 (-37%/decade) in China, while the emissions exhibited decreasing trends in Europe (-11%/decade) and the United States (-27%/decade) and an increasing trend in India (+23%/decade) during 2005—2017. A post peta-scale supercomputer such as post-K computer will facilitate the data assimilation calculation to produce tropospheric chemistry reanalysis data at 0.56-degree resolution for air pollutions on a megacity scale globally in a consistent way, which will benefit future study of atmospheric environment on various spatial scales.

Keywords: Data assimilation, Atmospheric chemistry, Atmospheric environment

©2019. Japan Geoscience Union. All Right Reserved.

The sensitivity to WRF shortwave radiation parameterizations in prediction of global horizontal irradiance for investigating interactions of atmosphere with croplands

*Ankur Srivastava[1], Sarita Kumari[1], Rajkumar Dhakar[2]

1. Indian Institute of Technology Delhi, 2. Indian Agriculture Research Institute

The present study intends to evaluate the Advanced Research Weather Research Forecating (ARW) model performance in representing the observed global horizontal irradiance (GHI) measurements while using different shortwave radiation (SWR) parameterization schemes. Two cases are considered, first case is ‘clear sky condition’ which includes model simulation of a clear/ cloudless day and second case is ‘all sky condition’ which includes model simulations of a cloudy and a rainy day. The above two cases are formulated on the basis that amount of incoming SWR will be different in each case owing to the differences in atmospheric conditions.
For the mentioned instances dates of 23rd February, 9th January and 12th March of 2016, which are clear, cloudy and rainy days respectively, are chosen for WRF model simulation. The shortwave radiation schemes that were evaluated are: Dudhia, Community Atmosphere Model (CAM), the updated Rapid Radiative Transfer Model (RRTMG), the updated Goddard and the
Goddard Fluid Dynamics Laboratory (GFDL) schemes. The model generated predictions are verified against the GHI measurements at weather station of Indian Agriculture Research Institute (IARI), New Delhi.
All schemes perform better under ‘clear sky condition’ i.e. for clear/cloudless day. For both the cases Dudhia scheme performs best with Mean Bias (MB) of 62.84 Wm^{-2} for clear day, 86.44 Wm^{-2} for cloudy day and 89.44 Wm^{-2} for rainy day. All-inclusive, the model derived predictions are over estimated in all the schemes.

Keywords: global horizontal irradiance , parameterization, shortwave radiation

©2019. Japan Geoscience Union. All Right Reserved.

The development of an atmospheric aerosol/chemistry–climate model, BCC_AGCM_CUACE2.0, and simulated effective radiative forcing of nitrate aerosols

*QI AN[1,2,4], Hua Zhang[2], Zhili Wang[2], Yi Liu[1,4], Bing Xie[3], Qianxia Liu[3], Zaizhi Wang[3], Sunling Gong[2]

1. LAGEO, IAP, CAS, 2. LaSW, CAMS, 3. NCC,CMA, 4. UCAS

As important components of total anthropogenic aerosols, nitrate aerosols have large impacts on aerosol radiative forcing and climate at regional and seasonal scales, but few current climate models coupled nitrate chemical modules online. This study developed a next-generation atmospheric aerosol/chemistry–climate model, the BCC_AGCM_CUACE2.0. Then, the performance of the model for nitrate was evaluated, and the direct radiative forcing (DRF) and effective radiative forcing (ERF) due to nitrate were simulated for the present day (2010), near future (2030) and middle future (2050) under the Representative Concentration Pathway (RCP) 4.5, 6.0, and 8.5 scenarios relative to the pre-industrial era (1850). The model reproduced the distributions and seasonal changes in nitrate loading well and simulated surface concentrations matched observations in Europe and North America. Current global mean annual loading of nitrates was predicted to increase by 1.12 mg m^{-2} relative to 1850, with the largest increases occurring in East Asia (3.89 mg m^{-2}), Europe (3.6 mg m^{-2}), and South Asia (1.86 mg m^{-2}). The current global mean annual ERF of nitrates was −0.21 W m^{-2} relative to 1850. Due to global reductions in pollutant emissions, the nitrate ERF values were predicted to decrease to −0.17 and −0.20 W m^{-2} in 2030, −0.07 and −0.18 W m^{-2} in 2050 for RCP4.5 and 6.0 relative to 1850, respectively. Under RCP8.5, nitrate ERF values were −0.24 and −0.19 W m^{-2} in 2030 and 2050, respectively. Although global mean nitrate values showed a declining trend, future nitrate loading remained high in East Asia and South Asia.

Keywords: Effective radiative forcing, Nitrate

©2019. Japan Geoscience Union. All Right Reserved.

Impacts of different types and intensities of El Niño events on winter aerosols over China

*Xiaochao Yu[1,2], Zhili Wang[2,1], Hua Zhang[2], Shuyun Zhao[3]

1. Collaborative Innovation Center on Forecast and Evaluation of Meteorological Disasters, Nanjing University of Information Science and Technology, Nanjing, 210044, China, 2. State Key Laboratory of Severe Weather and Key Laboratory of Atmospheric Chemistry of CMA, Chinese Academy of Meteorological Sciences, Beijing, 100081, China., 3. National Climate Center, China Meteorological Administration, Beijing, 100081, China

El Niño is a strong signal of interannual climate variability. The occurrence of an El Niño event may have an important impact on atmospheric pollutant concentrations in China through changes to the regional climate. This study quantitatively examines the differences among the effects of different types and intensities of El Niño events on winter mean aerosol concentration and severe haze days in China. It is found that Central Pacific (CP) El Niño events lead to larger increases in the aerosol burden over southern China relative to the same intensity of Eastern Pacific (EP) events. For El Niño events of the same type but with different intensities, moderate events induce large increases in surface aerosol concentrations over the entire eastern China, while strong and weak events lead to obvious decreases in the surface aerosol concentration over northern China. These differences are mainly attributed to changes in atmospheric circulation, with the resulting changes in aerosol mass transport occurring in response to the different types of El Niño event. Except for moderate CP events, all kinds of El Niño events lead to an increase in severe haze days in winter over northern China. Strong and weak EP El Niño events and weak CP El Niño events lead to an increase in severe haze days in winter over southern China. A change in the south-north transport of aerosols caused by El Niño events also play a dominate role in changing the occurrence of winter haze days in China.

Keywords: Eastern Pacific El Niño, Central Pacific El Niño, aerosol concentration, severe haze day

©2019. Japan Geoscience Union. All Right Reserved.

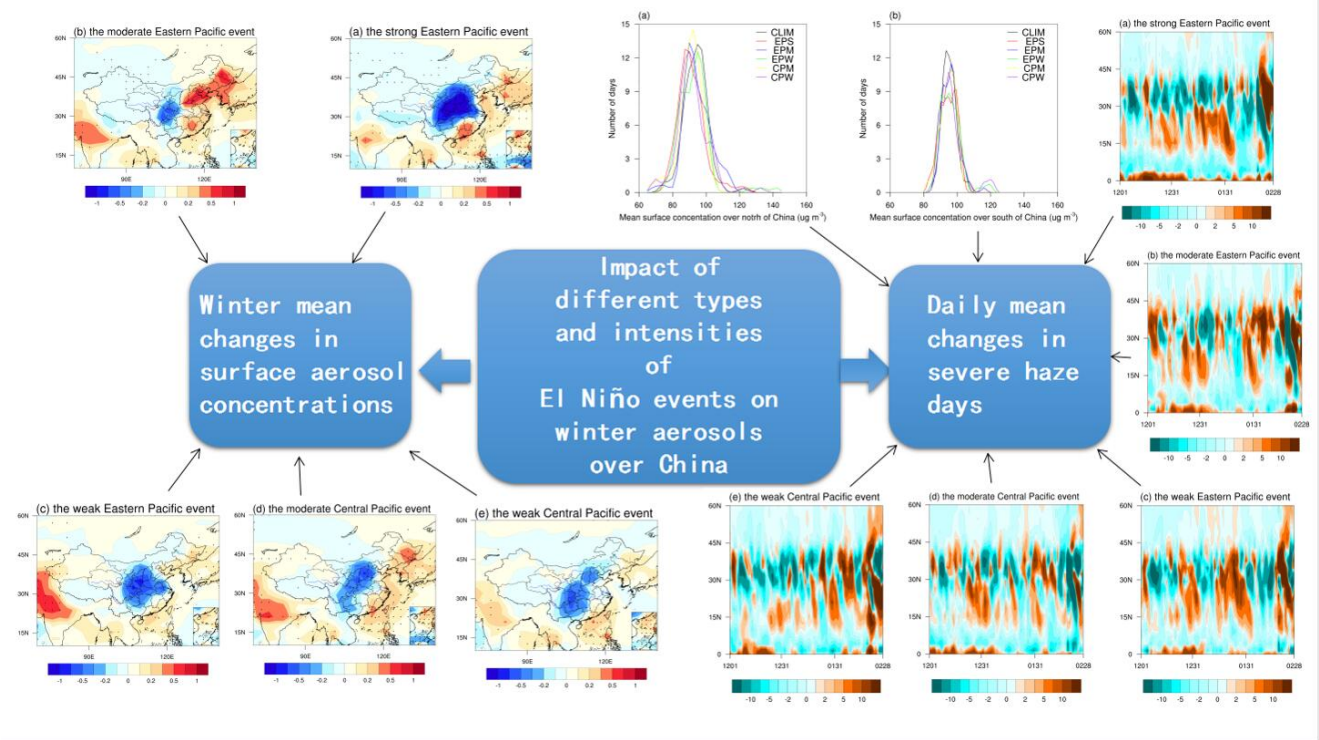

©2019. Japan Geoscience Union. All Right Reserved.

High Cloud Annual Variation and Its Responses to Global Warming in the NICAM AMIP Experiment

*Ying-Wen Chen[1], Masaki Satoh[1,2], Chihiro Kodama[2], Akira Noda[2], Yohei Yamada[2]

1. Atmospheric and Ocean Research Institute, The University of Tokyo , 2. Japan Agency for Marine-Earth Science and Technology

Uncertainties in climate sensitivity mainly come from the ambiguities in simulations of both high- and low-level clouds. The previous studies using NICAM’s short time simulation showed that the both the altitudes and amount of high clouds increase under the global warming condition, while other climate models show high cloud amount contrarily decreases.
Due to the progress in computer performance, long term climate simulation with $x < 20$ km becomes available. A pair of 25-year climate simulation (present and warming climate) with 14-km horizontal resolution (NICAM AMIP-like simulation, Kodama et al. 2015) has been performed by K computer. In this study, we analyze how the annual variation in high clouds is presented in the NICAM AMIP-like simulation. Satellite and in-situ data are used to investigate whether NICAM captures the observed responses of high clouds to the mean sea surface temperature (SST). Regressions between the high cloud amount variation and the SST variation is different with altitudes; positive regressions appear at altitudes above 100 hPa while negative regressions are found in altitudes below 100 hPa. The results are consistent with previous study based on observations (Zelinka and Hartmann 2011). Further analysis showed that the spatial pattern of high clouds is mainly associated with the El Nino response; as SST warmer, the high clouds shift in the eastern Pacific with higher. The increase of high clouds is associated with the increase of ice water content of cloud ice and snow. We argue that the response of high clouds to global warming is also explained by the change in the spatial distribution of the high clouds.

Keywords: Global Warming, Cloud-Resolving Model

©2019. Japan Geoscience Union. All Right Reserved.

Improvements in Simulating the Relationship between ENSO and East Asian Summer Rainfall in the CMIP5 Models

*Yuanhai FU[1], Riyu Lu[1]

1. IAP, CAS

There is a significant relationship between the preceding winter El Niño–Southern Oscillation (ENSO) and the subsequent East Asian summer rainfall (EASR), and this relationship is helpful for seasonal forecasting in East Asia. This study investigated the relationship between the preceding winter ENSO and EASR in the Coupled Model Intercomparison Project Phase 5 (CMIP5) models and compared the results with those from the CMIP3 models. In general, the CMIP5 models capture the ENSO–EASR relationship more realistically than the CMIP3 models. For instance, approximately two-thirds of the CMIP5 models capture the ENSO–EASR relationship, while less than one-third of the CMIP3 models capture the relationship. Further investigation suggests that the improvement could be attributed to simulating the physical processes of ENSO's impact on the EASR more realistically in the CMIP5 models, particularly the effect of ENSO on tropical Indian Ocean SST and the effect of Indian Ocean SST anomalies on the atmospheric convection over the Philippine Sea. However, there is large diversity in the ENSO–EASR relationship in the CMIP5 models, and most of the models underestimate the relationship. This underestimation comes from the underestimation of the physical processes, particularly from the underestimated impact of the atmospheric convection over the Philippine Sea on the EASR. The CMIP5 models that capture the ENSO–EASR relationship well/bad also show high/low skill in representing the physical processes.

Keywords: East Asian summer rainfall, ENSO, CMIP5 model

©2019. Japan Geoscience Union. All Right Reserved.

[E] Poster | A (Atmospheric and Hydrospheric Sciences)：A-OS Ocean Sciences & Ocean Environment

Wed. May 29, 2019 10:45 AM - 12:15 PM JST | Wed. May 29, 2019 1:45 AM - 3:15 AM UTC | Poster Hall International Exhibition Hall8, Makuhari Messe_4

[A-OS08] ECS-Kuroshio and Ryukyu Current System -Observation, modeling and theory-

convener:Hirohiko Nakamura(Kagoshima University, Faculy of Fisheries), Xiao-Hua Zhu(Second Institute of Oceanography)

The East China Sea (ECS) is separated from the North Pacific basin by the Ryukyu Islands. On each side of the Ryukyu Islands, there lies two western boundary currents -the Kuroshio on the northwest and the Ryukyu Current on the southeast. These two currents play an important role in the global substance cycle and have a remarkable impact on the climate and adjacent marginal seas. Our knowledge of the Kuroshio and the Ryukyu Current's dynamics, variability, and impact has advanced significantly over the last decade, because of recent international collaborative field programs, improvement in satellite measurements, and advancement in high-resolution numerical models. This session seeks contributions from ECS-Kuroshio and Ryukyu Current studies and will cover a wide range of topics of observation, modeling and theory. The dynamics of the Kuroshio and the Ryukyu Current's variability at all spatio-temporal scales, the influence of the Kuroshio on typhoons and climate, the interactions among the Kuroshio, Ryukyu Current and eddies, internal waves including near-internal waves and their interactions with background currents, and the water mass exchanges through the gaps between the Ryukyu Islands are welcome to be discussed in this session.

[AOS08-P01] Impact of the mesosacle eddies on the western boundary current over the entire western North Pacific

*Kako Shinichiro[1], Hirohiko Nakamura[2] (1.Graduate School of Science and Engineering, Kagoshima University, 2.Faculty of Fisheries, Kagoshima University)

[AOS08-P02] Glider observations of interleaving layers in the Kuroshio

*Sen Jan[1], Shih-Hong Wang[1], Kai-Chieh Yang[1], Yiing Jang Yang[1], Ming-Huei Chang[1] (1.Institute of Oceanography, National Taiwan Univ.)

[AOS08-P03] Bottom Pressure in the East China Sea -Observation and modeling

*Hua Zheng[1], Xiao-Hua Zhu[1], Hirohiko Nakamura[2], Jae-Hun Park[3], Chanhyung Jeon[4], Ruixiang Zhao[1], Ayako Nishina[2], Chuanzheng Zhang[1], Hanna Na[5], Ze-Nan Zhu[1], Hong Sik Min[6] (1.Second Institute of Oceanography, Ministry of Natural Resources, China, 2.Faculty of Fisheries, Kagoshima University, Kagoshima, Japan, 3.Department of Ocean Sciences, Inha University, Incheon, South Kore, 4.Department of Marine Science and Biological Engineering, Inha University, Incheon, Korea, 5.School of Earth and Environmental Sciences, Seoul National University, Seoul, Korea, 6.Ocean Circulation and Climate Research Center, Korea Institute of Ocean Science and Technology, Busan, Korea)

[AOS08-P04] A numerical study on the dynamics of seasonal velocity variation in the East China Sea

*ZHENLONG ZHANG[1], Nakamura Hirohiko[1], Xiao-Hua Zhu[2] (1.Kagoshima University, 2.Ministry of Natural Resources, CHINA.)

[AOS08-P05] Temporal and spatial velocity variations over the Kuroshio Extension, Kuroshio and Ryukyu Current System in 1982-2014

*YUXIANG QIAO[1], Hirohiko Nakamura[2], AYAKO NISHINA[2] (1.Kagoshima University, Graduate School of Fisheries, 2.Kagoshima University, Faculty of Fishries)

[AOS08-P06] Characteristics of water in the southern Okinawa Trough.

*Ayako Nishina[1], Hirohiko Nakamura[1], Jae-Hun Park[2], Xiao-Hua Zhu[3], Hong Sik Min[4], Hanna Na[5] (1.Kagoshima University, 2.Inha University, 3.Second Institute of Oceanography, 4.Korea Institute of Ocean Science and Technology, 5.Seoul National University)

Impact of the mesosacle eddies on the western boundary current over the entire western North Pacific

*Kako Shinichiro[1], Hirohiko Nakamura[2]

1. Graduate School of Science and Engineering, Kagoshima University, 2. Faculty of Fisheries, Kagoshima University

Although many previous studies have suggested that the mesoscale eddies affect the variations of the Kuroshio and Ryukyu current systems, the generated regions and paths to the western boundary have not been well explained yet. We constructed a mesosacle eddy tracking dataset using FORA-WNP30 in conjunction with Okubo-Weiss parameters to investigate the effects of eddies on the western boundary current over the entire North Pacific. We observed that cyclonic eddies with relatively long durations (>120 days) were mainly generated around the southern Kuroshio Extension region, while anti-cyclonic eddies were generated around the subtropical counter current. In addition, we found that the cyclonic eddies propagate westward along the Kuroshio region and reach the western boundary, while the anti-cyclonic eddies propagate westward from their regions of origin and thereafter reach the Kuroshio recirculation region and Ryukyu current. The comparison of the Ryukyu-current at a depth of 600 m and the number of times the meso-scale eddies passed over the Ryukyu current demonstrated that the weakening (strengthening) of the northward current in the northern part of the Ryukyu region was consistent with the number of times the cyclonic (anti-cyclonic) eddies passed over the northern part of the Ryukyu current.

Keywords: mesoscale eddy, Kuroshio, Ryukyu current

©2019. Japan Geoscience Union. All Right Reserved.

Glider observations of interleaving layers in the Kuroshio

*Sen Jan[1], Shih-Hong Wang[1], Kai-Chieh Yang[1], Yiing Jang Yang[1], Ming-Huei Chang[1]

1. Institute of Oceanography, National Taiwan Univ.

Interleaving layers (or thermohaline intrusions) were sometimes observed by repeated ship-based hydrographic surveys with coarse spacing between adjacent stations in the Kuroshio off Taiwan, but have never been examined in a dynamic context. A Seaglider was navigated along a triangle track east of Taiwan to complete two repeated high-resolution hydrographic observations from December 2016 to March 2017. Prominent interleaving layers were observed between dissimilar intermediate water masses across the Kuroshio. During the observations, a diple eddy pair and a relatively large anticyclonic eddy impinged on the offshore flank of the Kuroshio, respectively, which brought certain impacts on the formation and growth of the interleaving. Aside from the complicated physical processes in the upper 200 m, salinity profiles indicate that interleaving layers appeared within 500 and 800 m with vertical and horizontal length scales of O(50 m) and O(10-100 km), respectively. The time scale for the interleaving layers should be much less than 30 days, inferred from the discrepancy in the interleaving features between the two surveys. The instability analysis together with values of the Turner angle calculated from the hydrographic data suggests that the double-diffusive instability is the primary driving mechanism for the observed interleaving layers.

Keywords: Kuroshio, Interleaving, Double-diffusive instability, Glider observation

©2019. Japan Geoscience Union. All Right Reserved.

Bottom Pressure in the East China Sea -Observation and modeling

*Hua Zheng[1], Xiao-Hua Zhu[1], Hirohiko Nakamura[2], Jae-Hun Park[3], Chanhyung Jeon[4], Ruixiang Zhao[1], Ayako Nishina[2], Chuanzheng Zhang[1], Hanna Na[5], Ze-Nan Zhu[1], Hong Sik Min[6]

1. Second Institute of Oceanography, Ministry of Natural Resources, China, 2. Faculty of Fisheries, Kagoshima University, Kagoshima, Japan, 3. Department of Ocean Sciences, Inha University, Incheon, South Kore, 4. Department of Marine Science and Biological Engineering, Inha University, Incheon, Korea, 5. School of Earth and Environmental Sciences, Seoul National University, Seoul, Korea, 6. Ocean Circulation and Climate Research Center, Korea Institute of Ocean Science and Technology, Busan, Korea

A two-year ocean bottom pressure record acquired between June 2015 and June 2017 observed by two pressure-recording inverted echo sounders (PIESs) and five current and pressure-recording inverted echo sounders (CPIESs) deployed along a section southwest of the Kerama Gap showed a significant 21-day variability. This 21-day bottom pressure variability (P_{bot21}) was particularly strong from July 2016 to January 2017, and it showed a squared coherence of 0.72 with wind stress curl around the Yangtze estuary in the East China Sea (ECS) during this period with a nearly 3-day time lag. A barotropic ocean model demonstrated the generation, spread, and dissipation of P_{bot21}. The modeling results showed that the P_{bot21} was driven by wind stress curl on the continental shelf of the ECS, where depths are shallower than 100 m, and spread southeastward to the Ryukyu Island Chain (RIC). The P_{bot21} was generated and remained on the shallow continental shelf, and only little power spread toward the RIC; thus, whether the signal could be observed by the mooring array was related to where it was generated. Significant P_{bot21} was generated southeast of the Yangtze estuary and measured by the mooring array from July 2016 to January 2017. However, P_{bot21} generated northeast of the Yangtze estuary, far from the mooring section, from January 2016 to April 2016 was exhausted before reaching the mooring array due to the long distance. It is suggested that the spatial pattern of 21-day wind stress curl over the ECS strongly influences P_{bot21} near the RIC.

©2019. Japan Geoscience Union. All Right Reserved.

A numerical study on the dynamics of seasonal velocity variation in the East China Sea

*ZHENLONG ZHANG[1], Nakamura Hirohiko[1], Xiao-Hua Zhu[2]

1. Kagoshima University, 2. Ministry of Natural Resources, CHINA.

In our previous study, we investigated the seasonal velocity variations at different depths over the entire Kuroshio path. It showed that the upper layer (< ~500 m depth) velocity variation over the entire Kuroshio path has a coherent seasonal feature, which reaches a maximum in July and a minimum in autumn or winter, over most of the regions along the Kuroshio path. However, the lower layer velocity (> ~500 m depth, in the continental slope area from the east of Luzon Island to the east of the Ryukyu Island chain) shows a reversed seasonal variation with a maximum in winter. Several numerical experiments were carried out to clarify the essential mechanisms. Although it was shown that the local wind stress upon the current region is a key factor for the seasonal velocity variation in the upper layer, the detailed driving mechanism has been still unknown. Thus, we perform further numerical experiments to clarify the concreate mechanism in this study. Using a rectilinear regional model with idealized continental slope, we have successfully reproduced the seasonal velocity variation of the jet (the Kuroshio) by the seasonal wind stress variation over the jet. It turns out that the velocity of the jet increases (decreases) when the wind stress is directed to downstream (upstream) direction of the jet. We will report the concrete process underlying acceleration and deceleration processes of the upper layer velocity related to the local wind stress.

Keywords: Kuroshio, Seasonal variation

©2019. Japan Geoscience Union. All Right Reserved.

Temporal and spatial velocity variations over the Kuroshio Extension, Kuroshio and Ryukyu Current System in 1982-2014

*YUXIANG QIAO[1], Hirohiko Nakamura[2], AYAKO NISHINA[2]

1. Kagoshima University, Graduate School of Fisheries, 2. Kagoshima University, Faculty of Fishries

Four dimensional variational Ocean ReAnalysis for the Western North Pacific (FORA-WNP30) from 1982 to 2014 is used to investigate temporal and spatial velocity variations over the regions consisting of Kuroshio Extension (KE), Kuroshio and Ryukyu Current System (RCS). In order to identify such temporal and spatial features, we made Hovmöller diagrams at several depths, which display temporal variations of along-stream velocity along the current path from Luzon Island to KE region. In this study, we particularly examine long-term (> 1 year) variations for their regional characteristics (Luzon Island to KE region) and their vertical features (sea surface to 1000 m depth). The results revealed that 1) the KE is dominated by decadal signals while the upstream regions include clearer interannual signals in addition to decadal ones, 2) decadal variations in the KE tends to be almost out of phase to those variations in the upstream regions from Luzon Island to Izu-Ridge, and 3) the velocity variations at the sea surface tend to be similar to those variations at 1000 m depth.

Keywords: Kuroshio, Ryukyu Current, Kuroshio Extension, Velocity, Long-term variations

©2019. Japan Geoscience Union. All Right Reserved.

Characteristics of water in the southern Okinawa Trough.

*Ayako Nishina[1], Hirohiko Nakamura[1], Jae-Hun Park[2], Xiao-Hua Zhu[3], Hong Sik Min[4], Hanna Na[5]

1. Kagoshima University, 2. Inha University, 3. Second Institute of Oceanography, 4. Korea Institute of Ocean Science and Technology, 5. Seoul National University

The Okinawa Trough is a basin within the East China Sea, where maximum depth reaches 2300 m. There are two characteristic water masses in the Okinawa Trough. One is the high salinity water in the sub-surface layer shallower than 300 m and the other is the low salinity water in the intermediate layer from 400 m to 700 m. According to the previous studies, the former water is occupied by the South China Sea Tropical Water (SCSTW) and the Kuroshio Tropical Water (KTW), and the latter is dominated by modified water masses of the North Pacific Intermediate Water (NPIW) and the South China Sea Intermediate Water (SCSIW). However, in the previous studies, the southern part of the Okinawa Trough remains to be observed, and it should be confirmed whether the previous results can apply to the southern part.
In this study, water mass properties in the southern part of the Okinawa Trough are investigated in detail. We mainly used CTD data from T/V Kagoshima-maru cruises in Junes from 2013 to 2018. The high salinity waters in the sub-surface layer were classified into three groups: SCSTW, KTW and the tropical waters in the east of Ryukyu Islands chain. The low salinity water in the intermediate layer had a complicated distribution in which the low salinity water from the east of Taiwan and that from the Kerama Gap.

Keywords: Okinawa Trough, water mass

©2019. Japan Geoscience Union. All Right Reserved.

[E] Poster | A (Atmospheric and Hydrospheric Sciences)：A-OS Ocean Sciences & Ocean Environment

Wed. May 29, 2019 5:15 PM - 6:30 PM JST | Wed. May 29, 2019 8:15 AM - 9:30 AM UTC | Poster Hall International Exhibition Hall8, Makuhari Messe_11

[A-OS08] ECS-Kuroshio and Ryukyu Current System -Observation, modeling and theory-

convener:Hirohiko Nakamura(Kagoshima University, Faculy of Fisheries), Xiao-Hua Zhu(Second Institute of Oceanography)

The East China Sea (ECS) is separated from the North Pacific basin by the Ryukyu Islands. On each side of the Ryukyu Islands, there lies two western boundary currents -the Kuroshio on the northwest and the Ryukyu Current on the southeast. These two currents play an important role in the global substance cycle and have a remarkable impact on the climate and adjacent marginal seas. Our knowledge of the Kuroshio and the Ryukyu Current's dynamics, variability, and impact has advanced significantly over the last decade, because of recent international collaborative field programs, improvement in satellite measurements, and advancement in high-resolution numerical models. This session seeks contributions from ECS-Kuroshio and Ryukyu Current studies and will cover a wide range of topics of observation, modeling and theory. The dynamics of the Kuroshio and the Ryukyu Current's variability at all spatio-temporal scales, the influence of the Kuroshio on typhoons and climate, the interactions among the Kuroshio, Ryukyu Current and eddies, internal waves including near-internal waves and their interactions with background currents, and the water mass exchanges through the gaps between the Ryukyu Islands are welcome to be discussed in this session.

[AOS08-P01] Impact of the mesosacle eddies on the western boundary current over the entire western North Pacific

*Kako Shinichiro[1], Hirohiko Nakamura[2] (1.Graduate School of Science and Engineering, Kagoshima University, 2.Faculty of Fisheries, Kagoshima University)

[AOS08-P02] Glider observations of interleaving layers in the Kuroshio

*Sen Jan[1], Shih-Hong Wang[1], Kai-Chieh Yang[1], Yiing Jang Yang[1], Ming-Huei Chang[1] (1.Institute of Oceanography, National Taiwan Univ.)

[AOS08-P03] Bottom Pressure in the East China Sea -Observation and modeling

*Hua Zheng[1], Xiao-Hua Zhu[1], Hirohiko Nakamura[2], Jae-Hun Park[3], Chanhyung Jeon[4], Ruixiang Zhao[1], Ayako Nishina[2], Chuanzheng Zhang[1], Hanna Na[5], Ze-Nan Zhu[1], Hong Sik Min[6] (1.Second Institute of Oceanography, Ministry of Natural Resources, China, 2.Faculty of Fisheries, Kagoshima University, Kagoshima, Japan, 3.Department of Ocean Sciences, Inha University, Incheon, South Kore, 4.Department of Marine Science and Biological Engineering, Inha University, Incheon, Korea, 5.School of Earth and Environmental Sciences, Seoul National University, Seoul, Korea, 6.Ocean Circulation and Climate Research Center, Korea Institute of Ocean Science and Technology, Busan, Korea)

[AOS08-P04] A numerical study on the dynamics of seasonal velocity variation in the East China Sea

*ZHENLONG ZHANG[1], Nakamura Hirohiko[1], Xiao-Hua Zhu[2] (1.Kagoshima University, 2.Ministry of Natural Resources, CHINA.)

[AOS08-P05] Temporal and spatial velocity variations over the Kuroshio Extension, Kuroshio and Ryukyu Current System in 1982-2014

*YUXIANG QIAO[1], Hirohiko Nakamura[2], AYAKO NISHINA[2] (1.Kagoshima University, Graduate School of Fisheries, 2.Kagoshima University, Faculty of Fishries)

[AOS08-P06] Characteristics of water in the southern Okinawa Trough.

*Ayako Nishina[1], Hirohiko Nakamura[1], Jae-Hun Park[2], Xiao-Hua Zhu[3], Hong Sik Min[4], Hanna Na[5] (1.Kagoshima University, 2.Inha University, 3.Second Institute of Oceanography, 4.Korea Institute of Ocean Science and Technology, 5.Seoul National University)

Impact of the mesosacle eddies on the western boundary current over the entire western North Pacific

*Kako Shinichiro[1], Hirohiko Nakamura[2]

1. Graduate School of Science and Engineering, Kagoshima University, 2. Faculty of Fisheries, Kagoshima University

Although many previous studies have suggested that the mesoscale eddies affect the variations of the Kuroshio and Ryukyu current systems, the generated regions and paths to the western boundary have not been well explained yet. We constructed a mesosacle eddy tracking dataset using FORA-WNP30 in conjunction with Okubo-Weiss parameters to investigate the effects of eddies on the western boundary current over the entire North Pacific. We observed that cyclonic eddies with relatively long durations (>120 days) were mainly generated around the southern Kuroshio Extension region, while anti-cyclonic eddies were generated around the subtropical counter current. In addition, we found that the cyclonic eddies propagate westward along the Kuroshio region and reach the western boundary, while the anti-cyclonic eddies propagate westward from their regions of origin and thereafter reach the Kuroshio recirculation region and Ryukyu current. The comparison of the Ryukyu-current at a depth of 600 m and the number of times the meso-scale eddies passed over the Ryukyu current demonstrated that the weakening (strengthening) of the northward current in the northern part of the Ryukyu region was consistent with the number of times the cyclonic (anti-cyclonic) eddies passed over the northern part of the Ryukyu current.

Keywords: mesoscale eddy, Kuroshio, Ryukyu current

©2019. Japan Geoscience Union. All Right Reserved.

Glider observations of interleaving layers in the Kuroshio

*Sen Jan[1], Shih-Hong Wang[1], Kai-Chieh Yang[1], Yiing Jang Yang[1], Ming-Huei Chang[1]

1. Institute of Oceanography, National Taiwan Univ.

Interleaving layers (or thermohaline intrusions) were sometimes observed by repeated ship-based hydrographic surveys with coarse spacing between adjacent stations in the Kuroshio off Taiwan, but have never been examined in a dynamic context. A Seaglider was navigated along a triangle track east of Taiwan to complete two repeated high-resolution hydrographic observations from December 2016 to March 2017. Prominent interleaving layers were observed between dissimilar intermediate water masses across the Kuroshio. During the observations, a diple eddy pair and a relatively large anticyclonic eddy impinged on the offshore flank of the Kuroshio, respectively, which brought certain impacts on the formation and growth of the interleaving. Aside from the complicated physical processes in the upper 200 m, salinity profiles indicate that interleaving layers appeared within 500 and 800 m with vertical and horizontal length scales of O(50 m) and O(10-100 km), respectively. The time scale for the interleaving layers should be much less than 30 days, inferred from the discrepancy in the interleaving features between the two surveys. The instability analysis together with values of the Turner angle calculated from the hydrographic data suggests that the double-diffusive instability is the primary driving mechanism for the observed interleaving layers.

Keywords: Kuroshio, Interleaving, Double-diffusive instability, Glider observation

©2019. Japan Geoscience Union. All Right Reserved.

Bottom Pressure in the East China Sea -Observation and modeling

*Hua Zheng[1], Xiao-Hua Zhu[1], Hirohiko Nakamura[2], Jae-Hun Park[3], Chanhyung Jeon[4], Ruixiang Zhao[1], Ayako Nishina[2], Chuanzheng Zhang[1], Hanna Na[5], Ze-Nan Zhu[1], Hong Sik Min[6]

1. Second Institute of Oceanography, Ministry of Natural Resources, China, 2. Faculty of Fisheries, Kagoshima University, Kagoshima, Japan, 3. Department of Ocean Sciences, Inha University, Incheon, South Kore, 4. Department of Marine Science and Biological Engineering, Inha University, Incheon, Korea, 5. School of Earth and Environmental Sciences, Seoul National University, Seoul, Korea, 6. Ocean Circulation and Climate Research Center, Korea Institute of Ocean Science and Technology, Busan, Korea

A two-year ocean bottom pressure record acquired between June 2015 and June 2017 observed by two pressure-recording inverted echo sounders (PIESs) and five current and pressure-recording inverted echo sounders (CPIESs) deployed along a section southwest of the Kerama Gap showed a significant 21-day variability. This 21-day bottom pressure variability (P_{bot21}) was particularly strong from July 2016 to January 2017, and it showed a squared coherence of 0.72 with wind stress curl around the Yangtze estuary in the East China Sea (ECS) during this period with a nearly 3-day time lag. A barotropic ocean model demonstrated the generation, spread, and dissipation of P_{bot21}. The modeling results showed that the P_{bot21} was driven by wind stress curl on the continental shelf of the ECS, where depths are shallower than 100 m, and spread southeastward to the Ryukyu Island Chain (RIC). The P_{bot21} was generated and remained on the shallow continental shelf, and only little power spread toward the RIC; thus, whether the signal could be observed by the mooring array was related to where it was generated. Significant P_{bot21} was generated southeast of the Yangtze estuary and measured by the mooring array from July 2016 to January 2017. However, P_{bot21} generated northeast of the Yangtze estuary, far from the mooring section, from January 2016 to April 2016 was exhausted before reaching the mooring array due to the long distance. It is suggested that the spatial pattern of 21-day wind stress curl over the ECS strongly influences P_{bot21} near the RIC.

©2019. Japan Geoscience Union. All Right Reserved.

A numerical study on the dynamics of seasonal velocity variation in the East China Sea

*ZHENLONG ZHANG[1], Nakamura Hirohiko[1], Xiao-Hua Zhu[2]

1. Kagoshima University, 2. Ministry of Natural Resources, CHINA.

In our previous study, we investigated the seasonal velocity variations at different depths over the entire Kuroshio path. It showed that the upper layer (< ~500 m depth) velocity variation over the entire Kuroshio path has a coherent seasonal feature, which reaches a maximum in July and a minimum in autumn or winter, over most of the regions along the Kuroshio path. However, the lower layer velocity (> ~500 m depth, in the continental slope area from the east of Luzon Island to the east of the Ryukyu Island chain) shows a reversed seasonal variation with a maximum in winter. Several numerical experiments were carried out to clarify the essential mechanisms. Although it was shown that the local wind stress upon the current region is a key factor for the seasonal velocity variation in the upper layer, the detailed driving mechanism has been still unknown. Thus, we perform further numerical experiments to clarify the concreate mechanism in this study. Using a rectilinear regional model with idealized continental slope, we have successfully reproduced the seasonal velocity variation of the jet (the Kuroshio) by the seasonal wind stress variation over the jet. It turns out that the velocity of the jet increases (decreases) when the wind stress is directed to downstream (upstream) direction of the jet. We will report the concrete process underlying acceleration and deceleration processes of the upper layer velocity related to the local wind stress.

Keywords: Kuroshio, Seasonal variation

©2019. Japan Geoscience Union. All Right Reserved.

Temporal and spatial velocity variations over the Kuroshio Extension, Kuroshio and Ryukyu Current System in 1982-2014

*YUXIANG QIAO[1], Hirohiko Nakamura[2], AYAKO NISHINA[2]

1. Kagoshima University, Graduate School of Fisheries, 2. Kagoshima University, Faculty of Fishries

Four dimensional variational Ocean ReAnalysis for the Western North Pacific (FORA-WNP30) from 1982 to 2014 is used to investigate temporal and spatial velocity variations over the regions consisting of Kuroshio Extension (KE), Kuroshio and Ryukyu Current System (RCS). In order to identify such temporal and spatial features, we made Hovmöller diagrams at several depths, which display temporal variations of along-stream velocity along the current path from Luzon Island to KE region. In this study, we particularly examine long-term (> 1 year) variations for their regional characteristics (Luzon Island to KE region) and their vertical features (sea surface to 1000 m depth). The results revealed that 1) the KE is dominated by decadal signals while the upstream regions include clearer interannual signals in addition to decadal ones, 2) decadal variations in the KE tends to be almost out of phase to those variations in the upstream regions from Luzon Island to Izu-Ridge, and 3) the velocity variations at the sea surface tend to be similar to those variations at 1000 m depth.

Keywords: Kuroshio, Ryukyu Current, Kuroshio Extension, Velocity, Long-term variations

©2019. Japan Geoscience Union. All Right Reserved.

Characteristics of water in the southern Okinawa Trough.

*Ayako Nishina[1], Hirohiko Nakamura[1], Jae-Hun Park[2], Xiao-Hua Zhu[3], Hong Sik Min[4], Hanna Na[5]

1. Kagoshima University, 2. Inha University, 3. Second Institute of Oceanography, 4. Korea Institute of Ocean Science and Technology, 5. Seoul National University

The Okinawa Trough is a basin within the East China Sea, where maximum depth reaches 2300 m. There are two characteristic water masses in the Okinawa Trough. One is the high salinity water in the sub-surface layer shallower than 300 m and the other is the low salinity water in the intermediate layer from 400 m to 700 m. According to the previous studies, the former water is occupied by the South China Sea Tropical Water (SCSTW) and the Kuroshio Tropical Water (KTW), and the latter is dominated by modified water masses of the North Pacific Intermediate Water (NPIW) and the South China Sea Intermediate Water (SCSIW). However, in the previous studies, the southern part of the Okinawa Trough remains to be observed, and it should be confirmed whether the previous results can apply to the southern part.
In this study, water mass properties in the southern part of the Okinawa Trough are investigated in detail. We mainly used CTD data from T/V Kagoshima-maru cruises in Junes from 2013 to 2018. The high salinity waters in the sub-surface layer were classified into three groups: SCSTW, KTW and the tropical waters in the east of Ryukyu Islands chain. The low salinity water in the intermediate layer had a complicated distribution in which the low salinity water from the east of Taiwan and that from the Kerama Gap.

Keywords: Okinawa Trough, water mass

©2019. Japan Geoscience Union. All Right Reserved.

[E] Poster | A (Atmospheric and Hydrospheric Sciences)：A-OS Ocean Sciences & Ocean Environment

Wed. May 29, 2019 3:30 PM - 5:00 PM JST | Wed. May 29, 2019 6:30 AM - 8:00 AM UTC | Poster Hall International Exhibition Hall8, Makuhari Messe_7

[A-OS11] Continental-Oceanic Mutual Interaction: Planetary scale Material Circulation

convener:Yosuke Alexandre Yamashiki(Earth & Planetary Water Resources Assessment Laboratory Graduate School of Advanced Integrated Studies in Human Survivability Kyoto University), Yukio Masumoto(Graduate School of Science, The University of Tokyo), Swadhin Behera(Climate Variation Predictability and Applicability Research Group, Application Laboratory, JAMSTEC, 3173-25 Showa-machi, Yokohama 236-0001), Takanori Sasaki(Department of Astronomy, Kyoto University)

The main purpose of this session is to promote discussion on mutual interaction between Continental zone and Oceanic zone. The global-scale material circulation induced by River runoff through oceanic general circulation as major topic on Continental-Oceanic Interaction, where the ENSO / IOD influence into continental climate as major topics on Oceanic-Continental Interaction. Numerical simulation and field observation of radionuclide transport from continental zone into ocean and its potential impact is also important topics of this session. The session also extend discussion on planetary hydrology and oceanography focusing on subsurface ocean in Jupiter's moon & Ancient Martian Oceanography & Hydrology by possible application of terrestrial GCM into Ancient Mars.

[AOS11-P01] Remote Sensing of Chlorophyll-a and Submerged Aquatic Vegetation for a Freshwater Lake in Japan

*Shweta Yadav[1], Yamashiki Yosuke[1], Junichi Susaki[1], Kanako Ishikawa[2] (1.Kyoto University, 2.Lake Biwa Environmental Research Institute)

[AOS11-P02] Hydrological and Debris-flow simulation of Martian Surface in Hesperian & early Amazonian epoch

*Hiroaki Sato[2], Yosuke Alexandre Yamashiki[1], Ryusuke Kuroki[1], Hideaki Miyamoto[3], Ryodo Hemmi[3] (1.Earth & Planetary Water Resources Assessment Laboratory Graduate School of Advanced Integrated Studies in Human Survivability Kyoto University, 2.Faculty of Engineering, Kyoto University, 3.Graduate School of Engineering, The University of Tokyo)

[AOS11-P03] Global Lakes & reservoirs Repository and their application for terrestrial surface environment

*Yosuke Alexandre Yamashiki[1], Ryusuke Kuroki[1], Botong Gao[1], Hina Bando[2], Fuka Takagi[3], Shweta Yadav[4] (1.Earth & Planetary Water Resources Assessment Laboratory Graduate School of Advanced Integrated Studies in Human Survivability Kyoto University, 2.Faculty of Science, Kyoto University, 3.Faculty of Agriculture, Kyoto University, 4.Educational Unit for Studies on Connectivity of Hills, Humans and Ocean, Kyoto University)

[AOS11-P04] Numerical simulation of Tidal Heating using SPH and its application to inner sea formation

*keiya murashima[1], Yosuke Alexandre Yamashiki[1], Natsuki Hosono[2] (1.Kyoto University, 2.Japan Agency for Marine-Earth Science and Technology)

Remote Sensing of Chlorophyll-a and Submerged Aquatic Vegetation for a Freshwater Lake in Japan

*Shweta Yadav[1], Yamashiki Yosuke[1], Junichi Susaki[1], Kanako Ishikawa[2]

1. Kyoto University, 2. Lake Biwa Environmental Research Institute

Freshwater lakes, particularly shallow lakes often exhibit alternative vegetative states, a clear-water state dominated by submerged aquatic vegetation (SAV) and a turbid-water state dominated by phytoplankton. Phytoplankton and SAV constitute the base of the aquatic food web and are the primary driver of the biogeochemical process in both the freshwater and coastal water bodies. The abundance of phytoplankton biomass can potentially indicate the degree of eutrophication in a specific waterbody. On the other hand, the massive overgrowth of invasive SAV species can also pose a serious threat to the aquatic ecosystem. Conventional methods (eg. Site-specific Boat survey) used to monitor the large water bodies are often time-consuming and expensive. In this study, we used a remote sensing based approach to monitor SAV and phytoplankton of the Lake. A multi-spectral satellite image (Landsat-8 Operational Land Imager) was used to assess the phytoplankton concentration and SAV biomass. A spectral decomposing algorithm was used to estimate and quantify both phytoplankton and SAV. Based on the peak growth period of SAV in the lake, the estimations were limited to a certain period of the year (i.e. mainly August and September). The image was used to classify and map the SAV coverage area using the spectral mixture analysis. The SAV biomass estimation model was used to determine the biomass of the SAV classified pixels in the lake. The satellite-derived phytoplankton and SAV were validated using the in-situ measured data of the lake. The result indicates the time and location-specific variation in the dominance of the phytoplankton and SAV.

Keywords: Phytoplankton, Submerged Aquatic Vegetation, Remote Sensing, Lake Water Quality

©2019. Japan Geoscience Union. All Right Reserved.

Hydrological and Debris-flow simulation of Martian Surface in Hesperian & early Amazonian epoch

*Hiroaki Sato[2], Yosuke Alexandre Yamashiki[1], Ryusuke Kuroki[1], Hideaki Miyamoto[3], Ryodo Hemmi[3]

1. Earth & Planetary Water Resources Assessment Laboratory Graduate School of Advanced Integrated Studies in Human Survivability Kyoto University, 2. Faculty of Engineering, Kyoto University, 3. Graduate School of Engineering, The University of Tokyo

It is considered that the Mars in Noachian ecoch to early Amazonian was much warmer temperature than current condition, with atmosphere and ocean supported by its magnetic activity. Several valley which seems to be developed by ancient hydrological processes are obsered in Martian surface, is being considered to be built long time before. Some fluvial fun was formed during the following Hesperian to early Amazonian epoch, which is considered as much cooler and drier than Noachian epoch. In this study, we applied Hydro-debris 2D model into Martian surface in Hesperian epoch in order to try develping surface vallay formation throughout hydrological processes.

Sediment transport and associated small-scale debris-flow occurrence may be the key for valley formation, where might be the micro-habitable zone in ancient period. At the same time it is still uncertain how much precipitation and erosion should have been required to formulate such topography. Following the last year’ s calculation we attempted to compare several cases of debris flow experiments by changing hypothetical precipitation rate and erosive coefficients in the initially distributed regolith.

Keywords: Hesperian Epoch, Debris flow

©2019. Japan Geoscience Union. All Right Reserved.

Global Lakes & reservoirs Repository and their application for terrestrial surface environment

*Yosuke Alexandre Yamashiki[1], Ryusuke Kuroki[1], Botong Gao[1], Hina Bando[2], Fuka Takagi[3], Shweta Yadav[4]

1. Earth & Planetary Water Resources Assessment Laboratory Graduate School of Advanced Integrated Studies in Human Survivability Kyoto University, 2. Faculty of Science, Kyoto University, 3. Faculty of Agriculture, Kyoto University, 4. Educational Unit for Studies on Connectivity of Hills, Humans and Ocean, Kyoto University

Global Lakes & Reservoirs Repository (GLR) has been developed in order to list global scale freshwater storage focusing on Lakes & Reservoirs. In this presentation we'll introduce their application, combining this with the ecological model for lakes & reservoirs for their surface environmental assessment under different climatic conditions. A two-layer aquatic ecological model (consisted with three types of phytoplanktons & zooplankton) is linked for a number of global lakes for the evaluation of future trends of aquatic ecosystems, mainly focusing on phytoplankton growth. The application of the database, by coupling it with satellite remote sensing for monitoring aquatic environment, together with the three-dimensional lake & reservoir aquatic environment model, are also introduced in the database.

Keywords: GLR, Remote sensing of aquatic environment

©2019. Japan Geoscience Union. All Right Reserved.

Numerical simulation of Tidal Heating using SPH and its application to inner sea formation

*keiya murashima[1], Yosuke Alexandre Yamashiki[1], Natsuki Hosono[2]

1. Kyoto University, 2. Japan Agency for Marine-Earth Science and Technology

There are some traces of liquid in icy moons, such as a plume of vapor of Europa acquired by Hubble Space Telescope and tiger stripes of Enceladus observed by Cassini. Since liquid water is essential for the origin of life, it can be important to understand the development of inner sea and also the temperature distribution inside of such icy moons.

It is considered that the tidal heating caused by tidal acceleration melts the inner icy layer which results in the presence of liquid water beneath its surface. Thus, we aim at simulating the tidal heating of an icy moon by 3-dimensional numerical fluid calculation in Smoothed Particle Hydrodynamics (SPH) method. As the tidal heating model, we apply the viscosity model which was used for numerical calculation of tidal stripping.

It is confirmed that this viscosity model lead to qualitatively correct result about tidal disruption, but the possibility of its application to tidal heating is not validiated. Therefore, as a first step, we tried to compare the result of this simulation with the result which is estimated theoretically. We made a rotation of a differentiated Titan-sized tidally locked object around a Saturn-mass material point with the radius of orbit being 1.1 times larger than its Roche limit. We also considered how to applicate this simulation to the calculation of actual icy moons. We will report the progress.

Keywords: icy moon, tidal heating

©2019. Japan Geoscience Union. All Right Reserved.

[E] Poster | A (Atmospheric and Hydrospheric Sciences)：A-OS Ocean Sciences & Ocean Environment

Wed. May 29, 2019 5:15 PM - 6:30 PM JST | Wed. May 29, 2019 8:15 AM - 9:30 AM UTC | Poster Hall International Exhibition Hall8, Makuhari Messe_12

[A-OS11] Continental-Oceanic Mutual Interaction: Planetary scale Material Circulation

convener:Yosuke Alexandre Yamashiki(Earth & Planetary Water Resources Assessment Laboratory Graduate School of Advanced Integrated Studies in Human Survivability Kyoto University), Yukio Masumoto(Graduate School of Science, The University of Tokyo), Swadhin Behera(Climate Variation Predictability and Applicability Research Group, Application Laboratory, JAMSTEC, 3173-25 Showa-machi, Yokohama 236-0001), Takanori Sasaki(Department of Astronomy, Kyoto University)

The main purpose of this session is to promote discussion on mutual interaction between Continental zone and Oceanic zone. The global-scale material circulation induced by River runoff through oceanic general circulation as major topic on Continental-Oceanic Interaction, where the ENSO / IOD influence into continental climate as major topics on Oceanic-Continental Interaction. Numerical simulation and field observation of radionuclide transport from continental zone into ocean and its potential impact is also important topics of this session. The session also extend discussion on planetary hydrology and oceanography focusing on subsurface ocean in Jupiter's moon & Ancient Martian Oceanography & Hydrology by possible application of terrestrial GCM into Ancient Mars.

[AOS11-P01] Remote Sensing of Chlorophyll-a and Submerged Aquatic Vegetation for a Freshwater Lake in Japan

*Shweta Yadav[1], Yamashiki Yosuke[1], Junichi Susaki[1], Kanako Ishikawa[2] (1.Kyoto University, 2.Lake Biwa Environmental Research Institute)

[AOS11-P02] Hydrological and Debris-flow simulation of Martian Surface in Hesperian & early Amazonian epoch

*Hiroaki Sato[2], Yosuke Alexandre Yamashiki[1], Ryusuke Kuroki[1], Hideaki Miyamoto[3], Ryodo Hemmi[3] (1.Earth & Planetary Water Resources Assessment Laboratory Graduate School of Advanced Integrated Studies in Human Survivability Kyoto University, 2.Faculty of Engineering, Kyoto University, 3.Graduate School of Engineering, The University of Tokyo)

[AOS11-P03] Global Lakes & reservoirs Repository and their application for terrestrial surface environment

*Yosuke Alexandre Yamashiki[1], Ryusuke Kuroki[1], Botong Gao[1], Hina Bando[2], Fuka Takagi[3], Shweta Yadav[4] (1.Earth & Planetary Water Resources Assessment Laboratory Graduate School of Advanced Integrated Studies in Human Survivability Kyoto University, 2.Faculty of Science, Kyoto University, 3.Faculty of Agriculture, Kyoto University, 4.Educational Unit for Studies on Connectivity of Hills, Humans and Ocean, Kyoto University)

[AOS11-P04] Numerical simulation of Tidal Heating using SPH and its application to inner sea formation

*keiya murashima[1], Yosuke Alexandre Yamashiki[1], Natsuki Hosono[2] (1.Kyoto University, 2.Japan Agency for Marine-Earth Science and Technology)

Remote Sensing of Chlorophyll-a and Submerged Aquatic Vegetation for a Freshwater Lake in Japan

*Shweta Yadav[1], Yamashiki Yosuke[1], Junichi Susaki[1], Kanako Ishikawa[2]

1. Kyoto University, 2. Lake Biwa Environmental Research Institute

Freshwater lakes, particularly shallow lakes often exhibit alternative vegetative states, a clear-water state dominated by submerged aquatic vegetation (SAV) and a turbid-water state dominated by phytoplankton. Phytoplankton and SAV constitute the base of the aquatic food web and are the primary driver of the biogeochemical process in both the freshwater and coastal water bodies. The abundance of phytoplankton biomass can potentially indicate the degree of eutrophication in a specific waterbody. On the other hand, the massive overgrowth of invasive SAV species can also pose a serious threat to the aquatic ecosystem. Conventional methods (eg. Site-specific Boat survey) used to monitor the large water bodies are often time-consuming and expensive. In this study, we used a remote sensing based approach to monitor SAV and phytoplankton of the Lake. A multi-spectral satellite image (Landsat-8 Operational Land Imager) was used to assess the phytoplankton concentration and SAV biomass. A spectral decomposing algorithm was used to estimate and quantify both phytoplankton and SAV. Based on the peak growth period of SAV in the lake, the estimations were limited to a certain period of the year (i.e. mainly August and September). The image was used to classify and map the SAV coverage area using the spectral mixture analysis. The SAV biomass estimation model was used to determine the biomass of the SAV classified pixels in the lake. The satellite-derived phytoplankton and SAV were validated using the in-situ measured data of the lake. The result indicates the time and location-specific variation in the dominance of the phytoplankton and SAV.

Keywords: Phytoplankton, Submerged Aquatic Vegetation, Remote Sensing, Lake Water Quality

©2019. Japan Geoscience Union. All Right Reserved.

Hydrological and Debris-flow simulation of Martian Surface in Hesperian & early Amazonian epoch

*Hiroaki Sato[2], Yosuke Alexandre Yamashiki[1], Ryusuke Kuroki[1], Hideaki Miyamoto[3], Ryodo Hemmi[3]

1. Earth & Planetary Water Resources Assessment Laboratory Graduate School of Advanced Integrated Studies in Human Survivability Kyoto University, 2. Faculty of Engineering, Kyoto University, 3. Graduate School of Engineering, The University of Tokyo

It is considered that the Mars in Noachian ecoch to early Amazonian was much warmer temperature than current condition, with atmosphere and ocean supported by its magnetic activity. Several valley which seems to be developed by ancient hydrological processes are obsered in Martian surface, is being considered to be built long time before. Some fluvial fun was formed during the following Hesperian to early Amazonian epoch, which is considered as much cooler and drier than Noachian epoch. In this study, we applied Hydro-debris 2D model into Martian surface in Hesperian epoch in order to try develping surface vallay formation throughout hydrological processes.

Sediment transport and associated small-scale debris-flow occurrence may be the key for valley formation, where might be the micro-habitable zone in ancient period. At the same time it is still uncertain how much precipitation and erosion should have been required to formulate such topography. Following the last year’ s calculation we attempted to compare several cases of debris flow experiments by changing hypothetical precipitation rate and erosive coefficients in the initially distributed regolith.

Keywords: Hesperian Epoch, Debris flow

©2019. Japan Geoscience Union. All Right Reserved.

Global Lakes & reservoirs Repository and their application for terrestrial surface environment

*Yosuke Alexandre Yamashiki[1], Ryusuke Kuroki[1], Botong Gao[1], Hina Bando[2], Fuka Takagi[3], Shweta Yadav[4]

1. Earth & Planetary Water Resources Assessment Laboratory Graduate School of Advanced Integrated Studies in Human Survivability Kyoto University, 2. Faculty of Science, Kyoto University, 3. Faculty of Agriculture, Kyoto University, 4. Educational Unit for Studies on Connectivity of Hills, Humans and Ocean, Kyoto University

Global Lakes & Reservoirs Repository (GLR) has been developed in order to list global scale freshwater storage focusing on Lakes & Reservoirs. In this presentation we'll introduce their application, combining this with the ecological model for lakes & reservoirs for their surface environmental assessment under different climatic conditions. A two-layer aquatic ecological model (consisted with three types of phytoplanktons & zooplankton) is linked for a number of global lakes for the evaluation of future trends of aquatic ecosystems, mainly focusing on phytoplankton growth. The application of the database, by coupling it with satellite remote sensing for monitoring aquatic environment, together with the three-dimensional lake & reservoir aquatic environment model, are also introduced in the database.

Keywords: GLR, Remote sensing of aquatic environment

©2019. Japan Geoscience Union. All Right Reserved.

Numerical simulation of Tidal Heating using SPH and its application to inner sea formation

*keiya murashima[1], Yosuke Alexandre Yamashiki[1], Natsuki Hosono[2]

1. Kyoto University, 2. Japan Agency for Marine-Earth Science and Technology

There are some traces of liquid in icy moons, such as a plume of vapor of Europa acquired by Hubble Space Telescope and tiger stripes of Enceladus observed by Cassini. Since liquid water is essential for the origin of life, it can be important to understand the development of inner sea and also the temperature distribution inside of such icy moons.

It is considered that the tidal heating caused by tidal acceleration melts the inner icy layer which results in the presence of liquid water beneath its surface. Thus, we aim at simulating the tidal heating of an icy moon by 3-dimensional numerical fluid calculation in Smoothed Particle Hydrodynamics (SPH) method. As the tidal heating model, we apply the viscosity model which was used for numerical calculation of tidal stripping.

It is confirmed that this viscosity model lead to qualitatively correct result about tidal disruption, but the possibility of its application to tidal heating is not validiated. Therefore, as a first step, we tried to compare the result of this simulation with the result which is estimated theoretically. We made a rotation of a differentiated Titan-sized tidally locked object around a Saturn-mass material point with the radius of orbit being 1.1 times larger than its Roche limit. We also considered how to applicate this simulation to the calculation of actual icy moons. We will report the progress.

Keywords: icy moon, tidal heating

©2019. Japan Geoscience Union. All Right Reserved.

[E] Poster | A (Atmospheric and Hydrospheric Sciences)：A-HW Hydrology & Water Environment

Wed. May 29, 2019 3:30 PM - 5:00 PM JST | Wed. May 29, 2019 6:30 AM - 8:00 AM UTC | Poster Hall International Exhibition Hall8, Makuhari Messe_8

[A-HW23] Hydrology & Water Environment

convener:Isao Machida(Geological Survey of Japan), Dai Yamazaki(Institute of Industrial Sciences, The University of Tokyo), Takeshi Hayashi(Faculty of Education and Human Studies, Akita University), Keisuke Fukushi(Institute of Nature & Environmental Technology, Kanazawa University)

We focus on various issues of water cycle and environment and aim to answer questions of hydrological and earth system sciences including 1) surface, subsurface and evapotranspiration processes of water cycle; 2) natural and anthropogenic hydrothermal systems, 3) environments issues and studies on a watershed or global scale, 4) water-related issues with ecological, environmental, and geochemical aspects, and 5) other issues in hydrological sciences. This session welcomes presentations regarding various kinds of approaches and techniques such as field survey, remote sensing, isotope tracers, numerical simulation, and theoretical analysis.

[AHW23-P01] A multiobjective risk management model for real-time reservoir flood control operation

*Juan Chen[1,2], Ping-An Zhong[2], XinYu Wan[2], Yu Zhang[2] (1.College of Earth Sciences and Engineering, Hohai University, 2.College of Hydrology and Water Resources, Hohai University)

[AHW23-P02] Assessment of the Flow Regime of Roanoke River due to Climatic and Anthropogenic Activities

*Rahul Kumar Singh[1], Dr. Manoj Kumar Jain[1] (1.Indian Institute of Technology, Roorkee, India)

[AHW23-P03] Predictive Analysis of Climate, Water, Health and the Environment Nexus

*Abhishek [1], Deepika [2] (1.Technical University Dresden, GERMANY, 2.BPS Government Medical College for Women, Sonepat, INDIA)

[AHW23-P05] Severe droughts provide huge fuel for widespread wildfires in California in USA

*Linghua Qiu[1], Ji Chen[1], Haiyun Shi[2], Liqun Sun[3], Jun Niu[4] (1.the University of Hong Kong, 2.Southern University of Science and Technology, 3.Shenzhen Institutes of Advanced Technology, Chinese Academy of Sciences, 4.China Agricultural University)

[AHW23-P06] A comprehensive evaluation of MODIS-based water use efficiency with global eddy covariance flux data and a process model

*Shanshan YANG[1,2], Jiahua ZHANG[1], Sha ZHANG[1,2], Jingwen WANG[1,2], Yun BAI[1,2], Fengmei YAO[2], Huadong GUO[1] (1.Institute of Remote Sensing and Digital Earth, Chinese Academy of Sciences, 2.University of Chinese Academy of Sciences, Beijing, China)

[AHW23-P07] Impact of variability and anisotropy in the correlation decay distance for precipitation spatial interpolation in China

*yingxian zhang[1] (1.National Climate Center, China Meteorological Administration)

[AHW23-P08] New Record-Breaking Frequency of Annual Maximum Daily Precipitation of 58 stations in the whole Japan, an increasing of extreme values.

*Chhay Ngorn SEANG[1], Tomohito YAMADA[1] (1.Hokkaido University)

[AHW23-P09] Quantifying stemflow to better express its ecohydrological significance

*Shin'ichi Iida[1], Darryl E. Carlye-Moses[2], Sonja Germer[3], Pilar Llorens[4], Beate Michalzik[5], Kazuki Nanko[1], Alexander Tischer[5], Delphis F. Levia[6] (1.Department of Disaster Prevention, Meteorology and Hydrology, Forestry and Forest Products Research Institute, 2.Department of Geography and Environmental Studies, Thompson Rivers University, Kamloops, British Columbia, Canada, 3.Department of Bioengineering,

Leibniz Institute for Agricultural Engineering and Bioeconomy, Potsdam, Germany, 4.Institute of Environmental Assessment and Water Research (IDAEA-CSIC), Barcelona, Spain, 5.Soil Science, Institute of Geography, Friedrich Schiller University Jena, Jena, Germany, 6.Department of Geography and Department of Plant and Soil Sciences, University of Delaware, Newark, DE, USA)

[AHW23-P10] **Hydraulic analysis of overland flow caused by temporally varying rainfall**

*PING-CHENG HSIEH[1], Ming-Chang Wu[1] (1.National Chung Hsing University)

[AHW23-P11] A comparative Study on Water Environment of Isolated Islands - Focusing on Islands in Nagasaki Prefecture - (3)

*Go Yamaki[1], Koji Kodera[2], Kazuki Asami[1], Yoshihiro IGARI[1], Masaki Horiuchi[1] (1.Grad. Student, Hosei Univ., 2.Dep. of Geography, Hosei Univ.)

[AHW23-P12] **Water environment around Kusatsu-Shirane volcano and consideration of the effect of eruption in January 2018**

*Igari Yoshihiro[1], Koji Kodera[2], Kazuki Asami[1] (1.Grad.Student,Hosei Univ., 2.Dep.of Geography Hosei Univ.)

[AHW23-P13] Re-consideration of discharge rate of spring water in Lake Ezu, Kumamoto

*Kimpei Ichiyanagi[1], Kiyoshi Ide[1], Jun Shimada[1], Tsutomu Ichikawa[2] (1.Kumamoto University, 2.Tokai University)

[AHW23-P14] **Evaluating the efficacy of hydrologically and hydrodynamically driven methods of e-flow assessment for Upper Godavari River Basin, India**

*GAURAV KALIDAS PAKHALE[1], Jyoti Punjahari Nale[2], Ashvin Kumar Gosain[3], Rakesh Khosa[3] (1.PhD Research Scholar, Civil Engineering Department, Indian Institute of Technology, Delhi, 2.Project Advisor, IEWP, GIZ India, New Delhi, India, 3.Professor, Civil Engineering Department, Indian Institute of Technology, Delhi)

[AHW23-P15] Presence of pharmaceutical compounds in freshwater lakes and their impact on phytoplankton

*Nandakumar Kanavillil[1], Cassandra Fligg[1], Sreekumari Kurissery[1] (1.Lakehead University, Canada)

[AHW23-P16] **Novel approximate solutions for solute transport due to injections: considering the scale-dependent dispersion and non-integer flow dimension**

*Ye-Chen Lin[1], Hund-Der Yeh[1] (1.National Chiao Tung Univ.)

[AHW23-P17] Experimemtal study on the residual saturation of Porous Media using Pore Doublets Micromodel

*Chun-Wei Peng[1] (1.Taiwan National Chiao Tung University)

[AHW23-P18] Assessment of Synergy between Biomedical Waste and Shallow Groundwater Pollution

*Deepika [1], Abhishek [2] (1.BPS Government Medical College for Women, Sonepat, INDIA, 2.Technical University Dresden, GERMANY)

[AHW23-P19] Erosion and transport processes of earth surface materials in a reservoir-catchment system inferred from atmospheric radionuclides ^{7}Be and ^{210}Pb

*Mikiya Tsuruoka[1], Shinya Ochiai[2], Atsushi Matsuki[2], Seiya Nagao[2] (1.Graduate School of Natural Science and Technology, Kanazawa University, 2.Institute of Nature and Environmental Technology, Kanazawa University)

[AHW23-P20] Fluctuation of groundwater level in a sloping unconfined aquifer due to time varying recharge

*Ming-Chang Wu[1], Ping-Cheng Hsieh[1] (1.National Chung Hsing University)

[AHW23-P21] **Effect of cutoff wall on recharge water storage volume**

*Pei-hsun Tsai[1], Jung-hsing Tai[1] (1.Chaoyang University of Technology)

[AHW23-P22] **Studying Operation Parameters on Flat-Plate Membrane Bioreactor for Sewage Treatment**

*Jen Hung Chiu[1], Wen Chin Chen[1] (1.Studying Operation Parameters on Flat-Plate Membrane Bioreactor for Sewage Treatment)

[AHW23-P23] **Mine-water quality at a tertiary coalfield in India: Characterisation and treatment using novel polyvinyl alcohol (PVA) gel bioreactor**

*Aparna Dutta[1], Sudipta Sarkar[1] (1.Indian Institute of Technology Roorkee)

A multiobjective risk management model for real-time reservoir flood control operation

*Juan Chen[1,2], Ping-An Zhong[2], XinYu Wan[2], Yu Zhang[2]

1. College of Earth Sciences and Engineering, Hohai University, 2. College of Hydrology and Water Resources, Hohai University

Many uncertainties exit in the real-time reservoir flood control operation and bring risks to flood control decisions. A multiobjective optimization model is developed for the real-time risk management for the flood control operation of a reservoir system considering multiple uncertainties such as inflow forecast errors and outflow errors. The two competing objectives considered are: (1) minimizing the risk of reservoir upstream flooding and (2) minimizing the risk of downstream flooding. The optimization model seeks to find the operation schedules that satisfy the flood control objectives and simultaneously minimize the overall risks. The decision variables are the hourly reservoir releases. The formulated multiobjective optimization problem is nonlinear and non-convex, and is solved with an improved Non-dominated Sorting Genetic Algorithm-II (INSGA-II). We use a filtering algorithm to select representative non-dominated solutions from the Pareto front generated by INSGA-II to assist in real-time decision making. The proposed risk management model is applied to the Foziling reservoir in Huaihe river basin of China. The results show that the proposed method can provide a practical way to optimize the real-time flood control operation for risk management of a reservoir.

Keywords: Flood, Reservoir, Flood control operation, Risk assessment, Multiobjective optimization

©2019. Japan Geoscience Union. All Right Reserved.

Assessment of the Flow Regime of Roanoke River due to Climatic and Anthropogenic Activities

*Rahul Kumar Singh[1], Dr. Manoj Kumar Jain[1]

1. Indian Institute of Technology, Roorkee, India

The natural flow regime of many rivers around the world has been significantly altered due to climatic and anthropogenic modifications such as the construction of dams and reservoirs. The natural flow regime plays an important role in the development of the riverine ecosystem. Therefore, quantification of the extent of the alterations in the natural flow regime would be helpful in the river’ s ecological assessment. The Roanoke River in southeastern United States had one of the biggest and least disturbed forest ecosystems but due to climatic changes and anthropogenic actions such as construction of dam, artificial regulations of the natural flow regime, the overall riverine ecosystem has severely impacted. In this study, SWAT (Soil Water Assessment Tool) has been used to reconstruct the long-term unaltered streamflow for a hypothetical no-dam scenario condition, in order to assess the impact of climate change as well as due to construction of the John H Kerr reservoir on Roanoke River streamflow from 1956-2012. In order to simulate the unaltered streamflow series post construction of John H Kerr reservoir, 32 years (1916-1948) of observed gauge inflow prior to anthropogenic disturbance (due to construction of John H Kerr Reservoir) was used for calibration and validation of the parameters of the SWAT model. Historical land use and land cover backcasting data for the year 1938 has been used in the hydrological model to simulate the flow regime prior to construction of the dam and it was kept same during the whole simulation period. The SWAT model simulated observed gauge data with Nash-Sutcliffe efficiency coefficient (NSE) = 0.70, Percent bias (PBIAS) = 0.00 and the determination coefficient (R^2) = 0.73 during the calibration period (1916 - 1936), and performed equally better during the validation period (1937-1948) with NSE = 0.72, PBIAS = 0.00 and R^2 = 0.74. The indicators of hydrologic alteration (IHA) methodology has been used to assess the natural flow regime (no dam or reservoir moderated flow regime) characteristics under a simulated no-reservoir scenario (scenario1) and compare with the IHA results obtained based on the gauged streamflow downstream of the dam (scenario2). Hence, in case of scenario 1, the post-impact period has been taken as the simulated flow series using SWAT model from 1956-2012 and in case of scenario 2 the post-impact period has been taken as the gauged observed streamflow from 1956-2012 at Roanoke Rapids gauging station downstream of the reservoir. The pre-impact period for both the scenario was kept the same i.e. from 1912 to 1949. The results reveal that in case of the IHA assessment based on scenario 1, significant alterations have been observed in 5 out of 32 indicators compared to 13 out 32 indicators in case of scenario 2. The overall hydrologic alteration in case of scenario 1 was 45.65% and it was 55.17% in the case of scenario 2. The alteration during the scenario 1 could be attributed to the overall natural climatic variability. The results also indicate that flow variability in terms of high and low flows were better in scenario 1 compared to scenario 2 where the high flows were completely absorbed including the low pulse count and duration due to regulation in the flow. However, the reservoir operations enhanced the monthly flows including the multiday minima low flows. Thus, the present method can be treated as an easy-to-implement comprehensive approach for designing natural flow regimes to mimic the pre-impact flow condition in order to restore the ecosystem of modified rivers due to anthropogenic interventions.

Keywords: SWAT, IHA, Streamflow, Hydrologic Alteration, Ecosystem

©2019. Japan Geoscience Union. All Right Reserved.

Predictive Analysis of Climate, Water, Health and the Environment Nexus

*Abhishek -[1], Deepika -[2]

1. Technical University Dresden, GERMANY, 2. BPS Government Medical College for Women, Sonepat, INDIA

Amid the major demographic transition of developing world from a rural, agrarian society to an urban, industrial one, there is a need for predictive analytics of impact of the major biotic and abiotic stressors on the environmental constituents. The current study emphasizes the connections between climate, water, environment, and health and their interdependency followed by an impact assessment focusing on an urban environment. A data-driven hybrid framework for water resources assessment and management based on machine learning techniques was developed, calibrated and validated with the ground data for the sub-region scale of North-East Indian regime (mean spatial coordinates: 28° 38' 41.2800" N and 77° 13' 0.1956" E). The remote sensing data for land cover and land change were coupled with the climate model simulations to formulate the health risk assessment framework. The large ensemble of downscaled scenario based outputs including the effects of anthropogenic factors was used to drive the hybrid model framework.

Multi-dimensional Random Walk Metropolis (RWM) algorithms used to optimize the sample observations converged with an RMSE error of 0.18 with a range of 0.006. Pearson Product Moment Correlation coefficient range of all the ensemble members was 0.886-0.904. The prediction accuracy construed from 95 % model uncertainty bounds was 89-91 % for the constituent parameters. The sensitivity analysis revealed that the climate is the key parameter and is the most sensitive for all other linkage units followed by water availability and health factors. Comparative analysis of the simulated- and experimental results enforced comprehensive clarification of the assumptions made therein. By real-time monitoring and forecasting the vital impacts, this research will serve and benefit local policymakers and in the decision-making process, particularly regarding water resources vulnerability and future availability with significant economic consequences. The upscaling of the model form sub-regional to regional scale is well underway.

Keywords: Climate Change, Urbanization, RWM algorithm, Ensemble model

©2019. Japan Geoscience Union. All Right Reserved.

Severe droughts provide huge fuel for widespread wildfires in California in USA

*Linghua Qiu[1], Ji Chen[1], Haiyun Shi[2], Liqun Sun[3], Jun Niu[4]

1. the University of Hong Kong, 2. Southern University of Science and Technology, 3. Shenzhen Institutes of Advanced Technology, Chinese Academy of Sciences, 4. China Agricultural University

The frequently occurred large wildfires in California caught the public’ s attention in recent years and the ability to identify and prevent such disasters is pressing. The study built the rational relationship between soil moisture and vegetation based on remote sensing, hydrology and wildfire data during 2001-2017 in California. The purpose is to estimate the effects of droughts on wildfires and to detect the valid fuel for wildfires. The study results reported that severe droughts could cause huge fuel for wildfires and made them even much more widespread and longer sustained. The consequences could provide significant information for identification and prevention of future wildfires in California and even other regions in the world.

Keywords: Fuel, Wildfires, Droughts, Soil moisture, Vegetation

©2019. Japan Geoscience Union. All Right Reserved.

A comprehensive evaluation of MODIS-based water use efficiency with global eddy covariance flux data and a process model

*Shanshan YANG[1,2], Jiahua ZHANG[1], Sha ZHANG[1,2], Jingwen WANG[1,2], Yun BAI[1,2], Fengmei YAO[2], Huadong GUO[1]

1. Institute of Remote Sensing and Digital Earth, Chinese Academy of Sciences, 2. University of Chinese Academy of Sciences, Beijing, China

Ecosystem water use efficiency (WUE), defined as the ratio of gross primary productivity (GPP) to evapotranspiration (ET), is an important indicator to investigate the interaction between the terrestrial carbon and water cycles. The spatiotemporal patterns of WUE inferred from MODIS GPP and ET products and its responses to environmental factors have been analyzed, however, the accuracy of MODIS-derived WUE (MODIS WUE) has not been well evaluated. In this study, we evaluated monthly and annual MODIS WUE using global covariance flux data (FLUXNET2015 dataset) during 2000-2014, and conducted global intercomparisons (2001-2011) among annual WUE from MODIS, gridded FLUXNET (MTE) and a process model (BESS). Site scale (53 sites) evaluation results revealed that MODIS gave reliable estimates for GPP and ET, however, the performances of MODIS WUE was poor for monthly WUE (R2=0.14) and even worse for annual WUE (R2=0.08). MODIS WUE was generally underestimated with a bias of -0.21 gC kg-1 H2O (-8.43%) and RMSE of 1.20 gC kg-1 H2O for monthly WUE, and a bias of -0.28 gC kg-1 H2O (-11.31%) and RMSE of 0.98 gC kg-1 H2O for annual WUE. Among all land cover types, MODIS WUE performed relatively better in savannas and woody savannas for monthly WUE and grasslands for annual WUE, but significantly overestimated WUE in open shrublands. Likewise, MODIS WUE was obviously overestimated in hot and cold semiarid and arid climate zones. The global intercomparison results demonstrated that the spatial pattern of MODIS WUE was broadly similar to that of MTE and BESS WUE, except for the tropical and subtropical arid and semiarid areas. In these regions MODIS WUE showed extremely high values with large uncertainty and different linear trends compared with MTE and BESS WUE. These disagreements were mainly caused by the discrepancies in MODIS ET. Therefore, the uncertainty of MODIS WUE in the tropical arid and semiarid areas should be taken with caution when using MODIS WUE to investigate and interpret how WUE varies spatially and its responses to climate change. Furthermore, the accuracy of MODIS GPP and ET datasets should be paid extra attention since the quality of both GPP and ET would directly affect the WUE accuracy.

Keywords: Water use efficiency (WUE), Evaluation, Intercomparison, MODIS, FLUXNET, BESS

©2019. Japan Geoscience Union. All Right Reserved.

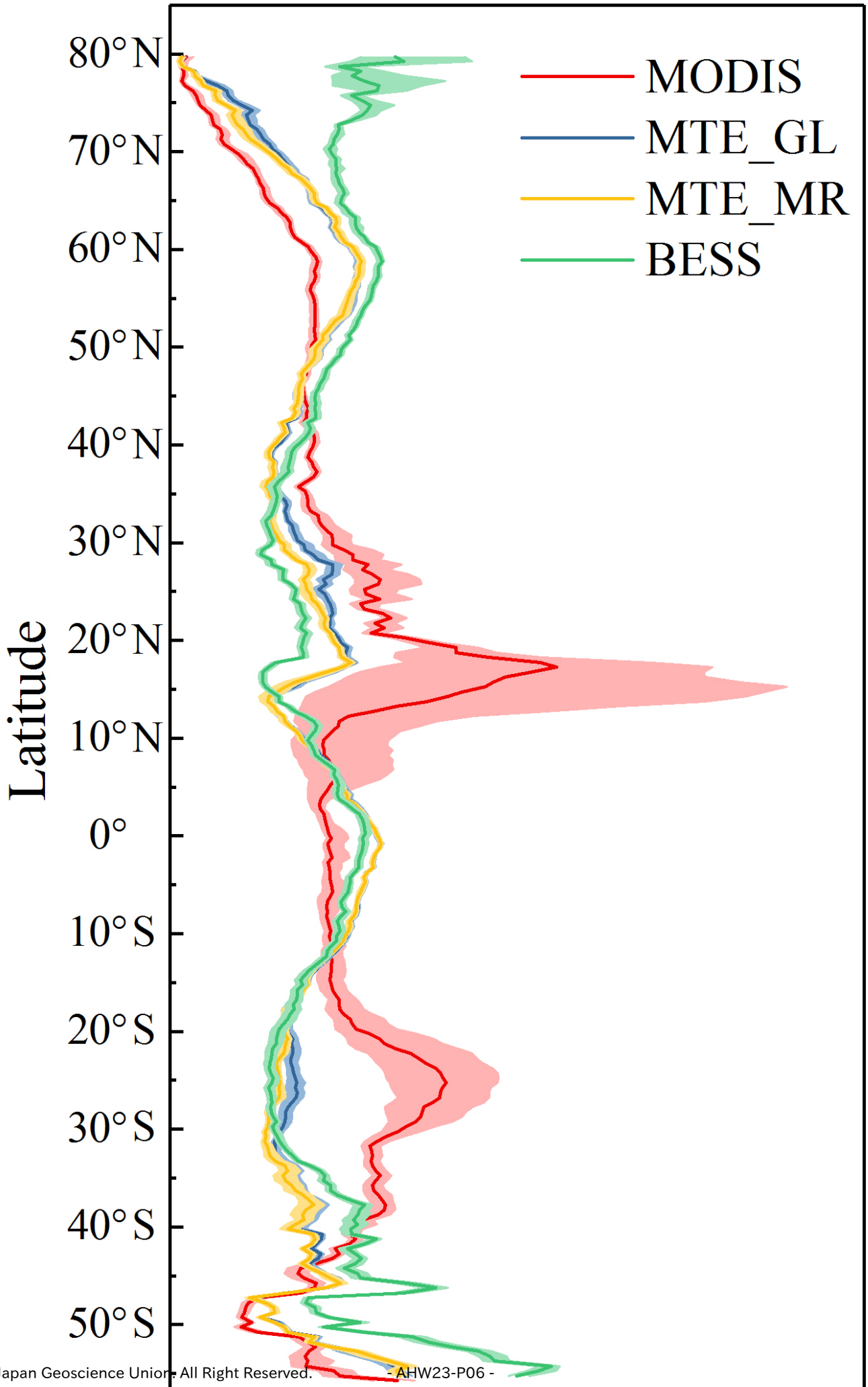

©2019. Japan Geoscience Union. All Right Reserved.

©2019. Japan Geoscience Union. All Right Reserved.

Impact of variability and anisotropy in the correlation decay distance for precipitation spatial interpolation in China

*yingxian zhang[1]

1. National Climate Center, China Meteorological Administration

The correlation decay distance (CDD) plays a key role in the angular-distance weighting (ADW) interpolation technique, being used as the searching radius to select correlated neighbors and to calculate the relative weights. The CDD of daily precipitation in China varies spatially and seasonally, and it presents anisotropic behavior, as a result of topography and the predominant atmospheric circulation. In general, CDD is largest in winter and smallest in summer, except for limited regions such as the Tibetan plateau. From a cross validation analysis, it is found that taking account of spatial and seasonal variations in CDD generally improves the ADW interpolation. Utilization of anisotropic CDDs increases the interpolation skill scores in regions with a dense monitoring network, significant elevation variation (southwestern China) or strongly anisotropic CDDs (Tibetan plateau).

Keywords: daily precipitation, correlation decay distance, ADW interpolation

©2019. Japan Geoscience Union. All Right Reserved.

New Record-Breaking Frequency of Annual Maximum Daily Precipitation of 58 stations in the whole Japan, an increasing of extreme values.

*Chhay Ngorn SEANG[1], Tomohito YAMADA[1]

1. Hokkaido University

The changes in daily temperature extremes in global scale have affected the weather and climate extreme events when there is an increase of greenhouse gas GHG compare to the industrialization in the 19th century (IPCC, 2014). Yamada et al. (2014) illustrate that the water vapor and convective instability follow the Clausius-Clapeyron-like rate of change with 99th percentile hourly precipitation intensity. Lehmann, J. et al. (2015), on another hand, studied globally the characteristic of precipitation change anomaly using a relation of the Clausius-Clapeyron model. By the way, the climate change tends to include another factor, which is more statistical base. The theory of record values in independent and identically distributed (i.i.d) random variable is studied more extensively and is more applicable with an assumption of stationary climate. The Clausius-Clapeyron equation is then also applicable base on the thermodynamic term which illustrates the relation of the temperature, vapor pressure and precipitation formation characteristic which also mentioned in the above previous studies. At the first stage, 58 stations of AMeDAS data with 117-years period across Japan are used for this analysis. The result shows that mean long-term precipitation of these 58 stations is higher than the mean value from theory i.i.d random variable of stationary climate. From this result, it can be implied that the change of precipitation in Japan is influenced by the drift term either of climate change or the heat island. In this case, the Clausius-Clapeyron equation is applied to identify the temperature term of change. This study tries to formulate a theory which more statistical base of climate drifts, non-stationary and non-identically to extreme events in accordance with time series. Clausius-Clapeyron Model and the Linear Drift Model is considered to form an empirical stochastically based on climate trend.

Keywords: Clausius-Clapeyron, New record Breaking, i.i.d

©2019. Japan Geoscience Union. All Right Reserved.

Quantifying stemflow to better express its ecohydrological significance

*Shin'ichi Iida[1], Darryl E. Carlye-Moses[2], Sonja Germer[3], Pilar Llorens[4], Beate Michalzik[5], Kazuki Nanko[1], Alexander Tischer[5], Delphis F. Levia[6]

1. Department of Disaster Prevention, Meteorology and Hydrology, Forestry and Forest Products Research Institute, 2. Department of Geography and Environmental Studies, Thompson Rivers University, Kamloops, British Columbia, Canada, 3. Department of Bioengineering, Leibniz Institute for Agricultural Engineering and Bioeconomy, Potsdam, Germany, 4. Institute of Environmental Assessment and Water Research (IDAEA-CSIC), Barcelona, Spain, 5. Soil Science, Institute of Geography, Friedrich Schiller University Jena, Jena, Germany, 6. Department of Geography and Department of Plant and Soil Sciences, University of Delaware, Newark, DE, USA

Stemflow is the flow of rainwater over the exterior of a tree stem to its base. Due to water balance calculations to obtain interception loss of forest stands, and the sometimes low percentage of stemflow as a function of rainfall, some literature ignores the ecohydrological significance of stemflow. However, stemflow is much more concentrated than throughfall per unit area. In recognition of the extreme amounts of water input to the small area around tree trunks, we advocate for two metrics to better express stemflow in relation to its ecohydrological importance: namely, the stand-scale funneling ratio and the stand-scale infiltration funneling ratio. We calculated these metrics based on measurements carried out in a tropical dry deciduous forest and a subpolar juvenile coniferous stand, and found that these are significantly larger than throughfall on both sites. The data cited from recent papers (n=34) showed that very small stand-scale amount of stemflow (approximately 0.5% on average) were necessary to make the stand-scale funneling ratio to be equal or more than unity. Moreover, the infiltration area of stemflow is generally < 0.2 m^2 due to the high infiltration capacity of top soil of forests, generally resulting in the stand-scale infiltration funneling ratio substantially greater than unity. Thus, stemflow is more effective for soil water recharge than throughfall. We recommend use of these metrics to better express ecohydrological importance of stemflow.

This presentation is based on the published paper as follows:
Carlye-Moses, D.E., Iida, S., Germer, S., Llorens, P., Michalzik, B., Nanko, K., Tischer, A., Levia, D.F. (2018): Expressing stemflow commensurate with its ecohydrological importance. Advances in Water Resources, 121, 472-479. Free open access article to: https://doi.org/10.1016/j.advwatres.2018.08.015

Keywords: Stemflow, Funneling ratio, Forest hydrology

©2019. Japan Geoscience Union. All Right Reserved.

Hydraulic analysis of overland flow caused by temporally varying rainfall

*PING-CHENG HSIEH[1], Ming-Chang Wu[1]

1. National Chung Hsing University

With the development of human civilization and population migration, we use many different types of pervious or impervious materials to cover the original surface. As a result, the surface friction and water permeability are reduced, resulting in increased flow velocity and runoff, and thus increasing the frequency and scale of flood occurrence. Therefore, predicting changes in overland flow caused by rainfall has become an important issue.

This study intends to simulate the overland flow under different rainfall patterns by the theory of diffusion wave model. The diffusion wave equation was used as the governing equation, and an analytical solution of the water depth by the generalized integral transformation method was presented. Since the values of the parameters used in previous research for diffusion wave models vary in an extensive range. In this study, the parameters were adjusted for each location to ensure the rationality of the simulation results according to the law of mass conservation.
The results show that for the non-uniform rainfall, the peak water depth and peak flow due to the post-peak rainfall are the largest, followed by the third quarter peak rainfall; whereas the average flow velocity of the mid-peak rainfall is the largest, followed by the third quarter peak rainfall. The peak water depth, peak flow rate and average flow rate due to the double peak rainfall are the smallest among the six rainfall patterns in this study.

Keywords: overland flow, nonuniform rainfall, diffusion wave

©2019. Japan Geoscience Union. All Right Reserved.

A comparative Study on Water Environment of Isolated Islands - Focusing on Islands in Nagasaki Prefecture - (3)

*Go Yamaki[1], Koji Kodera[2], Kazuki Asami[1], Yoshihiro IGARI[1], Masaki Horiuchi[1]

1. Grad. Student, Hosei Univ., 2. Dep. of Geography, Hosei Univ.

1. Introduction Research on islands in Nagasaki prefecture has hardly been investigated and research has been promoted since 2014 from Goto Island Islands, Tsushima, Iki, Hirado. For this time, we will clarify the water environment in each area from the relationship with land use and climate, and make it a foothold to clarify the material cycle of each island.

2. Target area Iki is rugged with a maximum altitude of 213 m, and there are numerous reservoirs in various parts of the island. In Tsushima, the altitude of the entire island is relatively high, and the mountains occupy about 89%. The Goto Islands Island consists of about 140 large and small islands, with large geological differences on each island. The Hirado Islands have many mountains while the fields are also relatively large. The population penetration rate of wastewater treatment in both areas is as low as 20-40%.

3. Research method Field survey was conducted 2 to 4 times a year from 2014 after organizing and examining existing research. On the site, water temperature, temperature, electric conductivity (EC), pH and RpH, COD were measured, and water was taken to measure the total organic carbon and the main dissolved components.

4. Results and discussion In Iki, the influence of agriculture appears in EC and TOC, but it is interesting that there is almost no effect of nitric acid. On the other hand, although many nitric acid was detected in the Goto Islands, it is thought that factors are due to paddy fields in Iki and upland fields in Goto Islands. Tsushima showed relatively low concentrations of EC and dissolved components, and seasonal changes also appeared. In Hirado Island, especially in the southern part, the geological influence is large in many places, the impact of sea salt is strong in Ikitsuki island and Azuchi Oshima. EC tends to rise in rainwater from October to March, pH tends to decrease. From the above, it is considered that the difference in the quality of the islands is greatly influenced by the difference of geology, topography and agricultural form.

Keywords: Iki island, Tsushima islands, Goto islands, Hirado islands, Water environment

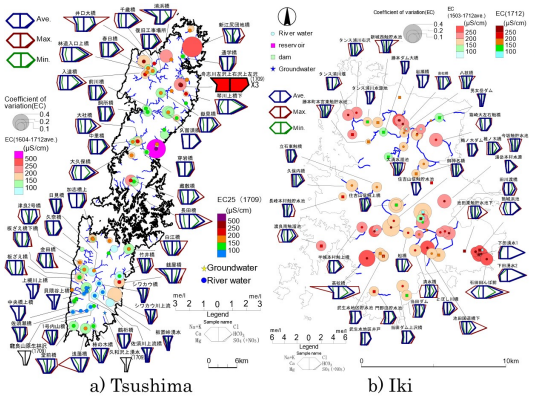

a) Tsushima b) Iki c) Hirado

Fig.1 Water quality

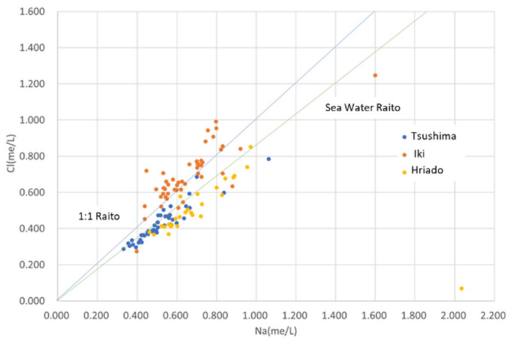

Fig.2 Na / Cl ratio

©2019. Japan Geoscience Union. All Right Reserved.

Water environment around Kusatsu-Shirane volcano and consideration of the effect of eruption in January 2018

*Igari Yoshihiro[1], Koji Kodera[2], Kazuki Asami[1]

1. Grad.Student,Hosei Univ., 2. Dep.of Geography Hosei Univ.

1. Introduction

The eruption (steam explosion) occurred in Mt.Motoshirane (One of Kusatsu-Shirane Volcano) on January 23, 2018. In this area, water quality survey of water environment began in May 2017 before the eruption. In addition to examining the influence on the water quality before and after the eruption, we studied the elution component of volcanic ash and the influence on the water environment. We also attempted to consider water quality forming factors in river water around Kusatsu-Shirane volcano.

2. Research method

We conducted about 21 field surveys from May 2017 to March 2019. The survey site is about 45 sites, centering on rivers flowing in the east and south of the mountain. Temperature, water temperature, pH, RpH, EC, and flow rate were measured locally, and the sampled sample was analyzed for the main dissolved components. In February 2018, we investigated the deposition situation and ash fall volume of volcanic ash and conducted sampling, and carried out dissolution experiment. In addition to rivers, field surveys and sampling of lakes and precipitation, snow cover, hot spring water were conducted.

3. Results and discussion

In Shirasuna River flowing to the east side of the mountain, groundwater and river water influenced by hot spring drainage and volcanic activity flow in from the tributary. There are points where the EC value fluctuates greatly, and it is influenced by the discharge and conduction of the dam which stores the neutralizing water of acidic rivers. In the Gando Swamp where the site of sulfur mine is located in the upstream part, the water quality is around pH:2.0, EC:6000 μS/cm. It is conceivable that the deposited volcanic ash affects the quality of the surrounding river due to snow melting water and precipitation.

Keywords: Mt.Kusatsu-Shirane, Volcano, Water environment, Eruption, Hot spring

©2019. Japan Geoscience Union. All Right Reserved.

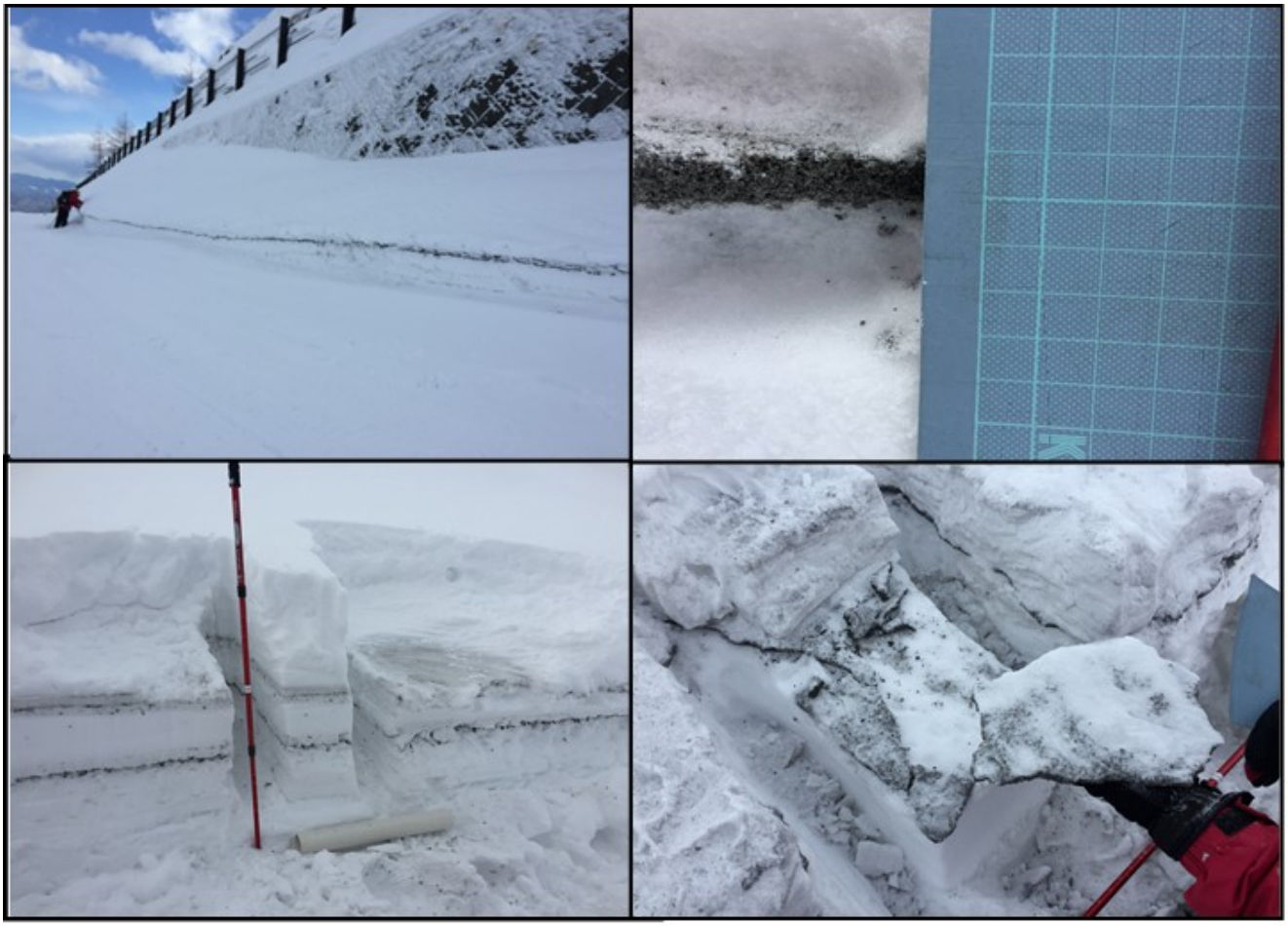

Picture.1 Ash fall in the east foot of Kusatsu-Shirane volcano (February 6, 2018)

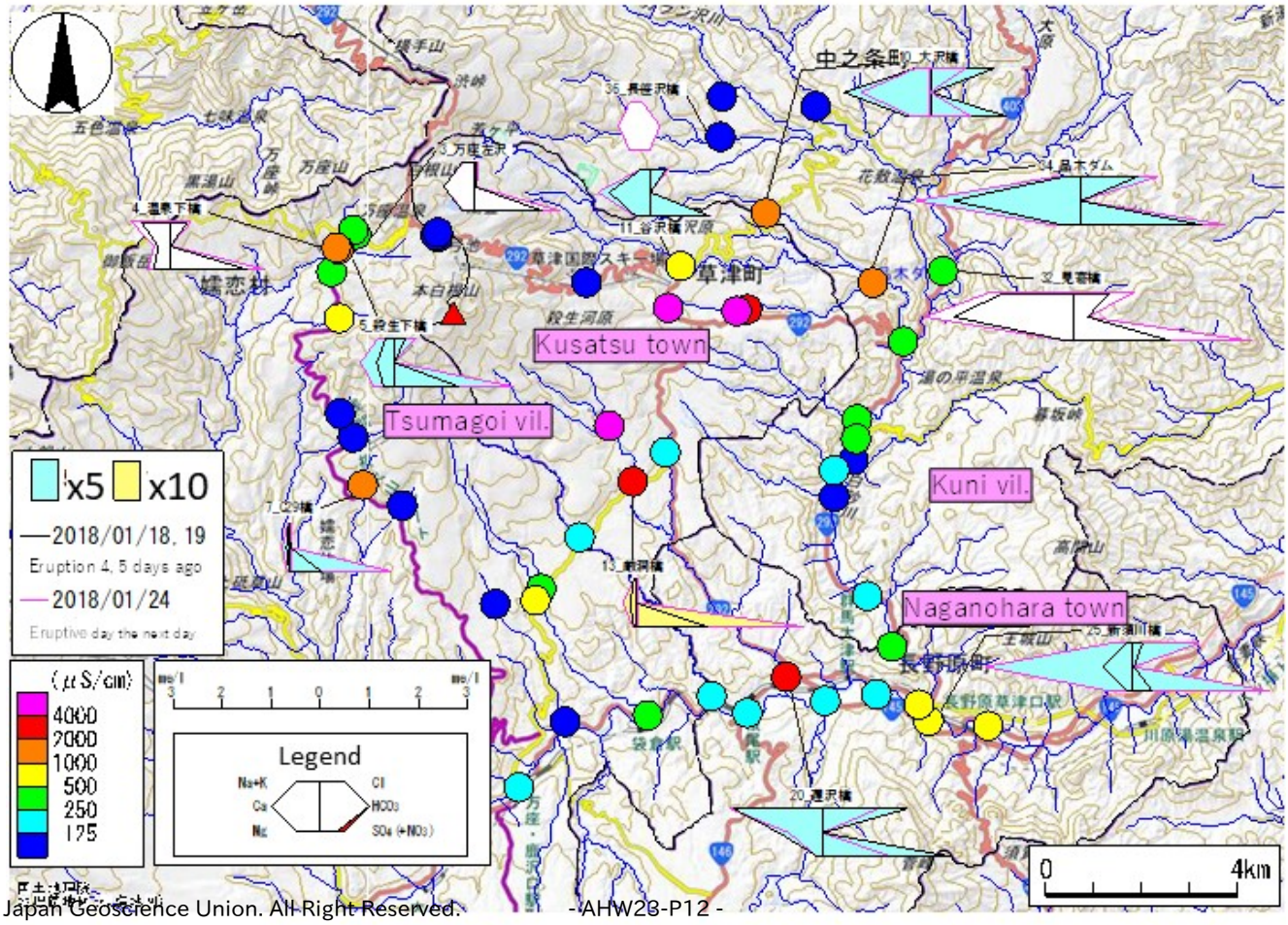

©2019. Japan Geoscience Union. All Right Reserved.

©2019. Japan Geoscience Union. All Right Reserved.

Re-consideration of discharge rate of spring water in Lake Ezu, Kumamoto

*Kimpei Ichiyanagi[1], Kiyoshi Ide[1], Jun Shimada[1], Tsutomu Ichikawa[2]

1. Kumamoto University, 2. Tokai University

In Kumamoto area, 100% of tap water is sourced from abundant groundwater. Recently, there is a great fear of groundwater level decreasing. To estimate discharge rete of spring water in Lake Ezu, the flow rate at 13 sites has been observed every month since December 1991. In previous studies, the total discharge rate of spring water was calculated by flow rates only at the most downstream, the most upper-stream, and incoming streams. In this study, total discharge rate from December 1991 to December 2014 was re-considered as a sum of three zones, that is upper-stream area, Kami-Ezu Lake, and Shimo-Ezu lake. When the discharge rate in each zone became negative, the case 1 where calculation was carried out with minus and the case 2 where it assumed to 0m^3/day were compared. As a result, total discharge rate gradually declined from about 450,000m^3/day in 1992 to about 360,000m^3/day (case 1) and to about 410,000m^3/day (case 2) in 2005. In July 2006, total discharge rate rapidly increased with heavy rainfall. After that, it had fluctuated about 400,000 to 500,000m^3/day in both cases. The discharge rate of Shimo-Ezu Lake sometimes became negative after 2003, and that averaged after July 2006 in case 2 was about 90,000m^3/day more than the case 1. As a result of comparing seasonal variability of discharge rate, monthly mean values of total and Shimo-Ezu Lake are low in April-May and high in October-November. However, monthly mean values of upper-stream area and Kami-Ezu Lake show no significant seasonal fluctuation. Monthly mean values of Shimo-Ezu Lake in August averaged after 2006 was about -14,000m^3/day in case 1 and about 32,000 m^3/day in case 2. Since negative value is not suitable to represent seasonal fluctuation, case 2 is proper to represent the discharge rate of spring water.

Keywords: spring water, Lake Ezu, long-term trend, seasonal variability

©2019. Japan Geoscience Union. All Right Reserved.

Evaluating the efficacy of hydrologically and hydrodynamically driven methods of e-flow assessment for Upper Godavari River Basin, India

*GAURAV KALIDAS PAKHALE[1], Jyoti Punjahari Nale[2], Ashvin Kumar Gosain[3], Rakesh Khosa[3]

1. PhD Research Scholar, Civil Engineering Department, Indian Institute of Technology, Delhi, 2. Project Advisor, IEWP, GIZ India, New Delhi, India, 3. Professor, Civil Engineering Department, Indian Institute of Technology, Delhi

In Peninsular India, pronounced seasonality in the precipitation and tropical semi-arid climate have compelled the tremendous development in the water resources sector. The major proportion of this fertile plateau falls in the rainshadow region of Western Ghats and is rightfully supported through enormous irrigation schemes which include the operation of several large reservoirs. These developments have resulted in alteration of various components of a natural hydrological regime like low as well as high flows. Environmental flows (e-flows), though acknowledged widely for their benefits, have not been attempted vigorously for peninsular river basins due to the prioritised issues related to water scarcity and disputes over water sharing. Also, many of these river streams have historically been known as non-perennial, thus further weakening the case of e-flows. Effectively, many recent e-flow assessments, have been observed to be elementary, quick and based on methods that are less intensive in terms of data and time requirements. In this view, the present study attempts to verify the efficiency of various hydrology and hydrodynamics-based e-flow assessment methods in one of such river basins, Upper Godavari River Basin. For this, hydrological observations of 16 sites with long term record availability (20 years or more) have been used and latest cross section data for these sites have been used for hydrodynamic computations.

Hydrological indices based on concepts like Percentage of Flow (POF) and Range of Variability Approach (RVA) have been estimated using a natural flow regime obtained from SWAT rainfall-runoff modelling. POF approaches like Tennant Method, Tessman Method, Variable Monthly Flow Methods are analysed while RVA approach has been analysed using Indicators of Hydrological Alteration (IHA) platform. These indices have been analysed for their feasibility and acceptability under the natural flow regime to understand the efficacy of these indices in providing optimum e-flow suggestions. Present observed flow regime has been juxtaposed with these indices to assess the present flow health in their comparison.

Hydrodynamic computations have been performed in HEC-RAS using 1-dimensional steady state conditions. Flow discharge versus flow depth, wetted perimeter, etc. relationships obtained for these study sites have been utilised to understand the critical flow levels which ensure the maximum bed inundations preferable for ecological sustainability. Wetted perimeter method of e-flow assessment has been evaluated for its suitability to provide the optimum e-flow suggestions. It has been found that hydrology based simple and quick methods of e-flow assessment fail the basic criteria of feasibility even under natural flow regime while hydrodynamic approach gives site-specific solutions which may not be relatable in longitudinal e-flow implementation.

Keywords: environmental flows, Range of Variability Approach, Wetted perimeter method

©2019. Japan Geoscience Union. All Right Reserved.

Presence of pharmaceutical compounds in freshwater lakes and their impact on phytoplankton

*Nandakumar Kanavillil[1], Cassandra Fligg[1], Sreekumari Kurissery[1]

1. Lakehead University, Canada

Historically, microalgae have been used as bio-indicators of aquatic health and this can be seen in several studies across the world. Often, at the bottom of the food chain microalgae constitute the primary producer of energy of many freshwater ecosystems. Diatoms, a group of microalgae, have been shown to exhibit extreme sensitivity to varying environmental parameters thereby making themselves an excellent candidate for studying the impacts of pollutants such as Pharmaceuticals and Personal Care Products (PPCPs). The contamination by PPCPs is common in our inland water bodies with a potential to get into our drinking water supply. This study explores the presence of PPCPs (Ibuprofen, 17-β Estradiol, and Triclosan) in the nearshore waters of Lake Simcoe, Ontario, Canada and their impacts on microalgal community. The study involved assessment of several environmental and algal parameters in the surrounding freshwater systems of three Waste Water Treatment Plants (WWTPs) that discharge their effluents *via* a creek/water channel to Lake Simcoe. Water samples were also drawn from a control location located away from the WWTPs. The results indicated that 1) PPCPs contamination is prevalent in the water outside of WWTPs (as far as the point of confluence with Lake Simcoe), and 2) The algal parameters varied according to the presence of PPCPs in the surface waters. Thus the study supported the growing concern of pharmaceutical contamination in the freshwater systems and its impacts on primary producers.

Keywords: Water quality, Bioindicators, Freshwater lakes, Pharmaceuticals, Phytoplankton

©2019. Japan Geoscience Union. All Right Reserved.

Novel approximate solutions for solute transport due to injections: considering the scale-dependent dispersion and non-integer flow dimension

*Ye-Chen Lin[1], Hund-Der Yeh[1]

1. National Chiao Tung Univ.

Prior research indicated that the flow dimension in a fractured medium may be of non-integer. In this article, we aim at developing a mathematical model for solute transport problems due to continuous or pulse injection in a non-integer dimensional flow field. The model allows the flow dimension ranging from linear flow to spherical flow. Our model also considers the effect of scale-dependent dispersion. The approximate solutions of the model are derived by applying the arrival times of mean and variance and validated through the comparison with finite-difference solutions of the present model. The results show that the approximate solutions give reasonable predictions when the value of dispersion or flow dimension is not large.

Keywords: solute transport, non-integer flow dimension, approximate solution, scale-dependent dispersion

©2019. Japan Geoscience Union. All Right Reserved.

Experimemtal study on the residual saturation of Porous Media using Pore Doublets Micromodel

*Chun-Wei Peng[1]

1. Taiwan National Chiao Tung University

In this study, we use a micromodel of PDM with different channel diameter ratios to study the fluid entrapment and mobilization. This study focuses on the evolution of the trapping and the amount of residuals saturation in the porous media. We observed the movement of wetting and non-wet liquids during the imbibition and drainage processes.We found that, with the low injection flow rates, the residual amount was strongly related to the contact angle; with the high injection flow rates, viscous force was dominated the trapping process. The results also showed that the liquids were trapped in the small tube for low injection rate, and in the large tube for the high injection rate. Our findings can help to control the residual saturation during water-flooding oil recovery, groundwater remediation, and the storage of carbon dioxide in deep subsurface.

©2019. Japan Geoscience Union. All Right Reserved.

Assessment of Synergy between Biomedical Waste and Shallow Groundwater Pollution

*Deepika -[1], Abhishek -[2]

1. BPS Government Medical College for Women, Sonepat, INDIA, 2. Technical University Dresden, GERMANY

Rapid urbanization and increasing population growth rate followed by the high rates of resource consumption patterns and increased waste generation have had an unintended negative impact on the prevailing environment. In a developing country like India where 50.34 % groundwater resources are not suitable for drinking as per WHO standards (United Nations, 2016), scrutinizing the open dumping of pathogenic biomedical waste becomes of paramount importance. Poor waste management practices pose a huge risk to the health of the public, patients, professionals and contribute to environmental degradation (land, air, and water pollution) if dumped untreated on the open ground. To assess this nexus, a prevalence study of the patients affected with waterborne diseases was conducted in a total of 35 hospitals comprising of government-, government-aided- and private hospitals of Ambala city. With a pronounced steppe climate, Ambala is located in North-Eastern (mean spatial coordinates: 30˚ 22' 41.4480" N and 76˚ 46' 36.1020" E) edge of Haryana, India. The city is drained by non-perennial streams and therefore the inhabitants depend solely on shallow groundwater resources for meeting their domestic water demand.

Data about the sources, quantity produced, treatment facilities, and awareness of biomedical waste, collected by questionnaire method based survey revealed that the mean waste generation was 8.08 kg/day with SD 5.371 kg/day. The biomedical waste consisted of approximately 1.2 % of the total municipal waste generated by the city and the patients affected with waterborne diseases were about 36 % of the total patients recorded. A latin hypercube Pareto distribution coupled with AMALGAM algorithm was employed for the initial sampling states of the proposals from the observed data (no. of patients). Thereafter, posterior estimates were generated using the Markov Chain Monte Carlo (MCMC) methods which showed a close fit with the observed and simulated data with RMSE 0.158. Furthermore, regression analysis with R^2=0.868 construed strong positive linear correlation between two variables viz. the number of patients and biomedical waste generated (and dumped). Recommendations are made for prioritizing the waste segregation and employing the indispensable management processes including waste treatment to avoid the further deterioration of the drinking water quality. The hospital authorities are advised to conduct the periodic seminars for enhancing awareness among the workforce from present 93.3 % to a maximum possible level.

Keywords: Groundwater, Biomedical waste, MCMC methods, Environmental awareness

©2019. Japan Geoscience Union. All Right Reserved.

Erosion and transport processes of earth surface materials in a reservoir-catchment system inferred from atmospheric radionuclides ^{7}Be and ^{210}Pb

*Mikiya Tsuruoka[1], Shinya Ochiai[2], Atsushi Matsuki[2], Seiya Nagao[2]

1. Graduate School of Natural Science and Technology, Kanazawa University, 2. Institute of Nature and Environmental Technology, Kanazawa University

Erosion and transport processes of earth surface materials are related to landform development in river catchment area and material discharge from the land area to the ocean. It is necessary to understand erosion and transport processes of earth surface materials to achieve proper management and prediction of river watershed and coastal area. However, since discharge behavior of earth surface materials in a large-scale river system is complicated by various processes, it is difficult to trace individual processes. On the other hand, earth surface materials eroded from catchment is transported and accumulated in reservoir. Therefore, discharge behavior of earth surface materials from catchment can be observed by monitoring of reservoir sediment. In this study, erosion and transport processes of earth surface materials in catchment were investigated based on atmospheric deposition flux to the catchment and sedimentation flux in the reservoir of ^{7}Be (half-life: 53 days) and ^{210}Pb (half-life: 22.3 years). From July 2016, rain water sample was collected every month with a collecting pan installed on the roof of Noto Atmospheric Observatory in Suzu City. ^{7}Be and ^{210}Pb in rain water were collected on ion exchange resins and measured with a Ge semiconductor detector to obtain atmospheric deposition fluxes. Sediment samples were collected with two sediment traps installed on the bottom of the reservoir (Shin-ike Reservoir) near the Noto Atmospheric Observatory at the same interval with rain sampling. Another trap was also set up in the middle layer (1.5 m above the bottom) since May 2018. Sediment samples were freeze-dried and measured with a Ge semiconductor detector to obtain sedimentation fluxes of ^{7}Be and ^{210}Pb. The atmospheric deposition fluxes of ^{7}Be and ^{210}Pb ranged 1.06-30.7 and 0.334-7.68 Bq/m^{2}/day, respectively. It shows clear seasonal fluctuation with high deposition in winter. The sedimentation fluxes of ^{7}Be in the bottom and middle layers were same level with the deposition flux. This result indicates that the contribution of ^{7}Be from the catchment is small. On the other hand, the sedimentation flux of ^{210}Pb in the middle layer was about 1.7-7.3 times higher than the atmospheric deposition flux of ^{210}Pb. This result suggests that sedimentation flux of ^{210}Pb in the middle layer reflects the contribution of ^{210}Pb from the catchment. The sedimentation flux of ^{210}Pb in the bottom layer was much higher than the atmospheric deposition flux, implying that sedimentation flux in the bottom was largely affected by resuspension in addition to the contribution of ^{210}Pb from the catchment. Residence time of these radionuclides in the reservoir-catchment system was estimated from the ^{7}Be/^{210}Pb$_{ex}$ ratios of rain water and sediment samples. The average residence times of the bottom layer samples and middle layer sample were estimated at 278 days and 141 days, respectively. This difference in the residence time may result from resuspension effect in the reservoir bottom.

Keywords: sediment, reservoir-catchment system, Be-7, Pb-210

©2019. Japan Geoscience Union. All Right Reserved.

Fluctuation of groundwater level in a sloping unconfined aquifer due to time varying recharge

*Ming-Chang Wu[1], Ping-Cheng Hsieh[1]

1. National Chung Hsing University

When a water-permeable slope is recharged by rainfall, the variation of the groundwater level is usually observed by setting up observation wells. However, the point observations are not sufficient to represent the vast domain of an aquifer and are constrained by the high cost of instrumentation and excavated wells. Therefore, the development of mathematical models for groundwater simulations can help us to understand the change of groundwater level more easily.
This study considers the variation of the groundwater level in a sloping aquifer with an impervious bottom. We divided the aquifer into two areas with and without rainfall recharge, and then use the nonlinear Boussinesq equation with a source term derived from the law of mass conservation. Analytical solutions to the nonlinear equation was acquired by the perturbation method for a finite region and a semi-infinite domain. After the transformation of variables, the general integral transformation method was used. The groundwater level varying with time under different factors (such as the dip angle of impervious bed, hydraulic conductivity, storage coefficient and different recharge rates) was discussed.
The present results were compared with the observed data from an observation well, and the difference in between was discussed. It is expected that the research results can better understand the physical mechanism of groundwater level change, and help to manage the groundwater.

Keywords: nonlinear Boussinesq equation, perturbation method, general integral transform method (GITM)

©2019. Japan Geoscience Union. All Right Reserved.

Effect of cutoff wall on recharge water storage volume

*Pei-hsun Tsai[1], Jung-hsing Tai[1]

1. Chaoyang University of Technology

Artificial groundwater recharge is used to increase groundwater in areas with water scarcity. Understanding the hydromechanical features of aquifers during groundwater withdrawal and recharge is necessary for managing groundwater resources effectively. In practice, an artificial pool can be used to collect surface runoff so that it infiltrates the aquifer and recharges groundwater. A cutoff wall can be constructed to seal recharge water and prevent it from flowing from the recharge area. Additional studies are required to understand the effect of the various parameters of cutoff walls on groundwater recharge. This study used the finite difference software FLAC 8.0 to examine the influence of the location and size of gaps of a cutoff wall on recharge water storage volume. Each aquifer was in an unsaturated state before groundwater recharging; therefore, groundwater recharge analyses were simulated by the two-phase flow in unsaturated porous media. The results revealed that when the groundwater layer was sand and the cutoff wall was not extended into the fully impermeable layer, the recharge water completely flowed from the gap between the bottom of the cutoff wall and the fully impermeable layer after stopping groundwater recharge. The recharge water volume related to the size of the gap at the bottom of the cutoff wall. When the cutoff wall was not extended into the groundwater layer, the cutoff wall did not intercept water. The gap at the top of the cutoff wall retained more recharge water compared with the gap at the bottom of the cutoff wall.

Keywords: Groundwater recharge, Cutoff wall, Water storage volume

©2019. Japan Geoscience Union. All Right Reserved.

Studying Operation Parameters on Flat-Plate Membrane Bioreactor for Sewage Treatment

*Jen Hung Chiu[1], Wen Chin Chen[1]

1. Studying Operation Parameters on Flat-Plate Membrane Bioreactor for Sewage Treatment

The flat-plate membrane bioreactor is applied to the domestic sewage treatment, which has a high quality of effluent than the traditional activated sludge process, and decreasing the susceptible of hair entanglement with the hollow fiber membrane. It has become a priority for recent sewage treatment applications.

A flat-plate membrane bioreactor pilot plant with a reaction volume of 4 m^3 was installed in the existing sewage treatment plant. In this research, the parallel treatment of the same influent water quality and hydraulic retention time was carried out to compare the treatment efficiency between the MBR and traditional activated sludge process, and the operational effects of the membrane flux were discussed.

With one year of long-term research, the average removal efficiencies of MBR process, regardless of the COD, SS and E.coli were over 99%, wchih was better than the activated sludge process only 90~95%. Meanwhile, the optimal operation mode of the MBR was obtained in the study. The aeration flow rate in the system was adjusted to 10~13 NL/min per film, the effluent flux was controlled under 50% of the maximum recommended flux of membrane with 9-minute operation and 1 minute stop in a cycle, there is no significant change in operating flux and pressure. These operational mode of MBR can extend the life time of membrane and effectively improve the application of flat-plate MBR to domestic sewage treatment.It is suggested that, in view of water treatment and resource sustainability, the flat plate MBR technology is feasible, and can serve as a green guide to the sewage treatment.

Keywords: Membrane Bioreactor, Flat-Plate Membrane, Sewage

©2019. Japan Geoscience Union. All Right Reserved.

Mine-water quality at a tertiary coalfield in India: Characterisation and treatment using novel polyvinyl alcohol (PVA) gel bioreactor

*Aparna Dutta[1], Sudipta Sarkar[1]

1. Indian Institute of Technology Roorkee

Nearly 78 percent of the total measured (proved) tertiary coal reserves of India is concentrated in the north-eastern state of Assam. The Tertiary coal of North–Eastern Coalfields (NEC) has been found to contain as high as 8% sulphur with varying percentage of pyrite, sulfate, organic and free sulphur. The pyrites are often associated with toxic heavy metals. Acid mine drainage (AMD) is generated when mining activities expose the pyrite and sulfides to atmospheric oxygen, moisture and micro-organisms that catalyse the oxidation process to release large amounts of sulfate into the mine water along with protons and dissolved metals. Microbial dissimilatory sulfate reduction (DSR) in the presence of a suitable organic carbon source can be engineered to treat such water. This study is significant because this region is rich in biodiversity and such mining impacted water may have adverse ecological impact, if discharged without appropriate treatment.The objective of the work is to characterise water samples collected from two open cast mines of Makum coalfield under NEC and evaluate the performance of a novel polyvinyl alcohol (PVA) gel packed bed bioreactor to treat the same. Sample collection, storage and physico-chemical analysis are carried out as per Standard methods of American Public Health Association. The biological treatment process is studied in a cylindrical continuous flow lab scale bioreactor under relevant acidic pH at different feed chemical oxygen demand (COD) to sulfate ratio and hydraulic retention time (HRT). Sludge from a lab scale anaerobic bioreactor treating very high sulfate industrial water is used as inoculum. The sulfate reducing microorganisms are enriched within the bioreactor in fed-batch mode using modified Postgate’ s medium for one month.Oxidation Reduction Potential (ORP), pH, sulfate removal, total inorganic carbon (TIC) and alkalinity produced are measured at the bioreactor outlet to evaluate the process performance. The mine water samples exhibit low pH, high sulfate, conductivity, dissolved solids, hardness, iron and manganese, which indicates the occurrence of AMD. The treatment process reduces the sulfate concentration and increases pH of the treated water. The use of highly porous PVA gel beads as packing material in the bioreactor treating sulfate rich acidic water imparts resilience to operational variation. The study evaluates the novel application of PVA gel beads to bioreactor for treating acidic mine waters from an ecologically important region. The research finding provides an understanding of the process for application to other biological AMD treatment configurations.

Keywords: acid mine drainage (AMD), polyvinyl alcohol (PVA), sulfate, sulfate reducing microorganism (SRM), dissimilatory sulfate reduction(DSR), pyrite

©2019. Japan Geoscience Union. All Right Reserved.

[E] Poster | A (Atmospheric and Hydrospheric Sciences)：A-HW Hydrology & Water Environment

Wed. May 29, 2019 5:15 PM - 6:30 PM JST | Wed. May 29, 2019 8:15 AM - 9:30 AM UTC | Poster Hall International Exhibition Hall8, Makuhari Messe_14

[A-HW23] Hydrology & Water Environment

convener:Isao Machida(Geological Survey of Japan), Dai Yamazaki(Institute of Industrial Sciences, The University of Tokyo), Takeshi Hayashi(Faculty of Education and Human Studies, Akita University), Keisuke Fukushi(Institute of Nature & Environmental Technology, Kanazawa University)

We focus on various issues of water cycle and environment and aim to answer questions of hydrological and earth system sciences including 1) surface, subsurface and evapotranspiration processes of water cycle; 2) natural and anthropogenic hydrothermal systems, 3) environments issues and studies on a watershed or global scale, 4) water-related issues with ecological, environmental, and geochemical aspects, and 5) other issues in hydrological sciences. This session welcomes presentations regarding various kinds of approaches and techniques such as field survey, remote sensing, isotope tracers, numerical simulation, and theoretical analysis.

[AHW23-P01] A multiobjective risk management model for real-time reservoir flood control operation

*Juan Chen[1,2], Ping-An Zhong[2], XinYu Wan[2], Yu Zhang[2] (1.College of Earth Sciences and Engineering, Hohai University, 2.College of Hydrology and Water Resources, Hohai University)

[AHW23-P02] Assessment of the Flow Regime of Roanoke River due to Climatic and Anthropogenic Activities

*Rahul Kumar Singh[1], Dr. Manoj Kumar Jain[1] (1.Indian Institute of Technology, Roorkee, India)

[AHW23-P03] Predictive Analysis of Climate, Water, Health and the Environment Nexus

*Abhishek [1], Deepika [2] (1.Technical University Dresden, GERMANY, 2.BPS Government Medical College for Women, Sonepat, INDIA)

[AHW23-P05] Severe droughts provide huge fuel for widespread wildfires in California in USA

*Linghua Qiu[1], Ji Chen[1], Haiyun Shi[2], Liqun Sun[3], Jun Niu[4] (1.the University of Hong Kong, 2.Southern University of Science and Technology, 3.Shenzhen Institutes of Advanced Technology, Chinese Academy of Sciences, 4.China Agricultural University)

[AHW23-P06] A comprehensive evaluation of MODIS-based water use efficiency with global eddy covariance flux data and a process model

*Shanshan YANG[1,2], Jiahua ZHANG[1], Sha ZHANG[1,2], Jingwen WANG[1,2], Yun BAI[1,2], Fengmei YAO[2], Huadong GUO[1] (1.Institute of Remote Sensing and Digital Earth, Chinese Academy of Sciences, 2.University of Chinese Academy of Sciences, Beijing, China)

[AHW23-P07] Impact of variability and anisotropy in the correlation decay distance for precipitation spatial interpolation in China

*yingxian zhang[1] (1.National Climate Center, China Meteorological Administration)

[AHW23-P08] New Record-Breaking Frequency of Annual Maximum Daily Precipitation of 58 stations in the whole Japan, an increasing of extreme values.

*Chhay Ngorn SEANG[1], Tomohito YAMADA[1] (1.Hokkaido University)

[AHW23-P09] Quantifying stemflow to better express its ecohydrological significance

*Shin'ichi Iida[1], Darryl E. Carlye-Moses[2], Sonja Germer[3], Pilar Llorens[4], Beate Michalzik[5], Kazuki Nanko[1], Alexander Tischer[5], Delphis F. Levia[6] (1.Department of Disaster Prevention, Meteorology and Hydrology, Forestry and Forest Products Research Institute, 2.Department of Geography and Environmental Studies, Thompson Rivers University, Kamloops, British Columbia, Canada, 3.Department of Bioengineering,

Leibniz Institute for Agricultural Engineering and Bioeconomy, Potsdam, Germany, 4.Institute of Environmental Assessment and Water Research (IDAEA-CSIC), Barcelona, Spain, 5.Soil Science, Institute of Geography, Friedrich Schiller University Jena, Jena, Germany, 6.Department of Geography and Department of Plant and Soil Sciences, University of Delaware, Newark, DE, USA)

[AHW23-P10] **Hydraulic analysis of overland flow caused by temporally varying rainfall**

*PING-CHENG HSIEH[1], Ming-Chang Wu[1] (1.National Chung Hsing University)

[AHW23-P11] A comparative Study on Water Environment of Isolated Islands - Focusing on Islands in Nagasaki Prefecture - (3)

*Go Yamaki[1], Koji Kodera[2], Kazuki Asami[1], Yoshihiro IGARI[1], Masaki Horiuchi[1] (1.Grad. Student, Hosei Univ., 2.Dep. of Geography, Hosei Univ.)

[AHW23-P12] **Water environment around Kusatsu-Shirane volcano and consideration of the effect of eruption in January 2018**

*Igari Yoshihiro[1], Koji Kodera[2], Kazuki Asami[1] (1.Grad.Student,Hosei Univ., 2.Dep.of Geography Hosei Univ.)

[AHW23-P13] Re-consideration of discharge rate of spring water in Lake Ezu, Kumamoto

*Kimpei Ichiyanagi[1], Kiyoshi Ide[1], Jun Shimada[1], Tsutomu Ichikawa[2] (1.Kumamoto University, 2.Tokai University)

[AHW23-P14] **Evaluating the efficacy of hydrologically and hydrodynamically driven methods of e-flow assessment for Upper Godavari River Basin, India**

*GAURAV KALIDAS PAKHALE[1], Jyoti Punjahari Nale[2], Ashvin Kumar Gosain[3], Rakesh Khosa[3] (1.PhD Research Scholar, Civil Engineering Department, Indian Institute of Technology, Delhi, 2.Project Advisor, IEWP, GIZ India, New Delhi, India, 3.Professor, Civil Engineering Department, Indian Institute of Technology, Delhi)

[AHW23-P15] Presence of pharmaceutical compounds in freshwater lakes and their impact on phytoplankton

*Nandakumar Kanavillil[1], Cassandra Fligg[1], Sreekumari Kurissery[1] (1.Lakehead University, Canada)

[AHW23-P16] **Novel approximate solutions for solute transport due to injections: considering the scale-dependent dispersion and non-integer flow dimension**

*Ye-Chen Lin[1], Hund-Der Yeh[1] (1.National Chiao Tung Univ.)

[AHW23-P17] Experimemtal study on the residual saturation of Porous Media using Pore Doublets Micromodel

*Chun-Wei Peng[1] (1.Taiwan National Chiao Tung University)

[AHW23-P18] Assessment of Synergy between Biomedical Waste and Shallow Groundwater Pollution

*Deepika [1], Abhishek [2] (1.BPS Government Medical College for Women, Sonepat, INDIA, 2.Technical University Dresden, GERMANY)

[AHW23-P19] Erosion and transport processes of earth surface materials in a reservoir-catchment system inferred from atmospheric radionuclides ^{7}Be and ^{210}Pb

*Mikiya Tsuruoka[1], Shinya Ochiai[2], Atsushi Matsuki[2], Seiya Nagao[2] (1.Graduate School of Natural Science and Technology, Kanazawa University, 2.Institute of Nature and Environmental Technology, Kanazawa University)

[AHW23-P20] Fluctuation of groundwater level in a sloping unconfined aquifer due to time varying recharge

*Ming-Chang Wu[1], Ping-Cheng Hsieh[1] (1.National Chung Hsing University)

[AHW23-P21] **Effect of cutoff wall on recharge water storage volume**

*Pei-hsun Tsai[1], Jung-hsing Tai[1] (1.Chaoyang University of Technology)

[AHW23-P22] **Studying Operation Parameters on Flat-Plate Membrane Bioreactor for Sewage Treatment**

*Jen Hung Chiu[1], Wen Chin Chen[1] (1.Studying Operation Parameters on Flat-Plate Membrane Bioreactor for Sewage Treatment)

[AHW23-P23] **Mine-water quality at a tertiary coalfield in India: Characterisation and treatment using novel polyvinyl alcohol (PVA) gel bioreactor**

*Aparna Dutta[1], Sudipta Sarkar[1] (1.Indian Institute of Technology Roorkee)

A multiobjective risk management model for real-time reservoir flood control operation

*Juan Chen[1,2], Ping-An Zhong[2], XinYu Wan[2], Yu Zhang[2]

1. College of Earth Sciences and Engineering, Hohai University, 2. College of Hydrology and Water Resources, Hohai University

Many uncertainties exit in the real-time reservoir flood control operation and bring risks to flood control decisions. A multiobjective optimization model is developed for the real-time risk management for the flood control operation of a reservoir system considering multiple uncertainties such as inflow forecast errors and outflow errors. The two competing objectives considered are: (1) minimizing the risk of reservoir upstream flooding and (2) minimizing the risk of downstream flooding. The optimization model seeks to find the operation schedules that satisfy the flood control objectives and simultaneously minimize the overall risks. The decision variables are the hourly reservoir releases. The formulated multiobjective optimization problem is nonlinear and non-convex, and is solved with an improved Non-dominated Sorting Genetic Algorithm-II (INSGA-II). We use a filtering algorithm to select representative non-dominated solutions from the Pareto front generated by INSGA-II to assist in real-time decision making. The proposed risk management model is applied to the Foziling reservoir in Huaihe river basin of China. The results show that the proposed method can provide a practical way to optimize the real-time flood control operation for risk management of a reservoir.

Keywords: Flood, Reservoir, Flood control operation, Risk assessment, Multiobjective optimization

©2019. Japan Geoscience Union. All Right Reserved.

Assessment of the Flow Regime of Roanoke River due to Climatic and Anthropogenic Activities

*Rahul Kumar Singh[1], Dr. Manoj Kumar Jain[1]

1. Indian Institute of Technology, Roorkee, India

The natural flow regime of many rivers around the world has been significantly altered due to climatic and anthropogenic modifications such as the construction of dams and reservoirs. The natural flow regime plays an important role in the development of the riverine ecosystem. Therefore, quantification of the extent of the alterations in the natural flow regime would be helpful in the river’ s ecological assessment. The Roanoke River in southeastern United States had one of the biggest and least disturbed forest ecosystems but due to climatic changes and anthropogenic actions such as construction of dam, artificial regulations of the natural flow regime, the overall riverine ecosystem has severely impacted. In this study, SWAT (Soil Water Assessment Tool) has been used to reconstruct the long-term unaltered streamflow for a hypothetical no-dam scenario condition, in order to assess the impact of climate change as well as due to construction of the John H Kerr reservoir on Roanoke River streamflow from 1956-2012. In order to simulate the unaltered streamflow series post construction of John H Kerr reservoir, 32 years (1916-1948) of observed gauge inflow prior to anthropogenic disturbance (due to construction of John H Kerr Reservoir) was used for calibration and validation of the parameters of the SWAT model. Historical land use and land cover backcasting data for the year 1938 has been used in the hydrological model to simulate the flow regime prior to construction of the dam and it was kept same during the whole simulation period. The SWAT model simulated observed gauge data with Nash-Sutcliffe efficiency coefficient (NSE) = 0.70, Percent bias (PBIAS) = 0.00 and the determination coefficient (R^2) = 0.73 during the calibration period (1916 - 1936), and performed equally better during the validation period (1937-1948) with NSE = 0.72, PBIAS = 0.00 and R^2 = 0.74. The indicators of hydrologic alteration (IHA) methodology has been used to assess the natural flow regime (no dam or reservoir moderated flow regime) characteristics under a simulated no-reservoir scenario (scenario1) and compare with the IHA results obtained based on the gauged streamflow downstream of the dam (scenario2). Hence, in case of scenario 1, the post-impact period has been taken as the simulated flow series using SWAT model from 1956-2012 and in case of scenario 2 the post-impact period has been taken as the gauged observed streamflow from 1956-2012 at Roanoke Rapids gauging station downstream of the reservoir. The pre-impact period for both the scenario was kept the same i.e. from 1912 to 1949. The results reveal that in case of the IHA assessment based on scenario 1, significant alterations have been observed in 5 out of 32 indicators compared to 13 out 32 indicators in case of scenario 2. The overall hydrologic alteration in case of scenario 1 was 45.65% and it was 55.17% in the case of scenario 2. The alteration during the scenario 1 could be attributed to the overall natural climatic variability. The results also indicate that flow variability in terms of high and low flows were better in scenario 1 compared to scenario 2 where the high flows were completely absorbed including the low pulse count and duration due to regulation in the flow. However, the reservoir operations enhanced the monthly flows including the multiday minima low flows. Thus, the present method can be treated as an easy-to-implement comprehensive approach for designing natural flow regimes to mimic the pre-impact flow condition in order to restore the ecosystem of modified rivers due to anthropogenic interventions.

Keywords: SWAT, IHA, Streamflow, Hydrologic Alteration, Ecosystem

©2019. Japan Geoscience Union. All Right Reserved.

Predictive Analysis of Climate, Water, Health and the Environment Nexus

*Abhishek -[1], Deepika -[2]

1. Technical University Dresden, GERMANY, 2. BPS Government Medical College for Women, Sonepat, INDIA

Amid the major demographic transition of developing world from a rural, agrarian society to an urban, industrial one, there is a need for predictive analytics of impact of the major biotic and abiotic stressors on the environmental constituents. The current study emphasizes the connections between climate, water, environment, and health and their interdependency followed by an impact assessment focusing on an urban environment. A data-driven hybrid framework for water resources assessment and management based on machine learning techniques was developed, calibrated and validated with the ground data for the sub-region scale of North-East Indian regime (mean spatial coordinates: 28° 38' 41.2800" N and 77° 13' 0.1956" E). The remote sensing data for land cover and land change were coupled with the climate model simulations to formulate the health risk assessment framework. The large ensemble of downscaled scenario based outputs including the effects of anthropogenic factors was used to drive the hybrid model framework.

Multi-dimensional Random Walk Metropolis (RWM) algorithms used to optimize the sample observations converged with an RMSE error of 0.18 with a range of 0.006. Pearson Product Moment Correlation coefficient range of all the ensemble members was 0.886-0.904. The prediction accuracy construed from 95 % model uncertainty bounds was 89-91 % for the constituent parameters. The sensitivity analysis revealed that the climate is the key parameter and is the most sensitive for all other linkage units followed by water availability and health factors. Comparative analysis of the simulated- and experimental results enforced comprehensive clarification of the assumptions made therein. By real-time monitoring and forecasting the vital impacts, this research will serve and benefit local policymakers and in the decision-making process, particularly regarding water resources vulnerability and future availability with significant economic consequences. The upscaling of the model form sub-regional to regional scale is well underway.

Keywords: Climate Change, Urbanization, RWM algorithm, Ensemble model

©2019. Japan Geoscience Union. All Right Reserved.

Severe droughts provide huge fuel for widespread wildfires in California in USA

*Linghua Qiu[1], Ji Chen[1], Haiyun Shi[2], Liqun Sun[3], Jun Niu[4]

1. the University of Hong Kong, 2. Southern University of Science and Technology, 3. Shenzhen Institutes of Advanced Technology, Chinese Academy of Sciences, 4. China Agricultural University

The frequently occurred large wildfires in California caught the public’ s attention in recent years and the ability to identify and prevent such disasters is pressing. The study built the rational relationship between soil moisture and vegetation based on remote sensing, hydrology and wildfire data during 2001-2017 in California. The purpose is to estimate the effects of droughts on wildfires and to detect the valid fuel for wildfires. The study results reported that severe droughts could cause huge fuel for wildfires and made them even much more widespread and longer sustained. The consequences could provide significant information for identification and prevention of future wildfires in California and even other regions in the world.

Keywords: Fuel, Wildfires, Droughts, Soil moisture, Vegetation

©2019. Japan Geoscience Union. All Right Reserved.

A comprehensive evaluation of MODIS-based water use efficiency with global eddy covariance flux data and a process model

*Shanshan YANG[1,2], Jiahua ZHANG[1], Sha ZHANG[1,2], Jingwen WANG[1,2], Yun BAI[1,2], Fengmei YAO[2], Huadong GUO[1]

1. Institute of Remote Sensing and Digital Earth, Chinese Academy of Sciences, 2. University of Chinese Academy of Sciences, Beijing, China

Ecosystem water use efficiency (WUE), defined as the ratio of gross primary productivity (GPP) to evapotranspiration (ET), is an important indicator to investigate the interaction between the terrestrial carbon and water cycles. The spatiotemporal patterns of WUE inferred from MODIS GPP and ET products and its responses to environmental factors have been analyzed, however, the accuracy of MODIS-derived WUE (MODIS WUE) has not been well evaluated. In this study, we evaluated monthly and annual MODIS WUE using global covariance flux data (FLUXNET2015 dataset) during 2000-2014, and conducted global intercomparisons (2001-2011) among annual WUE from MODIS, gridded FLUXNET (MTE) and a process model (BESS). Site scale (53 sites) evaluation results revealed that MODIS gave reliable estimates for GPP and ET, however, the performances of MODIS WUE was poor for monthly WUE (R2=0.14) and even worse for annual WUE (R2=0.08). MODIS WUE was generally underestimated with a bias of -0.21 gC kg-1 H2O (-8.43%) and RMSE of 1.20 gC kg-1 H2O for monthly WUE, and a bias of -0.28 gC kg-1 H2O (-11.31%) and RMSE of 0.98 gC kg-1 H2O for annual WUE. Among all land cover types, MODIS WUE performed relatively better in savannas and woody savannas for monthly WUE and grasslands for annual WUE, but significantly overestimated WUE in open shrublands. Likewise, MODIS WUE was obviously overestimated in hot and cold semiarid and arid climate zones. The global intercomparison results demonstrated that the spatial pattern of MODIS WUE was broadly similar to that of MTE and BESS WUE, except for the tropical and subtropical arid and semiarid areas. In these regions MODIS WUE showed extremely high values with large uncertainty and different linear trends compared with MTE and BESS WUE. These disagreements were mainly caused by the discrepancies in MODIS ET. Therefore, the uncertainty of MODIS WUE in the tropical arid and semiarid areas should be taken with caution when using MODIS WUE to investigate and interpret how WUE varies spatially and its responses to climate change. Furthermore, the accuracy of MODIS GPP and ET datasets should be paid extra attention since the quality of both GPP and ET would directly affect the WUE accuracy.

Keywords: Water use efficiency (WUE), Evaluation, Intercomparison, MODIS, FLUXNET, BESS

©2019. Japan Geoscience Union. All Right Reserved.

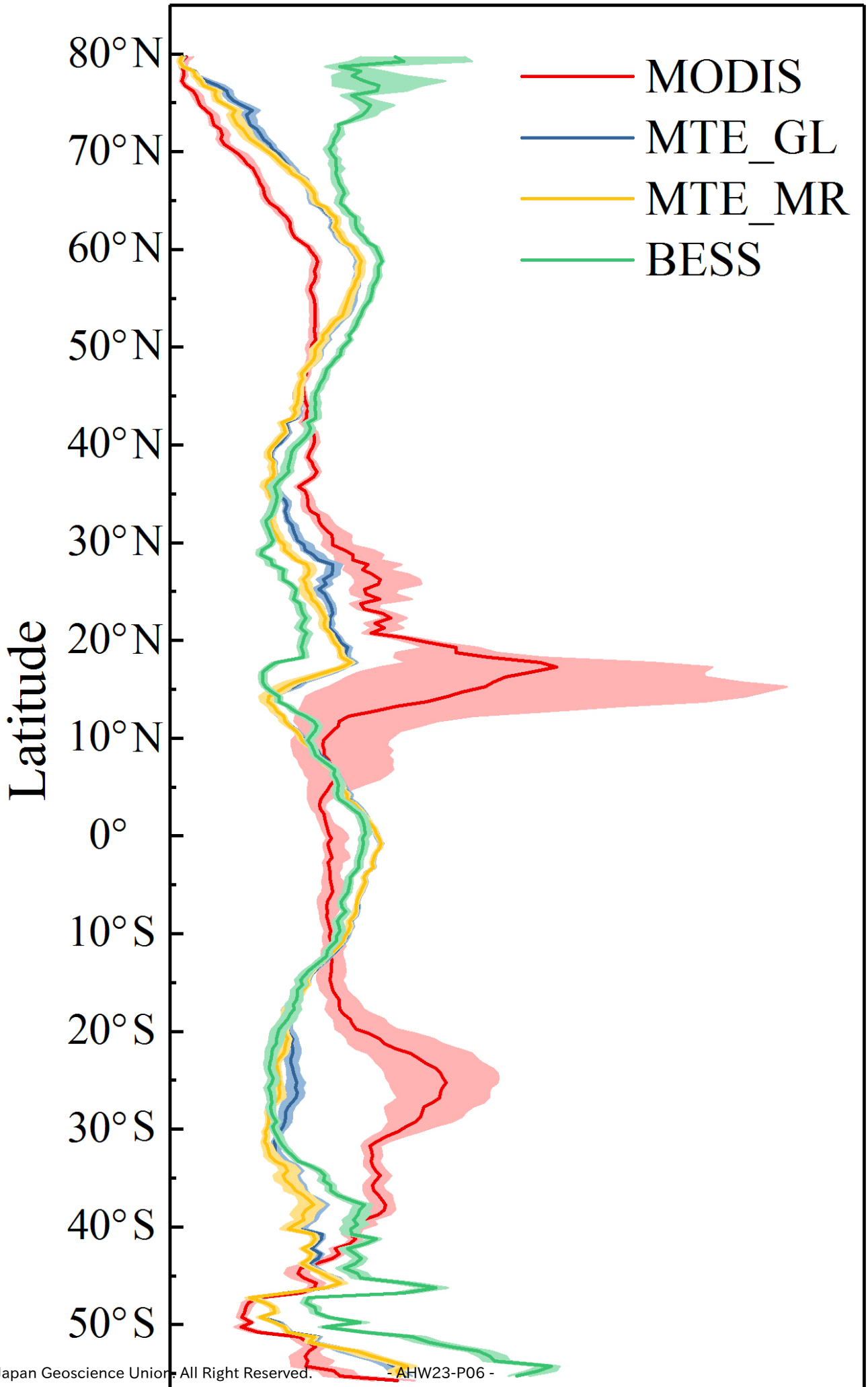

©2019. Japan Geoscience Union. All Right Reserved.

©2019. Japan Geoscience Union. All Right Reserved.

Impact of variability and anisotropy in the correlation decay distance for precipitation spatial interpolation in China

*yingxian zhang[1]

1. National Climate Center, China Meteorological Administration

The correlation decay distance (CDD) plays a key role in the angular-distance weighting (ADW) interpolation technique, being used as the searching radius to select correlated neighbors and to calculate the relative weights. The CDD of daily precipitation in China varies spatially and seasonally, and it presents anisotropic behavior, as a result of topography and the predominant atmospheric circulation. In general, CDD is largest in winter and smallest in summer, except for limited regions such as the Tibetan plateau. From a cross validation analysis, it is found that taking account of spatial and seasonal variations in CDD generally improves the ADW interpolation. Utilization of anisotropic CDDs increases the interpolation skill scores in regions with a dense monitoring network, significant elevation variation (southwestern China) or strongly anisotropic CDDs (Tibetan plateau).

Keywords: daily precipitation, correlation decay distance, ADW interpolation

©2019. Japan Geoscience Union. All Right Reserved.

New Record-Breaking Frequency of Annual Maximum Daily Precipitation of 58 stations in the whole Japan, an increasing of extreme values.

*Chhay Ngorn SEANG[1], Tomohito YAMADA[1]

1. Hokkaido University

The changes in daily temperature extremes in global scale have affected the weather and climate extreme events when there is an increase of greenhouse gas GHG compare to the industrialization in the 19th century (IPCC, 2014). Yamada et al. (2014) illustrate that the water vapor and convective instability follow the Clausius-Clapeyron-like rate of change with 99th percentile hourly precipitation intensity. Lehmann, J. et al. (2015), on another hand, studied globally the characteristic of precipitation change anomaly using a relation of the Clausius-Clapeyron model. By the way, the climate change tends to include another factor, which is more statistical base. The theory of record values in independent and identically distributed (i.i.d) random variable is studied more extensively and is more applicable with an assumption of stationary climate. The Clausius-Clapeyron equation is then also applicable base on the thermodynamic term which illustrates the relation of the temperature, vapor pressure and precipitation formation characteristic which also mentioned in the above previous studies. At the first stage, 58 stations of AMeDAS data with 117-years period across Japan are used for this analysis. The result shows that mean long-term precipitation of these 58 stations is higher than the mean value from theory i.i.d random variable of stationary climate. From this result, it can be implied that the change of precipitation in Japan is influenced by the drift term either of climate change or the heat island. In this case, the Clausius-Clapeyron equation is applied to identify the temperature term of change. This study tries to formulate a theory which more statistical base of climate drifts, non-stationary and non-identically to extreme events in accordance with time series. Clausius-Clapeyron Model and the Linear Drift Model is considered to form an empirical stochastically based on climate trend.

Keywords: Clausius-Clapeyron, New record Breaking, i.i.d

©2019. Japan Geoscience Union. All Right Reserved.

Quantifying stemflow to better express its ecohydrological significance

*Shin'ichi Iida[1], Darryl E. Carlye-Moses[2], Sonja Germer[3], Pilar Llorens[4], Beate Michalzik[5], Kazuki Nanko[1], Alexander Tischer[5], Delphis F. Levia[6]

1. Department of Disaster Prevention, Meteorology and Hydrology, Forestry and Forest Products Research Institute, 2. Department of Geography and Environmental Studies, Thompson Rivers University, Kamloops, British Columbia, Canada, 3. Department of Bioengineering, Leibniz Institute for Agricultural Engineering and Bioeconomy, Potsdam, Germany, 4. Institute of Environmental Assessment and Water Research (IDAEA-CSIC), Barcelona, Spain, 5. Soil Science, Institute of Geography, Friedrich Schiller University Jena, Jena, Germany, 6. Department of Geography and Department of Plant and Soil Sciences, University of Delaware, Newark, DE, USA

Stemflow is the flow of rainwater over the exterior of a tree stem to its base. Due to water balance calculations to obtain interception loss of forest stands, and the sometimes low percentage of stemflow as a function of rainfall, some literature ignores the ecohydrological significance of stemflow. However, stemflow is much more concentrated than throughfall per unit area. In recognition of the extreme amounts of water input to the small area around tree trunks, we advocate for two metrics to better express stemflow in relation to its ecohydrological importance: namely, the stand-scale funneling ratio and the stand-scale infiltration funneling ratio. We calculated these metrics based on measurements carried out in a tropical dry deciduous forest and a subpolar juvenile coniferous stand, and found that these are significantly larger than throughfall on both sites. The data cited from recent papers (n=34) showed that very small stand-scale amount of stemflow (approximately 0.5% on average) were necessary to make the stand-scale funneling ratio to be equal or more than unity. Moreover, the infiltration area of stemflow is generally < 0.2 m^2 due to the high infiltration capacity of top soil of forests, generally resulting in the stand-scale infiltration funneling ratio substantially greater than unity. Thus, stemflow is more effective for soil water recharge than throughfall. We recommend use of these metrics to better express ecohydrological importance of stemflow.

This presentation is based on the published paper as follows:
Carlye-Moses, D.E., Iida, S., Germer, S., Llorens, P., Michalzik, B., Nanko, K., Tischer, A., Levia, D.F. (2018): Expressing stemflow commensurate with its ecohydrological importance. Advances in Water Resources, 121, 472-479. Free open access article to: https://doi.org/10.1016/j.advwatres.2018.08.015

Keywords: Stemflow, Funneling ratio, Forest hydrology

©2019. Japan Geoscience Union. All Right Reserved.

Hydraulic analysis of overland flow caused by temporally varying rainfall

*PING-CHENG HSIEH[1], Ming-Chang Wu[1]

1. National Chung Hsing University

With the development of human civilization and population migration, we use many different types of pervious or impervious materials to cover the original surface. As a result, the surface friction and water permeability are reduced, resulting in increased flow velocity and runoff, and thus increasing the frequency and scale of flood occurrence. Therefore, predicting changes in overland flow caused by rainfall has become an important issue.

This study intends to simulate the overland flow under different rainfall patterns by the theory of diffusion wave model. The diffusion wave equation was used as the governing equation, and an analytical solution of the water depth by the generalized integral transformation method was presented. Since the values of the parameters used in previous research for diffusion wave models vary in an extensive range. In this study, the parameters were adjusted for each location to ensure the rationality of the simulation results according to the law of mass conservation.
The results show that for the non-uniform rainfall, the peak water depth and peak flow due to the post-peak rainfall are the largest, followed by the third quarter peak rainfall; whereas the average flow velocity of the mid-peak rainfall is the largest, followed by the third quarter peak rainfall. The peak water depth, peak flow rate and average flow rate due to the double peak rainfall are the smallest among the six rainfall patterns in this study.

Keywords: overland flow, nonuniform rainfall, diffusion wave

©2019. Japan Geoscience Union. All Right Reserved.

A comparative Study on Water Environment of Isolated Islands - Focusing on Islands in Nagasaki Prefecture - (3)

*Go Yamaki[1], Koji Kodera[2], Kazuki Asami[1], Yoshihiro IGARI[1], Masaki Horiuchi[1]

1. Grad. Student, Hosei Univ., 2. Dep. of Geography, Hosei Univ.

1. Introduction Research on islands in Nagasaki prefecture has hardly been investigated and research has been promoted since 2014 from Goto Island Islands, Tsushima, Iki, Hirado. For this time, we will clarify the water environment in each area from the relationship with land use and climate, and make it a foothold to clarify the material cycle of each island.

2. Target area Iki is rugged with a maximum altitude of 213 m, and there are numerous reservoirs in various parts of the island. In Tsushima, the altitude of the entire island is relatively high, and the mountains occupy about 89%. The Goto Islands Island consists of about 140 large and small islands, with large geological differences on each island. The Hirado Islands have many mountains while the fields are also relatively large. The population penetration rate of wastewater treatment in both areas is as low as 20-40%.

3. Research method Field survey was conducted 2 to 4 times a year from 2014 after organizing and examining existing research. On the site, water temperature, temperature, electric conductivity (EC), pH and RpH, COD were measured, and water was taken to measure the total organic carbon and the main dissolved components.

4. Results and discussion In Iki, the influence of agriculture appears in EC and TOC, but it is interesting that there is almost no effect of nitric acid. On the other hand, although many nitric acid was detected in the Goto Islands, it is thought that factors are due to paddy fields in Iki and upland fields in Goto Islands. Tsushima showed relatively low concentrations of EC and dissolved components, and seasonal changes also appeared. In Hirado Island, especially in the southern part, the geological influence is large in many places, the impact of sea salt is strong in Ikitsuki island and Azuchi Oshima. EC tends to rise in rainwater from October to March, pH tends to decrease. From the above, it is considered that the difference in the quality of the islands is greatly influenced by the difference of geology, topography and agricultural form.

Keywords: Iki island, Tsushima islands, Goto islands, Hirado islands, Water environment

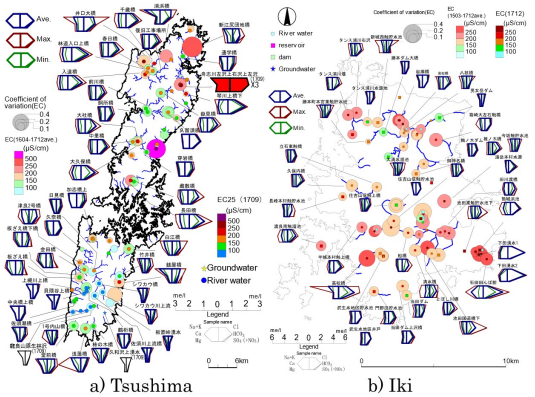

a) Tsushima b) Iki c) Hirado

Fig.1 Water quality

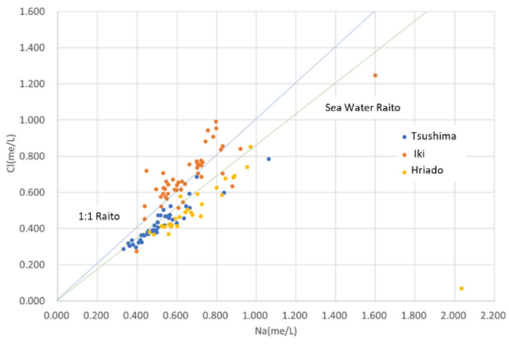

Fig.2 Na / Cl ratio

©2019. Japan Geoscience Union. All Right Reserved.

Water environment around Kusatsu-Shirane volcano and consideration of the effect of eruption in January 2018

*Igari Yoshihiro[1], Koji Kodera[2], Kazuki Asami[1]

1. Grad.Student,Hosei Univ., 2. Dep.of Geography Hosei Univ.

1. Introduction

The eruption (steam explosion) occurred in Mt.Motoshirane (One of Kusatsu-Shirane Volcano) on January 23, 2018. In this area, water quality survey of water environment began in May 2017 before the eruption. In addition to examining the influence on the water quality before and after the eruption, we studied the elution component of volcanic ash and the influence on the water environment. We also attempted to consider water quality forming factors in river water around Kusatsu-Shirane volcano.

2. Research method

We conducted about 21 field surveys from May 2017 to March 2019. The survey site is about 45 sites, centering on rivers flowing in the east and south of the mountain. Temperature, water temperature, pH, RpH, EC, and flow rate were measured locally, and the sampled sample was analyzed for the main dissolved components. In February 2018, we investigated the deposition situation and ash fall volume of volcanic ash and conducted sampling, and carried out dissolution experiment. In addition to rivers, field surveys and sampling of lakes and precipitation, snow cover, hot spring water were conducted.

3. Results and discussion

In Shirasuna River flowing to the east side of the mountain, groundwater and river water influenced by hot spring drainage and volcanic activity flow in from the tributary. There are points where the EC value fluctuates greatly, and it is influenced by the discharge and conduction of the dam which stores the neutralizing water of acidic rivers. In the Gando Swamp where the site of sulfur mine is located in the upstream part, the water quality is around pH:2.0, EC:6000 μS/cm. It is conceivable that the deposited volcanic ash affects the quality of the surrounding river due to snow melting water and precipitation.

Keywords: Mt.Kusatsu-Shirane, Volcano, Water environment, Eruption, Hot spring

©2019. Japan Geoscience Union. All Right Reserved.

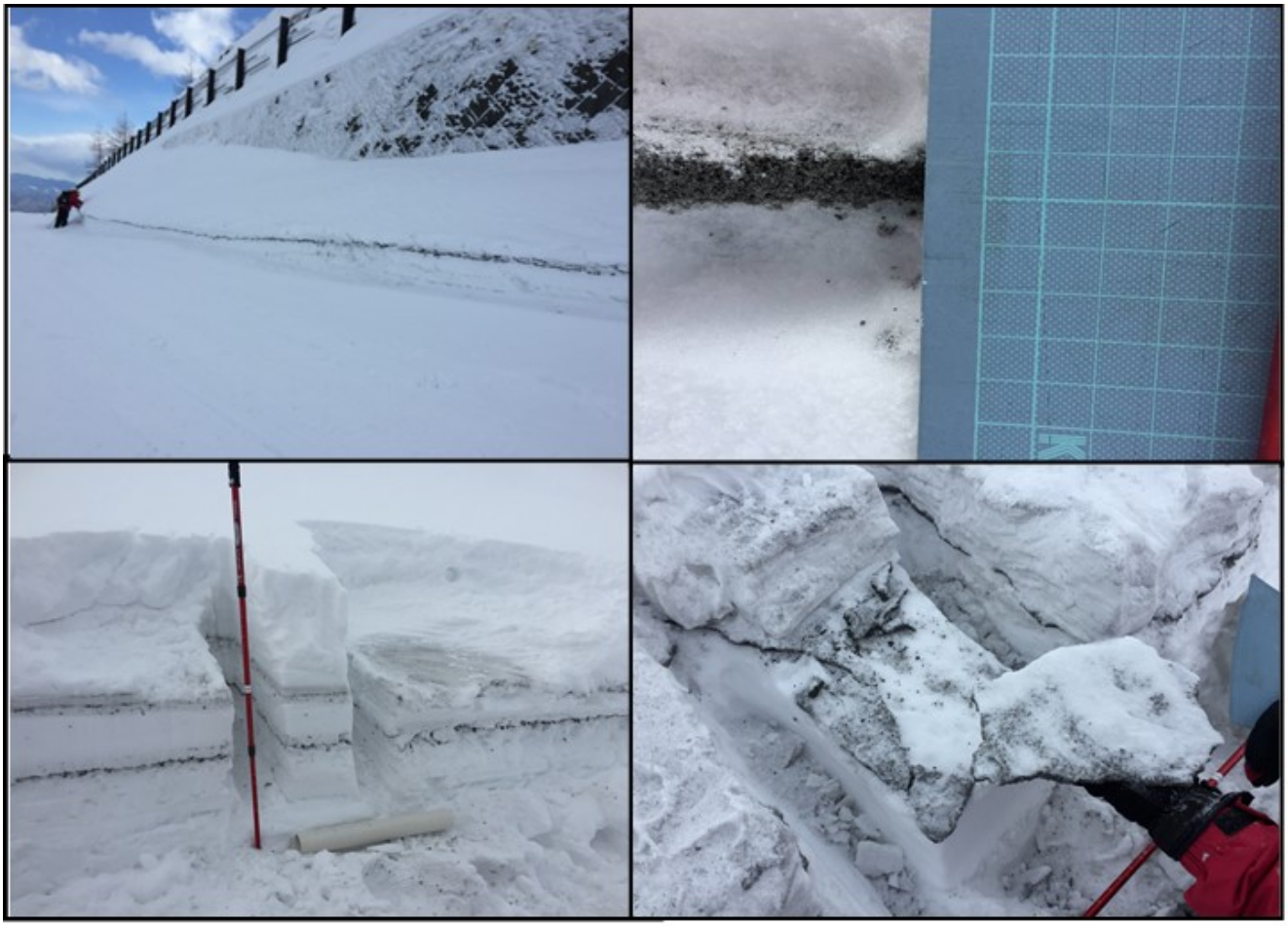

Picture.1 Ash fall in the east foot of Kusatsu-Shirane volcano (February 6, 2018)

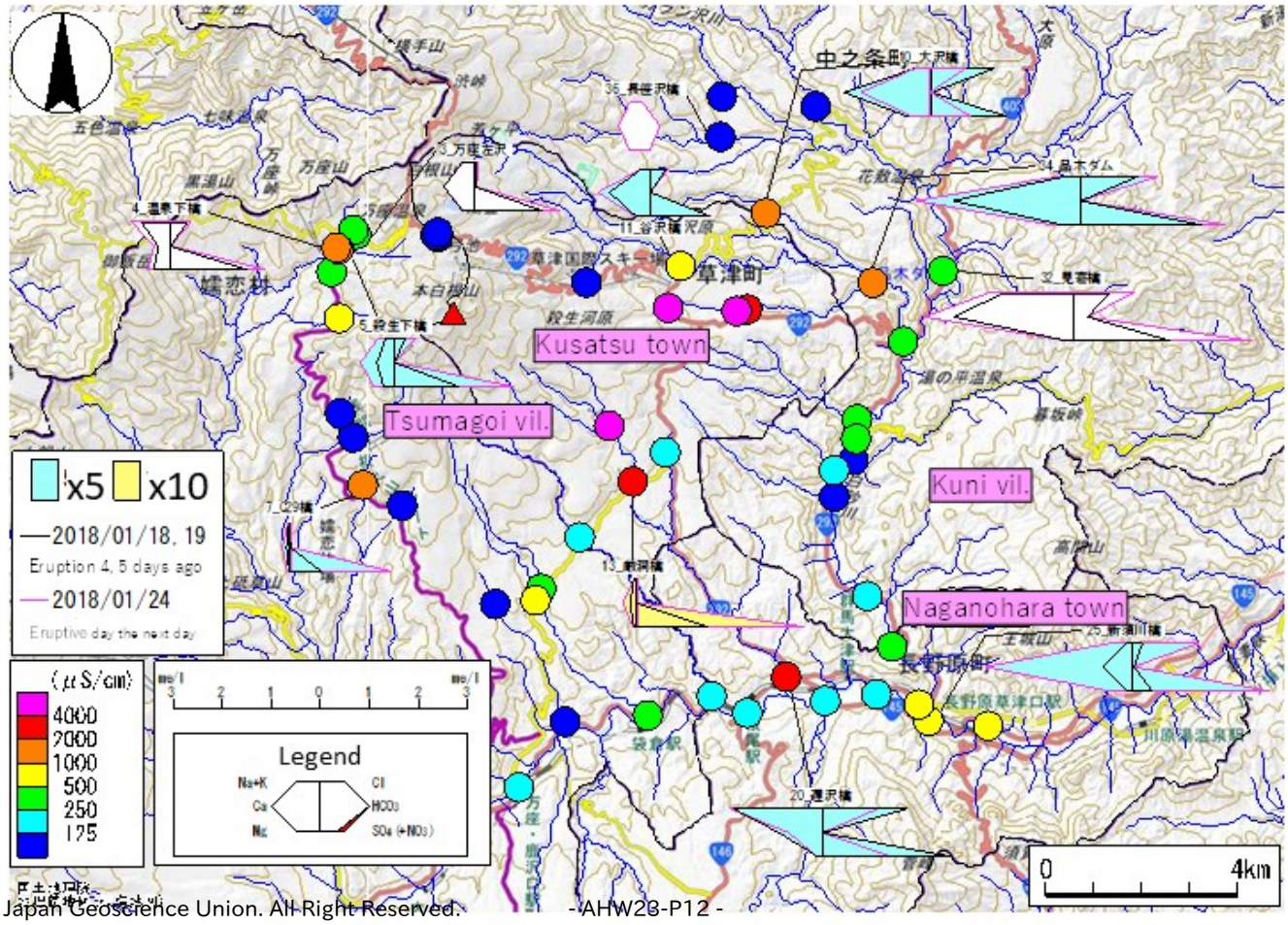

©2019. Japan Geoscience Union. All Right Reserved.

©2019. Japan Geoscience Union. All Right Reserved.

Re-consideration of discharge rate of spring water in Lake Ezu, Kumamoto

*Kimpei Ichiyanagi[1], Kiyoshi Ide[1], Jun Shimada[1], Tsutomu Ichikawa[2]

1. Kumamoto University, 2. Tokai University

In Kumamoto area, 100% of tap water is sourced from abundant groundwater. Recently, there is a great fear of groundwater level decreasing. To estimate discharge rete of spring water in Lake Ezu, the flow rate at 13 sites has been observed every month since December 1991. In previous studies, the total discharge rate of spring water was calculated by flow rates only at the most downstream, the most upper-stream, and incoming streams. In this study, total discharge rate from December 1991 to December 2014 was re-considered as a sum of three zones, that is upper-stream area, Kami-Ezu Lake, and Shimo-Ezu lake. When the discharge rate in each zone became negative, the case 1 where calculation was carried out with minus and the case 2 where it assumed to 0m^3/day were compared. As a result, total discharge rate gradually declined from about 450,000m^3/day in 1992 to about 360,000m^3/day (case 1) and to about 410,000m^3/day (case 2) in 2005. In July 2006, total discharge rate rapidly increased with heavy rainfall. After that, it had fluctuated about 400,000 to 500,000m^3/day in both cases. The discharge rate of Shimo-Ezu Lake sometimes became negative after 2003, and that averaged after July 2006 in case 2 was about 90,000m^3/day more than the case 1. As a result of comparing seasonal variability of discharge rate, monthly mean values of total and Shimo-Ezu Lake are low in April-May and high in October-November. However, monthly mean values of upper-stream area and Kami-Ezu Lake show no significant seasonal fluctuation. Monthly mean values of Shimo-Ezu Lake in August averaged after 2006 was about -14,000m^3/day in case 1 and about 32,000 m^3/day in case 2. Since negative value is not suitable to represent seasonal fluctuation, case 2 is proper to represent the discharge rate of spring water.

Keywords: spring water, Lake Ezu, long-term trend, seasonal variability

©2019. Japan Geoscience Union. All Right Reserved.

Evaluating the efficacy of hydrologically and hydrodynamically driven methods of e-flow assessment for Upper Godavari River Basin, India

*GAURAV KALIDAS PAKHALE[1], Jyoti Punjahari Nale[2], Ashvin Kumar Gosain[3], Rakesh Khosa[3]

1. PhD Research Scholar, Civil Engineering Department, Indian Institute of Technology, Delhi, 2. Project Advisor, IEWP, GIZ India, New Delhi, India, 3. Professor, Civil Engineering Department, Indian Institute of Technology, Delhi

In Peninsular India, pronounced seasonality in the precipitation and tropical semi-arid climate have compelled the tremendous development in the water resources sector. The major proportion of this fertile plateau falls in the rainshadow region of Western Ghats and is rightfully supported through enormous irrigation schemes which include the operation of several large reservoirs. These developments have resulted in alteration of various components of a natural hydrological regime like low as well as high flows. Environmental flows (e-flows), though acknowledged widely for their benefits, have not been attempted vigorously for peninsular river basins due to the prioritised issues related to water scarcity and disputes over water sharing. Also, many of these river streams have historically been known as non-perennial, thus further weakening the case of e-flows. Effectively, many recent e-flow assessments, have been observed to be elementary, quick and based on methods that are less intensive in terms of data and time requirements. In this view, the present study attempts to verify the efficiency of various hydrology and hydrodynamics-based e-flow assessment methods in one of such river basins, Upper Godavari River Basin. For this, hydrological observations of 16 sites with long term record availability (20 years or more) have been used and latest cross section data for these sites have been used for hydrodynamic computations.

Hydrological indices based on concepts like Percentage of Flow (POF) and Range of Variability Approach (RVA) have been estimated using a natural flow regime obtained from SWAT rainfall-runoff modelling. POF approaches like Tennant Method, Tessman Method, Variable Monthly Flow Methods are analysed while RVA approach has been analysed using Indicators of Hydrological Alteration (IHA) platform. These indices have been analysed for their feasibility and acceptability under the natural flow regime to understand the efficacy of these indices in providing optimum e-flow suggestions. Present observed flow regime has been juxtaposed with these indices to assess the present flow health in their comparison.

Hydrodynamic computations have been performed in HEC-RAS using 1-dimensional steady state conditions. Flow discharge versus flow depth, wetted perimeter, etc. relationships obtained for these study sites have been utilised to understand the critical flow levels which ensure the maximum bed inundations preferable for ecological sustainability. Wetted perimeter method of e-flow assessment has been evaluated for its suitability to provide the optimum e-flow suggestions. It has been found that hydrology based simple and quick methods of e-flow assessment fail the basic criteria of feasibility even under natural flow regime while hydrodynamic approach gives site-specific solutions which may not be relatable in longitudinal e-flow implementation.

Keywords: environmental flows, Range of Variability Approach, Wetted perimeter method

©2019. Japan Geoscience Union. All Right Reserved.

Presence of pharmaceutical compounds in freshwater lakes and their impact on phytoplankton

*Nandakumar Kanavillil[1], Cassandra Fligg[1], Sreekumari Kurissery[1]

1. Lakehead University, Canada

Historically, microalgae have been used as bio-indicators of aquatic health and this can be seen in several studies across the world. Often, at the bottom of the food chain microalgae constitute the primary producer of energy of many freshwater ecosystems. Diatoms, a group of microalgae, have been shown to exhibit extreme sensitivity to varying environmental parameters thereby making themselves an excellent candidate for studying the impacts of pollutants such as Pharmaceuticals and Personal Care Products (PPCPs). The contamination by PPCPs is common in our inland water bodies with a potential to get into our drinking water supply. This study explores the presence of PPCPs (Ibuprofen, 17-β Estradiol, and Triclosan) in the nearshore waters of Lake Simcoe, Ontario, Canada and their impacts on microalgal community. The study involved assessment of several environmental and algal parameters in the surrounding freshwater systems of three Waste Water Treatment Plants (WWTPs) that discharge their effluents *via* a creek/water channel to Lake Simcoe. Water samples were also drawn from a control location located away from the WWTPs. The results indicated that 1) PPCPs contamination is prevalent in the water outside of WWTPs (as far as the point of confluence with Lake Simcoe), and 2) The algal parameters varied according to the presence of PPCPs in the surface waters. Thus the study supported the growing concern of pharmaceutical contamination in the freshwater systems and its impacts on primary producers.

Keywords: Water quality, Bioindicators, Freshwater lakes, Pharmaceuticals, Phytoplankton

©2019. Japan Geoscience Union. All Right Reserved.

Novel approximate solutions for solute transport due to injections: considering the scale-dependent dispersion and non-integer flow dimension

*Ye-Chen Lin[1], Hund-Der Yeh[1]

1. National Chiao Tung Univ.

Prior research indicated that the flow dimension in a fractured medium may be of non-integer. In this article, we aim at developing a mathematical model for solute transport problems due to continuous or pulse injection in a non-integer dimensional flow field. The model allows the flow dimension ranging from linear flow to spherical flow. Our model also considers the effect of scale-dependent dispersion. The approximate solutions of the model are derived by applying the arrival times of mean and variance and validated through the comparison with finite-difference solutions of the present model. The results show that the approximate solutions give reasonable predictions when the value of dispersion or flow dimension is not large.

Keywords: solute transport, non-integer flow dimension, approximate solution, scale-dependent dispersion

©2019. Japan Geoscience Union. All Right Reserved.

Experimemtal study on the residual saturation of Porous Media using Pore Doublets Micromodel

*Chun-Wei Peng[1]

1. Taiwan National Chiao Tung University

In this study, we use a micromodel of PDM with different channel diameter ratios to study the fluid entrapment and mobilization. This study focuses on the evolution of the trapping and the amount of residuals saturation in the porous media. We observed the movement of wetting and non-wet liquids during the imbibition and drainage processes.We found that, with the low injection flow rates, the residual amount was strongly related to the contact angle; with the high injection flow rates, viscous force was dominated the trapping process. The results also showed that the liquids were trapped in the small tube for low injection rate, and in the large tube for the high injection rate. Our findings can help to control the residual saturation during water-flooding oil recovery, groundwater remediation, and the storage of carbon dioxide in deep subsurface.

©2019. Japan Geoscience Union. All Right Reserved.

Assessment of Synergy between Biomedical Waste and Shallow Groundwater Pollution

*Deepika -[1], Abhishek -[2]

1. BPS Government Medical College for Women, Sonepat, INDIA, 2. Technical University Dresden, GERMANY

Rapid urbanization and increasing population growth rate followed by the high rates of resource consumption patterns and increased waste generation have had an unintended negative impact on the prevailing environment. In a developing country like India where 50.34 % groundwater resources are not suitable for drinking as per WHO standards (United Nations, 2016), scrutinizing the open dumping of pathogenic biomedical waste becomes of paramount importance. Poor waste management practices pose a huge risk to the health of the public, patients, professionals and contribute to environmental degradation (land, air, and water pollution) if dumped untreated on the open ground. To assess this nexus, a prevalence study of the patients affected with waterborne diseases was conducted in a total of 35 hospitals comprising of government-, government-aided- and private hospitals of Ambala city. With a pronounced steppe climate, Ambala is located in North-Eastern (mean spatial coordinates: 30˚ 22' 41.4480" N and 76˚ 46' 36.1020" E) edge of Haryana, India. The city is drained by non-perennial streams and therefore the inhabitants depend solely on shallow groundwater resources for meeting their domestic water demand.

Data about the sources, quantity produced, treatment facilities, and awareness of biomedical waste, collected by questionnaire method based survey revealed that the mean waste generation was 8.08 kg/day with SD 5.371 kg/day. The biomedical waste consisted of approximately 1.2 % of the total municipal waste generated by the city and the patients affected with waterborne diseases were about 36 % of the total patients recorded. A latin hypercube Pareto distribution coupled with AMALGAM algorithm was employed for the initial sampling states of the proposals from the observed data (no. of patients). Thereafter, posterior estimates were generated using the Markov Chain Monte Carlo (MCMC) methods which showed a close fit with the observed and simulated data with RMSE 0.158. Furthermore, regression analysis with R^2=0.868 construed strong positive linear correlation between two variables viz. the number of patients and biomedical waste generated (and dumped). Recommendations are made for prioritizing the waste segregation and employing the indispensable management processes including waste treatment to avoid the further deterioration of the drinking water quality. The hospital authorities are advised to conduct the periodic seminars for enhancing awareness among the workforce from present 93.3 % to a maximum possible level.

Keywords: Groundwater, Biomedical waste, MCMC methods, Environmental awareness

©2019. Japan Geoscience Union. All Right Reserved.

Erosion and transport processes of earth surface materials in a reservoir-catchment system inferred from atmospheric radionuclides ^{7}Be and ^{210}Pb

*Mikiya Tsuruoka[1], Shinya Ochiai[2], Atsushi Matsuki[2], Seiya Nagao[2]

1. Graduate School of Natural Science and Technology, Kanazawa University, 2. Institute of Nature and Environmental Technology, Kanazawa University

Erosion and transport processes of earth surface materials are related to landform development in river catchment area and material discharge from the land area to the ocean. It is necessary to understand erosion and transport processes of earth surface materials to achieve proper management and prediction of river watershed and coastal area. However, since discharge behavior of earth surface materials in a large-scale river system is complicated by various processes, it is difficult to trace individual processes. On the other hand, earth surface materials eroded from catchment is transported and accumulated in reservoir. Therefore, discharge behavior of earth surface materials from catchment can be observed by monitoring of reservoir sediment. In this study, erosion and transport processes of earth surface materials in catchment were investigated based on atmospheric deposition flux to the catchment and sedimentation flux in the reservoir of ^{7}Be (half-life: 53 days) and ^{210}Pb (half-life: 22.3 years). From July 2016, rain water sample was collected every month with a collecting pan installed on the roof of Noto Atmospheric Observatory in Suzu City. ^{7}Be and ^{210}Pb in rain water were collected on ion exchange resins and measured with a Ge semiconductor detector to obtain atmospheric deposition fluxes. Sediment samples were collected with two sediment traps installed on the bottom of the reservoir (Shin-ike Reservoir) near the Noto Atmospheric Observatory at the same interval with rain sampling. Another trap was also set up in the middle layer (1.5 m above the bottom) since May 2018. Sediment samples were freeze-dried and measured with a Ge semiconductor detector to obtain sedimentation fluxes of ^{7}Be and ^{210}Pb. The atmospheric deposition fluxes of ^{7}Be and ^{210}Pb ranged 1.06-30.7 and 0.334-7.68 Bq/m^{2}/day, respectively. It shows clear seasonal fluctuation with high deposition in winter. The sedimentation fluxes of ^{7}Be in the bottom and middle layers were same level with the deposition flux. This result indicates that the contribution of ^{7}Be from the catchment is small. On the other hand, the sedimentation flux of ^{210}Pb in the middle layer was about 1.7-7.3 times higher than the atmospheric deposition flux of ^{210}Pb. This result suggests that sedimentation flux of ^{210}Pb in the middle layer reflects the contribution of ^{210}Pb from the catchment. The sedimentation flux of ^{210}Pb in the bottom layer was much higher than the atmospheric deposition flux, implying that sedimentation flux in the bottom was largely affected by resuspension in addition to the contribution of ^{210}Pb from the catchment. Residence time of these radionuclides in the reservoir-catchment system was estimated from the ^{7}Be/^{210}Pb$_{ex}$ ratios of rain water and sediment samples. The average residence times of the bottom layer samples and middle layer sample were estimated at 278 days and 141 days, respectively. This difference in the residence time may result from resuspension effect in the reservoir bottom.

Keywords: sediment, reservoir-catchment system, Be-7, Pb-210

©2019. Japan Geoscience Union. All Right Reserved.

Fluctuation of groundwater level in a sloping unconfined aquifer due to time varying recharge

*Ming-Chang Wu[1], Ping-Cheng Hsieh[1]

1. National Chung Hsing University

When a water-permeable slope is recharged by rainfall, the variation of the groundwater level is usually observed by setting up observation wells. However, the point observations are not sufficient to represent the vast domain of an aquifer and are constrained by the high cost of instrumentation and excavated wells. Therefore, the development of mathematical models for groundwater simulations can help us to understand the change of groundwater level more easily.
This study considers the variation of the groundwater level in a sloping aquifer with an impervious bottom. We divided the aquifer into two areas with and without rainfall recharge, and then use the nonlinear Boussinesq equation with a source term derived from the law of mass conservation. Analytical solutions to the nonlinear equation was acquired by the perturbation method for a finite region and a semi-infinite domain. After the transformation of variables, the general integral transformation method was used. The groundwater level varying with time under different factors (such as the dip angle of impervious bed, hydraulic conductivity, storage coefficient and different recharge rates) was discussed.
The present results were compared with the observed data from an observation well, and the difference in between was discussed. It is expected that the research results can better understand the physical mechanism of groundwater level change, and help to manage the groundwater.

Keywords: nonlinear Boussinesq equation, perturbation method, general integral transform method (GITM)

©2019. Japan Geoscience Union. All Right Reserved.

Effect of cutoff wall on recharge water storage volume

*Pei-hsun Tsai[1], Jung-hsing Tai[1]

1. Chaoyang University of Technology

Artificial groundwater recharge is used to increase groundwater in areas with water scarcity. Understanding the hydromechanical features of aquifers during groundwater withdrawal and recharge is necessary for managing groundwater resources effectively. In practice, an artificial pool can be used to collect surface runoff so that it infiltrates the aquifer and recharges groundwater. A cutoff wall can be constructed to seal recharge water and prevent it from flowing from the recharge area. Additional studies are required to understand the effect of the various parameters of cutoff walls on groundwater recharge. This study used the finite difference software FLAC 8.0 to examine the influence of the location and size of gaps of a cutoff wall on recharge water storage volume. Each aquifer was in an unsaturated state before groundwater recharging; therefore, groundwater recharge analyses were simulated by the two-phase flow in unsaturated porous media. The results revealed that when the groundwater layer was sand and the cutoff wall was not extended into the fully impermeable layer, the recharge water completely flowed from the gap between the bottom of the cutoff wall and the fully impermeable layer after stopping groundwater recharge. The recharge water volume related to the size of the gap at the bottom of the cutoff wall. When the cutoff wall was not extended into the groundwater layer, the cutoff wall did not intercept water. The gap at the top of the cutoff wall retained more recharge water compared with the gap at the bottom of the cutoff wall.

Keywords: Groundwater recharge, Cutoff wall, Water storage volume

©2019. Japan Geoscience Union. All Right Reserved.

Studying Operation Parameters on Flat-Plate Membrane Bioreactor for Sewage Treatment

*Jen Hung Chiu[1], Wen Chin Chen[1]

1. Studying Operation Parameters on Flat-Plate Membrane Bioreactor for Sewage Treatment

The flat-plate membrane bioreactor is applied to the domestic sewage treatment, which has a high quality of effluent than the traditional activated sludge process, and decreasing the susceptible of hair entanglement with the hollow fiber membrane. It has become a priority for recent sewage treatment applications.

A flat-plate membrane bioreactor pilot plant with a reaction volume of 4 m^3 was installed in the existing sewage treatment plant. In this research, the parallel treatment of the same influent water quality and hydraulic retention time was carried out to compare the treatment efficiency between the MBR and traditional activated sludge process, and the operational effects of the membrane flux were discussed.

With one year of long-term research, the average removal efficiencies of MBR process, regardless of the COD, SS and E.coli were over 99%, wchih was better than the activated sludge process only 90~95%. Meanwhile, the optimal operation mode of the MBR was obtained in the study. The aeration flow rate in the system was adjusted to 10~13 NL/min per film, the effluent flux was controlled under 50% of the maximum recommended flux of membrane with 9-minute operation and 1 minute stop in a cycle, there is no significant change in operating flux and pressure. These operational mode of MBR can extend the life time of membrane and effectively improve the application of flat-plate MBR to domestic sewage treatment.It is suggested that, in view of water treatment and resource sustainability, the flat plate MBR technology is feasible, and can serve as a green guide to the sewage treatment.

Keywords: Membrane Bioreactor, Flat-Plate Membrane, Sewage

©2019. Japan Geoscience Union. All Right Reserved.

Mine-water quality at a tertiary coalfield in India: Characterisation and treatment using novel polyvinyl alcohol (PVA) gel bioreactor

*Aparna Dutta[1], Sudipta Sarkar[1]

1. Indian Institute of Technology Roorkee

Nearly 78 percent of the total measured (proved) tertiary coal reserves of India is concentrated in the north-eastern state of Assam. The Tertiary coal of North–Eastern Coalfields (NEC) has been found to contain as high as 8% sulphur with varying percentage of pyrite, sulfate, organic and free sulphur. The pyrites are often associated with toxic heavy metals. Acid mine drainage (AMD) is generated when mining activities expose the pyrite and sulfides to atmospheric oxygen, moisture and micro-organisms that catalyse the oxidation process to release large amounts of sulfate into the mine water along with protons and dissolved metals. Microbial dissimilatory sulfate reduction (DSR) in the presence of a suitable organic carbon source can be engineered to treat such water. This study is significant because this region is rich in biodiversity and such mining impacted water may have adverse ecological impact, if discharged without appropriate treatment.The objective of the work is to characterise water samples collected from two open cast mines of Makum coalfield under NEC and evaluate the performance of a novel polyvinyl alcohol (PVA) gel packed bed bioreactor to treat the same. Sample collection, storage and physico-chemical analysis are carried out as per Standard methods of American Public Health Association. The biological treatment process is studied in a cylindrical continuous flow lab scale bioreactor under relevant acidic pH at different feed chemical oxygen demand (COD) to sulfate ratio and hydraulic retention time (HRT). Sludge from a lab scale anaerobic bioreactor treating very high sulfate industrial water is used as inoculum. The sulfate reducing microorganisms are enriched within the bioreactor in fed-batch mode using modified Postgate’ s medium for one month.Oxidation Reduction Potential (ORP), pH, sulfate removal, total inorganic carbon (TIC) and alkalinity produced are measured at the bioreactor outlet to evaluate the process performance. The mine water samples exhibit low pH, high sulfate, conductivity, dissolved solids, hardness, iron and manganese, which indicates the occurrence of AMD. The treatment process reduces the sulfate concentration and increases pH of the treated water. The use of highly porous PVA gel beads as packing material in the bioreactor treating sulfate rich acidic water imparts resilience to operational variation. The study evaluates the novel application of PVA gel beads to bioreactor for treating acidic mine waters from an ecologically important region. The research finding provides an understanding of the process for application to other biological AMD treatment configurations.

Keywords: acid mine drainage (AMD), polyvinyl alcohol (PVA), sulfate, sulfate reducing microorganism (SRM), dissimilatory sulfate reduction(DSR), pyrite

©2019. Japan Geoscience Union. All Right Reserved.

[E] Poster | A (Atmospheric and Hydrospheric Sciences)：A-CG Complex & General

Wed. May 29, 2019 10:45 AM - 12:15 PM JST | Wed. May 29, 2019 1:45 AM - 3:15 AM UTC | Poster Hall International Exhibition Hall8, Makuhari Messe_6

[A-CG35] Projection and detection of global environmental change

convener:Michio Kawamiya(Japan Agency for Marine-Earth Science and Technology), Hiroaki Tatebe(Japan Agency for Marine-Earth Science and Technology), Kaoru Tachiiri(Japan Agency for Marine-Earth Science and Technology)

Anthropogenic forcings on global environment are expected to cause intensification of extreme events, sea level rise, ocean acidification and deoxygenation, as well as large-scale ecosystem changes. The CMIP6 experimental protocol has been established based on which modeling groups across the world are starting to provide environmental projection data toward 6th IPCC assessment report due in 2021. Various new types of studies, such as event attribution and coupling of socio-economic processes and Earth system dynamics, are also emerging in the field of global change projection. In addition, observational studies are becoming increasingly more important for grasping changes in the global environment and evaluating model projections. Interactions and collaborations beyond boundaries of conventional scientific disciplines are desired for dealing with the issue of global changes. This session thus aims to deepen our understanding on global change, from both disciplinary and interdisciplinary viewpoints. This session is co-organized by AIMES - Future Earth project "Analysis, Integration and Modelling of the Earth System" (https://aimesproject.org/).

[ACG35-P01] World Regionalization of Climate Change (1961–2010)

*Shao Sun[1,2], Peijun Shi[2,3,4], Daoyi Gong[2], Tao Zhou[2] (1.National Climate Center, China Meteorological Administration, Beijing 100081, China, 2.State Key Laboratory of Earth Surface Processes and Resource Ecology, Beijing Normal University, Beijing 100875, China, 3.Key Laboratory of Environmental Change and Natural Disaster of Ministry of Education, Beijing Normal University, Beijing 100875, China, 4.Academy of Disaster Reduction and Emergency Management, Ministry of Civil Affairs & Ministry of Education, Beijing 100875, China)

[ACG35-P02] Quantifying and identifying future climate signal, noise, and internal variability at finer temporal scales

*Jongho Kim[1], Manh Van Doi[1] (1.University of Ulsan)

[ACG35-P03] Basic evaluation of MIROC6 and current status of CMIP6 experiments

*Hiroaki Tatebe[1] (1.Japan Agency for Marine-Earth Science and Technology)

[ACG35-P04] Synchronized increase of extreme cold and warm events in China during the recent global warming slowdown

*Xiubao Sun[1,3], Chunzai Wang[1], Guoyu Ren[2,3], Panfeng Zhang[2] (1.State Key Laboratory of Tropical Oceanography (LTO), South China Sea Institute of Oceanology(SCSIO), Chinese Academy of Sciences (CAS), 2.Department of Atmospheric Science, School of Environmental Studies, China University of Geosciences (CUG), 3.Laboratory for Climate Studies, National Climate Center (NCC), China Meteorological Administration (CMA))

[ACG35-P05] Quantification of thermodynamical and dynamical contributions to the anthropogenic influences on tropical cyclone rainfall extremes

*Cheng-Ta Chen[1], Shih-How Lo[1], Chung-Chieh Wang[1], Kazuhisa Tsuboki[2] (1.Department of Earth Sciences, National Taiwan Normal University, 2.Hydrospheric-Atmospheric Research Center, Nagoya University)

[ACG35-P06] Temporal Evolution of the Long-Term Distributional Biases of Climate Models as a Parameter for the Regional Evaluation of the Simulation of Climate Change

*Martin Gomez-Garcia[1], Akiko Matsumura[1], Shiro Hishinuma[1], Daikichi Ogawada[1] (1.Nippon Koei Co. Ltd., Reasearch and Development Center)

[ACG35-P07] A global simulation of bioenergy crop yield

*Zhipin Ai[1], Naota Hanasaki[1] (1.National Institute for Environmental Studies)

[ACG35-P08] Integrated Research Program for Advancing Climate Models - Theme B: national research program in Japan on earth system modeling

*Michio Kawamiya[1], Tomohiro Hajima[1], Kaoru Tachiiri[1], Jun'ichi Tsutsui[2], Tokuta Yokohata[3], Takashi Arakawa[4], Takahiro Inoue[4] (1.Japan Agency for Marine-Earth Science and Technology, 2.Central Research Institute of Electric Power Industry, 3.National Institute for Environmental Studies, 4.Research Organization for Information Science and Technology)

[ACG35-P09] Towards probabilistic climate projections based on the CMIP6 multi-model ensemble

*Junichi Tsutsui[1] (1.Central Research Institute of Electric Power Industry)

[ACG35-P10] Effect on the earth system of realizing 1.5 degree climate target by overshooting after reaching 2 degree level

*Kaoru Tachiiri[1], Herran Diego Silva[2], Xuanming Su[1], Michio Kawamiya[1] (1.Japan Agency for Marine-Earth Science and Technology, 2.Institute for Global Environmental Strategies)

[ACG35-P11] **Historical regional and sectoral contributions to climate change**

*Xuanming Su[1], Kaoru Tachiiri[1], Katsumasa TANAKA[2], Michio Watanabe[1] (1.Japan Agency for Marine-Earth Science and Technology, 2.National Institute for Environmental Studies)

[ACG35-P12] **Future projection of global climate, water, food, bio-energy, and land investigated with MIROC-INTEG: a global bio-geophysical land surface model with human components**

*Tokuta Yokohata[1], Yusuke Satoh[1], Tsuguki Kinoshita[2], Gen Sakurai[3], Yadu Pokhrel[4], Akihiko Ito[1], Etsushi Kato[5], Masashi Okada[1], Naota Hanasaki[1], Tomoko Nitta[6], Seita Emori[1] (1.National Institute for Environmental Studies, 2.Ibaraki University, 3.National Agriculture and Food Research Organization, 4.Michigan State University, 5.The Institute of Applied Energy, 6.University of Tokyo)

[ACG35-P13] **Downscaling a global agricultural land use model to country level for national SSP analysis**

*Wenchao Wu[1], Tomoko Hasegawa[1], Kiyoshi Takahashi[1], Shinichiro Fujimori[2] (1.National Institute for Environmental Studies, 2.Kyoto Univ.)

[ACG35-P14] Extreme Events and Emergent Trends in Marine Ecosystem Stressors under a historical/RCP8.5 Climate Change Pathway

*Keith Bradley Rodgers[1,2], Sarah Schlunegger[3], Richard Slater[3], Burke Hales[4], Axel Timmermann[1,2] (1.IBS Center for Climate Physics, Busan, South Korea, 2.Pusan National University, Busan, South Korea, 3.AOS Program, Princeton University, Princeton NJ, USA, 4.College of Ocean and Atmospheric Sciences, Oregon State Universitym, Corvallis, OR, USA)

World Regionalization of Climate Change (1961–2010)

*Shao Sun[1,2], Peijun Shi[2,3,4], Daoyi Gong[2], Tao Zhou[2]

1. National Climate Center, China Meteorological Administration, Beijing 100081, China, 2. State Key Laboratory of Earth Surface Processes and Resource Ecology, Beijing Normal University, Beijing 100875, China, 3. Key Laboratory of Environmental Change and Natural Disaster of Ministry of Education, Beijing Normal University, Beijing 100875, China, 4. Academy of Disaster Reduction and Emergency Management, Ministry of Civil Affairs & Ministry of Education, Beijing 100875, China

Existing climate regionalization aims to characterize the regional differences in climate based on years of the mean values of climate indices. However, with the accelerating climate change nowadays, existing climate regionalization cannot represent the regional difference of climate change, nor can it reflect the extreme weather and climate disasters and environmental risks incurred from climate changes. This paper utilizes the tendency value and fluctuation value of temperature and precipitation from 1961 to 2010 to identify the climate change quantitatively, and completes world regionalization of climate change (1961–2010) with administrative subdivisions of countries as the basic unit in combination with world's terrain feature. Level-I regionalization divides world's climate change (1961–2010) into twelve tendency zones based on the tendency of temperature and precipitation; level-II regionalization refers to twenty-eight fluctuation regions based on level-I regionalization according to the fluctuation of temperature and precipitation. Climate change regionalization provides a basis for countries and regions in the world to develop plans for adapting to climate change, especially for managing extreme weather and climate disasters and environmental risks.

Keywords: Climate change, Regionalization, Tendency, Fluctuation, World

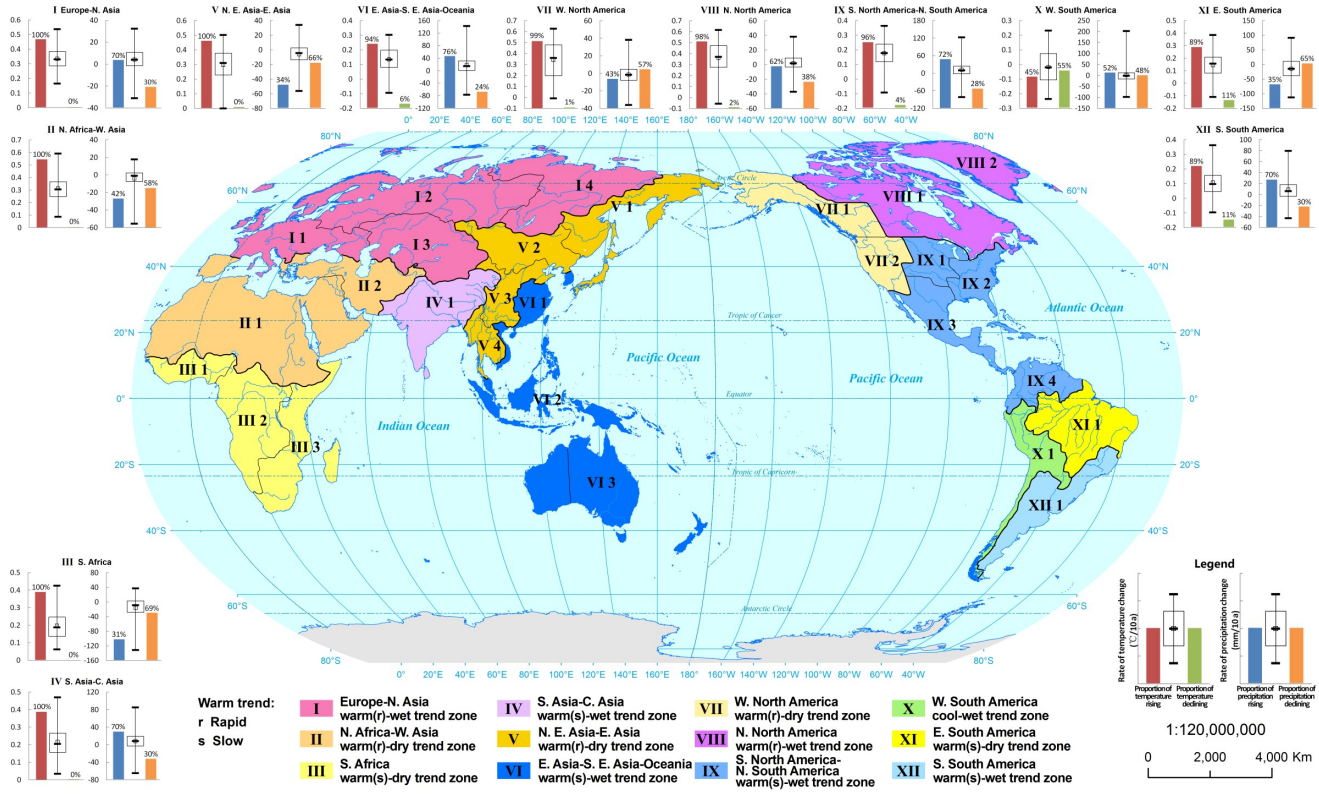

©2019. Japan Geoscience Union. All Right Reserved.

Quantifying and identifying future climate signal, noise, and internal variability at finer temporal scales

*Jongho Kim[1], Manh Van Doi[1]

1. University of Ulsan

Quantifying and identifying climate internal variability (CIV) plays an important role in climate change studies because of its irreducible and unpredictable characteristics. A large number of studies have addressed such an issue; however, the issue was only resolved at coarser resolution on the first order moments of few climate variables. Our recent study has estimated CIV of climate variables for a “current” period at finer spatial and temporal scales; however, whether CIV will change or remain constant in the future under the impact of representative concentration pathways (RCP45 and RCP85) is still questionable. To investigate how CIV will change in the future in both spatial pattern and magnitude, CIV is assessed over 30-year periods in both current and future periods with two scenarios in Korea by analyzing an ensemble of 100 simulations generated by an hourly weather generator. In this study, signal to noise ratio (SNR) used to evaluate the model performance will be applied to simulating ensemble for different periods. CIV is then estimated by two methods: “detrended” and “differenced”; SNR is estimated by “analysis of variance” and “trend analysis” methods. Both SNR and CIV are evaluated with four proposed matrices signifying rainfall volume, extremes and occurrence of rainfall. To consider the change of CIV in the future periods, t-test (test for mean difference) and f-test (test for variance difference) are applied to the ensemble of CIV. In this study, analyzing SNR’s values shows that the four proposed matrices are controlled by non-linear stochastic process and the change tend to increase in the future with increase of CO2 concentration. CIV is proved to change in the future periods under impact of CO2 scenarios. Spatial distribution of CIV’s change over future periods of which locations provides the important and useful information for decision making of water resources planning and proposing mitigation measures of disaster protection.

Acknowledgment:

This research was supported by the Water Management Research Program funded by Ministry of Environment of Korean government (127554), and by the Basic Science Research Program of the National Research Foundation of Korea funded by the Ministry of Education (2016R1D1A1B03931886).

Keywords: climate internal variability, signal to noise ratio, t-test, f-test

©2019. Japan Geoscience Union. All Right Reserved.

Basic evaluation of MIROC6 and current status of CMIP6 experiments

*Hiroaki Tatebe[1]

1. Japan Agency for Marine-Earth Science and Technology

The sixth version of the Model for Interdisciplinary Research on Climate (MIROC), called MIROC6, was cooperatively developed by a Japanese climate modeling community. Overall reproducibility of mean climate and internal climate variability in MIROC6 is better than that in the previous version (MIROC5). The tropical climate systems (e.g., summertime precipitation in the western Pacific and the eastward propagating Madden-Julian Oscillation) and the mid-latitude atmospheric circulations (e.g., the westerlies, the polar night jet, and troposphere-stratosphere interactions) are significantly improved in MIROC6. These improvements can be attributed to the newly implemented parameterization for shallow convective processes and to the directly resolved stratosphere. In the present study, simulated mean climate, internal climate variability in MIROC6 are evaluated and briefly summarized in comparison with MIROC5 and observations. Using MIROC6, designated simulations tackling a wide range of climate science issues, as well as seasonal-to-decadal climate predictions and future climate projections, are currently ongoing with an aim towards contributing to the sixth phase of the Coupled Model Intercomparison Project (CMIP6). Preliminary results of historical climate simulations from the middle of the 19th century, climate projections from the present to the end of the 21th century based on future scenarios of the Shared Socio-economic Pathways, and initialized climate predictions on seasonal-to-decadal timescales will be given in this talk.

Keywords: Climate model, CMIP6, climate projections/predictions

©2019. Japan Geoscience Union. All Right Reserved.

Synchronized increase of extreme cold and warm events in China during the recent global warming slowdown

*Xiubao Sun[1,3], Chunzai Wang[1], Guoyu Ren[2,3], Panfeng Zhang[2]

1. State Key Laboratory of Tropical Oceanography (LTO), South China Sea Institute of Oceanology(SCSIO), Chinese Academy of Sciences (CAS), 2. Department of Atmospheric Science, School of Environmental Studies, China University of Geosciences (CUG), 3. Laboratory for Climate Studies, National Climate Center (NCC), China Meteorological Administration (CMA)

From the end of 1990s to the middle of 2010s, global mean temperature experienced a process of warming slowdown. However, global warm extremes did not show the slowdown phenomenon during the recent global warming slowdown. Based on the observation data of 2362 land surface stations in China, we analyzed the cold and warm extremes changes over mainland China between global warming period (1961-1999) and warming slowdown period (2000-2014). Results indicate that the warming trend in the cold season (MAM and DJF) is significantly higher than that in the warm season (JJA and SON) in the period of global warming (1961-1999), while the warming trend in the warm season is significantly higher than that in the cold season in the period of global warming slowdown. That is, the trend of warm season and the cool season in China have reversed. At the same time, we also found that the synchronous increase occurrence of extreme warm events in summer (JJA) and extreme cold events in winter (DJF) leads to the seasonal trend reverse phenomenon, but there are differences in the spatial variation characteristics between cold and warm extremes. The increase of warm extremes in summer is mainly due to the strong increase of warm events in south China, while the increase of cold events in winter is due to the increase of cold events over China. Further, we also found that the variability of extreme temperature has increased more significantly in the warming slowdown period than that in global warming period. East Asian winter monsoon and summer monsoon both show enhanced characteristics during the global warming slowdown period, which indicates that the increase of sea-land temperature difference in summer and winter results in the synchronous increase of extreme cold and warm events by increasing the climate variability in China.

Keywords: Global warming, Global warming slowdown, Extreme warm events, Extreme cold events, Land-sea temperature difference

©2019. Japan Geoscience Union. All Right Reserved.

Quantification of thermodynamical and dynamical contributions to the anthropogenic influences on tropical cyclone rainfall extremes

*Cheng-Ta Chen[1], Shih-How Lo[1], Chung-Chieh Wang[1], Kazuhisa Tsuboki[2]

1. Department of Earth Sciences, National Taiwan Normal University, 2. Hydrospheric-Atmospheric Research Center, Nagoya University

The rainfall extremes and strong winds associated with tropical cyclones lead to significant damages and lost to where they make landfalling. Upward trend in term of financial lost was indicated for the past few decades from the report of major reinsurance firms. Whether the past anthropogenic warming played a significant role in such extreme event and their changes remained very controversial. On one hand, people argue it’s nearly impossible to attribute an individual extreme event to global warming. On the other hand, the increase of heavy rainfall is consistent with the expected effects of climate change on tropical cyclone. To diagnose possible anthropogenic contributions to the odds of heavy rainfall associated with tropical cyclone, we adapt an existing event attribution framework of modeling a ‘world that was’ and comparing it to a modeled ‘world that might have been’ for that same time but for the absence of historical anthropogenic drivers of climate. One limitation for applying such approach to high-impact weather system is that it will require models capable of capturing the essential processes lead to the studied extremes. Using a cloud system resolving model that can properly simulate the complicated interactions between tropical cyclone, large-scale background, topography, we first perform the ensemble ‘world that was’ simulations forced by the high resolution ECMWF YOTC analysis. We then re-simulate with the adjusted ‘world that might have been conditions’ by removing the regional atmospheric and oceanic forcing due to human influences estimated from the CMIP5 model ensemble mean conditions between all forcing and natural forcing only historical runs. Thus our findings are highly conditional on the driving analysis and adjustments therein, but the setup allows us to elucidate possible contribution of anthropogenic forcing to changes in the likelihood of heavy rainfall associated tropical cyclone. With only less than half of degree anthropogenic warming over the study area, we found that this forcing very likely (9 out of 10 cases) increase the risk of heavy rainfall event (grid rainfall greater than 33 mm per hour) by at least 16%. The role of dynamical processes that leads to precipitation extreme increases beyond the moisture content increase will be further analyzed and discussed.

Keywords: Tropical Cyclone, Extreme rainfall, extreme event attribution

©2019. Japan Geoscience Union. All Right Reserved.

Temporal Evolution of the Long-Term Distributional Biases of Climate Models as a Parameter for the Regional Evaluation of the Simulation of Climate Change

*Martin Gomez-Garcia[1], Akiko Matsumura[1], Shiro Hishinuma[1], Daikichi Ogawada[1]

1. Nippon Koei Co. Ltd., Reasearch and Development Center

Owing to the climate variability of the General Circulation Models (GCM), the discrepancy between their outputs and observational datasets at scales that range from hours to years is practically random. Thus, the associated errors need to be evaluated in terms of the long-term (multidecadal) distributional properties of the atmospheric variables. A recently developed bias-correction method corrects the systematic errors (i.e., biases) in the climate mean state and in three distributional measures of the daily and the interannual variability (namely the frequency of extremes, the skewness, and the scale of the variable at each timescale). The adjustment of these biases is done in such a way that the corrections at one timescale do not affect the probability distribution at another. Therefore, this bias-correction method is able to preserve the GCM-simulated climate trends and extensively reproduce the long-term frequency of the observed extreme weather (e.g. 98th percentile of wet days, maximum seasonal mean of surface temperature).

Generally, the bias-correction of GCMs faces the challenge of including the simulated changes of climate, which supposes alterations in not only the mean but also other aspects like the skewness and the frequency of extremes. The abovementioned bias-correction method includes the effect of the simulated climate change in the correction of the distributional biases. However, considering the coarse resolution of the GCMs and the imperfections in the parameterizations of the subgrid physical processes, the fundamental assumption that the distributional biases are predictable (i.e., stationary) is made.

In this study, we explored the possibility of evaluating the sensibility with which GCMs simulate the response of the earth-system components to external forcing (i.e., climate change) by comparing the temporal evolution of the distributional biases at different timescales over specific regions. For the short period in which the observed data was available, our results revealed that many CMIP5 GCMs are indeed able to simulate with a quasi-stationary bias the changes caused by climate change. Moreover, being able to identify the regions in which certain models do not show the errors with a systematic behavior in either the climate mean state, the daily variability or the interannual variability can be useful for the further development of climate models. We expect that with the data of the GCM outputs of the future phases of the CMIP project, the period in which the observed and the modeled data coincide becomes longer and, thus, our conclusions can be supported by more robust evidence.

Keywords: Bias correction of GCMs at different timescales, Climate trends and climate variability, Evaluation of the ability of GCMs to simulate climate change

©2019. Japan Geoscience Union. All Right Reserved.

A global simulation of bioenergy crop yield

*Zhipin Ai[1], Naota Hanasaki[1]

1. National Institute for Environmental Studies

Large-scale development of bioenergy is considered as an effective pathway to achieve the 2 degrees target of the Paris Agreement. To avoid the competition with food crops, so-called the second-generation bioenergy crops such as miscanthus and switchgrass are regarded as potential dedicated biomass crop. However, the models to estimate the yield of miscanthus and switchgrass at a global scale which enable analyzing the effects of irrigation water application are seldom seen as of today. Here, we firstly updated the crop module in the global hydrological model H08 for miscanthus and switchgrass. Then, we conducted a global simulation and validation of the yield for miscanthus and switchgrass at 0.5 degree. The results indicated that the updated H08 have a good ability in simulating the yield of perennial bioenergy crops, which provides a good foundation for further integrated assessment of the impacts of bioenergy crop production on water sector.

Acknowledgement: This research was supported by the Environment Research and Technology Development Fund (S-14-5) of the Environmental Restoration and Conservation Agency.

Keywords: Bioenergy, Crop yield, H08

©2019. Japan Geoscience Union. All Right Reserved.

Integrated Research Program for Advancing Climate Models - Theme B: national research program in Japan on earth system modeling

*Michio Kawamiya[1], Tomohiro Hajima[1], Kaoru Tachiiri[1], Jun'ichi Tsutsui[2], Tokuta Yokohata[3], Takashi Arakawa[4], Takahiro Inoue[4]

1. Japan Agency for Marine-Earth Science and Technology, 2. Central Research Institute of Electric Power Industry, 3. National Institute for Environmental Studies, 4. Research Organization for Information Science and Technology

The Integrated Research Program for Advancing Climate Models, or TOUGOU (abbreviation taken from its Japanese name), is a national project for projection of global change. Its aim to provide information for adaptation and mitigation, based on scientific evaluation of changes including those in extreme events and carbon cycle. The project was launched in April, 2017. While the entire program deals with a wide range of physical aspects and consequent impacts of climate change, Theme B (TOUGOU-B) focuses on the development of a state-of-the-art Earth system model (ESM) incorporating biogeochemical processes, such as sophisticated carbon and nitrogen cycles, as well as its application to exploring future socio-economic pathways of climate change mitigation. MIROC-ESM, an ESM developed under TOUGOU-B (and the previous SOUSEI-B) has been significantly improved since the 5th phase of coupled model intercomparison project (CMIP5), and has started to be run for CMIP6. During the three years since TOUGOU was launched, results have been obtained that may contribute to 6th Assessment Report (AR6) of Intergovernmental Panel on Climate Change (IPCC) including those on impacts of pyrogenic iron on oceanic ecosystem, assessment of the outcome of labor productivity change due to warming, and effects of high dust amount on surface temperature during the Last Glacial Maximum. Besides, efforts to secure ways to disseminate projection data are ongoing under TOUGOU-B. Specifically, collaboration has been established between climate modeling community in Japan and Data Integration and Analysis System (DIAS), a national IT project for environmental data, have been continuing, in order for Japan to participate in Earth System Grid Federation (ESGF). ESGF is an international cooperative activity to construct a data distributing system for climate related data such as CMIP6 outputs. Some of the details of these results will be explained in the presentation.

Keywords: IPCC, Earth system model , carbon cycle, socio-economic scenario, CMIP6, climate mitigation

©2019. Japan Geoscience Union. All Right Reserved.

Towards probabilistic climate projections based on the CMIP6 multi-model ensemble

*Junichi Tsutsui[1]

1. Central Research Institute of Electric Power Industry

Research on climate change mitigation uses a climate model emulator that represents the average and range over a specific multi-model ensemble of complex climate simulations. The Coupled Model Intercomparison Project (CMIP) has provided such multi-model ensembles, and its latest Phase 6 (CMIP6) results are being revealed. As a first step to applying the CMIP6 results to probabilistic climate projections, we focus on the distribution of key parameters representing atmospheric CO_2-induced forcing and transient temperature responses.

In this study, we develop a procedure to determine the forcing-response parameters of a complex climate model. We simultaneously fit a curve built on an impulse response function to the global mean time series of the model's surface temperature anomaly and top-of-atmosphere energy imbalance from two basic CO_2 -forced experiments, i.e., an abrupt quadrupling and a 1%-per-year increase in atmospheric CO_2 concentration. This scheme serves as an improved alternative to the widely-used regression method of Gregory et al. (2004). Furthermore, it makes a complete set of parameters to emulate the target model from which equilibrium climate sensitivity (ECS) and transient climate response (TCR) are derived. The properties of a multi-model ensemble are quantified through a statistical approach including a principal component analysis for the parameters.

The two CO_2-forced experiments are included in the set of common experiments which is designed to maintain continuity across different CMIP phases. Here, we compare the parameters of individual CMIP6 models with those of the previous-phase CMIP5 models. The parameters of the CMIP5 ensemble have several features. The ratio of TCR to ECS is distributed in the range of approximately 0.5 to 0.7, and for models with large ECS, the ratio tends to decrease. The scaling parameter for the effective radiative forcing of CO_2 varies from model to model and tends to be less than a reference value used in a conventional formula of CO_2 radiative forcing. Although the number of CMIP6 models is currently limited, their parameters show similar distributions within the CMIP5 ranges.

Keywords: climate sensitivity, effective radiative forcing, impulse response model, climate model emulator, ensemble climate experiment

©2019. Japan Geoscience Union. All Right Reserved.

Effect on the earth system of realizing 1.5 degree climate target by overshooting after reaching 2 degree level

*Kaoru Tachiiri[1], Herran Diego Silva[2], Xuanming Su[1], Michio Kawamiya[1]

1. Japan Agency for Marine-Earth Science and Technology, 2. Institute for Global Environmental Strategies

By using an Earth system model (ESM) with emissions and land use scenarios consistent with socio-economic projections from an integrated assessment model, the effect of overshooting to 1.5 degree target (in Celsius from pre-industrial periods) after reaching 2 degree level is investigated in selected indicators of the global environment. Unlike the internationally coordinated model intercomparison project, the scenario is developed for a specific climatic model. The ESM output results in delayed achievements for both of 1.5 and 2 degree targets in terms of global surface mean air temperature, but achieved before or around 2100 as expected when we use global mean surface temperature (for which sea surface temperature and surface air temperature are used for ocean and land, respectively) masked with observation areas. In the overshooting scenario more heat is absorbed by the ocean compared to a case without overshooting, but still we found significant difference between the two scenarios in Arctic sea ice, while in both scenarios corals seem difficult to survive the 21st century (when no thermal adaptation is assumed) . The difference in steric sea level rise between the scenarios is only below 2 cm in 2100. In addition, vegetation productivity in broad regions shows slight (~5%) increase. Emission pathways in the scenarios rely on a large amount of carbon sequestration. In the 2 degree scenario CO2 emissions in 2100 are slightly below zero, while for 1.5 degree scenario they are below -20 GtCO2.. When the Earth system has high climate sensitivity and TCRE, to reach the 1.5 degree target we need to take an overshooting temperature pathway, but in case the overshooting is large, difference in some indicators between 1.5 degree and 2 degree scenarios can be non-significant, which is an important indication in implementing adaptive mitigation in the coming decades.

Keywords: Earth system model, integrated assessment model, 1.5 degree target, 2 degree target, stabilization, overshooting

©2019. Japan Geoscience Union. All Right Reserved.

Historical regional and sectoral contributions to climate change

*Xuanming Su[1], Kaoru Tachiiri[1], Katsumasa TANAKA[2], Michio Watanabe[1]

1. Japan Agency for Marine-Earth Science and Technology, 2. National Institute for Environmental Studies

Regional or sectoral contributions to climate change are important in the formulation of climate change policy. After the industrial revolution, developed countries emit CO_2 and non-CO_2 greenhouse gases (GHGs), and the historical emissions are large; while developing countries contribute relative fewer emissions in historical period but increase significantly in recent years or visible future. To assess the contributions to climate change, using cumulative emissions is a general and direct method. However, such method may ignore the lifetime of GHGs since part of the GHGs sink into the biosphere, ocean, soil or diminish during biogeochemical cycles. In this study, we evaluate the historical regional and sectoral contributions to climate change by using an improved version of Simple Climate Model for OPTimization (SCM4OPT) with a normalized marginal method. Based on the results, we analyze ten major GHG emitting countries and 12 sectors.

First, current emissions with relative long lifetime like CO_2 and N_2O, from developing countries increase significantly, like China, India, Mexico and Brazil, however, their contributions to climate change are still relatively smaller, compared with the developed countries such as USA, Japan, Germany, Canada and UK, of which countries the cumulative emissions are in relatively larger scale and current emissions are already under controlled. We can conclude here that the GHGs with relatively long lifetime need to be controlled stringently to reduce the long-term effects on climate change. For CH_4, which has a relatively shorter lifetime, the contributions to climate change are closely related to emissions within recent decades. These imply that reductions on short lifetime emissions can make immediate alleviation regarding climate change.

Second, energy sector contributes most of the CO_2 emissions, and therefore contribute almost half to the climate change among all the sectors. However, for CH_4 and N_2O, agriculture sector contributes most of the emissions and therefore their contributions to climate change are remarkable. Reduction policiesneed to targetthesesectors. In addition, CO_2 from land transportation and CH_4 from waste treatment increase rapidly in recent years, attention also needs to be paid to these sectors for making climate change policies.

Keywords: region emissions, sector emissions, climate change contribution, simple climate model

©2019. Japan Geoscience Union. All Right Reserved.

Future projection of global climate, water, food, bio-energy, and land investigated with MIROC-INTEG: a global bio-geophysical land surface model with human components

*Tokuta Yokohata[1], Yusuke Satoh[1], Tsuguki Kinoshita[2], Gen Sakurai[3], Yadu Pokhrel[4], Akihiko Ito[1], Etsushi Kato[5], Masashi Okada[1], Naota Hanasaki[1], Tomoko Nitta[6], Seita Emori[1]

1. National Institute for Environmental Studies, 2. Ibaraki University, 3. National Agriculture and Food Research Organization, 4. Michigan State University, 5. The Institute of Applied Energy, 6. University of Tokyo

Future climate changes possibly affect water resources, food production, energy supply, and ecosystem services. It is critical to better understand the interactions between the changes in these complicated factors. While earth system models and integrated assessment models are applicable to explore this topic, parts of their natural and/or human processes tend to be simplified depending on their scope. As such, it still remains a challenge to realistically model the human-natural interface. In this context, the MIROC integrated terrestrial model (MIROC-INTEG) was developed. One of the features of MIROC-INTEG is that the natural ecosystem and human activity models are coupled to a global land surface model MATSIRO (Nitta et al. 2014, Journal of Climate), which is a component of a state-of-the-art global climate model, MIROC (Watanabe et al. 2010, Journal of Climate). As a natural ecosystem model, we use a global vegetation model, VISIT (Ito and Inatomi 2012, Biogeosciences). As human activity models, we use a global land-surface model with anthropogenic water regulation modules, HiGW-MAT (Pokhrel et al, 2012, Journal of Hydrometeorology), and a global crop model, PRYSBI2 (Sakurai et al, 2014, Scientific Reports). In HiGW-MAT, models of human water regulations such as water withdrawal from river, dam operation, and irrigation (Hanasaki et al. 2008, Hydrol. Earth Syst. Sci.) are incorporated to the above-mentioned global land surface model, MATSIRO. In PRYSBI2, the growth and yield of four crops (wheat, maize, soybean, rice) are calculated. In addition to these models, a global land use model (Terrestrial Land-use Model, TeLMO) is newly developed in the present study. TeLMO calculate the grid ratio of cropland (food and bio-energy crops), pasture, forest (managed and un-managed), as well as their transition. Output variables of each sub-model are passed to other sub-models during the time integration.
We will present an analysis of historical and future simulations with a focus on the interactions between water, food, energy, and land. In the historical simulations, we validated the model output such as irrigated water, crop yield, ecosystem productions, and cropland area by comparing to the observed or reanalysis data. In the future simulations, we investigated the role of uncertainties in climate (Representative Concentration Pathways) and socio-economic (Shared Socio-economic Pathways) scenarios. We also investigate the role of uncertainties in model parameters, and found that an uncertainty in the fertilization effect of crop growth model PRYSBI2 strongly affect uncertainty in future projection of crop yield and land use change in TeLMO. We found that future changes in precipitation and/or temperature possibly cause decrease in soil moisture, leading to decreases in crop yield (especially in high emission scenario such as RCP8.5). Decrease in crop yield bring about increase in crop land area, which also causes the increase in irrigation demands. Interaction between water, crop yield, and land use, as well as possible impacts on ecosystem service will be discussed in the presentation.

Keywords: Global Climate Model, Earth System Model, Human activity

©2019. Japan Geoscience Union. All Right Reserved.

Downscaling a global agricultural land use model to country level for national SSP analysis

*Wenchao Wu[1], Tomoko Hasegawa[1], Kiyoshi Takahashi[1], Shinichiro Fujimori[2]

1. National Institute for Environmental Studies, 2. Kyoto Univ.

The Shared Socioeconomic Pathways (SSPs) has been part of latest scenario framework developed by the climate change research society in the recent decade, serving the integrated analysis of future climate impacts, vulnerabilities, adaptation, and mitigation, in which the agriculture, food system and land use are important components. Multiple integrated assessment models (IAMs) have been used for the quantitative projections of future agriculture, food system and land use in the global scale. However, the tool and application of IAMs to the quantification of SSPs on regional or national level is limited. Meanwhile, there are growing needs for the quantification of SSPs on regional or national level for a more detailed understanding of agriculture, food, and land use, and their interactions with other nexus, such as energy, water, and biodiversity. One obstacle for such application is the coarse spatial resolution of global IAMs for land use module. This study aims to apply the Asian-Pacific Integrated Model/Platform for Land-Use and Environmental Model (AIM/PLUM) for the quantification of agriculture, food system, and land use in Japan under its national-specific SSPs narratives. To achieve this, a regional land use model, AIM/PLUM-Japan, was developed, by improving the spatial resolution to 0.05˚ (targeting 1km) from global model of 0.5˚. We combined the statistical production area data and spatial land use data to produce a refined base crop map. Agricultural land use could be downscaled to 0.05˚ resolution and gridded agricultural land use information could be generated using this model. Aside from providing quantitative land use information for Japan’ s SSPs, this study also contributes to the IAMs and SSPs societies by testing the applicability and feasibility of global IAMs, especially land use models, to the regional or national extension. For example, regional (national) SSPs quantifications for other regions could be easily implemented by a similar paradigm using AIM/PLUM.

Keywords: downscaling, land use, national SSP

©2019. Japan Geoscience Union. All Right Reserved.

Extreme Events and Emergent Trends in Marine Ecosystem Stressors under a historical/RCP8.5 Climate Change Pathway

*Keith Bradley Rodgers[1,2], Sarah Schlunegger[3], Richard Slater[3], Burke Hales[4], Axel Timmermann[1,2]

1. IBS Center for Climate Physics, Busan, South Korea, 2. Pusan National University, Busan, South Korea, 3. AOS Program, Princeton University, Princeton NJ, USA, 4. College of Ocean and Atmospheric Sciences, Oregon State Universitym, Corvallis, OR, USA

It is important to identify the degree to which climate change will impact ocean ecosystems over the 21st century. Over the last decade there has been increasing application of Earth System Models (ESMs) to project changes in ecosystem stressors (acidification, warming, and de-oxygenation) with a focus on surface and/or thermocline-integrated conditions. Recent efforts have made combined use of CMIP5 models, large ensemble simulations, and/or scenario sensitivity experiments to estimate uncertainties in future projections. Nevertheless very little to date has been done to evaluate how the frequency of extreme events with ecosystem stressors will respond to future climate perturbations. Here we consider for an ensemble suite of simulations with GFDL's ESM2M changes in the frequency of marine ecosystem extreme events over the 21stcentury. We focus on the contrast between the behavior at the ocean's surface vs. base of the ocean's euphotic zone, as these are both important horizons for ocean ecosystems, and on the contrast between the Time of Emergence of decadal trends vs. frequency changes of extreme events, as these are both important ecological timescales. Particular attention is devoted to acidification at the base of the euphotic zone, as this pertains to the life cycle of pteropods. Preliminary results indicate that in addition to the subpolar Northern Oceans and the Southern Ocean, the Large Marine Ecosystems (LME) regions of the eastern Pacific become increasingly exposed to corrosive waters over the 21stcentury.

Keywords: Climate Change, Ecosystem Stressors, Extreme Events, Large Ensemble

©2019. Japan Geoscience Union. All Right Reserved.

[E] Poster | A (Atmospheric and Hydrospheric Sciences)：A-CG Complex & General

Wed. May 29, 2019 5:15 PM - 6:30 PM JST | Wed. May 29, 2019 8:15 AM - 9:30 AM UTC | Poster Hall International Exhibition Hall8, Makuhari Messe_16

[A-CG35] Projection and detection of global environmental change

convener:Michio Kawamiya(Japan Agency for Marine-Earth Science and Technology), Hiroaki Tatebe(Japan Agency for Marine-Earth Science and Technology), Kaoru Tachiiri(Japan Agency for Marine-Earth Science and Technology)

Anthropogenic forcings on global environment are expected to cause intensification of extreme events, sea level rise, ocean acidification and deoxygenation, as well as large-scale ecosystem changes. The CMIP6 experimental protocol has been established based on which modeling groups across the world are starting to provide environmental projection data toward 6th IPCC assessment report due in 2021. Various new types of studies, such as event attribution and coupling of socio-economic processes and Earth system dynamics, are also emerging in the field of global change projection. In addition, observational studies are becoming increasingly more important for grasping changes in the global environment and evaluating model projections. Interactions and collaborations beyond boundaries of conventional scientific disciplines are desired for dealing with the issue of global changes. This session thus aims to deepen our understanding on global change, from both disciplinary and interdisciplinary viewpoints. This session is co-organized by AIMES - Future Earth project "Analysis, Integration and Modelling of the Earth System" (https://aimesproject.org/).

[ACG35-P01] World Regionalization of Climate Change (1961–2010)

*Shao Sun[1,2], Peijun Shi[2,3,4], Daoyi Gong[2], Tao Zhou[2] (1.National Climate Center, China Meteorological Administration, Beijing 100081, China, 2.State Key Laboratory of Earth Surface Processes and Resource Ecology, Beijing Normal University, Beijing 100875, China, 3.Key Laboratory of Environmental Change and Natural Disaster of Ministry of Education, Beijing Normal University, Beijing 100875, China, 4.Academy of Disaster Reduction and Emergency Management, Ministry of Civil Affairs & Ministry of Education, Beijing 100875, China)

[ACG35-P02] Quantifying and identifying future climate signal, noise, and internal variability at finer temporal scales

*Jongho Kim[1], Manh Van Doi[1] (1.University of Ulsan)

[ACG35-P03] Basic evaluation of MIROC6 and current status of CMIP6 experiments

*Hiroaki Tatebe[1] (1.Japan Agency for Marine-Earth Science and Technology)

[ACG35-P04] Synchronized increase of extreme cold and warm events in China during the recent global warming slowdown

*Xiubao Sun[1,3], Chunzai Wang[1], Guoyu Ren[2,3], Panfeng Zhang[2] (1.State Key Laboratory of Tropical Oceanography (LTO), South China Sea Institute of Oceanology(SCSIO), Chinese Academy of Sciences (CAS), 2.Department of Atmospheric Science, School of Environmental Studies, China University of Geosciences (CUG), 3.Laboratory for Climate Studies, National Climate Center (NCC), China Meteorological Administration (CMA))

[ACG35-P05] Quantification of thermodynamical and dynamical contributions to the anthropogenic influences on tropical cyclone rainfall extremes

*Cheng-Ta Chen[1], Shih-How Lo[1], Chung-Chieh Wang[1], Kazuhisa Tsuboki[2] (1.Department of Earth Sciences, National Taiwan Normal University, 2.Hydrospheric-Atmospheric Research Center, Nagoya University)

[ACG35-P06] Temporal Evolution of the Long-Term Distributional Biases of Climate Models as a Parameter for the Regional Evaluation of the Simulation of Climate Change

*Martin Gomez-Garcia[1], Akiko Matsumura[1], Shiro Hishinuma[1], Daikichi Ogawada[1] (1.Nippon Koei Co. Ltd., Reasearch and Development Center)

[ACG35-P07] A global simulation of bioenergy crop yield

*Zhipin Ai[1], Naota Hanasaki[1] (1.National Institute for Environmental Studies)

[ACG35-P08] Integrated Research Program for Advancing Climate Models - Theme B: national research program in Japan on earth system modeling

*Michio Kawamiya[1], Tomohiro Hajima[1], Kaoru Tachiiri[1], Jun'ichi Tsutsui[2], Tokuta Yokohata[3], Takashi Arakawa[4], Takahiro Inoue[4] (1.Japan Agency for Marine-Earth Science and Technology, 2.Central Research Institute of Electric Power Industry, 3.National Institute for Environmental Studies, 4.Research Organization for Information Science and Technology)

[ACG35-P09] Towards probabilistic climate projections based on the CMIP6 multi-model ensemble

*Junichi Tsutsui[1] (1.Central Research Institute of Electric Power Industry)

[ACG35-P10] Effect on the earth system of realizing 1.5 degree climate target by overshooting after reaching 2 degree level

*Kaoru Tachiiri[1], Herran Diego Silva[2], Xuanming Su[1], Michio Kawamiya[1] (1.Japan Agency for Marine-Earth Science and Technology, 2.Institute for Global Environmental Strategies)

[ACG35-P11] **Historical regional and sectoral contributions to climate change**

*Xuanming Su[1], Kaoru Tachiiri[1], Katsumasa TANAKA[2], Michio Watanabe[1] (1.Japan Agency for Marine-Earth Science and Technology, 2.National Institute for Environmental Studies)

[ACG35-P12] **Future projection of global climate, water, food, bio-energy, and land investigated with MIROC-INTEG: a global bio-geophysical land surface model with human components**

*Tokuta Yokohata[1], Yusuke Satoh[1], Tsuguki Kinoshita[2], Gen Sakurai[3], Yadu Pokhrel[4], Akihiko Ito[1], Etsushi Kato[5], Masashi Okada[1], Naota Hanasaki[1], Tomoko Nitta[6], Seita Emori[1] (1.National Institute for Environmental Studies, 2.Ibaraki University, 3.National Agriculture and Food Research Organization, 4.Michigan State University, 5.The Institute of Applied Energy, 6.University of Tokyo)

[ACG35-P13] **Downscaling a global agricultural land use model to country level for national SSP analysis**

*Wenchao Wu[1], Tomoko Hasegawa[1], Kiyoshi Takahashi[1], Shinichiro Fujimori[2] (1.National Institute for Environmental Studies, 2.Kyoto Univ.)

[ACG35-P14] Extreme Events and Emergent Trends in Marine Ecosystem Stressors under a historical/RCP8.5 Climate Change Pathway

*Keith Bradley Rodgers[1,2], Sarah Schlunegger[3], Richard Slater[3], Burke Hales[4], Axel Timmermann[1,2] (1.IBS Center for Climate Physics, Busan, South Korea, 2.Pusan National University, Busan, South Korea, 3.AOS Program, Princeton University, Princeton NJ, USA, 4.College of Ocean and Atmospheric Sciences, Oregon State Universitym, Corvallis, OR, USA)

World Regionalization of Climate Change (1961–2010)

*Shao Sun[1,2], Peijun Shi[2,3,4], Daoyi Gong[2], Tao Zhou[2]

1. National Climate Center, China Meteorological Administration, Beijing 100081, China, 2. State Key Laboratory of Earth Surface Processes and Resource Ecology, Beijing Normal University, Beijing 100875, China, 3. Key Laboratory of Environmental Change and Natural Disaster of Ministry of Education, Beijing Normal University, Beijing 100875, China, 4. Academy of Disaster Reduction and Emergency Management, Ministry of Civil Affairs & Ministry of Education, Beijing 100875, China

Existing climate regionalization aims to characterize the regional differences in climate based on years of the mean values of climate indices. However, with the accelerating climate change nowadays, existing climate regionalization cannot represent the regional difference of climate change, nor can it reflect the extreme weather and climate disasters and environmental risks incurred from climate changes. This paper utilizes the tendency value and fluctuation value of temperature and precipitation from 1961 to 2010 to identify the climate change quantitatively, and completes world regionalization of climate change (1961–2010) with administrative subdivisions of countries as the basic unit in combination with world's terrain feature. Level-I regionalization divides world's climate change (1961–2010) into twelve tendency zones based on the tendency of temperature and precipitation; level-II regionalization refers to twenty-eight fluctuation regions based on level-I regionalization according to the fluctuation of temperature and precipitation. Climate change regionalization provides a basis for countries and regions in the world to develop plans for adapting to climate change, especially for managing extreme weather and climate disasters and environmental risks.

Keywords: Climate change, Regionalization, Tendency, Fluctuation, World

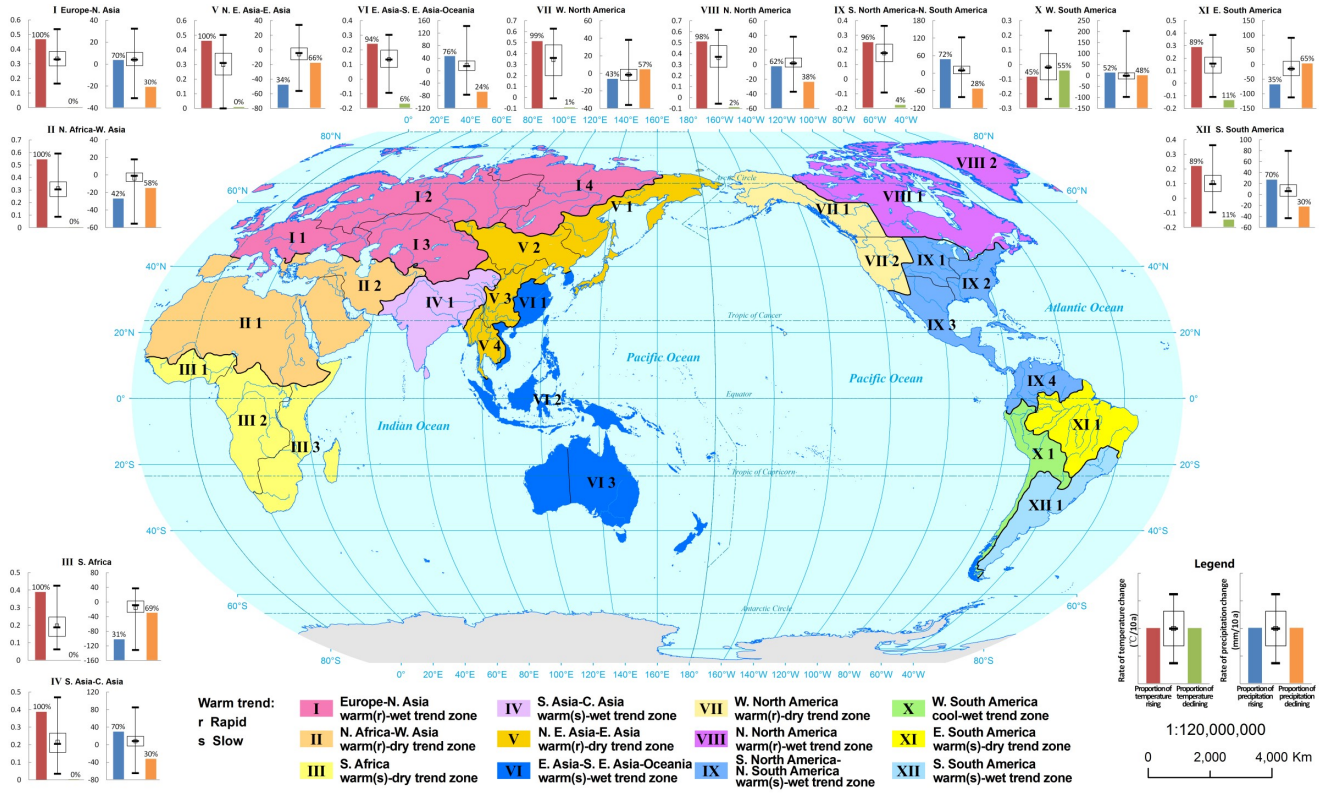

©2019. Japan Geoscience Union. All Right Reserved.

Quantifying and identifying future climate signal, noise, and internal variability at finer temporal scales

*Jongho Kim[1], Manh Van Doi[1]

1. University of Ulsan

Quantifying and identifying climate internal variability (CIV) plays an important role in climate change studies because of its irreducible and unpredictable characteristics. A large number of studies have addressed such an issue; however, the issue was only resolved at coarser resolution on the first order moments of few climate variables. Our recent study has estimated CIV of climate variables for a “current” period at finer spatial and temporal scales; however, whether CIV will change or remain constant in the future under the impact of representative concentration pathways (RCP45 and RCP85) is still questionable. To investigate how CIV will change in the future in both spatial pattern and magnitude, CIV is assessed over 30-year periods in both current and future periods with two scenarios in Korea by analyzing an ensemble of 100 simulations generated by an hourly weather generator. In this study, signal to noise ratio (SNR) used to evaluate the model performance will be applied to simulating ensemble for different periods. CIV is then estimated by two methods: “detrended” and “differenced”; SNR is estimated by “analysis of variance” and “trend analysis” methods. Both SNR and CIV are evaluated with four proposed matrices signifying rainfall volume, extremes and occurrence of rainfall. To consider the change of CIV in the future periods, t-test (test for mean difference) and f-test (test for variance difference) are applied to the ensemble of CIV. In this study, analyzing SNR’s values shows that the four proposed matrices are controlled by non-linear stochastic process and the change tend to increase in the future with increase of CO2 concentration. CIV is proved to change in the future periods under impact of CO2 scenarios. Spatial distribution of CIV’s change over future periods of which locations provides the important and useful information for decision making of water resources planning and proposing mitigation measures of disaster protection.

Acknowledgment:

This research was supported by the Water Management Research Program funded by Ministry of Environment of Korean government (127554), and by the Basic Science Research Program of the National Research Foundation of Korea funded by the Ministry of Education (2016R1D1A1B03931886).

Keywords: climate internal variability, signal to noise ratio, t-test, f-test

©2019. Japan Geoscience Union. All Right Reserved.

Basic evaluation of MIROC6 and current status of CMIP6 experiments

*Hiroaki Tatebe[1]

1. Japan Agency for Marine-Earth Science and Technology

The sixth version of the Model for Interdisciplinary Research on Climate (MIROC), called MIROC6, was cooperatively developed by a Japanese climate modeling community. Overall reproducibility of mean climate and internal climate variability in MIROC6 is better than that in the previous version (MIROC5). The tropical climate systems (e.g., summertime precipitation in the western Pacific and the eastward propagating Madden-Julian Oscillation) and the mid-latitude atmospheric circulations (e.g., the westerlies, the polar night jet, and troposphere-stratosphere interactions) are significantly improved in MIROC6. These improvements can be attributed to the newly implemented parameterization for shallow convective processes and to the directly resolved stratosphere. In the present study, simulated mean climate, internal climate variability in MIROC6 are evaluated and briefly summarized in comparison with MIROC5 and observations. Using MIROC6, designated simulations tackling a wide range of climate science issues, as well as seasonal-to-decadal climate predictions and future climate projections, are currently ongoing with an aim towards contributing to the sixth phase of the Coupled Model Intercomparison Project (CMIP6). Preliminary results of historical climate simulations from the middle of the 19th century, climate projections from the present to the end of the 21th century based on future scenarios of the Shared Socio-economic Pathways, and initialized climate predictions on seasonal-to-decadal timescales will be given in this talk.

Keywords: Climate model, CMIP6, climate projections/predictions

©2019. Japan Geoscience Union. All Right Reserved.

Synchronized increase of extreme cold and warm events in China during the recent global warming slowdown

*Xiubao Sun[1,3], Chunzai Wang[1], Guoyu Ren[2,3], Panfeng Zhang[2]

1. State Key Laboratory of Tropical Oceanography (LTO), South China Sea Institute of Oceanology(SCSIO), Chinese Academy of Sciences (CAS), 2. Department of Atmospheric Science, School of Environmental Studies, China University of Geosciences (CUG), 3. Laboratory for Climate Studies, National Climate Center (NCC), China Meteorological Administration (CMA)

From the end of 1990s to the middle of 2010s, global mean temperature experienced a process of warming slowdown. However, global warm extremes did not show the slowdown phenomenon during the recent global warming slowdown. Based on the observation data of 2362 land surface stations in China, we analyzed the cold and warm extremes changes over mainland China between global warming period (1961-1999) and warming slowdown period (2000-2014). Results indicate that the warming trend in the cold season (MAM and DJF) is significantly higher than that in the warm season (JJA and SON) in the period of global warming (1961-1999), while the warming trend in the warm season is significantly higher than that in the cold season in the period of global warming slowdown. That is, the trend of warm season and the cool season in China have reversed. At the same time, we also found that the synchronous increase occurrence of extreme warm events in summer (JJA) and extreme cold events in winter (DJF) leads to the seasonal trend reverse phenomenon, but there are differences in the spatial variation characteristics between cold and warm extremes. The increase of warm extremes in summer is mainly due to the strong increase of warm events in south China, while the increase of cold events in winter is due to the increase of cold events over China. Further, we also found that the variability of extreme temperature has increased more significantly in the warming slowdown period than that in global warming period. East Asian winter monsoon and summer monsoon both show enhanced characteristics during the global warming slowdown period, which indicates that the increase of sea-land temperature difference in summer and winter results in the synchronous increase of extreme cold and warm events by increasing the climate variability in China.

Keywords: Global warming, Global warming slowdown, Extreme warm events, Extreme cold events, Land-sea temperature difference

©2019. Japan Geoscience Union. All Right Reserved.

Quantification of thermodynamical and dynamical contributions to the anthropogenic influences on tropical cyclone rainfall extremes

*Cheng-Ta Chen[1], Shih-How Lo[1], Chung-Chieh Wang[1], Kazuhisa Tsuboki[2]

1. Department of Earth Sciences, National Taiwan Normal University, 2. Hydrospheric-Atmospheric Research Center, Nagoya University

The rainfall extremes and strong winds associated with tropical cyclones lead to significant damages and lost to where they make landfalling. Upward trend in term of financial lost was indicated for the past few decades from the report of major reinsurance firms. Whether the past anthropogenic warming played a significant role in such extreme event and their changes remained very controversial. On one hand, people argue it’s nearly impossible to attribute an individual extreme event to global warming. On the other hand, the increase of heavy rainfall is consistent with the expected effects of climate change on tropical cyclone. To diagnose possible anthropogenic contributions to the odds of heavy rainfall associated with tropical cyclone, we adapt an existing event attribution framework of modeling a ‘world that was’ and comparing it to a modeled ‘world that might have been’ for that same time but for the absence of historical anthropogenic drivers of climate. One limitation for applying such approach to high-impact weather system is that it will require models capable of capturing the essential processes lead to the studied extremes. Using a cloud system resolving model that can properly simulate the complicated interactions between tropical cyclone, large-scale background, topography, we first perform the ensemble ‘world that was’ simulations forced by the high resolution ECMWF YOTC analysis. We then re-simulate with the adjusted ‘world that might have been conditions’ by removing the regional atmospheric and oceanic forcing due to human influences estimated from the CMIP5 model ensemble mean conditions between all forcing and natural forcing only historical runs. Thus our findings are highly conditional on the driving analysis and adjustments therein, but the setup allows us to elucidate possible contribution of anthropogenic forcing to changes in the likelihood of heavy rainfall associated tropical cyclone. With only less than half of degree anthropogenic warming over the study area, we found that this forcing very likely (9 out of 10 cases) increase the risk of heavy rainfall event (grid rainfall greater than 33 mm per hour) by at least 16%. The role of dynamical processes that leads to precipitation extreme increases beyond the moisture content increase will be further analyzed and discussed.

Keywords: Tropical Cyclone, Extreme rainfall, extreme event attribution

©2019. Japan Geoscience Union. All Right Reserved.

Temporal Evolution of the Long-Term Distributional Biases of Climate Models as a Parameter for the Regional Evaluation of the Simulation of Climate Change

*Martin Gomez-Garcia[1], Akiko Matsumura[1], Shiro Hishinuma[1], Daikichi Ogawada[1]

1. Nippon Koei Co. Ltd., Reasearch and Development Center

Owing to the climate variability of the General Circulation Models (GCM), the discrepancy between their outputs and observational datasets at scales that range from hours to years is practically random. Thus, the associated errors need to be evaluated in terms of the long-term (multidecadal) distributional properties of the atmospheric variables. A recently developed bias-correction method corrects the systematic errors (i.e., biases) in the climate mean state and in three distributional measures of the daily and the interannual variability (namely the frequency of extremes, the skewness, and the scale of the variable at each timescale). The adjustment of these biases is done in such a way that the corrections at one timescale do not affect the probability distribution at another. Therefore, this bias-correction method is able to preserve the GCM-simulated climate trends and extensively reproduce the long-term frequency of the observed extreme weather (e.g. 98th percentile of wet days, maximum seasonal mean of surface temperature).

Generally, the bias-correction of GCMs faces the challenge of including the simulated changes of climate, which supposes alterations in not only the mean but also other aspects like the skewness and the frequency of extremes. The abovementioned bias-correction method includes the effect of the simulated climate change in the correction of the distributional biases. However, considering the coarse resolution of the GCMs and the imperfections in the parameterizations of the subgrid physical processes, the fundamental assumption that the distributional biases are predictable (i.e., stationary) is made.

In this study, we explored the possibility of evaluating the sensibility with which GCMs simulate the response of the earth-system components to external forcing (i.e., climate change) by comparing the temporal evolution of the distributional biases at different timescales over specific regions. For the short period in which the observed data was available, our results revealed that many CMIP5 GCMs are indeed able to simulate with a quasi-stationary bias the changes caused by climate change. Moreover, being able to identify the regions in which certain models do not show the errors with a systematic behavior in either the climate mean state, the daily variability or the interannual variability can be useful for the further development of climate models. We expect that with the data of the GCM outputs of the future phases of the CMIP project, the period in which the observed and the modeled data coincide becomes longer and, thus, our conclusions can be supported by more robust evidence.

Keywords: Bias correction of GCMs at different timescales, Climate trends and climate variability, Evaluation of the ability of GCMs to simulate climate change

©2019. Japan Geoscience Union. All Right Reserved.

A global simulation of bioenergy crop yield

*Zhipin Ai[1], Naota Hanasaki[1]

1. National Institute for Environmental Studies

Large-scale development of bioenergy is considered as an effective pathway to achieve the 2 degrees target of the Paris Agreement. To avoid the competition with food crops, so-called the second-generation bioenergy crops such as miscanthus and switchgrass are regarded as potential dedicated biomass crop. However, the models to estimate the yield of miscanthus and switchgrass at a global scale which enable analyzing the effects of irrigation water application are seldom seen as of today. Here, we firstly updated the crop module in the global hydrological model H08 for miscanthus and switchgrass. Then, we conducted a global simulation and validation of the yield for miscanthus and switchgrass at 0.5 degree. The results indicated that the updated H08 have a good ability in simulating the yield of perennial bioenergy crops, which provides a good foundation for further integrated assessment of the impacts of bioenergy crop production on water sector.

Acknowledgement: This research was supported by the Environment Research and Technology Development Fund (S-14-5) of the Environmental Restoration and Conservation Agency.

Keywords: Bioenergy, Crop yield, H08

©2019. Japan Geoscience Union. All Right Reserved.

Integrated Research Program for Advancing Climate Models - Theme B: national research program in Japan on earth system modeling

*Michio Kawamiya[1], Tomohiro Hajima[1], Kaoru Tachiiri[1], Jun'ichi Tsutsui[2], Tokuta Yokohata[3], Takashi Arakawa[4], Takahiro Inoue[4]

1. Japan Agency for Marine-Earth Science and Technology, 2. Central Research Institute of Electric Power Industry, 3. National Institute for Environmental Studies, 4. Research Organization for Information Science and Technology

The Integrated Research Program for Advancing Climate Models, or TOUGOU (abbreviation taken from its Japanese name), is a national project for projection of global change. Its aim to provide information for adaptation and mitigation, based on scientific evaluation of changes including those in extreme events and carbon cycle. The project was launched in April, 2017. While the entire program deals with a wide range of physical aspects and consequent impacts of climate change, Theme B (TOUGOU-B) focuses on the development of a state-of-the-art Earth system model (ESM) incorporating biogeochemical processes, such as sophisticated carbon and nitrogen cycles, as well as its application to exploring future socio-economic pathways of climate change mitigation. MIROC-ESM, an ESM developed under TOUGOU-B (and the previous SOUSEI-B) has been significantly improved since the 5th phase of coupled model intercomparison project (CMIP5), and has started to be run for CMIP6. During the three years since TOUGOU was launched, results have been obtained that may contribute to 6th Assessment Report (AR6) of Intergovernmental Panel on Climate Change (IPCC) including those on impacts of pyrogenic iron on oceanic ecosystem, assessment of the outcome of labor productivity change due to warming, and effects of high dust amount on surface temperature during the Last Glacial Maximum. Besides, efforts to secure ways to disseminate projection data are ongoing under TOUGOU-B. Specifically, collaboration has been established between climate modeling community in Japan and Data Integration and Analysis System (DIAS), a national IT project for environmental data, have been continuing, in order for Japan to participate in Earth System Grid Federation (ESGF). ESGF is an international cooperative activity to construct a data distributing system for climate related data such as CMIP6 outputs. Some of the details of these results will be explained in the presentation.

Keywords: IPCC, Earth system model , carbon cycle, socio-economic scenario, CMIP6, climate mitigation

©2019. Japan Geoscience Union. All Right Reserved.

Towards probabilistic climate projections based on the CMIP6 multi-model ensemble

*Junichi Tsutsui[1]

1. Central Research Institute of Electric Power Industry

Research on climate change mitigation uses a climate model emulator that represents the average and range over a specific multi-model ensemble of complex climate simulations. The Coupled Model Intercomparison Project (CMIP) has provided such multi-model ensembles, and its latest Phase 6 (CMIP6) results are being revealed. As a first step to applying the CMIP6 results to probabilistic climate projections, we focus on the distribution of key parameters representing atmospheric CO_2-induced forcing and transient temperature responses.

In this study, we develop a procedure to determine the forcing-response parameters of a complex climate model. We simultaneously fit a curve built on an impulse response function to the global mean time series of the model's surface temperature anomaly and top-of-atmosphere energy imbalance from two basic CO_2 -forced experiments, i.e., an abrupt quadrupling and a 1%-per-year increase in atmospheric CO_2 concentration. This scheme serves as an improved alternative to the widely-used regression method of Gregory et al. (2004). Furthermore, it makes a complete set of parameters to emulate the target model from which equilibrium climate sensitivity (ECS) and transient climate response (TCR) are derived. The properties of a multi-model ensemble are quantified through a statistical approach including a principal component analysis for the parameters.

The two CO_2-forced experiments are included in the set of common experiments which is designed to maintain continuity across different CMIP phases. Here, we compare the parameters of individual CMIP6 models with those of the previous-phase CMIP5 models. The parameters of the CMIP5 ensemble have several features. The ratio of TCR to ECS is distributed in the range of approximately 0.5 to 0.7, and for models with large ECS, the ratio tends to decrease. The scaling parameter for the effective radiative forcing of CO_2 varies from model to model and tends to be less than a reference value used in a conventional formula of CO_2 radiative forcing. Although the number of CMIP6 models is currently limited, their parameters show similar distributions within the CMIP5 ranges.

Keywords: climate sensitivity, effective radiative forcing, impulse response model, climate model emulator, ensemble climate experiment

©2019. Japan Geoscience Union. All Right Reserved.

Effect on the earth system of realizing 1.5 degree climate target by overshooting after reaching 2 degree level

*Kaoru Tachiiri[1], Herran Diego Silva[2], Xuanming Su[1], Michio Kawamiya[1]

1. Japan Agency for Marine-Earth Science and Technology, 2. Institute for Global Environmental Strategies

By using an Earth system model (ESM) with emissions and land use scenarios consistent with socio-economic projections from an integrated assessment model, the effect of overshooting to 1.5 degree target (in Celsius from pre-industrial periods) after reaching 2 degree level is investigated in selected indicators of the global environment. Unlike the internationally coordinated model intercomparison project, the scenario is developed for a specific climatic model. The ESM output results in delayed achievements for both of 1.5 and 2 degree targets in terms of global surface mean air temperature, but achieved before or around 2100 as expected when we use global mean surface temperature (for which sea surface temperature and surface air temperature are used for ocean and land, respectively) masked with observation areas. In the overshooting scenario more heat is absorbed by the ocean compared to a case without overshooting, but still we found significant difference between the two scenarios in Arctic sea ice, while in both scenarios corals seem difficult to survive the 21st century (when no thermal adaptation is assumed) . The difference in steric sea level rise between the scenarios is only below 2 cm in 2100. In addition, vegetation productivity in broad regions shows slight (~5%) increase. Emission pathways in the scenarios rely on a large amount of carbon sequestration. In the 2 degree scenario CO2 emissions in 2100 are slightly below zero, while for 1.5 degree scenario they are below -20 GtCO2.. When the Earth system has high climate sensitivity and TCRE, to reach the 1.5 degree target we need to take an overshooting temperature pathway, but in case the overshooting is large, difference in some indicators between 1.5 degree and 2 degree scenarios can be non-significant, which is an important indication in implementing adaptive mitigation in the coming decades.

Keywords: Earth system model, integrated assessment model, 1.5 degree target, 2 degree target, stabilization, overshooting

©2019. Japan Geoscience Union. All Right Reserved.

Historical regional and sectoral contributions to climate change

*Xuanming Su[1], Kaoru Tachiiri[1], Katsumasa TANAKA[2], Michio Watanabe[1]

1. Japan Agency for Marine-Earth Science and Technology, 2. National Institute for Environmental Studies

Regional or sectoral contributions to climate change are important in the formulation of climate change policy. After the industrial revolution, developed countries emit CO_2 and non-CO_2 greenhouse gases (GHGs), and the historical emissions are large; while developing countries contribute relative fewer emissions in historical period but increase significantly in recent years or visible future. To assess the contributions to climate change, using cumulative emissions is a general and direct method. However, such method may ignore the lifetime of GHGs since part of the GHGs sink into the biosphere, ocean, soil or diminish during biogeochemical cycles. In this study, we evaluate the historical regional and sectoral contributions to climate change by using an improved version of Simple Climate Model for OPTimization (SCM4OPT) with a normalized marginal method. Based on the results, we analyze ten major GHG emitting countries and 12 sectors.

First, current emissions with relative long lifetime like CO_2 and N_2O, from developing countries increase significantly, like China, India, Mexico and Brazil, however, their contributions to climate change are still relatively smaller, compared with the developed countries such as USA, Japan, Germany, Canada and UK, of which countries the cumulative emissions are in relatively larger scale and current emissions are already under controlled. We can conclude here that the GHGs with relatively long lifetime need to be controlled stringently to reduce the long-term effects on climate change. For CH_4, which has a relatively shorter lifetime, the contributions to climate change are closely related to emissions within recent decades. These imply that reductions on short lifetime emissions can make immediate alleviation regarding climate change.

Second, energy sector contributes most of the CO_2 emissions, and therefore contribute almost half to the climate change among all the sectors. However, for CH_4 and N_2O, agriculture sector contributes most of the emissions and therefore their contributions to climate change are remarkable. Reduction policiesneed to targetthesesectors. In addition, CO_2 from land transportation and CH_4 from waste treatment increase rapidly in recent years, attention also needs to be paid to these sectors for making climate change policies.

Keywords: region emissions, sector emissions, climate change contribution, simple climate model

©2019. Japan Geoscience Union. All Right Reserved.

Future projection of global climate, water, food, bio-energy, and land investigated with MIROC-INTEG: a global bio-geophysical land surface model with human components

*Tokuta Yokohata[1], Yusuke Satoh[1], Tsuguki Kinoshita[2], Gen Sakurai[3], Yadu Pokhrel[4], Akihiko Ito[1], Etsushi Kato[5], Masashi Okada[1], Naota Hanasaki[1], Tomoko Nitta[6], Seita Emori[1]

1. National Institute for Environmental Studies, 2. Ibaraki University, 3. National Agriculture and Food Research Organization, 4. Michigan State University, 5. The Institute of Applied Energy, 6. University of Tokyo

Future climate changes possibly affect water resources, food production, energy supply, and ecosystem services. It is critical to better understand the interactions between the changes in these complicated factors. While earth system models and integrated assessment models are applicable to explore this topic, parts of their natural and/or human processes tend to be simplified depending on their scope. As such, it still remains a challenge to realistically model the human-natural interface. In this context, the MIROC integrated terrestrial model (MIROC-INTEG) was developed. One of the features of MIROC-INTEG is that the natural ecosystem and human activity models are coupled to a global land surface model MATSIRO (Nitta et al. 2014, Journal of Climate), which is a component of a state-of-the-art global climate model, MIROC (Watanabe et al. 2010, Journal of Climate). As a natural ecosystem model, we use a global vegetation model, VISIT (Ito and Inatomi 2012, Biogeosciences). As human activity models, we use a global land-surface model with anthropogenic water regulation modules, HiGW-MAT (Pokhrel et al, 2012, Journal of Hydrometeorology), and a global crop model, PRYSBI2 (Sakurai et al, 2014, Scientific Reports). In HiGW-MAT, models of human water regulations such as water withdrawal from river, dam operation, and irrigation (Hanasaki et al. 2008, Hydrol. Earth Syst. Sci.) are incorporated to the above-mentioned global land surface model, MATSIRO. In PRYSBI2, the growth and yield of four crops (wheat, maize, soybean, rice) are calculated. In addition to these models, a global land use model (Terrestrial Land-use Model, TeLMO) is newly developed in the present study. TeLMO calculate the grid ratio of cropland (food and bio-energy crops), pasture, forest (managed and un-managed), as well as their transition. Output variables of each sub-model are passed to other sub-models during the time integration.
We will present an analysis of historical and future simulations with a focus on the interactions between water, food, energy, and land. In the historical simulations, we validated the model output such as irrigated water, crop yield, ecosystem productions, and cropland area by comparing to the observed or reanalysis data. In the future simulations, we investigated the role of uncertainties in climate (Representative Concentration Pathways) and socio-economic (Shared Socio-economic Pathways) scenarios. We also investigate the role of uncertainties in model parameters, and found that an uncertainty in the fertilization effect of crop growth model PRYSBI2 strongly affect uncertainty in future projection of crop yield and land use change in TeLMO. We found that future changes in precipitation and/or temperature possibly cause decrease in soil moisture, leading to decreases in crop yield (especially in high emission scenario such as RCP8.5). Decrease in crop yield bring about increase in crop land area, which also causes the increase in irrigation demands. Interaction between water, crop yield, and land use, as well as possible impacts on ecosystem service will be discussed in the presentation.

Keywords: Global Climate Model, Earth System Model, Human activity

©2019. Japan Geoscience Union. All Right Reserved.

Downscaling a global agricultural land use model to country level for national SSP analysis

*Wenchao Wu[1], Tomoko Hasegawa[1], Kiyoshi Takahashi[1], Shinichiro Fujimori[2]

1. National Institute for Environmental Studies, 2. Kyoto Univ.

The Shared Socioeconomic Pathways (SSPs) has been part of latest scenario framework developed by the climate change research society in the recent decade, serving the integrated analysis of future climate impacts, vulnerabilities, adaptation, and mitigation, in which the agriculture, food system and land use are important components. Multiple integrated assessment models (IAMs) have been used for the quantitative projections of future agriculture, food system and land use in the global scale. However, the tool and application of IAMs to the quantification of SSPs on regional or national level is limited. Meanwhile, there are growing needs for the quantification of SSPs on regional or national level for a more detailed understanding of agriculture, food, and land use, and their interactions with other nexus, such as energy, water, and biodiversity. One obstacle for such application is the coarse spatial resolution of global IAMs for land use module. This study aims to apply the Asian-Pacific Integrated Model/Platform for Land-Use and Environmental Model (AIM/PLUM) for the quantification of agriculture, food system, and land use in Japan under its national-specific SSPs narratives. To achieve this, a regional land use model, AIM/PLUM-Japan, was developed, by improving the spatial resolution to 0.05˚ (targeting 1km) from global model of 0.5˚. We combined the statistical production area data and spatial land use data to produce a refined base crop map. Agricultural land use could be downscaled to 0.05˚ resolution and gridded agricultural land use information could be generated using this model. Aside from providing quantitative land use information for Japan’ s SSPs, this study also contributes to the IAMs and SSPs societies by testing the applicability and feasibility of global IAMs, especially land use models, to the regional or national extension. For example, regional (national) SSPs quantifications for other regions could be easily implemented by a similar paradigm using AIM/PLUM.

Keywords: downscaling, land use, national SSP

©2019. Japan Geoscience Union. All Right Reserved.

Extreme Events and Emergent Trends in Marine Ecosystem Stressors under a historical/RCP8.5 Climate Change Pathway

*Keith Bradley Rodgers[1,2], Sarah Schlunegger[3], Richard Slater[3], Burke Hales[4], Axel Timmermann[1,2]

1. IBS Center for Climate Physics, Busan, South Korea, 2. Pusan National University, Busan, South Korea, 3. AOS Program, Princeton University, Princeton NJ, USA, 4. College of Ocean and Atmospheric Sciences, Oregon State Universitym, Corvallis, OR, USA

It is important to identify the degree to which climate change will impact ocean ecosystems over the 21st century. Over the last decade there has been increasing application of Earth System Models (ESMs) to project changes in ecosystem stressors (acidification, warming, and de-oxygenation) with a focus on surface and/or thermocline-integrated conditions. Recent efforts have made combined use of CMIP5 models, large ensemble simulations, and/or scenario sensitivity experiments to estimate uncertainties in future projections. Nevertheless very little to date has been done to evaluate how the frequency of extreme events with ecosystem stressors will respond to future climate perturbations. Here we consider for an ensemble suite of simulations with GFDL's ESM2M changes in the frequency of marine ecosystem extreme events over the 21stcentury. We focus on the contrast between the behavior at the ocean's surface vs. base of the ocean's euphotic zone, as these are both important horizons for ocean ecosystems, and on the contrast between the Time of Emergence of decadal trends vs. frequency changes of extreme events, as these are both important ecological timescales. Particular attention is devoted to acidification at the base of the euphotic zone, as this pertains to the life cycle of pteropods. Preliminary results indicate that in addition to the subpolar Northern Oceans and the Southern Ocean, the Large Marine Ecosystems (LME) regions of the eastern Pacific become increasingly exposed to corrosive waters over the 21stcentury.

Keywords: Climate Change, Ecosystem Stressors, Extreme Events, Large Ensemble

©2019. Japan Geoscience Union. All Right Reserved.

[E] Poster | H (Human Geosciences)：H-GM Geomorphology

Wed. May 29, 2019 3:30 PM - 5:00 PM JST | Wed. May 29, 2019 6:30 AM - 8:00 AM UTC | Poster Hall International Exhibition Hall8, Makuhari Messe_11

[H-GM03] Geomorphology

convener:Tsuyoshi Hattanji(Faculty of Life and Environmental Sciences, University of Tsukuba), Masayuki Seto(Fukushima Future Center for Regional Revitalization, Fukushima University)

The main subject of this session is interdisciplinary discussion on the whole range of themes relating to geomorphology, especially geomorphic processes, landform development and its relation to environmental changes, geomorphological hazards and their mitigation, relationships among geomorphic processes, other natural phenomena and human activities, and various techniques of geomorphological measurements and landform classification. All presentations and discussion of this session are made in English.

[HGM03-P01] Honeycomb Weathering (Tafoni) of Sandstone and Environmental Factors in Yonaguni Island, Okinawa Prefecture, Japan

*Takayuki Ogata[1] (1.Disaster Prevention Research Center for Island Regions, University of the Ryukyus)

[HGM03-P02] Colluvial deposits in first-order streams and channel head migration by shallow landslides: Case study in granitic basins, Asaminami, Hiroshima, Japan

*Tsuyoshi Hattanji[1], Ryuya Kodama[2], Takahisa Furuichi[3], Shoji Doshida[4], Yasushi Tanaka[5] (1.Faculty of Life and Environmental Sciences, University of Tsukuba, 2.former College of Geoscience, University of Tsukuba, 3.Hokkaido University, 4.National Research Institute of Fire and Disaster, 5.Komazawa University)

[HGM03-P03] Rock restrictions on topographical features of rivers: model experiment

*Yuta Takase[1], Noritaka Endo[1] (1.Kanazawa University)

[HGM03-P04] Stream power incision model and the stage of topographic equilibrium, using physical experiments

*Imamura Akihiro[1], Noritaka Endo[1] (1.Kanazawa University)

[HGM03-P05] Downstream variation in gravel size of the Tenjin River system

*Kazuaki Hori[1], Kazuya Yonehara[1] (1.Department of Geography, Graduate School of Environmental Studies, Nagoya University)

[HGM03-P06] Talus slope development in the time of deglaciation: a case study of the Rev Valley, SW Spitsbergen

*Krzysztof Senderak[1], Marta Kondracka[1], Bogdan Gądek[1] (1.Faculty of Earth Sciences, University of Silesia)

[HGM03-P07] Distribution of Large Benthic Foraminifers in one of Majuro's Conservation Areas – Drenmeo Island

*Benedict Yamamura[1], Kazuhiko Fujita[2], Melba White[3], Kyotak Ishiguro[3], Hironobu Kan[1] (1.Kyushu University, Integrated Sciences for Global Society - Research Center for Coastal Seafloor , 2.Department of Physics and Earth Sciences, University of the Ryukyus, 3.Marshall Islands Marine Resources Authority)

[HGM03-P08] Luminescence chronology of fluvial and marine records from subsurface sediment cores: An insight into the geomorphic evolution of Kaveri delta, India

*kartika goswami[1], Anbarasu Kumaresan[2], Sivakumar Krishnan[2], Senthil K. Sadasivam[2], Manoj Kumar Jaiswal[1] (1.Department of Earth Sciences, Indian Institute of Science Education and Reserach Kolkata, 2.National College Tiruchirappalli, India)

Honeycomb Weathering (Tafoni) of Sandstone and Environmental Factors in Yonaguni Island, Okinawa Prefecture, Japan

*Takayuki Ogata[1]

1. Disaster Prevention Research Center for Island Regions, University of the Ryukyus

Sandstone surfaces of Yonaguni Island (westernmost of the Ryukyu Arc) often show a honeycomb structure (tafoni) derived from physical disintegration in relation to salt weathering. Miocene sandstone (Yaeyama Group) is extensively exposed on the island surface, and forms sea cliffs along rocky coasts. The honeycomb structure is especially observed along the coasts where wave splashes produce wetting and drying processes assisted by strong wind and active evaporation. The geometry and density of tafoni seem to be controlled by vertical height from the sea level and horizontal distance of the coast line. Field observations at the rocky coasts of Yonaguni Island suggest that larger holes are developed along the north-faced coasts than the south-faced coasts, which depends mainly on the northeastern monsoon during the winter period.

Keywords: weathering, sandstone, rocky coast, tafoni, monsoon, Yaeyama group

©2019. Japan Geoscience Union. All Right Reserved.

Colluvial deposits in first-order streams and channel head migration by shallow landslides: Case study in granitic basins, Asaminami, Hiroshima, Japan

*Tsuyoshi Hattanji[1], Ryuya Kodama[2], Takahisa Furuichi[3], Shoji Doshida[4], Yasushi Tanaka[5]

1. Faculty of Life and Environmental Sciences, University of Tsukuba, 2. former College of Geoscience, University of Tsukuba, 3. Hokkaido University, 4. National Research Institute of Fire and Disaster, 5. Komazawa University

Relationship between dates of colluvial deposits and channel-head migration was examined in granitic mountains where a debris-flow disaster occurred in 2014. Topographic analysis using 1-m grid DEMs before and after the disaster indicates that post-event channel heads were located upslope from pre-event channel heads due to landslide or erosion by debris flow. Post-event channel heads with shallow landslides had strong inverse correlations between local slope and drainage area. Charcoal samples were collected in colluvial deposits of two post-event channel heads (A and B) where the channel heads migrated more than 50 m upslope with shallow landslides. The radiocarbon dates of the samples were 1162–1194 y BP for channel head A and 786 y BP for channel head B. Another sample was collected in colluvial deposits of a post-event channel head (C) with shallow landslide but no migration. The radiocarbon date of the sample at the channel head C was 670 y BP. These radiocarbon data explain contrasting intervals of landslide events in hollows. The channel head A with older radiocarbon dates has the longer interval of landslide events and therefore the valley head has been buried in longer distance (more than 50 m) along the channel since the last landslide event to 2014.

Keywords: High-resolution DEM, Micro-topography, Radiocarbon dating, Valley head

©2019. Japan Geoscience Union. All Right Reserved.

Rock restrictions on topographical features of rivers: model experiment

*Yuta Takase[1], Noritaka Endo[1]

1. Kanazawa University

Landforms of mountainous areas is developed by both downcutting and lateral erosion of rivers. For example, ingrown meanders develop when the lateral erosion is predominant, while entrenched meanders form when the downcutting is dominant. It is a generally accepted understanding that the relative superiority or inferiority between the downcutting and lateral erosion is determined by the uplift rate of the land, rock strength difference, riverbed gradient, deflection of flow in a channel, but the systematic discussion remains insufficient. In this study, we conducted flume experiments to investigate the relationship between bedrock strength and sinuosity, and the relationship between time series pattern of uplift and meandering development. We prepared a single channel that cut a uniform substrate in a two-dimensional flume. The substrates were made of the mixture of fine sand and clay, and we examined two types of substrate, hard and soft ones, which can be formed by changing the ratio of sand and clay (the mixure including more clay is harder). Uplift of the experimental land was realized by lowering a weir set at the downstream end of the channel, i.e. the base-level lowering.

Knickpoints were observed more frequently in the case of hard substrate, which is consistent with previous study (Grimaud, 2016). Sinuosity of the channel tended to be higher for the hard substrate than the soft substrate, which is seemingly opposite the conventional understanding, but can be attributed to sustainability of the channel shape due to erosion resistance of the hard substrate. In all the experiments, the sinuosity tended to be higher after the uplift ceased rather than during the period of uplift.

Keywords: labo, sinuosity, bedrock strength, knickpoint, uplift

©2019. Japan Geoscience Union. All Right Reserved.

Stream power incision model and the stage of topographic equilibrium, using physical experiments

*Imamura Akihiro[1], Noritaka Endo[1]

1. Kanazawa University

Bedrock rivers develop their landforms very slowly, compared with alluvial river, thus bedrock rivers and their surrounding topographies are expected to record long-term environmental changes such as tectonics and climate. The stream power incision model (SPIM) is an empirical model that expresses the erosion rate due to rivers by the product of two power functions of the contributing area and river bed slope. Using this equation with an uplift term, the differential equation of the temporal change in the altitude of riverbed is constituted. When applying the model to a natural drainage basin, the equilibrium state between erosion and uplift is often assumed, partially because the uplift rate is usually unknown. Under the assumption of equilibrium state, SPIM is reduced to the relationship in which the riverbed slope is a power function of the contributing area, known as Flint’s law, which is the basis of “slope-area analysis” to determine the concavity (equivalent to the ratio of two power exponents in SPIM). Usually the two power exponents in SPIM are presumed to be constant if lithology, climate, and other factors are the same. This postulation, however, is difficult to verify for natural landforms, because of heterogeneity of various kind of property within a single drainage basin and difficulty in evaluation of the incision rate.

This study investigates the relation between the incision rate and topographic properties in river basins, through the observation of small-sized physical experiments under well-controlled conditions. A flume used was 90×180 cm, and the substrate to be dissected composed of the uniform mixture of sand and clay was installed. Rainfall was simulated by supplying mist from 10 nozzles. Uplift was realized by lowering a weir that was installed at the downstream end of the flume and determined the base level. The landform was measured by photogrammetry using several hundred photos taken during intermission from rainfall for photographing.

We compared the results of (1) this and (2) the previous studies (Imamura and Endo, 2018) realizing different kinds of uplift: (1) sudden base level lowering from a stable state of basin, to observe the response processes of the landforms until the basin became stable again (about 5 hours); (2) Sudden change in the uplift rate, to observe the change from a stable state under constant uplift of 4.5 mm/h to a new stable state under faster uplift rate of 6.0 mm/h (about 6 hours).

The results of Experiment (1) showed that the incision rate decreased with time (presumably asymptotic to zero), while Experiment (2) always displayed a certain finite value of the incision rate. The power exponents in SPIM, m (for the contributing area) and n (for the slope) did not seem to be constant in both experiments. The ratio m/n also changed, but seemed to converge to a certain value in each experiment.

We evaluated the correlation of the incision rate with the fitted function for each measurement time. In Experiment (1), although the denudation rate decreased with time, the first half of the run time showed good correlations but the latter half showed the worse. By contrast, Experiment (2) exhibited increasing correlations in the latter half of the run. These results suggests that SPIM holds for dynamic equilibrium (tectonic steady state (Montgomery, 2001)) or the early stage of static quasi-equilibrium (erosional stead state (Montgomery, 2001)), but fails for mature or later stages in which a landform proceeds to a

©2019. Japan Geoscience Union. All Right Reserved.

peneplane.

Imamura and Endo, 2018. Incision rate, riverbed slope and contributing area of an experimental drainage basin. JPGU 2018 Abstract.

Montgomery, 2001, Slope distributions, threshold hillslopes, and steady-state topography. American Journal of Science, 301, 432–454.

Keywords: stream power model, laboratory experiment, bedrock river

©2019. Japan Geoscience Union. All Right Reserved.

Downstream variation in gravel size of the Tenjin River system

*Kazuaki Hori[1], Kazuya Yonehara[1]

1. Department of Geography, Graduate School of Environmental Studies, Nagoya University

Many researchers have studied downstream variation in river-bed material size and its controlling factors, because they are important to understand the evolution of fluvial landforms and drainage basin. Many of these studies have focused only on rivers flowing through mountains or alluvial plains. Thus, it is desirable to examine a much broader range, i.e. from head to mouth of a river. We investigated the downstream variation of gravel size and channel gradient in the Tenjin River system (Tenjin, Ogamo, and Mitoku rivers) located in the central part of Tottori prefecture, Japan. The Tenjin River is approximately 34 km in length and major tributaries, the Ogamo and Mitoku rivers, join the Tenjin River at approximately 7 km and 12 km upstream from the mouth, respectively. Mean gravel size tends to decrease toward the downstream between 5 and 23 km upstream from the Tenjin River mouth where exposed gravel bars are easily found. Channel gradient is usually less than 0.03 and its variation is relatively small in this range. On the other hand, exposed gravel bars are uncommon between 23 and 34 km upstream from the mouth. The channel gradient become larger (> 0.06) and shows large variation. Large boulders (> 500 mm) are distributed in the channel. The number of boulders, especially > 1000 mm, seems to be inversely proportional to the distance from the valley wall. Buffers along the rivers regulate the supply of boulders from the valley wall in the upper reaches and reduce the connectivity of sediment supply from the tributaries in the middle and lower reaches. Barriers typified by weirs reduce the connectivity in the longitudinal direction throughout the basin.

Keywords: sediment connectivity, grain size, channel gradient

©2019. Japan Geoscience Union. All Right Reserved.

Talus slope development in the time of deglaciation: a case study of the Rev Valley, SW Spitsbergen

*Krzysztof Senderak[1], Marta Kondracka[1], Bogdan Gądek[1]

1. Faculty of Earth Sciences, University of Silesia

Every high-mountain area is characterized by the occurrence of talus slopes. A process of development this kind of forms depends on among other things climatic conditions. Currently in Spitsbergen, we observe the deglaciation process caused climate changes. This causes that the evolution’ s tempo of all environments linked with glaciers is very high. It also concerns the talus slopes, which, in the last time, are more often used as key element to paleo-environmental reconstructions for last thousands. In this paper, we present the geophysical surveys of talus slopes conducted in the Rev Valley (SW Spitsbergen). The valley was shaped by glacier, which left behind among other things glacial lake and buried glacial ice in mixed slope-moraine material. Nowadays, the talus slopes in this valley develop under the typical conditions of periglacial environment. In the studies of 15 talus slopes we used the ground-penetrating radar (GPR) and electrical resistivity tomography method (ERT). The studies allowed to recognize the internal structure of talus slopes and to determine a character of their elements, such as thickness of slopes, permafrost table and a depth of active layer, present of buried glacial ice, sediementological structures caused by various deposition of material on the slope surface, and finally a shape of bedrock. A comparison obtained results indicates on relevant regularity in the development of internal structure of talus slopes. These are for example visible differences in the terms of present of permafrost, which is located from a depth 2-3 m in the oldest slopes to a depth 4-5 m in the youngest. On the other hands, the studies discovers the deviations from the typical evolution models. The buried glacial ice has not been survived in a younger forms, whereas it is present in these older slopes. Based on the results we created the proposition of model of talus slope evolution developing in a periglacial period. In this time the development of slopes characterize a very high variability, not much lower than in previous paraglacial period. This work was financed from the funds of the National Science Centre in Poland received by Krzysztof Senderak in the Preludium 12 project: Determination of the evolution of slopes of southern Spitsbergen on the background of climate changes (2016/23/N/ST10/00162).

Keywords: talus slope evolution, permafrost, deglaciation, electrical resistivity tomography (ERT), ground-penetrating radar (GPR)

©2019. Japan Geoscience Union. All Right Reserved.

Distribution of Large Benthic Foraminifers in one of Majuro's Conservation Areas –Drenmeo Island

*Benedict Yamamura[1], Kazuhiko Fujita[2], Melba White[3], Kyotak Ishiguro[3], Hironobu Kan[1]

1. Kyushu University, Integrated Sciences for Global Society - Research Center for Coastal Seafloor , 2. Department of Physics and Earth Sciences, University of the Ryukyus, 3. Marshall Islands Marine Resources Authority

Climate change is having a huge impact on the island formation. In this study, we examined the composition and distribution of large benthic foraminifers (LBF) from 12 chosen sample sites (see map) within and outside of Drenmeo islet, one of the designated conservation areas in Majuro atoll. Samples were collected from the area to further investigate the sand built-up between the conservation area and the adjacent islet. The preliminary findings showed that the area is predominantly composed of two island-building LBF, namely *Calcarina sp.* and *Amphistegina sp.* The final results from this study will help stakeholders to amend the management plan to include the adjacent islet under the current management plan.

Keywords: Drenmeo island, conservation area, large benthic foraminifers, management plan

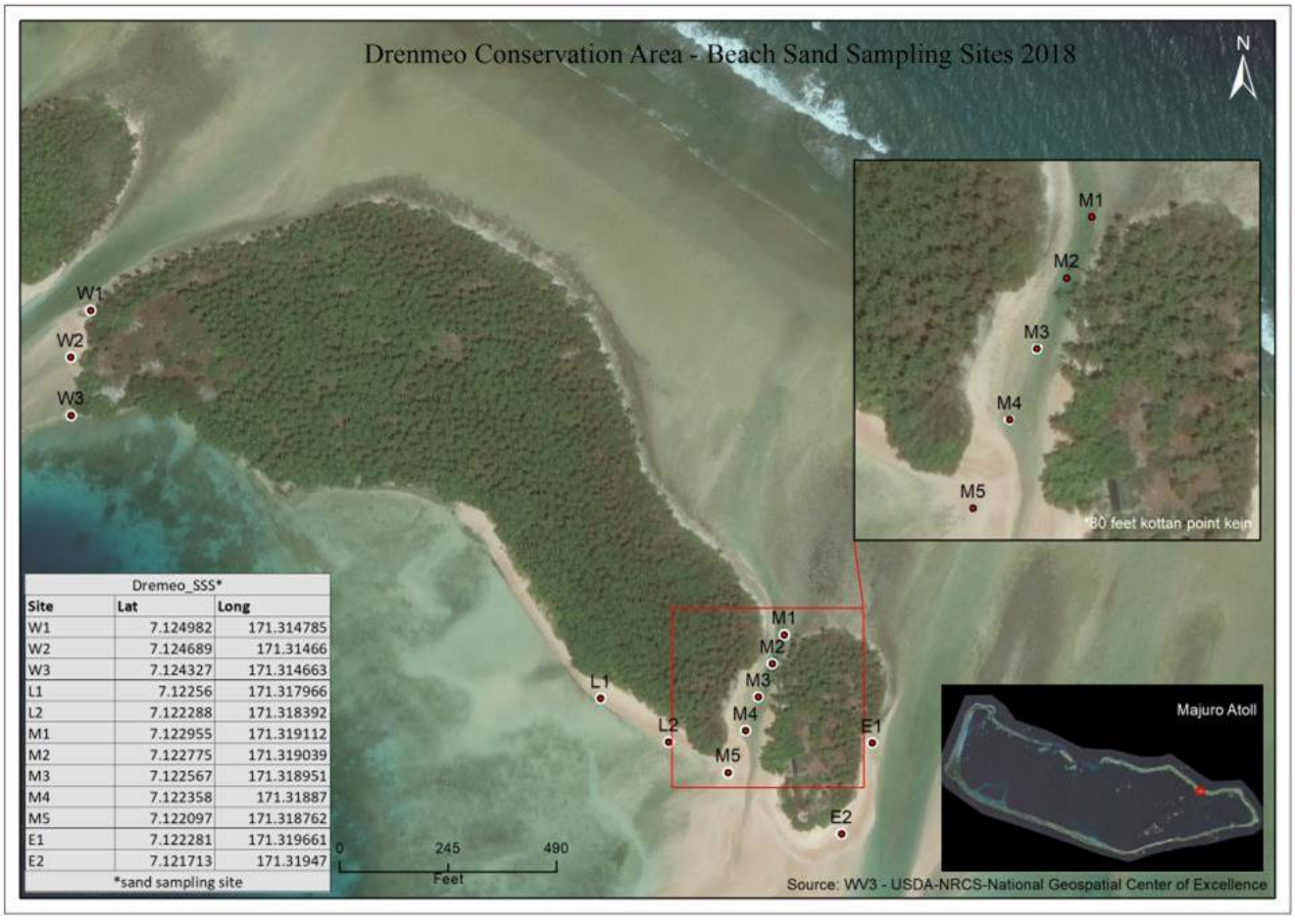

©2019. Japan Geoscience Union. All Right Reserved.

Luminescence chronology of fluvial and marine records from subsurface sediment cores: An insight into the geomorphic evolution of Kaveri delta, India

*kartika goswami[1], Anbarasu Kumaresan[2], Sivakumar Krishnan[2], Senthil K. Sadasivam[2], Manoj Kumar Jaiswal[1]

1. Department of Earth Sciences, Indian Institute of Science Education and Reserach Kolkata, 2. National College Tiruchirappalli, India

Long-term evolution of river deltas is a result of forcings (tectonics, climate, sea level, avulsion, compaction etc). We present the results of luminescence dating of sediments from four sediment cores (VKI, TNR, SY and KKI) of 25 m depth each, retrieved from the Kaveri delta in south India. The coring sites are ~2.5 km, ~11 km, ~17 km and ~20 km away from the present coastline respectively. The cores were analysed for OSL dating, 14C dating, lithology and microfossils and represent various stages of fluvial and marine activity in the region over the last ~150 ka. The chronology of the core closet to the coast (VKI) reflects eight major phases of increased sea level during the late quaternary period (142-140 ka, 104-100 ka, ~121 ka, 87-81 ka, 60-57 ka, 9-6 ka, ~5 ka and ~3 ka) partly coinciding with the global climate cycles MIS 6, MIS 5, MIS 3, MIS 1 respectively. During ~121 ka and 9-6 ka, marine transgression reached the core location to leave marine signatures in the forms of foraminifera. VKI core replicates the quaternary sea level curve, showing strong control of the sea in coastal deposition.

The oldest age of VKI is ~140 ka. The three cores situated further inland give oldest/bottom most ages of~120 ka. This indicates the coastal land has uplifted in the recent years with deeper sediments being encountered at relative shallower depth. The uplift is expected to occur around post 50 ka, creating a basin fill situation for riverine sediments to accumulate and restricting the delta to prograde. This is observed from the sedimentation pattern and robust chronology of the other three inland cores. Analysis of DEM also supported the occurrence of uplift. Thus, the present work examines the geomorphic evolution of Kaveri delta, an archive of fluvial, shoreline and tectonic activities.

Keywords: OSL Dating, Kaveri Delta , GIS, Foraminifera

©2019. Japan Geoscience Union. All Right Reserved.

[E] Poster | H (Human Geosciences)：H-GM Geomorphology

Wed. May 29, 2019 5:15 PM - 6:30 PM JST | Wed. May 29, 2019 8:15 AM - 9:30 AM UTC | Poster Hall International Exhibition Hall8, Makuhari Messe_18

[H-GM03] Geomorphology

convener:Tsuyoshi Hattanji(Faculty of Life and Environmental Sciences, University of Tsukuba), Masayuki Seto(Fukushima Future Center for Regional Revitalization, Fukushima University)

The main subject of this session is interdisciplinary discussion on the whole range of themes relating to geomorphology, especially geomorphic processes, landform development and its relation to environmental changes, geomorphological hazards and their mitigation, relationships among geomorphic processes, other natural phenomena and human activities, and various techniques of geomorphological measurements and landform classification. All presentations and discussion of this session are made in English.

[HGM03-P01] Honeycomb Weathering (Tafoni) of Sandstone and Environmental Factors in Yonaguni Island, Okinawa Prefecture, Japan

*Takayuki Ogata[1] (1.Disaster Prevention Research Center for Island Regions, University of the Ryukyus)

[HGM03-P02] Colluvial deposits in first-order streams and channel head migration by shallow landslides: Case study in granitic basins, Asaminami, Hiroshima, Japan

*Tsuyoshi Hattanji[1], Ryuya Kodama[2], Takahisa Furuichi[3], Shoji Doshida[4], Yasushi Tanaka[5] (1.Faculty of Life and Environmental Sciences, University of Tsukuba, 2.former College of Geoscience, University of Tsukuba, 3.Hokkaido University, 4.National Research Institute of Fire and Disaster, 5.Komazawa University)

[HGM03-P03] Rock restrictions on topographical features of rivers: model experiment

*Yuta Takase[1], Noritaka Endo[1] (1.Kanazawa University)

[HGM03-P04] Stream power incision model and the stage of topographic equilibrium, using physical experiments

*Imamura Akihiro[1], Noritaka Endo[1] (1.Kanazawa University)

[HGM03-P05] Downstream variation in gravel size of the Tenjin River system

*Kazuaki Hori[1], Kazuya Yonehara[1] (1.Department of Geography, Graduate School of Environmental Studies, Nagoya University)

[HGM03-P06] Talus slope development in the time of deglaciation: a case study of the Rev Valley, SW Spitsbergen

*Krzysztof Senderak[1], Marta Kondracka[1], Bogdan Gądek[1] (1.Faculty of Earth Sciences, University of Silesia)

[HGM03-P07] Distribution of Large Benthic Foraminifers in one of Majuro's Conservation Areas – Drenmeo Island

*Benedict Yamamura[1], Kazuhiko Fujita[2], Melba White[3], Kyotak Ishiguro[3], Hironobu Kan[1] (1.Kyushu University, Integrated Sciences for Global Society - Research Center for Coastal Seafloor , 2.Department of Physics and Earth Sciences, University of the Ryukyus, 3.Marshall Islands Marine Resources Authority)

[HGM03-P08] Luminescence chronology of fluvial and marine records from subsurface sediment cores: An insight into the geomorphic evolution of Kaveri delta, India

*kartika goswami[1], Anbarasu Kumaresan[2], Sivakumar Krishnan[2], Senthil K. Sadasivam[2], Manoj Kumar Jaiswal[1] (1.Department of Earth Sciences, Indian Institute of Science Education and Reserach Kolkata, 2.National College Tiruchirappalli, India)

Honeycomb Weathering (Tafoni) of Sandstone and Environmental Factors in Yonaguni Island, Okinawa Prefecture, Japan

*Takayuki Ogata[1]

1. Disaster Prevention Research Center for Island Regions, University of the Ryukyus

Sandstone surfaces of Yonaguni Island (westernmost of the Ryukyu Arc) often show a honeycomb structure (tafoni) derived from physical disintegration in relation to salt weathering. Miocene sandstone (Yaeyama Group) is extensively exposed on the island surface, and forms sea cliffs along rocky coasts. The honeycomb structure is especially observed along the coasts where wave splashes produce wetting and drying processes assisted by strong wind and active evaporation. The geometry and density of tafoni seem to be controlled by vertical height from the sea level and horizontal distance of the coast line. Field observations at the rocky coasts of Yonaguni Island suggest that larger holes are developed along the north-faced coasts than the south-faced coasts, which depends mainly on the northeastern monsoon during the winter period.

Keywords: weathering, sandstone, rocky coast, tafoni, monsoon, Yaeyama group

©2019. Japan Geoscience Union. All Right Reserved.

Colluvial deposits in first-order streams and channel head migration by shallow landslides: Case study in granitic basins, Asaminami, Hiroshima, Japan

*Tsuyoshi Hattanji[1], Ryuya Kodama[2], Takahisa Furuichi[3], Shoji Doshida[4], Yasushi Tanaka[5]

1. Faculty of Life and Environmental Sciences, University of Tsukuba, 2. former College of Geoscience, University of Tsukuba, 3. Hokkaido University, 4. National Research Institute of Fire and Disaster, 5. Komazawa University

Relationship between dates of colluvial deposits and channel-head migration was examined in granitic mountains where a debris-flow disaster occurred in 2014. Topographic analysis using 1-m grid DEMs before and after the disaster indicates that post-event channel heads were located upslope from pre-event channel heads due to landslide or erosion by debris flow. Post-event channel heads with shallow landslides had strong inverse correlations between local slope and drainage area. Charcoal samples were collected in colluvial deposits of two post-event channel heads (A and B) where the channel heads migrated more than 50 m upslope with shallow landslides. The radiocarbon dates of the samples were 1162–1194 y BP for channel head A and 786 y BP for channel head B. Another sample was collected in colluvial deposits of a post-event channel head (C) with shallow landslide but no migration. The radiocarbon date of the sample at the channel head C was 670 y BP. These radiocarbon data explain contrasting intervals of landslide events in hollows. The channel head A with older radiocarbon dates has the longer interval of landslide events and therefore the valley head has been buried in longer distance (more than 50 m) along the channel since the last landslide event to 2014.

Keywords: High-resolution DEM, Micro-topography, Radiocarbon dating, Valley head

©2019. Japan Geoscience Union. All Right Reserved.

Rock restrictions on topographical features of rivers: model experiment

*Yuta Takase[1], Noritaka Endo[1]

1. Kanazawa University

Landforms of mountainous areas is developed by both downcutting and lateral erosion of rivers. For example, ingrown meanders develop when the lateral erosion is predominant, while entrenched meanders form when the downcutting is dominant. It is a generally accepted understanding that the relative superiority or inferiority between the downcutting and lateral erosion is determined by the uplift rate of the land, rock strength difference, riverbed gradient, deflection of flow in a channel, but the systematic discussion remains insufficient. In this study, we conducted flume experiments to investigate the relationship between bedrock strength and sinuosity, and the relationship between time series pattern of uplift and meandering development. We prepared a single channel that cut a uniform substrate in a two-dimensional flume. The substrates were made of the mixture of fine sand and clay, and we examined two types of substrate, hard and soft ones, which can be formed by changing the ratio of sand and clay (the mixure including more clay is harder). Uplift of the experimental land was realized by lowering a weir set at the downstream end of the channel, i.e. the base-level lowering.

Knickpoints were observed more frequently in the case of hard substrate, which is consistent with previous study (Grimaud, 2016). Sinuosity of the channel tended to be higher for the hard substrate than the soft substrate, which is seemingly opposite the conventional understanding, but can be attributed to sustainability of the channel shape due to erosion resistance of the hard substrate. In all the experiments, the sinuosity tended to be higher after the uplift ceased rather than during the period of uplift.

Keywords: labo, sinuosity, bedrock strength, knickpoint, uplift

©2019. Japan Geoscience Union. All Right Reserved.

Stream power incision model and the stage of topographic equilibrium, using physical experiments

*Imamura Akihiro[1], Noritaka Endo[1]

1. Kanazawa University

Bedrock rivers develop their landforms very slowly, compared with alluvial river, thus bedrock rivers and their surrounding topographies are expected to record long-term environmental changes such as tectonics and climate. The stream power incision model (SPIM) is an empirical model that expresses the erosion rate due to rivers by the product of two power functions of the contributing area and river bed slope. Using this equation with an uplift term, the differential equation of the temporal change in the altitude of riverbed is constituted. When applying the model to a natural drainage basin, the equilibrium state between erosion and uplift is often assumed, partially because the uplift rate is usually unknown. Under the assumption of equilibrium state, SPIM is reduced to the relationship in which the riverbed slope is a power function of the contributing area, known as Flint’s law, which is the basis of “slope-area analysis” to determine the concavity (equivalent to the ratio of two power exponents in SPIM). Usually the two power exponents in SPIM are presumed to be constant if lithology, climate, and other factors are the same. This postulation, however, is difficult to verify for natural landforms, because of heterogeneity of various kind of property within a single drainage basin and difficulty in evaluation of the incision rate.

This study investigates the relation between the incision rate and topographic properties in river basins, through the observation of small-sized physical experiments under well-controlled conditions. A flume used was 90×180 cm, and the substrate to be dissected composed of the uniform mixture of sand and clay was installed. Rainfall was simulated by supplying mist from 10 nozzles. Uplift was realized by lowering a weir that was installed at the downstream end of the flume and determined the base level. The landform was measured by photogrammetry using several hundred photos taken during intermission from rainfall for photographing.

We compared the results of (1) this and (2) the previous studies (Imamura and Endo, 2018) realizing different kinds of uplift: (1) sudden base level lowering from a stable state of basin, to observe the response processes of the landforms until the basin became stable again (about 5 hours); (2) Sudden change in the uplift rate, to observe the change from a stable state under constant uplift of 4.5 mm/h to a new stable state under faster uplift rate of 6.0 mm/h (about 6 hours).

The results of Experiment (1) showed that the incision rate decreased with time (presumably asymptotic to zero), while Experiment (2) always displayed a certain finite value of the incision rate. The power exponents in SPIM, m (for the contributing area) and n (for the slope) did not seem to be constant in both experiments. The ratio m/n also changed, but seemed to converge to a certain value in each experiment.

We evaluated the correlation of the incision rate with the fitted function for each measurement time. In Experiment (1), although the denudation rate decreased with time, the first half of the run time showed good correlations but the latter half showed the worse. By contrast, Experiment (2) exhibited increasing correlations in the latter half of the run. These results suggests that SPIM holds for dynamic equilibrium (tectonic steady state (Montgomery, 2001)) or the early stage of static quasi-equilibrium (erosional stead state (Montgomery, 2001)), but fails for mature or later stages in which a landform proceeds to a

©2019. Japan Geoscience Union. All Right Reserved.

peneplane.

Imamura and Endo, 2018. Incision rate, riverbed slope and contributing area of an experimental drainage basin. JPGU 2018 Abstract.

Montgomery, 2001, Slope distributions, threshold hillslopes, and steady-state topography. American Journal of Science, 301, 432–454.

Keywords: stream power model, laboratory experiment, bedrock river

©2019. Japan Geoscience Union. All Right Reserved.

Downstream variation in gravel size of the Tenjin River system

*Kazuaki Hori[1], Kazuya Yonehara[1]

1. Department of Geography, Graduate School of Environmental Studies, Nagoya University

Many researchers have studied downstream variation in river-bed material size and its controlling factors, because they are important to understand the evolution of fluvial landforms and drainage basin. Many of these studies have focused only on rivers flowing through mountains or alluvial plains. Thus, it is desirable to examine a much broader range, i.e. from head to mouth of a river. We investigated the downstream variation of gravel size and channel gradient in the Tenjin River system (Tenjin, Ogamo, and Mitoku rivers) located in the central part of Tottori prefecture, Japan. The Tenjin River is approximately 34 km in length and major tributaries, the Ogamo and Mitoku rivers, join the Tenjin River at approximately 7 km and 12 km upstream from the mouth, respectively. Mean gravel size tends to decrease toward the downstream between 5 and 23 km upstream from the Tenjin River mouth where exposed gravel bars are easily found. Channel gradient is usually less than 0.03 and its variation is relatively small in this range. On the other hand, exposed gravel bars are uncommon between 23 and 34 km upstream from the mouth. The channel gradient become larger (> 0.06) and shows large variation. Large boulders (> 500 mm) are distributed in the channel. The number of boulders, especially > 1000 mm, seems to be inversely proportional to the distance from the valley wall. Buffers along the rivers regulate the supply of boulders from the valley wall in the upper reaches and reduce the connectivity of sediment supply from the tributaries in the middle and lower reaches. Barriers typified by weirs reduce the connectivity in the longitudinal direction throughout the basin.

Keywords: sediment connectivity, grain size, channel gradient

©2019. Japan Geoscience Union. All Right Reserved.

Talus slope development in the time of deglaciation: a case study of the Rev Valley, SW Spitsbergen

*Krzysztof Senderak[1], Marta Kondracka[1], Bogdan Gądek[1]

1. Faculty of Earth Sciences, University of Silesia

Every high-mountain area is characterized by the occurrence of talus slopes. A process of development this kind of forms depends on among other things climatic conditions. Currently in Spitsbergen, we observe the deglaciation process caused climate changes. This causes that the evolution’ s tempo of all environments linked with glaciers is very high. It also concerns the talus slopes, which, in the last time, are more often used as key element to paleo-environmental reconstructions for last thousands. In this paper, we present the geophysical surveys of talus slopes conducted in the Rev Valley (SW Spitsbergen). The valley was shaped by glacier, which left behind among other things glacial lake and buried glacial ice in mixed slope-moraine material. Nowadays, the talus slopes in this valley develop under the typical conditions of periglacial environment. In the studies of 15 talus slopes we used the ground-penetrating radar (GPR) and electrical resistivity tomography method (ERT). The studies allowed to recognize the internal structure of talus slopes and to determine a character of their elements, such as thickness of slopes, permafrost table and a depth of active layer, present of buried glacial ice, sediementological structures caused by various deposition of material on the slope surface, and finally a shape of bedrock. A comparison obtained results indicates on relevant regularity in the development of internal structure of talus slopes. These are for example visible differences in the terms of present of permafrost, which is located from a depth 2-3 m in the oldest slopes to a depth 4-5 m in the youngest. On the other hands, the studies discovers the deviations from the typical evolution models. The buried glacial ice has not been survived in a younger forms, whereas it is present in these older slopes. Based on the results we created the proposition of model of talus slope evolution developing in a periglacial period. In this time the development of slopes characterize a very high variability, not much lower than in previous paraglacial period. This work was financed from the funds of the National Science Centre in Poland received by Krzysztof Senderak in the Preludium 12 project: Determination of the evolution of slopes of southern Spitsbergen on the background of climate changes (2016/23/N/ST10/00162).

Keywords: talus slope evolution, permafrost, deglaciation, electrical resistivity tomography (ERT), ground-penetrating radar (GPR)

©2019. Japan Geoscience Union. All Right Reserved.

Distribution of Large Benthic Foraminifers in one of Majuro's Conservation Areas –Drenmeo Island

*Benedict Yamamura[1], Kazuhiko Fujita[2], Melba White[3], Kyotak Ishiguro[3], Hironobu Kan[1]

1. Kyushu University, Integrated Sciences for Global Society - Research Center for Coastal Seafloor , 2. Department of Physics and Earth Sciences, University of the Ryukyus, 3. Marshall Islands Marine Resources Authority

Climate change is having a huge impact on the island formation. In this study, we examined the composition and distribution of large benthic foraminifers (LBF) from 12 chosen sample sites (see map) within and outside of Drenmeo islet, one of the designated conservation areas in Majuro atoll. Samples were collected from the area to further investigate the sand built-up between the conservation area and the adjacent islet. The preliminary findings showed that the area is predominantly composed of two island-building LBF, namely *Calcarina sp.* and *Amphistegina sp.* The final results from this study will help stakeholders to amend the management plan to include the adjacent islet under the current management plan.

Keywords: Drenmeo island, conservation area, large benthic foraminifers, management plan

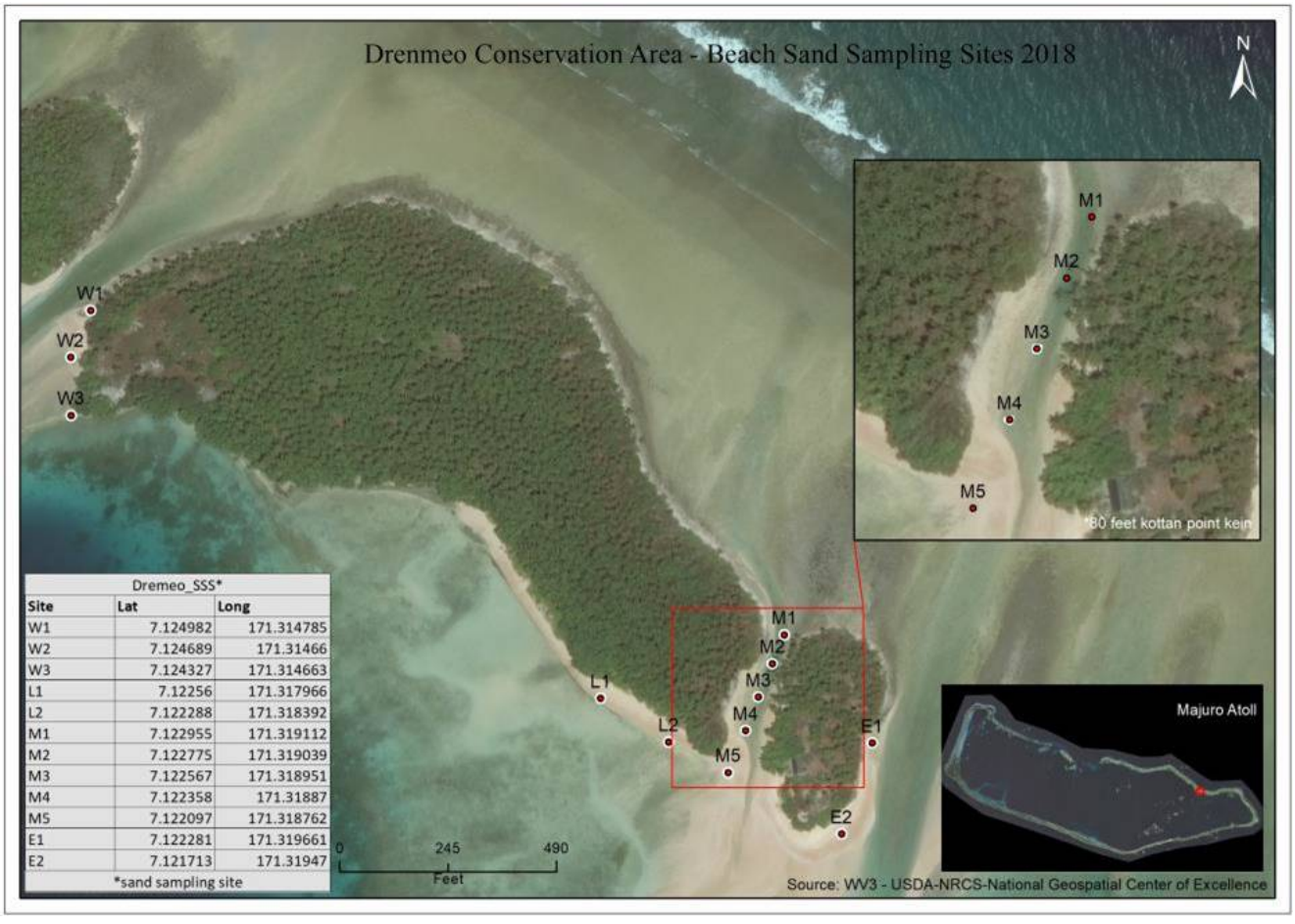

©2019. Japan Geoscience Union. All Right Reserved.

Luminescence chronology of fluvial and marine records from subsurface sediment cores: An insight into the geomorphic evolution of Kaveri delta, India

*kartika goswami[1], Anbarasu Kumaresan[2], Sivakumar Krishnan[2], Senthil K. Sadasivam[2], Manoj Kumar Jaiswal[1]

1. Department of Earth Sciences, Indian Institute of Science Education and Reserach Kolkata, 2. National College Tiruchirappalli, India

Long-term evolution of river deltas is a result of forcings (tectonics, climate, sea level, avulsion, compaction etc). We present the results of luminescence dating of sediments from four sediment cores (VKI, TNR, SY and KKI) of 25 m depth each, retrieved from the Kaveri delta in south India. The coring sites are ~2.5 km, ~11 km, ~17 km and ~20 km away from the present coastline respectively. The cores were analysed for OSL dating, 14C dating, lithology and microfossils and represent various stages of fluvial and marine activity in the region over the last ~150 ka. The chronology of the core closet to the coast (VKI) reflects eight major phases of increased sea level during the late quaternary period (142-140 ka, 104-100 ka, ~121 ka, 87-81 ka, 60-57 ka, 9-6 ka, ~5 ka and ~3 ka) partly coinciding with the global climate cycles MIS 6, MIS 5, MIS 3, MIS 1 respectively. During ~121 ka and 9-6 ka, marine transgression reached the core location to leave marine signatures in the forms of foraminifera. VKI core replicates the quaternary sea level curve, showing strong control of the sea in coastal deposition.

The oldest age of VKI is ~140 ka. The three cores situated further inland give oldest/bottom most ages of~120 ka. This indicates the coastal land has uplifted in the recent years with deeper sediments being encountered at relative shallower depth. The uplift is expected to occur around post 50 ka, creating a basin fill situation for riverine sediments to accumulate and restricting the delta to prograde. This is observed from the sedimentation pattern and robust chronology of the other three inland cores. Analysis of DEM also supported the occurrence of uplift. Thus, the present work examines the geomorphic evolution of Kaveri delta, an archive of fluvial, shoreline and tectonic activities.

Keywords: OSL Dating, Kaveri Delta , GIS, Foraminifera

©2019. Japan Geoscience Union. All Right Reserved.

[E] Poster | H (Human Geosciences)：H-DS Disaster geosciences

Wed. May 29, 2019 10:45 AM - 12:15 PM JST | Wed. May 29, 2019 1:45 AM - 3:15 AM UTC | Poster Hall International Exhibition Hall8, Makuhari Messe_7

[H-DS10] Natural hazards impacts on human society, economics and technological systems

convener:ELENA PETROVA(Lomonosov Moscow State University, Faculty of Geography), Hajime Matsushima(Research Faculty of Agriculture, Hokkaido University)

The last decade set a record for the number and scale of natural disasters and demonstrates high vulnerability of human society and technosphere to their impacts. The most serious consequences have the so-called natural-technological disasters in which natural hazards trigger accidents at technology and infrastructure such as nuclear power and chemical plants, oil refineries and pipelines, power supply systems, buildings, and roads. A distinctive feature of natural-technological events, such as of the 2011 Tohoku earthquake, is their multi-hazard and synergistic nature, which creates cascading impacts, resulting in simultaneous occurrences of myriad catastrophes. The main goal of this multidisciplinary session is to summarize case studies of relationships between natural hazards and technological disasters, their social and economic consequences; and to encourage a discussion about tools and methods to prevent disasters and to minimize their consequences, disaster reconstruction, and tourism for reconstruction, Eco-DRR, and green infrastructure.

[HDS10-P01] The 2018 Activity of Kamchatka Volcanoes and Danger to Aviation

*Olga Girina[1], Dmitry Melnikov[1], Alexander Manevich[1], Anton Nuzhdaev[1], Elena Petrova[2] (1.Institute of Volcanology and Seismology, Far East Division, Russian Academy of Sciences, 2.M.V. Lomonosov Moscow State University)

[HDS10-P02] Planning Methodology on the Effective Use of Green Infrastructure for Disaster Risk Reduction

★Invited Papers

*Keita Aragane[1], Satoshi Funakubo[1] (1.National Institute for Land Infrastructure Management)

[HDS10-P03] EMERGENCY CALL PATTERN IN PETROZAVODSK

*Boris Zalmanovich Belashev[1], Natalia Vladimirovna Krutskikh[1], Anna Aleksandrovna Gerasimova[1] (1.Karelian research center of Russian academy of science)

[HDS10-P04] IDENTIFYING “REGIMES” IN THE TIME SEQUENCES OF PROCESSES

*Boris Zalmanovich Belashev[1] (1.Karelian research center of Russian academy of science)

[HDS10-P05] Investigation of status and demand on public service of earthquake disaster mitigation in China

*Lina Dong[1], Weiping Lian[1], Weitao Chen[1] (1.Development Research Center, China Earthquake Administration)

[HDS10-P06] Analysis of Eco-DRR and Ecological Services using InVEST at the Disaster Areas of Kumamoto Earthquake

*Minghui Tang[1], Naoko Fujita[1] (1.Kyushu University)

[HDS10-P07] Transformation as praxis: Exploring socially just and transdisciplinary pathways to sustainability in marginal environments (TAPESTRY)

*Nobuhito Ohte[1], Lyla Mehta[2], Synne Movik[3], Devanathan Parthasarathy[4] (1.Department of Social Informatics, Graduate School of Informatics, Kyoto University, 2.Institute of Development Studies at the University of Sussex, 3.Department of Urban and Regional Planning, Norwegian University of Life Sciences, 4.Department of Humanities and Social Sciences, Indian Institute of Technology)

[HDS10-P08] Study for the Establishment of the Design for Disaster prevention through the survey of Recognition of tsunami disaster prevention from the viewpoint of green infrastructure in the coastal area of Kyushu-Pacific region.

*Shanshan Xu[1], Naoko Fujita[1], Minghui Tang[1] (1.Kyushu University)

[HDS10-P09] Design for Green Infrastructure: Analysis of Landscape change in the Kumamoto earthquake area

★Invited Papers

*Naoko Fujita[1] (1.Kyushu University)

The 2018 Activity of Kamchatka Volcanoes and Danger to Aviation

*Olga Girina[1], Dmitry Melnikov[1], Alexander Manevich[1], Anton Nuzhdaev[1], Elena Petrova[2]

1. Institute of Volcanology and Seismology, Far East Division, Russian Academy of Sciences, 2. M.V. Lomonosov Moscow State University

Strong explosive eruptions of volcanoes are the most dangerous for aircraft because they can produce in a few hours or days to the atmosphere and the stratosphere till several cubic kilometers of volcanic ash and aerosols. Ash plumes and the clouds, depending on the power of the eruption, the strength and wind speed, can travel thousands of kilometers from the volcano for several days, remaining hazardous to aircraft, as the melting temperature of small particles of ash below the operating temperature of jet engines.

There are 30 active volcanoes in the Kamchatka, and several of them are continuously active. Scientists of KVERT monitor Kamchatkan volcanoes since 1993. In 2018, three of these volcanoes (Sheveluch, Klyuchevskoy, Karymsky) had strong and moderate explosive eruptions.
The eruptive activity of Sheveluch volcano began since 1980 (growth of the lava dome) and is continuing at present. In 2018, strong explosions sent ash up to 10-11 km a.s.l. on 09 January, 26 and 30 December; and up to 6-7 km a.s.l. –on 09 November, and 12, 14, 26-27 and 29 December; ash plumes extended more 2000 km to the different directions of the volcano. Satellite data by KVERT showed a thermal anomaly over the volcano all year. Activity of the volcano was dangerous to international and local aviation.

The moderate explosive events (ash up to 5-6 km a.s.l.) of Klyuchevskoy volcano were observing from 01 till 18 January, on 08 May, and 06 and 15 June. Strong explosions sent ash up to 10.5 km a.s.l. on 14 May. Ash plumes extended more 350 km to the eastern and south-western directions from the volcano. Satellite data by KVERT showed a thermal anomaly over the volcano all year. Activity of the volcano was dangerous to international and local aviation.

The thermal anomaly over Karymsky volcano was recorded on satellite images from time to time, most brightly it manifested in January, May, June-August, September and December. According to visual and satellite data, at this time explosions rose ash up to 6.5 km a.s.l., ash plumes drifted for about 860 km to the different directions from the volcano. The most intense eruptive activity of the volcano was observed on 10, 14-20 and 26-31 July, besides, isolated strong explosive events were observed on 07 and 25 August, on 10-11, 22-23 and 30 September, and 01 December. The size of the ash clouds varied from 5-6 to 240 km. Activity of the volcano was dangerous to local aviation.
This work was supported by the Russian Science Foundation, project No. 16-17-00042.

Keywords: volcano, eruption, Kamchatka, danger to Aviation

©2019. Japan Geoscience Union. All Right Reserved.

Planning Methodology on the Effective Use of Green Infrastructure for Disaster Risk Reduction

*Keita Aragane[1], Satoshi Funakubo[1]

1. National Institute for Land Infrastructure Management

Green Infrastructure (GI) is a concept based on infrastructure development and land utilization that take advantage of natural environments' various functions for creating sustainable and attractive national land or regions. In Japan, since 2015, the concept of GI has been include in National Spatial Strategy, National Land Use Plan, and Priority Plan for Infrastructure Development, etc. Also, lessons learned from the Great East Japan Earthquake raised awareness of the need for more-comprehensive disaster risk reduction strategies in preparing for disasters that surpass worst-case scenarios. Additionally, there is concern over anticipated the Nankai Trough Earthquakes that might cause greater damage in near future, and increasingly frequent urban flooding owing to climate change. Thus, initiative for disaster risks reduction by utilizing GI's multiple functions in addition to approaches focusing on artificial infrastructure has become increasingly important.

This study aims to discuss planning methodology regarding the effective use of GI for disaster risk reduction in urban area by examining the “Green Master Plan (GMP)” through 72 case studies. In Japan, 680 municipal governments have developed GMPs as their basic policy for green space planning, management, and greening. These municipal governments in Japan are recommended to emphasize the viewpoint of disaster risk reduction in their GMPs, and to implement disaster risk reduction systematically through effective use of green spaces such as parks, roadside trees, waterways, private domestic gardens, agricultural land, and woodlands. Result from the case studies revealed that almost all GMPs designated green spaces such as parks as evacuation sites for mega-earthquakes or large-scale fires. Several GMPs were also found to present countermeasures that make effective use of GI for tsunami-related disasters and urban flooding.

Through these findings and through discussions with scholars at a workshop, we published “Technical Note on Green Infrastructure Planning for Urban Resilience” in June 2018. In this technical note, we explain six key points for developing GMPs that enhance the role of GI in disaster risk reduction: (1) combining various measures for disaster risk reduction by utilizing GI from a comprehensive perspective, (2) examining the role and combination of GI and other artificial infrastructure in urban disaster risk reduction, (3) building cooperative relationships with various stakeholders and citizens, (4) taking advantage of multiple functions of GI not only during disasters but also in normal times, (5) establishing a mechanism for maintaining and using GI from a long-term perspective, and (6) considering regional conditions and social situations.

Keywords: Green Infrastructure, Dsaster Risk Reduction, Green Master Plan

©2019. Japan Geoscience Union. All Right Reserved.

EMERGENCY CALL PATTERN IN PETROZAVODSK

*Boris Zalmanovich Belashev[1], Natalia Vladimirovna Krutskikh[1], Anna Aleksandrovna Gerasimova[1]

1. Karelian research center of Russian academy of science

The aim of the study is to analyze the emergency call distribution for Petrozavodsk, Russia, to obtain quantitative disease estimates and to assess the effect of environmental factors on them.

The study was based on medical statistical data and geophysical and geochemical monitoring. Environmental factors, such as magnetic storms and air and urban soil pollution, were assessed. The impersonified catalogue of emergency calls of Petrozavodsk Ambulance from 2015.1.1 to 2017.12.19, database of geomagnetic field variations at Petrozavodsk Geophysical Observatory, data on Kp index monitoring at the Laboratory of Tesis X-ray Astronomy at Lebedev Physical Institute, and the results of geochemical soil sampling in Petrozavodsk were used. Emergency call and geomagnetic activity distributions were constructed and processed in MATLAB computer mathematics system and Qgis software package. Analytical results were demonstrated on cardiovascular diseases.

The number of emergency call for patients with cardiac diseases in 2015-2017 is at about the same level. Seasonal factors affect the time distribution trends of calls for patients with essential hypertension, stenocardia and ischemic cardiac disease and do not affect the distribution trends of myocardial infarction and cerebral crisis. Time distribution spectra display a 25.6 day cycle similar to a geomagnetic activity period, two- and one-week cycles and cycles with periods of about 6, 4 and 3 days. Emergency calls for patients with myocardial infarction reflect the gender and age of the patients. The number of calls on weekends is typically low. On week-days, the number of calls at rush hours is maximum. The number of calls on days close to magnetic storms is not necessarily great. An elevated number of calls on these days for patients with stenocardia and myocardial infarction is observed.

The spatial distribution of the number of emergency calls were obtained using the Ambulance Geoinformation System. The system constructs the spatial distributions of the number of emergency team calls with known diagnoses for the streets and blocks of the city and is used to compare call frequency with district factors. With its help the link of distribution of quantity of calls of ambulance with diagnoses of cardiovascular diseases, bronchial asthma, vegeto-vascular dystonia, new growths, other diseases on districts of the city with the soils contamination indicated by the environmental hazard index –a total of the weighted average concentration values of As, Pb, Zn, Cd, Co, Cu, V, W is studied. No significant correlations between these values have been revealed.

3, 6-daily cycles in the analyzed ranges can be connected to thyroid gland hormone activity and a 4-day cycle to glucocorticoid hormone activity. Circadian rhythms are either thought to be general or to be due to the unwillingness of people to be sent to hospital or call for a doctor on weekends. In case of myocardial infarction, when help is needed urgently, the latter factor does not work, and a one-week cycle in the spectrum, showing the time dependence of the number of calls, is displayed.

This fact and the weekend effect can be understood, based on the properties of hydrocortisone. Stress from production activity stimulates the supply of the hormone into the blood, which rushes to the heart and muscles. When the heart fails to cope with the rush of blood, a cardiac disease becomes more acute.

©2019. Japan Geoscience Union. All Right Reserved.

As the hydrocortisone level in the blood on weekends and holidays declines, the number of emergency calls for patients with cardiovascular diseases decreases.

Peaks in the daily emergency call dynamics distribution on week-days are interpreted to be due to air pollution with car gases at rush hours (9-10 a.m., 1-2 and 6-7 p.m.) and an approximately one-hour delay caused by progress in disease and the need to apply for a doctor.
The emergency call distributions analyzed are highly informative, showing the complete dynamic disease pattern of the urban population.

Keywords: diseases, emergency call, patient, diagnose, magnetic storms, contamination

©2019. Japan Geoscience Union. All Right Reserved.

IDENTIFYING “REGIMES” IN THE TIME SEQUENCES OF PROCESSES

*Boris Zalmanovich Belashev[1]

1. Karelian research center of Russian academy of science

A process is represented as a sequence of “regimes” when describing climatic variations and complex systems, detecting the malfunctioning of instruments and illegal interference in computer and hardware networks. For natural, technological and social processes such representation is comfortable to detect precursors of disastrous events.
The shifts of “regimes” in the sequences are commonly detected by checking statistical hypotheses by Student’s test and tests of non-parametric statistics when comparing the characteristics of the sequence at one or another site. Algorithms often use a priori information, work in unstable fashion over short intervals and at sequences boundaries, find it hard to recognize the shifts and trends of “regimes”.
Widespread R-algorithm [1] analyze data consecutively in a sliding window, operate with a small number of parameters and filter off “red” noise. The boundary regimes it detect may reflect distortions characteristic of the beginning and end of measurements.
The goal of the present study is to develop B-algorithm which automatically recognizes stable “regimes” in time data sequences.
The main stages of the algorithm are clusterization, comparison and optimization. Clusterization preliminary divides a normalized time sequence into “regimes”. While comparing the characteristics of the “regimes”, the division obtained is re-estimated. The final model of division is formed during optimization, which minimizes the variance of deviations from the trends of the “regimes” by varying the internal boundaries of the sites.
The algorithm, developed as a software in the MATLAB computer mathematics system, fulfils procedures automatically, decreases the amount of a priori data, increases operation speed and brings solutions closer to optima.
The operation of B- and R-algorithms is exemplified by the PDO (Pacific Decade Oscillation) sequence of mean January temperatures [2].
In both algorithms the number of “regimes” and their approximate positions coincide. The delay of part of R-“regimes” emphasize the sensitivity of B-algorithm to new “regimes”. Discrepancies are connected with the last “regime” identified by R- and B-algorithms on 2 and 15 members of sequence, respectively.
B- algorithm can operate with constant, linear and complex trends.
B- and R-algorithms, applied to the time sequences of river runoff, solar and seismic activity and the sequences of the annual rings of trees, have provided new information on the stages of processes.
The simplified schematic “regime” representation of a process reveals trends commonly obscured by the abundance of details. B- algorithm identifies stable “regimes” and recognizes the shifts and trends of “regimes”. The use of MATLAB functions increases the potential of the algorithm, admits the fulfilment of procedures by various methods, brings solutions closer to optimum solutions and ensures high operation speed. The ability of the algorithm to automatically process data makes it suitable for working with extensive data in various earth sciences.
References:
1.Rodionov, S. (2006) Use of prewhitening in climate region shift detection. Geophysical Research Letters 33, L12707.
2.Pacific Decadal Oscillation Index Data.
https://www.rdocumentation.org/packages/rpdo/versions/0.2.5.

©2019. Japan Geoscience Union. All Right Reserved.

Keywords: time sequence, shift regime, algorithm, clusterization, comparision, optimization

©2019. Japan Geoscience Union. All Right Reserved.

Investigation of status and demand on public service of earthquake disaster mitigation in China

*Lina Dong[1], Weiping Lian[1], Weitao Chen[1]

1. Development Research Center, China Earthquake Administration

In order to make a comprehensive and systematic evaluation of the status and demands of public service of earthquake disaster mitigation, we launched an investigation with National Bureau of Statistics on the current situation of public service of earthquake disaster mitigation and the demands for it in 2018. The investigation was conducted in 31 provinces of China mainland using the Computer Assisted Telephone Interview(CATI) method and received 20078 valid samples in total.

The results indicate that 52.2% of the population have received the scientific knowledge education for earthquake disaster mitigation in Different levels. It shows that the public still possesses a high expectation of earthquake prediction and farmers have a low level of scientific knowledge of earthquake disaster mitigation. And TV, network, and the new media app such as wechat and weibo become the most important information channels for the public to obtain the earthquake related information. Furthermore, the degree of satisfaction evaluation of public service of earthquake disaster mitigation is marked on 81.22 points (the full mark is 100 points). And the most expectative services for the public are reconstruction, earthquake warning, and house earthquake resilience test. The results of the investigation have provided a scientific evidence for the government to provide better services of earthquake disaster mitigation and to make scientific knowledge popularization in a more scientific way.

Keywords: scientific knowledge popularization of earthquake disaster mitigation, public service, satisfaction evaluation

©2019. Japan Geoscience Union. All Right Reserved.

Analysis of Eco-DRR and Ecological Services using InVEST at the Disaster Areas of Kumamoto Earthquake

*Minghui Tang[1], Naoko Fujita[1]

1. Kyushu University

When compared with other countries in a global point of view, Japan is a country with high number of natural calamities, significant causalities, economic loss and damages by earthquakes, typhoons, and eruption. The damage is especially big when a hazard comes right after another one.

Complex disaster refers to the occurrence of multiple disasters instead of one. Such as, in 2016, Kumamoto prefecture was hit by earthquakes with magnitude as large as 7 and within another 2 months, by heavy rain and the damage was tremendous.

There is a huge number of researches on the eco-application of proceeding in various countries and it is vitally important to verify their validity. Here, InVEST refers to the ArcGIS tool for the integrated review for ecological services and its compensation.

This research focuses on the analysis of the changes of the land cover as reflected in satellite pictures of the whole Kumamoto prefecture taken after the complex disaster, the earthquake in April 2016 and heavy rain in June 2016. Also, it’ s a review on the ecological services with the use of InVEST. A special focus is paid on the review of the soil retention and the quality changes of the eco-habitant as reflection of the disaster damage reduction measures.

In addition, there is an analysis on the change of land coverage on area-unit level with Mashiki-machi, the epicenter, as the target. Furthermore, projection was plotted for the ecological services implemented as the reconstruction plan.

Keywords: Kumamoto Earthquake, Eco-DRR, Ecological services, Complex Disasters, local governments/local communities, InVEST

©2019. Japan Geoscience Union. All Right Reserved.

Transformation as praxis: Exploring socially just and transdisciplinary pathways to sustainability in marginal environments (TAPESTRY)

*Nobuhito Ohte[1], Lyla Mehta[2], Synne Movik[3], Devanathan Parthasarathy[4]

1. Department of Social Informatics, Graduate School of Informatics, Kyoto University, 2. Institute of Development Studies at the University of Sussex, 3. Department of Urban and Regional Planning, Norwegian University of Life Sciences, 4. Department of Humanities and Social Sciences, Indian Institute of Technology

Climate change related uncertainties are the main threats to the sustainability of societies and their environments. To tackle these challenges, systemic transformations are required. Our project focuses on three cases of transformation in marginal environments in India and Bangladesh, and is concerned with: How transformation happens through bottom up processes in these sites; and how they can be scaled up and facilitate wider societal changes. Both require transdisciplinary co-production and the praxis of transformation which presupposes change in social arrangements and reconstruction by individuals. Our project addresses issues concerning governance, wellbeing, identity and quality of life in relation to transformations to sustainability in a lower middle income country (India) and a least developed country (Bangladesh). Our results should help inform processes that ultimately improve the quality of life in marginal environments, and build action and capacity among all partners.

Keywords: Transformation, Sustainability, Marginal environment, Transdisciplinary study, India, Bangladesh

©2019. Japan Geoscience Union. All Right Reserved.

Study for the Establishment of the Design for Disaster prevention through the survey of Recognition of tsunami disaster prevention from the viewpoint of green infrastructure in the coastal area of Kyushu-Pacific region.

*Shanshan Xu[1], Naoko Fujita[1], Minghui Tang[1]

1. Kyushu University

Considering the possibility of Nankai Trough large-scale earthquake predicted to occur in the nearest future, the issue of the tsunami in the coastal area of Kyushu-Pacific region is becoming extremely important. Efforts to utilize the various functions of the ecosystem internationally for the society creation are expanding in recent years, and even in the situation of toughening of the land in Japan, the initiative to incorporate Green Infrastructure (GI) which utilizes the disaster prevention and reduction functions of the natural ecosystem are being observed. Also, during the process of self-help/mutual assistance action and disaster reconstruction at the time of disaster, attention is paid as regional ties are affected, which are being considered as Social capital (SC).

The purpose of this study is to clarify the actual situation of tsunami disaster prevention of Nankai Trough earthquake based on the viewpoint of GI. We conducted a questionnaire survey on tsunami disaster prevention and GI at local governments and local communities. After analyzing the questionnaire, we analyzed the needs of the self-governing president's disaster prevention measures, the problems of the area, and the deviation of the improved situation of municipalities' disaster prevention measures. A correlation analysis was conducted to grasp the relationship between the consciousness concerning GI utilization, the strength of regional linkage SC and the recognition of evacuation.

1. Misalignment between demand and maintenance situation desired by the region

Policy regarding the issue of disaster helpers was extracted as a gap between needs and maintenance situation. Regarding the needs of the soft pattern in disaster prevention, a lot of measures were taken by disaster support supporters, however as it comes from the municipality questionnaire results, the measures related to the introduction of the barrier-free system and evacuation action supporters were introduced only partially. Further improvement is necessary for welfare evacuation sites, measures against supporters requiring evacuation actions, barrier-free formation.

2. SC regarded from the viewpoint of the relationship between intentions to utilize GI and recognition on disaster.

©2019. Japan Geoscience Union. All Right Reserved.

Especially, the correlation coefficient was 0.701 between No.7 and No.6. This shows that those who responded that disaster can happen among residents can respond that regional ties are stronger. For items with a high correlation coefficient between No.3 and No.8, the correlation became 0.437. This means the respondents who answered that evacuation is possible for all area inhabitants including elderly people in case of disaster (flooding, earthquakes, and tsunami) are able to use local well water and spring water in the event of a disaster.

Between No.2 and No.4, the correlation coefficient became 3.380. This is because those who respond that they think they can fully utilize the resources of the area (resources such as firewood, foods that can be harvested in mountains) even in the event of disasters will escape by utilizing the nearby natural landforms such as plateaus and mountains for tsunami evacuation. Between No.2 and No.8, the correlation coefficient became 0.351. This is because it shows those who responded that they thought that they could escape by utilizing nearby plateau and mountains such as mountains during the tsunami evacuation, even if disasters (flood, earthquake, tsunami) occurred, everyone including the elderly in the area evacuated. Between No.2 and No.6, the correlation coefficient became 0.343. This indicates that those who responded that they believe that they can escape by utilizing nearby plateaus and mountains when evacuating the tsunami think that the connection of the community people is strong. Between No.3 and No.6, the correlation coefficient became 0.287. This indicates that those who responded as they thought they could use local well water and spring water at the time of a disaster replied that they think that the regional connection is stronger.

Based on the above, we clarified the SC from the viewpoint of the gap between the request and the maintenance situation the region desires and the relationship between the intention to utilize GI and the perception of disaster. The fact that utilization of natural resources such as well water and spring water and understanding that natural topography can be utilized for evacuation leads to a positive feeling making people believe it is possible for everyone to evacuate even if the tsunami comes, can be suggested from this study.

Keywords: the Design for Disaster prevention, tsunami disaster, green infrastructure, the coastal area of Kyushu-Pacific region, Nankai Trough large-scale earthquake

©2019. Japan Geoscience Union. All Right Reserved.

Design for Green Infrastructure: Analysis of Landscape change in the Kumamoto earthquake area

*Naoko Fujita[1]

1. Kyushu University

The concept of “Green Infrastructure” and “Eco-DRR” is developed in Europe and North America lately, and it started to spread around in Japan after the Tohoku earthquake and tsunami in 2011. Landscape ecology is parallel with this conceptually, as well as in terms of spatial scale. Its successful focused researches and social implementation are becoming pervasive.

The new concept is to solve various problems by local resources and pearls of wisdom, it connects local communities to the world while it’s mainly led by front liners and researchers in engineering and ecological fields that little attention is paid to the aspects of arts and designs. It’s still not well-penetrated despite the validity and functions of the concept are well verified. Thus, it’s vitally important to work on the insufficient.

The purpose of this research is to analyze the reconstruction plan prepared by the affected municipalities of the Kumamoto earthquake and compare the landscape change read from the plan and the actual landscape change actually occurred and make clear how the cities and nature have changed during the reconstruction process.

In this research, we firstly gathered and analyzed the earthquake reconstruction plans created by each local government for all 45 municipalities in Kumamoto prefecture. In this analysis, while studying each municipal original plan, we primarily focused on the background, features, and landscape references of the plan formulation. During this analysis, we grasped the relations between the reconstruction plan and the landscape change, and also clarified what exactly each local government emphasizes independently. As the next step, basing on the field survey, we analyzed the actual state of the landscape changes described in the plan. As a method, we took the photographs at places where the plans adopted by each municipality in Kumamoto prefecture were scheduled or executed, and after recording the current situation and the surrounding landscape, we made a comparison with the photographs taken at the same place in the past. By doing this, we revealed what kind of changes have occurred between the past and the present due to the disaster, and how they affected the surrounding landscape.

Among the 45 municipalities in downtown Kumamoto Prefecture, we found that earthquake reconstruction plan was formulated in 16 municipalities, and 5 municipalities planned to formulate. There were references that "consideration of the landscape when promoting housing improvement and infrastructure development" and "to consider the landscape from the tourism viewpoint". Also, there were plans to utilize the process of reconstruction itself as a resource for tourist attraction. Furthermore, as a result of analyzing the individual plans described in the reconstruction plan, the reference to landscape,

©2019. Japan Geoscience Union. All Right Reserved.

reference to the prediction of landscape change, reference to landscape protection exists in all 16 cities, towns, and villages. Totally 117 relevant plans have been found. Although many of them were intended to cope with the damage at the time of the disaster, there were several plans originally adopted by the local governments to make necessary improvements of the problems they had from the past by conducting disaster recovery.

The field survey was conducted for 16 municipalities in total in Kumamoto Prefecture. One year has passed since the earthquake disaster, and recovery works progressed in a wide range in Kumamoto Prefecture. In the recovery sites in various places, a secondary change of the landscape, which caused the recovery activity aimed at improving the convenience of life and safety, has already been taking place. Moreover, recovery works progressed also in Kumamoto castle which is also cultural asset and tourist attraction, as well as the station and the government office which are the center of town. As a result, we could confirm the change of landscape.

In this research, through the analysis of the reconstruction plan created by the municipalities affected by the Kumamoto earthquake and the field survey, from the viewpoint of Green Infrastructure, we could make clear the process of the landscape change occurred during the process of recovery/reconstruction of the living base, the tourist resources, the natural environment in the affected areas and its influence respectively. Although few local governments have formulated landscape-friendly reconstruction plans, to gain medium- and long-term benefits, we should make landscape-friendly reconstructions from the original planning stage. This is because it is the factor determining the richness of living base, tourism resources, and natural environment.

Keywords: Green Infrastructure, the Kumamoto earthquake , Design

©2019. Japan Geoscience Union. All Right Reserved.

[E] Poster | H (Human Geosciences)：H-DS Disaster geosciences

Wed. May 29, 2019 5:15 PM - 6:30 PM JST | Wed. May 29, 2019 8:15 AM - 9:30 AM UTC | Poster Hall International Exhibition Hall8, Makuhari Messe_21

[H-DS10] Natural hazards impacts on human society, economics and technological systems

convener:ELENA PETROVA(Lomonosov Moscow State University, Faculty of Geography), Hajime Matsushima(Research Faculty of Agriculture, Hokkaido University)

The last decade set a record for the number and scale of natural disasters and demonstrates high vulnerability of human society and technosphere to their impacts. The most serious consequences have the so-called natural-technological disasters in which natural hazards trigger accidents at technology and infrastructure such as nuclear power and chemical plants, oil refineries and pipelines, power supply systems, buildings, and roads. A distinctive feature of natural-technological events, such as of the 2011 Tohoku earthquake, is their multi-hazard and synergistic nature, which creates cascading impacts, resulting in simultaneous occurrences of myriad catastrophes. The main goal of this multidisciplinary session is to summarize case studies of relationships between natural hazards and technological disasters, their social and economic consequences; and to encourage a discussion about tools and methods to prevent disasters and to minimize their consequences, disaster reconstruction, and tourism for reconstruction, Eco-DRR, and green infrastructure.

[HDS10-P01] The 2018 Activity of Kamchatka Volcanoes and Danger to Aviation

*Olga Girina[1], Dmitry Melnikov[1], Alexander Manevich[1], Anton Nuzhdaev[1], Elena Petrova[2] (1.Institute of Volcanology and Seismology, Far East Division, Russian Academy of Sciences, 2.M.V. Lomonosov Moscow State University)

[HDS10-P02] Planning Methodology on the Effective Use of Green Infrastructure for Disaster Risk Reduction

★Invited Papers

*Keita Aragane[1], Satoshi Funakubo[1] (1.National Institute for Land Infrastructure Management)

[HDS10-P03] EMERGENCY CALL PATTERN IN PETROZAVODSK

*Boris Zalmanovich Belashev[1], Natalia Vladimirovna Krutskikh[1], Anna Aleksandrovna Gerasimova[1] (1.Karelian research center of Russian academy of science)

[HDS10-P04] IDENTIFYING “REGIMES” IN THE TIME SEQUENCES OF PROCESSES

*Boris Zalmanovich Belashev[1] (1.Karelian research center of Russian academy of science)

[HDS10-P05] Investigation of status and demand on public service of earthquake disaster mitigation in China

*Lina Dong[1], Weiping Lian[1], Weitao Chen[1] (1.Development Research Center, China Earthquake Administration)

[HDS10-P06] Analysis of Eco-DRR and Ecological Services using InVEST at the Disaster Areas of Kumamoto Earthquake

*Minghui Tang[1], Naoko Fujita[1] (1.Kyushu University)

[HDS10-P07] Transformation as praxis: Exploring socially just and transdisciplinary pathways to sustainability in marginal environments (TAPESTRY)

*Nobuhito Ohte[1], Lyla Mehta[2], Synne Movik[3], Devanathan Parthasarathy[4] (1.Department of Social Informatics, Graduate School of Informatics, Kyoto University, 2.Institute of Development Studies at the University of Sussex, 3.Department of Urban and Regional Planning, Norwegian University of Life Sciences, 4.Department of Humanities and Social Sciences, Indian Institute of Technology)

[HDS10-P08] Study for the Establishment of the Design for Disaster prevention through the survey of Recognition of tsunami disaster prevention from the viewpoint of green infrastructure in the coastal area of Kyushu-Pacific region.

*Shanshan Xu[1], Naoko Fujita[1], Minghui Tang[1] (1.Kyushu University)

[HDS10-P09] Design for Green Infrastructure: Analysis of Landscape change in the Kumamoto earthquake area

★Invited Papers

*Naoko Fujita[1] (1.Kyushu University)

The 2018 Activity of Kamchatka Volcanoes and Danger to Aviation

*Olga Girina[1], Dmitry Melnikov[1], Alexander Manevich[1], Anton Nuzhdaev[1], Elena Petrova[2]

1. Institute of Volcanology and Seismology, Far East Division, Russian Academy of Sciences, 2. M.V. Lomonosov Moscow State University

Strong explosive eruptions of volcanoes are the most dangerous for aircraft because they can produce in a few hours or days to the atmosphere and the stratosphere till several cubic kilometers of volcanic ash and aerosols. Ash plumes and the clouds, depending on the power of the eruption, the strength and wind speed, can travel thousands of kilometers from the volcano for several days, remaining hazardous to aircraft, as the melting temperature of small particles of ash below the operating temperature of jet engines.

There are 30 active volcanoes in the Kamchatka, and several of them are continuously active. Scientists of KVERT monitor Kamchatkan volcanoes since 1993. In 2018, three of these volcanoes (Sheveluch, Klyuchevskoy, Karymsky) had strong and moderate explosive eruptions.
The eruptive activity of Sheveluch volcano began since 1980 (growth of the lava dome) and is continuing at present. In 2018, strong explosions sent ash up to 10-11 km a.s.l. on 09 January, 26 and 30 December; and up to 6-7 km a.s.l. –on 09 November, and 12, 14, 26-27 and 29 December; ash plumes extended more 2000 km to the different directions of the volcano. Satellite data by KVERT showed a thermal anomaly over the volcano all year. Activity of the volcano was dangerous to international and local aviation.

The moderate explosive events (ash up to 5-6 km a.s.l.) of Klyuchevskoy volcano were observing from 01 till 18 January, on 08 May, and 06 and 15 June. Strong explosions sent ash up to 10.5 km a.s.l. on 14 May. Ash plumes extended more 350 km to the eastern and south-western directions from the volcano. Satellite data by KVERT showed a thermal anomaly over the volcano all year. Activity of the volcano was dangerous to international and local aviation.

The thermal anomaly over Karymsky volcano was recorded on satellite images from time to time, most brightly it manifested in January, May, June-August, September and December. According to visual and satellite data, at this time explosions rose ash up to 6.5 km a.s.l., ash plumes drifted for about 860 km to the different directions from the volcano. The most intense eruptive activity of the volcano was observed on 10, 14-20 and 26-31 July, besides, isolated strong explosive events were observed on 07 and 25 August, on 10-11, 22-23 and 30 September, and 01 December. The size of the ash clouds varied from 5-6 to 240 km. Activity of the volcano was dangerous to local aviation.
This work was supported by the Russian Science Foundation, project No. 16-17-00042.

Keywords: volcano, eruption, Kamchatka, danger to Aviation

©2019. Japan Geoscience Union. All Right Reserved.

Planning Methodology on the Effective Use of Green Infrastructure for Disaster Risk Reduction

*Keita Aragane[1], Satoshi Funakubo[1]

1. National Institute for Land Infrastructure Management

Green Infrastructure (GI) is a concept based on infrastructure development and land utilization that take advantage of natural environments' various functions for creating sustainable and attractive national land or regions. In Japan, since 2015, the concept of GI has been include in National Spatial Strategy, National Land Use Plan, and Priority Plan for Infrastructure Development, etc. Also, lessons learned from the Great East Japan Earthquake raised awareness of the need for more-comprehensive disaster risk reduction strategies in preparing for disasters that surpass worst-case scenarios. Additionally, there is concern over anticipated the Nankai Trough Earthquakes that might cause greater damage in near future, and increasingly frequent urban flooding owing to climate change. Thus, initiative for disaster risks reduction by utilizing GI's multiple functions in addition to approaches focusing on artificial infrastructure has become increasingly important.

This study aims to discuss planning methodology regarding the effective use of GI for disaster risk reduction in urban area by examining the “Green Master Plan (GMP)” through 72 case studies. In Japan, 680 municipal governments have developed GMPs as their basic policy for green space planning, management, and greening. These municipal governments in Japan are recommended to emphasize the viewpoint of disaster risk reduction in their GMPs, and to implement disaster risk reduction systematically through effective use of green spaces such as parks, roadside trees, waterways, private domestic gardens, agricultural land, and woodlands. Result from the case studies revealed that almost all GMPs designated green spaces such as parks as evacuation sites for mega-earthquakes or large-scale fires. Several GMPs were also found to present countermeasures that make effective use of GI for tsunami-related disasters and urban flooding.

Through these findings and through discussions with scholars at a workshop, we published “Technical Note on Green Infrastructure Planning for Urban Resilience” in June 2018. In this technical note, we explain six key points for developing GMPs that enhance the role of GI in disaster risk reduction: (1) combining various measures for disaster risk reduction by utilizing GI from a comprehensive perspective, (2) examining the role and combination of GI and other artificial infrastructure in urban disaster risk reduction, (3) building cooperative relationships with various stakeholders and citizens, (4) taking advantage of multiple functions of GI not only during disasters but also in normal times, (5) establishing a mechanism for maintaining and using GI from a long-term perspective, and (6) considering regional conditions and social situations.

Keywords: Green Infrastructure, Dsaster Risk Reduction, Green Master Plan

©2019. Japan Geoscience Union. All Right Reserved.

EMERGENCY CALL PATTERN IN PETROZAVODSK

*Boris Zalmanovich Belashev[1], Natalia Vladimirovna Krutskikh[1], Anna Aleksandrovna Gerasimova[1]

1. Karelian research center of Russian academy of science

The aim of the study is to analyze the emergency call distribution for Petrozavodsk, Russia, to obtain quantitative disease estimates and to assess the effect of environmental factors on them.

The study was based on medical statistical data and geophysical and geochemical monitoring. Environmental factors, such as magnetic storms and air and urban soil pollution, were assessed. The impersonified catalogue of emergency calls of Petrozavodsk Ambulance from 2015.1.1 to 2017.12.19, database of geomagnetic field variations at Petrozavodsk Geophysical Observatory, data on Kp index monitoring at the Laboratory of Tesis X-ray Astronomy at Lebedev Physical Institute, and the results of geochemical soil sampling in Petrozavodsk were used. Emergency call and geomagnetic activity distributions were constructed and processed in MATLAB computer mathematics system and Qgis software package. Analytical results were demonstrated on cardiovascular diseases.

The number of emergency call for patients with cardiac diseases in 2015-2017 is at about the same level. Seasonal factors affect the time distribution trends of calls for patients with essential hypertension, stenocardia and ischemic cardiac disease and do not affect the distribution trends of myocardial infarction and cerebral crisis. Time distribution spectra display a 25.6 day cycle similar to a geomagnetic activity period, two- and one-week cycles and cycles with periods of about 6, 4 and 3 days. Emergency calls for patients with myocardial infarction reflect the gender and age of the patients. The number of calls on weekends is typically low. On week-days, the number of calls at rush hours is maximum. The number of calls on days close to magnetic storms is not necessarily great. An elevated number of calls on these days for patients with stenocardia and myocardial infarction is observed.

The spatial distribution of the number of emergency calls were obtained using the Ambulance Geoinformation System. The system constructs the spatial distributions of the number of emergency team calls with known diagnoses for the streets and blocks of the city and is used to compare call frequency with district factors. With its help the link of distribution of quantity of calls of ambulance with diagnoses of cardiovascular diseases, bronchial asthma, vegeto-vascular dystonia, new growths, other diseases on districts of the city with the soils contamination indicated by the environmental hazard index –a total of the weighted average concentration values of As, Pb, Zn, Cd, Co, Cu, V, W is studied. No significant correlations between these values have been revealed.

3, 6-daily cycles in the analyzed ranges can be connected to thyroid gland hormone activity and a 4-day cycle to glucocorticoid hormone activity. Circadian rhythms are either thought to be general or to be due to the unwillingness of people to be sent to hospital or call for a doctor on weekends. In case of myocardial infarction, when help is needed urgently, the latter factor does not work, and a one-week cycle in the spectrum, showing the time dependence of the number of calls, is displayed.

This fact and the weekend effect can be understood, based on the properties of hydrocortisone. Stress from production activity stimulates the supply of the hormone into the blood, which rushes to the heart and muscles. When the heart fails to cope with the rush of blood, a cardiac disease becomes more acute.

©2019. Japan Geoscience Union. All Right Reserved.

As the hydrocortisone level in the blood on weekends and holidays declines, the number of emergency calls for patients with cardiovascular diseases decreases.

Peaks in the daily emergency call dynamics distribution on week-days are interpreted to be due to air pollution with car gases at rush hours (9-10 a.m., 1-2 and 6-7 p.m.) and an approximately one-hour delay caused by progress in disease and the need to apply for a doctor.
The emergency call distributions analyzed are highly informative, showing the complete dynamic disease pattern of the urban population.

Keywords: diseases, emergency call, patient, diagnose, magnetic storms, contamination

©2019. Japan Geoscience Union. All Right Reserved.

IDENTIFYING “REGIMES” IN THE TIME SEQUENCES OF PROCESSES

*Boris Zalmanovich Belashev[1]

1. Karelian research center of Russian academy of science

A process is represented as a sequence of “regimes” when describing climatic variations and complex systems, detecting the malfunctioning of instruments and illegal interference in computer and hardware networks. For natural, technological and social processes such representation is comfortable to detect precursors of disastrous events.
The shifts of “regimes” in the sequences are commonly detected by checking statistical hypotheses by Student’s test and tests of non-parametric statistics when comparing the characteristics of the sequence at one or another site. Algorithms often use a priori information, work in unstable fashion over short intervals and at sequences boundaries, find it hard to recognize the shifts and trends of “regimes”.
Widespread R-algorithm [1] analyze data consecutively in a sliding window, operate with a small number of parameters and filter off “red” noise. The boundary regimes it detect may reflect distortions characteristic of the beginning and end of measurements.
The goal of the present study is to develop B-algorithm which automatically recognizes stable “regimes” in time data sequences.
The main stages of the algorithm are clusterization, comparison and optimization. Clusterization preliminary divides a normalized time sequence into “regimes”. While comparing the characteristics of the “regimes”, the division obtained is re-estimated. The final model of division is formed during optimization, which minimizes the variance of deviations from the trends of the “regimes” by varying the internal boundaries of the sites.
The algorithm, developed as a software in the MATLAB computer mathematics system, fulfils procedures automatically, decreases the amount of a priori data, increases operation speed and brings solutions closer to optima.
The operation of B- and R-algorithms is exemplified by the PDO (Pacific Decade Oscillation) sequence of mean January temperatures [2].
In both algorithms the number of “regimes” and their approximate positions coincide. The delay of part of R-“regimes” emphasize the sensitivity of B-algorithm to new “regimes”. Discrepancies are connected with the last “regime” identified by R- and B-algorithms on 2 and 15 members of sequence, respectively.
B- algorithm can operate with constant, linear and complex trends.
B- and R-algorithms, applied to the time sequences of river runoff, solar and seismic activity and the sequences of the annual rings of trees, have provided new information on the stages of processes.
The simplified schematic “regime” representation of a process reveals trends commonly obscured by the abundance of details. B- algorithm identifies stable “regimes” and recognizes the shifts and trends of “regimes”. The use of MATLAB functions increases the potential of the algorithm, admits the fulfilment of procedures by various methods, brings solutions closer to optimum solutions and ensures high operation speed. The ability of the algorithm to automatically process data makes it suitable for working with extensive data in various earth sciences.
References:
1.Rodionov, S. (2006) Use of prewhitening in climate region shift detection. Geophysical Research Letters 33, L12707.
2.Pacific Decadal Oscillation Index Data.
https://www.rdocumentation.org/packages/rpdo/versions/0.2.5.

©2019. Japan Geoscience Union. All Right Reserved.

Keywords: time sequence, shift regime, algorithm, clusterization, comparision, optimization

©2019. Japan Geoscience Union. All Right Reserved.

Investigation of status and demand on public service of earthquake disaster mitigation in China

*Lina Dong[1], Weiping Lian[1], Weitao Chen[1]

1. Development Research Center, China Earthquake Administration

In order to make a comprehensive and systematic evaluation of the status and demands of public service of earthquake disaster mitigation, we launched an investigation with National Bureau of Statistics on the current situation of public service of earthquake disaster mitigation and the demands for it in 2018. The investigation was conducted in 31 provinces of China mainland using the Computer Assisted Telephone Interview(CATI) method and received 20078 valid samples in total.

The results indicate that 52.2% of the population have received the scientific knowledge education for earthquake disaster mitigation in Different levels. It shows that the public still possesses a high expectation of earthquake prediction and farmers have a low level of scientific knowledge of earthquake disaster mitigation. And TV, network, and the new media app such as wechat and weibo become the most important information channels for the public to obtain the earthquake related information. Furthermore, the degree of satisfaction evaluation of public service of earthquake disaster mitigation is marked on 81.22 points (the full mark is 100 points). And the most expectative services for the public are reconstruction, earthquake warning, and house earthquake resilience test. The results of the investigation have provided a scientific evidence for the government to provide better services of earthquake disaster mitigation and to make scientific knowledge popularization in a more scientific way.

Keywords: scientific knowledge popularization of earthquake disaster mitigation, public service, satisfaction evaluation

©2019. Japan Geoscience Union. All Right Reserved.

Analysis of Eco-DRR and Ecological Services using InVEST at the Disaster Areas of Kumamoto Earthquake

*Minghui Tang[1], Naoko Fujita[1]

1. Kyushu University

When compared with other countries in a global point of view, Japan is a country with high number of natural calamities, significant causalities, economic loss and damages by earthquakes, typhoons, and eruption. The damage is especially big when a hazard comes right after another one.

Complex disaster refers to the occurrence of multiple disasters instead of one. Such as, in 2016, Kumamoto prefecture was hit by earthquakes with magnitude as large as 7 and within another 2 months, by heavy rain and the damage was tremendous.

There is a huge number of researches on the eco-application of proceeding in various countries and it is vitally important to verify their validity. Here, InVEST refers to the ArcGIS tool for the integrated review for ecological services and its compensation.

This research focuses on the analysis of the changes of the land cover as reflected in satellite pictures of the whole Kumamoto prefecture taken after the complex disaster, the earthquake in April 2016 and heavy rain in June 2016. Also, it’ s a review on the ecological services with the use of InVEST. A special focus is paid on the review of the soil retention and the quality changes of the eco-habitant as reflection of the disaster damage reduction measures.

In addition, there is an analysis on the change of land coverage on area-unit level with Mashiki-machi, the epicenter, as the target. Furthermore, projection was plotted for the ecological services implemented as the reconstruction plan.

Keywords: Kumamoto Earthquake, Eco-DRR, Ecological services, Complex Disasters, local governments/local communities, InVEST

©2019. Japan Geoscience Union. All Right Reserved.

Transformation as praxis: Exploring socially just and transdisciplinary pathways to sustainability in marginal environments (TAPESTRY)

*Nobuhito Ohte[1], Lyla Mehta[2], Synne Movik[3], Devanathan Parthasarathy[4]

1. Department of Social Informatics, Graduate School of Informatics, Kyoto University, 2. Institute of Development Studies at the University of Sussex, 3. Department of Urban and Regional Planning, Norwegian University of Life Sciences, 4. Department of Humanities and Social Sciences, Indian Institute of Technology

Climate change related uncertainties are the main threats to the sustainability of societies and their environments. To tackle these challenges, systemic transformations are required. Our project focuses on three cases of transformation in marginal environments in India and Bangladesh, and is concerned with: How transformation happens through bottom up processes in these sites; and how they can be scaled up and facilitate wider societal changes. Both require transdisciplinary co-production and the praxis of transformation which presupposes change in social arrangements and reconstruction by individuals. Our project addresses issues concerning governance, wellbeing, identity and quality of life in relation to transformations to sustainability in a lower middle income country (India) and a least developed country (Bangladesh). Our results should help inform processes that ultimately improve the quality of life in marginal environments, and build action and capacity among all partners.

Keywords: Transformation, Sustainability, Marginal environment, Transdisciplinary study, India, Bangladesh

©2019. Japan Geoscience Union. All Right Reserved.

Study for the Establishment of the Design for Disaster prevention through the survey of Recognition of tsunami disaster prevention from the viewpoint of green infrastructure in the coastal area of Kyushu-Pacific region.

*Shanshan Xu[1], Naoko Fujita[1], Minghui Tang[1]

1. Kyushu University

Considering the possibility of Nankai Trough large-scale earthquake predicted to occur in the nearest future, the issue of the tsunami in the coastal area of Kyushu-Pacific region is becoming extremely important. Efforts to utilize the various functions of the ecosystem internationally for the society creation are expanding in recent years, and even in the situation of toughening of the land in Japan, the initiative to incorporate Green Infrastructure (GI) which utilizes the disaster prevention and reduction functions of the natural ecosystem are being observed. Also, during the process of self-help/mutual assistance action and disaster reconstruction at the time of disaster, attention is paid as regional ties are affected, which are being considered as Social capital (SC).

The purpose of this study is to clarify the actual situation of tsunami disaster prevention of Nankai Trough earthquake based on the viewpoint of GI. We conducted a questionnaire survey on tsunami disaster prevention and GI at local governments and local communities. After analyzing the questionnaire, we analyzed the needs of the self-governing president's disaster prevention measures, the problems of the area, and the deviation of the improved situation of municipalities' disaster prevention measures. A correlation analysis was conducted to grasp the relationship between the consciousness concerning GI utilization, the strength of regional linkage SC and the recognition of evacuation.

1. Misalignment between demand and maintenance situation desired by the region

Policy regarding the issue of disaster helpers was extracted as a gap between needs and maintenance situation. Regarding the needs of the soft pattern in disaster prevention, a lot of measures were taken by disaster support supporters, however as it comes from the municipality questionnaire results, the measures related to the introduction of the barrier-free system and evacuation action supporters were introduced only partially. Further improvement is necessary for welfare evacuation sites, measures against supporters requiring evacuation actions, barrier-free formation.

2. SC regarded from the viewpoint of the relationship between intentions to utilize GI and recognition on disaster.

©2019. Japan Geoscience Union. All Right Reserved.

Especially, the correlation coefficient was 0.701 between No.7 and No.6. This shows that those who responded that disaster can happen among residents can respond that regional ties are stronger. For items with a high correlation coefficient between No.3 and No.8, the correlation became 0.437. This means the respondents who answered that evacuation is possible for all area inhabitants including elderly people in case of disaster (flooding, earthquakes, and tsunami) are able to use local well water and spring water in the event of a disaster.

Between No.2 and No.4, the correlation coefficient became 3.380. This is because those who respond that they think they can fully utilize the resources of the area (resources such as firewood, foods that can be harvested in mountains) even in the event of disasters will escape by utilizing the nearby natural landforms such as plateaus and mountains for tsunami evacuation. Between No.2 and No.8, the correlation coefficient became 0.351. This is because it shows those who responded that they thought that they could escape by utilizing nearby plateau and mountains such as mountains during the tsunami evacuation, even if disasters (flood, earthquake, tsunami) occurred, everyone including the elderly in the area evacuated. Between No.2 and No.6, the correlation coefficient became 0.343. This indicates that those who responded that they believe that they can escape by utilizing nearby plateaus and mountains when evacuating the tsunami think that the connection of the community people is strong. Between No.3 and No.6, the correlation coefficient became 0.287. This indicates that those who responded as they thought they could use local well water and spring water at the time of a disaster replied that they think that the regional connection is stronger.

Based on the above, we clarified the SC from the viewpoint of the gap between the request and the maintenance situation the region desires and the relationship between the intention to utilize GI and the perception of disaster. The fact that utilization of natural resources such as well water and spring water and understanding that natural topography can be utilized for evacuation leads to a positive feeling making people believe it is possible for everyone to evacuate even if the tsunami comes, can be suggested from this study.

Keywords: the Design for Disaster prevention, tsunami disaster, green infrastructure, the coastal area of Kyushu-Pacific region, Nankai Trough large-scale earthquake

©2019. Japan Geoscience Union. All Right Reserved.

Design for Green Infrastructure: Analysis of Landscape change in the Kumamoto earthquake area

*Naoko Fujita[1]

1. Kyushu University

The concept of “Green Infrastructure” and “Eco-DRR” is developed in Europe and North America lately, and it started to spread around in Japan after the Tohoku earthquake and tsunami in 2011. Landscape ecology is parallel with this conceptually, as well as in terms of spatial scale. Its successful focused researches and social implementation are becoming pervasive.

The new concept is to solve various problems by local resources and pearls of wisdom, it connects local communities to the world while it’s mainly led by front liners and researchers in engineering and ecological fields that little attention is paid to the aspects of arts and designs. It’s still not well-penetrated despite the validity and functions of the concept are well verified. Thus, it’s vitally important to work on the insufficient.

The purpose of this research is to analyze the reconstruction plan prepared by the affected municipalities of the Kumamoto earthquake and compare the landscape change read from the plan and the actual landscape change actually occurred and make clear how the cities and nature have changed during the reconstruction process.

In this research, we firstly gathered and analyzed the earthquake reconstruction plans created by each local government for all 45 municipalities in Kumamoto prefecture. In this analysis, while studying each municipal original plan, we primarily focused on the background, features, and landscape references of the plan formulation. During this analysis, we grasped the relations between the reconstruction plan and the landscape change, and also clarified what exactly each local government emphasizes independently. As the next step, basing on the field survey, we analyzed the actual state of the landscape changes described in the plan. As a method, we took the photographs at places where the plans adopted by each municipality in Kumamoto prefecture were scheduled or executed, and after recording the current situation and the surrounding landscape, we made a comparison with the photographs taken at the same place in the past. By doing this, we revealed what kind of changes have occurred between the past and the present due to the disaster, and how they affected the surrounding landscape.

Among the 45 municipalities in downtown Kumamoto Prefecture, we found that earthquake reconstruction plan was formulated in 16 municipalities, and 5 municipalities planned to formulate. There were references that "consideration of the landscape when promoting housing improvement and infrastructure development" and "to consider the landscape from the tourism viewpoint". Also, there were plans to utilize the process of reconstruction itself as a resource for tourist attraction. Furthermore, as a result of analyzing the individual plans described in the reconstruction plan, the reference to landscape,

©2019. Japan Geoscience Union. All Right Reserved.

reference to the prediction of landscape change, reference to landscape protection exists in all 16 cities, towns, and villages. Totally 117 relevant plans have been found. Although many of them were intended to cope with the damage at the time of the disaster, there were several plans originally adopted by the local governments to make necessary improvements of the problems they had from the past by conducting disaster recovery.

The field survey was conducted for 16 municipalities in total in Kumamoto Prefecture. One year has passed since the earthquake disaster, and recovery works progressed in a wide range in Kumamoto Prefecture. In the recovery sites in various places, a secondary change of the landscape, which caused the recovery activity aimed at improving the convenience of life and safety, has already been taking place. Moreover, recovery works progressed also in Kumamoto castle which is also cultural asset and tourist attraction, as well as the station and the government office which are the center of town. As a result, we could confirm the change of landscape.

In this research, through the analysis of the reconstruction plan created by the municipalities affected by the Kumamoto earthquake and the field survey, from the viewpoint of Green Infrastructure, we could make clear the process of the landscape change occurred during the process of recovery/reconstruction of the living base, the tourist resources, the natural environment in the affected areas and its influence respectively. Although few local governments have formulated landscape-friendly reconstruction plans, to gain medium- and long-term benefits, we should make landscape-friendly reconstructions from the original planning stage. This is because it is the factor determining the richness of living base, tourism resources, and natural environment.

Keywords: Green Infrastructure, the Kumamoto earthquake , Design

©2019. Japan Geoscience Union. All Right Reserved.

[E] Poster | H (Human Geosciences)：H-TT Technology & Techniques

Wed. May 29, 2019 1:45 PM - 3:15 PM JST | Wed. May 29, 2019 4:45 AM - 6:15 AM UTC | Poster Hall International Exhibition Hall8, Makuhari Messe_2

[H-TT21] Non-destructive techniques applied to stone cultural heritage

convener:Chiaki T. Oguchi(Institute for Environmental Science and Technology, Graduate School of Science and Engineering, Saitama University), Celine Elise Thomachot-Schneider(Groupe d'etude des environnements naturels, anthropiques et archeologiques - Universite de Reims-Champagne-Ardenne (France)), Wonsuh Song(Waseda University), Miguel Gomez-Heras(Universidad Autonoma de Madrid)

Non-destructive and non-invasive techniques applying to cultural heritage made of stones, soils and earthen materials have been significantly developed over past years, and thus, the interest in such techniques has greatly increased. Here, we focus the session on new devices, new protocols and new data treatments that allow better understanding of weathering mechanisms, decay states and response to treatments.
A few topics would be listed as follows: 1) The development of new techniques and devices in cultural heritage and new protocols using non-destructive techniques; 2) The application of these techniques and protocols on indoor and outdoor case studies and laboratory studies; 3) The assessment of weathering mechanisms, weathering kinetics, decay state, and response to treatments; and 4) The modeling and simulation of decay processes.

[HTT21-P01] Comparison and Analysis of GNSS-RTK Combined with 3D LiDAR Technology on Monument Maintenance Project

*Lih-Shinn Hwang[1], Chien-Hua Chiu[1], Chien-Wen Wang[1], Hsiao-Hung Chen[1] (1.National Defense Univ.)

[HTT21-P02] Non-destructive field measurement for investigation of deteriorated parts of an artificial cave

Kaisei Sakane[1], *Chiaki T. Oguchi[1], Yasuhiko TAMURA[2] (1.Institute for Environmental Science and Technology, Graduate School of Science and Engineering, Saitama University, 2.The Exective Committee for the Preservation of Taya Cavern)

[HTT21-P03] Ultra-portable thermal cameras for moisture detection

*Miguel Gomez-Heras[1], Laura Lopez-Gonzalez[2], Maria Teresa Gil-Muñoz[3] (1.Universidad Autonoma de Madrid, 2.Artfabrik, 3.Universidad Complutense de Madrid)

[HTT21-P04] A laboratory experiment on stone decay by combination of salt and ice crystallization

*Masato Sato[1], Tsuyoshi Hattanji[2] (1.Graduate School of Life and environmental Sciences, 2.Faculty of Life and EnvironmentalSciences, University of Tsukuba)

[HTT21-P05] Study of the micro-climatic monitoring on the Saint-Remi Basilica (Rheims, France)

*Emilie Huby[1], Celine Elise Thomachot-Schneider[1], Patricia Vazquez[1], Gilles Fronteau[1] (1.Universite de Reims-Champagne-Ardenne)

Comparison and Analysis of GNSS-RTK Combined with 3D LiDAR Technology on Monument Maintenance Project

*Lih-Shinn Hwang[1], Chien-Hua Chiu[1], Chien-Wen Wang[1], Hsiao-Hung Chen[1]

1. National Defense Univ.

The Precision is the first face problem in the restoration and preservation of Monument Maintenance Project. It may be that the initial coordinates of the position cannot be effectively determined by each object of historical antiquities or buildings, which seriously affects the proportional position when the combination is later reconstructed; or because the relative relationship with the natural environment is neglected, the restoration project is time consuming and even there may be errors that cannot be recovered.
Therefore, external reference control points play an important role in the 3D laser scanning operation of historical antiquities or buildings. Especially for long-term monitoring, it almost determines the accuracy of the following article scanning.
However, due to the unexpected situation on the spot, there are often control points lost, and there is a need for a rebuild-point project, which affects the 3D scanning operation of the later cultural relics. Rebuild-point project requires not only consistent precision, but also convenience and speed. This team takes the ancient house of Li-Tengfang, a national monument, as an example. When this term is studying on the restoration and preservation of Monument Maintenance Project, it is, and proposes newly method of rebuild-point project by comparison. A new method based on the viewpoint of engineering measurement is proposed to improve the lack of traditional operations.
The experimental results show that the GNSS-RTK rapidly-precise-positioning technology can replace the traditional static-measurement to practice rebuild-point project, and the 3D LiDAR ground control measurement which accuracy is enough can also be used as a reference for the other control points. Under the premise of high efficiency and constant accuracy, our team not only successfully introduced the concept of engineering measurement into the restoration and preservation of Monument Maintenance Project, but also completed the all 3D laser scanning operation on Li-Tengfang ancient house. All research processes can be provided to relevant units for reference.

Keywords: Monument Maintenance Project, Rebuild-point project, GNSS-RTK rapidly-precise-positioning positioning, 3D LiDAR Ground control measurement

©2019. Japan Geoscience Union. All Right Reserved.

Non-destructive field measurement for investigation of deteriorated parts of an artificial cave

Kaisei Sakane[1], *Chiaki T. Oguchi[1], Yasuhiko TAMURA[2]

1. Institute for Environmental Science and Technology, Graduate School of Science and Engineering, Saitama University, 2. The Exective Committee for the Preservation of Taya Cavern

Non-destructive measurements are useful methods for evaluating weathering degree without any damage on geoarchaeological sites. The present study aims to extract the deteriorated parts by using Silver Schmidt hammer and ultrasonic measurement on the Taya cave in Yokohama city. It is a manmade cave excavated from Kamakura to late Edo periods. Many sculptures and reliefs were carved on the surface of the cave wall made of soft rock. The cave has a complex three-layer structure with a total length of 570 m. Firstly, distribution maps showing cracks and exfoliation parts were created. Then, the points showing low rebound values and slow ultrasonic rates were plotted on the same map. After these on-site measurements, many dangerous parts were turned out within the worship route.

Keywords: Taya Cave, Silver Schmidt Test, Ultrasonic Rate

©2019. Japan Geoscience Union. All Right Reserved.

Ultra-portable thermal cameras for moisture detection

*Miguel Gomez-Heras[1], Laura Lopez-Gonzalez[2], Maria Teresa Gil-Muñoz[3]

1. Universidad Autonoma de Madrid, 2. Artfabrik, 3. Universidad Complutense de Madrid

Thermal imaging technology has grown and costs have decreased exponentially from 1987, when the first portable commercially available radiometric system appeared. Several firms produce nowadays ultra-portable thermal cameras that can be fitted in smartphones and tablets, giving resolutions of thermal images up to 320x240 p at a low cost. This facilitates the use of this tool for practitioners as a part of assessment of the state of conservation of heritage buildings and control and monitoring of conservation measurements. Moisture detection is a particular case in which thermal imaging is useful. This communication presents a case study of ultra-portable thermal camera usage for moisture detection and monitoring in two north-facing chapels in the ambulatory of the 14th to 16th Century Cathedral of Palencia (Spain). [Supported by Top Heritage (P2018/NMT-4372) programe from the Regional Government of Madrid (Spain)]

Keywords: Infrared Termography, Non-Destructive Testing, Moisture

©2019. Japan Geoscience Union. All Right Reserved.

A laboratory experiment on stone decay by combination of salt and ice crystallization

*Masato Sato[1], Tsuyoshi Hattanji[2]

1. Graduate School of Life and environmental Sciences, 2. Faculty of Life and EnvironmentalSciences, University of Tsukuba

A laboratory weathering experiment simulating combination of salt and ice crystallization was carried out using four types of rocks (porous tuff, dense tuff, dense sandstone, and porous andesite) with three types of salts (sodium chloride, sodium sulfate, or magnesium sulfate). The rock specimens were subjected to freeze-thaw cycles in a climatic cabinet where air temperature ranged from -30℃ to 10℃ within 24 hours. Prior to the freeze-thaw experiment, the specimens were immersed in saturated salt solutions at 10˚C or distilled water for 72 hours, and covered with foil for preventing the specimens from drying.
The specimens immersed in saturated salt solutions showed greater weight losses, reductions in Equotip rebound value and longitudinal wave velocity and surface expansion than those immersed in distilled water. Saturated solution of magnesium sulfate induced the greatest damage on rock specimens, although magnesium sulfate has been regarded as an inactive salt in the previous freeze-thaw experiments in which rock specimen were partly immersed in salt solution with dilute or mild concentration. Sodium sulfate induced rock damages comparable with sodium chloride. Sodium and magnesium sulfate crystallized from saturated solution and induced rock expansion prior to freezing. These salt crystals may fill micro-pores in rock and facilitates rock expansion and breakdown due to freezing.

Keywords: alt weathering, frost weathering, freeze-thaw, surface hardness, longitudinal wave velocity, surface expansion

©2019. Japan Geoscience Union. All Right Reserved.

Study of the micro-climatic monitoring on the Saint-Remi Basilica (Rheims, France)

*Emilie Huby[1], Celine Elise Thomachot-Schneider[1], Patricia Vazquez[1], Gilles Fronteau[1]

1. Universite de Reims-Champagne-Ardenne

Historical buildings are subjected to weathering through different factors such as temperature and humidity variations, that have a direct influence on different weathering processes. Insolation produces thermal expansion differences within the stone creating stresses at grain boundaries that can lead to disaggregation. If water is involved, a low temperature can cause the freezing of water inducing ice expansion and cryosuction. These repetitive stresses can damage the stone through fatigue failure. The measurement of environmental parameters on site is essential in order to study the weathering of the stone in its particular environment and anticipate risk areas.
To identify the micro-climatic conditions on a monument, an in situ monitoring was achieved on the Saint-Remi Basilica of Rheims, listed as a UNESCO World Heritage site. A sensor network was set up on the two towers of the monument in December 2017: fourteen temperature-humidity i-Buttons facing different directions, at different heights and recording with a time step of 1 hour, or a time step of 2 minutes for short measurement campaigns.
The data obtained by the sensor network highlighted the microclimates on the building. The height of the measured points had no significant impact on the results, whereas the orientation of the façade had an influence on the surface temperature. This was directly related to the longer solar exposure of the stone throughout the day and allowed to identify micro-climates. The façades exposed to the sun (South, East in the morning, West in the afternoon) present higher temperatures and lower relative humidity compared to the shadowed areas (North, East in the afternoon, West in the morning, other shadowed zones). The relative humidity measured was linked to the temperature: a temperature increase induces a humidity decrease. A mean difference of temperature between South and North of 2,7˚C with a maximum of 18˚C and a mean difference of relative humidity of 4,3% with a maximum of 48% were observed.
Climatic cycles on different time ranges were identified: an annual cycle alternating between winter and summer, a daily cycle due to sun exposure and short cycles identified during short term monitoring. These short abrupt variations of temperature (1-2˚C) on façades lasted between 5 and 40 minutes and were due to cloud cover and/or wind-speed. Four typical days inducing strains were identified: sunny days with a temperature increase superior to 10˚C, rainy days inducing wet/dry cycles, frost days presenting frost/thaw cycles and stormy days where a sudden rain on heated stones caused abrupt temperature and humidity variations. A year can thus be fragmented in those 4 categorized days. This repartition of typical days over a year depended on the micro-climatic variations previously identified: the shadowed zones experienced less sunny days and more rainy days.
This study of climatic monitoring will help anticipate the stone weathering on the Saint-Remi Basilica. The monitoring will continue for the next two years in order to obtain reproducible data and will be coupled with an infrared thermography monitoring. The strains corresponding to the four identified types of day are reproduced through accelerated ageing experiments using the parameters recorded on site. From the repartition of these typical days in one year, this will allow to estimate the behavior of a stone during a year on a sun-exposed façade and on a shadowed zone of the Basilica. The final goal is to be able to anticipate the stone weathering on the monument and identify risk areas.

Keywords: weathering processes, micro-climate, Saint-Remi Basilica, in situ monitoring

©2019. Japan Geoscience Union. All Right Reserved.

©2019. Japan Geoscience Union. All Right Reserved.

[E] Poster | H (Human Geosciences)：H-TT Technology & Techniques

Wed. May 29, 2019 5:15 PM - 6:30 PM JST | Wed. May 29, 2019 8:15 AM - 9:30 AM UTC | Poster Hall International Exhibition Hall8, Makuhari Messe_23

[H-TT21] Non-destructive techniques applied to stone cultural heritage

convener:Chiaki T. Oguchi(Institute for Environmental Science and Technology, Graduate School of Science and Engineering, Saitama University), Celine Elise Thomachot-Schneider(Groupe d'etude des environnements naturels, anthropiques et archeologiques - Universite de Reims-Champagne-Ardenne (France)), Wonsuh Song(Waseda University), Miguel Gomez-Heras(Universidad Autonoma de Madrid)

Non-destructive and non-invasive techniques applying to cultural heritage made of stones, soils and earthen materials have been significantly developed over past years, and thus, the interest in such techniques has greatly increased. Here, we focus the session on new devices, new protocols and new data treatments that allow better understanding of weathering mechanisms, decay states and response to treatments.
A few topics would be listed as follows: 1) The development of new techniques and devices in cultural heritage and new protocols using non-destructive techniques; 2) The application of these techniques and protocols on indoor and outdoor case studies and laboratory studies; 3) The assessment of weathering mechanisms, weathering kinetics, decay state, and response to treatments; and 4) The modeling and simulation of decay processes.

[HTT21-P01] Comparison and Analysis of GNSS-RTK Combined with 3D LiDAR Technology on Monument Maintenance Project

*Lih-Shinn Hwang[1], Chien-Hua Chiu[1], Chien-Wen Wang[1], Hsiao-Hung Chen[1] (1.National Defense Univ.)

[HTT21-P02] Non-destructive field measurement for investigation of deteriorated parts of an artificial cave

Kaisei Sakane[1], *Chiaki T. Oguchi[1], Yasuhiko TAMURA[2] (1.Institute for Environmental Science and Technology, Graduate School of Science and Engineering, Saitama University, 2.The Exective Committee for the Preservation of Taya Cavern)

[HTT21-P03] Ultra-portable thermal cameras for moisture detection

*Miguel Gomez-Heras[1], Laura Lopez-Gonzalez[2], Maria Teresa Gil-Muñoz[3] (1.Universidad Autonoma de Madrid, 2.Artfabrik, 3.Universidad Complutense de Madrid)

[HTT21-P04] A laboratory experiment on stone decay by combination of salt and ice crystallization

*Masato Sato[1], Tsuyoshi Hattanji[2] (1.Graduate School of Life and environmental Sciences, 2.Faculty of Life and EnvironmentalSciences, University of Tsukuba)

[HTT21-P05] Study of the micro-climatic monitoring on the Saint-Remi Basilica (Rheims, France)

*Emilie Huby[1], Celine Elise Thomachot-Schneider[1], Patricia Vazquez[1], Gilles Fronteau[1] (1.Universite de Reims-Champagne-Ardenne)

Comparison and Analysis of GNSS-RTK Combined with 3D LiDAR Technology on Monument Maintenance Project

*Lih-Shinn Hwang[1], Chien-Hua Chiu[1], Chien-Wen Wang[1], Hsiao-Hung Chen[1]

1. National Defense Univ.

The Precision is the first face problem in the restoration and preservation of Monument Maintenance Project. It may be that the initial coordinates of the position cannot be effectively determined by each object of historical antiquities or buildings, which seriously affects the proportional position when the combination is later reconstructed; or because the relative relationship with the natural environment is neglected, the restoration project is time consuming and even there may be errors that cannot be recovered.
Therefore, external reference control points play an important role in the 3D laser scanning operation of historical antiquities or buildings. Especially for long-term monitoring, it almost determines the accuracy of the following article scanning.
However, due to the unexpected situation on the spot, there are often control points lost, and there is a need for a rebuild-point project, which affects the 3D scanning operation of the later cultural relics. Rebuild-point project requires not only consistent precision, but also convenience and speed. This team takes the ancient house of Li-Tengfang, a national monument, as an example. When this term is studying on the restoration and preservation of Monument Maintenance Project, it is, and proposes newly method of rebuild-point project by comparison. A new method based on the viewpoint of engineering measurement is proposed to improve the lack of traditional operations.
The experimental results show that the GNSS-RTK rapidly-precise-positioning technology can replace the traditional static-measurement to practice rebuild-point project, and the 3D LiDAR ground control measurement which accuracy is enough can also be used as a reference for the other control points. Under the premise of high efficiency and constant accuracy, our team not only successfully introduced the concept of engineering measurement into the restoration and preservation of Monument Maintenance Project, but also completed the all 3D laser scanning operation on Li-Tengfang ancient house. All research processes can be provided to relevant units for reference.

Keywords: Monument Maintenance Project, Rebuild-point project, GNSS-RTK rapidly-precise-positioning positioning, 3D LiDAR Ground control measurement

©2019. Japan Geoscience Union. All Right Reserved.

Non-destructive field measurement for investigation of deteriorated parts of an artificial cave

Kaisei Sakane[1], *Chiaki T. Oguchi[1], Yasuhiko TAMURA[2]

1. Institute for Environmental Science and Technology, Graduate School of Science and Engineering, Saitama University, 2. The Exective Committee for the Preservation of Taya Cavern

Non-destructive measurements are useful methods for evaluating weathering degree without any damage on geoarchaeological sites. The present study aims to extract the deteriorated parts by using Silver Schmidt hammer and ultrasonic measurement on the Taya cave in Yokohama city. It is a manmade cave excavated from Kamakura to late Edo periods. Many sculptures and reliefs were carved on the surface of the cave wall made of soft rock. The cave has a complex three-layer structure with a total length of 570 m. Firstly, distribution maps showing cracks and exfoliation parts were created. Then, the points showing low rebound values and slow ultrasonic rates were plotted on the same map. After these on-site measurements, many dangerous parts were turned out within the worship route.

Keywords: Taya Cave, Silver Schmidt Test, Ultrasonic Rate

©2019. Japan Geoscience Union. All Right Reserved.

Ultra-portable thermal cameras for moisture detection

*Miguel Gomez-Heras[1], Laura Lopez-Gonzalez[2], Maria Teresa Gil-Muñoz[3]

1. Universidad Autonoma de Madrid, 2. Artfabrik, 3. Universidad Complutense de Madrid

Thermal imaging technology has grown and costs have decreased exponentially from 1987, when the first portable commercially available radiometric system appeared. Several firms produce nowadays ultra-portable thermal cameras that can be fitted in smartphones and tablets, giving resolutions of thermal images up to 320x240 p at a low cost. This facilitates the use of this tool for practitioners as a part of assessment of the state of conservation of heritage buildings and control and monitoring of conservation measurements. Moisture detection is a particular case in which thermal imaging is useful. This communication presents a case study of ultra-portable thermal camera usage for moisture detection and monitoring in two north-facing chapels in the ambulatory of the 14th to 16th Century Cathedral of Palencia (Spain). [Supported by Top Heritage (P2018/NMT-4372) programe from the Regional Government of Madrid (Spain)]

Keywords: Infrared Termography, Non-Destructive Testing, Moisture

©2019. Japan Geoscience Union. All Right Reserved.

A laboratory experiment on stone decay by combination of salt and ice crystallization

*Masato Sato[1], Tsuyoshi Hattanji[2]

1. Graduate School of Life and environmental Sciences, 2. Faculty of Life and EnvironmentalSciences, University of Tsukuba

A laboratory weathering experiment simulating combination of salt and ice crystallization was carried out using four types of rocks (porous tuff, dense tuff, dense sandstone, and porous andesite) with three types of salts (sodium chloride, sodium sulfate, or magnesium sulfate). The rock specimens were subjected to freeze-thaw cycles in a climatic cabinet where air temperature ranged from -30℃ to 10℃ within 24 hours. Prior to the freeze-thaw experiment, the specimens were immersed in saturated salt solutions at 10˚C or distilled water for 72 hours, and covered with foil for preventing the specimens from drying.
The specimens immersed in saturated salt solutions showed greater weight losses, reductions in Equotip rebound value and longitudinal wave velocity and surface expansion than those immersed in distilled water. Saturated solution of magnesium sulfate induced the greatest damage on rock specimens, although magnesium sulfate has been regarded as an inactive salt in the previous freeze-thaw experiments in which rock specimen were partly immersed in salt solution with dilute or mild concentration. Sodium sulfate induced rock damages comparable with sodium chloride. Sodium and magnesium sulfate crystallized from saturated solution and induced rock expansion prior to freezing. These salt crystals may fill micro-pores in rock and facilitates rock expansion and breakdown due to freezing.

Keywords: alt weathering, frost weathering, freeze-thaw, surface hardness, longitudinal wave velocity, surface expansion

©2019. Japan Geoscience Union. All Right Reserved.

Study of the micro-climatic monitoring on the Saint-Remi Basilica (Rheims, France)

*Emilie Huby[1], Celine Elise Thomachot-Schneider[1], Patricia Vazquez[1], Gilles Fronteau[1]

1. Universite de Reims-Champagne-Ardenne

Historical buildings are subjected to weathering through different factors such as temperature and humidity variations, that have a direct influence on different weathering processes. Insolation produces thermal expansion differences within the stone creating stresses at grain boundaries that can lead to disaggregation. If water is involved, a low temperature can cause the freezing of water inducing ice expansion and cryosuction. These repetitive stresses can damage the stone through fatigue failure. The measurement of environmental parameters on site is essential in order to study the weathering of the stone in its particular environment and anticipate risk areas.
To identify the micro-climatic conditions on a monument, an in situ monitoring was achieved on the Saint-Remi Basilica of Rheims, listed as a UNESCO World Heritage site. A sensor network was set up on the two towers of the monument in December 2017: fourteen temperature-humidity i-Buttons facing different directions, at different heights and recording with a time step of 1 hour, or a time step of 2 minutes for short measurement campaigns.
The data obtained by the sensor network highlighted the microclimates on the building. The height of the measured points had no significant impact on the results, whereas the orientation of the façade had an influence on the surface temperature. This was directly related to the longer solar exposure of the stone throughout the day and allowed to identify micro-climates. The façades exposed to the sun (South, East in the morning, West in the afternoon) present higher temperatures and lower relative humidity compared to the shadowed areas (North, East in the afternoon, West in the morning, other shadowed zones). The relative humidity measured was linked to the temperature: a temperature increase induces a humidity decrease. A mean difference of temperature between South and North of 2,7˚C with a maximum of 18˚C and a mean difference of relative humidity of 4,3% with a maximum of 48% were observed.
Climatic cycles on different time ranges were identified: an annual cycle alternating between winter and summer, a daily cycle due to sun exposure and short cycles identified during short term monitoring. These short abrupt variations of temperature (1-2˚C) on façades lasted between 5 and 40 minutes and were due to cloud cover and/or wind-speed. Four typical days inducing strains were identified: sunny days with a temperature increase superior to 10˚C, rainy days inducing wet/dry cycles, frost days presenting frost/thaw cycles and stormy days where a sudden rain on heated stones caused abrupt temperature and humidity variations. A year can thus be fragmented in those 4 categorized days. This repartition of typical days over a year depended on the micro-climatic variations previously identified: the shadowed zones experienced less sunny days and more rainy days.
This study of climatic monitoring will help anticipate the stone weathering on the Saint-Remi Basilica. The monitoring will continue for the next two years in order to obtain reproducible data and will be coupled with an infrared thermography monitoring. The strains corresponding to the four identified types of day are reproduced through accelerated ageing experiments using the parameters recorded on site. From the repartition of these typical days in one year, this will allow to estimate the behavior of a stone during a year on a sun-exposed façade and on a shadowed zone of the Basilica. The final goal is to be able to anticipate the stone weathering on the monument and identify risk areas.

Keywords: weathering processes, micro-climate, Saint-Remi Basilica, in situ monitoring

©2019. Japan Geoscience Union. All Right Reserved.

©2019. Japan Geoscience Union. All Right Reserved.

[E] Poster | H (Human Geosciences)：H-CG Complex & General

Wed. May 29, 2019 3:30 PM - 5:00 PM JST | Wed. May 29, 2019 6:30 AM - 8:00 AM UTC | Poster Hall International Exhibition Hall8, Makuhari Messe_15

[H-CG25] International Comparison of Landscape Appreciation

convener:Anastasia Petrova(Institute of Oriental Studies of the Russian Academy of Sciences), yoji aoki(Open University of Japan)

Evaluation of landscape has been developed in a variety of fields, such as geography, landscape architecture, nature protection, and some others. Landscape appreciation is a complex and sophisticated psychological phenomenon. There is no consensus among researchers on what the phenomenon of "landscape" truly is, how people physiologically and mentally experience it, which human attributes affect the perception of it, and why it is apprehended the way it is. The concept of landscape appreciation has yet to be clearly defined and there is a lack of agreement on evaluation methods, the factors that determine landscape preferences, the steps in appreciation, and so forth. This session aims to discuss the research findings of landscape evaluation in various fields, including geography, geomorphology, landscape planning, architecture, engineering, social sciences, environmental psychology, meteorology, phenology, and so on.

[HCG25-P01] The Globally Important Agricultural Heritage of Aso from the perspective of landscape and its supporting systems

*REIKO MACHIDA[1] (1.TOKYO UNIVERSITY OF AGRICULTURE)

[HCG25-P02] Hazardous natural phenomena and weather conditions appreciation in Russian landscape painting

*ELENA PETROVA[1] (1.Lomonosov Moscow State University, Faculty of Geography)

[HCG25-P03] Trends of evaluation items to landscape appreciation until 2017 in the English journals

*yoji aoki[1], keisuke mukagai[2], Anastasia Petrova[3] (1.Open University of Japan, 2.Nagano University, 3.Institute of Oriental Studies, Russian Academy of Sciences)

The Globally Important Agricultural Heritage of Aso from the perspective of landscape and its supporting systems

*REIKO MACHIDA[1]

1. TOKYO UNIVERSITY OF AGRICULTURE

Globally Important Agricultural Heritage Systems (GIAHS) is a partnership initiative of the Food and Agriculture Organization of the United Nations which began in 2002 with the aim to identify, support and safeguard remarkable land use systems and landscapes that are rich in globally significant biological diversity evolving from the co-adaptation of a community with its environment and its needs and aspirations for sustainable development. There are 19 countries and 45 areas around the world, and among them 9 areas in Japan that are listed as GIAHS at present.The Aso area located in Northern Kyusyu features the world's largest caldera, which is 25 km wide from north to south and 18 km from east to west and grassland landscapes. The vast grasslands of the Aso area have been managed throughout history by local agricultural activities such as controlled burning, mowing and pasturage since the Heian period. The historical land use in Aso has been a balanced combination of rice fields at the caldera floor, forestry and fungiculture at the foot of the caldera, and grazing pasture at the top of caldera, which is carried out in harmony with the environment. The management of the Aso grasslands for sustainable agriculture have been recognized and certified as Globally Important Agricultural Heritage Systems (GIAHS) in 2013.In terms of landscape, the values of Aso as Globally Important Agricultural Heritage System are the dynamic grassland landscapes of the large caldera, the historical paddies and rice terraces, which vary in size from small to large as a result of the local human activities. There are beautiful rural landscapes on various scales.However, the productivity oriented rural development and the division of land has been having a negative impact on the landscape value of the GIAHS. There are cases of rice paddies and buildings that contribute to the landscape value being lost. From such cases, it is evident that the landscape structures that should be protected since they are GIHS are not recognized widely enough.This study investigated the landscape value and landscape structure as GIAHS and its value supports landscape policy. As a result, it became clear that the landscape structure of Minamiaso village consist of the traditional combination of grasslands and paddy fields retains significant wildlife habitat and picturesque agricultural landscapes. It has become clear that development activities do not influence to landscape in large-scale, however development activities as land readjustment project influenced to landscape in small and medium-scale. "Landscape planning" "Landscape agricultural development plan" can support the landscape structure in small and medium -scale. It is important to plan the land use for the landscape value of GIAHS.

Keywords: Globally Important Agricultural Heritage Systems (GIAHS), Landscape, Landscape Planning

©2019. Japan Geoscience Union. All Right Reserved.

Hazardous natural phenomena and weather conditions appreciation in Russian landscape painting

*ELENA PETROVA[1]

1. Lomonosov Moscow State University, Faculty of Geography

The fixation of various natural phenomena by landscape artists of different historical periods in different regions and countries has not only purely aesthetic interest, but also particular interest to science. During the period of Romanticism that has spread in the European and Russian art in the 19th century, Russian art turned to real living nature. Landscapes of the native country began to play a dominant role in the formation of landscape image. Romanticism aroused interest not only in the picturesque and exotic landscapes, but also in the majestic forces of nature. Volcanic eruptions, earthquakes, storms, thunderstorms, floods, and other natural hazards were new motifs for artists of that time. Romantic artists were inclined to exaggerate the power and destructive forces of natural phenomena they portrayed, elevating any event of this kind to the rank of a natural disaster. Often, they portrayed the rather ordinary storm, thunderstorm, flood as a universal natural catastrophe, comparable, perhaps, only to the biblical flood. What to say about really extraordinary events. Most vividly, the theme of the turbulent, dramatic landscape was developed in the works by Aivazovsky who quite realistically showed the sea element in various stages of its manifestation - from complete calm to the strongest storm. Being in Italy, Russian artists could not disregard such an extraordinary event as the violent eruption of the volcano Vesuvius, which occurred in 1822; many have captured it in their landscape images.

Thanks to the rapid development of scientific knowledge and discoveries in the field of geosciences, including meteorology, artists were encouraged to observe various atmospheric phenomena and weather conditions. Gradually, the sky ceased to be depicted simply as a smooth blue background, as was customary in the tradition of classicism; carefully traced clouds of various types, shapes and shades began to appear in pictures. In addition, various evaporations, fogs, haze, etc. became objects of the landscape image. Romantic artists were little interested in depicting winter and snow, despite the fact that the cold season with a steady snow cover continues in Russia for almost half a year from November to early April. The painting “Russian Winter” (1827) by Nikifore Krylov became perhaps the first winter landscape image in Russian painting. Krylov depicted a somewhat naive, but quite real, winter landscape on the bank of the Tosna River in the vicinity of St. Petersburg, which he painted from life. He was able to reliably convey the atmosphere of the Russian winter: a valley covered with snow, a frozen river, a dark strip of forest in the distance and the peasants with their daily affairs on the road down to the river in the foreground. The first bright and joyful snow-covered landscape image was created, apparently, by Alexey Savrasov in his famous painting “The Rooks Have Come Back” (1871). The spring snow melting and sparkling in the sun became later the favorite motif of the Russian painting. Comparative analysis of landscape pictures can be an important tool, in addition to scientific methods, in studying the nature and dynamics of various hazardous natural processes and phenomena, including hydrological and meteorological ones in conditions of changing climate.

Keywords: hazardous natural phenomena , weather conditions , landscape painting, landscape images

©2019. Japan Geoscience Union. All Right Reserved.

Trends of evaluation items to landscape appreciation until 2017 in the English journals

*yoji aoki[1], keisuke mukagai[2], Anastasia Petrova[3]

1. Open University of Japan, 2. Nagano University, 3. Institute of Oriental Studies, Russian Academy of Sciences

Introduction
We have considered trends of landscape appreciation since JpGU2013-2018. According to the definition of landscape phenomena proposed by Prof. O. Shinohara (Fig. 1), we reported the trends of studies in each part of the phenomena.

Aoki, Y. (1999) described the first landscape evaluation using psychometrical methods to be pioneered by Peterson, G.L. (1967). Before this development, they tried to find the landscape appreciation using various descriptors. They were mostly belonging to the literature or the paintings. As for the literature, the first description of mountain was found in Francesco Petrarca in 1336 of France (Kondo, T. 2002). But his description has no reliable evidence to ensure the landscape. In the field of art, Albrecht Altdorfer drew the first natural landscape in the beginning of 15th century of Germany (Cavaliere, B. 1989). But we could not measure the physical data from his picture. The literature and the art found the beauty of natural landscape by these examples. They recorded the aesthetic beauty in landscape (Thiel, P. 1968).

Jay Appleton (1980) explained the scientific reason of the landscape phenomena with physical data, e.g. geomorphysical data and meteorological data. He explained the landscape phenomena of two pictures, Constable's Weymouth Bay and Constable's sunset study of Hampstead Heath. His approach must be the scientific based explanation to find psychological phenomena of landscape using the geology and meteorology. But the psychological phenomena could deviate by the person observed and the results must be happened statistically. So the process of the landscape phenomena should be explained by stochastic process of psychology. Then scientists developed psychological approach to it.

Here, we summarize the appreciation item (the third component of the landscape phenomena).

1. The developments to establish the psychological scale of appraisal

In the trial of psychometrical method, Ekman & Kuennapas (1962) tested the difference of Nominal scale and Interval scale, and the development of SD method promoted to use many adjectives in the visual complexities (Berlyne & Peckham 1966). Hart & Graham (1967) considered “How to rate & rank landscape”.

In the development of the psychological scale, Heise (1969) tested the scale -3 to 3, and Zube, Anderson & Pitt (1973) used the numerical scale 3 to 14.

2. The psychological evaluation item of preference

Kaplan, Kaplan, & Wendt (1972) proposed to use preference for the landscape appreciation. Compared to the results obtained by SD method, “preference” is easy to understand among different cultural back ground and was popularized in many countries.

©2019. Japan Geoscience Union. All Right Reserved.

3. The developments and the use of SD method

As for the SD method proposed by Osgood & Suci (1955), it employed many pairs of adjectives to evaluate landscape and provided detailed impressions of landscape. The largest number of 240 adjectives was tested by Craik (1975). The results were too complicated and scientists would like to summarize the results. SBE (Terry & Boster 1976), AVQ (Arriaza etc. 2004) and others were statistical aggregation examples of this trial and the example of meaningful aggregation was “Coherence, Complexity, Legibility and Mystery” proposed by Kaplan (1987). These indicators were tested with the relation to the preference and other appreciations by many scientists (Stamps III 2004, and so on.).

4. Method of monetary term evaluation

Monetary term is another evaluation of landscapes and sometimes used in the physical planning (Fukahori & Kubota 2003).

5. Items based on the human behavior of landscape evaluation

The origin of the landscape appreciation was explained from the animal behavior of predation (Appleton 1975). This theory had discussed for a long time. And this behavior might propose a base appreciation of landscape (Aoki & Kitamura 2001). Consideration on the human activities, the reason of visit (Andereck et al. 1989) and the visitability (Abdulkarim & Nasar 2014) were examined and the photographing (Oku & Fukamachi 2006, Sugimoto 2013) were reported.

6. Other appraisals

There are many appreciation descriptors and even now the scientists are finding new descriptors (Collier & Scott 2008). Until now, we could find examples of this trial in absorption (Berlyne 1958), quietness (Womble & Studebaker 1981), beauty (Hull IV, Buhyoff & Daniel 1984), size (Coeterier 1994), fear and stress (Nasar & Jones 1997), positive and negative (Ryan 1998), aggression and violence (Kuo 2001), satisfaction (Kaplan & Austin 2004), overcrowding (Manning & Freimund 2004), openness (Dramstad et al. 2006), ugly (Ruell, Halleux & Teller 2013), and other descriptions.

Keywords: landscape appreciation, appreciation items, until 2017

©2019. Japan Geoscience Union. All Right Reserved.

Table Historical review of landscape appreciation items

Interesting subject	Name of authors	Year
Development of the SD method	Osgood, C.E. and Suci, G.J.	1955
absorption	Berlyne, D.E.,	1958
descriptive appreciation as aesthetic beauty	Thiel, P.,	1961
difference of Nominal scale and Interval scale	Ekman, G. and Kuennapas, T.	1962
SD method	Wright, B. and Rainwater, L.	1962
description	Halprin, L.,	1965
absorption	Berlyne, D.E. and Peckham, S.	1966
description	Noe, S. and Abernathy, B.L.	1966
landscape type	Hart W. J. and William W. Graham,	1967
absorption	Wohlwill, J.F.	1968
numerical scale from -3 to +3	Heise, D.R.,	1969
aesthetic and emotional	Shafer, E.L. and Mietz, J.	1969
objectivity	Craik, K.H.	1972
preference	Kaplan, S., Kaplan, R. and Wendt, J.S.	1972
scaling	Acking, C.A and Sorte, G.J.	1973
numerical scale from 3 to 14	Zube, E.H., Anderson, T. and Pitt, D.	1973
prospect-refuge theory	Appleton, J.	1975
SD method with 240 pairs of adjectives	Craik, K.H.	1975
SBE method; normalization of the results	Daniel, T.C. and Boster, R.S.	1976
monetary	McConnell, K.E.,	1977
SD method	Pedersen, D.M.	1978
SD method	Shuttleworth, S.	1980
preference	Nasar, J.L.,	1981
meaning	Russell, J.A. and Ward, L.M.	1981
quiet	Womble, P. and Studebaker, S.	1981
quiet	Hammitt, W.E.,	1982
preference	Mudrak, L.Y.,	1983
preference	Nasar, J.L.,	1983
SD method	Ruiz, J.P. and Gonzalez-Bernaldez, F.	1983
scenic beauty	Hull IV, R.B., Buhyoff, G.J. and Daniel, T.C.	1984
needs and fears	Talbot, J.F. and Kaplan, R.	1984
preference	Herzog, T.R.	1985
SD method	Abello, R.P., Bernaldez, F.G. and Galiano, E.F.	1986
preference	Talbot, J.F. and Kaplan, R.	1986
survey paper: Coherence, Complexity, Legibility, Mystery	Kaplan, S.	1987
SD method	Kobayashi, M., Higashiyama, J. and Kawasaki, K.	1987
preference	Talbot, J.F., Bardwell, L.V. and Kaplan, R.	1987
monetary	Anderson, L.M. and Cordell, H.K.	1988
preference	Herzog, T. and Smith, G.A.	1988
motivation to visit	Andereck, K. et al.	1989
evaluation by monetary term	Daniel, T.C., et al.	1989
SD method	Kaplan, R., Kaplan, S. and Brown, T.	1989
SD method	Ruiz, M. and Ruiz, J.P.	1989
preference	Gimblett, H.R.	1990
monetary	Green, C.H., et al.	1990
motivation to visit	Uysal, M., McDonald, C.D. and Reid, L.J.	1990
quiet	Ulrich, R.S. et al.	1991
preference	Chokor, B.A	1992
preference	Herzog, T.	1992
refuge provides shelter	Hudson, B.J.	1992
effect to land price	Orland, B., Vinning, J. and Ebreo, A.	1992
familiarity	Purcell, A.T.	1992
description: literature works	Ikeda, T. and Konno, A.	1993
size of space	Coeterier, J.F.,	1994
identity	Hull IV, R.B., Lam, M. and Vigo, G.	1994
preference	Stamps III, A.E.	1994
preference	Strumse, E.	1994
preference	Sullivan III, W.C.,	1994
prospect-refuge theory reviewed	Appleton, J.,	1995
motivation to visit	Cha, S., McCleary, K.W. and Uysal, M.	1995
preference	Mealey, L.	1995
preference on tree form	Sommer, R. and Summit, J.	1995
preference	Herzog, T.R. and Gale, T.A.	1996
scenic preference in Finland	Karjalainen, E.	1996
scaling	Tahvanainen, L., Tyrvainen, L. and Nousiainen, I.	1996
Notation for a Participatory Envirotecture	Thiel, P.,	1996
fear and stress	Nasar, J.L. and Jones, K.M.	1997
landscape preferences of USA, Ireland, Senegal	Newell, P.B.	1997
quiet	Caffyn, A. and Prosser, B.	1998
preference	Herzog, T.R.,	1998
consistency of evaluation by rank order and graphical scale	Karjalainen, E. and Komulainen, M.	1998
preference	Kuo, F.E., Bacaicoa, M. and Sullivan, W.C.	1998
preference and naturalness using Scrub-forest, wide-close view, nature-altered	Purcell, A.T. and Lamb, R.J.	1998
positive and negative scenery of river frontland	Ryan, R.L.	1998
monetary	Tyrvainen, L. and Vaananen, H.	1998
preference	Brown, T.J., Kaplan R. and Quaderer, G.	1999
tranquility and preference	Herzog, T.R. and Barnes, G.J.	1999
preference	Summit, J. and Sommer, R.	1999
landscape preference in Australia	Herzog, T.R. et al	2000
landscape preference in Israel	Misgav, A.	2000
Phylogenic and Ontogenic evolution of landscape appreciation	Aoki, Y. and Kitamura, S.	2001
correlation between preference and likeliness	Hagerhall, C.M.	2001
motivation of ecological behavior	Hartig, T.	2001
aggression and violence	Kuo, F.E.,	2001
preference and danger	Herzog, T.R. and Kutzli, G.E.	2002
landscape preference in Norway	Kaltenborn, B.P. and Bjerke, T.	2002
positive and negative scenery of rural living	Ryan, R.L.,	2002
comparison of VOC and SBE	Franco, D. et al.	2003
cost and amenity level of road scenery	Fukahori, K. and Kubota, Y.	2003
preference	Herzog, T.R. and Leverich, O.L.	2003
AVQ index for visual quality	Arriaza, M. et al.	2004
preference	Herzog, T.R. and Kropscott, L.S.	2004
satisfaction of nature	Kaplan, R. and Austin, M.E.	2004
over crowding by photo montage method	Manning, R.E. and Freimund, W.A	2004
SBE difference 1976-1996	Palmer, J.F.	2004
preference did not correlate to mystery, complexity, legibility, coherence	Stamps, III, A.E.	2004
preference and danger by visibility	Herzog, T.R., & Kirk, K.M.	2005
preference by pair comparison	Rodiek, S.D. and Fried, J.T.	2005
proper openness, student and locals	Dramstad, W.E., et al.	2006
essential features for scenic beauty	Ergin, A., Williams, A.T. and Micallef, A.	2006
landscape preferred in Turkey	Kaplan, A., Taskin, T. and Onenc, A.,	2006
photographing by activity	Oku, H., & Fukamachi, K.	2006
disturbance, naturalness, visual scale, place identity in the photographs	Tveit, M., Ode, A. and Fry, G.	2006
mystery did not affect preference	Herzog, T.R. and Bryce, A.G.,	2007
words interested in the interview	Collier, M.J. and Scott, M.J.	2008
preference of transportation system; vegetation, distance, side fascia affected	Bernasconi, C. et al.	2009
beautiful high mountain, Sherpa appreciate flora, ugly garbage site no vegetation at Everest	Beza, B.B.	2010
species-rich of middle ground affect like of alpine landscape	Lindemann-Matthies, P. et al.	2010
naturalness, unity affect preference of Spruce forest landscape in Turkey	Eroglu, E. and Acar, C.	2011
surprise and Mystery affect preference, Turkey find Mystery at curved street	Nasar, J.L. and Cubukcu, E.	2011
ugly impression of brown fields and montage support improvement in Belgium	Ruelle, C., Halleux, J.-M. & Teller, J.	2013
Visitability	Abdulkarim, D. and Nasar, J. L.	2014
oppressiveness	Asgarzadeh, M. et al.	2014
threat	Chiang, Y-C., Nasal, J. and Ko, C-C.	2014
variance affected by evaluation value	Kalivoda, O. et al.	2014
forest and park affected stress relief	Tyrvainen, L., Ojala, A., Korpela, K. Lanki, T., Tsunetsugu, Y., Kagawa, T.	2014
proper understorey affect preference	van der Wal, R., Miller, D., Irvine, J., Fiorini, S., Amar, A., Yearley, S. Gill, R. & Dandy, N.	2014
openness	Weitkamp, G., Lammeren, R. and Bregt, A.	2014
risk of bushfire	Gill, N. et al.	2015
water use affect landscaping preference	Hayden, L., et al	2015
panorama tree cover density affect to preference	Jiang, B., et al.	2015
green roof affect restorativeness	Lee, K.E., Williams,K.J.H., Sargent, L.D., Williams, N.S.G., Johnson, K.A	2015
aesthetic, morphological condition and ecological integrity	McCormick, A, Fisher, K. and Brierley, G.	2015
water, reed, litter, dead wood affected preference	Eder, R., & Arnberger, A.	2016
tree coverage affect stress recovery	Jiang, B., Li, D., Larsen, L. & Sullivan, W.C.	2016
visual realism and sound affect preference	Lindquist, M., Lange, E. & Kang J.	2016
change of motivation	Shalev, I.	2016
cultural values in visual object	Sowinska-Swierkosz, B.N., Chmielewski, T.J.	2016
visual green reduces noise annoyance	Van Renterghem, T. & Botteldooren, D.	2016
public litter and fishing litter affect preference	Wyles, K.J., Pahl, S. Thomas, K. & Thompson, R.	2016
disorder affect fear of crime	Biasi, Alaina De	2017
nature contact reduce depression, anxiety, stress in outside experience	Brooks, A.M. et al.	2017
biodiversity affected preference	Cracknell, D. et. al.	2017
dead wood affected preference	Gundersen, V., Stange, E.E., Kaltenborn, B.P. Vistad	2017
EAB infestation affect crime, theft, breaking entering, property crime	Kondo, M.C., Han, S., Donovan, G.H., MacDonald, J.M.	2017
preference increase 4bit designed complexinformation entropy values	Kuper, R.	2017
wind generator affect to EEG (electroencephalographic)	Murcia, G. et al.	2017
natural scenery affect change of heart rate by CT scan	Zijlstra, E. et. Al.	2017
attributes affected to landscape aesthetic value of CVM	Dupras, J. et al.	2018
point elements affect preference	Haefner, K. et al.	2018
dense vegetation preferred in city	Harris, V. et al.	2018
motivation of park visit	Hecke, Linde, et al.	2018
firing affect emotional wellbeing	Knez, I. et al.	2018
mature oak with anemone preferred	Nielsen, A.B., Gundersen, V.S. & Jensen, F.S.	2018
traditional landscape preferred by residents in central Alps	Pecher, C., et al.	2018
photo points located by GIS	Sugimoto, K.	2018
setting and arrangement affect restrativeness	Tabrizian, P., et al.	2018
forest preference of 4 seasons	Bravo-Vargas, V. et al.	2019

behavioral consideration
developments in scaling
monetary approaches
use of preference
developments in SD method
other appreciation

©2019. Japan Geoscience Union. All Right Reserved.

[E] Poster | H (Human Geosciences)：H-CG Complex & General

Wed. May 29, 2019 5:15 PM - 6:30 PM JST | Wed. May 29, 2019 8:15 AM - 9:30 AM UTC | Poster Hall International Exhibition Hall8, Makuhari Messe_24

[H-CG25] International Comparison of Landscape Appreciation

convener:Anastasia Petrova(Institute of Oriental Studies of the Russian Academy of Sciences), yoji aoki(Open University of Japan)

Evaluation of landscape has been developed in a variety of fields, such as geography, landscape architecture, nature protection, and some others. Landscape appreciation is a complex and sophisticated psychological phenomenon. There is no consensus among researchers on what the phenomenon of "landscape" truly is, how people physiologically and mentally experience it, which human attributes affect the perception of it, and why it is apprehended the way it is. The concept of landscape appreciation has yet to be clearly defined and there is a lack of agreement on evaluation methods, the factors that determine landscape preferences, the steps in appreciation, and so forth. This session aims to discuss the research findings of landscape evaluation in various fields, including geography, geomorphology, landscape planning, architecture, engineering, social sciences, environmental psychology, meteorology, phenology, and so on.

[HCG25-P01] The Globally Important Agricultural Heritage of Aso from the perspective of landscape and its supporting systems

*REIKO MACHIDA[1] (1.TOKYO UNIVERSITY OF AGRICULTURE)

[HCG25-P02] Hazardous natural phenomena and weather conditions appreciation in Russian landscape painting

*ELENA PETROVA[1] (1.Lomonosov Moscow State University, Faculty of Geography)

[HCG25-P03] Trends of evaluation items to landscape appreciation until 2017 in the English journals

*yoji aoki[1], keisuke mukagai[2], Anastasia Petrova[3] (1.Open University of Japan, 2.Nagano University, 3.Institute of Oriental Studies, Russian Academy of Sciences)

The Globally Important Agricultural Heritage of Aso from the perspective of landscape and its supporting systems

*REIKO MACHIDA[1]

1. TOKYO UNIVERSITY OF AGRICULTURE

Globally Important Agricultural Heritage Systems (GIAHS) is a partnership initiative of the Food and Agriculture Organization of the United Nations which began in 2002 with the aim to identify, support and safeguard remarkable land use systems and landscapes that are rich in globally significant biological diversity evolving from the co-adaptation of a community with its environment and its needs and aspirations for sustainable development. There are 19 countries and 45 areas around the world, and among them 9 areas in Japan that are listed as GIAHS at present.The Aso area located in Northern Kyusyu features the world's largest caldera, which is 25 km wide from north to south and 18 km from east to west and grassland landscapes. The vast grasslands of the Aso area have been managed throughout history by local agricultural activities such as controlled burning, mowing and pasturage since the Heian period. The historical land use in Aso has been a balanced combination of rice fields at the caldera floor, forestry and fungiculture at the foot of the caldera, and grazing pasture at the top of caldera, which is carried out in harmony with the environment. The management of the Aso grasslands for sustainable agriculture have been recognized and certified as Globally Important Agricultural Heritage Systems (GIAHS) in 2013.In terms of landscape, the values of Aso as Globally Important Agricultural Heritage System are the dynamic grassland landscapes of the large caldera, the historical paddies and rice terraces, which vary in size from small to large as a result of the local human activities. There are beautiful rural landscapes on various scales.However, the productivity oriented rural development and the division of land has been having a negative impact on the landscape value of the GIAHS. There are cases of rice paddies and buildings that contribute to the landscape value being lost. From such cases, it is evident that the landscape structures that should be protected since they are GIHS are not recognized widely enough.This study investigated the landscape value and landscape structure as GIAHS and its value supports landscape policy. As a result, it became clear that the landscape structure of Minamiaso village consist of the traditional combination of grasslands and paddy fields retains significant wildlife habitat and picturesque agricultural landscapes. It has become clear that development activities do not influence to landscape in large-scale, however development activities as land readjustment project influenced to landscape in small and medium-scale. "Landscape planning" "Landscape agricultural development plan" can support the landscape structure in small and medium -scale. It is important to plan the land use for the landscape value of GIAHS.

Keywords: Globally Important Agricultural Heritage Systems (GIAHS), Landscape, Landscape Planning

©2019. Japan Geoscience Union. All Right Reserved.

Hazardous natural phenomena and weather conditions appreciation in Russian landscape painting

*ELENA PETROVA[1]

1. Lomonosov Moscow State University, Faculty of Geography

The fixation of various natural phenomena by landscape artists of different historical periods in different regions and countries has not only purely aesthetic interest, but also particular interest to science. During the period of Romanticism that has spread in the European and Russian art in the 19th century, Russian art turned to real living nature. Landscapes of the native country began to play a dominant role in the formation of landscape image. Romanticism aroused interest not only in the picturesque and exotic landscapes, but also in the majestic forces of nature. Volcanic eruptions, earthquakes, storms, thunderstorms, floods, and other natural hazards were new motifs for artists of that time. Romantic artists were inclined to exaggerate the power and destructive forces of natural phenomena they portrayed, elevating any event of this kind to the rank of a natural disaster. Often, they portrayed the rather ordinary storm, thunderstorm, flood as a universal natural catastrophe, comparable, perhaps, only to the biblical flood. What to say about really extraordinary events. Most vividly, the theme of the turbulent, dramatic landscape was developed in the works by Aivazovsky who quite realistically showed the sea element in various stages of its manifestation - from complete calm to the strongest storm. Being in Italy, Russian artists could not disregard such an extraordinary event as the violent eruption of the volcano Vesuvius, which occurred in 1822; many have captured it in their landscape images.

Thanks to the rapid development of scientific knowledge and discoveries in the field of geosciences, including meteorology, artists were encouraged to observe various atmospheric phenomena and weather conditions. Gradually, the sky ceased to be depicted simply as a smooth blue background, as was customary in the tradition of classicism; carefully traced clouds of various types, shapes and shades began to appear in pictures. In addition, various evaporations, fogs, haze, etc. became objects of the landscape image. Romantic artists were little interested in depicting winter and snow, despite the fact that the cold season with a steady snow cover continues in Russia for almost half a year from November to early April. The painting “Russian Winter” (1827) by Nikifore Krylov became perhaps the first winter landscape image in Russian painting. Krylov depicted a somewhat naive, but quite real, winter landscape on the bank of the Tosna River in the vicinity of St. Petersburg, which he painted from life. He was able to reliably convey the atmosphere of the Russian winter: a valley covered with snow, a frozen river, a dark strip of forest in the distance and the peasants with their daily affairs on the road down to the river in the foreground. The first bright and joyful snow-covered landscape image was created, apparently, by Alexey Savrasov in his famous painting “The Rooks Have Come Back” (1871). The spring snow melting and sparkling in the sun became later the favorite motif of the Russian painting. Comparative analysis of landscape pictures can be an important tool, in addition to scientific methods, in studying the nature and dynamics of various hazardous natural processes and phenomena, including hydrological and meteorological ones in conditions of changing climate.

Keywords: hazardous natural phenomena , weather conditions , landscape painting, landscape images

©2019. Japan Geoscience Union. All Right Reserved.

Trends of evaluation items to landscape appreciation until 2017 in the English journals

*yoji aoki[1], keisuke mukagai[2], Anastasia Petrova[3]

1. Open University of Japan, 2. Nagano University, 3. Institute of Oriental Studies, Russian Academy of Sciences

Introduction
We have considered trends of landscape appreciation since JpGU2013-2018. According to the definition of landscape phenomena proposed by Prof. O. Shinohara (Fig. 1), we reported the trends of studies in each part of the phenomena.

Aoki, Y. (1999) described the first landscape evaluation using psychometrical methods to be pioneered by Peterson, G.L. (1967). Before this development, they tried to find the landscape appreciation using various descriptors. They were mostly belonging to the literature or the paintings. As for the literature, the first description of mountain was found in Francesco Petrarca in 1336 of France (Kondo, T. 2002). But his description has no reliable evidence to ensure the landscape. In the field of art, Albrecht Altdorfer drew the first natural landscape in the beginning of 15th century of Germany (Cavaliere, B. 1989). But we could not measure the physical data from his picture. The literature and the art found the beauty of natural landscape by these examples. They recorded the aesthetic beauty in landscape (Thiel, P. 1968).

Jay Appleton (1980) explained the scientific reason of the landscape phenomena with physical data, e.g. geomorphysical data and meteorological data. He explained the landscape phenomena of two pictures, Constable's Weymouth Bay and Constable's sunset study of Hampstead Heath. His approach must be the scientific based explanation to find psychological phenomena of landscape using the geology and meteorology. But the psychological phenomena could deviate by the person observed and the results must be happened statistically. So the process of the landscape phenomena should be explained by stochastic process of psychology. Then scientists developed psychological approach to it.

Here, we summarize the appreciation item (the third component of the landscape phenomena).

1. The developments to establish the psychological scale of appraisal

In the trial of psychometrical method, Ekman & Kuennapas (1962) tested the difference of Nominal scale and Interval scale, and the development of SD method promoted to use many adjectives in the visual complexities (Berlyne & Peckham 1966). Hart & Graham (1967) considered “How to rate & rank landscape”.

In the development of the psychological scale, Heise (1969) tested the scale -3 to 3, and Zube, Anderson & Pitt (1973) used the numerical scale 3 to 14.

2. The psychological evaluation item of preference

Kaplan, Kaplan, & Wendt (1972) proposed to use preference for the landscape appreciation. Compared to the results obtained by SD method, “preference” is easy to understand among different cultural back ground and was popularized in many countries.

©2019. Japan Geoscience Union. All Right Reserved.

3. The developments and the use of SD method

As for the SD method proposed by Osgood & Suci (1955), it employed many pairs of adjectives to evaluate landscape and provided detailed impressions of landscape. The largest number of 240 adjectives was tested by Craik (1975). The results were too complicated and scientists would like to summarize the results. SBE (Terry & Boster 1976), AVQ (Arriaza etc. 2004) and others were statistical aggregation examples of this trial and the example of meaningful aggregation was “Coherence, Complexity, Legibility and Mystery” proposed by Kaplan (1987). These indicators were tested with the relation to the preference and other appreciations by many scientists (Stamps III 2004, and so on.).

4. Method of monetary term evaluation

Monetary term is another evaluation of landscapes and sometimes used in the physical planning (Fukahori & Kubota 2003).

5. Items based on the human behavior of landscape evaluation

The origin of the landscape appreciation was explained from the animal behavior of predation (Appleton 1975). This theory had discussed for a long time. And this behavior might propose a base appreciation of landscape (Aoki & Kitamura 2001). Consideration on the human activities, the reason of visit (Andereck et al. 1989) and the visitability (Abdulkarim & Nasar 2014) were examined and the photographing (Oku & Fukamachi 2006, Sugimoto 2013) were reported.

6. Other appraisals

There are many appreciation descriptors and even now the scientists are finding new descriptors (Collier & Scott 2008). Until now, we could find examples of this trial in absorption (Berlyne 1958), quietness (Womble & Studebaker 1981), beauty (Hull IV, Buhyoff & Daniel 1984), size (Coeterier 1994), fear and stress (Nasar & Jones 1997), positive and negative (Ryan 1998), aggression and violence (Kuo 2001), satisfaction (Kaplan & Austin 2004), overcrowding (Manning & Freimund 2004), openness (Dramstad et al. 2006), ugly (Ruell, Halleux & Teller 2013), and other descriptions.

Keywords: landscape appreciation, appreciation items, until 2017

©2019. Japan Geoscience Union. All Right Reserved.

Table Historical review of landscape appreciation items

Interesting subject	Name of authors	Year
Development of the SD method	Osgood, C.E. and Suci, G.J.	1955
absorption	Berlyne, D.E.,	1958
descriptive appreciation as aesthetic beauty	Thiel, P.,	1961
difference of Nominal scale and Interval scale	Ekman, G. and Kuennapas, T.	1962
SD method	Wright, B. and Rainwater, L.	1962
description	Halprin, L.,	1965
absorption	Berlyne, D.E. and Peckham, S.	1966
description	Noe, S. and Abernathy, B.L.	1966
landscape type	Hart W. J. and William W. Graham,	1967
absorption	Wohlwill, J.F.	1968
numerical scale from -3 to +3	Heise, D.R.,	1969
aesthetic and emotional	Shafer, E.L. and Mietz, J.	1969
objectivity	Craik, K.H.	1972
preference	Kaplan, S., Kaplan, R. and Wendt, J.S.	1972
scaling	Acking, C.A and Sorte, G.J.	1973
numerical scale from 3 to 14	Zube, E.H., Anderson, T. and Pitt, D.	1973
prospect-refuge theory	Appleton, J.	1975
SD method with 240 pairs of adjectives	Craik, K.H.	1975
SBE method; normalization of the results	Daniel, T.C. and Boster, R.S.	1976
monetary	McConnell, K.E.,	1977
SD method	Pedersen, D.M.	1978
SD method	Shuttleworth, S.	1980
preference	Nasar, J.L.,	1981
meaning	Russell, J.A. and Ward, L.M.	1981
quiet	Womble, P. and Studebaker, S.	1981
quiet	Hammitt, W.E.,	1982
preference	Mudrak, L.Y.,	1983
preference	Nasar, J.L.,	1983
SD method	Ruiz, J.P. and Gonzalez-Bernaldez, F.	1983
scenic beauty	Hull IV, R.B., Buhyoff, G.J. and Daniel, T.C.	1984
needs and fears	Talbot, J.F. and Kaplan, R.	1984
preference	Herzog, T.R.	1985
SD method	Abello, R.P., Bernaldez, F.G. and Galiano, E.F.	1986
preference	Talbot, J.F. and Kaplan, R.	1986
survey paper: Coherence, Complexity, Legibility, Mystery	Kaplan, S.	1987
SD method	Kobayashi, M., Higashiyama, J. and Kawasaki, K.	1987
preference	Talbot, J.F., Bardwell, L.V. and Kaplan, R.	1987
monetary	Anderson, L.M. and Cordell, H.K.	1988
preference	Herzog, T. and Smith, G.A.	1988
motivation to visit	Andereck, K. et al.	1989
evaluation by monetary term	Daniel, T.C., et al.	1989
SD method	Kaplan, R., Kaplan, S. and Brown, T.	1989
SD method	Ruiz, M. and Ruiz, J.P.	1989
preference	Gimblett, H.R.	1990
monetary	Green, C.H., et al.	1990
motivation to visit	Uysal, M., McDonald, C.D. and Reid, L.J.	1990
quiet	Ulrich, R.S. et al.	1991
preference	Chokor, B.A	1992
preference	Herzog, T.	1992
refuge provides shelter	Hudson, B.J.	1992
effect to land price	Orland, B., Vinning, J. and Ebreo, A.	1992
familiarity	Purcell, A.T.	1992
description: literature works	Ikeda, T. and Konno, A.	1993
size of space	Coeterier, J.F.,	1994
identity	Hull IV, R.B., Lam, M. and Vigo, G.	1994
preference	Stamps III, A.E.	1994
preference	Strumse, E.	1994
preference	Sullivan III, W.C.,	1994
prospect-refuge theory reviewed	Appleton, J.,	1995
motivation to visit	Cha, S., McCleary, K.W. and Uysal, M.	1995
preference	Mealey, L.	1995
preference on tree form	Sommer, R. and Summit, J.	1995
preference	Herzog, T.R. and Gale, T.A.	1996
scenic preference in Finland	Karjalainen, E.	1996
scaling	Tahvanainen, L., Tyrvainen, L. and Nousiainen, I.	1996
Notation for a Participatory Envirotecture	Thiel, P.,	1996
fear and stress	Nasar, J.L. and Jones, K.M.	1997
landscape preferences of USA, Ireland, Senegal	Newell, P.B.	1997
quiet	Caffyn, A. and Prosser, B.	1998
preference	Herzog, T.R.,	1998
consistency of evaluation by rank order and graphical scale	Karjalainen, E. and Komulainen, M.	1998
preference	Kuo, F.E., Bacaicoa, M. and Sullivan, W.C.	1998
preference and naturalness using Scrub-forest, wide-close view, nature-altered	Purcell, A.T. and Lamb, R.J.	1998
positive and negative scenery of river frontland	Ryan, R.L.	1998
monetary	Tyrvainen, L. and Vaananen, H.	1998
preference	Brown, T.J., Kaplan R. and Quaderer, G.	1999
tranquility and preference	Herzog, T.R. and Barnes, G.J.	1999
preference	Summit, J. and Sommer, R.	1999
landscape preference in Australia	Herzog, T.R. et al	2000
landscape preference in Israel	Misgav, A.	2000
Phylogenic and Ontogenic evolution of landscape appreciation	Aoki, Y. and Kitamura, S.	2001
correlation between preference and likeliness	Hagerhall, C.M.	2001
motivation of ecological behavior	Hartig, T.	2001
aggression and violence	Kuo, F.E.,	2001
preference and danger	Herzog, T.R. and Kutzli, G.E.	2002
landscape preference in Norway	Kaltenborn, B.P. and Bjerke, T.	2002
positive and negative scenery of rural living	Ryan, R.L.,	2002
comparison of VOC and SBE	Franco, D. et al.	2003
cost and amenity level of road scenery	Fukahori, K. and Kubota, Y.	2003
preference	Herzog, T.R. and Leverich, O.L.	2003
AVQ index for visual quality	Arriaza, M. et al.	2004
preference	Herzog, T.R. and Kropscott, L.S.	2004
satisfaction of nature	Kaplan, R. and Austin, M.E.	2004
over crowding by photo montage method	Manning, R.E. and Freimund, W.A	2004
SBE difference 1976-1996	Palmer, J.F.	2004
preference did not correlate to mystery, complexity, legibility, coherence	Stamps, III, A.E.	2004
preference and danger by visibility	Herzog, T.R., & Kirk, K.M.	2005
preference by pair comparison	Rodiek, S.D. and Fried, J.T.	2005
proper openness, student and locals	Dramstad, W.E., et al.	2006
essential features for scenic beauty	Ergin, A., Williams, A.T. and Micallef, A.	2006
landscape preferred in Turkey	Kaplan, A., Taskin, T. and Onenc, A.,	2006
photographing by activity	Oku, H., & Fukamachi, K.	2006
disturbance, naturalness, visual scale, place identity in the photographs	Tveit, M., Ode, A. and Fry, G.	2006
mystery did not affect preference	Herzog, T.R. and Bryce, A.G.,	2007
words interested in the interview	Collier, M.J. and Scott, M.J.	2008
preference of transportation system; vegetation, distance, side fascia affected	Bernasconi, C. et al.	2009
beautiful high mountain, Sherpa appreciate flora, ugly garbage site no vegetation at Everest	Beza, B.B.	2010
species-rich of middle ground affect like of alpine landscape	Lindemann-Matthies, P. et al.	2010
naturalness, unity affect preference of Spruce forest landscape in Turkey	Eroglu, E. and Acar, C.	2011
surprise and Mystery affect preference, Turkey find Mystery at curved street	Nasar, J.L. and Cubukcu, E.	2011
ugly impression of brown fields and montage support improvement in Belgium	Ruelle, C., Halleux, J.-M. & Teller, J.	2013
Visitability	Abdulkarim, D. and Nasar, J. L.	2014
oppressiveness	Asgarzadeh, M. et al.	2014
threat	Chiang, Y-C., Nasal, J. and Ko, C-C.	2014
variance affected by evaluation value	Kalivoda, O. et al.	2014
forest and park affected stress relief	Tyrvainen, L., Ojala, A., Korpela, K. Lanki, T., Tsunetsugu, Y., Kagawa, T.	2014
proper understorey affect preference	van der Wal, R., Miller, D., Irvine, J., Fiorini, S., Amar, A., Yearley, S. Gill, R. & Dandy, N.	2014
openness	Weitkamp, G., Lammeren, R. and Bregt, A.	2014
risk of bushfire	Gill, N. et al.	2015
water use affect landscaping preference	Hayden, L., et al	2015
panorama tree cover density affect to preference	Jiang, B., et al.	2015
green roof affect restorativeness	Lee, K.E., Williams,K.J.H., Sargent, L.D., Williams, N.S.G., Johnson, K.A	2015
aesthetic, morphological condition and ecological integrity	McCormick, A, Fisher, K. and Brierley, G.	2015
water, reed, litter, dead wood affected preference	Eder, R., & Arnberger, A.	2016
tree coverage affect stress recovery	Jiang, B., Li, D., Larsen, L. & Sullivan, W.C.	2016
visual realism and sound affect preference	Lindquist, M., Lange, E. & Kang J.	2016
change of motivation	Shalev, I.	2016
cultural values in visual object	Sowinska-Swierkosz, B.N., Chmielewski, T.J.	2016
visual green reduces noise annoyance	Van Renterghem, T. & Botteldooren, D.	2016
public litter and fishing litter affect preference	Wyles, K.J., Pahl, S. Thomas, K. & Thompson, R.	2016
disorder affect fear of crime	Biasi, Alaina De	2017
nature contact reduce depression, anxiety, stress in outside experience	Brooks, A.M. et al.	2017
biodiversity affected preference	Cracknell, D. et. al.	2017
dead wood affected preference	Gundersen, V., Stange, E.E., Kaltenborn, B.P. Vistad	2017
EAB infestation affect crime, theft, breaking entering, property crime	Kondo, M.C., Han, S., Donovan, G.H., MacDonald, J.M.	2017
preference increase 4bit designed complexinformation entropy values	Kuper, R.	2017
wind generator affect to EEG (electroencephalographic)	Murcia, G. et al.	2017
natural scenery affect change of heart rate by CT scan	Zijlstra, E. et. Al.	2017
attributes affected to landscape aesthetic value of CVM	Dupras, J. et al.	2018
point elements affect preference	Haefner, K. et al.	2018
dense vegetation preferred in city	Harris, V. et al.	2018
motivation of park visit	Hecke, Linde, et al.	2018
firing affect emotional wellbeing	Knez, I. et al.	2018
mature oak with anemone preferred	Nielsen, A.B., Gundersen, V.S. & Jensen, F.S.	2018
traditional landscape preferred by residents in central Alps	Pecher, C., et al.	2018
photo points located by GIS	Sugimoto, K.	2018
setting and arrangement affect restrativeness	Tabrizian, P., et al.	2018
forest preference of 4 seasons	Bravo-Vargas, V. et al.	2019

behavioral consideration
developments in scaling
monetary approaches
use of preference
developments in SD method
other appreciation

©2019. Japan Geoscience Union. All Right Reserved.

[E] Poster | S (Solid Earth Sciences)：S-IT Science of the Earth's Interior & Techtonophysics

Wed. May 29, 2019 10:45 AM - 12:15 PM JST | Wed. May 29, 2019 1:45 AM - 3:15 AM UTC | Poster Hall International Exhibition Hall8, Makuhari Messe_8

[S-IT26] New perspectives on the geodynamics of East Asia

convener:Timothy B Byrne(University of Connecticut), Asuka Yamaguchi(Atomosphere and Ocean Research Institute, The University of Tokyo), Jonny Wu(University of Houston), Kyoko Okino(Atmosphere and Ocean Research Institute, The University of Tokyo)

The Pacific, Indo-Australia and Eurasian plates converge around the Philippine Sea plates in south and East Asia, resulting in one of the most tectonically active regions on earth. The area is also geologically and tectonically complex with numerous active tectonic environments, ranging from subduction to collision, and a long history of plate boundary interactions. The last decade has yielded a wide range of new observations, including detailed geologic data and high resolution crustal to mantle imaging. Here we seek oral and poster presentations that bear on the geologic history and geophysical character of modern and ancient plates in East Asia and their interactions since the Mesozoic. We also invite geodynamic models that integrate these diverse datasets into a more holistic view of this dynamic environment.

[SIT26-P01] Geochemical characteristics of effusive rocks (greenstones) in the Hidaka Belt, Hokkaido, Japan

*Toru Yamasaki[1], Futoshi Nanayama[1] (1.Geol. Survey of Japan (AIST))

[SIT26-P02] Large gas reservoir in continental back-arc basin, revealed by automatic seismic velocity analysis in the Okinawa Trough

*Kota Mukumoto[1], Takeshi Tsuji[1], Andri Hendriyana[1] (1.Kyushu University)

[SIT26-P03] Characterize coseismic deformation of Mw 7.5 Palu earthquake in a triple junction in Sulawesi, Indonesia

*MIN-CHIEN TSAI[1], Ying-Hui Yang[2], Chun-Ying Chiu[3], Jyr-Ching Hu[3] (1.Seismological center, Central Weather Bureau, Taipei, Taiwan, R.O.C., 2.School of Civil Engineering and Architecture, Southwest Petroleum University, Chengdu, China, 3.Department of Geosciences, National Taiwan University, Taipei, Taiwan, R.O.C.)

Geochemical characteristics of effusive rocks (greenstones) in the Hidaka Belt, Hokkaido, Japan

*Toru Yamasaki[1], Futoshi Nanayama[1]

1. Geol. Survey of Japan (AIST)

Igneous rocks in a subduction complex typically occur as greenstones, and petrological and geochemical investigations of such greenstones can provide important insights into the oceanic magmatism, origin of the accretionary complex, and growth of the continental margin. The Hidaka Belt in Central Hokkaido, Japan consists of an early Paleogene subduction complex, referred to as the Hidaka Supergroup (HSG), dominated by clastic rocks. Locally, the terrigenous sediments of the HSG were intruded by the contemporary, normal-type mid-ocean ridge basalts (“*in situ*N-MORBs”) that were formed at an oceanic ridge near the Eurasian continent (Miyashita and Katsushima, 1986: GSJ). The southern area of the HSG has been referred to as the Nakanogawa Group (NKG), which gradually leads to the high-temperature Hidaka metamorphic belt (HMB) in the western part. The lower sequence of the HMB consists mainly of high-grade metabasites, which are assumed to be equivalent to the N-MORBs in the HSG, based on their geochemical features. Recently, Yamasaki and Nanayama (2018a: Lithos) reported about the unique Daimaruyama greenstones from the NKG, formed by an immature intra-oceanic arc-type volcanism. In addition, highly-alkaline basalts, presumably formed at the seamount, exist as exotic blocks in the NKG and are named as Tachiiwa blocks (Owada et al., 1992: JMPEG). In fact, the N-MORBs in the HSG and the Tachiiwa alkaline rocks are characterized by the whole-rock major and minor element geochemistry, but the trace element geochemistry, including the rare earth elements (REEs), has not been reported yet for these rocks. Therefore, we collected 18 samples of greenstones from the entire Hidaka Belt and examined their whole-rock major and trace element geochemistry.

Including those in our previous reports (Yamasaki and Nanayama, 2018a, b: JpGU Abs.), there are three distinct types of greenstones in the Hidaka Belt. The first type are the MORB-type greenstones which show relatively flat chondrite-normalized (CN) REE patterns and N-MORB-normalized (NMN) multi-element patterns with Ti/V = 26–53 and Zr/Nb = 21–117. Although Miyashita and Kiminami (1999: MemGSJ) showed the flat NMN minor element (Nb, P, Zr, Ti, and Y) patterns of basalts from the northern HSG, trace element patterns of the MORB-type rocks in this study show rather light REE (LREE)-rich NMN multi-element patterns. The second type are the ocean island basalt (OIB)-type greenstones. The NMN multi-element and CN REE patterns for this type of greenstones show a gentle slope up to the left, with Ti/V>62 and Zr/Nb<15. The third type are the Daimaruyama greenstones. This type of greenstones show similar NMN multi-element patterns and CN REE patterns to those in the OIB-type, but with a clear relative depletion of Nb, Ta, and Ti. In addition, their Ti-V relations are similar to those in the MORB-type greenstones.

MORB-type greenstones are distributed from the northernmost part of the HSG to the southern Rakko River area in the NKG. OIB-type greenstones occur in the Tachiiwa block and the Rakko River area. Daimaruyama greenstones occur only in the Daimaruyama megablock in the NKG. Since the Tachiiwa and Daimaruyama blocks are presumably derived from the neighboring Tokoro Belt, the absence of the OIB-type and Daimaruyama greenstones in the northern HSG implies a difference in provenance between the HSG and NKG. The MORB-type greenstones do not show the typical N-MORB-type (LREE-depleted) trace element patterns, whereas the metabasite in the HMB shows the typical N-MORB-type geochemical features. In addition, the distribution of the MORB-type greenstones is separated from the metabasites of

©2019. Japan Geoscience Union. All Right Reserved.

the HMB in the southern Hidaka Belt. These lines of evidence suggest that the protolith of the HMB is not an equivalent of the “*in-situ*MORB” in the HSG, and is probably an accreted fragment of the older oceanic plate.

Keywords: Hidaka Belt, greenstones, trace elements

©2019. Japan Geoscience Union. All Right Reserved.

Large gas reservoir in continental back-arc basin, revealed by automatic seismic velocity analysis in the Okinawa Trough

*Kota Mukumoto[1], Takeshi Tsuji[1], Andri Hendriyana[1]

1. Kyushu University

P-wave velocity acquired from seismic reflection data allows us to quantify submarine geological structures. In the Iheya North Knoll of the Okinawa Trough, intense hydrothermal activity occurs due to continental rifting. The hydrothermal system in the Iheya North Knoll has been explored by geophysical surveys, geochemical measurements and drilling campaign. Based on these surveys, gas reservoir could be considered to exist around the Iheya North Knoll. However, gas reservoir around the Iheya North Knoll has not been identified in previous studies. Here we show P-wave velocity structure derived from automatic velocity analysis of multi-channel seismic reflection data. P-wave velocity is sensitive to free gas in sediments. Therefore, P-wave velocity is key information to quantify gas distribution in sediments. Automatic velocity analysis estimated P-wave velocity structure with remarkable high spatial and temporal resolution. The P-wave velocity structure revealed gas reservoirs around the Iheya North Knoll. Although many gas components can be generated by magmatic activity, hydrothermal alteration of organic-rich sediments and biogenic processes, CH_4 and CO_2 could be major gas components which is derived by hydrothermal system in marine sediment. Therefore, main gas components could be CH_4 or CO_2. The strong amplitude reflector above the gas reservoir could be the interface between CH_4 hydrate and gas, because the depth of strong amplitude reflector is well consistent with pressure-temperature conditions of the phase transition. If the main gas component is CH_4, the gas reservoir could be important as resource. Whereas, if the gas reservoir includes CO_2, the gas distribution could be important to consider carbon flux between earth and ocean. Furthermore, widely distributed gas reservoir may influence on the chemical components of hydrothermal fluids in the Iheya North Knoll.

Keywords: Seismic reflection data, Okinawa Trough, Gas reservoir

©2019. Japan Geoscience Union. All Right Reserved.

Characterize coseismic deformation of Mw 7.5 Palu earthquake in a triple junction in Sulawesi, Indonesia

*MIN-CHIEN TSAI[1], Ying-Hui Yang[2], Chun-Ying Chiu[3], Jyr-Ching Hu[3]

1. Seismological center, Central Weather Bureau, Taipei, Taiwan, R.O.C., 2. School of Civil Engineering and Architecture, Southwest Petroleum University, Chengdu, China, 3. Department of Geosciences, National Taiwan University, Taipei, Taiwan, R.O.C.

We first use SAR satellite data to map the coseismic deformation for the 2018 Mw=7.5 strike-slip earthquake of 28 September 2018 in Palu, Sulawesi, Indonesia. The seismogenic fault is a left-lateral a strike-slip event along the Palu-Koro fault at shallow depth that occurred within the interior of the Molucca Sea microplate, which is part of the Sunda plate. We use D-InSAR technique with ALOS-2 descending orbit radar images to characterize coseismic and deformation pattern induced by Palu earthquake.We also plan to use with sub-pixel correlation form Sentinel-2 and Planet imagery to map the surface rupture area and the coseismic offsets in order to provide the near-field deformation data located in decorrelation zone from the D-InSAR result. Thus we can inverse the distribution of slip on the fault patches. In addition, we also calculate the Coulomb stress transfer for assessing the stress increasing and shadow on the major fault systems, such as the active Poso Fault Zone and Mamuju –Lariang Active Fault Zone. In particular, we will assess the seismic potential by Coulomb stress transfer in Minahasa Active Subduction Zone together with two events with Mw 7.9 and Mw 7.0 happened on 1996/01/01 and 1996/07/22. We try to assess the seismogenic potential in terms of interseismic slip rate, slip rate deficit and coupling ratio for the Palu-Koro fault system in a triple junction of the Sulawesi island.

Keywords: InSAR , pixel offset , Palu earthquake, Triple junction

©2019. Japan Geoscience Union. All Right Reserved.

[E] Poster | S (Solid Earth Sciences)：S-IT Science of the Earth's Interior & Techtonophysics

Wed. May 29, 2019 5:15 PM - 6:30 PM JST | Wed. May 29, 2019 8:15 AM - 9:30 AM UTC | Poster Hall International Exhibition Hall8, Makuhari Messe_28

[S-IT26] New perspectives on the geodynamics of East Asia

convener:Timothy B Byrne(University of Connecticut), Asuka Yamaguchi(Atomosphere and Ocean Research Institute, The University of Tokyo), Jonny Wu(University of Houston), Kyoko Okino(Atmosphere and Ocean Research Institute, The University of Tokyo)

The Pacific, Indo-Australia and Eurasian plates converge around the Philippine Sea plates in south and East Asia, resulting in one of the most tectonically active regions on earth. The area is also geologically and tectonically complex with numerous active tectonic environments, ranging from subduction to collision, and a long history of plate boundary interactions. The last decade has yielded a wide range of new observations, including detailed geologic data and high resolution crustal to mantle imaging. Here we seek oral and poster presentations that bear on the geologic history and geophysical character of modern and ancient plates in East Asia and their interactions since the Mesozoic. We also invite geodynamic models that integrate these diverse datasets into a more holistic view of this dynamic environment.

[SIT26-P01] Geochemical characteristics of effusive rocks (greenstones) in the Hidaka Belt, Hokkaido, Japan

*Toru Yamasaki[1], Futoshi Nanayama[1] (1.Geol. Survey of Japan (AIST))

[SIT26-P02] Large gas reservoir in continental back-arc basin, revealed by automatic seismic velocity analysis in the Okinawa Trough

*Kota Mukumoto[1], Takeshi Tsuji[1], Andri Hendriyana[1] (1.Kyushu University)

[SIT26-P03] Characterize coseismic deformation of Mw 7.5 Palu earthquake in a triple junction in Sulawesi, Indonesia

*MIN-CHIEN TSAI[1], Ying-Hui Yang[2], Chun-Ying Chiu[3], Jyr-Ching Hu[3] (1.Seismological center, Central Weather Bureau, Taipei, Taiwan, R.O.C., 2.School of Civil Engineering and Architecture, Southwest Petroleum University, Chengdu, China, 3.Department of Geosciences, National Taiwan University, Taipei, Taiwan, R.O.C.)

Geochemical characteristics of effusive rocks (greenstones) in the Hidaka Belt, Hokkaido, Japan

*Toru Yamasaki[1], Futoshi Nanayama[1]

1. Geol. Survey of Japan (AIST)

Igneous rocks in a subduction complex typically occur as greenstones, and petrological and geochemical investigations of such greenstones can provide important insights into the oceanic magmatism, origin of the accretionary complex, and growth of the continental margin. The Hidaka Belt in Central Hokkaido, Japan consists of an early Paleogene subduction complex, referred to as the Hidaka Supergroup (HSG), dominated by clastic rocks. Locally, the terrigenous sediments of the HSG were intruded by the contemporary, normal-type mid-ocean ridge basalts (“*in situ*N-MORBs”) that were formed at an oceanic ridge near the Eurasian continent (Miyashita and Katsushima, 1986: GSJ). The southern area of the HSG has been referred to as the Nakanogawa Group (NKG), which gradually leads to the high-temperature Hidaka metamorphic belt (HMB) in the western part. The lower sequence of the HMB consists mainly of high-grade metabasites, which are assumed to be equivalent to the N-MORBs in the HSG, based on their geochemical features. Recently, Yamasaki and Nanayama (2018a: Lithos) reported about the unique Daimaruyama greenstones from the NKG, formed by an immature intra-oceanic arc-type volcanism. In addition, highly-alkaline basalts, presumably formed at the seamount, exist as exotic blocks in the NKG and are named as Tachiiwa blocks (Owada et al., 1992: JMPEG). In fact, the N-MORBs in the HSG and the Tachiiwa alkaline rocks are characterized by the whole-rock major and minor element geochemistry, but the trace element geochemistry, including the rare earth elements (REEs), has not been reported yet for these rocks. Therefore, we collected 18 samples of greenstones from the entire Hidaka Belt and examined their whole-rock major and trace element geochemistry.

Including those in our previous reports (Yamasaki and Nanayama, 2018a, b: JpGU Abs.), there are three distinct types of greenstones in the Hidaka Belt. The first type are the MORB-type greenstones which show relatively flat chondrite-normalized (CN) REE patterns and N-MORB-normalized (NMN) multi-element patterns with Ti/V = 26–53 and Zr/Nb = 21–117. Although Miyashita and Kiminami (1999: MemGSJ) showed the flat NMN minor element (Nb, P, Zr, Ti, and Y) patterns of basalts from the northern HSG, trace element patterns of the MORB-type rocks in this study show rather light REE (LREE)-rich NMN multi-element patterns. The second type are the ocean island basalt (OIB)-type greenstones. The NMN multi-element and CN REE patterns for this type of greenstones show a gentle slope up to the left, with Ti/V>62 and Zr/Nb<15. The third type are the Daimaruyama greenstones. This type of greenstones show similar NMN multi-element patterns and CN REE patterns to those in the OIB-type, but with a clear relative depletion of Nb, Ta, and Ti. In addition, their Ti-V relations are similar to those in the MORB-type greenstones.

MORB-type greenstones are distributed from the northernmost part of the HSG to the southern Rakko River area in the NKG. OIB-type greenstones occur in the Tachiiwa block and the Rakko River area. Daimaruyama greenstones occur only in the Daimaruyama megablock in the NKG. Since the Tachiiwa and Daimaruyama blocks are presumably derived from the neighboring Tokoro Belt, the absence of the OIB-type and Daimaruyama greenstones in the northern HSG implies a difference in provenance between the HSG and NKG. The MORB-type greenstones do not show the typical N-MORB-type (LREE-depleted) trace element patterns, whereas the metabasite in the HMB shows the typical N-MORB-type geochemical features. In addition, the distribution of the MORB-type greenstones is separated from the metabasites of

©2019. Japan Geoscience Union. All Right Reserved.

the HMB in the southern Hidaka Belt. These lines of evidence suggest that the protolith of the HMB is not an equivalent of the “*in-situ*MORB” in the HSG, and is probably an accreted fragment of the older oceanic plate.

Keywords: Hidaka Belt, greenstones, trace elements

©2019. Japan Geoscience Union. All Right Reserved.

Large gas reservoir in continental back-arc basin, revealed by automatic seismic velocity analysis in the Okinawa Trough

*Kota Mukumoto[1], Takeshi Tsuji[1], Andri Hendriyana[1]

1. Kyushu University

P-wave velocity acquired from seismic reflection data allows us to quantify submarine geological structures. In the Iheya North Knoll of the Okinawa Trough, intense hydrothermal activity occurs due to continental rifting. The hydrothermal system in the Iheya North Knoll has been explored by geophysical surveys, geochemical measurements and drilling campaign. Based on these surveys, gas reservoir could be considered to exist around the Iheya North Knoll. However, gas reservoir around the Iheya North Knoll has not been identified in previous studies. Here we show P-wave velocity structure derived from automatic velocity analysis of multi-channel seismic reflection data. P-wave velocity is sensitive to free gas in sediments. Therefore, P-wave velocity is key information to quantify gas distribution in sediments. Automatic velocity analysis estimated P-wave velocity structure with remarkable high spatial and temporal resolution. The P-wave velocity structure revealed gas reservoirs around the Iheya North Knoll. Although many gas components can be generated by magmatic activity, hydrothermal alteration of organic-rich sediments and biogenic processes, CH_4 and CO_2 could be major gas components which is derived by hydrothermal system in marine sediment. Therefore, main gas components could be CH_4 or CO_2. The strong amplitude reflector above the gas reservoir could be the interface between CH_4 hydrate and gas, because the depth of strong amplitude reflector is well consistent with pressure-temperature conditions of the phase transition. If the main gas component is CH_4, the gas reservoir could be important as resource. Whereas, if the gas reservoir includes CO_2, the gas distribution could be important to consider carbon flux between earth and ocean. Furthermore, widely distributed gas reservoir may influence on the chemical components of hydrothermal fluids in the Iheya North Knoll.

Keywords: Seismic reflection data, Okinawa Trough, Gas reservoir

©2019. Japan Geoscience Union. All Right Reserved.

Characterize coseismic deformation of Mw 7.5 Palu earthquake in a triple junction in Sulawesi, Indonesia

*MIN-CHIEN TSAI[1], Ying-Hui Yang[2], Chun-Ying Chiu[3], Jyr-Ching Hu[3]

1. Seismological center, Central Weather Bureau, Taipei, Taiwan, R.O.C., 2. School of Civil Engineering and Architecture, Southwest Petroleum University, Chengdu, China, 3. Department of Geosciences, National Taiwan University, Taipei, Taiwan, R.O.C.

We first use SAR satellite data to map the coseismic deformation for the 2018 Mw=7.5 strike-slip earthquake of 28 September 2018 in Palu, Sulawesi, Indonesia. The seismogenic fault is a left-lateral a strike-slip event along the Palu-Koro fault at shallow depth that occurred within the interior of the Molucca Sea microplate, which is part of the Sunda plate. We use D-InSAR technique with ALOS-2 descending orbit radar images to characterize coseismic and deformation pattern induced by Palu earthquake.We also plan to use with sub-pixel correlation form Sentinel-2 and Planet imagery to map the surface rupture area and the coseismic offsets in order to provide the near-field deformation data located in decorrelation zone from the D-InSAR result. Thus we can inverse the distribution of slip on the fault patches. In addition, we also calculate the Coulomb stress transfer for assessing the stress increasing and shadow on the major fault systems, such as the active Poso Fault Zone and Mamuju –Lariang Active Fault Zone. In particular, we will assess the seismic potential by Coulomb stress transfer in Minahasa Active Subduction Zone together with two events with Mw 7.9 and Mw 7.0 happened on 1996/01/01 and 1996/07/22. We try to assess the seismogenic potential in terms of interseismic slip rate, slip rate deficit and coupling ratio for the Palu-Koro fault system in a triple junction of the Sulawesi island.

Keywords: InSAR , pixel offset , Palu earthquake, Triple junction

©2019. Japan Geoscience Union. All Right Reserved.

[E] Poster | S (Solid Earth Sciences)：S-GC Geochemistry

Wed. May 29, 2019 10:45 AM - 12:15 PM JST | Wed. May 29, 2019 1:45 AM - 3:15 AM UTC | Poster Hall International Exhibition Hall8, Makuhari Messe_9

[S-GC40] Volatile Cycles in the Deep Earth - from Subduction Zone to Hot Spot

convener:Hirochika Sumino(Department of Basic Science, Graduate School of Arts and Sciences, The University of Tokyo), Takeshi Hanyu(Japan Agency for Marine-Earth Science and Technology, Department of Solid Earth Geochemistry), Yuji Sano(Division of Ocean and Earth Systems, Atmosphere and Ocean Research Institute, University of Tokyo), Gray E Bebout(Lehigh University)

Volatiles play an important role in the geodynamics and chemical differentiation in the mantle and crust by drastically changing mineral stability and rheological behavior. Fractionation-processes such as partial melting, hydration, and dehydration are all controlled by volatiles in the rocks. A significant portion of the volatiles in the Earth has been thought to be present in the atmosphere and oceans as a consequence of extensive degassing during accretion and subsequent mantle degassing. On the other hand, it has been recently recognized that substantial amounts of volatiles are recycled back into the mantle at subduction zones, where intensive devolatilization of descended materials during arc magma generation was once thought to act as an effective "subduction barrier". However, fundamental questions still remain, such as: how are volatiles species distributed throughout the early and present Earth? What are the mechanisms for, and rate at which, volatiles are fluxed between the atmosphere, crust, and mantle? And what role have volatiles played in driving the evolution of the Earth? The possible role of the core in storing primordial volatiles is also poorly constrained. We therefore welcome contributions from experimental, observational, and modeling studies that help shed light on the deep cycles of volatiles, such as hydrogen, carbon, nitrogen, noble gases, halogens and sulfur. We particularly encourage studies linking the behavior of multiple volatile elements and their isotopic compositions. Studies investigating the linkage between volatile and solid geochemical tracers, the phase equilibria of volatile-bearing mantle assemblages, and the effect of volatiles on the physical properties of the mantle are also welcome.

[SGC40-P01] Continental growth models demystified

*Jun Korenaga[1] (1.Department of Geology and Geophysics, Yale University)

[SGC40-P02] Mass-independent sulfur isotope signature from the 2.7 Ga Belingwe komatiite: Recycling of crustal material in Archean

*Yusuke Kubota[1], Yuichiro Ueno[1,2,3], Kenji Shimizu[3], Fumihiro Matsuura[2], Akira Ishikawa[1,3] (1.Department of Earth and Planetary Sciences, Tokyo Institute of Technology, 2.Earth-Life Science Institute, Tokyo Institute of Technology, 3.Japan Agency for Marine-Earth Science and Technology (JAMSTEC))

[SGC40-P03] Determination of halogens in some standard materials using the neutron irradiation noble gas mass spectrometric technique

*Hirochika Sumino[1], Masahiro Kobayashi[2], Takehiko Saito[3], Keisuke Nagao[3] (1.Department of Basic Science, Graduate School of Arts and Sciences, The University of Tokyo, 2.Tokyo Metropolitan Industrial Technology Research Institute, 3.Geochemical Research Center, Graduate School of Science, University of Tokyo)

[SGC40-P04] FTIR spectroscopy and noble gas mass spectrometry for a single olivine grain

*Sota Niki[1], Hirochika Sumino[2], Masahiro Kobayashi[3], Hiroyuki Kagi[1], Takafumi Hirata[1], Chris J. Ballentine[4] (1.Geochemical Research Center, Grad. School of Science, Univ. of Tokyo, 2.Dept. of Basic Science, Grad. School of Arts and Sciences, Univ. of Tokyo, 3.Tokyo Metropolitan Industrial Technology Research Institute, 4.Dept. of Earth Sciences, Univ. of Oxford)

[SGC40-P05] New halogen incorporation mechanism in serpentine group minerals: Crystal chemical consideration

*Masami Kanzaki[1] (1.Institute for Planetary Matereials, Okayama University)

[SGC40-P06] Mineralogical and geochemical characteristics of cuttings from Taketomi hot spring

*Noriyuki Shingaki[1], Tomohiro Toki[1], Syogo Oshima[2], Masaaki chinen[3], Arito Sakaguchi[4], Naoto Takahata[5], Yuji Sano[5], Shirai Kotaro[5], Kentaro Tanaka[5] (1.University of the Ryukyus , 2.West Japan Engineering Consultants, Inc., 3.MicroRange, 4.Faculty of Science, Yamaguchi University, 5.Atmosphere and Ocean Research Institute, The University of Tokyo)

[SGC40-P07] Variation of helium isotope compositions at Lake Mashu

*Takanori Kagoshima[1], Yuji Sano[1], Atsushi Tanaka[2] (1.Atmosphere and Ocean Research Institute, University of Tokyo, 2.National Institute for Environmental Studies)

[SGC40-P08] Helium isotopes in Tachibana Bay and Shimabara Bay, Nagasaki

*Ma. Teresa Escobar[1], Yama Tomonaga[2], Hajime Obata[1], Shigenobu Takeda[3], Naoto Takahata[1], Yuji Sano[1] (1.Atmosphere and Ocean Research Institute, University of Tokyo, Kashiwanoha, Kashiwa, Chiba, Japan, 2.Eawag,, Swiss Federal Institute of Aquatic Science and Technology, Department of Water Resources and Drinking Water, Überlandstrasse 133 CH-8600 ,Dübendorf, Switzerland, 3.Graduate School of Fisheries and Environmental Sciences, Nagasaki University, Nagasaki, Japan)

Continental growth models demystified

*Jun Korenaga[1]

1. Department of Geology and Geophysics, Yale University

So far proposed models of continental growth exhibit bewildering diversity, but this diversity is rather superficial. By understanding how different growth models are built and what they are meant to constrain, we can gain deeper insight into the evolution of continental crust as well as the dynamics of the early Earth. There are three kinds of growth models: crust-based, mantle-based, and others. Crust-based models provide only the lower bound on net crustal growth, and mantle-based models aim at constraining net crustal growth itself. Other models are also about net crustal growth, but they are subject to greater uncertainty. In the presence of crustal recycling, crust-based models are expected to be different from mantle-based models, and more important, the difference between these two kinds of models provides important constraints on the operation of plate tectonics in the early Earth. Some popular misconceptions in the recent literature are also discussed.

Keywords: Continental crust, Plate tectonics, Chemical differentiation

©2019. Japan Geoscience Union. All Right Reserved.

Mass-independent sulfur isotope signature from the 2.7 Ga Belingwe komatiite: Recycling of crustal material in Archean

*Yusuke Kubota[1], Yuichiro Ueno[1,2,3], Kenji Shimizu[3], Fumihiro Matsuura[2], Akira Ishikawa[1,3]

1. Department of Earth and Planetary Sciences, Tokyo Institute of Technology, 2. Earth-Life Science Institute, Tokyo Institute of Technology, 3. Japan Agency for Marine-Earth Science and Technology (JAMSTEC)

Recycling of the Earth's crustal material has long been discussed mainly through the radiogenic isotopes of modern Ocean Island Basalts (OIB). Recent finding of Sulfur Mass Independent Fractionation (S-MIF) from HIMU and EM I basalts supports recycling of crustal material in mantle (Cabral et al., 2013; Delavault et al., 2016). Since photochemical reactions under reducing Archean atmosphere are thought to be a plausible process of large S-MIF generation (Farquhar et al., 2001; Farquhar and Wings, 2003), these discoveries demonstrated that the S-MIF is a useful signature for tracing Archean crustal material. However, it has been difficult to estimate when the subduction started in the history of the Earth. Here, we report multiple sulfur isotope analysis of the 2.7 Ga Belingwe komatiites and related rocks, which has potential to elucidate earlier subduction or recycling of crustal material before 2.7 Ga. The Belingwe komatiite are one of the best-preserved Archean komatiites in the world. The results show clear S-MIF signature in several komatiites and basalts. Sulfide minerals in the S-MIF bearing samples occur as pyrrhotite and chalcopyrite scattered within groundmass around the quenched olivine and pyroxene crystals, indicating that the sulfides crystalized at the time of eruption. The original nature of the sulfide is also supported by the correlation between sulfur contents and magnesium number. Based on Nd, Sr, and Pb isotope composition measured in the previous study (Shimizu et al., 2005), the S-MIF bearing komatiites and basalts are likely to be derived from depleted mantle source, whereas more enriched samples do not show S-MIF. Therefore, the S-MIF component is not likely derived from assimilated crust at the time of the komatiite volcanism, but originally incorporated in the depleted source mantle. Consequently, our results suggest that subduction of S-MIF bearing surface material into the mantle had been operated at least prior to 2.7 Ga.

Keywords: Sulfur mass independent fractionation, Mantle geochemistry, Komatiite, Archean

©2019. Japan Geoscience Union. All Right Reserved.

Determination of halogens in some standard materials using the neutron irradiation noble gas mass spectrometric technique

*Hirochika Sumino[1], Masahiro Kobayashi[2], Takehiko Saito[3], Keisuke Nagao[3]

1. Department of Basic Science, Graduate School of Arts and Sciences, The University of Tokyo, 2. Tokyo Metropolitan Industrial Technology Research Institute, 3. Geochemical Research Center, Graduate School of Science, University of Tokyo

Halogens are among the most powerful tracers of volatile cycling in subduction zones, because of (i) the large contrast in concentrations between the surface and interior of the Earth [1], (ii) their high affinities to gas- and fluid-phases relative to mineral [2], (iii) distinct elemental and/or isotopic compositions in each reservoir in the Earth [3-7]. However, few analytical techniques can determine trace amounts of halogens, particularly bromine and iodine in mantle-derived samples. Consequently, there have been relatively few previous studies of halogens in mantle-derived samples.

The neutron irradiation noble gas mass spectrometric technique (NI-NGMS) is capable of measuring very low concentrations of halogens (<1 ppb) in very small samples (<1 mg). The NI-NGMS is an extension of the Ar-Ar and I-Xe dating methods [8-10]. Halogens (chlorine, bromine, and iodine) and other elements (potassium, calcium, barium, and uranium) are converted to corresponding isotopes of argon, krypton, and xenon by neutron irradiation in a nuclear reactor. The noble gas isotopes in neutron-irradiated samples are analyzed by noble gas mass spectrometry. Irradiation conditions such as neutron fluence are monitored using standard materials of the Ar-Ar and I-Xe dating methods. Relatively high cross-sections of halogens for neutron capture and high sensitivity of noble gas mass spectrometry enable determination of trace amounts of halogens using NI-NGMS.

We report new halogen concentrations determined for scapolite standards and geological reference materials distributed by Geological Survey of Japan and US Geological Survey using NI-NGMS. Consistent results with those regarded as reference values were obtained from scapolite standards, which indicate that the scapolite standards are reliable in halogen analysis. On the other hand, the halogen concentrations obtained from geological reference materials are systematically lower than the reference values for samples with low concentrations of halogens. The higher concentrations reported for the geological reference materials probably result from contamination on the sample surface during preparation of these reference materials. We also propose a fluorine determination method using NI-NGMS based on neon systematics, although reliable determination of fluorine has been thought to be impossible.

[1] Pyle & Mather, *Chem. Geol.* 2009. [2] Bureau *et al.*, *GCA* 2016. [3] Sumino *et al.*, *EPSL* 2010. [4] Chavrit *et al.*, *GCA* 2016. [5] Kobayashi *et al.*, *EPSL* 2017. [6] Kendrick *et al.*, *Nature Geosci.* 2017. [7] Kobayashi *et al.*, *G-cubed* 2019. [8] Turner, *JGR* 1965. [9] Kendrick, *Chem. Geol.* 2012. [10] Ruzié-Hamilton *et al.*, *Chem. Geol.* 2016.

Keywords: Halogen, Noble gas, Nuetron irradiation, Noble gas mass spectrometry

©2019. Japan Geoscience Union. All Right Reserved.

FTIR spectroscopy and noble gas mass spectrometry for a single olivine grain

*Sota Niki[1], Hirochika Sumino[2], Masahiro Kobayashi[3], Hiroyuki Kagi[1], Takafumi Hirata[1], Chris J. Ballentine[4]

1. Geochemical Research Center, Grad. School of Science, Univ. of Tokyo, 2. Dept. of Basic Science, Grad. School of Arts and Sciences, Univ. of Tokyo, 3. Tokyo Metropolitan Industrial Technology Research Institute, 4. Dept. of Earth Sciences, Univ. of Oxford

Volatiles have been degassed from the mantle and recycled back into the mantle at subduction zones. Water is the main component of volatiles and plays a key role in dynamics of the subduction zones because even a small water content in rocks has an influence on the physical and chemical properties of the rocks (e.g. friction coefficient, melting point, etc.) which are closely related to phenomena studied in earth sciences including volcanic or seismic activities. It is still unclear to what extent of water have been subducted into the mantle and released to the Earth’ s surface. To elucidate the volatile recycling, noble gases are powerful tracers because they have unique compositions in geochemical reservoirs. Previous researches have mainly reported results of bulk analysis of mantle peridotites. On the contrary, in this study, FTIR measurements and noble gas analysis of a single olivine grain were conducted to determine the noble gas concentrations in fluid inclusions.

The olivine samples used for this study were separated from mantle xenoliths collected from an intraplate setting (Hualalai in Hawaii) and two subduction zones (the Avacha volcano in the Kamchatka arc and the Pinatubo volcano in the Luzon arc). The Hualalai olivine was expected to show mantle-derived noble gas compositions (Kobayashi et al., G-cubed 2019) and was used for checking the accuracy of noble gas analysis. The Avacha and Pinatubo olivines contained H_2O-rich fluid inclusions and the noble gas concentrations in the inclusions had been estimated from salinities, and halogen and noble gas compositions (Kobayashi et al., EPSL 2017). The Avacha and Pinatubo olivines were used to confirm the accuracy of the analytical method used in this study for determining the noble gas concentrations in the inclusions.

FTIR measurements were conducted to determine the H_2O concentration in the Avacha and Pinatubo olivines. The mantle xenoliths were crushed into 0.5 to 2 mm and olivine grains were separated. The olivine grains were embedded in resin (Ortho Bright) and polished to a thickness of several hundred micrometers. The weight of samples was 0.7 to 16 mg. The H_2O concentration was calculated from the absorbance at 3404 cm^{-1}. After the FTIR measurements, resin was removed from each grain by heating at 50ºC and dissolving in acetone.

Noble gas analysis was conducted using multicollector noble gas mass spectrometers (Helix SFT and Argus, Thermo Fisher Scientific). After the sample loading into a laser heating cell, the cell was baked out with pumping to desorb atmospheric noble gases to achieve low blank levels required for single-grain analysis. Consequently, noble gases were extracted by laser heating (Fusion Diode Stepped Heating System, Teledyne CETAC) at about 1000 ºC for 5 minutes. The gases released from samples were purified by removing active gases using a getter, and then, absorbed on two cryo-traps (one was for helium and neon and the other was for argon, krypton, and xenon). Each noble gas was desorbed from the trap at a certain temperature and introduced into the mass spectrometers. Helium was measured with Helix SFT and other noble gases were measured with Argus. The abundances and isotopic ratios of noble gases in a

©2019. Japan Geoscience Union. All Right Reserved.

single olivine grain were obtained. The accuracy of the isotopic ratios was checked by the Hualalai samples.

The noble gas concentrations in the inclusions obtained will be compared with the previous bulk analysis to discuss the accuracy of the method in this study. This method of determining the noble gas concentrations in fluid inclusions from single-grain analysis has a potential to clarify the heterogeneity of the mantle volatiles in terms of a single-grain mineral and the flux quantification during the volatile recycling.

Keywords: noble gas, FTIR spectroscopy, mantle

©2019. Japan Geoscience Union. All Right Reserved.

New halogen incorporation mechanism in serpentine group minerals: Crystal chemical consideration

*Masami Kanzaki[1]

1. Institute for Planetary Matereials, Okayama University

Introduction: Recent geochemical studies revealed that serpentinites contain a significant amount of halogens. However, how halogen ions are incorporated into serpentinites is not well understood. Commonly assumed mechanism is "OH^- substitution" in serpentine group minerals (chrysotile, lizardite and antigorite). Although this mechanism will be fine for F, but may not be adequate for larger halogens (Cl, Br, I). Here, I propose new halogen incorporation mechanism in lizardite and antigorite from crystal chemical point of view.

Calculation methods: In order to assess present new incorporation model, first-principles calculation was conducted. Quantum-Espresso package was used to optimize the halogen incooporated model structures. In the present study, lizardite and antigorite (*m*=17 polysome) are considered. For our proposed mechanism, charge balance should be observed; so $Mg^{2+} = X^- + Al^{3+}$ substitution (X^- = halogen) is assumed to introduce halogen to a vacant site. For lizardite, enthalpy difference between two models (OH^- substitution and our model) was calculated for following equation: $Mg_2AlSi_2O_8XH_2 + H_2O = Mg_2AlSi_2O_9XH_4$. Former corresponds to the OH substituted model (with Al introduced), and latter corresponds to our new model. Although this comparison is crude (as free H_2O is included in the equation), it could provide systematic trend with kinds of halogen atoms. Since antigorite has a very large unit cell and many vacant sites, only $Mg^{2+} = Cl^- + Al^{3+}$ substitute in five vacant sites are considered so far.

Results and Discussion: From close inspection of crystal structures of lizardite and antigorite, vacant sites ideal for halogens are identified. The vacant sites are surrounded by four protons (of OH^-) forming elongated tetrahedon (i.e., XH_4^{3+}) if halogen is located. Such vacant sites provide local structure similar to halogen ions in aqueous solution.

In order to further assess present incorporation mechanism, first-principles calculations of lizardite and antigorite containing halogens in those sites were conducted. The structural optimizations confirmed that halogens could be well accommodated into the tetrahedral vacant sites in lizardite. The calculated enthalpy difference between OH substitution and present models in lizardite revealed that larger halogens prefer our model over the OH substitution model. There is sinlge vacant site in lizardite, but antigorite (*m*=17) has 17 crystallographically different vacant sites. Most sites have local structures more or less similar to that of lizardite (locating in 6-membered SiO_4 ring). But there is another kind of vacant site which is locating in 8-membered SiO_4 ring. This local structure is surrounded by six protons, but it can be regareded as two tetrahedral proton sites with edge sharing. Substitution of Cl^- to this site (one of tetrahedral sites) showed lower enthalpy compared to those of other lizardite-like sites, and can accept more larger ions. Therefore, Cl^- (and other larger halogens) will prefet this site in antigorite (*m*=17). Not all antogorite polysomes have this site.

Present study suggests that our new proposed incorporation mechanism is promising, and it should be further studied experimentally. Present new incorporation mechanism would be important to understand elemental partition behavior of halogens in subduction zones.

Keywords: halogen site, serpentine, crystal chemistry, incorporation mechanism, elemental partition

©2019. Japan Geoscience Union. All Right Reserved.

Mineralogical and geochemical characteristics of cuttings from Taketomi hot spring

*Noriyuki Shingaki[1], Tomohiro Toki[1], Syogo Oshima[2], Masaaki chinen[3], Arito Sakaguchi[4], Naoto Takahata[5], Yuji Sano[5], Shirai Kotaro[5], Kentaro Tanaka[5]

1. University of the Ryukyus , 2. West Japan Engineering Consultants, Inc., 3. MicroRange, 4. Faculty of Science, Yamaguchi University, 5. Atmosphere and Ocean Research Institute, The University of Tokyo

It is important to grasp carbon cycle on the earth’ s surface for thinking about global environmental change. A hot spring with a maximum temperature of 64℃ is venting with gas containing 70% of methane from several spots on the seafloor at depth of 22 m at 1 km northeast off Taketomi Island. Based on methane and helium isotope ratios in the venting gas, the influence of magmatic gas has been pointed out. In spite of Taketomi Island located on the trench side from island arc, magmatic gas is venting. It suggests the forearc where magma cannot generate, might form new supply path of carbon from the Earth’ s interior. The mass balance from new supply path of carbon may change estimation of carbon cycle on earth’ s surface. Therefore, the purpose of this study is to elucidate venting mechanism and quantitative grasp of magmatic gas from forearc, and the history of hot spring activities will be investigated to predict future activities.

In 2017, the hot spring was drilled up to depth of 940 m in Taketomi Island. The cuttings with muddy water were sampled every 10 m. The thin sections were prepared from cuttings to be observed using polarization microscope, and the chemical compositions of grains were analyzed by SEM-EDX. The ground samples were analyzed for mineral and chemical compositions by XRD and EDX. The clay minerals gathered by levitation were measured for half-value width of illite using XRD. He and CO_2 contained in samples that were crashed in vacuum were measured for isotope ratios by mass spectrometer. Calcite and dolomite collected from the cuttings were measured for the carbon and oxygen isotope ratios by mass spectrometer. The vitrinite in the cuttings was separated by a heavy liquid, and the reflectance was measured by a reflecting microscope.

In the microscopy, the stratum was roughly divided two formations; cryptocrystalline quartz layer and sand stone layer. Carbonaceous materials were observed in most of the stratum. Dolomite was limitedly observed in the vicinity of 800 m. In the XRD analysis, Quartz was detected at all depth. Calcite was detected at shallower depth than 30 m, and dolomite was detected only around 800 m. As a result of the EDX analysis, silicon was the most dominant in all layers, and especially, it was contained around 0-100 m, 300 m and around 900 m over 80%. There was a layer that contained much calcium. Around 0-30 m, 400-500 m and around 800 m, calcite was contained 15 % or more. The half-value width of illite was large, 0.8 $\Delta^\circ 2\theta$, in only 10 m surface, and as low as 0.2 to 0.4 $\Delta^\circ 2\theta$ below 50 m. Vitrinite reflectance was around 5% in the whole layer, close to measurement limit. The helium content was 10^{-14}-10^{-11} mol per 1g of cuttings, and tended to increase with increasing depth. The highest content was detected at 800 m depth. The helium isotope ratio($^3He/^4He$)have value of 0.4-3.6 times that of atmosphere, and tended to increase with increasing depth. Particularly, it was higher at 100 m, 300-400 m and 700-800 m. The CO_2 content per gram of cuttings, was in the range of 10^{-8}-10^{-6} mol in most layers, but it showed

©2019. Japan Geoscience Union. All Right Reserved.

higher values at 400 m and 800 m depth. the water tended to decrease with increasing depth, and showed especially high values at 400 m and 900 m. The carbon isotope ratio ($\delta^{13}C$) of calcite was -4.7‰ VPDB, and the oxygen isotope ratio ($\delta^{18}O$) is -16.3‰VPDB. The $\delta^{13}C$ value of dolomite was -1‰VPDB, and the $\delta^{18}O$ value was -10.9‰VPDB. The $\delta^{13}C$ value of CO_2 from cuttings at 800 m was -7.3‰VPDB, which contained sufficiently amount of carbon to measure carbon isotope ratio.

Keywords: Taketomi Island, Hot spring, cuttings, vitrinite reflectance, carbon cycle, helium isotope

©2019. Japan Geoscience Union. All Right Reserved.

Variation of helium isotope compositions at Lake Mashu

*Takanori Kagoshima[1], Yuji Sano[1], Atsushi Tanaka[2]

1. Atmosphere and Ocean Research Institute, University of Tokyo, 2. National Institute for Environmental Studies

Helium-3 is one of the most sensitive geochemical tracers which reflects addition of mantle components to gas and fluids in volcanic hydrothermal systems, and $^{3}He/^{4}He$ ratios may be useful to assess temporal change of hydrothermal activity at volcanic lakes. Lake Mashu is a caldera lake which formed around 7000 years ago in Hokkaido. Igarashi et al. (1992) measured He and Ne isotopes in water of Lake Mashu, and concluded that the depth profile of isotopic compositions reflect injection of mantle-derived He due to hot spring activity at the lake bottom. After that, there is no subsequent study reporting He isotope data. The lack of observational data may be due to difficulty of water sampling at caldera lakes. Igarashi et al. (1992) collected water samples into copper tubes. However, this method requires heavy and large sampling tools, and people who can transfer water and seal the tubes properly. In May and September 2017, we investigated Lake Mashu in order to check volcanic activity and practical sampling methods for caldera lakes. We collected water using a Niskin bottle at several depths (surface to 210 m) around the deepest point (211 m). Collected water was immediately transferred into lead-glass containers with vacuum valves at both ends. In Atmosphere and Ocean Research Institute, dissolved gases were extracted by the head space method, and introduced into a purification vacuum line. In the line, He and Ne were purified for isotope analyses. $^{3}He/^{4}He$ and $^{4}He/^{20}Ne$ ratios were measured using Helix-SFT and QMS, respectively. The highest $^{3}He/^{4}He$ ratios were observed at 205-210 m depth, indicating that injection of fluids with the high $^{3}He/^{4}He$ ratio at the bottom. The linear correlation between $^{4}He/^{20}Ne$ and $^{3}He/^{20}Ne$ ratios in water samples indicated mixing of two components: injected fluids and the atmosphere. The estimated $^{3}He/^{4}He$ ratio of the fluid end member was indistinguishable from the value reported by Igarashi et al. (1992), implying a possibility that there was no significant change in volcanic activity at Lake Mashu in the past 30 years.

Keywords: Helium isotope, Volcanic lake, Lake Mashu

©2019. Japan Geoscience Union. All Right Reserved.

Helium isotopes in Tachibana Bay and Shimabara Bay, Nagasaki

*Ma. Teresa Escobar[1], Yama Tomonaga[2], Hajime Obata[1], Shigenobu Takeda[3], Naoto Takahata[1], Yuji Sano[1]

1. Atmosphere and Ocean Research Institute, University of Tokyo, Kashiwanoha, Kashiwa, Chiba, Japan, 2. Eawag,, Swiss Federal Institute of Aquatic Science and Technology, Department of Water Resources and Drinking Water, Ü berlandstrasse 133 CH-8600 ,Dübendorf, Switzerland, 3. Graduate School of Fisheries and Environmental Sciences, Nagasaki University, Nagasaki, Japan

Noble gases are powerful tracers to study physical transport processes in aquatic system. Moreover, helium isotopes have been shown to be very useful to infer the origin of fluids. Shimabara Peninsula is located on western side of the Beppu-Shimabara graben in Kyushu, SW Japan. In the region, there are some hot springs and groundwaters which indicate magmatic helium with high 3He/4He ratio. Although some researchers report helium isotopic ratio on land, there is no data in the sea.

The surrounding bays around Shimabara Peninsula in Nagasaki were recently studied for the existence of hydrothermal springs and vents. Physico-chemical properties characteristic of hydrothermal activity were detected on the seafloor. For this study, we use helium isotopes to detect the occurrence of hydrothermal springs on the seafloor in both Tachibana Bay and Shimabara Bay. Samples were collected using a CTD-CMS system and analyzed using a Noble Gas Mass Spectrometer. Our data supplements the discovery of hydrothermal venting along known faults on the seafloor. We present the results of noble gas measurements conducted on water samples and discuss the relationship between our observations and the tectonic setup of the surrounding region.

Keywords: Helium Isotopes, Hydrothermal vents, Tachibana Bay

©2019. Japan Geoscience Union. All Right Reserved.

[E] Poster | S (Solid Earth Sciences)：S-GC Geochemistry

Wed. May 29, 2019 5:15 PM - 6:30 PM JST | Wed. May 29, 2019 8:15 AM - 9:30 AM UTC | Poster Hall International Exhibition Hall8, Makuhari Messe_31

[S-GC40] Volatile Cycles in the Deep Earth - from Subduction Zone to Hot Spot

convener:Hirochika Sumino(Department of Basic Science, Graduate School of Arts and Sciences, The University of Tokyo), Takeshi Hanyu(Japan Agency for Marine-Earth Science and Technology, Department of Solid Earth Geochemistry), Yuji Sano(Division of Ocean and Earth Systems, Atmosphere and Ocean Research Institute, University of Tokyo), Gray E Bebout(Lehigh University)

Volatiles play an important role in the geodynamics and chemical differentiation in the mantle and crust by drastically changing mineral stability and rheological behavior. Fractionation-processes such as partial melting, hydration, and dehydration are all controlled by volatiles in the rocks. A significant portion of the volatiles in the Earth has been thought to be present in the atmosphere and oceans as a consequence of extensive degassing during accretion and subsequent mantle degassing. On the other hand, it has been recently recognized that substantial amounts of volatiles are recycled back into the mantle at subduction zones, where intensive devolatilization of descended materials during arc magma generation was once thought to act as an effective "subduction barrier". However, fundamental questions still remain, such as: how are volatiles species distributed throughout the early and present Earth? What are the mechanisms for, and rate at which, volatiles are fluxed between the atmosphere, crust, and mantle? And what role have volatiles played in driving the evolution of the Earth? The possible role of the core in storing primordial volatiles is also poorly constrained. We therefore welcome contributions from experimental, observational, and modeling studies that help shed light on the deep cycles of volatiles, such as hydrogen, carbon, nitrogen, noble gases, halogens and sulfur. We particularly encourage studies linking the behavior of multiple volatile elements and their isotopic compositions. Studies investigating the linkage between volatile and solid geochemical tracers, the phase equilibria of volatile-bearing mantle assemblages, and the effect of volatiles on the physical properties of the mantle are also welcome.

[SGC40-P01] Continental growth models demystified

*Jun Korenaga[1] (1.Department of Geology and Geophysics, Yale University)

[SGC40-P02] Mass-independent sulfur isotope signature from the 2.7 Ga Belingwe komatiite: Recycling of crustal material in Archean

*Yusuke Kubota[1], Yuichiro Ueno[1,2,3], Kenji Shimizu[3], Fumihiro Matsuura[2], Akira Ishikawa[1,3] (1.Department of Earth and Planetary Sciences, Tokyo Institute of Technology, 2.Earth-Life Science Institute, Tokyo Institute of Technology, 3.Japan Agency for Marine-Earth Science and Technology (JAMSTEC))

[SGC40-P03] Determination of halogens in some standard materials using the neutron irradiation noble gas mass spectrometric technique

*Hirochika Sumino[1], Masahiro Kobayashi[2], Takehiko Saito[3], Keisuke Nagao[3] (1.Department of Basic Science, Graduate School of Arts and Sciences, The University of Tokyo, 2.Tokyo Metropolitan Industrial Technology Research Institute, 3.Geochemical Research Center, Graduate School of Science, University of Tokyo)

[SGC40-P04] FTIR spectroscopy and noble gas mass spectrometry for a single olivine grain

*Sota Niki[1], Hirochika Sumino[2], Masahiro Kobayashi[3], Hiroyuki Kagi[1], Takafumi Hirata[1], Chris J. Ballentine[4] (1.Geochemical Research Center, Grad. School of Science, Univ. of Tokyo, 2.Dept. of Basic Science, Grad. School of Arts and Sciences, Univ. of Tokyo, 3.Tokyo Metropolitan Industrial Technology Research Institute, 4.Dept. of Earth Sciences, Univ. of Oxford)

[SGC40-P05] New halogen incorporation mechanism in serpentine group minerals: Crystal chemical consideration

*Masami Kanzaki[1] (1.Institute for Planetary Matereials, Okayama University)

[SGC40-P06] Mineralogical and geochemical characteristics of cuttings from Taketomi hot spring

*Noriyuki Shingaki[1], Tomohiro Toki[1], Syogo Oshima[2], Masaaki chinen[3], Arito Sakaguchi[4], Naoto Takahata[5], Yuji Sano[5], Shirai Kotaro[5], Kentaro Tanaka[5] (1.University of the Ryukyus , 2.West Japan Engineering Consultants, Inc., 3.MicroRange, 4.Faculty of Science, Yamaguchi University, 5.Atmosphere and Ocean Research Institute, The University of Tokyo)

[SGC40-P07] Variation of helium isotope compositions at Lake Mashu

*Takanori Kagoshima[1], Yuji Sano[1], Atsushi Tanaka[2] (1.Atmosphere and Ocean Research Institute, University of Tokyo, 2.National Institute for Environmental Studies)

[SGC40-P08] Helium isotopes in Tachibana Bay and Shimabara Bay, Nagasaki

*Ma. Teresa Escobar[1], Yama Tomonaga[2], Hajime Obata[1], Shigenobu Takeda[3], Naoto Takahata[1], Yuji Sano[1] (1.Atmosphere and Ocean Research Institute, University of Tokyo, Kashiwanoha, Kashiwa, Chiba, Japan, 2.Eawag,, Swiss Federal Institute of Aquatic Science and Technology, Department of Water Resources and Drinking Water, Überlandstrasse 133 CH-8600 ,Dübendorf, Switzerland, 3.Graduate School of Fisheries and Environmental Sciences, Nagasaki University, Nagasaki, Japan)

Continental growth models demystified

*Jun Korenaga[1]

1. Department of Geology and Geophysics, Yale University

So far proposed models of continental growth exhibit bewildering diversity, but this diversity is rather superficial. By understanding how different growth models are built and what they are meant to constrain, we can gain deeper insight into the evolution of continental crust as well as the dynamics of the early Earth. There are three kinds of growth models: crust-based, mantle-based, and others. Crust-based models provide only the lower bound on net crustal growth, and mantle-based models aim at constraining net crustal growth itself. Other models are also about net crustal growth, but they are subject to greater uncertainty. In the presence of crustal recycling, crust-based models are expected to be different from mantle-based models, and more important, the difference between these two kinds of models provides important constraints on the operation of plate tectonics in the early Earth. Some popular misconceptions in the recent literature are also discussed.

Keywords: Continental crust, Plate tectonics, Chemical differentiation

©2019. Japan Geoscience Union. All Right Reserved.

Mass-independent sulfur isotope signature from the 2.7 Ga Belingwe komatiite: Recycling of crustal material in Archean

*Yusuke Kubota[1], Yuichiro Ueno[1,2,3], Kenji Shimizu[3], Fumihiro Matsuura[2], Akira Ishikawa[1,3]

1. Department of Earth and Planetary Sciences, Tokyo Institute of Technology, 2. Earth-Life Science Institute, Tokyo Institute of Technology, 3. Japan Agency for Marine-Earth Science and Technology (JAMSTEC)

Recycling of the Earth's crustal material has long been discussed mainly through the radiogenic isotopes of modern Ocean Island Basalts (OIB). Recent finding of Sulfur Mass Independent Fractionation (S-MIF) from HIMU and EM I basalts supports recycling of crustal material in mantle (Cabral et al., 2013; Delavault et al., 2016). Since photochemical reactions under reducing Archean atmosphere are thought to be a plausible process of large S-MIF generation (Farquhar et al., 2001; Farquhar and Wings, 2003), these discoveries demonstrated that the S-MIF is a useful signature for tracing Archean crustal material. However, it has been difficult to estimate when the subduction started in the history of the Earth. Here, we report multiple sulfur isotope analysis of the 2.7 Ga Belingwe komatiites and related rocks, which has potential to elucidate earlier subduction or recycling of crustal material before 2.7 Ga. The Belingwe komatiite are one of the best-preserved Archean komatiites in the world. The results show clear S-MIF signature in several komatiites and basalts. Sulfide minerals in the S-MIF bearing samples occur as pyrrhotite and chalcopyrite scattered within groundmass around the quenched olivine and pyroxene crystals, indicating that the sulfides crystalized at the time of eruption. The original nature of the sulfide is also supported by the correlation between sulfur contents and magnesium number. Based on Nd, Sr, and Pb isotope composition measured in the previous study (Shimizu et al., 2005), the S-MIF bearing komatiites and basalts are likely to be derived from depleted mantle source, whereas more enriched samples do not show S-MIF. Therefore, the S-MIF component is not likely derived from assimilated crust at the time of the komatiite volcanism, but originally incorporated in the depleted source mantle. Consequently, our results suggest that subduction of S-MIF bearing surface material into the mantle had been operated at least prior to 2.7 Ga.

Keywords: Sulfur mass independent fractionation, Mantle geochemistry, Komatiite, Archean

©2019. Japan Geoscience Union. All Right Reserved.

Determination of halogens in some standard materials using the neutron irradiation noble gas mass spectrometric technique

*Hirochika Sumino[1], Masahiro Kobayashi[2], Takehiko Saito[3], Keisuke Nagao[3]

1. Department of Basic Science, Graduate School of Arts and Sciences, The University of Tokyo, 2. Tokyo Metropolitan Industrial Technology Research Institute, 3. Geochemical Research Center, Graduate School of Science, University of Tokyo

Halogens are among the most powerful tracers of volatile cycling in subduction zones, because of (i) the large contrast in concentrations between the surface and interior of the Earth [1], (ii) their high affinities to gas- and fluid-phases relative to mineral [2], (iii) distinct elemental and/or isotopic compositions in each reservoir in the Earth [3-7]. However, few analytical techniques can determine trace amounts of halogens, particularly bromine and iodine in mantle-derived samples. Consequently, there have been relatively few previous studies of halogens in mantle-derived samples.

The neutron irradiation noble gas mass spectrometric technique (NI-NGMS) is capable of measuring very low concentrations of halogens (<1 ppb) in very small samples (<1 mg). The NI-NGMS is an extension of the Ar-Ar and I-Xe dating methods [8-10]. Halogens (chlorine, bromine, and iodine) and other elements (potassium, calcium, barium, and uranium) are converted to corresponding isotopes of argon, krypton, and xenon by neutron irradiation in a nuclear reactor. The noble gas isotopes in neutron-irradiated samples are analyzed by noble gas mass spectrometry. Irradiation conditions such as neutron fluence are monitored using standard materials of the Ar-Ar and I-Xe dating methods. Relatively high cross-sections of halogens for neutron capture and high sensitivity of noble gas mass spectrometry enable determination of trace amounts of halogens using NI-NGMS.

We report new halogen concentrations determined for scapolite standards and geological reference materials distributed by Geological Survey of Japan and US Geological Survey using NI-NGMS. Consistent results with those regarded as reference values were obtained from scapolite standards, which indicate that the scapolite standards are reliable in halogen analysis. On the other hand, the halogen concentrations obtained from geological reference materials are systematically lower than the reference values for samples with low concentrations of halogens. The higher concentrations reported for the geological reference materials probably result from contamination on the sample surface during preparation of these reference materials. We also propose a fluorine determination method using NI-NGMS based on neon systematics, although reliable determination of fluorine has been thought to be impossible.

[1] Pyle & Mather, *Chem. Geol.* 2009. [2] Bureau *et al.*, *GCA* 2016. [3] Sumino *et al.*, *EPSL* 2010. [4] Chavrit *et al.*, *GCA* 2016. [5] Kobayashi *et al.*, *EPSL* 2017. [6] Kendrick *et al.*, *Nature Geosci.* 2017. [7] Kobayashi *et al.*, *G-cubed* 2019. [8] Turner, *JGR* 1965. [9] Kendrick, *Chem. Geol.* 2012. [10] Ruzié-Hamilton *et al.*, *Chem. Geol.* 2016.

Keywords: Halogen, Noble gas, Nuetron irradiation, Noble gas mass spectrometry

©2019. Japan Geoscience Union. All Right Reserved.

FTIR spectroscopy and noble gas mass spectrometry for a single olivine grain

*Sota Niki[1], Hirochika Sumino[2], Masahiro Kobayashi[3], Hiroyuki Kagi[1], Takafumi Hirata[1], Chris J. Ballentine[4]

1. Geochemical Research Center, Grad. School of Science, Univ. of Tokyo, 2. Dept. of Basic Science, Grad. School of Arts and Sciences, Univ. of Tokyo, 3. Tokyo Metropolitan Industrial Technology Research Institute, 4. Dept. of Earth Sciences, Univ. of Oxford

Volatiles have been degassed from the mantle and recycled back into the mantle at subduction zones. Water is the main component of volatiles and plays a key role in dynamics of the subduction zones because even a small water content in rocks has an influence on the physical and chemical properties of the rocks (e.g. friction coefficient, melting point, etc.) which are closely related to phenomena studied in earth sciences including volcanic or seismic activities. It is still unclear to what extent of water have been subducted into the mantle and released to the Earth’ s surface. To elucidate the volatile recycling, noble gases are powerful tracers because they have unique compositions in geochemical reservoirs. Previous researches have mainly reported results of bulk analysis of mantle peridotites. On the contrary, in this study, FTIR measurements and noble gas analysis of a single olivine grain were conducted to determine the noble gas concentrations in fluid inclusions.

The olivine samples used for this study were separated from mantle xenoliths collected from an intraplate setting (Hualalai in Hawaii) and two subduction zones (the Avacha volcano in the Kamchatka arc and the Pinatubo volcano in the Luzon arc). The Hualalai olivine was expected to show mantle-derived noble gas compositions (Kobayashi et al., G-cubed 2019) and was used for checking the accuracy of noble gas analysis. The Avacha and Pinatubo olivines contained H_2O-rich fluid inclusions and the noble gas concentrations in the inclusions had been estimated from salinities, and halogen and noble gas compositions (Kobayashi et al., EPSL 2017). The Avacha and Pinatubo olivines were used to confirm the accuracy of the analytical method used in this study for determining the noble gas concentrations in the inclusions.

FTIR measurements were conducted to determine the H_2O concentration in the Avacha and Pinatubo olivines. The mantle xenoliths were crushed into 0.5 to 2 mm and olivine grains were separated. The olivine grains were embedded in resin (Ortho Bright) and polished to a thickness of several hundred micrometers. The weight of samples was 0.7 to 16 mg. The H_2O concentration was calculated from the absorbance at 3404 cm^{-1}. After the FTIR measurements, resin was removed from each grain by heating at 50ºC and dissolving in acetone.

Noble gas analysis was conducted using multicollector noble gas mass spectrometers (Helix SFT and Argus, Thermo Fisher Scientific). After the sample loading into a laser heating cell, the cell was baked out with pumping to desorb atmospheric noble gases to achieve low blank levels required for single-grain analysis. Consequently, noble gases were extracted by laser heating (Fusion Diode Stepped Heating System, Teledyne CETAC) at about 1000 ºC for 5 minutes. The gases released from samples were purified by removing active gases using a getter, and then, absorbed on two cryo-traps (one was for helium and neon and the other was for argon, krypton, and xenon). Each noble gas was desorbed from the trap at a certain temperature and introduced into the mass spectrometers. Helium was measured with Helix SFT and other noble gases were measured with Argus. The abundances and isotopic ratios of noble gases in a

©2019. Japan Geoscience Union. All Right Reserved.

single olivine grain were obtained. The accuracy of the isotopic ratios was checked by the Hualalai samples.

The noble gas concentrations in the inclusions obtained will be compared with the previous bulk analysis to discuss the accuracy of the method in this study. This method of determining the noble gas concentrations in fluid inclusions from single-grain analysis has a potential to clarify the heterogeneity of the mantle volatiles in terms of a single-grain mineral and the flux quantification during the volatile recycling.

Keywords: noble gas, FTIR spectroscopy, mantle

©2019. Japan Geoscience Union. All Right Reserved.

New halogen incorporation mechanism in serpentine group minerals: Crystal chemical consideration

*Masami Kanzaki[1]

1. Institute for Planetary Matereials, Okayama University

Introduction: Recent geochemical studies revealed that serpentinites contain a significant amount of halogens. However, how halogen ions are incorporated into serpentinites is not well understood. Commonly assumed mechanism is "OH^- substitution" in serpentine group minerals (chrysotile, lizardite and antigorite). Although this mechanism will be fine for F, but may not be adequate for larger halogens (Cl, Br, I). Here, I propose new halogen incorporation mechanism in lizardite and antigorite from crystal chemical point of view.

Calculation methods: In order to assess present new incorporation model, first-principles calculation was conducted. Quantum-Espresso package was used to optimize the halogen incooporated model structures. In the present study, lizardite and antigorite (*m*=17 polysome) are considered. For our proposed mechanism, charge balance should be observed; so $Mg^{2+} = X^- + Al^{3+}$ substitution (X^- = halogen) is assumed to introduce halogen to a vacant site. For lizardite, enthalpy difference between two models (OH^- substitution and our model) was calculated for following equation: $Mg_2AlSi_2O_8XH_2 + H_2O = Mg_2AlSi_2O_9XH_4$. Former corresponds to the OH substituted model (with Al introduced), and latter corresponds to our new model. Although this comparison is crude (as free H_2O is included in the equation), it could provide systematic trend with kinds of halogen atoms. Since antigorite has a very large unit cell and many vacant sites, only $Mg^{2+} = Cl^- + Al^{3+}$ substitute in five vacant sites are considered so far.

Results and Discussion: From close inspection of crystal structures of lizardite and antigorite, vacant sites ideal for halogens are identified. The vacant sites are surrounded by four protons (of OH^-) forming elongated tetrahedon (i.e., XH_4^{3+}) if halogen is located. Such vacant sites provide local structure similar to halogen ions in aqueous solution.

In order to further assess present incorporation mechanism, first-principles calculations of lizardite and antigorite containing halogens in those sites were conducted. The structural optimizations confirmed that halogens could be well accommodated into the tetrahedral vacant sites in lizardite. The calculated enthalpy difference between OH substitution and present models in lizardite revealed that larger halogens prefer our model over the OH substitution model. There is sinlge vacant site in lizardite, but antigorite (*m*=17) has 17 crystallographically different vacant sites. Most sites have local structures more or less similar to that of lizardite (locating in 6-membered SiO_4 ring). But there is another kind of vacant site which is locating in 8-membered SiO_4 ring. This local structure is surrounded by six protons, but it can be regareded as two tetrahedral proton sites with edge sharing. Substitution of Cl^- to this site (one of tetrahedral sites) showed lower enthalpy compared to those of other lizardite-like sites, and can accept more larger ions. Therefore, Cl^- (and other larger halogens) will prefet this site in antigorite (*m*=17). Not all antogorite polysomes have this site.

Present study suggests that our new proposed incorporation mechanism is promising, and it should be further studied experimentally. Present new incorporation mechanism would be important to understand elemental partition behavior of halogens in subduction zones.

Keywords: halogen site, serpentine, crystal chemistry, incorporation mechanism, elemental partition

©2019. Japan Geoscience Union. All Right Reserved.

Mineralogical and geochemical characteristics of cuttings from Taketomi hot spring

*Noriyuki Shingaki[1], Tomohiro Toki[1], Syogo Oshima[2], Masaaki chinen[3], Arito Sakaguchi[4], Naoto Takahata[5], Yuji Sano[5], Shirai Kotaro[5], Kentaro Tanaka[5]

1. University of the Ryukyus , 2. West Japan Engineering Consultants, Inc., 3. MicroRange, 4. Faculty of Science, Yamaguchi University, 5. Atmosphere and Ocean Research Institute, The University of Tokyo

It is important to grasp carbon cycle on the earth’ s surface for thinking about global environmental change. A hot spring with a maximum temperature of 64℃ is venting with gas containing 70% of methane from several spots on the seafloor at depth of 22 m at 1 km northeast off Taketomi Island. Based on methane and helium isotope ratios in the venting gas, the influence of magmatic gas has been pointed out. In spite of Taketomi Island located on the trench side from island arc, magmatic gas is venting. It suggests the forearc where magma cannot generate, might form new supply path of carbon from the Earth’ s interior. The mass balance from new supply path of carbon may change estimation of carbon cycle on earth’ s surface. Therefore, the purpose of this study is to elucidate venting mechanism and quantitative grasp of magmatic gas from forearc, and the history of hot spring activities will be investigated to predict future activities.

In 2017, the hot spring was drilled up to depth of 940 m in Taketomi Island. The cuttings with muddy water were sampled every 10 m. The thin sections were prepared from cuttings to be observed using polarization microscope, and the chemical compositions of grains were analyzed by SEM-EDX. The ground samples were analyzed for mineral and chemical compositions by XRD and EDX. The clay minerals gathered by levitation were measured for half-value width of illite using XRD. He and CO_2 contained in samples that were crashed in vacuum were measured for isotope ratios by mass spectrometer. Calcite and dolomite collected from the cuttings were measured for the carbon and oxygen isotope ratios by mass spectrometer. The vitrinite in the cuttings was separated by a heavy liquid, and the reflectance was measured by a reflecting microscope.

In the microscopy, the stratum was roughly divided two formations; cryptocrystalline quartz layer and sand stone layer. Carbonaceous materials were observed in most of the stratum. Dolomite was limitedly observed in the vicinity of 800 m. In the XRD analysis, Quartz was detected at all depth. Calcite was detected at shallower depth than 30 m, and dolomite was detected only around 800 m. As a result of the EDX analysis, silicon was the most dominant in all layers, and especially, it was contained around 0-100 m, 300 m and around 900 m over 80%. There was a layer that contained much calcium. Around 0-30 m, 400-500 m and around 800 m, calcite was contained 15 % or more. The half-value width of illite was large, 0.8 $\Delta^\circ 2\theta$, in only 10 m surface, and as low as 0.2 to 0.4 $\Delta^\circ 2\theta$ below 50 m. Vitrinite reflectance was around 5% in the whole layer, close to measurement limit. The helium content was 10^{-14}-10^{-11} mol per 1g of cuttings, and tended to increase with increasing depth. The highest content was detected at 800 m depth. The helium isotope ratio($^3He/^4He$)have value of 0.4-3.6 times that of atmosphere, and tended to increase with increasing depth. Particularly, it was higher at 100 m, 300-400 m and 700-800 m. The CO_2 content per gram of cuttings, was in the range of 10^{-8}-10^{-6} mol in most layers, but it showed

©2019. Japan Geoscience Union. All Right Reserved.

higher values at 400 m and 800 m depth. the water tended to decrease with increasing depth, and showed especially high values at 400 m and 900 m. The carbon isotope ratio ($\delta^{13}C$) of calcite was -4.7‰ VPDB, and the oxygen isotope ratio ($\delta^{18}O$) is -16.3‰VPDB. The $\delta^{13}C$ value of dolomite was -1‰VPDB, and the $\delta^{18}O$ value was -10.9‰VPDB. The $\delta^{13}C$ value of CO_2 from cuttings at 800 m was -7.3‰VPDB, which contained sufficiently amount of carbon to measure carbon isotope ratio.

Keywords: Taketomi Island, Hot spring, cuttings, vitrinite reflectance, carbon cycle, helium isotope

©2019. Japan Geoscience Union. All Right Reserved.

Variation of helium isotope compositions at Lake Mashu

*Takanori Kagoshima[1], Yuji Sano[1], Atsushi Tanaka[2]

1. Atmosphere and Ocean Research Institute, University of Tokyo, 2. National Institute for Environmental Studies

Helium-3 is one of the most sensitive geochemical tracers which reflects addition of mantle components to gas and fluids in volcanic hydrothermal systems, and $^{3}He/^{4}He$ ratios may be useful to assess temporal change of hydrothermal activity at volcanic lakes. Lake Mashu is a caldera lake which formed around 7000 years ago in Hokkaido. Igarashi et al. (1992) measured He and Ne isotopes in water of Lake Mashu, and concluded that the depth profile of isotopic compositions reflect injection of mantle-derived He due to hot spring activity at the lake bottom. After that, there is no subsequent study reporting He isotope data. The lack of observational data may be due to difficulty of water sampling at caldera lakes. Igarashi et al. (1992) collected water samples into copper tubes. However, this method requires heavy and large sampling tools, and people who can transfer water and seal the tubes properly. In May and September 2017, we investigated Lake Mashu in order to check volcanic activity and practical sampling methods for caldera lakes. We collected water using a Niskin bottle at several depths (surface to 210 m) around the deepest point (211 m). Collected water was immediately transferred into lead-glass containers with vacuum valves at both ends. In Atmosphere and Ocean Research Institute, dissolved gases were extracted by the head space method, and introduced into a purification vacuum line. In the line, He and Ne were purified for isotope analyses. $^{3}He/^{4}He$ and $^{4}He/^{20}Ne$ ratios were measured using Helix-SFT and QMS, respectively. The highest $^{3}He/^{4}He$ ratios were observed at 205-210 m depth, indicating that injection of fluids with the high $^{3}He/^{4}He$ ratio at the bottom. The linear correlation between $^{4}He/^{20}Ne$ and $^{3}He/^{20}Ne$ ratios in water samples indicated mixing of two components: injected fluids and the atmosphere. The estimated $^{3}He/^{4}He$ ratio of the fluid end member was indistinguishable from the value reported by Igarashi et al. (1992), implying a possibility that there was no significant change in volcanic activity at Lake Mashu in the past 30 years.

Keywords: Helium isotope, Volcanic lake, Lake Mashu

©2019. Japan Geoscience Union. All Right Reserved.

Helium isotopes in Tachibana Bay and Shimabara Bay, Nagasaki

*Ma. Teresa Escobar[1], Yama Tomonaga[2], Hajime Obata[1], Shigenobu Takeda[3], Naoto Takahata[1], Yuji Sano[1]

1. Atmosphere and Ocean Research Institute, University of Tokyo, Kashiwanoha, Kashiwa, Chiba, Japan, 2. Eawag,, Swiss Federal Institute of Aquatic Science and Technology, Department of Water Resources and Drinking Water, Ü berlandstrasse 133 CH-8600 ,Dübendorf, Switzerland, 3. Graduate School of Fisheries and Environmental Sciences, Nagasaki University, Nagasaki, Japan

Noble gases are powerful tracers to study physical transport processes in aquatic system. Moreover, helium isotopes have been shown to be very useful to infer the origin of fluids. Shimabara Peninsula is located on western side of the Beppu-Shimabara graben in Kyushu, SW Japan. In the region, there are some hot springs and groundwaters which indicate magmatic helium with high 3He/4He ratio. Although some researchers report helium isotopic ratio on land, there is no data in the sea.

The surrounding bays around Shimabara Peninsula in Nagasaki were recently studied for the existence of hydrothermal springs and vents. Physico-chemical properties characteristic of hydrothermal activity were detected on the seafloor. For this study, we use helium isotopes to detect the occurrence of hydrothermal springs on the seafloor in both Tachibana Bay and Shimabara Bay. Samples were collected using a CTD-CMS system and analyzed using a Noble Gas Mass Spectrometer. Our data supplements the discovery of hydrothermal venting along known faults on the seafloor. We present the results of noble gas measurements conducted on water samples and discuss the relationship between our observations and the tectonic setup of the surrounding region.

Keywords: Helium Isotopes, Hydrothermal vents, Tachibana Bay

©2019. Japan Geoscience Union. All Right Reserved.

[E] Poster | S (Solid Earth Sciences)：S-CG Complex & General

Wed. May 29, 2019 10:45 AM - 12:15 PM JST | Wed. May 29, 2019 1:45 AM - 3:15 AM UTC | Poster Hall International Exhibition Hall8, Makuhari Messe_10

[S-CG48] Science of slow earthquakes: Toward unified understandings of whole earthquake process

convener:Satoshi Ide(Department of Earth an Planetary Science, University of Tokyo), Hitoshi Hirose(Research Center for Urban Safety and Security, Kobe University), Kohtaro Ujiie(Graduate School of Life and Environmental Sciences, University of Tsukuba), Takahiro Hatano(Earthquake Research Institute, University of Tokyo)

Accumulating observational studies on various types of slow deformation events, such as tectonic tremors, very low frequency events, and slow slip events, portrays some universal characteristics in generally complex behavior, including interaction among events and influence by various outer loadings. Some of these phenomena seem to have causal relation with the occurrence of very large earthquakes. A unified understanding of these slow and fast earthquake processes requires an approach integrating geophysics, seismology, geodesy, geology, and non-equilibrium statistical physics. We welcome presentations based on, but not limited to, geophysical observation, data analysis, analytical theory, numerical simulation, field study, and laboratory experiments.

[SCG48-P01] Off the Kii Peninsula Shallow Low Frequency Earthquake in 2004 revealed by Ocean Bottom Seismometer

*Koji Tamaribuchi[1], Akio Kobayashi[1], Takahito Nishimiya[1], Satoshi Annoura[2] (1.Meteorological Research Institute, 2.Japan Meteorological Agency)

[SCG48-P02] The development of pressure vessel on gouges for rock deformation at seismic rates under water-saturated conditions

*Wei-Ting Lin[1], Li-Wei Kuo[1], Wen-Jie Wu[1], Jia-Jyun Dong[1], Yi-Hung Huang[2] (1.National Central University, 2.MATSUKI HYDRAULIC INDUSTRIAL CO. LTD)

[SCG48-P03] Spatial variations of shallow very low-frequency earthquake activity along the Nankai Trough based on CMT inversion using the 3D heterogeneous model

*Shunsuke Takemura[1], Takanori Matsuzawa[1], Akemi Noda[1], Takashi Tonegawa[2], Youichi Asano[1], Takeshi Kimura[1], Katsuhiko Shiomi[1] (1.National Research Institute for Earth Science and Disaster Resilience, 2.Japan Agency for Marine-Earth Science and Technology)

[SCG48-P04] Evaluation of Magnitude and Characteristics of Seismicity of Low Frequency Earthquakes in Parkfield

*Miki Aso[1,3], Naofumi Aso[2], Satoshi Ide[1] (1.Department of Earth and Planetary Science, The University of Tokyo, 2.Tokyo Institute of Technology, School of Science, 3.OYO RMS Corporation)

[SCG48-P05] Tectonic tremor catalog in the Tohoku-Hokkaido-Oki region using S-net

*Satoshi Ide[1], Tomoaki Nishikawa[2], Takanori Matsuzawa[3], Kazuaki Ohta[2], Naoki Uchida[4], Takuya NISHIMURA[2] (1.Department of Earth an Planetary Science, University of Tokyo, 2.Disaster Prevention Research Institute, Kyoto University, 3.National Research Institute for Earth Science and Disaster Resilience, 4.Graduate School of Science and International Research Institute of Disaster Science, Tohoku University)

[SCG48-P06] Spontaneous Slow Slip and Runaway Slip in Laboratory

*Miki Takahashi[1] (1.Institute of Earthquake and Volcano Geology, Geological Survey of Japan, AIST)

[SCG48-P07] Hydration and amorphization of quartz rocks during high-velocity frictional sliding: An examination of fault gouge from friction experiments of synthetic quartz

*Yuko Onoe[1], Hirotaka Iida[2], Akito Tsutsumi[1], Aki Takigawa[1] (1.Graduate School of Science, Kyoto University, 2.Geothermal Engineering Co., Ltd.)

[SCG48-P08] Constraining S Wave Velocity of the Source Region of Shallow Very Low-Frequency Earthquakes

*Takeshi Akuhara[1], Takashi Tonegawa[2] (1.Earthquake Research Institute, The University of Tokyo, 2.Research and Development center for Earthquake and Tsunami, Japan Agency for Marine-Earth Science and Technology)

[SCG48-P09] **Quantitative relationship between aseismic slip propagation speed and frictional properties**

*Keisuke Ariyoshi[1], Jean-Paul Ampuero[2,3], Roland Burgmann[4], Toru Matsuzawa[5], Akira Hasegawa[5], Ryota Hino[5], Takane Hori[1] (1.Japan Agency for Marine-Earth Science and Technology, 2.Université Côte d'Azur, 3.California Institute of Technology, 4.University of California, Berkeley, 5.Graduate School of Science, Tohoku University)

[SCG48-P10] Comprehensive detection of very low frequency earthquakes off the Pacific coasts of Hokkaido and Tohoku, northeastern Japan

*Satoru Baba[1], Akiko Takeo[1], Kazushige Obara[1], Takanori Matsuzawa[2], Takuto Maeda[3] (1.Earthquake Research Institute, University of Tokyo, 2.National Research Institute for Earth Science and Disaster Resilience, 3.Graduate School of Science and Technology, Hirosaki University)

[SCG48-P11] **Spatio-temporal evolution of long- and short-term slow slip events in the Tokai region, central Japan estimated from a very dense GNSS network, during 1997-2017**

*Hiromu Sakaue[1], Takuya NISHIMURA[2], Jun'ichi Fukuda[3], Teruyuki Kato[4] (1.Graduate School of Science, Kyoto University, 2.Disaster Prevention Research Institute Kyoto University, 3.Earthquake Research Institute,The University of Tokyo, 4.Hot Springs Research Institute of Kanagawa Prefecture)

[SCG48-P12] Broadband excitation of acoustic emission in granular stick-slip : experiments and spectral analyses

*Hidekazu Fukumizu[1], Ikuro Sumita[2] (1.Earth and Environmental Science Course, Division of Natural System, Graduate school of Natural Science and Technology, Kanazawa University, 2.School of Geosciences and Civil Engineering, Kanazawa University)

[SCG48-P13] Episodic tremor and slip silently invades strongly locked megathrust in the Nankai Trough

*Masayuki Kano[1], Aitaro Kato[2], Kazushige Obara[2] (1.Graduate school of science, Tohoku University, 2.Earthquake Research Institute, The University of Tokyo)

[SCG48-P14] Spatial distribution of the electrical resistivity beneath western part of Shikoku Island where long-term SSE events have repeatedly occurred

*Makoto Uyeshima[1], Maki Hata[1], Hiroshi Ichihara[2], Ryokei Yoshimura[3], Koki Aizawa[4] (1.Earthquake Research Institute, The University of Tokyo, 2.Graduate School of Environmental Studies, Nagoya University, 3.Disaster Prevention Research Institute, Kyoto University, 4.Institute of Seismology and Volcanology, Faculty of Sciences, Kyushu University)

[SCG48-P15] Variations of scaling relationships for shallow tremor observed along the Nankai trough

*Masaru Nakano[1], Suguru Yabe[1] (1.Japan Agency for Marine-Earth Science and Technology)

[SCG48-P16] Low-frequency earthquakes triggered by teleseismic surface waves by Ryukyu subduction zone.

Ayumi Kinjo[1], *Mamoru Nakamura[1] (1.Faculty of Science, University of the Ryukyus)

[SCG48-P17] Detection of small surface displacement accompanying deep low-frequency tremor in Shikoku region, southwest Japan

*Yutaro Okada[1], Takao Tabei[2] (1.Faculty of Science, Kochi University, 2.Faculty of Science and Technology, Kochi University)

[SCG48-P18] Long-term temporal change in crustal resistivity beneath western Shikoku

*Futoshi Yamashita[1], Yoshimori Honkura[1] (1.National Research Institute for Earth Science and Disaster Resilience)

[SCG48-P19] Slow decay of postseismic deformation compared with aftershocks following the 2011 Tohoku-oki Earthquake

*Yuta Mitsui[1], Shunsuke Morikami[2] (1.Department of Geosciences, Shizuoka University, 2.Formerly at Graduate School of Science and Technology, Shizuoka University)

[SCG48-P20] Serpentinite dehydration in subduction shear zones formed at source depths of slow earthquakes

*Yasushi Mori[1], Miki Shigeno[1], Kohtaro Ujiie[2], Kazuya Noro[2], Tadao Nishiyama[3] (1.Kitakyushu Museum of Natural History and Human History, 2.University of Tsukuba, 3.Kumamoto University)

[SCG48-P21] Earthquake swarms following very low-frequency earthquakes in the central Ryukyu Trench

*Mamoru Nakamura[1] (1.Faculty of Science, University of the Ryukyus)

[SCG48-P22] Seismic imaging in the central Nankai trough, off Shionomisaki to Kii channel

*Yasuyuki Nakamura[1], Shuichi Kodaira[1], Tetsuo No[1], Yuka Kaiho[1], Gou Fujie[1], Seiichi Miura[1], Kazuya Shiraishi[1] (1.Japan Agency for Marine Earth Science and Technology)

[SCG48-P23] Attempt to Detect Intra-plate SSEs Based on F3 Solution of GEONET

*Yusaku Tanaka[1] (1.Earthquake Research Institute)

[SCG48-P24] A new hydrothermal, low to high speed rotary-shearing apparatus: Reproduction of slow/megathrust earthquakes in laboratory

*Takehiro Hirose[1], Wataru Tanikawa[1], Yohei Hamada[1], Keishi Okazaki[1] (1.Kochi Institute for Core Sample Research, Japan Agency for Marine-Earth Science and Technology)

[SCG48-P25] Very low-frequency earthquakes in western Shikoku remotely triggered by the 2016 Mw5.9 off-Kii Peninsula earthquake

*Masatoshi Miyazawa[1] (1.Disaster Prevention Research Institute, Kyoto University)

[SCG48-P26] **Underground structure around source region of slow earthquakes in western Shikoku obtained by receiver function analysis**

Akira Hikita[1], Aitaro Kato[1], *Kazushige Obara[1], Akiko Takeo[1], Takeshi Akuhara[1] (1.Earthquake Research Institute, The University of Tokyo)

[SCG48-P27] Hypocenter determination of deep low frequency tremors beneath the Kii Peninsula by backprojection of seismic array data

*Kodai Sagae[1], Hisashi Nakahara[1], Takeshi Nishimura[1], Kazutoshi Imanishi[2] (1.Graduate School of Science,Tohoku University, 2.National Institute of Advanced Industrial Science and Technology (AIST))

[SCG48-P28] Triggered tremors and stress perturbations due to surface waves

*Ryohei Ikeda[1], Naoki Suda[1] (1.Hiroshima University)

[SCG48-P29] Numerical modeling of long- and shallow slow slip events including shallow region in Hyuganada and western Nankai, Japan

*Takanori Matsuzawa[1], Bunichiro Shibazaki[2] (1.National Research Institute for Earth Science and Disaster Resilience, 2.Building Research Institute)

[SCG48-P30] Further evidence for the influence of a subducting-ridge on the spatial strain accumulation and release pattern in the shallow eastern Nankai Trough, based on VLFE distribution

*Akiko Toh[1], Chen Wan-Jou [2], Doug Dreger[3], Wu-Cheng Chi[2], Satoshi Ide[1] (1.University of Tokyo, 2.Institute of Earth Sciences, Academia Sinica, 3.UC Berkeley)

[SCG48-P31] Evidence for semi-brittle flow in mantle-wedge serpentinites under high pore fluid pressure and their implications for deep low frequency earthquakes

Kengo Kataoka[1], Yurina Nagata[1], *Ken-ichi Hirauchi[1], Ryosuke Oyanagi[2], Atsushi Okamoto[3], Katsuyoshi Michibayashi[4] (1.Department of Geosciences, Faculty of Science, Shizuoka University, 2.Japan Agency for Marine-Earth Science and Technology, 3.Graduate School of Environmental studies, Tohoku University, 4.Department of Earth and Planetary Sciences, Nagoya University)

[SCG48-P32] Spatial distribution of slow slip events off the Boso peninsula from 1996 to 2018 under sparsity constraints

*Ryoko Nakata[1], Hideitsu Hino[2], Tatsu Kuwatani[3,4], Takahiro Akiyama[5], Shoichi Yoshioka[6], Masato Okada[7], Takane Hori[1] (1.Japan Agency for Marine-Earth Science and Technology, 2.The Institute of Statistical Mathematics, 3.Department of Solid Earth Geochemistry, Japan Agency for Marine-Earth Science and Technology, 4.PRESTO, Japan Science and Technology Agency, 5.Graduate School of Science, Kobe University, 6.Research Center for Urban Safety and Security, Kobe University, 7.Graduate School of Frontier Sciences, The University of Tokyo)

[SCG48-P33] Marine electromagnetic observations around a slow earthquake region in the western Nankai trough

*Hiroshi Ichihara[1], Tada-nori Goto[2], Tetsuo Matsuno[3], Noriko Tada[4], Shinya Sato[2] (1.Earthquake and Volcano Research Center, Nagoya University, 2.Graduate School of Engineering, Kyoto University, 3.Ocean Bottom Exploration Center, Kobe University, 4.JAMSTEC)

[SCG48-P34] Dynamics of precipitating injection fronts inside of structured medium

*Yutaka Sumino[1], Shunsuke Tanaka[1], Miyuki Kunihiro[1] (1.Tokyo University of Science)

[SCG48-P35] Permeability changes of simulated low permeable fault rocks induced by intermediate velocity friction test

*Wataru Tanikawa[1] (1.Japan Agency for Marine-Earth Science and Technology, Kochi Instutute for Core Sample Research)

[SCG48-P36] Modified relation between the coupling and tremor rates around the Shikoku region

*Tadafumi Ochi[1] (1.Institute of Earthquake and Volcano Geology, Geological Survey of Japan, The National Institute of Advanced Industrial Science and Technology)

[SCG48-P37] Spatiotemporal distribution of regular and very low-frequency earthquakes in the northern part of the Ryukyu subduction zone

*Youichi Asano[1], Kazuhiko Goto[2], Hiroshi Yakiwara[3], Shuichiro Hirano[3] (1.National Research Institute for Earth Science and Disaster Resilience, 2.Association for the development of earthquake prediction,

3.Nansei-toko Observatory for Earthquakes and Volcanoes, Kagoshima University)

[SCG48-P38] Possible tectonic tremor activities near the VLFE epicenters in the Sanriku-Oki region in 2011

*Hidenobu Takahashi[1], Ryota Hino[1], Yusaku Ohta[1], Naoki Uchida[1], Syuichi Suzuki[1], Masanao Shinohara[2], Takanori Matsuzawa[3] (1.Graduate school of Science Tohoku University , 2.Earthquake Research Institute, University of Tokyo, 3.National Research Institute for Earth Science and Disaster Resilience)

[SCG48-P39] Heterogeneous structure around a region of slow earthquake activity off Ibaraki prefecture along the Japan Trench

*Kimihiro Mochizuki[1], Tomoaki Yamada[1], Masanao Shinohara[1], Ryota Hino[2], Ryosuke Azuma[2], Yoshihiro Ito[3], Yoshio Murai[4], Kenji Uehira[5], Toshinori Sato[6] (1.ERI, Univ. of Tokyo, 2.Graduate School of Science, Tohoku Univ., 3.DPRI, Kyoto Univ., 4.Faculty of Science, Hokkaido Univ., 5.NIED, 6.Graduate School of Science, Chiba Univ.)

[SCG48-P40] Shallow low-frequency tremor triggered by nearby moderate earthquakes off Sanriku

*Sachiko Tanaka[1], Takanori Matsuzawa[1], Youichi Asano[1] (1.National Research Institute for Earth Science and Disaster Resilience)

[SCG48-P41] Slow slip events in the Bungo Channel over 15 years as inferred from GNSS data (1996-2011)

Takatoshi Yokoi[1], *SHINICHI MIYAZAKI[1], Hiromu Sakaue[1], Jun'ichi Fukuda[2] (1.Graduate School of Science, Kyoto University, 2.Earthquake Research Institute, The University of Tokyo)

[SCG48-P42] Investigations of sensor orientation and a possibility of detecting crustal deformation based on accelerometer records of S-net

*Ryota Takagi[1], Naoki Uchida[1], Takashi NAKAYAMA[1], Ryosuke Azuma[1], Akira Ishigami[1], Tomomi Okada[1], Yusaku Ohta[1], Ryota Hino[1] (1.Research Center for Prediction of Earthquakes and Volcanic Eruptions, Graduate School of Science, Tohoku University)

[SCG48-P43] Spatiotemporal variation of released seismic energy from shallow low-frequency tremor in Hyuga-nada, revealed by ocean bottom seismological observation

*Yusuke Yamashita[1], Saki Watanabe[2], Tomoaki Yamada[3], Masanao Shinohara[3], Takeshi Matsushima[2] (1.Disaster Prevention Research Institute, Kyoto University, 2.Institute of Seismology and Volcanology, Kyushu University, 3.Earthquake Research Institute, The University of Tokyo)

[SCG48-P44] Unified description of fast and slow earthquakes using velocity strengthening patches

*So Ozawa[1], Takahiro Hatano[1] (1.Earthquake Research Institute, the University of Tokyo)

[SCG48-P45] The b-value of the earthquake swarm activities accompanied by the Boso slow slip events

*Yuki Noda[1], Hitoshi Hirose[2,1] (1.Department of Planetology, Faculty of Science, Kobe University , 2.Research Center for Urban Safety and Security, Kobe University)

[SCG48-P46] **Three-dimensional thermal modeling associated with subduction of the Philippine Sea plate at the Ryukyu Trench, and its relation to the occurrence of interplate seismic events**

*Nobuaki Suenaga[1], Shoichi Yoshioka[2,1], Yinfeng Ji[3] (1.Graduate School of Science, Kobe University, Japan, 2.Research Center for Urban Safety and Security, Kobe University, Japan, 3.Chinese Academy of Science, Beijin, China)

Off the Kii Peninsula Shallow Low Frequency Earthquake in 2004 revealed by Ocean Bottom Seismometer

*Koji Tamaribuchi[1], Akio Kobayashi[1], Takahito Nishimiya[1], Satoshi Annoura[2]

1. Meteorological Research Institute, 2. Japan Meteorological Agency

The 2004 off the Kii Peninsula earthquakes (Mj7.1, 7.4) occurred near the Nankai trough axis, southeast off the Kii Peninsula, Japan, on September 5, 2004. After the earthquakes, the Meteorological Research Institute conducted OBS observation to examine the aftershock distribution accurately. Although the analysis was limited to hypocenter relocation of "ordinary aftershocks", no analysis was done for slow events. In this study, it is shown that many low-frequency earthquakes (LFEs) occurred in "ordinary aftershocks" from the detailed inspection of our observation. During the observation period, the frequency of LFE gradually decreased. Since P- and S-arrival times are unclear, it is difficult to determine the distribution of the hypocenter accurately. However, by using the Amplitude Source Location (ASL; Battaglia and Aki, 2003), the LFEs are located between a splay fault and trench axis. The 2004 OBS stations are located east of the DONET, and many LFEs are detected in the 2004 OBS network. In addition, there are many very-low-frequency events (VLFEs) in the F-net waveforms with very-low-frequency band-pass filter (0.02 - 0.05 Hz) during the observation period. We found that the identified LFEs were associated with VLFEs since their amplitudes seemed to be correlated. This means that the LFEs and VLFEs show the same phenomenon. Our observations might contribute to reveal the relationship between ordinary aftershocks, slow-events, and megathrust events such as Nankai trough earthquake.

Keywords: LFE, OBS, 2004 off the Kii Peninsula earthquakes

©2019. Japan Geoscience Union. All Right Reserved.

The development of pressure vessel on gouges for rock deformation at seismic rates under water-saturated conditions

*Wei-Ting Lin[1], Li-Wei Kuo[1], Wen-Jie Wu[1], Jia-Jyun Dong[1], Yi-Hung Huang[2]

1. National Central University, 2. MATSUKI HYDRAULIC INDUSTRIAL CO. LTD

To understand earthquake mechanism and fault behavior during earthquake ruptures, experimentalists commonly conduct rock deformation tests with rotary shear apparatus (e.g., low-to high-velocity rock friction experiment, LHVR) which allow deformed at seismic rates. In general, the materials utilized for rotary shear apparatus are both cohesive rocks (e.g., gabbro and carbonate) and incohesive rocks (natural fault gouges and synthetic rock powders), while the latter are deformed at seismic rates and, commonly at low normal stresses (0.5 to 2 MPa confining with a plastic Teflon ring). However, using Teflon rings has issues of gouge extrusion and chemical contamination, in particular, at high normal stresses (>3MPa) and water-saturated condition, and the obtained mechanical data and associated experimental products seem to be questionable. Here we develop a metal pressure vessel for LHVR to deform gouges at seismic rates and, importantly, expand the normal stress capability (up to 15 MPa) and under water-saturated condition. Our results show the resistance from the pressure vessel itself (metal-to-metal contact) is extremely low (friction coefficient ≈0.02), and the result of kaolinite is similar to the previously published data. In particular, both gouge-extrusion and water-leaking was not observed deformed at a normal stress of 15 MPa and equivalent velocity 1 m/s. The designed pressure vessel could fill the gap of experimental conditions among the current used pressure vessels and complete the understanding of fault ruptures.

Keywords: pressure vessel, water-saturated condition, fault gouge, rotary shear experiment

©2019. Japan Geoscience Union. All Right Reserved.

Spatial variations of shallow very low-frequency earthquake activity along the Nankai Trough based on CMT inversion using the 3D heterogeneous model

*Shunsuke Takemura[1], Takanori Matsuzawa[1], Akemi Noda[1], Takashi Tonegawa[2], Youichi Asano[1], Takeshi Kimura[1], Katsuhiko Shiomi[1]

1. National Research Institute for Earth Science and Disaster Resilience, 2. Japan Agency for Marine-Earth Science and Technology

To reveal structural properties around the Philippine Sea plate boundary, we investigated spatial variation of shallow very low-frequency earthquake (SVLFE) activity along the Nankai Trough. By using F-net velocity seismograms for periods of 20-50s, we conducted centroid moment tensor (CMT) inversion of SVLFEs detected by array analysis of Asano et al. (2008 EPS). Our CMT method is basically same as in Takemura et al. (2018 GRL). Source grids were assumed on the boundary of the Philippine Sea plate at horizontal intervals of 0.1°. Green's functions from source grids to F-net stations were evaluated by finite-difference method simulations of seismic wave propagation within the 3D heterogeneous structure model of Takemura et al. (2019 PAGEOPH).

We applied our CMT method to SVLFEs occurred from June 2003 to May 2018. Almost of CMT solutions are low-angle thrust faulting mechanism occurred around the accretionary prism toe. We evaluated spatial variations of SVLFE activity along the Nankai trough by calculating cumulative moment at each source grid. The areas with large cumulative moments appeared near the trench axis of off the Cape Muroto, the Kii Channel and the southeastern Kii Peninsula. We found spatial correlations between cumulative moment, slip-deficit rate (Noda et al. 2018 JGR) and *S*-wave velocities (Tonegawa et al. 2017 Nature Comm.) around the Philippine Sea plate boundary. Such spatial correlations suggest that SVLFEs are effectively activated by mechanically weakening due to pore fluid at surrounding area of strongly locked zone of the Philippine Sea plate.

Acknowledgement
NIED F-net broadband velocity seismograms were used. The catalogs of slow earthquakes were downloaded from the website of slow earthquake database (Kano et al., 2018 SRL). Finite-different method simulations were conducted on the Earth Simulator at the JAMSTEC.

Keywords: Nankai Trough, Shallow very low-frequency earthquake, CMT inversion, Pore fluid pressure, Slip deficit rate

©2019. Japan Geoscience Union. All Right Reserved.

Evaluation of Magnitude and Characteristics of Seismicity of Low Frequency Earthquakes in Parkfield

*Miki Aso[1,3], Naofumi Aso[2], Satoshi Ide[1]

1. Department of Earth and Planetary Science, The University of Tokyo, 2. Tokyo Institute of Technology, School of Science, 3. OYO RMS Corporation

Over a million tectonic low frequency earthquakes (LFEs) have been found in Parkfield along the San Andreas Fault, as 88 families by Shelly and Hardebeck [2010]. Thanks to enormous event detection, interesting characteristics focusing on their event amplitudes have been reported such as the spatial variation along the fault, the exponential frequency distribution for each family, and the relationship with recurrence time [Shelly and Hardebeck, 2010; Shelly, 2010]. However, the relative size of families has not been quantified accurately, because we have to consider various factors such as radiation pattern depending on focal mechanisms, attenuation during wave propagation, and site amplification effects. For quantitative comparison of scale among differently located events, here we estimate the absolute magnitude of each event considered those effects.

We estimate the seismic moment Mo [Nm] and moment magnitude Mw of all LFE events in the catalog of Shelly [2017]. We first stack seismograms of over one million events in the catalog to improve the signal-to-noise (S/N) ratio. Then, we evaluate the absolute amplitude of the original seismograms using the stacked waveforms. Specifically, we evaluate seismic moment Mo by assuming focal mechanisms of each family, attenuation quality factor, site effect estimated by Aso et al. [2019, submitted to JpGU meeting, “Variations of Focal Mechanisms of Low Frequency Earthquake in Parkfield”], and the source time function estimated by Thomas et al. [2016]. Note that we consider the frequency-limited seismic moment Mo, though it is not exactly the same as the original definition of seismic moment measured at a lower frequency than the minimum frequency contained in one phenomenon.

As previously reported by reported by Shelly and Hardebeck [2010], LFEs in the southern part has larger magnitude. We also find that shallower events are smaller than deeper events.

Similarly, most of the frequency distribution for each family shows an exponential distribution which is also reported for LFEs in Cascadia [Sweet et al., 2014] and New Zealand [Chamberlain et al., 2014].

By comparing size and recurrence interval, the events during LFE burst (seconds interval) tend to be larger than the first event of burst, which occurs after hours-to-days quiescence. A similar tendency is found in tremor burst occurring with a longer time scale (~1-week-long) than that of LFEs (~1-minute-long) [Yabe and Ide, 2014]. These might suggest some temporal change in fault rheology and/or some characteristic spatiotemporal behavior such as Brownian slow earthquake processes [Ide, 2008].

Keywords: San Andreas Fault, Parkfield, seismicity, waveform stacking, low frequency earthquake, amplitude evaluation

©2019. Japan Geoscience Union. All Right Reserved.

Tectonic tremor catalog in the Tohoku-Hokkaido-Oki region using S-net

*Satoshi Ide[1], Tomoaki Nishikawa[2], Takanori Matsuzawa[3], Kazuaki Ohta[2], Naoki Uchida[4], Takuya NISHIMURA[2]

1. Department of Earth an Planetary Science, University of Tokyo, 2. Disaster Prevention Research Institute, Kyoto University, 3. National Research Institute for Earth Science and Disaster Resilience, 4. Graduate School of Science and International Research Institute of Disaster Science, Tohoku University

Recently, various slow earthquakes have discovered in the subduction zone off Tohoku and Hokkaido regions along the Japan Trench. In this presentation, we report the detection of tectonic tremors using the Seafloor Observation Network for Earthquakes and Tsunamis along the Japan Trench (S-net), operated by The National Research Institute for Earth Science and Disaster Resilience (NIED).

We used continuous seismograms from August 2016 to August 2018 recorded by short-period sensors at 150 S-net stations. The original data were converted to envelope waveforms and analyzed using the envelope correlation method coded by Ide (2010), for each 300 s time windows with 150 s overlap. Since the results included many ordinary earthquakes with short durations, we regarded the events with durations longer than 20 s as tremors. This number is twice longer than that used for deep tremors in western Japan, reflecting the long-lasting waves in ocean bottom observation.

We found that the detection completeness is not high due to the high seismic activity in the Japan Trench, especially after the occurrence of large earthquakes, with numerous aftershocks falsely detected. We therefore divided the study area into 18 overlapping sub-regions that cover the locations of tremor activity to solve this problem. We detected tremors in each sub-region and merged the results into one catalogue by removing one of any two events within 10 s and 1 degree of each other, depending on their root-mean-square errors. Some tremor-like signals were found near the triple junction off the Boso Peninsula at approximately 34.8˚N. However, visual inspection revealed these events to be ordinary earthquakes, which we excluded from our tremor catalogue. The resultant tremor catalogue will be available in Slow Earthquake Database (Kano et al., 2018).

Keywords: tectonic tremor, slow earthquake, ocean bottom seismometer, S-net, Japan trench

©2019. Japan Geoscience Union. All Right Reserved.

Spontaneous Slow Slip and Runaway Slip in Laboratory

*Miki Takahashi[1]

1. Institute of Earthquake and Volcano Geology, Geological Survey of Japan, AIST

Earthquake nucleation and propagation involves the acceleration of slip on a fault from a background, quasi-static, low-velocity state towards meter-per-second values. From shear experiments using brine-saturated simulated gouge composed of 80:20 wt.% mixtures of halite and muscovite (following e.g. Niemeijer & Spiers, 2007, JGR), Takahashi et al., [2017, G-cubed] recently reported a switch in the dominant deformation process, from distributed viscous flow (pressure solution creep) to localized brittle deformation, at a critical velocity V_c (~20 μm/sec). The direct effect which is normally observed upon perturbations in sliding rate disappears for $V > V_c$, suggesting that runaway fault-slip may be achieved when the sliding velocity exceeds V_c.
At relatively low shear stress, flow mechanisms, such as pressure solution creep and dislocation creep, will be fast enough to effectively suppress slip acceleration. However, with increasing the shear stress, there may be a velocity range in which flow mechanisms still works but not as effective. Hypothesizing that, under constant shear stress boundary conditions, this may lead to spontaneous acceleration followed by deceleration, analogous to a slow slip event. Moreover, imposing the constant shear stress with equal or larger value of the maximum strength of the simulated gouge, I also hypothesize that slip acceleration may proceed as $V > V_c$, inducing a dynamic weakening.
To address these hypotheses, I conducted torque-controlled rotary shear experiments, using brine-saturated, 80:20 wt % mixtures of halite (grain size < 75 μm) and muscovite (grain size < 33 μm) powders. Approximately 1.65 g of the gouge mixture was sandwiched between two teethed steel piston rings, forming an initially 1 mm thick layer. The piston rings had an inner diameter of 38 mm, and an outer diameter of 50 mm. I used a high-velocity rotary shear apparatus designed by T. Shimamoto [e.g., Togo and Shimamoto, 2012], and now installed at the Geological Survey of Japan (GSJ). The apparatus was modified to enable torque control with an accuracy of ±0.002 in the friction coefficient (μ), at a normal stress of 5 MPa. Rotation displacement is measured using a potentiometer installed close to the piston ring at the rotating side.
A preliminary result shows the velocity evolution after stepwise changes in the shear stress. At low shear stresses, corresponding to the pressure solution creep-controlled regime, transient increasing velocity towards a steady-state values suggests stable sliding. At $\mu \approx 0.6$, the simulated gouge shows spontaneous acceleration to $V \approx 1$ μm/sec, followed by deceleration. Lastly, under a constant shear stress condition equivalent to $\mu = 0.67$, spontaneous slip acceleration occurred followed by dynamic weakening at $V \approx V_c = 20$ μm/sec. More experiments and microstructural observations will help to elucidate the relationship between the critical velocity and the switch among dominant deformation mechanisms.

Keywords: shear stress control test, spontaneous acceleration/deceleration, dynamic weakening

©2019. Japan Geoscience Union. All Right Reserved.

Hydration and amorphization of quartz rocks during high-velocity frictional sliding: An examination of fault gouge from friction experiments of synthetic quartz

*Yuko Onoe[1], Hirotaka Iida[2], Akito Tsutsumi[1], Aki Takigawa[1]

1. Graduate School of Science, Kyoto University, 2. Geothermal Engineering Co., Ltd.

Various types of rocks and fault gouges display weakening of frictional strength at high-velocities, and in many cases, it is caused by high-temperature faulting processes such as frictional melting and thermal decomposition of fault materials. On the other hand, siliceous rocks display weakening of frictional strength at relatively slow slip velocity of ~1 mm/s. This weakening is a specific phenomenon because frictional heat is not sufficient to induce the high-temperature transformation reactions in this slip velocity range [Di Toro et al., 2004]. Goldsby and Tullis [2002] proposed gel lubrication model to explain the weakening of siliceous rocks; in which model frictional weakening likely results from production and shearing of hydrated amorphous silica layer along a fault in quartz rocks. But the relationship between the frictional weakening and hydration and amorphization of fault gouge is not clear yet.

This study aims to elucidate the mechanism of the frictional weakening observed for siliceous rocks. We conducted a series of friction experiments on synthetic quartz samples using a rotary-shear, intermediate-to high-velocity friction testing machine. Experiments were carried out under a constant normal stress condition of 1.5 MPa and at slip velocities of 5 μm/s, 10 μm/s, 105 μm/s, 1 mm/s, 10 mm/s and 105 mm/s. In this study effect of drying the sample on the frictional behavior were examined by introducing dry air to the chamber of the sample. After the friction tests, the gouge material on the slip surfaces were collected and analyzed by FTIR.

The frictional behavior of the synthetic quartz differs between room humidity and dry conditions; velocity weakening was observed for both conditions, however, velocity weakening starts at lower slip velocities for the dry experiments. Under DRY conditions, the frictional weakening occurs at slip velocity around 10 μm/s. From the results of the FTIR analysis, hydration of the gouge is confirmed for all the samples tested in this study. The FTIR result also indicates that the faster the slip velocity, the more the crystal structure of the gouge is destructed.
It is showed that under both DRY and Room Humidity conditions, at least the gouge generated on the friction surface of the sample which showed slip weakening is hydrated, consistent with the weakening model of Goldsby and Tullis [2002].

©2019. Japan Geoscience Union. All Right Reserved.

Constraining S Wave Velocity of the Source Region of Shallow Very Low-Frequency Earthquakes

*Takeshi Akuhara[1], Takashi Tonegawa[2]

1. Earthquake Research Institute, The University of Tokyo, 2. Research and Development center for Earthquake and Tsunami, Japan Agency for Marine-Earth Science and Technology

Shallow very low-frequency earthquakes (VLFEs), which are believed to occur in the vicinity of megathrusts, have been often associated with elevated pore fluid pressure. Lines of evidence for this idea include a small amount of stress drop, high tidal sensitivity, and reduced P wave velocity inferred from active source seismic surveys. Revealing the physical properties of the source region of shallow VLFEs will lead to a better understanding of their generation mechanisms. However, the challenge lies in the difficulty of acquiring S wave velocity in fine resolution.

Recent achievements by the authors may help overcome this issue. Akuhara et al. (2019) developed a robust technique to estimate Green's functions of receiver side structures from offshore seismograms, which are typically ill-conditioned due to water reverberations. Tonegawa et al. (2017) inverted Rayleigh wave admittance (i.e., a ratio of ground displacement to hydraulic pressure) for shallow S wave velocity structures beneath DONET seafloor observatories at the Nankai Trough subduction zone. Their velocity models show low-velocity zones that characterize the source regions of shallow VLFEs. However, a smoothing constraint imposed on the models renders their interpretation somewhat difficult.

This study presents preliminary results from transdimensional inversion of receiver-side Green's function estimated by the method of Akuhara et al. (2019), where we adopt a prior constraint by the velocity models of Tonegawa et al. (2017). Complementary to the Rayleigh admittance, the Green's function approach is sensitive to velocity contrasts and thus will offer an improved resolution.

Keywords: shallow very low frequency earthquake, seismic velocity structure, ocean bottom seismometer, bayesian analysis

©2019. Japan Geoscience Union. All Right Reserved.

Quantitative relationship between aseismic slip propagation speed and frictional properties

*Keisuke Ariyoshi[1], Jean-Paul Ampuero[2,3], Roland Burgmann[4], Toru Matsuzawa[5], Akira Hasegawa[5], Ryota Hino[5], Takane Hori[1]

1. Japan Agency for Marine-Earth Science and Technology, 2. Université Côte d'Azur, 3. California Institute of Technology, 4. University of California, Berkeley, 5. Graduate School of Science, Tohoku University

Recent observations show evidence of propagation of postseismic slip, whose propagation speed may contain information about the mechanical properties of faults. Here, we develop a new analytical relationship between the propagation speed of aseismic slip transients and fault frictional properties, modeled by a rate- and state-dependent friction law. The relationship explains the propagation speed of afterslip in 3-D numerical simulations to first order. Based on this relationship, we identify systematic dependencies of afterslip propagation speed on effective normal stress σ and frictional properties (the coefficients a and a-b which quantify the instantaneous and the steady-state velocity-dependence of friction, respectively, and the characteristic slip distance d_c of fault state evolution). Lower values of the parameter $A=a\sigma$ cause faster propagation in areas where the passage of the postseismic slip front induces large shear stress changes $\Delta\tau$ compared to A, which are typically located near the mainshock rupture. In areas where $\Delta\tau/A$ is small, typically more distant from the mainshock, afterslip propagation speed is more sensitive to (a-b) σ. The propagation speed is proportional to initial slip velocity and inversely proportional to d_c. The relationship developed here should be useful to constrain the frictional properties of faults based on observed propagation speeds, independently of rock laboratory experiments, which can then be used in predictive numerical simulations of aseismic slip phenomena.

Keywords: rate- and state-dependent friction, effective normal stress, stress perturbation

©2019. Japan Geoscience Union. All Right Reserved.

Comprehensive detection of very low frequency earthquakes off the Pacific coasts of Hokkaido and Tohoku, northeastern Japan

*Satoru Baba[1], Akiko Takeo[1], Kazushige Obara[1], Takanori Matsuzawa[2], Takuto Maeda[3]

1. Earthquake Research Institute, University of Tokyo, 2. National Research Institute for Earth Science and Disaster Resilience, 3. Graduate School of Science and Technology, Hirosaki University

Very low frequency earthquakes (VLFEs), classified as one type of slow earthquakes, occur near seismogenic zones. VLFEs off the Pacific coasts of Hokkaido and Tohoku in northeastern Japan occur around subducting plate interfaces near trenches. Asano et al. (2008) found VLFEs in the off-Tokachi region, the southern part of the Pacific coast of Hokkaido along the Kuril Trench, by array signal processing using high-sensitivity accelerometers of Hi-net operated by National Research Institute for Earth Science and Disaster Resilience (NIED). In recent years, VLFEs off the Pacific coast of Tohoku were found by visually checking broadband seismograms of F-net operated by NIED and other events were detected by the matched-filter technique using waveforms of detected events as templates (Matsuzawa et al., 2015). However, the number of detected VLFEs may have been limited because of the small number of the VLFE templates in previous studies. Baba et al. (2018, SSJ) set four virtual epicenters off the Pacific coasts of Hokkaido and Tohoku and detected VLFEs by the matched-filter technique using numerically simulated waveforms as templates. We extended virtual epicentral gridsto make more comprehensive detection of VLFEs.

We used continuous seismograms of F-net seismometers from January 2003 to July 2018 after applying a band-pass filter of 0.02–0.05 Hz. We set 123 virtual epicentral grids off the Pacific coasts of Hokkaido and Tohoku, and computed the synthetic waveform from the source at each virtual epicenter by the finite difference method with a three-dimensional velocity structure model, namely, Japan Integrated Velocity Structure Model (Koketsu et al., 2012). The fault mechanisms were assumed to be consistent with the geometry of the plate boundary and a plate motion model, NUVEL-1A. We then calculated station- and component-averaged cross-correlation coefficients (averaged CC) between synthetic waveforms and the data of F-net seismograms every 1 s, and selected the events which have averaged CC above nine times of the median absolute deviation of the distribution. This method is, however, sensitive to regular earthquakes and teleseismic events as well. We then excluded the signal of regular earthquakes by discarding events with the amplitudes of more than 160 nm/s at 1-2 Hz in vertical components at the nearest stations. Moreover, to remove teleseismic events, we used the USGS earthquake catalog and discarded events with high amplitudes and low averaged cross-correlation coefficients.

VLFE activities in the off-Tokachi and off-Aomori regions show synchronized episodic bursts in the interval of several months. VLFEs in the off-Tokachi region was rapidly increased by the afterslip of the 2003 Tokachi-Oki earthquake. Those in the off-Iwate and off-Ibaraki regions, located out of the coseismic slip area of the 2011 off the Pacific coast of Tohoku Earthquake (hereinafter, the Tohoku earthquake), were also rapidly increased by the afterslip of the Tohoku earthquake. VLFE activity in the off-Miyagi region is characterized by episodic bursts in the interval of several months to one year before the Tohoku earthquake, but it became low since then. VLFE activity in the off-Fukushima region show dramatic increase after an Mw 6.9 earthquake at off-Fukushima on July 19, 2008. In the off-Miyagi and off-Fukushima regions, located within or at the edge of the coseismic slip area of the Tohoku earthquake, VLFE activity has been low since the Tohoku earthquake probably because the earthquake released the

©2019. Japan Geoscience Union. All Right Reserved.

stress almost completely. These results suggest that VLFEs are sensitive to the stress perturbation and can be a slip meter that reflect spatiotemporal change of the interplate slip, as has been indicated by previous studies. Consequently, one possible cause of these episodic VLFE bursts in the off-Tokachi, off-Aomori and off-Miyagi regions may be the intermittent release of small portion of stress accumulated by interplate locking between plates in the interval of several months to one year. The interval of episodic bursts is shorter than a periodicity of slow slips ranging from 1 to 6 years off the Pacific coasts of Tohoku indicated by Uchida et al. (2016).

©2019. Japan Geoscience Union. All Right Reserved.

Spatio-temporal evolution of long- and short-term slow slip events in the Tokai region, central Japan estimated from a very dense GNSS network, during 1997-2017

*Hiromu Sakaue[1], Takuya NISHIMURA[2], Jun'ichi Fukuda[3], Teruyuki Kato[4]

1. Graduate School of Science, Kyoto University, 2. Disaster Prevention Research Institute Kyoto University, 3. Earthquake Research Institute,The University of Tokyo, 4. Hot Springs Research Institute of Kanagawa Prefecture

The long-term slow slip events (SSEs) have been reported on the subducting Philippine Sea Plate in the Tokai region, central Japan during 2001-2005 and 2013-2016. Many short-term slow slip events have been also observed there since 1996. We analyzed GNSS data from 1997 to 2017 to estimate spatiotemporal distribution of interplate slip associated with these SSEs in this study. The GIPSY-OASIS II software (version 6.1) was used to estimate daily coordinates of GNSS stations operated by GSI and JUNCO (the Japanese University Consortium for GPS Research). It is well known that GNSS time series have many systematic signals and noises that do not result from SSEs. They include, for example, seasonal variations, co- and post-seismic deformation of the 2004 southeast off Kii Peninsula earthquakes (M_w 7.3/7.4), the 2008 Ibaraki-ken-oki earthquake (M_w6.9), the 2008 Fukushima-ken-oki earthquake (M_w7.0) and the 2011 Tohoku-oki earthquake (M_w9.0), and crustal deformation of volcanic activity on the northern Izu Islands in 2000. After removing them, we applied a modified Network Inversion Filter (NIF) [Fukuda et al., 2008] to estimate daily slip and slip rate on the subduction plate interface.
Our results suggest that not only long-term SSEs (M_w~7.1 and M_w~6.7) in 2000-2005 and 2013-2016, but also short-term SSEs (M_w<6.1). The maximum estimated daily slip rates for short-term SSEs are an order of magnitude larger than those of the long-term SSE, and peak slip for short-term SSEs migrates along strike with LFTs synchronously. It suggests that LFTs are loaded directly by SSEs, and that slip rate regulates LFT genesis. We will present the change of back slip rate between inter short-term SSEs and characteristics of short-term SSEs (e.g. slip rates and recurrence interval) depending on the occurrence of long-term SSE.

Keywords: slow slip event, Tokai region, GNSS

©2019. Japan Geoscience Union. All Right Reserved.

Broadband excitation of acoustic emission in granular stick-slip : experiments and spectral analyses

*Hidekazu Fukumizu[1], Ikuro Sumita[2]

1. Earth and Environmental Science Course, Division of Natural System, Graduate school of Natural Science and Technology, Kanazawa University, 2. School of Geosciences and Civil Engineering, Kanazawa University

Slow slip and tremor are observed to occur simultaneously (e.g., Rogers and Dragert, Science, 2003). Such observation can be modelled using granular stick-slip experiments which show that the timing of the slips and acoustic emission (AE) are well correlated (e.g., Johnson et al., GRL, 2013, Jiang et al. GRL, 2017). AE waveforms are complex (e.g., Michlmayr & Or, Gran. Matt., 2014), and we do not fully understand the details of the temporal change of AE during the slip. Here we report the results of granular stick-slip experiments which focus on how their spectra depend on the shear rate, particle size and container size.

We shear glass beads contained in a stainless steel beaker using a rotating viscometer to which a vane spindle is attached (Higashi and Sumita, JGR, 2009), and measure the shear stress and AE at 200kHz. We use broadband accelerometers and microphones to measure AE. Four accelerometers are attached at the outer rim of the beaker, and each are separated by an angle of 90 degrees.

We integrate the acceleration to obtain AE velocity –time series data and analyze their characteristics in broad band. We find that although AE has a broad spectrum, the spectra show that there are two characteristic frequency (f) components ; a high-f (of the order of 100 Hz) and a low-f (of the order of 10Hz) components. The velocity waveforms recorded at antipodal positions, show that the high-f components are in phase, whereas the low-f components are of the opposite phase. This indicates that the mechanism which excite these components differ : the high-f component may correspond to AE excited by particle rearrangement, whereas the low-f component may correspond to the translational motion of the container. Indeed we find that the frequency of the low-f component depends on the container size.

We also conducted experiments using a rheometer in a parallel-plate setup and confirmed that these two different components exist. When the particle size becomes larger, the amplitude of the shear stress and the AE velocity increases. Furthermore we find that the mean frequency of the normalized power spectra rose to a higher frequency, thus correlating with the stress increase.

Our experiments indicate that AE is excited in broadband, and that their frequency components can be used to infer the interparticle stress. Such excitation appear to be analogous to tremors and very low frequency earthquakes that are also excited simultaneously.

Keywords: granular matter, stick-slip, acoustic emission, earthquake, tremor

©2019. Japan Geoscience Union. All Right Reserved.

Episodic tremor and slip silently invades strongly locked megathrust in the Nankai Trough

*Masayuki Kano[1], Aitaro Kato[2], Kazushige Obara[2]

1. Graduate school of science, Tohoku University, 2. Earthquake Research Institute, The University of Tokyo

Recent seismic and geodetic observations in subduction zones have revealed that slow earthquakes have preceded some large earthquakes (e.g., Kato et al., 2012; Mavrommatis et al., 2014; Ruiz et al., 2014). Characterization of slow earthquakes and their relation to large earthquakes provides important clues to constrain a wide spectrum of slip rates on tectonic faults. In this study, we report new evidence of a slow slip transient at the downdip edge of the strongly locked seismogenic zone in the western Nankai Trough in southwest Japan based on GNSS time series. This slow slip transient was remotely excited during an episodic tremor and slip at the downdip extension of the locked zone. Through this remote triggering, the frequent occurrence of the deep episodic tremor and slip invades the strongly locked megathrust zone and may intermittently increase the probability of large earthquakes in the Nankai Trough.

Acknowledgments

We used GNSS data provided by the Geospatial Information Authority of Japan. This study was supported by the JSPS KAKENHI Grant Number JP15K17743 in Grant-in-Aid for Young Scientists (B), JP18K03796 in Grant-in-Aid for Scientific Research (C), JP16H06473 and JP16H06474 in Scientific Research on Innovative Areas “Science of Slow Earthquakes.”

Keywords: Slow slip events, Slow earthquakes, Western Shikoku, GNSS

©2019. Japan Geoscience Union. All Right Reserved.

Spatial distribution of the electrical resistivity beneath western part of Shikoku Island where long-term SSE events have repeatedly occurred

*Makoto Uyeshima[1], Maki Hata[1], Hiroshi Ichihara[2], Ryokei Yoshimura[3], Koki Aizawa[4]

1. Earthquake Research Institute, The University of Tokyo, 2. Graduate School of Environmental Studies, Nagoya University, 3. Disaster Prevention Research Institute, Kyoto University, 4. Institute of Seismology and Volcanology, Faculty of Sciences, Kyushu University

In the Bungo channel area at the western margin of the Nankai megathrust rupture zones, the long-term slow slip events (SSE) repeatedly occurred about every 6 or 7 years. Since the last large-scale SSE event occurred in 2010, we will have a next large event soon. In order to obtain the electrical resistivity structure in the vicinity of the SSE area and examine its temporal change, we have started the Network-MT survey in the western part of the Shikoku Island facing the Bungo channel since April, 2016. Just before beginning of the observation, a tiny-scale SSE event occurred in the Bungo-channel (Ozawa, 2017, Hirose et al., 2018). We selected 17 areas in the western part of the Shikoku Island and installed 3 or 4 electrodes in the respective areas. The electrical potential differences with typical electrode spacing of several km are measured by using metallic telephone line network. We also measure the geomagnetic field at two stations in the target region. With the aid of the BIRRP code (Chave and Thomson, 2004), we could estimate the frequency-domain Network-MT response functions of good quality between the voltage difference and the magnetic field. The Network-MT response functions were directly inverted to estimate the 3-D resistivity structure in this area with the aid of the DASOCC Network-MT 3-D inversion code (Siripunvaraporn, Uyeshima & Egbert, 2004).

Conductive portions are commonly detected in the mid-crust of the target region. Their roots are just on the upper surface of the subducting Philippine Sea slab. This may suggest dehydration there. Among the spatial distribution of resistivity, that of seismic P-wave attenuation (Kita and Matsubara, 2016), and that of SSE slips (e.g. Ozawa et al., 2013, Yoshioka et al., 2015, Hirose et al., 2018), some mutually related features are detected. Low Qp (high attenuation) areas tend to correspond to highly conductive areas. The low Qp and highly conductive area are detected just above the subducting slab and outside of the SSE area. Inside the SSE area, while Qp takes generally high values, a patchy conductive area is detected in overall resistive background structure.

This study is supported by JSPS KAKENHI Grand Number JP16H06475 in Scientific Research on Innovative Areas "Science of Slow Earthquakes". It is also partly supported by the Ministry of Education, Culture, Sports, Science and Technology (MEXT) of Japan, under its Earthquake and Volcano Hazards Observation and Research Program. We acknowledge staffs of the Nippon Telegraph and Telephone WEST Corporation for their cordial support in the survey. We also thank H. Abe, A. Takeuchi and Y. Suwa for their help in preparing and installing instruments.

Keywords: slow slip event beneath the Bungo Channel, 3-D resistivity structure, Network-MT observation

©2019. Japan Geoscience Union. All Right Reserved.

Variations of scaling relationships for shallow tremor observed along the Nankai trough

*Masaru Nakano[1], Suguru Yabe[1]

1. Japan Agency for Marine-Earth Science and Technology

Scaling relationships of seismic phenomena is one of keys to understand the source processes. Size distributions of slow earthquakes as low-frequency earthquakes (LFEs), non-volcanic tremor (NVT), very-low-frequency earthquakes (VLFE), and slow-slip events (SSEs) have been studied in many locations. Some studies showed that the size distribution follow an exponential law (e.g. Watanabe et al., 2007; Hiramatsu et al., 2008; Chestler and Creager, 2017), while others showed that power law distributions better explain the observations (e.g. Kao et al., 2010; Bostock et al., 2015; Nakamura and Sunagawa, 2015).

Most of previous studies are for slow earthquakes that occur in regions deeper than the source region of megathrust earthquakes, and only a limited number of studies have been carried out for shallow slow earthquakes beneath accretionary prism as observed along the Nankai trough. Although observed characteristics of shallow and deep ones are very similar, physical conditions as temperature and pressure much differs in these region.

In our previous studies (Nakano et al., 2018SSJ, AGU), we obtained the result that shallow tremor follows a power law distribution with b values of about 1. In this study, we further analyzed tremor activities beneath the Muroto fore-arc basin. using data from DONET2. We estimated the seismic energy of tremor signals using the same method as our previous studies, during intensive activities starting in September 2015, April 2016, February 2017, and February 2018. The source region of each activity is different from each other, spanning between off Shiono-Misaki and off Cape Muroto.

The size distribution of each activity mostly follow power-law distributions, but the b value varies from 0.7 and 1.7. We note that the activity in 2016 is also well fitted by an exponential law, probably due to narrow range of observed event size distribution. Similar result has been obtained in the 2018 activity in Kumano. The size distribution deviate from a power law for largest events as observed in Kumano activities. This deviation at larger events would be due to limited system size, expected from the theoretical stochastic model of tremor by Ide and Yabe (2018). The upper limit of event size, and accordingly the system size, varies from activity to activity.

We also investigated the relation between the seismic energy and duration of tremor events. The relation also follows a power law, with slopes of 2.0 to 2.6 in Kumano, and 1.5 to 3.3 in Muroto. These values are again consistent with the expectation value of 2 from the model of Ide and Yabe (2018).

These investigations represent that the scaling relationships of shallow tremor are mostly consistent with the 2D PCA model by Ide and Yabe (2018). Further studies would be necessary to reproduce the observed variations of the scaling parameters.

Acknowledgments: We used DONET data and JMA and USGS earthquake catalogs in the analysis. This research was supported by JSPS KAKENHI Grant Number 16H06477 in Scientific Research on Innovative Areas “Science of Slow Earthquakes”

Keywords: DONET, Nankai trough, earthquake size distributions

©2019. Japan Geoscience Union. All Right Reserved.

Low-frequency earthquakes triggered by teleseismic surface waves by Ryukyu subduction zone.

Ayumi Kinjo[1], *Mamoru Nakamura[1]

1. Faculty of Science, University of the Ryukyus

We investigated low-frequency earthquakes (LFEs) in the Ryukyu Trench region that were triggered by surface waves from teleseismic earthquakes. Although these LFEs in the southwestern Ryukyu arc have previously been explored by Chao et al. (2016), their hypocenter distribution is not known in detail.

We selected 50 earthquakes from January 2004 to December 2016, which had magnitudes greater than 7.5 and epicentral distances between 9–150˚. We used the waveforms of 6 broadband seismometers in the Ryukyu arc from F-net (NIED) to analyze the surface waves. We also used the waveforms of 20 short-period seismometers in the Ryukyu arc from the Japan Meteorological Agency to detect trace LFEs in Ryukyu Island and determine their hypocenters.

The LFEs in the Yaeyama and Okinawa regions were observed. In the former region, during the passage of the surface waves, spindle-shaped LFE waveforms were first observed at Hateruma (south of Yaeyama Islands), and later at other stations in the Yaeyama region. Similarly, for the latter region, during the passage of the surface waves, spindle-shaped LFE waveforms were first observed at ZMM or Tamagusuku (south of Okinawa Island), and later at other stations in the Okinawa region. These observations suggest that the sources of the triggered LFEs were near or south of Hateruma and Tamagusuku.

We subsequently determined the hypocenters of the triggered LFEs. We computed the LFE travel-time difference between two stations using cross-correlations of the waveforms (Obara, 2002). The travel-time difference of waveforms of the LFEs corresponded to travel-time difference of the S-phase because S-waves were dominant in the LFEs, and P-waves were weak. The hypocenters were determined using the grid search method (Chao et al., 2013). In the Yaeyama region, the LFE hypocenters were mainly distributed near Hateruma Island. In the Okinawa region, they were distributed south of Okinawa Island. These positions are similar to the positions of the LFE hypocenters that accompany very low frequency earthquakes (LFE-VLFEs). This suggests that faulting in a cluster of LFE-VLFEs would be active with dynamic stress change.

In the Okinawa and Yaeyama regions, LFEs are triggered when the peak ground velocity of the surface wave is greater than 0.1 cm/s. This threshold value is similar to that for LFEs in Taiwan (Chao et al., 2013), suggesting that the weak friction coefficient at the plate interface of the Ryukyu Trench is similar to that in Taiwan.

Keywords: low frequency earthquake, surface wave, Ryukyu Trench

©2019. Japan Geoscience Union. All Right Reserved.

Detection of small surface displacement accompanying deep low-frequency tremor in Shikoku region, southwest Japan

*Yutaro Okada[1], Takao Tabei[2]

1. Faculty of Science, Kochi University, 2. Faculty of Science and Technology, Kochi University

In many subduction zones in the world, several types of slow earthquakes occur with different depths on the plate interface and some of them are accompanied by surface displacement. In this study, we focus on small surface displacements coincident with non-volcanic deep low-frequency tremor in Shikoku region in the Nankai subduction zone, southwest Japan.

We use daily coordinates time series from 107 GEONET stations located in Shikoku and tremor catalog compiled by NIED (Maeda and Obara, 2009; Obara et al., 2010) in the period from Jan. 1 2004 to Dec. 31 2008. Since GNSS coordinates changes due to the Bungo Channel long-term slow slip events are well reproduced by S-shaped logistic function, we use the same function to extract small displacement coincident with tremor activity. At first, we convert horizonal components into N50°W direction after removing annual and semiannual variations and common-mode errors. Next, we fit the logistic function to a data segment with variable time window of 5, 7, and 9 days and estimate an amplitude of the function. The fitting is checked by a correlation coefficient between the observation and calculation. We apply this fitting for entire data period at all stations sliding data segment. Finally, we extract displacement when the amplitude of the fitted logistic function exceeds a certain criterion (1.8 mm in this study) and the correlation coefficient is large enough. If the extracted displacement is coincident with tremor activity within 30 m from the GNSS station, we adopt it as the tremor-related displacement. As a result, 225 events are adopted.

Spatial pattern of the tremor-related displacement seems to be related with the location and mechanism of the tremor event though closer inspection is needed. However, we extract much more small displacements by fitting a logistic function, of which the source is unknown. The logistic function is effective to reproduce transient displacement of the surface but we need to reconsider noise reduction of GNSS time series, time constant of logistic function, time window of the fitting, and so on.

Keywords: GNSS, southwest Japan, Deep low frequency tremor

©2019. Japan Geoscience Union. All Right Reserved.

Long-term temporal change in crustal resistivity beneath western Shikoku

*Futoshi Yamashita[1], Yoshimori Honkura[1]

1. National Research Institute for Earth Science and Disaster Resilience

In southwest Japan, various slow earthquakes such as deep low-frequency tremor and short/long-term slow slip events occur at the subducting plate interface (e.g. Obara and Kato, 2016, Scinence). In western Shikoku, Magneto-telluric (MT) survey was carried out along the dip direction of subducting Philippine Sea plate. The survey revealed an existence of low-resistivity structure in the lower crust in this region (Yamashita and Obara, 2009, AGU). In order to investigate a relationship between this characteristic structure and the activity of slow earthquakes, NIED has been carrying out continuous MT observations in western Shikoku since 2008. Here we show the observational records over 10 years and then discuss a relationship between observed temporal change in crustal resistivity and activity of the long-term slow slip event (L-SSE). Two observational sites KBN and IKT are available as of 2019. Qualities of data recorded at these sites are relatively fine. However, in order to improve the quality for discussing subtle change in MT parameters, we apply a data processing method same as Honkura *et al.* (2013, Nature comm.); we use only data whose coherency between electric and magnetic field is higher than a threshold. The lowest frequency of processed data is 0.00028 Hz. The processed MT parameters, apparent resistivity and phase, do not show any long-term temporal changes at KBN site even after temporal stops of observation over some months. On the other hand, apparent resistivity at IKT site, which is around 10 km southwest away from KBN site, shows temporal reduction at a frequency lower than 0.0022 Hz between 2010 and the middle of 2012. It is known that L-SSE occurred beneath the Bungo Channel in 2010 (e.g. Yoshioka *et al.*, 2015, GJI), which could induce resistivity change in the lower crust and then it might be detected by our MT observation.

Keywords: Crustal resistivity, Long-term slow slip event, Magneto-telluric method

©2019. Japan Geoscience Union. All Right Reserved.

Slow decay of postseismic deformation compared with aftershocks following the 2011 Tohoku-oki Earthquake

*Yuta Mitsui[1], Shunsuke Morikami[2]

1. Department of Geosciences, Shizuoka University, 2. Formerly at Graduate School of Science and Technology, Shizuoka University

In the literature, decays of postseismic deformation rates of large earthquakes were almost comparable to aftershock decays for subduction earthquakes (e.g. Hsu et al. (2006), Lange et al. (2014)). They are characterized by the modified Omori law with p~1, which means "afterslip-triggerred aftershocks". In this study, we focus on the 2011 Tohoku-oki megathrust earthquake using GNSS and seismicity data. On the basis of high-rate analysis of RINEX data and the F3 solution provided by the Geographical Survey Institute (GSI), we clarify the characteristics of postseismic deformation and aftershocks up to five orders of magnitude of time scale. We find that the p value for the postseismic deformation (p_m) is ~0.7, by contrast, that for the aftershocks (p_n) is ~1. Because a rate-and-state-friction model (Helmstetter and Shaw (2009)) predicted $p_m>=p_n$, another or an additional physical mechanism is necessary to explain the data of $p_m<p_n$. One important mechanism is viscoelastic relaxation of asthenosphere, thus we try fitting the postseismic deformation data by combination of afterslip and viscoelastic relaxation (a model of Suito (2017)). The fitting is not poor but fails to reproduce the Omori-like decay. More complex combination models may improve the fitting, but would not make simple Omori-like power-law decays. We need more sophisticated physical model to represent the decay characteristics of postseismic deformation.

Keywords: aftershocks, postseismic deformation, afterslip, viscoelastic relaxation, the 2011 Tohoku Earthquake

©2019. Japan Geoscience Union. All Right Reserved.

Serpentinite dehydration in subduction shear zones formed at source depths of slow earthquakes

*Yasushi Mori[1], Miki Shigeno[1], Kohtaro Ujiie[2], Kazuya Noro[2], Tadao Nishiyama[3]

1. Kitakyushu Museum of Natural History and Human History, 2. University of Tsukuba, 3. Kumamoto University

Long-term slow slip events (L-SSEs) and episodic tremor and slip (ETS) occur along the subduction plate boundary at depths of 30–45 km (Obara, 2002; Shelly et al., 2006). These deep slow earthquakes are probably induced by high pore-fluid pressure. Based on geological study, we propose that the high pore-fluid pressure can be produced by metasomatic dehydration of serpentinite in subduction shear zones at source depths of deep slow earthquakes.

The Nishisonogi metamorphic rocks in Kyushu, Japan, are part of a Late Cretaceous subduction complex metamorphosed at $P \approx 1$ GPa and $T \approx 470$ ˚C. The P-T conditions are close to those of source depths of deep slow earthquakes. Serpentinite mélanges intercalated with the metamorphic rocks contain blocks of metabasite, metapelite and albitite. The mélange matrix consists of chlorite-actinolite schist (CAS), talc schist and schistose serpentinite. Intense shear deformation is concentrated in the CAS, and the serpentinite mélanges have the characteristics of anastomosing shear zones.

Bulk chemical composition of the rocks suggests that the CAS is the metasomatized mixture of serpentinite and metabasite. In addition, chemical mass balance indicates considerable dehydration during the CAS formation, along with a slight increase of solid volume. These findings suggest that the CAS formation involves the build-up of pore-fluid pressure. The high pore-fluid pressure results in the concentration of shear deformation into the weakened CAS.

Dehydration of serpentinite probably plays a key role in deep slow earthquakes (Poulet et al., 2014; Okazaki and Katayama, 2015). Thermal dehydration of serpentinite occurs at ~600 ˚C along the subduction plate boundary (Auzende et al., 2006), which is much higher temperature than that of source depths of deep slow earthquakes. In contrast, metasomatic dehydration of serpentinite described here could occur at source depths of deep slow earthquakes.

Auzende, A-L., et al., 2006, EJM, 18, 21–33. Obara, K., 2002, Science, 296, 1679–1681. Okazaki, K., Katayama, I, 2015, GRL, 42, 1099–1104. Poulet, T., et al., 2014, JGR, 119, 4606–4625. Shelly, D.R., et al., 2006, Nature, 442, 188–191.

Keywords: serpentinite mélange, shear zone, dehydration, pore fluid pressure, Nishisonogi metamorphic rocks, deep slow earthquakes

©2019. Japan Geoscience Union. All Right Reserved.

Earthquake swarms following very low-frequency earthquakes in the central Ryukyu Trench

*Mamoru Nakamura[1]

1. Faculty of Science, University of the Ryukyus

Earthquake swarms occur frequently from Amami Island to Okinawa Island, near the axis of the central Ryukyu Trench. These earthquake swarms recur every few years and typically followed swarms of very-low frequency earthquakes (VLFE) that occur in a similar area. I have investigated the relationship between the VLFEs and the subsequent earthquake swarms in the central Ryukyu Trench, using the earthquake catalog provided by the Japan Meteorological Agency (JMA). For the VLFEs, I used the catalog by Nakamura and Sunagawa (2015) and the extended catalog to December 2018.

Results show that the VLFE swarms occurred approximately one month before the subsequent earthquake swarms began near the trench axis in this region. Previous noteworthy earthquake swarms occurred on August 2005 (with a maximum magnitude of 4.7), April 2009 (with a maximum magnitude of 5.1), May 2016 (with a maximum magnitude of 5.6), and September 2018 (with a maximum magnitude of 6.2).

Prior to the earthquake swarm that occurred in August 2005, a VLFE swarm started near Okinawa Island three months before and its activity moved intermittently from Okinawa Island to Amami Island. In the case of the earthquake swarm that occurred in April 2009, a VLFE swarm started near Amami Island and the subsequent swarm occurred two weeks after the start of the VLFE swarm. The location of the VLFE swarm moved intermittently closer to Okinawa Island. In the case of the earthquake swarm that occurred on May 2016, the VLFE swarm started near Amami Island and its active cluster moved intermittently towards Okinawa Island. The subsequent earthquake swarm started near the trench axis, approximately twenty days after the occurrence of the VLFE swarm. In the case of the earthquake swarm that occurred in September 2018, the VLFE swarm started near Okinoerabu Island (the midpoint between Amami Island and Okinawa Island) and the activity moved intermittently to Okinawa Island. The earthquake swarm occurred approximately twenty-five days after the start of the VLFE swarm. The location of the cluster of the 2018 earthquake swarm was slightly landward from the trench axis.

The faulting associated with these earthquake swarms was of normal type, corresponding to intra-slab earthquakes in the subducting Philippine Sea plate. I calculated the Coulomb Failure Stress (delta-CFS) assuming that a small slow slip event (SSE) occurred on the plate interface. Our results show that the positive delta-CFS that accelerated the normal faulting could not have occurred in the subducted slab near the trench axis until the slip of the SSE had reached close to the trench axis. This suggests that the SSE propagated from Amami Island to Okinawa Island accompanying the activation of the VLFE swarm, the slip of the SSE then propagated close to the trench axis, and the normal-faulting earthquake swarm in the slab was induced by the positive delta-CFS caused by the SSE.

Keywords: Very low frequency earthquake, Ryukyu Trench, Earthquake swarm

©2019. Japan Geoscience Union. All Right Reserved.

Seismic imaging in the central Nankai trough, off Shionomisaki to Kii channel

*Yasuyuki Nakamura[1], Shuichi Kodaira[1], Tetsuo No[1], Yuka Kaiho[1], Gou Fujie[1], Seiichi Miura[1], Kazuya Shiraishi[1]

1. Japan Agency for Marine Earth Science and Technology

Shallow very low frequency events (sVLFE) have been reported in the Nankai Trough subduction zone recently. In the central part of the Nankai trough, sVLFE were observed off Kii channel and Shinomisaki, but not reported in the area between them, off western Kii peninsula. We conducted a seismic survey with R/V *Kaimei* in November and December 2018 in Nankai subduction zone off Kii channel to Shonomisaki to investigate the structural features and its possible relationship to the sVLFE. R/V *Kaimei* fired 10600 $inch^3$ air gun array at every 50 m and a streamer cable (4.3 km at shortest, 5.7 km at longest) recorded the seismic signals. We acquired 23 seismic profiles with the length of ~ 75 km in dip direction at 4 km line separation and four profiles of ~ 90 km in strike direction at the shallowest part of the subduction zone. In addition, seven dip profiles with the length of 35 km were acquired off Kii channel to cover the lowermost part of the landward slope densely. The streamer cable was towed at a depth of 25 m to relatively enhance the lower frequency signals for better imaging of the deeper structure. Preliminary processed seismic profiles exhibited the structural variation in the survey area. Deformation of the hanging wall sediments and decollement were well imaged especially ~ 20 –30 km from the trough axis. Top of subducting Philippine Sea plate can be observed through ~ 40 –50 km from the trough axis in some of the obtained profiles. A pair of apparently low angle deep strong reflections were imaged at ~ 7 –8 s two-way time around 40 - 50 km from the trough axis off the western Kii peninsula, which was located slightly east and landward of the area with sVLFE. The shallowest part of the subduction zone in the area where the recent sVLFE activity was not reported, a slope basin with younger sediments deposited over the body of the accretionary prism is imaged, and the deformation was not observed in the slope basin. This suggests the thrust faults within the accretionary prism have not been active recently in this area. We will further process acquired data to obtain clearer seismic images and discuss the structural features and its connection to the observed seismological events in the Nankai Trough.

Keywords: Nankai Trough, seismic imaging

©2019. Japan Geoscience Union. All Right Reserved.

Attempt to Detect Intra-plate SSEs Based on F3 Solution of GEONET

*Yusaku Tanaka[1]

1. Earthquake Research Institute

Slow earthquakes have been detected all over the world and providing new insights into earthquakes. However, most of slow slip events (SSEs) were detected only on plate boundaries and intra-plate SSE was detected only once in Hokkaido. Thus, I attempt to detect intra-plate SSEs all over Japan using F3 solution of GEONET by GSI. I analyze the F3 data with six steps, i.e., (1) removing outliers by setting a term of mean + two times standard deviation for 1/4+1/4 year before-and-after each datum except for the datum itself and considering it is an outlier when it is out of the term, (2) removing disconnections estimated from the offsets and linear trends of 60+60 days before-and-after each datum with the least square method, (3) searching statistically significant temporal changes of the trends by using AIC, (4) cheking visually the time series in which the temporal changes are detected, (5) estimating the displacements from the trend chagnes, and (6) verifying the deformations by numerical calculation by setting rectangular faults.

As of 18th Feb 2019, my study has proceeded to the step (4). In the JpGU meeting, I will report the results of this analysis.

Keywords: crustal deformation, slow slip event, geonet

©2019. Japan Geoscience Union. All Right Reserved.

A new hydrothermal, low to high speed rotary-shearing apparatus: Reproduction of slow/megathrust earthquakes in laboratory

*Takehiro Hirose[1], Wataru Tanikawa[1], Yohei Hamada[1], Keishi Okazaki[1]

1. Kochi Institute for Core Sample Research, Japan Agency for Marine-Earth Science and Technology

Earthquakes involve a wide range of slip rates, from slow/aseismic to fast/seismic slip along faults. Thus, frictional properties of faults over wide slip rates (nm/s to m/s), in particular under hydrothermal conditions similar to those expected in seismogenic zones are essential for a unified understanding of all earthquake events. A new hydrothermal, low to high speed rotary-shearing apparatus has been installed at Kochi/JAMSTEC, in order to study the fault constitutive properties at slow to fast slip rates and the physicochemical mechanisms underlying mechanical responses. The apparatus is currently capable of applying slip rates from 100 nm/s to 2 m/s, normal stress up to 55 MPa, fluid pressure up to 120 MPa and temperature up to 450oC with infinite displacement. We have been improving the apparatus to work as we intended. In pilot tests, we used metamorphic rocks (pelitic and green schists) as starting materials that are potentially distributed at and below seismogenic zones along hot and young subduction zones. We will present our preliminary results with the basic design of the apparatus.

Keywords: friction, hydrothermal, slow to fast slip

©2019. Japan Geoscience Union. All Right Reserved.

Very low-frequency earthquakes in western Shikoku remotely triggered by the 2016 Mw5.9 off-Kii Peninsula earthquake

*Masatoshi Miyazawa[1]

1. Disaster Prevention Research Institute, Kyoto University

Slow tectonic events are known to be sensitive to external stress perturbations due to passing seismic waves and earth tides. High-amplitude surface waves from large earthquakes have transiently triggered low-frequency earthquakes (LFEs) and slow slip events (SSEs) in subduction zones. However, dynamic triggering of very low-frequency (VLF) earthquakes during the arrival of seismic waves from a large, distant earthquake has not been observed. Because both the VLF earthquake and the surface wave have similar characteristic periods, remote triggering is not easily detected by using existing methods. We developed a particle filter/smoother for time series analysis combined with Markov chain Monte-Carlo methods, to detect seismic signals and estimate the maximum likelihood source parameters of VLF events that might have been remotely triggered. We apply this method to seismic data from the Mw5.9 earthquake, which occurred on 1 April 2016 (UTC), off Kii Peninsula. We found that six VLF events with magnitudes about 4, likely occurred in the seismogenic regions of ambient LFEs, and were likely triggered by the arrivals of high-amplitude surface waves. The triggering stress changes are from 0.4 to 1.5 kPa, which are similar to the values for LFEs triggering reported previously. Since there were no triggered LFEs in western Shikoku following the 2016 earthquake, these VLF earthquakes are more sensitive to stress changes caused by surface waves from large earthquakes.

Keywords: Very low-frequency earthquake, Remote triggering

©2019. Japan Geoscience Union. All Right Reserved.

Underground structure around source region of slow earthquakes in western Shikoku obtained by receiver function analysis

Akira Hikita[1], Aitaro Kato[1], *Kazushige Obara[1], Akiko Takeo[1], Takeshi Akuhara[1]

1. Earthquake Research Institute, The University of Tokyo

Various types of slow earthquakes have been observed at subduction zones surrounding the Pacific Ocean. It has been suggested that elevated pore fluid pressure plays an essential role in the generation of slow earthquakes because low velocity or high Vp/Vs zones have been also reported along the plate boundaries where they occur. In Tokai region of the Nankai subduction zone, Kato et al. (2010) revealed that long-term slow slip event (SSE) occurs at the boundary between the continental lower crust and the subducting Philippine Sea plate and episodic tremor and slip (ETS) occurs between the mantle wedge and the subducting plate. Kato et al (2010) also revealed that oceanic crust indicates higher Vp/Vs in the long-term SSE region than in the ETS region. In contrast, Toya et al. (2017) reported that the oceanic crust indicates higher Vp/Vs in the ETS region than in the long-term SSE region in western Shikoku of the same subduction zone. In this study, we revealed configurations of continental Moho discontinuity and subducting oceanic crust and investigated relationship between slow earthquakes and the surrounding seismic velocity structure by receiver function analysis using a dense seismic array in western Shikoku.

As a result, continuous continental Moho and oceanic crust are clearly imaged along both north-south and east-west oriented seismic lines. The plate boundary in the south part, where the distinct continental Moho is not imaged, has steeper slope than the north part along the north-south line. ETS occurs between the mantle wedge and the subducting plate, and long-term SSE occurs along a contact between the continental crust and the oceanic crust.
We show that the oceanic crust indicates much higher Vp/Vs than the hanging wall by using also the reverberation phases. This high Vp/Vs means the elevated fluid pore pressure within oceanic crust due to dehydration. Vp/Vs in the oceanic crust is higher in the deep part of the long-term SSE region than in the ETS region like as the case of Tokai. It is assumed that fluid would accumulate within the oceanic crust owing to low permeability of the continental crust in the long-term SSE region. In contrast, serpentinization of the mantle wedge just above the ETS region could reduce fluid pressure in the oceanic crust. Furthermore, Vp/Vs in the oceanic crust becomes lower in the deeper part beyond the ETS depths, suggesting that eclogization is completed at the depths.

Keywords: Receiver function, episodic tremor and slip, long-term slow slip event, low seismic velocity layer

©2019. Japan Geoscience Union. All Right Reserved.

Hypocenter determination of deep low frequency tremors beneath the Kii Peninsula by backprojection of seismic array data

*Kodai Sagae[1], Hisashi Nakahara[1], Takeshi Nishimura[1], Kazutoshi Imanishi[2]

1. Graduate School of Science,Tohoku University, 2. National Institute of Advanced Industrial Science and Technology (AIST)

A seismic array analysis enables us to detect weak signals if they are coherent. In Cascadia, a high accuracy hypocenter determination of tremors has been carried out by using dense seismic arrays (e.g.,Ghosh et al.,2012). In Southwest Japan, previous studies (e.g.,Ueno et al.,2010) applied the **MU**ltiple **SI**gnal **C**lassification (MUSIC) method (Schmidt,1986) to data of surface seismic arrays at Western Shikoku and carried out the hypocenter determination. However, a quantitative threshold for event detection was not considered. Sagae et al.,(2018 SSJ) introduced an event detection threshold based on the coherence of waveforms among stations, and improved tremor detection by using a surface seismic array installed by AIST at the Kii Peninsula. We applied the MUSIC method to this data in times when tremor events were detected and estimated slownesses and arrival azimuths of tremor signals. Their temporal variations suggested tremor migration. However, we did not carry out hypocenter determination. In this study, we determine hypocenters of tremors by backprojection using the estimated slownesses and arrival azimuths.
The surface seismic array installed by AIST at the Kii Peninsula was composed of 39 three component velocity sensors with a natural frequency of 2.0 Hz and a sampling frequency of 200 Hz. This array had an aperture of about 1.5 km and the sensors were arranged in a cross shape with interval spacings of 50~100 m. We analyze data for 1 year (between July 7,2013 and July 7,2014), because the number of sensors is stable in this period.
We focus on a frequency of 3Hz, which is within the tremor's dominant frequency band of 2-10 Hz. Data processing is described as follows. (1) We calculate averaged coherence of waveforms for all station's pairs. (2) We detect tremor events by setting a detection threshold based on the averaged coherence. (3) We estimate slownesses and arrival azimuths by applying the MUSIC method to the data when tremors are detected. (4) We project them back to the plate boundary (Hirose et al.,2008) and determine source locations by using S wave velocity model JMA2001 (Ueno et al.,2002).
We detected 5 periods of high tremor activities during the 1 year period. We compared the hypocenter distributions determined by our method and those of AIST tremor catalogue which were determined from an envelope cross correlation method. Temporal variation of tremors in this study were almost consistent with the AIST catalogue. We were also able to detect about 2.5 times as many events as the AIST catalogue. It is easier to identify temporal variation of tremors in more detail because our study improved temporal resolution up to 10 sec.
We projected temporal variations of tremor distributions into along-strike and along-dip directions. The results show tremors tend to migrate along the strike in time scales of several days with migration velocities of 6.0~9.3 km/day. Along-dip migrations of tremors with a short timescale of several hours are also detected. When we focused on the initial part of tremor activities, tremors tend to start in deeper parts and gradually migrate to shallow parts. These migration velocities were estimated to be about 1.0 km/hr (24 km/day) in the up-dip direction.
In this study, we were able to improve tremor detection by setting the event detection threshold based on the coherence of seismograms for stations pairs in a surface seismic array. Thanks to this, we were able to locate 2.5 times more tremors than the conventional method. We made it easier to keep track of tremor migrations by improving the temporal resolution of hypocenter determination to 10 sec.
We used the plate boundary model (Hirose et al.,2008). We downloaded the AIST catalogue from Slow

©2019. Japan Geoscience Union. All Right Reserved.

Earthquake Database (Kano et al.,2018).

Keywords: Deep low frequency tremor, Seismic array analysis, Backprojection, MUSIC method, Kii Peninsula, Hypocenter determination

©2019. Japan Geoscience Union. All Right Reserved.

Triggered tremors and stress perturbations due to surface waves

*Ryohei Ikeda[1], Naoki Suda[1]

1. Hiroshima University

Surface waves radiated from distant large earthquakes sometimes trigger a series of deep non-volcanic tremors with intervals of 20-30 seconds, which are the same as dominant periods of surface waves [e.g. Miyazawa & Brodsky 2008]. Understanding the triggering mechanism is important because it provides us clues to the slip process occurring along the transition zone of subducting plate interface. Dynamic stress perturbations due to surface waves that triggered tremors were estimated on the order of 1 to 10 kPa [e.g. Chao & Obara 2016]. To study the relationship between triggered tremors and stress perturbations due to surface waves, we computed theoretical dynamic stresses due to surface waves from large earthquakes by using observed and theoretical surface waves.

We focused on the triggered tremors in the western Shikoku region of the Nankai subduction zone. Most of them occurred in two clusters where tectonic tremors actively occur. We computed theoretical dynamic stress perturbations due to surface waves from 106 earthquakes between 2004 and 2016 with moment magnitudes of 7.0 or grater. The receiver points at which the stress components were computed are at the plate boundary below the N.TSAF and N.KWBH stations, which are the nearest stations of the triggered tremors in F-net and Hi-net, respectively. PREM [Dziewonski & Anderson 1981] and Global CMT catalog [Dziewonski et al. 1981; Ekstrom et al. 2012] were used for the Earth model and the seismic sources for computing theoretical surface waves. Source time functions were approximated with triangular functions whose half durations are equal to the centroid time lags.

The stress change at the plate boundary by the surface wave was estimated based on the method of Spudich et al. (1995). This method consists of two stages: (1) Estimate the stress at the surface from the observed ground velocity and (2) Estimate the stress at the plate boundary from the stress at the surface estimated in (1). In these estimations, we used theoretical proportional relations between the ground velocity and the surface stress and those between the surface and the deep stresses in the frequency domain, which were obtained from the theoretical surface waves. We used the N.TSAF and N.KWBH records as the observed ground velocity. The records from the latter were corrected using the method of Maeda et al. (2011).

The stress components in the source coordinates were transformed to the stress normal to the plate interface and the stress along the possible slip direction of tremor source. The normal and slip directions were obtained from the model plate interface [Baba et al. 2002; Nakajima & Hasegawa 2007; Hirose et al. 2008] and plate convergence vectors [Miyazaki & Heki 2001]. We computed waveforms of the Coulomb failure function (ΔCFF) using a frictional coefficient of 0.2 at periods between 20 and 50 seconds.

©2019. Japan Geoscience Union. All Right Reserved.

Results from the N.TSAF records show that the maximum ΔCFF for the events that triggered tremors are greater than 0.5 kPa. The magnitudes of triggering earthquakes are greater than 7.5. ΔCFFs were generally overestimated when we used the corrected N.KWBH records because the correction did not well work, in particular, for the earthquakes with magnitudes less than 7.5. The important point is that not all of the events that provided the stress perturbations greater than 0.5 kPa triggered tremors. This shows that the stress perturbation due to surface waves cannot be the unique triggering condition: other conditions, for example, stress perturbations due to possible background slow slip events and/or high pore fluid pressure are required.

©2019. Japan Geoscience Union. All Right Reserved.

Numerical modeling of long- and shallow slow slip events including shallow region in Hyuganada and western Nankai, Japan

*Takanori Matsuzawa[1], Bunichiro Shibazaki[2]

1. National Research Institute for Earth Science and Disaster Resilience, 2. Building Research Institute

Recent studies reported deep long-term slow slip events (SSEs) in the Hyuganada and western Nankai region (e.g., Kobayashi, 2014; Takagi et al., 2016; Ozawa. 2017). Shallow SSEs are also recently reported with low-frequency tremor and very low-frequency earthquakes (e.g., Araki et al., 2017; Nakano et al., 2018). In our previous study, we have numerically reproduced recurring deep long- and short-term SSEs in the Shikoku region (Matsuzawa et al., 2013), considering the actual distribution of slow earthquakes and configuration of the subducting Philippine Sea plate. We aim to reproduce deep long- and short-term SSEs and shallow SSEs in a single numerical model applying a similar approach in Matsuzawa et al. (2013).

We adopt a rate- and state-dependent friction law (RS-law) with cutoff velocities. We assume that (a-b) value in the RS-law is negative within the deep short-term SSE region, and positive outside that region. The deep short-term SSE region is modeled based on the actual distribution of deep low frequency tremor. Deep long-term SSE region is assumed based on the geodetic observation (Hirose et al., 2011). To focus on the Hyuganada and western Nankai region, we assume stable sliding region with positive (a-b) in the south of the Kyushu-Palau ridge. We also assume low cutoff velocity at the depth shallower than 9 km to reproduce shallow SSEs. Low effective normal stress is assumed at the depth of SSEs. Temporal evolution of slip velocity is numerically simulated, introducing elastic response and realistic configuration of the plate interface.

In terms of deep long-term SSEs in Hyuganada, a simple extension of the long-term SSE region in the Bungo Channel cannot reproduce the segments of observed SSEs. Narrowed long-term SSE region in the dip direction between Bungo and southern Hyuganada can reproduce three observed segments of SSEs, i.e., Bungo, northern Hyuganada, and southern Hyuganada. In addition, recurring shallow SSEs along trench in Hyuganada and off Ashizuri are reproduced in our result. Megathrust earthquakes are divided into two regions; off Shikoku and Hyuganada in our result. The segments of these large earthquakes may be attributed to the long-term SSE region in the Bungo Channel. Our model comprehensively reproduces various SSEs and megathrust earthquakes, including newly found long-term SSEs.

Keywords: Slow Earthquake, Slow Slip Event, Hyuganada

©2019. Japan Geoscience Union. All Right Reserved.

Further evidence for the influence of a subducting-ridge on the spatial strain accumulation and release pattern in the shallow eastern Nankai Trough, based on VLFE distribution

*Akiko Toh[1], Chen Wan-Jou [2], Doug Dreger[3], Wu-Cheng Chi[2], Satoshi Ide[1]

1. University of Tokyo, 2. Institute of Earth Sciences, Academia Sinica, 3. UC Berkeley

We investigated the distribution and focal mechanisms of very low frequency earthquakes (VLFEs) located in the shallow part of the eastern Nankai trough. While they are mainly explained as low angle thrust faulting along the plate boundary (Sugioka et al., 2012; Nakano et al, 2016), along the strike variation in their distribution has also been observed, likely caused by a subducting-ridge (Toh et al., 2018). Such variations could be closely related to the strain release pattern, or the tsunamigenic potential, of this region, thus warrant a further comprehensive study.

We used 3 component records of broadband ocean bottom seismometers equipped in Dense Oceanfloor Network system for Earthquakes and Tsunamis 1 (DONET1). Records of VLFE activities that occurred immediately beneath the network in 2015, 2016 and 2017 for 1-2 weeks each year, are used. Through visual inspections, we detected 335 VLFEs whose signals are observed at least 6 stations on vertical component filtered between 16-32s.

Instead of estimating the source parameters for one after another for all the events, we searched for densely located event groups inferred by similarities of the maximum amplitude variations measured per event, and, so far, worked only on the grouped events. The purpose of this event selection process is to get an overview of the distribution using the simple quantity (i.e. max. amplitude variation) that can be evaluated for every VLFE, and to avoid a bias that may be caused by eliminating events that are merely difficult to process (i.e. do not fit synthetic waveforms) mostly due to complicated long source time functions that characterize VLFEs. The grouping is conducted by a hieratical density-based clustering method HDBSCAN (Campello et al., 2003), and 197 events were grouped into 26 groups that consists of 2 to 35 events.

We determined the centroid origin time, location and 5-component of moment tensor of VLFEs that maximize the normalized variance reduction (VR) between the observed and synthetic velocity waveforms. The waveforms are bandpass filtered either between 16-32s or 20-50s, depending on signal duration and S/N per event. The time and location are grid-searched at intervals of 0.01 degree in horizontal, 1 km in depth between 5 and 10km bsl., and 1 s in time. At each grid, the moment tensor is estimated using the code TDMT_INV (Dreger, 2003) that conducts full-waveform linearized inversion in time domain. Green’s functions are calculated using the code by Herrmann (2013) based on wavenumber integration. We used a 1D structural model based on a 2D model obtained by an active source survey (Nakanishi et al., 2008). Although the 1D structure is assumed, the large variations in station elevation (1.9-4.3 km bsl) are considered in Green’s function calculations.

We obtained 50 events with good VR (>65%). Among the 26 groups, 6 groups ended up with no events of high VR, mostly due to being located outside of the network. Almost all the VLFEs are reasonably explained by low angle thrust faulting. From the obtained distribution, the strong influence of the subduction-ridge located on the northwestern side of DONET1 is inferred. On the southwestern side

©2019. Japan Geoscience Union. All Right Reserved.

where there is no ridge-subduction, VLFEs are distributed beneath outer-ridge toward the trench axis. The estimated depths for the ones located beneath the outer-ridge are deep (7–10km with median at 8km), which are consistent with the depth of the plate boundary of this area. In contrast, on the northeastern side, VLFEs are mostly distributed landward of outer-ridge and their estimated depth are shallow (5–8km with the median at 7km) as previously suggested (To et al., 2015). The shallow depths can be explained by the uplifted plate boundary in this area due to the subducting-ridge. Furthermore, they are located to landward of the peak of the subducting-ridge, which can be reasonably explained by the change in shear stresses and pore pressures caused by the subducting-ridge.

Keywords: Nankai trough, Very low frequency earthquake (VLFE), Accretionary prism, HDBSCAN, Broadband ocean bottom seismometer

©2019. Japan Geoscience Union. All Right Reserved.

Evidence for semi-brittle flow in mantle-wedge serpentinites under high pore fluid pressure and their implications for deep low frequency earthquakes

Kengo Kataoka[1], Yurina Nagata[1], *Ken-ichi Hirauchi[1], Ryosuke Oyanagi[2], Atsushi Okamoto[3], Katsuyoshi Michibayashi[4]

1. Department of Geosciences, Faculty of Science, Shizuoka University, 2. Japan Agency for Marine-Earth Science and Technology, 3. Graduate School of Environmental studies, Tohoku University, 4. Department of Earth and Planetary Sciences, Nagoya University

In southwest Japan, deep low frequency earthquakes occur at the base of the shallow serpentinized mantle wedge. In order to understand deformation styles of the mantle wedge serpentinite, we conducted structural and petrological analysis of a paleo-mantle wedge body that has experienced serpentinization at pressure–temperature conditions corresponding to source areas of low-frequency earthquakes, in the Sanbagawa belt, central Shikoku. The serpentinite body has a block-in-matrix structure that result from pervasive fragmentation. At outcrop and thin section scales, the distribution of blocks follows a power law distribution with exponent $2.32 < D < 2.37$ (2-D). The block has experienced complete serpentinization, characterized by randomly-oriented antigorite aggregates. The matrix also consists of antigorite, which was formed due to dissolution–precipitation process of the block in the presence of H_2O. Antigorite aggregates in the matrix along localized shear planes is characterized by a strong crystallographic preferred orientation with a dominant [010](001) slip system, suggesting dislocation glide on (001) planes. We suggest that deep slow earthquakes occur by semi-plastic deformation of the serpentinized mantle wedge, under low effective normal stresses.

Keywords: slow earthquakes, low frequency earthquake, mantle wedge, serpentinite

©2019. Japan Geoscience Union. All Right Reserved.

Spatial distribution of slow slip events off the Boso peninsula from 1996 to 2018 under sparsity constraints

*Ryoko Nakata[1], Hideitsu Hino[2], Tatsu Kuwatani[3,4], Takahiro Akiyama[5], Shoichi Yoshioka[6], Masato Okada[7], Takane Hori[1]

1. Japan Agency for Marine-Earth Science and Technology, 2. The Institute of Statistical Mathematics, 3. Department of Solid Earth Geochemistry, Japan Agency for Marine-Earth Science and Technology, 4. PRESTO, Japan Science and Technology Agency, 5. Graduate School of Science, Kobe University, 6. Research Center for Urban Safety and Security, Kobe University, 7. Graduate School of Frontier Sciences, The University of Tokyo

We estimated spatial distribution of the six slow slip events (SSEs) off the Boso peninsula, central Japan, from 1996 to 2018. We have applied an inversion method called fused regularization, a type of sparsity constraint, suitable for detecting discontinuous changes in the model parameters, for evaluation function [Nakata et al., 2017]. In this study, to shorten calculation time, we used a type of approximation method by Obuchi and Kabashima [2016] to search hyperparameters, not LOO-CV (leave-one-out cross validation).

From our tentative results, the maximum slips for the 2002, 2011 and 2018 SSEs were large, and the 1996, 2007 and 2013 SSEs were small. The slip distributions of the 2011 and 2018 SSEs seem to be distributed southward than 2002. It is confirmed by numerical experiments that the difference in slip distribution is not due to GNSS station distribution.

Furthermore, we are conducting numerical simulation of earthquake generation cycles, which modelling SSEs off the Boso peninsula and M~8 earthquakes along the Sagami Trough. We will discuss slip distributions of SSEs and locked area during an interseismic period.

©2019. Japan Geoscience Union. All Right Reserved.

Marine electromagnetic observations around a slow earthquake region in the western Nankai trough

*Hiroshi Ichihara[1], Tada-nori Goto[2], Tetsuo Matsuno[3], Noriko Tada[4], Shinya Sato[2]

1. Earthquake and Volcano Research Center, Nagoya University, 2. Graduate School of Engineering, Kyoto University, 3. Ocean Bottom Exploration Center, Kobe University, 4. JAMSTEC

Slow earthquakes have been believed to relate to fraction of pore fluid around plate boundary. Thus, imaging of electrical resistivity (conductivity) distribution is essential to understand slow earthquakes. However, many of SSE areas are distributed beneath the ocean, we need marine electromagnetic (EM) observations. In this presentation, we report preliminary results of marine EM observations in the western part of Nankai Trough (off Miyazaki prefecture and off western Kochi prefecture, Japan) where SSEs, VLF events and regular earthquakes (e.g. 1968 off-Hyuga earthquake, M7.5) are known. We deployed eight ocean bottom electro-magnetometers (OBEMs) and recovered seven of them between 2017 and 2018. In addition to EM fields, two OBEMs measure absolute pressure to detect short period crustal deformations caused by SSE. We estimated high quality magnetotelluric responses based on Chave and Thomson (2004). However, the responses show strong three-dimensionality of resistivity distribution and strong coast effect (e.g. Key and Constable, 2011). They indicate that we need to apply three-dimensional imaging techniques for seafloor magnetotelluric data.

Keywords: Slow earthquake, magnetotelluric, OBEM, Nankai trough, off Miyazaki

©2019. Japan Geoscience Union. All Right Reserved.

Dynamics of precipitating injection fronts inside of structured medium

*Yutaka Sumino[1], Shunsuke Tanaka[1], Miyuki Kunihiro[1]

1. Tokyo University of Science

Recent study on a slow earthquake elucidates that the migration of water within a mantle wedge may play relevant roles[1]. The flow inside of confined geometry, such as within a soil, is often described by the Darcy’s law, where flow velocity is described by the gradient of fluid pressure. Interestingly, however, the water within a mantle wedge contains large amount of solid contents, and hence, a precipitation can be formed within the water[2]. For this reason, the dynamics of fluid flow under the effect of precipitation reaction should be explored.

Based on the above motivation, we explored the 2-dimensional confined chemical garden[3] as an analogue experiment for the fluid flow within a mantle wedge[4]. The system consists of two fluids with a quasi-two dimensional thin cell, so called a Hele-Shaw cell. The cell was filled with a fluid, and the other fluid is injected from the center of the cell. The flow in a Hele-Shaw cell can be described by the Darcy’s law. Furthermore, the mixing of these fluids leads to the precipitation. Thus, the flow observed in 2-dimensional confined chemical garden system is analogous to the one of water in a mantle wedge with precipitation formation.

Our previous study[4] showed that a filamentous pattern appears when the injection speed is high enough, whereas the symmetrical circular front was formed for lower injection speed. This results indicates that the propagation radius of injection front can be drastically different depending on the injection speed. In addition, the number of moving filaments saturate whose value is proportional to the injection speed. Such tendency can be understood with our boundary model adopting the effect Laplace pressure and the conservation of precipitation at the boundary. The model further predicts existence of optimal curvature for the moving front with which the required pressure for the motion is minimum. The curvature, and the speed of the optimal boundary motion is independent of the injection speed. These experimental and theoretical study thus worked well in the 2-dimensional Hele-Shaw cell. However, actual condition in a mantle wedge should have quenched structure, which is absent in a Hele-Shaw cell.

In order to fill the gap between actual condition in a mantle wedge and our analogue experiments, we modified our Hele-Shaw cell to have periodic pillar structure. As a control parameter, we changed the pillar to pillar distance, w, as shown in attached figure. The filament pattern showed meandering motion without pillar structures ($w = \infty$). We found that the filament pattern showed straight motion especially when w agreed with the typical filament width. Our modified mathematical model adopting nonlinear response of permeability with precipitation density numerically reproduced such experimental results. This results indicates that the propagation distance of injected fluid can be modified by the locally quenched disorder within a mantle wedge.

In this paper, we show detailed setup for experiments, as well as mathematical model.

[1] A. Tanaka et al. Earth, Planets and Space 70, 25 (2018).
[2] K. Ujiie, et al., *Geophys. Res. Lett.* **45**, 5371–5379 (2018).

©2019. Japan Geoscience Union. All Right Reserved.

[3] F. Haudin et al., *Proc. Natl. Acad. Sci. U.S.A.* **111**, 17363–17367 (2014).
[4] S. Wagatsuma, et, al., *Phys. Rev. E* **95**,052220 (2017).

Keywords: injection, fluid, precipitation

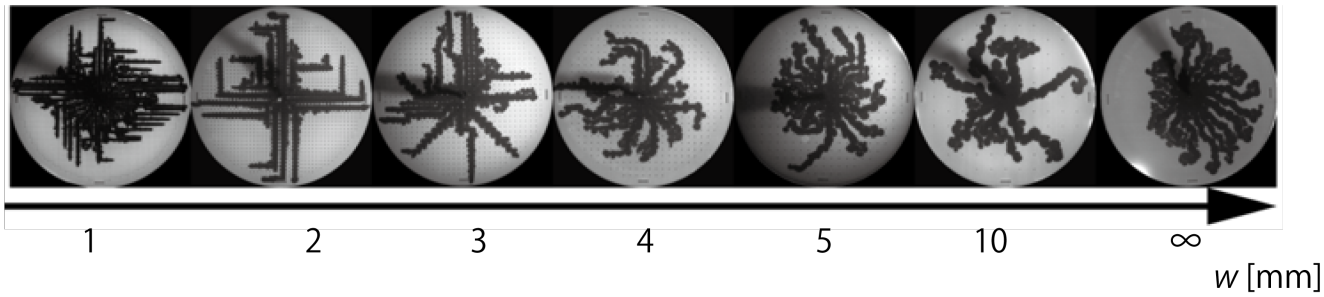

©2019. Japan Geoscience Union. All Right Reserved.

Permeability changes of simulated low permeable fault rocks induced by intermediate velocity friction test

*Wataru Tanikawa[1]

1. Japan Agency for Marine-Earth Science and Technology, Kochi Instutute for Core Sample Research

Earthquake events often associate with fluctuations of flow rate, pore pressure and pore fluid chemistry at a subsurface of earthquake rupture zones. The co-seismic hydrological changes are explained by changes in fluid permeability of fault zones during earthquakes, and the permeability change plays an important role for dynamic fault processes as well. Therefore, we newly designed a system to estimate water permeability changes during and after low to high velocity shear deformation using a rotary shear apparatus and simulated fault rocks.

A pair of hollow cylindrical samples made by low permeable Belfast dolerite and Aji granite were used as test specimens. To calculate permeability, a radial flow from the inner wall to the outer wall of the specimen was induced by applying a differential pore pressure (0.01 to 0.2 MPa) between inner and outer walls. We performed friction tests at normal stress of 2 MPa, rotation speed from 0.0003 to 0.6 m/s, and slip displacement of 1 m.

The results showed that permeability increased during sliding at every slip velocity condition, and higher velocity friction caused more abrupt increase in permeability. After the end of sliding, permeability gradually decreased with time and then became nearly constant value. Reduction rate of permeability 5 min after slip increased with slip rate. Fiction coefficient was decreased with sliding velocity. Frictional heating is a key to explain slip velocity dependence of permeability (flow rate). Temperature rise caused by frictional heating will reduce fluid viscosity, therefore, apparent permeability reduction after sliding can be explained by an increase in fluid viscosity by cooling. Pore pressure build-up by frictional heating can increase aperture, therefore, this process can explain permeability enhancement during sliding and velocity dependences on permeability increase and friction coefficient.

Keywords: permeability, friction coefficient, frictional heating

©2019. Japan Geoscience Union. All Right Reserved.

Modified relation between the coupling and tremor rates around the Shikoku region

*Tadafumi Ochi[1]

1. Institute of Earthquake and Volcano Geology, Geological Survey of Japan, The National Institute of Advanced Industrial Science and Technology

In Ochi and Takeda (2018, EPS), I examined the relation between the interplate coupling velocity and the number of deep low-frequency tremors in the same place around the Shikoku region, southwest Japan. I found that there were some spot-like points where the coupling and the tremor count were well correlated, and that the regression line required the coupling rate to be the plate convergence rate in this region under conditions of zero tremor count rate. One of the problems to be resolved is the interpretation of the first matter 'spot-like points' mentioned above. According to the pairs of time series of the coupling rate and tremor count rate, some pairs show a time delay, and the others show a small fluctuation in the tremor count rate that seems to be independent of the coupling rate. It is interesting that whether the an ill-correlation just comes from an oversimple model of the linear regression I used in the previous study, or really reflects some physical background. In order to answer this question, I construct the model which allows the fluctuation in the tremor count rate that is independent from the coupling rate and observe the fitness of the model. At this time, some trial models that allow the shorter period fluctuation in the tremor count rate than in the coupling rate and temporal change in the period achieve clear correlations. In the presentation, I will show the results of the various trials.

Keywords: Interplate coupling, Low-frequency tremor

©2019. Japan Geoscience Union. All Right Reserved.

Spatiotemporal distribution of regular and very low-frequency earthquakes in the northern part of the Ryukyu subduction zone

*Youichi Asano[1], Kazuhiko Goto[2], Hiroshi Yakiwara[3], Shuichiro Hirano[3]

1. National Research Institute for Earth Science and Disaster Resilience, 2. Association for the development of earthquake prediction, 3. Nansei-toko Observatory for Earthquakes and Volcanoes, Kagoshima University

We have investigated detailed spatiotemporal distribution of regular and very low-frequency (VLF) earthquakes including an Mw 6.3 interplate event near Tanegashima along the Ryukyu trench on Jun. 08, 2019. This earthquake was followed four Mw4-5 class regular and many VLF earthquakes by the end of Jan., 2019. At first we estimated centroid moment tensors of these regular and several VLF earthquakes, respectively, from broadband seismograms recorded at the NIED F-net and temporally observation stations. In the next step, the known VLF earthquakes were selected to be template events for searching unknown VLF earthquakes from continuous seismograms. If there are several candidates of VLF earth quake, we select the most coherent event with a maximum cross-correlation coefficient averaged over all stations in every 180 seconds. Finally we estimated locations of the selected events from phase shift of the wavelets between the template and these selected events. Obtained result shows that activity of VLF earthquakes after the Mw 6.3 earthquake was started in the adjacent area east of this Mw 6.3 earthquake; however, the following Mw4-5 regular earthquakes occurred south of this area in the period of Jan. 25-30, 2019. In this period, the front of the VLF activity migrated toward east from these Mw4-5 events. Such a spatiotemporal distribution of regular and VLF earthquakes suggests that the after slip of the Mw 6.3 and/or an SSE caused these regular and VLF earthquakes.

Acknowledgment

This study is partly supported by JSPS KAKENHI Grant Number JP16H06473.

Keywords: very low-frequency earthquake, Ryukyu subduction zone

©2019. Japan Geoscience Union. All Right Reserved.

Possible tectonic tremor activities near the VLFE epicenters in the Sanriku-Oki region in 2011

*Hidenobu Takahashi[1], Ryota Hino[1], Yusaku Ohta[1], Naoki Uchida[1], Syuichi Suzuki[1], Masanao Shinohara[2], Takanori Matsuzawa[3]

1. Graduate school of Science Tohoku University , 2. Earthquake Research Institute, University of Tokyo, 3. National Research Institute for Earth Science and Disaster Resilience

Recently various kind of slow earthquakes have been discovered along the Japan Trench subduction zone. Prior to the occurrence of the 2011 Tohoku-oki earthquake, occurrence of slow slip events associated with migration of small earthquake epicenters and tectonic tremors was reported near the hypocenter of the Tohoku-Oki earthquake (e.g. Kato et al., 2012; Ito et al., 2015; Katakami et al., 2018). As a different type of a slow-earthquake family, Very Low Frequency Earthquakes (VLFEs) have been detected in more broad areas (Matsuzawa et al., 2015). Takahashi et al. (in prep.) detected the seismic signals from the VLFEs by short-period ocean bottom seismograms (OBS) deployed in the vicinity of the VLFE epicenters in the Sanriku-Oki region, just after the Tohoku-Oki earthquake. They further identified a number of VLFE-like events, not recognized by the onshore data. Here, we report on possible tectonic tremor activities in the same area based on the OBS data after the 2011 Tohoku-oki earthquake.
We detected four sequences of continuous rises of amplitudes on the OBS records. Each of the sequence has a duration of ~ half a day. The sequences were composed of numerous wave trains with good correlations in their growths and decays in observed amplitudes among the stations, but no distinct P- or S-wave onsets were identified for individual wave trains. Interestingly, the spatial variation of the wave trains amplitudes is similar to those of the previously identified VLFEs. These observations suggest that the sequences were composed of small seismic events closely located each other and to the known VLFEs. It is also notable that some of the VLFE-like events discovered by the OBS data were contained in the sequences. We regard the discovered sequence as a kind of tectonic tremor activity and will inspect their characteristics, such as frequency content and its variability, to clarify their nature and discuss their relevance to slow slip events along the shallow subduction interface, which might promote the activities.

Keywords: tectonic tremor, Sanriku−oki

©2019. Japan Geoscience Union. All Right Reserved.

Heterogeneous structure around a region of slow earthquake activity off Ibaraki prefecture along the Japan Trench

*Kimihiro Mochizuki[1], Tomoaki Yamada[1], Masanao Shinohara[1], Ryota Hino[2], Ryosuke Azuma[2], Yoshihiro Ito[3], Yoshio Murai[4], Kenji Uehira[5], Toshinori Sato[6]

1. ERI, Univ. of Tokyo, 2. Graduate School of Science, Tohoku Univ., 3. DPRI, Kyoto Univ., 4. Faculty of Science, Hokkaido Univ., 5. NIED, 6. Graduate School of Science, Chiba Univ.

Large earthquakes of magnitude (M) ~7 have repeatedly occurred in the Ibaraki-oki region, about 100 km offshore of the Ibaraki prefecture along the Japan Trench, at a constant interval of ~20 years. Mochizuki et al. (2008) conducted a marine seismic survey and revealed that there exists a subducted seamount in the region. They also conducted an offshore seismic observation using ocean bottom seismometers (OBSs) to show that the seismicity in the region can be seen off of the subducted seamount, but not along the plate interface over it. They found that the location of the subducted seamount did not agree with the focal region of the repeating M7 earthquakes. From these results, they argued that the plate interface over the subducted seamount does not constitute an asperity of the repeating M7 earthquakes. Wang and Bilek (2011) introduced an idea that the seamount subduction causes formation of a fracture network within the overriding plate, and such a fracture network would prevent accumulation of large strain energy along the plate interface over the subducted seamount to generate large earthquakes. In addition to the repeating M7 earthquakes, recent studies (e.g. Matsuzawa et al., 2015; Nishikawa and Ide, 2018) have reported activity of slow earthquakes in the region. Relationship between activity of various types of earthquakes and structural features around the plate interface is one of the key topics to better understand controlling factors over earthquake types to be generated.

Recent studies in the Hikurangi subduction margin off the North Island of New Zealand show spatial relationship between variety of fault slips and topographic features of the plate interface. Wallace et al. (2016) successfully observed a large slow slip event just beneath an offshore array of ocean bottom pressure gauges, and precisely determined its slip distribution. They revealed that its slip propagation appeared to have circumvented subducted seamounts that have been imaged by magnetic anomalies as well as seismic reflection sections. Todd et al. (2018), for the first time, detected offshore tremor activity in the Hikurangi margin. The activity appears to have started just after the cessation of the slow slip, and its spatial distribution is only limited within regions of subducted seamounts. These results show that distributions of slow slip and tremor activity do not appear coincident, and thus the physical properties of the plate interface may be different. Further seismic surveys are supposed to provide vital information on structural variations that control physical characteristics of the plate interface.

In February, 2011, we acquired wide-angle reflection and refraction seismic data using 21 OBSs along a 150 km transect in the Ibaraki-oki region during the KH11-2 R/V Hakuho-maru cruise. We also included data from an OBS array that had already been deployed for a long-term seismic observation above the subduction front of the subducted seamount. Thus, we could construct a dense OBS profile above the subducted seamount with a receiver interval of ~3 km to achieve a high spatial resolution, whereas the largest interval is 10 km near both ends of the profile. First arrivals from the airgun sources can be traced up to ~95 km on most of the OBSs. The OBS record sections show significant heterogeneity that may include very rough structural features of the subducting oceanic crust along strike. Such heterogeneity may control seismic activity in the region.

©2019. Japan Geoscience Union. All Right Reserved.

Keywords: Ibaraki-oki, Active source seismic survey, Heterogeneous structure

©2019. Japan Geoscience Union. All Right Reserved.

Shallow low-frequency tremor triggered by nearby moderate earthquakes off Sanriku

*Sachiko Tanaka[1], Takanori Matsuzawa[1], Youichi Asano[1]

1. National Research Institute for Earth Science and Disaster Resilience

In the region off Sanriku, we have observed shallow low-frequency tremor, which occurs between the 12 km and 20 km depth contours of the plate interface, applying an envelope correlation method (Obara, 2002) to the records from the Seafloor observation network for earthquakes and tsunamis along the Japan Trench (S-net) (Tanaka et al., 2018). Several episodes of tremor, each of which lasted for half a day to six days, were detected in 2017, with intervals of one to three months. In the present study, we found tremor triggered by nearby moderate earthquakes. On July 24, 2017, an Mw 5.6 earthquake, showing reverse faulting consistent with the slip on the plate interface, occurred at the downdip end of the tremor zone off Sanriku, which was the largest event within 100 km of that tremor zone in the year. Immediately after the Mw 5.6 earthquake, coherent tremor signals were identified at surrounding stations. These signals continued for 20 hours, and the locations of their sources spanned 40 km along strike and 50 km along dip. Similar triggered tremor was observed following an Mw 5.1 earthquake on July 22, two days before the Mw 5.6 earthquake. This tremor activity was smaller and shorter than that triggered by the Mw 5.6 earthquake; tremor was localized to an area of 20 km by 15 km, and lasted for twelve hours. After a quiescence of nearly one day, the Mw 5.6 earthquake occurred at an adjacent area and triggered tremor was detected again. Triggering of tremor by moderate interplate earthquakes in or very close to the tremor zone we observed may imply small-scale (~ a few kilometers) heterogeneities in frictional properties on the plate interface in the area.

Keywords: shallow low-frequency tremor, triggered tremor, Japan Trench

©2019. Japan Geoscience Union. All Right Reserved.

Slow slip events in the Bungo Channel over 15 years as inferred from GNSS data (1996-2011)

Takatoshi Yokoi[1], *SHINICHI MIYAZAKI[1], Hiromu Sakaue[1], Jun'ichi Fukuda[2]

1. Graduate School of Science, Kyoto University, 2. Earthquake Research Institute, The University of Tokyo

We estimated space-time evolution of inter-plate slip and slip velocity associated with slow slip events (SSE) in the Bungo Channel over 15 years between January 1, 1996 and February 28, 2011, from GNSS data.

We use GNSS time series at 80 stations around the Bungo Channel out of GEONET stations. Time series were obtained with GIPSY-OASIS II software by Nishimura (personal communication). We removed data during SSE and estimated secular velocities, annual and semi-annual seasonal variations, and offsets associated with earthquakes, SSEs and instrumental events. Then we remove contributions of those components from time series with SSE to prepare time series for the inversion. We constructed plate interface based on iso-depth data by Baba et al. (2002) and Hirose et al. (2008), and setup the model region that is 200km long east to west and 280km long north to south. The model region was subdivided into 719 small triangular patches. We employed the inversion method based on the Monte Carlo Mixture Kalman Filter (Fukuda et al. 2008) and estimated slip and slip velocities on the fault continuously over 15 years.

First, Long-term slow slip events (L-SSE hereafter) that lasted for several months were inferred in 1997, 2003 and 2010 as obtained by, such as, Ozawa et al. (2012, 2017) and Yoshioka et al. (2015). In addition to basic characteristics described in these previous studies, short-term slow slip events (S-SSE hereafter) were inferred just before or just after the main slip event. This result suggests that stress perturbations by SSEs trigger other SSEs. Therefore the inferred cumulative moment in this study was smaller than previous studies because we successfully excluded contributions from S-SSEs. Second, S-SSEs have repeatedly occurred with the interval of about three or four months over 15 years. Those S-SSE were located at depths of about 30-40km and associated with low frequency tremors.

In this presentation, we focus space-time evolutions of L-SSE in 2010 and S-SSE in 2005.

Keywords: Slow slip in the Bungo Channel, crustal deformation, Monte Carlo Mixture Kalman Filter

©2019. Japan Geoscience Union. All Right Reserved.

Investigations of sensor orientation and a possibility of detecting crustal deformation based on accelerometer records of S-net

*Ryota Takagi[1], Naoki Uchida[1], Takashi NAKAYAMA[1], Ryosuke Azuma[1], Akira Ishigami[1], Tomomi Okada[1], Yusaku Ohta[1], Ryota Hino[1]

1. Research Center for Prediction of Earthquakes and Volcanic Eruptions, Graduate School of Science, Tohoku University

Seafloor Observation Network for Earthquakes and Tsunamis along the Japan Trench (S-net) of National Research Institute for Earth Science and Disaster Resilience (NIED) will greatly improve our knowledge of subsurface structure beneath offshore region along Japan trench and understanding of regular and slow earthquakes on the subducting plate boundary. We estimated the orientations of S-net sensors that are fundamental information for further data analysis and investigated the possibility of detecting crustal deformation based on accelerometer records.

We determined three parameters of sensor orientations: tilt angle of the long axis of a cable, rotation angle around the long axis, azimuth of the long axis. We estimated the tilt and rotation angles by assuming the DC components of accelerometers record the gravitational acceleration. The tilt and rotation angles slightly vary within the range of 0.01-0.1 degree during the period from 2016 to 2018 except for coseismic steps of rotation angles larger than 1 degree due to the M6.4 off Sanriku earthquake (August 20, 2016) and M7.4 off Fukushima earthquake (November 20, 2016). The long-axis azimuths are estimated by particle motions of long-period Rayleigh waves. We used the accelerometer records in 30-100 s of 7-14 teleseismic earthquakes with Mw 7.0-8.2. The azimuths are constrained in the range of 5-10 degrees. After correcting waveforms based on the estimated sensor orientation, we found coherent waveforms within the whole S-net stations and separation of Rayleigh and Love waves in radial and transverse components.

The capability of the DC components of accelerometers implies a possibility to detect crustal deformation from accelerometer records. We made time series of tilt and rotation angle with the sampling rate of one hour. During the period without offsets partly due to earthquakes, the root-mean-square (RMS) amplitudes of tilt and rotation angles are about 2 micro radians at most stations. The buried stations shallower than 1500 m show smaller variations and RMS amplitudes are about 0.2 micro radians. Some buried stations show tidal response with amplitude of about 1 micro radians. Since the maximum tilt change of land stations by a slow slip event (SSE) near the Boso Peninsula is about 1 micro radians, it might be possible to detect crustal deformation due to similar SSEs based on the accelerometer records.

Acknowledgement: We used continuous records of S-net managed by NIED. We thank NIED for providing the data.

Keywords: S-net, Sensor orientation, Crustal deformation, Slow slip, Tilt observation

©2019. Japan Geoscience Union. All Right Reserved.

Spatiotemporal variation of released seismic energy from shallow low-frequency tremor in Hyuga-nada, revealed by ocean bottom seismological observation

*Yusuke Yamashita[1], Saki Watanabe[2], Tomoaki Yamada[3], Masanao Shinohara[3], Takeshi Matsushima[2]

1. Disaster Prevention Research Institute, Kyoto University, 2. Institute of Seismology and Volcanology, Kyushu University, 3. Earthquake Research Institute, The University of Tokyo

In this study, we estimate the released seismic energy by shallow low-frequency tremors (shallow tremors) and clarify spatiotemporal variation of shallow tremor activity in Hyuga-nada, east off Kyushu. We used the data obtained from the temporal ocean bottom seismological observation for 3 months in 2013 [Yamashita *et al*., 2015] and long-term ocean bottom seismological observation from 2014 to 2017. The source location and released seismic energy of each shallow tremor was simultaneously estimated by Hybrid Envelope Cross-correlation Method [Maeda and Obara, 2009]. Observation data were obtained by the long-term continuous ocean bottom seismic observation in Hyuga-nada from 2013 to 2017. Site amplification factors were estimated by the coda normalization method [e.g., Sato and Fehler, 1998].

Spatial distribution of released seismic energy rate (energy rate) shows a heterogeneity although the average value of that is generally 10^4 J/s. The regions where the energy rate is relatively small are roughly coincident with the subducting or passed areas of the Kyushu-Palau Ridge. This result suggests that the structure and/or shape of the subducting plate such as seamounts or ridges may have an effect on the frictional property of the shallow plate interface. The 2013 activity was similar characteristics of shallow tremor location in space and time as the previous study, including two migrations episode. In addition, the characteristics of the released seismic energy were revealed as follows: (1) the energy rate was large at the both initiation point and the front of the migration, (2) the total released energy amount of the first migration was larger than that of the second migration, (3) both migrations were stopped at the region of small amount of released energy. Migration episode occurred while the 2015 activity and similar characteristics were documented.

Migration speed of shallow tremor is a few times faster, and energy rate of that is one or two orders of magnitude greater than the deep tremor. Applying the model of Ando *et al*. [2010, 2012] and Yabe and Ide [2014] to the result in this study, the average fault strength of shallow tremor is stronger than that of deep tremor, which leads up to a faster fault slip both brittle and ductile area. As a result, migration speed may become to be faster than deep tremor.

Acknowledgements: This study is supported by the research project for compound disaster mitigation on the great earthquakes and tsunami around the Nankai trough region, the MEXT of Japan, and JSPS KAKENHI Grant Number JP16H06471, JP16H06472. We thank Dr. Takuto Maeda for valuable discussions and comments. The observation data in 2013 obtained by T/S Nagasaki-maru. We used the JMA unified earthquake catalog and the seismic data obtained by Kagoshima University.

Keywords: Shallow low frequency tremor, Shallow slow earthquake, Ocean bottom seismological observation

©2019. Japan Geoscience Union. All Right Reserved.

©2019. Japan Geoscience Union. All Right Reserved.

Unified description of fast and slow earthquakes using velocity strengthening patches

*So Ozawa[1], Takahiro Hatano[1]

1. Earthquake Research Institute, the University of Tokyo

In a prevalent view, seismicity in subduction zones is governed by the distribution of the frictional properties of the plate interface. Regions with velocity-weakening (VW) friction generate earthquakes, whereas velocity-strengthening (VS) regions creep aseismically. Although most models consider isolated VW regions (patches) from the idea of asperities (e.g. Dublanchet et al., 2013), isolated VS patches also would exist given the frictional properties on faults are inferred to be complex and hierarchical. Therefore, the role of VS patches is to be studied.

Here we perform 3-D numerical simulation of the seismic cycle of faults governed by the rate and state friction law with the aging law. We distribute randomly circular VS patches on a VW background. We mainly focus on the effect of the ratio of VS and VW areas.

In our preliminary simulation, we identified two important effects. First, the VS patches act as the “stability barriers” during dynamic rupture propagation, which makes the rupture process more complicated than a single propagating crack. Rupture decelerates by encountering a stability barrier, followed by reacceleration due to overcoming the barrier. Such a process gives rise to multiple rupture fronts in the slipping area.

Second, dynamic rupture is inhibited by increasing the number of VS patches, and the fault slips aseismically with strong fluctuation in slip velocity. This is because there are no enough VW regions to accelerate the slip to dynamic rupture. Although a similar mechanism for slow earthquakes is proposed by Skarbek et al. (2012) and Yabe & Ide (2017), our 3-D modeling enables detailed studies on the spatiotemporal evolution of slip. In the presentation, we further discuss our results in the context of the dynamic scaling of rupture growth and the phenomenological law of slow earthquakes.

Keywords: Slow earthquake, Rate and state friction

©2019. Japan Geoscience Union. All Right Reserved.

The b-value of the earthquake swarm activities accompanied by the Boso slow slip events

*Yuki Noda[1], Hitoshi Hirose[2,1]

1. Department of Planetology, Faculty of Science, Kobe University , 2. Research Center for Urban Safety and Security, Kobe University

Slow slip events (SSEs) which are accompanying earthquake swarms repeatedly occur at intervals of about 2 to 7 years off Boso Peninsula (e.g., Sagiya, 2004; Hirose et al., 2012, 2014; Fukuda, 2018). These SSEs and swarms are thought to occur on the upper boundary of the subducting Philippine Sea plate.

As a statistical property of earthquakes, Gutenberg-Righter’ s law is well-known, that is, the relationship between the magnitude and the logarithm of occurrence frequency of earthquakes is expressed well with a straight line a-bM (Gutenberg and Richter, 1944). Although the b-value (slope of the line) often takes values around 1, there are many reports about the temporal changes of the b-value. For example, a decade-scale b-value decrease prior to the 2011 Tohoku Earthquake is reported (Nanjo et al., 2012). Although the relationship between the temporal change of b-value and aseismic slip is suggested, but the lack of near field geodetic observations prevents the direct evidence for the relationship. Here we examine the b-value of the earthquake swarms accompanied by the Boso SSEs, of which the aseismic slip is revealed by geodetic observations.

In this study, we estimate the b-value of the earthquake swarms in 2002, 2007, 2011 and 2014. We use the JMA unified earthquake catalog. As a preliminary analysis, we investigated the earthquakes with focal depths of 5 km to 40 km occurring at 35.05˚ to 35.56˚N in latitude and 140.15˚ to 140.73˚E in longitude. Eventually, “event period” estimated in the previous studies of the crustal deformation by geodetic observation does not necessarily agree with the period of the swarms occurring at the same time. Therefore, in this research, “event period” was redefined from seismic activity and used. In other words, we extracted swarms including a SSE period from crustal deformation studies and the time when the seismicity rate (the number of earthquakes per unit time) is significantly higher than the other time is defined as “event period”. In addition, the period other than the event period is defined as “inter-swarm period”.

We find that the b-values in the event periods tend to be lower than that during inter-swarm period. In more detail, different trends that seem to correspond to the difference in slip zone and location of earthquake activity of each SSE (Hirose et al. 2014) are seen in the b-values for the event periods. A seismic activity near the southern coast of the Boso Peninsula was hardly observed in the 2007 event period, whereas an active seismic activity was seen there in the 2011 event period. In order to clarify the dependence of the b-value on the difference in the location of the earthquakes, we divided the survey area into two areas, that is, the northern area (area A) and the southern area (area B). The seismic activity is observed in all event periods in the area A, whereas an active seismic activity is observed only in the event periods of 2002 and 2011 in the area B. Then a b- value is estimated in each period in the same way. As a result, for the earthquakes occurred in the northern region (area A), there is a tendency that the b-value in each of the event periods is lower by about 0.2-0.4 than that during inter-swarm. On the other hand, such a tendency is not observed in the southern area (area B). Such differences in the northern and southern regions may suggest that the effects of stress changes caused by SSEs vary from region to region.

©2019. Japan Geoscience Union. All Right Reserved.

Keywords: Gutenberg-Richter's law

©2019. Japan Geoscience Union. All Right Reserved.

Three-dimensional thermal modeling associated with subduction of the Philippine Sea plate at the Ryukyu Trench, and its relation to the occurrence of interplate seismic events

*Nobuaki Suenaga[1], Shoichi Yoshioka[2,1], Yinfeng Ji[3]

1. Graduate School of Science, Kobe University, Japan, 2. Research Center for Urban Safety and Security, Kobe University, Japan, 3. Chinese Academy of Science, Beijin, China

Interplate seismic events such as short-term slow slip evens (S-SSEs) (Nakamura, 2017), low-frequency earthquakes (LFEs) (Ando et al., 2012), and shallow very low-frequency earthquakes (VLFEs) (Nakamura et al., 2015) have been identified at the Ryukyu Trench, southwestern Japan. As the specific characteristics of these distributions, depths where S-SSEs and LFEs occur at the plate interface beneath the Okinawa island, whose depth is ranging from 15 km to 25 km, is about 10-20 km shallower than that beneath the Yaeyama islands, whose depth is ranging from 35 km to 50 km.

In this study, we constructed three-dimensional parallelepiped thermal convection model associated with subduction of the Philippine Sea (PHS) plate beneath the Amurian (AM) plate at the Ryukyu subduction zone. We considered subduction history of the PHS plate in the model region, referring to the plate rotation model (Mathews et al., 2016). We performed the numerical simulation as the time-dependent problem in the last 15 Myr to elucidate relationships among calculated thermal structures, dehydrations from the subducting plate, and the interplate seismic events. We used observed heat flow data to constrain thermal structures.

As a result at 0 Ma, we found that interplate temperature where S-SSEs and LFEs occur beneath the Yaeyama islands is lower than that beneath the Okinawa island when compared with the same depth along the direction of the trench axis. This is mainly because the convergence rate (PHS-AM) becomes gradually fast toward the southwest. Therefore, interplate temperatures where S-SSEs and LFEs occur were estimated ranging from 500℃ to 700℃ both beneath the Okinawa island and the Yaeyama islands.

We also calculated water content distribution within the PHS plate, using the calculated thermal structures and the phase diagram of MORB in an oceanic crust (Omori et al., 2008) and ultramafic rock in a slab mantle (Hacker et al., 2003). As for dehydration of MORB, we found that epidote eclogite transforms into amphibole eclogite in the neighboring area where S-SSEs and LFEs occur beneath the Okinawa island, and amphibole eclogite transforms into eclogite beneath the Yaeyama islands. The former and the latter dehydrate a total amount of 1.4 wt% and 0.7 wt% associated with their phase transformations, respectively.

Keywords: three dimensional thermal modeling

©2019. Japan Geoscience Union. All Right Reserved.

[E] Poster | S (Solid Earth Sciences)：S-CG Complex & General

Wed. May 29, 2019 5:15 PM - 6:30 PM JST | Wed. May 29, 2019 8:15 AM - 9:30 AM UTC | Poster Hall International Exhibition Hall8, Makuhari Messe_33

[S-CG48] Science of slow earthquakes: Toward unified understandings of whole earthquake process

convener:Satoshi Ide(Department of Earth an Planetary Science, University of Tokyo), Hitoshi Hirose(Research Center for Urban Safety and Security, Kobe University), Kohtaro Ujiie(Graduate School of Life and Environmental Sciences, University of Tsukuba), Takahiro Hatano(Earthquake Research Institute, University of Tokyo)

Accumulating observational studies on various types of slow deformation events, such as tectonic tremors, very low frequency events, and slow slip events, portrays some universal characteristics in generally complex behavior, including interaction among events and influence by various outer loadings. Some of these phenomena seem to have causal relation with the occurrence of very large earthquakes. A unified understanding of these slow and fast earthquake processes requires an approach integrating geophysics, seismology, geodesy, geology, and non-equilibrium statistical physics. We welcome presentations based on, but not limited to, geophysical observation, data analysis, analytical theory, numerical simulation, field study, and laboratory experiments.

[SCG48-P01] Off the Kii Peninsula Shallow Low Frequency Earthquake in 2004 revealed by Ocean Bottom Seismometer

*Koji Tamaribuchi[1], Akio Kobayashi[1], Takahito Nishimiya[1], Satoshi Annoura[2] (1.Meteorological Research Institute, 2.Japan Meteorological Agency)

[SCG48-P02] The development of pressure vessel on gouges for rock deformation at seismic rates under water-saturated conditions

*Wei-Ting Lin[1], Li-Wei Kuo[1], Wen-Jie Wu[1], Jia-Jyun Dong[1], Yi-Hung Huang[2] (1.National Central University, 2.MATSUKI HYDRAULIC INDUSTRIAL CO. LTD)

[SCG48-P03] Spatial variations of shallow very low-frequency earthquake activity along the Nankai Trough based on CMT inversion using the 3D heterogeneous model

*Shunsuke Takemura[1], Takanori Matsuzawa[1], Akemi Noda[1], Takashi Tonegawa[2], Youichi Asano[1], Takeshi Kimura[1], Katsuhiko Shiomi[1] (1.National Research Institute for Earth Science and Disaster Resilience, 2.Japan Agency for Marine-Earth Science and Technology)

[SCG48-P04] Evaluation of Magnitude and Characteristics of Seismicity of Low Frequency Earthquakes in Parkfield

*Miki Aso[1,3], Naofumi Aso[2], Satoshi Ide[1] (1.Department of Earth and Planetary Science, The University of Tokyo, 2.Tokyo Institute of Technology, School of Science, 3.OYO RMS Corporation)

[SCG48-P05] Tectonic tremor catalog in the Tohoku-Hokkaido-Oki region using S-net

*Satoshi Ide[1], Tomoaki Nishikawa[2], Takanori Matsuzawa[3], Kazuaki Ohta[2], Naoki Uchida[4], Takuya NISHIMURA[2] (1.Department of Earth an Planetary Science, University of Tokyo, 2.Disaster Prevention Research Institute, Kyoto University, 3.National Research Institute for Earth Science and Disaster Resilience, 4.Graduate School of Science and International Research Institute of Disaster Science, Tohoku University)

[SCG48-P06] Spontaneous Slow Slip and Runaway Slip in Laboratory

*Miki Takahashi[1] (1.Institute of Earthquake and Volcano Geology, Geological Survey of Japan, AIST)

[SCG48-P07] Hydration and amorphization of quartz rocks during high-velocity frictional sliding: An examination of fault gouge from friction experiments of synthetic quartz

*Yuko Onoe[1], Hirotaka Iida[2], Akito Tsutsumi[1], Aki Takigawa[1] (1.Graduate School of Science, Kyoto University, 2.Geothermal Engineering Co., Ltd.)

[SCG48-P08] Constraining S Wave Velocity of the Source Region of Shallow Very Low-Frequency Earthquakes

*Takeshi Akuhara[1], Takashi Tonegawa[2] (1.Earthquake Research Institute, The University of Tokyo, 2.Research and Development center for Earthquake and Tsunami, Japan Agency for Marine-Earth Science and Technology)

[SCG48-P09] **Quantitative relationship between aseismic slip propagation speed and frictional properties**

*Keisuke Ariyoshi[1], Jean-Paul Ampuero[2,3], Roland Burgmann[4], Toru Matsuzawa[5], Akira Hasegawa[5], Ryota Hino[5], Takane Hori[1] (1.Japan Agency for Marine-Earth Science and Technology, 2.Université Côte d'Azur, 3.California Institute of Technology, 4.University of California, Berkeley, 5.Graduate School of Science, Tohoku University)

[SCG48-P10] Comprehensive detection of very low frequency earthquakes off the Pacific coasts of Hokkaido and Tohoku, northeastern Japan

*Satoru Baba[1], Akiko Takeo[1], Kazushige Obara[1], Takanori Matsuzawa[2], Takuto Maeda[3] (1.Earthquake Research Institute, University of Tokyo, 2.National Research Institute for Earth Science and Disaster Resilience, 3.Graduate School of Science and Technology, Hirosaki University)

[SCG48-P11] **Spatio-temporal evolution of long- and short-term slow slip events in the Tokai region, central Japan estimated from a very dense GNSS network, during 1997-2017**

*Hiromu Sakaue[1], Takuya NISHIMURA[2], Jun'ichi Fukuda[3], Teruyuki Kato[4] (1.Graduate School of Science, Kyoto University, 2.Disaster Prevention Research Institute Kyoto University, 3.Earthquake Research Institute,The University of Tokyo, 4.Hot Springs Research Institute of Kanagawa Prefecture)

[SCG48-P12] Broadband excitation of acoustic emission in granular stick-slip : experiments and spectral analyses

*Hidekazu Fukumizu[1], Ikuro Sumita[2] (1.Earth and Environmental Science Course, Division of Natural System, Graduate school of Natural Science and Technology, Kanazawa University, 2.School of Geosciences and Civil Engineering, Kanazawa University)

[SCG48-P13] Episodic tremor and slip silently invades strongly locked megathrust in the Nankai Trough

*Masayuki Kano[1], Aitaro Kato[2], Kazushige Obara[2] (1.Graduate school of science, Tohoku University, 2.Earthquake Research Institute, The University of Tokyo)

[SCG48-P14] Spatial distribution of the electrical resistivity beneath western part of Shikoku Island where long-term SSE events have repeatedly occurred

*Makoto Uyeshima[1], Maki Hata[1], Hiroshi Ichihara[2], Ryokei Yoshimura[3], Koki Aizawa[4] (1.Earthquake Research Institute, The University of Tokyo, 2.Graduate School of Environmental Studies, Nagoya University, 3.Disaster Prevention Research Institute, Kyoto University, 4.Institute of Seismology and Volcanology, Faculty of Sciences, Kyushu University)

[SCG48-P15] Variations of scaling relationships for shallow tremor observed along the Nankai trough

*Masaru Nakano[1], Suguru Yabe[1] (1.Japan Agency for Marine-Earth Science and Technology)

[SCG48-P16] Low-frequency earthquakes triggered by teleseismic surface waves by Ryukyu subduction zone.

Ayumi Kinjo[1], *Mamoru Nakamura[1] (1.Faculty of Science, University of the Ryukyus)

[SCG48-P17] Detection of small surface displacement accompanying deep low-frequency tremor in Shikoku region, southwest Japan

*Yutaro Okada[1], Takao Tabei[2] (1.Faculty of Science, Kochi University, 2.Faculty of Science and Technology, Kochi University)

[SCG48-P18] Long-term temporal change in crustal resistivity beneath western Shikoku

*Futoshi Yamashita[1], Yoshimori Honkura[1] (1.National Research Institute for Earth Science and Disaster Resilience)

[SCG48-P19] Slow decay of postseismic deformation compared with aftershocks following the 2011 Tohoku-oki Earthquake

*Yuta Mitsui[1], Shunsuke Morikami[2] (1.Department of Geosciences, Shizuoka University, 2.Formerly at Graduate School of Science and Technology, Shizuoka University)

[SCG48-P20] Serpentinite dehydration in subduction shear zones formed at source depths of slow earthquakes

*Yasushi Mori[1], Miki Shigeno[1], Kohtaro Ujiie[2], Kazuya Noro[2], Tadao Nishiyama[3] (1.Kitakyushu Museum of Natural History and Human History, 2.University of Tsukuba, 3.Kumamoto University)

[SCG48-P21] Earthquake swarms following very low-frequency earthquakes in the central Ryukyu Trench

*Mamoru Nakamura[1] (1.Faculty of Science, University of the Ryukyus)

[SCG48-P22] Seismic imaging in the central Nankai trough, off Shionomisaki to Kii channel

*Yasuyuki Nakamura[1], Shuichi Kodaira[1], Tetsuo No[1], Yuka Kaiho[1], Gou Fujie[1], Seiichi Miura[1], Kazuya Shiraishi[1] (1.Japan Agency for Marine Earth Science and Technology)

[SCG48-P23] Attempt to Detect Intra-plate SSEs Based on F3 Solution of GEONET

*Yusaku Tanaka[1] (1.Earthquake Research Institute)

[SCG48-P24] A new hydrothermal, low to high speed rotary-shearing apparatus: Reproduction of slow/megathrust earthquakes in laboratory

*Takehiro Hirose[1], Wataru Tanikawa[1], Yohei Hamada[1], Keishi Okazaki[1] (1.Kochi Institute for Core Sample Research, Japan Agency for Marine-Earth Science and Technology)

[SCG48-P25] Very low-frequency earthquakes in western Shikoku remotely triggered by the 2016 Mw5.9 off-Kii Peninsula earthquake

*Masatoshi Miyazawa[1] (1.Disaster Prevention Research Institute, Kyoto University)

[SCG48-P26] **Underground structure around source region of slow earthquakes in western Shikoku obtained by receiver function analysis**

Akira Hikita[1], Aitaro Kato[1], *Kazushige Obara[1], Akiko Takeo[1], Takeshi Akuhara[1] (1.Earthquake Research Institute, The University of Tokyo)

[SCG48-P27] Hypocenter determination of deep low frequency tremors beneath the Kii Peninsula by backprojection of seismic array data

*Kodai Sagae[1], Hisashi Nakahara[1], Takeshi Nishimura[1], Kazutoshi Imanishi[2] (1.Graduate School of Science,Tohoku University, 2.National Institute of Advanced Industrial Science and Technology (AIST))

[SCG48-P28] Triggered tremors and stress perturbations due to surface waves

*Ryohei Ikeda[1], Naoki Suda[1] (1.Hiroshima University)

[SCG48-P29] Numerical modeling of long- and shallow slow slip events including shallow region in Hyuganada and western Nankai, Japan

*Takanori Matsuzawa[1], Bunichiro Shibazaki[2] (1.National Research Institute for Earth Science and Disaster Resilience, 2.Building Research Institute)

[SCG48-P30] Further evidence for the influence of a subducting-ridge on the spatial strain accumulation and release pattern in the shallow eastern Nankai Trough, based on VLFE distribution

*Akiko Toh[1], Chen Wan-Jou [2], Doug Dreger[3], Wu-Cheng Chi[2], Satoshi Ide[1] (1.University of Tokyo, 2.Institute of Earth Sciences, Academia Sinica, 3.UC Berkeley)

[SCG48-P31] Evidence for semi-brittle flow in mantle-wedge serpentinites under high pore fluid pressure and their implications for deep low frequency earthquakes

Kengo Kataoka[1], Yurina Nagata[1], *Ken-ichi Hirauchi[1], Ryosuke Oyanagi[2], Atsushi Okamoto[3], Katsuyoshi Michibayashi[4] (1.Department of Geosciences, Faculty of Science, Shizuoka University, 2.Japan Agency for Marine-Earth Science and Technology, 3.Graduate School of Environmental studies, Tohoku University, 4.Department of Earth and Planetary Sciences, Nagoya University)

[SCG48-P32] Spatial distribution of slow slip events off the Boso peninsula from 1996 to 2018 under sparsity constraints

*Ryoko Nakata[1], Hideitsu Hino[2], Tatsu Kuwatani[3,4], Takahiro Akiyama[5], Shoichi Yoshioka[6], Masato Okada[7], Takane Hori[1] (1.Japan Agency for Marine-Earth Science and Technology, 2.The Institute of Statistical Mathematics, 3.Department of Solid Earth Geochemistry, Japan Agency for Marine-Earth Science and Technology, 4.PRESTO, Japan Science and Technology Agency, 5.Graduate School of Science, Kobe University, 6.Research Center for Urban Safety and Security, Kobe University, 7.Graduate School of Frontier Sciences, The University of Tokyo)

[SCG48-P33] Marine electromagnetic observations around a slow earthquake region in the western Nankai trough

*Hiroshi Ichihara[1], Tada-nori Goto[2], Tetsuo Matsuno[3], Noriko Tada[4], Shinya Sato[2] (1.Earthquake and Volcano Research Center, Nagoya University, 2.Graduate School of Engineering, Kyoto University, 3.Ocean Bottom Exploration Center, Kobe University, 4.JAMSTEC)

[SCG48-P34] Dynamics of precipitating injection fronts inside of structured medium

*Yutaka Sumino[1], Shunsuke Tanaka[1], Miyuki Kunihiro[1] (1.Tokyo University of Science)

[SCG48-P35] Permeability changes of simulated low permeable fault rocks induced by intermediate velocity friction test

*Wataru Tanikawa[1] (1.Japan Agency for Marine-Earth Science and Technology, Kochi Instutute for Core Sample Research)

[SCG48-P36] Modified relation between the coupling and tremor rates around the Shikoku region

*Tadafumi Ochi[1] (1.Institute of Earthquake and Volcano Geology, Geological Survey of Japan, The National Institute of Advanced Industrial Science and Technology)

[SCG48-P37] Spatiotemporal distribution of regular and very low-frequency earthquakes in the northern part of the Ryukyu subduction zone

*Youichi Asano[1], Kazuhiko Goto[2], Hiroshi Yakiwara[3], Shuichiro Hirano[3] (1.National Research Institute for Earth Science and Disaster Resilience, 2.Association for the development of earthquake prediction,

3.Nansei-toko Observatory for Earthquakes and Volcanoes, Kagoshima University)

[SCG48-P38] Possible tectonic tremor activities near the VLFE epicenters in the Sanriku-Oki region in 2011

*Hidenobu Takahashi[1], Ryota Hino[1], Yusaku Ohta[1], Naoki Uchida[1], Syuichi Suzuki[1], Masanao Shinohara[2], Takanori Matsuzawa[3] (1.Graduate school of Science Tohoku University , 2.Earthquake Research Institute, University of Tokyo, 3.National Research Institute for Earth Science and Disaster Resilience)

[SCG48-P39] Heterogeneous structure around a region of slow earthquake activity off Ibaraki prefecture along the Japan Trench

*Kimihiro Mochizuki[1], Tomoaki Yamada[1], Masanao Shinohara[1], Ryota Hino[2], Ryosuke Azuma[2], Yoshihiro Ito[3], Yoshio Murai[4], Kenji Uehira[5], Toshinori Sato[6] (1.ERI, Univ. of Tokyo, 2.Graduate School of Science, Tohoku Univ., 3.DPRI, Kyoto Univ., 4.Faculty of Science, Hokkaido Univ., 5.NIED, 6.Graduate School of Science, Chiba Univ.)

[SCG48-P40] Shallow low-frequency tremor triggered by nearby moderate earthquakes off Sanriku

*Sachiko Tanaka[1], Takanori Matsuzawa[1], Youichi Asano[1] (1.National Research Institute for Earth Science and Disaster Resilience)

[SCG48-P41] Slow slip events in the Bungo Channel over 15 years as inferred from GNSS data (1996-2011)

Takatoshi Yokoi[1], *SHINICHI MIYAZAKI[1], Hiromu Sakaue[1], Jun'ichi Fukuda[2] (1.Graduate School of Science, Kyoto University, 2.Earthquake Research Institute, The University of Tokyo)

[SCG48-P42] Investigations of sensor orientation and a possibility of detecting crustal deformation based on accelerometer records of S-net

*Ryota Takagi[1], Naoki Uchida[1], Takashi NAKAYAMA[1], Ryosuke Azuma[1], Akira Ishigami[1], Tomomi Okada[1], Yusaku Ohta[1], Ryota Hino[1] (1.Research Center for Prediction of Earthquakes and Volcanic Eruptions, Graduate School of Science, Tohoku University)

[SCG48-P43] Spatiotemporal variation of released seismic energy from shallow low-frequency tremor in Hyuga-nada, revealed by ocean bottom seismological observation

*Yusuke Yamashita[1], Saki Watanabe[2], Tomoaki Yamada[3], Masanao Shinohara[3], Takeshi Matsushima[2] (1.Disaster Prevention Research Institute, Kyoto University, 2.Institute of Seismology and Volcanology, Kyushu University, 3.Earthquake Research Institute, The University of Tokyo)

[SCG48-P44] Unified description of fast and slow earthquakes using velocity strengthening patches

*So Ozawa[1], Takahiro Hatano[1] (1.Earthquake Research Institute, the University of Tokyo)

[SCG48-P45] The b-value of the earthquake swarm activities accompanied by the Boso slow slip events

*Yuki Noda[1], Hitoshi Hirose[2,1] (1.Department of Planetology, Faculty of Science, Kobe University , 2.Research Center for Urban Safety and Security, Kobe University)

[SCG48-P46] **Three-dimensional thermal modeling associated with subduction of the Philippine Sea plate at the Ryukyu Trench, and its relation to the occurrence of interplate seismic events**

*Nobuaki Suenaga[1], Shoichi Yoshioka[2,1], Yinfeng Ji[3] (1.Graduate School of Science, Kobe University, Japan, 2.Research Center for Urban Safety and Security, Kobe University, Japan, 3.Chinese Academy of Science, Beijin, China)

Off the Kii Peninsula Shallow Low Frequency Earthquake in 2004 revealed by Ocean Bottom Seismometer

*Koji Tamaribuchi[1], Akio Kobayashi[1], Takahito Nishimiya[1], Satoshi Annoura[2]

1. Meteorological Research Institute, 2. Japan Meteorological Agency

The 2004 off the Kii Peninsula earthquakes (Mj7.1, 7.4) occurred near the Nankai trough axis, southeast off the Kii Peninsula, Japan, on September 5, 2004. After the earthquakes, the Meteorological Research Institute conducted OBS observation to examine the aftershock distribution accurately. Although the analysis was limited to hypocenter relocation of "ordinary aftershocks", no analysis was done for slow events. In this study, it is shown that many low-frequency earthquakes (LFEs) occurred in "ordinary aftershocks" from the detailed inspection of our observation. During the observation period, the frequency of LFE gradually decreased. Since P- and S-arrival times are unclear, it is difficult to determine the distribution of the hypocenter accurately. However, by using the Amplitude Source Location (ASL; Battaglia and Aki, 2003), the LFEs are located between a splay fault and trench axis. The 2004 OBS stations are located east of the DONET, and many LFEs are detected in the 2004 OBS network. In addition, there are many very-low-frequency events (VLFEs) in the F-net waveforms with very-low-frequency band-pass filter (0.02 - 0.05 Hz) during the observation period. We found that the identified LFEs were associated with VLFEs since their amplitudes seemed to be correlated. This means that the LFEs and VLFEs show the same phenomenon. Our observations might contribute to reveal the relationship between ordinary aftershocks, slow-events, and megathrust events such as Nankai trough earthquake.

Keywords: LFE, OBS, 2004 off the Kii Peninsula earthquakes

©2019. Japan Geoscience Union. All Right Reserved.

The development of pressure vessel on gouges for rock deformation at seismic rates under water-saturated conditions

*Wei-Ting Lin[1], Li-Wei Kuo[1], Wen-Jie Wu[1], Jia-Jyun Dong[1], Yi-Hung Huang[2]

1. National Central University, 2. MATSUKI HYDRAULIC INDUSTRIAL CO. LTD

To understand earthquake mechanism and fault behavior during earthquake ruptures, experimentalists commonly conduct rock deformation tests with rotary shear apparatus (e.g., low-to high-velocity rock friction experiment, LHVR) which allow deformed at seismic rates. In general, the materials utilized for rotary shear apparatus are both cohesive rocks (e.g., gabbro and carbonate) and incohesive rocks (natural fault gouges and synthetic rock powders), while the latter are deformed at seismic rates and, commonly at low normal stresses (0.5 to 2 MPa confining with a plastic Teflon ring). However, using Teflon rings has issues of gouge extrusion and chemical contamination, in particular, at high normal stresses (>3MPa) and water-saturated condition, and the obtained mechanical data and associated experimental products seem to be questionable. Here we develop a metal pressure vessel for LHVR to deform gouges at seismic rates and, importantly, expand the normal stress capability (up to 15 MPa) and under water-saturated condition. Our results show the resistance from the pressure vessel itself (metal-to-metal contact) is extremely low (friction coefficient ≈0.02), and the result of kaolinite is similar to the previously published data. In particular, both gouge-extrusion and water-leaking was not observed deformed at a normal stress of 15 MPa and equivalent velocity 1 m/s. The designed pressure vessel could fill the gap of experimental conditions among the current used pressure vessels and complete the understanding of fault ruptures.

Keywords: pressure vessel, water-saturated condition, fault gouge, rotary shear experiment

©2019. Japan Geoscience Union. All Right Reserved.

Spatial variations of shallow very low-frequency earthquake activity along the Nankai Trough based on CMT inversion using the 3D heterogeneous model

*Shunsuke Takemura[1], Takanori Matsuzawa[1], Akemi Noda[1], Takashi Tonegawa[2], Youichi Asano[1], Takeshi Kimura[1], Katsuhiko Shiomi[1]

1. National Research Institute for Earth Science and Disaster Resilience, 2. Japan Agency for Marine-Earth Science and Technology

To reveal structural properties around the Philippine Sea plate boundary, we investigated spatial variation of shallow very low-frequency earthquake (SVLFE) activity along the Nankai Trough. By using F-net velocity seismograms for periods of 20-50s, we conducted centroid moment tensor (CMT) inversion of SVLFEs detected by array analysis of Asano et al. (2008 EPS). Our CMT method is basically same as in Takemura et al. (2018 GRL). Source grids were assumed on the boundary of the Philippine Sea plate at horizontal intervals of 0.1°. Green's functions from source grids to F-net stations were evaluated by finite-difference method simulations of seismic wave propagation within the 3D heterogeneous structure model of Takemura et al. (2019 PAGEOPH).

We applied our CMT method to SVLFEs occurred from June 2003 to May 2018. Almost of CMT solutions are low-angle thrust faulting mechanism occurred around the accretionary prism toe. We evaluated spatial variations of SVLFE activity along the Nankai trough by calculating cumulative moment at each source grid. The areas with large cumulative moments appeared near the trench axis of off the Cape Muroto, the Kii Channel and the southeastern Kii Peninsula. We found spatial correlations between cumulative moment, slip-deficit rate (Noda et al. 2018 JGR) and *S*-wave velocities (Tonegawa et al. 2017 Nature Comm.) around the Philippine Sea plate boundary. Such spatial correlations suggest that SVLFEs are effectively activated by mechanically weakening due to pore fluid at surrounding area of strongly locked zone of the Philippine Sea plate.

Acknowledgement
NIED F-net broadband velocity seismograms were used. The catalogs of slow earthquakes were downloaded from the website of slow earthquake database (Kano et al., 2018 SRL). Finite-different method simulations were conducted on the Earth Simulator at the JAMSTEC.

Keywords: Nankai Trough, Shallow very low-frequency earthquake, CMT inversion, Pore fluid pressure, Slip deficit rate

©2019. Japan Geoscience Union. All Right Reserved.

Evaluation of Magnitude and Characteristics of Seismicity of Low Frequency Earthquakes in Parkfield

*Miki Aso[1,3], Naofumi Aso[2], Satoshi Ide[1]

1. Department of Earth and Planetary Science, The University of Tokyo, 2. Tokyo Institute of Technology, School of Science, 3. OYO RMS Corporation

Over a million tectonic low frequency earthquakes (LFEs) have been found in Parkfield along the San Andreas Fault, as 88 families by Shelly and Hardebeck [2010]. Thanks to enormous event detection, interesting characteristics focusing on their event amplitudes have been reported such as the spatial variation along the fault, the exponential frequency distribution for each family, and the relationship with recurrence time [Shelly and Hardebeck, 2010; Shelly, 2010]. However, the relative size of families has not been quantified accurately, because we have to consider various factors such as radiation pattern depending on focal mechanisms, attenuation during wave propagation, and site amplification effects. For quantitative comparison of scale among differently located events, here we estimate the absolute magnitude of each event considered those effects.

We estimate the seismic moment Mo [Nm] and moment magnitude Mw of all LFE events in the catalog of Shelly [2017]. We first stack seismograms of over one million events in the catalog to improve the signal-to-noise (S/N) ratio. Then, we evaluate the absolute amplitude of the original seismograms using the stacked waveforms. Specifically, we evaluate seismic moment Mo by assuming focal mechanisms of each family, attenuation quality factor, site effect estimated by Aso et al. [2019, submitted to JpGU meeting, “Variations of Focal Mechanisms of Low Frequency Earthquake in Parkfield”], and the source time function estimated by Thomas et al. [2016]. Note that we consider the frequency-limited seismic moment Mo, though it is not exactly the same as the original definition of seismic moment measured at a lower frequency than the minimum frequency contained in one phenomenon.

As previously reported by reported by Shelly and Hardebeck [2010], LFEs in the southern part has larger magnitude. We also find that shallower events are smaller than deeper events.

Similarly, most of the frequency distribution for each family shows an exponential distribution which is also reported for LFEs in Cascadia [Sweet et al., 2014] and New Zealand [Chamberlain et al., 2014].

By comparing size and recurrence interval, the events during LFE burst (seconds interval) tend to be larger than the first event of burst, which occurs after hours-to-days quiescence. A similar tendency is found in tremor burst occurring with a longer time scale (~1-week-long) than that of LFEs (~1-minute-long) [Yabe and Ide, 2014]. These might suggest some temporal change in fault rheology and/or some characteristic spatiotemporal behavior such as Brownian slow earthquake processes [Ide, 2008].

Keywords: San Andreas Fault, Parkfield, seismicity, waveform stacking, low frequency earthquake, amplitude evaluation

©2019. Japan Geoscience Union. All Right Reserved.

Tectonic tremor catalog in the Tohoku-Hokkaido-Oki region using S-net

*Satoshi Ide[1], Tomoaki Nishikawa[2], Takanori Matsuzawa[3], Kazuaki Ohta[2], Naoki Uchida[4], Takuya NISHIMURA[2]

1. Department of Earth an Planetary Science, University of Tokyo, 2. Disaster Prevention Research Institute, Kyoto University, 3. National Research Institute for Earth Science and Disaster Resilience, 4. Graduate School of Science and International Research Institute of Disaster Science, Tohoku University

Recently, various slow earthquakes have discovered in the subduction zone off Tohoku and Hokkaido regions along the Japan Trench. In this presentation, we report the detection of tectonic tremors using the Seafloor Observation Network for Earthquakes and Tsunamis along the Japan Trench (S-net), operated by The National Research Institute for Earth Science and Disaster Resilience (NIED).

We used continuous seismograms from August 2016 to August 2018 recorded by short-period sensors at 150 S-net stations. The original data were converted to envelope waveforms and analyzed using the envelope correlation method coded by Ide (2010), for each 300 s time windows with 150 s overlap. Since the results included many ordinary earthquakes with short durations, we regarded the events with durations longer than 20 s as tremors. This number is twice longer than that used for deep tremors in western Japan, reflecting the long-lasting waves in ocean bottom observation.

We found that the detection completeness is not high due to the high seismic activity in the Japan Trench, especially after the occurrence of large earthquakes, with numerous aftershocks falsely detected. We therefore divided the study area into 18 overlapping sub-regions that cover the locations of tremor activity to solve this problem. We detected tremors in each sub-region and merged the results into one catalogue by removing one of any two events within 10 s and 1 degree of each other, depending on their root-mean-square errors. Some tremor-like signals were found near the triple junction off the Boso Peninsula at approximately 34.8˚N. However, visual inspection revealed these events to be ordinary earthquakes, which we excluded from our tremor catalogue. The resultant tremor catalogue will be available in Slow Earthquake Database (Kano et al., 2018).

Keywords: tectonic tremor, slow earthquake, ocean bottom seismometer, S-net, Japan trench

©2019. Japan Geoscience Union. All Right Reserved.

Spontaneous Slow Slip and Runaway Slip in Laboratory

*Miki Takahashi[1]

1. Institute of Earthquake and Volcano Geology, Geological Survey of Japan, AIST

Earthquake nucleation and propagation involves the acceleration of slip on a fault from a background, quasi-static, low-velocity state towards meter-per-second values. From shear experiments using brine-saturated simulated gouge composed of 80:20 wt.% mixtures of halite and muscovite (following e.g. Niemeijer & Spiers, 2007, JGR), Takahashi et al., [2017, G-cubed] recently reported a switch in the dominant deformation process, from distributed viscous flow (pressure solution creep) to localized brittle deformation, at a critical velocity V_c (~20 μm/sec). The direct effect which is normally observed upon perturbations in sliding rate disappears for $V > V_c$, suggesting that runaway fault-slip may be achieved when the sliding velocity exceeds V_c.
At relatively low shear stress, flow mechanisms, such as pressure solution creep and dislocation creep, will be fast enough to effectively suppress slip acceleration. However, with increasing the shear stress, there may be a velocity range in which flow mechanisms still works but not as effective. Hypothesizing that, under constant shear stress boundary conditions, this may lead to spontaneous acceleration followed by deceleration, analogous to a slow slip event. Moreover, imposing the constant shear stress with equal or larger value of the maximum strength of the simulated gouge, I also hypothesize that slip acceleration may proceed as $V > V_c$, inducing a dynamic weakening.
To address these hypotheses, I conducted torque-controlled rotary shear experiments, using brine-saturated, 80:20 wt % mixtures of halite (grain size < 75 μm) and muscovite (grain size < 33 μm) powders. Approximately 1.65 g of the gouge mixture was sandwiched between two teethed steel piston rings, forming an initially 1 mm thick layer. The piston rings had an inner diameter of 38 mm, and an outer diameter of 50 mm. I used a high-velocity rotary shear apparatus designed by T. Shimamoto [e.g., Togo and Shimamoto, 2012], and now installed at the Geological Survey of Japan (GSJ). The apparatus was modified to enable torque control with an accuracy of ±0.002 in the friction coefficient (μ), at a normal stress of 5 MPa. Rotation displacement is measured using a potentiometer installed close to the piston ring at the rotating side.
A preliminary result shows the velocity evolution after stepwise changes in the shear stress. At low shear stresses, corresponding to the pressure solution creep-controlled regime, transient increasing velocity towards a steady-state values suggests stable sliding. At $\mu \approx 0.6$, the simulated gouge shows spontaneous acceleration to $V \approx 1$ μm/sec, followed by deceleration. Lastly, under a constant shear stress condition equivalent to $\mu = 0.67$, spontaneous slip acceleration occurred followed by dynamic weakening at $V \approx V_c = 20$ μm/sec. More experiments and microstructural observations will help to elucidate the relationship between the critical velocity and the switch among dominant deformation mechanisms.

Keywords: shear stress control test, spontaneous acceleration/deceleration, dynamic weakening

©2019. Japan Geoscience Union. All Right Reserved.

Hydration and amorphization of quartz rocks during high-velocity frictional sliding: An examination of fault gouge from friction experiments of synthetic quartz

*Yuko Onoe[1], Hirotaka Iida[2], Akito Tsutsumi[1], Aki Takigawa[1]

1. Graduate School of Science, Kyoto University, 2. Geothermal Engineering Co., Ltd.

Various types of rocks and fault gouges display weakening of frictional strength at high-velocities, and in many cases, it is caused by high-temperature faulting processes such as frictional melting and thermal decomposition of fault materials. On the other hand, siliceous rocks display weakening of frictional strength at relatively slow slip velocity of ~1 mm/s. This weakening is a specific phenomenon because frictional heat is not sufficient to induce the high-temperature transformation reactions in this slip velocity range [Di Toro et al., 2004]. Goldsby and Tullis [2002] proposed gel lubrication model to explain the weakening of siliceous rocks; in which model frictional weakening likely results from production and shearing of hydrated amorphous silica layer along a fault in quartz rocks. But the relationship between the frictional weakening and hydration and amorphization of fault gouge is not clear yet.

This study aims to elucidate the mechanism of the frictional weakening observed for siliceous rocks. We conducted a series of friction experiments on synthetic quartz samples using a rotary-shear, intermediate-to high-velocity friction testing machine. Experiments were carried out under a constant normal stress condition of 1.5 MPa and at slip velocities of 5 μm/s, 10 μm/s, 105 μm/s, 1 mm/s, 10 mm/s and 105 mm/s. In this study effect of drying the sample on the frictional behavior were examined by introducing dry air to the chamber of the sample. After the friction tests, the gouge material on the slip surfaces were collected and analyzed by FTIR.

The frictional behavior of the synthetic quartz differs between room humidity and dry conditions; velocity weakening was observed for both conditions, however, velocity weakening starts at lower slip velocities for the dry experiments. Under DRY conditions, the frictional weakening occurs at slip velocity around 10 μm/s. From the results of the FTIR analysis, hydration of the gouge is confirmed for all the samples tested in this study. The FTIR result also indicates that the faster the slip velocity, the more the crystal structure of the gouge is destructed.
It is showed that under both DRY and Room Humidity conditions, at least the gouge generated on the friction surface of the sample which showed slip weakening is hydrated, consistent with the weakening model of Goldsby and Tullis [2002].

©2019. Japan Geoscience Union. All Right Reserved.

Constraining S Wave Velocity of the Source Region of Shallow Very Low-Frequency Earthquakes

*Takeshi Akuhara[1], Takashi Tonegawa[2]

1. Earthquake Research Institute, The University of Tokyo, 2. Research and Development center for Earthquake and Tsunami, Japan Agency for Marine-Earth Science and Technology

Shallow very low-frequency earthquakes (VLFEs), which are believed to occur in the vicinity of megathrusts, have been often associated with elevated pore fluid pressure. Lines of evidence for this idea include a small amount of stress drop, high tidal sensitivity, and reduced P wave velocity inferred from active source seismic surveys. Revealing the physical properties of the source region of shallow VLFEs will lead to a better understanding of their generation mechanisms. However, the challenge lies in the difficulty of acquiring S wave velocity in fine resolution.

Recent achievements by the authors may help overcome this issue. Akuhara et al. (2019) developed a robust technique to estimate Green's functions of receiver side structures from offshore seismograms, which are typically ill-conditioned due to water reverberations. Tonegawa et al. (2017) inverted Rayleigh wave admittance (i.e., a ratio of ground displacement to hydraulic pressure) for shallow S wave velocity structures beneath DONET seafloor observatories at the Nankai Trough subduction zone. Their velocity models show low-velocity zones that characterize the source regions of shallow VLFEs. However, a smoothing constraint imposed on the models renders their interpretation somewhat difficult.

This study presents preliminary results from transdimensional inversion of receiver-side Green's function estimated by the method of Akuhara et al. (2019), where we adopt a prior constraint by the velocity models of Tonegawa et al. (2017). Complementary to the Rayleigh admittance, the Green's function approach is sensitive to velocity contrasts and thus will offer an improved resolution.

Keywords: shallow very low frequency earthquake, seismic velocity structure, ocean bottom seismometer, bayesian analysis

©2019. Japan Geoscience Union. All Right Reserved.

Quantitative relationship between aseismic slip propagation speed and frictional properties

*Keisuke Ariyoshi[1], Jean-Paul Ampuero[2,3], Roland Burgmann[4], Toru Matsuzawa[5], Akira Hasegawa[5], Ryota Hino[5], Takane Hori[1]

1. Japan Agency for Marine-Earth Science and Technology, 2. Université Côte d'Azur, 3. California Institute of Technology, 4. University of California, Berkeley, 5. Graduate School of Science, Tohoku University

Recent observations show evidence of propagation of postseismic slip, whose propagation speed may contain information about the mechanical properties of faults. Here, we develop a new analytical relationship between the propagation speed of aseismic slip transients and fault frictional properties, modeled by a rate- and state-dependent friction law. The relationship explains the propagation speed of afterslip in 3-D numerical simulations to first order. Based on this relationship, we identify systematic dependencies of afterslip propagation speed on effective normal stress σ and frictional properties (the coefficients a and a-b which quantify the instantaneous and the steady-state velocity-dependence of friction, respectively, and the characteristic slip distance d_c of fault state evolution). Lower values of the parameter $A=a\sigma$ cause faster propagation in areas where the passage of the postseismic slip front induces large shear stress changes $\Delta\tau$ compared to A, which are typically located near the mainshock rupture. In areas where $\Delta\tau/A$ is small, typically more distant from the mainshock, afterslip propagation speed is more sensitive to (a-b) σ. The propagation speed is proportional to initial slip velocity and inversely proportional to d_c. The relationship developed here should be useful to constrain the frictional properties of faults based on observed propagation speeds, independently of rock laboratory experiments, which can then be used in predictive numerical simulations of aseismic slip phenomena.

Keywords: rate- and state-dependent friction, effective normal stress, stress perturbation

©2019. Japan Geoscience Union. All Right Reserved.

Comprehensive detection of very low frequency earthquakes off the Pacific coasts of Hokkaido and Tohoku, northeastern Japan

*Satoru Baba[1], Akiko Takeo[1], Kazushige Obara[1], Takanori Matsuzawa[2], Takuto Maeda[3]

1. Earthquake Research Institute, University of Tokyo, 2. National Research Institute for Earth Science and Disaster Resilience, 3. Graduate School of Science and Technology, Hirosaki University

Very low frequency earthquakes (VLFEs), classified as one type of slow earthquakes, occur near seismogenic zones. VLFEs off the Pacific coasts of Hokkaido and Tohoku in northeastern Japan occur around subducting plate interfaces near trenches. Asano et al. (2008) found VLFEs in the off-Tokachi region, the southern part of the Pacific coast of Hokkaido along the Kuril Trench, by array signal processing using high-sensitivity accelerometers of Hi-net operated by National Research Institute for Earth Science and Disaster Resilience (NIED). In recent years, VLFEs off the Pacific coast of Tohoku were found by visually checking broadband seismograms of F-net operated by NIED and other events were detected by the matched-filter technique using waveforms of detected events as templates (Matsuzawa et al., 2015). However, the number of detected VLFEs may have been limited because of the small number of the VLFE templates in previous studies. Baba et al. (2018, SSJ) set four virtual epicenters off the Pacific coasts of Hokkaido and Tohoku and detected VLFEs by the matched-filter technique using numerically simulated waveforms as templates. We extended virtual epicentral gridsto make more comprehensive detection of VLFEs.

We used continuous seismograms of F-net seismometers from January 2003 to July 2018 after applying a band-pass filter of 0.02–0.05 Hz. We set 123 virtual epicentral grids off the Pacific coasts of Hokkaido and Tohoku, and computed the synthetic waveform from the source at each virtual epicenter by the finite difference method with a three-dimensional velocity structure model, namely, Japan Integrated Velocity Structure Model (Koketsu et al., 2012). The fault mechanisms were assumed to be consistent with the geometry of the plate boundary and a plate motion model, NUVEL-1A. We then calculated station- and component-averaged cross-correlation coefficients (averaged CC) between synthetic waveforms and the data of F-net seismograms every 1 s, and selected the events which have averaged CC above nine times of the median absolute deviation of the distribution. This method is, however, sensitive to regular earthquakes and teleseismic events as well. We then excluded the signal of regular earthquakes by discarding events with the amplitudes of more than 160 nm/s at 1-2 Hz in vertical components at the nearest stations. Moreover, to remove teleseismic events, we used the USGS earthquake catalog and discarded events with high amplitudes and low averaged cross-correlation coefficients.

VLFE activities in the off-Tokachi and off-Aomori regions show synchronized episodic bursts in the interval of several months. VLFEs in the off-Tokachi region was rapidly increased by the afterslip of the 2003 Tokachi-Oki earthquake. Those in the off-Iwate and off-Ibaraki regions, located out of the coseismic slip area of the 2011 off the Pacific coast of Tohoku Earthquake (hereinafter, the Tohoku earthquake), were also rapidly increased by the afterslip of the Tohoku earthquake. VLFE activity in the off-Miyagi region is characterized by episodic bursts in the interval of several months to one year before the Tohoku earthquake, but it became low since then. VLFE activity in the off-Fukushima region show dramatic increase after an Mw 6.9 earthquake at off-Fukushima on July 19, 2008. In the off-Miyagi and off-Fukushima regions, located within or at the edge of the coseismic slip area of the Tohoku earthquake, VLFE activity has been low since the Tohoku earthquake probably because the earthquake released the

©2019. Japan Geoscience Union. All Right Reserved.

stress almost completely. These results suggest that VLFEs are sensitive to the stress perturbation and can be a slip meter that reflect spatiotemporal change of the interplate slip, as has been indicated by previous studies. Consequently, one possible cause of these episodic VLFE bursts in the off-Tokachi, off-Aomori and off-Miyagi regions may be the intermittent release of small portion of stress accumulated by interplate locking between plates in the interval of several months to one year. The interval of episodic bursts is shorter than a periodicity of slow slips ranging from 1 to 6 years off the Pacific coasts of Tohoku indicated by Uchida et al. (2016).

©2019. Japan Geoscience Union. All Right Reserved.

Spatio-temporal evolution of long- and short-term slow slip events in the Tokai region, central Japan estimated from a very dense GNSS network, during 1997-2017

*Hiromu Sakaue[1], Takuya NISHIMURA[2], Jun'ichi Fukuda[3], Teruyuki Kato[4]

1. Graduate School of Science, Kyoto University, 2. Disaster Prevention Research Institute Kyoto University, 3. Earthquake Research Institute,The University of Tokyo, 4. Hot Springs Research Institute of Kanagawa Prefecture

The long-term slow slip events (SSEs) have been reported on the subducting Philippine Sea Plate in the Tokai region, central Japan during 2001-2005 and 2013-2016. Many short-term slow slip events have been also observed there since 1996. We analyzed GNSS data from 1997 to 2017 to estimate spatiotemporal distribution of interplate slip associated with these SSEs in this study. The GIPSY-OASIS II software (version 6.1) was used to estimate daily coordinates of GNSS stations operated by GSI and JUNCO (the Japanese University Consortium for GPS Research). It is well known that GNSS time series have many systematic signals and noises that do not result from SSEs. They include, for example, seasonal variations, co- and post-seismic deformation of the 2004 southeast off Kii Peninsula earthquakes (M_w 7.3/7.4), the 2008 Ibaraki-ken-oki earthquake (M_w6.9), the 2008 Fukushima-ken-oki earthquake (M_w7.0) and the 2011 Tohoku-oki earthquake (M_w9.0), and crustal deformation of volcanic activity on the northern Izu Islands in 2000. After removing them, we applied a modified Network Inversion Filter (NIF) [Fukuda et al., 2008] to estimate daily slip and slip rate on the subduction plate interface.
Our results suggest that not only long-term SSEs (M_w~7.1 and M_w~6.7) in 2000-2005 and 2013-2016, but also short-term SSEs (M_w<6.1). The maximum estimated daily slip rates for short-term SSEs are an order of magnitude larger than those of the long-term SSE, and peak slip for short-term SSEs migrates along strike with LFTs synchronously. It suggests that LFTs are loaded directly by SSEs, and that slip rate regulates LFT genesis. We will present the change of back slip rate between inter short-term SSEs and characteristics of short-term SSEs (e.g. slip rates and recurrence interval) depending on the occurrence of long-term SSE.

Keywords: slow slip event, Tokai region, GNSS

©2019. Japan Geoscience Union. All Right Reserved.

Broadband excitation of acoustic emission in granular stick-slip : experiments and spectral analyses

*Hidekazu Fukumizu[1], Ikuro Sumita[2]

1. Earth and Environmental Science Course, Division of Natural System, Graduate school of Natural Science and Technology, Kanazawa University, 2. School of Geosciences and Civil Engineering, Kanazawa University

Slow slip and tremor are observed to occur simultaneously (e.g., Rogers and Dragert, Science, 2003). Such observation can be modelled using granular stick-slip experiments which show that the timing of the slips and acoustic emission (AE) are well correlated (e.g., Johnson et al., GRL, 2013, Jiang et al. GRL, 2017). AE waveforms are complex (e.g., Michlmayr & Or, Gran. Matt., 2014), and we do not fully understand the details of the temporal change of AE during the slip. Here we report the results of granular stick-slip experiments which focus on how their spectra depend on the shear rate, particle size and container size.

We shear glass beads contained in a stainless steel beaker using a rotating viscometer to which a vane spindle is attached (Higashi and Sumita, JGR, 2009), and measure the shear stress and AE at 200kHz. We use broadband accelerometers and microphones to measure AE. Four accelerometers are attached at the outer rim of the beaker, and each are separated by an angle of 90 degrees.

We integrate the acceleration to obtain AE velocity –time series data and analyze their characteristics in broad band. We find that although AE has a broad spectrum, the spectra show that there are two characteristic frequency (f) components ; a high-f (of the order of 100 Hz) and a low-f (of the order of 10Hz) components. The velocity waveforms recorded at antipodal positions, show that the high-f components are in phase, whereas the low-f components are of the opposite phase. This indicates that the mechanism which excite these components differ : the high-f component may correspond to AE excited by particle rearrangement, whereas the low-f component may correspond to the translational motion of the container. Indeed we find that the frequency of the low-f component depends on the container size.

We also conducted experiments using a rheometer in a parallel-plate setup and confirmed that these two different components exist. When the particle size becomes larger, the amplitude of the shear stress and the AE velocity increases. Furthermore we find that the mean frequency of the normalized power spectra rose to a higher frequency, thus correlating with the stress increase.

Our experiments indicate that AE is excited in broadband, and that their frequency components can be used to infer the interparticle stress. Such excitation appear to be analogous to tremors and very low frequency earthquakes that are also excited simultaneously.

Keywords: granular matter, stick-slip, acoustic emission, earthquake, tremor

©2019. Japan Geoscience Union. All Right Reserved.

Episodic tremor and slip silently invades strongly locked megathrust in the Nankai Trough

*Masayuki Kano[1], Aitaro Kato[2], Kazushige Obara[2]

1. Graduate school of science, Tohoku University, 2. Earthquake Research Institute, The University of Tokyo

Recent seismic and geodetic observations in subduction zones have revealed that slow earthquakes have preceded some large earthquakes (e.g., Kato et al., 2012; Mavrommatis et al., 2014; Ruiz et al., 2014). Characterization of slow earthquakes and their relation to large earthquakes provides important clues to constrain a wide spectrum of slip rates on tectonic faults. In this study, we report new evidence of a slow slip transient at the downdip edge of the strongly locked seismogenic zone in the western Nankai Trough in southwest Japan based on GNSS time series. This slow slip transient was remotely excited during an episodic tremor and slip at the downdip extension of the locked zone. Through this remote triggering, the frequent occurrence of the deep episodic tremor and slip invades the strongly locked megathrust zone and may intermittently increase the probability of large earthquakes in the Nankai Trough.

Acknowledgments

We used GNSS data provided by the Geospatial Information Authority of Japan. This study was supported by the JSPS KAKENHI Grant Number JP15K17743 in Grant-in-Aid for Young Scientists (B), JP18K03796 in Grant-in-Aid for Scientific Research (C), JP16H06473 and JP16H06474 in Scientific Research on Innovative Areas “Science of Slow Earthquakes.”

Keywords: Slow slip events, Slow earthquakes, Western Shikoku, GNSS

©2019. Japan Geoscience Union. All Right Reserved.

Spatial distribution of the electrical resistivity beneath western part of Shikoku Island where long-term SSE events have repeatedly occurred

*Makoto Uyeshima[1], Maki Hata[1], Hiroshi Ichihara[2], Ryokei Yoshimura[3], Koki Aizawa[4]

1. Earthquake Research Institute, The University of Tokyo, 2. Graduate School of Environmental Studies, Nagoya University, 3. Disaster Prevention Research Institute, Kyoto University, 4. Institute of Seismology and Volcanology, Faculty of Sciences, Kyushu University

In the Bungo channel area at the western margin of the Nankai megathrust rupture zones, the long-term slow slip events (SSE) repeatedly occurred about every 6 or 7 years. Since the last large-scale SSE event occurred in 2010, we will have a next large event soon. In order to obtain the electrical resistivity structure in the vicinity of the SSE area and examine its temporal change, we have started the Network-MT survey in the western part of the Shikoku Island facing the Bungo channel since April, 2016. Just before beginning of the observation, a tiny-scale SSE event occurred in the Bungo-channel (Ozawa, 2017, Hirose et al., 2018). We selected 17 areas in the western part of the Shikoku Island and installed 3 or 4 electrodes in the respective areas. The electrical potential differences with typical electrode spacing of several km are measured by using metallic telephone line network. We also measure the geomagnetic field at two stations in the target region. With the aid of the BIRRP code (Chave and Thomson, 2004), we could estimate the frequency-domain Network-MT response functions of good quality between the voltage difference and the magnetic field. The Network-MT response functions were directly inverted to estimate the 3-D resistivity structure in this area with the aid of the DASOCC Network-MT 3-D inversion code (Siripunvaraporn, Uyeshima & Egbert, 2004).

Conductive portions are commonly detected in the mid-crust of the target region. Their roots are just on the upper surface of the subducting Philippine Sea slab. This may suggest dehydration there. Among the spatial distribution of resistivity, that of seismic P-wave attenuation (Kita and Matsubara, 2016), and that of SSE slips (e.g. Ozawa et al., 2013, Yoshioka et al., 2015, Hirose et al., 2018), some mutually related features are detected. Low Qp (high attenuation) areas tend to correspond to highly conductive areas. The low Qp and highly conductive area are detected just above the subducting slab and outside of the SSE area. Inside the SSE area, while Qp takes generally high values, a patchy conductive area is detected in overall resistive background structure.

This study is supported by JSPS KAKENHI Grand Number JP16H06475 in Scientific Research on Innovative Areas "Science of Slow Earthquakes". It is also partly supported by the Ministry of Education, Culture, Sports, Science and Technology (MEXT) of Japan, under its Earthquake and Volcano Hazards Observation and Research Program. We acknowledge staffs of the Nippon Telegraph and Telephone WEST Corporation for their cordial support in the survey. We also thank H. Abe, A. Takeuchi and Y. Suwa for their help in preparing and installing instruments.

Keywords: slow slip event beneath the Bungo Channel, 3-D resistivity structure, Network-MT observation

©2019. Japan Geoscience Union. All Right Reserved.

Variations of scaling relationships for shallow tremor observed along the Nankai trough

*Masaru Nakano[1], Suguru Yabe[1]

1. Japan Agency for Marine-Earth Science and Technology

Scaling relationships of seismic phenomena is one of keys to understand the source processes. Size distributions of slow earthquakes as low-frequency earthquakes (LFEs), non-volcanic tremor (NVT), very-low-frequency earthquakes (VLFE), and slow-slip events (SSEs) have been studied in many locations. Some studies showed that the size distribution follow an exponential law (e.g. Watanabe et al., 2007; Hiramatsu et al., 2008; Chestler and Creager, 2017), while others showed that power law distributions better explain the observations (e.g. Kao et al., 2010; Bostock et al., 2015; Nakamura and Sunagawa, 2015).

Most of previous studies are for slow earthquakes that occur in regions deeper than the source region of megathrust earthquakes, and only a limited number of studies have been carried out for shallow slow earthquakes beneath accretionary prism as observed along the Nankai trough. Although observed characteristics of shallow and deep ones are very similar, physical conditions as temperature and pressure much differs in these region.

In our previous studies (Nakano et al., 2018SSJ, AGU), we obtained the result that shallow tremor follows a power law distribution with b values of about 1. In this study, we further analyzed tremor activities beneath the Muroto fore-arc basin. using data from DONET2. We estimated the seismic energy of tremor signals using the same method as our previous studies, during intensive activities starting in September 2015, April 2016, February 2017, and February 2018. The source region of each activity is different from each other, spanning between off Shiono-Misaki and off Cape Muroto.

The size distribution of each activity mostly follow power-law distributions, but the b value varies from 0.7 and 1.7. We note that the activity in 2016 is also well fitted by an exponential law, probably due to narrow range of observed event size distribution. Similar result has been obtained in the 2018 activity in Kumano. The size distribution deviate from a power law for largest events as observed in Kumano activities. This deviation at larger events would be due to limited system size, expected from the theoretical stochastic model of tremor by Ide and Yabe (2018). The upper limit of event size, and accordingly the system size, varies from activity to activity.

We also investigated the relation between the seismic energy and duration of tremor events. The relation also follows a power law, with slopes of 2.0 to 2.6 in Kumano, and 1.5 to 3.3 in Muroto. These values are again consistent with the expectation value of 2 from the model of Ide and Yabe (2018).

These investigations represent that the scaling relationships of shallow tremor are mostly consistent with the 2D PCA model by Ide and Yabe (2018). Further studies would be necessary to reproduce the observed variations of the scaling parameters.

Acknowledgments: We used DONET data and JMA and USGS earthquake catalogs in the analysis. This research was supported by JSPS KAKENHI Grant Number 16H06477 in Scientific Research on Innovative Areas “Science of Slow Earthquakes”

Keywords: DONET, Nankai trough, earthquake size distributions

©2019. Japan Geoscience Union. All Right Reserved.

Low-frequency earthquakes triggered by teleseismic surface waves by Ryukyu subduction zone.

Ayumi Kinjo[1], *Mamoru Nakamura[1]

1. Faculty of Science, University of the Ryukyus

We investigated low-frequency earthquakes (LFEs) in the Ryukyu Trench region that were triggered by surface waves from teleseismic earthquakes. Although these LFEs in the southwestern Ryukyu arc have previously been explored by Chao et al. (2016), their hypocenter distribution is not known in detail.

We selected 50 earthquakes from January 2004 to December 2016, which had magnitudes greater than 7.5 and epicentral distances between 9–150˚. We used the waveforms of 6 broadband seismometers in the Ryukyu arc from F-net (NIED) to analyze the surface waves. We also used the waveforms of 20 short-period seismometers in the Ryukyu arc from the Japan Meteorological Agency to detect trace LFEs in Ryukyu Island and determine their hypocenters.

The LFEs in the Yaeyama and Okinawa regions were observed. In the former region, during the passage of the surface waves, spindle-shaped LFE waveforms were first observed at Hateruma (south of Yaeyama Islands), and later at other stations in the Yaeyama region. Similarly, for the latter region, during the passage of the surface waves, spindle-shaped LFE waveforms were first observed at ZMM or Tamagusuku (south of Okinawa Island), and later at other stations in the Okinawa region. These observations suggest that the sources of the triggered LFEs were near or south of Hateruma and Tamagusuku.

We subsequently determined the hypocenters of the triggered LFEs. We computed the LFE travel-time difference between two stations using cross-correlations of the waveforms (Obara, 2002). The travel-time difference of waveforms of the LFEs corresponded to travel-time difference of the S-phase because S-waves were dominant in the LFEs, and P-waves were weak. The hypocenters were determined using the grid search method (Chao et al., 2013). In the Yaeyama region, the LFE hypocenters were mainly distributed near Hateruma Island. In the Okinawa region, they were distributed south of Okinawa Island. These positions are similar to the positions of the LFE hypocenters that accompany very low frequency earthquakes (LFE-VLFEs). This suggests that faulting in a cluster of LFE-VLFEs would be active with dynamic stress change.

In the Okinawa and Yaeyama regions, LFEs are triggered when the peak ground velocity of the surface wave is greater than 0.1 cm/s. This threshold value is similar to that for LFEs in Taiwan (Chao et al., 2013), suggesting that the weak friction coefficient at the plate interface of the Ryukyu Trench is similar to that in Taiwan.

Keywords: low frequency earthquake, surface wave, Ryukyu Trench

©2019. Japan Geoscience Union. All Right Reserved.

Detection of small surface displacement accompanying deep low-frequency tremor in Shikoku region, southwest Japan

*Yutaro Okada[1], Takao Tabei[2]

1. Faculty of Science, Kochi University, 2. Faculty of Science and Technology, Kochi University

In many subduction zones in the world, several types of slow earthquakes occur with different depths on the plate interface and some of them are accompanied by surface displacement. In this study, we focus on small surface displacements coincident with non-volcanic deep low-frequency tremor in Shikoku region in the Nankai subduction zone, southwest Japan.

We use daily coordinates time series from 107 GEONET stations located in Shikoku and tremor catalog compiled by NIED (Maeda and Obara, 2009; Obara et al., 2010) in the period from Jan. 1 2004 to Dec. 31 2008. Since GNSS coordinates changes due to the Bungo Channel long-term slow slip events are well reproduced by S-shaped logistic function, we use the same function to extract small displacement coincident with tremor activity. At first, we convert horizonal components into N50°W direction after removing annual and semiannual variations and common-mode errors. Next, we fit the logistic function to a data segment with variable time window of 5, 7, and 9 days and estimate an amplitude of the function. The fitting is checked by a correlation coefficient between the observation and calculation. We apply this fitting for entire data period at all stations sliding data segment. Finally, we extract displacement when the amplitude of the fitted logistic function exceeds a certain criterion (1.8 mm in this study) and the correlation coefficient is large enough. If the extracted displacement is coincident with tremor activity within 30 m from the GNSS station, we adopt it as the tremor-related displacement. As a result, 225 events are adopted.

Spatial pattern of the tremor-related displacement seems to be related with the location and mechanism of the tremor event though closer inspection is needed. However, we extract much more small displacements by fitting a logistic function, of which the source is unknown. The logistic function is effective to reproduce transient displacement of the surface but we need to reconsider noise reduction of GNSS time series, time constant of logistic function, time window of the fitting, and so on.

Keywords: GNSS, southwest Japan, Deep low frequency tremor

©2019. Japan Geoscience Union. All Right Reserved.

Long-term temporal change in crustal resistivity beneath western Shikoku

*Futoshi Yamashita[1], Yoshimori Honkura[1]

1. National Research Institute for Earth Science and Disaster Resilience

In southwest Japan, various slow earthquakes such as deep low-frequency tremor and short/long-term slow slip events occur at the subducting plate interface (e.g. Obara and Kato, 2016, Scinence). In western Shikoku, Magneto-telluric (MT) survey was carried out along the dip direction of subducting Philippine Sea plate. The survey revealed an existence of low-resistivity structure in the lower crust in this region (Yamashita and Obara, 2009, AGU). In order to investigate a relationship between this characteristic structure and the activity of slow earthquakes, NIED has been carrying out continuous MT observations in western Shikoku since 2008. Here we show the observational records over 10 years and then discuss a relationship between observed temporal change in crustal resistivity and activity of the long-term slow slip event (L-SSE). Two observational sites KBN and IKT are available as of 2019. Qualities of data recorded at these sites are relatively fine. However, in order to improve the quality for discussing subtle change in MT parameters, we apply a data processing method same as Honkura *et al.* (2013, Nature comm.); we use only data whose coherency between electric and magnetic field is higher than a threshold. The lowest frequency of processed data is 0.00028 Hz. The processed MT parameters, apparent resistivity and phase, do not show any long-term temporal changes at KBN site even after temporal stops of observation over some months. On the other hand, apparent resistivity at IKT site, which is around 10 km southwest away from KBN site, shows temporal reduction at a frequency lower than 0.0022 Hz between 2010 and the middle of 2012. It is known that L-SSE occurred beneath the Bungo Channel in 2010 (e.g. Yoshioka *et al.*, 2015, GJI), which could induce resistivity change in the lower crust and then it might be detected by our MT observation.

Keywords: Crustal resistivity, Long-term slow slip event, Magneto-telluric method

©2019. Japan Geoscience Union. All Right Reserved.

Slow decay of postseismic deformation compared with aftershocks following the 2011 Tohoku-oki Earthquake

*Yuta Mitsui[1], Shunsuke Morikami[2]

1. Department of Geosciences, Shizuoka University, 2. Formerly at Graduate School of Science and Technology, Shizuoka University

In the literature, decays of postseismic deformation rates of large earthquakes were almost comparable to aftershock decays for subduction earthquakes (e.g. Hsu et al. (2006), Lange et al. (2014)). They are characterized by the modified Omori law with p~1, which means "afterslip-triggerred aftershocks". In this study, we focus on the 2011 Tohoku-oki megathrust earthquake using GNSS and seismicity data. On the basis of high-rate analysis of RINEX data and the F3 solution provided by the Geographical Survey Institute (GSI), we clarify the characteristics of postseismic deformation and aftershocks up to five orders of magnitude of time scale. We find that the p value for the postseismic deformation (p_m) is ~0.7, by contrast, that for the aftershocks (p_n) is ~1. Because a rate-and-state-friction model (Helmstetter and Shaw (2009)) predicted $p_m>=p_n$, another or an additional physical mechanism is necessary to explain the data of $p_m<p_n$. One important mechanism is viscoelastic relaxation of asthenosphere, thus we try fitting the postseismic deformation data by combination of afterslip and viscoelastic relaxation (a model of Suito (2017)). The fitting is not poor but fails to reproduce the Omori-like decay. More complex combination models may improve the fitting, but would not make simple Omori-like power-law decays. We need more sophisticated physical model to represent the decay characteristics of postseismic deformation.

Keywords: aftershocks, postseismic deformation, afterslip, viscoelastic relaxation, the 2011 Tohoku Earthquake

©2019. Japan Geoscience Union. All Right Reserved.

Serpentinite dehydration in subduction shear zones formed at source depths of slow earthquakes

*Yasushi Mori[1], Miki Shigeno[1], Kohtaro Ujiie[2], Kazuya Noro[2], Tadao Nishiyama[3]

1. Kitakyushu Museum of Natural History and Human History, 2. University of Tsukuba, 3. Kumamoto University

Long-term slow slip events (L-SSEs) and episodic tremor and slip (ETS) occur along the subduction plate boundary at depths of 30–45 km (Obara, 2002; Shelly et al., 2006). These deep slow earthquakes are probably induced by high pore-fluid pressure. Based on geological study, we propose that the high pore-fluid pressure can be produced by metasomatic dehydration of serpentinite in subduction shear zones at source depths of deep slow earthquakes.

The Nishisonogi metamorphic rocks in Kyushu, Japan, are part of a Late Cretaceous subduction complex metamorphosed at $P \approx 1$ GPa and $T \approx 470$ ˚C. The P-T conditions are close to those of source depths of deep slow earthquakes. Serpentinite mélanges intercalated with the metamorphic rocks contain blocks of metabasite, metapelite and albitite. The mélange matrix consists of chlorite-actinolite schist (CAS), talc schist and schistose serpentinite. Intense shear deformation is concentrated in the CAS, and the serpentinite mélanges have the characteristics of anastomosing shear zones.

Bulk chemical composition of the rocks suggests that the CAS is the metasomatized mixture of serpentinite and metabasite. In addition, chemical mass balance indicates considerable dehydration during the CAS formation, along with a slight increase of solid volume. These findings suggest that the CAS formation involves the build-up of pore-fluid pressure. The high pore-fluid pressure results in the concentration of shear deformation into the weakened CAS.

Dehydration of serpentinite probably plays a key role in deep slow earthquakes (Poulet et al., 2014; Okazaki and Katayama, 2015). Thermal dehydration of serpentinite occurs at ~600 ˚C along the subduction plate boundary (Auzende et al., 2006), which is much higher temperature than that of source depths of deep slow earthquakes. In contrast, metasomatic dehydration of serpentinite described here could occur at source depths of deep slow earthquakes.

Auzende, A-L., et al., 2006, EJM, 18, 21–33. Obara, K., 2002, Science, 296, 1679–1681. Okazaki, K., Katayama, I, 2015, GRL, 42, 1099–1104. Poulet, T., et al., 2014, JGR, 119, 4606–4625. Shelly, D.R., et al., 2006, Nature, 442, 188–191.

Keywords: serpentinite mélange, shear zone, dehydration, pore fluid pressure, Nishisonogi metamorphic rocks, deep slow earthquakes

©2019. Japan Geoscience Union. All Right Reserved.

Earthquake swarms following very low-frequency earthquakes in the central Ryukyu Trench

*Mamoru Nakamura[1]

1. Faculty of Science, University of the Ryukyus

Earthquake swarms occur frequently from Amami Island to Okinawa Island, near the axis of the central Ryukyu Trench. These earthquake swarms recur every few years and typically followed swarms of very-low frequency earthquakes (VLFE) that occur in a similar area. I have investigated the relationship between the VLFEs and the subsequent earthquake swarms in the central Ryukyu Trench, using the earthquake catalog provided by the Japan Meteorological Agency (JMA). For the VLFEs, I used the catalog by Nakamura and Sunagawa (2015) and the extended catalog to December 2018.

Results show that the VLFE swarms occurred approximately one month before the subsequent earthquake swarms began near the trench axis in this region. Previous noteworthy earthquake swarms occurred on August 2005 (with a maximum magnitude of 4.7), April 2009 (with a maximum magnitude of 5.1), May 2016 (with a maximum magnitude of 5.6), and September 2018 (with a maximum magnitude of 6.2).

Prior to the earthquake swarm that occurred in August 2005, a VLFE swarm started near Okinawa Island three months before and its activity moved intermittently from Okinawa Island to Amami Island. In the case of the earthquake swarm that occurred in April 2009, a VLFE swarm started near Amami Island and the subsequent swarm occurred two weeks after the start of the VLFE swarm. The location of the VLFE swarm moved intermittently closer to Okinawa Island. In the case of the earthquake swarm that occurred on May 2016, the VLFE swarm started near Amami Island and its active cluster moved intermittently towards Okinawa Island. The subsequent earthquake swarm started near the trench axis, approximately twenty days after the occurrence of the VLFE swarm. In the case of the earthquake swarm that occurred in September 2018, the VLFE swarm started near Okinoerabu Island (the midpoint between Amami Island and Okinawa Island) and the activity moved intermittently to Okinawa Island. The earthquake swarm occurred approximately twenty-five days after the start of the VLFE swarm. The location of the cluster of the 2018 earthquake swarm was slightly landward from the trench axis.

The faulting associated with these earthquake swarms was of normal type, corresponding to intra-slab earthquakes in the subducting Philippine Sea plate. I calculated the Coulomb Failure Stress (delta-CFS) assuming that a small slow slip event (SSE) occurred on the plate interface. Our results show that the positive delta-CFS that accelerated the normal faulting could not have occurred in the subducted slab near the trench axis until the slip of the SSE had reached close to the trench axis. This suggests that the SSE propagated from Amami Island to Okinawa Island accompanying the activation of the VLFE swarm, the slip of the SSE then propagated close to the trench axis, and the normal-faulting earthquake swarm in the slab was induced by the positive delta-CFS caused by the SSE.

Keywords: Very low frequency earthquake, Ryukyu Trench, Earthquake swarm

©2019. Japan Geoscience Union. All Right Reserved.

Seismic imaging in the central Nankai trough, off Shionomisaki to Kii channel

*Yasuyuki Nakamura[1], Shuichi Kodaira[1], Tetsuo No[1], Yuka Kaiho[1], Gou Fujie[1], Seiichi Miura[1], Kazuya Shiraishi[1]

1. Japan Agency for Marine Earth Science and Technology

Shallow very low frequency events (sVLFE) have been reported in the Nankai Trough subduction zone recently. In the central part of the Nankai trough, sVLFE were observed off Kii channel and Shinomisaki, but not reported in the area between them, off western Kii peninsula. We conducted a seismic survey with R/V *Kaimei* in November and December 2018 in Nankai subduction zone off Kii channel to Shonomisaki to investigate the structural features and its possible relationship to the sVLFE. R/V *Kaimei* fired 10600 $inch^3$ air gun array at every 50 m and a streamer cable (4.3 km at shortest, 5.7 km at longest) recorded the seismic signals. We acquired 23 seismic profiles with the length of ~ 75 km in dip direction at 4 km line separation and four profiles of ~ 90 km in strike direction at the shallowest part of the subduction zone. In addition, seven dip profiles with the length of 35 km were acquired off Kii channel to cover the lowermost part of the landward slope densely. The streamer cable was towed at a depth of 25 m to relatively enhance the lower frequency signals for better imaging of the deeper structure. Preliminary processed seismic profiles exhibited the structural variation in the survey area. Deformation of the hanging wall sediments and decollement were well imaged especially ~ 20 –30 km from the trough axis. Top of subducting Philippine Sea plate can be observed through ~ 40 –50 km from the trough axis in some of the obtained profiles. A pair of apparently low angle deep strong reflections were imaged at ~ 7 –8 s two-way time around 40 - 50 km from the trough axis off the western Kii peninsula, which was located slightly east and landward of the area with sVLFE. The shallowest part of the subduction zone in the area where the recent sVLFE activity was not reported, a slope basin with younger sediments deposited over the body of the accretionary prism is imaged, and the deformation was not observed in the slope basin. This suggests the thrust faults within the accretionary prism have not been active recently in this area. We will further process acquired data to obtain clearer seismic images and discuss the structural features and its connection to the observed seismological events in the Nankai Trough.

Keywords: Nankai Trough, seismic imaging

©2019. Japan Geoscience Union. All Right Reserved.

Attempt to Detect Intra-plate SSEs Based on F3 Solution of GEONET

*Yusaku Tanaka[1]

1. Earthquake Research Institute

Slow earthquakes have been detected all over the world and providing new insights into earthquakes. However, most of slow slip events (SSEs) were detected only on plate boundaries and intra-plate SSE was detected only once in Hokkaido. Thus, I attempt to detect intra-plate SSEs all over Japan using F3 solution of GEONET by GSI. I analyze the F3 data with six steps, i.e., (1) removing outliers by setting a term of mean + two times standard deviation for 1/4+1/4 year before-and-after each datum except for the datum itself and considering it is an outlier when it is out of the term, (2) removing disconnections estimated from the offsets and linear trends of 60+60 days before-and-after each datum with the least square method, (3) searching statistically significant temporal changes of the trends by using AIC, (4) cheking visually the time series in which the temporal changes are detected, (5) estimating the displacements from the trend chagnes, and (6) verifying the deformations by numerical calculation by setting rectangular faults.

As of 18th Feb 2019, my study has proceeded to the step (4). In the JpGU meeting, I will report the results of this analysis.

Keywords: crustal deformation, slow slip event, geonet

©2019. Japan Geoscience Union. All Right Reserved.

A new hydrothermal, low to high speed rotary-shearing apparatus: Reproduction of slow/megathrust earthquakes in laboratory

*Takehiro Hirose[1], Wataru Tanikawa[1], Yohei Hamada[1], Keishi Okazaki[1]

1. Kochi Institute for Core Sample Research, Japan Agency for Marine-Earth Science and Technology

Earthquakes involve a wide range of slip rates, from slow/aseismic to fast/seismic slip along faults. Thus, frictional properties of faults over wide slip rates (nm/s to m/s), in particular under hydrothermal conditions similar to those expected in seismogenic zones are essential for a unified understanding of all earthquake events. A new hydrothermal, low to high speed rotary-shearing apparatus has been installed at Kochi/JAMSTEC, in order to study the fault constitutive properties at slow to fast slip rates and the physicochemical mechanisms underlying mechanical responses. The apparatus is currently capable of applying slip rates from 100 nm/s to 2 m/s, normal stress up to 55 MPa, fluid pressure up to 120 MPa and temperature up to 450oC with infinite displacement. We have been improving the apparatus to work as we intended. In pilot tests, we used metamorphic rocks (pelitic and green schists) as starting materials that are potentially distributed at and below seismogenic zones along hot and young subduction zones. We will present our preliminary results with the basic design of the apparatus.

Keywords: friction, hydrothermal, slow to fast slip

©2019. Japan Geoscience Union. All Right Reserved.

Very low-frequency earthquakes in western Shikoku remotely triggered by the 2016 Mw5.9 off-Kii Peninsula earthquake

*Masatoshi Miyazawa[1]

1. Disaster Prevention Research Institute, Kyoto University

Slow tectonic events are known to be sensitive to external stress perturbations due to passing seismic waves and earth tides. High-amplitude surface waves from large earthquakes have transiently triggered low-frequency earthquakes (LFEs) and slow slip events (SSEs) in subduction zones. However, dynamic triggering of very low-frequency (VLF) earthquakes during the arrival of seismic waves from a large, distant earthquake has not been observed. Because both the VLF earthquake and the surface wave have similar characteristic periods, remote triggering is not easily detected by using existing methods. We developed a particle filter/smoother for time series analysis combined with Markov chain Monte-Carlo methods, to detect seismic signals and estimate the maximum likelihood source parameters of VLF events that might have been remotely triggered. We apply this method to seismic data from the Mw5.9 earthquake, which occurred on 1 April 2016 (UTC), off Kii Peninsula. We found that six VLF events with magnitudes about 4, likely occurred in the seismogenic regions of ambient LFEs, and were likely triggered by the arrivals of high-amplitude surface waves. The triggering stress changes are from 0.4 to 1.5 kPa, which are similar to the values for LFEs triggering reported previously. Since there were no triggered LFEs in western Shikoku following the 2016 earthquake, these VLF earthquakes are more sensitive to stress changes caused by surface waves from large earthquakes.

Keywords: Very low-frequency earthquake, Remote triggering

©2019. Japan Geoscience Union. All Right Reserved.

Underground structure around source region of slow earthquakes in western Shikoku obtained by receiver function analysis

Akira Hikita[1], Aitaro Kato[1], *Kazushige Obara[1], Akiko Takeo[1], Takeshi Akuhara[1]

1. Earthquake Research Institute, The University of Tokyo

Various types of slow earthquakes have been observed at subduction zones surrounding the Pacific Ocean. It has been suggested that elevated pore fluid pressure plays an essential role in the generation of slow earthquakes because low velocity or high Vp/Vs zones have been also reported along the plate boundaries where they occur. In Tokai region of the Nankai subduction zone, Kato et al. (2010) revealed that long-term slow slip event (SSE) occurs at the boundary between the continental lower crust and the subducting Philippine Sea plate and episodic tremor and slip (ETS) occurs between the mantle wedge and the subducting plate. Kato et al (2010) also revealed that oceanic crust indicates higher Vp/Vs in the long-term SSE region than in the ETS region. In contrast, Toya et al. (2017) reported that the oceanic crust indicates higher Vp/Vs in the ETS region than in the long-term SSE region in western Shikoku of the same subduction zone. In this study, we revealed configurations of continental Moho discontinuity and subducting oceanic crust and investigated relationship between slow earthquakes and the surrounding seismic velocity structure by receiver function analysis using a dense seismic array in western Shikoku.

As a result, continuous continental Moho and oceanic crust are clearly imaged along both north-south and east-west oriented seismic lines. The plate boundary in the south part, where the distinct continental Moho is not imaged, has steeper slope than the north part along the north-south line. ETS occurs between the mantle wedge and the subducting plate, and long-term SSE occurs along a contact between the continental crust and the oceanic crust.
We show that the oceanic crust indicates much higher Vp/Vs than the hanging wall by using also the reverberation phases. This high Vp/Vs means the elevated fluid pore pressure within oceanic crust due to dehydration. Vp/Vs in the oceanic crust is higher in the deep part of the long-term SSE region than in the ETS region like as the case of Tokai. It is assumed that fluid would accumulate within the oceanic crust owing to low permeability of the continental crust in the long-term SSE region. In contrast, serpentinization of the mantle wedge just above the ETS region could reduce fluid pressure in the oceanic crust. Furthermore, Vp/Vs in the oceanic crust becomes lower in the deeper part beyond the ETS depths, suggesting that eclogization is completed at the depths.

Keywords: Receiver function, episodic tremor and slip, long-term slow slip event, low seismic velocity layer

©2019. Japan Geoscience Union. All Right Reserved.

Hypocenter determination of deep low frequency tremors beneath the Kii Peninsula by backprojection of seismic array data

*Kodai Sagae[1], Hisashi Nakahara[1], Takeshi Nishimura[1], Kazutoshi Imanishi[2]

1. Graduate School of Science,Tohoku University, 2. National Institute of Advanced Industrial Science and Technology (AIST)

A seismic array analysis enables us to detect weak signals if they are coherent. In Cascadia, a high accuracy hypocenter determination of tremors has been carried out by using dense seismic arrays (e.g.,Ghosh et al.,2012). In Southwest Japan, previous studies (e.g.,Ueno et al.,2010) applied the **MU**ltiple **SI**gnal **C**lassification (MUSIC) method (Schmidt,1986) to data of surface seismic arrays at Western Shikoku and carried out the hypocenter determination. However, a quantitative threshold for event detection was not considered. Sagae et al.,(2018 SSJ) introduced an event detection threshold based on the coherence of waveforms among stations, and improved tremor detection by using a surface seismic array installed by AIST at the Kii Peninsula. We applied the MUSIC method to this data in times when tremor events were detected and estimated slownesses and arrival azimuths of tremor signals. Their temporal variations suggested tremor migration. However, we did not carry out hypocenter determination. In this study, we determine hypocenters of tremors by backprojection using the estimated slownesses and arrival azimuths.
The surface seismic array installed by AIST at the Kii Peninsula was composed of 39 three component velocity sensors with a natural frequency of 2.0 Hz and a sampling frequency of 200 Hz. This array had an aperture of about 1.5 km and the sensors were arranged in a cross shape with interval spacings of 50~100 m. We analyze data for 1 year (between July 7,2013 and July 7,2014), because the number of sensors is stable in this period.
We focus on a frequency of 3Hz, which is within the tremor's dominant frequency band of 2-10 Hz. Data processing is described as follows. (1) We calculate averaged coherence of waveforms for all station's pairs. (2) We detect tremor events by setting a detection threshold based on the averaged coherence. (3) We estimate slownesses and arrival azimuths by applying the MUSIC method to the data when tremors are detected. (4) We project them back to the plate boundary (Hirose et al.,2008) and determine source locations by using S wave velocity model JMA2001 (Ueno et al.,2002).
We detected 5 periods of high tremor activities during the 1 year period. We compared the hypocenter distributions determined by our method and those of AIST tremor catalogue which were determined from an envelope cross correlation method. Temporal variation of tremors in this study were almost consistent with the AIST catalogue. We were also able to detect about 2.5 times as many events as the AIST catalogue. It is easier to identify temporal variation of tremors in more detail because our study improved temporal resolution up to 10 sec.
We projected temporal variations of tremor distributions into along-strike and along-dip directions. The results show tremors tend to migrate along the strike in time scales of several days with migration velocities of 6.0~9.3 km/day. Along-dip migrations of tremors with a short timescale of several hours are also detected. When we focused on the initial part of tremor activities, tremors tend to start in deeper parts and gradually migrate to shallow parts. These migration velocities were estimated to be about 1.0 km/hr (24 km/day) in the up-dip direction.
In this study, we were able to improve tremor detection by setting the event detection threshold based on the coherence of seismograms for stations pairs in a surface seismic array. Thanks to this, we were able to locate 2.5 times more tremors than the conventional method. We made it easier to keep track of tremor migrations by improving the temporal resolution of hypocenter determination to 10 sec.
We used the plate boundary model (Hirose et al.,2008). We downloaded the AIST catalogue from Slow

©2019. Japan Geoscience Union. All Right Reserved.

Earthquake Database (Kano et al.,2018).

Keywords: Deep low frequency tremor, Seismic array analysis, Backprojection, MUSIC method, Kii Peninsula, Hypocenter determination

©2019. Japan Geoscience Union. All Right Reserved.

Triggered tremors and stress perturbations due to surface waves

*Ryohei Ikeda[1], Naoki Suda[1]

1. Hiroshima University

Surface waves radiated from distant large earthquakes sometimes trigger a series of deep non-volcanic tremors with intervals of 20-30 seconds, which are the same as dominant periods of surface waves [e.g. Miyazawa & Brodsky 2008]. Understanding the triggering mechanism is important because it provides us clues to the slip process occurring along the transition zone of subducting plate interface. Dynamic stress perturbations due to surface waves that triggered tremors were estimated on the order of 1 to 10 kPa [e.g. Chao & Obara 2016]. To study the relationship between triggered tremors and stress perturbations due to surface waves, we computed theoretical dynamic stresses due to surface waves from large earthquakes by using observed and theoretical surface waves.

We focused on the triggered tremors in the western Shikoku region of the Nankai subduction zone. Most of them occurred in two clusters where tectonic tremors actively occur. We computed theoretical dynamic stress perturbations due to surface waves from 106 earthquakes between 2004 and 2016 with moment magnitudes of 7.0 or grater. The receiver points at which the stress components were computed are at the plate boundary below the N.TSAF and N.KWBH stations, which are the nearest stations of the triggered tremors in F-net and Hi-net, respectively. PREM [Dziewonski & Anderson 1981] and Global CMT catalog [Dziewonski et al. 1981; Ekstrom et al. 2012] were used for the Earth model and the seismic sources for computing theoretical surface waves. Source time functions were approximated with triangular functions whose half durations are equal to the centroid time lags.

The stress change at the plate boundary by the surface wave was estimated based on the method of Spudich et al. (1995). This method consists of two stages: (1) Estimate the stress at the surface from the observed ground velocity and (2) Estimate the stress at the plate boundary from the stress at the surface estimated in (1). In these estimations, we used theoretical proportional relations between the ground velocity and the surface stress and those between the surface and the deep stresses in the frequency domain, which were obtained from the theoretical surface waves. We used the N.TSAF and N.KWBH records as the observed ground velocity. The records from the latter were corrected using the method of Maeda et al. (2011).

The stress components in the source coordinates were transformed to the stress normal to the plate interface and the stress along the possible slip direction of tremor source. The normal and slip directions were obtained from the model plate interface [Baba et al. 2002; Nakajima & Hasegawa 2007; Hirose et al. 2008] and plate convergence vectors [Miyazaki & Heki 2001]. We computed waveforms of the Coulomb failure function (ΔCFF) using a frictional coefficient of 0.2 at periods between 20 and 50 seconds.

©2019. Japan Geoscience Union. All Right Reserved.

Results from the N.TSAF records show that the maximum ΔCFF for the events that triggered tremors are greater than 0.5 kPa. The magnitudes of triggering earthquakes are greater than 7.5. ΔCFFs were generally overestimated when we used the corrected N.KWBH records because the correction did not well work, in particular, for the earthquakes with magnitudes less than 7.5. The important point is that not all of the events that provided the stress perturbations greater than 0.5 kPa triggered tremors. This shows that the stress perturbation due to surface waves cannot be the unique triggering condition: other conditions, for example, stress perturbations due to possible background slow slip events and/or high pore fluid pressure are required.

©2019. Japan Geoscience Union. All Right Reserved.

Numerical modeling of long- and shallow slow slip events including shallow region in Hyuganada and western Nankai, Japan

*Takanori Matsuzawa[1], Bunichiro Shibazaki[2]

1. National Research Institute for Earth Science and Disaster Resilience, 2. Building Research Institute

Recent studies reported deep long-term slow slip events (SSEs) in the Hyuganada and western Nankai region (e.g., Kobayashi, 2014; Takagi et al., 2016; Ozawa. 2017). Shallow SSEs are also recently reported with low-frequency tremor and very low-frequency earthquakes (e.g., Araki et al., 2017; Nakano et al., 2018). In our previous study, we have numerically reproduced recurring deep long- and short-term SSEs in the Shikoku region (Matsuzawa et al., 2013), considering the actual distribution of slow earthquakes and configuration of the subducting Philippine Sea plate. We aim to reproduce deep long- and short-term SSEs and shallow SSEs in a single numerical model applying a similar approach in Matsuzawa et al. (2013).

We adopt a rate- and state-dependent friction law (RS-law) with cutoff velocities. We assume that (a-b) value in the RS-law is negative within the deep short-term SSE region, and positive outside that region. The deep short-term SSE region is modeled based on the actual distribution of deep low frequency tremor. Deep long-term SSE region is assumed based on the geodetic observation (Hirose et al., 2011). To focus on the Hyuganada and western Nankai region, we assume stable sliding region with positive (a-b) in the south of the Kyushu-Palau ridge. We also assume low cutoff velocity at the depth shallower than 9 km to reproduce shallow SSEs. Low effective normal stress is assumed at the depth of SSEs. Temporal evolution of slip velocity is numerically simulated, introducing elastic response and realistic configuration of the plate interface.

In terms of deep long-term SSEs in Hyuganada, a simple extension of the long-term SSE region in the Bungo Channel cannot reproduce the segments of observed SSEs. Narrowed long-term SSE region in the dip direction between Bungo and southern Hyuganada can reproduce three observed segments of SSEs, i.e., Bungo, northern Hyuganada, and southern Hyuganada. In addition, recurring shallow SSEs along trench in Hyuganada and off Ashizuri are reproduced in our result. Megathrust earthquakes are divided into two regions; off Shikoku and Hyuganada in our result. The segments of these large earthquakes may be attributed to the long-term SSE region in the Bungo Channel. Our model comprehensively reproduces various SSEs and megathrust earthquakes, including newly found long-term SSEs.

Keywords: Slow Earthquake, Slow Slip Event, Hyuganada

©2019. Japan Geoscience Union. All Right Reserved.

Further evidence for the influence of a subducting-ridge on the spatial strain accumulation and release pattern in the shallow eastern Nankai Trough, based on VLFE distribution

*Akiko Toh[1], Chen Wan-Jou [2], Doug Dreger[3], Wu-Cheng Chi[2], Satoshi Ide[1]

1. University of Tokyo, 2. Institute of Earth Sciences, Academia Sinica, 3. UC Berkeley

We investigated the distribution and focal mechanisms of very low frequency earthquakes (VLFEs) located in the shallow part of the eastern Nankai trough. While they are mainly explained as low angle thrust faulting along the plate boundary (Sugioka et al., 2012; Nakano et al, 2016), along the strike variation in their distribution has also been observed, likely caused by a subducting-ridge (Toh et al., 2018). Such variations could be closely related to the strain release pattern, or the tsunamigenic potential, of this region, thus warrant a further comprehensive study.

We used 3 component records of broadband ocean bottom seismometers equipped in Dense Oceanfloor Network system for Earthquakes and Tsunamis 1 (DONET1). Records of VLFE activities that occurred immediately beneath the network in 2015, 2016 and 2017 for 1-2 weeks each year, are used. Through visual inspections, we detected 335 VLFEs whose signals are observed at least 6 stations on vertical component filtered between 16-32s.

Instead of estimating the source parameters for one after another for all the events, we searched for densely located event groups inferred by similarities of the maximum amplitude variations measured per event, and, so far, worked only on the grouped events. The purpose of this event selection process is to get an overview of the distribution using the simple quantity (i.e. max. amplitude variation) that can be evaluated for every VLFE, and to avoid a bias that may be caused by eliminating events that are merely difficult to process (i.e. do not fit synthetic waveforms) mostly due to complicated long source time functions that characterize VLFEs. The grouping is conducted by a hieratical density-based clustering method HDBSCAN (Campello et al., 2003), and 197 events were grouped into 26 groups that consists of 2 to 35 events.

We determined the centroid origin time, location and 5-component of moment tensor of VLFEs that maximize the normalized variance reduction (VR) between the observed and synthetic velocity waveforms. The waveforms are bandpass filtered either between 16-32s or 20-50s, depending on signal duration and S/N per event. The time and location are grid-searched at intervals of 0.01 degree in horizontal, 1 km in depth between 5 and 10km bsl., and 1 s in time. At each grid, the moment tensor is estimated using the code TDMT_INV (Dreger, 2003) that conducts full-waveform linearized inversion in time domain. Green’s functions are calculated using the code by Herrmann (2013) based on wavenumber integration. We used a 1D structural model based on a 2D model obtained by an active source survey (Nakanishi et al., 2008). Although the 1D structure is assumed, the large variations in station elevation (1.9-4.3 km bsl) are considered in Green’s function calculations.

We obtained 50 events with good VR (>65%). Among the 26 groups, 6 groups ended up with no events of high VR, mostly due to being located outside of the network. Almost all the VLFEs are reasonably explained by low angle thrust faulting. From the obtained distribution, the strong influence of the subduction-ridge located on the northwestern side of DONET1 is inferred. On the southwestern side

©2019. Japan Geoscience Union. All Right Reserved.

where there is no ridge-subduction, VLFEs are distributed beneath outer-ridge toward the trench axis. The estimated depths for the ones located beneath the outer-ridge are deep (7–10km with median at 8km), which are consistent with the depth of the plate boundary of this area. In contrast, on the northeastern side, VLFEs are mostly distributed landward of outer-ridge and their estimated depth are shallow (5–8km with the median at 7km) as previously suggested (To et al., 2015). The shallow depths can be explained by the uplifted plate boundary in this area due to the subducting-ridge. Furthermore, they are located to landward of the peak of the subducting-ridge, which can be reasonably explained by the change in shear stresses and pore pressures caused by the subducting-ridge.

Keywords: Nankai trough, Very low frequency earthquake (VLFE), Accretionary prism, HDBSCAN, Broadband ocean bottom seismometer

©2019. Japan Geoscience Union. All Right Reserved.

Evidence for semi-brittle flow in mantle-wedge serpentinites under high pore fluid pressure and their implications for deep low frequency earthquakes

Kengo Kataoka[1], Yurina Nagata[1], *Ken-ichi Hirauchi[1], Ryosuke Oyanagi[2], Atsushi Okamoto[3], Katsuyoshi Michibayashi[4]

1. Department of Geosciences, Faculty of Science, Shizuoka University, 2. Japan Agency for Marine-Earth Science and Technology, 3. Graduate School of Environmental studies, Tohoku University, 4. Department of Earth and Planetary Sciences, Nagoya University

In southwest Japan, deep low frequency earthquakes occur at the base of the shallow serpentinized mantle wedge. In order to understand deformation styles of the mantle wedge serpentinite, we conducted structural and petrological analysis of a paleo-mantle wedge body that has experienced serpentinization at pressure–temperature conditions corresponding to source areas of low-frequency earthquakes, in the Sanbagawa belt, central Shikoku. The serpentinite body has a block-in-matrix structure that result from pervasive fragmentation. At outcrop and thin section scales, the distribution of blocks follows a power law distribution with exponent $2.32 < D < 2.37$ (2-D). The block has experienced complete serpentinization, characterized by randomly-oriented antigorite aggregates. The matrix also consists of antigorite, which was formed due to dissolution–precipitation process of the block in the presence of H_2O. Antigorite aggregates in the matrix along localized shear planes is characterized by a strong crystallographic preferred orientation with a dominant [010](001) slip system, suggesting dislocation glide on (001) planes. We suggest that deep slow earthquakes occur by semi-plastic deformation of the serpentinized mantle wedge, under low effective normal stresses.

Keywords: slow earthquakes, low frequency earthquake, mantle wedge, serpentinite

©2019. Japan Geoscience Union. All Right Reserved.

Spatial distribution of slow slip events off the Boso peninsula from 1996 to 2018 under sparsity constraints

*Ryoko Nakata[1], Hideitsu Hino[2], Tatsu Kuwatani[3,4], Takahiro Akiyama[5], Shoichi Yoshioka[6], Masato Okada[7], Takane Hori[1]

1. Japan Agency for Marine-Earth Science and Technology, 2. The Institute of Statistical Mathematics, 3. Department of Solid Earth Geochemistry, Japan Agency for Marine-Earth Science and Technology, 4. PRESTO, Japan Science and Technology Agency, 5. Graduate School of Science, Kobe University, 6. Research Center for Urban Safety and Security, Kobe University, 7. Graduate School of Frontier Sciences, The University of Tokyo

We estimated spatial distribution of the six slow slip events (SSEs) off the Boso peninsula, central Japan, from 1996 to 2018. We have applied an inversion method called fused regularization, a type of sparsity constraint, suitable for detecting discontinuous changes in the model parameters, for evaluation function [Nakata et al., 2017]. In this study, to shorten calculation time, we used a type of approximation method by Obuchi and Kabashima [2016] to search hyperparameters, not LOO-CV (leave-one-out cross validation).

From our tentative results, the maximum slips for the 2002, 2011 and 2018 SSEs were large, and the 1996, 2007 and 2013 SSEs were small. The slip distributions of the 2011 and 2018 SSEs seem to be distributed southward than 2002. It is confirmed by numerical experiments that the difference in slip distribution is not due to GNSS station distribution.

Furthermore, we are conducting numerical simulation of earthquake generation cycles, which modelling SSEs off the Boso peninsula and M~8 earthquakes along the Sagami Trough. We will discuss slip distributions of SSEs and locked area during an interseismic period.

©2019. Japan Geoscience Union. All Right Reserved.

Marine electromagnetic observations around a slow earthquake region in the western Nankai trough

*Hiroshi Ichihara[1], Tada-nori Goto[2], Tetsuo Matsuno[3], Noriko Tada[4], Shinya Sato[2]

1. Earthquake and Volcano Research Center, Nagoya University, 2. Graduate School of Engineering, Kyoto University, 3. Ocean Bottom Exploration Center, Kobe University, 4. JAMSTEC

Slow earthquakes have been believed to relate to fraction of pore fluid around plate boundary. Thus, imaging of electrical resistivity (conductivity) distribution is essential to understand slow earthquakes. However, many of SSE areas are distributed beneath the ocean, we need marine electromagnetic (EM) observations. In this presentation, we report preliminary results of marine EM observations in the western part of Nankai Trough (off Miyazaki prefecture and off western Kochi prefecture, Japan) where SSEs, VLF events and regular earthquakes (e.g. 1968 off-Hyuga earthquake, M7.5) are known. We deployed eight ocean bottom electro-magnetometers (OBEMs) and recovered seven of them between 2017 and 2018. In addition to EM fields, two OBEMs measure absolute pressure to detect short period crustal deformations caused by SSE. We estimated high quality magnetotelluric responses based on Chave and Thomson (2004). However, the responses show strong three-dimensionality of resistivity distribution and strong coast effect (e.g. Key and Constable, 2011). They indicate that we need to apply three-dimensional imaging techniques for seafloor magnetotelluric data.

Keywords: Slow earthquake, magnetotelluric, OBEM, Nankai trough, off Miyazaki

©2019. Japan Geoscience Union. All Right Reserved.

Dynamics of precipitating injection fronts inside of structured medium

*Yutaka Sumino[1], Shunsuke Tanaka[1], Miyuki Kunihiro[1]

1. Tokyo University of Science

Recent study on a slow earthquake elucidates that the migration of water within a mantle wedge may play relevant roles[1]. The flow inside of confined geometry, such as within a soil, is often described by the Darcy’s law, where flow velocity is described by the gradient of fluid pressure. Interestingly, however, the water within a mantle wedge contains large amount of solid contents, and hence, a precipitation can be formed within the water[2]. For this reason, the dynamics of fluid flow under the effect of precipitation reaction should be explored.

Based on the above motivation, we explored the 2-dimensional confined chemical garden[3] as an analogue experiment for the fluid flow within a mantle wedge[4]. The system consists of two fluids with a quasi-two dimensional thin cell, so called a Hele-Shaw cell. The cell was filled with a fluid, and the other fluid is injected from the center of the cell. The flow in a Hele-Shaw cell can be described by the Darcy’s law. Furthermore, the mixing of these fluids leads to the precipitation. Thus, the flow observed in 2-dimensional confined chemical garden system is analogous to the one of water in a mantle wedge with precipitation formation.

Our previous study[4] showed that a filamentous pattern appears when the injection speed is high enough, whereas the symmetrical circular front was formed for lower injection speed. This results indicates that the propagation radius of injection front can be drastically different depending on the injection speed. In addition, the number of moving filaments saturate whose value is proportional to the injection speed. Such tendency can be understood with our boundary model adopting the effect Laplace pressure and the conservation of precipitation at the boundary. The model further predicts existence of optimal curvature for the moving front with which the required pressure for the motion is minimum. The curvature, and the speed of the optimal boundary motion is independent of the injection speed. These experimental and theoretical study thus worked well in the 2-dimensional Hele-Shaw cell. However, actual condition in a mantle wedge should have quenched structure, which is absent in a Hele-Shaw cell.

In order to fill the gap between actual condition in a mantle wedge and our analogue experiments, we modified our Hele-Shaw cell to have periodic pillar structure. As a control parameter, we changed the pillar to pillar distance, w, as shown in attached figure. The filament pattern showed meandering motion without pillar structures ($w = \infty$). We found that the filament pattern showed straight motion especially when w agreed with the typical filament width. Our modified mathematical model adopting nonlinear response of permeability with precipitation density numerically reproduced such experimental results. This results indicates that the propagation distance of injected fluid can be modified by the locally quenched disorder within a mantle wedge.

In this paper, we show detailed setup for experiments, as well as mathematical model.

[1] A. Tanaka et al. Earth, Planets and Space 70, 25 (2018).
[2] K. Ujiie, et al., *Geophys. Res. Lett.* **45**, 5371–5379 (2018).

©2019. Japan Geoscience Union. All Right Reserved.

[3] F. Haudin et al., *Proc. Natl. Acad. Sci. U.S.A.* **111**, 17363–17367 (2014).
[4] S. Wagatsuma, et, al., *Phys. Rev. E* **95**,052220 (2017).

Keywords: injection, fluid, precipitation

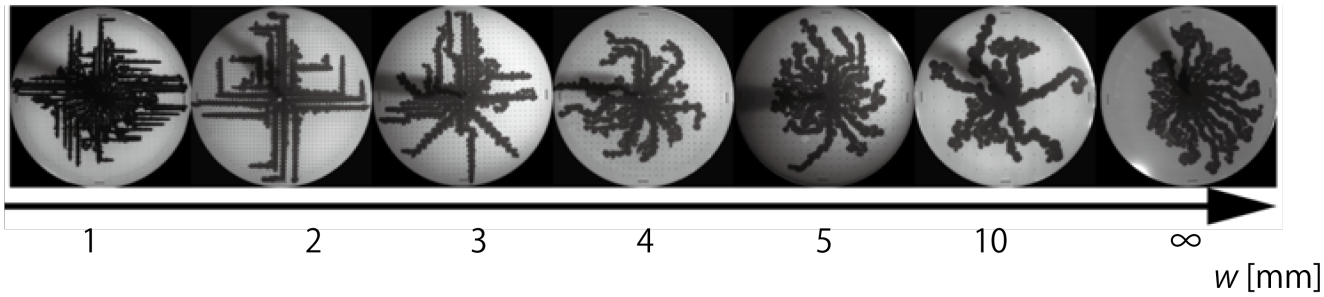

©2019. Japan Geoscience Union. All Right Reserved.

Permeability changes of simulated low permeable fault rocks induced by intermediate velocity friction test

*Wataru Tanikawa[1]

1. Japan Agency for Marine-Earth Science and Technology, Kochi Instutute for Core Sample Research

Earthquake events often associate with fluctuations of flow rate, pore pressure and pore fluid chemistry at a subsurface of earthquake rupture zones. The co-seismic hydrological changes are explained by changes in fluid permeability of fault zones during earthquakes, and the permeability change plays an important role for dynamic fault processes as well. Therefore, we newly designed a system to estimate water permeability changes during and after low to high velocity shear deformation using a rotary shear apparatus and simulated fault rocks.

A pair of hollow cylindrical samples made by low permeable Belfast dolerite and Aji granite were used as test specimens. To calculate permeability, a radial flow from the inner wall to the outer wall of the specimen was induced by applying a differential pore pressure (0.01 to 0.2 MPa) between inner and outer walls. We performed friction tests at normal stress of 2 MPa, rotation speed from 0.0003 to 0.6 m/s, and slip displacement of 1 m.

The results showed that permeability increased during sliding at every slip velocity condition, and higher velocity friction caused more abrupt increase in permeability. After the end of sliding, permeability gradually decreased with time and then became nearly constant value. Reduction rate of permeability 5 min after slip increased with slip rate. Fiction coefficient was decreased with sliding velocity. Frictional heating is a key to explain slip velocity dependence of permeability (flow rate). Temperature rise caused by frictional heating will reduce fluid viscosity, therefore, apparent permeability reduction after sliding can be explained by an increase in fluid viscosity by cooling. Pore pressure build-up by frictional heating can increase aperture, therefore, this process can explain permeability enhancement during sliding and velocity dependences on permeability increase and friction coefficient.

Keywords: permeability, friction coefficient, frictional heating

©2019. Japan Geoscience Union. All Right Reserved.

Modified relation between the coupling and tremor rates around the Shikoku region

*Tadafumi Ochi[1]

1. Institute of Earthquake and Volcano Geology, Geological Survey of Japan, The National Institute of Advanced Industrial Science and Technology

In Ochi and Takeda (2018, EPS), I examined the relation between the interplate coupling velocity and the number of deep low-frequency tremors in the same place around the Shikoku region, southwest Japan. I found that there were some spot-like points where the coupling and the tremor count were well correlated, and that the regression line required the coupling rate to be the plate convergence rate in this region under conditions of zero tremor count rate. One of the problems to be resolved is the interpretation of the first matter 'spot-like points' mentioned above. According to the pairs of time series of the coupling rate and tremor count rate, some pairs show a time delay, and the others show a small fluctuation in the tremor count rate that seems to be independent of the coupling rate. It is interesting that whether the an ill-correlation just comes from an oversimple model of the linear regression I used in the previous study, or really reflects some physical background. In order to answer this question, I construct the model which allows the fluctuation in the tremor count rate that is independent from the coupling rate and observe the fitness of the model. At this time, some trial models that allow the shorter period fluctuation in the tremor count rate than in the coupling rate and temporal change in the period achieve clear correlations. In the presentation, I will show the results of the various trials.

Keywords: Interplate coupling, Low-frequency tremor

©2019. Japan Geoscience Union. All Right Reserved.

Spatiotemporal distribution of regular and very low-frequency earthquakes in the northern part of the Ryukyu subduction zone

*Youichi Asano[1], Kazuhiko Goto[2], Hiroshi Yakiwara[3], Shuichiro Hirano[3]

1. National Research Institute for Earth Science and Disaster Resilience, 2. Association for the development of earthquake prediction, 3. Nansei-toko Observatory for Earthquakes and Volcanoes, Kagoshima University

We have investigated detailed spatiotemporal distribution of regular and very low-frequency (VLF) earthquakes including an Mw 6.3 interplate event near Tanegashima along the Ryukyu trench on Jun. 08, 2019. This earthquake was followed four Mw4-5 class regular and many VLF earthquakes by the end of Jan., 2019. At first we estimated centroid moment tensors of these regular and several VLF earthquakes, respectively, from broadband seismograms recorded at the NIED F-net and temporally observation stations. In the next step, the known VLF earthquakes were selected to be template events for searching unknown VLF earthquakes from continuous seismograms. If there are several candidates of VLF earth quake, we select the most coherent event with a maximum cross-correlation coefficient averaged over all stations in every 180 seconds. Finally we estimated locations of the selected events from phase shift of the wavelets between the template and these selected events. Obtained result shows that activity of VLF earthquakes after the Mw 6.3 earthquake was started in the adjacent area east of this Mw 6.3 earthquake; however, the following Mw4-5 regular earthquakes occurred south of this area in the period of Jan. 25-30, 2019. In this period, the front of the VLF activity migrated toward east from these Mw4-5 events. Such a spatiotemporal distribution of regular and VLF earthquakes suggests that the after slip of the Mw 6.3 and/or an SSE caused these regular and VLF earthquakes.

Acknowledgment

This study is partly supported by JSPS KAKENHI Grant Number JP16H06473.

Keywords: very low-frequency earthquake, Ryukyu subduction zone

©2019. Japan Geoscience Union. All Right Reserved.

Possible tectonic tremor activities near the VLFE epicenters in the Sanriku-Oki region in 2011

*Hidenobu Takahashi[1], Ryota Hino[1], Yusaku Ohta[1], Naoki Uchida[1], Syuichi Suzuki[1], Masanao Shinohara[2], Takanori Matsuzawa[3]

1. Graduate school of Science Tohoku University , 2. Earthquake Research Institute, University of Tokyo, 3. National Research Institute for Earth Science and Disaster Resilience

Recently various kind of slow earthquakes have been discovered along the Japan Trench subduction zone. Prior to the occurrence of the 2011 Tohoku-oki earthquake, occurrence of slow slip events associated with migration of small earthquake epicenters and tectonic tremors was reported near the hypocenter of the Tohoku-Oki earthquake (e.g. Kato et al., 2012; Ito et al., 2015; Katakami et al., 2018). As a different type of a slow-earthquake family, Very Low Frequency Earthquakes (VLFEs) have been detected in more broad areas (Matsuzawa et al., 2015). Takahashi et al. (in prep.) detected the seismic signals from the VLFEs by short-period ocean bottom seismograms (OBS) deployed in the vicinity of the VLFE epicenters in the Sanriku-Oki region, just after the Tohoku-Oki earthquake. They further identified a number of VLFE-like events, not recognized by the onshore data. Here, we report on possible tectonic tremor activities in the same area based on the OBS data after the 2011 Tohoku-oki earthquake.
We detected four sequences of continuous rises of amplitudes on the OBS records. Each of the sequence has a duration of ~ half a day. The sequences were composed of numerous wave trains with good correlations in their growths and decays in observed amplitudes among the stations, but no distinct P- or S-wave onsets were identified for individual wave trains. Interestingly, the spatial variation of the wave trains amplitudes is similar to those of the previously identified VLFEs. These observations suggest that the sequences were composed of small seismic events closely located each other and to the known VLFEs. It is also notable that some of the VLFE-like events discovered by the OBS data were contained in the sequences. We regard the discovered sequence as a kind of tectonic tremor activity and will inspect their characteristics, such as frequency content and its variability, to clarify their nature and discuss their relevance to slow slip events along the shallow subduction interface, which might promote the activities.

Keywords: tectonic tremor, Sanriku−oki

©2019. Japan Geoscience Union. All Right Reserved.

Heterogeneous structure around a region of slow earthquake activity off Ibaraki prefecture along the Japan Trench

*Kimihiro Mochizuki[1], Tomoaki Yamada[1], Masanao Shinohara[1], Ryota Hino[2], Ryosuke Azuma[2], Yoshihiro Ito[3], Yoshio Murai[4], Kenji Uehira[5], Toshinori Sato[6]

1. ERI, Univ. of Tokyo, 2. Graduate School of Science, Tohoku Univ., 3. DPRI, Kyoto Univ., 4. Faculty of Science, Hokkaido Univ., 5. NIED, 6. Graduate School of Science, Chiba Univ.

Large earthquakes of magnitude (M) ~7 have repeatedly occurred in the Ibaraki-oki region, about 100 km offshore of the Ibaraki prefecture along the Japan Trench, at a constant interval of ~20 years. Mochizuki et al. (2008) conducted a marine seismic survey and revealed that there exists a subducted seamount in the region. They also conducted an offshore seismic observation using ocean bottom seismometers (OBSs) to show that the seismicity in the region can be seen off of the subducted seamount, but not along the plate interface over it. They found that the location of the subducted seamount did not agree with the focal region of the repeating M7 earthquakes. From these results, they argued that the plate interface over the subducted seamount does not constitute an asperity of the repeating M7 earthquakes. Wang and Bilek (2011) introduced an idea that the seamount subduction causes formation of a fracture network within the overriding plate, and such a fracture network would prevent accumulation of large strain energy along the plate interface over the subducted seamount to generate large earthquakes. In addition to the repeating M7 earthquakes, recent studies (e.g. Matsuzawa et al., 2015; Nishikawa and Ide, 2018) have reported activity of slow earthquakes in the region. Relationship between activity of various types of earthquakes and structural features around the plate interface is one of the key topics to better understand controlling factors over earthquake types to be generated.

Recent studies in the Hikurangi subduction margin off the North Island of New Zealand show spatial relationship between variety of fault slips and topographic features of the plate interface. Wallace et al. (2016) successfully observed a large slow slip event just beneath an offshore array of ocean bottom pressure gauges, and precisely determined its slip distribution. They revealed that its slip propagation appeared to have circumvented subducted seamounts that have been imaged by magnetic anomalies as well as seismic reflection sections. Todd et al. (2018), for the first time, detected offshore tremor activity in the Hikurangi margin. The activity appears to have started just after the cessation of the slow slip, and its spatial distribution is only limited within regions of subducted seamounts. These results show that distributions of slow slip and tremor activity do not appear coincident, and thus the physical properties of the plate interface may be different. Further seismic surveys are supposed to provide vital information on structural variations that control physical characteristics of the plate interface.

In February, 2011, we acquired wide-angle reflection and refraction seismic data using 21 OBSs along a 150 km transect in the Ibaraki-oki region during the KH11-2 R/V Hakuho-maru cruise. We also included data from an OBS array that had already been deployed for a long-term seismic observation above the subduction front of the subducted seamount. Thus, we could construct a dense OBS profile above the subducted seamount with a receiver interval of ~3 km to achieve a high spatial resolution, whereas the largest interval is 10 km near both ends of the profile. First arrivals from the airgun sources can be traced up to ~95 km on most of the OBSs. The OBS record sections show significant heterogeneity that may include very rough structural features of the subducting oceanic crust along strike. Such heterogeneity may control seismic activity in the region.

©2019. Japan Geoscience Union. All Right Reserved.

Keywords: Ibaraki-oki, Active source seismic survey, Heterogeneous structure

©2019. Japan Geoscience Union. All Right Reserved.

Shallow low-frequency tremor triggered by nearby moderate earthquakes off Sanriku

*Sachiko Tanaka[1], Takanori Matsuzawa[1], Youichi Asano[1]

1. National Research Institute for Earth Science and Disaster Resilience

In the region off Sanriku, we have observed shallow low-frequency tremor, which occurs between the 12 km and 20 km depth contours of the plate interface, applying an envelope correlation method (Obara, 2002) to the records from the Seafloor observation network for earthquakes and tsunamis along the Japan Trench (S-net) (Tanaka et al., 2018). Several episodes of tremor, each of which lasted for half a day to six days, were detected in 2017, with intervals of one to three months. In the present study, we found tremor triggered by nearby moderate earthquakes. On July 24, 2017, an Mw 5.6 earthquake, showing reverse faulting consistent with the slip on the plate interface, occurred at the downdip end of the tremor zone off Sanriku, which was the largest event within 100 km of that tremor zone in the year. Immediately after the Mw 5.6 earthquake, coherent tremor signals were identified at surrounding stations. These signals continued for 20 hours, and the locations of their sources spanned 40 km along strike and 50 km along dip. Similar triggered tremor was observed following an Mw 5.1 earthquake on July 22, two days before the Mw 5.6 earthquake. This tremor activity was smaller and shorter than that triggered by the Mw 5.6 earthquake; tremor was localized to an area of 20 km by 15 km, and lasted for twelve hours. After a quiescence of nearly one day, the Mw 5.6 earthquake occurred at an adjacent area and triggered tremor was detected again. Triggering of tremor by moderate interplate earthquakes in or very close to the tremor zone we observed may imply small-scale (~ a few kilometers) heterogeneities in frictional properties on the plate interface in the area.

Keywords: shallow low-frequency tremor, triggered tremor, Japan Trench

©2019. Japan Geoscience Union. All Right Reserved.

Slow slip events in the Bungo Channel over 15 years as inferred from GNSS data (1996-2011)

Takatoshi Yokoi[1], *SHINICHI MIYAZAKI[1], Hiromu Sakaue[1], Jun'ichi Fukuda[2]

1. Graduate School of Science, Kyoto University, 2. Earthquake Research Institute, The University of Tokyo

We estimated space-time evolution of inter-plate slip and slip velocity associated with slow slip events (SSE) in the Bungo Channel over 15 years between January 1, 1996 and February 28, 2011, from GNSS data.

We use GNSS time series at 80 stations around the Bungo Channel out of GEONET stations. Time series were obtained with GIPSY-OASIS II software by Nishimura (personal communication). We removed data during SSE and estimated secular velocities, annual and semi-annual seasonal variations, and offsets associated with earthquakes, SSEs and instrumental events. Then we remove contributions of those components from time series with SSE to prepare time series for the inversion. We constructed plate interface based on iso-depth data by Baba et al. (2002) and Hirose et al. (2008), and setup the model region that is 200km long east to west and 280km long north to south. The model region was subdivided into 719 small triangular patches. We employed the inversion method based on the Monte Carlo Mixture Kalman Filter (Fukuda et al. 2008) and estimated slip and slip velocities on the fault continuously over 15 years.

First, Long-term slow slip events (L-SSE hereafter) that lasted for several months were inferred in 1997, 2003 and 2010 as obtained by, such as, Ozawa et al. (2012, 2017) and Yoshioka et al. (2015). In addition to basic characteristics described in these previous studies, short-term slow slip events (S-SSE hereafter) were inferred just before or just after the main slip event. This result suggests that stress perturbations by SSEs trigger other SSEs. Therefore the inferred cumulative moment in this study was smaller than previous studies because we successfully excluded contributions from S-SSEs. Second, S-SSEs have repeatedly occurred with the interval of about three or four months over 15 years. Those S-SSE were located at depths of about 30-40km and associated with low frequency tremors.

In this presentation, we focus space-time evolutions of L-SSE in 2010 and S-SSE in 2005.

Keywords: Slow slip in the Bungo Channel, crustal deformation, Monte Carlo Mixture Kalman Filter

©2019. Japan Geoscience Union. All Right Reserved.

Investigations of sensor orientation and a possibility of detecting crustal deformation based on accelerometer records of S-net

*Ryota Takagi[1], Naoki Uchida[1], Takashi NAKAYAMA[1], Ryosuke Azuma[1], Akira Ishigami[1], Tomomi Okada[1], Yusaku Ohta[1], Ryota Hino[1]

1. Research Center for Prediction of Earthquakes and Volcanic Eruptions, Graduate School of Science, Tohoku University

Seafloor Observation Network for Earthquakes and Tsunamis along the Japan Trench (S-net) of National Research Institute for Earth Science and Disaster Resilience (NIED) will greatly improve our knowledge of subsurface structure beneath offshore region along Japan trench and understanding of regular and slow earthquakes on the subducting plate boundary. We estimated the orientations of S-net sensors that are fundamental information for further data analysis and investigated the possibility of detecting crustal deformation based on accelerometer records.

We determined three parameters of sensor orientations: tilt angle of the long axis of a cable, rotation angle around the long axis, azimuth of the long axis. We estimated the tilt and rotation angles by assuming the DC components of accelerometers record the gravitational acceleration. The tilt and rotation angles slightly vary within the range of 0.01-0.1 degree during the period from 2016 to 2018 except for coseismic steps of rotation angles larger than 1 degree due to the M6.4 off Sanriku earthquake (August 20, 2016) and M7.4 off Fukushima earthquake (November 20, 2016). The long-axis azimuths are estimated by particle motions of long-period Rayleigh waves. We used the accelerometer records in 30-100 s of 7-14 teleseismic earthquakes with Mw 7.0-8.2. The azimuths are constrained in the range of 5-10 degrees. After correcting waveforms based on the estimated sensor orientation, we found coherent waveforms within the whole S-net stations and separation of Rayleigh and Love waves in radial and transverse components.

The capability of the DC components of accelerometers implies a possibility to detect crustal deformation from accelerometer records. We made time series of tilt and rotation angle with the sampling rate of one hour. During the period without offsets partly due to earthquakes, the root-mean-square (RMS) amplitudes of tilt and rotation angles are about 2 micro radians at most stations. The buried stations shallower than 1500 m show smaller variations and RMS amplitudes are about 0.2 micro radians. Some buried stations show tidal response with amplitude of about 1 micro radians. Since the maximum tilt change of land stations by a slow slip event (SSE) near the Boso Peninsula is about 1 micro radians, it might be possible to detect crustal deformation due to similar SSEs based on the accelerometer records.

Acknowledgement: We used continuous records of S-net managed by NIED. We thank NIED for providing the data.

Keywords: S-net, Sensor orientation, Crustal deformation, Slow slip, Tilt observation

©2019. Japan Geoscience Union. All Right Reserved.

Spatiotemporal variation of released seismic energy from shallow low-frequency tremor in Hyuga-nada, revealed by ocean bottom seismological observation

*Yusuke Yamashita[1], Saki Watanabe[2], Tomoaki Yamada[3], Masanao Shinohara[3], Takeshi Matsushima[2]

1. Disaster Prevention Research Institute, Kyoto University, 2. Institute of Seismology and Volcanology, Kyushu University, 3. Earthquake Research Institute, The University of Tokyo

In this study, we estimate the released seismic energy by shallow low-frequency tremors (shallow tremors) and clarify spatiotemporal variation of shallow tremor activity in Hyuga-nada, east off Kyushu. We used the data obtained from the temporal ocean bottom seismological observation for 3 months in 2013 [Yamashita *et al*., 2015] and long-term ocean bottom seismological observation from 2014 to 2017. The source location and released seismic energy of each shallow tremor was simultaneously estimated by Hybrid Envelope Cross-correlation Method [Maeda and Obara, 2009]. Observation data were obtained by the long-term continuous ocean bottom seismic observation in Hyuga-nada from 2013 to 2017. Site amplification factors were estimated by the coda normalization method [e.g., Sato and Fehler, 1998].

Spatial distribution of released seismic energy rate (energy rate) shows a heterogeneity although the average value of that is generally 10^4 J/s. The regions where the energy rate is relatively small are roughly coincident with the subducting or passed areas of the Kyushu-Palau Ridge. This result suggests that the structure and/or shape of the subducting plate such as seamounts or ridges may have an effect on the frictional property of the shallow plate interface. The 2013 activity was similar characteristics of shallow tremor location in space and time as the previous study, including two migrations episode. In addition, the characteristics of the released seismic energy were revealed as follows: (1) the energy rate was large at the both initiation point and the front of the migration, (2) the total released energy amount of the first migration was larger than that of the second migration, (3) both migrations were stopped at the region of small amount of released energy. Migration episode occurred while the 2015 activity and similar characteristics were documented.

Migration speed of shallow tremor is a few times faster, and energy rate of that is one or two orders of magnitude greater than the deep tremor. Applying the model of Ando *et al*. [2010, 2012] and Yabe and Ide [2014] to the result in this study, the average fault strength of shallow tremor is stronger than that of deep tremor, which leads up to a faster fault slip both brittle and ductile area. As a result, migration speed may become to be faster than deep tremor.

Acknowledgements: This study is supported by the research project for compound disaster mitigation on the great earthquakes and tsunami around the Nankai trough region, the MEXT of Japan, and JSPS KAKENHI Grant Number JP16H06471, JP16H06472. We thank Dr. Takuto Maeda for valuable discussions and comments. The observation data in 2013 obtained by T/S Nagasaki-maru. We used the JMA unified earthquake catalog and the seismic data obtained by Kagoshima University.

Keywords: Shallow low frequency tremor, Shallow slow earthquake, Ocean bottom seismological observation

©2019. Japan Geoscience Union. All Right Reserved.

©2019. Japan Geoscience Union. All Right Reserved.

Unified description of fast and slow earthquakes using velocity strengthening patches

*So Ozawa[1], Takahiro Hatano[1]

1. Earthquake Research Institute, the University of Tokyo

In a prevalent view, seismicity in subduction zones is governed by the distribution of the frictional properties of the plate interface. Regions with velocity-weakening (VW) friction generate earthquakes, whereas velocity-strengthening (VS) regions creep aseismically. Although most models consider isolated VW regions (patches) from the idea of asperities (e.g. Dublanchet et al., 2013), isolated VS patches also would exist given the frictional properties on faults are inferred to be complex and hierarchical. Therefore, the role of VS patches is to be studied.

Here we perform 3-D numerical simulation of the seismic cycle of faults governed by the rate and state friction law with the aging law. We distribute randomly circular VS patches on a VW background. We mainly focus on the effect of the ratio of VS and VW areas.

In our preliminary simulation, we identified two important effects. First, the VS patches act as the “stability barriers” during dynamic rupture propagation, which makes the rupture process more complicated than a single propagating crack. Rupture decelerates by encountering a stability barrier, followed by reacceleration due to overcoming the barrier. Such a process gives rise to multiple rupture fronts in the slipping area.

Second, dynamic rupture is inhibited by increasing the number of VS patches, and the fault slips aseismically with strong fluctuation in slip velocity. This is because there are no enough VW regions to accelerate the slip to dynamic rupture. Although a similar mechanism for slow earthquakes is proposed by Skarbek et al. (2012) and Yabe & Ide (2017), our 3-D modeling enables detailed studies on the spatiotemporal evolution of slip. In the presentation, we further discuss our results in the context of the dynamic scaling of rupture growth and the phenomenological law of slow earthquakes.

Keywords: Slow earthquake, Rate and state friction

©2019. Japan Geoscience Union. All Right Reserved.

The b-value of the earthquake swarm activities accompanied by the Boso slow slip events

*Yuki Noda[1], Hitoshi Hirose[2,1]

1. Department of Planetology, Faculty of Science, Kobe University , 2. Research Center for Urban Safety and Security, Kobe University

Slow slip events (SSEs) which are accompanying earthquake swarms repeatedly occur at intervals of about 2 to 7 years off Boso Peninsula (e.g., Sagiya, 2004; Hirose et al., 2012, 2014; Fukuda, 2018). These SSEs and swarms are thought to occur on the upper boundary of the subducting Philippine Sea plate.

As a statistical property of earthquakes, Gutenberg-Righter’ s law is well-known, that is, the relationship between the magnitude and the logarithm of occurrence frequency of earthquakes is expressed well with a straight line a-bM (Gutenberg and Richter, 1944). Although the b-value (slope of the line) often takes values around 1, there are many reports about the temporal changes of the b-value. For example, a decade-scale b-value decrease prior to the 2011 Tohoku Earthquake is reported (Nanjo et al., 2012). Although the relationship between the temporal change of b-value and aseismic slip is suggested, but the lack of near field geodetic observations prevents the direct evidence for the relationship. Here we examine the b-value of the earthquake swarms accompanied by the Boso SSEs, of which the aseismic slip is revealed by geodetic observations.

In this study, we estimate the b-value of the earthquake swarms in 2002, 2007, 2011 and 2014. We use the JMA unified earthquake catalog. As a preliminary analysis, we investigated the earthquakes with focal depths of 5 km to 40 km occurring at 35.05˚ to 35.56˚N in latitude and 140.15˚ to 140.73˚E in longitude. Eventually, “event period” estimated in the previous studies of the crustal deformation by geodetic observation does not necessarily agree with the period of the swarms occurring at the same time. Therefore, in this research, “event period” was redefined from seismic activity and used. In other words, we extracted swarms including a SSE period from crustal deformation studies and the time when the seismicity rate (the number of earthquakes per unit time) is significantly higher than the other time is defined as “event period”. In addition, the period other than the event period is defined as “inter-swarm period”.

We find that the b-values in the event periods tend to be lower than that during inter-swarm period. In more detail, different trends that seem to correspond to the difference in slip zone and location of earthquake activity of each SSE (Hirose et al. 2014) are seen in the b-values for the event periods. A seismic activity near the southern coast of the Boso Peninsula was hardly observed in the 2007 event period, whereas an active seismic activity was seen there in the 2011 event period. In order to clarify the dependence of the b-value on the difference in the location of the earthquakes, we divided the survey area into two areas, that is, the northern area (area A) and the southern area (area B). The seismic activity is observed in all event periods in the area A, whereas an active seismic activity is observed only in the event periods of 2002 and 2011 in the area B. Then a b- value is estimated in each period in the same way. As a result, for the earthquakes occurred in the northern region (area A), there is a tendency that the b-value in each of the event periods is lower by about 0.2-0.4 than that during inter-swarm. On the other hand, such a tendency is not observed in the southern area (area B). Such differences in the northern and southern regions may suggest that the effects of stress changes caused by SSEs vary from region to region.

©2019. Japan Geoscience Union. All Right Reserved.

Keywords: Gutenberg-Richter's law

©2019. Japan Geoscience Union. All Right Reserved.

Three-dimensional thermal modeling associated with subduction of the Philippine Sea plate at the Ryukyu Trench, and its relation to the occurrence of interplate seismic events

*Nobuaki Suenaga[1], Shoichi Yoshioka[2,1], Yinfeng Ji[3]

1. Graduate School of Science, Kobe University, Japan, 2. Research Center for Urban Safety and Security, Kobe University, Japan, 3. Chinese Academy of Science, Beijin, China

Interplate seismic events such as short-term slow slip evens (S-SSEs) (Nakamura, 2017), low-frequency earthquakes (LFEs) (Ando et al., 2012), and shallow very low-frequency earthquakes (VLFEs) (Nakamura et al., 2015) have been identified at the Ryukyu Trench, southwestern Japan. As the specific characteristics of these distributions, depths where S-SSEs and LFEs occur at the plate interface beneath the Okinawa island, whose depth is ranging from 15 km to 25 km, is about 10-20 km shallower than that beneath the Yaeyama islands, whose depth is ranging from 35 km to 50 km.

In this study, we constructed three-dimensional parallelepiped thermal convection model associated with subduction of the Philippine Sea (PHS) plate beneath the Amurian (AM) plate at the Ryukyu subduction zone. We considered subduction history of the PHS plate in the model region, referring to the plate rotation model (Mathews et al., 2016). We performed the numerical simulation as the time-dependent problem in the last 15 Myr to elucidate relationships among calculated thermal structures, dehydrations from the subducting plate, and the interplate seismic events. We used observed heat flow data to constrain thermal structures.

As a result at 0 Ma, we found that interplate temperature where S-SSEs and LFEs occur beneath the Yaeyama islands is lower than that beneath the Okinawa island when compared with the same depth along the direction of the trench axis. This is mainly because the convergence rate (PHS-AM) becomes gradually fast toward the southwest. Therefore, interplate temperatures where S-SSEs and LFEs occur were estimated ranging from 500℃ to 700℃ both beneath the Okinawa island and the Yaeyama islands.

We also calculated water content distribution within the PHS plate, using the calculated thermal structures and the phase diagram of MORB in an oceanic crust (Omori et al., 2008) and ultramafic rock in a slab mantle (Hacker et al., 2003). As for dehydration of MORB, we found that epidote eclogite transforms into amphibole eclogite in the neighboring area where S-SSEs and LFEs occur beneath the Okinawa island, and amphibole eclogite transforms into eclogite beneath the Yaeyama islands. The former and the latter dehydrate a total amount of 1.4 wt% and 0.7 wt% associated with their phase transformations, respectively.

Keywords: three dimensional thermal modeling

©2019. Japan Geoscience Union. All Right Reserved.

[E] Poster | M (Multidisciplinary and Interdisciplinary)：M-GI General Geosciences, Information Geosciences & Simulations

Wed. May 29, 2019 10:45 AM - 12:15 PM JST | Wed. May 29, 2019 1:45 AM - 3:15 AM UTC | Poster Hall International Exhibition Hall8, Makuhari Messe_11

[M-GI30] Data assimilation: A fundamental approach in geosciences

convener:Shin ya Nakano(The Institute of Statistical Mathematics), Yosuke Fujii(Meteorological Research Institute, Japan Meteorological Agency), SHINICHI MIYAZAKI(Graduate School of Science, Kyoto University), Takemasa Miyoshi(RIKEN)

Data assimilation is an inversion approach to estimate the evolution of a system by utilizing a constraint given by a dynamical simulation model. Data assimilation is now widely used not only in meteorology and oceanography but also other fields of geosciences such as hydrology, solid earth science, and space science. This session aims at providing an opportunity for discussion on data assimilation studies among researchers of various field of geosciences. We encourage contributions addressing novel methods and theoretical developments of data assimilation. Contributions dealing with useful applications of data assimilation are also welcome.

[MGI30-P01] Superposition of atmospheric states using information redundancy for Numerical Weather Prediction

*Toshiyuki Ishibashi[1] (1.Meteorological Research Institute/Japan Meteorological Agency)

[MGI30-P02] **Numerical Weather Prediction Experiments using a Coupled Atmosphere-Ocean Data Assimilation System in JMA/MRI** (3)

*Toshiyuki Ishibashi[1], Takeshi Iriguchi[1], Yosuke Fujii[1], Tamaki Yasuda[1], Yuhei Takaya[1], Naoki Saito[1], Toshikazu Onogi[1] (1.Meteorological Research Institute/Japan Meteorological Agency)

[MGI30-P03] **Accurate estimation of posterior error covariance in a 4D-Var inverse analysis**

*Yosuke Niwa[1,2], Yosuke Fujii[2,3] (1.National Institute for Environmental Studies, 2.Meteorological Research Institute, Japan Meteorological Agency, 3.The Institute of Statistical Mathematics)

[MGI30-P04] Assimilation CO_2 concentration data in the Kanto region using AIST-MM model and for the estimation of CO_2 emissions

*Yutaka Arai[1], Ryoichi Imasu[1], Hiroaki Kondo[2], Yosuke Niwa[3] (1.Atmosphere and Ocean Research Institute, The University of Tokyo, 2.National Institute of Advanced Industrial Science and Technology, 3.National Institute for Environmental Studies, Independent Administrative Institutions)

[MGI30-P05] **Application of data assimilation method on parameter estimation of flow and nutrient behavior in watershed model**

*Yosuke Horie[1] (1.Nippon Koei Co., Ltd.)

[MGI30-P06] Bayesian inference of grain growth prediction via multi-phase-field models

*Shin-ichi Ito[1], Hiromichi Nagao[1], Takashi Kurokawa[1], Tadashi Kasuya[1], Junya Inoue[1] (1.The University of Tokyo)

[MGI30-P07] GNSS data assimilation for the Bungo channel Long-term SSEs using Ensemble Kalman Filter (EnKF)

*Megumi Fujita[1], Takuya NISHIMURA[2], Kazuro Hirahara[3], SHINICHI MIYAZAKI[1] (1.Graduate School of Science , Kyoto University, 2.Disaster Prevention Research Institute, Kyoto University, 3.Institute of Education, Research and Regional Cooperation for crisis Management Shikoku, Kagawa University)

[MGI30-P08] A data assimilation library with Python for parallel computing

*Shin ya Nakano[1], Yuya Ariyoshi[2], Tomoyuki Higuchi[1] (1.The Institute of Statistical Mathematics, 2.Faculty of Engineering, Nippon Bunri University)

Superposition of atmospheric states using information redundancy for Numerical Weather Prediction

*Toshiyuki Ishibashi[1]

1. Meteorological Research Institute/Japan Meteorological Agency

Atmospheric state analysis is a difficult scientific problem due to our limited ability in computation and observation, and analysed atmospheric states are fluctuating around the true state. The purpose of this paper is to analyse atmospheric state as a superposition of possible atmospheric states using information redundancy, and evaluate its accuracy in the context of numerical weather prediction (NWP). This atmospheric state analysis approach has two novel aspects. First, it uses only real atmospheric information, and no-artificial perturbations unlike existing ensemble based methods. Second, it does not require specific error structures of our knowledge of the atmosphere. We performed this method on a global numerical weather prediction system of Japan Meteorological Agency. The experimental results show the method can clearly reduce forecast root means square errors about 3-5% in average within 2 day forecast compared to existing methods (CNTL). Furthermore, forecast RMSEs of ensemble means of ensemble forecasts using only a few members generated by this method are significantly smaller than CNTL from the forecast initial time.

©2019. Japan Geoscience Union. All Right Reserved.

Numerical Weather Prediction Experiments using a Coupled Atmosphere-Ocean Data Assimilation System in JMA/MRI (3)

*Toshiyuki Ishibashi[1], Takeshi Iriguchi[1], Yosuke Fujii[1], Tamaki Yasuda[1], Yuhei Takaya[1], Naoki Saito[1], Toshikazu Onogi[1]

1. Meteorological Research Institute/Japan Meteorological Agency

An atmosphere-ocean coupled data assimilation system (CDAS) has been developed at the JMA/MRI to investigate feasibility of a CDAS as a future DAS for seamless numerical prediction including both numerical weather prediction (NWP) and numerical seasonal climate prediction (NCP), and for reanalysis of the atmosphere-ocean. Our CDAS (**MRI-CDA1**) has two features. 1) It composed of the JMA operational systems, the global atmospheric DAS (MRI-NAPEX) based on 4D-Var, the global ocean DAS (MOVE-G2) based on 3D-Var, and the atmosphere- ocean coupled global forecast model (CGCM: JMA/MRI-CGCM2). 2) Coupling strategy is “weak coupling” with two different data assimilation window lengths for the atmosphere and ocean. Here, “weak coupling” denotes the approximation that ignores correlations of atmosphere and ocean background forecast errors. Following the previous reports in JpGU2018 and JpGU-AGU joint meeting 2017 (Ishibashi et al. 2018; 2017), we will report basic property of MRI-CDA1 in NWP.

©2019. Japan Geoscience Union. All Right Reserved.

Accurate estimation of posterior error covariance in a 4D-Var inverse analysis

*Yosuke Niwa[1,2], Yosuke Fujii[2,3]

1. National Institute for Environmental Studies, 2. Meteorological Research Institute, Japan Meteorological Agency, 3. The Institute of Statistical Mathematics

The four-dimensional variational method (4D-Var) is one prominent data assimilation/inversion method. However, it is a non-trivial task for a conventional 4D-Var to estimate a posterior error variance-covariance matrix. This study developed a method to estimate a posterior error variance-covariance matrix especially focusing on its off-diagonal elements, i.e., covariance. Off-diagonal elements are usually difficult to be estimated but provide error correlations that are beneficial for interpreting optimized parameter variations. The method was developed within a 4D-Var framework using a quasi-Newton method with the Broyden–Fletcher–Goldfarb–Shanno (BFGS) formula. This study newly introduces numerical techniques that ensure conjugacy among the set of increment vector pairs in the BFGS formula. Through application to an inverse problem of atmospheric CO_2, the developed method was evaluated with three diagnostic measures and compared against existing methods. The evaluation revealed that the developed method could provide accurate estimates of the posterior variance-covariance matrix, in terms not only of the diagonal but also of the off-diagonal elements. Although far more expensive than optimal state estimation, the computational efficiency was found reasonable for practical use, especially in conjunction with an ensemble approach.

Keywords: inversion, data assimilation, posterior error covariance

©2019. Japan Geoscience Union. All Right Reserved.

Assimilation CO_2 concentration data in the Kanto region using AIST-MM model and for the estimation of CO_2 emissions

*Yutaka Arai[1], Ryoichi Imasu[1], Hiroaki Kondo[2], Yosuke Niwa[3]

1. Atmosphere and Ocean Research Institute, The University of Tokyo, 2. National Institute of Advanced Industrial Science and Technology, 3. National Institute for Environmental Studies, Independent Administrative Institutions

Atmospheric carbon dioxide (CO_2) known as greenhouse gas is the most important gas for global warming. For the reason, there have been many researches about CO_2 such as model calculations, satellite observations and direct observations recently. As computer spec get higher, the CO_2 model has been more improved and 3D distributions of CO_2 has been calculated in more detail. In Japan, the satellite observation has been high resolution by satellite, Greenhouse Observing SATellite-2 (GOSAT-2). But in urban area, CO_2 distributions are complicated because of complexed CO_2 emission source and sink around the area. Especially, in the Kanto district mega city, Tokyo is located, CO_2 emissions from power plants and human activities are very huge. Furthermore, around the city there are forests and mountains which strongly affect to CO_2 concentrations in the atmosphere through their respiration and photosynthesis. In case to calculate such the district with high spatial resolutions, the models are required to be able to represent the temporal and spatial variations of the respiration and photosynthesis of the plants precisely. It has been also pointed out that representativeness of the vertical transport of CO_2 in the models is a key subject. About satellite observations, it is not always possible to observe CO2 distributions because of to be influenced by the weather and the frequencies of them are limited, and what ca be observed are not 3 dimensional but 2 dimensional namely vertical column densities of CO_2. On the other hand, the accuracy of the in-situ observations, is best, but there are very limited observation points. These are obstacles to grasping the detailed behavior of CO_2 concentration.

In this study, a regional transport model, AIST-MM has been used to investigate the behavior of CO_2 concentrations in Kanto district (Kondo et al., 2001). Firstly, AIST-MM computes CO_2 concentrations in the outer area (630 km×550 km), and then calculates CO_2 concentrations in the inner area (216 km×216 km) using the results from the former.
Firstly, the model was improved to be able to calculate the CO_2 seasonal variations through a year in order to estimate CO_2 emission source which contained large error. It was found that AIST-MM had uncertainty in the part of plant activities especially respiration in summer. As the calculation of plant respiration strongly depends on the temperature, when the temperature becomes high, the respiration of plants unrealistically increases. So the plant respiration parameter was tuned.
In order to compensate for the CO_2 influx from outside of the calculation region, the result of a global model, NICAM-TM (GL5) were used as the boundary conditions when calculating outer region. This modification led to improve the calculation of the vertical transport.
Furthermore, constant sea surface temperature was replaced with the satellite observation data derived from AVHRR-AMSR. In order to improve the simulating performance, we adjusted many detailed emission information by distinguishing between holidays and weekdays.
Secondly, Local Ensemble Transform Kalman Filter (LETKF) which is one of data assimilation methods is adapted to the adjusted AIST-MM and try to calculate CO_2 concentrations using in-situ observations, satellite observations, and ground remote sensing observations. In the near future, the CO_2 emissions will be estimated using Kalman smoother method.

©2019. Japan Geoscience Union. All Right Reserved.

Keywords: regional CO2 transport model, plant respiration, data assimilation, Local Ensemble Transform Kalman Filter, Kanto region

©2019. Japan Geoscience Union. All Right Reserved.

Application of data assimilation method on parameter estimation of flow and nutrient behavior in watershed model

*Yosuke Horie[1]

1. Nippon Koei Co., Ltd.

In schemes for nutrient reduction from watershed such as Japanese total volume control framework on nutrient or master plan for sewerage system propagation, hydrologic and nutrient behavior in watershed is critical to make an effective plan to fulfill environmental standard of water body. However, there are many uncertainties in constructing a watershed model as follows. First, observation frequency of concentration of water quality, which is a target of such scheme on nutrient reduction, is not enough because they can be obtained in public water quality observation system only about once a month. Second, pollutant load unit, which is used for quantifying pollutant load from watershed, can be fluctuated from place to place. Third, there are many parameters of watershed models which should be calibrated. To resolve these problems, this study applied EnKF, one of data assimilation method, to SWAT (Soil and Water Assessment Tools) model, which can simulate hydrologic and nutrient cycle in watershed, and conducted parameter estimation to achieve more robust result from watershed model under the uncertainties above.

Keywords: Data assimilation, watershed model, water quality simulation, SWAT

©2019. Japan Geoscience Union. All Right Reserved.

Bayesian inference of grain growth prediction via multi-phase-field models

*Shin-ichi Ito[1], Hiromichi Nagao[1], Takashi Kurokawa[1], Tadashi Kasuya[1], Junya Inoue[1]

1. The University of Tokyo

We propose a Bayesian inference methodology to evaluate unobservable parameters involved in multi-phase-field models with the aim of accurately predicting the observed grain growth, such as in metals and rocks. This approach integrates models and a set of observational image data of grain structures. Since the set of image data is not a time series, directly applying conventional inference techniques that require time series as the input data is difficult. The key idea in our methodology to overcome this difficulty is to construct a time series with an appropriate statistic that characterizes static image data of grain structures. Our methodology implements the empirical Bayes method. It can estimate not only a probability density function of the parameters but also an initial phase-field, which is generally unobservable in real experiments. After validating the proposed method through numerical tests using synthetic data, we apply it to real experimental images of grain structures in a steel alloy. The proposed method properly estimates unobservable parameters together with their uncertainties, and successfully selects the initial phase-field that best explains the experimental data from among candidate initial phase-fields.

Keywords: Grain growth, Bayesian inference, Data assimilation, Phase-field model

©2019. Japan Geoscience Union. All Right Reserved.

GNSS data assimilation for the Bungo channel Long-term SSEs using Ensemble Kalman Filter (EnKF)

*Megumi Fujita[1], Takuya NISHIMURA[2], Kazuro Hirahara[3], SHINICHI MIYAZAKI[1]

1. Graduate School of Science , Kyoto University, 2. Disaster Prevention Research Institute, Kyoto University, 3. Institute of Education, Research and Regional Cooperation for crisis Management Shikoku, Kagawa University

Long-term Slow Slip Events (L-SSEs) in the Bungo channel, southwest Japan occur in the down-dip side of the seismogenic zones on the megathrust plate interface. Although L-SSEs release accumulated strain in the L-SSE zones, they can increase strain in the up-dip seismogenic locked zones. Therefore, better understanding of the temporal evolution of L-SSEs is very important for earthquake hazard assessment. Hirahara, and Nishikiori (JpGU, 2018) developed a method for estimating slip evolution and frictional properties on L-SSE area in the Bungo channel, by applying a data assimilation method EnKF (Ensemble Kalman Filter), which has been developed in meteorology and oceanology, to the synthetic GNSS data. Although they used the surface velocity data as GNSS data, the actual data which we can observe at GNSS station is the surface displacement data, not surface velocity data. In order to apply EnKF to the actual GNSS observational data, we conducted two numerical experiments, as follows.

i)We used the surface velocity data converted from the synthetic surface displacement data as observational data.

ii) We used the surface displacement data, not the surface velocity data as observational data.

We used the same model settings in above two numerical experiments as Hirahara and Nishikiori (2018) did. Firstly, we set a plane fault in homogeneous isotropic elastic body, whose angle of dip is 15 degrees. The frictional force on the plane fault follows a Rate and State Friction (RSF) law with an aging law [Dieterich,1979; Ruina,1983]. We set a velocity weakening (A-B<0) circular patch, whose radius R is 35 km, in the velocity strengthen (A-B>0) fault plane. We reproduced the observed L-SSEs in the Bungo Channel, using the frictional parameters in such a way that R is smaller than the critical nucleation size R_c [Rubin and Ampuero (2005), Chen and Lapusta (2009)]. Secondly, we considered the effect the seismogenic locked zones in the up-dip side of the L-SSEs zone. We set a locked zone at the up-dip of the L-SSE fault, whose back-slip rate is 6.0 cm/yr.

As the common analysis settings, we selected several pairs of frictional parameters in a wide range of parameter space which reproduce L-SSEs for the initial ensemble members of frictional parameters. We made the daily synthetic GNSS surface displacement data for 93 GEONET stations around the Bungo channel by calculating the surface displacements using true synthetic frictional parameters and adding random Gaussian noise. We set the assimilation interval to 10 days.

In experiment i), we calculated 31 day moving averages of the synthetic GNSS displacement data, and we obtained the surface velocities at GNSS stations from the derivatives of a 150-day cubic spline function fitting the moving averaged surface displacements. Then we applied EnKF to the obtained surface velocities and we successfully estimated slip evolution and frictional parameters. This result suggests this method for converting the surface displacement data into the surface velocity data at GNSS stations might be applicable.

©2019. Japan Geoscience Union. All Right Reserved.

In experiment ii), we applied EnKF to the synthetic GNSS displacement data directly. When we conducted experiment ii), we changed some analysis settings for stabilizing the assimilation. Firstly, when the slip velocity at the center of fault plane is low, we added larger random noise to the innovations artificially. Secondly, when the slip velocity at the center of fault plane is high, we reduced the assimilation interval to 1 day and introduced additive inflation to prevent the prediction errors from being too small. As a result, we also successfully estimated slip evolution and frictional parameters using the surface displacements, although the experiment sometime fails depending on the start timing of the analysis. Therefore, this method has not been fully stabilized yet, and we need to improve it for robust estimation.

Finally, we applied EnKF to the real GNSS data before the 2011 Tohoku-oki earthquake in the same settings as experiment i) and ii) respectively. We corrected offsets of major earthquakes and antenna changes in the GNSS data. However, both experiments stopped during the assimilation due to negative slip velocities. It manifests an importance of correction of GNSS data including removing annual and semiannual components for a stable assimilation of real GNSS data. Furthermore, we need to consider the realistic model settings including the geometry of the subducting Philippine Sea plate interface and distribution of both L-SSE and locked zones.

Acknowledgement: We used GNSS of GEONET provided by the Geospatial Information Authority of Japan (GSI).

Keywords: GNSS, Ensemble Kalman Filter (EnKF), Long-term SSEs, the Bungo channel

©2019. Japan Geoscience Union. All Right Reserved.

A data assimilation library with Python for parallel computing

*Shin ya Nakano[1], Yuya Ariyoshi[2], Tomoyuki Higuchi[1]

1. The Institute of Statistical Mathematics, 2. Faculty of Engineering, Nippon Bunri University

Parallel computing is essential to reduce the computational time in the ensemble-based data assimilation. However, it requires skills in parallel programming. It is sometimes a hard task to attain high computational efficiency with ensemble-based data assimilation. In particular, the particle filter (PF) algorithm, which is applicable to nonlinear and/or non-Gaussian problems, contains a procedure difficult to parallelize.
It is thus challenging to achieve high computational efficiency with the PF even for experienced users.

We have developed a Python library named P-cubed (Python Parallelized Particle Filter Library), that enables us to use parallel-ready PF algorithms with high parallel efficiency. Now we are also planning to attach a module of other data assimilation algorithms such as the ensemble Kalman filter to this library. In this presentation, we introduce the parallelized PF algorithms which are already available in P-cubed and explain the design and characteristics of the library. Future prospects of this library will also be discussed.

Keywords: data assimilation, particle filter, parallel computing, Python

©2019. Japan Geoscience Union. All Right Reserved.

[E] Poster | M (Multidisciplinary and Interdisciplinary)：M-GI General Geosciences, Information Geosciences & Simulations

Wed. May 29, 2019 5:15 PM - 6:30 PM JST | Wed. May 29, 2019 8:15 AM - 9:30 AM UTC | Poster Hall International Exhibition Hall8, Makuhari Messe_37

[M-GI30] Data assimilation: A fundamental approach in geosciences

convener:Shin ya Nakano(The Institute of Statistical Mathematics), Yosuke Fujii(Meteorological Research Institute, Japan Meteorological Agency), SHINICHI MIYAZAKI(Graduate School of Science, Kyoto University), Takemasa Miyoshi(RIKEN)

Data assimilation is an inversion approach to estimate the evolution of a system by utilizing a constraint given by a dynamical simulation model. Data assimilation is now widely used not only in meteorology and oceanography but also other fields of geosciences such as hydrology, solid earth science, and space science. This session aims at providing an opportunity for discussion on data assimilation studies among researchers of various field of geosciences. We encourage contributions addressing novel methods and theoretical developments of data assimilation. Contributions dealing with useful applications of data assimilation are also welcome.

[MGI30-P01] Superposition of atmospheric states using information redundancy for Numerical Weather Prediction

*Toshiyuki Ishibashi[1] (1.Meteorological Research Institute/Japan Meteorological Agency)

[MGI30-P02] **Numerical Weather Prediction Experiments using a Coupled Atmosphere-Ocean Data Assimilation System in JMA/MRI** (3)

*Toshiyuki Ishibashi[1], Takeshi Iriguchi[1], Yosuke Fujii[1], Tamaki Yasuda[1], Yuhei Takaya[1], Naoki Saito[1], Toshikazu Onogi[1] (1.Meteorological Research Institute/Japan Meteorological Agency)

[MGI30-P03] **Accurate estimation of posterior error covariance in a 4D-Var inverse analysis**

*Yosuke Niwa[1,2], Yosuke Fujii[2,3] (1.National Institute for Environmental Studies, 2.Meteorological Research Institute, Japan Meteorological Agency, 3.The Institute of Statistical Mathematics)

[MGI30-P04] Assimilation CO_2 concentration data in the Kanto region using AIST-MM model and for the estimation of CO_2 emissions

*Yutaka Arai[1], Ryoichi Imasu[1], Hiroaki Kondo[2], Yosuke Niwa[3] (1.Atmosphere and Ocean Research Institute, The University of Tokyo, 2.National Institute of Advanced Industrial Science and Technology, 3.National Institute for Environmental Studies, Independent Administrative Institutions)

[MGI30-P05] **Application of data assimilation method on parameter estimation of flow and nutrient behavior in watershed model**

*Yosuke Horie[1] (1.Nippon Koei Co., Ltd.)

[MGI30-P06] Bayesian inference of grain growth prediction via multi-phase-field models

*Shin-ichi Ito[1], Hiromichi Nagao[1], Takashi Kurokawa[1], Tadashi Kasuya[1], Junya Inoue[1] (1.The University of Tokyo)

[MGI30-P07] GNSS data assimilation for the Bungo channel Long-term SSEs using Ensemble Kalman Filter (EnKF)

*Megumi Fujita[1], Takuya NISHIMURA[2], Kazuro Hirahara[3], SHINICHI MIYAZAKI[1] (1.Graduate School of Science , Kyoto University, 2.Disaster Prevention Research Institute, Kyoto University, 3.Institute of Education, Research and Regional Cooperation for crisis Management Shikoku, Kagawa University)

[MGI30-P08] A data assimilation library with Python for parallel computing

*Shin ya Nakano[1], Yuya Ariyoshi[2], Tomoyuki Higuchi[1] (1.The Institute of Statistical Mathematics, 2.Faculty of Engineering, Nippon Bunri University)

Superposition of atmospheric states using information redundancy for Numerical Weather Prediction

*Toshiyuki Ishibashi[1]

1. Meteorological Research Institute/Japan Meteorological Agency

Atmospheric state analysis is a difficult scientific problem due to our limited ability in computation and observation, and analysed atmospheric states are fluctuating around the true state. The purpose of this paper is to analyse atmospheric state as a superposition of possible atmospheric states using information redundancy, and evaluate its accuracy in the context of numerical weather prediction (NWP). This atmospheric state analysis approach has two novel aspects. First, it uses only real atmospheric information, and no-artificial perturbations unlike existing ensemble based methods. Second, it does not require specific error structures of our knowledge of the atmosphere. We performed this method on a global numerical weather prediction system of Japan Meteorological Agency. The experimental results show the method can clearly reduce forecast root means square errors about 3-5% in average within 2 day forecast compared to existing methods (CNTL). Furthermore, forecast RMSEs of ensemble means of ensemble forecasts using only a few members generated by this method are significantly smaller than CNTL from the forecast initial time.

©2019. Japan Geoscience Union. All Right Reserved.

Numerical Weather Prediction Experiments using a Coupled Atmosphere-Ocean Data Assimilation System in JMA/MRI (3)

*Toshiyuki Ishibashi[1], Takeshi Iriguchi[1], Yosuke Fujii[1], Tamaki Yasuda[1], Yuhei Takaya[1], Naoki Saito[1], Toshikazu Onogi[1]

1. Meteorological Research Institute/Japan Meteorological Agency

An atmosphere-ocean coupled data assimilation system (CDAS) has been developed at the JMA/MRI to investigate feasibility of a CDAS as a future DAS for seamless numerical prediction including both numerical weather prediction (NWP) and numerical seasonal climate prediction (NCP), and for reanalysis of the atmosphere-ocean. Our CDAS (**MRI-CDA1**) has two features. 1) It composed of the JMA operational systems, the global atmospheric DAS (MRI-NAPEX) based on 4D-Var, the global ocean DAS (MOVE-G2) based on 3D-Var, and the atmosphere- ocean coupled global forecast model (CGCM: JMA/MRI-CGCM2). 2) Coupling strategy is “weak coupling” with two different data assimilation window lengths for the atmosphere and ocean. Here, “weak coupling” denotes the approximation that ignores correlations of atmosphere and ocean background forecast errors. Following the previous reports in JpGU2018 and JpGU-AGU joint meeting 2017 (Ishibashi et al. 2018; 2017), we will report basic property of MRI-CDA1 in NWP.

©2019. Japan Geoscience Union. All Right Reserved.

Accurate estimation of posterior error covariance in a 4D-Var inverse analysis

*Yosuke Niwa[1,2], Yosuke Fujii[2,3]

1. National Institute for Environmental Studies, 2. Meteorological Research Institute, Japan Meteorological Agency, 3. The Institute of Statistical Mathematics

The four-dimensional variational method (4D-Var) is one prominent data assimilation/inversion method. However, it is a non-trivial task for a conventional 4D-Var to estimate a posterior error variance-covariance matrix. This study developed a method to estimate a posterior error variance-covariance matrix especially focusing on its off-diagonal elements, i.e., covariance. Off-diagonal elements are usually difficult to be estimated but provide error correlations that are beneficial for interpreting optimized parameter variations. The method was developed within a 4D-Var framework using a quasi-Newton method with the Broyden–Fletcher–Goldfarb–Shanno (BFGS) formula. This study newly introduces numerical techniques that ensure conjugacy among the set of increment vector pairs in the BFGS formula. Through application to an inverse problem of atmospheric CO_2, the developed method was evaluated with three diagnostic measures and compared against existing methods. The evaluation revealed that the developed method could provide accurate estimates of the posterior variance-covariance matrix, in terms not only of the diagonal but also of the off-diagonal elements. Although far more expensive than optimal state estimation, the computational efficiency was found reasonable for practical use, especially in conjunction with an ensemble approach.

Keywords: inversion, data assimilation, posterior error covariance

©2019. Japan Geoscience Union. All Right Reserved.

Assimilation CO_2 concentration data in the Kanto region using AIST-MM model and for the estimation of CO_2 emissions

*Yutaka Arai[1], Ryoichi Imasu[1], Hiroaki Kondo[2], Yosuke Niwa[3]

1. Atmosphere and Ocean Research Institute, The University of Tokyo, 2. National Institute of Advanced Industrial Science and Technology, 3. National Institute for Environmental Studies, Independent Administrative Institutions

Atmospheric carbon dioxide (CO_2) known as greenhouse gas is the most important gas for global warming. For the reason, there have been many researches about CO_2 such as model calculations, satellite observations and direct observations recently. As computer spec get higher, the CO_2 model has been more improved and 3D distributions of CO_2 has been calculated in more detail. In Japan, the satellite observation has been high resolution by satellite, Greenhouse Observing SATellite-2 (GOSAT-2). But in urban area, CO_2 distributions are complicated because of complexed CO_2 emission source and sink around the area. Especially, in the Kanto district mega city, Tokyo is located, CO_2 emissions from power plants and human activities are very huge. Furthermore, around the city there are forests and mountains which strongly affect to CO_2 concentrations in the atmosphere through their respiration and photosynthesis. In case to calculate such the district with high spatial resolutions, the models are required to be able to represent the temporal and spatial variations of the respiration and photosynthesis of the plants precisely. It has been also pointed out that representativeness of the vertical transport of CO_2 in the models is a key subject. About satellite observations, it is not always possible to observe CO2 distributions because of to be influenced by the weather and the frequencies of them are limited, and what ca be observed are not 3 dimensional but 2 dimensional namely vertical column densities of CO_2. On the other hand, the accuracy of the in-situ observations, is best, but there are very limited observation points. These are obstacles to grasping the detailed behavior of CO_2 concentration.

In this study, a regional transport model, AIST-MM has been used to investigate the behavior of CO_2 concentrations in Kanto district (Kondo et al., 2001). Firstly, AIST-MM computes CO_2 concentrations in the outer area (630 km×550 km), and then calculates CO_2 concentrations in the inner area (216 km×216 km) using the results from the former.
Firstly, the model was improved to be able to calculate the CO_2 seasonal variations through a year in order to estimate CO_2 emission source which contained large error. It was found that AIST-MM had uncertainty in the part of plant activities especially respiration in summer. As the calculation of plant respiration strongly depends on the temperature, when the temperature becomes high, the respiration of plants unrealistically increases. So the plant respiration parameter was tuned.
In order to compensate for the CO_2 influx from outside of the calculation region, the result of a global model, NICAM-TM (GL5) were used as the boundary conditions when calculating outer region. This modification led to improve the calculation of the vertical transport.
Furthermore, constant sea surface temperature was replaced with the satellite observation data derived from AVHRR-AMSR. In order to improve the simulating performance, we adjusted many detailed emission information by distinguishing between holidays and weekdays.
Secondly, Local Ensemble Transform Kalman Filter (LETKF) which is one of data assimilation methods is adapted to the adjusted AIST-MM and try to calculate CO_2 concentrations using in-situ observations, satellite observations, and ground remote sensing observations. In the near future, the CO_2 emissions will be estimated using Kalman smoother method.

©2019. Japan Geoscience Union. All Right Reserved.

Keywords: regional CO2 transport model, plant respiration, data assimilation, Local Ensemble Transform Kalman Filter, Kanto region

©2019. Japan Geoscience Union. All Right Reserved.

Application of data assimilation method on parameter estimation of flow and nutrient behavior in watershed model

*Yosuke Horie[1]

1. Nippon Koei Co., Ltd.

In schemes for nutrient reduction from watershed such as Japanese total volume control framework on nutrient or master plan for sewerage system propagation, hydrologic and nutrient behavior in watershed is critical to make an effective plan to fulfill environmental standard of water body. However, there are many uncertainties in constructing a watershed model as follows. First, observation frequency of concentration of water quality, which is a target of such scheme on nutrient reduction, is not enough because they can be obtained in public water quality observation system only about once a month. Second, pollutant load unit, which is used for quantifying pollutant load from watershed, can be fluctuated from place to place. Third, there are many parameters of watershed models which should be calibrated. To resolve these problems, this study applied EnKF, one of data assimilation method, to SWAT (Soil and Water Assessment Tools) model, which can simulate hydrologic and nutrient cycle in watershed, and conducted parameter estimation to achieve more robust result from watershed model under the uncertainties above.

Keywords: Data assimilation, watershed model, water quality simulation, SWAT

©2019. Japan Geoscience Union. All Right Reserved.

Bayesian inference of grain growth prediction via multi-phase-field models

*Shin-ichi Ito[1], Hiromichi Nagao[1], Takashi Kurokawa[1], Tadashi Kasuya[1], Junya Inoue[1]

1. The University of Tokyo

We propose a Bayesian inference methodology to evaluate unobservable parameters involved in multi-phase-field models with the aim of accurately predicting the observed grain growth, such as in metals and rocks. This approach integrates models and a set of observational image data of grain structures. Since the set of image data is not a time series, directly applying conventional inference techniques that require time series as the input data is difficult. The key idea in our methodology to overcome this difficulty is to construct a time series with an appropriate statistic that characterizes static image data of grain structures. Our methodology implements the empirical Bayes method. It can estimate not only a probability density function of the parameters but also an initial phase-field, which is generally unobservable in real experiments. After validating the proposed method through numerical tests using synthetic data, we apply it to real experimental images of grain structures in a steel alloy. The proposed method properly estimates unobservable parameters together with their uncertainties, and successfully selects the initial phase-field that best explains the experimental data from among candidate initial phase-fields.

Keywords: Grain growth, Bayesian inference, Data assimilation, Phase-field model

©2019. Japan Geoscience Union. All Right Reserved.

GNSS data assimilation for the Bungo channel Long-term SSEs using Ensemble Kalman Filter (EnKF)

*Megumi Fujita[1], Takuya NISHIMURA[2], Kazuro Hirahara[3], SHINICHI MIYAZAKI[1]

1. Graduate School of Science , Kyoto University, 2. Disaster Prevention Research Institute, Kyoto University, 3. Institute of Education, Research and Regional Cooperation for crisis Management Shikoku, Kagawa University

Long-term Slow Slip Events (L-SSEs) in the Bungo channel, southwest Japan occur in the down-dip side of the seismogenic zones on the megathrust plate interface. Although L-SSEs release accumulated strain in the L-SSE zones, they can increase strain in the up-dip seismogenic locked zones. Therefore, better understanding of the temporal evolution of L-SSEs is very important for earthquake hazard assessment. Hirahara, and Nishikiori (JpGU, 2018) developed a method for estimating slip evolution and frictional properties on L-SSE area in the Bungo channel, by applying a data assimilation method EnKF (Ensemble Kalman Filter), which has been developed in meteorology and oceanology, to the synthetic GNSS data. Although they used the surface velocity data as GNSS data, the actual data which we can observe at GNSS station is the surface displacement data, not surface velocity data. In order to apply EnKF to the actual GNSS observational data, we conducted two numerical experiments, as follows.

i)We used the surface velocity data converted from the synthetic surface displacement data as observational data.

ii) We used the surface displacement data, not the surface velocity data as observational data.

We used the same model settings in above two numerical experiments as Hirahara and Nishikiori (2018) did. Firstly, we set a plane fault in homogeneous isotropic elastic body, whose angle of dip is 15 degrees. The frictional force on the plane fault follows a Rate and State Friction (RSF) law with an aging law [Dieterich,1979; Ruina,1983]. We set a velocity weakening (A-B<0) circular patch, whose radius R is 35 km, in the velocity strengthen (A-B>0) fault plane. We reproduced the observed L-SSEs in the Bungo Channel, using the frictional parameters in such a way that R is smaller than the critical nucleation size R_c [Rubin and Ampuero (2005), Chen and Lapusta (2009)]. Secondly, we considered the effect the seismogenic locked zones in the up-dip side of the L-SSEs zone. We set a locked zone at the up-dip of the L-SSE fault, whose back-slip rate is 6.0 cm/yr.

As the common analysis settings, we selected several pairs of frictional parameters in a wide range of parameter space which reproduce L-SSEs for the initial ensemble members of frictional parameters. We made the daily synthetic GNSS surface displacement data for 93 GEONET stations around the Bungo channel by calculating the surface displacements using true synthetic frictional parameters and adding random Gaussian noise. We set the assimilation interval to 10 days.

In experiment i), we calculated 31 day moving averages of the synthetic GNSS displacement data, and we obtained the surface velocities at GNSS stations from the derivatives of a 150-day cubic spline function fitting the moving averaged surface displacements. Then we applied EnKF to the obtained surface velocities and we successfully estimated slip evolution and frictional parameters. This result suggests this method for converting the surface displacement data into the surface velocity data at GNSS stations might be applicable.

©2019. Japan Geoscience Union. All Right Reserved.

In experiment ii), we applied EnKF to the synthetic GNSS displacement data directly. When we conducted experiment ii), we changed some analysis settings for stabilizing the assimilation. Firstly, when the slip velocity at the center of fault plane is low, we added larger random noise to the innovations artificially. Secondly, when the slip velocity at the center of fault plane is high, we reduced the assimilation interval to 1 day and introduced additive inflation to prevent the prediction errors from being too small. As a result, we also successfully estimated slip evolution and frictional parameters using the surface displacements, although the experiment sometime fails depending on the start timing of the analysis. Therefore, this method has not been fully stabilized yet, and we need to improve it for robust estimation.

Finally, we applied EnKF to the real GNSS data before the 2011 Tohoku-oki earthquake in the same settings as experiment i) and ii) respectively. We corrected offsets of major earthquakes and antenna changes in the GNSS data. However, both experiments stopped during the assimilation due to negative slip velocities. It manifests an importance of correction of GNSS data including removing annual and semiannual components for a stable assimilation of real GNSS data. Furthermore, we need to consider the realistic model settings including the geometry of the subducting Philippine Sea plate interface and distribution of both L-SSE and locked zones.

Acknowledgement: We used GNSS of GEONET provided by the Geospatial Information Authority of Japan (GSI).

Keywords: GNSS, Ensemble Kalman Filter (EnKF), Long-term SSEs, the Bungo channel

©2019. Japan Geoscience Union. All Right Reserved.

A data assimilation library with Python for parallel computing

*Shin ya Nakano[1], Yuya Ariyoshi[2], Tomoyuki Higuchi[1]

1. The Institute of Statistical Mathematics, 2. Faculty of Engineering, Nippon Bunri University

Parallel computing is essential to reduce the computational time in the ensemble-based data assimilation. However, it requires skills in parallel programming. It is sometimes a hard task to attain high computational efficiency with ensemble-based data assimilation. In particular, the particle filter (PF) algorithm, which is applicable to nonlinear and/or non-Gaussian problems, contains a procedure difficult to parallelize.
It is thus challenging to achieve high computational efficiency with the PF even for experienced users.

We have developed a Python library named P-cubed (Python Parallelized Particle Filter Library), that enables us to use parallel-ready PF algorithms with high parallel efficiency. Now we are also planning to attach a module of other data assimilation algorithms such as the ensemble Kalman filter to this library. In this presentation, we introduce the parallelized PF algorithms which are already available in P-cubed and explain the design and characteristics of the library. Future prospects of this library will also be discussed.

Keywords: data assimilation, particle filter, parallel computing, Python

©2019. Japan Geoscience Union. All Right Reserved.

[E] Poster | M (Multidisciplinary and Interdisciplinary)：M-TT Technology & Techniques

Wed. May 29, 2019 1:45 PM - 3:15 PM JST | Wed. May 29, 2019 4:45 AM - 6:15 AM UTC | Poster Hall International Exhibition Hall8, Makuhari Messe_6

[M-TT45] Cryoseismology - a new proxy for detecting surface environmental variations of the Earth -

convener:Genti Toyokuni(Research Center for Prediction of Earthquakes and Volcanic Eruptions, Graduate School of Science, Tohoku University), Masaki Kanao(National Institute of Polar Research), Seiji Tsuboi(JAMSTEC, Center for Earth Information Science and Technology)

Several kinds of environmental signals associated with ocean - cryosphere - solid earth systems have recently been detected in bi-polar regions. Ice-related seismic motions for small magnitude events are generally named ice-quakes (ice-shocks) and can be generated by glacially related dynamics. Such kinds of cryoseismic sources are classified into the movements of ice sheets, sea-ice, oceanic tide-cracks, icebergs and the calving fronts of ice caps. Cryoseismic waves are likely to be influenced by variations in environmental conditions, and the continuous study of their time-space variability provides indirect evidence of climate change. As glacial earthquakes are the most prominent phenomena found recently in polar regions, in particular on the Greenland in this 21st century, the new innovative studies from seismology are expected by long-term monitoring under extreme conditions in the Earth's environment.

Taking these issues into account, the conveners are willing to invite many contributions to a special session on "Cryoseismology", which will cover the recent achievements on glacial related seismic events and associated phenomenon observed in polar regions. It is particularly encouraged to have contributions based on seismic signals involving the dynamics of ice sheets, sea-ice, and icebergs and glaciers. Although the glacial earthquakes are the most prominent evidence found recently in polar regions, all related topics involving polar seismology are welcome, such as studies of crust and mantle structure in the area, comparison of tectonic and glacier-related seismicity, recent triggered earthquakes and active volcanoes, glacial isostatic adjustment (GIA), harmonic tremor associated with cryoseismic events, etc. This session has been held every year since 2015, and was held as Union Session last year.

[MTT45-P01] Application of neural network and theoretical seismograms as training data to locate ice quakes

*Seiji Tsuboi[1], DAISUKE SUGIYAMA[1] (1.JAMSTEC, Center for Earth Information Science and Technology)

[MTT45-P02] **P-wave tomography beneath Greenland**

*Takaya Matsuno[1], Genti Toyokuni[1], Dapeng Zhao[1] (1.Research Center for Prediction of Earthquakes and Volcanic Eruptions, Graduate School of Science, Tohoku University)

[MTT45-P03] **Seismic observations in Greenland by a joint USA and Japanese GLISN team (2011–2018)**

*Genti Toyokuni[1], Masaki Kanao[2], Seiji Tsuboi[3], Yoko Tono[4] (1.RCPEVE, Tohoku Univ., 2.NIPR, 3.JAMSTEC, 4.ERI, Univ. Tokyo)

Application of neural network and theoretical seismograms as training data to locate ice quakes

*Seiji Tsuboi[1], DAISUKE SUGIYAMA[1]

1. JAMSTEC, Center for Earth Information Science and Technology

We have applied numerically computed theoretical seismograms and deep machine learning to locate earthquakes. We calculate theoretical seismograms for realistic three-dimensional Earth model and use these seismograms to create seismic wave propagation images at the surface of the Earth. Then we use these images as training dataset of convolutional neural network. We build neural networks for determination of hypocentral parameters, such as epicenter, depth, origin time and magnitude, and applied these networks to actual seismograms to examine if this procedure works to locate earthquake and determine magnitude. Although the number of earthquakes is small and the regional extent is quite limited, the results demonstrate that it is feasible to locate earthquakes by using this approach. Advantages of using this approach to locate earthquakes and determine magnitude are; accuracy of hypocenter parameters can be increased by accumulating theoretical seismograms for various earthquake location and size as learning dataset of deep machine learning; three dimensional Earth structure can be included without additional computational cost to locate earthquakes. Here we will discuss a possibility of applying this methodology to locate ice quakes, which happen in and near the ice sheet.

Keywords: icequakes, hypocenter determination, synthetic seismograms

©2019. Japan Geoscience Union. All Right Reserved.

P-wave tomography beneath Greenland

*Takaya Matsuno[1], Genti Toyokuni[1], Dapeng Zhao[1]

1. Research Center for Prediction of Earthquakes and Volcanic Eruptions, Graduate School of Science, Tohoku University

The Greenland landmass has a long and complex tectonic history (~4 billion years). However, most of the continent is covered by the extensive inland ice cap, so it was hard to access its geology and the underlying tectonics. The Greenland Ice Sheet Monitoring Network (GLISN) is an international project by 11 countries to establish a seismic network in and around Greenland (Toyokuni et al., 2014). The project was initiated in 2009, and now it provides broadband, continuous, and real-time seismic data recorded at 33 stations. In this study we aim to investigate the 3-D upper mantle structure beneath Greenland by using the GLISN data.

We inverted a number of P-wave arrival-time data of both local and teleseismic events, observed at 30 GLISN stations, to estimate a 3-D P-wave velocity (Vp) model beneath Greenland and surrounding regions. All of the GLISN arrival-time data are downloaded from the Bulletins of the International Seismological Centre. We used the seismic tomography method by Zhao et al. (2012).

In the polar region, if grid nodes are arranged on the basis of equatorial coordinates, distance between two adjacent nodes in the same latitude decreases as it gets closer to the pole. To overcome this problem, we converted our study region from the equatorial coordinates to the ecliptic coordinates. This scheme enables us to solve tomographic equations in quasi-Cartesian coordinates (e.g., Kobayashi & Zhao, 2004; Gupta et al., 2009; Takenaka et al., 2017). We set up a 3-D grid with a horizontal grid interval of 2° and a vertical grid interval of 15–30 km (at depths of 5–700 km).

The results of this study are summarized as follows.
(1) There is a prominent low-Vp anomaly beneath Iceland (depth < 500 km), which is related to the current Iceland plume.
(2) In the shallow mantle (40-250 km depths) beneath central and offshore eastern Greenland, Vp is relatively lower than those in the other inland areas of Greenland in the depth range, which may reflect the ancient motion path of the Iceland plume. This feature coincides with known basalt areas at central western and eastern coasts of Greenland.

References:
Kobayashi, R. & D. Zhao (2004) PEPI, 141, 167–181.
Gupta, S., D. Zhao & S. Rai (2009) Gondwana Res, 16, 109–118.
Takenaka, H. et al. (2017) EPS, 69, 67.
Toyokuni, G. et al. (2014) Antarctic Record, 58, 1–18.
Zhao, D. et al. (2012) GJI, 190, 816–828.

Keywords: Seismic tomography, Greenland, Iceland plume, GLISN project

©2019. Japan Geoscience Union. All Right Reserved.

Seismic observations in Greenland by a joint USA and Japanese GLISN team (2011–2018)

*Genti Toyokuni[1], Masaki Kanao[2], Seiji Tsuboi[3], Yoko Tono[4]

1. RCPEVE, Tohoku Univ., 2. NIPR, 3. JAMSTEC, 4. ERI, Univ. Tokyo

The Greenland Ice Sheet (GrIS) is a huge storehouse of water on Earth, and has the potential to raise the global sea level by approximately 7 m if completely melted. Although researchers have been mainly studying the GrIS surface snowmelt as a response to climate warming, recent progress in ice-core drilling, remote sensing, and theoretical analyses has turned a spotlight on its basal conditions. However, the traditional observation techniques, such as ice-core drilling and ice-penetrating radar, provide only discontinuous information in both time and space.

Seismic observation is now drawing widespread attention as an alternative method for monitoring the GrIS. The Greenland Ice Sheet Monitoring Network (GLISN), an international project between 11 countries that began in 2009, now provides broadband, continuous, and real-time seismic data from 33 stations in and around Greenland. Japan is a partner country from when the GLISN project was launched, and has been sending an expedition team every year since 2011. In 2011, a joint USA and Japanese GLISN team installed the dual seismic–GPS station ICESG-GLS2 in the middle of the GrIS. During 2012–2018, we conducted maintenance of three stations on the GrIS (station codes: ICESG-GLS2, DY2G-GLS1, and NEEM-GLS3), and three stations on bedrock in coastal areas (NUUK, DBG, and SOEG). We had succeeded in real-time transmission of broad-band and continuous seismic waveform data from the three ice stations. It was the first time in the world that the seismic data with such a high sampling rate are transferred from the ice sheet. The data is now open to public and available from the IRIS Data Management Center (http://www.iris.edu/ds/nodes/dmc/). This presentation will summarize our field activities for 2011–2018, and introduce the future field plans.

Acknowledgments: The Japanese GLISN team has been supported by research grants from JSPS (24403006).

Keywords: GLISN project, Seismic observation, Greenland Ice Sheet

©2019. Japan Geoscience Union. All Right Reserved.

[E] Poster | M (Multidisciplinary and Interdisciplinary)：M-TT Technology & Techniques

Wed. May 29, 2019 5:15 PM - 6:30 PM JST | Wed. May 29, 2019 8:15 AM - 9:30 AM UTC | Poster Hall International Exhibition Hall8, Makuhari Messe_40

[M-TT45] Cryoseismology - a new proxy for detecting surface environmental variations of the Earth -

convener:Genti Toyokuni(Research Center for Prediction of Earthquakes and Volcanic Eruptions, Graduate School of Science, Tohoku University), Masaki Kanao(National Institute of Polar Research), Seiji Tsuboi(JAMSTEC, Center for Earth Information Science and Technology)

Several kinds of environmental signals associated with ocean - cryosphere - solid earth systems have recently been detected in bi-polar regions. Ice-related seismic motions for small magnitude events are generally named ice-quakes (ice-shocks) and can be generated by glacially related dynamics. Such kinds of cryoseismic sources are classified into the movements of ice sheets, sea-ice, oceanic tide-cracks, icebergs and the calving fronts of ice caps. Cryoseismic waves are likely to be influenced by variations in environmental conditions, and the continuous study of their time-space variability provides indirect evidence of climate change. As glacial earthquakes are the most prominent phenomena found recently in polar regions, in particular on the Greenland in this 21st century, the new innovative studies from seismology are expected by long-term monitoring under extreme conditions in the Earth's environment.

Taking these issues into account, the conveners are willing to invite many contributions to a special session on "Cryoseismology", which will cover the recent achievements on glacial related seismic events and associated phenomenon observed in polar regions. It is particularly encouraged to have contributions based on seismic signals involving the dynamics of ice sheets, sea-ice, and icebergs and glaciers. Although the glacial earthquakes are the most prominent evidence found recently in polar regions, all related topics involving polar seismology are welcome, such as studies of crust and mantle structure in the area, comparison of tectonic and glacier-related seismicity, recent triggered earthquakes and active volcanoes, glacial isostatic adjustment (GIA), harmonic tremor associated with cryoseismic events, etc. This session has been held every year since 2015, and was held as Union Session last year.

[MTT45-P01] Application of neural network and theoretical seismograms as training data to locate ice quakes

*Seiji Tsuboi[1], DAISUKE SUGIYAMA[1] (1.JAMSTEC, Center for Earth Information Science and Technology)

[MTT45-P02] **P-wave tomography beneath Greenland**

*Takaya Matsuno[1], Genti Toyokuni[1], Dapeng Zhao[1] (1.Research Center for Prediction of Earthquakes and Volcanic Eruptions, Graduate School of Science, Tohoku University)

[MTT45-P03] **Seismic observations in Greenland by a joint USA and Japanese GLISN team (2011–2018)**

*Genti Toyokuni[1], Masaki Kanao[2], Seiji Tsuboi[3], Yoko Tono[4] (1.RCPEVE, Tohoku Univ., 2.NIPR, 3.JAMSTEC, 4.ERI, Univ. Tokyo)

Application of neural network and theoretical seismograms as training data to locate ice quakes

*Seiji Tsuboi[1], DAISUKE SUGIYAMA[1]

1. JAMSTEC, Center for Earth Information Science and Technology

We have applied numerically computed theoretical seismograms and deep machine learning to locate earthquakes. We calculate theoretical seismograms for realistic three-dimensional Earth model and use these seismograms to create seismic wave propagation images at the surface of the Earth. Then we use these images as training dataset of convolutional neural network. We build neural networks for determination of hypocentral parameters, such as epicenter, depth, origin time and magnitude, and applied these networks to actual seismograms to examine if this procedure works to locate earthquake and determine magnitude. Although the number of earthquakes is small and the regional extent is quite limited, the results demonstrate that it is feasible to locate earthquakes by using this approach. Advantages of using this approach to locate earthquakes and determine magnitude are; accuracy of hypocenter parameters can be increased by accumulating theoretical seismograms for various earthquake location and size as learning dataset of deep machine learning; three dimensional Earth structure can be included without additional computational cost to locate earthquakes. Here we will discuss a possibility of applying this methodology to locate ice quakes, which happen in and near the ice sheet.

Keywords: icequakes, hypocenter determination, synthetic seismograms

©2019. Japan Geoscience Union. All Right Reserved.

P-wave tomography beneath Greenland

*Takaya Matsuno[1], Genti Toyokuni[1], Dapeng Zhao[1]

1. Research Center for Prediction of Earthquakes and Volcanic Eruptions, Graduate School of Science, Tohoku University

The Greenland landmass has a long and complex tectonic history (~4 billion years). However, most of the continent is covered by the extensive inland ice cap, so it was hard to access its geology and the underlying tectonics. The Greenland Ice Sheet Monitoring Network (GLISN) is an international project by 11 countries to establish a seismic network in and around Greenland (Toyokuni et al., 2014). The project was initiated in 2009, and now it provides broadband, continuous, and real-time seismic data recorded at 33 stations. In this study we aim to investigate the 3-D upper mantle structure beneath Greenland by using the GLISN data.

We inverted a number of P-wave arrival-time data of both local and teleseismic events, observed at 30 GLISN stations, to estimate a 3-D P-wave velocity (Vp) model beneath Greenland and surrounding regions. All of the GLISN arrival-time data are downloaded from the Bulletins of the International Seismological Centre. We used the seismic tomography method by Zhao et al. (2012).

In the polar region, if grid nodes are arranged on the basis of equatorial coordinates, distance between two adjacent nodes in the same latitude decreases as it gets closer to the pole. To overcome this problem, we converted our study region from the equatorial coordinates to the ecliptic coordinates. This scheme enables us to solve tomographic equations in quasi-Cartesian coordinates (e.g., Kobayashi & Zhao, 2004; Gupta et al., 2009; Takenaka et al., 2017). We set up a 3-D grid with a horizontal grid interval of 2° and a vertical grid interval of 15–30 km (at depths of 5–700 km).

The results of this study are summarized as follows.
(1) There is a prominent low-Vp anomaly beneath Iceland (depth < 500 km), which is related to the current Iceland plume.
(2) In the shallow mantle (40-250 km depths) beneath central and offshore eastern Greenland, Vp is relatively lower than those in the other inland areas of Greenland in the depth range, which may reflect the ancient motion path of the Iceland plume. This feature coincides with known basalt areas at central western and eastern coasts of Greenland.

References:
Kobayashi, R. & D. Zhao (2004) PEPI, 141, 167–181.
Gupta, S., D. Zhao & S. Rai (2009) Gondwana Res, 16, 109–118.
Takenaka, H. et al. (2017) EPS, 69, 67.
Toyokuni, G. et al. (2014) Antarctic Record, 58, 1–18.
Zhao, D. et al. (2012) GJI, 190, 816–828.

Keywords: Seismic tomography, Greenland, Iceland plume, GLISN project

©2019. Japan Geoscience Union. All Right Reserved.

Seismic observations in Greenland by a joint USA and Japanese GLISN team (2011–2018)

*Genti Toyokuni[1], Masaki Kanao[2], Seiji Tsuboi[3], Yoko Tono[4]

1. RCPEVE, Tohoku Univ., 2. NIPR, 3. JAMSTEC, 4. ERI, Univ. Tokyo

The Greenland Ice Sheet (GrIS) is a huge storehouse of water on Earth, and has the potential to raise the global sea level by approximately 7 m if completely melted. Although researchers have been mainly studying the GrIS surface snowmelt as a response to climate warming, recent progress in ice-core drilling, remote sensing, and theoretical analyses has turned a spotlight on its basal conditions. However, the traditional observation techniques, such as ice-core drilling and ice-penetrating radar, provide only discontinuous information in both time and space.

Seismic observation is now drawing widespread attention as an alternative method for monitoring the GrIS. The Greenland Ice Sheet Monitoring Network (GLISN), an international project between 11 countries that began in 2009, now provides broadband, continuous, and real-time seismic data from 33 stations in and around Greenland. Japan is a partner country from when the GLISN project was launched, and has been sending an expedition team every year since 2011. In 2011, a joint USA and Japanese GLISN team installed the dual seismic–GPS station ICESG-GLS2 in the middle of the GrIS. During 2012–2018, we conducted maintenance of three stations on the GrIS (station codes: ICESG-GLS2, DY2G-GLS1, and NEEM-GLS3), and three stations on bedrock in coastal areas (NUUK, DBG, and SOEG). We had succeeded in real-time transmission of broad-band and continuous seismic waveform data from the three ice stations. It was the first time in the world that the seismic data with such a high sampling rate are transferred from the ice sheet. The data is now open to public and available from the IRIS Data Management Center (http://www.iris.edu/ds/nodes/dmc/). This presentation will summarize our field activities for 2011–2018, and introduce the future field plans.

Acknowledgments: The Japanese GLISN team has been supported by research grants from JSPS (24403006).

Keywords: GLISN project, Seismic observation, Greenland Ice Sheet

©2019. Japan Geoscience Union. All Right Reserved.